RTA4680012 ศ.ดร.สมชาติ โสภณรณฤทธิ์



รายงานวิจัยฉบับสมบูรณ์

โครงการการพัฒนา/ปรับปรุงผลิตภัณฑ์อาหาร/เกษตรโดยการผสมผสานเทคนิคการอบแห้งที่หลากหลาย

เล่มที่ 1

โดย สมชาติ โสภณรณฤทธิ์ และคณะ

กันยายน 2549

สัญญาเลขที่ RTA4680012

รายงานวิจัยฉบับสมบูรณ์

โครงการการพัฒนา/ปรับปรุงผลิตภัณฑ์อาหาร/เกษตรโดยการผสมผสานเทคนิคการอบแห้งที่หลากหลาย

เล่มที่ 1

คณะผู้วิจัย		สังกัด
1. ศ.ดร.สมชาติ	โสภณรณฤทธิ์	มจธ.
2. รศ. วารุณี	เตีย	มจธ.
3. รศ.ดร.สมเกียรติ	ปรัชญาวรากร	มจธ.
4. ผศ.ดร.อดิศักดิ์	นาถกรณกุล	มจธ.
5. ผศ.ดร.สักกมน	เทพหัสดิน ณ อยุธยา	มจธ.
6. ดร.ธนิต	สวัสดิเสวี	มจธ.
7. ผศ.ดร.ฐานิตย์	เมธิยานนท์	ม.มหานคร
8. ผศ.ดร.ชัยยงค์	เตชะไพโรจน์	ม.ศิลปากร
9. ผศ.ดร.เจริญพร	เลิศสถิตธนากร	ม.มหาสารคาม
10. ผศ.ดร.สัมพันธ์	ฤทธิเดช	ม.มหาสารคาม
11. ผศ.ดร.ณัฐพล	ภูมิสะอาด	ม.มหาสารคาม
12. ผศ.ดร.ทรงชัย	วิริยะอำไพวงศ์	ม.มหาสารคาม
13. ผศ.ดร.อำไพศักดิ์	ทีบุญมา	ม.อุบลราชธานี
14. ดร.จินดาพร	จำรัสเลิศลักษณ์	ม.มหาสารคาม

15. นักศึกษาปริญญาเอก 17 คน และปริญญาโท 40 คน

สนับสนุนโดยสำนักงานกองทุนสนับสนุนการวิจัย

กิตติกรรมประกาศ

คณะนักวิจัยใคร่ขอขอบคุณสำนักงานกองทุนสนับสนุนการวิจัย ที่ให้การสนับสนุนโครงการเมธีวิจัยอาวุโส สกว. ระยะที่ 2 - การพัฒนา/ปรับปรุงผลิตภัณฑ์อาหาร/เกษตรโดยการผสมผสานเทคนิคการอบแห้งที่หลากหลาย นอกจากนี้ยังใคร่ขอขอบคุณหน่วยงานต่าง ๆ ที่ให้ความร่วมมือเป็นอย่างดี ได้แก่ บริษัทไร้ซ์เอ็นจิเนียริ่งซัพพลาย จำกัด บริษัทจักรวาลเทคโนโลยีเกษตร จำกัด สถาบันวิจัยอาหารและพัฒนาผลิตภัณฑ์ มหาวิทยาลัยเกษตรศาสตร์ สถาบันวิจัยข้าว กรมวิชาการเกษตร และท้ายสุด โรงสีข้าวคุ้งหลีจัน ที่ได้ให้การสนับสนุนงานวิจัยด้านการทดสอบเครื่องต้นแบบ

บทสรุปผู้บริหาร

กระทรวงอุตสาหกรรมรายงานไว้ว่า ประเทศไทยส่งออกอาหารแห้งปีละหลายพันล้านบาท นอกจากนี้ยังส่งออกข้าวปีละกว่าแสนล้านบาท การอบแห้งเป็นกระบวนการสำคัญในสายการผลิตของผลิตภัณฑ์เหล่านี้ เทคนิคการอบแห้งมีหลากหลาย เช่น การใช้ลมร้อน ไอน้ำร้อนยวดยิ่ง ปั๊มความร้อน รังสีอินฟราเรดไกล รังสีไมโครเวฟ ภายใต้ความดันบรรยากาศ หรือต่ำกว่า/สูงกว่า บรรยากาศ การใช้สารดูดความชื้น การผสมผสานเทคนิคที่หลากหลายสามารถพัฒนาผลิตภัณฑ์ใหม่ ปรับปรุงคุณภาพ และหรือลดต้นทุนการผลิต เช่นผลิตภัณฑ์ประเภทเนื้อสัตว์และผลไม้ที่มีความกรอบคล้ายกับของที่ได้จากการทอด แต่ต่างกันที่ไม่มีน้ำมันเพิ่มเติมในผลิตภัณฑ์ การผลิตข้าวนึ่งโดยใช้ไอน้ำยวดยิ่งช่วยลดขั้นตอน/กรรมวิธี การผลิต ทำให้ประหยัดเวลาและค่าใช้จ่าย

ห้องปฏิบัติการวิจัยเทคโนโลยีการอบแห้ง คณะพลังงานและวัสดุ มหาวิทยาลัยเทคโนโลยีพระจอมเกล้าธนบุรี ได้รับการสนับสนุนจากสำนักงานกองทุนสนับสนุนการวิจัยอย่างต่อเนื่องเป็นเวลาหลายปี มีนักวิจัยที่ชำนาญการอบแห้งผลิตภัณฑ์อาหาร/เกษตร จำนวนมาก เป็นแหล่งรวบรวมความเชี่ยวชาญสหสาขาวิชา ได้แก่ วิศวกรรมศาสตร์สาขาต่าง ๆ วิทยาศาสตร์และเทคโนโลยีการอาหาร เป็นแหล่งพึ่งพิงทางความรู้และเทคโนโลยีด้านการอบแห้งให้กับภาคเอกชนและภาคราชการ มีการให้คำปรึกษาตามคำร้องขออย่างสม่ำเสมอ รวมถึงการจัดอบรมทางวิชาการเพื่อเผยแพร่ความรู้ใหม่ ๆ ที่ได้จากการวิจัย

ผลงานเด่นของห้องปฏิบัติการวิจัยเทคโนโลยีการอบแห้งได้แก่ การร่วมมือกับภาคเอกชนพัฒนาเครื่องต้นแบบสำหรับอบแห้งข้าวเปลือก ผักและผลไม้ จนนำไปสู่การจดสิทธิบัตร ผลิตขาย และส่งออกอย่างแพร่หลาย ตัวอย่างเช่น เครื่องอบแห้งข้าวเปลือกแบบฟลูอิไดซ์เบด เตาเผาแกลบไซโคลน เครื่องอบแห้งปั๊มความร้อน เครื่องอบแห้ง LPG ปัจจุบันเน้นงานการพัฒนากรรมวิธีการผลิตข้าวนึ่ง/ข้าวขาว ผักและผลไม้อบแห้งคุณภาพสูง ประโยชน์ที่ได้รับจากงานวิจัยข้างต้นได้แก่ การลดความสูญเสียของผลิตผลการเกษตร การเพิ่มมูลค่าผลผลิต การสนับสนุนการส่งออก/ทดแทนการนำเข้า และการสนับสนุนนโยบายครัวของโลก

โครงการวิจัยเทคโนโลยีการอบแห้งนี้มีวัตถุประสงค์เพื่อ เพิ่มขีดความสามารถในการวิจัยของกลุ่มนักวิจัยในห้องปฏิบัติการวิจัยเทคโนโลยีการอบแห้ง คณะพลังงานและวัสดุ มหาวิทยาลัยเทคโนโลยีพระจอมเกล้าธนบุรี โดยมีเป้าหมายสูงสุดในการยกระดับความสามารถให้ทัดเทียมกับระดับนานาชาติ เทคโนโลยีการอบแห้งที่เน้นได้แก่ การอบแห้งเมล็ดพืชและอาหารโดยเทคนิคต่าง ๆ ดังที่ได้กล่าวมาแล้วข้างต้น นอกจากเป้าหมายเพื่อตีพิมพ์เผยแพร่ในวารสารนานาชาติแล้ว ยังมีเป้าหมายให้มีการนำผลงานไปผลิตขายและใช้งานในภาคอุตสาหกรรมด้วย

โดยการทำงานเป็นทีมในรูปแบบของปิรามิด คือมีฐานของปิรามิดเป็นนักศึกษาปริญญาโทและปริญญาเอก มีอาจารย์ผู้ช่วยอยู่ระหว่างฐานและยอดของปิรามิด ซึ่งมีหัวหน้ากลุ่มวิจัยคอยดูแลให้คำแนะนำปรึกษา ในขณะใดขณะหนึ่งจะมีนักศึกษาปริญญาโทประมาณ 15 คน ระดับปริญญาเอกประมาณ 8 คน ทำวิทยานิพนธ์ มีอาจารย์ร่วมกลุ่มวิจัยกว่า 10 คน มีการประชุมวิชาการร่วมกันระหว่างนักศึกษาและอาจารย์ทุกสัปดาห์ อาจารย์ที่มีอาวุโสน้อยจะทำหน้าที่เป็นอาจารย์ที่ปรึกษาร่วมกับอาจารย์ที่อาวุโสกว่าทางวิชาการ อาจารย์เหล่านี้จะเรียนรู้การทำงานอย่างเป็นทีมจากกระบวนการนี้ ทุก ๆ คนในห้องปฏิบัติการวิจัยมีความรับผิดชอบต่อการเขียนบทความวิจัยเพื่อตีพิมพ์เผยแพร่ โดยเฉพาะในวารสารนานาชาติ นอกจากการทำงานร่วมกันเป็นทีมภายในห้องปฏิบัติการวิจัยของตัวเองแล้ว ยังร่วมกันทำงานวิจัยกับภาคอุตสาหกรรมในการผลิตเครื่องอบแห้งต้นแบบ และกับสถาบันวิจัยอื่นที่มีความชำนาญเฉพาะด้านด้วย

หัวข้อการวิจัยส่วนใหญ่เกี่ยวข้องกับเทคโนโลยีการอบแห้ง หากแบ่งตามผลิตภัณฑ์ที่สำคัญ ได้แก่ เมล็ดพืชจำพวกข้าว ข้าวโพด ถั่วเหลือง ผักและผลไม้ สมุนไพร เนื้อสัตว์ แต่อาจแบ่งตามลักษณะของ

เทคโนโลยีการอบแห้ง ได้แก่ การอบแห้งโดยใช้ลมร้อน หรือไอน้ำร้อนยวดยิ่ง การอบแห้งโดยเทคนิคฟลูอิไดเซชัน และเทคนิคสเปาเต็ดเบด การอบแห้งโดยใช้ปั๊มความร้อน การอบแห้งโดยใช้สารดูดความชื้น การอบแห้งโดยใช้รังสีอินฟราเรดไกล การอบแห้งภายใต้สภาวะความดันต่ำ การอบแห้งโดยการผสมผสานเทคนิคการอบแห้งหลายแบบ นอกจากนี้ยังทำการวิจัยด้านการใช้พลังงานหมุนเวียนจากมวลชีวภาพ และการประหยัดพลังงานในการอบแห้ง

โครงการวิจัยนี้ประสบผลสำเร็จเกินเป้าหมายที่ตั้งไว้ คือได้ผลงานตีพิมพ์ในวารสารนานาชาติ จำนวน 28 เรื่อง (ไม่นับที่อยู่ระหว่างการตีพิมพ์) ในวารสารในประเทศจำนวน 13 เรื่อง ในรายงานการประชุมทางวิชาการนานาชาติ จำนวน 15 เรื่อง และในรายงานการประชุมทางวิชาการในประเทศ จำนวน 60 เรื่อง บางบทในหนังสือ 1 บท สิทธิบัตรการประดิษฐ์ระหว่างการตรวจสอบจำนวน 1 เรื่อง มีนักศึกษาระดับปริญญาเอกและปริญญาโทจบการศึกษา 8 คน และ 31 คน ตามลำดับ นอกจากประสบความสำเร็จทางด้านผลงานทางวิชาการแล้ว ยังสามารถขยายผลไปสู่ภาคอุตสาหกรรมเมล็ดพืช และอุตสาหกรรมผักและผลไม้ โดยมีบริษัทเอกชนผลิตขายเครื่องอบแห้งแบบฟลูอิไดซ์เบดสำหรับข้าวเปลือก ข้าวนึ่ง ข้าวโพด และถั่วเหลือง เตาเผาแกลบแบบไซโคลน เครื่องอบแห้งปั๊มความร้อน และเครื่องอบแห้งลมร้อนสำหรับอุตสาหกรรมผักและผลไม้แห้ง รวมถึงระบบเป่าลมเย็นข้าวเปลือกในไซโล

ที่สำคัญไม่น้อยไปกว่าผลที่ได้จากโครงการข้างต้นคือ การพัฒนากลุ่มวิจัยจากสหสาขาวิชา ให้ทำงานกันเป็นทีม รวมแล้ว 71 คน ตลอดระยะเวลา 3 ปี โดยทำงานร่วมกับสถาบันวิจัยอื่น และภาคอุตสาหกรรมด้วย

บทคัดย่อ

รหัสโครงการ: RTA4680012

ชื่อโครงการ: (ภาษาไทย) การพัฒนา/ปรับปรุงผลิตภัณฑ์อาหาร/เกษตรโดยการผสมผสานเทคนิคการอบแห้งที่หลากหลาย

(ภาษาอังกฤษ) **Development and Improvement of Agricultural and Food Products with Combination of Various Drying Techniques**

คณะผู้วิจัย (รวม 71คน):

1. ศ.ดร. สมชาติ โสภณรณฤทธิ์ สายวิชาเทคโนโลยีพลังงาน คณะพลังงานและวัสดุ มจธ. หัวหน้าโครงการ
2. รศ.วารุณี เตีย สายวิชาเทคโนโลยีการจัดการพลังงาน คณะพลังงานและวัสดุ มจธ.
3. รศ.ดร.สมเกียรติ ปรัชญาวรากร ภาควิชาวิศวกรรมเคมี คณะวิศวกรรมศาสตร์ มจธ.
4. ผศ.ดร.อดิศักดิ์ นาถกรณกุล สายวิชาเทคโนโลยีพลังงาน คณะพลังงานและวัสดุ มจธ.
5. ผศ.ดร.สักกมน เทพหัสดิน ณ อยุธยา ภาควิชาวิศวกรรมอาหาร คณะวิศวกรรมศาสตร์ มจธ.
6. ดร.ธนิตย์ สวัสดิเสวี สายวิชาเทคโนโลยีอุณหภาพ คณะพลังงานและวัสดุ มจธ.
7. ดร.ฐานิตย์ เมธิยานนท์ ภาควิชาวิศวกรรมเครื่องกล คณะวิศวกรรมศาสตร์ มหาวิทยาลัยเทคโนโลยีมหานคร (ปัจจุบันดำรงตำแหน่ง ผ.ศ.)
8. ดร.ชัยยงค์ เตชะไพโรจน์ คณะวิศวกรรมศาสตร์และเทคโนโลยี มหาวิทยาลัยศิลปากร (ปัจจุบันดำรงตำแหน่ง ผ.ศ.)
9. ดร.เจริญพร เลิศสถิตธนากร คณะวิศวกรรมศาสตร์ มหาวิทยาลัยหาสารคาม (1 ต.ค. 2546 – 30 ก.ย. 2548) (ปัจจุบันดำรงตำแหน่ง ผ.ศ.)
10. ดร.สัมพันธ์ ฤทธิเดช คณะวิศวกรรมศาสตร์ มหาวิทยาลัยมหาสารคาม (1 ต.ค. 2546 – 30 ก.ย. 2547) (ปัจจุบันดำรงตำแหน่ง ผ.ศ.)
11. ดร.ณัฐพล ภูมิสะอาด คณะวิศวกรรมศาสตร์ มหาวิทยาลัยมหาสารคาม (1 ต.ค. 2546 – 30 ก.ย. 2548) (ปัจจุบันดำรงตำแหน่ง ผ.ศ.)
12. ดร.ทรงชัย วิริยะอำไพวงศ์ คณะวิศวกรรมศาสตร์ มหาวิทยาลัยมหาสารคาม (1 ก.ค. 2547 -) (ปัจจุบันดำรงตำแหน่ง ผ.ศ.)
13. ดร.อำไพศักดิ์ ทีบุญมา คณะวิศวกรรมศาสตร์ มหาวิทยาลัยอุบลราชธานี (1 ก.ค. 2547 -) (ปัจจุบันดำรงตำแหน่ง ผ.ศ.)
14. ดร.จินดาพร จำรัสเลิศลักษณ์ คณะวิศวกรรมศาสตร์ มหาวิทยาลัยมหาสารคาม (1 ก.ค. 2549 -)
15. นักศึกษาปริญญาเอก 17 คน และนักศึกษาปริญญาโท 40 คน

e-mail: Somchart.sop@kmutt.ac.th

สาขาวิชาที่ทำการวิจัย: เทคโนโลยีพลังงาน/ เทคโนโลยีหลังการเก็บเกี่ยว

งบประมาณทั้งโครงการ: อนุมัติ 6.0 ล้านบาท ใช้จริงประมาณ 4 ล้านบาท

ระยะเวลาดำเนินงาน: 1 ตุลาคม 2546 - 30 กันยายน 2549

วัตถุประสงค์:

โครงการนี้มีวัตถุประสงค์โดยรวมเพื่อพัฒนาบุคคลากรทางการวิจัยโดยเน้นการพัฒนาอาจารย์นักวิจัยรุ่นใหม่ มีเป้าหมายในการผลิตบัณฑิตระดับปริญญาโท-เอก จำนวนผลงานวิจัยตีพิมพ์ในวารสารนานาชาติ และการนำผลงานวิจัยไปใช้ประโยชน์ได้จริงในภาคธุรกิจอุตสาหกรรม

วิธีการ:

ในขณะใดขณะหนึ่งจะมีนักศึกษาปริญญาโทประมาณ 15 คน ระดับปริญญาเอกประมาณ 8 คน ทำวิทยานิพนธ์ มีการประชุมวิชาการร่วมกันระหว่างนักศึกษาและอาจารย์ทุกสัปดาห์ อาจารย์ที่มีอาวุโสน้อยจะทำหน้าที่เป็นอาจารย์ที่ปรึกษาร่วมกับอาจารย์ที่อาวุโสกว่าทางวิชาการ อาจารย์เหล่านี้จะเรียนรู้การทำงานอย่างเป็นทีมจากกระบวนการนี้ ทุก ๆ คนในห้องปฏิบัติการวิจัยมีความรับผิดชอบต่อการเขียนบทความวิจัยเพื่อตีพิมพ์เผยแพร่ โดยเฉพาะในวารสารนานาชาติ นอกจากการทำงานร่วมกันเป็นทีมภายในห้องปฏิบัติการวิจัยของตัวเองแล้ว ยังร่วมกันทำงานวิจัยกับภาคอุตสาหกรรมในการผลิตเครื่องอบแห้งต้นแบบ และกับสถาบันวิจัยอื่นที่มีความชำนาญเฉพาะด้านด้วย

หัวข้อการวิจัยส่วนใหญ่เกี่ยวข้องกับเทคโนโลยีการอบแห้ง หากแบ่งตามผลิตภัณฑ์ที่สำคัญ ได้แก่ เมล็ดพืชจำพวกข้าว ข้าวโพด ถั่วเหลือง ผักและผลไม้ สมุนไพร เนื้อสัตว์ แต่อาจแบ่งตามลักษณะของเทคโนโลยีการอบแห้ง ได้แก่ การอบแห้งโดยใช้ลมร้อนหรือไอน้ำร้อนยวดยิ่ง การอบแห้งโดยเทคนิคฟลูอิไดเซชันและเทคนิคสเปาเต็ดเบด การอบแห้งโดยใช้ปั๊มความร้อน การอบแห้งโดยใช้สารดูดความชื้น การอบแห้งโดยใช้รังสีอินฟราเรดไกล การอบแห้งภายใต้สภาวะความดันต่ำ การอบแห้งโดยการผสมผสานเทคนิคการอบแห้งหลายแบบ นอกจากนี้ยังทำการวิจัยด้านการใช้พลังงานหมุนเวียนจากมวลชีวภาพ และการประหยัดพลังงานในการอบแห้ง

ผล :

โครงการวิจัยนี้ประสบผลสำเร็จเกินเป้าหมายที่ตั้งไว้ คือได้ผลงานตีพิมพ์ในวารสารนานาชาติจำนวน 28 เรื่อง (ไม่นับที่อยู่ระหว่างการตีพิมพ์) ในวารสารในประเทศจำนวน 13 เรื่อง ในรายงานการประชุมทางวิชาการนานาชาติ จำนวน 15 เรื่อง และในรายงานการประชุมทางวิชาการในประเทศ จำนวน 60 เรื่อง บางบทในหนังสือ 1 บท สิทธิบัตรการประดิษฐ์ระหว่างการตรวจสอบจำนวน 1 เรื่อง มีนักศึกษาระดับปริญญาเอกและปริญญาโทจบการศึกษา 8 คน และ 31 คน ตามลำดับ นอกจากประสบความสำเร็จทางด้านผลงานทางวิชาการแล้ว ยังสามารถขยายผลไปสู่ภาคอุตสาหกรรมเมล็ดพืชและอุตสาหกรรมผักและผลไม้ โดยมีบริษัทเอกชนผลิตขายเครื่องอบแห้งแบบฟลูอิไดซ์เบดสำหรับข้าวเปลือก ข้าวนึ่ง ข้าวโพด และถั่วเหลือง เตาเผาแกลบแบบไซโคลน เครื่องอบแห้งปั๊มความร้อน และเครื่องอบแห้งลมร้อนสำหรับอุตสาหกรรมผักและผลไม้แห้ง รวมถึงระบบเป่าลมเย็นข้าวเปลือกในไซโล

วิจารณ์และสรุป :

1. ได้ตีพิมพ์ผลงานวิจัยในวารสารนานาชาติจำนวน 28 เรื่อง มีค่า impact factor รวม 29.085
2. ใช้เงินวิจัยสำหรับโครงการนี้รวมประมาณ 4 ล้านบาท คิดเป็นค่าใช้จ่ายประมาณ 143,000 บาท ต่อบทความในวารสารานานาชาติ 1 เรื่อง
3. ได้ตีพิมพ์ผลงานวิจัยในวารสารในประเทศจำนวน 15 เรื่อง หากคิดให้บทความในวารสารในประเทศจำนวน 2 เรื่อง เทียบเท่ากับบทความในวารสารนานาชาติจำนวน 1 เรื่อง จะได้บทความเทียบเท่าวารสารนานาชาติจำนวน 9 เรื่อง คิดเป็นค่าใช้จ่ายประมาณ 123,000 บาท ต่อบทความเทียบเท่าวารสารนานาชาติ 1 เรื่อง
4. ผลงานวิจัยที่นำไปสู่ภาคอุตสาหกรรมสามารถก่อประโยชน์อย่างสูง เช่น ลดค่าใช้จ่ายในการอบแห้ง เพิ่มสมรรถนะการอบแห้ง และยกระดับคุณภาพของผลิตภัณฑ์ นอกจากนี้ยังสร้างรายได้ให้กับประเทศจากการส่งออกเครื่องอบแห้งแบบฟลูอิไดซ์เบดและเตาแกลบแบบไซโคลน
5. ได้ค้นพบผลพลอยได้จากการใช้ไอน้ำร้อนยวดยิ่งสำหรับอบแห้งข้าวเปลือก ผัก ผลไม้ และเนื้อสัตว์ โดยเฉพาะกับข้าวเปลือก ซึ่งนำไปสู่การค้นพบกระบวนการผลิตข้าวนึ่งแบบใหม่ ที่ลดเวลาการทำงาน มีค่าใช้จ่ายต่ำ
6. ได้พัฒนาแบบจำลองทางคณิตศาสตร์สำหรับระบบอบแห้งแบบต่าง ๆ จนสามารถนำไปสู่การหาเงื่อนไขการออกแบบ และเงื่อนไขการทำงานที่เหมาะสมที่สุด
7. ที่สำคัญที่สุดคือการพัฒนากลุ่มวิจัยจากสหสาขาวิชาให้ทำงานกันเป็นทีม รวม 71 คนในระยะเวลา 3 ปี

คำสำคัญ : การอบแห้ง, ความดันต่ำ, คุณภาพ, แบบจำลองทางคณิตศาสตร์, ปั๊มความร้อน, ผัก, ผลไม้, ฟลูอิไดซ์เบด, เมล็ดพืช, รังสีอินฟราเรดไกล, สารดูดความชื้น, อาหาร, ไอน้ำร้อนยวดยิ่ง

ABSTRACT

Project code: RTA4680012

Project title: Development and Improvement of Agricultural and Food Products with Combination of Various Drying Techniques

Investigators (71 people):

Investigators		Organization
1. Prof.Dr.Somchart	Soponronnarit	Division of Energy Technology, School of Energy and Materials, KMUTT (Head of project)
2. Assoc.Prof.Warunee	Tia	Division of Energy Management Technology, School of Energy and Materials, KMUTT
3. Assoc.Prof.Dr.Somkiat	Prachayawara-korn	Division of Chemical Engineering, Faculty of Engineering, KMUTT
4. Asst.Prof.Dr.Adisak	Nathakaranakule	Division of Energy Technology, School of Energy and Materials, KMUTT
5. Asst.Prof.Sakamon	Devahastin	Division of Food Engineering, Faculty of Engineering, KMUTT
6. Dr.Thanit	Swasdisevi	Division of Thermal Technology, School of Energy and Materials, KMUTT KMUTT
7. Asst.Prof.Dr.Thanid	Madhiyanon	Department of Mechanical Engineering, Faculty of Engineering, University of Technology Mahanakorn
8. Asst.Prof.Dr.Chaiyong	Taechapairoj	Faculty of Engineering and Technology, Silpakorn University
9. Asst.Prof.Dr.Chareonporn	Lertsatitthanakorn	Faculty of Engineering, Marasarakham University
10. Asst.Prof.Dr.Sampan	Rittidech	Faculty of Engineering, Marasarakham University
11. Asst.Prof.Dr.Nattapol	Poomsa-ad	Faculty of Engineering, Marasarakham University
12. Asst.Prof.Dr.Songchai	Wiriyaumpaiwong	Faculty of Engineering, Marasarakham University
13. Asst.Prof.Dr.Umphisak	Teeboonma	Faculty of Engineering, Ubonratchathani University
14. Asst.Prof.Dr.Jindaporn	Jamradloedluk	Faculty of Engineering, Marasarakham University
15. Seventeen doctoral and forty master students		

Email Address: Somchart.sop@kmutt.ac.th

Research field: Energy technology/ Post-harvest technology

Project fund: Six million baht approved, about four million baht actual payments

Project period: 1 October 2003 – 30 September 2006

Objectives:

The objective of the Project "Development and Improvement of Agricultural and Food Products with Combination of Various Drying Techniques" is to enhance the research capabilities of the lecturers and researchers involved in the project, and to produce numbers of graduated doctoral and master students as well as international journal publications and transfer research outputs to industrial sections and commercialization.

Methodology:

During each semester, there are about 15 master and 8 doctoral students working in the project. Project meeting was arranged weekly for discussion between the students and supervisors who co-operated under senior-supported advisor system. All colleagues had a responsibility to publish the knowledge from his/her researches especially in cited international journals. Collaboration was also made with industrial sectors to produce prototyped dryer and with expertise research institutes.

Research topics of the project are mostly in the field of drying technology. Research topics separated by products are emphasized on grains (i.e. paddy, corn, and soybean), vegetable, fruit, herb and meat. The topics are also separated by drying technology into hot air and superheated steam drying, fluidized bed and spouted bed drying, heat pump drying, drying using adsorbent, far-infrared drying, drying under low pressure and drying by combined techniques. Renewable energy from biomass and drying energy saving are also included in the research topics of the project.

Results:

The success of this project is beyond the proposed target. The outputs of the project are 28 publications in international journals (excluding some papers in print), 13 publications in national journals, 15 papers in international proceedings, 60 papers in national proceedings, and one chapter in one book. One patent of invention is on pending status. Eight doctoral and 31 master students in the project have been graduated. Besides the academic outputs, the knowledge of the project is also transferred to industrial sectors in grain, vegetable and fruit drying. Private companies have been produced and commercialized fluidized bed dryers for drying paddy, parboiled rice, corn and soybean; rice-husk cyclonic furnace; heat pump and hot air dryer for fruit and vegetable drying industries; and cool air ventilation system in a paddy silo.

Discussion and Conclusion:

1. Twenty eight papers have been published in international journals with overall impact factor (2004) of 29.085.
2. The overall budget used in this project is about 4 million baht and is about equivalent to 143,000 baht per an international journal paper.
3. Fifteen papers have been published in national journals. If two national journal papers are set to be equivalent to one international journal paper, it costs about 123,000 baht per an equivalent international journal paper.
4. Research outputs transferred to industrial sectors resulted in high benefit to these sectors, such as saving drying energy, improving drying performance and dried products' qualities. This technology transfer also produced more incomes from exporting fluidized bed dryers and rice-husk cyclonic furnaces.
5. Advantages of using superheated steam for drying paddy, vegetable, fruit and meat were found from this research. This drying technique has a trend to use for developing new drying processes, especially new techniques for producing parboiled rice which have low drying cost and short drying time.
6. Mathematical models of studied drying techniques have been developed to the level that can be used for optimizing drying designs and operations.
7. The most success of the project is the cooperation of 71 researchers from multi branches of knowledge for three years.

Key words: adsorbent, drying, far-infrared, fluidization, fruit, grain, heat pump, low pressure, mathematical model, quality, superheated steam, vegetable, food.

รายงานการวิจัย

1. ปัญหาที่ทำการวิจัยและความสำคัญของปัญหา

เทคนิคการอบแห้งมีหลากหลาย เช่น การใช้ลมร้อน ไอน้ำร้อนยวดยิ่ง ปั๊มความร้อน รังสีอินฟราเรด ไกล รังสีไมโครเวฟ ภายใต้ความดันบรรยากาศ หรือต่ำกว่า/สูงกว่า บรรยากาศ การผสมผสานเทคนิคที่หลากหลายสามารถพัฒนาผลิตภัณฑ์ใหม่ ปรับปรุงคุณภาพ และหรือลดต้นทุนการผลิต เช่นผลิตภัณฑ์ประเภทเนื้อสัตว์และผลไม้ที่มีความกรอบคล้ายกับของที่ได้จากการทอด แต่ต่างกันที่ไม่มีน้ำมันเพิ่มในผลิตภัณฑ์ การผลิตข้าวนึ่งโดยใช้ไอน้ำยวดยิ่งช่วยลดขั้นตอน/กรรมวิธี การผลิต ทำให้ประหยัดเวลาและค่าใช้จ่าย

ห้องปฏิบัติการวิจัยเทคโนโลยีการอบแห้ง คณะพลังงานและวัสดุ มหาวิทยาลัยเทคโนโลยีพระจอมเกล้าธนบุรี ได้รับการสนับสนุนจากสำนักงานกองทุนสนับสนุนการวิจัยอย่างต่อเนื่องเป็นเวลาหลายปี มีนักวิจัยที่ชำนาญการอบแห้งผลิตภัณฑ์อาหาร/เกษตร จำนวนมาก เป็นแหล่งรวบรวมความเชี่ยวชาญสหสาขาวิชา ได้แก่ วิศวกรรมศาสตร์สาขาต่าง ๆ วิทยาศาสตร์และเทคโนโลยีการอาหาร ห้องปฏิบัติการวิจัยเทคโนโลยีการอบแห้งเป็นแหล่งพึ่งพิงทางความรู้และเทคโนโลยีด้านการอบแห้งให้กับภาคเอกชนและภาคราชการ มีการให้คำปรึกษาตามคำร้องขออย่างสม่ำเสมอ รวมถึงการจัดอบรมทางวิชาการเพื่อเผยแพร่ความรู้ใหม่ ๆ ที่ได้จากการวิจัย

ผลงานเด่นของห้องปฏิบัติการวิจัยเทคโนโลยีการอบแห้งได้แก่ การร่วมมือกับภาคเอกชนพัฒนาเครื่องต้นแบบสำหรับอบแห้งข้าวเปลือก ผักและผลไม้ จนนำไปสู่การจดสิทธิบัตรและผลิตขายและส่งออกอย่างแพร่หลาย ตัวอย่างเช่น เครื่องอบแห้งข้าวเปลือกแบบฟลูอิไดซ์เบด เตาเผาแกลบไซโคลน เครื่องอบแห้งปั๊มความร้อน ปัจจุบันเน้นงานการพัฒนากรรมวิธีการผลิตข้าวนึ่ง/ข้าวขาว ผักและผลไม้อบแห้งคุณภาพสูง ประโยชน์ที่ได้รับจากงานวิจัยข้างต้นได้แก่ การลดความสูญเสียของผลิตผลการเกษตร การเพิ่มมูลค่าผลผลิต การสนับสนุนการส่งออก/ทดแทนการนำเข้า และการสนับสนุนนโยบายครัวของโลก

2. วัตถุประสงค์

โครงการนี้มีวัตถุประสงค์โดยรวมเพื่อพัฒนาบุคคลากรทางการวิจัยโดยเน้นการพัฒนาอาจารย์นักวิจัยรุ่นใหม่ มีเป้าหมายในการผลิตบัณฑิตระดับปริญญาโท-เอก จำนวนผลงานวิจัยตีพิมพ์ในวารสารนานาชาติ และการนำผลงานวิจัยไปใช้ประโยชน์ได้จริงในภาคธุรกิจอุตสาหกรรม โดยมีวัตถุประสงค์จำเพาะดังนี้

1. ฝึกฝนอาจารย์ นักวิจัยรุ่นใหม่/ปานกลาง ประมาณ 7 คนตลอดโครงการ
2. ผลิตบัณฑิตปริญญาโทเน้นการวิจัย 6 คน/ปี รวม 18 คนตลอดโครงการ
3. ผลิตบัณฑิตปริญญาเอกเน้นการวิจัย 1.3 คน/ปี รวม 4 คนตลอดโครงการ
4. ตีพิมพ์ผลงานวิจัยในวารสารนานาชาติ 4 เรื่อง/ปี รวม 12 เรื่องตลอดโครงการ และตีพิมพ์ในวารสารในประเทศ 4 เรื่อง/ปี รวม 12 เรื่องตลอดโครงการ
5. นำผลงานวิจัยไปใช้งานในภาคธุรกิจอุตสาหกรรม 1 เรื่อง/ปี รวม 3 เรื่องตลอดโครงการ และจดสิทธิบัตร 1 เรื่อง

3. ระเบียบวิธีวิจัย

ในขณะใดขณะหนึ่งจะมีนักศึกษาปริญญาโทประมาณ 15 คน ระดับปริญญาเอกประมาณ 8 คน ทำวิทยานิพนธ์ ทุกสัปดาห์จะมีการประชุมวิชาการร่วมกันระหว่างนักศึกษาและอาจารย์ อาจารย์ที่มีอาวุโสน้อยจะทำหน้าที่เป็นอาจารย์ที่ปรึกษาร่วมกับอาจารย์ที่อาวุโสกว่าทางวิชาการ อาจารย์เหล่านี้จะเรียนรู้การทำงานอย่างเป็นทีมจากกระบวนการเหล่านี้ ทุก ๆ คนในห้องปฏิบัติการมีความรับผิดชอบต่อการเขียนบทความวิจัยเพื่อตีพิมพ์เผยแพร่โดยเฉพาะในวารสารนานาชาติ นอกจากนี้ยังร่วมมือกับภาคอุตสาหกรรมในการผลิตเครื่องต้นแบบอบแห้ง และกับสถาบันวิจัยอื่นที่มีความชำนาญเฉพาะด้านด้วย รายละเอียดของบุคลากรมีดังนี้

อาจารย์ร่วมโครงการวิจัยเต็มเวลา

1. ศ.ดร. สมชาติ โสภณรณฤทธิ์ สายวิชาเทคโนโลยีพลังงาน คณะพลังงานและวัสดุ มจธ. หัวหน้าโครงการ
2. รศ.วารุณี เตีย สายวิชาเทคโนโลยีการจัดการพลังงาน คณะพลังงานและวัสดุ มจธ.
3. รศ.ดร.สมเกียรติ ปรัชญาวรากร ภาควิชาวิศวกรรมเคมี คณะวิศวกรรมศาสตร์ มจธ. ได้รับทุนพัฒนานักวิจัยหน้าใหม่ สกว. ทุนเมธีวิจัย สกว. และ ทุนคปก. สกว.
4. ผศ.ดร.อดิศักดิ์ นาถกรณกุล สายวิชาเทคโนโลยีพลังงาน คณะพลังงานและวัสดุ มจธ. ได้รับทุนพัฒนานักวิจัยหน้าใหม่ สกว.

อาจารย์ร่วมโครงการวิจัยบางเวลา

1. ผศ.ดร.สักกมน เทพหัสดิน ณ อยุธยา ภาควิชาวิศวกรรมอาหาร คณะวิศวกรรมศาสตร์ มจธ. ได้รับทุนพัฒนานักวิจัยหน้าใหม่ สกว. ทุนเมธีวิจัย สกว. และ ทุนคปก. สกว.
2. ดร.ธนิดย์ สวัสดิเสวี สายวิชาเทคโนโลยีอุณหภาพ คณะพลังงานและวัสดุ มจธ. ได้รับทุนพัฒนานักวิจัยหน้าใหม่ สกว.
3. ดร.ฐานิดย์ เมธิยานนท์ ภาควิชาวิศวกรรมเครื่องกล คณะวิศวกรรมศาสตร์ มหาวิทยาลัยเทคโนโลยีมหานคร (ปัจจุบันดำรงตำแหน่ง ผ.ศ.) ได้รับทุนพัฒนานักวิจัยหน้าใหม่ สกว.
4. ดร.ชัยยงค์ เตชะไพโรจน์ คณะวิศวกรรมศาสตร์และเทคโนโลยี มหาวิทยาลัยศิลปากร (ปัจจุบันดำรงตำแหน่ง ผ.ศ.) ได้รับทุนพัฒนานักวิจัยหน้าใหม่ สกว.
5. ดร.เจริญพร เลิศสถิตธนากร คณะวิศวกรรมศาสตร์ มหาวิทยาลัยมหาสารคาม (1 ต.ค. 2546 – 30 ก.ย. 2548) (ปัจจุบันดำรงตำแหน่ง ผ.ศ.) ได้รับทุนพัฒนานักวิจัยหน้าใหม่ สกว.
6. ดร.สัมพันธ์ ฤทธิเดช คณะวิศวกรรมศาสตร์ มหาวิทยาลัยมหาสารคาม (1 ต.ค. 2546 – 30 ก.ย. 2547) (ปัจจุบันดำรงตำแหน่ง ผ.ศ.) ได้รับทุนพัฒนานักวิจัยหน้าใหม่ สกว. และเตรียมทำสัญญารับทุนเมธีวิจัย สกว.
7. ดร.ณัฐพล ภูมิสะอาด คณะวิศวกรรมศาสตร์ มหาวิทยาลัยมหาสารคาม (1 ต.ค. 2546 – 30 ก.ย. 2548) (ปัจจุบันดำรงตำแหน่ง ผ.ศ.) ได้รับทุนพัฒนานักวิจัยหน้าใหม่ สกว.
8. ดร.ทรงชัย วิริยะอำไพวงศ์ คณะวิศวกรรมศาสตร์ มหาวิทยาลัยมหาสารคาม (1 ก.ค. 2547 -) (ปัจจุบันดำรงตำแหน่ง ผ.ศ.) ได้รับทุนพัฒนานักวิจัยหน้าใหม่ สกว.
9. ดร.อำไพศักดิ์ ทีบุญมา คณะวิศวกรรมศาสตร์ มหาวิทยาลัยอุบลราชธานี (1 ก.ค. 2547 -) (ปัจจุบันดำรงตำแหน่ง ผ.ศ.) ได้รับทุนพัฒนานักวิจัยหน้าใหม่ สกว.

10. ดร.จินดาพร จำรัสเลิศลักษณ์ คณะวิศวกรรมศาสตร์ มหาวิทยาลัยมหาสารคาม (1 ก.ค. 2549 -) ได้รับทุนพัฒนานักวิจัยหน้าใหม่ สกว.

นักศึกษาปริญญาเอกร่วมในโครงการวิจัย

1. นายชัยยงค์ เตชะไพโรจน์ (จบการศึกษา)
   การอบแห้งข้าวเปลือกโดยเทคนิคฟลูอิไดซ์เบดด้วยไอน้ำร้อนยวดยิ่ง
2. นายยุทธนา ฏิระวณิชกุลย์ (จบการศึกษา)
   การจัดการข้าวเปลือกชื้นโดยการอบแห้งในที่เก็บภายใต้สภาวะอากาศร้อนชื้น
3. นางสุภาวรรณ ฏิระวณิชกุลย์ (จบการศึกษา)
   ผลของอุณหภูมิที่มีต่อการอบแห้งข้าวเปลือก
4. นายวทัญญู รอดประพัฒน์ (จบการศึกษา)
   การพัฒนาเครื่องต้นแบบการอบแห้งข้าวเปลือกด้วยเทคนิคฟลูอิไดเซชันโดยใช้ไอน้ำร้อนยวดยิ่ง
5. นางยุวนารี นามสงวน (จบการศึกษา)
   การอบแห้งกุ้งด้วยเทคนิคไอน้ำร้อนยวดยิ่งร่วมกับปั๊มความร้อน
6. นายนเรศ มีโส (จบการศึกษา)
   การอบแห้งข้าวเปลือกด้วยเทคนิคฟลูอิไดเซชันร่วมกับรังสีอินฟราเรดไกล
7. น.ส.จินดาพร จำรัสเลิศลักษณ์ (จบการศึกษา) (เป็นผลงานในทุน คปก. แบบกลุ่มวิจัย สกว.)
   การอบแห้งผลไม้ด้วยไอน้ำร้อนยวดยิ่ง
8. นายกิตติศักดิ์ วิธินันทกิตต์ (จบการศึกษา)
   การอบแห้งข้าวเปลือกโดยใช้แกลบดูดซับความชื้น
9. นายณรงค์ อึ้งกิมบัวน
   การอบแห้งเนื้อสัตว์ด้วยไอน้ำร้อนยวดยิ่ง
10. นายกิตติ สถาพรประสาธน์
    การอบแห้งสลัดจ์โดยเทคนิคกระแสชน
11. นายปกรณ์ เหลืองมาลาวัฒน์
    การอบแห้งด้วยฮีทปั๊มและรังสีอินฟราเรดไกล
12. นายฉัตรชัย นิมมน
    การอบแห้งโดยไอน้ำร้อนยวดยิ่งร่วมกับรังสีอินฟราเรดไกลภายใต้ความดันต่ำ
13. นายวุฒิกรณ์ จริยตันติเวทย์
    การผลิตข้าวนึ่งโดยการพ่นไอน้ำก่อนการอบแห้งด้วยเทคนิคฟลูอิไดเซชัน
14. น.ส.ดลฤดี ใจสุทธิ์
    อิทธิพลของอุณหภูมิที่มีต่อจลนพลศาสตร์ของการอบแห้งข้าวเปลือกและคุณภาพข้าวกล้องและข้าวขาวที่ได้จากการอบแห้งด้วยเทคนิคฟลูอิไดเซชัน
15. น.ส.รดิยา ธุวพาณิชยานันท์
    การอบแห้งแผ่นโฟมกล้วยสุกด้วยเครื่องอบแห้งแบบถาด
16. น.ส.ชลิดา เนียมนุ้ย
    ปรากฏการณ์ถ่ายเทและการเปลี่ยนแปลงสมบัติทางกายภาพระหว่างการแปรรูปและการเก็บรักษากุ้ง

17. นายประสาน สถิตย์เรืองศักดิ์

การพัฒนาเตาเผาชีวมวลร่วมกับถ่านหินโดยใช้เทคนิคฟลูอิไดซ์เบดแบบห้องเผาไหม้สั้น

นักศึกษาปริญญาโทร่วมโครงการวิจัย

1. นายปกรณ์ เหลืองมาลาวัฒน์ (จบการศึกษา)

การพัฒนาแบบจำลองทางคณิตศาสตร์ของการทำความเย็นข้าวเปลือก

2. นายณรงค์ศักดิ์ แก้วนิล (จบการศึกษา)

เงื่อนไขที่เหมาะสมสำหรับการอบแห้งกระเทียม

3. นายเฉลิมพร เอี่ยมมิ (จบการศึกษา)

การผลิตข้าวหอมนึ่งด้วยกระบวนผสมผสาน

4. นส.พิมพร แจ้งพลอย (จบการศึกษา)

นโยบายการวิจัยพลังงานหมุนเวียน

5. นายเชษฐ์ โชติบุญ (จบการศึกษา)

การจำลองแบบทางคณิตศาสตร์ของการถ่ายเทความร้อนและมวลในไซโลเก็บข้าวเปลือก

6. นายศรีมา แจ้คำ (จบการศึกษา)

การอบแห้งอาหารด้วยปั๊มความร้อนและ FIR

7. น.ส.สุนียพร พรหมดวง (จบการศึกษา)

การอบแห้งสมุนไพรด้วยปั๊มความร้อน

8. น.ส.ปวีณา ปรัชญาวสิน (จบการศึกษา)

การทดลองอบแห้งถั่วเหลืองด้วยไอน้ำร้อนยวดยิ่ง

9. นายพยุงศักดิ์ ท่าไม้สุข (จบการศึกษา)

การอบแห้งข้าวสุกเพื่อผลิตข้าวพร้อมกิน

10. นายสุทธิศักดิ์ แก้วนก (จบการศึกษา)

การอบแห้งกระเทียมระยะที่สอง

11. น.ส.รติยา สุวพานิชยานันท์ (จบการศึกษา)

การถ่ายเทความร้อนและมวลในการอบแห้งเมล็ดถั่วเหลือง

12. นายรัฐพร บัวขม (จบการศึกษา)

การอบแห้งเมล็ดกาแฟสดด้วยไอน้ำร้อนยวดยิ่ง

13. นายอธิคม จิรจินดาเลิศ (จบการศึกษา)

การผลิตข้าวกล้องนึ่งโดยเทคนิคฟลูอิไดเซชัน

14. นายปรีดา ปรากฏมาก (จบการศึกษา)

การประยุกต์เครือข่ายรูพรุนในการอบแห้งเมล็ดพืช

15. นายประสาน สถิตย์เรืองศักดิ์ (จบการศึกษา)

การผลิตเชื้อเพลิงแข็งอัดแท่ง

16. น.ส.อุบลวรรณ ชนะภัย (จบการศึกษา)

แบบจำลองทางคณิตศาสตร์ของการอบแห้งเมล็ดถั่วเหลืองด้วยไอน้ำร้อนยวดยิ่ง

17. น.ส.ภาวิกา วงศ์แก้ว (จบการศึกษา)

การลดความชื้นของข้าวเปลือกโดยใช้แกลบบด

18. นายธนากร บูรณเพชร (จบการศึกษา) (ผลงานในฐานะนักวิจัยพี่เลี้ยงทุนพัฒนานักวิจัยหน้าใหม่ สกว.)
อิทธิพลของอุณหภูมิที่มีผลต่อการอบแห้งใบหม่อน
19. นายวิริยะ แดงทน (จบการศึกษา) (ผลงานในฐานะนักวิจัยพี่เลี้ยงทุนพัฒนานักวิจัยหน้าใหม่ สกว.)
ท่อความร้อนสั้นปลายปิดสำหรับอุ่นอากาศในเครื่องอบแห้ง
20. นายมนตรี มนตรีพิลา (จบการศึกษา) (ผลงานในฐานะนักวิจัยพี่เลี้ยงทุนพัฒนานักวิจัยหน้าใหม่ สกว.)
การอบแห้งข้าวเหนียวนึ่งสุกโดยใช้ไอน้ำร้อนยวดยิ่ง
21. นายวรวิทย์ กรัยวณิชย์กุล
การอบแห้งเนื้อไก่ด้วยไอน้ำร้อนยวดยิ่ง (จบการศึกษา)
22. นายพีระวัตร์ ทองนอก (จบการศึกษา)
การออกแบบและทดสอบเตาแกลบแบบไซโคลนร่วมกับฟลูอิไดเซชัน
23. นายฤทธิไกร งามชุ่ม (จบการศึกษา)
การอบแห้งแบบสุญญากาศร่วมกับรังสีอินฟราเรดไกล
24. นายวรุต ยุทธชัย (จบการศึกษา)
อิทธิพลการแช่ที่มีต่อการลดลงของสารต่อต้านโภชนาการในเมล็ดถั่วเหลืองที่อบแห้งโดยเทคนิคฟลูอิไดเซชัน
25. นายศิริวัฒ ศิลป์ประเสริฐ (จบการศึกษา)
การอบแห้งเนื้อวัวด้วยไอน้ำร้อนยวดยิ่ง
26. นายพลสันต์ วงษ์ศรี (จบการศึกษา)
การปรับปรุงและทดสอบเครื่องต้นแบบอบแห้งอาหารโดยใช้ไอน้ำร้อนยวดยิ่ง
27. นายเกียรติศักดิ์ จงสุวรรณรักษ์ (จบการศึกษา)
การพัฒนาแบบจำลองทางคณิตศาสตร์สามมิติสำหรับการเก็บรักษาข้าวเปลือกในไซโลเหล็กทรงกระบอก
28. นายเสริมพงษ์ อดิเรกรัตน์ (จบการศึกษา)
การอบแห้งอาหารโดยใช้ลมร้อนร่วมกับซิลิกาเจล
29. นายภูมิใจ สะอาดชม (จบการศึกษา)
แบบจำลองทางคณิตศาสตร์ของการอบแห้งด้วยรังสีอินฟราเรดภายใต้ความดันต่ำ
30. นส.นภาภรณ์พลายโถ (จบการศึกษา) (ผลงานในฐานะนักวิจัยพี่เลี้ยงทุนพัฒนานักวิจัยหน้าใหม่สกว.)
ผลของการพรีทรีทเมนต์ที่มีต่อจลนพลศาสตร์การอบแห้งและคุณภาพของกล้วยแผ่น
31. น.ส.มัทนียา เชี่ยวเวช (จบการศึกษา)
การเร่งข้าวเก่าโดยการอบแห้งแบบฟลูอิไดเซชันร่วมกับการเก็บในที่อับอากาศ
32. นายมานะ สุยะรา
อิทธิพลของระดับความสุกที่มีต่อจลนพลศาสตร์การอบแห้งและคุณภาพของกล้วยแผ่น
33. นายสมคิด โฆษิตพันธวงศ์
อิทธิพลของเวลาและอุณหภูมิการแช่ที่มีต่อการผลิตข้าวนึ่งโดยใช้เทคนิคฟลูอิไดเซชันที่ใช้ไอน้ำร้อนยวดยิ่ง
34. นายวีระ ศรีอาริยะกุล
อิทธิพลของการพ่นไอน้ำที่มีต่อการผลิตข้าวนึ่งโดยใช้เทคนิคฟลูอิไดเซชันที่ใช้อากาศร้อน
35. นายอนุชา ใจกล้า
เงื่อนไขที่เหมาะสมของการอบแห้งโดยเทคนิคฟลูอิไดเซชันสำหรับการรักษาคุณภาพ

36. นายปัญญา ตีระกิจวัฒนา

การให้ความร้อนกับถั่วเหลืองโดยใช้เทคนิคฟลูอิไดเซชันร่วมกับการพ่นไอน้ำก่อนเพื่อลดสารต่อต้านโภชนาการ

37. น.ส.พรสิกาณฐ์ ใจบุญ

การทดสอบเปรียบเทียบการอบแห้งลำไยด้วยเทคนิคต่างๆ

38. น.ส.จารุวรรณ กุลวิศว

การศึกษาอิทธิพลของเงื่อนไขการอบแห้งที่มีต่อคุณภาพกล้วยแผ่น

39. นายคำพัน บัวละพัน

การศึกษาเงื่อนไขการอบแห้งที่มีผลต่อการพองตัวของกล้วยแผ่น

40. น.ส.ศกุนตลา ภู่เจริญ

การวิเคราะห์การใช้พลังงานในการผลิตเอธานอลโดยใช้วัตถุดิบต่างชนิด

4. ผลงาน

ผลงานวิจัยโดยสรุปมีดังนี้

1. ผลงานวิจัยที่ตีพิมพ์เผยแพร่

- บทความวิจัยในวารสารนานาชาติ จำนวน 28 เรื่อง รวมค่าแฟคเตอร์ผลกระทบ (Impact factor) = 29.085 โครงการนี้มีค่าใช้จ่ายโดยประมาณ 4 ล้านบาท ดังนั้นค่าใช้จ่ายที่ใช้ในการตีพิมพ์ผลงานในวารสารนานาชาติเท่ากับ 143,000 บาท/เรื่อง
- บทความวิจัยในวารสารในประเทศ จำนวน 13 เรื่อง
- บางบทในหนังสือ จำนวน 1 บท
- บทความวิจัยในรายงานการประชุมทางวิชาการนานาชาติ จำนวน 15 เรื่อง
- บทความวิจัยในรายงานการประชุมทางวิชาการในประเทศ จำนวน 60 เรื่อง

2. สิทธิบัตร

มีสิทธิบัตรที่อยู่ระหว่างการดำเนินการขอจดในประเทศไทย จำนวน 1 เรื่อง

3. ผลงานด้านการพัฒนาบุคลากรวิจัย

- ฝึกฝนอาจารย์ 13 คน นักศึกษาปริญญาเอก 17 คน นักศึกษาปริญญาโท 40 คน ทำงานร่วมกันเป็นทีมแบบสหสาขาวิชา มีนักศึกษาปริญญาเอกและปริญญาโทจบการศึกษา 8 และ 31 คน ตามลำดับ
- อาจารย์ที่ร่วมกลุ่มวิจัยได้รับทุนวิจัยจาก สกว. ดังนี้ ทุนพัฒนานักวิจัยหน้าใหม่ 12 ทุน ทุนเมธีวิจัย 2 ทุน กำลังจะได้รับทุนเมธีวิจัยอีก 1 ทุน ทุน คปก. 2 ทุน
- อาจารย์ที่ร่วมกลุ่มวิจัยได้รับการเลื่อนตำแหน่งทางวิชาการจำนวน 7 คน

4. ผลงานที่นำไปใช้ในภาคอุตสาหกรรม

- มีผลงานวิจัยที่นำไปใช้ในภาคอุตสาหกรรมหลายเรื่อง บางเรื่องเป็นงานวิจัยเพิ่มเติมจากโครงการเมธีวิจัยอาวุโส ระยะที่ 1 ผลงานหลักได้แก่ เครื่องอบแห้งข้าวเปลือกแบบฟลูอิไดซ์เบดเตาเผาแกลบไซโคลน เครื่องอบแห้งด้วยปั๊มความร้อน เครื่องอบแห้งด้วย LPG นอกจากนี้ยังมีผลงานที่แนะนำกับภาคอุตสาหกรรมจนสามารถผลิตขาย ได้แก่ ระบบทำความเย็นข้าวเปลือกในไซโล และได้พัฒนาต้นแบบที่มีศักยภาพเชิงพาณิชย์ ได้แก่ เครื่องอบแห้งข้าวเปลือกด้วยเทคนิคฟลูอิไดเซชันโดยใช้ไอน้ำร้อนยวดยิ่ง และเครื่องอบแห้งผลิตภัณฑ์อาหารโดยใช้ปั๊มความร้อนร่วมกับรังสีอินฟราเรดไกล
- ให้คำปรึกษากับภาคอุตสาหกรรม จำนวน 15 เรื่อง

รายละเอียดของผลงานวิจัยมีดังนี้

1 Research Publication, Book Chapter and Patent:

International Journal Papers:

1. Wiriyaumpaiwong, S., Soponronnarit, S. and Prachayawarakorn, S. 2003. Soybean drying by two-dimensional spouted bed. Drying Technology-An International Journal 21(9) 1739-1761. (IF = 0.987)
2. Prachayawarakorn, S., Sawanduanpen, S., Saynampheung, S., Poolpatarachewin, T., Soponronnarit, S. and Nathakaranakule, A. 2004. Kinetics of colour change during storage of dried garlic slices as affected by relative humidity and temperature. Journal of Food Engineering 62, 1-7. (IF = 1.22)
3. Tirawanichakul, Y., Prachayawarakorn, S., Varanyanon, W. and Soponronnarit, S. 2004. Simulation and grain quality for in-store drying of paddy. Journal of Food Engineering 64, 405-415. (IF = 1.22)
4. Meeso, N., Nathakaranakule, A., Madhiyanon, T. and Soponronnarit, S. 2004. Influence of FIR irradiation on paddy moisture reduction and milling quality after fluidized bed drying. Journal of Food Engineering 65, 293-301. (IF = 1.22)
5. Wiriyaumpaiwong, S., Soponronnarit, S. and Prachayawarakorn, S. 2004. Comparative study of heating process for full-fat soybeans. Journal of Food Engineering 65,371-382. (IF = 1.22)
6. Prachayawarakorn, S., Soponronnarit, S., Wetchacama, S. and Chinnabun, K. 2004. Methodology of enhancing drying rate and improving maize quality in a fluidized-bed dryer. Journal of Stored Products Research 40, 379-393. (1.044)
7. Taechapairoj, C., Prachayawarakorn, S. and Soponronnarit, S. 2004. Characteristics of rice dried in superheated-steam fluidized-bed. Drying Technology-An International Journal 22(4), 719-743. (IF = 0.987)

8. Namsanguan, Y., Tia, W., Devahastin, S. and Soponronnarit, S. 2004. Drying kinetics and quality of shrimp under different two-stage drying processes. Drying Technology-An International Journal 22(4), 759-778. (IF = 0.987)
9. Tirawanichakul, S., Prachayawarakorn, S., Varanyanon, W., Tungtrakul, P. and Soponronnarit, S. 2004. Effect of fluidized bed drying temperature on various quality attributes of paddy. Drying Technology-An International Journal 22(7), 1731-1754. (IF = 0.987)
10. Devahastin, S., Suvarnakuta, P., Soponronnarit, S., Mujumdar, A.S., 2004. A comparative study of low-pressure superheated steam and vacuum drying of a heat-sensitive material. Drying Technology–An International Journal 22(8), 1845-1867. (IF = 0.987) (เป็นผลงานในฐานะนักวิจัยพี่เลี้ยงทุนพัฒนานักวิจัยหน้าใหม่ สกว.)
11. Prachayawarakorn, S., Prachayawasin, P. and Soponronnarit, S. 2004. Effective diffusivity and kinetics of urease inactivation and color change during processing of soybeans with superheated-steam fluidized bed. Drying Technology-An International Journal 22(9), 2095-2118. (IF = 0.987) (เป็นผลงานในฐานะนักวิจัยพี่เลี้ยงทุนพัฒนานักวิจัยหน้าใหม่ สกว.)
12. Prachayawarakorn, S., Poomsa-ad, N. and Soponronnarit, S. 2005. Quality maintenance and economy with high-temperature paddy-drying process. Journal of Stored Products Research 41, 333-351. (1.044)
13. Suvarnakuta, P., Devahastin, S., Soponronnarit, S., Mujumdar, A.S., 2005. Drying kinetics and inversion temperature in a low-pressure superheated steam drying system. Industrial & Engineering Chemistry Research 44(6), 1934-1941 (IF = 1.424). (เป็นผลงานในฐานะนักวิจัยพี่เลี้ยงทุนพัฒนานักวิจัยหน้าใหม่ สกว.)
14. Poomsa-ad, N., Soponronnarit, S., Prachayawarakorn, S. and Terdyothin, A. 2005. Investigations on head-rice yield and operating time in the fluidized-bed drying process : Experiment and simulation. Journal of Stored Products Research 41, 387-400. (1.044)
15. Prachayawarakorn, S., Choteboon, C. and Soponronnarit, S. 2005. Simultaneous momentum, heat and mass transfer with color change during paddy storage in silo. Drying Technology-An International Journal 23(1&2), 205-223. (IF = 0.987)
16. Namsanguan, Y., Tichangtong, S., Tia, W., Soponronnarit, S. and Devahastin, S. 2005. Simulation of a mixed air and superheated steam drying system. Drying Technology-An International Journal 23(1&2), 225-248. (IF = 0.987)
17. Madhiyanon, T. and Soponronnarit, S. 2005. High temperature spouted bed paddy drying with varied downcomer air flows and moisture contents: Effects on drying kinetics, critical moisture content, and milling quality. Drying Technology-An International Journal 23(3), 473-495. (IF = 0.987) (เป็นผลงานในฐานะนักวิจัยพี่เลี้ยงทุนพัฒนานักวิจัยหน้าใหม่ สกว.)
18. Rittidech, S., Dangeton, W. and Soponronnarit, S. 2005. Closed-ended oscillating heat-pipe (CEOHP) air-preheater for energy thrift in a dryer. Applied Energy 81, 198-208. (0.378) (เป็นผลงานในฐานะนักวิจัยพี่เลี้ยงทุนพัฒนานักวิจัยหน้าใหม่ สกว.)

19. Prachayawarakorn, S., Tia, W., Poopaiboon, K. and Soponronnarit, S. 2005. Comparison of performances of pulsed and conventional fluidized-bed dryers. Journal of Stored Products Research 41, 479-497. (1.044)
20. Rordprapat, W., Nathakaranakule, A., Tia, W. and Soponronnarit, S. 2005. Comparative study of fluidized bed paddy drying using hot air and superheated steam. Journal of Food Engineering 71, 28-36. (IF = 1.209)
21. Lertsatitthanakorn, C., Rerngwongwitaya, S. and Soponronnarit, S. 2006. Field experiments and economic evaluation of an evaporative cooling system in a silkworm rearing house. Biosystems Engineering 93, 213-219. (IF=0.496) (เป็นผลงานในฐานะนักวิจัยพี่เลี้ยงทุนพัฒนานักวิจัยหน้าใหม่ สกว.)
22. Soponronnarit, S., Nathakaranakule, A., Jirajindalert, A. and Taechapairoj, C., 2006. Parboiling brown rice using superheated steam fluidization technique. Journal of Food Engineering 75, 423-432. (IF = 1.209)
23. Taechapairoj, C., Prachayawarakorn, S., and Soponronnarit, S., 2006. Modelling of parboiled rice in superheated steam fluidized bed. Journal of Food Engineering 76, 411-419. (IF=1.209)
24. Prachayawarakorn, S., Kaewnin, N., Natahkaranakule, A. and Soponronnarit, S. 2006. Effects of peeled and unpeeled garlic cloves on the changes of drying rate and quality. Drying Technology-An International Journal 24(1), 65-75. (IF=0.987)
25. Prachayawarakorn, S., Prachayawasin, P. and Soponronnarit, S. 2006. Heating process of soybean using hot-air and superheated-steam fluidized-bed dryers. LWT-Food Sci Technol 39, 770-778. (IF=0.818)
26. Madhiyanon, T., Techaprasan, A. and Soponronnarit, S. 2006. Mathematical models based on heat transfer and coupled heat and mass transfer for rapid high temperature treatment in fluidized bed: application for grain heat disinfestations. International Journal of Heat and Mass Transfer 49, 2277-2290. (IF=1.22)
27. Prachayawarakorn, S., Ruengnarong, S. and Soponronnarit, S. 2006. Characteristics of heat transfer in two-dimensional spouted bed. Journal of Food Engineering 76, 327-333. (IF=1.209)
28. Witinantakit, K., Prachayawarakorn, S., Nathakaranakule, A. and Soponronnarit, S. 2006. Paddy drying using adsorption technique: experiments and simulation. Drying Technology-An International Journal 24, 609-617. (IF=0.987)

Local Journal Papers:

1. Wanichsumran, S., Tungtrakul, P., Waranyanon, W. and Soponronnarit, S. 2003. Increased yield in head rice of poor quality paddy by combined soaking and fluidized bed drying. The Journal of the Royal Institute of Thailand 28(4), 1160-1169 (in Thai).
2. Madhiyanon, T., Piriyarungroj, N., Nathakarannakule, A. and Soponronnarit, S. 2003. The vortexing-fluidized bed combustor cold model : experimental study of air – rice husk flow

behavior. Research and Development Journal of Engineering Institute of Thailand, 14(4), 59-67 (in Thai). (เป็นผลงานในฐานะที่ปรึกษาและวิจัยร่วม)

3. Leungmalawat, P., Nathakarannakule, A. and Soponronnarit, S. 2004. Developing a mathematical model of paddy cooling system. The Journal of the Royal Institute of Thailand 29(1), 64-77 (in Thai).
4. Soponronnarit, S., Taechapairoj, C. and Prachayawarakorn, S. 2004. A new technique for the manufacture of steamed rice. The Journal of the Royal Institute of Thailand 29(1), 78-86 (in Thai).
5. Chaioranan, A., Soponronnarit, S. and Tia, W. 2004. Water heating using heat pump. Research and Development Journal of Engineering Institute of Thailand, 15(2), 31-37 (in Thai).
6. Tia, W., Jangploy, P., Sakunpongmalee and Soponronnarit, S. 2004. Status and research trends on biomass energy in Thailand. The Journal of the Royal Institute of Thailand 29(3), 557-567 (in Thai).
7. Madhiyanon, T., Piriyarungroj and Soponronnarit, S. 2004. A novel vortex-fluidized bed combustor with two combustion chambers for rice husk fuel. Songklanakarin J. Sci. Technol. 26(6), 875-893 (in Thai). (เป็นผลงานในฐานะที่ปรึกษาและวิจัยร่วม)
8. Soponronnarit, S. and Prachayawarakorn, S. 2004. Mathematical modelling and simulation of fluidized-bed drying, tempering and ventilation of grains. KKU Engineering Journal 32(1), 1-14.
9. Eiammi, C., Tangtrakul, P., Tachapairoj, C. and Soponronnarit, S. 2004. Combination process of steaming and drying for parboiling aromatic rice. Thai Society of Agricultural Engineering Journal 11(1), 24-33 (in Thai).
10. Soponronnarit, S., Jirajindalert, Nathakaranakule, A., Taechapairoj, C. 2005. Parboiling brown rice using superheated steam fluidization technique. The Journal of the Royal Institute of Thailand 30(1), 76-91 (in Thai).
11. Rordprapat, W., Nathakaranakule, A., Tia, W. and Soponronnarit, S. 2005. Development of a superheated-steam-fluidized-bed dryer for parboiled rice. The Journal of the Royal Institute of Thailand 30(2), 363-378 (in Thai).
12. Tia, W., Jangploy, P., Sakunpongmalee and Soponronnarit, S. 2004. Status and research trends on renewable energy in Thailand. The Journal of the Royal Institute of Thailand 30(3), 659-677 (in Thai).
13. Taechapairoj, C., Sinprasert, S., Prachayawarakorn, S. and Soponronnarit, S. 2005. Effect of drying medium on drying kinetics and beef quality. The Journal of the Royal Institute of Thailand 30(4), 970-987 (in Thai).

Book Chapters:

1. Soponronnarit, S. and Prachayawarakorn, S. 2003. Research and development work on paddy drying in South-east Asia. Lectures and Workshop Exercises on Drying of Agricultural and Marines Products. Eds: Ghin, Y.B. et al., ASEAN SCNCER, pp.87-112.

Keynote/Invited speaker in Conferences/Symposiums:

1. Soponronnarit, S. 2003. Fluidised bed grain drying. Proceedings of the 3rd Asia-Pacific Drying Conference, 1-3 September 2003, Asian Institute of Technology, Bangkok, Thailand, pp. 55-71 (keynote paper).
2. Soponronnarit, S. 2003. Fluidised bed grain drying. Presented at the International Seminar on Grain Drying in South Asia, 1-2 Dec. 2003, Durgapur, India (keynote paper).
3. Soponronnarit, S. and Prachayawarakorn, S. 2004. Mathematical modelling anc simulation of fluidized-bed drying, tempering and ventilation of grains. Proc. 15th International Symposium on Transport Phenomena (ISTP-15), 9th-13th May 2004, Bangkok, Thailand, pp. 8-14 (keynote paper).
4. Soponronnarit, S. and Prachayawarakorn, S. 2004. Mathematical modelling and simulation of fluidized-bed drying, tempering and ventilation of grains. Presented at The 18th Conference on Mechanical Engineering Network of Thailand, Khonkaen ,18-20 Oct. 2004. Also in KKU Engineering Journal 32(1), 1-14.
5. Tia, W., Jangploy, P., Sakunpongmalee, K. and Soponronnarit, S. 2005. Status and research trends on renewable energy in Thailand. CD-Rom Proceedings of the 1st Energy Network Conference, Pattaya, 11-13 May 2005, 18 p. (invited paper in Thai).
6. Soponronnarit, S. and Prachayawarakorn, S. 2005. Research and development work on paddy drying in South-East Asia. Paper presented at the 3rd National Technical Seminar on Post-harvest/Post-production Technology, Cha-am, 10-11 Oct. 2005 (keynote paper).
7. Soponronnarit, S., Prachayawarakorn, S. and Taechapairoj, C. 2005. New method for producing parboiled rice under high-temperature superheated-steam fluidization. Proc. of the 4th Asia Pacific Drying Conference, 13-15 Dec. 2005, Kolkata, India (invited paper).
8. Soponronnarit, S. and Prachayawarakorn, S. 2006. Research and development work on paddy drying in South-East Asia. In CD-Rom Proc. of the 7th National Conference of the Thai Society of Agricultural Engineering, 23-24 Jan. 2006, Marasarakham, pp. 15-31 (keynote paper).

International Conference Papers:

1. Namsanguan, Y., Tia, W., Devahastin and S. Soponronnarit, S. 2003. Drying kinetics and quality of shrimp undergoing two-stage superheated steam and heat pump drying. Proceedings of the 3rd Asia-Pacific Drying Conference, 1-3 September 2003, Asian Institute of Technology, Bangkok, Thailand, pp. 457-467.
2. Tirawanichakul, S., Prachayawarakorn, S., Varanyanond, W. and Soponronnarit, S. 2003. Diffusion model of a wide drying temperature range for fluidized bed paddy drying. Proceedings of the 3rd Asia-Pacific Drying Conference, 1-3 September 2003, Asian Institute of Technology, Bangkok, Thailand, pp. 657-666.

3. Jamradloedluk, J., Nathkaranakule, A., Soponronnarit, S. and Prachayawarakorn, S. 2003. Drying of durian slices in superheated steam and hot air. Proceedings of the 3rd Asia-Pacific Drying Conference, 1-3 September 2003, Asian Institute of Technology, Bangkok, Thailand, pp. 667-677. (เป็นผลงานในฐานะอาจารย์ที่ปรึกษาร่วมทุน คปก. สกว.)
4. Uengkimbuan, N., Soponronnarit, S., Prachayawarakorn, S. and Nathkaranakule, A. 2003. Comparative study of pork dried using superheated steam and hot air. Proceedings of the 3rd Asia-Pacific Drying Conference, 1-3 September 2003, Asian Institute of Technology, Bangkok, Thailand, pp. 679-691. (เป็นผลงานในฐานะอาจารย์ที่ปรึกษาร่วมทุน คปก. สกว.)
5. Rordprapat, W., Nathkaranakule, A., Tia, W. and Soponronnarit, S. 2003. Effect of soaking time and drying media on qualities of paddy dried by fluidization technique. Proceedings of the 3rd Asia-Pacific Drying Conference, 1-3 September 2003, Asian Institute of Technology, Bangkok, Thailand, pp. 693-704.
6. Meeso, N., Nathakaranakule, A., Madhiyanon, T. and Soponronnarit, S. 2003. Effect of far-infrared radiation and tempering on subsequent drying of paddy by fluidization technique. Proceedings of the 3rd Asia-Pacific Drying Conference, 1-3 September 2003, Asian Institute of Technology, Bangkok, Thailand, pp. 705-720.
7. Sathapornprasath, K., Devahastin, S. and Soponronnarit, S. 2004. Effects of operating conditions on the overall performance of an air and superheated steam-operated impinging stream dryer. Proc. 15th International Symposium on Transport Phenomena (ISTP-15), 9th-13th May 2004, Bangkok, Thailand, pp. 55-59.
8. Suvarnakuta, P., Devahastin, S., Soponronnarit, S. and Mujumdar, A.S. 2004. Drying rate and inversion temperatures of porous particles undergoing low-pressure superheated steam and vacuum drying. Proc. 15th International Symposium on Transport Phenomena (ISTP-15), 9th-13th May 2004, Bangkok, Thailand, pp. 60-64. (เป็นผลงานในฐานะนักวิจัยพี่เลี้ยงทุนพัฒนานักวิจัยหน้าใหม่ สกว.)
9. Rittidech, S., Soponronnarit, S. and Dangeton, W. 2004. Effect of hot gas temperature and working fluid on effectiveness of a closed-end oscillating heat pipe air-preheater for dryer. Proc. 15th International Symposium on Transport Phenomena (ISTP-15), 9th-13th May 2004, Bangkok, Thailand, pp. 65-72. (เป็นผลงานในฐานะนักวิจัยพี่เลี้ยงทุนพัฒนานักวิจัยหน้าใหม่ สกว.)
10. Prachayawarakorn, S., Ruengnarong, S. and Soponronnarit, S. 2004. Characteristics of heat transfer in two-dimentional spouted bed. Proc. 15th International Symposium on Transport Phenomena (ISTP-15), 9th-13th May 2004, Bangkok, Thailand, pp. 73-78.
11. Tirawanichakul, Y., Prachayawarakorn, S., Varanyanon, W. and Soponronnarit, S. 2004. In-store paddy drying under tropical atmostsphere: strategy and quality aspects. Proc. 15th International Symposium on Transport Phenomena (ISTP-15), 9th-13th May 2004, Bangkok, Thailand, pp. 431-437.
12. Prachayawarakorn, S., Choteboon, C. and Soponronnarit, S. 2004. Moisture transport and change of yellowness of paddy during storage. Proc. 15th International Symposium on Transport Phenomena (ISTP-15), 9th-13th May 2004, Bangkok, Thailand, pp. 609-614.

13. Jamradloedluk, J., Nathakaranakule, A., Soponronnarit, S. and Prachayawarakorn, S. 2005. Modelling of dehydration and redehydration kinetics of durian. Proc. 2nd Int. Conf. on Innovations in Food Processing Technology and Engineering, 11-13 Jan. 2005, Bangkok, Thailand, pp. 267-277.
14. Witinantakit, K., Prachayawarakorn, S., Nathakaranakule, A. and Soponronnarit, S. 2005. Drying of paddy using rice husk as adsorbent. Proc. 2nd Int. Conf. on Innovations in Food Processing Technology and Engineering, 11-13 Jan. 2005, Bangkok, Thailand, pp. 312-319.
15. Uengkimbuan, N., Soponronnarit, S., Prachayawarakorn, S. and Nathakaranakule, A. 2005. Drying kinetics and physical properties of dried pork using two-stage techniques. Proc. 2nd Int. Conf. on Innovations in Food Processing Technology and Engineering, 11-13 Jan. 2005, Bangkok, Thailand, pp. 320-328.

Local Conference Papers:

1. Madhiyanon, T., Piriyarungroj, N., Nathakarannakule, A. and Soponronnarit, S. 2003. Development of a vortexing-fluidized bed combustor for rice husk fuel. CD Rom Proc. the 17th Conference on Mechanical Engineering Network of Thailand, KMITNB-Prachinburi., 15-17 Oct. 2003, 9 p (in Thai). (เป็นผลงานในฐานะที่ปรึกษาและวิจัยร่วม)
2. Madhiyanon, T., Baingam, M. and Soponronnarit, S. 2003. Solid fuel producing from sawdust by extrusion technique. CD Rom Proc. the 17th Conference on Mechanical Engineering Network of Thailand, KMITNB-Prachinburi., 15-17 Oct. 2003, 6 p (in Thai). (เป็นผลงานในฐานะที่ปรึกษาและวิจัยร่วม)
3. Madhiyanon, T. and Soponronnarit, S. 2003. High temperature spouted bed grain drying with various downcomer-airflow. CD Rom Proc. the 17th Conference on Mechanical Engineering Network of Thailand, KMITNB-Prachinburi., 15-17 Oct. 2003, 12 p (in Thai). (เป็นผลงานในฐานะนักวิจัยพี่เลี้ยงทุนพัฒนานักวิจัยหน้าใหม่ สกว.)
4. Jamradloedluk, J., Soponronnarit, S., Nathakaranakule, A., and Prachayawarakorn, S. 2004. Compressive behaviors of durian slices during hot air and superheated steam drying. Proc. the 5th Technical Conference of Thai Society of Agricultural Engineering, 26-27 April 2004, Bangkok, pp. 1-7. (เป็นผลงานในฐานะอาจารย์ที่ปรึกษาร่วมทุน คปก. สกว.)
5. Uengkimbuan, N., Soponronnarit, S., Prachayawarakorn, S., and Nathakaranakule, A. 2004. Pork drying using superheated steam and hot air. Proc. the 5th Technical Conference of Thai Society of Agricultural Engineering, 26-27 April 2004, Bangkok, pp. 8-14 (in Thai). (เป็นผลงานในฐานะอาจารย์ที่ปรึกษาร่วมทุน คปก. สกว.)
6. Witinantakit, K., Nathakaranakule, A., Prachayawarakorn, S., and Soponronnarit, S. 2004. Drying of paddy using rice husk as an adsorption medium. Proc. the 5th Technical Conference of Thai Society of Agricultural Engineering, 26-27 April 2004, Bangkok, pp. 15-21 (in Thai).
7. Jaekum., S., Nathakaranakule, A., Prachayawarakorn, S., and Soponronnarit, S. 2004. Fruit and hurb drying using combined techniques of heat pump and far-infared radiation. Proc. the 5th

Technical Conference of Thai Society of Agricultural Engineering, 26-27 April 2004, Bangkok, pp. 22-28 (in Thai).

8. Tia, W., Soponronnarit, S., and Athasart, S. 2004. Cogeneration potential of a parboiled rice mill. Proc. the 5th Technical Conference of Thai Society of Agricultural Engineering, 26-27 April 2004, Bangkok, pp. 29-35 (in Thai).
9. Prachayawasin, P., Soponronnarit, S., and Prachayawarakorn, S. 2004. Soybean drying using superheated steam fluidized bed. Proc. the 5th Technical Conference of Thai Society of Agricultural Engineering, 26-27 April 2004, Bangkok, pp. 36-43 (in Thai).
10. Kaewnin, N., Prachayawarakorn, S., Soponronnarit, S., and Nathakaranakule, A. 2004. Appropriate strategy for drying garlic. Proc. the 5th Technical Conference of Thai Society of Agricultural Engineering, 26-27 April 2004, Bangkok, pp. 44-51 (in Thai).
11. Iam-mi, ch., Tungtrakul, P., Taechapairoj, Ch., and S., Soponronnarit. 2004. The drying for parboiling aromatic rice using superheated-steam fluidized bed. Proc. the 5th Technical Conference of Thai Society of Agricultural Engineering, 26-27 April 2004, Bangkok, pp. 52-61 (in Thai).
12. Prakotmak, P., Soponronnarit, S. and Prachayawarakorn, S. 2004. Effect of pore size distribution on water transport inside porous materials. Proc. the 5th Technical Conference of Thai Society of Agricultural Engineering, 26-27 April 2004, Bangkok, pp. 62-69 (in Thai).
13. Teeboonma, U. and Soponronnarit, S. 2004. Heat pump drying design using optimization technique. Proc. the 5th Technical Conference of Thai Society of Agricultural Engineering, 26-27 April 2004, Bangkok, pp. 70-77 (in Thai).
14. Buranapetch, T., Soponronnarit, S., and Poomsa-add. N. 2004. Equilibrium moisture content and drying kinetics of mulberry leaves. Proc. the 5th Technical Conference of Thai Society of Agricultural Engineering, 26-27 April 2004, Bangkok, pp. 125-131 (in Thai). (เป็นผลงานในฐานะนักวิจัยพี่เลี้ยงทุนพัฒนานักวิจัยหน้าใหม่ สกว.)
15. Teeboonma, U. and Soponronnarit, S. 2004. Comparative assessment of R134a, R407C, and R410A as alternatives to R22. Proc. the 5th Technical Conference of Thai Society of Agricultural Engineering, 26-27 April 2004, Bangkok, pp. 139-146.
16. Sathitruangsak, P., Soponronnarit, S. and Madhiyanon, T. 2004. Briquette fuel product from coconut shell by extrusion technique using molass as binder. CD Rom Proc., The 18th Conference on Mechanical Engineering Network of Thailand, Khonkaen, 18-20 Oct. 2004, 7p. (in Thai).
17. Madhiyanon, T., Sathitruangsak, P. and Soponronnarit, S. 2004. A study of influences of binder treated from wheat straw on physical properties of fuel briquette. CD Rom Proc., The 18th Conference on Mechanical Engineering Network of Thailand, Khonkaen, 18-20 Oct. 2004, 5p. (in Thai).
18. Madhiyanon, T., Piriyarungroj, N., Thongnork, P. and Soponronnarit, S. 2004. Vortexing-fluidized bed combustor (VFBC) : Part I Effects of primary air on performance of combustor. CD Rom

Proc. The 18th Conference on Mechanical Engineering Network of Thailand, Khonkaen , 18-20 Oct. 2004, 9p. (in Thai). (เป็นผลงานในฐานะที่ปรึกษาและวิจัยร่วม)

19. Madhiyanon, T., Piriyarungroj, N., Thongnork, P. and Soponronnarit, S. 2004. Vortexing-fluidized bed combustor (VFBC) : Part II Effects of secondary air on performance of combustor. CD Rom Proc. The 18th Conference on Mechanical Engineering Network of Thailand, Khonkaen , 18-20 Oct. 2004, 9p. (in Thai). (เป็นผลงานในฐานะที่ปรึกษาและวิจัยร่วม)
20. Thuwapanichayanan, R., Soponronnarit, S. and Prachawarakorn, S. 2004. Mathematical model for fluidized bed drying using superheated steam. CD Rom Proc. The 18th Conference on Mechanical Engineering Network of Thailand, Khonkaen, 18-20 Oct. 2004, 6p. (in Thai).
21. Dangton, W., Rittidech, S. and Soponronnarit, S. 2004 Performance tests of a closed-end oscillation heat pipe air preheater for dryer. CD Rom Proc. The 18th Conference on Mechanical Engineering Network of Thailand, Khonkaen, 18-20 Oct. 2004, 8p. (in Thai). (เป็นผลงานในฐานะนักวิจัยพี่เลี้ยงทุนพัฒนานักวิจัยหน้าใหม่ สกว.)
22. Montripila, M., Soponronnarit, S. and Poomsa-ad, N. 2004. Drying kinetics of cooked glutinous rice using superheated steam and hot air. CD Rom Proc. The 18th Conference on Mechanical Engineering Network of Thailand, Khonkaen, 18-20 Oct. 2004, 6p. (in Thai). (เป็นผลงานในฐานะนักวิจัยพี่เลี้ยงทุนพัฒนานักวิจัยหน้าใหม่ สกว.)
23. Jutajan, W., Soponronnarit, S., Siriamornpun, S. and Poomsa-Ad, N. 2005. Physical properties of cooking glutinous rice after drying. In CD-Rom Proc. of the Technical Conference of the Thai Society of Agricultural Engineering, Bangkok, 30th-31st March 2005, pp. 379-386 (in Thai).
24. Sathapomprasath, K., Devahastin, S. and Soponronnarit, S. 2005. Effects of operating conditions on the overall performance of impinging stream dryer. In CD-Rom Proc. of the Technical Conference of the Thai Society of Agricultural Engineering, Bangkok, 30th-31st March 2005, pp. 463-471.
25. Witinantakit, K., Prachayawarakorn, S., Nathkaranakule, A. and Soponronnarit, S. 2005. Modeling of paddy drying using rice husk as adsorption medium. In CD-Rom Proc. of the Technical Conference of the Thai Society of Agricultural Engineering, Bangkok, 30th-31st March 2005, pp. 472-482 (in Thai).
26. Jamradloedluk, J., Nathkaranakule, A., Soponronnarit, S. and Prachayawarakorn, S. 2005. Rehydration kinetics of dried durian. In CD-Rom Proc. of the Technical Conference of the Thai Society of Agricultural Engineering, Bangkok, 30th-31st March 2005, pp. 483-490.
27. Tachapiroch, C., Prachayawarakorn, S., Trangtrakoon, P., Tarmaisuk, P. and Soponronnarit, S. 2005. The effect of drying on instant rice properties. In CD-Rom Proc. of the Technical Conference of the Thai Society of Agricultural Engineering, Bangkok, 30th-31st March 2005, pp. 491-498 (in Thai).
28. Uengkimbuan, N., Soponronnarit, S., Prachayawarakorn, S. and Nathkaranakule, A. 2005. Drying kinetics and physical properties of pork dried using two-stage techniques. In CD-Rom Proc. of the Technical Conference of the Thai Society of Agricultural Engineering, Bangkok, 30th-31st March 2005, pp. 499-506 (in Thai).

29. Wongkaew, P., Prachayawarakorn, S., Nathkaranakule, A. and Soponronnarit, S. 2005. Effects of bulk density of rice husk and mixing ratio on drying characteristics of paddy. In CD-Rom Proc. of the Technical Conference of the Thai Society of Agricultural Engineering, Bangkok, 30th-31st March 2005, pp. 507-518 (in Thai).
30. Buakhom, R., Soponronnarit, S. and Prachayawarakorn, S. 2005. Drying of coffee berries using heat pump and hot air. In CD-Rom Proc. of the Technical Conference of the Thai Society of Agricultural Engineering, Bangkok, 30th-31st March 2005, pp. 519-529 (in Thai).
31. Ngamchum, R., Swasdisevi, T., Devahastin, S. and Soponronnarit, S. 2005. Cavendish drying with far infrared–vacuum dryer. In CD-Rom Proc. of the Technical Conference of the Thai Society of Agricultural Engineering, Bangkok, 30th-31st March 2005, pp. 530-542 (in Thai).
32. Kraiwanichkul, W., Nathkaranakule, A. and Soponronnarit, S. 2005. Chicken drying using superheated steam combined with heat pump. In CD-Rom Proc. of the Technical Conference of the Thai Society of Agricultural Engineering, Bangkok, 30th-31st March 2005, pp. 543-554 (in Thai).
33. Yuttachai, W., Soponronnarit, S. and Prachayawarakorn, S. 2005. Effect of soaking on urease inactivation and protein solubility in soybean during treatment with hot air fluidized bed drying. In CD-Rom Proc. of the Technical Conference of the Thai Society of Agricultural Engineering, Bangkok, 30th-31st March 2005, pp. 555-565 (in Thai).
34. Kaewnok, S., Prachayawarakorn, S., Nathkaranakule, A. and Soponronnarit, S. 2005. Effects of temperature on drying characteristics and quality of garlic clove. In CD-Rom Proc. of the Technical Conference of the Thai Society of Agricultural Engineering, Bangkok, 30th-31st March 2005, pp. 566-576 (in Thai).
35. Madhiyanon, T., Adirekrut, S., Sathitruangsak, P. and Soponronnarit, S. 2005. A study of coconut drying using hot air combined with desiccant. In CD-Rom Proc. of the Technical Conference of the Thai Society of Agricultural Engineering, Bangkok, 30th-31st March 2005, pp. 577-586 (in Thai).
36. Chanapai, U., Soponronnarit, S. and Prachayawarakorn, S. 2005. Mathematical modeling for a single soybean drying with superheated steam and hot air. In CD-Rom Proc. of the Technical Conference of the Thai Society of Agricultural Engineering, Bangkok, 30th-31st March 2005, pp. 587-601 (in Thai).
37. Namsanguan, Y., Tia, W., Devahastin, S. and Soponronnarit, S. 2005. Characteristics of shrimp dried by two-stage drying technique at different drying conditions. In CD-Rom Proc. of the Technical Conference of the Thai Society of Agricultural Engineering, Bangkok, 30th-31st March 2005, pp. 620-629 (in Thai).
38. Kitikhun, C., Soponronnarit, S., Teeboonma, U. and Wiriyaumpaiwong, S. 2005. Production of steam for domestic industry using traveling grate combustor as heat source. In CD-Rom Proc. of the Technical Conference of the Thai Society of Agricultural Engineering, Bangkok, 30th-31st March 2005, pp. 858-867 (in Thai).

39. Madhiyanon, T., Sathitruangsak, P., Thongnork, P., Soponronnarit, S. and Wongchang, T. 2005. A short combustion chamber fluidized-bed combustor: Part I. Effects of primary air on combustor performance. In CD-Rom Proceedings of the 19th Conference of Mechanical Engineering Network of Thailand, 19-21 October 2005, 8p.
40. Madhiyanon, T., Sathitruangsak, P., Wongchang, T. and Soponronnarit, S. 2005. A short combustion chamber fluidized-bed combustor: Part II. Effects of upper secondary air on combustor performance. In CD-Rom Proceedings of the 19th Conference of Mechanical Engineering Network of Thailand, 19-21 October 2005, 9p.
41. Madhiyanon, T., Lapirattanakun, A., Sathitruangsak, P. and Soponronnarit, S. 2005. Vortexing-fluidized bed combustor: The performance and gas distribution, within a combustor. In CD-Rom Proceedings of the 19th Conference of Mechanical Engineering Network of Thailand, 19-21 October 2005, 15p.
42. Madhiyanon, T., Sathitruangsak, P. and Soponronnarit, S. 2005. Study of solid fuel produced from ground anthracite by extrusion technique. In CD-Rom Proceedings of the 19th Conference of Mechanical Engineering Network of Thailand, 19-21 October 2005, 6p.
43. Madhiyanon, T., Sathitruangsak, P., Adirekrut, S. and Soponronnarit, S. 2005. A coconut drying kinetics comparison between drying in a combined hot air-desiccant system and a hot air system. In CD-Rom Proceedings of the 19th Conference of Mechanical Engineering Network of Thailand, 19-21 October 2005, 8p.
44. Madhiyanon, T., Sathitruangsak, P., Adirekrut, S. and Soponronnarit, S. 2005. A study of the influences of drying air relative humidity in a combined hot air-desiccant dryer. In CD-Rom Proceedings of the 19th Conference of Mechanical Engineering Network of Thailand, 19-21 October 2005, 10p.
45. Yangwo, P., Wiriyaumpaiwong, S. and Soponronnarit, S. 2006. Multi-stage reduction of moisture of paddy by using tapioca flour as adsorption media. In CD-Rom Proc. of the 7th National Conference of the Thai Society of Agricultural Engineering, Mahasarakham Univ., 23rd-24th January 2006, pp.381-388 (in Thai).
46. Rikham, K., Wiriyaumpaiwong, S. and Soponronnarit, S. 2006. Multi-stage reduction of moisture of paddy by using rice husk as adsorption media. In CD-Rom Proc. of the 7th National Conference of the Thai Society of Agricultural Engineering, Mahasarakham Univ., 23rd-24th January 2006, pp.389-395 (in Thai).
47. Witinantakit, K., Prachayawarakorn, S., Nathkaranakule, A. and Soponronnarit, S. 2006. Multi-pass drying of paddy using rice husk. In CD-Rom Proc. of the 7th National Conference of the Thai Society of Agricultural Engineering, Mahasarakham Univ., 23rd-24th January 2006, pp.396-402 (in Thai).
48. Jamradloedluk, J., Soponronnarit, S., Nathakaranakule, A. and Prachayawarakorn, S. 2006. Adsorption isotherms of durian flour undergoing three different drying techniques. In CD-Rom Proc. of the 7th National Conference of the Thai Society of Agricultural Engineering, Mahasarakham Univ., 23rd-24th January 2006, pp.403-410 (in Thai).

49. Wongsri, P., Swasdsevi, T., Prachayawarakon, S. and Soponronnarit, S. 2006. Superheated steam pork meat drying. In CD-Rom Proc. of the 7th National Conference of the Thai Society of Agricultural Engineering, Mahasarakham Univ., 23rd-24th January 2006, pp.437-446 (in Thai).
50. Plytho, N., Prachayawarakorn, S., Tia, W. and Soponronnarit, S. 2006. Effect of pretreatment on drying kinetics and quality of banana slices. In CD-Rom Proc. of the 7th National Conference of the Thai Society of Agricultural Engineering, Mahasarakham Univ., 23rd-24th January 2006, pp.447-455 (in Thai).
51. Nimmol, C., Devahastin, S., Swasdisevi, T. and Soponronnarit, S. 2006. Drying of carrot by far-infrared radiation under vacuum condition. In CD-Rom Proc. of the 7th National Conference of the Thai Society of Agricultural Engineering, Mahasarakham Univ., 23rd-24th January 2006, pp.456-463 (in Thai).
52. Thuwapanichayanan, R., Prachayawarakorn, S., and Soponronnarit, S. 2006. Drying of foam-mat ripe bananas. In CD-Rom Proc. of the 7th National Conference of the Thai Society of Agricultural Engineering, Mahasarakham Univ., 23rd-24th January 2006, pp.464-472 (in Thai).
53. Sinprasert, S., Taechapairoj, C., Prachayawarakorn, S. and Soponronnarit, S. 2006. Investigation of drying kinetics of beef dried using superheated steam and hot air. In CD-Rom Proc. of the 7th National Conference of the Thai Society of Agricultural Engineering, Mahasarakham Univ., 23rd-24th January 2006, pp.473-481 (in Thai).
54. Chiawwet, M., Prachayawarakorn, S., Tungtrakul, P. and Soponronarit, S. 2006. Accelerating aging of paddy using fluidized bed drying followed by tempering. In CD-Rom Proc. of the 7th National Conference of the Thai Society of Agricultural Engineering, Mahasarakham Univ., 23rd-24th January 2006, pp.482-490 (in Thai).
55. Jaisut, D., Prachayawarakorn, S., Varanyanond, W., Tungtrakul, P. and Soponronnarit, S. 2006. Producing high quality brown rice using fluidization technique. In CD-Rom Proc. of the 7th National Conference of the Thai Society of Agricultural Engineering, Mahasarakham Univ., 23rd-24th January 2006, pp.491-499 (in Thai).
56. Meeso, N., Nathakaranakule, A., Madhiyanon, T. and Soponronnarit, S. 2006. Feasibility study of combined FIR and hot-air convection in fluidized bed paddy dryiong. In CD-Rom Proc. of the 7th National Conference of the Thai Society of Agricultural Engineering, Mahasarakham Univ., 23rd-24th January 2006, pp.500-507 (in Thai).
57. Jariyatontivait, W., Prachayawarakorn, S., Teachapairoj, C. and Soponronnarit, S. 2006. Effects of soaking time and pre-steaming for production of parboiled rice using hot air fluidized bed. In CD-Rom Proc. of the 7th National Conference of the Thai Society of Agricultural Engineering, Mahasarakham Univ., 23rd-24th January 2006, pp.508-515 (in Thai).
58. Luangmalawat, P., Nathakaranakule, A., Prachayawarakorn, S., Tungtrakul, P. and Soponronnarit, S. 2006. Effect of drying methods on quality of cooked rice. In CD-Rom Proc. of the 7th National Conference of the Thai Society of Agricultural Engineering, Mahasarakham Univ., 23rd-24th January 2006, pp.516-524 (in Thai).
59. Madhiyanon, T., Sathitruangsak, P., Adirekrut, S. and Soponronnarit, S. 2006. A study of coconut drying kinetics by fluidized bed technique. In CD-Rom Proc. of the 7th National Conference of the Thai Society of Agricultural Engineering, Mahasarakham Univ., 23rd-24th January 2006, pp.525-530 (in Thai).

60. Jamradloedluk, J., Soponronnarit, S., Nathakaranakule, A. and Prachayawarakorn, S. 2006. Physical and pasting properties of durian flour obtained by different drying methods. In CD-Rom Proc. of the 7th National Conference of the Thai Society of Agricultural Engineering, Mahasarakham Univ., 23rd-24th January 2006, pp.566-572 (in Thai).

Patents:

1. Equipment and processes in steaming and drying cereal grains using superheated steam fluidization technique. Patent (Invention) pending No. 083492.

2 ผลงานที่นำไปใช้ในอุตสาหกรรม:

ผลงานที่นำไปใช้ในอุตสาหกรรมที่ต่อเนื่องจากโครงการที่แล้ว

1. เครื่องอบแห้งข้าวเปลือกแบบฟลูอิไดซ์เบด บริษัทเอกชนที่ร่วมวิจัยได้ผลิตจำหน่ายแล้วประมาณ 250 เครื่อง โดยมียอดจำหน่ายปีละประมาณ 25 เครื่อง ปัจจุบันมีหลายบริษัทผลิตจำหน่ายอย่างแพร่หลาย
2. เตาเผาแกลบไซโคลน บริษัทเอกชนที่ร่วมวิจัยได้ผลิตจำหน่ายแล้วประมาณ 250 เครื่อง โดยมียอดจำหน่ายปีละประมาณ 25 เครื่อง ปัจจุบันมีหลายบริษัทผลิตจำหน่ายอย่างแพร่หลาย
3. เครื่องอบแห้งปั๊มความร้อน บริษัทเอกชนที่ร่วมวิจัยได้ผลิตจำหน่ายแล้วประมาณ 25 เครื่อง
4. เครื่องอบแห้งแบบตู้โดยใช้ LPG บริษัทเอกชนที่ร่วมวิจัยได้ผลิตจำหน่ายแล้วประมาณ 25 เครื่อง

ผลงานที่นำไปใช้ในอุตสาหกรรมในโครงการนี้

1. ได้ให้คำปรึกษากับคุณณรงค์ศักดิ์ ภู่ธนะพิบูล บริษัทเทอร์โมดูลซัพพลาย แอนด์ เซอร์วิส จำกัด กทม. เรื่องการทำความเย็นข้าวเปลือกที่เก็บรักษาในไซโล ปัจจุบันได้ผลิตขายให้กับโรงสีข้าวหลายแห่ง
2. ได้จัดสร้างเครื่องต้นแบบเครื่องอบแห้งข้าวเปลือกแบบฟลูอิไดซ์เบดโดยใช้ไอน้ำร้อนยวดยิ่ง
3. ได้จัดสร้างเครื่องต้นแบบเครื่องอบแห้งปั๊มความร้อนร่วมกับรังสีอินฟราเรดไกล

ผลงานที่นำไปใช้ในอุตสาหกรรมในโครงการนี้ในรูปแบบที่ปรึกษาโครงการวิจัย/ร่วมวิจัย

1. เตาเผาไหม้วอร์เทค-ฟลูอิไดซ์เบด อยู่ระหว่างการสร้าง (ดูภาคผนวก)
2. การผลิตเชื้อเพลิงแท่งแข็งจากถ่านกะลามะพร้าวโดยเทคนิคเอ็กทรูชัน ได้ถ่ายทอดเทคโนโลยี (ดูภาคผนวก)

การให้คำปรึกษากับภาคธุรกิจอุตสาหกรรม

- 31 มกราคม 2547 คุณสุรเชษฐ์ บุษบกแก้ว จังหวัดลำพูน ขอคำปรึกษาเกี่ยวกับการใช้เตาผาแกลบที่ใช้กับเครื่องอบแห้งลำไยขนาดใหญ่ อัตราความร้อนจากเตาประมาณ 1 MW

- 29 มีนาคม 2547 ห้างหุ้นส่วนจำกัดไทยฟิลเตอร์เทค กทม. โดย คุณวิโรจน์ จิระกรานนท์ ปรึกษาวิธีการอบแห้งขี้แป้งจากโรงงานแป้งมันสำปะหลัง
- 12 กรกฎาคม 2547 โรงงานน้ำมันมะพร้าวมงคลเจริญทรัพย์ 2 จังหวัดราชบุรี โดย คุณอนุวัตน์ คงอุดม-เกียรติ ปรึกษาวิธีการอบแห้งเนื้อมะพร้าวโดยใช้ความร้อนจากเตาเผาฟืน
- 12 กรกฎาคม 2547 โรงสีศิริภิญโญ จังหวัดฉะเชิงเทรา โดย คุณพิเชษฐ์ โตนิติวงศ์ ปรึกษาเรื่อง การออกแบบเตาแกลบเพื่อใช้กับเครื่องอบแห้งข้าวเปลือก
- 16 กรกฎาคม 2547 ส่วนส่งเสริมวิศวกรรมเกษตร กรมส่งเสริมการเกษตร โดย คุณจงรักษ์ งามดี ขอคำปรึกษาวิธีการปรับปรุงการไหลของลมร้อนในเครื่องอบแห้งแบบตู้ ซึ่งภายในบรรจุถาดใส่ผลิตภัณฑ์ เพื่อให้ลมร้อนไหลอย่างสม่ำเสมอ
- 18 กันยายน 2547 บริษัทเทอร์โมคูลซัพพลาย แอนด์ เซอร์วิส จำกัด กทม. โดย คุณณรงค์ศักดิ์ ภู่ธนะ-พิบูล ปรึกษาเรื่องการทำความเย็นข้าวเปลือกที่เก็บรักษาในไซโล ได้รับรายงานว่าได้ผลิตขายให้กับโรงสีข้าวหลายแห่ง
- 8 เมษายน 2548 กลุ่มผู้ประกอบการโรงสีจากสามประเทศในอเมริกากลาง ได้แก่ เม็กซิโก โคลัมเบีย และเวเนซูเอลา จำนวน 8 คน เข้าเยี่ยมชมงานวิจัยด้านการอบแห้งข้าวเปลือกที่ห้องปฏิบัติการวิจัยเทคโนโลยีการอบแห้ง คณะพลังงานและวัสดุ มจธ.
- 22 เมษายน 2548 บริษัทธนาคูณอินเตอร์เนชั่นแนล จำกัด กทม. โดยคุณวิมล เสือเปรม ปรึกษาเกี่ยวกับการระบายอากาศในไซโลเก็บข้าวเปลือกขนาด 1,000 ตัน
- 19 พฤษภาคม 2548 กลุ่มบริษัทธรรมสรณ์ กทม. โดย คุณธิติโตวิวัฒน์ และคุณชจร สมสาย ปรึกษาวิธีการนึ่งและอบแห้งขยะอินทรีย์ภายใต้ความดันสูง
- 1 มิถุนายน 2548 กลุ่มบริษัทธรรมสรณ์ กทม. ปรึกษาเป็นครั้งที่ 2
- 16 มิถุนายน 2548 กลุ่มบริษัทธรรมสรณ์ กทม. ปรึกษาเป็นครั้งที่ 3
- 20 มิถุนายน 2548 บริษัทแอดวานซ์ คอมบัสชั่น เอ็นจิเนียริ่ง จำกัด กทม. โดย คุณวีระชัย วชิรเกยูร และบริษัท ยูโร-ไทย เอ็นจิเนียริ่ง จำกัด โดยคุณวรชัย นิเวศวิวัฒน์ ปรึกษาวิธีการอบแห้งลำไย
- 24 สิงหาคม 2548 ผู้ประกอบการโรงสีที่ใหญ่ที่สุดในโลกจากประเทศสหรัฐอเมริกา (Riceland Food Inc.) จำนวน 4 คน เข้าเยี่ยมชมงานวิจัยด้านการอบแห้งข้าวเปลือกที่ห้องปฏิบัติการวิจัยเทคโนโลยีการอบแห้ง คณะพลังงานและวัสดุ มจธ.
- 10 พฤศจิกายน 2548 บริษัทร็อคเอเชีย จำกัด จังหวัดฉะเชิงเทรา โดยคุณปรีชา แซ่ลิ่ม ปรึกษาวิธีการอบแห้งเยื่อเปลือกไม้เพื่อเป็นเชื้อเพลิง
- 27 พฤษภาคม 2549 บริษัทเทอร์โมคูลซัพพลาย แอนด์ เซอร์วิส จำกัด กทม. โดย คุณณรงค์ศักดิ์ ภู่ธนะ-พิบูล ปรึกษาเรื่องการผลิตเครื่องอบแห้งแบบปั๊มความร้อนเพื่อขาย

3 รายชื่อนักศึกษาที่ทำวิทยานิพนธ์แล้วเสร็จ:

1. นายปกรณ์ เหลืองมาลาวัฒน์ ต.ค. 46 วศ.ม. เทคโนโลยีการจัดการพลังงาน มจธ. "การพัฒนาแบบจำลองทางคณิตศาสตร์ของการทำความเย็นข้าวเปลือก"
2. นายเฉลิมพร เอี่ยมมิ ต.ค. 46 วศ.ม. เทคโนโลยีพลังงาน มจธ. "การรวมกระบวนการผลิตของการนึ่งข้าวและการอบแห้งข้าวนึ่งสำหรับข้าวหอม"

3. นายณรงค์ศักดิ์ แก้วนิล พ.ย. 46 วศ.ม. เทคโนโลยีพลังงาน มจธ. "การการศึกษาหาแนวทางการอบแห้งกระเทียมที่เหมาะสม"
4. นายชัยยงค์ เตชะไพโรจน์ ต.ค. 46 วศ.ม. เทคโนโลยีอุณหภาพ มจธ. "การอบแห้งข้าวเปลือกโดยเทคนิคฟลูอิไดซ์เบดด้วยไอน้ำร้อนยวดยิ่ง"
5. นายเชษฐ์ โชติบุญ ต.ค. 46 วศ.ม. เทคโนโลยีพลังงาน มจธ. "การจำลองทางคณิตศาสตร์ของการเก็บข้าวเปลือกในถังเก็บโลหะ"
6. นายศรีมา แจ้คำ พ.ย. 46 วศ.ม. เทคโนโลยีพลังงาน มจธ. "การอบแห้งสมุนไพรโดยใช้ปั๊มความร้อนร่วมกับอินฟราเรดไกล"
7. นางสาวพิมพร แจ้งพลอย ธ.ค. 46 วศ.ม. เทคโนโลยีการจัดการพลังงาน มจธ. "แนวทางการวิจัยพลังงานชีวมวลและพลังน้ำขนาดเล็กสำหรับประเทศไทย"
8. นายยุทธนา ฏิระวณิชย์กุล ม.ค. 47 ปร.ด. เทคโนโลยีพลังงาน มจธ. "การจัดการข้าวเปลือกชื้นโดยการอบแห้งในที่เก็บภายใต้สภาวะอากาศร้อนชื้น"
9. นางสาวปาวีณา ปรัชญาวศิน มี.ค. 47 วศ.ม. วิศวกรรมเคมี มจธ. "การศึกษาผลของการอบแห้งด้วยอากาศร้อนและไอน้ำร้อนยวดยิ่งที่มีต่อคุณภาพของถั่วเหลือง" (เป็นผลงานในฐานะนักวิจัยพี่เลี้ยงทุนพัฒนานักวิจัยหน้าใหม่ สกว.)
10. นายธนากร บูรณเพชร พ.ค. 47 วศ.ม. เทคโนโลยีพลังงาน มมส. "อิทธิพลของอุณหภูมิที่มีผลต่อการอบแห้งใบหม่อน" (เป็นผลงานในฐานะนักวิจัยพี่เลี้ยงทุนพัฒนานักวิจัยหน้าใหม่ สกว.)
11. นายประสาน สถิตย์เรืองสวัสดิ์ มิ.ย. 47 วศ.ม. เทคโนโลยีการจัดการพลังงาน มจธ. "การออกแบบและทดสอบสกรูอัดสำหรับผลิตเชื้อเพลิงแข็งอัดแท่ง"
12. นายสุทธิศักดิ์ แก้วนก มิ.ย. 47 วศ.ม. เทคโนโลยีพลังงาน มจธ. "อิทธิพลของอุณหภูมิและรูปทรงที่มีผลต่อการอบแห้งและคุณภาพของกระเทียม"
13. นางสาวสุนียพร พรหมดวง มิ.ย. 47 วศ.ม. เทคโนโลยีการจัดการพลังงาน มจธ. "การอบแห้งตะไคร้ด้วยปั๊มความร้อน"
14. นายพยุงศักดิ์ ท่าไม้สุข มิ.ย. 47 วศ.ม. เทคโนโลยีพลังงาน มจธ. "การอบแห้งข้าวสุกเพื่อผลิตเป็นข้าวกึ่งสำเร็จรูป"
15. นายอธิคม จิรจินดาเลิศ มิ.ย. 47 วศ.ม. เทคโนโลยีการจัดการพลังงาน มจธ. "การนึ่งข้าวกล้องด้วยไอน้ำร้อนยวดยิ่ง"
16. นายปรีดา ปรากฏมาก มิ.ย. 47 วศ.ม. เทคโนโลยีการจัดการพลังงาน มจธ. "อิทธิพลของการกระจายขนาดท่อที่มีต่อการเคลื่อนที่ของน้ำในวัสดุรูพรุน"
17. นางสาวรติยา ธุวพาณิชยนันท์ ก.ค. 47 วศ.ม. เทคโนโลยีการจัดการพลังงาน มจธ. "แบบจำลองทางคณิตศาสตร์การอบแห้งถั่วเหลืองโดยเทคนิคฟลูอิไดซ์เบดด้วยไอน้ำร้อนยวดยิ่งและอากาศร้อน"
18. นายรัฐพร บัวขม ก.ค. 47 วศ.ม. เทคโนโลยีการจัดการพลังงาน มจธ. "การอบแห้งเมล็ดกาแฟสดโดยใช้ปั๊มความร้อนและลมร้อน"
19. น.ส.อุบลวรรณ ชนะภัย ต.ค. 47 วศ.ม. เทคโนโลยีอุณหภาพ มจธ. "แบบจำลองทางคณิตศาสตร์การอบแห้งถั่วเหลืองเมล็ดเดี่ยวโดยเทคนิคฟลูอิไดซ์เบดด้วยไอน้ำร้อนยวดยิ่งและอากาศร้อน"
20. นายวิริยะ แดงทน พ.ย. 47 วศ.ม. เทคโนโลยีพลังงาน มมส. "ท่อความร้อนสั้นปลายปิดสำหรับอุ่นอากาศในเครื่องอบแห้ง" (เป็นผลงานในฐานะนักวิจัยพี่เลี้ยงทุนพัฒนานักวิจัยหน้าใหม่ สกว.)
21. นายมนตรี มนตรีพิลา พ.ย. 47 วศ.ม. เทคโนโลยีพลังงาน มมส. "การอบแห้งข้าวเหนียวนึ่งสุกโดยใช้ไอน้ำร้อนยวดยิ่ง" (เป็นผลงานในฐานะนักวิจัยพี่เลี้ยงทุนพัฒนานักวิจัยหน้าใหม่ สกว.)

22. น.ส.ภาวิกา วงศ์แก้ว พ.ย. 47 วศ.ม. เทคโนโลยีพลังงาน มจธ. "การอบแห้งข้าวเปลือกโดยใช้แกลบเป็นสารดูดความชื้น"
23. นางยุวนารี นามสงวน ต.ค. 47 ปร.ด. เทคโนโลยีอุณหภาพ มจธ. "การอบแห้งกุ้งโดยใช้ไอน้ำร้อนยวดยิ่งตามด้วยปั๊มความร้อน"
24. นายวทัญญู รอดประพัฒน์ พ.ย. 47 ปร.ด. เทคโนโลยีอุณหภาพ มจธ. "การพัฒนาเครื่องต้นแบบอบแห้งข้าวเปลือกแบบฟลูอิไดซ์เบดโดยใช้ไอน้ำร้อนยวดยิ่ง"
25. นางสุภาวรรณ ฏิระวณิชย์กุล ธ.ค. 47 ปร.ด. เทคโนโลยีพลังงาน มจธ. "การศึกษาปัจจัยของอุณหภูมิที่ใช้ในการอบแห้งต่อสมบัติทางเคมีและทางกายภาพบางประการของข้าวเปลือกขึ้น"
26. นายนเรศ มีโส พ.ค. 48 ปร.ด. เทคโนโลยีอุณหภาพ มจธ. "การประยุกต์ใช้รังสีอินฟราเรดไกลในกระบวนการอบแห้งข้าวเปลือก"
27. นายพีระวัตร์ ทองนอก ก.พ. 48 วศ.ม. เทคโนโลยีอุณหภาพ มจธ. "เตาเผาไหม้ชีวมวลฟลูอิไดซ์เบดแบบห้องเผาไหม้สั้นโดยไม่ใช้วัสดุเฉื่อยผสมลงในเบด : ออกแบบสร้างและทดสอบ"
28. นายวรุต ยุทธชัย เม.ย. 48 วศ.ม. เทคโนโลยีพลังงาน มจธ. "อิทธิพลของการบำบัดขั้นต้นและอุณหภูมิอบแห้งที่มีต่อการลดลงของเอนไซม์ยูรีเอสและการละลายโปรตีนในถั่วเหลืองโดยใช้เทคนิคฟลูอิไดเซชัน"
29. นายฤทธิไกร งามซุ่ม เม.ย. 48 วศ.ม. เทคโนโลยีพลังงาน มจธ. "การออกแบบสร้างและทดสอบเครื่องอบแห้งสุญญากาศร่วมกับรังสีอินฟราเรดไกล"
30. นายวรวิทย์ กรัยวณิชย์กุล เม.ย. 48 วศ.ม. เทคโนโลยีการจัดการพลังงาน มจธ. "การอบแห้งเนื้อไก่ด้วยไอน้ำร้อนยวดยิ่งร่วมกับปั๊มความร้อน"
31. นายศิริวัฒ ศิลป์ประเสริฐ ก.ค. 48 วศ.ม. เทคโนโลยีการจัดการพลังงาน มจธ. " การอบแห้งเนื้อวัวด้วยไอน้ำร้อนยวดยิ่ง"
32. นายพลสันต์ วงษ์ศรี ก.ย. 48 วศ.ม. เทคโนโลยีการจัดการพลังงาน มจธ. "การอบแห้งเนื้อหมูด้วยไอน้ำร้อนยวดยิ่ง"
33. นายเสริมพงษ์ อดิเรกรัตน์ ต.ค. 48 วศ.ม. เทคโนโลยีการจัดการพลังงาน มจธ. "การอบแห้งอาหารโดยใช้ลมร้อนร่วมกับสารดูดความชื้น"
34. นางสาวจินดาพร จำรัสเลิศลักษณ์ ต.ค. 48 ปร.ด. เทคโนโลยีอุณหภาพ มจธ. "การศึกษาเปรียบเทียบการอบแห้งทุเรียนด้วยเทคนิคต่างๆ" (เป็นผลงานในทุน คปก. แบบกลุ่มวิจัย สกว.)
35. นายเกียรติศักดิ์ จงสุวรรณรักษ์ เม.ย. 49 วศ.ม. เทคโนโลยีพลังงาน มจธ. "การพัฒนาแบบจำลองทางคณิตศาสตร์สามมิติของการเก็บรักษาข้าวเปลือกในไซโลเหล็กทรงกระบอก"
36. นางสาวนภาพร พลายโถ เม.ย. 49 วศ.ม. เทคโนโลยีพลังงาน มจธ. "อิทธิพลของการพรีทรีทเมนต์ที่มีต่อจลนพลศาสตร์การอบแห้งและคุณภาพของกล้วยแผ่น" (เป็นผลงานในฐานะนักวิจัยพี่เลี้ยงทุนพัฒนานักวิจัยหน้าใหม่ สกว.)
37. นางสาวมัทนียา เชี่ยวเวช พ.ค. 49 วศ.ม. เทคโนโลยีพลังงาน มจธ. "การเร่งความเก่าของข้าวเปลือกโดยใช้เทคนิคในการอบแบบฟลูอิไดซ์เบดร่วมกับการเทมเปอร์"
38. นายภูมิใจ สอาดโฉม พ.ค. 49 วศ.ม. เทคโนโลยีพลังงาน มจธ. "การจำลองทางคณิตศาสตร์ของการอบแห้งกล้วยหอมทองด้วยระบบสุญญากาศร่วมกับรังสีอินฟราเรดไกล"
39. นายกิตติศักดิ์ วิธินันทกิตต์ มิย. 49 ปร.ด. เทคโนโลยีอุณหภาพ มจธ. "การอบแห้งข้าวเปลือกโดยใช้สารดูดความชื้น"

4 กิจกรรมอื่น ๆที่เกี่ยวข้อง

Keynote/Invited speakers,

- The 3rd Asia-Pacific Drying Conference, 1-3 September 2003, Asian Institute of Technology, Bangkok, Thailand.
- The International Seminar on Grain Drying in South Asia, 1-2 Dec. 2003, Durgapur, India.
- The 15th International Symposium on Transport Phenomena (ISTP-15), Bangkok, Thailand, 9-14th May 2004,
- The 18th Mechanical Engineering Network Conference, Khonkaen, Thailand, 18-20th Oct. 2004.
- The 1st Energy Network Conference, Pattaya, Thailand, 11-13th May 2005.
- The 1st Technical Conference of Mahasarakham University, Thailand, 1st-2nd Sep. 2005.
- The 3rd National Technical Conference on Post-harvest Technology, Cha-am, Thailand, 10-11th Oct. 2005.
- The 4th Asia Pacific Drying Conference (ADC 05), 12-15th Dec. 2005, Kolkata, India.
- The 7th National Agricultural Engineering Conference, Marasarakham University, Thailand, 23rd-24th Jan. 2006.
- Technology and Innovation for Sustainable Development Conference, Khonkaen, Thailand, 25-27th Jan. 2006.

ทำวิจัยร่วม

ทำวิจัยด้านการอบแห้งข้าวเปลือกร่วมกับ Japan International Research Center for Agricultural Sciences โดยร่วมกับกรมวิชาการเกษตร และสถาบันวิจัยอาหารและพัฒนาผลิตภัณฑ์ มหาวิทยาลัยเกษตรศาสตร์ (1 ตุลาคม 2546 – 31 มีนาคม 2548)

เป็นวิทยากรรับเชิญบรรยายเกี่ยวกับงานวิจัย

- สสวท เรื่อง การสร้างเครือข่ายงานวิจัย, 2004
- สกว เรื่อง การเขียนบทความวิจัย, 2004
- SIIT เรื่อง Key features for successful research, 2004
- Expert consultation on post-harvest technologies for ensuring food safety and value addition for enhanced income, Asia-Pacific Association of Agricultural Research Institutions, Bangkok, 1-3 Dec. 2004.
- สกว เรื่อง New Technique for Producing Parboiled Rice, การประชุม นักวิจัยหน้าใหม่พบเมธีวิจัยอาวุโส สกว, 14-16 ม.ค. 2548

- โรงงานยาสูบ เรื่อง สถานภาพและแนวทางการพัฒนาพลังงานทดแทน 6 ก.ย. 2548
- บวท ผู้ดำเนินการเสวนา เรื่อง การพัฒนาพลังงานที่ยั่งยืนสำหรับประเทศไทย ที่ มทส 19 ต.ค. 2548

เป็นกรรมการเกี่ยวกับงานวิจัย

- Advisory panel of International Drying Symposium
- Board member of Section IV: Post-harvest Technology and Process Engineering, Congre International de Genie Rural (CIGR)
- Editorial member of International Energy Journal
- Editorial member of Asian Journal of Energy and Environment
- Editorial member of Engineering Journal, Khonkaen University
- Editorial member of the Journal of the Royal Institute of Thailand

ภาคผนวก

โครงการที่มีส่วนร่วมกับภาคอุตสาหกรรม

โดย ผศ. ดร.ฐานิตย์ เมธิยานนท์ (หัวหน้าโครงการ)
ภาควิชาวิศวกรรมเครื่องกล คณะวิศวกรรมศาสตร์ มหาวิทยาลัยเทคโนโลยีมหานคร

โครงการที่มีส่วนร่วมกับภาคอุตสาหกรรม มีอยู่ด้วยกันสี่โครงการ

1. โครงการ : เตาเผาไหม้วอร์เทค-ฟลูอิไดซ์เบดในระดับอุตสาหกรรม
   ผู้ประกอบการที่ร่วมโครงการ : บ. เกษตรไทยอินเตอร์ (22) จำกัด
   ลักษณะความร่วมมือ : ทางคณะผู้วิจัยได้ทำการพัฒนาเตาเผาไหม้วอร์เทค-ฟลูอิไดซ์เบด (VFBC) ในระดับอุตสาหกรรมขนาด 9 MW_{th} โดยการออกแบบเตาเผาไหม้วอร์เทค-ฟลูอิไดซ์เบด (VFBC) ในระดับอุตสาหกรรมนี้ได้นำข้อมูลพื้นฐานที่จำเป็นต่อการออกแบบและสร้างเตามาจากการศึกษาและวิจัยเตาเผาไหม้วอร์เทค-ฟลูอิไดซ์เบด (VFBC) ในระดับห้องปฏิบัติการ ซึ่งทางภาคอุตสาหกรรมรับหน้าที่ในการก่อสร้างตัวเตา โดยหลังจากที่ก่อสร้างแล้วเสร็จ ทางคณะวิจัยและทางภาคอุตสาหกรรมได้ร่วมกันทดสอบสมรรถนะและการทำงานของเตาเผาไหม้
   ความก้าวหน้า : จากการที่ได้ทำการทดสอบสมรรถนะของเตาเผาไหม้วอร์เทค-ฟลูอิไดซ์เบดในระดับอุตสาหกรรมพบว่าสมรรถนะใกล้เคียงกับเตาเผาไหม้วอร์เทค-ฟลูอิไดซ์เบด (VFBC) ในระดับห้องปฏิบัติการ โดยประสิทธิภาพเชิงความร้อนของเตาเผาไหม้มีค่าใกล้เคียงกันทุกเงื่อนไขการทดลองโดยมีค่าระหว่าง 90-95% (เตาเผาไหม้วอร์เทค-ฟลูอิไดซ์เบดระดับห้องปฏิบัติการพบว่ามีค่าอยู่ในช่วง 75-94% เมื่อเข้าสู่สภาวะคงตัว) ได้ค่าภาระความร้อนเตาเผาไหม้และพิกัดเตาที่ทดสอบโดยมีค่ามากที่สุดเท่ากับ 0.67 MW_{th}/m^3 และ 7.5 MW_{th} ทั้งนี้พบว่า ทางภาคอุตสาหกรรมพอใจกับภาระความร้อนที่เตาอุตสาหกรรมทำได้อยู่ในปัจจุบันคือ 0.67 $MW_{th}m^{-3}$ โดยสูงกว่าที่เตาไซโคลนที่ทางภาคอุตสาหกรรมผลิตอยู่ ซึ่งทำได้เพียง 0.25 $MW_{th}m^{-3}$ โดยสามารถนำ VFBC นี้ไปใช้เป็นต้นกำลังให้กับอุตสาหกรรมที่ต้องการแหล่งพลังงานความร้อนในกระบวนการผลิตโดยเฉพาะอุตสาหกรรมโรงสีข้าวในประเทศไทย ซึ่งหลังจากได้ประชุมกับทางภาคอุตสาหกรรมถึงประเด็นที่จะนำ VFBC ไปใช้ในภาคอุตสาหกรรมโรงสีพบว่า ในระยะ 2-3 ปีที่ผ่านมาโรงสีต่างๆได้ขยายกำลังผลิตและสั่งซื้อเครื่องอบแห้งพร้อมกับเตาเผาไหม้เป็นจำนวนมาก ทำให้ปัจจุบันตลาดของเตาเผาไหม้ที่ใช้แกลบเป็นเชื้อเพลิงเริ่มอิ่มตัว ทางคณะวิจัยหาทางออกโดยการนำเชื้อเพลิงชีวมวลชนิดอื่นมาเผาไหม้แทน เช่น ซังข้าวโพด เหง้ามันสำปะหลัง ทลายปาล์มเพื่อที่จะเป็นการเปิดกว้างในการที่จะนำ VFBC ไปใช้ในอุตสาหกรรมด้านอื่น

2. โครงการ : การผลิตเชื้อเพลิงแท่งแข็งจากถ่านกะลามะพร้าวโดยเทคนิคเอ็กทรูชัน
   ผู้ประกอบการที่ร่วมโครงการ : บ. สามัคคี คำเนิน คาร์บอน จำกัด
   ลักษณะความร่วมมือ : ทางคณะผู้วิจัยได้ถ่ายทอดเทคโนโลยีทั้งในส่วนของรูปแบบสกรูอัดซึ่งช่วยให้สามารถลดขั้นตอนในการผลิตลงได้ และในส่วนของการเลือกใช้ตัวประสานที่เหมาะสมเพื่อเพิ่มความแข็งแรงให้กับเชื้อเพลิงแท่งทำให้ไม่แตกหักง่ายขณะทำการเผาไหม้ จากการถ่ายทอดเทคโนโลยีในเรื่องสกรูอัด ทำให้ทางโรงงานสามารถลดขั้นตอนในการผลิตลงได้ครึ่งหนึ่งจากการที่ต้องทำการอัดรีดถึงสองครั้งก็เหลือเพียงครั้งเดียว นอกจากนี้ยังทำให้โรงงานสามารถผลิตเชื้อเพลิงจากผงถ่านกะลามะพร้าวได้ 100% ซึ่งเป็นที่

ต้องการของตลาดต่างประเทศ ในส่วนของตัวประสานซึ่งคณะผู้วิจัยแนะนำให้ใช้กากน้ำตาลแทนแป้งมันที่ทางโรงงานใช้อยู่ ขณะนี้ทางโรงงานกำลังดำเนินการทดสอบอยู่ นอกจากนี้ คาดว่าภายในเร็วๆ นี้ ทางคณะผู้วิจัยจะนำเครื่องอัดรีดเชื้อเพลิงแท่งที่ออกแบบและจัดสร้างไว้ นำไปทดสอบการใช้งานจริงที่โรงงาน

ความก้าวหน้า : ในขณะนี้ทางคณะผู้วิจัยได้นำเครื่องผลิตแท่งเชื้อเพลิงไปทดสอบในภาคอุตสาหกรรม ซึ่งพบว่าอัตราการผลิตที่ได้ประมาณ 5 ตันต่อวัน (อัดภายในขั้นตอนเดียว) และความแข็งแรงของแท่งเชื้อเพลิงที่ผลิตได้นั้นมีค่า ประมาณ 1.5 MPa ซึ่งเกินมาตรฐานของการค้าขายเชิงพาณิชย์ที่ 0.375 MPa โดยเครื่องผลิตแท่งเชื้อเพลิงที่สร้างขึ้นนี้ยังสามารถนำไปใช้ผลิตแท่งเชื้อเพลิงจากวัตถุดิบชนิดอื่น ๆ ได้อีกด้วย เช่น ผงถ่านหินแอนทราไซต์ ผงถ่านไม้ยางพารา รวมถึงผงถ่านซังข้าวโพด นอกจากนี้คณะผู้วิจัยยังได้ออกแบบเครื่องผลิตแท่งเชื้อเพลิงในรูปแบบใหม่ที่สามารถปรับเปลี่ยนขนาดของแท่งเชื้อเพลิงได้ระหว่าง 38 – 50 mm ทำให้มีความยืดหยุ่นในการใช้งานได้มากขึ้น และได้ส่งเข้าประกวดในโครงการรางวัลนวัตกรรมแห่งประเทศไทยครั้งที่ 5 ซึ่งได้รับรางวัลรองชนะเลิศอันดับสอง หลังจากนั้นก็ได้มีการติดต่อจากราชการ เพื่อจะนำเครื่องไปทำการแสดง และจากภาคเอกชนเพื่อขอเยี่ยมชมงาน รวมถึงมีการสั่งเครื่องผลิตแท่งเชื้อเพลิงเพื่อจะนำไปใช้ในการประกอบธุรกิจอีกด้วย

3. โครงการ 1.เตาเผาไหม้วอร์เทค-ฟลูอิไดซ์เบด (VFBC) ในระดับห้องปฏิบัติการ
2. เตาเผาไหม้ฟลูอิไดซ์เบดแบบห้องเผาไหม้สั้นที่ไม่ใช้วัสดุเฉื่อยผสมในเบด (FBC)

ผู้ประกอบการที่คาดว่าจะร่วมโครงการ : บริษัทร่วมทุนจัดการพลังงาน จำกัด

ลักษณะความร่วมมือ : เป็นการร่วมวิจัยเพื่อที่จะหาความเป็นไปได้ในการนำ VFBC และ FBC ไปใช้กับเชื้อเพลิงชีวมวลชนิดอื่น โดยเป้าหมายของบริษัทคือสร้างโรงไฟฟ้าที่ใช้เชื้อเพลิงชีวมวลเป็นหลักซึ่งโรงไฟฟ้าที่จะดำเนินการสร้างนั้นจะมีลักษณะของระบบผลิตไฟฟ้าความร้อนร่วม (Cogeneration) และเข้าร่วมกับโครงการผู้ผลิตไฟฟ้ารายเล็ก (SPP) สำหรับเชื้อเพลิงที่ได้รับความสนใจอยู่ในขณะนี้คือ ทลายปาล์ม และซังข้าวโพด โดยในการดำเนินโครงการนี้จะสอดคล้องกับนโยบายของสำนักนโยบายและแผนพลังงานแห่งชาติที่ส่งเสริมให้มีการใช้เชื้อเพลิงชีวมวลแทนเชื้อเพลิงฟอสซิล

ความก้าวหน้า : ตอนนี้ยังอยู่ในช่วงประเมินโครงการ

4. โครงการ 1.เตาเผาไหม้วอร์เทค-ฟลูอิไดซ์เบด (VFBC) ในระดับห้องปฏิบัติการ
2. เตาเผาไหม้ฟลูอิไดซ์เบดแบบห้องเผาไหม้สั้นที่ไม่ใช้วัสดุเฉื่อยผสมในเบด (FBC)

ผู้ประกอบการที่คาดว่าจะร่วมโครงการ : บริษัทยูนิค ไมนิ่ง เซอร์วิสเซส มหาชนจำกัด

ลักษณะความร่วมมือ : ทางคณะวิจัยได้ทำการศึกษาการเผาไหม้เชื้อเพลิงผสมระหว่างถ่านหินบดบิทูมินัสกับเชื้อเพลิงชีวมวล โดยจะร่วมมือจากทางบริษัทยูนิค ไมนิ่ง เซอร์วิสเซส มหาชน จำกัด โดยที่มาของโครงการนี้คือ บริษัทมีเศษถ่านหินบิทูมินัสขนาด 0-10 mm อยู่เป็นจำนวนมาก แต่ยังไม่ถูกนำไปใช้ประโยชน์เท่าที่ควร ประกอบกับปัญหาของการกักเก็บเชื้อเพลิงชีวมวลที่ต้องใช้เนื้อที่มากและการขาดแคลนเชื้อเพลิงชีวมวลในช่วงที่ไม่ใช่ฤดูกาลเก็บเกี่ยวของภาคอุตสาหกรรมที่ใช้ชีวมวลเป็นเชื้อเพลิงอยู่ในปัจจุบัน สำหรับรูปแบบของความร่วมมือ คือ ทางบริษัทจะสนับสนุนถ่านหินบิทูมินัสในการทดลอง ซึ่งหากมีแนวโน้มที่ดีก็จะขยายไปสู่ภาคอุตสาหกรรมที่มีการใช้งานเครื่องกำเนิดไอน้ำที่ใช้เชื้อเพลิงชีวมวล ดังนั้นทางบริษัทจึงมีความสนใจที่จะนำถ่านหินบดบิทูมินัสขนาด 0-10 mm มาเผาไหม้ร่วมกับเชื้อเพลิงชีวมวลภายใน VFBCและFBC ในสัดส่วน (ความร้อน) ไม่เกิน 25 (ถ่านหิน): 75 (ชีวมวล) ตามข้อกำหนดของสำนักงานนโยบายและแผนพลังงานแห่งชาติ (สนพ.)

ความก้าวหน้า : ขณะนี้กำลังอยู่ในขั้นตอนการวิจัยในระดับห้องปฏิบัติการ

DRYING TECHNOLOGY
Vol. 21, No. 9, pp. 1735–1757, 2003

Soybean Drying by Two-Dimensional Spouted Bed

Songchai Wiriyaumpaiwong,[1,*] Somchart Soponronnarit,[1] and Somkiat Prachayawarakorn[2]

[1]School of Energy and Materials, and [2]Faculty of Engineering, King Mongkut's University of Technology Thonburi, Thungkru, Bangkok, Thailand

ABSTRACT

Urease activity, cracking, and breakage are important factors in considering the quality of raw soybean for feed meal industries. A two-dimensional spouted bed dryer was investigated to determine its capability for thermally inactivating the urease enzyme and maintaining its other qualities. The experimental results have shown that the drying kinetics of soybean in a two-dimensional spouted bed dryer are of the form described in the thin layer drying. The expression for the model parameter in Newton's law of cooling equation accounting for the moisture contents and inlet air temperatures was developed. The initial moisture content and inlet air temperature conditions cause cracks in the kernels. The strong collision between kernels and

*Correspondence: Songchai Wiriyaumpaiwong, School of Energy and Materials, King Mongkut's University of Technology Thonburi, Pracha-utit Rd., Thungkru, Bangkok 10140, Thailand; E-mail: wsongchai@hotmail.com.

DOI: 10.1081/DRT-120025506
0737-3937 (Print); 1532-2300 (Online)
Copyright © 2003 by Marcel Dekker, Inc.
www.dekker.com

deflector because of high superficial velocity leads to high percentage of broken soybeans in the spout region. However, the velocity of 15.9 m/s can reduce the breakage below 5%. The inactivation of urease at low-to-moderate moisture content is suitably described by the first order kinetics. The modified Monod equation is applied when the moisture content is higher than 26% dry basis due to the inhibitory effect of water content on the inactivation rate. To complete urease inactivation and maintain protein quality, the temperatures of 150°C should be used.

Key Words: Grain; Inactivation; Protein; Urease; Trypsin.

INTRODUCTION

Soybean has long been used as a primary protein source in human foods and animal diets. Soybean proteins are used as human foods in a variety of forms, such as infant formulas, flour, protein isolates and concentrates, and textured fibers. New soy foods has been continually developed.[1,2] The demand of soy foods is increasingly important because of low cholesterol and high protein in soybean. However, raw soybeans cannot immediately be utilized because they contain the anti-nutritional factors i.e., trypsin inhibitors, hemagglutinins, and saponins.[3] These substances seriously affect the growth of animals.[4] Proper processing of soybean treatment requires control of moisture content, temperature, and processing time[5] to inactivate such factors. Adequate moisture and temperature during processing facilitates destruction of the anti-nutritional factors.

There are four major processes to inactivate the anti-nutritional factors such as extrusion, infrared roast, hot-air treatment and solid-particulate treatment. The different heat treatments provide dissimilar results. White et al.[6] and Faber and Zimmerman[7] found that the weight gain and growth of baby chicken were higher with the extruded soybeans than with the infrared roasted soybeans. Solid-particulate treatment produced excellent results in terms of feed efficiency.[8]

Recently, several works have been studied about the fluidized bed technique for eliminating the trypsin inhibitor in soybeans.[9,10] In their works, the urease measurement was used as an indirect indicator for inactivating the trypsin inhibitors since its analysis is simple. It showed a positive result of reduction in urease activity to acceptable limit of 0.3 pH rise or lower by using temperature higher than 120°C. This standard level is applied for the feed meal products.[11]

In addition to the urease activity, the crack of kernels is also an important part, particularly drying at high temperatures. To avoid grain cracking too high, soybeans should not be dried below 23.5% from initial 33.5% dry-basis.[10,12] Another approach that might replace fluidized bed technique is the spouted bed. This technique is suitable for coarse particles that will be difficult to be fluidized completely. In the present work, a two-dimensional spouted bed dryer shown in Fig. 1 is used. By this approach, particles are speeded up and carried by a very high air velocity from the bottom of drying chamber through a spout zone until impacting with a deflector and then falling down to the top of bed in the downcomer zone. The high air velocity together with high temperature in the spout zone provides the rapid moisture transfer from particles to air although the contact time is very short. In the downcomer, air and particles move in counter-current flow. Particles mix strongly at the bottom of this zone due to their movement to entrain into spout. Such a cyclic movement is the main characteristic of the spouted bed dryer.[13-15]

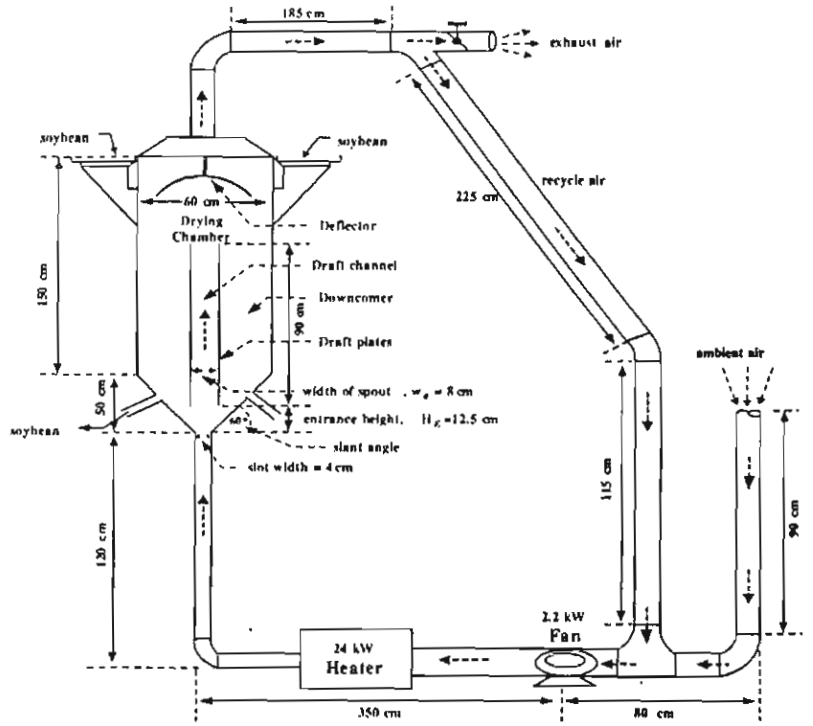


Figure 1. Schematic diagram of two-dimensional spouted bed dryer.

The aim of this work is to investigate moisture reduction and urease inactivation of raw soybeans in two-dimensional spouted bed dryer. The effects of moisture content and temperature on the other soybean qualities such as cracking and breakage, and protein are also reported.

MATERIALS AND METHODS

Spouted Bed Dryer

The schematic diagram of a two-dimensional spouted bed dryer with draft plates is shown in Fig. 1. The inlet cross sectional area of $4 \times 15\,cm^2$, drying chamber of $60 \times 15 \times 50\,cm^3$, spout width of 8 cm and entrance height of 12.5 cm were used. The selected values of spouted width and entrance height could maintain the transport of soybean to spout region and the spouting behavior. A 24 kW electrical heater was equipped to heat the air. A PID controller was used to control the temperature with an accuracy of ±1°C. A backward-curved blade centrifugal fan driven by a 2.2 kW motor was used to supply hot air into the dryer. An airflow rate was controlled by a variable speed unit. In the operation, the equipments were first heated until the temperatures reached the desired level. The heated air is then forced through the spouted bed dryer in which 90% of total airflow passed between draft plates, with the rest flowing through the downcomer. After that, some of the exhaust air was delivered to atmosphere and the remaining was recycled and then mixed with fresh air.

To get rid of the dead zone, the slanted base was fixed at an angle of 60° as recommended by Passos et al.[16] Kalwar et al.[17] found a serious dead region at the bottom for the slant angle lower than 30°. A deflector was installed for entrapping the entrainment of solid particles at a height of 142 cm from the base. At this height, the grain bed depth could be maintained at the same level for both the downcomer sides.

Quality

Soybeans were rewetted to obtain the desired moisture content and kept in a temperature-controlled room between 8 and 10°C for 5 or 7 days to ensure uniform moisture content throughout the kernels. Before starting the experiments, the soybeans were placed in ambient condition until grain temperature rose to room temperature. The soybeans were

then treated with heat by using the two-dimensional spouted bed dryer, as shown in Fig. 1. The grains were dried at inlet temperatures of 120, 130, 140, or 150°C controlled at ± 1°C. The air velocity varied in the range of 15.86 and 20.50 m/s with a fixed hold up of 25 kg, corresponding to the bed height of 60 cm. The initial moisture contents of interest were 14, 22, and 28% dry basis. Samples were taken from the dryer at drying times of 0, 5, 10, 15, 20, 25, and 30 min. The moisture content determination was determined at a temperature of 103°C in an electrical oven for 72 h, according to ASA standard.[11]

The urease activity was determined by following AACC method 22–90.[18] Experimental data was expressed as pH difference. The pH difference values were then converted to percentage of urease inactivation using equation proposed by Savage et al.[19] According to AOCS method Aa 5–38,[20] the percentage of crude protein content can be calculated by percentage of nitrogen multiplied by nitrogen-to-protein factor (6.25) and the percentage of nitrogen in soybean was estimated by Kjeldahl method, using a TKN analyzer. Protein solubility indicated the dispersion of proteins in 0.2% KOH solution. The nitrogen in the supernatant was determined by the Kjeldahl method. According to ASA standard,[11] protein solubility should be in the range of 70–85%. If its value is lower than 70%, it represents overcooked soybean, but if higher than 85%, soybean is insufficiently cooked. Protein solubility was calculated by

$$\text{Protein solubility} = \frac{\text{nitrogen of the supernatant in 0.2\% KOH solution}}{\text{crude protein}} \times 100 \quad (1)$$

In addition to the above quality parameter, cracking and breakage were inspected visually by sorting out the cracked or broken kernels with fluorescent light using a 200-g sample. At the beginning, the soybean kernels had a sound quality. The percentages of cracking and breakage can be calculated by the following equations:

$$\%\ \text{Cracking} = \frac{\text{weight of cracked kernel}}{\text{weight of sample}} \times 100 \quad (2)$$

$$\%\ \text{Breakage} = \frac{\text{weight of broken kernel}}{\text{weight of sample}} \times 100 \quad (3)$$

All analysis was performed in duplicate and the average value was presented in this work.

Thin Layer Drying Models

The drying rates in a drafted two-dimensional spouted bed are greatly affected by the inlet air temperature. The sensible heat gain and following moisture evaporation mostly occur between draft plates. The full exposure of individual grains to gas stream in a draft channel results in thermodynamic equilibrium to justify the condition for thin layer concept. Therefore, the drying rates for grains were correlated in the form of thin layer model. There are several thin layer models to predict the drying rate of cereal grains such as Newton's Law of Cooling, and the models of Page[21] and Sharaf-Eldeen et al.[22] In this research, three models were fitted to the experimental data to obtain the suitable model for predicting the drying rate in the spouted bed dryer. The three models are:

Newton's Law of Cooling:

$$MR = \exp(-k_1 t) \tag{4}$$

where k_1 is the drying constant (min^{-1}) and t is the drying time (min). MR in Eq. (1) is the moisture ratio defined as $(M - M_{eq})/(M_{in} - M_{eq})$ where M is the moisture at time t (decimal dry basis), M_{in} is the initial moisture content (decimal dry basis) and M_{eq} is the equilibrium moisture content (decimal dry basis). In calculating the moisture ratio (MR), we assumed M_{eq} to be zero because of low relative humidity at the temperature above the normal boiling point.[23]

Page's[21] Equation:

$$MR = \exp(-k_2 t^n) \tag{5}$$

where k_2 and n are the drying constants.

Sharaf-Eldeen et al.'s[22] Equation (two-component model):

$$MR = A\exp(-k_3 t) + B\exp(-k_4 t) \tag{6}$$

where k_3, k_4, A, B are the drying constants.

Kinetic Model of Urease Inactivation

The behavior of urease inactivation during drying was very complicated. It was mostly affected by initial moisture content. The inactivation rate started a relative increase at early drying period for the low-to-moderate moisture content. With the high moisture content, however, the reaction rate was inhibited. The kinetics of urease inactivation was therefore accounted for such behaviors by the first order for the low-to-moderate moisture content and the modified Monod models for high moisture content.

The Modified Monod equation[24]

$$U = \exp(c_1 \cdot t)/[K + \exp(c_2 \cdot t)] \tag{7}$$

The first order kinetic model

$$dU/dt = -k(U - U_e) \tag{8}$$

where U is the degree of urease inactivation, t is the inactivation time, c_1, K, c_2, U_e, and k are the inactivation constants. For a batch system, integration of Eq. (8) becomes

$$(U - U_e)/(U_o - U_e) = \exp(-kt) \tag{9}$$

where U_o is the degree of inactivation at $t = 0$. All of the constants in Eqs. (7) and (8) were statistically fitted to the function of initial moisture content and inlet air temperature using a nonlinear regression. c_1, K, c_2, U_e, and k in Eqs. (7) and (8) are given by the following equations:

$$c_1 \text{ and } c_2 = b_1 \cdot M_i/\exp(b_2 \cdot T) \tag{10}$$

$$K = M_i^{b3} \cdot T^{b4} \cdot \exp(b_5/T) \tag{11}$$

$$U_e \text{ and } k = b_6 + (b_7 \cdot M_i) + (b_8 \cdot T) + (b_9 \cdot M_i \cdot T) \tag{12}$$

where M_i and T are the initial moisture content (percent dry basis) and the inlet temperature (K), respectively.

RESULTS AND DISCUSSION

Effects of Temperature on Reduction of Moisture Content

Figure 2 shows the reduction of moisture content at different drying conditions. It is evident that the movement of moisture from the inside kernel to outside has a high potential capability with high inlet air temperature because of a large driving force of heat transfer. The change in moisture content with time follows the exponential decay, implying that the internal resistance controls the moisture movement. This resistance strictly limits the moisture movement at low moisture content. As shown in Fig. 2c, the average drying rates at 14% d.b. is very slow, for example,

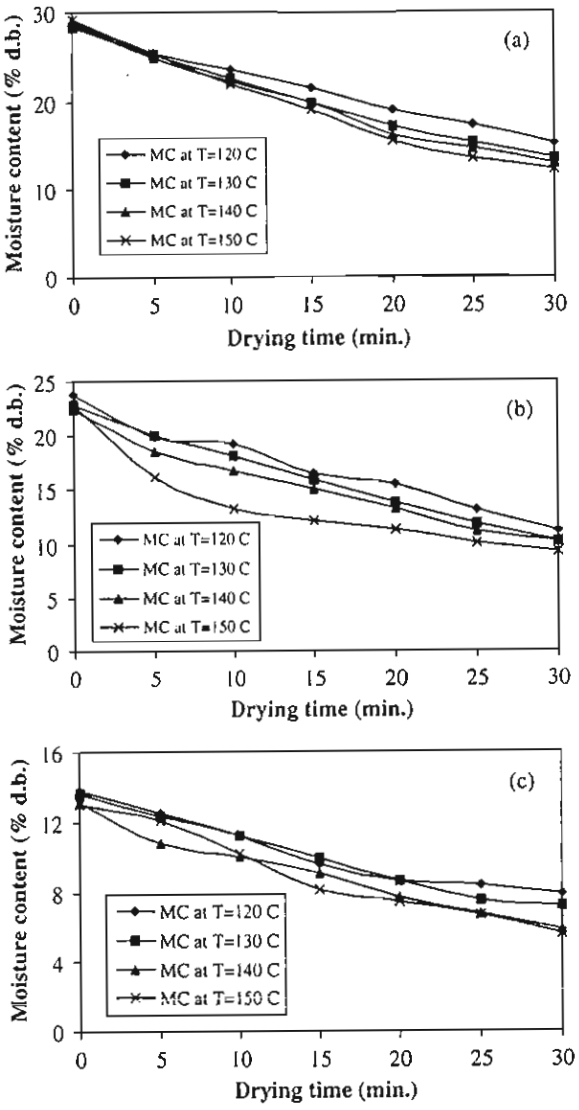


Figure 2. Relationship of moisture reduction with drying time at initial moisture contents of (a) 28% d.b., (b) 22% d.b, and (c) 14% d.b.

7% reduction of moisture content for 30 min at 150°C. The internal resistance, however, becomes less important for the higher range of moisture content since a large portion of moisture exists near the exterior surface which can be removed easily while the kernels are being drawn through the spout region where the mixing of grains and air is rigorous. This can be indicated by the slope of moisture curve shown in Figs. 2a and b for the moisture contents of 28 and 22% d.b., respectively.

Moisture Ratio (MR) Fitting

To find a relationship for each thin layer model between the drying constants and the independent variables, the drying constants were correlated with a function of inlet air temperature (T) and initial moisture content (M_i). The functions developed for drying constants of each model were then substituted into the original one. A nonlinear technique was used for estimating the constant parameters. The prediction of each model was generated for all the drying runs and compared with the collected data of each run. Typical graph of this comparison for some illustrative drying conditions is shown in Figs. 3a–c. The results of fitting three proposed models were then evaluated based on r^2 and the mean sum of squares of the errors (MSE). The MSE can be expressed by[25]

$$\mathrm{MSE} = \frac{\sum_{i=1}^{n} (\mathrm{MR}_{\mathrm{obs}} - \mathrm{MR}_{\mathrm{pre}})}{n - z} \tag{13}$$

where $\mathrm{MR}_{\mathrm{obs}}$ is the moisture content ratio from the experiment, $\mathrm{MR}_{\mathrm{pre}}$ is the predicted moisture ratio, n is the number of data points, and z is the number of unknown parameters. The values of r^2, MSE and drying constants for three proposed models for soybean drying are shown in Table 1. It is very clear that the three proposed models predicts the moisture content almost the same magnitude and approaching to the experimentally determined values. For ease of practical use, however, Newton's law of cooling is the suitable equation for calculating the MR.

Effect of Air Velocity on Cracking and Breakage

The cracking and breakage of soybean kernels were in the V-shaped fissures, as observed from the experiments. This result is similar to that reported by several workers.[10,26,27] Figure 4a shows the percentage of the cracked kernels at different air velocities and a 142 cm deflector height. The fracture on soybean kernels develops progressively with

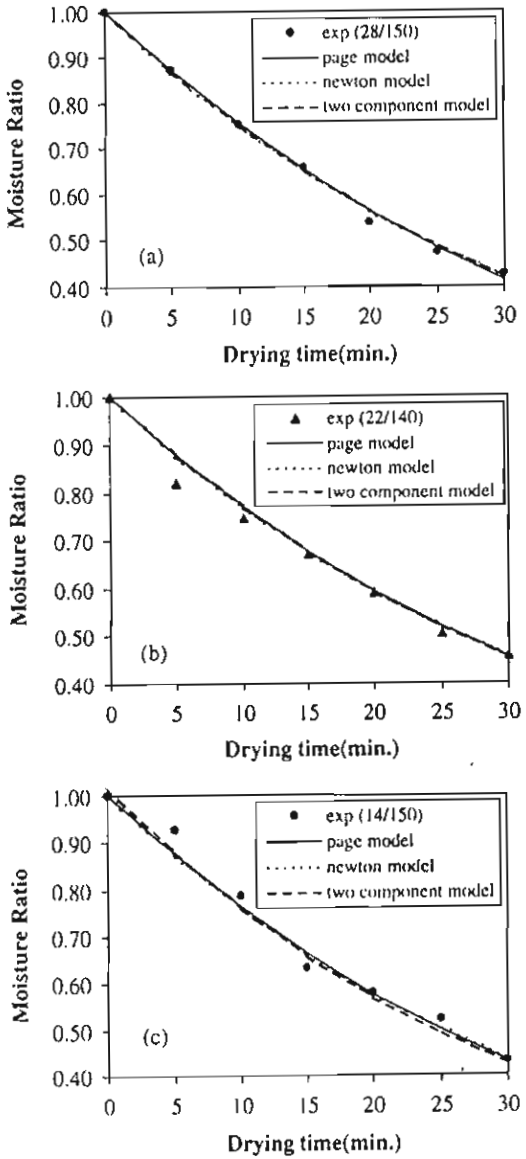


Figure 3. Comparison of predicted MR to experimental data at different drying conditions. (a) Initial moisture content of 28% d.b. and 150°C, (b) 22% d.b. and 140°C, and (c) 14% d.b. and 150°C.

Table 1. Drying constants and comparison of r^2 and MSE of each empirical model.

Models	Drying constants	r^2	MSE
Newton's law of cooling	$k_1 = 0.7652\ M_i^{0.0559}$	0.9862	0.00036
$MR = \exp(-k_1 t)$	$\exp(-1467.12/T)$		
Page's equation	$k_2 = 0.0347$	0.9869	0.00067
	$\exp(-142.0664/T)$		
$MR = \exp(-k_2 t^n)$	$n = 2.7985\ M_i^{0.0183}$		
	$\exp(-440.6973/T)$		
Two component model	$A = 0.8425\ M_i^{-5.2938}$	0.9862	0.00001
	$\exp(-405.3663/T)$		
$MR = A\exp(k_3 t) + B\exp(k_4 t)$	$k_3 = -2.5999$		
	$\exp(663.9915/T)$		
	$B = 1.3278\ M_i^{-0.0148}$		
	$\exp(-96.8986/T)$		
	$k_4 = -1.5147$		
	$\exp(-1674.9034/T)$		

reduction in moisture content, in particular at the early drying period showing the rapid development of crack kernels. When considering the influence of air velocities at the spout region, it shows that the percentage of the cracked kernel is slightly affected by the superficial velocity. At the final moisture content of 16% dry basis, the percentages of the cracked kernels at the superficial air velocities of 15.86, 17.12, and 20.5 m/s were 71, 72, and 75, respectively.

Figure 4b shows final moisture content versus the percentage of breakage, showing the severe effect of superficial air velocity on the percentage of the broken kernels. The soybean kernels are prone to break at high velocity, for example, the percentage of the broken kernels at 16% dry basis was higher than 10% at 20.5 m/s and less than 5% at 15.86 m/s. Such higher amounts of the broken kernels at higher air velocity is due to the combined effects of the strong impact of soybean kernel with deflector and drying rate, the latter playing a minor role since the drying rate at such velocities is essentially identical.

Effects of Moisture Content and Temperature on Percentages of Cracking and Breakage

To minimize the effect of the collision between kernels and deflector, the superficial air velocity was kept at 15.86 m/s throughout

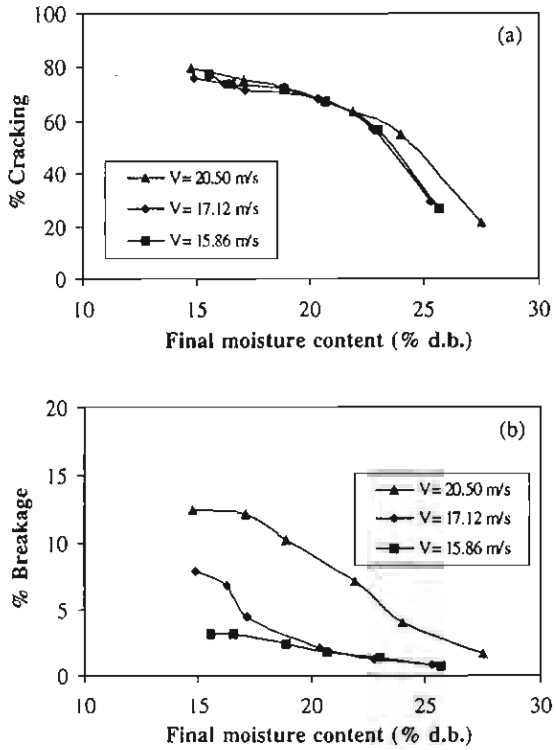


Figure 4. Effect of air velocities on (a) the percentage of cracking and (b) breakage at a fixed temperature of 130°C, initial moisture content of 28% d.b. and a deflector height of 142 cm.

the experiments. The percentages of the cracked and broken kernels obtained at temperatures of 120–150°C and initial moisture contents of 14–28% dry basis are shown in Fig. 5a–c, indicating the strong dependence of the percentages of the cracked and broken kernels on the final moisture contents and inlet air temperatures. Either the reduction of final moisture content or the increase in inlet air temperature directs toward the increase in the percentage of the fissured kernels.

As shown in Fig. 5a–b, at initial moisture contents of 22 and 28% dry basis, the percentages of fissures at the end are between 58 and 61% for the cracking and 3–4% for the breakage. Such amounts of fissure kernels are comparable to those obtained by the fluidized bed technique as reported by Soponronnarit et al.[10] However, when soybeans were dried from 14.0% dry basis, the percentages of cracking and breakage

are respectively 10–14.4% and 1.2–2.0% as shown in Fig. 5c. According to the results shown in Fig. 5, they suggest that the drying rate greatly affect the crack and breakage formations in the soybean kernels. Higher drying rate, directly related to the combination of higher inlet air

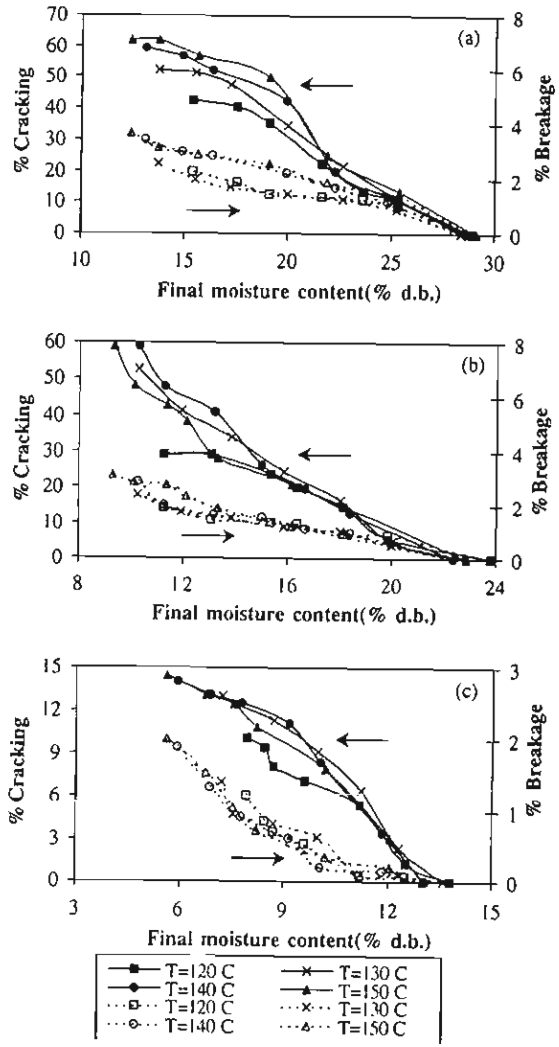


Figure 5. Percentage of cracking and breakage vs. final moisture content for the initial moisture contents of (a) 28% d.b., (b) 22% d.b., and (c) 14% d.b.

temperature and initial moisture content, provides the larger amount of the cracked and broken kernels.

As shown in Figs. 4a–b, the percentages of cracking and breakage at the end of drying for the temperature of 130°C and air velocity of 15.9 m/s (77% for cracking and 3.2% for breakage) is higher than that at the corresponding conditions shown in Fig. 5a (52% cracking and 2.54% for breakage). This can be attributed to the different moisture contents of soybean before rewetting, in which the moisture contents for the nonrewetting soybeans in Figs. 4 and 5 were 12 and 14% dry basis, respectively. The soybean rewetted from 12 to 28% dry basis leads to greater swelling than that rewetted from 14 to 28% dry basis. Thus, the grains adsorbed more water have a weaker strength, causing by a swelling of the cells at the surface layers which induces the gradient of forces between the surface and inner portion of the kernels.[28]

Urease Activity and Percentage of Urease Inactivation

The experimental results of urease activity and percentage of urease inactivation at different drying conditions are shown in Fig. 6a–c. The urease enzyme, measured by pH rise in an ammonia solution, was about 2.2–2.5, which is a typical value for raw soybeans. The pH difference was then converted to the percentage of urease inactivation by an equation proposed by Savage et al.[19] As presented in this figure, the urease activity reduces monotonically with drying time for any moisture content, except for the initial moisture content of 28% dry basis that shows a slow decline of urease activity for the first 15 min and a more rapid decrease afterwards. The behavior of urease activity is opposite to that of its inactivation showing the increase in amount of the inactive urease enzyme.

Inactivation of urease enzyme is very complicated and requires precise control of related parameters. The effective urease inactivation requires the adequate heat and moisture content for a given drying time. At temperatures of 120 and 130°C shown in Fig. 6, the inactivation of urease is insufficient for any initial moisture content, except for 28% dry basis showing the acceptable level with 97% urease inactivation, corresponding to the urease activity less than 0.3 pH difference. The accomplishment was performed within drying time of 30 min, at which the final moisture content was in the range from 14 to 15% dry basis. At the temperatures higher than 130°C, however, the urease enzyme is inactivated in 30 min for any initial moisture content (97% inactivation). The final moisture contents at 30 min for the initial moisture contents

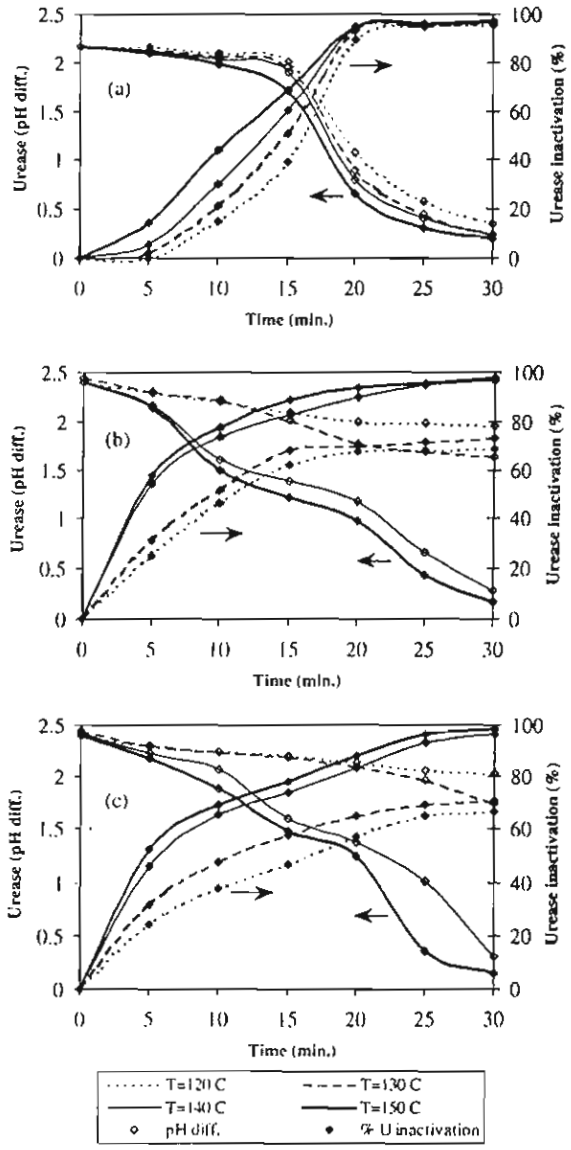


Figure 6. Effect of drying time on the urease activity and percentage of urease inactivation at different initial moisture content of (a) 28%, (b) 22%, and (c) 14% d.b.

between 14 and 28% dry basis were in the respective range of 7–12.5% dry basis.

Results indicate that the spouted bed is applicable to inactivate urease enzyme in soybean kernels. However, when compared with the previous works in which soybeans were dried by fluidized bed technique,[9,10] the drying time in the spouted bed requires much longer for achieving the inactivated urease enzyme. The inactivation times at moisture content of 22% dry basis and temperature of 140°C, for example, needs at least 30 min for the spouted bed dryer whilst it needed only 10 min for the fluidized bed dryer. The longer inactivation time is due to the effect of tempering of grains in the downcomer.

Kinetics of Urease Inactivation Fitting

The data of percentage of urease inactivation at different drying conditions was used for analysis. A nonlinear procedure was used to estimate the model parameters, c_1, K, c_2, in Eq. (7) and U_e, k, in Eq. (8). A set of empirical models were generated for c_1, K, c_2, U_e, and k but only one was chosen for each kinetics parameter based on a compromise between the goodness of fit as indicated by the coefficient of determination and MSE.

The estimated constant parameters (b_1–b_9), r^2 for each model parameters and MSE for each model are shown in Table 2. Note that the first order kinetics model was analyzed from the sets of data obtained under the conditions of initial moisture content between 14 and 22% dry basis and temperatures between 120 and 150°C. For low-to-moderate moisture content, because of inhibitory effect of higher moisture content on the urease inactivation, the modified Monod equation was fitted with the set of data at 28% dry basis.

The proposed correlations for c_1, K, c_2, k, and U_e were then substituted into Eqs. (7) and (9) to calculate the urease inactivation. It was found that both kinetic models describe the urease inactivation reasonably well compared to the experimental data as shown in Fig. 7. In Figs. 8–11, the sensitivity of temperature and initial moisture content to the urease inactivation is presented. The Modified Monod and the first order kinetic prediction results are covered through the range of moisture content from 26 to 30% and from 14 to 25% dry basis, respectively. Insufficient inactivation often occurs when using low temperature and moisture content even though inactivation rates are relatively faster at the early period as shown in Fig. 10, comparing to those shown in

Table 2. Estimated constants in equations (8), (9) and (10).

	Modified Monod equation			First order kinetic model	
Constants	c_1	K	c_2	U_e	k
b_1	2.39588	—	2.41301	—	—
b_2	0.01301	—	0.01302	—	—
b_3	—	11.62190	—	—	—
b_4	—	−11.47016	—	—	—
b_5	—	14126.82346	—	—	—
b_6	—	—	—	−2.58181	−0.40940
b_7	—	—	—	8.47817E−03	1.14487E−03
b_8	—	—	—	1.63242E−03	−2.47649E−02
b_9	—	—	—	−5.72912E−06	6.89432E−05
r^2	0.9972	0.9999	0.9969	0.8459	0.9760
MSE		0.00115		0.00157	

Figs. 8 and 9. They also indicate that the inhibitory effect of moisture content on the urease inactivation as illustrated in Fig. 9 becomes less important when the initial moisture content of soybean approaches 26% dry basis since the inactivation rate calculated from Eq. (7) is almost superimposed to that found by using Eq. (9) after drying time of 15 min.

Effects of Temperature on Soybean Protein

Destruction of anti-nutrition factors using higher temperature may cause the reduction of amount of protein. Therefore, it is necessary to check the amount of protein after heat treatment. The total crude proteins before and after heat treatment and protein solubility are shown in Table 3. The amount of crude protein in raw soybeans for all lots varied between 38 and 43. After 30 min, the amount of protein in the soybeans at different inlet temperatures is insignificantly changed as compared to the reference ones, indicating the properly processed soybeans. However, the protein solubility at inlet temperature of 120°C is still high, showing the insufficiently cooked soybeans. To make sure soybeans are properly cooked; protein solubility in the range of 70–85% and the complete urease inactivation (97%), inlet temperature should not be lower than 150°C.

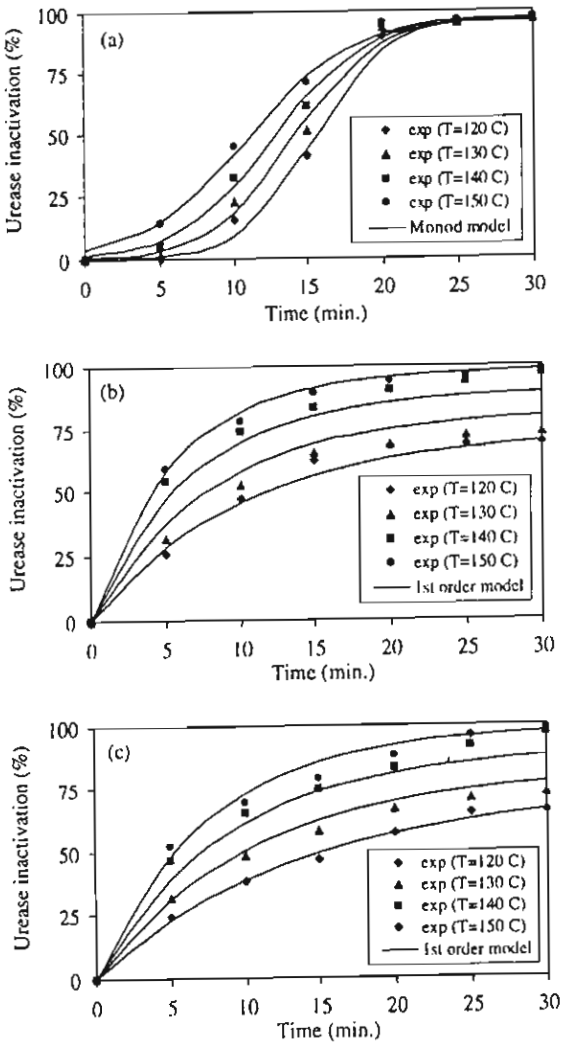


Figure 7. Predicted lines and data points of inactivation at different initial moisture contents (a) 28%, (b) 22%, and (c) 14% d.b.

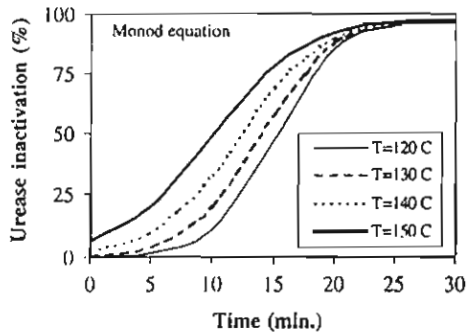


Figure 8. Influence of variation of temperature on the predicted inactivation at initial moisture content of 28% d.b.

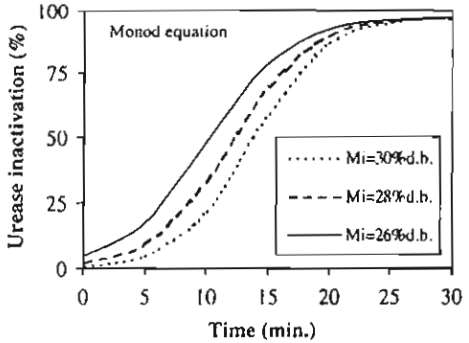


Figure 9. Influence of variation of initial moisture content on the predicted inactivation (inlet air temperature of 140°C).

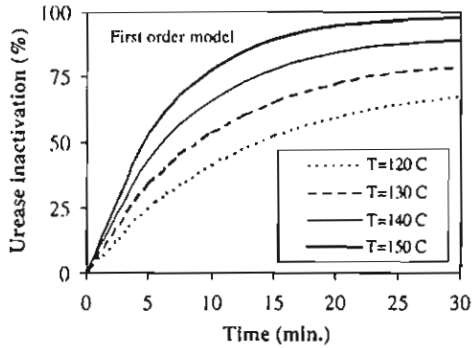


Figure 10. Influence of variation of temperature on the predicted inactivation at initial moisture content of 18% d.b.

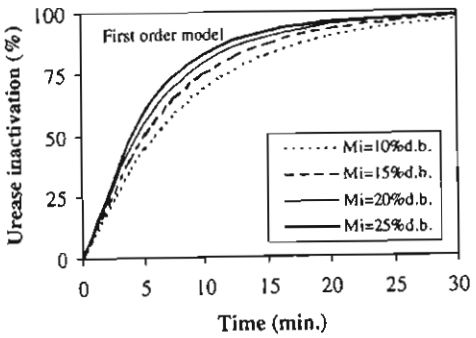


Figure 11. Influence of variation of initial moisture content on the predicted inactivation (inlet air temperature of 150°C).

Table 3. Crude protein content of soybeans at different operating conditions.

	IMC 28% d.b.		IMC 22% d.b.		IMC 14% d.b.	
Temp. (°C)	Protein after drying (%)	Protein solubility (%)	Protein after drying (%)	Protein solubility (%)	Protein after drying (%)	Protein solubility (%)
120	37.16	89.41	39.03	91.99	41.78	90.61
130	38.04	NA	43.45	NA	41.29	NA
140	38.04	81.22	40.70	74.64	42.17	80.65
150	38.14	81.96	39.81	73.80	42.27	73.95
	Initial protein 38.44–38.93		Initial protein 40.80–43.75		Initial protein 42.37–43.84	

Note: temp. = inlet air temperature and IMC = initial moisture content.
NA = Not available.

CONCLUSIONS

- Drying kinetics for soybeans in two-dimensional spouted bed can be described by Newton's law of cooling with adequate accuracy and its equation is very tractable.
- The development of fissuring on the kernels is mainly caused by the combination of moisture content and inlet temperature. The high air velocity in the spouted region results in the large amounts of broken and cracked kernels due to the powerful impact between the kernels and deflector.

- Two-dimensional spouted bed dryer can be fully complied with a requirement of both soybean drying and inactivation of urease enzyme, along with the protein content to be maintained, as long as the operating temperature is 150°C.
- The kinetics of inactivation of urease enzyme can be suitably described by the first order reaction for the initial moisture contents lower than 26% dry basis. At higher initial moisture content of 26% dry basis, the application of the first order kinetic model was switched to the Modified Monod equation for predicting the kinetics of urease inactivation.

ACKNOWLEDGMENTS

The authors would like to thank the Thailand Research Fund for supporting this work.

REFERENCES

1. Lin, K. Expanding soybean food utilization. Food Technology **2000**, *54*, 46–58.
2. Singh, R.; Singh, G.; Chanhan, G.S. Nutritional evaluation of soy-fortified biscuits. Journal Food Science Technology **2000**, *37*, 162–164.
3. Cheong, Y.L. *Fullfat Soybean Meal Production and Utilization*; Technical Bulletin of American Soybean Association: Singapore, 1997.
4. Stephenson, E.L.; Tollet, L. Processing of soybeans for broiler feeding. Feedstuffs **1960**, *31*, 8.
5. Wright, K.N. Soybean meal processing and quality control. Journal American Oil Chemists' Society **1981**, *58*, 294–300.
6. White, C.L.; Greene, D.E.; Waldroup, P.W.; Stephenson, E.L. The use of unextracted soybeans for chicks. Poultry Science **1967**, *46*, 1180–1185.
7. Faber, J.L.; Zimmerman, D.R. Evaluation of infrared-roasted and extruder-processed soybeans in baby pig diets. Journal of Animal Science **1973**, *36*, 902–907.
8. Raghavan, G.S.V.; Harper, J.M. Nutritive value of salt-bed roasted soybeans for broiler chicks. Poultry Science **1974**, *53* (2), 547–553.

9. Osella, C.A.; Gordo, N.A.; González, R.J.; Tosi, E.; Ré, E. Soybean heat-treated using a fluidized bed. Lebensm. Wiss u.—Technology **1997**, *30*, 676–680.
10. Soponronnarit, S.; Swasdisevi, T.; Wetchacama, S.; Wutiwiwatchai, W. Fluidized bed drying of soybeans. Journal Stored Products Research **2001**, *37*, 133–151.
11. ASA. *Fullfat Soybeans Handbook of American Soybean Association*; Singapore, 1990.
12. Barrozo, M.A.S.; Murata, V.V.; Costa, S.M. The drying of soybean seeds in countercurrent and concurrent moving bed dryer. Drying Technology **1998**, *16* (9&10), 2033–2048.
13. Madhiyanon, T.; Soponronnarit, S.; Tia, W. A two-region mathematical model for batch drying of grains in a two-dimensional spouted bed. Drying Technology **2001**, *19* (6), 1045–1064.
14. El-Naas, M.H.; Rognon, S.; Legros, R.; Mayer, R.C. Hydrodynamics and mass transfer in a spouted bed dryer. Drying Technology **2000**, *18* (1&2), 323–340.
15. Devahastin, S.; Mujumdar, A.S.; Raghavan, G.S.V. Diffusion-controlled batch drying of particles in a novel roatating jet annular spouted bed. Drying Technology **1998**, *16* (3–5), 525–544.
16. Passos, M.L.; Mujumdar, A.S.; Raghavan, V.G.S. Spouted beds for drying: principles and design considerations. Advances in Drying **1987**, *4*, 359–397.
17. Kalwar, M.I.; Kudra, T.; Raghavan., G.S.V.; Mujumdar, A.S. Drying of grains in a drafted two-dimensional spouted bed. Journal Food Proc. Eng. **1991**, *3*, 321–332.
18. AACC. *Approved Method of the American Association of Cereal Chemist*, 9th Ed.; AACC: St. Paul, MN, 1995.
19. Savage, W.D.; Wei, L.S.; Sutherland, J.W.; Schmidt, S.J. Biologically active components inactivation and protein insolubilization during heat processing of soybeans. Journal of Food Science **1995**, *60*, 164–168.
20. AOCS. *Official and Tentative Methods of the American Oil Chemists' Society*, 3rd Ed.; AOCS: Campaign, IL, 1984.
21. Page, G.E. Factors Influencing the Maximum Rate of Drying Shelled Corn in Layers. Unpublished M.S. thesis, Purdue University, West Lafayette, IN, 1949.
22. Sharaf-Eldeen, Y.I.; Blaisel, J.L.; Hamdy, M.Y. A model for ear corn drying. Transaction of the American Society of Agricultural Engineers **1980**, *27*, 195–200.

shirmp in superheated steam and hot air. Drying Technology **2002**, *20* (3), 669–684.
24. Lee, J.M. *Biochemical Engineering*; Englewood Cliffs: NJ, 1992.
25. López, A.; Piqué, M.T.; Romero, A.; Aletá, N. Modelling of walnut sorption isotherms. Ital. J. Food Sci. **1998**, *1* (10), 67–74.
26. Jia, C.-C.; Sun, D.-W.; Cao, C.-W. Mathematical simulation of stresses within a corn kernel during drying. Drying Technology **2000**, *18* (4), 887–906.
27. Overhults, D.G.; White, G.M.; Hamilton, H.E.; Ross, I.J. Drying soybean with heated air. Transaction of American Society of Agricultural Engineers **1973**, *16*, 112–113.
28. Grosh, G.M.; Milner, M. Water penetration and internal cracking in tempered wheat grains. Cereal Chemistry **1959**, *36*, 260.

ELSEVIER

Journal of Food Engineering 62 (2004) 1–7

JOURNAL OF FOOD ENGINEERING

www.elsevier.com/locate/jfoodeng

Kinetics of colour change during storage of dried garlic slices as affected by relative humidity and temperature

Somkiat Prachayawarakorn [a,*], Saijai Sawangduanpen [a], Supranee Saynampheung [a], Thitikorn Poolpatarachewin [a], Somchart Soponronnarit [b], Adisak Nathakarakule [b]

[a] *Department of Chemical Engineering, King Mongkut's University of Technology Thonburi, Suksawat 48 Road, Bangkok 10140, Thailand*
[b] *School of Energy and Materials, King Mongkut's University of Technology Thonburi, Suksawat 48 Road, Bangkok 10140, Thailand*

Received 27 October 2002; accepted 13 May 2003

Abstract

The influence of relative humidity and temperature on colour changes in garlic slices has been investigated. The lab colour parameters, lightness, redness and yellowness, were used to determine the colour changes in the environments of isothermal heating at 20, 37 and 50 °C and relative humidity at 30%, 70% and 90%. The experimental results have shown that temperature and relative humidity greatly affect the redness, yellowness and lightness. A first-order kinetic model is an appropriate representation for describing the changes in the experimental values of the lightness and redness. In contrast to the redness and lightness, the yellowness is described by a first-order kinetics in series, characterised the rise in the yellowness to a maximum value followed by a decrease. According to the experimental results indicated by total colour difference, the maximum browning rate occurs at 70% relative humidity.
© 2003 Elsevier Ltd. All rights reserved.

Keywords: Garlic; Browning reaction; Colour kinetics

1. Introduction

Garlic is a semi-perishable spicy herb, used as a primary ingredient for preparing the various kinds of native food in Asia. The moisture content of fresh harvested garlic is approximately 162% (dry basis) and the garlic is then dried by sun drying or convective drying to maintain its quality for prolonged storage. The drying process and phenomenological changes that occur during drying prominently affect the product quality attributes such as colour and texture (Ambrose & Sreenarayanan, 1998). In general, garlic that meets the required market specification appears light brown or creamy-white in colour.

The colour, one of the most important qualities of acceptance for products, reflects a sensation to the human eye and visual examination is the common method of assessing product colour. The change of product colour is caused by the reactive components in the food activated during the drying process. Colour development is the result of various reactions such as non-enzymatic browning reactions and pigment destruction (Cornwell & Wrolstad, 1981; Wong & Stanton, 1992). It results in undesirable colour, odour, flavour changes and lowering of nutritive value (Toribio & Betusawa, 1978). In non-enzymatic browning reactions, the browning rates are closely related to temperature and relative humidity (Labuza & Saltmarch, 1981; Rapusas & Driscoll, 1995; Samaniego-Esguerra, Boag, & Robertson, 1991; Soponronnarit, Srisubati, & Yoovidhya, 1998). Maximum stability of dried foods can be obtained by dehydrating and maintaining them at the monolayer moisture content.

Colour can be characterised by spectrophotometer at any wavelength. For example, 420 nm is one of the wavelengths most frequently used for juices. Colour determination can also be detected by a tristimulus colourimeter in terms of redness, yellowness and lightness. The latter is the simplest instrumental method and it has been previously proved to be valuable in describing discolouration and providing useful information for quality control of food products (Feng & Tang, 1998; Garza, Ibarz, Pagan, & Giner, 1999; Krokida, Tsami, & Urbricain, 1998; Maskan, 2001).

* Corresponding author. Tel.: +662-4270-9221; fax: +662-428-3534.
E-mail address: somkiat.pra@kmutt.ac.th (S. Prachayawarakorn).

0260-8774/$ - see front matter © 2003 Elsevier Ltd. All rights reserved.
doi:10.1016/S0260-8774(03)00163-8

In the present work, the kinetics of the browning reaction in garlic slices is determined quantitatively using the colourimetry and the generalised kinetic models for L-, a- and b-values are then proposed to describe its colour change with environmental conditions as well as with time. The kinetic parameters are correlated empirically with a modified Arrhenius-type equation. The kinetic models proposed in this present study, in association with heat and mass transfer equations, enables us to predict the changes in colour during garlic drying. It also can be used to identify an appropriate drying condition in order to obtain high quality dried garlic.

2. Material and methods

Dry garlic bulbs obtained from the local market were sliced to a uniform size of $15\times15\times3$ mm^3. The dry garlic slices were rewetted to the desired moisture content of 1.6 dry basis and kept in cold storage at 5 ± 0.5 °C for a week. To follow the colour development with relative humidity and temperature levels, the static method was employed. In this work, three levels of temperature, 20, 37 and 50 °C, and four levels of relative humidity, 30%, 50%, 70% and 90% for each temperature were used for determining the browning kinetics of the garlic slices. This temperature range is relevant to commercial practice.

A series of saturated salt solutions was prepared in order to obtain the required relative humidity. The salt solutions used were $MgCl_2\cdot6H_2O$, $Mg(NO_3)_2\cdot6H_2O$, NaCl and $BaCl_2$ and the corresponding water activity levels were prepared from the data reported by Gustafson (1972). Samples were left on a wire screen placed inside airtight containers, which were then sealed and kept in temperature-controlled incubators, temperature fluctuation being ±1 °C. To ensure the uniform moisture content, the garlic slices were spread in a single layer with a mass of 4.2 g. Samples were removed at different exposure time intervals to measure their colour.

The degree of browning is represented by the values of L, a and b, measured by a JP-700 Hunterlab Juki colourimeter. The colourimeter was calibrated each time with a standard reference having a value of L, a and b corresponding to 97.76, −0.06 and −0.3, respectively. The values of a and b range from −60 to +60. The positive values of a and b represent redness and yellowness respectively and the negative values of a and b show the respective greenness and blueness. The value of lightness can vary between 0 and 100, with the highest one showing the highest lightness of the sample. Five pieces of sample were used to measure the colours, each of which were measured at five different surface positions. The results reported throughout this work were based on the average value.

3. Results and discussion

3.1. Change of L-, a- and b-values

Garlic samples initially had a creamy-white colour. This colour was represented by a L-value between 66 and 68, an a-value between −3.77 and −3.16 and a- b-value between 14.3 and 16.2. Figs. 1–3 show respectively the L-, a- and b-values at different levels of relative humidity and temperature, indicating the dissimilar patterns of the individual lab colour parameter over the exposure time. For the lightness, the L-value rapidly and linearly drops during the early period whilst the a- and b-values increase as shown in Fig. 1(a)–(c). After a long exposure time, the changes in the lightness and redness become rather slower. The yellowness presented in Fig. 3(a)–(c) exhibits the opposite behaviour, that is, after rising to a maximum value, the b-value then reduces with time. This suggests that destruction of yellow pigments takes place. The disappearance rate in the latter period varies rapidly especially at high temperature and relative humidity.

As seen in Fig. 1(a)–(c), changing L-value seems to be independent of relative humidity at relative humidities lower than 50%. Similar results are found for the redness and yellowness. These results reveal that the relative humidity is not an important factor in accelerating colour change when the relative humidity is lower than 50%. However, under such low humidity, the temperature will have a greater effect; garlic had slightly more yellowness and redness as well as becoming darker with increase in temperature.

When the relative humidity is higher than 50%, the trends of change in all the Hunter parameters are still similar to those mentioned above, but the rate change for each one is faster and now dependent on the relative humidity, in addition to the temperature effect. However, when the relative humidity is higher than a certain level, the colour changes, instead of increasing, become smaller and comparable to that at lower humidity. This can be seen in the case of 90% relative humidity compared to that at 70%.

The changes in colour values, L, a and b, for garlic under different levels of relative humidity and temperature appear to have different behaviours and it is difficult to describe such changes by a single kinetic model. A first-order reaction was chosen to describe the changes of L- and a-values. This can be expressed by the following equation:

$$\frac{x_{eq}-x(t)}{x_{eq}-x_0}=\exp(-kt), \tag{1}$$

where x and x_0 are the a- or L-values at time t and at the beginning, k is the reaction constant (min^{-1}). X_{eq} is the equilibrium value at infinite time and can be determined by linear regression. For the b-value, first-order reaction

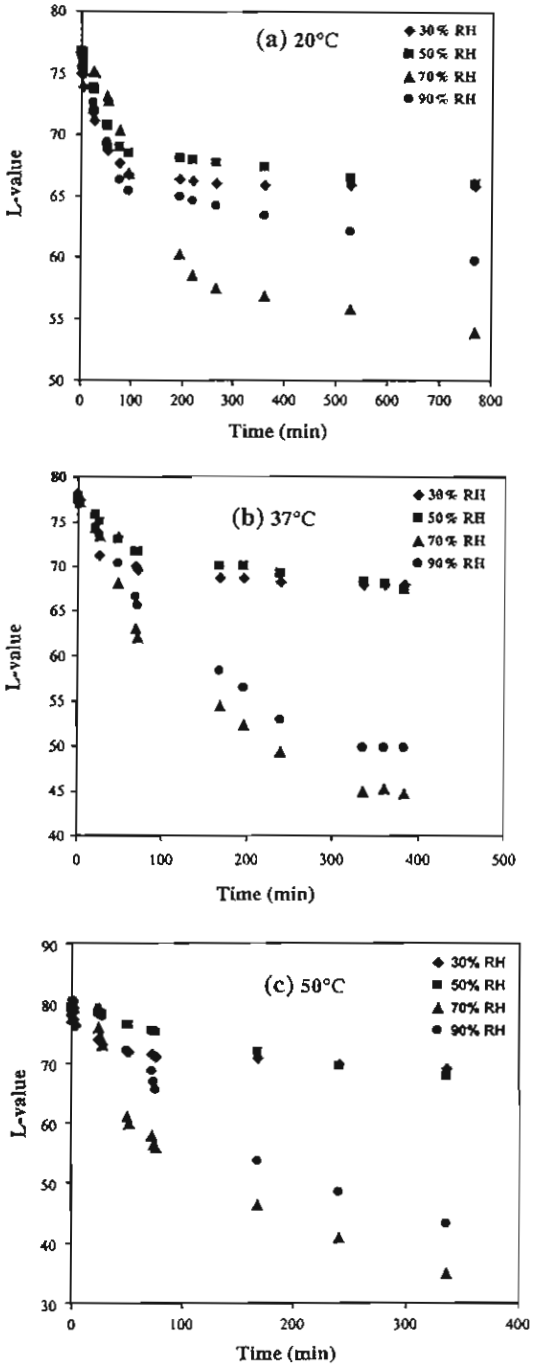


Fig. 1. Change of lightness at different levels of relative humidity and temperature.

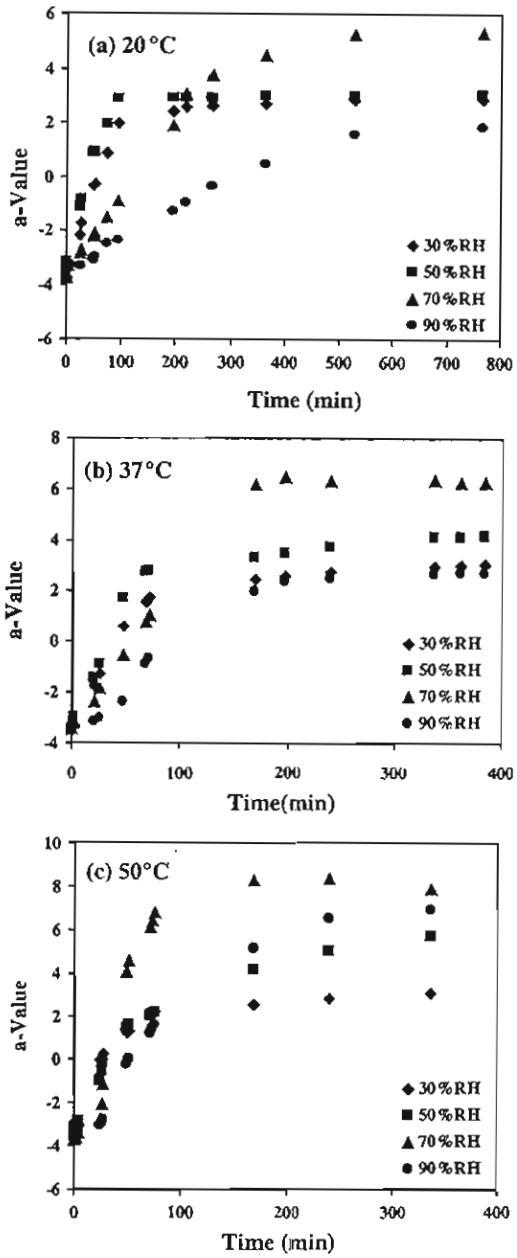


Fig. 2. Change of redness at different levels of relative humidity and temperature.

kinetics is not suitable to describe the change in the yellowness because there are two different behaviours, the rate of formation and rate of disappearance. Accordingly, a combined kinetic equation is proposed, in which the kinetics reactions are considered to consist of two series steps, the first and second steps, corresponding to colour formation and degradation, followed by a first-order reaction. The combined kinetics model can thus be expressed by

$$b(t) = ck_1\left[\frac{\exp(-k_{b1}t)}{k_{b2}-k_{b1}} + \frac{\exp(-k_{b2}t)}{k_{b1}-k_{b2}}\right] + b_0\exp(-k_{b2}t), \tag{2}$$

where k_{b1} and k_{b2} are the reaction constants (min^{-1}), b_0 is the b-value at $t = 0$ and c is the constant. If b_0 becomes zero, Eq. (2) will then be reduced to the equation as reported by Levenspiel (1999). As may be expected, the

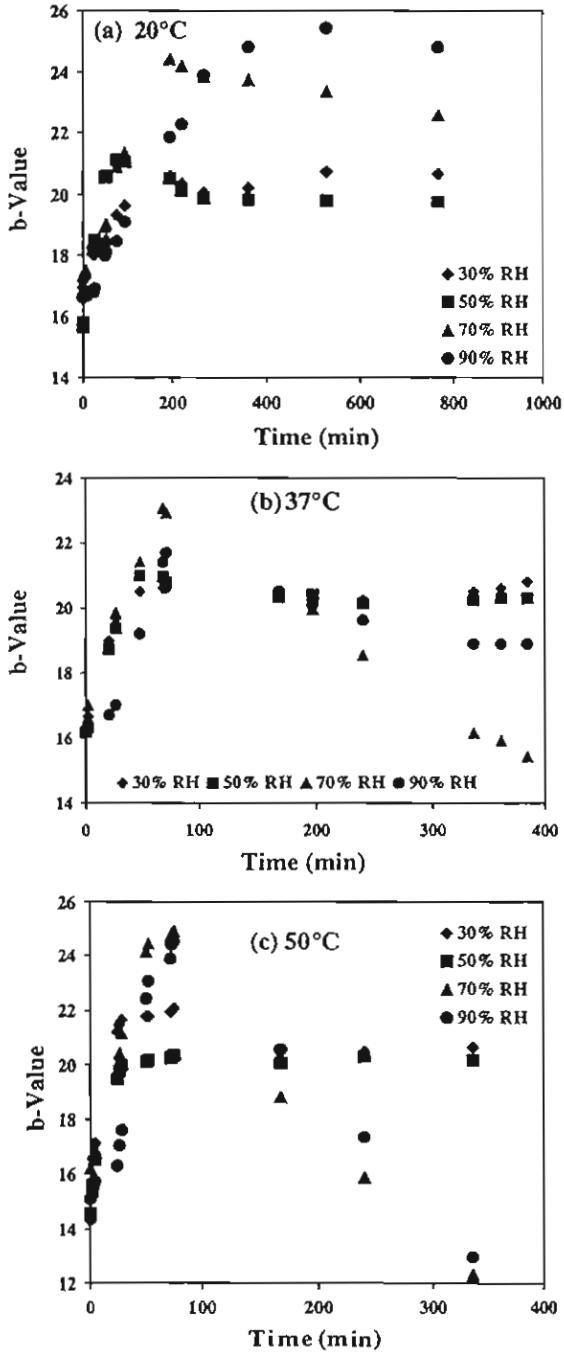


Fig. 3. Change of yellowness at different levels of relative humidity and temperature.

values of k_{b1} and k_{b2} govern the locations of maximum yellowness. The time at which the maximum b-value occurs is thus

$$t_{max} = \frac{1}{k_{b2} - k_{b1}} \ln \left[\frac{k_{b2}}{k_{b1}} \{1 - b_0(k_{b2} - k_{b1})\} \right]. \quad (3)$$

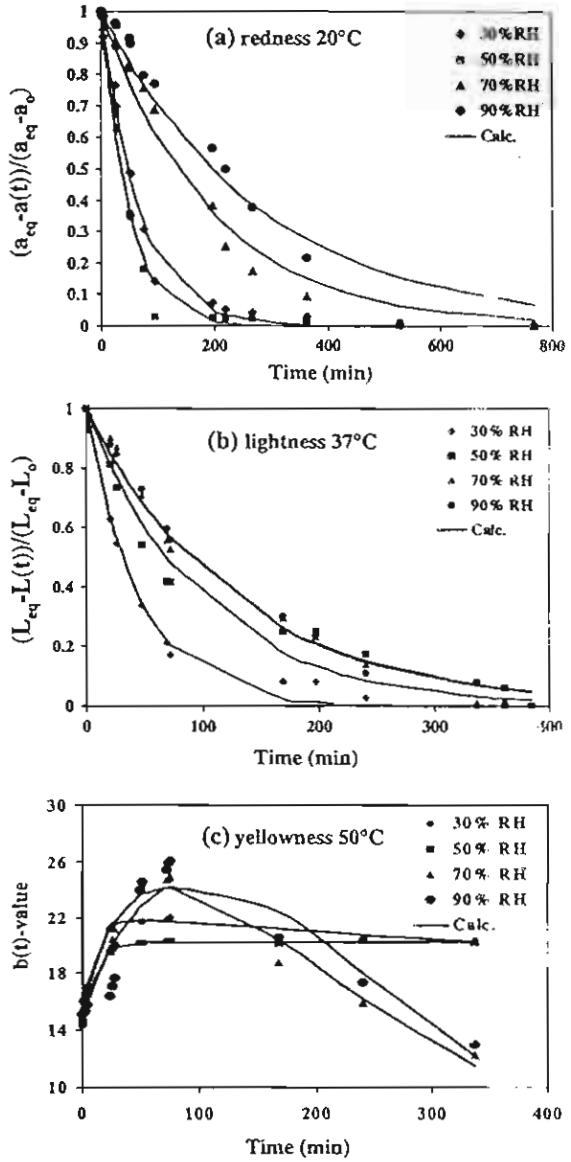


Fig. 4. Colour changes of garlic at different levels of relative humidity and temperature.

Substituting t_{max} in Eq. (3) into Eq. (2), we obtain the following equation for calculating the maximum b-value:

$$b_{max} = c\left(\frac{k_{b2}}{k_{b1}}(1 + b_0(k_{b1} - k_{b2})\right)^{k_{b2}/(k_{b1}-k_{b2})} \times \left[1 - b_0 k_{b2} + \frac{b_0}{c}\right]. \quad (4)$$

By regression of experimental data with Eq. (1) for a- and L-values and Eq. (2) for b-value, reaction constants were obtained from garlic placed in various temperature and relative humidity environments. The predicted and experimental colour parameters for some conditions are illustrated in Fig. 4(a)–(c) for redness, lightness and

yellowness, respectively, showing the proposed models capable of predicting the colour changes. The solid line of calculated lightness at 30% relative humidity shown in Fig. 4b is superimposed with the one at 50%.

In order to obtain the functional relationships between constant parameters in the equations of L-, a- and b-values and operating conditions, the empirical models were developed by non-linear regression analysis. The correlation equations, along with their coefficients of determinations (R^2) and residual sum of squares (RSS), for each colour parameter are given as follows:

Redness:

$$k_a = \left(4.68 - \frac{84.13}{RH} - \frac{523.97}{T}\right)\exp\left(-\frac{2279.64}{T} + \frac{558.98}{RH} + \frac{13.856^2}{RH} - \frac{1.298T}{RH}\right),$$

$$R^2 = 0.90,\ \mathrm{RSS} = 0.005, \tag{5}$$

$$a_{eq} = (307.7 + 0.2326T)\exp[0.000065RH - \exp(-0.0196RH + 0.2723)] - 2.585RH,$$

$$R^2 = 0.96,\ \mathrm{RSS} = 0.81. \tag{6}$$

Lightness:

$$k_L = (0.00000298)\exp\left(\frac{2177.04}{T} + \frac{279.872}{RH} - \frac{69329.7}{RH{\cdot}T}\right),$$

$$R^2 = 0.96,\ \mathrm{RSS} = 0.0022, \tag{7}$$

$$L_{eq} = \frac{\left(347.39 - 0.7940T - \frac{4840.55}{RH}\right)\exp(0.24182RH) + 8.83\times 10^8}{13131500 + \exp(0.2418RH)},$$

$$R^2 = 0.99, \mathrm{RSS} = 1.66. \tag{8}$$

Yellowness:

$$k_{b1} = \left(0.90386 + \frac{129.4451}{T} - \frac{90.74128}{RH} + \frac{1908.852}{RH^2} - \frac{3884.178}{RH{\cdot}T}\right)\exp\left(-\frac{3252.927}{T} + \frac{542.3706}{RH} + \frac{886.3580}{RH^2}\right),$$

$$R^2 = 0.98,\ \mathrm{RSS} = 0.004, \tag{9}$$

$$k_{b2} = (127.96954)\exp\left[\left(\frac{-4376.0011}{T}\right) + \exp\left(\frac{239.7552}{RH} - \frac{11608.7}{RH^2}\right)\right],$$

$$R^2 = 0.98,\ \mathrm{RSS} = 0.003, \tag{10}$$

$$c = (31.70352 - 0.204875T + 0.000333T^2) \times \exp[-0.03741RH + \exp(0.010838RH + 1.19392)] - 0.105791RH,$$

$$R^2 = 0.98,\ \mathrm{RSS} = 0.003, \tag{11}$$

where T is the absolute temperature and RH is the percentage of relative humidity.

When garlic is exposed to different relative humidity and temperature levels for a very long time, it becomes darker, in particular at high relative humidity and temperature which shows a low calculated L_{eq}-value, lower than that at the mild conditions shown in Fig. 5. In addition to low luminosity, the garlic loses its yellow pigment and becomes redder when held at higher relative humidity and temperature. The redness behaviour at equilibrium can be seen in Fig. 6 and it exhibits the highest value at a relative humidity between 70% and 80% for any temperature.

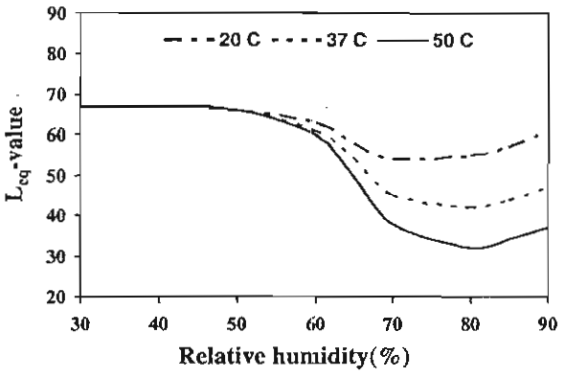


Fig. 5. Prediction of L_{eq}-value at different levels of relative humidity and temperature.

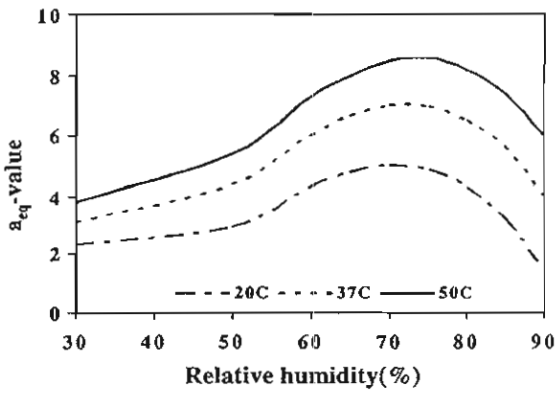


Fig. 6. Prediction of a_{eq}-value at different levels of relative humidity and temperature.

3.2. Maximum yellowness (b_{max})

The required time to obtain the maximum yellowness was found to range from 50 to 480 min depending on the relative humidity and temperature; the shorter time being obtained with higher temperatures and lower relative humidity levels. The b_{max}-value presented in Fig. 7 indicates that the increase in relative humidity and temperature induces more yellowness in garlic, except for the temperature of 37 °C at which shows lower b_{max} over the relative humidity range.

3.3. Change of ΔE

Total colour difference (ΔE) was calculated from the Hunter parameters, L, a and b, using the Hunter–Scotfield equation:

$$\Delta E = \sqrt{(L(t) - L_0)^2 + (a(t) - a_0)^2 + (b(t) - b_0)^2}, \quad (12)$$

where $L(t)$, $a(t)$ and $b(t)$ are respectively the lightness, redness and yellowness at time t in minutes. The total colour difference is shown in Fig. 8(a)–(c) showing that the value of ΔE is dependent on the temperature and relative humidity. The ΔE-value obtained at any temperature is noticeably higher for the high relative humidity condition than for the low one although the increase in the ΔE-value for the latter case in the early period seems to be higher, especially at a temperature of 20 °C. This behaviour can be explained by the state of the bound water and the solute mobility. At low humidity, the moisture content of garlic falls quickly before reactive species can reach each other. Therefore, the ΔE-values for the low humidity levels of 30% and 50% are almost equal and relatively low compared to the values at higher humidity levels. These results clearly indicate that the relative humidity at low levels plays an important role in retarding the browning reactions. When considering the temperature effect, it appears that the total colour difference is slightly depended on the temperature when the relative humidity is lower than 50%.

For the high humidity, on the other hand, the loss of moisture content is slow and the water inside the garlic acts as a solvent. As a result, as the temperature increases, the reactive species can dissolve in the water so that their potential mobility and reactivity become higher, resulting in higher ΔE values as represented in

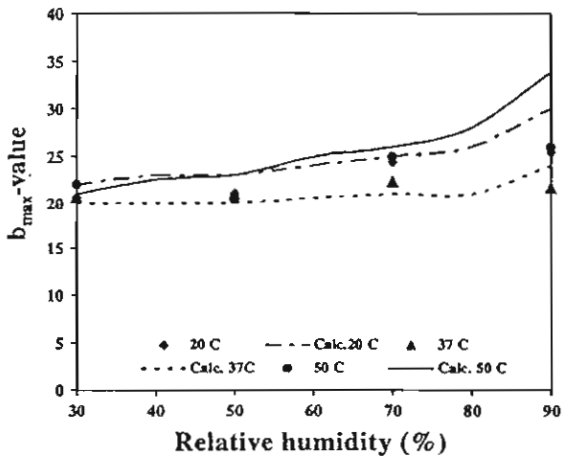


Fig. 7. Comparison of b_{max}-value obtained from the experiment and calculation by Eq. (4).

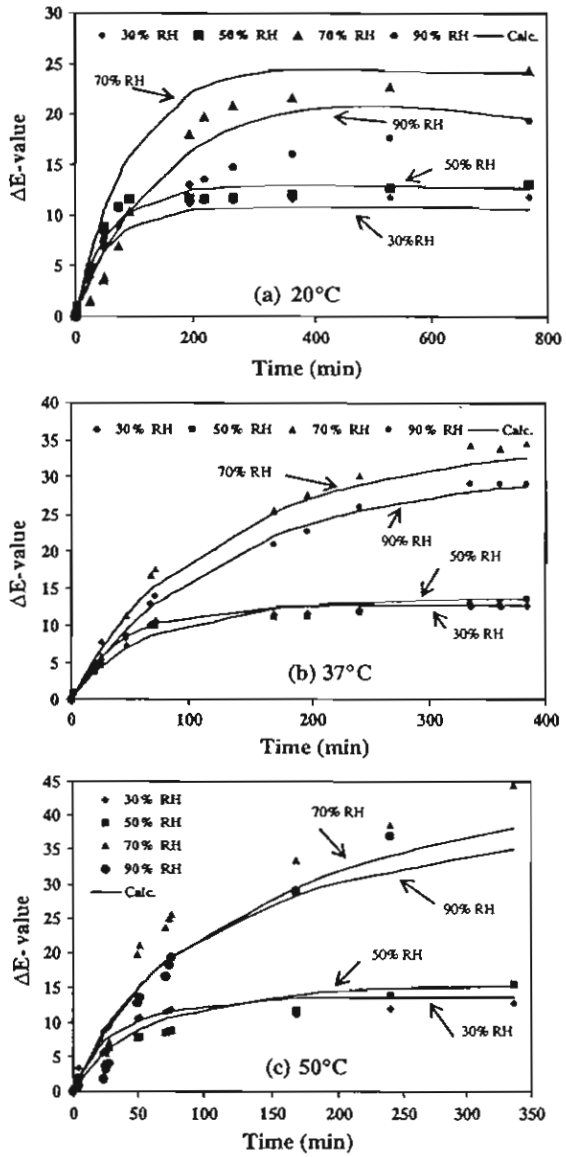


Fig. 8. Change of ΔE-value at different relative humidity and temperature levels.

Fig. 8(a)–(c) for the 70% relative humidity. As the relative humidity is higher than 70%, the opposite result to those mentioned above becomes evident. The lowering of ΔE-value is noticed with increase in relative humidity. This result can be explained by the fact that that there exists a large amount of water in the garlic and the dilution of reactive species inhibits the browning rate.

According to the experimental results at various relative humidity levels, the maximum browning rate for the garlic occurs at 70% relative humidity. This result is similar to the work reported by Rapusas and Driscoll (1995) who studied the browning rate in the dehydrated food product and observed the occurrence of maximum browning rate ranging from 65 to 75% relative humidity. Thus, to keep the low browning rate, use low relative humidity and temperature for storage or dehydration.

As shown in Fig. 8, the proposed empirical kinetics models for L, a and b, which are used to calculate the total colour difference by Eq. (12), can reasonably predict the changes in total colour difference under various operating conditions.

4. Conclusion

Three colour parameters, lightness (L), redness (a), and yellowness (b), were used to investigate the changes in colour of garlic. The lightness, redness and yellowness were found to be dependent on relative humidity and temperature. The reduction in the lightness and increase in the redness with time can suitably be described by a first-order kinetics model. For yellowness, it rises to a maximum value, after which it declines, and such characteristics of the yellowness-time curve can be represented by first-order reactions in series. The reaction rate constants for the L, a and b kinetic equations are empirically correlated with relative humidity and temperature in the ranges of 30–90% and 20–50 °C, respectively. As indicated by the total colour difference, there exists a maximum browning rate for garlic which was isothermally heated at a relative humidity of 70%.

Acknowledgements

The authors would like to thank King Mongkut's University of Technology Thonburi and The Thailand Research Fund for their financial support.

References

Ambrose, D. C. P., & Sreenarayanan, V. V. (1998). Studies on the dehydration of garlic. *Journal of Food Science Technology, 35*, 242.

Cornwell, C. J., & Wrolstad, R. E. (1981). Causes of browning in pear juice concentrate during storage. *Journal of Food Science, 46*, 515.

Feng, H., & Tang, J. (1998). Microwave finish drying of diced apples in a spouted bed. *Journal of Food Engineering, 63*, 679.

Garza, S., Ibarz, A., Pagan, J., & Giner, J. (1999). Non-enzymatic browning in peach puree during heating. *Food Research International, 32*, 335.

Gustafson, F.C. (1972). Equilibrium moisture content of shelled corn from 50 °F to 155 °F. Unpublished master of science thesis, University of Illinois, Urbana, USA.

Krokida, M. K., Tsami, E., & Urbricain, M. J. (1998). Kinetics on colour changes during drying of some fruits and vegetables. *Drying Technology, 16*(3–5), 667.

Labuza, T. P., & Saltmarch, M. (1981). The nonenzymatic browning reaction as affected by water in foods. In L. B. Rockland, & G. F. Stewart (Eds.), *Water activity: influences on food quality* (p. 605). New York: Academic Press.

Levenspiel, O. (1999). Chemical reaction engineering (third ed., p. 53). USA: John Wiley & Sons.

Maskan, M. (2001). Kinetics of colour change of kiwi fruits during hot air and microwave drying. *Journal of Food Engineering, 48*, 169.

Rapusas, R. S., & Driscoll, R. H. (1995). Kinetics of non-enzymatic browning in onion slices during isothermal heating. *Journal of Food Engineering, 24*, 417.

Samaniego-Esguerra, C. M., Boag, I. F., & Robertson, G. L. (1991). Kinetics of quality deterioration in dried onions and green beans as a function of temperature and water activity. *Lebensmittel Wissenshaft und Technologie, 24*, 53.

Soponronnarit, S., Srisubati, N., & Yoovidhya, T. (1998). Effect of temperature and relative humidity on yellowing rate of paddy. *Journal of Stored Product Research, 34*(4), 323.

Toribio, J. L., & Betusawa, M. (1978). Heat induced browning of clarified apple juice at high temperatures. *Journal of Food Science, 51*, 172.

Wong, M., & Stanton, D. W. (1992). Effect of removal of amino acids and phenolic compounds on non-enzymatic browning in stored kiwi fruit juice concentrates. *Lebensmittel Wissenshaft und Technologie, 26*, 138.

ELSEVIER

Journal of Food Engineering 64 (2004) 405–415

JOURNAL OF FOOD ENGINEERING

www.elsevier.com/locate/jfoodeng

Simulation and grain quality for in-store drying of paddy

Yutthana Tirawanichakul [a,*], Somkiat Prachayawarakorn [b,1], Warunee Varanyanond [c,2], Somchart Soponronnarit [a,3]

[a] *Drying Technology Research Laboratory, School of Energy and Materials, King Mongkut's University of Technology Thonburi, ThungKru, Prachautit Rd., Bangkok 10140, Thailand*

[b] *Department of Chemical Engineering, Faculty of Engineering, King Mongkut's University of Technology Thonburi (KMUTT), ThungKru, Prachautit Rd., Bangkok 10140, Thailand*

[c] *The Institute of Food Research and Product Development (IFRPD), Kasetsart University, Chatuchak, Thailand*

Received 8 February 2003; accepted 13 September 2003

Abstract

Quality of product obtained from dehydration process is important to consumer and food manufacturer. Experiment results from the in-store drying technique using ambient air temperature have shown that the head rice yield, stickiness and whiteness of samples dried from initial moisture contents of 18.5–20.6% to 13.3 ± 0.6% wet basis at temperature of 30 ± 4 °C and specific airflow rates of 0.65–1.5 m^3/min m^3 of paddy reduces but hardness increases. As compared with the qualities of control samples which were gently dried by ambient air aeration in thin layer dryer, they are all slightly different. A near-equilibrium drying model incorporating the yellowing kinetics of paddy is proposed which takes accounts of the experimental observations. The model is reasonable to predict the experimental data. The simulation results indicate that the degree of whiteness depends on temperature, relative humidity, loading capacity and airflow rate. The relative humidity lower than 70% and specific airflow rate higher than 0.75 m^3/min m^3 of paddy are recommended.

© 2003 Elsevier Ltd. All rights reserved.

Keywords: In-store drying; Microstructure; Near equilibrium model; Rice quality

1. Introduction

Freshly harvested paddy may contain the water around 18–26% wet basis. The management of highly moist paddy during the harvesting period is a serious problem in Asian countries because high humidity conditions can encourage the excessive mould growth and the high respiration rate from grain. Consequently, the dry matter of grain is lost and heat liberated from its respiration and biological activities may accelerate rice yellowing (Soponronnarit & Nathakaranakule, 1990). To obtain high quality of paddy and prevent all the above problems, moisture content of paddy must be reduced to moisture content of 12.0–14.0% wet basis. The in-store paddy drying, which is well known as a fixed-bed drying, is the most common method used for the purpose of paddy drying. To ensure a high head rice yield and a high germination rate of rice, the recommended drying temperature should not exceed 43 °C (Soponronnarit & Preechakul, 1990).

Physical quality index used for considering quality of rice is the head rice yield and the rice yellowing. Many researchers have studied on physical quality in terms of yellowness or whiteness (Bason, Gras, Banks, & Esteves, 1990; Gras & Bason, 1989; Gras, Banks, Bason, & Arriola, 1989; Phillips, Widjaja, Wallbridge, & Cooke, 1988; Quitco, 1982; Soponronnarit, Srisubati, & Yoovidhya, 1998; Yap, Juiliano, & Perez, 1988). The yellowing of rice was mainly caused by either non-enzymatic reactions or enzymatic reactions. The enzymatic reactions induced by the fungal metabolites might be expected to produce the distinctly yellowed individual rice kernel while the non-enzymatic browning reaction might cause the overall change in hue. For non-enzymatic reactions, the water activity and temperature play an important role in accelerating the yellowing of rice

* Corresponding author. Tel.: +1-662-4708695-6x112; fax: +1-662-4279062/8746364/4708623.

E-mail addresses: tyutthan@hotmail.com (Y. Tirawanichakul), isomarit@cc.kmutt.ac.th (S. Soponronnarit).

[1] Tel.: +1-662-4709220-35x206.

[2] Tel.: +1-662-9428629-35.

[3] Tel.: +1-662-4708695-6x111; fax: +1-662-4708623/4279062.

0260-8774/$ - see front matter © 2003 Elsevier Ltd. All rights reserved.
doi:10.1016/j.jfoodeng.2003.09.001

kernels while oxygen shows a minor effect. In addition to such factors, variety and ageing also have some effects.

The effect of various postharvest treatments on chemical and physicochemical properties of rice were investigated by using texture profile (Juliano, 1985; Ngamchuen, Lamaimaat, & Kanchana, 1985), microstructure (Inprasit & Noomhorm, 2001; Zhou, Robards, Helliwell, & Blanchard, 2002), sensory analysis (Ngamchuen et al., 1985; Jean, Meullenet, Bradley, Griffin, & Daniels, 1999) and thermal analysis (Ohtsubo, Toyoshima, & Okadome, 1998; Ong & Blanshard, 1995). The low-temperature fixed-bed drying takes long time to reduce the moisture content of paddy. This long period of drying looks like as the storage duration. Storage duration and temperature had profound effects on the sensory analysis, texture profiles and chemical property (Gras & Bason, 1989; Jean et al., 1999; Ngamchuen et al., 1985; Zhou et al., 2002). A few studies have been conducted on effect of fixed-bed drying at low temperature on quality.

The objective of this paper is to investigate the quality of paddy obtained by in-store drying technique. The mathematical model developed by Soponronnarit and Nathakaranakule (1990) is used for predicting moisture content and degrees of yellowness represented in the form of value of whiteness. In addition, the physical quality, physicochemical quality, microstructure and germination are also determined.

2. Materials and methods

2.1. In-store drying system

Fig. 1 illustrates the schematic diagram of in-store dryer and its components. A deep bed dryer is composed of a cylindrical bin with a diameter of 0.75 m and height of 2.75 m, a blower and an electrical heating unit (in case of control relative humidity of inlet drying air temperature, the air will be heated but it is not used in these experiments). However, the electrical heating unit was shut off during the experiment. In the experiments, the bed depth of paddy was fixed at 1.0 m. Ambient air flow rates of 0.93, 0.65, 1.20 and 1.50 $m^3/min\,m^3$ of paddy for experiment Nos. 1, 2, 3 and 4, respectively, were blown through the grain bed. The outlet air was then delivered to the atmosphere. The desired air flow rate was controlled by the combination of a frequency inverter and a butterfly valve.

2.2. Methods

2.2.1. Paddy drying condition

Suphanburi 1, the long grain *indica* variety with a high amylose content of 27–29% provided by Rice Research Station at Pathumthani province, Thailand, was used in the experiments. To obtain the uniform moisture content, fresh paddy was rewetted by spraying water and then mixed and kept in a cold storage at the tem-

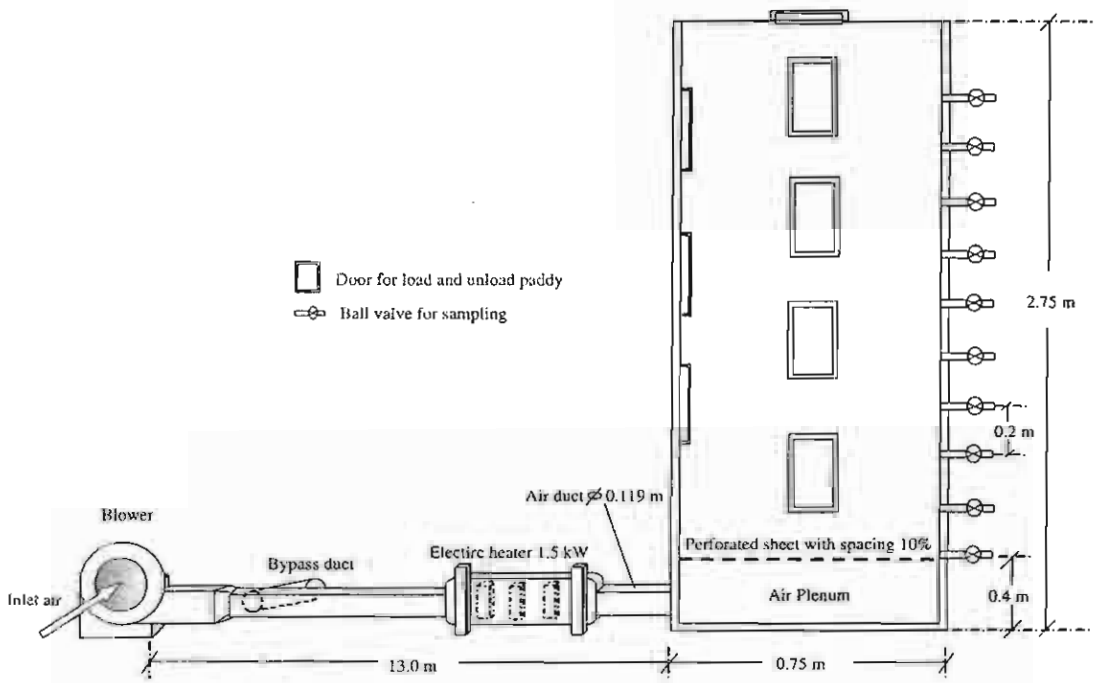


Fig. 1. Schematic diagram of in-store dryer [the electrical heaters were shut off in this work].

perature of 4–8 °C for a week. Before running the experiments, paddy was placed at the ambient environment until its temperature was closed to ambient air temperature. The initial moisture contents were 20.1% wet basis for experiment No. 1 and experiment No. 3, 18.5% wet basis for experiment No. 2 and 19.5% wet basis for experiment No. 4. The moisture content of paddy was determined by using AOAC standard method (AOAC, 1995). During the experiments, inlet air, moisture content, grain temperature and outlet air were recorded. Paddy sample was taken out from the bin for determining head rice yield and whiteness of rice. Moisture content of the sample was determined in every 5 day, except for the first 3 day of the experiment that it was checked in every 24 h. To avoid disturbance of drying process, the sampling for determining head rice yield was done in every 5 days. The grain temperature, dry bulb and wet bulb temperatures were measured by K-type thermocouple, which were continuously monitored by a Yogokawa data logger with a precision of ±0.1 °C. Air relative humidity was determined from dry and wet bulb temperatures. Air velocity was measured by a hot wire anemometer with a precision of ±0.1 m/s.

2.2.2. Quality of paddy

Quality of paddy from the fixed-bed experiments were characterized by head rice yield, whiteness, pasting properties and texture properties, germination and compared with the control one, for which paddy lied in a single layer was dried by ambient air ventilation. The details on each method were reported in the following items.

2.2.2.1. Head rice yield. The method of head rice yield determination was followed as by the guideline of USDA method (USDA, 1988). Percentage of head rice yield was reported as the average value of two replications. The relative head rice yield is referred to the ratio of head rice yield obtained from the dried sample to that from the control sample.

2.2.2.2. Whiteness of rice. The rice whiteness was measured by the light reflectance at the surface of rice kernel using a Satake milling meter. Before measuring, the meter was calibrated with standard pure white magnesium oxide powder. The initial yellowness value was measured in Hunter *b* unit by using Data Color meter and used as an input parameter for calculating the rice whiteness [see Eq. (16)].

2.2.2.3. Microstructure study. The structure of rice kernels were characterized with a Phillips 535-M scanning electron microscope at 10–20 kV. Before scanning, the milled rice samples were cut in cross section. Then, the samples were glued on the metal stubs for the stable supporting and were coated with gold (~30 nm thick) to become the electrical conductor for electron attachment during scanning.

2.2.2.4. Texture measurement. Hardness and stickiness of rice were determined by a bench-top Texture analyzer model TA-XT2*i* (Stable Micro Systems Ltd.). A 30 g portion of each dry-milled head rice sample was put in an aluminum cylindrical cup (diameter of 7 cm and height of 7 cm) and rice sample was rinsed twice with distilled water and the distilled water was added in an amount equal to a 1:1.7 ratio of rice to water by weight. After cooking cycle, the sample was then taken out and cooled down to room temperature for 1 h. The cooked rice sample was taken from the middle of cup and this portion (50.0 ± 0.1 g) was placed 1 cm equidistant from each other on the base of the Texture analyzer. The initial height of the compression probe (Ottawa cell) was set at 120 mm. During the compression, the test speed was 0.5 mm/s. The maximum force required to compress the cooked rice to 90% of initial portion height 10 mm measured as hardness. The initial height of the compression probe (Ottawa cell) was set at 120 mm. The pretest speed of probe was 1.5 mm/s. During the compression, the test speed was set up at 0.5 mm/s and the post test speed in retraction period was 10 mm/s. In the other words, the hardness was the height of the force peak on the first compression. For measuring stickiness value, the cylindrical probe P50 was used in this work. The texture profile analysis used for determining hardness and stickiness of cooked rice was recorded in kilogram.

2.2.2.5. Pasting property. The pasting properties of hydrothermally treated rice flour samples were determined using a Rapid Visco Analyzer [RVA] (Newport Scientific Ltd., Warriewood, NSW, Australia Model 3D) with approved method 61-02 (AACC, 2000). Viscosity of rice flour was reported as the average value of two replications. A heating and cooling cycle was used at a constant shear rate where the sample was equilibrated at 35 °C for 2 min and heated up to 95 °C at the rate of 11.8 °C/min, held at 95 °C for 2.5 min and cooled down to 35 °C at the same rate. The RVA parameters measured as peak viscosity (the maximum hot paste viscosity), holding strength (the trough at the minimum hot paste viscosity), final viscosity (the viscosity at the end of the test after cooling to 50 °C), setback (the final viscosity minus peak viscosity), peak time (min) and pasting temperature (°C). Those of RVA parameters were expressed in Rapid Visco Unit (1 RVU $\approx 10^{-2}$ cP).

2.2.2.6. Germination of rice. The mature paddy samples were chosen and kept at room environment for 4 weeks before germination test. The germination test of dried paddy and control paddy was done following the method of the Rice Research Station, Pathumthani

province, Thailand. Two hundred mature kernels were placed in a Petri disc added with the distilled water of 200 ml and then were left for a week. A percentage of paddy germination, defined as the ratio of number of germinated seeds to total seeds and multiplied by 100, was represented. Percentage of paddy germination was reported as the average value of triplicate.

2.3. Mathematical model

Mathematical simulation of grain drying has been studied and the models for deep bed grain drying could be divided into the 3 models as follows: non-equilibrium model (Brooker, Bakker-Arkema, & Hall, 1992), near-equilibrium model (Soponronnarit, 1988; Soponronnarit & Chinsakolthanakorn, 1990; Soponronnarit & Nathakaranakule, 1990; Thompson, Peart, & Foster, 1968) and logarithmic model (Barre, Baughman, & Hamdy, 1971; Hukill, 1947). The mathematical deep bed paddy drying model used in this work is based on a near-equilibrium model, which has been developed by Soponronnarit (1988). In this model, it supposes that the temperatures of air and grain are in thermal equilibrium at a certain grain layer and a small time interval. The main equations of model are as follows.

2.3.1. Energy balance equation for a thin layer

In the model, the grain bed is composed of series of thin layer. For a given thin layer, the energy equation is derived based on the first law of Thermodynamics by assuming that heat loss is very small and can be negligible. Thus, the sum of changes of the internal energy in the control volume of a thin bed and enthalpy of flowing stream is equal to zero. The following equation can thus be written as (Soponronnarit, 1988)

$$c_a T_o + (2502 + c_v T_o) W_o + R c_{pw} \theta_o = c_a T_f + (2502 + c_v T_f) W_f + R c_{pw} T_f \quad (1)$$

where c is the specific heat capacity (kJ/kg °C), T is the air temperature (°C), θ_o is the grain temperature (°C), W is the absolute humidity (kg H_2O/kg dry air), and R is the ratio of dry grain mass to dry air mass (kg dry matter/kg dry air) with subscripts: 'a' is the dry air, 'f' is the after drying, 'o' is the before drying, 'pw' is the wet grain, and 'v' is the water vapor.

2.3.2. Mass balance equation for a thin layer

The assumption is that water vapor evaporated from the thin layer is equal to the changes of water vapor in flowing stream. The equation of mass balance can thus be written as (Soponronnarit, 1988)

$$W_f - W_o = (M_o - M_f) R \quad (2)$$

where M is the grain moisture content (decimal dry basis).

The moisture equilibrium for paddy is given by Henderson's equation (Henderson, 1952) as follows:

$$M_{eq} = \left(\frac{1}{100}\right)\left[\frac{\ln(1 - RH)}{\{C(1.8T + 491.7)\}}\right]^{1/N} \quad (3)$$

where M_{eq} is the equilibrium moisture content (decimal dry basis), T and RH are the air temperature (°C) and relative humidity (in decimal), respectively, and C and N are the arbitrary constants depending upon agricultural material (dimensionless).

For paddy, the values of C and N are -7.87×10^{-6} and 2.088, respectively.

2.3.3. Thin layer drying equation

An empirical thin layer drying equation developed by Agrawal and Singh (1977) is used. It can be written as the following equation:

$$MR = \left(\frac{M - M_{eq}}{M_{in} - M_{eq}}\right) = \exp(-xt^y) \quad (4)$$

where

$$x = 0.02958 - 0.44565 RH_o + 0.01215 T_o \quad (5)$$

$$y = 0.13365 + 1.93653 RH_o - 1.77431 RH_o^2 + 0.009468 T_o \quad (6)$$

where RH_o is the relative humidity of air before drying (in decimal), M_{in} is the initial grain moisture content (decimal dry basis), and t is the drying time (h).

2.3.4. Energy balance at fan

Temperature rise of air while flowing across a fan is determined by applying the first law of thermodynamics for steady state flow process. Eq. (7) is used for calculating temperature rise of air across fan given by (Soponronnarit, 1988)

$$\dot{m} c_a \Delta T_s = \frac{\dot{m} P}{\rho_a E_f} \quad (7)$$

where $\dot{m}$ is the air mass flow rate (kg/s), ΔT_s is the temperature rise of air while flowing across a fan (°C), ρ_a is the air density (kg/m^3), P is the pressure (kPa), and E_f is the fan efficiency, 0.60 (in decimal).

Shaft power for driving fan can be calculated by the following equation (Soponronnarit, 1988):

$$BP = (q)(\Delta P_t)/E_m \quad (8)$$

where BP is the shaft power (kW), q is the volumetric air flow rate (m^3/s), ΔP_t is the total pressure loss of system (kPa), and E_m is the mechanical efficiency (in decimal).

2.3.5. Dry matter loss

The dry matter loss (DML) equation for paddy used in the present work was obtained from Seib, Pfost, Sukaboi, Rao, and Burroughs (1980), showing that the loss of dry matter depends on grain temperature and

moisture content. The dry matter loss equation can be written in the following empirical form:

$$\mathrm{DML} = 1 - \exp[\mathrm{TERM}] \tag{9}$$

in which

$$\mathrm{TERM} = 0.001889\left(\frac{t}{1000}\right)^{0.7101} \times \exp[0.0274(1.8\theta - 28)]\exp[31.63(M_w - 0.14)] \tag{10}$$

where DML is the dry matter loss (in decimal), t is the drying time (h), θ is the long grain temperature (°C), and M_w is the long grain moisture content (decimal dry basis).

Carbon-dioxide and water vapor are the by-products from the respiration reaction. A 1% of dry matter loss per kilogram of dry matter produces about 0.15778 MJ of heat. Therefore, the heat and moisture liberated from respiration was calculated by the following equations (Seib et al., 1980):

$$\Delta T_h = 15778\mathrm{DML}/c_{pw} \tag{11}$$

$$\Delta M_h = 0.6\mathrm{DML} \tag{12}$$

where ΔT_h is the temperature rise of grain (°C), and ΔM_h is the moisture rise of grain (decimal dry basis).

The heat from this respiration process was important. In the simulation program, there is an optional condition for simulation with and without heat of grain respiration.

2.3.6. Shrinkage of paddy

The shrinkage of bulk paddy's equation for long grain rice with a validation of moisture content from 12.0% dry basis to 39% dry basis developed by Preechakul (1986) is given by

$$v = 0.001997 + 0.0012M \tag{13}$$

where v is the the volume per kilogram of dry matter (m^3/kg), and M is the moisture content of paddy (decimal dry basis).

2.3.7. Yellowness of rice kernel

The yellowing rate of paddy was explained by temperature and water activity and the following empirical equations are used to predict the change in the yellow color developed by Soponronnarit et al. (1998) as

$$\frac{db}{dt_d} = k \tag{14}$$

and

$$\ln k = 71.87 - 25.32(\mathrm{RH}) - \frac{25919.13}{T_k} + \frac{10712.78(\mathrm{RH})}{T_k} \tag{15}$$

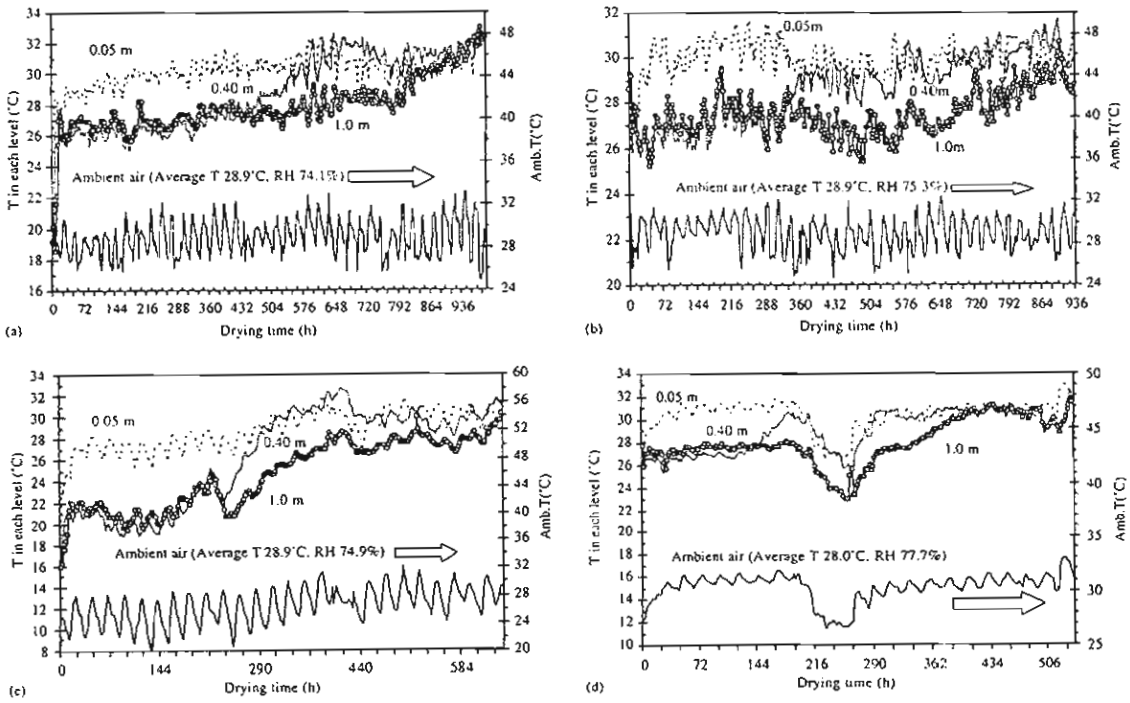


Fig. 2. Evolution of temperature profile during drying at different air flow rates (Amb. means ambient air): (a) experiment No. 1 (0.93 m^3/min m^3 of paddy); (b) experiment No. 2 (0.65 m^3/min m^3 of paddy); (c) experiment No. 3 (1.20 m^3/min m^3 of paddy); (d) experiment No. 4 (1.50 m^3/min m^3 of paddy).

where b is the yellowness of rice (Hunter b unit), t_d is the time (day), k is the constant value for the yellowing rate (Hunter b unit/day), RH is the relative humidity (in decimal), and T_k is the temperature (K).

From the experimental data, the empirical equation of rice whiteness (W_h) was formulated by a linear regression relation to the yellowness of rice as given by (Soponronnarit et al., 1998)

$$W_h = 85.1 - 3.36b \tag{16}$$

where W_h is the whiteness of rice.

Finally, the average moisture content and the average whiteness can be determined by Eqs. (17) and (18), respectively.

$$\overline{M}_{av} = \frac{\int_0^L M(x)\,dx}{\int_0^L dx} \tag{17}$$

$$\overline{W}_{hav} = \frac{\int_0^L W_h(x)\,dx}{\int_0^L dx} \tag{18}$$

where $\overline{M}_{av}$ is the average moisture content of paddy (% wet basis), $\overline{W}_{hav}$ is the average whiteness of rice kernel, $M(x)$ is the moisture content of paddy (% wet basis), $W_h(x)$ is the whiteness of rice in each bed depth, and dx is the bed depth (m).

The yellowness of paddy in each thin layer is calculated during drying time by using the air temperature and air relative humidity, which were in the thermal equilibrium with thin layer of grain kernel. The average moisture content and the average whiteness can be calculated by Eqs. (17) and (18), respectively.

2.4. Grain drying system program

The mathematical model of Grain Drying System Program (GDS) incorporating the Eqs. (14)–(16) was written by QBASIC language. The input parameters were composed of initial grain moisture content, grain temperature, inlet ambient air temperature, airflow rate and relative humidity.

The major assumption was that there exists thermal equilibrium between grain and drying air and the outlet drying air condition from the first thin layer is used as the input drying air condition for the next layer and the same calculation procedure is made for all thin layers with advancing time step.

3. Results and discussion

3.1. Moisture profile and energy consumption

Fig. 2(a)–(d) shows the evolution of temperatures during drying period for all experiments. The inlet air temperature and relative humidity change with time in range of 30 ± 4 °C and $76 \pm 8\%$, respectively. As seen from these figures, the temperature during early drying period is relatively higher at the bottom level than at the upper level. When a particular period of drying time elapses, depending on the specific air flow rate and initial moisture content of paddy, the temperatures at the lower and upper parts of bed approach together. The phenomena of temperature change is correlated with the change of moisture profiles presented in Fig. 3(a) and (b), showing that drying zone starts from the bottom and then moves towards the top layer of paddy. At the end of drying, the moisture content of paddy at various levels is close to 13.3% wet basis. According to these results, they indicate that the transfer of heat and mass is in the equilibrium stage at the drying end.

In Fig. 3(a) and (b), they also show that the proposed model can predict the moisture content at various bed levels and is in a good agreement with the experimental results. In this calculation, the respiration effect and experimental weather data is used to predict the moisture change.

Fig. 4(a)–(d) intends to show the average moisture content prediction, which are included and excluded

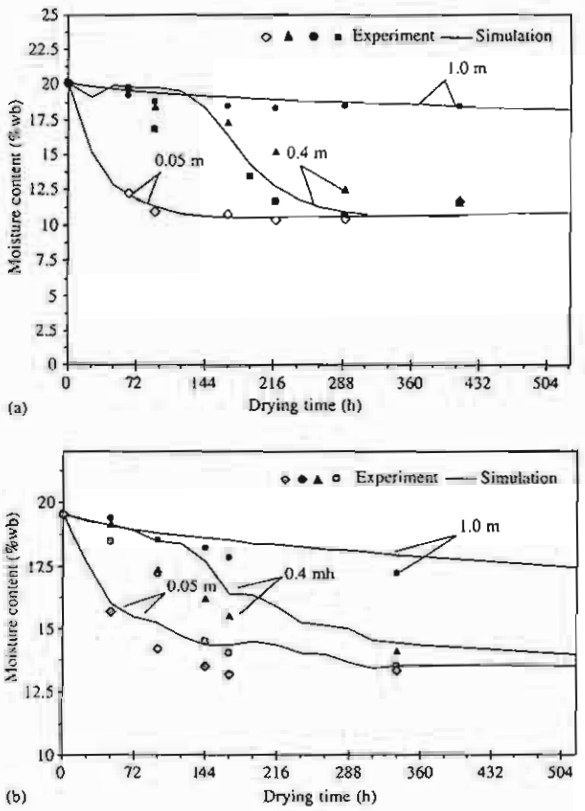


Fig. 3. Moisture profile in fix-bed drying at various specific air flow rates (including respiration): (a) experiment No. 3 (M_i 20.1% w.b., M_f 14% w.b., 1.20 m³/min m³ of paddy); (b) experiment No. 4 (M_i 19.5% w.b., M_f 13.7% w.b., 1.50 m³/min m³ of paddy).

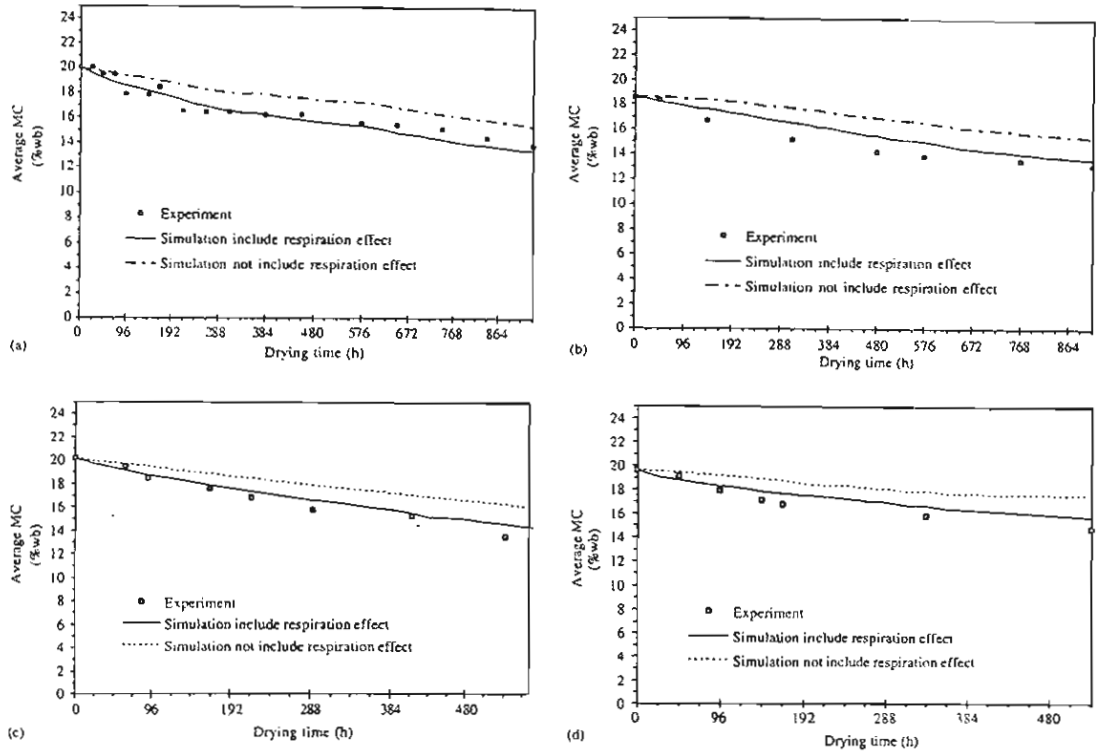


Fig. 4. Comparison of moisture prediction using the model including and excluding the respiration effect: (a) experiment No. 1 (M_i 20.1% w.b., M_f 14.4% w.b., 0.93 $m^3/min\,m^3$ of paddy); (b) experiment No. 2 (M_i 18.5% w.b., M_f 13.3% w.b., 0.65 $m^3/min\,m^3$ of paddy); (c) experiment No. 3 (M_i 20.1% w.b., M_f 14.0% w.b., 1.20 $m^3/min\,m^3$ of paddy); (d) experiment No. 4 (M_i 19.5% w.b., M_f 13.7% w.b., 1.50 $m^3/min\,m^3$ of paddy).

Table 1
Comparison of energy consumption between experiments and simulations of various drying strategies (grain bed depth 1.0 m, M_i 18.5–20.6% wet basis and M_f 13.3 ± 0.7% wet basis)

Descriptions	Simulated results of energy consumption, MJ/kg of water evaporated	Experimental results of energy consumption, MJ/kg of water evaporated	Simulated results of energy from respiration effect, [% DML] MJ/kg of water evaporated
Exp. 1: 0.93 $m^3/min\,m^3$ of paddy	0.07	0.09	0.80 [0.80]
Exp. 2: 0.65 $m^3/min\,m^3$ of paddy	0.11	0.11	2.00 [0.90]
Exp. 3: 1.20 $m^3/min\,m^3$ of paddy	0.09	0.08	1.07 [0.66]
Exp. 4: 1.50 $m^3/min\,m^3$ of paddy	0.13	0.09	1.01 [0.73]

respiration effect for the calculation of experiment Nos. 1, 2, 3 and 4, respectively. The simulation including the respiration effect shows the moisture content predictions more accuracy than the excluding one. This is because heat liberated from grain respiration increases the air temperature while air flows through the bed, thus allowing the more potential capability to remove the moisture inside the paddy.

The specific energy consumption reported in this work covers only the mechanical energy used for driving the fan. The energy consumption from the experiments shown in Table 1 is in a range of 0.08–0.11 MJ/kg of water evaporated for the specific air flow rate at 0.65–1.50 $m^3/min\,m^3$ of paddy. The prediction of specific energy consumption from the model has a similar trend to the experimental values.

From the prediction of DML value, energy liberation of grain respiration corresponding to dry matter loss of 0.66–0.9% is about 0.8–2.0 MJ/kg of water evaporated (as given in Table 1). These amounts of energy are the main energy source used for evaporating water.

3.2. Paddy qualities

3.2.1. Head rice yield and whiteness

The average head rice yield of paddy samples at the beginning was about 40% for the first two experiments and 51% for the latter two experiments. The value of

Table 2
Physical quality and physicochemical quality of Suphanburi 1 rice variety dried by in-store dryer

Drying strategy	Hardness (kg)	Stickiness (kg)	Peak viscosity (RVU)	Final viscosity (RVU)	Relative head rice yield	Average whiteness	Germination (%)
Control rice EXP-1	16.66 ± 4.25	–[a]	293.33	380.50	1	50.3	–[a]
After drying EXP-1	23.87 ± 5.28	–[a]	304.58	389.67	0.93	48.8	–[a]
Control rice EXP-2	16.14 ± 1.89	−0.11 ± 0.04	246.58	286.01	1	49.8	97.2
After drying EXP-2	22.84 ± 3.43	−0.07 ± 0.06	266.81	311.47	0.94	49.0	96.3
Control rice EXP-3	20.18 ± 0.69	−0.17 ± 0.04	239.00	261.25	1	51.1	97.7
After drying EXP-3	19.28 ± 0.04	−0.14 ± 0.03	255.17	272.17	0.95	49.3	96.8
Control rice EXP-4	16.86 ± 0.48	−0.29 ± 0.06	247.39	267.61	1	51.2	97.7
After drying EXP-4	17.61 ± 0.03	−0.29 ± 0.01	313.72	264.77	0.98	50.1	97.2

[a] Not available.

relative head rice yield after drying for all experiments was in between 0.93 and 0.98 as shown in Table 2. This indicates that the low drying temperature with low specific air flow rate of 0.65–1.5 $m^3/min\,m^3$ of paddy does not affect the head rice yield ($p < 0.05$).

Fig. 5(a) shows the change in the whiteness of rice kernel during drying at bed depths of 0.05–0.8 m for experiment No. 1. It seems that the value of whiteness at the bottom part, where the grain contacts with the low relative humidity, is slightly higher than at the upper part even at the upper part of paddy bed the rice whiteness is slightly lower than the lower part, the whiteness value still be acceptable in the market (>45). The similar behavior is also found in the experiment Nos. 2–4. However, the difference of whiteness at various bed levels is insignificant ($p < 0.05$), so that the average value of rice whiteness is presented. Fig. 5(b) shows the change in whiteness of rice kernel with drying time, indicating that the grain drying model incorporating the yellowing rate of rice is reasonable to predict the change in the whiteness during drying. The average value of rice whiteness for each experiment is shown in Table 2 indicates that the whiteness obtained the experiments slightly changes, comparing to that from the control sample.

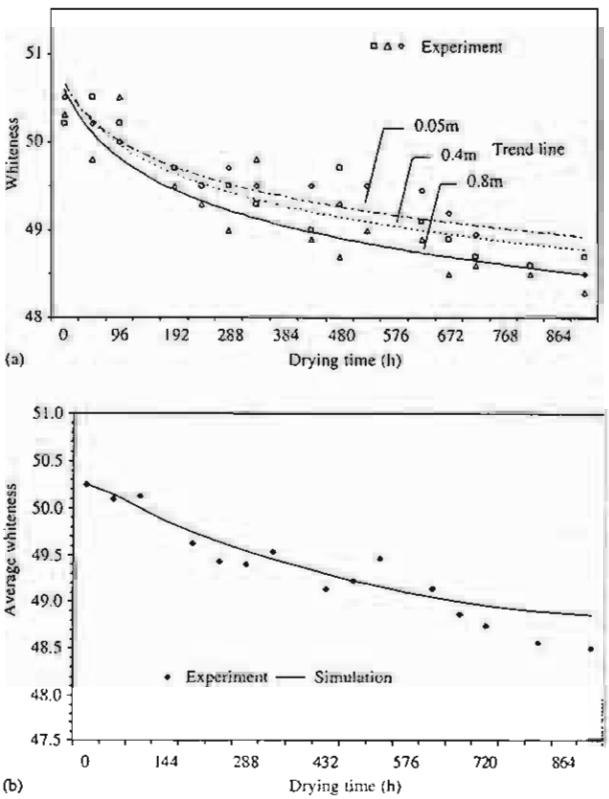


Fig. 5. The change of rice whiteness during drying: (a) whiteness value in each bed depth for experiment No. 1 (0.93 $m^3/min\,m^3$ of paddy); (b) whiteness value in each level of paddy bed depth for experiment No. 3 (1.20 $m^3/min\,m^3$ of paddy).

3.2.2. Microstructure of rice

Fig. 6(a) and (b) shows examples of the microstructure of Suphanburi 1 rice kernel in cross section area before and after in-store drying of the rice samples, respectively. As shown in Fig. 6(a), the small granular shapes of rice samples with diameters of 4–8 μm are starch granules. The morphologies of starch granules do not change with the low temperature drying technique although drying time takes very long.

3.2.3. Texture and pasting property

Table 2 presents the physical quality and physicochemical quality of dried rice compared to that of the

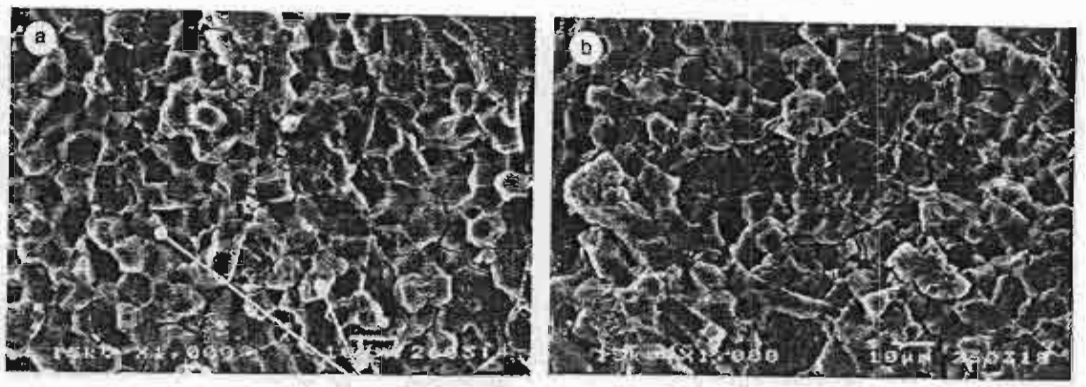


Fig. 6. Scanning electron micrograph of rice kernel in cross section view before and after in-store drying using ambient air at volumetric flow rate 0.65 $m^3/min\,m^3$ of paddy (Suphanburi 1 variety): (a) before drying (control rice); (b) after drying.

control one. The hardness value increases whilst the stickiness slightly decreases. The change in the hardness correlates with the final viscosity, as shown in Table 2. The peak viscosity and final viscosity after drying relatively increase, however, the value of the final viscosity remains higher than the corresponding value of peak viscosity in all the cases. The long period of drying using ambient air ventilation can take the paddy aged like as the storage duration of paddy in ambient environment. This result is similar to the previous works reported by some researchers (Inprasit & Noomhorm, 2001; Juliano, 1985; Zhou et al., 2002). The change in hardness and stickiness from texture analysis correlates with the increase in final and peak viscosities of rice flour.

The germination of paddy was determined and average percentage for germination of rice was about 97.5 ± 0.2% for control paddy and 96.8 ± 0.4% for dried paddy, respectively. Thus, it can be concluded that the in-store drying by ambient air ventilation does not affect the germination of rice.

3.3. Drying strategy by GDS program

To investigate the proper drying condition for low-temperature air drying, simulation model (GDS program) had been performed at air temperatures of 30–40 °C, relative humidity (RH) of 60–90%, paddy bed depths of 1.8–3.6 m, initial moisture content of 18–20% wet basis, whiteness value of 48 at the beginning, specific air flow rates ranging of 0.35–1.0 $m^3/min\,m^3$ of paddy and the limiting value of the dry matter loss is lower than 0.5%.

3.3.1. Whiteness–relative humidity of ambient air

The relation between whiteness and relative humidity of ambient air is shown in Fig. 7. It indicates that at air temperature of 30 °C, the average whiteness is slightly changed with relative humidity between 60% and 90%.

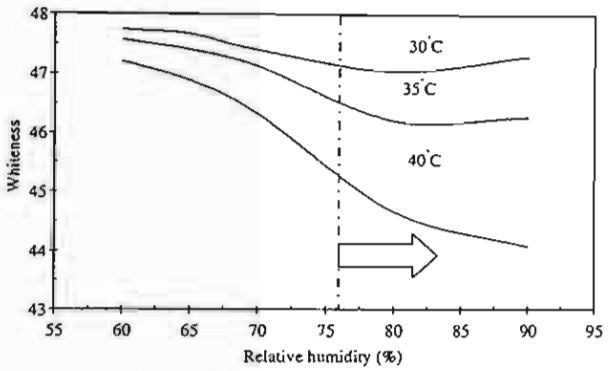


Fig. 7. The simulated values of whiteness of rice during various ambient air conditions of in-store paddy drying at the flow rate of 0.5 $m^3/min\,m^3$ of paddy.

But, at temperatures of 35 and 40 °C, the average whiteness values show the large change when RH of inlet air is higher than 70%. This can be explained that as the temperature increases, the reactive species can more dissolve in the water so that their potential mobility and reactivity become higher, resulting in the large change in whiteness of rice. For determination of whiteness value in the mathematical model, the rice whiteness is inversely related to the yellowness of rice and this yellowing is depended on the temperature and relative humidity. Thus, paddy drying among the high relative humidity and high temperature can encourage the decrease of rice whiteness. This change of whiteness is also discussed by Gras et al. (1989), Phillips et al. (1988) and Bason et al. (1990). Moreover, the prediction results show that the average final moisture content of paddy cannot be reduced to 14% wet basis because of high relative humidity.

3.3.2. Whiteness–specific air flow rate

Fig. 8 shows the change in the value of rice whiteness with air flow rate of 0.35–1.0 $m^3/min\,m^3$ of paddy,

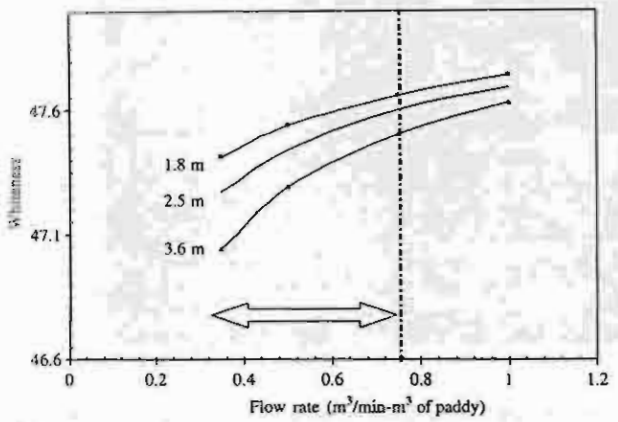


Fig. 8. The simulated values of whiteness of rice versus air flow rate of air of in-store paddy drying in different bed depths with RH 70%; initial moisture content (M_i) of 18% w.b.; final moisture content (M_f) of 14.0% w.b.

indicating that using high air flow rate results in high value of the rice whiteness. Besides the air flow rate, the whiteness also depends on the loading capacity: higher loading, corresponding to higher bed depth, shows the lower whiteness. This is because at low flow rate between 0.35 and 0.5 m^3/min m^3 of paddy and slow drying rate, the heat liberated from grain respiration causes the yellowing of rice kernels, especially at high bed depth. For the high air flow rate of 0.75 and 1.0 m^3/min m^3 of paddy, the heat from respiration is easy to deliver to the atmosphere. Moreover, the DML with air flow rate below of 0.75 m^3/min m^3 of paddy is higher than 0.5%. From these simulations, the recommended specific air flow rate should be higher than 0.75 m^3/min m^3 of paddy.

4. Conclusions

1. The in-store paddy drying using near ambient air temperature has a slight effect on the head rice yield and yellowing of the rice kernel. The value of hardness increases slightly whilst that of the stickiness decreases slightly due to drying.
2. The grain drying model including the yellowing kinetics can suitably describe the change in moisture content and rice whiteness occurring in the deep bed drying.
3. The simulation including the respiration effect shows the higher accuracy of average moisture content of rice at given drying time than that excluding respiration effect predictions. Thus, in the low temperature in-store drying, the energy liberated during the respiration of product is a dominant factor to reduce its moisture content.
4. The drying temperatures between 30 and 40 °C, along with the relative humidity lower than 70%, are recommended. For the in-store paddy drying, the suitable specific air flow rate should not be lower than 0.75 m^3/min m^3 of paddy.

Acknowledgements

The authors wish to express their sincere thanks to the Thailand Research Fund (TRF). The authors also thank to the Japan International Research Center for Agricultural Sciences (JIRCAS) for financial support, the Institute of Food Research and Product Development (IFRPD) at Kasetsart University, Thailand for testing of rice qualities and Institute of Technology Rajchamongkrala, Headquarter, Pathumthani, Thailand for rice whiteness testing.

References

AACC (2000). Approved methods of the AACC. The 10th American Association of Cereal Chemists, St. Paul, MN, USA.

Agrawal, Y. C., & Singh, R. P. (1977). Thin-layer drying studies on short-grain rough ice. ASAE Paper No. 77-3531, ASAE, St. Joseph, MI, pp. 330–350.

AOAC (1995). *Official methods of analysis* (15th ed.). Washington, DC: Association of Official Analytical Chemists.

Barre, H. J., Baughman, G. R., & Hamdy, M. Y. (1971). Application of the logarithmic model to cross-flow deep-bed drying. *Transactions of the ASAE, 14*(6), 1061–1064.

Bason, M. L., Gras, P. W., Banks, H. J., & Esteves, L. A. (1990). A qualitative study of the influences of temperature, water activity and storage atmosphere on the yellowing of paddy endosperm. *Journal of Cereal Science, 12*, 193–201.

Brooker, D. B., Bakker-Arkema, F. W., & Hall, C. W. (1992). *Drying and storage of grain and oilseeds*. New York: Van Nostrand Reinhold, pp. 206–240.

Gras, P. W., & Bason, M. L. (1989). Biochemical effects of storage atmospheres on grain and grain quality. *ACIAR Proceeding No. 25, Fumigation and controlled atmosphere storage of grain*, pp. 83–91.

Gras, P. W., Banks, H. J., Bason, M. L., & Arriola, L. P. (1989). A qualitative study of the influences of temperature, water activity and storage atmosphere on the yellowing of milled rice. *Journal of Cereal Science, 9*, 77–89.

Henderson, S. M. (1952). A basic concept of equilibrium. *Agricultural Engineering, 33*, 29–31.

Hukill, W. V. (1947). Basic principles in drying corn and grain sorghum. *Agricultural Engineering, 28*(8), 335–338, 340.

Inprasit, C., & Noomhorm, N. (2001). Effect of drying air temperature and grain temperature of different types of dryer and operation on rice quality. *Drying Technology, 19*(2), 389–404.

Juliano, B. O. (1985). Rice: Chemistry and technology. American Association of Cereal Chemists, USA, 774 pp.

Jean, F., Meullenet, C., Bradley, P. M., Griffin, K., & Daniels, M. J. (1999). Effects of rough rice drying and storage conditions on sensory profiles of cooked rice. *Cereal Chemistry, 76*(4), 483–486.

Ngamchuen, K., Lamaimaat, N., & Kanchana, N. (1985). Changes in cooking and eating qualities of rice during long-term storage. In *Proceedings of the 8th ASEAN technical seminar on grain post-harvest technology* (pp. 165–187). Manila Hotel, Philippines.

Ong, M. H., & Blanshard, J. M. V. (1995). Texture determinants of cooked, parboiled rice II: physicochemical properties and leaching behaviour of rice. *Journal of Cereal Science, 21*, 261–269.

Ohtsubo, K., Toyoshima, H., & Okadome, H. (1998). Quality assay of rice using traditional and novel tools. *Cereal Foods World, 43*(4), 203–206.

Phillips, S., Widjaja, S., Wallbridge, A., & Cooke, R. (1988). Rice yellowing post-harvest drying by aeration and during storage. *Journal of Stored Products Research, 24*, 173–181.

Preechakul, P. (1986). A study on in-store drying of paddy (2nd phase). Master thesis, School of Energy and Materials, King Mongkut's Institute of Technology Thonburi, Bangkok, Thailand, 115 pp.

Quitco, R. T. (1982). Studies of fungal infection and heating of paddy. In *Proceedings GASGA seminar, paddy deterioration in the humid tropics* (pp. 52–56). Baquio, Phillippines, GTZ, Eschborn.

Seib, P. A., Pfost, H. B., Sukaboi, A., Rao, V. S., & Burroughs, R. B. (1980). Spoilage of rough rice as measured by carbon dioxide evolution. In *Proceedings of the 3rd annual workshop on grain post-harvest technology*. Kuala Lumpur, January 29–30.

Soponronnarit, S. (1988). Energy model of grain drying system. *ASEAN Journal on Science and Technology for Development, 5*(2), 43–68.

Soponronnarit, S., & Chinsakolthanakorn, S. (1990). Effect of heat and water from respiration on drying rate and energy consumption. *ASEAN Journal for Science and Technology for Development, 7*, 65–83.

Soponronnarit, S., & Nathakaranakule, A. (1990). Field experience of in-store drying of paddy under tropical climates. In *Proceedings of the 13th ASEAN seminar on grain postharvest tech.* (pp. 183–196). Brunei Darussalam, 4–7 September.

Soponronnarit, S., & Preechakul, P. (1990). Experiments on in-store and batch drying of paddy: quality of product. *Kasetsart University Science Journal, 24*, 367–388 (in Thai).

Soponronnarit, S., Srisubati, N., & Yoovidhya, T. (1998). Effect of temperature and relative humidity on yellowing rate of paddy. *Journal of Stored Products Research, 34*(4), 323–330.

Thompson, T. L., Peart, R. M., & Foster, G. H. (1968). Mathematical simulation of corn drying—a new model. *Transaction of ASAE, 11*(4), 582–586.

USDA (1988). Grain grade procedure. Federal Grain Inspection Service, Washington, DC, USA.

Yap, A. B., Juiliano, B. O., & Perez, C. M. (1988). Artificial yellowing of rice at 60 °C. In *Proceeding group, the source of yellow grains in rice* (pp. 153–157). Myc. Centralbl, 3.

Zhou, Z., Robards, K., Helliwell, S., & Blanchard, C. (2002). Ageing of stored rice: changes in chemical and physical attributes. *Journal of Cereal Science, 35*, 65–78.

ELSEVIER

Journal of Food Engineering 65 (2004) 293–301

JOURNAL OF FOOD ENGINEERING

www.elsevier.com/locate/jfoodeng

Influence of FIR irradiation on paddy moisture reduction and milling quality after fluidized bed drying

Naret Meeso [a,*], Adisak Nathakaranakule [a], Thanid Madhiyanon [b], Somchart Soponronnarit [a]

[a] *School of Energy and Materials, King Mongkut's University of Technology Thonburi, Bangkok 10140, Thailand*
[b] *Department of Mechanical Engineering, Mahanakorn University of Technology, Bangkok 10530, Thailand*

Received 29 August 2003; accepted 26 January 2004

Abstract

The influence of far-infrared (FIR) irradiation in multi-stage paddy drying process on moisture reduction and milling quality has been experimentally studied. The process, running in series, comprised fluidized bed drying, FIR irradiation, tempering and ambient air ventilation. The experimental results showed that the critical moisture content after the fluidized bed drying was around 23% d.b. whereas incorporating with the FIR irradiation could continuously reduced the moisture content to 21% d.b. without affecting paddy head rice yield and whiteness. Under the intensity of FIR irradiation, wet paddy was more sensitive than dry paddy. However, to maintain head rice yield, moisture equalization by a subsequent tempering stage was still required. Studying the microstructure of rice kernels and the pasting behavior of rice flours showed the presence of partial gelatinization resulted in the improvement of head rice yield.
© 2004 Elsevier Ltd. All rights reserved.

Keywords: Ambient air ventilation; Far-infrared irradiation; Fluidized bed; Tempering

1. Introduction

Two-stage paddy drying; fast dried in a fluidized bed dryer and then slowly dried by in-storage drying to moisture contents of 23% dry basis (d.b.) and 16% d.b. respectively, was recommended by Soponronnarit (1995) to maintain paddy qualities, such as head rice yield and whiteness. Poomsa-ad, Soponronnarit, Terdyothin, and Prachayawarakron (2001) suggested that the moisture content of paddy, after drying by a fluidized bed dryer, should not be less than 22.5% d.b. in order to maintain or in some cases to increase the head rice yield. High temperature use in the first stage, led to the development of a moisture gradient inside each grain kernel, and resulted in cracking and breakage of the paddy kernels. This problem can be solved by introducing a tempering process between the two stages in order to increase or maintain the paddy head rice yield and reduce the paddy moisture content in the second stage (Soponronnarit, Wetchacama, Swasdisevi, & Poomsa-ad, 1999; Steffe, Singh, & Bakshi, 1979). The benefit of the tempering process depended on two main factors; tempering temperature and time (Poomsa-ad, Soponronnarit, Prachayawarakron, & Terdyothin, 2002; Steffe & Singh, 1980).

The fluidized bed paddy dryer that is suitable for high moisture grain (i.e. from 35% to 23% d.b.) has been widely used in more than 10 countries. However, in maintaining the head rice yield, paddy moisture reduction must be limited. According to the mechanism of FIR drying, heat is generated deep inside the grain and tends to be selectively absorbed in the regions with high moisture content. Thus the vapour pressure would be the largest in these regions, and the moisture diffusion will be in the direction toward the areas of lower vapour pressure such as the grain surface (Afzal & Abe, 1998; Afzal, Abe, & Hikida, 1999; Ratti & Mujumdar, 1995; Sakai & Hanzawa, 1994). Therefore, it may be possible to apply FIR irradiation in the drying process to lower this limit. Suitable wavelengths for medium paddy kernels were in the range of 2.9–9.5 μm for FIR (Bekki,

* Corresponding author. Tel./fax: +662-470-8663.
E-mail address: n_meeso@hotmail.com (N. Meeso).

0260-8774/$ - see front matter © 2004 Elsevier Ltd. All rights reserved.
doi:10.1016/j.jfoodeng.2004.01.033

1991). The depth of penetration of FIR in grains was just under 1–2 mm (Datta & Ni, 2002; Nindo, Kudo, & Bekki, 1995; Sandu, 1986). Hence, FIR was suitable for small grains, such as paddy or wheat. In addition, temperature of the FIR radiator, distance between the FIR radiator and the grain bed, initial grain moisture content and drying time significantly affected grain temperatures. However, FIR radiator temperature and radiator height had no significant effect on grain final moisture content (Fasina, Tyler, & Pickard, 1998).

Recently, the concept of FIR irradiation application immediately after convective warm air (approximately 40 °C) drying of paddy has been utilized in the paddy industry in Japan especially for the recirculating batch dryer (Bekki, 1991; Institute of Agricultural Machinery, Japan, 2003). It is believed to save energy consumption and obtained better product quality. In contrast to the FIR irradiation technique, much higher air temperature (approximately 120–150 °C) is usually used for paddy drying with the fluidization technique in the Thai rice industry. Thus, FIR irradiation was introduced in the production line, just after fluidized bed drying to improve the paddy quality. The purpose of this study was to experimentally investigate the influence of FIR irradiation on moisture reduction and milling qualities of paddy.

2. Materials and methods

2.1. Experimental apparatus

The experimental apparatus consisted of a batch-type fluidized bed dryer, a box-type FIR dryer, a tempering glass bottle and an ambient air ventilator as follows:

The batch-type fluidized bed dryer shown in Fig. 1, comprised a cylindrical drying chamber, a 12 kW electrical heater, a centrifugal fan driven by 1.5 kW motor. The drying temperature was controlled by a PID controller giving an accuracy of ±1 °C.

The box-type FIR dryer, shown in Fig. 2, comprised a radiative chamber and air vents at the back of a chamber. A ceramic infrared heater had a diameter of 1.7 cm, a length of 60 cm, and maximum power of 800 W. Its surface temperature was controlled by ON-OFF controller. An acrylic sample tray had dimensions of $50 \times 60 \times 1.5$ cm.

The tempering glass bottle had a diameter and a height of 12 and 10 cm respectively. It could be closed completely and kept in a hot-air oven at a temperature equal to the paddy temperature after the fluidized bed drying.

The ambient air ventilator had a diameter of 20 cm and a sample tray made of wire mesh. Air velocity,

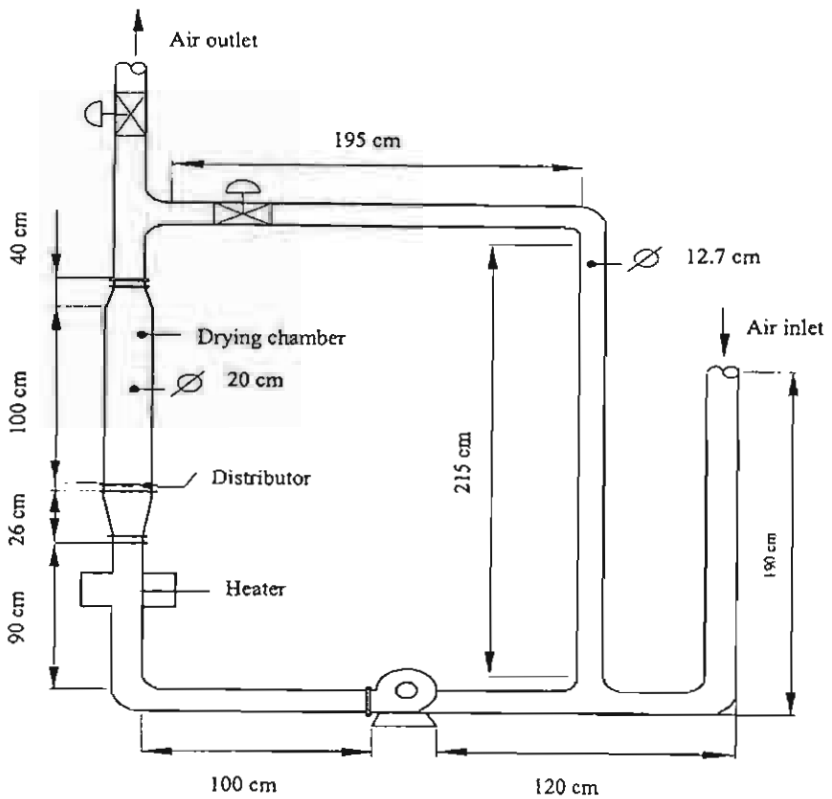


Fig. 1. Schematic diagram of a batch-type fluidized bed dryer.

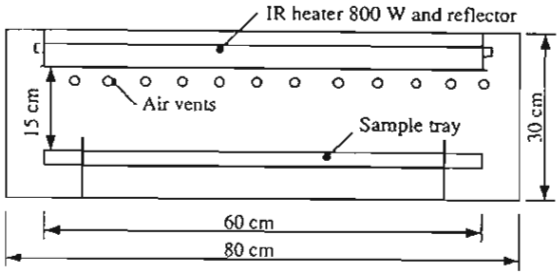


Fig. 2. Schematic diagram of a box-type FIR dryer.

ventilated throughout the tray, was measured by hot-wire anemometer (accuracy of ±0.1 m/s).

The temperatures of grain, drying air and ambient conditions were measured by K-type thermocouples connected to a data logger with an accuracy of ±1 °C.

2.2. Experimental procedure

The multi-stage drying process in each experiment was operated in series. It comprised fluidized bed (FB) drying, FIR irradiation, tempering (TEM) and ambient air ventilation (AAV). The experiments were divided into six conditions as shown in Table 1.

In the drying process, paddy was dried by a fluidized bed dryer at 150 °C for 1–2 min. Then, it was moved immediately into the sample tray as a single layer of grain and irradiated in a FIR dryer at intensities of 0.310 and 0.707 W/cm^2 for 0.5–1 min. After that, it was tempered in the tempering glass bottle for 20 min before being exposed in ambient air with velocity of 0.15 m/s for 30 min.

Fresh harvested paddy (Supanburi 1) was rewetted to about 30.0–34.0% d.b. and kept in a cooling room at 3–5 °C for 7 days. Before starting the experiments, the paddy was left in ambient air until its temperature was close to ambient temperature.

Paddy samples were taken after each stage of the drying process, except after the tempering stage, for measuring moisture content and quality. The moisture contents of paddy were determined by drying three samples in a hot-air oven at 103 °C for 72 h (AACC, 1995). The paddy qualities in terms of head rice yield (HRY) and whiteness (Wh) were tested by the test method of the Ministry of Agriculture and Cooperatives, Thailand and measured using a KETT whiteness tester model C-300 respectively. The head rice yield was also presented in terms of relative head rice yield, which is the ratio of head rice yield obtained from the aforementioned drying processes to the head rice yield obtained from ambient air drying.

The change in microstructure of rice kernels during the multi-stage drying process was observed by scanning electron microscopy (SEM) (JSM-5600 Low vacuum, JEOL Co. Ltd.) at 15 kV. The polished rice kernels (before and after each drying process) were broken along the cross-sectional axis, placed on adhesive tape attached to a SEM stub, coated with gold-palladium then examined, and photographed.

A rapid visco analyzer (RVA) (Newport Scientific Instrument, Narrabean N.S.W., Australia) was used to

Table 1
The experimental conditions of the paddy drying process

The drying process		The conditional numbers					
		A	B	C	D	E	F
FB	Air temperature (°C)[a]	150	150	150	150	150	150
	Bed thickness (cm)[a]	9.5	9.5	9.5	9.5	9.5	9.5
	Air velocity (m/s)[a]	2.6	2.6	2.6	2.6	2.6	2.6
	Time (min)	1	1	1.5	1.5	2	2
FIR	Average radiative intensity (W/cm^2)	0.312	0.707	0.310	0.689	0.310	0.310
	Bed thickness	–[b]	–[b]	–[b]	–[b]	–[b]	–[b]
	Average load of radiative chamber ($kg_{dry\ paddy}$/W)	2.0	0.9	2.1	0.9	2.1	2.1
	Distance between heater-paddy (cm)[c]	15	15	15	15	15	15
	Time (min)	1	1	0.5	0.5	0.5	0.5
TEM	Temperature (°C)	75	75	80	80	85	–
	Time (min)	20	20	20	20	20	–
AAV	Bed thickness (cm)[a]	3	3	3	3	3	3
	Air velocity (m/s)[a]	0.15	0.15	0.15	0.15	0.15	0.15
	Time (min)	30	30	30	30	30	30

[a] Recommended by Poomsa-ad et al. (2001).
[b] Corresponding to a paddy single layer of 1.1 $kg_{wet\ paddy}$.
[c] Recommended by Afzal et al. (1999).

investigate the pasting behavior of milled rice flour according to the AACC (1995, standard method). Rice flour (3 g on % d.b.) was placed in water (25 ml) in the canister and mixed thoroughly. The operating temperature was first maintained at 50 °C for 1.5 min to allow a uniform temperature and then raised to 95 °C at a rate of 12 °C/min. The sample was maintained at 95 °C for 2.5 min, then cooled to 50 °C at a rate of 12 °C/min. After the sample was maintained at 50 °C for 1.5 min., the pasting behavior was specifically measured as the temperature where viscosity first increased by 2 rapid visco units (RVU) over a 20 s period and by the peak viscosity. These are needed in order to investigate the gelatinization of rice flour during the multi-stage drying process.

3. Results and discussion

3.1. Moisture reduction

The moisture content evaluations in the paddy drying processes shown in Figs. 3–6 show the change in moisture content of paddy after fluidized bed drying, FIR irradiation, tempering and ambient air ventilation with processing time.

Focusing on the FIR irradiation stage, the experimental results clearly showed that FIR intensities aided removing moisture from paddy, which still had high moisture contents after the fluidized bed drying stage, by approximately 1.5–2.6% d.b. (Fig. 3). These drying curves indicated that the moisture content of paddy was significantly reduced with higher radiation intensity. However, the radiation intensity had no influence on moisture reduction of paddy with low moisture contents particularly for moisture contents less than 23% d.b. (Fig. 4). This was illustrated by comparing the moisture reduction between radiation drying with an FIR intensity of about 0.7 W cm^{-2} and that of about 0.3 W cm^{-2} as shown in Figs. 3 and 4. The result in Table 1 was also indicated that the moisture reduction increased with the decrease of the load of radiative chamber. The amount of radiation energy absorbed by paddy was directly proportional to the amount of water contained inside the paddy kernel. However, drying effectiveness of FIR irradiation covered a wide range of paddy moisture contents after fluidized bed drying, i.e. 26%, 23% and 21% d.b. as shown in Figs. 3–5 respectively.

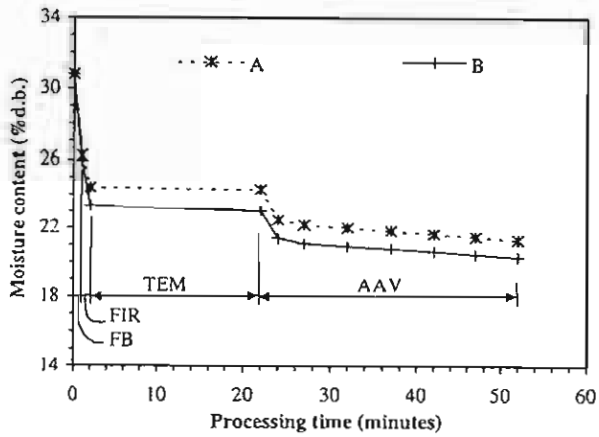


Fig. 3. Evolution of moisture content of paddy during conditions: (A) FB (150 °C, 1 min), FIR (0.312 W cm^{-2}, 1 min), TEM (75 °C, 20 min) and AAV (30 min, ambient air condition: 29.2 °C, 70% RH). (B) FB (150 °C, 1 min), FIR (0.707 W cm^{-2}, 1 min), TEM (75 °C, 20 min) and AAV (30 min, ambient air condition: 29.2 °C, 70% RH).

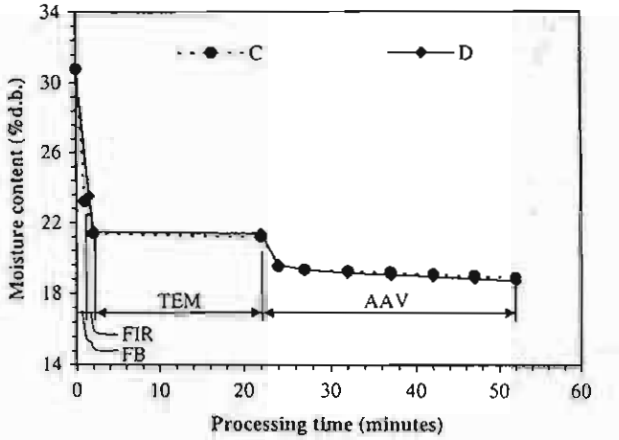


Fig. 4. Evolution of moisture content of paddy during conditions: (C) FB (150 °C, 1.5 min), FIR (0.310 W cm^{-2}, 0.5 min), TEM (80 °C, 20 min) and AAV (30 min, ambient air condition: 29.2 °C, 70% RH). (D) FB (150 °C, 1.5 min), FIR (0.689 W cm^{-2}, 0.5 min), TEM (80 °C, 20 min) and AAV (30 min, ambient air condition: 29.2 °C, 70% RH).

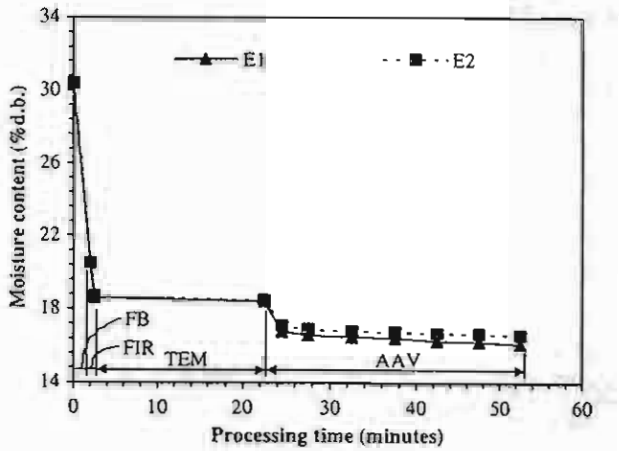


Fig. 5. Evolution of moisture content of paddy during conditions: (E1) FB (150 °C, 2 min), FIR (0.310 W cm^{-2}, 0.5 min), TEM (85 °C, 20 min) and AAV (30 min, ambient air condition: 29.6 °C, 67% RH). (E2) is repeated experiment of E1 conditions.

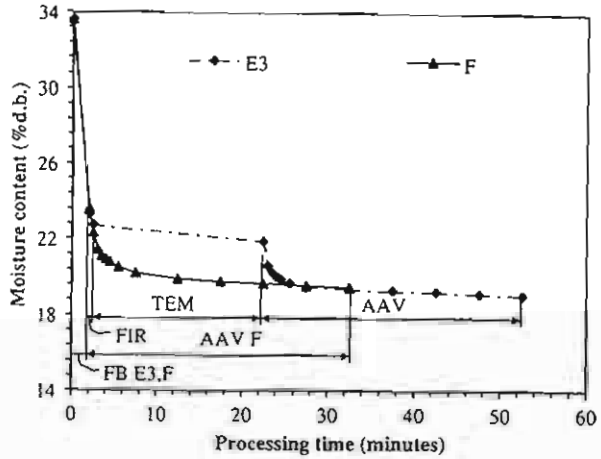


Fig. 6. Evolution of moisture content of paddy during conditions: (E3) FB (150 °C, 2 min), FIR (0.310 W cm^{-2}, 0.5 min), TEM (85 °C, 20 min) and AAV (30 min, ambient air condition: 29.6 °C, 67% RH). (F) FB (150 °C, 2 min), FIR (0.310 W cm^{-2}, 0.5 min) and AAV (30 min, ambient air condition: 29.6 °C, 67% RH).

During the transition period from the tempering to the ambient air ventilation period indicated by the drying curves in Figs. 3–5, the moisture content dropped progressively within 5 min after exposure to ambient air and thereafter it reduced gradually. Fig. 6 reflected the influence of FIR irradiation on moisture reduction in the ventilation stage by comparing the drying curves between the multi-stage drying processes with and without tempering stage after the FIR irradiation stage. The slopes of curve E (with a tempering stage) and curve F (without a tempering stage) during the ventilation period were almost the same. This meant that the multistage drying with the existence of a tempering stage after the FIR irradiation stage did not provide more benefit in moisture reduction in the ventilation stage compared with that without the tempering stage. It may be inferred that the mechanism of FIR irradiation, which may support redistribution of moisture inside paddy kernels, may be somewhat analogous to the tempering mechanism. However, the milling quality and especially the head rice yield was quite different between the two cases, which will be discussed in the next section.

3.2. Milling qualities

3.2.1. Head rice yield

The head rice yield of paddy under each experimental condition is shown in Tables 2–5. The relationship between head rice yield and moisture content after each drying stage were plotted and shown in Figs. 7–9. A relative head rice yield over 100% could be achieved if the moisture content of paddy after fluidized bed drying was not less than 23% d.b. (Fig. 7). This limitation of paddy moisture content confirmed the results of Poomsa-ad et al. (2001). After passing the FIR irradiation stage, the results revealed the possibility of further paddy moisture content reduction to approximately 21% d.b., whereas the relative head rice yield was still maintained over 100%. (Fig. 8). An improvement in head rice yield in the drying process was mainly due to the rapid increase in paddy grain temperature during the fluidized bed stage (Table 6) to the temperature level of partial gelatinization (68–78 °C depending on the types of paddy (Sanders, 1996)). Meanwhile, during FIR irradiation which probably functioned as a partial tempering process, the radiation energy absorbed by moisture inside a paddy kernel aided moisture migration from inside to outside the paddy kernel. Thus, moisture removal and moisture leveling were occurring simultaneously. The latter resulted in decreasing moisture gradient as well as the stresses development within the kernel, hence head rice yield was maintained. Decreasing the moisture content lower than those limits (23% d.b. by fluidized bed drying and 21% d.b. by FIR irradiation after fluidized bed drying) resulted in more grain damage, as the stresses inside the paddy kernels increased due to high moisture and temperature gradients. In the experiments, when paddy transited from the tempering stage to the ventilation stage, no change in head rice yield was assumed. Therefore, head rice yield after ambient air ventilation shown in Tables 2–5 was

Table 2
Evolution of milling quality of paddy during conditions A and B

Drying process	The conditional numbers			
	A		B	
	HRY (%)	Wh	HRY (%)	Wh
Initial quality	52.2	50.4	52.2	50.4
Quality after FB	56.9	50.9	55.7	50.6
Quality after FIR	55.9	50.7	56.9	46.1
Quality after TEM	NA	NA	NA	NA
Quality after AAV	57.7	49.4	56.7	51.1

A: FB (150 °C, 1 min), FIR (0.312 W cm^{-2}, 1 min), TEM (75 °C, 20 min) and AAV (30 min, ambient air condition: 29.2 °C, 70.0% RH).
B: FB (150 °C, 1 min), FIR (0.707 W cm^{-2}, 1 min), TEM (75 °C, 20 min) and AAV (30 min, ambient air condition: 29.2 °C, 70.0% RH).
NA: non-available.

Table 3
Evolution of milling quality of paddy during conditions C and D

Drying process	The conditional numbers			
	C		D	
	HRY (%)	Wh	HRY (%)	Wh
Initial quality	52.2	50.4	52.2	50.4
Quality after FB	55.4	50.3	55.8	50.0
Quality after FIR	52.2	50.0	54.7	50.4
Quality after TEM	NA	NA	NA	NA
Quality after AAV	55.8	49.8	56.6	50.3

C: FB (150 °C, 1.5 min), FIR (0.310 W cm^{-2}, 0.5 min), TEM (80 °C, 20 min) and AAV (30 min, ambient air condition: 29.2 °C, 70.0% RH).
D: FB (150 °C, 1.5 min), FIR (0.689 W cm^{-2}, 0.5 min), TEM (80 °C, 20 min) and AAV (30 min, ambient air condition: 29.2 °C, 70.0% RH).
NA: non-available.

Table 4
Evolution of milling quality of paddy during conditions E1 and E2

Drying process	The conditional numbers			
	E1		E2	
	HRY (%)	Wh	HRY (%)	Wh
Initial quality	54.2	51.6	54.2	51.6
Quality after FB	31.0	47.7	27.8	48.4
Quality after FIR	20.0	45.4	21.9	46.4
Quality after TEM	NA	NA	NA	NA
Quality after AAV	46.6	48.7	47.1	48.6

E1: FB (150 °C, 2 min), FIR (0.310 W cm^{-2}, 0.5 min), TEM (85 °C, 20 min) and AAV (30 min, ambient air condition: 29.6 °C, 67.0% RH).
E2 is repeated experiment of E1 conditions.
NA: non-available.

Table 5
Evolution of milling quality of paddy during conditions E3 and F

Drying process	The conditional numbers			
	E3		F	
	HRY (%)	Wh	HRY (%)	Wh
Initial quality	47.3	52.4	47.3	52.4
Quality after FB	48.7	49.3	47.0	48.8
Quality after FIR	45.8	48.4	45.2	47.1
Quality after TEM	NA	NA	–	–
Quality after AAV	47.9	47.3	30.0	46.2

E3: FB (150 °C, 2 min), FIR (0.310 W cm^{-2}, 0.5 min), TEM (85 °C, 20 min) and AAV (30 min, ambient air condition: 29.6 °C, 67.0% RH).
F: FB (150 °C, 2 min), FIR (0.310 W cm^{-2}, 0.5 min) and AAV (30 min, ambient air condition: 29.6 °C, 67.0% RH).
NA: non-available.

representative for head rice yield after tempering. As the tempering temperatures of these conditions (75–80 °C) were in the range of gelatinization temperatures, head rice yields was slightly improved because of a continuous gelatinization reaction during tempering. This reason could be confirmed by much improvement of head rice yields of paddy in condition E (Table 4 and Fig. 9).

For the multi-stage drying process without tempering after the FIR irradiation stage (condition F in Table 5), the result showed that head rice yield was significantly reduced because of sudden cooling at the beginning of the ventilation stage. Therefore, moisture relaxation during the tempering process before ventilation was recommended for maintaining grain quality. This also indicated that even though FIR irradiation may support moisture redistribution inside the kernel, moisture redistribution could not completely occur without the tempering process.

The change in the microstructure of the gelatinized kernel samples during condition D was observed by

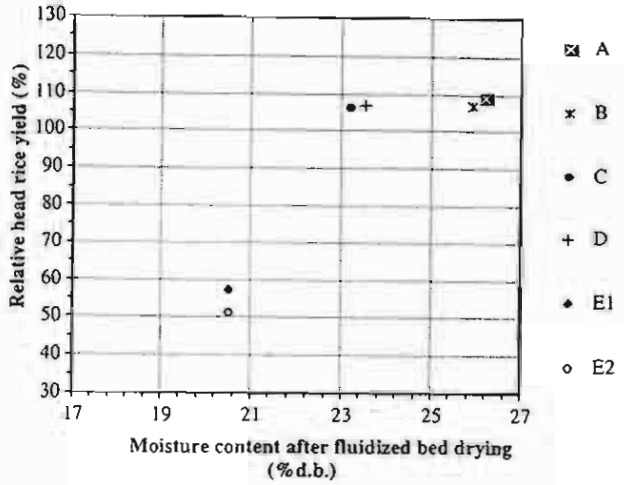


Fig. 7. The relationship between moisture content after fluidized bed drying and relative head rice yield.

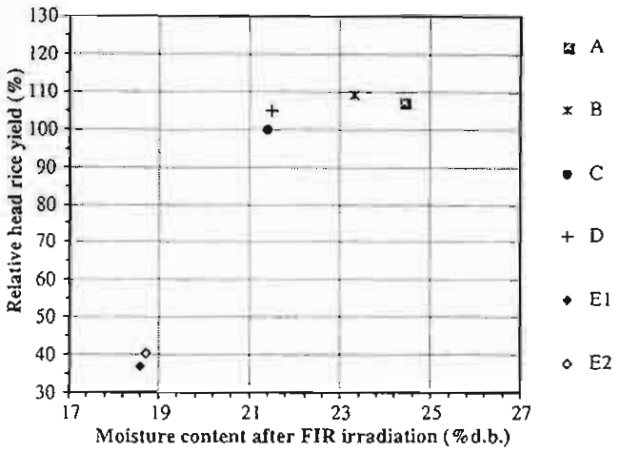


Fig. 8. The relationship between moisture content after FIR irradiation and relative head rice yield.

SEM (Fig. 10). This figure has an enlarged photograph of the kernels, in cross-sectional view. Fig. 10a showed a cross-sectional view of the kernel before drying that had the distinctive structure of starch granules spreading throughout. During fluidized bed drying, the kernel temperature rose rapidly, starch granules swelled,

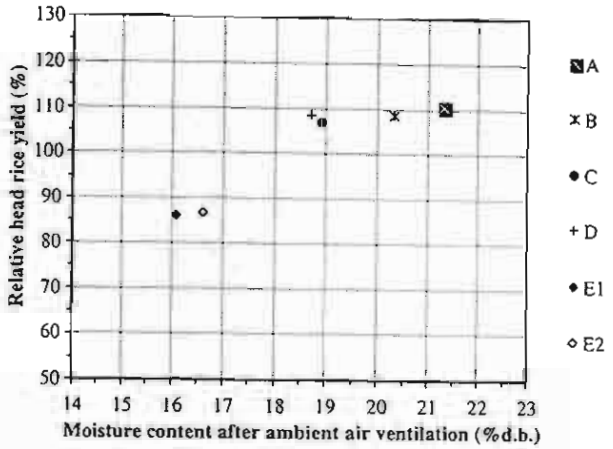


Fig. 9. The relationship between moisture content after ambient air ventilation and relative head rice yield.

absorbing surrounding moisture, and gelatinized. This gelatinization existed at the surface of starch granules and is called partial gelatinization (Fig. 10b). The granule surface gelatinization existed continuously in the FIR irradiation and tempering stages (Fig. 10c and d). Therefore, it was proven that, in the multi-stage drying, starch gelatinization certainly occurred in the rice kernels, and could support head rice yield maintenance.

In order to confirm the explanation in the previous section, the gelatinization of rice kernel samples during condition D was again investigated using RVA, as shown in Fig. 11. The pasting curve of milled rice flour before drying had a pasting temperature and a peak viscosity of 75.2 °C and 191.2 RVU, respectively. Reduction in the peak viscosity to 167.4 RVU after the fluidized bed drying stage indicated that the gelatinization has partially occurred in the rice kernel during fluidized bed drying. Similar to the rice flour after fluidized bed drying, the peak viscosity after the respective FIR irradiation and tempering stages had the slight difference, approximately 160.5 and 150.6 RVU. These results may support the explanation of gelatinization in the rice kernels, even though the reduction in peak viscosity after the fluidized bed drying stage, FIR irradiation and tempering stage were not significantly different.

Table 6
Average grain temperature of paddy after fluidized bed drying and FIR irradiation

Condition no.	FB drying			FIR irradiation		
	Drying temperature (°C)	Time (min)	Average grain temperature (°C)	Radiative chamber temperature (°C)	Time (min)	Average grain temperature (°C)
A	150	1	75	80	1	55.2
B	150	1	75	150	1	60.7
C	150	1.5	80	80	0.5	57.4
D	150	1.5	80	150	0.5	64
E, F	150	2	85	80	0.5	68

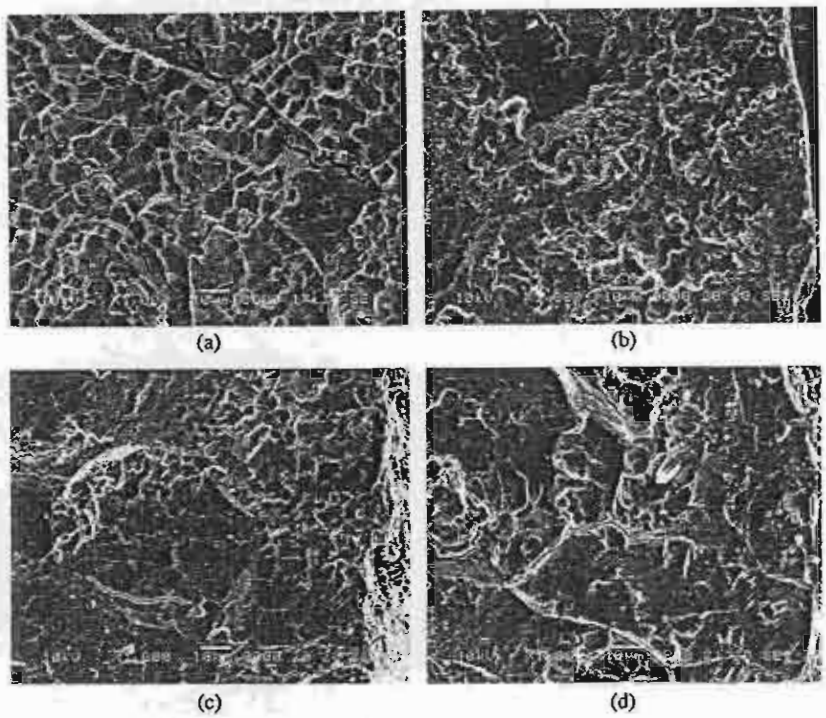


Fig. 10. Photos of cross-section of kernels during condition D: (a) before drying, (b) after fluidized bed drying, (c) after FIR irradiation and (d) after ambient air ventilation.

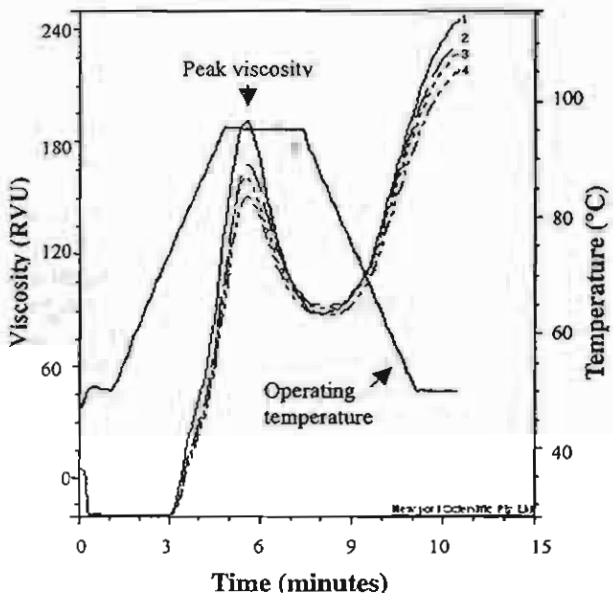


Fig. 11. Pasting curves of milled rice flour during condition D: (1) before drying, (2) after fluidized bed drying, (3) after FIR irradiation and (4) after ambient air ventilation.

3.2.2. *Whiteness*

The results of paddy whiteness are shown in Tables 2–5, indicated that whiteness of paddy after each drying stage was not significantly changed. Its value was approximately 50, which is in a good commercial criterion.

4. Conclusions

Intensity of FIR was more effective in moisture reduction of wet paddy than dry paddy. The moisture content of paddy from the fluidized bed drying stage was limited to not lower than 23% d.b. but with integrating FIR irradiation into the paddy drying process, the moisture content could be further reduced to around 21% d.b. without any significant grain damage. Nevertheless, tempering was still necessary to achieve high head rice yield for the multi-stage drying process. Studying the microstructure of rice kernels and the pasting behavior of rice flours indicated partial gelatinization during fluidized bed drying, FIR irradiation and tempering processes reflected in head rice yield improvement.

Acknowledgements

The authors would like to thank the Thailand Research Fund for financial support, Pathumtani Rice Research Center for testing quality of milling and Department of Microbiology, King Mongkut's Uni-

versity of Technology Thonburi for providing a FIR dryer.

References

AACC (1995). Approved method of the American Association of Cereal Chemists (9th ed.). St. Paul, MN.

Afzal, T. M., & Abe, T. (1998). Diffusion in potato during for infrared radiation drying. *Journal of Food Engineering, 37*, 353–365.

Afzal, T. M., Abe, T., & Hikida, Y. (1999). Energy and quality aspects during combined FIR-convective drying of barley. *Journal of Food Engineering, 42*, 177–182.

Bekki, E. (1991). Rough rice drying with a far-infrared panel heater. *Journal of the Japanese Society of Agricultural Machinery, 53*(1), 55–63 (in Japanese).

Datta, A. K., & Ni, H. (2002). Infrared and hot-air-assisted microwave heating of foods for control of surface moisture. *Journal of Food Engineering, 51*, 355–364.

Fasina, O. O., Tyler, R. T., & Pickard, M. D. (1998). Modelling the infrared radiative heating of agriculture crops. *Drying Technology, 16*(9&10), 2065–2082.

Institute of Agricultural Machinery, Japan (2003). Recirculating batch grain dryer using far-infrared radiation. http://www.brain.go.jp/Organ/sei0301e.htm.

Nindo, C. I., Kudo, Y., & Bekki, E. (1995). Test model for studying sun drying of rough rice using far-infrared radiation. *Drying Technology, 13*(1&2), 225–238.

Poomsa-ad, N., Soponronnarit, S., Terdyothin, A., & Prachayawarakron, S. (2001). Head rice yield after drying by fluidization technique and tempering. In *Proceedings of ADC 2001* (pp. 717–726). Penang, Malaysia.

Poomsa-ad, N., Soponronnarit, S., Prachayawarakron, S., & Terdyothin, A. (2002). Effect of tempering on subsequent drying of paddy using fluidization technique. *Drying Technology, 20*(1), 195–210.

Ratti, C., & Mujumdar, A. S. (1995). Infrared drying. In A. S. Mujumdar (Ed.), *Handbook of Industrial Drying* (pp. 567–588). New York: Marcel Dekker.

Sakai, N., & Hanzawa, T. (1994). Applications and advances in far-infrared heating in Japan. *Trends in Food Science and Technology, 5*, 357–362.

Sanders, J. P. M. (1996). Starch manufacturing in the world. In: Advanced Post Academic Course on Tapioca Starch Technology, AIT, Bangkok, Thailand.

Sandu, C. (1986). Infrared radiative drying in food engineering: a process analysis. *Biotechnology Progress, 2*, 109–119.

Soponronnarit, S. (1995). Strategy for managing moist paddy. *The Royal Institute Journal, 20*(4), 115–125 (in Thai).

Soponronnarit, S., Wetchacama, S., Swasdisevi, T., & Poomsa-ad, N. (1999). Managing moist paddy by drying tempering and ambient air ventilation. *Drying Technology, 17*(1&2), 335–344.

Steffe, J. F., & Singh, R. P. (1980). Theoretical and practical aspects of rough rice tempering. *Transactions of the ASAE, 23*, 775–782.

Steffe, J. F., Singh, R. P., & Bakshi, A. S. (1979). Influence of tempering time and cooling on rice milling yields and moisture removal. *Transactions of the ASAE, 22*, 1214–1218.

ELSEVIER

Journal of Food Engineering 65 (2004) 371–382

JOURNAL OF FOOD ENGINEERING

www.elsevier.com/locate/jfoodeng

Comparative study of heating processes for full-fat soybeans

Songchai Wiriyaumpaiwong [a,*], Somchart Soponronnarit [b], Somkiat Prachayawarakorn [c]

[a] *Faculty of Engineering, Mahasarakham University, Kamreang, Kuntarawichai, Mahasarakham 44150, Thailand*
[b] *School of Energy and Materials, King Mongkut's University of Technology Thonburi, Pracha-utit Rd., Thungkru, Bangkok 10140, Thailand*
[c] *Faculty of Engineering, King Mongkut's University of Technology Thonburi, Pracha-utit Rd., Thungkru, Bangkok 10140, Thailand*

Received 24 July 2003; accepted 26 January 2004

Abstract

Heating is very important to inactivate anti-nutritional factors and enhance quality of soybean products. Four heating techniques i.e. extrusion, fluidized bed, spouted bed and infrared radiation have been investigated along with their performances, regarding moisture reduction, urease inactivation, protein solubility and lysine. The rate of moisture diffusion for soybean kernel in the spouted bed and infrared dryer was described by a semi-empirical drying equation for which the drying constant was determined using non-linear regression. The experimental results have shown that the water mobility is more rapidly accelerated by infrared radiation. Every technique has a potential to reduce the urease activity to the standard range, with the quantity of remaining lysine being insignificantly different ($p < 0.05$) under the testing conditions. The extent of urease inactivation in each technique depends on the moisture content, time and temperature, the latter being the most important factor. High moisture content induces rapid urease inactivation for the soybeans treated by the convection and radiation-type equipments. Conversely, inhibited inactivation is encountered with the extruded soybeans due to the strong cohesive forces amongst ground soybeans at a higher moisture content of 24% d.b., inducing poor mixing behaviour in the barrel. The results from the lab- and commercial-scale equipment are shown to have higher soluble protein content in 0.2% KOH for the infrared-treated soybeans, comparing to the other techniques. Extrusion consumed the largest quantity of energy followed by the fluidized bed with no recycled air and the micronizer becomes the most effective energy utilization.
© 2004 Elsevier Ltd. All rights reserved.

Keywords: Anti-nutritional factors; Protein solubility; Urease; Soybean

1. Introduction

Osborne and Mendel (1917) first proposed the necessity of heating raw soybeans in order to improve their nutritional values since raw soybeans contain anti-nutritional factors, i.e. trypsin inhibitors, hemagglutinins, lectins and saponins, which cause ineffective food utilization, thereby depressing the growth rate of animals (Hensen, Flores, Tanksley, & Knabe, 1987; Liener, 1994; Vandergrift, Knabe, Tanksley, & Anderson, 1983). Methods of heat treatment used in the feed meal industries can generally be divided into three techniques: radiation, conduction and convection (Fasina, Tyler, Pickard, Hua Zheng, & Wang, 2001; Mustakas & Griffin, 1964; Soponronnarit, Swasdisevi, Wetchacama, & Wutiwiwatchai, 2001).

Within radiation techniques, infrared is one of the common methods. Infrared radiation is not entirely a surface heating method, but the energy rather penetrates inside the kernel in a non-contact mode. Two conventional types of infrared radiators are commercially used, namely, electric radiators and gas-fired radiators, the latter mostly available to the feed meal industries. For conduction heating, the material is heated at the surface and heat is thereafter transferred to the interior of the material. Solids are directly contacted with the energy source. Extrusion employs this heating method to inactivate such anti-nutritional factors (Camire, Camire, & Krumhar, 1990; Mustakas & Griffin, 1964). In this process, whole or ground soybeans receive the heat not only from the barrel wall, but also from the friction forces between screw and barrel while being passed through the barrel. The extruder is operated in a continuous manner at high temperature for a relatively short time. Some experimental works have shown that soybeans treated by extrusion yield higher weight gain

* Corresponding author.
E-mail address: wsongchai@hotmail.com (S. Wiriyaumpaiwong).

0260-8774/$ - see front matter © 2004 Elsevier Ltd. All rights reserved.
doi:10.1016/j.jfoodeng.2004.01.036

and animal growth than the infrared roasted soybeans (Faber & Zimmerman, 1973; White, Greene, Waldroup, & Stephenson, 1967).

Convective heating involves the transfer of heat between the kernels and the heating media, in which heat from the media is conveyed to the kernels. Heating efficiency depends on how well the media and kernels contact. Fluidized bed and spouted bed heating systems are two of the most popular convective heating techniques. A rigorous mixing between solids and media occur in these heating systems, consequently enhancing heat and mass transfer rates. The important characteristics of fluidization and spouted bed are that the particles are suspended in the medium and move randomly like a fluid. This behaviour makes it less variable in quality. The use of a hot air temperature above 120 °C for the fluidized bed can reduce the urease activity to a pH difference of 0.3 or lower (Osella, Gordo, González, Tosi, & Ré, 1997; Soponronnarit et al., 2001). This value is an upper limit which is still safe for the feed meal products (ASA, 1990) and the lower limit should not be below 0.02 pH difference: if lower, it becomes overcooked.

In the present work, three processes were used on a laboratory-scale to investigate the urease inactivation and protein solubility of soybeans. These were spouted bed, infrared radiation and twin-screw extrusion. Besides the urease inactivation and protein solubility, the drying rate was studied using only the spouted bed and infrared radiation since the moisture contents at any time of extrusion process cannot be measured. In addition, the three different heat treatments being operated in the feed meal industries were comparatively studied. These were micronization, single-screw extrusion and fluidized bed. Their performance was evaluated in terms of energy consumption in addition to their urease activity and protein solubility. It was anticipated that this work would lead to an understanding of the behaviour of urease inactivation for each heat treatment technique and give some information about what technique should be appropriate for treating the raw soybeans for the feed milling or related industries.

2. Materials and methods

2.1. Heat treatment technique

2.1.1. Fluidized bed

An industrial-scale fluidized bed dryer with a feed rate of 2 ton/h capacity as shown in Fig. 1 was used, consisting of a drying chamber with a dimension of $0.7 \times 2.1 \times 1.3$ m^3. A diesel oil burner was used to heat the air with an average temperature of 164.5 °C. A thermostat was used to control the temperature with an accuracy of ±1 °C. A backward curved blade centrifugal fan driven by a 50 kW motor was used to supply hot air to the dryer. The exhausted air was discharged to the atmosphere. Grain in the drying chamber was forced by the hot air to move forward until it reached the dryer exit.

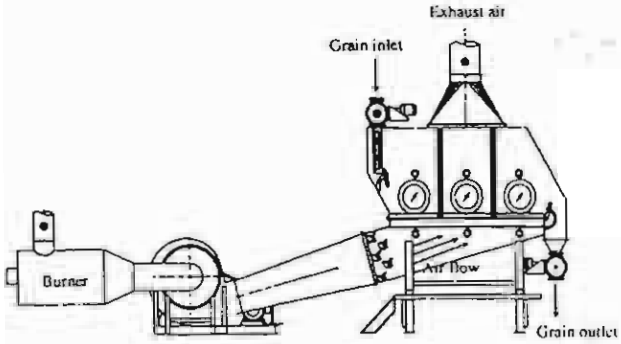


Fig. 1. Schematic diagram of fluidized bed dryer (industry).

2.1.2. Spouted bed

The schematic diagram of a two-dimensional spouted bed dryer with draft plates in a laboratory-scale unit is shown in Fig. 2. The inlet cross sectional area was 4×15 cm^2, drying chamber $60 \times 15 \times 50$ cm^3, spout width 8 cm and entrance height 12.5 cm. The selected values of spout width and entrance height were appropriate for steadily maintaining the spouting behaviour and the transport of soybeans from the downcomer to the spout region, where intensive mixing between hot air and soybeans takes place. A 24 kW electrical heater was used to heat the air. A PID controller handled temperature with an accuracy of ±1 °C. A backward-curved blade centrifugal type fan driven by a 2.2 kW motor was used to supply hot air into the dryer. The airflow rate was controlled by a variable speed unit. The heated air flowed through the spouted bed dryer in which 90% of total airflow rate passed between the draft plates, with the remaining proportion flowing through the downcomer. After that, some of the exhaust air was discharged to the atmosphere and the remaining air was recycled and then mixed with fresh air.

2.1.3. Extrusion

The extruders used in this study were the single-screw type for soybean treatment on a commercial-scale (95 kW insta-pro model 2500) and a counter-rotating, intermeshing twin-screw type for the laboratory-scale experiments (4.8 kW Thermo Haake). Fig. 3 shows the schematic diagram of the commercial single-screw extruder with a pre-conditioner. The pre-conditioner is an additional part and acts as a pre-heating unit for the product before it enters the system, thereby increasing the extruder capacity and reducing the wear and tear on the machine. A steam jacket in the pre-conditioner was

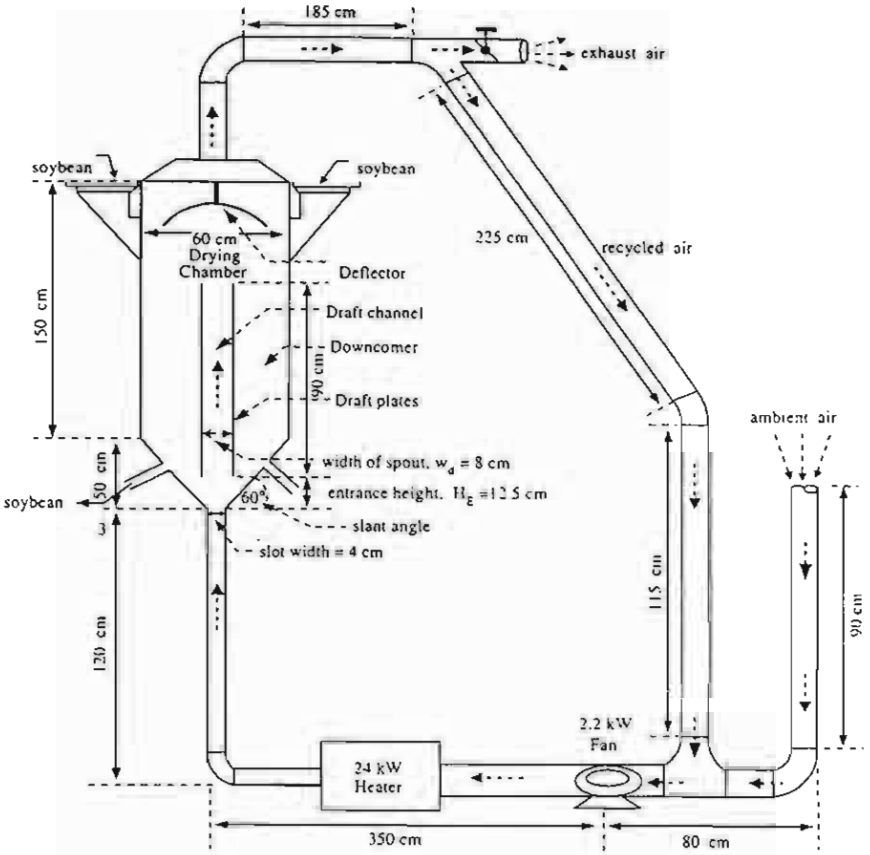


Fig. 2. Schematic diagram of a two-dimensional spouted bed dryer (lab-scale).

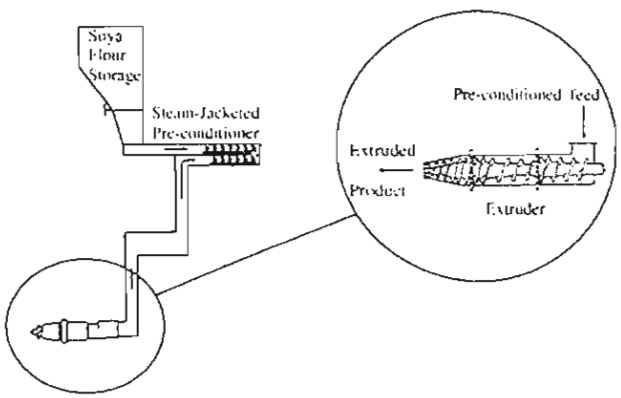


Fig. 3. Schematic diagram of single-screw extruder with a pre-conditioner (industry).

fed with low-pressure steam (0.9 MPa). The product was then forced through a barrel with variable screw configurations and eventually reached a die at the end of the barrel. The heat generated from the friction and shearing forces in the extruder barrel typically raised the temperature to 104–115 °C at a feed rate of 1 ton/h, corresponding to a retention time of 2.9 min. In the laboratory experiment, the extruder used was the twin-screw type for which the screw configuration is shown in Fig. 4. At the inter-screw region, it exhibited very complex flow. This would induce the shear and extensional flows required for mixing. The twin-screw extruder consists of a barrel, a 4.8 kW motor to drive the screws and a 1 kW electrical heater.

2.1.4. Infrared radiation

Both an industrial-scale micronizer and a laboratory-scale single layer infrared dryer were used. The micronizer, with a capacity of 1.5 ton/h as shown in Fig. 5, consisted of the three main components, namely, a

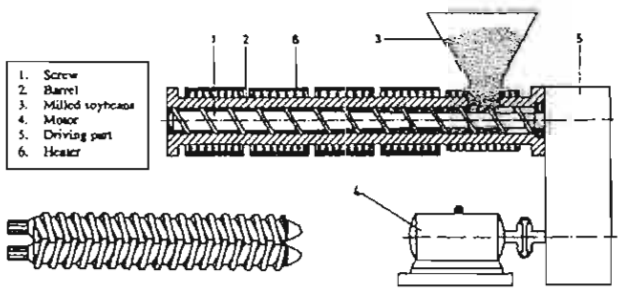


Fig. 4. Schematic diagram of twin-screw extruder (laboratory).

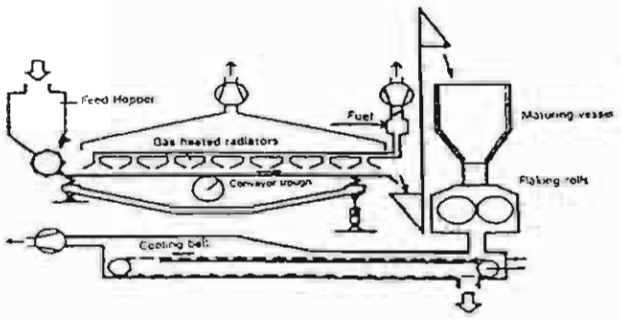


Fig. 5. Schematic diagram of micronizer being operated in feed meal industry (Micro Red 20 purchased from Micronizing Company (UK) Limited).

feeder, vibrating unit and infrared radiation source. This generated infrared wavelengths of 1.8–3.4 μm. Radiation is emitted when ceramic tiles are heated by the ignition of a pre-mixed air and natural gas or LPG. Soybeans, moved on the vibrating screen, driven by a 6 kW motor, then absorbed the energy from the heated ceramics. The environmental temperature within chamber was approximately 180–220 °C which was high enough to eliminate the anti-nutritional factors. For the laboratory infrared equipment, the system contains a drying chamber fitted with two 650 W electrical infrared bulbs and a tray to hold the soybeans. The temperature used in the experiments was in the range of 100–160 °C, the highest temperature that the components of dryer could withstand without any damage. A schematic diagram for the single layer infrared dryer is shown in Fig. 6.

2.2. Materials

2.2.1. Commercial-scale operation

Raw soybeans, with a moisture content of 12% d.b., used for producing the animal feed, were stored in silos in order to prepare the raw material before treating by the fluidized bed dryer and micronizer. Soybeans treated by these techniques possessed full kernels. The residence times of soybeans in the processes were approximately 3–4 min for the micronizer and 10 min for the fluidized bed. However, the kernels were ground to soy flour for the extrusion process due to the constraint of the screw gap. The initial moisture content ranged from 13% to 14% d.b. for the extrusion. The moisture contents of samples were determined at a temperature of 103 °C for 72 h, according to ASA standard (1990). The product temperature was measured by using a type K thermocouple submerged into the grains in the container at the end of the heating system.

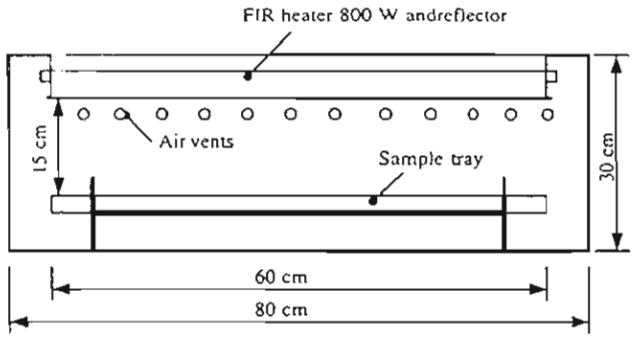


Fig. 6. Schematic diagram of single layer infrared dryer (laboratory).

2.2.2. Laboratory-scale operation

Soybeans were rewetted to obtain moisture contents between 14% and 28% d.b. and then kept in a temperature-controlled room between 8 and 10 °C for 5 or 7 days. Before starting the experiments, the soybeans were placed in ambient condition until the grain temperature rose to room temperature.

2.3. Thin layer drying model

Drying of most agricultural materials occurs in the falling rate period, during which diffusion mechanisms dominate. When the main resistance to the water diffusion inside a kernel occurs at the outer layer of the kernel, a semi-empirical grain drying model can reasonably be used to describe its transport. In the model, the rate of moisture loss of a single kernel surrounded by air is proportional to the difference between the kernel moisture and its equilibrium moisture content, and the drying rate can thus be expressed by

$$\frac{d\overline{M}}{dt} \doteq -k(\overline{M} - M_{eq}) \tag{1}$$

By integrating Eq. (1) from time 0 to t, corresponding to moisture content change from M_{in} to M, the grain drying equation is obtained as

$$\frac{\overline{M}(t) - M_{eq}}{\overline{M}_{in} - M_{eq}} = \exp(-kt) \tag{2}$$

where k is the drying constant, $\overline{M}_{in}$ is the initial moisture content and M_{eq} is the equilibrium moisture content. The drying constant relies upon the heat treatment used, in addition to temperature and moisture content. The equilibrium moisture content for drying at above the normal boiling point temperature may be reasonably assumed to be zero.

2.4. Quality

Urease activity was determined by following the AACC method 22–90 (AACC, 1995). Urease was used as a measure of the level of trypsin inhibitor (Cheong, 1997). The difference between the pH of the test sample and the pH of the blank was used as an index of urease

Table 1
The operating condition of each heating process

Processing method	Raw materials	IMC (% d.b.)	Temperature[a] (°C)
Twin-screw extruder (laboratory)	Milled soya flour	18, 24, 27	100, 110, 120, 130, 140
Spouted bed (TDSB) (laboratory)	Full-fat soybean	14, 22, 28	120, 130, 140, 150
Single layer infrared dryer (laboratory)	Full-fat soybean	18, 24, 27	100, 120, 140, 160
Single-screw extruder (commercial-scale)	Milled soya flour	13	104–115
FBD (commercial-scale)	Full-fat soybean	12	160–170
Micronizer (commercial-scale)	Full-fat soybean	11.4	180–220

Note: FBD: Fluidized bed dryer; TDSB: Two-dimensional spouted bed; IMC: Initial moisture content.
[a] Accuracy of temperature controller ±1 °C.

activity. The pH difference value was measured by the Mettler pH meter (Model No. DELTA 340) and was then converted to the percentage of urease inactivation by the equation proposed by Savage, Wei, Sutherland, and Schmidt (1995). The acceptable level of pH difference should be in the range lower than 0.3, corresponding to the urease inactivation of 97%.

According to AOCS method Aa 5-38 (AOCS, 1984), the percentage of crude protein can be calculated by percentage of nitrogen multiplied by a nitrogen-to-protein factor (6.25) and the percentage of nitrogen in the soybean was estimated by the Kjeldahl method, using a TKN analyzer (Model No. Antek 9000N). Protein solubility indicates the level of protein dispersion in a 0.2% KOH solution. According to Cheong (1997), protein solubility should be in a normal range between 70% and 85%. If its value is lower than 70%, it means the soybean is overcooked, but if higher than 85%, soybean is insufficiently cooked. Protein solubility is calculated by

$$\text{Protein solubility} = \frac{\text{nitrogen of the supernatant in 0.2\%KOH solution}}{\text{crude protein}} \times 100 \quad (3)$$

In addition, the lysine in soy protein was also analyzed by the AccQ-Tag method. Soybean sample was hydrolyzed at 110 °C for 22 h with AccQ-Flour reagent. Finally, it was analyzed by high performance liquid chromatography (Model No. Waters Lambda-Max 481).

The experimental conditions for treating soybeans in each process are shown in Table 1.

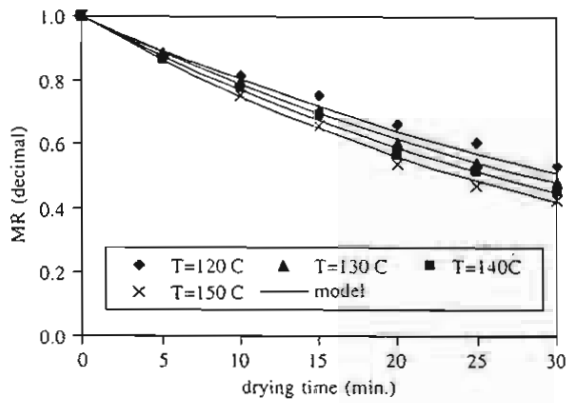


Fig. 7. Comparison of moisture ratio between experiment (dots) and prediction (lines) at different temperature and initial moisture content of 28% dry basis using two-dimensional spouted bed (lab-scale).

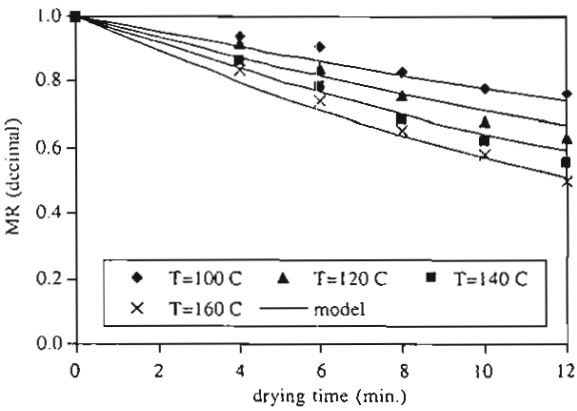


Fig. 8. Comparison of moisture ratio between experiment (dots) and prediction (lines) at different temperature and initial moisture content of 24% dry basis using single layer infrared dryer (lab-scale).

3. Results and discussions

3.1. Reduction of moisture content

The drying rates of the soybeans in the spouted bed and single layer infrared dryer at different inlet air temperatures are shown in Figs. 7 and 8 respectively. The characteristics of the drying curves from such heating methods are very similar, the moisture exhibiting a typically decrease with drying time, but the rate of moisture removal by spouted bed is noticeably lower, as indicated by the slope of the drying curve. The lower drying rate is due to the fact that the energy from the hot air is conducted to the water inside the kernel via the complex physical structure of the food material and this structure resists the heat transport. In addition, the

inherent characteristics of the spouted bed that consists of spout and downcomer regions result in slow water transport inside the kernels since the kernels stay in the downcomer, where the rates of heat and mass transfer are very poor, for a relatively longer time than that spent in the spout region. The influence of temperature on the drying rate can also be observed in these figures: the higher the temperature the faster the moisture decrease, as expected. This factor has a profound effect whilst the initial moisture content has a lesser contribution. The data of moisture effect was not shown here.

Knowing the experimental value of moisture content at various times and conditions, the drying constant was determined using a non-linear regression approach. To obtain this parameter, the drying constant formulation was correlated with temperature and initial moisture content in the following form:

$$k = AM_{in}^{B}\exp(-E/T_{abs}) \tag{4}$$

where T_{abs} is the absolute temperature (K) and A, B and E are the constant parameters, all of which depend on the heating technique. Substituting Eq. (2) into Eq. (1), it was then fitted to the experimental data by a single-step regression. The results of regression analysis using the original data are shown in Table 2, with the values of R^2 and MSE, demonstrating the adequacy of the proposed model. The mean sum squares of error (MSE) is defined as (López, Piqué, Romero, & Aletá, 1998)

$$\mathrm{MSE} = \frac{\sum_{i=1}^{n}(MR_{obs} - MR_{pre})^2}{n - z} \tag{5}$$

where MR_{obs} is the experimental moisture ratio, MR_{pre} is the predicted moisture ratio, n is the number of data points and z is the number of unknown parameters. As seen in Figs. 7 and 8, the thin layer drying reasonably predicted the data over the drying conditions.

The result of the calculated drying constants at various temperatures for the spouted bed and infrared heating is shown in Fig. 9, indicating a significantly higher value of the drying constant for the infrared heating compared to that for the spouted bed. Moreover, the drying constant for the infrared heating was strongly affected by temperature whilst it was only slightly changed for the spouted bed. These results emphasize that the infrared technique shows a higher potential capability for removing water and its capability is more effective when operated at higher temperature, as indicated by the positive slope in Fig. 9. The experimental results for the other initial moisture contents show the same trend as found in Fig. 9.

Table 2
Drying constants of spouted bed and single infrared dryer (lab-scale)

Processing method	A	B	E	R^2	MSE
Spouted bed dryer	0.7652	0.0559	−1467.12	0.98	0.0004
Single layer infrared dryer	6.72705	−0.22633	−2212.67	0.97	0.0005

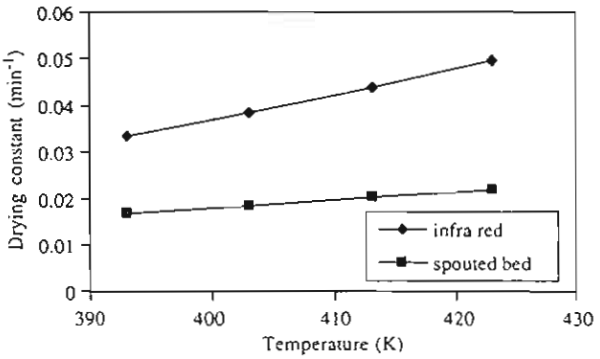


Fig. 9. Relationship between drying constant and inlet air temperature when using two-dimensional spouted bed and single layer infrared dryer (M_{in} = 18% d.b.).

3.2. Urease activity and urease inactivation

Figs. 10 and 11 show the urease activity, measured as pH difference, and the percentage of urease inactivation in the soybeans treated by the respective spouted bed and single layer infrared techniques. The urease activity of raw soybeans is approximately 2.2–2.5 at the beginning and reduced with drying time. In some cases, insufficient inactivation occurs, in particular when raw soybeans with a low initial moisture content are treated at a low temperature for a certain period. This can be observed from the soybeans at initial moisture contents below 24% d.b. which were treated by the spouted bed at a lower temperature of 130 °C and infrared radiation at a lower temperature of 120 °C. The percentage of urease inactivation at the end is between 60% and 80% for times of 30 min in the spouted bed and 12 min in the infrared. Since the treated soybeans became brown in colour, we were not interested in examining them at longer treating times although it was expected that the pH difference would decrease to acceptable limit.

Adequate inactivation, implying a pH difference lower than 0.3, can be accomplished in the raw soybeans at 22–24% d.b. using a temperature of 140 °C for 30 min in the spouted bed and 12 min in the infrared. Under such heating conditions, the moisture content at the end was about 14% or 15% d.b. at which it is safe for long-term storage. When the initial moisture content increased beyond 24% d.b., the treating temperature or the treating time for sufficient inactivation can be reduced. It needs 30 min at 120 °C and 25 min at 130–140 °C for the spouted bed as well as 10 min at 140–160 °C for the infrared technique. The reduction in such operating parameters is due to the fact that high initial moisture favours rapid cooking (Wright, 1981).

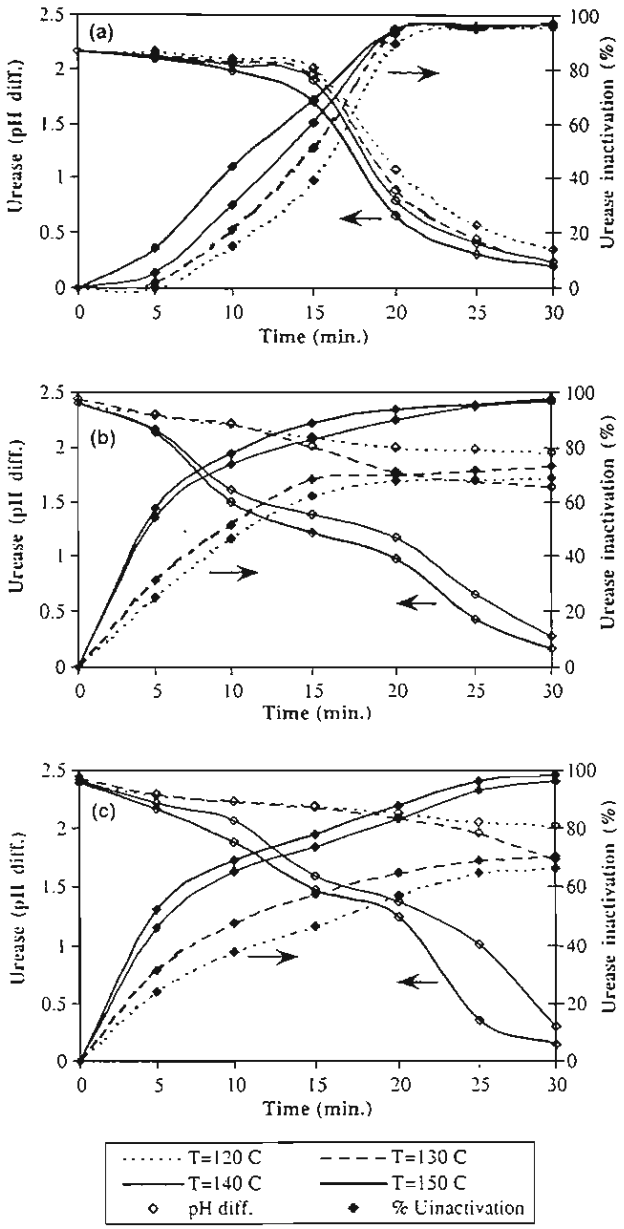


Fig. 10. Effect of moisture on the urease activity and percentage of urease inactivation for two-dimensional spouted bed dryer (a) 28%, (b) 22% and (c) 14% d.b.

In addition to the lab-scale test, we also examined the dry soybean quality after treating in large-scale equipment at commercial sites. The result from the industrial-scale micronizer is shown in Table 5 and reveals that an environmental temperature between 180 and 220 °C, corresponding to a grain temperature of 119–122 °C, yields a pH difference of 0.1–0.16 at treating times of less than 5 min. For the continuous fluidized bed dryer, in which the kernels are rigorously mixed, the colour of the treated soybeans was rather brown and their pH difference fell into the acceptable range, being between 0.21

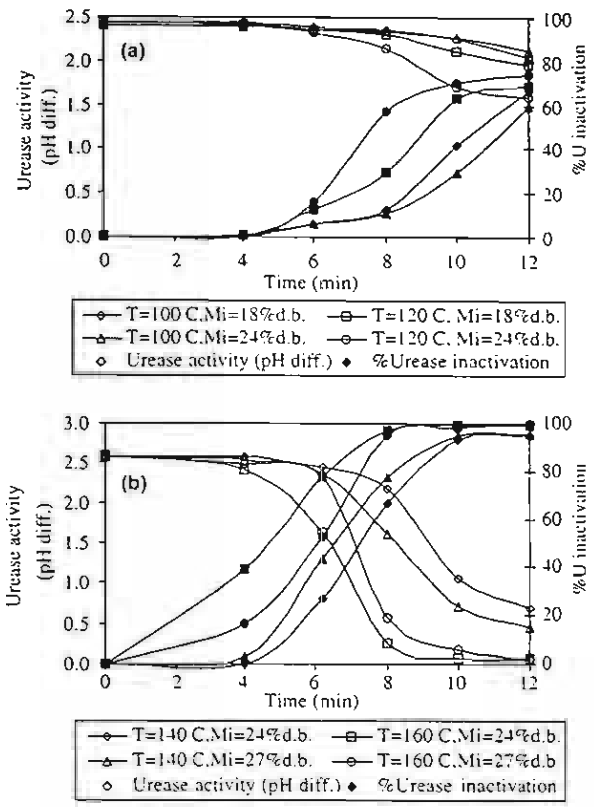


Fig. 11. Urease activity (pH difference) and urease inactivity using single layer infrared dryer (lab-scale). (a) Operating at dryer room temperature of 100 and 120 °C and initial moisture content of 18% and 24% d.b. (b) Operating at dryer room temperature of 140 and 160 °C and initial moisture content of 24% and 27% d.b.

and 0.27 for treatment time of 10 min using inlet air temperatures of 164.5 °C as shown in Table 6. These data also indicate that the extent of urease inactivation at the exit from the dryer is almost uniform although there is a certain degree of mixing of solid particles while being moved in the dryer. To avoid the undesirable colour, temperatures below 160 °C can be employed, but for inactivating urease, times should be longer than 10 min (Osella et al., 1997). This suggestion is for dry soybean. For moist soybeans, it requires treatment times shorter than 10 min.

These findings demonstrate that intensive heating techniques i.e. fluidized bed and infrared require a relatively short treatment time for the inactivation whilst mild heating techniques like a spouted bed takes longer. The time required was approximately 25 min at 150 °C and 30 min at 140 °C. The longer time for the spouted bed is caused by the particles remaining in the downcomer due to the low airflow rate in this region.

Extrusion technique is distinctly different to the above-mentioned techniques in that the raw soybean kernels must be ground before passing through the extruder. The operating conditions for the twin-screw

extruder and analytical results after passing the extruder are presented in Table 3. The retention time varied between 2.2 and 4.8 min, depending on the screw speed, and the heating temperature was in the range of 100–140 °C corresponding to product temperatures of 91–130 °C, respectively. The results of final moisture content and urease activity of the extruded soybeans are within the range recommended by the American Soybean Association (1990), except for run nos. 1 and 8, both of which had pH differences that were nearly as high as raw soybeans. This implies that the urease is not inactivated at product temperatures below 100 °C even though the retention time or initial moisture content increased. When the product temperature is 100 °C, corresponding to a heating temperature of 110 °C or higher, the pH difference of the treated samples lies in the standard range.

In addition to the temperature, the initial moisture content also had some effects. The degree of urease inactivation for the extruded soybeans trends to contradict those results from the spouted bed and infrared systems: using soy flour with initial moisture content higher than 24% d.b. inhibits the urease inactivation as shown in Table 3. The corresponding values of pH difference become higher but still fall into the desirable range for feed meal products, except for run no. 17. These results clearly indicated that the addition of water into the soybean flour is unnecessary since an excessive quantity of water in soy flour causes a dense agglomeration of flour between the gap of the screws. The subsequent dispersion of soy flour within the barrel is not mixed well, so that the product unevenly absorbs the heat generated in the barrel. High moisture content also caused unstable operation. The extruder was automatically shut off, as is obvious from the experiment at a moisture content of 26% d.b. for run no. 24. Similar results for the urease inactivation were also found with the single-screw extruder as presented in Table 4, the pH difference being between 0.01 and 0.04.

3.3. Protein solubility

In addition to the urease activity, protein solubility is also an important parameter that characterizes the protein quality of soybean. During heating, in order to inactivate the anti-nutritional factors, proteins are denatured and protein aggregates are formed. The protein solubility of raw soybean in the present study was approximately 92.8% and it was reduced after heat treatment. The magnitude of its reduction depended on

Table 3
The operating condition and analytical results after passing extruder (lab-scale)

Run no.	Screw speed (rpm)	Residence time (min)	Temperature (°C)		Moisture (% d.b.)		Urease activity (pH diff.)	Protein solubility (%)
			Heating temperature	Product temperature	Inlet	Outlet		
1	100	3.4	100	91	18.1	15.8	2.27	83.0
2	100	3.4	120	112	18.1	14.8	0.03	78.8
3	100	3.4	140	129	18.1	10.1	0.01	72.8
4	120	2.2	110	100	23.8	19.9	0.19	84.3
5	120	2.2	120	109	23.8	18.1	0.06	81.4
6	120	2.2	130	118	23.8	17.1	0.07	79.8
7	120	2.2	140	130	23.8	11.4	0.09	71.7
8	100	3.4	100	92	24.4	20.8	2.29	NA
9	100	3.4	110	103	24.4	20.0	0.01	NA
10	100	3.4	120	111	24.4	18.7	0.02	NA
11	100	3.4	130	121	24.4	17.6	0.02	NA
12	100	3.4	140	130	24.4	11.5	0.01	NA
13	80	4.8	110	100	24.4	18.8	0.05	NA
14	80	4.8	120	111	24.4	17.2	0.03	NA
15	80	4.8	130	120	24.4	15.3	0.03	NA
16	80	4.8	140	131	24.4	11.1	0.02	NA
17	120	2.2	110	100	26.9	21.8	0.36	81.4
18	120	2.2	120	113	26.9	18.3	0.24	78.6
19	120	2.2	130	119	26.9	16.3	0.26	75.9
20	120	2.2	140	128	26.9	12.0	0.14	73.3
21	100	3.4	110	100	26.9	20.7	0.15	NA
22	100	3.4	120	112	26.9	17.3	0.15	NA
23	100	3.4	130	118	26.9	15.8	0.21	NA
24	100	–	140	–	26.9	–	–	–

Note: Urease activity (pH difference) of raw soybean = 2.33–2.46.

Table 4
Full-fat soy flour analysis after passing single screw extruder (commercial-scale)

Time (min)	Temperature (°C)		Moisture content (% d.b.)		Urease activity (pH change)	Protein solubility (%)
	Pre-conditioner	Product	Inlet	Outlet		
15	89	105	12.9	11.4		
30	88	104	13.0	11.6	0.04	79.3
45	91	108	13.4	12.1		
60	92	111	14.1	12.5	0.04	76.4
75	92	110	12.9	11.3		
90	92	111	12.7	11.1	0.03	75.0
105	94	113	12.9	11.6		
120	93	115	13.5	11.3	0.03	72.8
135	93	114	13.3	11.8		
150	92	112	12.9	11.4	0.01	75.6
165	92	113	12.9	11.2		
180	92	112	12.8	11.7	0.01	76.2

the heating process and operating conditions, i.e. temperature and time.

The results of protein solubility for the soybeans treated by different types of laboratory-scale heating processes are shown in Fig. 12. The data presented were measured at the ends of the experiment, namely, after 30 min in the spouted bed, 3.4 min in the extruder and 12 min in the infrared. It is evident that the protein solubility for the soybeans treated by various thermal processes declines to the recommended range, except that of soybeans processed with the spouted bed and infrared at 120 °C which was above 85%. However, this temperature is not high enough to inactivate the urease to the level lower than 0.3 pH difference within a given time. To maintain the product in the range of 70–85% together with the acceptable pH difference, soybeans should therefore be treated at a temperature higher than 140 °C.

As noticed, the quality from each technique is rather different; the higher protein solubility is obtained with the single layer infrared and spouted bed (78–89%) and the lower one is obtained from the screw extruder (74–78%). This can be seen easily at 140 °C where the quantity of soluble protein in 0.2% KOH solution ranges between 82% and 84% for the spouted bed and infrared and becomes lower for the extruded soybeans with a value of 73%. The lower soluble proteins are attributed to the grounded soybeans absorbing the heat uniformly, unlike the other two techniques where the full kernels retard the heat penetration. Moreover, this effect results in a higher degree of urease inactivation, along with shorter treating time, when compared to the other heating techniques at the same temperature. To obtain a higher protein solubility, while maintaining an adequate level of urease inactivation, the extruder should not be operated at a temperature higher than 130 °C. The results of heat treatment by the spouted bed and infrared radiation indicated that the infrared seems to be a more attractive technique since the rates of water transport and urease inactivation using this approach are enhanced, along with a high soluble protein content.

Fig. 12 also shows the influence of temperature on the protein solubility, indicating the lower amount of soluble proteins associated with higher temperature. This is

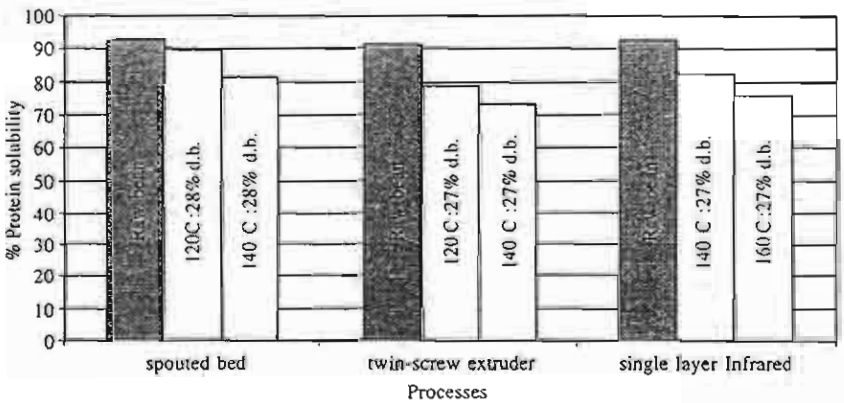


Fig. 12. Comparisions of the percentage of protein solubility between two-dimensional spouted bed, single layer infrared dryer and twin-screw extruder (lab-scale).

expected since when more thermal energy is transferred, the treating temperature is increased.

The change in protein solubility of dry soybeans after treating with the single-screw extruder, micronizer and fluidized bed dryer is shown in Tables 4–6, respectively. The protein solubility of soybeans from each heat treatment technique varies in a range of 73–85%, implying properly cooked soybeans. The soluble proteins of treated soybeans, when compared with those obtained from the extruder and fluidized bed, are relatively higher with the micronizer. From a qualitative point of view, these results are in accordance with the one from the lab-scale infrared dryer as illustrated in Fig. 12, showing higher protein solubility.

3.4. Lysine

Some interesting conditions of each process for inactivating urease enzyme were chosen to determine the remaining lysine as follows: 130 °C, 18% d.b. and 2.2 min for the twin-screw extruder; 140 °C, 14% d.b. and 10 min for the fluidized bed dryer; 140 °C, 14% d.b. and 30 min for the spouted bed dryer; and 160 °C, 18% d.b. and 12 min for the single layer infrared dryer. Table 7 shows the remaining lysine in the soybeans after treatment with the twin-screw extruder, fluidized bed, spouted bed and infrared driers. The percentage of lysine was 5.25% for untreated soybeans and was decreased by 0.8–1.2% in each heat treatment technique. The statistical analysis using a t-test approach indicated that the amounts of remaining lysine from such techniques were insignificantly different ($p < 0.05$).

Table 5
Full-fat soybean analysis after passing the micronizer (commercial-scale)

Time (min)	Product temperature (°C)	Moisture content (% d.b.)		Urease activity (pH change)	Protein solubility (%)
		Inlet	Outlet		
15	121	11.6	6.9		
30	120	11.5	6.8	0.10	83.5
45	122	11.6	7.0		
60	120	11.5	6.9	0.10	84.8
75	119	11.5	7.1		
90	120	11.6	7.1	0.10	85.9
105	121	11.6	6.7		
120	121	11.5	6.9	0.12	74.1
135	122	11.6	7.0		
150	119	11.6	7.0	0.16	76.8
165	120	11.6	6.9		
180	120	11.5	6.9	0.16	82.2

Table 6
Full-fat soybean analysis after fluidized bed heating process (commercial-scale)

Time (min)	Moisture content (% d.b.)		Urease activity (pH change)	Protein solubility (%)
	Inlet	Outlet		
15	11.8	0.8		
30	11.9	0.9	0.25	77.6
45	11.9	1.2		
60	12.3	1.3	0.21	74.4
75	11.9	1.0		
90	11.8	1.0	0.26	74.4
105	12.1	1.4		
120	12.3	1.6	0.27	75.6
135	12.3	1.5		
150	12.4	1.6	0.24	72.6
165	12.3	1.4		
180	12.3	1.4	0.26	74.6

3.5. Energy consumption

Table 8 shows the energy consumptions of commercial-scale equipment, i.e. extruder, micronizer and fluidized bed dryer for inactivating the urease in the dry soybeans. The electrical energy consumption represented in the table was calculated by multiplying by a factor of 2.6, a conversion factor for converting secondary to primary energy, with the experimentally measured electrical energy. It can be seen that the extruder consumed about 928 MJ/ton of product, which is 1.5 times of the thermal energy utilized. The opposite results were obvious with the fluidized bed dryer and micronizer where both types of equipment use high levels of thermal energy, with amounts of 550 MJ/ton of product for the micronizer and 911 MJ/ton of product for the fluidized bed.

In calculating the energy cost, we assumed that LPG gas cost was 20 baht/kg and electricity cost was 3 baht/kW h (42.3 baht = 1$). The calculated total energy costs were 260, 429, 547 baht/ton of product for the micronizer, fluidized bed dryer, single-screw extruder, respectively, the first technique providing the lowest operating cost. The energy cost for the fluidized bed was relatively high since the industrial dryer did not have an air recycling system although the exhaust air had a temperature higher than 100 °C and, therefore, a high reuse potential. The ineffectively utilized energy consumption is a consequence. However, if the exhaust air was fully recycled, the thermal energy might possibly have savings of 74%, compared to no air recirculation. The resulting total energy cost would be reduced and become lower than that spent in the micronizer and extruder by approximately 39% and 71%, respectively.

In addition to the energy cost, attention should be paid to the equipment cost as well. As informed by the feed milling industries, fluidized bed dryer, micronizer and extruder, all of which have a capacity of 1–1.5 ton/h, cost 375,000, 13,000,000 and 3,200,000 baht, respectively (SPM animal feed and Saha farm company limited). According to this information including the energy cost and the quality of treated soybeans, it is likely that

Table 7
Percent lysine in soybean after treatment for twin-screw extruder, fluidized bed, spouted bed, and single layer infrared dryer (lab-scale)

Heating processes	% Lysine
Untreated soybean	5.25
Heat treatment with two-dimensional spouted bed dryer[a]	4.15
Heat treatment with single layer infrared dryer[b]	4.05
Heat treatment with fluidized bed dryer[c]	4.45
Heat treatment with twin screw extruder[d]	4.15

[a] Heating temperature of 140 °C and initial moisture content of 14% d.b. for 30 min.
[b] Heating temperature of 160 °C and initial moisture content of 18% d.b. for 12 min.
[c] Heating temperature of 140 °C and initial moisture content of 14% d.b. for 10 min.
[d] Heating temperature of 130 °C and initial moisture content of 18% d.b. for 2.2 min.

Table 8
Energy consumption of commercial-scale extruder, micronizer, and fluidized bed soybean dryer (FBD)

Items	Extruder	Micronizer	FBD	FBD (assumed fully recycle)
Testing hours	3	3	3	
Capacity (ton/h)[a]	1	1.5	2	
Treatment temperature (°C)[a]	110	120	148	
Inlet moisture content (% d.b.)[a]	13	12	12	
Outlet moisture content (% d.b.)[a]	12	7	1	
Electrical energy consumed (MJ/ton of product)	928	94	204	204
Thermal energy consumed (MJ/ton of product)	625	550	911	233

[a] Average value.

fluidized bed technique is the most attractive alternative technique for replacing conventional methods such as extrusion and infrared radiation.

4. Conclusions

The rate of water removal in soybean during the course of drying by spouted bed and infrared techniques shows a remarkable difference, the latter exhibiting more potential. Such difference is shown by the drying constant, which can be statistically determined by the semi-empirical drying equation. The drying constant was correlated with moisture content and temperature in a modified Arrhenius form. Both factors also importantly affect the urease inactivation where high moisture content and temperature induce rapid inactivation for the soybeans treated by the spouted bed and infrared radiation whilst the first factor results in slow inactivation for the extruded soybeans. The results of the soybeans treated by spouted bed, extruders, fluidized bed and infrared radiation show that each heat treatment technique appears to be capable of satisfactorily inactivating urease, but provides radical differences in the amounts of soluble proteins, the highest protein solubility being produced by the infrared treatment whilst the lowest one was obtained by extrusion. The amounts of lysine remaining after treatment by the different techniques were similar. The experimental results from the feed milling industries showed that the highest total energy used for treating soybeans was required by the extruder followed by the fluidized bed technique with the micronizer requiring the least amount. There is a high possibility of using the fluidized bed with an air recirculation system for inactivating anti-nutritional factors and improving energy utilization.

Acknowledgements

The authors would like to thank the Thailand Research Fund for the financial support this work. In addition, we wish to thank the SPM animal feed company limited and the Saha farm company limited for their cooperation while working at industrial sites.

References

AACC. *Approved method of the American Association of Cereal Chemist (9th ed.)*. St. Paul, MN: AACC, 1995.
AOCS. *Official and Tentative Methods of the American Oil Chemists' Society (3rd ed.)*. Campaign, IL: AOCS, 1984.
ASA. *Fullfat Soybeans Handbook of American Soybean Association*. Singapore, 1990.
Camire, M. E., Camire, A., & Krumhar, K. (1990). Chemical and nutritional changes in foods during extrusion. *Critical Review in Food Science and Nutrition, 29*, 35–57.
Cheong, Y.L. (1997). Fullfat soybean meal production and utilization. *Technical Bulletin of American Soybean Association*, Singapore.

Faber, J. L., & Zimmerman, D. R. (1973). Evaluation of infrared-roasted and extruder-processed soybeans in baby pig diets. *Journal of Animal Science, 36*, 902–907.

Fasina, O., Tyler, B., Pickard, M., Hua Zheng, G., & Wang, N. (2001). Effect of infrared heating on the properties of legume seeds. *International Journal of Food Science and Technology, 36*, 79–90.

Hensen, B. C., Flores, E. S., Tanksley, T. D., Jr., & Knabe, D. A. (1987) Effect of different heat treatments during processing of soybean meal on nursery and growing pig performance. *Journal of Animal Science, 65*, 1283–1291.

Liener, I. E. (1994). Implications of antinutritional components in soybean foods. *Critical Review in Food Science and Nutrition, 34*. 31–67.

López, A., Piqué, M. T., Romero, A., & Aletá, N. (1998). Modelling of Walnut Sorption Isotherms. *Italian Journal of Food Science, 1*(10), 67–74.

Mustakas, G. C., & Griffin, E. L., Jr. (1964). Production and nutritional evaluation of extrusion-cooked full-fat soybean flour. *The Journal of the American Oil Chemist' Society, 41*, 607–614.

Osborne, T. B., & Mendel, L. B. (1917). The use of soybean as food. *Journal of Biological Chemistry, 32*, 369.

Osella, C. A., Gordo, N. A., González, R. J., Tosi, E., & Ré, E. (1997). Soybean heat-treated using a fluidized bed. *Lebensmittel-Wissenschaft & Technologie, 30*, 676–680.

Savage, W. D., Wei, L. S., Sutherland, J. W., & Schmidt, S. J. (1995). Biologically active components inactivation and protein insolubilization during heat processing of soybeans. *Journal of Food Science, 60*, 164–168.

Soponronnarit, S., Swasdisevi, T., Wetchacama, S., & Wutiwiwatchai, W. (2001). Fluidised bed drying of soybeans. *Journal Stored Products Research, 37*, 133–151.

Vandergrift, W. L., Knabe, D. A., Tanksley, T. D., Jr., & Anderson, S. A. (1983). Digestibility of nutrients in raw and heated soyflakes for pigs. *Journal of Animal Science, 57*(5), 1215–1224.

White, C. L., Greene, D. E., Waldroup, P. W., & Stephenson, E. L. (1967). The use of unextracted soybeans for chicks. *Poultry Science, 46*, 1180–1185.

Wright, K. N. (1981). Soya meal. *JAOCS*, 294–300.

Available online at www.sciencedirect.com
SCIENCE DIRECT®
PERGAMON
Journal of Stored Products Research 40 (2004) 379–393
Journal of STORED PRODUCTS RESEARCH
www.elsevier.com/locate/jspr

Methodology for enhancing drying rate and improving maize quality in a fluidised-bed dryer

Somkiat Prachayawarakorn[a,*], Somchart Soponronnarit[b], Somboon Wetchacama[b], Kongsak Chinnabun[b]

[a] *Department of Chemical Engineering, Faculty of Engineering, King Mongkut's University of Technology Thonburi, Suksawat 48Rd, Tungkru, Bangkok 10140, Thailand*

[b] *School of Energy and Materials, King Mongkut's University of Technology Thonburi, Suksawat, 48Rd, Tungkru, Bangkok 10140, Thailand*

Accepted 30 January 2003

Abstract

A theoretical diffusion model for a single maize (*Zea mays* L.) kernel has been developed to describe moisture migration during drying and tempering stages. The effective diffusivity was determined experimentally at a range of temperatures between 90°C and 170°C with initial moisture contents of 37% and 43% dry-basis. The functional relationship between the diffusivity and temperature is analogous to a modified Arrhenius equation.

Two-stage drying including tempering between stages provides not only faster removal of moisture, but also a reduced number of stress cracks when compared to single-stage drying. However, the colour of the maize appears darker and more intense with longer tempering periods. To maintain maize quality and to reduce energy consumption, the results from the experiments and simulations are limited to temperatures of less than 150°C; high-moisture maize should be dried to 23% dry-basis and then tempered for 40 min.

The ambient-air velocity for cooling the tempered maize in a range between 0.075 and 0.375 m/s does not affect the maize quality as measured by the number of stress cracks and colour.
© 2003 Elsevier Science Ltd. All rights reserved.

Keywords: Ambient-air ventilation; Diffusion model; Fluidised bed; Quality; Tempering

1. Introduction

The main production of maize (*Zea mays* L.) in Thailand occurs in the rainy season. During this period, the moisture content of harvested maize is between 20% and 23% wet-basis. On some

*Corresponding author. Tel.: +66-2-4709220.
E-mail address: somkiat.pra@kmutt.ac.th (S. Prachayawarakorn).

0022-474X/03/$ - see front matter © 2003 Elsevier Science Ltd. All rights reserved.
doi:10.1016/S0022-474X(03)00029-8

occasions, it can be up to 25% wet-basis. A rapid moisture-removal rate is a necessary step in the prevailing hot and humid climate to achieve a safe moisture level and to inhibit the growth of microorganisms such as *Aspergillus flavus* Link ex Fr. and *Aspergillus parasiticus* Speare which are frequently found in maize from cultivation areas (Siriacha et al., 1991). Hot-air drying is likely to be an appropriate approach. Amongst the commercial dryer types, the fluidised-bed dryer is one that can suitably be applied (Mourad et al., 1995; Soponronnarit et al., 1997a).

With this technique, a stream of hot air is blown through a bed of solid particles which then behave like a liquid and can flow randomly along a bed with fluid-like properties. Solid particles are in intimate contact with the drying medium so that the temperature is rather uniform throughout the bed, although dispersion results in the moisture contents of individual grains being non-uniform. This provides advantages in that the inlet air temperature and superficial air velocity can be as high as possible. The resulting heat and mass transfer between solid and drying air are extreme, and hence some portions of the moisture concentrated near the grain surface can be transported rapidly through the environment whereas the inner surface is still wet, producing a large moisture gradient inside the grain. The moisture of the kernel is very difficult to remove in spite of the high convective mass transfer and the high capability of drying air, thus requiring rapid consumption of energy. In addition to energy consumption, such high drying rates in the fluidised bed may result in serious detrimental effects on maize quality. Thus, when maize is subjected to hot air for extended times, the dried maize surface becomes more and more brittle and eventually cracks or fractures. Soponronnarit et al. (1997b, 2001) investigated the effect of high temperatures (more than 100°C) on the physical damage to maize and soybean and reported that significant increases in stress cracks and in breakability occurred at reduced moisture contents.

Similarly, some early work on maize drying using a fixed-bed dryer showed that stress cracks increased with drying temperature, and conversely, reduced with increased humidity (Thompson and Foster, 1963; White and Ross, 1972; Otten et al., 1984; Estrada and Litchfield, 1993; Davidson et al., 2000). In their work, the temperature was in a range of 40°C to 100°C.

In addition to experimental studies, a theoretical framework has also been developed to explain qualitatively how crack generation develops in the porous materials while the material is being dried. It appears that moisture gradients are the main cause of the generation of the shrinkage stresses (Musielak, 2000). The kernels are in tension near the surface of the dried body, and in compression at the centre of the solid. If the relative humidity of the drying medium decreases with the increased temperature, then the stresses are considerably higher at higher values of the drying-medium temperatures.

In addition to stress cracking and breakage, the change in colour of the kernel caused by thermal effects is also important, particularly when drying involves very high temperatures. The colours in terms of a (red) and b (yellow) values measured on the Hunter scale were significantly affected by drying time (Soponronnarit et al., 1997b). The change of colour may result in a rapid drop in price and it is rejected by the food industries if premium quality is needed.

These considerations motivated us to explore methods of improving the process of fluidised-bed maize drying. One common approach used in the grain industry is tempering between drying stages. Some authors refer to this technique as dryeration. In the tempering stage, the maize leaving the dryer is kept in a closed bin with no air ventilation. During this period, moisture will not evaporate through the grain surface but is redistributed to achieve a uniform moisture content

throughout the kernel. Drying of paddy with tempering was investigated by Steffe and Singh (1980) who reported that head-rice yield could be improved as compared with single stage drying.

In the process of tempering, basic information that is needed in practice is how long the grain should be tempered to ensure a uniform moisture content. This is accomplished by formulating a mathematical model that enables the simulation of moisture movement inside the kernel. The model should be validated by experiments so that it can conveniently be used for engineering calculation.

The drawback of either semi-empirical or empirical models, which have frequently been used by some authors (Satayaprasert and Vanishsriwatana, 1992; Soponronnarit et al., 1997c), is that they do not provide the details of changing local moisture content inside the maize with time. Consequently, after the end of the first drying period, the spatial concentration profile is not known, thereby not allowing prediction of the change of moisture content during tempering. In the present work, we have developed a theoretical diffusion model that enables the moisture-content distribution to be determined during both drying and tempering. This allows investigation of the uniformity of moisture concentration everywhere inside the maize kernels after they have been dried for a given period. For simplicity, we used a sphere model to describe the maize kernel geometry. The effective diffusion coefficient was assumed to be the same for each component of the maize kernel, such as endosperm and pericarp. In addition to developing the mathematical model, we also examined how the tempering periods and cooling rates affect the quality of maize in terms of stress cracking and colour.

Since the establishment of commercial fluidised-bed dryers in Thailand, some industries have used this dryer type for maize drying. As high an operating temperature as possible is usually adopted to achieve the highest throughput and to avoid aflatoxin B-1 production, which is prevalent in tropical regions. Therefore, the principal experiments were conducted at the high end of the temperature range. The results of this work will therefore be of value in practical applications.

2. Mathematical model

In this work, the maize kernel is assumed to be composed of a homogeneous body at the macroscopic level, and the volume of maize kernel does not change during drying and tempering processes. When the maize is immersed in the drying air, the liquid starts diffusing through the maize surface, neglecting the convective effect inside the maize kernel, so that Fick's second law of diffusion can then be applied to describe the moisture movement inside the sphere-shaped maize as given by the following equation:

$$\frac{\partial M}{\partial t} = D_{eff}\left(\frac{\partial^2 M}{\partial r^2} + \frac{2}{r}\frac{\partial M}{\partial r}\right) \tag{1}$$

where M is the moisture content of maize in dry-basis units, D_{eff} is the effective diffusion coefficient (m^2/s) accounting for heterogeneous media, t is the drying time (s) and r is the distance in the radius direction (m^2).

Initially, the moisture content is assumed to be spatially uniform. When the maize is being subjected to drying, moisture around the exterior surface evaporates immediately and approaches

equilibrium with the surrounding air. This behaviour is substantially correct for drying maize at a high superficial air velocity and a high inlet temperature. Typically, as in the drying of other porous solids, the water content is removed most quickly from the peripheral regions of the kernel and more slowly from the interior. The initial and boundary conditions of internal resistance are:

$$t = 0, \quad 0 \leqslant r \geqslant a, \quad M = M_{in} \tag{2}$$

$$t > 0, \quad r = 0, \quad \frac{\partial M}{\partial r} = 0 \tag{3}$$

$$t > 0, \quad r = a, \quad M = M_{eq} \tag{4}$$

where M_{in} is the initial moisture content, M_{eq} is the equilibrium moisture content and a is the equivalent radius of sphere (m). The moisture profile along the radius positions when Eq. (1) is solved algebraically with the above initial and boundary conditions is given by the following equation:

$$\frac{M(r,t) - M_{eq}}{M_{in} - M_{eq}} = \frac{2a}{\pi} \sum_{p=1}^{\infty} \frac{(-1)^n}{rp} \sin \frac{p\pi r}{a} \exp\left(-\frac{p^2 \pi^2 D_{eff} t}{a^2}\right) \tag{5a}$$

After integrating the analytical solution of Eq. (5a) over the volume of the sphere and dividing by the total volume, the average moisture content throughout the kernel is expressed as

$$MR(t) = \frac{6}{\pi^2} \sum_{p=1}^{\infty} \left(\frac{1}{p^2}\right) \exp\left[-p^2 \pi^2 \frac{D_{eff}}{a^2} t\right] \tag{5b}$$

where p is the number of series terms, $MR(t)$ is the ratio of the remaining driving force of concentration to total driving force of concentration, $(M(t) - M_{eq})/(M_{in} - M_{eq})$. We found that 5 or 6 terms of the infinite series represented by Eq. (5b) were sufficient to represent the results over the drying period. The moisture equilibrium equation for maize is (Pudpong et al., 1990)

$$1 - RH = \exp(-3.074 \times 10^{-5}(T + 273.15)(100 M_{eq})^{1.8156}) \tag{5c}$$

where RH and T (°C) are the relative humidity and temperature of air, respectively. The proposed equation was obtained experimentally in a range of temperatures and relative humidities between 35°C and 65°C and 10% and 90%, respectively. Such conditions were lower than the range used in the present work, but it can still be used for calculating the moisture reduction as will be seen in Fig. 3 because of the very low equilibrium moisture content in our experimental conditions.

After passing through the fluidised bed, maize was collected in an airtight container maintained at the same temperature as that of the grains. This is known as tempering. To predict the change of moisture concentration profiles during tempering, the concentration gradient along the radius at the end of the drying period must be known. They are used as initial values at the beginning of the tempering process. In addition, the maize surface is assumed to be impermeable to moisture transport throughout the tempering period. The initial and boundary conditions during the tempering period are given by the following equations:

$$t = 0, \quad 0 \leqslant r \leqslant a, \quad M = M(r), \tag{6}$$

$$t > 0, \quad r = 0, \quad \frac{\partial M}{\partial r} = 0, \tag{7}$$

$$t > 0, \quad r = a, \quad \frac{\partial M}{\partial r} = 0 \tag{8}$$

Due to the complexity of Eq. (1) with the above-mentioned boundary conditions, a numerical solution is sought. A sphere is divided into N intervals and the distance between the nodes is h (m), and the time step used in calculation is k (s). Thus, a finite difference approximation of Eq. (1) is expressed by

$$\gamma M_i^{j+1} - \beta M_{i-1}^{j+1} - \sigma M_{i+1}^{j+1} - \beta M_{i-1}^{j} - \psi M_i^j - \sigma M_{i+1}^j = 0 \tag{9}$$

where

$$\alpha = \frac{kD_{eff}}{2h^2} \tag{10}$$

$$\beta = \alpha\left(\frac{i-2}{i-1}\right) \tag{11}$$

$$\gamma = 1 + 2\alpha \tag{12}$$

$$\sigma = \alpha\left(\frac{i}{i-1}\right) \tag{13}$$

$$\psi = 1 - 2\alpha \tag{14}$$

Subscripts i and superscripts j refer, respectively, to the spatial nodal grid index and the nodal temporal grid index. Eq. (9) is used to calculate the internal node concentrations starting from $i=2$ until N, the number of intervals in the sphere. To solve the boundary conditions given by Eqs. (7) and (8), substituting the Crank–Nicolson formula yields, respectively, the following equations:

for $i = 1$ (at sphere centre),

$$(1 + 6\alpha)M_1^{j+1} - (1 - 6\alpha)M_1^j - 6\alpha(M_2^{j+1} + M_2^j) = 0 \tag{15}$$

for $i = N + 1$ (at the impermeable surface),

$$(1 + 2\alpha)M_{N+1}^{j+1} - (1 - 2\alpha)M_{N+1}^j - (2\alpha)(M_N^{j+1} + M_N^j) = 0 \tag{16}$$

Values of parameters required to simulate the change in moisture profile during tempering by such equations can be summarised as follows:

1. An equivalent radius for the maize kernel is 4 mm.
2. The effective diffusion equation for maize as a function of moisture content and inlet-air temperature is expressed as

$$D_{eff} = 4.70 \times 10^{-5} \exp(-2.971M)\exp\left(-\frac{4171.3}{273 + T}\right) \tag{17}$$

where T is the inlet-air temperature (°C). Eq. (17) is obtained from the drying experiments at temperatures between 90°C and 170°C. The details will be discussed below.

3. Materials and methods

3.1. Drying kinetics

A batch-fluidised-bed dryer was used to study the drying kinetics and quality of maize. To fully understand the mechanism of moisture transfer inside the grain, a maize bed depth of 2 cm was used throughout these experiments. If the bed depth is too thick, then there may be transfer of water between kernels and a more elaborate model would be needed. However, this is not the main subject of our work. The superficial air velocity was limited to 3 m/s. The chosen velocity, which was beyond the minimum fluidisation velocity of maize (1.8 m/s; Soponronnarit et al., 1997c), ensured that the convection resistance to mass transfer would be insignificant. To determine the effective diffusion coefficient, the experiments were carried out at temperatures of 90°C, 110°C, 130°C, 150°C and 170°C with two levels of initial moisture content, 27% and 30% wet-basis. To obtain the desired moisture content, the maize was rewetted and kept in a temperature-controlled room between 5°C and 10°C for 7 days to allow for water to penetrate into the grains. Samples drawn from the dryer every minute were then placed in a hot-air oven at a constant temperature of 103°C for 72 h to determine their moisture content, using the method of the Association of Official Agricultural Chemists (Anon., 1960).

3.2. Tempering

After a first-stage drying at 150°C for 6 min for 43% dry-basis initial moisture content and 4 min for 37% dry-basis, maize was placed in a well-sealed container. During this stage, the maize was maintained at the same temperature as the maize leaving the bed for periods of 10, 20 30, 40 and 50 min. The tempered maize was then dried by the fluidised-bed dryer under the same drying conditions as employed previously for periods of 5 min. Eventually, the maize was tested for physical damage.

To study the effect of cooling rates, the maize dried under the conditions described and tempered for 40 min was ventilated immediately by ambient-air velocities of 0.075, 0.15, 0.225, 0.3 and 0.375 m/s without drying at the second stage. The reason for selecting this tempering period is explained below.

Before these experiments, the fresh maize was shelled carefully by hand to ensure that every kernel was sound and not cracked.

3.3. Quality tests

The amount of stress-cracked grain and the colour were of particular interest in testing maize quality in the rapid-drying approach using high temperature. For the stress cracks, visual inspection under light was employed using a 200 g sample of maize. Each kernel was assigned to one of two classes: cracks (multiple and single) and completeness. The percentage in each class was normalised by dividing the weight of maize kernels in each category by the total weight. Multiple cracking was often found in this work. A colour meter, Juki JP 7100p, was used to determine the grain surface colours. a, b and L values in the Hunter system correspond to red, yellow and lightness, respectively.

4. Results and discussion

4.1. Effective diffusion coefficients

Fig. 1 shows the moisture reduction of maize with time for different inlet-air temperatures, indicating that larger amounts of moisture can be removed when the maize is dried at higher inlet-air temperatures. During the early drying period, the slope of the drying curve is very steep and it continually declines with a longer drying time, suggesting that the water inside the kernel is difficult to remove and that internal diffusion is the main factor in controlling the moisture movement inside the maize kernel.

Moisture diffusion depends strongly on the temperature and frequently also on the moisture content. The dependence of effective diffusivity on temperature is often modelled by an equation of Arrhenius form:

$$\text{Model 1}: \quad D_{eff} = A_1 \exp\left\{\frac{-C_1}{R(T+273)}\right\} \tag{18}$$

where A_1 (m^2/s) is called pre-exponential factor, C_1 (kJ/kmol) is the activation energy and R (kJ/kmol/K) is the universal gas constant. In the case where effective diffusivity is independent of the moisture content, A_1 has a constant value. In contrast, when the moisture content contributes to an effective diffusion coefficient, A_1 varies with moisture content. In the absence of a theoretical explanation of the changing value of A_1 with moisture content, an empirical equation has often been used (Mulet et al., 1989; Ulku and Uckan, 1986). In the present work, the following diffusion equation including Eq. (18) was used to correlate the effective diffusion coefficient with inlet temperature and moisture content:

$$\text{Model 2}: \quad D_{eff} = A_2 \exp(B_2 M)\exp\left[-\frac{C_2}{R(273+T)}\right] \tag{19}$$

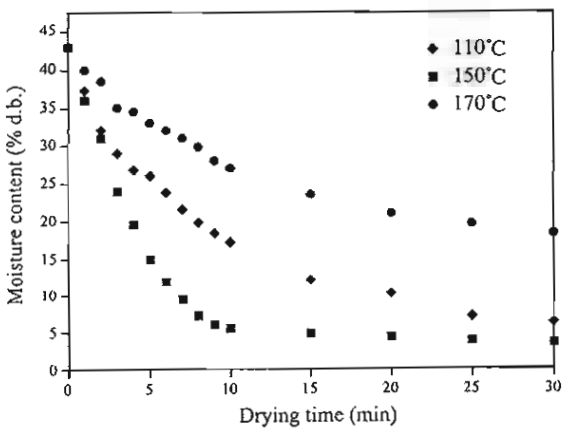


Fig. 1. Change of moisture content at different inlet-air temperatures during first-stage drying (initial moisture content of 43% dry-basis).

Table 1
Coefficients of diffusion models

Model	A	B	C	Coefficient of determination
1	1.992×10^{-4}	NA	599.4	0.9568
2	4.700×10^{-5}	−2.971	501.7	0.9734

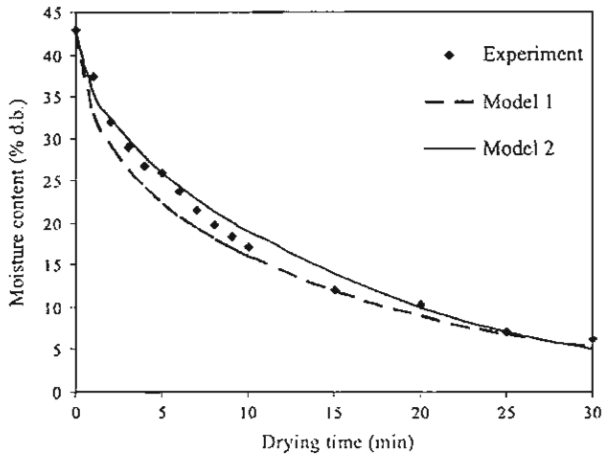


Fig. 2. Comparison of predicted moisture content from diffusion models with the experimental results (inlet-air temperature of 150°C).

A non-linear regression was applied to determine the coefficients in each model by substituting the above diffusion equations into Eq. (5b). The accuracy of the models was evaluated by examining the values of the coefficient of determination (R^2), which was defined as

$$R^2 = 1 - \frac{\sum_{i=1}^{z}(M_{\text{calculated}} - M_{\text{experiment}})^2}{\sum_{i=1}^{z}(M_{\text{experiment}})^2 - \sum_{i=1}^{z}(M_{\text{experiment}})^2/(z-k)} \tag{20}$$

where z and k are the numbers of data points and parameters in the diffusion model, respectively. The coefficients obtained from the fitting are shown in Table 1.

As seen from Table 1, the activation energy for maize varies in the range of 500–600 kJ/kmol, depending upon the diffusion model employed. Model 2 adequately describes moisture reduction over a long drying period as represented in Fig. 2.

4.2. *Effects of tempering period on moisture reduction*

The purpose of collecting the moisture contents for two-stage drying was to validate the data with the theoretical drying–tempering equations. In predicting moisture content at the second stage of drying, the moisture profile along the radius at the end of tempering was used as the initial condition for calculating the moisture reduction in this stage. It is shown in Fig. 3 that the

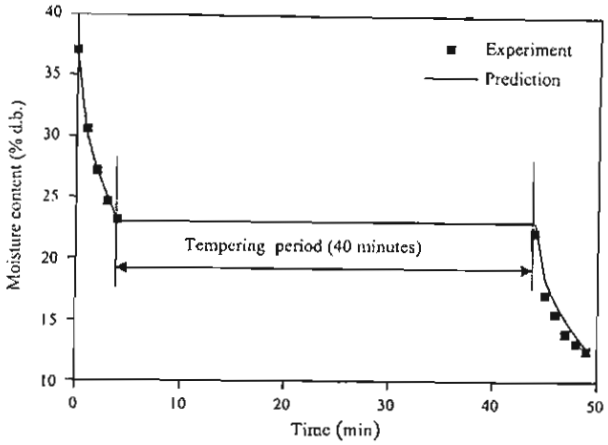


Fig. 3. Comparison of simulated moisture content with the experimental results for two-stage drying including tempering between stages (inlet-air temperature of 150°C).

agreement between the proposed drying–tempering equations and the experimental results is very good.

In the tempering process, large differences in moisture content between the surface and the centre of maize kernel during the early period can be encountered. After a sufficiently long period, the moisture redistributes and ultimately equalises throughout the kernel. To evaluate the time for moisture balance during such stage, a tempering index, TI, was recommended. The definition of this index is expressed by

$$TI = \frac{M_s(t) - M_s(t=0)}{M_s(t=\infty) - M_s(t=0)} \tag{21}$$

where M_s is the surface concentration and t is the tempering time (s). The tempering index was introduced initially by Sabbath (1970). The surface concentration after an infinite tempering period is equivalent to the mean concentration at the end of the first drying pass that is calculated by the following equation:

$$M_s(t=\infty) = \bar{M} = \frac{\int_0^a M(r) r^2 \, dr}{\int_0^a r^2 \, dr} \tag{22}$$

where $\bar{M}$ is the mean concentration, $M(r)$ is the moisture profile, r is the distance along the radius (m) and a is the radius of sphere (m). This equivalence is a result of the assumption that there is no moisture loss from the surface during the tempering.

The tempering–drying models were utilised to study the effect of tempering period on moisture removal. In our case study, maize having an initial moisture content of 43% dry-basis was dried at an inlet temperature of 150°C for 6 min followed by tempering at different periods, with subsequent drying at the same temperature as the previous one. The simulation results clearly indicate the advantages of having the tempering stage in the drying process as it not only reduces the drying time but also reduces the energy consumption. In Fig. 4, we plotted only the moisture content with the drying time, ignoring the tempering time. It is shown that as the tempering period

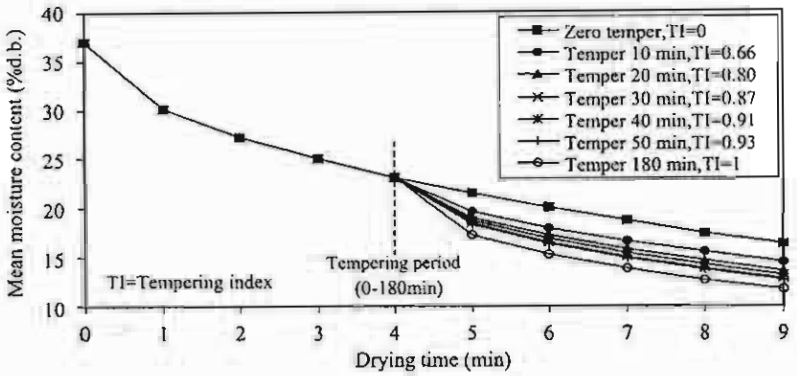


Fig. 4. Simulated results of the effect of tempering periods on moisture removal for two-stage drying (inlet-air temperature of 150°C and initial moisture content of 43% dry-basis).

is provided between two-stage drying, better moisture transport is accomplished. When predicting the moisture content at the start of second-stage drying, the tempering time is an important factor in determining the final moisture content. As shown in Fig. 4, as the tempering period increases from 0 to 180 min, the final moisture content decreases from 18.4% dry-basis to 13.7% dry-basis. This can be explained by the fact that tempering results in moisture transport from the interior to the surface of kernel, and consequently, the water near the surface can be removed easily when subjected to drying conditions again.

As indicated in Fig. 4, when maize was tempered for more than 40 min, corresponding to a tempering index higher than 0.9, the reduction of moisture content at the second stage is almost of the same magnitude as the case of maize tempered for 180 min. It seems that the moisture gradient becomes insignificantly different and does not affect the drying rate. For 37% dry-basis initial moisture content, the results of simulation are similar to Fig. 4.

In the remaining sections, we are concerned with how the grain quality is affected when the tempering stage was included in the process, by comparison with single-stage drying. The experiments for testing maize quality were limited to 150°C in order to maintain the drying capacity as high as possible. The effect of relative humidity on the stress cracks has not been considered since the relative humidity was very low (<5%) at high temperatures. In fact, this factor is also important for low-temperature drying (Estrada and Litchfield, 1993), reducing stress cracking with higher humidity.

4.3. Effect of tempering periods on maize qualities

In studying the effect of tempering on stress cracks and colour, maize was dried first to 19% or 18% dry-basis and then tempered for different periods, with subsequent drying. The final moisture content in all cases varied in a small range between 13% and 16% dry-basis, depending upon tempering period.

Fig. 5 shows the percentage of stress-cracked grain by weight against tempering periods for two initial moisture contents, 37% and 43% dry-basis. Note that zero tempering means that the moist

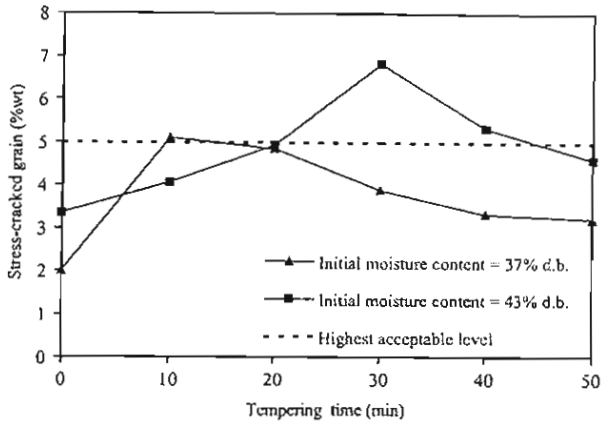


Fig. 5. Percentage of stress-cracked grain at different tempering periods (inlet-air temperature of 150°C for first-stage drying).

maize was dried to the desired moisture content by single-stage drying, and a standard value for cracking that is acceptable should not be higher than 5% as recommended by Soponronnarit et al. (1997b). In reducing moisture content to 15% dry-basis with no tempering, initial moisture content is one of the factors contributing to stress cracking. As shown in Fig. 5, the stress cracks for initial moisture contents of 37% and 43% reach, respectively, 3.8% and 6.2% of the kernels by weight when they are zero at the beginning. The latter would be graded as poorer quality maize. The cracked maize is caused by the non-uniform shrinkage within the maize kernel inducing stresses higher than the failure strength of the kernel. Cracking first manifested itself at the surface and then progressed inwards as the drying process continued.

When two-stage drying with tempering between stages was employed, however, stress cracking was reduced to an acceptable level. In addition, tempering for any longer time did not reduce the severity of stress cracking. This trend also appeared in the case of maize with lower moisture contents.

At present, the standard colour of yellow maize kernels used in the grain industry in Thailand has not been formally established as a criterion of quality. Traders use their experience and expertise to consider colour quality. According to Soponronnarit et al. (1999), the criterion has been established based on the maize samples that passed the quality test in the commercial market. The premium quality of colour is as follows: L and b should not be lower than 47.7 and 23.5, respectively, and a should not be higher than 9.7. Fig. 6 shows the maize surface colour represented in the form of L, b and a values, after it has passed the second stage of drying from initial moisture contents of 37% and 43% dry-basis. The data shown in this figure were obtained at the same conditions as in Fig. 5 indicating that colours do not change significantly with the increased tempering period from those of untempered maize. L decreases continuously with increased tempering period and the values of a and b are almost constant in the early period with subsequent higher values after 30 min. According to these results, both the tempering period and heat used to maintain temperature during tempering cause the poorer colour. However, the colour quality of tempered maize is still better than the standard level.

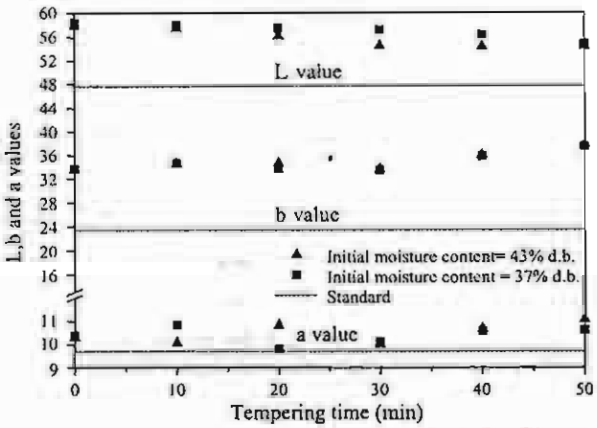


Fig. 6. Colours of maize surface at different tempering periods (values of L, b and a represent lightness, yellowness and redness, respectively).

4.4. *Effect of cooling rate on maize qualities*

After maize was tempered for 40 min, it was assumed that the moisture-content gradient inside the kernel was very small, corresponding to a tempering index of 0.9 as previously shown in Fig. 4. The tempered maize was subsequently cooled at different cooling rates. It was found that the cooling rate insignificantly affected the drying rate, implying that internal diffusion controlled moisture movement. The moisture content can be reduced by 2 points from 22.5% dry-basis down to 20% or 21% dry-basis during cooling, higher than the desired value of 16% dry-basis for safe storage. In view of this, the moisture gradient inside the kernel shows an insignificant variation, whereas the temperature gradient due to cooling was more pronounced. Such large gradients of temperature may lead to stress cracks in the maize kernel. Fortunately, this plays a minor role in the cracking of maize as evidenced by Fig. 7 which shows that the percentage of cracked maize changes slightly with the degrees of cooling rate, 3.3–4.7% for 37% moisture content and 4.0–5.3% for 43% moisture content. This can be explained by the shrinkage of the maize kernel due to moisture removal during the cooling period being very small and thus the stress that appears in this period is low. This behaviour is somewhat similar to drying during the very early period, in which the amount of moisture removed from the material is very small, so that physical damage in terms of breaking and cracking is small (Soponronnarit et al., 2001; Soponronnarit and Prachayawarakorn, 1994).

The data represented in Fig. 8 were obtained under identical conditions to those in Fig. 7. The cooling rates do not cause discolouration of maize kernels: the values of a, b and L are unchanged.

5. Conclusions and recommendations

- Moisture movement inside the maize kernel during drying is controlled by internal diffusion. The effective diffusivity depends on the temperature and moisture content and can be described adequately by the modified Arrhenius equation.

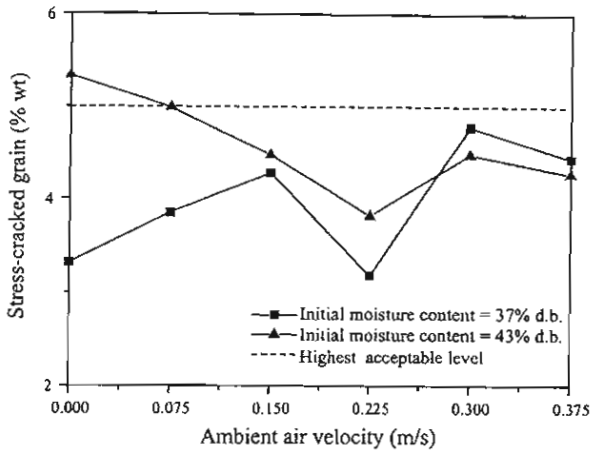


Fig. 7. Effect of cooling rates on stress-cracked grain (inlet-air temperature of 150°C for first-stage drying and tempering period of 40 min).

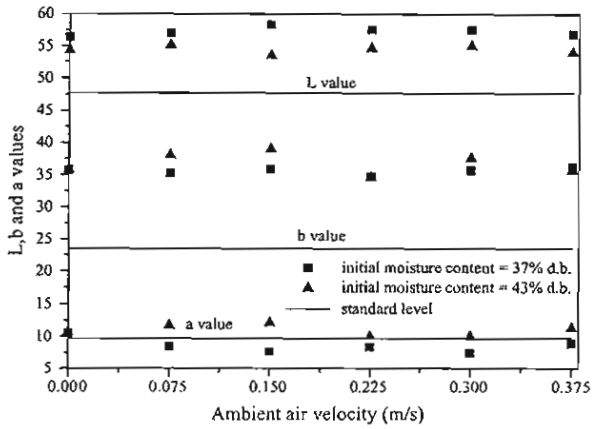


Fig. 8. Influence of cooling rates on maize surface colour (inlet-air temperature of 150°C for first-stage drying and tempering period of 40 min).

- A theoretical diffusion equation for a single sphere, that assumes the maize kernel is homogeneous at the macroscopic level, is used to simulate drying and tempering. The proposed equation is validated for moisture data over the range of the first and second drying stages in fluidised-bed drying
- The tempering period is the most important factor determining the extent of moisture removal during the second drying period. The amount of moisture removal is enhanced when the tempering stage is completed, allowing uniformity of concentration throughout the maize kernel. In reducing the moisture content from 37% or 43% dry-basis to 23% dry-basis using an inlet temperature of 150°C and drying periods of 4 or 6 min depending on its moisture content, a tempering period of 40 min is sufficiently long to provide the most efficient energy utilisation.

To be useful for the grain industry, more research work is needed to explore the appropriate tempering time for a wider range of inlet-air temperatures and initial moisture contents.

- Tempering reduces maize cracking but a longer tempering period causes the colour of maize to become more intense and darker.
- Ambient-air velocity in the range of 0.075–0.375 m/s flowing through the tempered maize insignificantly affects the above-mentioned maize qualities.

Acknowledgements

The authors thank The Thailand Research Fund for financial support of this work.

References

Anon., 1960. Official and Tentative Methods of Analysis of the Association of Official Agricultural Chemists, 9th Edition. Association of Official Agricultural Chemists, Washington, DC.

Davidson, V.J., Noble, S.D., Brown, R.B., 2000. Effects of drying air temperature and humidity on stress cracks and breakage of corn kernels. Journal of Agricultural Engineering Research 77, 303–308.

Estrada, J.A., Litchfield, J.B., 1993. High humidity drying of corn: effect on drying rate and product quality. Drying Technology 11, 65–84.

Mourad, M., Hemati, M., Laguérie, C., 1995. The drying of corn in a flotation fluidised-bed: an experimental study of the drying rate. Chemical Engineering Journal 59, 221–228.

Mulet, A., Berna, A., Rossello, C., 1989. Drying of carrots. I. Drying models. Drying Technology 7, 536–557.

Musielak, G., 2000. Influence of the drying medium parameters on drying induced stresses. Drying Technology 18, 561–581.

Otten, L., Brown, R.B., Reid, W.S., 1984. Drying of white beans—effect of temperature and relative humidity on seed coat damage. Canadian Journal of Agricultural Engineering 26, 101–104.

Pudpong, A., Soponronnarit, S., Tia, V., 1990. The study of parameters for corn drying. Thailand Engineering Journal 4, 95–101.

Sabbath, M.A., 1970. Convective heat transfer coefficient and tempering effects on cooling rate of shelled corn. Ph.D. Thesis, Purdue University, Lafayette, IN.

Satayaprasert, C., Vanishsriwatana, V., 1992. Drying corn in fluidised-bed. Thailand Engineering Journal 44, 76–79.

Siriacha, P., Tanboon-Ek, P., Buangsuwon, D., 1991. Aflatoxin in maize in Thailand. In: Champ, B.R., Highley, E., Hocking, A.D., Pitt, J.I. (Eds), Fungi and Mycotoxins in Stored Products: Proceeding of an International Conference, Bangkok, Thailand, 23–26 April, ACIAR Proceedings No. 36, pp. 187–193.

Soponronnarit, S., Prachayawarakorn, S., 1994. Optimum strategy for fluidised-bed paddy drying. Drying Technology 12, 1667–1686.

Soponronnarit, S., Kittiporn, K., Prachayawarakorn, S., 1997a. Appropriate operating parameters for fluidised-bed corn drying. Regional Energy Resources Information Center International Energy Journal 19, 1–13.

Soponronnarit, S., Pongtornkulpanich, A., Prachayawarakorn, S., 1997b. Maize quality after drying by fluidisation technique at high temperature. Drying Technology 15, 2577–2586.

Soponronnarit, S., Pongtornkulpanich, A., Prachayawarakorn, S., 1997c. Drying characteristics of maize in fluidised-bed dryer. Drying Technology 15, 1603–1615.

Soponronnarit, S., Wetchacama, S., Swasdisevi, T., Chotijukdikuld, P., 1999. Effects of drying, tempering and ambient air ventilation on quality and moisture reduction of corn. Drying Technology 17, 1227–1238.

Soponronnarit, S., Swasdisevi, T., Wetchacama, S., Wutiwiwatchai, W., 2001. Fluidised-bed drying of soybeans. Journal of Stored Products Research 37, 133–151.

Steffe, J.F., Singh, R.P., 1980. Theoretical and practical aspects of rough rice tempering. Transactions of the American Society of Agricultural Engineers 23, 775–781.

Thompson, R.A., Foster, G.H., 1963. Stress cracks and breakage in artificially dried maize. USDA Marketing Research Report 631, pp. 139–142.

Ulku, S., Uckan, G., 1986. Corn drying in fluidised-beds. In: Mujumdar, A.S. (Ed.), Drying'86. 2. Hemisphere. Springer, London, New York, pp. 531–536.

White, G.M., Ross, I.J., 1972. Discoloration and stress cracking in white corn as affected by drying temperature and cooling rate. Transactions of the American Society of Agricultural Engineers 15, 504–507.

DRYING TECHNOLOGY
Vol. 22, No. 4, pp. 719–743, 2004

Characteristics of Rice Dried in Superheated-Steam Fluidized-Bed

Chaiyong Taechapairoj,[1,*] Somkiat Prachayawarakorn,[2] and Somchart Soponronnarit[1]

[1]School of Energy and Materials and
[2]Faculty of Engineering, King Mongkut's University of Technology, Thonburi, Suksawat, Bangkok, Thailand

ABSTRACT

Characteristic properties of rice in a superheated-steam fluidized-bed dryer have been investigated using RVA, DSC, and SEM. The experimental results have shown that the reduction in moisture content from 41–42.5 to 25% d.b. using steam temperatures of 150–170°C was initially linear with drying time followed by the exponential decay when the moisture content was below 25% d.b. During the latter period, the water transport was controlled by the internal diffusion. Condensation of steam, along with the use of high temperature, enabled the development of gel layer as obvious from SEM. The formed gel layer caused the very low effective diffusivity

*Correspondence: Chaiyong Taechapairoj, School of Energy and Materials, King Mongkut's University of Technology, Thonburi, Suksawat 48 Road, Bangkok 10140, Thailand; E-mail: chaiyong_t@yahoo.com.

DOI: 10.1081/DRT-120034259
Copyright © 2004 by Marcel Dekker, Inc.
0737-3937 (Print); 1532-2300 (Online)
www.dekker.com

when compared with the case of no gel formation in paddy kernel. The pasting properties and DSC measurements have shown that paddy dried at a higher temperature and a thinner bed depth provided a greater extent of gelatinization during the drying time, the first factor showing a profound effect. Kinetics of gelatinization is reasonably described by the zero-order reaction. For the paddy quality, the head rice yield was 70% higher than the reference value and color of white rice became yellow and low luminous after reducing moisture content to 18% d.b. The percentage of white belly was less than 1.5%.

Key Words: Gelatinization; Superheated steam; White belly.

INTRODUCTION

Parboiled rice is made from fresh paddy, which is subjected to a hydrothermal treatment. In the traditional parboiling process, paddy is steeped in water until attaining the moisture content between 42 and 54% dry basis (d.b.). This stage is taken overnight or longer in water at ambient temperature. It is then followed by boiling or steaming the steeped rice at 100°C to gelatinize the starch, resulting in the grain swelling and the hull's lemma and palea separating. The parboiled rice is then cooled and dried before storing and milling. In the modern process, the stages are similar to the first one, except for the soaking stage in which paddy is immersed in hot water in order to reduce the sour odour and accelerate transport of water into kernel.[1] During steaming, the nutrients from the bran layer penetrate into the endosperm and consequently, some of the vitamins existing inside the rice kernels are sealed due to the formation of gel layer.[2] Parboiled rice is therefore a more nutritious form of rice than the white rice.

However, the above-mentioned parboiling processes are not very convenient in practice since they consist of many steps. An attempt to reduce them is a main objective in the present work and a possible way is that of using superheated-steam. With this medium, we expect that both steaming and drying stages can be integrated into a single stage if the gelatinizing condition and moisture removal stage are well organized. The superheated-steam drying has been widely recognized in many applications.[3–5] Recent studies have reported some advantages of superheated-steam drying[6,7]: high drying rate and deodorization of products.

The purpose of the present work is to produce the rice parboiling by using superheated-steam as a drying media in fluidized-bed dryer. The characteristics of dried paddy such as pasting properties, microstructure, and lipid content are investigated. In addition, the head rice yield and whiteness of paddy are also determined.

MATERIALS AND METHODS

Sample Preparation

Long grain paddy of Chainat1 (CNT1) variety from the Rice Experiment Station at Ayutthaya Province, Thailand, was used in the present investigation. In preparation, it was followed by a traditional method where paddy was cleaned and soaked at a temperature of 80°C for 3.5 h. Then, the water was drained out and the paddy was tempered at the same tank for 1 h prior to drying.

Drying

After soaking, paddy samples were dried with a batch superheated steam fluidized dryer as shown in Fig. 1. The system of the fluidized-bed dryer consists of five main components: a cylindrical chamber with a 15 cm inner diameter and a 100 cm height, a 13.5 kW electrical heater for converting saturated steam to the superheated steam, a backward-curved blade centrifugal fan driven by a 2.2 kW motor, a reverse flow cyclone, and a small boiler with a 31 kg/h capacity of generated steam. A PID controller with an accuracy of ± 1°C was used to control steam temperature. Before using steam for drying, hot air was used for warming up the system until the temperature in every part reached the desired temperature. Then, the steam was replaced accordingly. The steam generator was generated the saturated steam at 106 kPa (absolute pressure) with the corresponding temperature of 100°C. When the saturated steam was flowed through the electrical heaters, the additional heat was supplied to raise the steam temperature up to the required level. It was subsequently flowed through the fluidized bed dryer. The dust particles and the immature grains being suspended in the exhaust steam were collected at the cyclone. Finally, the cleaning exhaust steam was reused again.

The experimental conditions were set up as follows: initial moisture contents of 41–42.5% d.b., bed depths of 10–15 cm, superheated steam

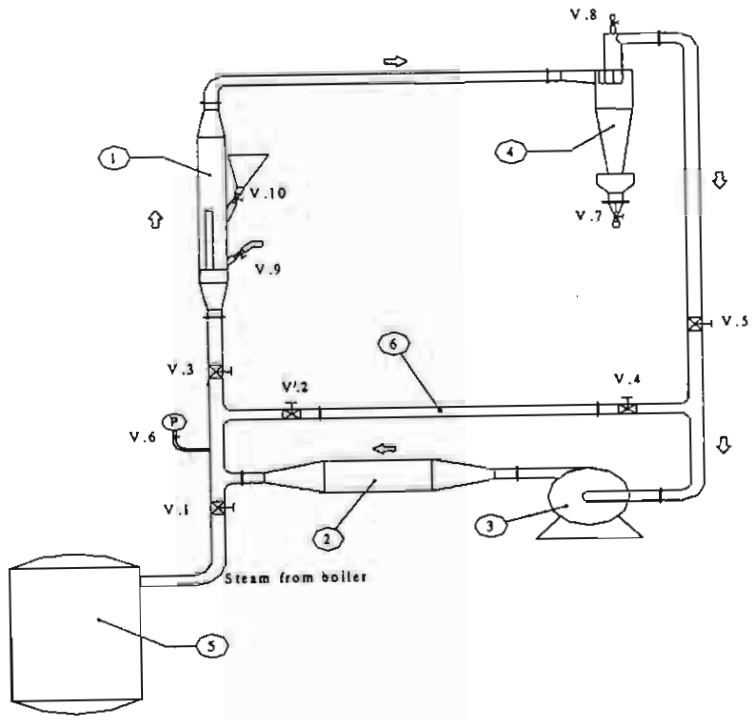


Figure 1. A schematic diagram of the superheated-steam system: (1) fluidized bed dryer; (2) heater; (3) fan; (4) cyclone; (5) boiler; (6) bypass line; P = pressure guage, and V = valve.

temperatures of 150–170°C, a fixed superficial velocity of 3.1 m/s. Temperatures at different positions of drying chamber were measured by Chromel-Alumel thermocouples (Type K) connected to a data logger with an accuracy of ± 1°C. The paddy, with a mass 1 kg, was dried until reaching the predetermined time and then withdrawn from dryer at the valve V.9 to determine the moisture content and grain temperature. In grain temperature measurement, the paddy kernels were fully packed in a well-insulated container. After that, the sample was kept in polypropylene bag and left in the environment condition until the grain temperature approached ambient temperature. Then, it was spread on a sieve and ventilated by an ambient airflow rate until its moisture content reached 16% dry basis. Finally, a 300 g sample was kept in a seal plastic bag for 2 weeks before testing head rice yield, whiteness and white belly.

The moisture content of paddy was determined by an electrical air oven at a temperature of 103°C for 72 h. Paddy quality in terms of head rice yield and whiteness was determined quantitatively and compared to the reference sample (paddy dried by the ambient air). The methods were followed with the guideline of the Ministry of Agriculture and Cooperatives, Thailand. Head rice is defined as milled rice having kernel length at least three-fourths of its original length. The head rice yield was calculated from the mass of white rice that remains as head rice after milling divided by the mass of paddy sample.

The color of rice samples was measured by a Kett digital whiteness meter (Model C-300). Before measuring the color of sample, the whiteness meter was calibrated with a white colored reference, presenting a standard value of 86.3.

Scanning Electron Microscopy

Structural changes of kernels were investigated by scanning electron microscopy (SEM) (S-4500, Hitachi, Tokyo, Japan). The rice kernel was broken along the cross-sectional axis. Samples were placed on adhesive tape attached to a circular aluminum specimen stub, coated with gold layer using a sputter-coater (Hitachi E-1010 10N, Tokyo, Japan), and photographed at an accelerator potential of 15 kV.

RVA Measurement

All rice flour samples were prepared by grinding rice with a laboratory model hammer mill (Retsch Mühle, type SK1, Germany) with a mesh opening of 800 μm. Pasting properties of rice flour were determined by a Rapid Visco Analyser model-4 (Newport Scientific Pty Ltd., Warriewood, Australia) utilizing Thermocline. Following AACC Method 61-02,[8] the sample (3 g, 14% moisture basis) was mixed with distilled water in a RVA aluminum canister to make the total weight of slurry 28 g. The mixture was stirred at 900 rpm for 10 s and then changed to 160 rpm. The mixture was held at 50°C for 1 min and then heated to 95°C at 12°C/min. After that, holding at 95°C was 2.5 min, followed by cooling down to 50°C at 12°C/min and kept for 2.1 min. These tests were done in duplication. A plot of paste viscosity in arbitrary RVA unit (RVU) vs. time was used to determine the peak viscosity (PV), temperature at peak viscosity (P_{temp}), trough final viscosity (FV), breakdown viscosity (BKV = PV − trough), and setback viscosity

(SBV = FV – trough). The first point at which the viscosity increases to 1 RVU/s or faster is defined as the onset gelatinization temperature of rice flour (P_{Temp}). Peak viscosity (PV) indicates the water-biding capacity of mixture. It is often correlated with the final product quality, and also provides an indication of the viscous load likely to be encountered by a cook. Breakdown viscosity measures the degree of disintegration of the granules or paste stability. Setback viscosity is a measure of gelling or retrogradation tendency.[9]

Lipid Content

Lipid content was determined using the method of Folch et al.,[10] with some modifications for the rice flour extraction. Parboiled rice flour was extracted with chloroform–methanol (2:1 by volume). The suspension was shaken for 5 min and settled for 30 min before decanted through folded filter paper. Filtrate was added with one-fourth of water and shaken to create two immiscible liquid phases. The lower and upper phases were composed of chloroform–methanol–water in the corresponding proportions of 86:14:1 and 3:48:47 (by volume), respectively. The final lipid extract was evaporated at 35°C under stream of oxygen-free nitrogen.

Differential Scanning Calorimetry Analysis

Gelatinization properties of parboiled rice flours were analyzed by using a differential scanning calorimeter (DSC Pyris-I, Perkin-Elmer, Norwalk, CT, USA). The calibration was periodically performed using indium (heat of fusion of 28.41 J/g and 156.66°C of melting temperature). Flour samples (~3 mg each) were weighed in sample pans, mixed with distilled water (~9 μL). The sample pan was sealed and allowed to stand for 1 h at room temperature.[11] The sample was held isothermally at 30°C for 1 min, and then scanned at a heating rate of 5°C/min until the temperature raise to 100°C. The calorimetric measures were made by duplications. The enthalpy change (ΔH) was evaluated using the Thermal Analyzer (TA) Instruments analysis software program. The degree of gelatinization (DG) of rice flour was calculated by the following equation[12]:

$$DG(\%) = [1 - (\Delta H_{pg}/\Delta H_{raw})] \times 100 \quad (1)$$

where ΔH_{pg} and raw ΔH_{raw} are the enthalpies of gelatinized and raw rice grains, respectively.

Drying Kinetics

In the present study, paddy kernels fully adsorbed water which is formed a thin liquid film around the external surface, namely unbound moisture. When exposed to superheated steam, this unbound water can be removed easily and water evaporation rate can thus be simply expressed by

$$\frac{d(M(t) - M_{eq}/M_{in} - M_{eq})}{dt} = k \quad (2)$$

where $M(t)$ is the moisture content at time t (d.b.), M_{eq} is the equilibrium moisture content, M_{in} is the initial moisture content, k is the drying constant (s^{-1}) and t is the drying time (s^{-1}). The drying constant depends upon the operating parameters.

When the moisture content has reached a value of M_c, the critical moisture content, the film thickness of moisture at the surface has been reduced by evaporation, so that further drying causes the formation of dry surface. This gives rise to the part of falling rate period in which the evaporation rate can be calculated by

$$\frac{M(t) - M_{eq}}{M_c - M_{eq}} = \frac{8}{\pi^2}\sum_{i=1}^{\infty}\frac{1}{(2i-1)}\exp\left[-(2i-1)^2\frac{\pi^2}{4b}\left(\frac{D_{eff}(t-t_c)}{b}\right)\right] + 4\sum_{i=1}^{\infty}\frac{1}{\alpha_i^2 R^2}\exp\left(-D_{eff}\alpha_i^2(t-t_c)\right) \quad (3)$$

where R is the radius of cylinder, b is the half thickness, t_c is the drying time at the critical point, and α_i are the positive roots of the equation $J_0(R\alpha_i) = 0$. Equation (3) was used by Poomsa-ad et al.[13] in order to describe the moisture transport inside paddy kernel, assuming cylindrical shape, which governs the drying behavior.

Gelatinization Kinetics

Food systems usually follow either a zero or first order kinetics.[14] A plot of C vs. t gives a straight line for zero-order reaction (Eq. (4)),

whereas for first-order reaction (Eq. (5)), a plot of log C vs. t yields a straight line. The slope of the line is equal to the rate constant.

$$-C = kt + C_0 \tag{4}$$

$$-\log C = kt + \log C_0 \tag{5}$$

where C and C_0 are the percentage of ungelatinized rice flour at time t and 0, respectively, k is the rate constant (s^{-1}) and t is the drying time (s).

The temperature dependence of the rate constant can be explained by an Arrhenius type relationship:

$$k = k_a \exp(-E_a/RT_{abs}) \tag{6}$$

where R is the universal gas constant and T_{abs} is the absolute temperature. The activation energy (E_a) can be obtained from the slope of the plot of ln k vs. the reciprocal of process temperature (T_{abs}). The regression results were shown that the determined activation energy was slightly changed with bed depth, showing 13% difference between the lowest and highest bed depths, whilst the value of k_a was very sensitive to the bed depth, the largest difference being 60% in present work, the activation energy is, therefore, assumed to be constant and the pre-exponential factor (k_a) is correlated with the following form:

$$k_a = F + GH_b + IHb^2 \tag{7}$$

where F, G, and I are the constant parameters and H_b is the bed depth (cm).

RESULTS AND DISCUSSION

Drying Curve

Figure 2 shows the relationship between the grain temperature, moisture content, and drying time. At the initial stage of drying, there is a region where the uptake of moisture into grains can be observed, typically of the order of 1–2% moisture content dry basis, since the flowing steam contacting with a low initial temperature of paddy is condensed. The amount of water uptake is slightly dependent on the steam temperature, as observed from the experiments.

Because of rapid release of heat vaporisation by condensation, the grain temperature rapidly increases. As shown in Fig. 2a, the grain temperature is slightly above 80°C in the first minute of drying time and

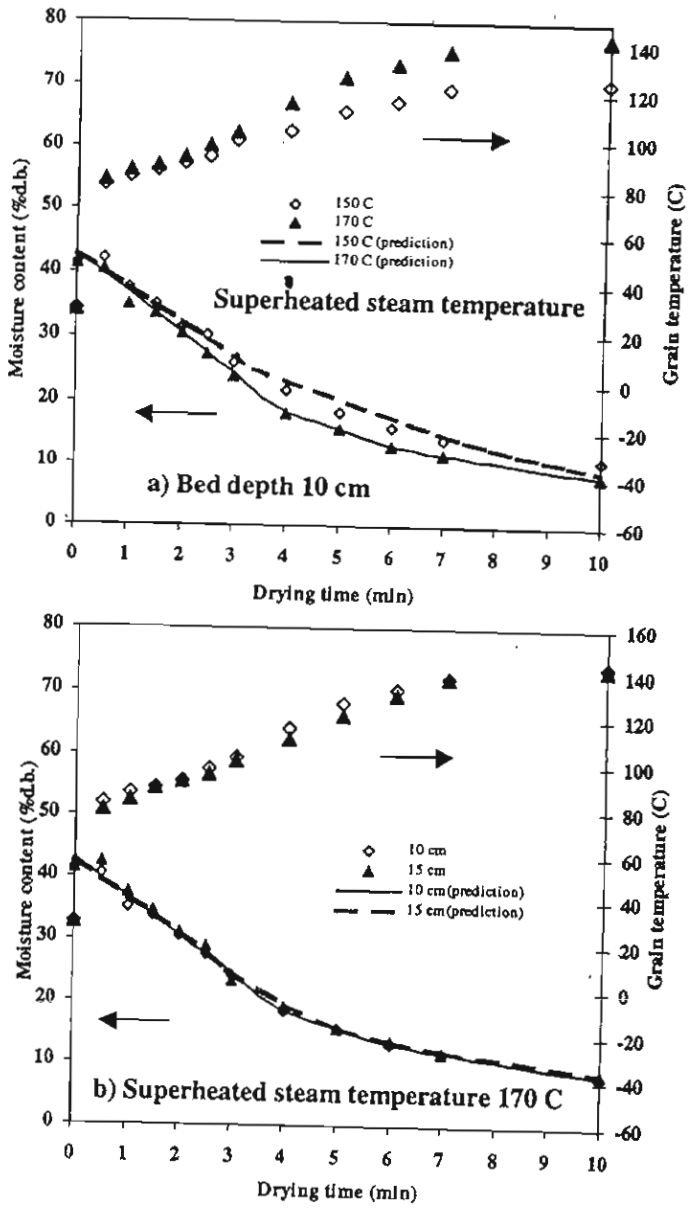


Figure 2. Variation in moisture content and grain temperature with time at different bed depths and inlet superheated-steam temperatures.

then relatively rises to 100°C in 3 or 4 min. During this period, more than a half of rice starch is gelatinized as can be seen in Fig. 6 and all of the heat is used to vaporise the water that exists inside the paddy and the condensing water that was not adsorbed by grains. Afterwards, the grain temperature rapidly increases and higher grain temperatures follow with higher steam temperatures, resulting in the relative difference of moisture content.

Due to very high initial moisture content, together with steam condensation, the moisture reduction of paddy at the early drying period is linear with time and it is described by the following equation:

$$MR = (0.08991V - 1.1886 \times 10^{-5}T - 2.268 \times 10^{-4}VT + 0.00314)\,t + 1.03674 \qquad (R^2 = 0.975) \tag{8}$$

where MR is the moisture ratio $(M(t) - M_{eq}/M_{in} - M_{eq})$, V is the specific mass velocity (kg steam s^{-1}/kg dry matter), T is the superheated steam temperature (K), and t is the time (s). The drying rate in this period is affected by the temperature and specific mass velocity: higher drying rates will follow with higher temperature and specific mass velocity, the first one being more important. Such linear decrease proceeds to the critical moisture content, after which it falls into the exponential decline. The critical moisture content of paddy was approximately 25% d.b. and independent of drying conditions. Equation (8) is valid at the temperature of 423–443K and the specific mass velocity of 0.024–0.038 kg $kg^{-1}_{dry\ matter}$ s^{-1}.

In the period of the exponential decline, the effective diffusivity of paddy was determined by using Eq. (3). Figure 3 shows the experimentally determined effective diffusivity at various bed depths and steam temperatures. The value of effective diffusivity is in the range of 3.0×10^{-10}–4.2×10^{-10} m^2/s for the temperatures of 150–170°C. As expected, the effective diffusivity increases with the increase of drying temperature. The bed depth does not remarkably affect the effective diffusivity obtained for each temperature, implying that the values obtained are the intrinsic ones. The experimental relationship between drying temperature and D_{eff} has been established using the Arrhenius-type equation,

$$D_{eff} = 3.02087 \times 10^{-7}\exp\left(\frac{-24318.4}{RT}\right), \qquad R^2 = 0.925 \tag{9}$$

Equation (9), with a R^2-value of 0.925 and an absolute mean error of 1.0025×10^{-11}, is reasonably fitted with the experimental data, as indicated by the solid line in Fig. 3.

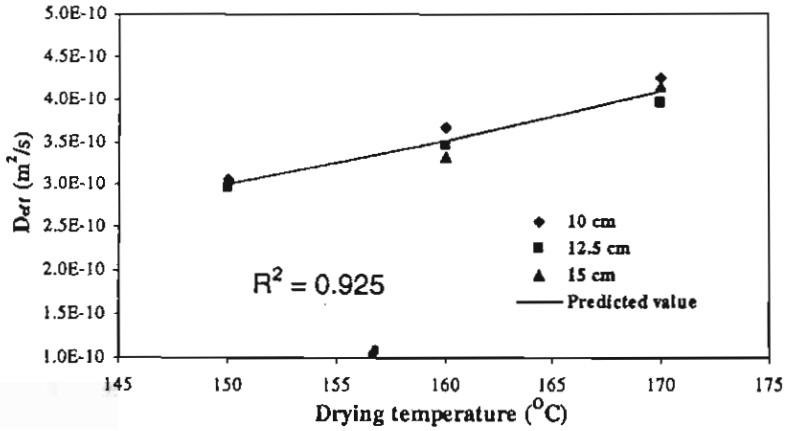


Figure 3. Experimental and predicted values of effective diffusivity (superheated steam).

Comparing to Poomsa-ad's work,[13] the effective diffusion of paddy is atleast 15 times lower when dried in the superheated steam than when dried in the hot air under the same dryer type. The effective diffusion of paddy dried in hot air fluidized-bed dryer[13] is given by

$$D_{eff} = 5.41141 \times 10^{-6}\exp\left(\frac{-28436.4}{RT}\right) \tag{10}$$

The prediction of moisture reduction of paddy using D_{eff} in Eqs. (9) and (10) is shown in Fig. 4 that the drying rate in the falling rate period for the use of superheated steam as drying medium is significantly lower over the drying time. The lower drying rate is due to the formation of gel layer starting from the exterior surface and moving towards the interior, thereby allowing the internal spaces to be reduced. This gel layer retards the diffusing water. The evidence of the gel formation will be discussed later with the results of differential scanning calorimeter and RVA measurements and morphology of rice kernel using scanning electron microscopy.

Pasting Behavior

Pasting curve of viscosity determined by RVA represents the viscosity of starch during heating cycle, which shows the molecular

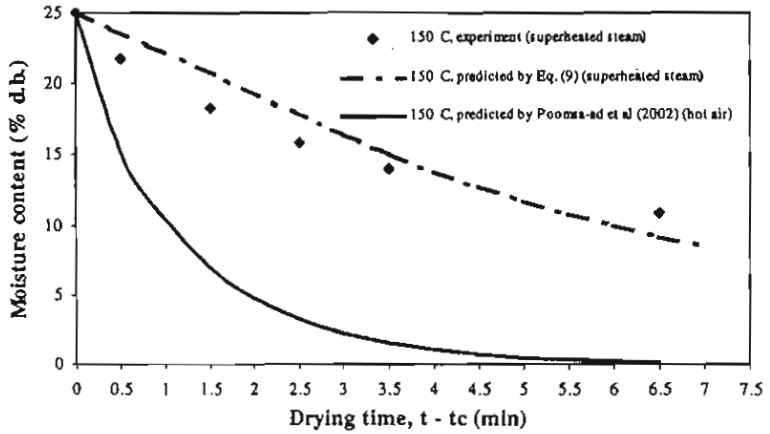


Figure 4. Comparison of predicted and experimental drying curve for paddy drying at 150°C.

events occurring in the starch granules. The integrity of starch granules and hydration properties resulting from the native properties of starch, or from the molecular interactions during drying can therefore be easily investigated by measuring the pasting properties of rice flour before and after treatments. The typical RVA viscographs and viscosity properties of pastes prepared from the raw rice and dried rice are shown in Figs. 5a and b. The pasting properties are significantly affected by the temperature, except for bed depth, and the characteristic properties are totally different from those of the raw rice. The rate of increasing viscosity of dried rice flour during heating period, as indicated by the slope, is very low when dried at 150, 160, and 170°C. The resulting gelatinization temperature becomes higher, approximately 90°C for the dried rice and 80°C for the raw rice, and the peak viscosity is lower. The higher gelatinization temperature is due to retrogradation of dried rice causing reassociation of starch molecules. Consequently, the reassociated starch structure is resistance to water penetration and thus required more energy for water absorption during the heating period in RVA testing.

Table 1 presents a summary of the effect of temperature on the pasting properties of treated rice flour. The PV, BKV, FV, and SBV of treated rice flour are remarkably smaller than those of the raw rice flour. The differences between the raw rice flour and dried rice flour increase with increase in temperature because the degrees of reassociation of starch molecules depend on the degree of heat treatment. This is indicated

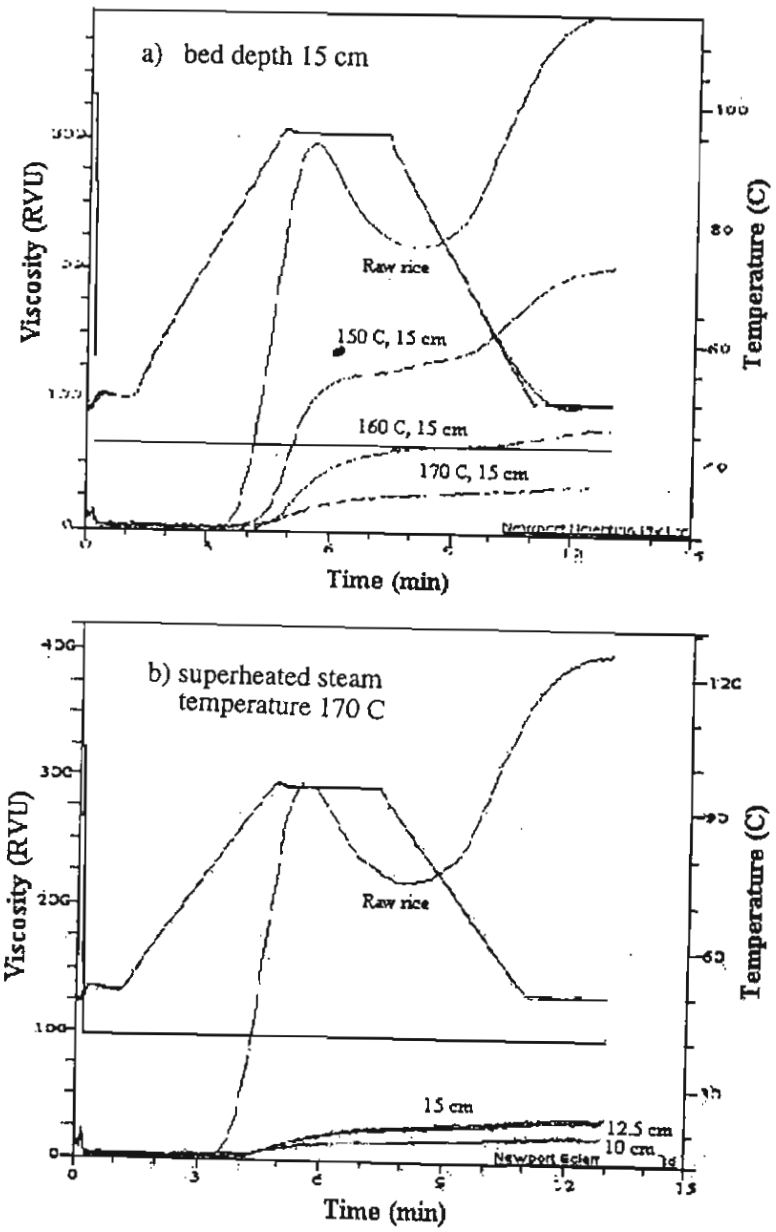


Figure 5. Viscograph of raw rice flour and rice flour dried by superheated steam.

Table 1. Pasting properties of raw and dried flour.

	PV (rvu)	Trough (rvu)	BKV (rvu)	FV (rvu)	SBV (rvu)	P_{Temp} (°C)
Raw rice	296	218	78	399	181	79.9
150°C 15 cm	120	113	7	205	92	89.7
160°C 15 cm	57	47	10	81	34	88
170°C 15 cm	25	20	5	35	15	89.7
170°C 12.5 cm	23	19	4	32	13	89.7
170°C 10 cm	14	12	2	21	9	89.7

by the decrease of PV and FV with increase in temperature. The treated samples possess low firmness texture, as indicated by the low FV and SBV.

Kinetics of Gelatinization

Figure 6 illustrated the DSC thermal curve for rice drying at temperature of 160°C and bed depth of 15 cm, showing the increase in degree of gelatinization of rice four with drying time. At the drying time of 5 min, heat flow line is almost parallel with x-axis, implying the nearly completed gelatinization of starch. Degree of ungelatinization of rice flour during superheated steam drying as a function of drying time at different temperatures and bed depths is shown in Fig. 7. A certain degree of starch gelatinization, approximately 20%, occurred before starting the experiment because of the soaking effect. The degree of ungelatinization is linearly decreased with drying time and is almost zero after the drying time passed by 5–6 min at steam temperatures of 150–160°C and 4 min at 170°C.

The experimental data were used to fit with Eqs. (4) and (5). The prediction results for the zero and first order reactions show in Figs. 7 and 8, respectively. The kinetics of gelatinization of paddy during drying in the superheated-steam fluidized-bed dryer is reasonably described by the zero-order kinetic reaction, as indicated by R^2 and absolute mean error values which are respectively 0.97 and 3.66 for the zero order whilst 0.80 and 45.3 for the first order. These findings oppose to the previous works reported in the literature as a first-order reaction.[15–19] The reason has not yet cleared. However, it might be possible that the gelatinization

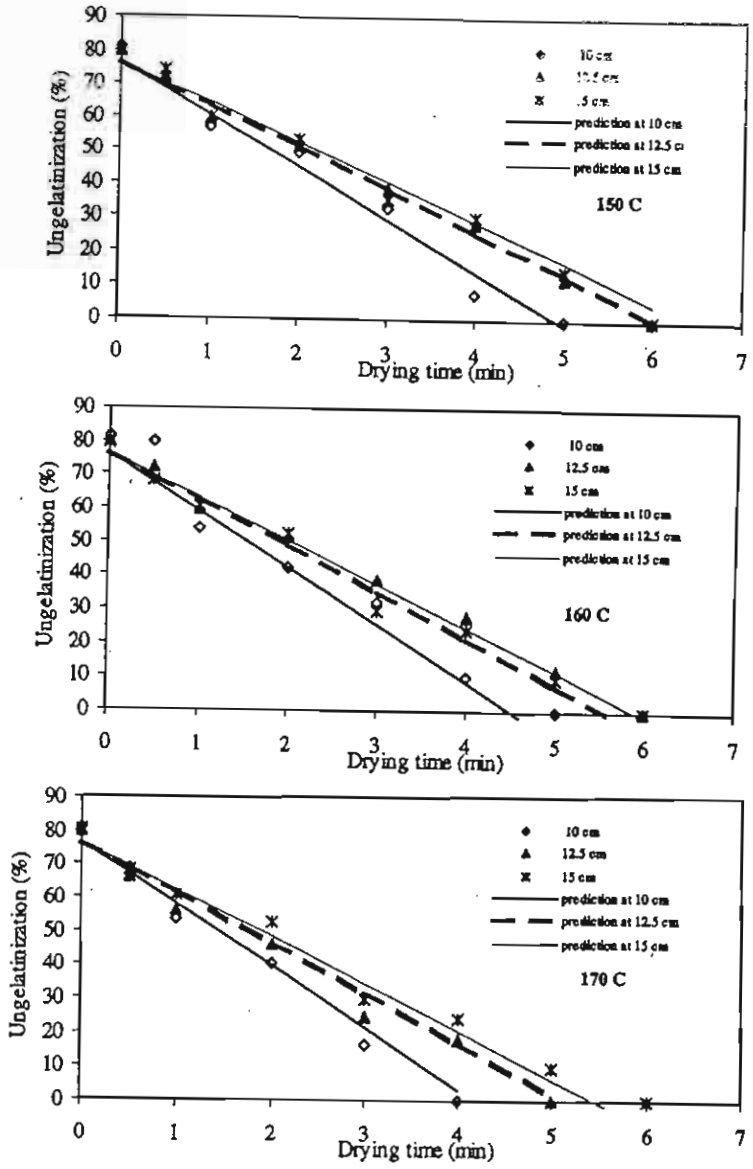


Figure 6. Zero-order reaction kinetics of gelatinization of rice at different temperatures and bed depths.

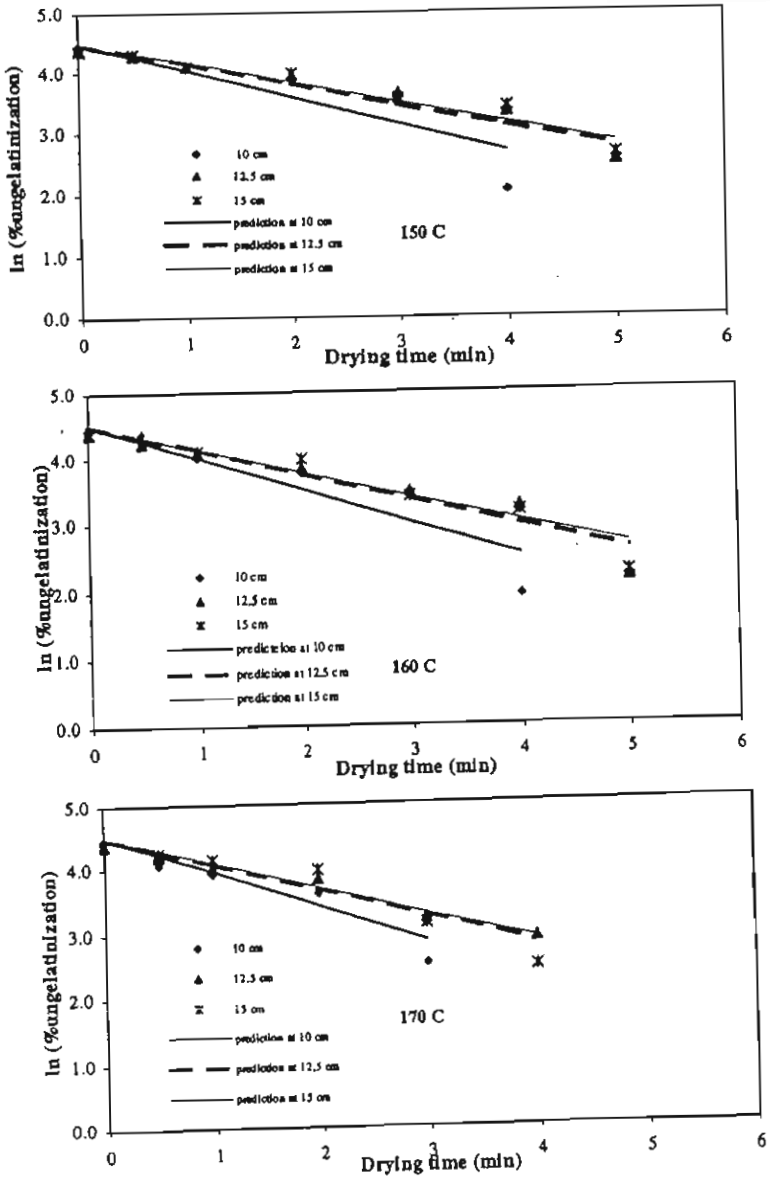


Figure 7. First-order reaction kinetics of gelatinization of rice at different temperatures and bed depths.

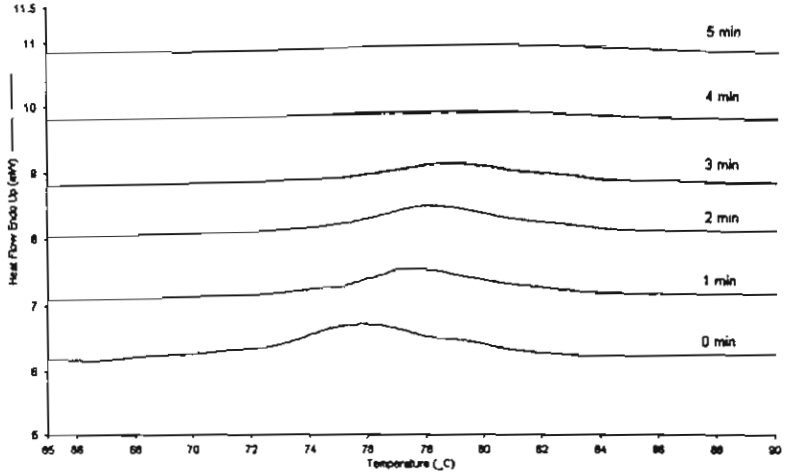


Figure 8. DSC thermal curves for rice drying at temperature of 160°C and bed depth of 15 cm. The water content of all samples was 70% (w/w).

Table 2. Zero-order reaction rate constant for the gelatinization of treated rice.

Drying temperature (°C)	Zero-order reaction rate constant, k (s^{-1})		
	10 cm	12.5 cm	15 cm
150	0.25	0.20	0.20
160	0.28	0.22	0.22
170	0.31	0.24	0.24

kinetics of starch granules they investigated was carried out in a limited range of slightly above normal boiling point temperature and the resulting time required for the complete gelatinization took longer than 20 min, but this work performed in a very shorter time, at least five times.

The apparent rate constants for the zero-order reaction (k) at various drying conditions are presented in Table 2. The apparent rate varies with the temperature and bed depth, the first factor showing a positive effect, in which the rate increases with temperature, whilst the latter shows a negative effect. The relationships between the apparent rate constant and

Table 3. Nonlinear regression analysis of zero-order and first-order

Model	I	G	J	E_a/R	R^2
Zero	−30.34026	3.1920113	−0.109836	−1518.626	0.97
First	−2.630565	0.3054912	−0.010674	−1654.481	0.80

the involving parameters are described by Eqs. (7) and (8), of which the constant parameters determined by the nonlinear regression are given in Table 3. The activation energy for paddy is in order of 12.63 kJ/mol in the temperature range of 150–170°C.

Scanning Electron Microscopy

The microstructure of the starch granules is shown in Fig. 9. Before drying as shown in Fig. 9a, the starch granules spreads throughout the cross-sectional surface. When dried at any drying temperature (150–170°C), the starch granules swelled, absorbed surrounding moisture, and gelatinized, leading to lose its granular appearance. The rice kernels were consequently observed as smoother appearance on the entire cross-sectional microstructure as represented in Figs. 9b–d.

Head Rice Yield

The relationship between head rice yield and final moisture content in the superheated-steam fluidized-bed dryer at different drying conditions is shown in Fig. 10. The head rice yield slightly changes when the paddy is dried from 41–42.5% to 18% d.b. The head rice obtained is in the narrow range of 65–70, which is 70% higher than that of the control samples. The higher head rice yield is because the swelling effect causes the starch granules approaching together and thus resistant to deformation by strengthening the intra-molecular binding forces. This explanation can be indicated by the low SBV, FV, and trough of dried rice flour in RVA measurement. However, when the moisture content reduces below 18% d.b., the head rice yield rapidly decreases. This may be caused by the prevalent contribution of stress forces taking place by moisture gradient, leading to fissure development inside the grain kernels.

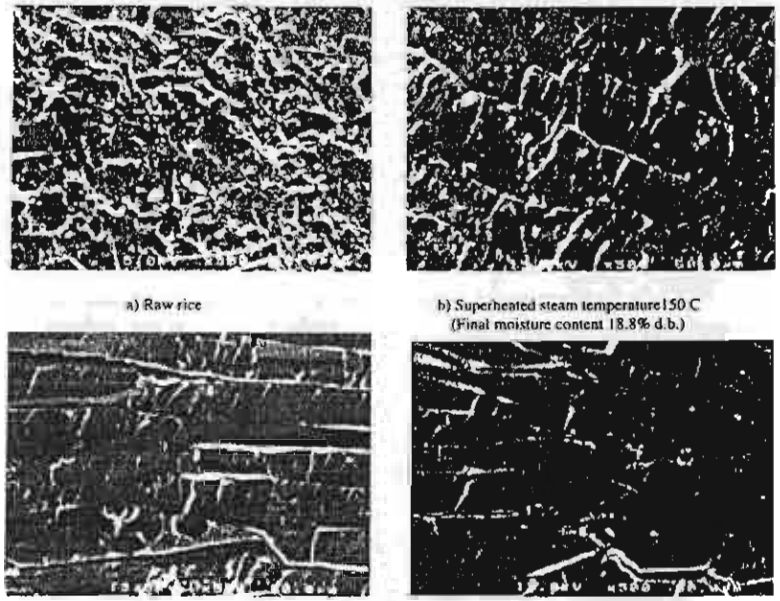
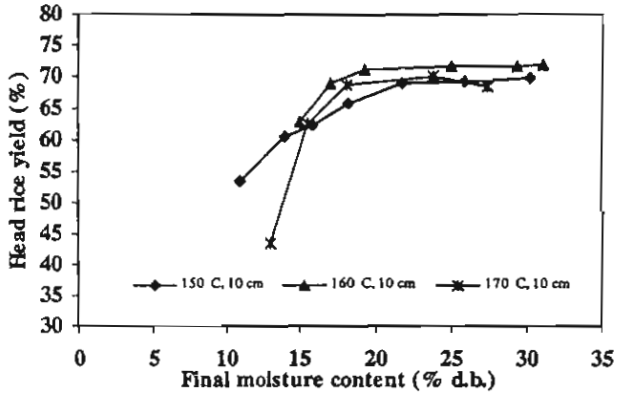


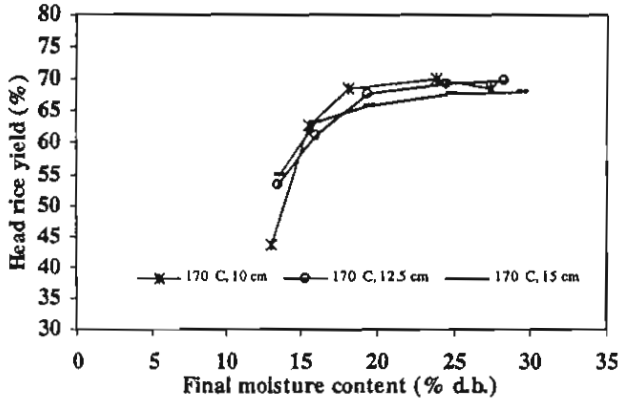
Figure 9. Effect of steam temperature on microstructure.

White Belly

Kernel that has an opaque white area higher than 50% of its total area is taken into account as white belly category, according to Thai Standard Rice.[20] The percentage of white belly shown in Fig. 10 was calculated by the number of white belly kernels divided by the total number of head rice kernels. The percentage of white belly kernels reduces with decrease in final moisture content or, in other words, with increase in drying time. When drying temperature is changed, the percentage of white belly is changed in a way that higher temperature provides the smaller number of white belly kernels as shown in Fig. 11a. The bed depth has a rather small effect, with the value lying between 1 and 2% for the bed depths of 10–15 cm as illustrated in Fig. 10b for 170°C. According to the white belly results, it may be indirectly used to indicate how well the grain kernels can be gelatinized, besides the accurate method.



a) Bed depth 10 cm

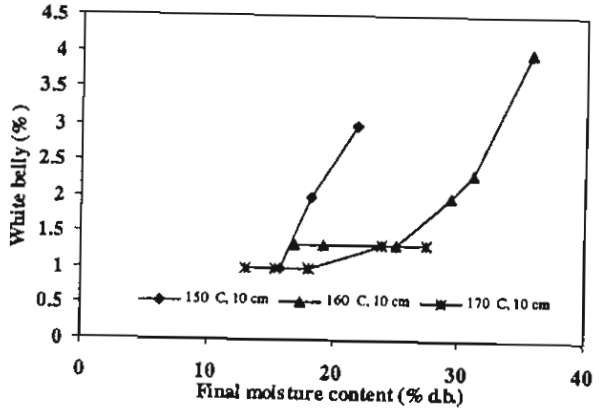


b) Superheated steam temperature 170 C

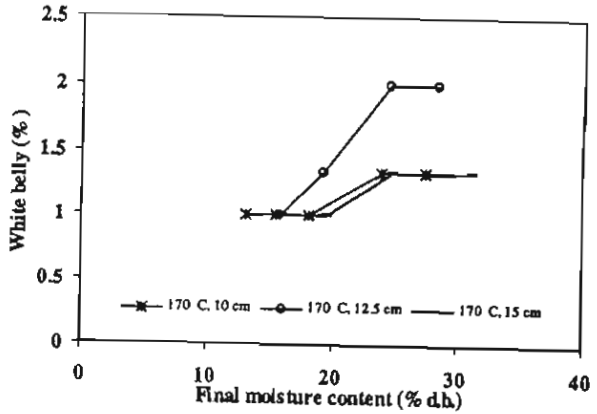
Figure 10. Relationship between head rice yield and final moisture content during drying in superheated steam (initial moisture content = 41.5–42.5% d.b.).

Rice Whiteness

The change of the color of samples at steam temperatures of 150, 160, and 170°C and initial moisture content of 42% d.b. is shown in Figs. 12a and b. The rice whiteness at the first 2 min of drying steeply drops from the original values, 41–43, to approximately 30. Such a rapid change



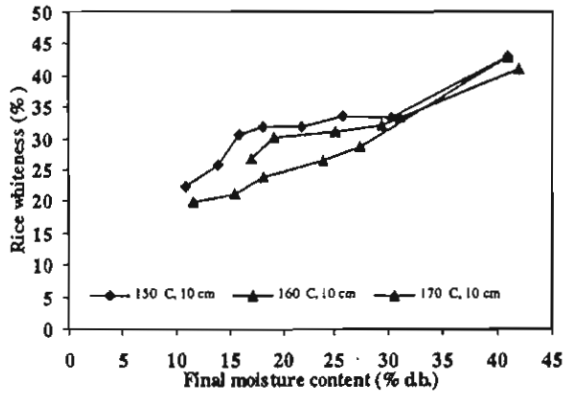
a) Bed depth 10 cm



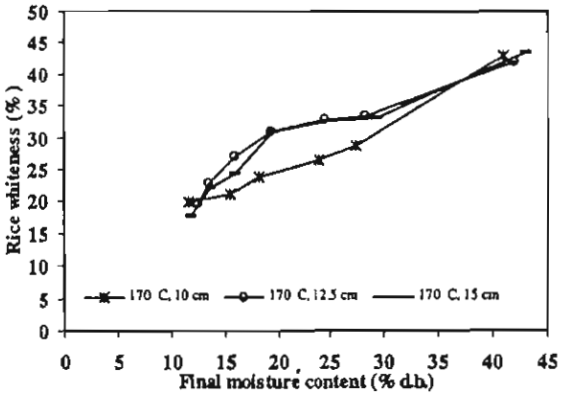
b) Superheated steam temperature 170 C

Figure 11. Relationship between percentage of white belly and final moisture content during drying in superheated steam (initial moisture content = 41.5–42.5% d.b.).

in the color is due to the steam condensation onto the paddy surface. The resulting bran and color pigments covered around kernel are dissolved and then adsorbed by the endosperm: the amounts of bran after milling for the dried samples are in order of 5.3–7.1%, which is approximately two times lower than the original value of the reference samples. In



a) Bed depth 10 cm



b) Superheated steam temperature 170 C

Figure 12. Relationship between rice whiteness and final moisture content during drying in superheated steam (initial moisture content = 41.5–42.5% d.b.).

addition to the result of bran, we also tested the lipid content as presented in Table 4, showing higher lipid contents in the dried rice than in the raw rice. This was due to the absorption of lipid from bran layer to endosperm of grain during drying as mention earlier. Thus, greater amount of lipid was removed with bran of raw rice compared to that of dried sample.

Table 4. Lipid content for dried rice at various temperatures and bed depths.

		Lipid content (%$g/g_{dry\ matter\ flour}$)
Raw white rice		0.2 ± 0.02
Rice		
150°C	10 cm	0.4 ± 0.03
	12.5 cm	0.23 ± 0.04
	15 cm	0.23 ± 0.04
160°C	10 cm	0.43 ± 0.03
	12.5 cm	0.3 ± 0.04
	15 cm	0.21 ± 0.03
170°C	10 cm	0.65 ± 0.02
	12.5 cm	0.35 ± 0.02
	15 cm	0.21 ± 0.03

In addition to the dissolved pigments, the color development might be caused by nonenzymatic Browning reaction. This reaction seems to be enhanced by high grain temperature as shown in Fig. 11a, where the higher temperature causes the lower whiteness. For the bed depth effect, the slightly low value of whiteness is obtained with the use of thin bed depth.

CONCLUSIONS

The characteristics of pasting properties of rice dried by superheated-steam fluidized-bed drying under temperatures, 150–170°C, and bed depths, 10, 12.5, and 15 cm, were determined. Drying rate was initially constant and exponentially decreased after the moisture content was lower than 25% d.b. During superheated steam drying, the gel formation occurred throughout the kernel resulting in the starch molecules closely packed together, as revealed by SEM micrograph. This provided the limitation of the water transport inside the paddy, resulting in low value of effective diffusivity when compared to the case of no gel development. DSC measurement indicated that the kinetics of gelatinization is described by the zero-order reaction. The values of peak viscosity, breakdown viscosity of dried rice were lower than those of the raw rice. Rice whiteness was apparently darkened at high temperature. In addition to such qualities, the percentage of white belly kernels decreased with the increase in inlet drying temperature. To maintain high head rice yield,

it is recommended that the final moisture content of paddy should not be dried lower than 18% dry basis.

ACKNOWLEDGMENTS

The authors would like to express their sincere thanks to the Thailand Research Fund for financial support, Faculty of Engineering and Industrial Technology Silpakorn University for supporting RVA instrument, Division of Agricultural Engineering, Department of Agriculture for testing quality of milling, and Pathum Thani Rice Research Center for testing the physical quality of rice. Phillip Semiconductor (Thailand) for supporting SEM instrument.

REFERENCES

1. Gariboldi, F. Rice parboiling. *FAO Agricultural Development Paper No. 97*; Food and Agriculture Organization of the United Nations: Rome, Italy, 1974.
2. Dimopoulos, J.S.; Muller, H.G. Effect of processing conditions on protein extraction and composition and on some other physicochemical characteristics of parboiled rice. Cereal Chemistry **1972**, *49*, 54–62.
3. Blasco, R.; Alvarez, P.I. Flash drying of fish meals with superheated steam: isothermal process. Drying Technology **1995**, *17* (4–5), 775–790.
4. Iyota, H.; Nishimura, N.; Nomura, T.; Konishi, Y.; Yoshida, K. *Effect of Initial Steam Condensation on Color Changes of Potatoes During Drying in Superheated Steam*, Proceedings of the 13th International Drying Symposium; Beijing, China, Aug 27–30, 2002; Vol. B, 1352–1359.
5. Looi, A.Y.; Golonka and Rhodes, M. Drying kinetics of single porous particles in superheated steam under pressure. Chem. Eng. J. **2002**, *87* (3), 329–338.
6. Iyota, H.; Nishimura, N.; Onuma, T.; Nomura, T. Drying of sliced raw potatoes in superheated steam and hot air. Drying Technology **2001**, *19* (7), 1411–1424.
7. Tatermoto, Y.; Mawatari, Y.; Sakurai, K.; Noda, K.; Komatsu, N. *Drying Characteristics of Pours Material in Superheated Steam Fluidized Bed*, Proceedings of the 13th International Drying Symposium; Beijing, China, Aug 27–30, 2002; Vol. A, 624–633.

8. AACC. *Approved Method of the American Association of Cereal Chemists*, 8th Ed.; American Association of Cereal Chemists: St. Paul, MN, 1995.
9. Dengate, H.N. Swelling pasting, and gelling of wheat starch. In *Advances in Cereal Science and Technology*; Pomeranz, Y., Ed.; American Associated Cereal Chemistry, St. Paul: MN, USA, 1984; Vol. 6, 49–82.
10. Folch, J.; Lees, M.; Sloane-Stanley, G.H. A simple method for isolation and purification of total lipids from animal tissues. J. Bio. Chem. **1957**, *226*, 497–509.
11. Normand, F.L.; Mashall, W.E. Differential scanning calorimetry of whole grain milled rice and milled rice and milled rice flour. Cereal Chemistry **1989**, *66* (4), 317–320.
12. Marshall, W.E.; Wadsworth, J.I.; Verma, L.R.; Velupillai, L. Determining the degree of gelatinization in parboiled rice: comparison of a subjective and an objective method. Cereal Chemistry **1993**, *70*, 226–230.
13. Poomsa-ad, N.; Soponronnarit, S.; Prachayawarakorn, S.; Terdyothin. Effect of tempering on subsequent drying of paddy using fluidization. Drying Technology **2002**, *20* (1), 195–210.
14. Arabshahi, A.; Lund, D.B. Consideration in calculating kinetic parameters from experimental data. J. Food Proc. Engng. **1985**, *7*, 239–251.
15. Okechukwu, P.E.; Rao, M.A. Influence of granule size on viscosity of cornstarch suspension. J. Texture Studies **1995**, *26*, 501–516.
16. Bakshi, A.S.; Singh, R.P. Kinetics of water diffusion and starch gelatinization during rice parboiling. J. Food Science **1980**, *45*, 1387–1392.
17. Suzuki, K.; Kubota, K.; Omichi, M.; Hosaka, H. Kinetic studies on cooking of rice. J. Food Science **1976**, *41*, 1180–1183.
18. Lund, D.B.; Wirakartakusumah, M. A model for starch gelatinization phenomena. In *Engineering and Food*; McKenna, B.M., Ed.; Engineering Science in the Food Industry: London, UK, 1984; Vol. 1, 425–435.
19. Turhan, M; Gunasekaran, S. Kinetic of in situ and in vitro gelatinization of hard and soft wheat starches during cooking in water. J. Food Eng. **2002**, *52*, 1–7.
20. *Ministry of Commerce*; Thai Standard Rice: Thailand, 1997 http://203.151.17.19/document/grain/english/standard.htm, last revised on 20 June 2002.

DRYING TECHNOLOGY
Vol. 22, No. 4, pp. 759–778, 2004

Drying Kinetics and Quality of Shrimp Undergoing Different Two-Stage Drying Processes

Yuvanaree Namsanguan,[1,*] Warunee Tia,[1] Sakamon Devahastin,[2] and Somchart Soponronnarit[1]

[1]School of Energy and Materials and
[2]Department of Food Engineering, King Mongkut's University of Technology Thonburi, Bangkok, Thailand

ABSTRACT

An innovative two-stage drying concept is presented in this article. The work considered drying of shrimp using a superheated steam dryer followed by a heat pump (SSD/HPD) or a hot air dryer (SSD/AD) both from drying kinetics and dried product quality points of view. The experiments were performed using the first-stage superheated steam drying temperature of 140°C while the second-stage heat pump drying (or hot air drying) was performed at 50°C. The moisture content of shrimp at the end of the superheated steam

*Correspondence: Yuvanaree Namsanguan, School of Engineering and Materials, King Mongkut's University of Technology Thonburi, 91 Pracha U-tid Road, Bangkok 10140, Thailand; Fax: 662-470-8663; E-mail: yuvanaree@yahoo.com.

DOI: 10.1081/DRT-120034261
0737-3937 (Print); 1532-2300 (Online)
Copyright © 2004 by Marcel Dekker, Inc.
www.dekker.com

drying stage was varied between 30 and 40% (w.b.). The effect of tempering between SSD/HPD was also investigated. Shrinkage, color, rehydration behavior, texture (toughness and hardness), and microstructure of dried shrimp were measured. The results showed that SSD/HPD dried shrimp had much lower degree of shrinkage, higher degree of rehydration, better color, less tough and softer, and more porous than single-stage SSD dried shrimp. It was also found that SSD/AD gave redder shrimp compared to shrimp dried in a single-stage superheated steam dryer. No improvement in terms of shrinkage and rehydration behavior was observed, however.

Key Words: Color; Hybrid drying; Rehydration behavior; SEM; Shrinkage; Texture.

INTRODUCTION

Shrimp is one of the most popular seafood products available. Traditionally, a production of dried shrimp is performed in a small-scale, mostly at a household level, and sun drying, roasting in an opened air, or alternating with dryer have been used mostly to dry shrimp. Due to very high domestic and export demands, however, a way to improve the dried shrimp production that would yield dried shrimp of superior quality at a high drying rate and lower energy consumption is desired. The preferred quality of dried shrimp is red-orange color, low shrinkage, little tough but rather soft.

The production of dried shrimp can be mainly divided into two steps: boiling raw shrimp in NaCl solution (in order to deactivate microbial growth) and then drying. For shrimp drying the use of a superheated steam dryer (SSD) seems very attractive since boiling and drying can be performed in a single step due to the use of superheated steam as the drying medium. Another advantage of using SSD to dry shrimp, and hence be able to eliminate the boiling step, is that there is no nutritional loss during boiling.[1] The color and shrinkage were also found to be better than shrimp dried in a conventional hot air dryer (AD). Other advantages of using SSD to dry shrimp include the ability to obtain the dried product that has lower degree of shrinkage, which is due to expanded vapor inside the product during rapid drying leading to a highly porous structure.[2–5] It is found, however, that although the higher steam temperature leads to more and larger pores, the elevated steam temperature corresponds to a higher modulus of deformation (hardness) of the dried product.

Albeit the above-mentioned advantages, the use of higher steam temperature may cause the thermal damage of food or some other biological products such as structural degradation, discoloration and protein denaturation.[6,7] Drying product at a higher steam temperature for an extended period of time may also damage its porous structure. In the case of meat product such as shrimp, thermal denaturation of muscle (myofibrillar proteins) and shrinkage of collagen experienced during dehydration can also result in a tightening and stiffening of its structure.

To alleviate the aforementioned problem, various new drying techniques have been proposed and reported over the past decade such as hybrid or multi-stage drying. For example, the two-step SSD/AD (superheated steam drying followed by hot air drying) was recommended by Chen et al.[7] for drying silk cocoon. Since all a product of improper silk quality was obtained when drying was conducted solely in superheated steam. Innovatively, combining a superheated steam dryer and a heat pump dryer (HPD) may have a potential for improving the quality of the final dried product as well as reducing the energy consumption due to enhanced drying rates. SSD can produce a product with high porous structure at a higher drying rate during the first stage of drying; HPD could then be used to maintain the shape and preserve the color of the drying product.[8–15]

The purpose of the present work was to study a two-stage SSD/HPD (superheated steam drying followed by heat pump drying). The effect of tempering between these two stages of drying was also investigated in order to possibly reduce the drying time. The drying characteristics, along with various quality attributes of dried shrimp, i.e., shrinkage, color, texture (toughness and hardness), rehydration behavior and microstructure, were investigated. In addition, SSD/AD was also investigated and compared with SSD/HPD and SSD/HPD with tempering.

MATERIALS AND METHODS

Equipment

Figure 1 shows a schematic diagram of the close-loop superheated steam drying system used in the present study. The unit consisted of a steam generator, a steam superheater rated at 13.5 kW, a $0.3 \times 0.3 \times 0.1$ m^3 cabinet dryer and a backward-curved blade centrifugal fan, which was used to circulate the drying steam through the dryer. Drying was performed at a pressure slightly above the atmospheric pressure.

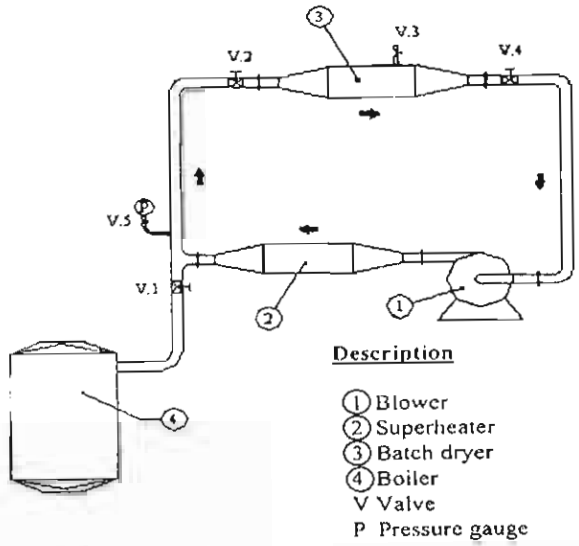


Figure 1. A schematic diagram of the superheated steam dryer used.

A schematic diagram of the close-loop heat pump dryer using R134a refrigerant, which was also used in the present study, is shown in Fig. 2. The unit consisted of a 0.5 kW reciprocating compressor, a 1 kW evaporator, a 1.8 kW internal condenser and a 1.1 kW external condenser. The evaporator bypass air ratio was fixed at 52%.

For air-drying experiments, drying was performed in an open-circuit hot air dryer. An AD unit used consisted of an air heater rated at 4 kW, a $0.4 \times 0.4 \times 0.4\ m^3$ cabinet dryer and a 1.5 kW centrifugal fan. Both steam and air (in HPD and AD) were forced to flow in parallel with a series of wire screens where the samples sat upon in each dryer. Temperatures of all drying media were measured by type-*k* thermocouples connected to a data logger with an accuracy of ±1°C.

Drying of Shrimp

One kilogram of raw shrimp (*Penaeidae*) was used in each drying test. Before drying raw shrimp was washed and dipped in NaCl solution (2% W/V) at room temperature for 30 min. The sample was then placed proportionally on three wire screens. The weight of shrimp was measured

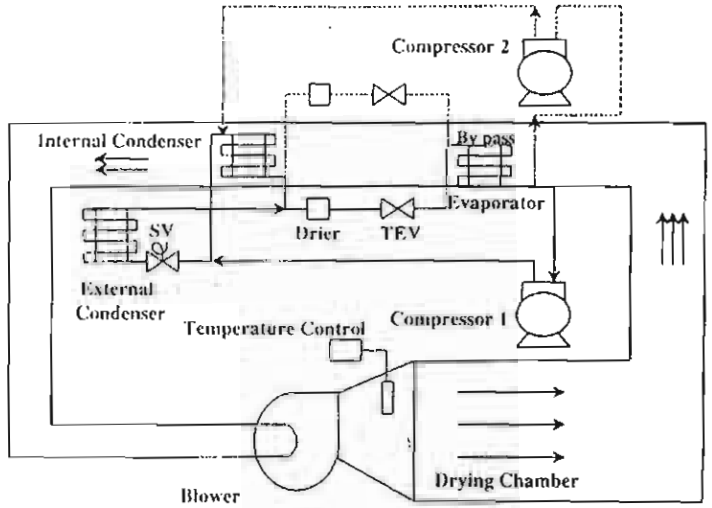


Figure 2. A schematic diagram of the heat pump dryer used (SV = solenoid value, TEV = thermostatic expansion value).

by a digital balance (an accuracy of ±0.1 g) at every 15 min interval during drying. Drying was carried out first in an SSD and later in an HPD. The inlet steam temperature of 140°C and the steam velocity of 2.08 ± 0.2 m/s were used in all experiments. For an HPD unit drying was performed at the drying air temperature and air velocity of 50°C and 0.91 m/s, respectively. The moisture content of dried shrimp after SSD was termed intermediate moisture content (IMC), and was varied between 30 ± 2.4 and 40 ± 2.1% (w.b.). For comparison shrimp was also dried solely using SSD. Another set of experiments involved using SSD/HPD but with a tempering period in between. During tempering shrimp was placed in a tightly sealed container and kept at 60°C with the tempering time of 60 min. Drying conditions used for the SSD/HPD with tempering experiments were the same as those used in the SSD/HPD experiments with no tempering.

Finally, drying was also carried out first in an SSD and later in an AD. For SSD/AD experiments, the first-stage drying conditions and IMCs were the same as those in SSD/HPD experiments. The air temperature and air velocity used in the second-stage air dryer were set at 50°C and 0.87 m/s, respectively.

Shrinkage Measurement

The measurement of shrinkage was performed by manually measuring the sizes of dried shrimp samples obtained from different drying processes (SSD, SSD/HPD, SSD/HPD with tempering, and SSD/AD) using a vernier (by measuring each sample at three positions: length, width, and thickness). The equivalent spherical diameter of each sample was then determined and compared. Ten samples were taken for measurement for each experimental condition. All experiments were performed in duplicate. Percentage of shrinkage was then calculated by:

$$\% \text{ shrinkage} = \frac{Z_o - Z_f}{Z_o} \times 100 \quad (1)$$

where Z_o and Z_f are respectively the sizes of shrimp at the beginning and at the end of each drying experiment.

Color Measurement

Colors of the dried samples were assessed using a colorimeter (Juki JP 7100, Juki Corporation, Tokyo, Japan). The color system used was Hunter Lab where "L" is a measure of lightness, "a" is a measure of redness (-a implies greenness), and "b" is a measure of yellowness (-b implies blueness). For each drying experiment color measurements were taken on five dried and deshelled samples at three positions: P1 (by the head) to P3 (by the tail). The average of 15 measurements of each color parameter (L, a, b) was reported. All experiments were performed in duplicate.

Texture Measurement

Texture of dried and deshelled samples was analyzed by shear test and uniaxial compression test. The shear test was carried out using a TA-XT2i Texture Analyzer (Stable Micro Systems, Haslemere, England). The force required to cut through an individual dried shrimp was measured using a Warner-Bratzler (WB) shear blade with an angular triangular slot cutting edge. The crosshead speed used was 2 mm/s and the distance travelled by the blade through the whole sample thickness and through the base plate slot was 20 mm. The maximum shear force was recorded. Three measurements were taken each at three positions (near head, center, and near tail). Fifteen samples were analyzed and the mean value of 45 measurements was reported.

A uniaxial compression test was performed using an Instron Universal Testing Machine model 4301 (Instron Limited, High Wycombe, England). The crosshead speed used was 50 mm/min and the specimens were compressed to 50% of their original thickness. The values of maximum force reported were the mean of 30 measurements.

The two textural tests were carried out by shearing and compressing the samples perpendicular to the muscle fiber axis and were performed in duplicate.

Microstructure Measurement

The microstructure of dried shrimp samples was analyzed by a JEOL Scanning Electron Microscope (model JSM-5600LV, JEOL Ltd., Tokyo, Japan) with an accelerating voltage of 10 kV. The samples were cut perpendicular to their body longitudinal direction and their cross sections (transverse sections) were observed.

Rehydration Measurement

Dried shrimp samples were rehydrated by immersing them in hot water at 100°C. The samples were drained and their sizes were measured by a vernier at 1 min interval for 10 min. The expanded size, due to absorbed water, was then expressed as the degree of rehydration. The slope of the plot between the degree of rehydration and the rehydration time was defined as the rate of rehydration.

All experiment data were analyzed using an analysis of variance (ANOVA). Differences among mean values were established using the Duncan test. Mean values were considered significantly different when $p < 0.05$.

RESULTS AND DISCUSSION

Drying Curves

The drying curves of shrimp undergoing SSD and two-stage SSD/HPD are shown in Fig. 3. By varying the intermediate moisture content

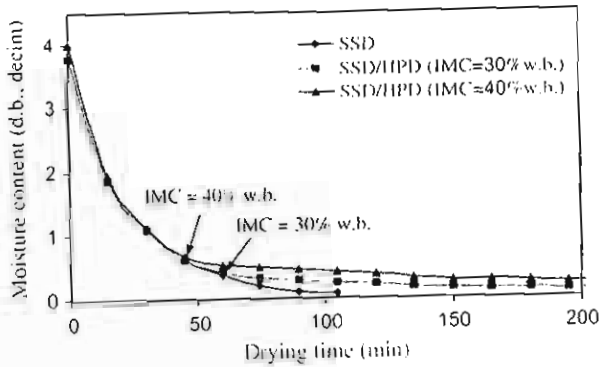


Figure 3. Drying curves of shrimp undergoing purely SSD and SSD/HPD. *(View this art in color at www.dekker.com.)*

(IMC) between 30 and 40% (w.b.), the final moisture content of shrimp of about 20% (w.b.) was reached in approximately 100 and 180 min, respectively. It can be seen from this figure that purely SSD resulted in the highest rate of moisture reduction as compared with the other drying techniques tested here. The moisture content of shrimp of about 20% (w.b.) was reached in approximately 70 min since the whole drying process was performed at a higher medium temperature.

To reduce the drying time of SSD/HPD, tempering between these two stages of drying was included. Figure 4 represents the effect of tempering on the second-stage HPD drying curves. After passing through the tempering stage, shrimp dried faster during the second-stage HPD. As shown in Fig. 4, the linearized second-stage HPD drying curves illustrate the effect of tempering on the second-stage drying rate by comparing the specific drying constant, K, which is equal to the slope of the plots between $\ln[M - M_{eq}]/[M_{in} - M_{eq}]$ against time, where M is the moisture content of shrimp and the subscripts "in" and "eq" are initial and equilibrium, respectively. Higher values of K were obtained for shrimp undergoing tempering for both IMC's (Figs. 4(a) and (b)) implying higher drying rates. The faster moisture removal is due probably to the redistribution of moisture inside the product. The moisture inside the shrimp body transported to the exterior surface and concentrated near this surface, so it could be removed more easily when drying was continued again. It was found that SSD/HPD with tempering could save about 14 and 12% of the net drying time for the corresponding IMCs of about 30 and 40% (w.b.), respectively.

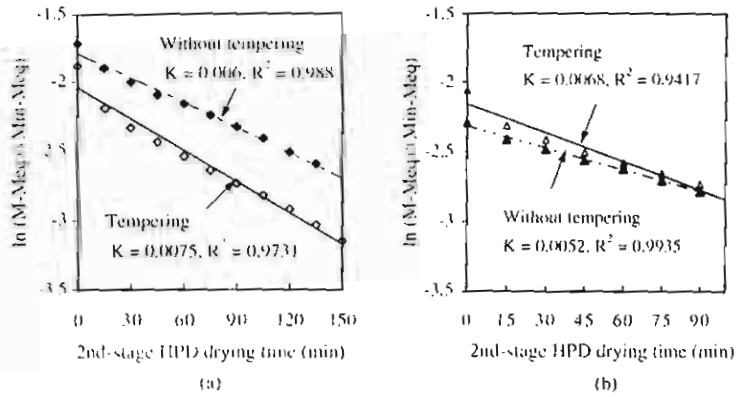


Figure 4. Linearized second-stage HPD drying curves: K = specific drying constant (dotted line were experimental and dashed line were calculated data). (a) IMC about 40% w.b., (b) IMC about 30% w.b. *(View this art in color at www.dekker.com.)*

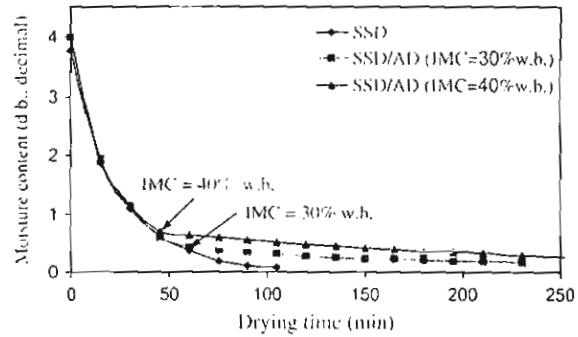


Figure 5. Drying curves of shrimp undergoing purely SSD and SSD/AD. *(View this art in color at www.dekker.com.)*

Figure 5 shows the drying curves for the case of SSD/AD. The moisture content of shrimp reached 20% (w.b.) in approximately 135 and 250 min for the corresponding IMCs of about 30 and 40% (w.b.), respectively. In terms of the drying time, as shown in Fig. 6, SSD/HPD was found to be 1.4–1.5 times faster than SSD/AD at the same IMCs. This is due to the use of low-humidity drying air in an HPD; SSD/HPD is thus a faster drying process compared with SSD/AD. Compared to

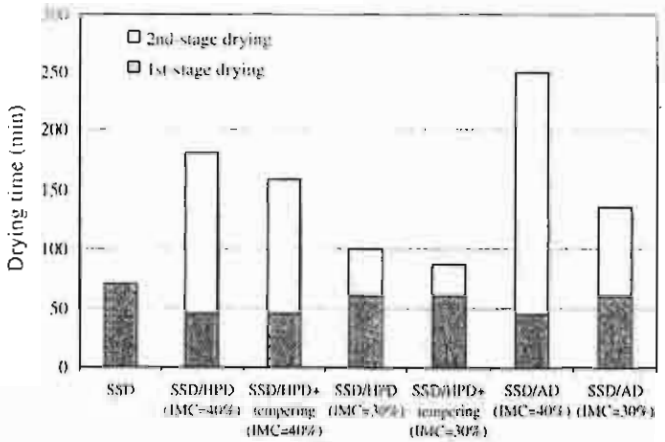


Figure 6. Net drying time of dried shrimp undergoing different drying techniques (reached to the final moisture content of about 20% (w.b.)). *(View this art in color at www.dekker.com.)*

purely SSD, it was observed that the drying time increased slightly in the case of SSD/HPD at lower IMCs but increased significantly in the case of SSD/AD at higher IMCs. For the same two-stage drying process, i.e., SSD/HPD or SSD/AD, it was found that the lower IMC used, the shorter the drying time required. For the same value of IMC used, the drying time required to reach the desired final moisture content differs significantly for the case of SSD/HPD and SSD/AD, however.

Shrinkage

During drying foods undergo volume changes either by shrinkage, which is due to the removal of water from the drying material or by expansion, which is due to the gas generation or pore formation.[16] Different drying techniques thus provide different degrees of volume changes. Normally, the muscle fibers shrink as they lose moisture during drying.

Table 1 shows the results of shrinkage of shrimp that underwent different drying techniques investigated. Shrinkage was found to be lower in the case of SSD/HPD as compared to the case of purely SSD. Although superheated steam drying is known to have a potential to

Table 1. Percentage of shrinkage of shrimp undergoing different drying techniques.*

Drying technique	Shrinkage (%)
SSD	37.50 ± 7.50^{b}
SSD/HPD (IMC ≈ 40% w.b.)	$31.20 \pm 5.67^{a,b}$
SSD/HPD + tempering (IMC ≈ 40% w.b.)	35.79 ± 4.64^{b}
SSD/HPD (IMC ≈ 30% w.b.)	21.47 ± 7.36^{a}
SSD/HPD + tempering (IMC ≈ 30% w.b.)	23.81 ± 6.39^{a}
SSD/AD (IMC ≈ 40% w.b.)	48.07 ± 8.87^{c}
SSD/AD (IMC ≈ 30% w.b.)	35.53 ± 7.19^{b}

*Data are means ± standard deviations.
[a,b,c]Means in the same column with different superscripts are significantly different ($p < 0.05$).

reduce the degree of shrinkage of the drying product due to the evolution of vapor inside the product that expands into cells, leading to a normally porous dried product.[12, 51] drying product at higher steam temperature for an extended period of time may damage the porous structure and hence leads to a less porous product when comparing with the product undergoing SSD/HPD. When separating drying into the first-stage drying at high steam temperature and the second-stage HPD at lower air temperature, it was observed that most pores or space network inside the products developed during superheated steam drying were better maintained during the second-stage HPD due to the use of lower air temperature. Using HPD as the second-stage drying thus helps maintaining the shape of product better than using only SSD.

Similarly, the degree of shrinkage of shrimp undergoing SSD/HPD with tempering was found to be lower than that of purely SSD; similar trends to SSD/HPD were observed, but tempering seemed to yield a product with slightly higher degree of shrinkage than that obtained from the process with no tempering. It is possible that some shrinkage occurred during the tempering period.

The degree of shrinkage of SSD/AD dried shrimp when IMC ≈ 40% (w.b.) was much higher, while that of SSD/AD when IMC ≈ 30% (w.b.) was found to be almost equal to that of purely SSD. It can be concluded that SSD/AD gives no improvement in terms of shrinkage of dried shrimp over that of purely SSD. A possible reason for this is that SSD/AD took longer drying time, especially at higher IMCs. Furthermore, hot air drying is normally known as the cause of shrinkage itself as confirmed

by several previous works such as those of Prachayawarakorn et al.[11] and Posomboon.[17]

It was also noticed that the lower the intermediate moisture content, the lower the degree of shrinkage. This may be ascribed to the fact that changing the process from SSD at higher moisture contents resulted in a lower degree of pore development. Thus, when the drying was continued with HPD, the materials shrink easier. Drying time is also a significant factor in determining the degree of shrinkage; it takes longer time to dry products with higher IMCs in an HPD so these products tend to shrink more than those with lower IMCs.

Colors

Dried shrimp samples that were processed by different drying techniques were distinguishable based on both visual and instrumental assessments of their colors. Instrumentally, as shown in Table 2, the "a" and "b" values of samples dried in both SSD/HPD and SSD/HPD with tempering were higher compared to samples dried in purely SSD while the values of "L" were lower. Since the intense red orange color indicates the good quality of dried shrimp, it can be said that SSD/HPD and SSD/HPD with tempering have a potential to improve the color of dried shrimp in terms of higher a and b values, and lower L value. In the case of SSD/HPD, it is possible that the two-stage drying process helps preventing color degradation, which may result from the use of higher steam temperature for an extended period of time in SSD; low drying

Table 2. Values of "a," "b," and "L" of dried shrimp samples.

Sample	Colors		
	a	b	L
SSD	6.05^{d}	12.80^{b,c}	41.98^{a}
SSD/HPD (IMC ≈ 40% w.b.)	10.82^{a}	13.64^{a,b}	34.89^{b}
SSD/HPD + tempering (IMC ≈ 40% w.b.)	11.47^{a}	14.95^{a}	36.48^{b}
SSD/HPD (IMC ≈ 30% w.b.)	6.80^{c,d}	13.12^{b}	36.32^{b}
SSD/HPD + tempering (IMC ≈ 30% w.b.)	7.33^{b,c}	13.28^{b}	35.18^{b}
SSD/AD (IMC ≈ 40% w.b.)	5.97^{d}	11.34^{c}	42.08^{a}
SSD/AD (IMC ≈ 30% w.b.)	8.19^{b}	9.75^{d}	35.25^{b}

^{a,b,c,d}Means in the same column with different superscripts are significantly different ($p < 0.05$)

temperature in the second-stage HPD helps preserving the color of the dried products. As confirmed by many researchers HPD itself is known to provide excellent product color[9,11,12,18] and hence is a good candidate for the second-stage drying. Switching the process from SSD to HPD at higher moisture contents yields products of better color since doing so implies shorter exposure of shrimp to the higher drying temperature. In this work, the initial values of a, b, and L were −0.42, −0.97, and 32.15, respectively.

Shrimp dried by SSD/HPD with tempering also possessed similar color trends to that dried by SSD/HPD; the two-stage drying with tempering yielded products that were redder and more yellow than products obtained from the process without tempering since tempering reducing the HPD drying time. Moreover, based on the sensory evaluation, it was found that shrimp undergoing SSD/HPD and SSD/HPD with tempering was more transparent and glossy than purely SSD samples. This is due to the shorter drying period at higher steam temperature.

On the other hand, SSD/AD gave reversed results compared to SSD/HPD. Shrimp that was dried using this technique seemed to have no color improvement compared to SSD. Since SSD/AD took longer time to dry shrimp due to the disadvantages of high humidity air, color could not be preserved. Dried shrimp that had an IMC ≈ 30% (w.b.) was markedly redder compared to that had an IMC ≈ 40% (w.b.), however. This is due to the shorter second-stage drying time at lower IMCs mentioned earlier.

In the case of pure hot air drying, the color of dried shrimp is not acceptable if high air temperatures (over 140°C) are used[17] while the color is not acceptable when the drying temperature is over 160°C for SSD.[11] A two-stage SSD/HPD is therefore a possible way to eliminate this limitation; a higher steam temperature is used only in the first-stage SSD to increase the drying rate while the rest of drying is conducted in a lower-temperature environment.

Texture

Textural properties of dried shrimp samples were measured in terms of shear strength or maximum shear force (Fig. 7) and maximum force in compression test (Fig. 8). The shear strength is an indicator of the toughness of the product whereas the compressive force is an indicator of the hardness. Shear strength can describe the maximum force needed to cut the product in human mouth by the front teeth while hardness measures the force needed to destruct the product by the molars.

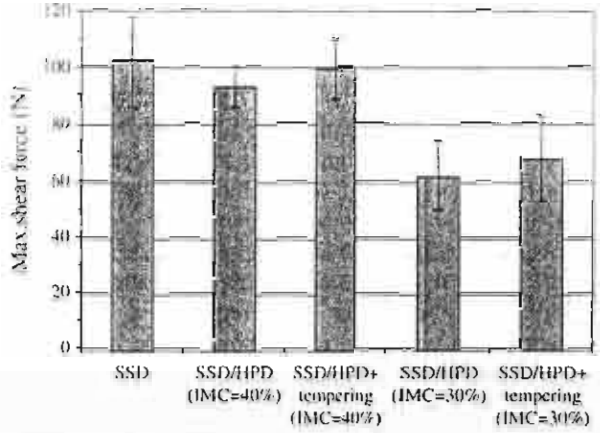


Figure 7. Shear strength of dried shrimp undergoing different drying techniques (vertical lines indicate standard deviations). *(View this art in color at www.dekker.com.)*

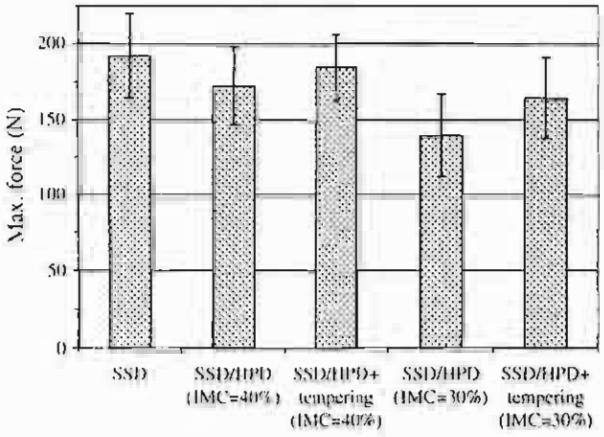


Figure 8. Hardness of dried shrimp undergoing different drying techniques (vertical lines indicate standard deviations). *(View this art in color at www.dekker.com.)*

From the experiments it was found that the shear strength required to cut dried shrimp undergoing SSD/HPD and SSD/HPD with tempering was lower than that required for SSD samples, especially when IMC $\approx 30\%$ (w.b.); the texture of SSD/HPD dried shrimp was less tough than

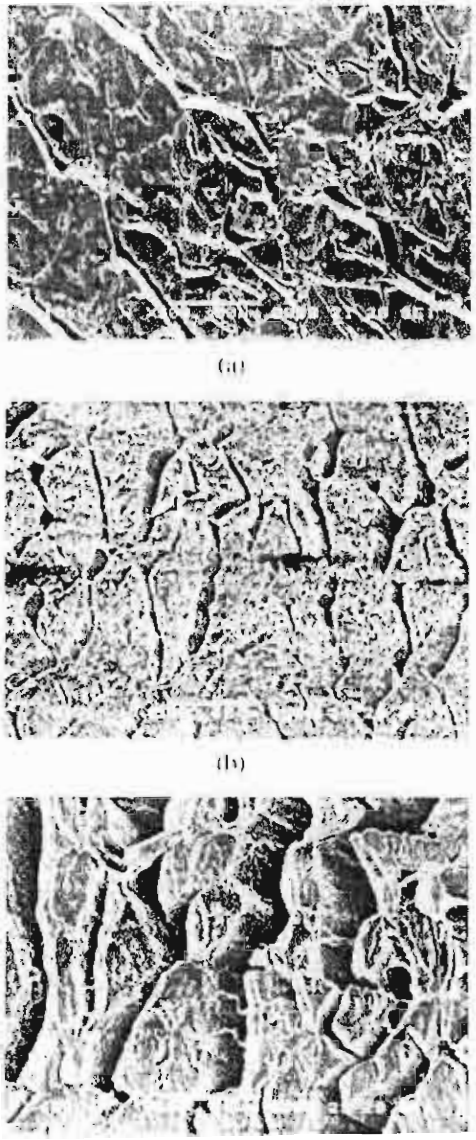
that of SSD samples (Fig. 7). Similarly, shrimp undergoing SSD/HPD and SSD/HPD with tempering was softer than that dried by purely SSD (Fig. 8). Evidently, toughness and hardness are closely related; a direct relationship was found between instrumental shear force (toughness) and compressive force (hardness) measurements for all different dried samples tested.

Based on the instrumental evaluation it was found that the texture of dried shrimp samples obtained from two-stage SSD/HPD with and without tempering was less tough and softer than that of samples obtained from the single-stage SSD. This is due to the shorter period of high-temperature drying, which leads to less tough and softer dried product. It is also known that temperature changes the solubility of the meat protein; high temperature in food processing often attributes to increased protein coagulation resulting in the toughening of the meat fibers.[19] The texture of dried shrimp also seems to have a direct relationship with shrinkage; the lower the degree of shrinkage, the less tough and softer the dried product.

Microstructure

Figure 9 shows the microstructure of dried shrimp samples obtained from different drying processes (SSD and SSD/HPD) while Figs. 10(a) and (b) compare the microstructure of dried samples undergoing SSD/HPD with and without tempering. Microscopically, all scanned sets of dried shrimp muscle tissue had nearly the same pattern in their structure organization. However, there was an enormous system of pore between the muscle fibers of shrimp undergoing SSD/HPD, especially at IMC $\approx 30\%$ (w.b.) (Fig. 9(c)) while there was much less pore space inside the muscle fibers of shrimp undergoing single-stage SSD (Fig. 9(a)). SSD samples seemed to have a tightening structure of muscle fibers due to its exposure to an extended period of high-temperature drying. For the effect of tempering it was observed that some shrinkage occurred during the tempering period. As shown in Fig. 10 shrimp undergoing SSD/HPD with tempering had less space inside its muscle fibers than samples that did not go through the tempering period.

Generally, dried products with more porous structure often have lower density as well as lower degree of shrinkage. As evidenced by SEM photographs and the results on shrinkage discussed earlier, larger pore space resulted in a lower degree of shrinkage. Besides, this pore space system affects the texture of shrimp; more space inside the muscle fibers resulted in a softer shrimp. SSD/HPD samples were thus the least tough

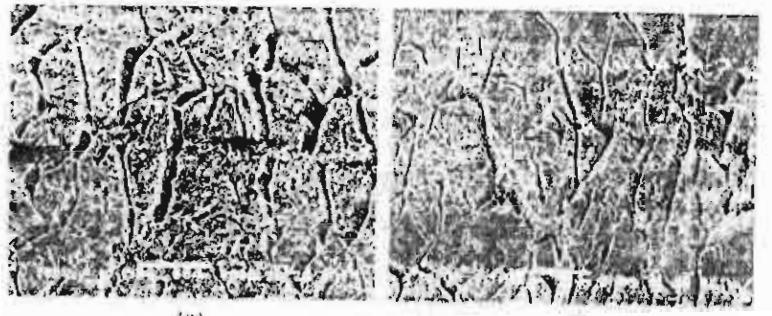


(a)

(b)

(c)

Figure 9. Effects of different drying processes on microstructure of dried shrimp (transverse sections). (a) SSD, (b) SSD HPD (IMC ~ 40% w.b.), and (c) SSD HPD (IMC ~ 30% w.b.).



(a) (b)

Figure 10. Effects of tempering between SSD and HPD on microstructure of dried shrimp (IMC ~ 40% w.b.) (transverse sections). (a) SSD HPD and (b) SSD HPD with tempering.

and the softest. This is probably the reason for the direct correlation between shrinkage and textural properties of dried shrimp.

Rehydration Behavior

Figure 11 illustrates the rehydration behavior of dried shrimp samples obtained from different drying methods at rehydrating temperature of 100 C. The trends are similar for all sample sets tested. Higher rehydration rates were observed at the beginning of the process, as expected. Also, it was found that SSD HPD produced samples had higher degree of rehydration compared to samples dried using other techniques. An adversely relationship was also found between the degree of rehydration and that of shrinkage.

Generally, it is accepted that the degree of rehydration is dependent on the degree of cellular and structural disruption[20,21] and the nature of internal porous structure and mechanical properties of dried materials will influence the water uptake during their rehydration. The space system provides necessary avenues for conveying water to the muscle fibers, which are indispensible during rehydration.[22] Form SEM photographs, it is clear that the structural pattern of dried shrimp tissue is directly related to its rehydratability. SSD HPD dried shrimp had higher degree of rehydration than dried samples obtained from the other drying methods studied.

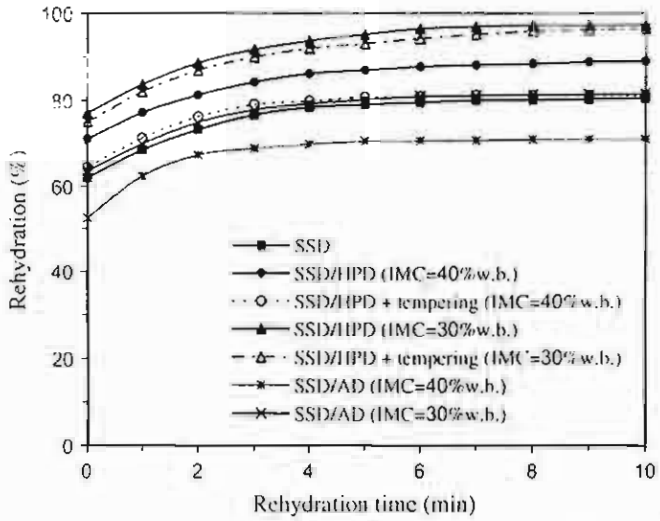


Figure 11. Rehydration curves of dried shrimp samples obtained from different drying processes. *(View this art in color at www.dekker.com.)*

CONCLUSION

SSD/HPD is a new alternative for two-stage drying, which has proved to yield a product of better quality; degree of shrinkage, rehydration potential, color, textural properties, and microstructure of shrimp undergoing this newly proposed drying scheme were greatly improved as compared to samples undergoing a single-stage SSD. An enormous system of pore space between the muscle fibers of sample undergoing SSD/HPD was also observed as compared to sample undergoing only SSD.

A two-stage drying (SSD/HPD) with a tempering period in between was also tested. It was found that the drying rate during the second-stage HPD could be improved when the tempering treatment between the two drying stages was included. In addition, a two-stage SSD/AD was tested and it was found that the process led to some quality improvement viz. redder products but no improvement was observed in terms of shrinkage and rehydration behavior.

An appropriate selection of drying conditions viz. drying temperature and intermediate moisture content between the two drying stages presents an effective way to improve dried product quality in many ways. For this study, the optimum IMC ≈ 30% (w.b.) was found to improve many attributes of quality of dried shrimp.

ACKNOWLEDGMENTS

The authors would like to express their sincere appreciation to the Thailand Research Fund (TRF) for supporting this study financially.

REFERENCES

1. Prachayawarakorn, S.; Soponronnarit, S.; Wetchacama, S.; Jaisut, D. Desorption isotherms and drying characteristics of shrimp in superheated steam and hot air. Drying Technology **2002**, *20* (3), 669–684.
2. Caixeta, A.T.; Moreira, R.G.; Castell-Perez, M.E. Impingement drying of potato chips. Journal of Food Process Engineering **2002**, *25*, 63–90.
3. Elustondo, D. Drying foodstuff with superheated steam. Drying Technology **2002**, *20* (1), 235–237.
4. Moreira, R.G. Impingement drying of foods using hot air and superheated steam. Journal of Food Engineering **2001**, *49*, 291–295.
5. Seyed-Yagoobi, J.; Li, Y.B.; Moreira, R.G.; Yamsaengsung, R. Superheated steam impingement drying of tortilla chips. Drying Technology **1999**, *17* (1–2), 191–213.
6. Mujumdar, A.S. Superheated steam drying. *Handbook of Industrial Drying*; Pub. Marcel Dekker Inc.: New York, 1995.
7. Chen, S.-R.; Chen, J.-Y.; Mujumdar, A.S. A preliminary study of steam drying of silkworm cocoons. Drying Technology **1992**, *10* (1), 251–260.
8. Sosle, V.; Raghavan, G.S.V.; Kittler, R. Low-temperature drying using a versatile heat pump dehumidifier. Drying Technology **2003**, *21* (3), 539–554.
9. Alves-Filho, O. Combined innovative heat pump drying technologies and new cold extrusion techniques for production of instant foods. Drying Technology **2002**, *20* (8), 1541–1557.
10. Chua, K.J.; Chou, S.K.; Ho, J.C.; Hawlader, M.N.A. Heat pump drying: recent developments and future trends. Drying Technology **2002**, *20* (8), 1579–1610.

11. Perera, C.O. *Modified Atmosphere Heat Pump Drying of Food Products*, Proceedings of the 2nd Asian-Oceania Drying Conference (ADC '01), Pulau Pinang, Malaysia, Aug 20–22, 2001; 469–476.
12. Strommen, I. *Heat Pump Drying, New Development and Applications*, Proceedings of the 2nd Asian-Oceania Drying Conference (ADC '01), Pulau Pinang, Malaysia, Aug 20–22, 2001; 102–113.
13. Prasertsan, S.; Saen-saby, P. Heat pump drying of agricultural materials. Drying Technology **1998**, *16* (1–2), 235–250.
14. Chou, S.K.; Hawlader, M.N.A.; Ho, J.C.; Wijeysundrea, N.E.; Chua, K.J. *Heat Pump Drying Systems*, Proceedings of the 4th ASEAN Science and Technology Week, Science and Technology: The Future of ASEAN, Bangkok, Thailand, Aug 21–Sept 1, 1995; 266–276.
15. Young, G.; Sirchall, S; Mason, R. *Heat Pump Drying of Food Products—Prediction of Performance and Energy Efficiency*, Proceedings of the 4th ASEAN Science and Technology Week, Science and Technology: The Future of ASEAN, Bangkok, Thailand, Aug 21–Sept 1, 1995; 240–247.
16. Rahman, M.S. Toward prediction of porosity in foods during drying: a brief review. Drying Technology **2001**, *19* (1), 1–13.
17. Posomboon, W. Processing Effect on Quality of Dried Shrimp. Master thesis, Asian Institute of Technology, Bangkok, Thailand, 1998.
18. Chua, K.J.; Mujumdar, A.S.; Chou, S.K.; Hawlader, M.N.A; Ho, J.C. Convective drying of banana, guava and potato pieces: effect of cyclical variations of air temperature on drying kinetics and color change. Drying Technology **2000**, *18* (4–5), 907–936.
19. Bouton, R.E.; Harris, P.V. The effect of cooking temperature and time on some mechanical properties of meat. Journal of Food Science **1972**, *37*, 140–144.
20. Krokida, M.K; Morinos-Kouris, D. Rehydration kinetics of dehydrated products. Journal of Food Engineering **2003**, *57*, 1–7.
21. Moorjani, M.N.; Dani, N.P. Textural and reconstitutional properties of freeze-dried shrimp. Food Technology **1968**, *22*, 886–888.
22. Wang, H.; Auerbach, E.; Bates, V.; Doty, D.M.; Kraybill, H.R. A histology and histochemical study of beef dehydration. IV. Characteristics of muscle tissues dehydrated by freeze-drying techniques. Food Research **1954**, *19*, 543–556.

DRYING TECHNOLOGY
Vol. 22, No. 7, pp. 1731–1754, 2004

Effect of Fluidized Bed Drying Temperature on Various Quality Attributes of Paddy

Supawan Tirawanichakul,[1,*] Somkiat Prachayawarakorn,[2] Warunee Varanyanond,[3] Patcharee Tungtrakul,[3] and Somchart Soponronnarit[1]

[1]School of Energy and Materials and
[2]Faculty of Engineering, King Mongkut's University of Technology, Thonburi, Bangkok, Thailand
[3]Institute of Food Research and Product Development, Kasetsart University, Bangkean, Bangkok, Thailand

ABSTRACT

As reported by many researchers, it was found that fluidized bed paddy drying using high drying air temperatures of over 100°C affected the head rice yield and whiteness of dried rice. However, only a few studies on fluidized bed paddy drying with drying air temperatures below 100°C were so far reported. The main objective of this work was therefore to study the effect of fluidized bed drying air temperature on various quality parameters of Suphanburi 1 and

*Correspondence: Supawan Tirawanichakul, School of Energy and Materials, King Mongkut's University of Technology, Thonburi, Bangkok 10140, Thailand; Fax: +662-470-8623; E-mail: supawanvachiramon@hotmail.com.

DOI: 10.1081/DRT-200025634
0737-3937 (Print); 1532-2300 (Online)
Copyright © 2004 by Marcel Dekker, Inc.
www.dekker.com

Pathumthani 1 *Indica* rice. Paddy was dried from the initial moisture contents of 25.0, 28.8, and 32.5% dry basis to 22.5 ± 1.2% dry basis using inlet drying air temperatures between 40 and 150°C at 10°C step. After fluidized bed drying, paddy was tempered and followed by ambient air aeration until its final moisture content was reduced to 16.3 ± 0.5% dry basis. The results showed that the head rice yield of Suphanburi 1 was significantly related to the inlet drying temperature and initial moisture content whilst there was no significant relationship between the head rice yield, drying temperature and initial moisture content for Pathumthani 1. The whiteness of the two rice varieties was slightly decreased with increase in drying air temperature and initial moisture content. It was also found that the hardness of both cooked rice varieties exhibited insignificant difference ($p < 0.05$) comparing to rewetted rice, which was gently dried by ambient air aeration in thin layer. The thermal analysis by DSC also showed that partial gelatinization occurred during drying at higher temperatures. Using inlet drying air temperatures in the range of 40–150°C therefore did not affected the quality of cooked rice and paddy. The milling quality of paddy was also well maintained.

Key Words: Amylose; High-temperature drying; Rice quality; Sensory evaluation.

INTRODUCTION

The management of highly moist paddy with moisture content of over 22% dry basis is an extremely serious problem in tropical countries since high humid air condition can accelerate an excessive mould growth, and yellowing of grains.[1–4] To prevent paddy deterioration, rapid reduction of moisture is essential and hot air drying seems to be the most appropriate drying technique under such weather condition. Some previous researches recommended that high moisture content of paddy should be first reduced to 22% dry basis within 24 h by hot air drying (using high temperature and short drying time) and then followed by natural air drying at lower temperature.[5,6] However, the use of heated air may damage some important grain qualities that are susceptible to thermal damage such as head rice yield, whiteness, physicochemical properties, and nutritional values.[7–9]

Hot air fluidized bed drying is one of the drying techniques that provides faster moisture reduction and uniformity of drying. The rapid drop in moisture content can, however, develop stresses inside the kernel, causing the reduction of head rice yield.[10] The head rice yield reduction decreases the value of rice since broken rice has lower commercial values than the complete one. To reduce the thermal stresses and maintain the full kernel, tempering stage is recommended after the first stage of drying.[11–14]

Although fluidized-bed dryer is well recognised in the grain industries, not much work is devoted to determining how this type dryer affects the quality of rice, especially in the low drying temperature range. Therefore, the main objective of this article was to investigate the effects of drying temperature and initial moisture content of paddy on various quality attributes of long grain rice varieties containing high and low amylose contents. The physical qualities tested were head rice yield, whiteness of rice, microstructure of rice kernel, and germination. The chemical properties of rice were determined in terms of amylose content and protein. The texture of cooked rice as well as the thermogram of rice determined using a differential scanning calorimetry (DSC) was investigated. Finally, overall acceptability of cooked rice by sensory evaluation was also determined.

EXPERIMENTAL SET-UP, MATERIALS, AND METHODS

1. Experimental Set-up

Figure 1 shows the schematic diagram of a batch fluidized bed dryer used in the present study. The dryer consists of a cylindrical shaped drying chamber, a 16 kW electric heating unit and a backward curved blade centrifugal fan driven by a 1.5 kW motor. The inlet drying air temperature was controlled by a PID controller with an accuracy of ±1°C. A mechanical variable speed unit was used for regulating air flow rate. A constant air velocity of 2.5 m/s was used for the bed of rice of 9.5 cm. The final moisture content required in the present study was approximately 22.5% dry basis as recommended by Poomsa-ad et al.[6]

2. Materials

Two varieties of long grain rough rice (Suphanburi 1 and Pathumthani 1) provided by the Rice Research Institute at Pathumthani province, Thailand, were rewetted, mixed, and kept in a cold storage at a temperature range of 4–6°C for one week prior to the

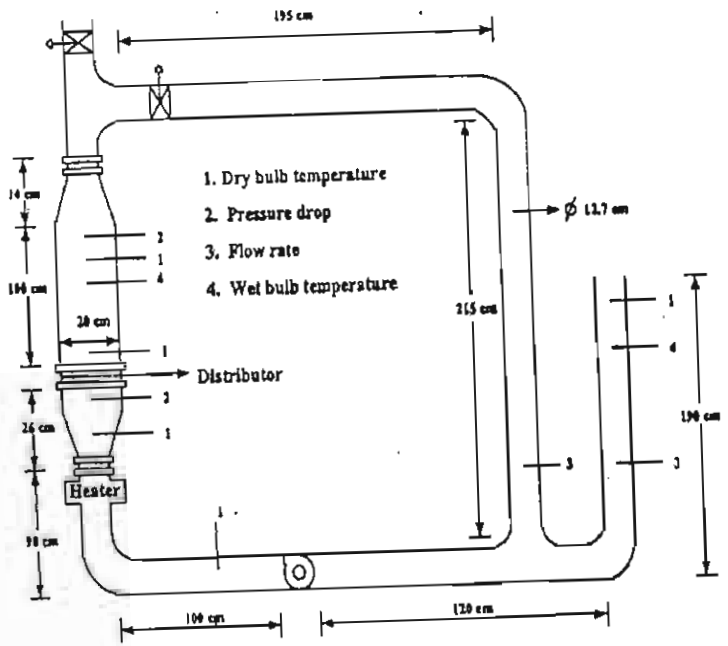


Figure 1. A schematic diagram of a batch fluidized bed dryer.

start of each experiment. The desired initial moisture content of rewetted paddy was about 25–33% dry basis. The local varieties of Suphanburi 1 and Pathumthani 1 contain amylose contents of 25–27% and 15–18%, respectively. Before starting the experiments, paddy was placed in an ambient environment until the thermal equilibrium was reached.

2. Methods

2.1. Paddy Drying Condition

Figure 2 illustrates a schematic diagram of the drying schedule used in this work. Wet paddy was first dried using a fluidized bed dryer by varying inlet air temperatures between 40 and 150°C with 10°C increment. It was subsequently tempered for 30 min.[15] During tempering, dried paddy was placed in a sealed glass bottle with an o-ring and kept in an oven at the same temperature as the grain

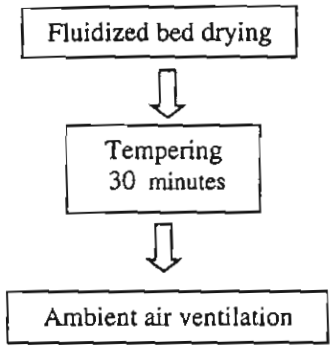


Figure 2. A schematic diagram of a fluidized bed drying system.

temperature. The tempering process was performed to relax some of thermal stresses developed during the first-stage drying.

To measure the grain temperature, paddy sample was taken out from the fluidized bed drying chamber at the end of drying time, corresponding to the final moisture content as aforementioned, and then measured when it was kept in the well-insulated vessel. This temperature was used for the tempering grain. By this measuring, it was concluded that at the inlet drying air temperature ranges of 40 to 90°C, the average grain temperature corresponded to the range of 38 to 75°C, respectively. For the inlet drying air temperature ranges of 100 to 150°C, the average grain temperature was in the range of 83 to 89°C, respectively.

After tempering paddy was taken out of the sealed bottle and ventilated immediately with a constant ambient airflow rate of 0.15 m/s until its moisture content reached 16.3 ± 0.5% dry basis as recommended by Soponronnarit.[16] A K-type thermocouple used for measuring the temperature of the bed was connected to a data logger with an accuracy of ±1°C. The determination of paddy moisture content was performed according to the AOAC method.[17] Air velocity was measured by a hot wire anemometer with a precision of ±0.1 m/s.

2.2. Quality of Rice

All qualities of rice samples after drying were determined comparing to the rewetted rice sample (so-called control rice), which was gently dried by ambient air ventilation in thin-layer. The various qualities of paddy

were analyzed as follows:

(a) Head Rice Yield

The determination of head rice yield was performed according to the USDA method.[18] Head rice yield was calculated by dividing the head rice weight by the initial rough rice weight. This value was determined in duplicate.

(b) Microstructure and Thermal Property of Rice

The microstructure of rice kernel was characterized by a scanning electron microscope (SEM) (JEOL, model LV5600, England) at 10–20 kV. The magnification range was 200–4000 times.

Thermal analysis of rice flour was determined by differential scanning calorimetry (DSC) (Perkin Elmer, model DSC-7, Norwalk, USA). The rice flour sample was heated from 40 to 95°C at a scanning rate of 10°C/min. From the DSC curve, the onset temperature, peak temperature, conclusion temperature, and transition enthalpy were recorded. The degree of gelatinization of hydrothermally-treated rice flour was calculated by the following equation[19]:

$$SG(\%) = \left(1 - \left[\frac{\Delta H}{\Delta H_c}\right]\right) \times 100 \quad (1)$$

where SG = degree of gelatinization (%)

ΔH = transition enthalpy of treated rice (J/g (dry weight basis))

ΔH_c = transition enthalpy of control rice (J/g (dry weight basis))

(c) Whiteness of Rice

The whiteness of milled rice was measured by a Satake milling meter model MM-113 (Japan). This value was determined in duplicate.

(d) Germination of Paddy

Before germination testing, dried mature paddy samples were kept at ambient air environment for 6 weeks. The mature paddy samples (200 seeds) were then used for each test. The germination test followed the guidelines given by the Rice Research Institute at Pathumthani province, Thailand. The experiments were performed in triplicate.

(e) Chemical Quality of Rice

Amylose was determined by simplified assay iodine colorimetric method of Juliano.[20] The content of protein was quantified as described by AOAC method.[17] These value was determined in duplicate.

(f) Textural Property of Cooked Rice

Hardness of cooked rice was determined by a bench-top texture analyzer model TA-XT2*i* (Stable Micro Systems Ltd., USA). A 30 g portion of each milled head rice sample was placed in an aluminum cylindrical cup (diameter of 7 cm and height of 7 cm). Before cooking, the rice sample was washed, rinsed, and then cooked with distilled water at rice-to-water weight ratios of 1:1.5 for Pathumthani 1 and 1:1.7 for Suphanburi 1.[21,22]

The initial height of the compression probe (Ottawa cell) was set at 120 mm and the pretest speed, test speed, and post speed of probe were 1.5, 0.5, and 10 mm/s, respectively. The maximum force required for compressing cooked rice to 90% of the initial height of 10 mm was indicated as the hardness of cooked rice. The hardness value was represented by the mean of 5 replications and the average value was expressed in kilogram unit.

(i) Sensory Evaluation of Cooked Rice

For determination of the cooking quality, 100 g of head rice was washed with tap water and cooked in an electric cooker at a rice-to-water ratio of 1:1.8 by weight.[22] The quality of cooked rice was evaluated on the basis of its palatability. Eight trained panelists from the Institute of Food Research and Product Development, Kasetsart University, Thailand were invited to evaluate the overall acceptability of cooked rice using hedonic scale of 1–9 with the following scales: 1 = extremely dislike, 2 = very much dislike, 3 = moderately dislike, 4 = slightly dislike, 5 = like nor dislike, 6 = slightly like, 7 = moderately like, 8 = very much like, and 9 = extremely like. Analysis of variance (ANOVA) and Duncan's new multiple range test (DMRT) were used to evaluate the effects of inlet drying air temperature on the quality of rice at 95% confidence limit ($p < 0.05$).

RESULTS AND DISCUSSION

1. Moisture Content and Drying Rate

For all experiments, the moisture content of paddy after the first stage drying was set at 22.5 ± 1.2% dry basis to avoid significant fissuring and subsequent breakage of rice. However, this moisture level is still not safe for long-term storage and hence paddy needs to be dried further. Reducing moisture content from this level to 16% dry basis can be

achieved by many means technique. In common practice paddy would be tempered at a suitable temperature[15,23] and dried by any low-temperature drying technique until the desired final moisture content of paddy of 14–16% dry basis is reached.[13,15]

Thus, in this work, the tempering process at grain temperature was performed and the tempered duration was fixed at 30 min. After tempering, paddy sample was thin-layer dried immediately by ambient air ventilation until the final moisture content was in range of 14–16% dry basis, resulting in minimal breakage and consequently a high head rice yield.[23]

Figures 3(a) shows the drying rates of paddy at three initial moisture levels of 25.0, 28.8, and 32.5% dry basis for Suphanburi 1 at inlet drying air temperatures of 40–150°C. It can be seen that the drying rates seem to be independent of an initial moisture content, indicating that the main part of moisture content, above 25.0% dry basis, existed only on the exterior surface, thus allowing easier water removal without any interference of disordered void spaces inside grain kernel during drying. As is seen in Fig. 3(b), the changes of drying rates for Pathumthani 1 with inlet air temperatures of 40–150°C and three initial moisture contents of 25.0, 28.8, and 32.5% dry basis show a similar trend to that found for Suphanburi 1.

2. Quality of Rice

(a) Head Rice Yield of Rice

Figure 4 shows the relationship between inlet drying air temperature and head rice yield. The head rice yield after rewetting reduces to lower level than that obtained before rewetting for both rice varieties. However, the amount of head rice yield reduction depends on the rice variety as observed from the experiments; Suphanburi 1 variety, which contains higher amylose content has larger amount of broken kernel although the head rice yield of both varieties before rewetting was nearly the same.

When paddy kernels were subjected to drying at different air temperatures, the changing of head rice yield was rather complicated. For Suphanburi 1 variety, as can be seen in Fig. 4(a), at air temperatures below 80°C or grain temperatures below 70°C, head rice yield of paddy samples at three different initial moisture contents of 25.0, 28.8, and 32.5% dry basis was insignificantly different, (when compared with the gently dried control sample) the values were between 43 and 45%. The maintained head rice yield could be explained by two possible reasons.

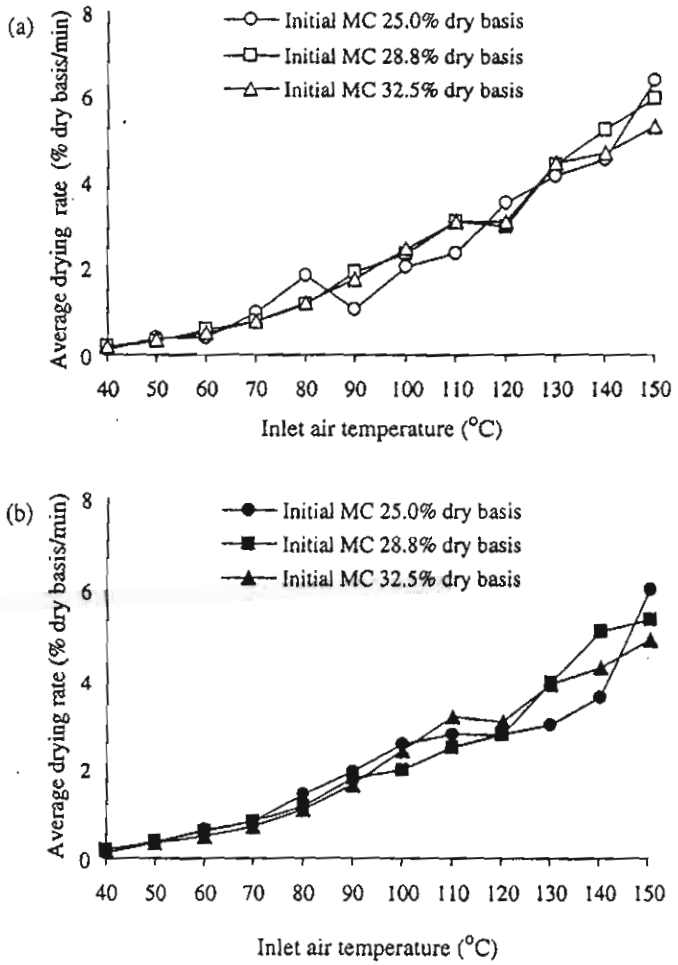


Figure 3. Effect of inlet air temperature on average drying rate of Suphanburi 1 and Pathumthani 1: initial moisture contents were in the range of 25.0–32.5% dry basis and final moisture content of 22.0 ± 1.2% dry basis (after fluidized bed drying). (a) Suphanburi 1, (b) Pathumthani 1.

Firstly, at low drying air temperatures of 40–50°C, which corresponded to the grain temperatures of 38–46°C, the moisture gradient developed inside a grain kernel during slow moisture reduction from any level to 22.5% dry basis was not sufficiently large to develop fissures. This is

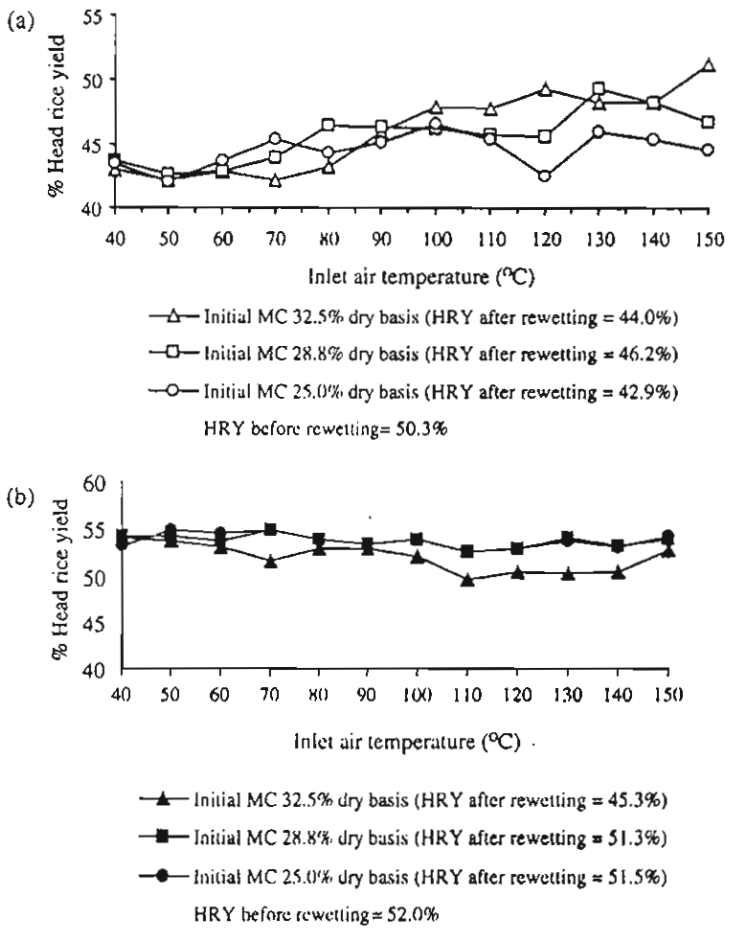


Figure 4. Effect of inlet air temperature on head rice yield of Suphanburi 1 and Pathumthani 1: initial moisture contents were in the range of 25.0–32.5% dry basis and final moisture contents of 22.0 ± 1.2% dry basis (after fluidized bed drying). (a) Suphanburi 1, (b) Pathumthani 1.

reason why drying and tempering at the drying air temperatures below the glass transition temperature did not cause significant fissuring and subsequent breakage of rice.[23,25]

For drying temperatures in the range of 60 to 70°C, even though the moisture gradient was sufficiently large and hence induced stresses inside

the kernel, tempering could still prevent the head rice yield reduction since paddy was tempered at temperatures above 50°C. Under this condition, paddy was in its rubbery state,[23] thus starch existed as a rubbery material with higher expansion coefficients.[26,27] Several researchers have reported that paddy drying at temperatures above 50°C could be detrimental to head rice yield if the moisture content drops larger than 3 percentages of moisture content in one drying pass and when tempering is not included between drying stages.[14,23,28,29] However, in this study, the moisture content of paddy sample was removed around 6.8–10.5% during for the first-stage drying and hence the head rice yield was not reduced when paddy was tempered at its own grain temperature after fluidized bed drying. Moreover, the tempering duration of 30 min used in this study was sufficient large to remove large portion of moisture content. Consequently, some of proteins or lipids might interact with amylose and carbonyl compounds presented in paddy,[30] resulting in subsequent improvement of milling resistance of paddy.[31,32]

The change of head rice yield of paddy dried at a higher temperature of 80°C was quite different to that dried at lower temperatures, however. At 80°C, the head rice yield was improved, particularly at an initial moisture content of 32.5% dry basis; even higher than 47% as can be seen in Fig. 4(a). This value was indeed higher than that of control sample. The larger percentage head rice yield for high temperature treated samples implies stronger intra-granular binding forces, which make the kernel more resistant to abrasive forces during milling. This improvement of binding forces amongst granules is caused by their swelling together with the leaching out of amylose molecule from starch granules into aqueous substrates.[33] The swollen granules were then gelatinized, but only partially, since the water content inside the kernel in the present study was not enough for a complete gelatinization.

It is interesting to note that, at each level of initial moisture content, the change of head rice yield with inlet drying air temperature for Pathumthani 1, which contains lower amylose content, was insignificantly different over the entire drying temperature range; the values laid between 53 and 55% for an initial moisture contents of 25.0 and 28.8% dry basis and between 52 and 54% for an initial moisture content of 32.5% dry basis. Such changes were not similar to those found for Suphanburi 1 variety, especially when drying at higher temperatures in which the head rice yield did not show an increasing trend although a high initial moisture content of 32.5% dry basis was employed. According to these results, it may be indicated that the amylose content significantly contributes to the improved intra-granular forces during

gelatinization; the lower the amount of amylose, the lower the binding forces are.

As shown in Fig. 4(b), the head rice yield for Pathumthani 1 sample with an initial moisture content of 32.5% dry basis and dried at a higher temperature of 80°C was lower than that of the other two initial moisture contents. The lower amount of full kernel was due to the dominant contribution of stresses, which consequently induced an irreversible structural damage although partial gelatinization occurred during drying. This change was not similar to Suphanburi 1 samples in which the head rice yield became higher with the initial moisture content.

(b) Microstructure and Thermal Analysis of Rice

To confirm the aforementioned occurrence of gelatinization, the microstructure of rice samples was examined by means of scanning electron microscopy (SEM). The gelatinization enthalpy was also determined by differential scanning calorimetry (DSC).

The results of SEM observation of the morphological changes of starch granules of Suphanburi 1 variety at various drying temperatures are shown in Figs. 5(a–d). As can be seen in Fig. 5(a), the starch granules in endosperms of control sample showed clearly the characteristically irregular polygons with diameters of 4–8 μm, while Figs. 5(b–d) show the morphology of starch granules of dried rice kernel at inlet drying air temperatures of 40, 120, and 150°C, respectively. Drying at low inlet air

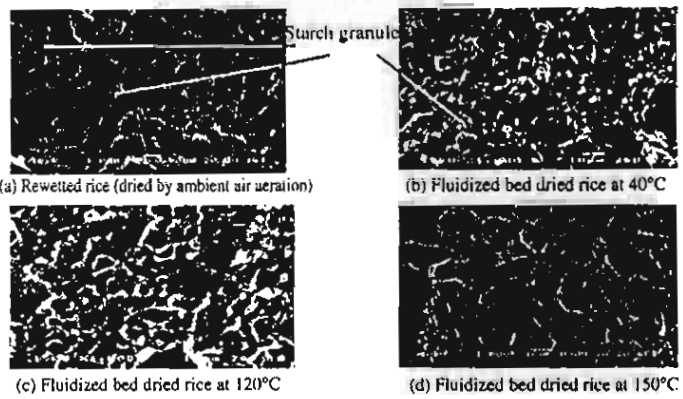


Figure 5. Scanning electron micrographs of Suphanburi 1 (initial MC = 32.5% dry basis) at various inlet air temperatures.

temperature of 40°C does not change the conformation of starch granules, as can be seen in Fig. 5(b), comparing to the morphology of starch granules of the control sample (Fig. 5(a)).

As can be observed in Figs. 5(c–d), during drying at high inlet drying air temperatures of 120 and 150°C (the average grain temperature was in range of 83 to 89°C), starch granules obviously exhibited swelling. This is due to the fact that the bonding between amylose and amylopectin molecules in starch granules was relaxed around their gelatinization temperatures of 68–78°C[34] and leaching of amylose from starch granules led to partial gelatinization.[7,35] These combined characteristics of the granule segments to form network-like structures contributed to the strong gel formation. The structure of starch granules eventually disintegrated and adjacent starch granules fused together to form the composite clusters with homogeneous interior and low well defined polygonal boundaries. The rice kernel appeared as dense and smooth layer throughout its cross-sectional area as shown in Fig. 5(d).

The above-mentioned partial gelatinization agreed well with the DSC results manifested by a certain degree of gelatinization as shown in Table 1, which shows the gelatinization and thermal properties of Suphanburi 1 and Pathumthani 1 rice varieties. The degree of gelatinization of both rice varieties after drying at 150°C was different from that of the reference sample. The higher degree of gelatinization was observed in rice that had higher initial moisture content and the longer drying time. The percentage degree of gelatinization for Suphanburi 1 and Pathumthani 1 calculated by Eq. (1) were in the range of 42–55% for the initial moisture content of 32.5% dry basis and less than 20% for the lower initial moisture content of 28.8% dry basis.

(c) Whiteness of Rice

Figure 6 shows the effects of drying air temperature and initial moisture content on the whiteness of rice for Suphanburi 1 and Pathumthani 1. After rewetting, the whiteness value of Pathumthani 1 rice sample remained the same as before rewetting whilst the color of Suphanburi 1 rice sample became less luminous, with the average whiteness value of 49.8. As paddy was subjected to drying at various drying air temperatures, the whiteness of Pathumthani 1 with initial moisture contents of 25.0, 28.8, and 32.5% dry basis showed an insignificant difference amongst each other at drying temperatures below 80°C and was equivalent to its original value of the control sample. On the other hand, the change in whiteness for Suphanburi 1 was

Table 1. Gelatinization properties of rice flour of Suphanburi 1 and Pathumthani 1 varieties.

Rice variety	Initial MC % dry basis	Inlet air temp. (°C)	Transition temp (°C) T_{onset}	T_{peak}	$T_{conclude}$	ΔH (J/g)[a]	% Degree of gelatinization
Suphanburi 1	32.5	Control	71.5	76.4	81.4	7.1	
		150	78.1	85.0	89.5	3.2	54.9
	28.8	Control	71.2	77.2	85.1	6.7	
		150	73.0	78.1	85.5	5.2	22.3
Pathumthani 1	32.5	Control	61.5	73.6	85.6	7.4	
		150	59.4	75.2	82.6	4.3	41.9
	28.8	Control	71.2	77.2	82.2	6.7	
		150	69.5	76.2	81.8	4.4	26.7

Note: control = Rewetted rice which was gently dried by ambient air ventilation in thin-layer.
[a]Based on dry starch weight.

Figure 6. Effect of inlet air temperature on whiteness of Suphanburi 1 and Pathumthani 1: initial moisture contents were in the range of 25.0–32.5% dry basis and final moisture content of 22.0 ± 1.2% dry basis (after fluidized bed drying). (a) Suphanburi 1, (b) Pathumthani 1. *(View image in color online.)*

rather sensitive to initial moisture content, with the lowest brightness being for the initial moisture content of 32.5% dry basis.

At a higher temperature of 80°C and at lower initial moisture content, changes in whiteness for both rice varieties were less pronounced. For paddy samples that had an initial moisture content of 25.0% dry basis, The value of whiteness varied between 49.8 and 51.3 for Suphanburi 1 and between 44.1 and 46.2 for Pathumthani 1. For paddy

samples with an initial moisture content of 28.8% dry basis, the values of whiteness varied between 50.3 and 52.1 for Suphanburi 1 and between 44.7 and 46.5 for Pathumthani 1 over the drying temperature range of 80 to 150°C. Most of these results indicated that the drying temperature range of 40–150°C along with the low initial moisture contents of rice samples of 25.0 and 28.8% dry basis for both rice varieties did not significantly affect the whiteness of rice ($p < 0.05$). However, a steep decrease in whiteness with increasing air temperature for the samples with a high initial moisture content of 32.5% dry basis for both rice varieties was evident. This can be explained by the effects of the longer drying time and the Maillard nonenzymatic browning reaction.[1,3,7] At this high initial moisture content, drying took longer time than that required by the sample that had lower initial moisture contents of 25.0 and 28.8% dry basis. In addition, the Maillard browning reaction rate was accelerated when the drying temperature increased. In contrast, their mobility and reactivity inside the paddy samples that had low initial moisture content were restricted, even though the temperature was risen. The resulting browning rate was thus retarded. In addition to the limitation of reactive biological components in seeds, the improved whiteness of rice samples was also due to the shorter drying time required for samples with lower initial moisture content. However, for all experiments, the whiteness values were within an acceptable range for the commercial purpose.[13]

(d) Germination of Paddy

Figures 7(a) and 7(b) show respectively the average percentage of germination for paddy with three initial moisture contents of 25.0, 28.8, and 32.5% dry basis for Suphanburi 1 and Pathumthani 1 rice varieties. The germination of both paddy varieties dried with hot air in the temperature range of 40–60°C was in range of 90–98%, with no significant difference between the dried paddy and the control paddy ($p < 0.05$). At the drying air temperature of 70°C the germination of paddy was only found in samples that had initial moisture contents of 25.0 and 28.8% dry basis, however.

When an inlet drying air temperature was higher than 80°C, the degradation of viability was high and the resulting germination of paddy samples of any initial moisture content did not occur. This is due to the fact that the gelatinization of starch granules was partially formed, thereby allowing the rice kernel to lose its biological activity in embryo. However, the germination of both paddy varieties dried using inlet drying

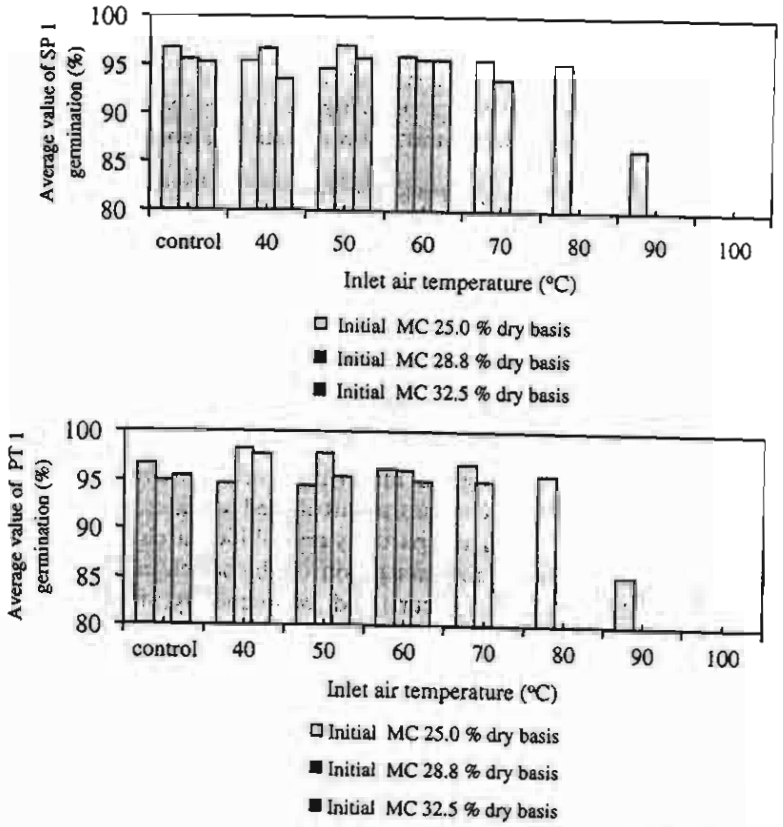


Figure 7. Effect of inlet air temperature on percent germination of Suphanburi 1 and Pathumthani 1: initial moisture contents were in the range of 25.0–32.5% dry basis and final moisture content of 22.0 ± 1.2% dry basis (after fluidized bed drying). (a) Suphanburi 1, (b) Pathumthani 1. *(View image in color online.)*

air temperatures below 60°C, was not significantly changed comparing to its control sample.

(e) Chemical Quality of Rice

Based on the determination of the chemical quality of the two rice varieties, it was found that the inlet drying air temperatures of 40–150°C had no significant effect on both amylose and protein contents of the

samples; the average amylose contents of rice before and after drying were in the range of 25.0 ± 2.8 and 14.5 ± 2.3% (dry weight basis) for Suphanburi 1 and Pathumthani 1, respectively. The average value of protein content was in the range of 7.50 ± 0.05 and 7.99 ± 0.05% (dry weight basis) for Suphanburi 1 and Pathumthani 1, respectively.

(f) Textural Property of Cooked Rice

Figures 8(a) and 8(b) show the hardness of cooked rice samples dried at different temperatures. The hardness of thermally untreated samples was 32.77 kg for Suphanburi 1 variety and 16.39 kg for Pathumthani 1. The difference in hardness is attributed to amylose content presented in paddy. When a certain amount of water was added to the sample and the rewetted sample was then gently dried, the hardness changed in a way that the samples with higher initial moisture contents had higher hardness, except for the range of initial moisture contents between 25 and 28.8% dry basis. These changes are attributed to water, which acts as plasticizer of the amorphous and partially crystalline starch systems. This subsequently facilitates the reorganization of the starch crystallites and amylose-lipid complexes to occur, and consequently, influences the textural properties of paddy.[36,37]

As can be seen in Fig. 8(a), the hardness of cooked Suphanburi 1 rice samples at each initial moisture content was insignificantly different from that of the control sample ($p < 0.05$). At an initial moisture content of 25.0% dry basis, the harness of cooked rice samples was between 34 and 37 kg, indicating the small variation with the drying air temperature while the trend of hardness was different for the samples that had initial moisture contents of 28.8% dry basis and 32.5% dry basis; the hardness values ranged between 31 and 40 kg when using drying air temperatures of 40–150°C.

Similarly, as can be seen in Fig. 8(b), the hardness of cooked Pathumthani 1 sample tended to be related to the initial moisture content whilst there was no significant difference among those samples dried at different drying air temperatures ($p < 0.05$). The hardness values of Pathumthani 1 rice sample at 32.5% dry basis, ranging between 19 and 24 kg, were above those of the samples that had initial moisture contents of 25.0 and 28.8% dry basis, which had the values of hardness vary in the range of 18–21 kg.

The results showed that the hardness of cooked rice increased with an increased initial moisture content. The reasons for these changes might be due to partial gelatinization of rice kernel and interaction between starch, lipid, and protein.[38]

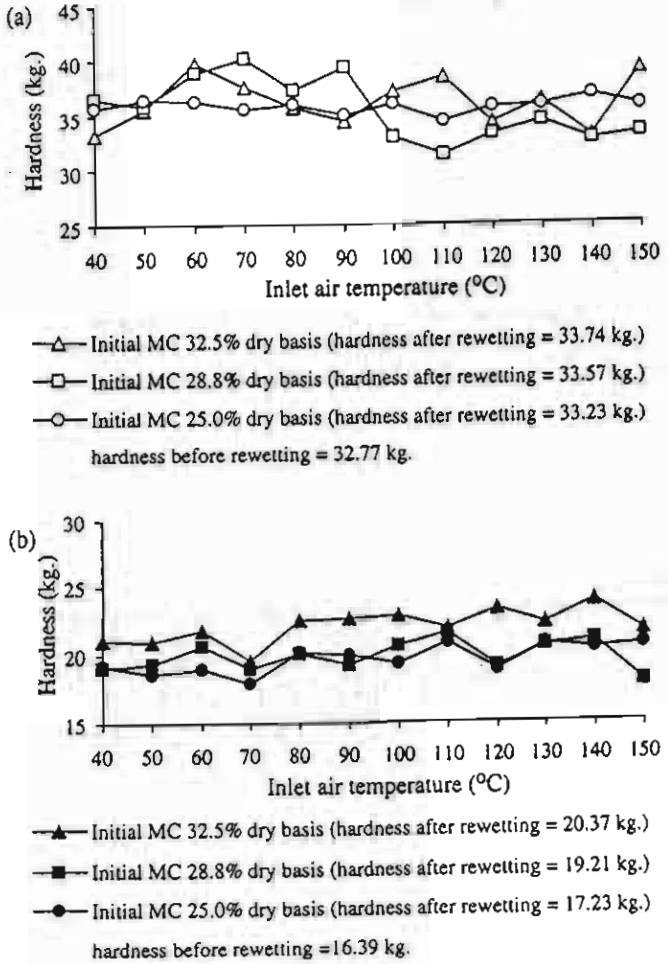


Figure 8. Effect of inlet air temperature on hardness of Suphanburi 1 and Pathumthani 1: initial moisture contents were in the range of 25.0–32.5% dry basis and final moisture content of 22.0 ± 1.2% dry basis (after fluidized bed drying). (a) Suphanburi 1, (b) Pathumthani 1.

(i) Sensory Evaluation

Table 2 shows the hedonic score of an overall acceptability of cooked Suphanburi 1 and Pathumthani 1 rice samples. The results show that for

Table 2. Effect of inlet drying air temperature on overall acceptability of cooked rice of Suphanburi 1 and Pathumthani 1 varieties.

	Overall acceptability of cooked rice					
Inlet air temp. (°C)	Initial MC: Pathumthani 1			Initial MC: Suphanburi 1		
	25.0% (dry basis)	28.8% (dry basis)	32.5% (dry basis)	25.0% (dry basis)	28.8% (dry basis)	32.5% (dry basis)
Control	6.94b	5.98a	4.96b	6.46a	4.53a	4.97a
40	7.54a	6.40a	8.38a	5.54a	4.57a	4.43b
60	7.21b	5.44b	7.92a	5.17b	4.55a	5.05a
80	7.18b	5.27b	7.83a	5.58a	4.46a	4.67a
100	7.37a	6.32a	4.96b	5.38b	4.05b	4.38b
120	7.52a	5.82b	6.63b	4.63b	4.05b	4.67a
140	7.52a	5.77b	4.92b	4.58b	4.51a	4.13b
150	7.37a	5.86a	7.08a	4.67b	4.86a	4.09b

Note: The same letter in the same column indicates no significant difference at $p < 0.05$.

Control = Rewetted rice which was gently dried by ambient air ventilation in thin-layer.

The meaning of hedonic score is as follows:

Hedonic scale from 1–9:

1 = Extremely dislike.
2 = Very much dislike.
3 = Moderately dislike.
4 = Slightly dislike.
5 = Like nor dislike
6 = Slightly like.
7 = Moderately like.
8 = Very much dislike.
9 = Extremely like.

all experiments except Pathumthani 1 with an initial moisture content of 25.0% dry basis, the overall acceptability was in preference scores, from 4.05 to 5.54, representing like nor dislike. The overall acceptability for Pathumthani 1 with an initial moisture content of 25.0% dry basis was in preference scores, from 4.92 to 8.38, which means like nor dislike to very much like. It can be concluded that the inlet drying air temperature and initial moisture content had an insignificantly change the overall acceptability of cooked rice comparing to the rewetted rice (control sample).

CONCLUSIONS

In this study the effect of inlet drying air temperature on various qualities of rice was experimentally investigated. It was found that paddy, either low- and high-amylose content varieties, which had initial moisture contents of 25.0–32.5% dry basis, and was subjected to fluidized bed drying at temperatures between 40–150°C could maintain high head rice yield comparing to the control rice samples.

The head rice yield of Suphanburi 1 samples, which have high amylose content, was significantly related to the inlet drying air temperature and initial moisture content whilst the head rice yield of Pathumthani 1 samples, which have lower amylose content, did not tend to be associated with the inlet drying air temperature as well as the initial moisture content. However, it was found that the whiteness of both rice varieties that had initial moisture contents of 25.0–32.5% dry basis slightly decreased with an increase in inlet drying air temperature; the effect was more pronounced at inlet drying air temperatures of over 80°C and the initial moisture content of 32.5% dry basis.

The germination of both paddy varieties dried at inlet drying air temperatures below 60°C was not significantly changed comparing to their control samples. When inlet drying air temperatures were higher than 80°C, however, germination of paddy samples of any initial moisture contents did not occur due to partial gelatinization of starch granules. This partial gelatinization at inlet drying air temperatures of over 90°C caused some effects on the morphology, endothermic energy of rice flour, hardness, and head rice yield of rice samples. Moreover, the overall acceptability of both cooked rice samples after drying had an insignificant correlation with inlet drying air temperature, initial moisture content, and rice variety comparing to those of control samples.

ACKNOWLDGMENTS

The authors wish to express their sincere thanks to the Thailand Research Fund (TRF) and the Japan International Research Center for Agricultural Sciences (JIRCAS) for their financial support and to the Institute of Food Research and Product Development (IFRPD) of Kasetsart University, Thailand for testing rice qualities and to the Institute of Technology Rajchamongkrala, Headquarter, Pathumthani, Thailand for rice whiteness testing.

REFERENCES

1. Gras, P.W.; Banks, H.J.; Bason, M.L.; Arriola, L.P. A qualitative study of the influences of temperature, water activity and storage atmosphere on the yellowing of milled rice. J. Cereal Science **1989**, *9*, 77–89.
2. Bason, M.L.; Gras, P.W.; Banks, H.J.; Esteves, L.A. A qualitative study of the influences of temperature, water activity and storage atmosphere on the yellowing of paddy endosperm. J. Cereal Science **1990**, *12*, 193–201.
3. Soponronnarit, S.; Srisubati, N.; Yoovidhya, T. Effect of temperature and relative humidity on yellowing rate of paddy. J. Stored Prod. Res. **1998**, *34* (4), 323–330.
4. Yap, A.B.; Juiliano, B.O.; Perez, C.M. Artificial yellowing of rice at 60°C. Proceedings Group, The Source of Yellow Grains in Rice, Myc. Centralbl **1988**, *3*, 153–157.
5. Driscoll, R.H.; Adamczak, T. Drying systems for the humid tropics. In bulk handling and storage of grain in the humid tropics. ACIAR Proceedings **1988**, *22*, 58–68.
6. Poomsa-ad, N.; Soponronnarit, S.; Terdyothin, A.; Prachayawarakorn, S. *Head Rice Yield after Drying by Fluidization Technique and Tempering*, Proceedings of the 2nd Asian-Oceania Drying Conference, Batu-Feringhai, Penang, Malaysia, Aug 20–22, 2001.
7. Inprasit, C.; Noomhorm, N. Effect of drying air temperature and grain temperature of different types of dryer and operation on rice quality. Drying Technology **2001**, *19* (2), 389–404.
8. Bonazzi, C.; du Peuty, M.A.; Themelin, A. Influence of drying conditions on the processing quality of rough rice. Drying Technology **1997**, *15* (3&4), 1141–1157.
9. Daniel, M.J.; Marks, B.P.; Siebenmorgen, T.J.; Mcnew, R.W.; Meullenet, J.F. Effects of long-grain rough rice storage history on end-use quality. J. Food Sci. **1998**, *63* (5), 832–835.
10. Soponronnarit, S.; Prachayawarakorn, S. Optimum strategy for fluidized bed paddy drying. Drying Technology **1994**, *12* (7), 1667–1686.
11. Steffe, J.F.; Singh, R.P.; Bakshi, A.S. Influence of tempering time and cooling on rice milling yields and moisture removal. Trans. of the ASAE **1979**, *22*, 1214–1218, 1224.
12. Zhang, Q.; Litchfield, J.B. An optimization of intermittent corn drying in a laboratory scale thin layer dryer. Drying Technology **1991**, *9* (1), 233–244.

13. Soponronnarit, S.; Wetchama, S.; Swasdisevi, T.; Poomsa-ad, N. Managing moist paddy by drying, tempering and ambient air ventilation. Drying Technology **1999**, *17* (1&2), 335–344.
14. Cnossen, A.G.; Jimenez, M.J.; Siebenmorgen, T.J. Rice fissuring response to high drying and tempering temperatures. J. Food Eng. **2003**, *59*, 61–69.
15. Poomsa-ad, N.; Soponronnarit, S.; Prachayawarakorn, S.; Terdyotin, A. Effect of tempering on subsequent drying of paddy using fluidisation technique. Drying Technology **2002**, *20* (1), 195–210.
16. Soponronnarit, S. *Drying in Bulk Storage of High Moisture Grains in the Kingdom of Thailand*, Final report submitted to Australian Centre for International Agricultural Research, Canberra, 1987.
17. AOAC. *Official Methods of Analysis, Association of Official Analytical Chemists*, 15th Ed; Washington, D.C., USA, 1995.
18. USDA. *Grain Grade Procedure*; Federal Grain Inspection Service: Washington, DC, USA, 1988.
19. Marshall, W.E.; Wadsworth, J.I.; Verma, L.R.; Velupillai, L. Determination the degree of gelatinization in parboiled rice: comparison of a subjective and an objective methods. Cereal Chem. **1993**, *70*, 226–230.
20. Juliano, B.O. A simplified assay for mill-rice amylose. Cereal Sci. Today **1971**, *16*, 334–338.
21. Kongseree, N. *Training Course in Standardization and Quality of HoomDokMali Rice*; Rice Research Station: Pathumthani, Thailand, 22–24 Dec. 1995.
22. Tungtrakul, P. *Quality and Physicochemical Properties of Rice Related to Rice Noodle*, United Nations University Research Fellowship Report; Tsukuba, Japan, 1997.
23. Cnossen, A.G.; Siebenmorgen, T.J. The glass transition temperature concept in rice drying and tempering: effect on milling quality. Trans. of the ASAE **2000**, *23* (6), 1661–1667.
24. Perdon, A.A. Amorphous State Transition in Rice during the Drying Process, Ph.D. diss., Fayetteville, Ark, Department of Food Science, University of Arkansas, USA, 1999.
25. Siebenmorgen, T.J.; Perdon, A.A. *Applying Glass Transition Principle to Explain Fissure Formation during Drying Process*, Presented in the 1999 Int. Starch Tech. Conf., Urbana, June 7–9, 1999; Volume III.
26. Slade, L.; Levine, H. A polymer science approach to structure/property relationships in aqueous food systems: non-equilibrium

behavior of carbohydrate-water systems. In *Water Relationships in Foods*; Levine, H., Slade, L., Eds.; Plenum Press: New York, USA, 1991; 29–101.
27. Slade, L.; Levine, H. Glass transitions and water-food structure interactions. Adv. Food Nutrit. Res. **1995**, *38*, 103–269.
28. Kunze, O.R. Fissuring of the rice grain after heated air drying. Trans. of the ASAE **1979**, *22* (5), 1197–1202, 1207.
29. Aquerre, R.; Suarez, C.; Viollaz, P.E. Effect of drying on the quality of milled rice. J. of Food Tech. **1986**, *21*, 75–80.
30. Eliasson, A.C. Interactions between starch and lipids studied by DSC. Thermochimica Acta **1994**, *246*, 343–356.
31. Moritaka, S.; Yasumatsu, K. Studies on cereals X. The effect of sulfhydryl groups on storage deterioration of milled rice. Eiyo To Shokuryo **1972**, *25*, 59–62.
32. Teo, C.H.; Abd. Karim, A.; Cheah, P.B.; Norziah, M.H.; Seow, C.C. On the roles of protein and starch in the aging of non-waxy rice flour. Food Chem. **2000**, *69*, 229–236.
33. Swinkels, J.J.M. Starch, source, chemistry and physics. In *Starch Conversion Technology*; van Beynum, G.M.A., Roels, J.A., Eds.; Marcel Dekker, Inc.: New York, USA, 1985; 31–35.
34. Sander, J.P.M. Starch manufacturing in the world. In *Advanced Post Academic Course on Tapioca Starch Technology*; AIT Center: Bangkok, Thailand; 22–26 Jan & 19–23 Feb 1996.
35. Miah, K.M.A.; Haque, A.; Douglass, M.P.; Clarke, B. Parboiling of rice part I: effect of hot soaking time on quality of milled rice. Int. J. of Food Sci. and Tech. **2002**, *37*, 527–537.
36. Juliano, B.O. *Rice: Chemistry and Technology*, 2nd Ed.; American Association of Cereal Chemists, Inc., St. Paul: Minnesota, USA, 1985; 774.
37. Beynum, G.M.A.; Roels, J.A. *Starch Conversion Technology*; Marcel Dekker, Inc.: USA, 1985; 40–41.
38. Parnsakhorn, S. *The Effect of Steaming Treatment on Accelerated Aging of Rough Rice*. M.E. thesis, School of Environment, Resource and Development, Asian Institute of Technology, Bangkok, Thailand, 2001.

DRYING TECHNOLOGY
Vol. 22, No. 8, pp. 1845–1867, 2004

A Comparative Study of Low-Pressure Superheated Steam and Vacuum Drying of a Heat-Sensitive Material

S. Devahastin,[1,*] P. Suvarnakuta,[1] S. Soponronnarit,[2] and A. S. Mujumdar[3]

[1]Department of Food Engineering and
[2]School of Energy and Materials, King Mongkut's,
University of Technology Thonburi, Bangkok, Thailand
[3]Department of Mechanical Engineering,
National University of Singapore, Singapore

ABSTRACT

Using carrot cubes as a model heat-sensitive material, experimental investigations were conducted to examine the drying kinetics and various quality parameters of the dried product undergoing both low-pressure superheated steam and vacuum drying. Effects of operating parameters such as pressure and temperature on the drying characteristics as well as quality attributes, i.e., volume, shrinkage,

*Correspondence: S. Devahastin, Department of Food Engineering, King Mongkut's University of Technology Thonburi, 91 Pracha u-tid Road, Bangkok 10140, Thailand; Fax: 662 470 9240; E-mail: sakamon.dev@kmutt.ac.th.

DOI: 10.1081/LDRT-200032818
Copyright © 2004 by Marcel Dekker, Inc.
0737-3937 (Print); 1532-2300 (Online)
www.dekker.com

apparent density, color, and rehydration behavior, of the dried product underwent the two drying processes were also evaluated and compared. Although low-pressure steam drying required longer dwell time to achieve the same final moisture content than vacuum drying, some of the quality attributes were superior to those obtained in vacuum drying.

Key Words: Apparent density; Carrot; Color; Rehydration behavior; Shrinkage; Volume.

INTRODUCTION

During the past decade the idea of using superheated steam to dry food has been derived from other drying applications, e.g., paper drying,[1–3] coal drying,[4] wood particles drying,[5] sludge,[6] and beat pulp drying.[7,8] The notable advantages of superheated steam drying (SSD) that are of interest to food industry include the absence of oxidative reactions (e.g., enzymatic browning, lipid oxidation) due to lack of oxygen, high drying rates in both constant and falling rate periods, depending on steam temperature and pressure, and its ability to yield a higher porosity dried product due to an evolution of steam within the product. Moreover, SSD strips more of the acids that contribute to an undesirable taste or aroma of the products.[9]

Despite the many advantages of SSD as mentioned earlier, several limitations, especially when applying it to drying heat-sensitive materials like foods and bioproducts, are still present. Since most foods or other heat-sensitive products melt, undergo glass transition or are damaged at the saturation temperature of superheated steam corresponding to the atmospheric or higher pressures, one possible way to prevent the products from being damaged in a high-temperature environment of SSD is to operate a dryer at reduced pressure.[9–11] Lowering the dryer operating pressure is a feasible option that not only preserves the quality of the dried product, but may also enhance the drying rate as well.[9,12–15] However, very little is reported on low-pressure (or sub-atmospheric) superheated steam drying of foodstuffs both from drying kinetics and dried product quality points of view.

Chen *et al.*[16] performed a laboratory-scale testing of a sub-atmospheric pressure superheated steam drying of silk cocoons (at temperature around 45°C) and found that this drying technique helped improving the quality of silk produced in terms of the brightness and strength of fiber. The increased cost of steam drying was therefore

justified by the additional credit received for the enhanced quality of the silk.

Pang and Dakin[17] studied the drying rates and temperature profiles of stacks of softwood lumber undergoing vacuum SSD in a Moldrup kiln. The superheated steam temperature used was 90°C and had a circulating velocity of 10 m/s. Vacuum SSD was found to yield lower drying rates of whole lumber stack than those obtained using hot moist air. This is due to the fact that the wood temperatures in a vacuum SSD were lower than those used in hot air drying. However, the defects of the dried product such as kiln brown stain and drying stresses were lower. To reduce the drying time in a vacuum SSD, it was recommended that a higher steam circulating velocity (more than 10 m/s) be used.

Elustondo et al.[11] studied sub-atmospheric pressure superheated steam drying of foodstuffs both experimentally and theoretically. Wood slab, shrimp, banana, apple, potato and cassava slices were dried using the steam pressures of 10,000–20,000 Pa, the steam temperatures of 60–90°C and the steam circulating velocities of 2–6 m/s. A semi-empirical mathematical model was also developed based on a theoretical drying mechanism, which assumed that the water removal was carried out by evaporation in a moving boundary allowing the vapor to flow through the dry layer built as drying proceeded to predict the drying characteristics of foodstuffs undergoing this drying operation. A simplified expression, which has two experimentally determined parameters, was derived and used to predict the drying rate of the tested samples. A model proposed was found to predict the drying kinetics reasonably well. No mention about the dried product quality is given, however.

The present work was therefore aimed at the design, fabrication and testing of a cabinet-type low-pressure superheated steam dryer and to investigate the influence of various operating parameters on the drying and heat transfer characteristics as well as various quality attributes of a heat-sensitive food product (carrot) undergoing this drying operation. Comparison was also made with the similar sets of information obtained from vacuum drying experiments conducted in the same drying chamber.

EXPERIMENTAL SET-UP, MATERIALS AND METHODS

Experimental Set-up

A schematic diagram of the low-pressure superheated steam dryer and its accessories is shown in Fig. 1. The dryer consists of a stainless

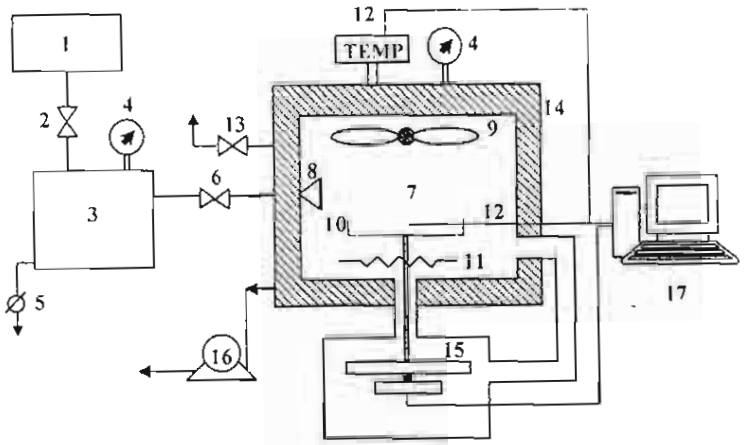


Figure 1. A schematic diagram of the overall experimental set-up. 1, boiler; 2, steam valve; 3, steam reservoir; 4, pressure gauge; 5, steam trap; 6, steam regulator; 7, drying chamber; 8, steam inlet and distributor; 9, electric fan; 10, sample holder; 11, electric heater; 12, on-line temperature sensor and logger; 13, vacuum break-up valve; 14, insulator; 15, on-line weight indicator and logger; 16, vacuum pump; 17, PC with installed data acquisition card.

steel drying chamber, insulated carefully with rock wool, with an inner dimension of $45 \times 45 \times 45\,cm^3$; a steam reservoir, which received the steam from the boiler and maintained its pressure at around 200 kPa (gage); and a liquid ring vacuum pump (Nash, model ET32030, Germany), which was used to maintain the vacuum in the drying chamber. Steam trap was installed to reduce the excess steam condensation in the reservoir. An electric heater, rated at 1.5 kW, which was controlled by a PID controller (Omron, model E5CN, Japan) was installed in the drying chamber to control the steam temperature and to minimize the condensation of steam in the drying chamber during the start-up period; with the use of a heater the initial steam condensation during the start-up period was reduced considerably. A variable-speed electric fan was used to disperse steam throughout the drying chamber. The steam inlet was made into a cone shape and was covered with a screen to also help distribution of the steam in the chamber. The sample holder was made of a stainless steel screen with a dimensions of $12 \times 12\,cm^2$. The change of the weight of the sample was detected

continuously (at 30 s intervals) using a load cell (Minebea, model Ucg-3 kg, Japan), which was installed in a smaller chamber connected to the drying chamber by a flexible hose (in order to maintain the same vacuum pressure as that in the drying chamber), and also to an indicator and recorder (AND A&D Co., model AD 4329, Japan). The temperatures of the steam and of the drying sample were also measured continuously using type K thermocouples, which were connected to an expansion board (Omega Engineering, model no. EXP-32, USA). Thermocouple signals were then multiplexed to a data acquisition card (Omega Engineering, model no. CIO-DAS16Jr., USA) installed in a PC. LABTECH NOTEBOOK software (version 12.1, Laboratory Technologies Corp., USA) was then used to read and record the temperature data.

Materials and Methods

Fresh carrot was obtained from a local supermarket and stored at 4°C. Prior to the start of each experiment carrot was peeled and diced into $1\,cm^3$ cubes. To perform a drying experiment approximately 35 cubes of carrot (about 40 g) were placed on the sample holder. The drying chamber was then sealed tightly. Valve 2 was opened to allow the steam from the boiler to flow into the reservoir; the steam pressure was maintained at about 200 kPa (gage) in the reservoir. A vacuum pump was then switched on to evacuate the drying chamber to the desired operating pressure and the steam regulator was opened to slowly flash the steam into the drying chamber. Due to the low-pressure environment of the chamber the steam became superheated. An electric heater was used to maintain the steam temperature at a desired drying temperature. At the end of the drying process the break-up valve was opened to allow the air into the drying chamber (to regain an atmospheric condition) before opening up the chamber door and loading off the dried product.

For vacuum drying experiments the same experimental set-up was used but without the application of steam to the drying chamber. The same operating conditions were therefore achievable. The experiments were performed at the following conditions: steam absolute pressures of 7, 10, and 13 kPa; steam temperatures of 60, 70, and 80°C. The flow rate of steam into the drying chamber (in the case of SSD) was maintained at about 26 kg/h and the speed of the fan was fixed at 2100 rpm.

Volume and Apparent Density Measurements

The measurement of the sample volume (V) was performed using a liquid pycnometer with n-heptane as the working liquid. The apparent density (ρ_{app}) of the sample was also readily obtained using this technique. The volume and apparent density of the sample were calculated according to the following equations:

$$V = \frac{[m_{Ph} - m_P] - [m_{Phs} - m_P - m_s]}{\rho_h} \quad (1)$$

$$\rho_{app} = \frac{\text{weight of sample in air}}{V} \quad (2)$$

where m_{Ph}, m_P, m_{Phs}, and m_s are respectively masses of a pycnometer filled with n-heptane, empty pycnometer, pycnometer with sample and n-heptane, and mass of the sample. ρ_h is the density of n-heptane. The average values of five samples were reported. All measurements were performed in duplicate.

Shrinkage Measurement

Five samples were used for a shrinkage measurement of each experimental condition. Shrinkage was expressed in terms of the percentage change of the volume of the original sample volume.

$$\%\text{shrinkage} = \frac{V_i - V}{V_i} \times 100 \quad (3)$$

where V_i and V are respectively the volumes of carrot at the beginning and at the end of each drying experiment. The average values of five samples were reported. All measurements were performed in duplicate.

Rehydration Ability

The rehydration ratio (R) of the dried sample was determined by immersing dried carrot sample in hot water at 100°C for 10 min. The sample was then drained and its volumes, both before and after immersion, were measured by a pycnometer. The rehydration ratio of the dried carrot was calculated by:

$$R = \frac{V_{after}}{V} \quad (4)$$

where V_{after} and V are respectively the volumes of dried carrot after and before immersion in hot water, respectively. The average valves of five samples were reported and all measurements were performed in duplicate.

Color Measurement

Colors of the samples were measured in a Hunter Lab color system using a colorimeter (Juki, model JP 7100, Japan). For each drying experiment the color measurement was performed on five dried samples and the color values were compared with those of fresh samples. All experiments were performed in duplicate and the average values were then reported. The color changes (L and a values only) were calculated by:

$$\Delta L = \frac{L - L_i}{L_i} \quad \text{and} \quad \Delta a = \frac{a - a_i}{a_i} \quad (5)$$

where L and a represent the lightness and redness of the dried sample, respectively. L_i and a_i are respectively the lightness and redness of the fresh carrot sample.

All experimental data were analyzed using an analysis of variance (ANOVA). Tukey's test was employed to establish the multiple comparisons of mean values. Mean values were considered significantly different when $p < 0.05$. From reproducibility tests the reproducibility values of the volume, density, percentage of shrinkage, rehydration ratio, Δa, and ΔL were within ± 1.8, 2.5, 4.2, 12.8, 6.1, and 5.5%, respectively.

RESULTS AND DISCUSSION

Drying and Heat Transfer Characteristics of Carrot

After the low-pressure superheated steam dryer was fabricated it was tested to ensure that the distribution of the steam temperature within the drying chamber was uniform. It was found from this study that the maximum difference of the steam temperature within the drying chamber was within ± 3 C. The dryer was then used to conduct both low-pressure

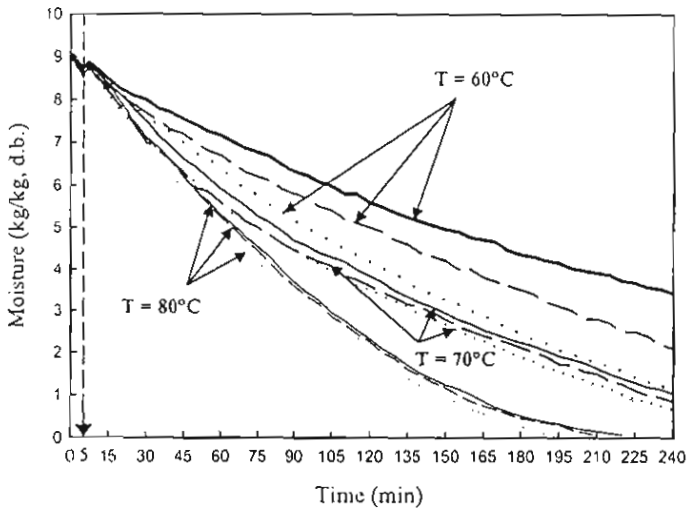


Figure 2. Drying curves of carrot undergoing LPSSD during the first 4 h of experiments (Legends used are the same as in Fig. 3).

superheated steam drying (LPSSD) and conventional vacuum drying experiments.

Carrot that had an initial moisture content of about 9 kg/kg (d.b.) (or about 90% w.b.) was dried to a final moisture content of about 0.07 kg/kg (d.b.) (or about 6.5% w.b.) in the dryer using both low-pressure superheated steam and conventional vacuum drying. The drying curves of carrot undergoing LPSSD are shown in Fig. 2; a slight decrease in the moisture content during the first 5 min of the process was due to the initialization of the chamber pressure and of the load cell. Drying indeed started at about 5 min after the weight was initially recorded. It can be seen in this figure that all samples gained a small amount of moisture during the first few minutes of drying (after the above-mentioned 5 min) for all drying conditions due to steam condensation. This phenomenon is indeed typical of superheated steam drying[8,9] although, in this study, the drying chamber was preheated at 50°C during the first 5 min of the process. Nevertheless, the condensation of steam was rather negligible if the operating pressure was low; for example, the samples gained moisture of about 1.4, 1.3, and 1% when drying at 60, 70, and 80°C at 7 kPa, respectively. Accordingly, the restoration time, which

Table 1. Average drying times of LPSSD and vacuum drying of carrot at various operating conditions.

	Temperature (°C)		
Pressure (kPa)	60	70	80
Drying time of LPSSD (min)			
7	389	280	198
10	N/A	290	210
13	N/A	317	230
Drying time of vacuum drying (min)			
7	235	205	159
10	241	223	175
13	255	265	206

N/A implies that, at this condition, the final carrot moisture content of 0.07 kg/kg (d.b.) was not achievable.

is the time by which the original mass has returned to its original value[18] was 5, 4 and 4 min for drying at 60, 70, and 80°C at 7 kPa, respectively.

Table 1 lists the drying times of all LPSSD and vacuum drying experiments. It can be seen from this table and also from Fig. 2 that the effect of temperature on the drying rates was greater than the effect of pressure in the case of LPSSD, especially at higher drying temperatures. The effect of operating pressure was less clear even at lower temperature (60°C) for the case of vacuum drying, as can be seen in Fig. 3, however. This may probably due to the fact that the steam thermal properties were affected by temperature to a larger extent than those of air, especially at lower drying temperatures. No initial condensation was also observed, as expected, in the case of vacuum drying. It can also be seen that the moisture decreased faster at a higher temperature than at a lower temperature because the temperature difference between the sample and the medium at a higher drying temperature was greater than that at a lower temperature. For example, an increase of the drying temperature from 60 to 80°C led to a reduction in the drying time of about 49 and 32% in the case of LPSSD and vacuum drying at an operating pressure of 7 kPa, respectively. In addition, it was observed that the moisture content decreased faster, especially in the case of LPSSD at lower drying temperatures, at lower pressures since water in carrot boiled and evaporated at lower temperatures; a decrease of the pressure from 13 to 7 kPa, for example, led to a reduction of the drying time by 14 and

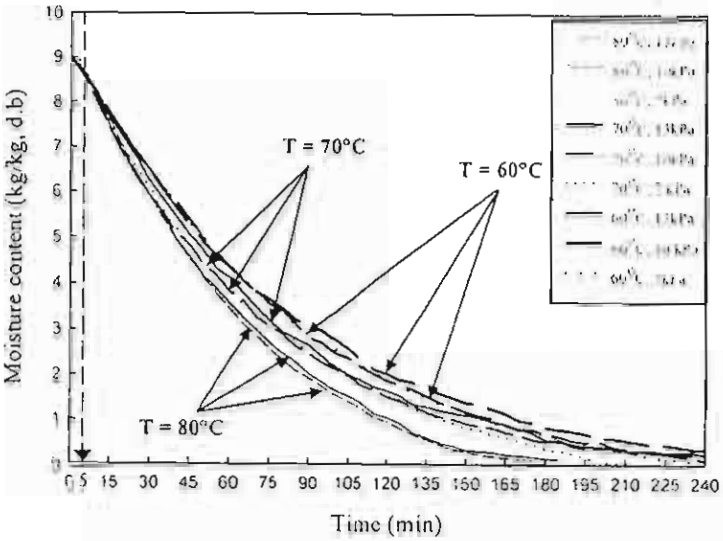


Figure 3. Drying curves of carrot undergoing vacuum drying during the first 4 h of experiments.

23% in the case of LPSSD and vacuum drying at a temperature of 80°C, respectively. Performing LPSSD experiments at higher pressures and lower temperatures also led to another problem, i.e., it was not able to dry carrot to the required moisture content of 0.07 kg/kg (d.b.) because there was an excessive amount of steam condensation in the drying chamber.

It was found that the drying times of vacuum drying were shorter than those of LPSSD (at the same pressure) for all conditions tested. This is probably due to the fact that the electric heater was used more often during vacuum drying since it was the only source of energy for drying. This might increase the amount of radiation absorbed by the carrot surfaces, thus explaining the higher drying rate during vacuum drying. The initial steam condensation on the product surface might also contribute to the longer drying times for the case of LPSSD. The differences between the two sets of drying times, however, were smaller at higher drying temperatures. Raising the drying temperature further would eventually lead to equal rates of drying at an inversion temperature (due to increased temperature difference between the

steam and the product as well as a reduction of the initial steam condensation). This could not be done in this case, however, as it would adversely affect the quality of the dried carrot.

Figure 4 illustrates changes of moisture content and temperature of carrot undergoing LPSSD at some selected conditions. It can be seen in this figure that the shapes of the drying and temperature curves were affected by both the drying temperature and pressure. At lower drying temperatures (say, at 60 and 70°C) the temperature of carrot changed suddenly from its initial value (after initial adjustment) and remained rather constant at the boiling temperature of water corresponding to the operating pressure until the first falling rate period drying ended (drying rate data are not shown here for the sake of brevity). Beyond this point, the carrot temperature rose again and finally approached the temperature of the drying medium. As the medium temperature increased (at the same operating pressure) it can be seen (for example, from Fig. 4c) that the period of constant product temperature was shorter; the product temperature rose almost steadily from its initial value to the medium temperature. At the same drying temperature, however, increasing of the operating pressure led to a lower rate of drying but a longer period of constant product temperature (as can be seen from Figs. 4c and d). It may depend both on the characteristics of the drying product and on these effects to determine the optimum operating conditions of an LPSSD.

Figure 5 shows the evolutions of moisture content and temperature of carrot undergoing vacuum drying at the same operating conditions as those used for LPSSD shown in Fig. 4. It can be seen from this figure that the drying and heat transfer behavior of carrot undergoing vacuum drying was quite different from that of LPSSD; the product temperature, in this case, rose almost steadily from its initial value to the medium temperature. However, the rates of moisture reduction in the case of vacuum drying were higher than those belonged to LPSSD, especially at lower drying temperatures as mentioned earlier.

Attempts were also made to compare the present data with a similar set of data available in the literature, i.e., the processes of freeze drying, air drying and microwave vacuum drying of carrot, in terms of the average drying rates over the whole period of drying.[19] It was found that the lowest drying rates obtained in the present study (which corresponded to using LPSSD at 60°C and 7 kPa) of 1.38 kg water kg^{-1} dry matter h^{-1} was, as expected, lower than that achievable by microwave vacuum drying (19.1 kg water kg^{-1} dry matter h^{-1}) but was still higher than those obtained by air drying and freeze drying of blanched carrot slices (1.31 and 0.013 kg water kg^{-1} dry matter h^{-1}, respectively). It should be

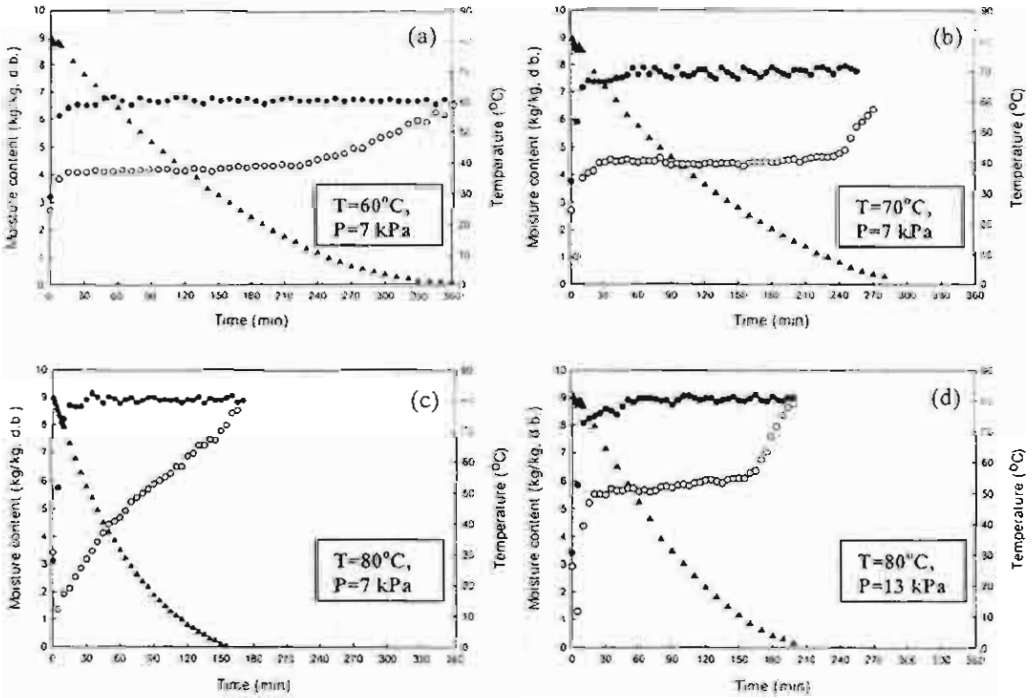


Figure 4. Changes in moisture content and temperature of carrot undergoing LPSSD at different operating conditions. ▲ moisture content; ● steam temperature; O sample temperature.

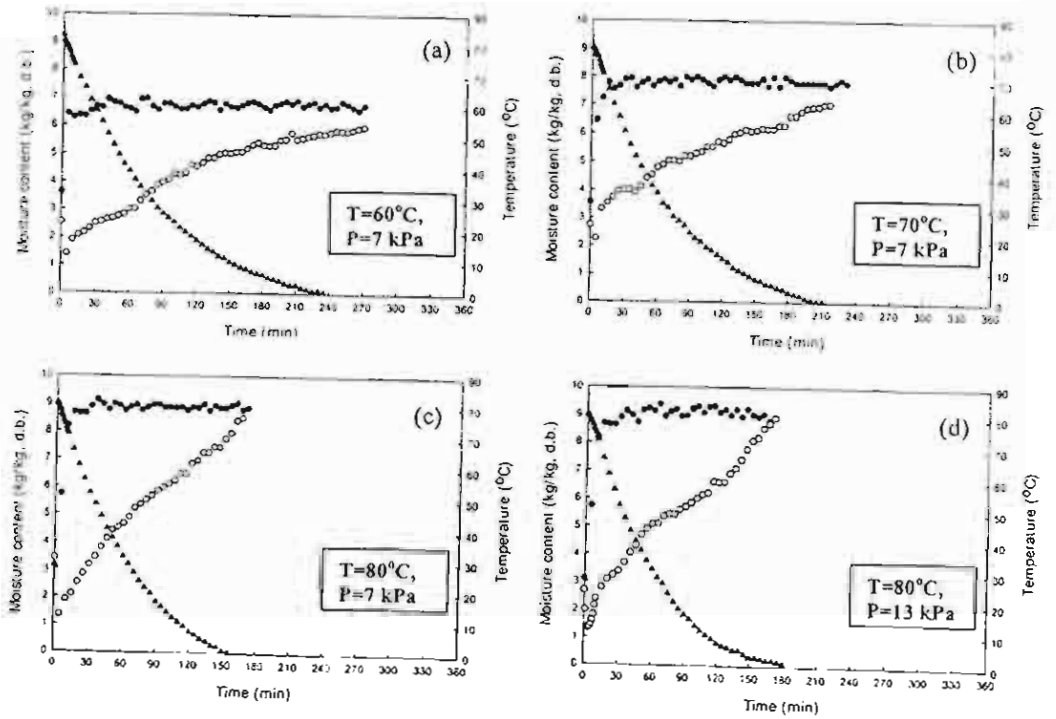


Figure 5. Changes in moisture content and temperature of carrot undergoing vacuum drying at different operating conditions. ▲ moisture content; ● steam temperature; O sample temperature.

noted that it is easier to dry blanched carrot than fresh carrot used in the present study. The carrot slices used by Lin et al.[19] also had less thickness (4 mm) than that used in our study as well.

. Volume, Apparent Density, Shrinkage, and Rehydration Behavior of Carrot

Table 2 illustrates the effects of the drying temperature and pressure of both LPSSD and vacuum drying on various physical properties of carrot, i.e., volume, density, shrinkage, and rehydration behavior. It was found that the volume of dried carrot was inversely proportional to its apparent density; carrot that had lower apparent density has larger volume, as expected. It can be seen also that the volume and apparent density of dried carrot undergoing both drying techniques slightly decreased and increased, respectively, as the operating pressure increased. This is due to the fact that pressure affects the percentage of air pores developed in the final dried products[20]; both properties changed only slightly in this case, however, because of the narrow range of operating pressures tested. Different drying techniques as well as the drying temperature also did not have much effect on the volume and density of the final dried products in this case. This is in accordance with the results reported by Krokida et al.[21] who compared the apparent density of dried carrot and other dried food products undergoing convective hot-air, microwave, freeze, and osmotic drying; it was found in their work that the operating pressure significantly affected the apparent density of the dried products than did the other operating parameters. Lowering the pressure during subatmospheric drying (both LPSSD and vacuum drying) also helped preventing the structural collapse of foods, especially in the case of carrot.

Table 2 also shows the results of shrinkage of carrot undergoing different drying techniques and operating conditions. Like the apparent density, shrinkage values correlated directly with the volume of dried carrot. It can be seen from Table 2 that the percentage of shrinkage of LPSSD and vacuum dried carrot was similar although superheated steam drying is known to have a potential to reduce the degree of shrinkage of the drying product due to an evolution of vapor inside the product that expands into cells, leading to a normally porous dried product.[15,22,23] This improvement in terms of shrinkage may only be seen clearly when comparing the dried product obtained with that dried by a conventional atmospheric hot air drying.

Table 2. Physical properties of carrot undergoing LPSSD and vacuum drying at different drying conditions.

Drying process	Temperature (°C)	Pressure (kPa)	Volume (cm^3)	Density (g/cm^3)	Shrinkage (%)	Rehydration ratio
LPSSD	$T = 60$ °C	7	0.092 ± 0.002^{d}	1.43 ± 0.03^{a}	90.80 ± 0.09^{ab}	5.19 ± 0.08^{f}
		10	N/A	N/A	N/A	N/A
		13	N/A	N/A	N/A	N/A
	$T = 70$ °C	7	0.092 ± 0.008^{d}	1.42 ± 0.02^{a}	90.77 ± 0.09^{a}	5.21 ± 0.09^{fg}
		10	0.087 ± 0.01^{a}	1.50 ± 0.04^{d}	91.21 ± 0.07^{de}	5.10 ± 0.14^{de}
		13	0.086 ± 0.004^{a}	1.51 ± 0.06^{de}	91.23 ± 0.10^{eh}	4.94 ± 0.04^{d}
	$T = 80$ °C	7	0.093 ± 0.009^{c}	1.43 ± 0.11^{ab}	90.8 ± 0.09^{ab}	5.23 ± 0.15^{h}
		10	0.09 ± 0.006^{b}	1.44 ± 0.01^{b}	90.82 ± 0.06^{b}	5.19 ± 0.05^{f}
		13	0.088 ± 0.008^{ab}	1.45 ± 0.08^{c}	91.09 ± 0.02^{f}	5.15 ± 0.07^{e}
Vacuum drying	$T = 60$ °C	7	0.092 ± 0.009^{c}	1.42 ± 0.1^{ab}	90.85 ± 0.11^{cd}	4.39 ± 0.18^{b}
		10	0.09 ± 0.012^{b}	1.43 ± 0.04^{ab}	90.97 ± 0.14^{d}	4.17 ± 0.16^{a}
		13	0.09 ± 0.007^{b}	1.43 ± 0.03^{ab}	90.99 ± 0.08^{d}	4.10 ± 0.04^{a}
	$T = 70$ °C	7	0.092 ± 0.003^{c}	1.43 ± 0.07^{ab}	90.82 ± 0.04^{b}	4.51 ± 0.03^{bc}
		10	0.091 ± 0.004^{bc}	1.40 ± 0.09^{a}	91.08 ± 0.04^{cf}	4.47 ± 0.09^{c}
		13	0.091 ± 0.01^{bc}	1.43 ± 0.02^{ab}	90.93 ± 0.05^{d}	4.13 ± 0.07^{b}
	$T = 80$ °C	7	0.092 ± 0.002^{c}	1.42 ± 0.04^{ab}	90.79 ± 0.04^{a}	4.82 ± 0.04^{de}
		10	0.092 ± 0.009^{c}	1.42 ± 0.12^{ab}	90.82 ± 0.11^{b}	4.56 ± 0.15^{c}
		13	0.09 ± 0.009^{b}	1.42 ± 0.07^{ab}	90.95 ± 0.09^{d}	4.51 ± 0.13^{c}

[a,b,c,d,e,f,g]In the same column with different superscripts means that the values are significantly different ($p < 0.05$).
N/A implies that, at this condition, the final carrot moisture content of 0.07 kg/kg (d.b.) was not achievable.

As mentioned earlier, carrot that was dried at various temperatures but at the same pressure in LPSSD and vacuum dryer had similar values of the final volume and apparent density and similar degrees of shrinkage. Although it is known that the temperature directly affects the shrinkage property of the dried product because high temperature drying results in a higher moisture gradient within the material and so higher internal stresses, which leads to a larger degree of shrinkage, the effect of temperature on shrinkage was not indeed much significant in this case, both for the cases of LPSSD and vacuum drying. This is probably due to the fact that the differences in drying temperature used might not be large enough to cause significant differences in shrinkage. This is in accordance with the results of Ratti[24] who also found that the shrinkage characteristics were independent of drying conditions over a limited range of drying temperature.

It should be noted, however, that although the values of shrinkage of carrot that underwent LPSSD and vacuum drying were similar, the shrinkage patterns resulted from the two different drying processes were quite different. Carrot that underwent vacuum drying tended to shrink nonuniformly. This characteristic is indeed rather typical of most food products.[25] In a more rapid drying (as in the case of vacuum drying when compared with LPSSD) the surface of the drying product became dry and rigid long before the center had dried out; the center dried and shrank much later than the outer surface did and pulled away from the rigid surface layers and caused a nonuniform shrinkage. Drying carrot in LPSSD, however, led to a more uniform shrinkage; in this case shrinkage seemed to occur because the carrot structure could not support its own weight and hence collapsed under gravitational force in the absence of moisture.[26] This is because LPSSD offered a milder drying condition (since the drying chamber was moister than in the case of vacuum drying). Dense or rigid large formation might not as much be formed in the case of LPSSD as in the case of vacuum drying. The photographs of carrot cubes both after drying and after rehydration are shown in Fig. 6

Regarding the rehydration ability of carrot undergoing both drying processes it can be seen in Table 2 that carrot that underwent LPSSD had much better rehydration capability than that vacuum dried. This is also due to the formation of dense layers in the case of vacuum drying, which led to nonuniform shrinkage mentioned earlier; the rather dense and rigid layers prevented the re-adsorption of water and hence led to lower degrees of rehydration. This can also be seen from SEM photographs of Figs. 7a and b, which show the microstructure of LPSSD and vacuum dried carrot, respectively. It is seen from these figures that carrot that underwent vacuum drying developed a rather dense layer and its pore

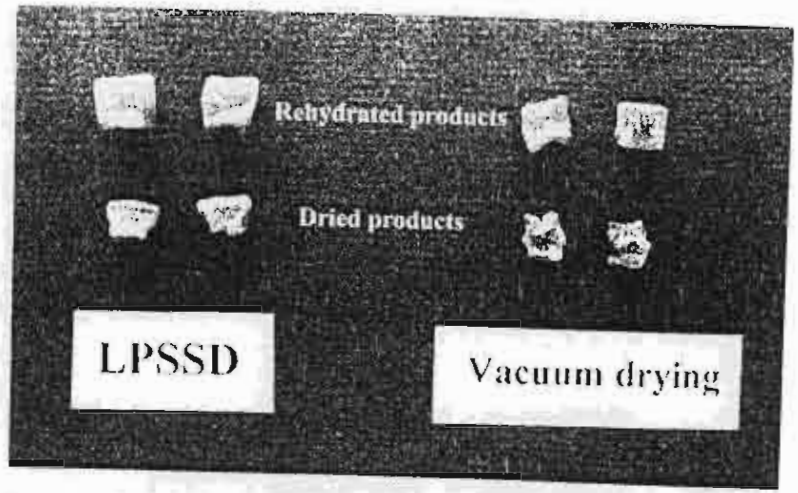


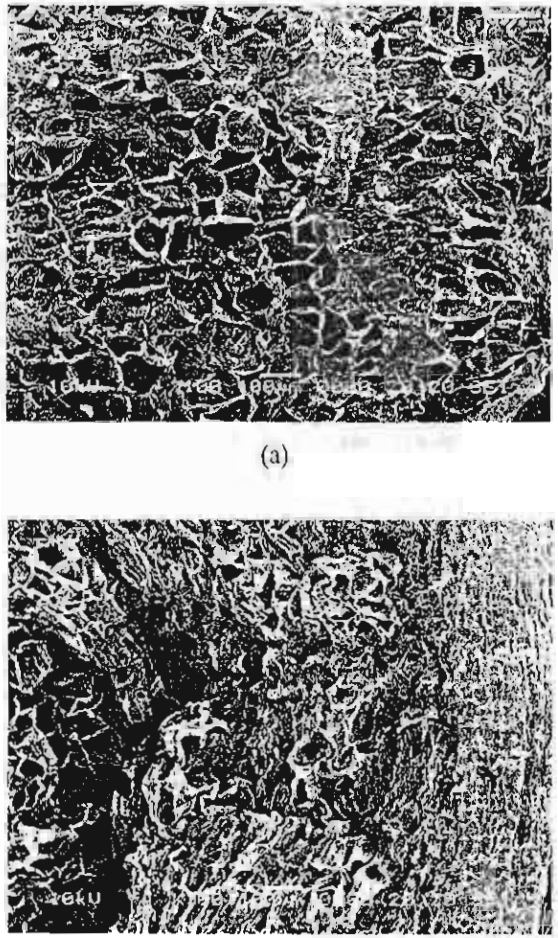
Figure 6. Photographs of carrot cubes both after drying and after rehydration.

distribution was rather nonuniform comparing with carrot that underwent LPSSD (see Figs. 8a and b), which also did not have dense layer that prevented re-adsorption of water. It was also found that, in general, there existed an adverse relationship between the degree of rehydration and that of shrinkage.

Color Parameters

The changes of color parameters (Δa and ΔL) of carrot undergoing LPSSD and vacuum drying are listed in Table 3. It was observed that all dried carrot was redder than fresh carrot as can be seen from the positive Δa values. This is probably due to the concentration of color pigments in carrot when moisture is removed. On the other hand, it was observed that almost all drying conditions (for both LPSSD and vacuum drying) yielded dried carrot with negative ΔL values, which implied that the dried carrot was slightly darker than the fresh one.

It can be observed from Table 3 that, when comparing the effects of different drying methods, LPSSD yielded carrot of redder and lighter colors than those obtained by vacuum drying. These results were similar to those reported by Caixeta et al.[27] who compared the color values of potato chips undergoing impingement superheated steam drying and hot air drying. It was also found that lower drying temperatures gave redder

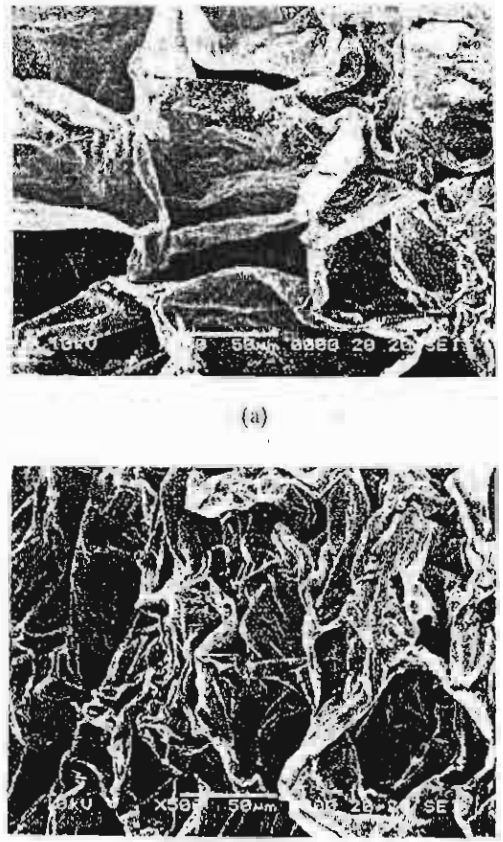


(a)

(b)

Figure 7. SEM photographs of carrot undergoing (a) LPSSD, (b) vacuum drying.

and lighter dried carrot. This may be due to the fact that red color is attributed to the presence of β carotenes[19] and the degradation of β carotene in carrot is inversely proportional to the drying temperature.[28] Operating pressure seems to have only a small effect on the colors of the dried carrot, however.



(a)

(b)

Figure 8. SEM photographs showing pore distribution of carrot undergoing (a) LPSSD, (b) vacuum drying.

CONCLUSIONS

Detailed experimental evaluation of low-pressure superheated steam drying showed that, despite lower drying rates due to poorer convective heat transfer under reduced pressures, the process gave superior quality dried product compared to that obtained using conventional vacuum drying. It was observed that the effect of operating pressure was less significant than that of steam temperature. It is interesting to note that

Table 3. Average values of Δa and ΔL of carrot undergoing LPSSD and vacuum drying at different operating conditions.

Drying process	Temperature (°C)	Pressure (kPa)	Δa	ΔL
LPSSD	$T=60$°C	7	0.2 ± 0.04^{e}	0.01 ± 0.02^{f}
		10	N/A	N/A
		13	N/A	N/A
	$T=70$°C	7	0.17 ± 0.02^{d}	-0.04 ± 0.03^{e}
		10	0.16 ± 0.06^{d}	-0.04 ± 0.02^{e}
		13	0.16 ± 0.04^{d}	-0.04 ± 0.04^{e}
	$T=80$°C	7	0.15 ± 0.01^{c}	-0.06 ± 0.08^{d}
		10	0.15 ± 0.01^{c}	-0.09 ± 0.17^{abc}
		13	0.15 ± 0.06^{c}	-0.08 ± 0.11^{cd}
Vaccum drying	$T=60$°C	7	0.10 ± 0.02^{ab}	-0.05 ± 0.03^{de}
		10	0.10 ± 0.02^{ab}	-0.06 ± 0.03^{d}
		13	0.09 ± 0.02^{ab}	-0.1 ± 0.08^{ab}
	$T=70$°C	7	0.07 ± 0.06^{a}	-0.09 ± 0.02^{a}
		10	0.07 ± 0.05^{a}	-0.1 ± 0.04^{ab}
		13	0.07 ± 0.1^{a}	-0.1 ± 0.03^{ab}
	$T=80$°C	7	0.07 ± 0.01^{a}	-0.1 ± 0.06^{ab}
		10	0.07 ± 0.04^{a}	-0.1 ± 0.03^{ab}
		13	0.07 ± 0.07^{a}	-0.1 ± 0.02^{ab}

[a,b,c,d,e,f]In the same column with different superscripts means that the values are significantly different ($p<0.05$).
N/A implies that, at this condition, the final carrot moisture content of 0.07 kg/kg (d.b.) was not achievable.

the operating pressure and temperature affected the shapes of the drying rate and temperature curves differently in steam drying and vacuum drying. The two drying techniques yielded differing structural and optical properties of the dried product. Steam drying provided better rehydration and a redder dried carrot than that obtained in vacuum drying over the operating parameter ranges studied.

NOMENCLATURE

m_p	Mass of an empty pycnometer (g)
m_{Ph}	Mass of a pycnometer filled with *n*-heptane (g)
m_{Phs}	Mass of a pycnometer with sample and *n*-heptane (g)
m_s	Masses of the sample (g)
R	Rehydration ratio (–)
V	Volume (cm^3)
V_i	Volume of fresh carrot (cm^3)

Greek Letters

ρ_{app}	Apparent density (g/cm^3)
ρ_h	Density of *n*-heptane (g/cm^3)

ACKNOWLEDGMENTS

The authors would like to express their sincere appreciation to the Thailand Research Fund (TRF) and the International Foundation for Science (Sweden) for supporting this study financially.

REFERENCES

1. Mujumdar, A.S. *Recent Developments in Drying*, Annual Conference of the Indian Institute of Chemical Engineering, Madras, India, 1981.
2. Cui, W.K.; Mujumdar, A.S. Paper drying—an overview of developments. In *Drying of Solids*; Mujumdar, A.S., Ed.; Wiley Eastern: New Delhi, 1986; 142–156.
3. Douglas, W.J.M. Drying paper in superheated steam. Drying Technology **1994**, *12* (6), 1341–1355.
4. Potter, O.E.; Beeby, C. Modelling tube to bed heat transfer in fluidized bed steam drying. In *Drying '86*; Mujumdar, A.S., Ed.; Hemisphere: Washington, 1986; Vol. 2, 595–603.
5. Salin, J.G. Steam drying of wood particles for particleboard. In *Drying'86*; Mujumdar, A.S., Ed.; Hemisphere: Washington, 1986; Vol. 2, 572–574.
6. Mujumdar, A.S. Superheated steam drying. In *Handbook of Industrial Drying*; Mujumdar, A.S., Ed.; Marcel Dekker, Inc.: New York, 1995; 1071–1086.
7. Urbaniec, K.; Malczewski, J. Experimental investigations of beet pulp drying in superheated steam under pressure. Drying Technology **1997**, *15* (6–8), 2005–2011.

8. Tang, Z.; Cenkowski, S.; Muir, W.E. Dehydration of sugar-beet pulp in superheated steam and hot air. Transactions of the ASAE **2000**, *43* (3), 685–689.
9. Mujumdar, A.S. Superheated steam drying—technology of the future. In *Mujumdar's Practical Guide to Industrial Drying*; Devahastin, S., Ed.; Exergex: Brossard, Canada, 2000; 115–138.
10. Kumar, P.; Mujumdar, A.S. Superheated-steam drying: a bibliography. Drying Technology **1990**, *8* (1), 195–205.
11. Elustondo, D.; Elustondo, M.P.; Urbicain, M.J. Mathematical modeling of moisture evaporation from foodstuffs exposed to subatmospheric pressure superheated steam. Journal of Food Engineering **2001**, *49* (1), 15–24.
12. Shibata, H.; Mada, J.; Shinohara, H. Drying mechanism of sintered spheres of glass beads in superheated steam. Industrial & Engineering Chemistry Research **1988**, *27* (12), 2353–2362.
13. Shibata, H.; Mada, J.; Funatsu, K. Prediction of drying curves on sintered spheres of glass beads in superheated steam under vacuum. Industrial & Engineering Chemistry Research **1990**, *29* (4), 614–617.
14. Senda, Y.; Bando, Y.; Yasuda, K.; Nakamura, M.; Sugimura, Y.; Shibata, M. *Development of Superheated Steam Dryer at Reduced Pressure*, Proceedings of the 1st Asia-Pacific Drying Conference, Bali, Indonesia, 2001; 247–256.
15. Elustondo, D.M.; Mujumdar, A.S.; Urbicain, M.J. Optimum operating conditions in drying foodstuffs with superheated steam. Drying Technology **2002**, *20* (2), 381–402.
16. Chen, S.R.; Chen, J.Y.; Mujumdar, A.S. Preliminary study of steam drying of silkworm cocoons. Drying Technology **1992**, *10* (1), 251–260.
17. Pang, S.; Dakin, M. Drying rate and temperature profile for superheated steam vacuum drying and moist air drying of softwood lumber. Drying Technology **1999**, *17* (6), 1135–1147.
18. Iyota, H.; Nishimura, N.; Yoshida, M.; Nomura, T. Simulation of superheated steam drying considering initial steam condensation. Drying Technology **2001**, *19* (7), 1425–1440.
19. Lin, T.M.; Durance, T.D.; Scaman, C.H. Characterization of vacuum microwave, air and freeze dried carrot slices. Food Research International **1998**, *31* (2), 111–117.
20. Krokida, M.K.; Maroulis, Z. Quality changes during drying of food materials. In *Drying Technology in Agriculture and Food Science*; Mujumdar, A.S., Ed.; Science Publishers, Inc.: Enfield, 2000; 61–106.

21. Krokida, M.K.; Oreopoulou, V.; Maroulis, Z.B. Modeling shrinkage and porosity during vacuum dehydration. International Journal of Food Science and Technology **1997**, *32* (6), 445–458.
22. Seyed-Yagoobi, J.; Li, Y.B.; Moreira, R.G.; Yamsaengsang, R. Superheated steam impingement drying of tortilla chips. Drying Technology **1999**, *17* (1&2), 191–213.
23. Moreira, R.G. Impingement drying of foods using hot air and superheated steam. Journal of Food Engineering **2001**, *49* (4), 291–295.
24. Ratti, C. Shrinkage during drying of foodstuffs. Journal of Food Engineering **1994**, *23* (1), 91–95.
25. Potter, N.N.; Hotchkiss, J.H. *Food science*, 5th Ed.; An Aspen Publication: Gaithersburg, 1998.
26. Achanta, S.; Okos, M.R. Quality changes during drying of food polymers. In *Drying Technology in Agriculture and Food Science*; Mujumdar, A.S., Ed.; Science Publishers, Inc.: Enfield, 2000; 133–147.
27. Caixeta, A.T.; Moreira, R.; Castell-Perez, M.E. Impingement drying of potato chips. Journal of Food Process Engineering **2002**, *25* (1), 63–90.
28. Pan, Y.K.; Zhao, L.J.; Dong, Z.X.; Mujumdar, A.S.; Kudra, T. Intermittent drying of carrot in a vibrated fluid bed: effect on product quality. Drying Technology **1999**, *17* (10), 2323–2340.

DRYING TECHNOLOGY
Vol. 22, No. 9, pp. 2095–2118, 2004

Effective Diffusivity and Kinetics of Urease Inactivation and Color Change During Processing of Soybeans with Superheated-Steam Fluidized Bed

Somkiat Prachayawarakorn,[1,*] Paveena Prachayawasin,[1] and Somchart Soponronnarit[2]

[1]Department of Chemical Engineering, [2]School of Energy and Materials, King Mongkut's University of Technology, Thonburi, Bangkok, Thailand

ABSTRACT

Influences of temperature and moisture content on diffusional transport property and kinetics of both urease inactivation and color change during soybean treatment with superheated steam in the temperatures of 120–150°C were investigated. The experimental results have shown that the effective diffusivity and apparent rates of such reactions are related to temperature in a way that the rates of

*Correspondence: Somkiat Prachayawarakorn, Department of Chemical Engineering, King Mongkut's University of Technology, Thonburi, Suksawat 48 Road, Bangkok 10140, Thailand; E-mail: somkiat.pra@kmutt.ac.th.

DOI: 10.1081/LDRT-200034265 0737-3937 (Print); 1532-2300 (Online)
Copyright © 2004 by Marcel Dekker, Inc. www.dekker.com

water transport, urease inactivation, and brown pigment formation are higher with higher temperature. In addition, these rates are also enhanced by increasing moisture content, except for the browning reaction that is inhibited by this factor due to the dilution effect. The reduction in urease activity is reasonably described by modified first-order reaction and the color change of soybeans is characterized by three Hunter parameters in which the changes of *L*-, *a*- and *b*-values are followed according to zero-order, modified Monod and first-order reactions, respectively. The kinetics of inactivation and color change, along with the experimental data of protein solubility and lysine content, have been suggested that the soybean should be treated with superheated steam at the temperature ranging from 120 to 135°C. The superheated-steam fluidized-bed technique can simultaneously be applied for both drying and inactivating such components in soybeans by a single operation when the initial moisture content falls within a suitable range, approximately lower than 20%d.b. At elevated initial moisture contents, two-stage drying technique is recommended in order to avoid excessive cooked soybeans.

Key Words: Color; Legume; Superheated steam; Trypsin; Urease.

INTRODUCTION

Legumes are valuable potential source of good-quality protein that is used as a main ingredient of animal feed and are increasingly important in human nutrition. Soybean is the most important legumes in relation to total world legume production because of its relative cheapness and high protein content. However, the utilization of nutritional value of soybean is limited due to the presence of certain antinutritional factors, such as trypsin inhibitor, hemagglutinins, saponins, and urease. Trypsin inhibitor inhibits the growth rate by 30–50% and causes the pancreatic hypertrophic response in animals when raw soybean meal is fed.[1] Urease enzyme, which catalyzes the urea converted into ammonia and carbon dioxide, does not affect on the physiological functions in humans, but is toxic to animals when fed with raw soybean meal. These antinutritional factors are destroyed by thermal processing methods such as roasting, cooking/autoclaving, micronization, and extrusion.[2–5] In addition to elimination of such factors, the thermal treatments improve nutritional value through conversion of native protein into more digestible denaturated forms.[6]

Roasting, one of the most frequently used techniques, involves cooking of soybeans using heated air with temperature above the normal boiling point of water. There are several roasting methods, ranging from salt bed roasting, rotary dryer similar to a common grain dryer. These methods provide nonuniform degree of cooking since the poor contact between grains and medium is encountered. The nonuniform cooking can be diminished by using fluidized-bed technique by which the hot-air stream with a sufficiently high velocity is forced through grain bed and consequently, the particles are suspended in hot air and move randomly within the bed. Besides the improvement of cooking, this technique gives rise to inactivation of the trypsin inhibitors and urease enzyme without losses of nutritional values in particular lysine.[7,8] In the present work, however, superheated-steam is chosen as heating media, in stead of hot air, to eliminate the antinutritional factors. Use of superheated steam is an attractive technology that offers improved thermal efficiency, thereby gaining improvements in economy and minimising environmental impact.[9,10] In addition to these advantages, the waste heat and water vapor evaporated from product can be recovered and used in other processes. The idea of using superheated steam to destroy the antinutrients originates from its unique characteristic, that is, the superheated steam is condensed when it is contacted with cold surface of material, thus releasing latent heat along with a rapid increase in particle temperature. With such peculiar phenomenon, it motivates us to quantify the effect of superheated steam in destroying antinutritive substances and simultaneously maintaining the high protein solubility.

Although treatment by thermal processes is able to reduce the levels of antinutritional factors satisfactorily, color deterioration of the product is unavoidable since temperature is an important factor in accelerating the formation of brown pigment, thus resulting in poor product quality. In general, the soybean color after processing should be yellow or light brown. The kinetics of color change is therefore a subject to be considered in the present investigation, in addition to the kinetics of urease inactivation.

MATERIALS AND METHODS

Samples

Dry soybeans, with moisture content of 13.5% d.b., were purchased from the local market and then adjusted to initial moisture contents of 19.5% and 36% by adding the required calculated amount of water.

The rewetted samples were kept in the cold storage room at 8-10°C for a week in order to allow water to penetrate uniformly into every part of the kernel.

Equipments

Figure 1 shows a schematic diagram of a superheated-steam fluidized-bed system. A fluidized-bed dryer has a cylindrical shape with a dimension of 15 cm diameter and 100 cm height. The saturated steam generated from a small boiler, with a capacity of 31 kg/h at the condition of 100°C and 106 kPa absolute pressure, flows through the dryer forced

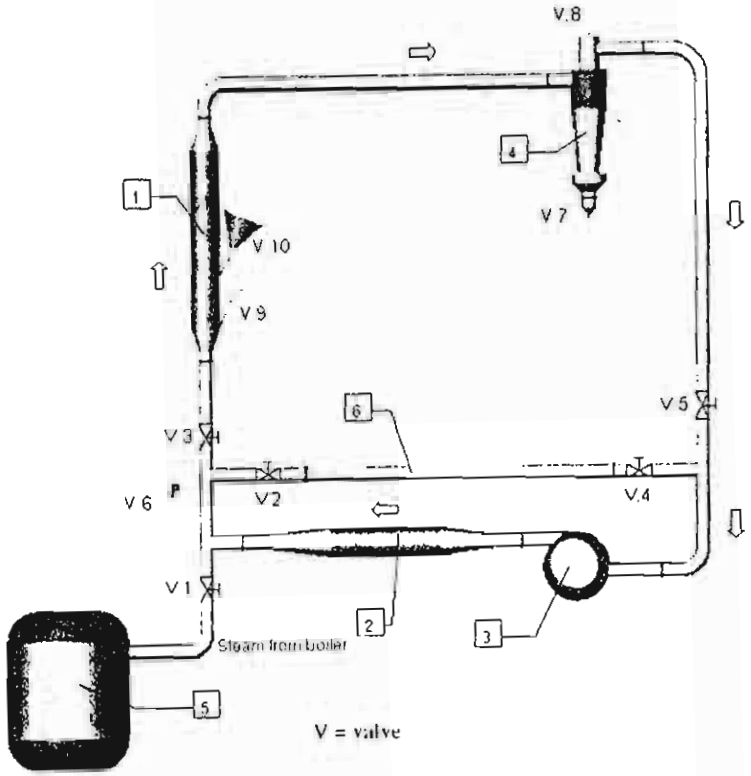


Figure 1. Schematic diagram of superheated-steam fluidized-bed system. (1) fluidized-bed dryer, (2) heater unit, (3) fan, (4) cyclone, (5) boiler (6) bypass line.

by a backward-curved blade centrifugal fan driven by a 2.2 kW motor. Before reaching the dryer, the saturated steam was passed through 13.5 kW electrical heaters to rise its temperature up to the desired level. This accordingly changed the saturated vapor into the superheated steam. The steam flow rate required for fluidizing the solid particles was precisely controlled by a frequency inverter and the desired superficial velocity at the drying chamber inlet was fixed at 3.2 m/s, which is 1.7 times higher than the minimum fluidizing velocity for soybean particle.[7] The steam velocity was measured by a pitot static tube.

The designed system can be used either for hot air or steam. In the superheated steam operation, the hot air is initially used for warming up the equipments and steam ducts of the system in order to prevent water condensation. The warming up period was stopped when the temperature in every part of the system reached the desired level and the steam was replaced accordingly by opening a valve V.1. At the same time, the air was delivered to atmosphere via a valve V.8 and this valve was closed again when the experiment was started. During the drying period, the steam flowing out of the dryer is directed to a reverse flow cyclone to collect the small particles being suspended in the fluid stream. The cleaned steam was reused again.

Before starting the experiments, samples were taken out from the storage room and left in the ambient condition until the grain temperature approached the ambient temperature. Amount 1 kg of soybeans, corresponding to a bed depth of 10 cm, was then dried at temperatures of 120, 135, and 150°C. A PID controller, with an accuracy of ±1°C, was used to maintain the steam temperature at the drying chamber inlet. Temperature at different positions within the drying chamber was monitored by a data logger with an accuracy of ±1°C. The sample was taken from the dryer at valve V.9 to examine the moisture content, urease activity, and quality. The moisture content of soybean was determined by drying in an electrical oven at 103°C for 72 h.[11]

Urease Activity Measurement

Urease test measures the activity of urease after processing. This test is an indirect method to indicate the level of trypsin inhibitor since rate of its inactivation becomes almost identical to that of trypsin inactivation.[8,12] It measures the change of pH which results from the urease enzyme converting the urea to ammonia. The determination of urease activity was followed by the direction of AACC method 22-90.[13] The pH difference of raw soybeans throughout the experiments was

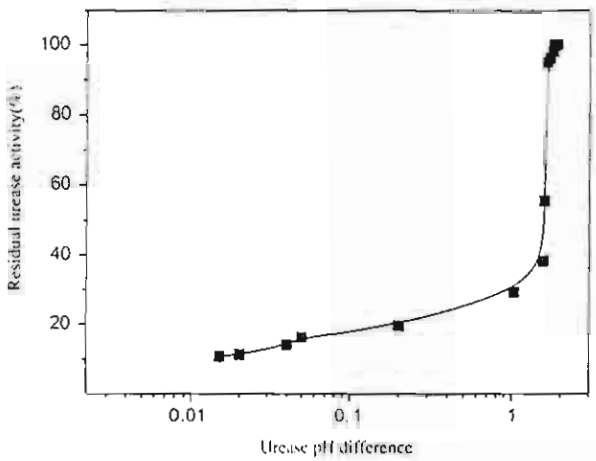


Figure 2. Relationship between pH difference and residual urease activity.

approximately 1.9. The relationship between pH difference and percent residual urease activity is given in Fig. 2. This figure was achieved by taking the samples dried at various drying times to measure the pH difference and the residual urease activity. The residual urease activity determination was followed with Rasmussen's method.[14] The reaction time for urease enzyme to develop ammonia was 60 min. The residual urease activity is expressed as the ratio of milliequivalents of ammonia produced from urea per gram of thermally treated soybeans to that obtained from raw soybeans. In uncooked soybean, ammonia was produced with an approximate value of 5 milliequivalents/g.

As shown in Fig. 2, the change in pH difference is not proportional to that of percent residual urease activity, with a steep rise in the residual urease activity at the pH difference higher than unity. From ASA standard, the adequately cooked soybeans possess the urease values in the range of 0.02 to 0.3 pH difference[11] and the corresponding percent residual urease activity is between 10 and 20%.

Colour Measurement

A Minolta CR-300 tristumulus colorimeter was used to determine the L, a, b values of samples. In Hunter Lab Color Space, the L-value presents the degree of lightness or darkness. The chromatic proportion of

the color space is based on rectangular Cartesian coordinates (a, b), with red represented by $+a$, green represented $-a$, yellow by b and blue by $-b$. The L-value gives a spectrum in the range from 0 to 100, with the highest value showing whiteness whereas the lowest value indicates the blackness. The a- and b-values represent the same spectrum range from -60 to 60. Before the color measurements, the colorimeter was standardized each time with a black and a white ceramic plates. The color was measured for soybeans thermally treated at various drying times, temperatures and initial moisture contents. Before measuring, the dried soybeans in each set were finely grounded using a mixer and then spread on a plate.

Protein Solubility Measurement

Protein solubility was determined according to the AOCS method BA 10-63.[15] This method involves the dispersion of proteins in 0.2% KOH solution. The protein solubility is defined as the ratio between nitrogen content in the supernatant after extraction with 0.2% KOH and total nitrogen content of material. The total nitrogen content and the nitrogen content in the supernatant were performed by Kjeldahl method.

Lysine Measurement

Lysine content in soybean was analyzed by AccQ-Tag method.[16] The grounded soybean was hydrolyzed with HCl solution at 110°C for 22 h and was then derivatized with 6-aminoquinolyl-N-hydroxysuccinimidyl carbamate (AccQ-Flour reagent). The lysine content was eventually determined by a high performance liquid chromatography.

Moisture Diffusion

In the present study, a method of slopes was applied to study the effect of moisture content on the effect diffusivity, D_{eff}.[17,18] Determination of effective diffusivity was written based on the Fick's second law equation, under the initial and boundary conditions that the moisture distribution inside a soybean kernel was specially uniform at the beginning; and the moisture at the exterior surface, after drying has started, rapidly vaporized reaching almost zero value since the temperature used

for drying was above the normal boiling point. The solution of Fick's equation for sphere-shaped soybean is given by[19]

$$\frac{M(t)}{M_{in}} = \frac{6}{\pi^2}\sum_{n=1}^{\infty}\frac{1}{n^2}\exp\left(-\frac{n^2\pi^2 D_{eff}t}{r^2}\right) \quad (1)$$

where, $M(t)$ is the moisture content at time t (dry basis, kg H_2O/kg dry matter), and M_{in} is the initial moisture content, D_{eff} is the effective diffusivity (m^2/s), t is the drying time (s) and r is the sphere radius (m). To determine the effective diffusivity along the change in moisture content with drying time, it can be accomplished by differentiating Eq. (1) with respect to t, yielding

$$\frac{d(M(t)/M_{in})}{dt} = -\frac{6D_{eff}}{r^2}\sum_{n=1}^{\infty}\exp\left(-\frac{n^2\pi^2 D_{eff}t}{r^2}\right) \quad (2)$$

The slope of experimental drying curve was known at every time and used as input parameter on the left hand side of Eq. (2) and the effective diffusivity was then estimated. The main assumptions of Eq. (2) were that the moisture transport occurred only in the radial direction and the sample was homogeneous, without shrinkage during drying.

Kinetics of Urease Inactivation

Inactivation of urease enzyme during thermal treatment by superheated steam was assumed to follow the modified first-order kinetics expressed as

$$C = (C_o - C_{eq})\exp(-kt) + C_{eq} \quad (3)$$

where, C_o is the activity of urease enzyme at the beginning (dimensionless), k is the apparent rate constant (min^{-1}). C_{eq} is the equilibrium activity and can be determined by a linear regression.

Kinetics of Color Change

The color change of thermally treated soybean is caused by the non-enzymatic browning reaction, where the interaction between carbonyl compounds (sugars and carbohydrates) and amine compounds (amino acids and proteins) has occurred. In addition, it is possibly produced by the structural deformation of pigments. There have been numerous

research studies on the kinetics of color changes during storage and processing.[20-22] Generally, the apparent rate change of color is presented by the zero- or first-order kinetics. As observed from the experiments, the change of individual color parameters, representing by L-, a- and b-values, with time appears to be clearly different and hence, different kinetic models are used to describe their changes. A zero-order reaction is chosen to describe the change of L-value and it is expressed by

$$L = L_o + (-k_L t) \quad (4)$$

where, k_L is the rate constant for the L-value, min^{-1}, L is the L-value at time t and L_o is the initial L-value. For the b-value, a first-order reaction is adopted and it is given by

$$b = b_o\exp(-k_b t) \quad (5)$$

where, k_b is the rate constant for the b-value, min^{-1}, b is the b-value at time t and b_o is the initial b-value. A modified Monod equation is accounted for the change of a-value and it is written as

$$a = \frac{a_o c\exp(k_a t)}{c + a_o\exp(k_a t)} \quad (6)$$

where, k_a is the rate constant for the a-value, a_o is the initial a-value and c is the constant value related to the equilibrium a-value. If $c \gg a_o\exp(k_a t)$, Eq. (6) then approaches Eq. (5).

Adequacy of Model

Several criteria for adequacy of fit such as coefficient of determination (r^2) and residual sum of squares (RSS) were used to choose the appropriate models for the effective diffusivity, urease enzyme, and color changes. The RSS can be calculated by the following equation:

$$RSS = \sum_{i=1}^{n}(Z_{exp,i} - Z_{cal,i})^2 \quad (7)$$

where, Z_{exp} is the experimental value of the dependent variable, Z_{cal} is the calculated value from the model and n is the total number of experimental data. The best model describing the transport property and quality change was selected as the one with the highest coefficient of correlation and the least value of RSS.

RESULTS AND DISCUSSION

Change of Moisture Content

Figure 3 shows the change of moisture content at three initial moisture contents of 13.5, 19.5, and 36% d.b., all of which were dried at a temperature of 120°C. The characteristic curve of moisture content during superheated steam drying is different to that found with the conventional hot air drying. Two phenomena are observed in the superheated steam drying, which are the moisture uptake period followed by the evaporation period whereas only latter period is found with the hot air.

In the first period, the steam is in close contact with the bed of particles having a lower temperature which causes the steam to be condensed. The amount of moisture uptake is related to the initial moisture content and superheated steam temperature. The first period can be seen in Fig. 3, which shows the condensation period in the first 2 min of drying time and the amount of moisture content increased from the beginning to the highest point is approximately 4% d.b. for an initial moisture content of 14% d.b. and less than 3% d.b. for the higher initial moisture contents. The lowering of moisture uptake at higher moisture content is probably due to the higher occupancy of water in the

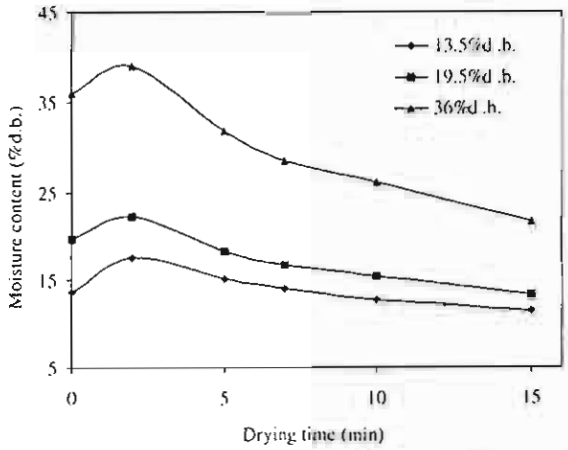


Figure 3. Change of moisture content at three different initial moisture contents (inlet superheated steam temperature of 120°C).

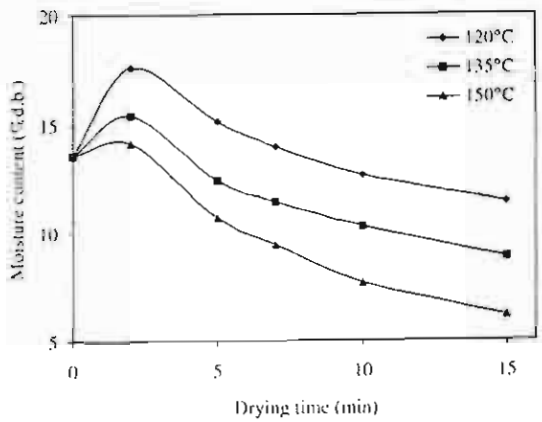


Figure 4. Change of moisture content at three different inlet steam temperatures (initial moisture content of 13.5% d.b.).

void spaces of the kernel, so that the less condensed water can penetrate into the kernel. In addition to this effect of high moisture content, the lower quantity of moisture uptake is obvious with higher inlet superheated steam as shown in Fig. 4: the moisture uptake into the samples in the superheated steam temperatures at 120, 135, and 150°C are 4.0, 1.8, and 0.6% d.b., respectively. The possible explanation of these results is due to the higher degree of superheat, resulting in a smaller amount of condensed steam.

When the evaporation period starts, transport of moisture is in the diffusion controlled region, as indicated by the exponential decay of moisture characteristic curve. The drying rate in this region is dependent on moisture content and temperature. An increase in initial moisture content or inlet steam temperature increases the soybean drying rate, as shown by the slopes of the characteristic curves in Figs. 3 and 4, respectively.

Change of Bed Temperature

Figure 5 illustrates the change in bed temperature for the samples at different initial moisture contents using the inlet steam temperature of 120°C. The bed temperature is strikingly increased for a short period and then rises gradually for the remaining drying time, corresponding to the

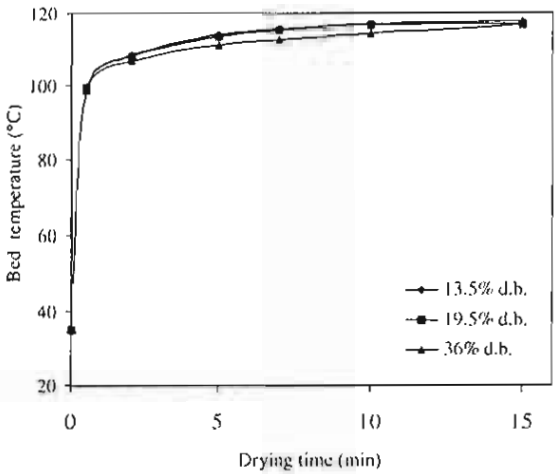


Figure 5. Change of bed temperature at different initial moisture contents (inlet superheated steam temperature of 120°C).

evaporation period. The rapid rise in temperature is attributed to the release of latent heat from the condensing steam, thus fast heating the kernels. As illustrated in Fig. 5, the bed temperatures during condensation period are in the range of 98 and 100°C, the lowest temperature corresponding to the initial moisture content of 36% d.b. The condensed steam did not take seriously the operational problem in this case but it produced the desirable result of soybean product quality, with the rapid inactivation of urease enzyme. For a few minutes of drying, the residual urease activity fell off by 100% to the range of 10 to 96%, depending upon the inlet temperature and initial moisture content. The details will be given in the section of urease inactivation.

Moisture Diffusivity

Data from a particular evaporation period of the drying experiment were analysed for calculating the effective diffusion coefficient. Figure 6 shows the relationship between the effective diffusion coefficient and moisture content at various temperatures. Values vary considerably from 1.8×10^{-11} to 1.5×10^{-8} m^2/s. D_{eff} have high values in the early stages of evaporation period, where the moisture content is high, and then

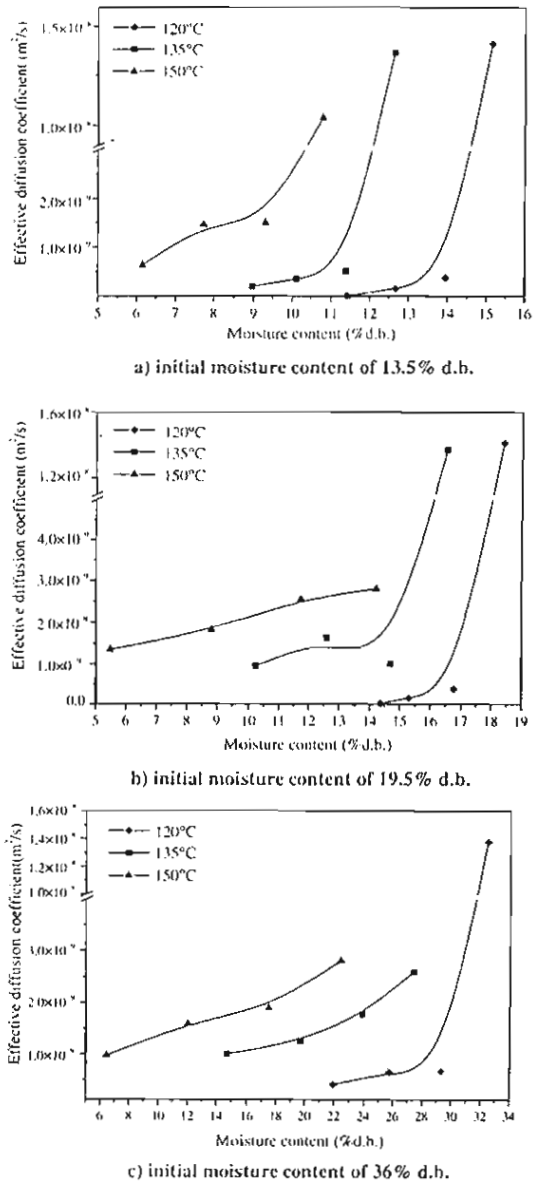


Figure 6. Relationships between effective diffusion coefficient and moisture content at different steam temperatures.

becomes monotonically decreasing in the later stages, where the moisture content appears to be lower. The decrease of D_{eff} at lower moisture content may be due to the complex structure of the kernel restricting the transport of water from the interiors to the exteriors. In addition to moisture effect, the effective diffusion coefficient also varies with temperature by a way that the diffusivity increases with increase in temperature.

It is noted that for some dying conditions, viz., at temperatures of 120 or 135°C and initial moisture content of 13.5 or 19.5% d.b., the effective diffusion coefficient is very high particularly at the beginning of evaporation period. This high value corresponds to the reduction in moisture content from the peak to the next data point, suggesting that the condensed steam only penetrates into the kernel around the outer layer during this short period of condensation. Accordingly, when the evaporation period starts, the moisture is removed easily without the interference of soybean structure and leads to extremely high drying rates.

In order to obtain the representative model for the effective diffusivity, the values of D_{eff} were fitted with an empirical equation treating D_{eff} as the dependent variable with temperature and moisture content as the independent variables. The analysis of the data using a non-linear regression technique suggests the following form:

$$D_{eff} = \left[5.4364 \times 10^{-20} + 5.111 \times 10^{-18} M^2\right] \exp(0.057318T) \qquad (8)$$

where, D_{eff} is the effective diffusion coefficient, m^2/s, T is the bed temperature, K. The values of R^2 and RSS for Eq. (3) are 0.8 and 1×10^{-18}, respectively.

Urease Activity

Figure 7 depicts some illustrative residual urease activity curves of soybeans at initial moisture content of 19.5% d.b. and inlet steam temperatures of 120–150°C. This enzyme is progressively destroyed by heat, whereby a sharp decline in urease activity occurs at the early period of drying, except for the conditions where the samples at initial moisture contents of 13.5 and 19.5 % d.b. are dried at lower temperature of 135°C, and a slow reduction is a consequence. This figure also shows the faster rate of inactivation at the higher temperature, as would be expected because more thermal energy is being transferred when drying temperature is increased. The inactivation results for the samples at the initial moisture contents of 13.5 and 36% d.b. showed the same fashion as in Fig. 7, but the rate of inactivation amongst their initial moisture

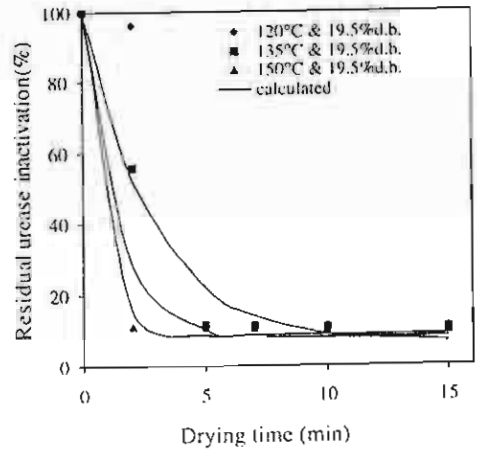


Figure 7. Change in residual urease activity versus time at different inlet steam temperatures.

contents was not identical even though the inlet steam temperature was the same, a relatively faster rate of inactivation for the samples at higher moisture content. These results can clearly be seen in Fig. 8, presenting the apparent reaction rate constant for the inactivation versus bed temperature. These reaction constants were obtained from statistical fitting of Eq. (3) to the residual urease activity data.

To reduce the residual urease activity to an acceptable range, it required 7–8 min at a temperature of 120°C and became shorter at the higher temperature for the initial moisture content of 13.5% d.b. The treatment time was decreased as the initial moisture content increased, with the treatment time of 5 min at temperatures of 120–135°C and 2 min at the temperature of 150°C for the moisture content of 19.5% d.b. In addition, for the initial moisture content of 36% d.b., the treatment time was only about 2 min, which is long enough for inactivating the urease enzyme under the above-mentioned temperature range.

Figure 8 demonstrates how the temperature and initial moisture content can cause a rapid inactivation of urease through the thermal treatment with fluidized bed. Large differences in the patterns of inactivation are observed between such operating parameters. The influence of temperature plays an important role in accelerating the urease inactivation for soybean containing low to moderate moisture contents, in particular at the initial moisture content of 19.5% d.b. showing a large

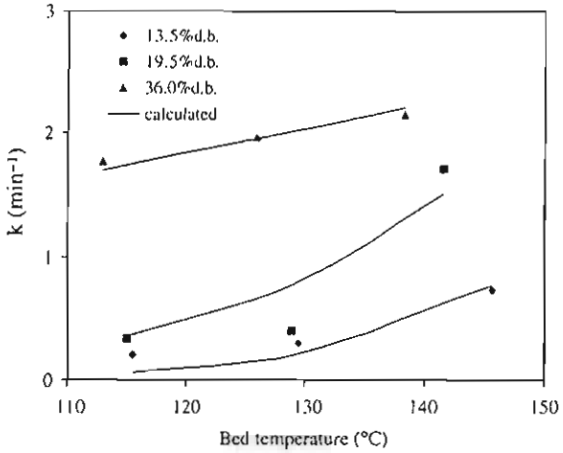


Figure 8. Apparent rate constant for inactivating urease enzyme at different temperatures and initial moisture contents.

increase in the reaction rate constant from 0.43 to 1.7 min^{-1} when the corresponding bed temperature rises from 113 to 140°C. This effect turns into lesser importance for the higher initial moisture content, as indicated by a linear increase in the apparent reaction rate constant with increasing temperature for soybean sample at 36% d.b. At such high initial moisture content, the prevalent contribution of moisture initially present in soybeans induces the rapid inactivation in the first 2 min of drying, by which the residual urease activity lies between 15 and 17% after soybeans are treated with temperature in the range studied.

The rate constant and equilibrium activity are empirically correlated with the initial moisture content and bed temperature, and their relationships are given by the following equations:

$$k = \left(5.7696 \times 10^{-18} + 1.3531 \times 10^{-16} M_{in} - \frac{8.59758 \times 10^{-15}}{T}\right) \times \exp(-0.245571 T M_{in} + 97.7304 M_{in} + 0.09702 T) \quad (9)$$

$$C_{eq} = (-0.047523 + 0.071742 M_{in}^2 + 0.000122 T) \times \exp\left(-\frac{978.15 M_{in}}{T} + \frac{3227.286}{T}\right) \quad (10)$$

As shown in Fig. 7, the kinetic model of urease inactivation proposed, along with its constant parameters in Eqs. (9) and (10), can reasonably predict the experimental data.

Color Changes

The changes in color of a product reflect a sensation to human eye and the visual examination is often used to evaluate product color. The *L*-, *a*- and *b*-values of soybean at the beginning are respectively 85.71, 0.38 and 24.33, presenting yellow color. Figure 9 shows the change in the behaviors of *L*-, *a*- and *b*-values for soybeans dried at various steam temperatures, with a progressive decrease of the *L*-value whilst the increase of the *a*- and *b*-values with the increased drying time are evident. The decrease in *L*-value upon heating is attributed to the formation of brown pigments, as a result of Maillard reaction. The linear behaviour of the lightness suggests a zero-order kinetic model.

In addition to the *L*-value, *a*- and *b*-values are also used to indicate characteristics of brown pigments formed by heat treatment. The change of *a*-value is initially slow and followed by a rapid raise of the level of redness. To explain the whole range of redness, the change of a-value follows the Monod kinetic reaction. For the *b*-value, it exponentially increases according to the first-order reaction kinetics. The reaction rate constants of the *L*-, and *b*-values were determined by a linear regression technique whereas the rate constant of the *a*-value was determined by a nonlinear regression because of nonlinearity of Eq. (6). The experimentally determined reaction rate constants are presented in Fig. 10 to show the effect of temperature on their reaction rate constants. The results indicate that the reaction speeds of the color parameters increase with increased temperature. The increase in the reaction speed of the individual color parameters has a difference of magnitude in which the fast reaction speed is the lightness followed by the redness, and the slowest speed is the yellowness. From this figure, it can be seen that the initial moisture content has some effect on the color of soybeans during heat treatment. This influence on the color change is different to that found with the urease inactivation in a way that the higher moisture content slows down the rate of brown pigment formation, as interpreted by lower reaction rate constants of both lightness and redness shown in Figs. 10a and b. The moisture content is not influential to the yellowness change for soybeans. The slow development of brown color is attributed to the fact that the lower concentration of the reactive compounds inside the food material retards the browning rate and this lower concentration

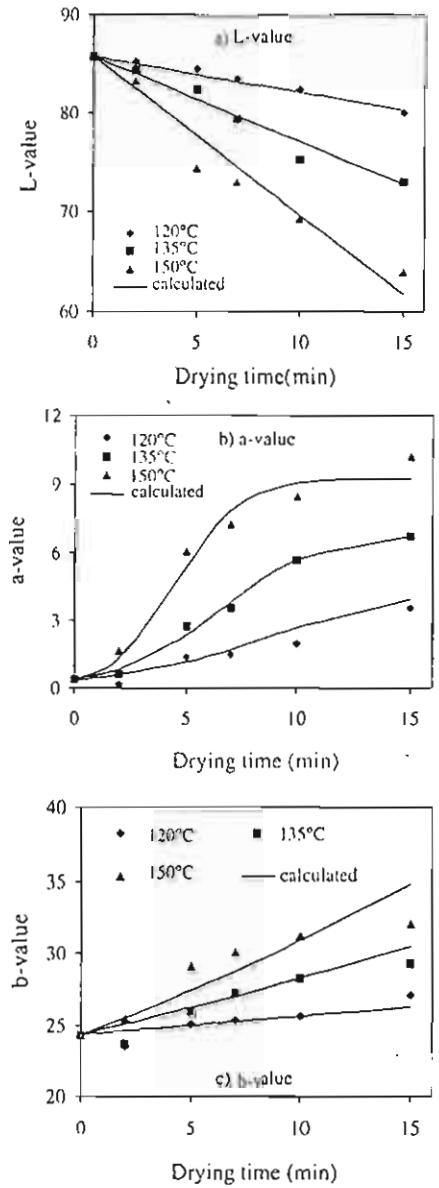


Figure 9. Changes in colour parameters versus drying time for different inlet superheated steam temperatures (initial moisture content of 13.5% d.b.).

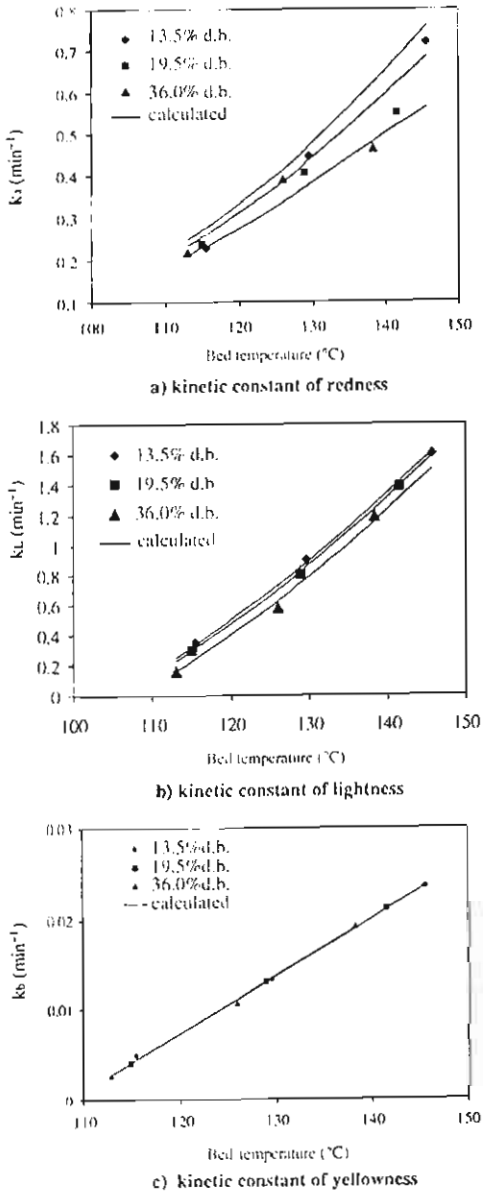


Figure 10. Effect of initial moisture content on colour parameters at various bed temperatures.

effect seems to be more dominant than the effect of reactant mobility, which has higher motivation at elevated initial moisture contents. The effect of water content on the browning rate for food materials has been reported by several workers.[20,23] The results found from their investigations were similar to this finding.

According to the experimental results, such reaction rate constants of the L-, a- and b-values were empirically correlated with the relevant parameters by the following equations:

$$\text{For } L\text{-value} \quad k_L = (-200.35 - 6.8356M_{in} + 0.53253T)\exp\left(-\frac{1087.66}{T}\right)$$

$$R^2 = 0.99, \quad \text{RSS} = 0.004 \tag{11}$$

$$\text{For } b\text{-value} \quad k_b = (-0.2435 + 6.4 \times 10^{-4}T)\exp\left(-\frac{5.3 \times 10^{-5}}{T}\right)$$

$$R^2 = 0.99, \quad \text{RSS} = 0.0127 \tag{12}$$

$$\text{For } a\text{-value} \quad k_a = [1.5 \times 10^9 - 1.1343 \times 10^8 M_{in} - 3.2052 \times 10^6 T]\exp\left(-\frac{8019}{T}\right)$$

$$R^2 = 0.96, \quad \text{RSS} = 0.007 \tag{13}$$

$$c = \left(-66.6919 + 0.181201T + \frac{3417.06M_{in}}{T}\right) \times \exp\left[1.5M_{in} - \frac{898.370M_{in}}{T}\right]$$

$$R^2 = 0.95, \quad \text{RSS} = 0.2267 \tag{14}$$

The result for the changes of L-, a- and b-values, calculated by using Eqs. (11)–(14), with drying time are depicted in Fig. 9, suggested that the proposed models can predict the color parameters in a good agreement with the experimental results over a wide range of drying condition.

Protein Solubility

For determining the amount of soluble proteins, some treated soybean samples that contain the level of urease activity lower than the required standard limit were analysed. Changes in protein solubility of

Table 1. Protein solubility and lysine content of soybeans treated with superheated steam at various temperatures.

Initial moisture content (%d.b.)	Inlet steam temperature (°C)	Treating time (min)	Moisture content after treatment (%d.b.)	Protein solubility (%)	ΔpH	Lysine content (mg/g of soybean)
Raw soybeans	---		--	94.3	1.9	2.85
13.5	120	7	14.0	85.7	0.2	2.80
	135	5	12.4	71.7	0.03	2.76
	150	5	10.7	54.9	0.04	NA
19.5	120	5	18.3	85.2	0.04	2.67
		15	16.7	75.3	0.005	NA
	135	5	16.5	82.3	0.01	2.71
		7	14.8	76.7	0.005	NA
	150	2	18.9	83.8	0.02	NA
		5	14.1	72.9	0.015	2.82
36	120	2	38.9	80.6	0.05	NA
	135	2	34.1	81.4	0.025	NA
		15	14.7	59.4	0	NA
	150	2	31.6	75.3	0.02	NA
		10	11.4	53.6	0	NA

soybeans treated at different operating conditions are shown in Table 1. The protein solubility is about 94.3% for raw soybeans and it is decreased faster when the soybeans were subjected to contact with steam at higher temperatures and for longer times. The reduction in protein solubility is caused by the destruction of helical regions of the proteins and subsequent disulfide bond, which links between amino acid groups. Consequently, the proton of hydrogen in water molecules inside proteins will react with the sulfur of disulfide to form as sulfhydryl. However, the formation of sulfhydryl is not stable and protein molecules will aggregate with the neighbouring molecules by disulfide bond, leading to the larger molecules of protein and the subsequent reduction in their dispersability in water.

As shown in Table 1, for the low initial moisture content of 13.5% d.b., the inlet steam temperature of 120°C is sufficiently high enough to inactivate the urease enzyme and the treating time is taken only 7 min, which is four times shorter than the use of the same technique but the hot

air replaced the superheated steam.[7,8] Using this temperature, the protein solubility and lysine content maintain at the satisfactory levels of 85% and 2.80 mg/g soybean, respectively. In addition, the color of treated soybeans does not changed much from the beginning, with the values of 83, 1.45, and 25 for the respective lightness, redness, and yellowness related parameters. However, the higher temperature of 120°C is not recommended because of lower protein solubility than the desirable range.

When the superheated steam was introduced to the moist soybeans, it beneficially provides shorter time for inactivation together with high protein solubility and lysine content. Unfortunately, their moisture contents at that treating time are still higher than the level for the extended storage. They therefore need to further dry to the safe moisture content. As can be seen from Table 1, the superheated steam can comply with both requirements, drying and urease inactivation, for soybeans at initial moisture content of 19.5% d.b. while preserving their nutritional value and yellow color as long as the inlet steam temperature varies between 120 and 135°C. At elevated initial moisture content, two-stage drying, where the soybean is treated with superheated steam at such a temperature range for a certain time to inactivate the urease enzyme and then followed with low-temperature hot-air drying to prevent the denaturation of protein and brown color development, should be applied.

CONCLUSION

Soybean treatment using superheated-steam fluidized-bed technique was examined. Steam was initially condensed onto the kernel surface which enables grains to adsorb it. An amount of condensed steam related to steam temperature and initial moisture content in a way that high steam inlet temperature and high initial moisture content reduced the quantity of condensing steam. During evaporation period, the transport of water is governed by internal diffusion and the rate of water removal depends on the temperature and moisture content, the first factor being the most important. During its operation, the urease activity and the color of soybeans, described by three Hunter parameters *L*-, *a*- and *b*-values, are also changed. The rates of urease inactivation and brown pigment formation, corresponding to the decrease of *L*-value and increases of *a*- and *b*-values, were enhanced by increasing temperature. In addition, the inactivation rate was faster whereas the change rates of *L*- and *a*-values became slower with higher initial moisture content, except for the *b*-value which showed an insignificant change. To inactivate the urease enzyme while maintaining soybean qualities in terms of protein solubility, lysine and color, inlet steam temperature should not exceed 135°C; with 120°C being the minimum required for treating dry soybean. Furthermore, this technique can be acted as the simultaneous operation of inactivating urease and removing water in a single operation for the moist soybean at a certain level.

ACKNOWLEDGMENT

The authors would like to thank the Thailand Research Fund for supporting this work.

REFERENCES

1. Rackis, J.J.; Wolf, W.I.; Baker, E.C. Protease inhibitors in plant foods: content and inactivation. In *Nutritional and Toxicological Significance of Enzyme Inhibitors in Foods*; Friedmann, M., Ed.; Plenum Press: New York, 1986.
2. Abd El-Hady, E.A.; Habiba, R.A. Effect of soaking and extrusion conditions on antinutrients and protein digestibility of legume seeds. Lebensm-Wiss. U.-Technol. **2003**, *36*, 285–293.
3. Alonso, R.; Grant, G.; Dewey, P.; Marzo, F. Nutritional assessment in vitro and in vitro of raw and extruded peas (Pisum sativum). Journal of Agricultural and Food Chemistry **2000**, *68*, 2286–2290.
4. Cheong, Y.L. Fullfat soybean meal production and utilization. *Technical Bulletin of American Soybean Association*, Singapore, 1997.
5. Raghavan, G.S.V.; Harper, J.M. Nutritive value of salt-bed roasted soybeans for broiler chicks. Poultry Science **1974**, *53* (2), 547–553.
6. Valle, F.R. Nutritional qualities of soya protein as affected by processing. Journal American Oil Chemists' Society **1981**, *58* (3), 419 429.
7. Soponronnarit, S.; Swasdisevi, T.; Wetchacama, S.; Wutiwiwatchai, W. Fluidised bed drying of soybeans. Journal of Stored Products Research **2001**, *37*, 133 151.
8. Osella, C.A.; Gordo, N.A.; González, R.J.; Tosi, E.; Ré, E. Soybean heat-treated using a fluidised bed. Lebensm. Wiss u.-Technology **1997**, *30*, 676 680.
9. Salin, J.G. Steam drying of wood for improved particle board and lower energy consumption. Paper and Timber **1988**, *9*, 806–810.

10. Heinrich, S.; Krüger, G.; Mörl, L. Modelling of the batch treatment of wet granular solids with superheated steam in fluidised beds. Journal of Chemical Engineering Processing **1999**, *38*, 131–142.
11. ASA. *Fullfat Soybeans Handbook of American Soybean Association*; Singapore, 1990.
12. Baker, E.C.; Mustakas, G.C. Heat inactivation of trypsin inhibitor, lipoxgygenase and urease in soybeans: Effect of acid and base additives. Journal of the American Oil Chemists' Society **1973**, *50*, 137–141.
13. AACC. *Approved method of the American Association of Cereal Chemist*, 9th ed.; AACC: St. Paul, MN, 1995.
14. Rasmussen. 2002, Determination of residual urease activity. http://www.analytichem.com/Applications/Kjeldah/.
15. American Oil Chemists' Society (AOCS). Protein solubility index. AOCS Official method BA **1979**, 10–63.
16. AccQ-Tag Instruction Manual. *Lysine determination*. Manual no. WAT052874, Revo April, 1993.
17. Saravacos, G.D.; Raouzeos, G.S. Diffusivity of moisture in air drying of raisins. In *Drying'86*; Mujumdar, A.S., Ed.; McGrawHill: Hemisphere, 1986; Vol. 2, 487–491.
18. Ramesh, M.N. Moisture transfer properties of cooked rice during drying. Lebensm. Wiss u.-Technology **2003**, *36*, 245–255.
19. Crank, J. *The Mathematics of Diffusion*, 2nd ed.; Oxford University Press: Oxford, 1975.
20. Rapusas, R.S.; Driscoll, R.H. Kinetics of non-enzymatic browning in onion slices during isothermal heating. Journal of Food Engineering **1995**, *24*, 417–429.
21. Krokida, M.K.; Tsami, E.; Urbricain, M.J. Kinetics on colour changes during drying of some fruits and vegetables. Drying Technology **1998**, *16* (3–5), 667.
22. Avila, I.M.L.B.; Silva, C.L.M. Modeling kinetics of thermal degradation of colour in peach puree. Journal of Food Engineering **1999**, *39*, 161–166.
23. Prachayawarakorn, S.; Sawangduanpen, S.; Saynampheung, S.; Poolpatarachewin, T.; Soponronnarit, S.; Nathakarakule, A. Kinetics of colour change during storage of dried garlic slices as affected by relative humidity and temperature. Journal of Food Engineering **2004**, *62*, 1–7.

Available online at www.sciencedirect.com
SCIENCE DIRECT
Journal of Stored Products Research 41 (2005) 333–351
Journal of STORED PRODUCTS RESEARCH
www.elsevier.com/locate/jspr

Quality maintenance and economy with high-temperature paddy-drying processes

Somkiat Prachayawarakorn[a,*], Nattapol Poomsa-ad[b], Somchart Soponronnarit[c]

[a]*Faculty of Engineering, King Mongkut's University of Technology Thonburi, Suksawat 48 Road, Bangkok 10140, Thailand*
[b]*Faculty of Engineering and Computer Science, Mahasarakham University, Mahasarakham 44150, Thailand*
[c]*School of Energy and Materials, King Mongkut's University of Technology Thonburi, Suksawat 48 Road, Bangkok 10140, Thailand*

Accepted 25 May 2004

Abstract

Drying processes result in some loss of product quality. Three drying systems for paddy were investigated for their effects on head-rice yield and whiteness. Fluidised-bed drying, tempering and ambient air ventilation units were the main components, but they were arranged differently in each drying system. Heat- and mass-transfer equations were applied to predict the change in moisture content for each drying system. Both the experiments and simulations indicated that the two sub-drying systems (system No. 2) with tempering and ventilation as elements of each stage yielded higher drying capacity and thermal efficiency than the single drying system (system No. 1), in which paddy was treated with the drying, tempering and ventilation units only once. The proportion of full kernels and value of the whiteness obtained from both drying systems were not significantly different. System No. 3, where grains after the first tempering were dried immediately by the second fluidised-bed dryer with no ventilation unit, produced poor head-rice yield and colour and was unacceptable for producing white rice.
© 2004 Elsevier Ltd. All rights reserved.

Keywords: Dehydration; Fluidisation; Grain; Head rice; Mathematical model

*Corresponding author. Tel.: +662-4270-9221; fax: +662-428-3534.
E-mail address: somkiat.pra@kmutt.ac.th (S. Prachayawarakorn).

0022-474X/$ - see front matter © 2004 Elsevier Ltd. All rights reserved.
doi:10.1016/j.jspr.2004.05.001

Nomenclature

C_a	specific heat of dry air, kJ/kg °C
C_v	specific heat of water vapour, kJ/kg °C
C_{pw}	specific heat of moist paddy, kJ/kg °C
D_{eff}	effective diffusivity, m^2/s
h_{fg}	latent heat of water, kJ/kg
I_c	tempering index, decimal
M	moisture content, dry-basis decimal
M_{eq}	equilibrium moisture content, dry-basis decimal
$M_{i,av}$	average inlet moisture content, dry-basis decimal
$M_{i,n}$	inlet moisture content at *n*th element, dry-basis decimal
$M_{f,n}$	outlet moisture content at *n*th element, dry-basis decimal
$M_{s,t}$	surface moisture content at time *t*, dry-basis decimal
$\dot{m}_i$	mass flow rate of dry fresh air, kg/s
$\dot{m}_p$	mass flow rate of dry matter, kg/s
$\dot{m}_{mix}$	mass flow rate of dry air, kg/s
$\dot{m}_{rc}$	mass flow rate of dry air in the recycle line, kg/s
l	half length of cylinder axis, m
$\dot{Q}$	thermal energy consumption, kJ/s
P	pressure drop across fan, Pa
R	ratio of dry mass of grain to mass of air, kg dry matter/kg dry air
R_t	ratio of dry mass of grain to mass of air at ventilation unit, kg dry matter/kg dry air
r	distance in radial direction, m
r_o	radius of paddy, m
SHC	specific thermal energy consumption, MJ/kg water evaporated
SPC	specific electrical energy consumption, MJ/kg water evaporated
T_{abs}	absolute temperature, K
T_b	temperature at the fan exit, °C
$T_{f,n}$	exhaust temperature at *n*th element, °C
T_{fl}	exhaust temperature, °C
T_{ft}	outlet air temperature at ventilation unit, °C
T_{mix}	inlet air temperature, °C
T_x	temperature at the fan inlet, °C
t	time, s
V_p	particle volume, m^3
$W_{f,n}$	humidity ratio at *n*th element exit, kg water/kg dry air
W_{fl}	humidity ratio at fluidised-bed dryer exit, kg water/kg dry air
W_i	humidity ratio of fresh air, kg water/kg dry air
W_{mix}	humidity ratio at fluidised-bed dryer inlet, kg water/kg dry air
W_{ft}	outlet humidity ratio at the ventilation unit, kg water/kg dry air
z	distance along the axis direction, m

θ_{in}	grain temperature, °C
ρ_{air}	air density, kg/m^3
ϕ	relative humidity, fraction
η_{fan}	fan efficiency, decimal

1. Introduction

The drying process involves transfers of heat and mass between media and solid materials, in which heat from the media is convected to the particles present in the dryer vapourising the water inside the particles. This phenomenon is very complicated and causes irreversible change in the physical and chemical properties of food materials such as colour, cracking and viscosity (Avila and Silva, 1999; Peplinski et al., 1994; Wiset et al., 2000). Such changes give lower quality and reduce price. For rice, whole kernels, one of the most important qualities, have a higher commercial value than broken ones. Therefore, industry requires milled rice with a larger proportion of full kernels.

Numerous studies on breakage in paddy kernels have reported that kernel breakage is dependent on a number of factors such as grain properties, environmental conditions for milling grains, and drying approaches (Kunze, 1972; Nguyen and Kunze, 1984; Siebenmorgen et al., 1998; Inprasit and Noomhorm, 2001). Breakage is a result of the development of stress cracks inside kernels, causing grains to have lower resistance to milling. Stress cracks are induced by non-uniform distribution of temperature and moisture. Thermal stresses usually occur during the heating period and become smaller afterwards. Subsequently, stresses from the moisture gradient are increasingly important. Paddy kernels that experience large moisture differences between their interiors and exteriors are prone to cracking. Conditions most favourable for stress cracking occur when the grain is subjected to high heat- and mass-transfer rates.

Fluidised-bed techniques, where solid particles and fluid media are in a good contact over the entire bed, can generate a large amount of broken rice (Sutherland and Ghaly, 1990; Soponronnarit and Prachayawarakorn, 1994). This problem motivated us to investigate the approach of taking the moisture content of paddy down to 16.5% dry basis while maintaining head-rice yield. The other two important factors, grain colour and energy consumption, were also explored as the fluidised-bed dryers are operated at high temperatures to accelerate moisture movement inside kernels. High temperatures may encourage change in the colour of paddy from white to yellow and may consume a large amount of energy if the management or the drying process is inappropriate. In the present study, experiments and mathematical simulation were conducted to determine the process for paddy drying that meets the requirements for high quality and less energy consumption.

2. Materials and methods

In the experimental work, paddy was dried using three different configurations of the drying process, each of which consisted of three main units, a fluidised-bed dryer, a tempering unit and

ambient-air ventilation. The tempering unit was responsible for grain relaxation after drying. Previous studies had shown that if drying was operated in a single step without tempering, very low yields of whole kernels would result (Steffe and Singh, 1980; Soponronnarit et al., 1999). During the tempering stage, it is believed that moisture distribution inside kernels becomes almost uniform, resulting in high yields of full kernels.

The ambient-air ventilation cooled the grain to stop formation of yellow pigment. Yellowing can be a severe problem in rice drying because temperature stimulates the development of rice yellowness, a non-enzymatic browning reaction (Taweerattanapanish et al., 1999; Soponronnarit et al., 1998; Yap et al., 1988). Ventilation was stopped when the grain temperature approached or was slightly above ambient-air temperature.

Details of the proposed drying systems are shown in Fig. 1. System No. 1 was the simplest system, in which paddy was first dried in the fluidised-bed dryer and then held temporarily in the tempering unit, after which it was ventilated with ambient air. System No. 2 contained two sub-drying systems, in each of which the components were arranged as in system No. 1. The two sub-drying systems were connected in series with a tempering unit between the sub-systems to equalise the moisture content inside the kernels before they passed through the second fluidised-bed dryer. In system No. 3, grains after relaxing in the first tempering unit were dried immediately by the second fluidised-bed dryer without ambient-air ventilation. To prevent water condensation in the grain bulks, grains were ventilated by ambient air before taking them to the storage area as shown in Fig. 1 for each drying system. This is an additional advantage to that mentioned in the above section.

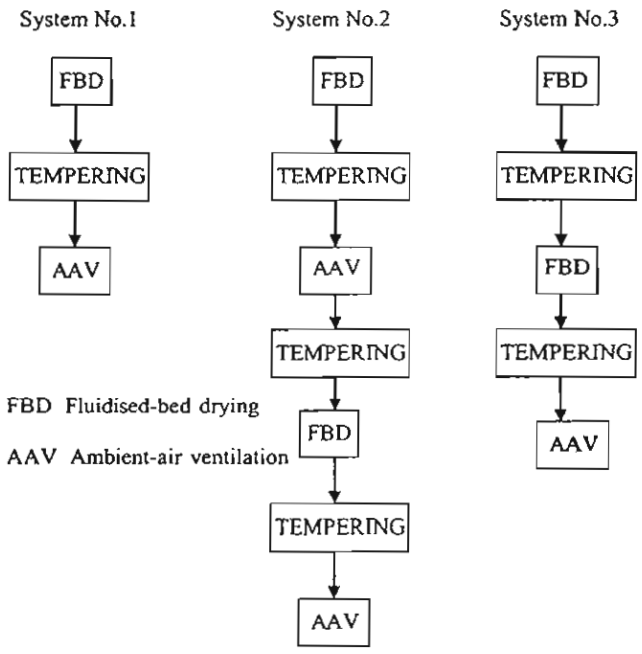


Fig. 1. Plan of three paddy-drying systems.

Details of experimental conditions for each drying system are presented in Tables 1–3. Paddy qualities in terms of head-rice yield and whiteness were determined quantitatively after treatment with the drying systems.

2.1. Equipment

2.1.1. Paddy preparation

Paddy was freshly harvested from the central region of Thailand with an average moisture content of 20% dry basis. The paddy was rewetted, mixed and kept in a cool storage at a temperature of 3–5 °C for 5–7 days. Two initial moisture contents of 30% and 35% dry basis were used. Before starting the experiment, the cooled paddy was placed in the ambient atmosphere until its temperature was close to that of ambient-air temperature.

2.2.2. Fluidised-bed drying

Experiments on quality were carried out with a batch fluidised-bed dryer. Drying conditions for all systems involved a superficial air velocity of 2.3 m/s, a bed thickness of 10 cm and temperatures of 130 and 150 °C. The inlet temperature was controlled by a proportional integral derivative controller with an accuracy of ± 1 °C. Drying time, i.e., residence time in the dryer, varied from 1 to 4 min, depending on the drying system.

2.2.3. Tempering

During tempering, the paddy was held in a completely sealed glass bottle with a diameter of 12 cm and a height of 10 cm and kept in an oven at the grain temperature obtained from the previous stage between 15 and 45 min. When tempering was complete, the samples were ventilated by ambient air or passed through the second fluidised-bed dryer depending on the drying system being investigated. For the second drying, the paddy was dried at the same temperature as the first one.

2.2.4. Ambient-air ventilation

The fixed-bed ventilator used in this study consisted of a cylindrical chamber with an inner diameter of 20 cm with a paddy bed height of 3 cm. The paddy was ventilated for at least 20–30 min using ambient air at a velocity of 0.125 m/s.

2.2. Measurement of moisture content

Samples were collected before and after passing through each process and the moisture content was determined from the weight loss of samples held in a hot-air oven at 103 °C for 72 h.

2.3. Quality of paddy

After completion of each drying system, the paddy was kept in a plastic bag for a week in a cool storage room at a temperature of 3–5 °C. A 125 g sample was then dehusked, milled and the whole kernels separated from the broken rice by a screen device. The head-rice yield was defined as the mass of unbroken rice kernels (a length longer than 80% of the whole kernel length was

Table 1
Experimental conditions and results of moisture content, relative head-rice yield and whiteness for drying system No. 1

Run No.	Initial moisture content (% dry basis)	Fluidised-bed drying conditions		Tempering time (min)	Ventilation time (min)	Moisture content after ventilation (% dry basis)	Relative head-rice yield (%)	Whiteness (%)
		Temperature (°C)	Time (min)					
1	35	150	3	0	20	19.5	1.5	40.6
2	35	150	3	15	20	18.5	80.5	41.6
3	35	150	3	30	20	18.3	110.2	40.1
4	35	150	3	45	20	18.4	108.3	39.5
5	35	130	4	0	20	19.7	3.0	41.2
6	35	130	4	15	20	18.5	60.5	40.6
7	35	130	4	30	20	18.4	103.2	40.3
8	35	130	4	45	20	18.4	105.3	39.8
9	30	150	2.5	0	20	18.5	3.5	41.5
10	30	150	2.5	15	20	17.8	95.3	41.2
11	30	150	2.5	30	20	17.5	108.2	41.3
12	30	150	2.5	45	20	17.6	106.4	40.8
13	30	130	3	0	20	18.9	5.0	41.8
14	30	130	3	15	20	17.8	73.8	41.3
15	30	130	3	30	20	17.7	101.2	41.9
16	30	130	3	45	20	17.6	105.3	38.2

Note: reference head-rice yield, 46.3%; reference whiteness, 44.0.

Table 2
Experimental conditions for drying system No. 2

		Reference code			
		a	b	c	d
Initial moisture content (% dry basis)		35	30	35	30
Fluidised-bed drying					
The first stage	Temperature (°C)	150	150	130	130
	Time (min)	1.5	1.5	2.0	2.0
	Bed thickness	10	10	10	10
	Tempering time (min)	15	15	20	20
	Ventilation time (min)	30	30	30	30
The second stage	Temperature (°C)	150	150	130	130
	Time (min)	1.0	1.0	1.5	1.5
	Bed thickness (cm)	7.5	7.5	7.5	7.5
	Tempering time (min)	15	15	20	20
	Ventilation time (min)	30	30	30	30

Table 3
Experimental results of moisture content, relative head-rice yield and whiteness for different reference codes in Table 2

Drying strategy	Tempering time between the first and the second stage (min)	Moisture content after passing the second FBD (% dry basis)	Relative head-rice yield (%)	Whiteness
	0	19.6	107.6	40.2
	15	19.5	109.6	39.5
a	30	19.6	102.5	40.0
	60	19.6	107.6	39.6
	120	19.4	106.4	39.2
	0	18.5	100.0	40.1
	15	18.3	102.6	39.8
b	30	18.3	104.4	39.6
	60	18.5	110.4	39.4
	120	18.2	98.7	39.6
	0	20.4	104.7	40.5
	15	20.6	108.9	40.2
c	30	20.5	103.4	39.8
	60	20.2	98.8	39.7
	120	20.3	103.9	40.0
	0	19.6	94.5	40.3
	15	19.4	98.2	39.9
d	30	19.3	95.8	40.0
	60	19.5	93.2	39.7
	120	19.2	96.4	40.0

Note: Reference head-rice yield, 47.6%; reference whiteness, 43.5; FBD, fluidised-bed drying.

acceptable) after milling, divided by the mass of paddy before milling. The control sample was prepared by drying paddy from its initial moisture content to 16% dry basis using ambient temperature. This took around 16 h. The results were presented as relative head-rice yield, defined as the ratio of head rice obtained from each system to that from the control sample.

A commercial whiteness meter (Kett C-300) was used for measuring the colour. Before measuring, it was standardised with pure white magnesium oxide powder which had a value of 86.3. The whiteness values of samples before treating were between 46.8 and 47.6.

2.4. Mathematical model for drying system

The state of moist grains present in each unit of the drying process such as drying, tempering and ventilation was different. A mathematical model for each unit was formulated to describe its behaviour. The models developed in conjunction with the head-rice equation allowed estimation of the energy consumption for each drying treatment.

2.4.1. Dryer unit

The first unit involved simultaneous heat and mass transfer in which air was used to convey heat to the grains to evaporate their moisture and then take the water vapour away. In the fluidised-bed dryer, there was dispersion of grain. The simplified analysis used in the present study assumed that the grain movement along the axial direction was a plug flow and the subsequent moisture content of paddy was reduced following this direction. To describe such results, the grain bed was divided into a series of N small sets. Two governing equations, Eqs. (1) and (2), for a differential volume as shown in Fig. 2, along with a theoretical diffusion equation for a single kernel as given by Eq. (3), were used in the model. Eqs. (1) and (2) were written based on energy and mass balances for a small interval of time Δt and a single compartment:

$$W_{f,n} = R(M_{i,n} - M_{f,n}) + W_{mix}, \tag{1}$$

where $W_{f,n}$ was the humidity ratio at nth element exit (kg water/kg dry air), R was the ratio of dry mass of grain to mass of air (kg dry matter/kg dry air), $M_{i,n}$ was the inlet moisture content at nth element (dry-basis decimal), $M_{f,n}$ was the outlet moisture content at nth element and W_{mix} was the humidity ratio at the fluidised-bed dryer inlet.

$$T_{f,n} = (C_a T_{mix} + W_{mix}(h_{fg} + C_v T_{mix}) - W_{mix} h_{fg} + RC_{pw}\theta_{in})/(C_a + W_{f,n}C_v + RC_{pw}), \tag{2}$$

where $T_{f,n}$ was the exhaust temperature at nth element (°C), T_{mix} was the inlet air temperature, C_a was the specific heat of dry air (kJ/kg °C), C_v was the specific heat of water vapour, C_{pw} was the specific heat of moist paddy, h_{fg} was the latent heat of water (kJ/kg) and θ_{in} was the grain temperature. The moisture transport inside the paddy, assuming a cylindrical shape, can be described by

$$\frac{\partial M}{\partial t} = D_{eff}\left[\frac{\partial^2 M}{\partial r^2} + \left(\frac{1}{r}\right)\frac{\partial M}{\partial r} + \frac{\partial^2 M}{\partial z^2}\right], \tag{3}$$

where M was the moisture content, D_{eff} was the effective diffusivity (m^2/s), t was the drying time (s), r was the distance in a radial direction (m) and z was the distance along the axis direction

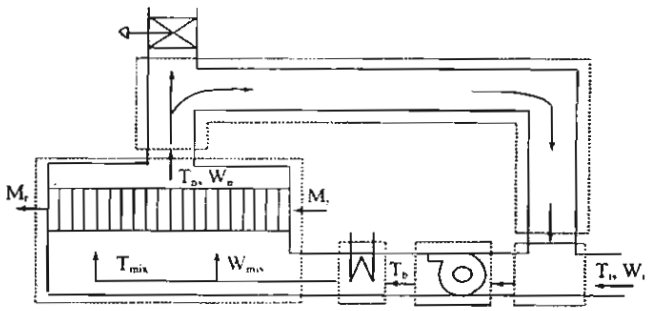


Fig. 2. Schematic diagram of continuous fluidised-bed dryer. *Note*: M_i, inlet moisture content of paddy; M_f, outlet moisture content of paddy; T_b, temperature at the fan exit; T_{f1}, exhaust air temperature; T_i, ambient air temperature; T_{mix}, inlet air temperature; W_i, humidity ratio of ambient air; W_{f1}, humidity ratio of exhaust air; W_{mix}, humidity ratio of inlet air.

(m).The effective diffusion coefficient for paddy was given by Poomsa-ad et al. (2002):

$$D_{eff} = 5.41141 \times 10^{-6} \exp\left(-\frac{28436.4}{T_{abs}}\right), \tag{4}$$

where T_{abs} was the absolute temperature (K). Eq. (4) was obtained from the experiments that were carried out at a thin bed depth of 3 cm. Using this bed depth, the inlet-air temperature was slightly reduced and thus Eq. (4) was statistically fitted with the inlet-air temperature. The equilibrium moisture equation of Laithong (1987) used in the present study was

$$1 - \phi = \exp\{(-4.584 \times 10^{-6}) T_{abs} (100 M_{eq})^{2.397}\}, \tag{5}$$

where ϕ was the relative humidity (fraction) and M_{eq} was the equilibrium moisture content. In order to solve Eq. (3), the following conditions were assumed: (1) the initial moisture content was uniform throughout the kernel; (2) the air was at equilibrium with the moisture content at the surface and both ends of the solid particle over the drying time; and (3) the moisture content of paddy had a maximum value at the central region during drying. The average temperature between inlet- and outlet-air temperatures was used as the input parameter for calculating the effective diffusion coefficient because the temperature of the inlet air entering the drying chamber dropped due to the relatively thick bed depth used in the experiments (10 cm). If the outlet or inlet temperature was used, the relatively large differences between the calculated moisture contents and experimental values were obvious. The outlet temperature can be calculated by Eq. (2), assuming thermal equilibrium between the kernels and exhaust air.

To obtain the moisture distribution in a paddy kernel, the finite difference was applied to solve Eq. (3). The grain shape was divided into a constant number of elements with 80 nodes of length and 10 nodes of radius. The average moisture content, M_{av}, throughout the kernel at time t was determined by the following equation:

$$M_{av} = \frac{1}{V_p} \iint 2\pi r M(r, z, t)\, dr\, dz, \tag{6}$$

where V_p was the particle volume (m^3). The algorithm for solving the set of equations (Eqs. (1)–(6)) followed an iteration procedure commencing with an assumed absolute humidity ratio at the drying chamber inlet. This procedure was similar to that developed by Soponronnarit et al. (1996). After obtaining the set of solutions for each compartment, the average outlet absolute-humidity ratio, W_{f1}, and exhaust-air temperature, T_{f1}, were then calculated by arithmetic means. Time steps for paddy movement through a small element in the dryer were calculated from the residence time of paddy divided by N.

By conservation of mass around the hypothetical volume where the recycled air and fresh air are mixed together, the humidity ratio at the inlet was calculated by

$$W_{mix} = (1 - \frac{\dot{m}_{rc}}{\dot{m}_{mix}})W_i + \frac{\dot{m}_{rc}}{\dot{m}_{mix}} W_{f1}, \tag{7}$$

where $\dot{m}_{rc}$ was the mass flow rate of dry air in the recycle line (kg/s), $\dot{m}_{mix}$ was the mass flow rate of dry air at the fluidised-bed dryer inlet, W_i was the humidity ratio of fresh air and W_{f1} was the humidity ratio at the fluidised-bed dryer exit.

The amount of energy consumed for heating the moist air to the desired temperature was calculated by

$$\dot{Q} = \dot{m}_{mix}(C_a + C_v W_{mix})(T_{mix} - T_b), \tag{8}$$

where $\dot{Q}$ was the thermal energy consumption (kJ/s) and T_b was the temperature at the fan exit. Before determining the thermal energy consumption, T_b must be known. To accomplish this, the conservation of energy was applied around the hypothetical volume and the temperature at the fan inlet was

$$T_x = \frac{\dot{m}_i(C_a + C_v W_i)T_i + \dot{m}_{rc}(C_a + C_v W_{f1})T_{f1}}{\dot{m}_{mix}(C_a + C_v W_{mix})}, \tag{9}$$

where T_x was the temperature at the fan inlet and T_i was the temperature of fresh air. Thus, the temperature at the fan exit, T_b, was given by

$$T_b = T_x + \frac{P\dot{m}_{mix}}{\rho_{air}\eta_{fan}C_a}, \tag{10}$$

where P was the pressure drop across the fan (Pa), ρ_{air} was the air density (kg/m^3) and η_{fan} was the fan efficiency (decimal).

In the case of no air recycling, T_x was replaced by T_i. In the present study, the amount of energy consumed was represented by the specific energy. The specific heat consumption was given by

$$SHC = \frac{\dot{Q}}{\dot{m}_p(M_{i,av} - M_{f,av})1000}, \tag{11}$$

where SHC was the specific thermal energy consumption (MJ/kg water evaporated), $M_{i,av}$ was the average inlet moisture content and $M_{f,av}$ was the average moisture content at the dryer outlet. The

specific electrical energy for the fan was given by

$$SPC = P\left(\frac{\dot{m}_{mix}/\rho_{air}\eta_{fan}}{\dot{m}_p(M_{i,av} - M_{f,av})1000}\right), \tag{12}$$

where SPC was the specific electrical energy consumption (MJ/kg water evaporated), $\dot{m}_p$ was the mass flow rate of dry matter (kg/s) and η_{fan} was the fan efficiency. η_{fan} was about 0.8.

2.4.2. Tempering unit

The drying processes shown in Fig. 1 were interrupted when the partially dried grains were in the tempering unit. In this temporary stop, the grains were not subjected to contact with hot air and the subsequent moisture and temperature gradients inside the individual kernels had less variation.

During tempering, the moisture in the interior of grains will move to the exterior surface, but it does not evaporate to the environment. The transport of moisture can be described by the moisture diffusion equation, which is similar to Eq. (3). In order to solve this equation, the initial and boundary conditions must be known:

$$t = 0, \quad M = M(r, z), \tag{13}$$

$$t > 0, r = r_0, \quad \frac{\partial M}{\partial r} = 0, \tag{14}$$

$$z = \pm l, \quad \frac{\partial M}{\partial z} = 0, \tag{15}$$

$$t > 0, \quad r = 0, \quad \frac{\partial M}{\partial r} = 0. \tag{16}$$

where r_0 was the radius of paddy (m) and l was the half length of cylinder axis (m). Eq. (13) was the initial condition obtained from the end of the previous section. Eqs. (14) and (16) were similar but did not have the same physical meaning: Eq. (14) showed the maximum moisture content at the centre whilst the other represented the state of water that cannot vapourise through the exterior surface.

When the grains were in the tempering unit, time was an important parameter for uniformly distributed moisture content. Theoretically, the uniform distribution of moisture, corresponding to the tempering index of unity, required infinite time. The tempering index was defined by several workers (Steffe and Singh, 1980; Zhang and Litchfield, 1991; Tolaba et al., 1999) as

$$I_c = \frac{M_{s,t} - M_{s,t=0}}{M_{s,t=\infty} - M_{s,t=0}}, \tag{17}$$

where I_c was the tempering index (decimal) and $M_{s,t}$ was the surface moisture content at time t. This index strongly affected the next drying stage: the lower the tempering indices, the smaller the drying rates. Poomsa-ad et al. (2002), however, found that the drying rate at an index higher than 0.95 was almost the same as that at unity. It is thus reasonable to say that an index of 0.95 was an appropriate value for tempering the paddy.

2.4.3. Ambient-air ventilation unit

In the tempering section, the grains were tempered at the temperature of the outlet grain temperature from the dryer, usually higher than 80 °C where the fluidised-bed dryer was operated at a temperature higher than 100 °C. At such temperatures, it was necessary to reduce the grain temperature to ambient temperature before storage or passing to the following step. First, if not ventilated, the moisture around the grain surface would have evaporated to the air space and the grain temperature dropped. This situation would have encouraged water vapour flow in the bin which could have condensed when it came into contact with cooler surfaces. This in turn could cause wet spots during storage, which could induce the growth of microorganisms. The second reason was to inhibit the development of yellow pigment and to avoid the paddy becoming darkened.

While air was passed through the heated grains, there was simultaneous heat and mass transfer from the grain to air, making the air slightly warmer and more humid. The heat-transfer phenomenon in this unit was opposite to that occurring in the dryer section. Assuming that the air flowed through a thin bed in the cross-flow dryer, the outlet-air temperature, T_{fl}, was given by

$$T_{fl} = (C_a T_i + W_i(h_{fg} + C_v T_i) - W_i h_{fg} + R_t C_{pw}\theta_{in})/(C_a + W_{fl} C_v + R_t C_{pw}), \quad (18)$$

where R_t was the ratio of dry mass of grain to mass of air in the ventilation unit (kg dry matter/kg dry air) and W_{fl} was the outlet humidity ratio of the ventilation unit. Using such a simplified assumption, the properties of air changed insignificantly along the bed height, thereby providing economic computation by a single-step approach. The moisture transport was calculated by using Eq. (3) again, with the following initial and boundary conditions:

$$t = 0, \quad M = M(r, z), \quad (19)$$

$$t > 0, r = r_0, \quad M = M_{eq}, \quad (20)$$

$$z = \pm\ell, \quad M = M_{eq}. \quad (21)$$

In the determination of moisture reduction, the grain temperature was used in Eq. (4), instead of the inlet-air temperature, because the grain temperature at the beginning of ventilation was 50 °C higher than the ambient-air temperature.

3. Results and discussion

3.1. Experimental results of the drying performance and final quality

The experimental results from system No. 1 are shown in Table 1. In this system, the outlet moisture content after fluidised-bed drying was limited to approximately 22% dry basis. At this moisture level, the drying times varied from 2.5 to 4 min depending upon the inlet temperature and moisture content. The system that did not have tempering after drying gave very low relative head-rice yields. Values were between 1.5% and 5% as shown in Table 1 for run Nos. 1, 5, 9 and 13 despite the time in the fluidised-bed dryer being very short. This result emphasised the necessity for tempering in the drying system. Such low head-rice yields were caused by the combined effects of moisture and temperature gradients, with the latter being dominant because of the thermal

stresses set up when the heated grain contacted cooler air. The significant improvement in head-rice quality with tempering, however, became evident. Higher head-rice yields related to higher tempering times as illustrated for run Nos. 2 and 3 for the tempering times of 15 and 30 min, which produced 80.5% and 110.2% relative head-rice yield, respectively. Similar results were found at other temperatures and initial moisture contents. The high head-rice yield is attributed to less moisture stresses after tempering and the partial formation of gel in paddy kernels when the moist grains were tempered at temperatures higher than 80 °C.

Table 1 illustrates that tempering for longer than a certain period does not increase head-rice yield, but does result in milled rice becoming darker. A tempering time of 30 min was enough for redistribution of moisture inside individual kernels, while luminosity and whiteness of the milled rice were still acceptable. The values of whiteness for paddy tempered at such a recommended tempering time were higher than 40.

It is interesting to note that the final moisture content after ventilation was lower for the tempered paddy than for paddy not tempered. This resulted from the moisture gradient produced inside the paddy in the drying unit becoming less variable after tempering and consequently the water was removed more easily when the paddy was ventilated. This is an advantage of tempering and can accordingly provide more economic energy utilisation. This drying system is now used in some rice industries.

Paddy dried by system Nos. 2 and 3 exhibited different qualities from that dried by system No. 1 as presented in Tables 3 and 4, respectively. The two sub-drying processes in system No. 2 provided premium quality, with high values of head-rice yield and whiteness, while system No. 3, with ambient-air ventilation only in the last step, gave poor quality. The colour of the milled rice had relatively more yellowness and darkness with the values falling in the range of 35–37, compared with a reference value of 45.5 for the gently dried paddy. Milled rice with a colour below 40 is not preferred by the domestic market. This result indicates that the grain should be ventilated immediately as otherwise the colour becomes a severe problem.

The colour of the milled rice in system No. 2 was similar to that from system No. 1. For whole kernels, the values of head-rice yield obtained from both systems were not significantly different if the grains treated with system No. 1 were tempered for longer than 30 min.

Table 3 illustrates that after ambient ventilation in the first drying stage of system No. 2, further tempering did not significantly affect the head-rice yield. The relative head-rice yield obtained from the experiments varied from 94% to 110%. These results indicated that the forces between compression and tension acting on the kernels during ventilation were not significantly different because of the relatively small moisture reduction which resulted in less shrinkage at the exterior surface. System No. 2 thus yielded sound quality paddy and a tempering period between the two drying stages was not necessary.

3.2. *An appropriate drying system*

The experimental data from Soponronnarit et al. (2001) were compared with those obtained here. In their work, the experimental results were obtained from a continuous fluidised-bed dryer operated in the rice industry under different drying conditions. Results are presented in Table 5 showing that each predicted parameter such as outlet moisture content and energy consumption was in good agreement with the experimentally determined values.

Table 4
Experimental conditions and results of relative head-rice yield and whiteness for drying system No. 3

Run no.	Initial moisture content (% d.b.)	The first FBD drying condition Temperature/ time (°C/min)	Tempering time (min)	The second FBD drying condition Temperature/ time (°C/min)	Tempering time (min)	Ambient air ventilation(min)	Relative head-rice yield (%)	Whiteness
1	35	150/2.0	15	150/1.0	15	30	77.9	35.4
2	35	150/2.0	30	150/1.0	30	30	77.1	35.4
3	35	150/2.0	15	130/1.5	15	30	84.3	37.0
4	35	130/2.5	15	130/1.5	15	30	80.9	36.8
5	35	130/2.5	15	130/1.5	30	30	83.3	35.4
6	30	150/2.0	15	150/1.0	15	30	82.3	35.2
7	30	150/2.0	30	150/1.0	30	30	81.2	34.3
8	30	130/2.0	15	130/1.5	15	30	78.3	37.8
9	30	130/2.5	30	130/1.5	30	30	77.9	36.1

Note: Reference head-rice yield, 47.6%; reference whiteness, 45.5; FBD, fluidised-bed drying.

Table 5
Comparison between experiments and simulations for industrial-scale fluidised-bed dryer (after Soponronnarit et al., 2001)

Run no.	Drying temperature (°C)	Feed rate (tonnes/h)	Bed height (m)	M_{in} %dry basis	M_f (%d.b.)		*SHC* (MJ/kg of water)		*SPC* (MJ/kg of water)	
					Exp.	Sim.	Exp.	Sim.	Exp.	Sim.
1	130	3.12	0.115	25.9	22.5	22.1	6.45	5.31	0.9	0.88
2	140	4.72	0.147	26.7	23.3	23.6	4.83	4.05	0.73	0.81
3	150	6.42	0.119	25.9	23.3	23.0	4.93	4.83	0.7	0.55
4	150	6.09	0.15	25.9	23.7	22.8	6.7	5.01	0.85	0.69
5	150	5.1	0.15	26.1	23.4	22.9	6.01	5.02	0.79	0.72
6	130	4.82	0.115	26.8	23.7	23.7	5.47	4.68	0.77	0.74
7	140	4.82	0.115	24.1	20.7	20.9	4.69	5.15	0.66	0.74
8	150	4.82	0.115	28.0	23.0	24.0	3.8	4.78	0.48	0.56

Note: *SHC* = Specific thermal energy consumption; *SPC* = Specific electrical energy consumption; M_{in} = Initial moisture content; M_f = Final moisture content

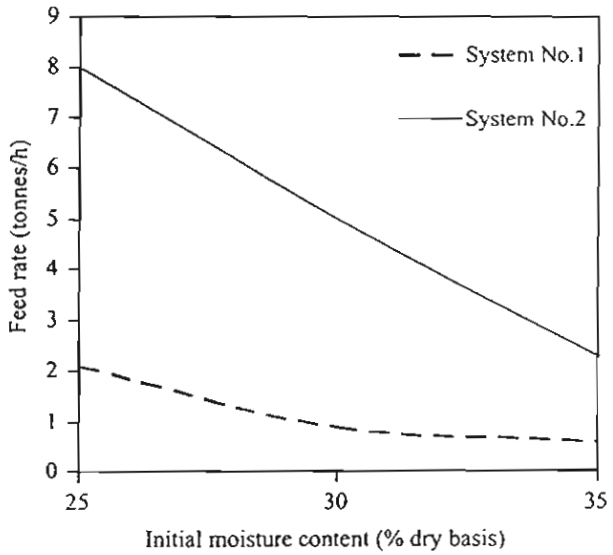


Fig. 3. Feed rates at different initial moisture contents for system Nos. 1 and 2.

Simulations were then made with the drying system Nos. 1 and 2 to determine the most suitable drying process. System No. 3 was not considered, as it did not reach the standard for producing white rice. In simulating system No. 2, the tempering step between the two sub-drying systems was not included. The criteria quantifying performance were energy consumption and drying capacity. In the simulations, drying temperature was limited to 150 °C, bed depth was fixed at 10 cm corresponding to the holding capacity of 60 kg, superficial air velocity was 2.3 m/s and ratio of recycled air was 0.85. The tempering index of 0.95 was chosen for the required time to represent

idealised moisture equalisation inside kernels. In addition to such constraints, grains must be cooled to room temperature in the ventilation unit and the final moisture content at the last unit of each system must be lower than 17.5% dry basis.

Trial and error was used to estimate the feed rate needed to acquire the desired moisture level at process end. Fig. 3 shows the results of calculated feed rates at different initial moisture contents. Feed rate reduced with increase in initial moisture content as the drying time took longer with a higher initial moisture content. The feed rate for system No. 2 was at least 4 times higher than that for system No. 1, implying more potential for water removal. The higher drying capacity was due to the tempering units that enabled the remaining moisture after drying to move towards the grain surface. The surface moisture could therefore be removed quickly when the grains reached the next stage. The advantage of the tempering units complies not only with high drying capacity, but also with energy saving, in particular, the thermal energy that is consumed in the thermal dehydration process. The total specific heat consumption for system No. 2 was, for example, 4.75 MJ/kg water evaporated at 35% dry basis whilst it was 7.32 MJ/kg water evaporated for system No. 1. The energy consumption at the other moisture contents for system Nos. 1 and 2 are shown in Tables 6 and 7, respectively. It can be seen that the thermal energy utilisation of system

Table 6
Simulation results of drying system No. 1

	Case 1	Case 2	Case 3
Initial moisture content (% dry basis)	25	30	35
Feed rate (tonnes/h)	2.1	0.9	0.6
The FBD drying condition			
Drying temp (°C)	150	150	150
Bed height (m)	0.1	0.1	0.1
Air velocity (m/s)	2.3	2.3	2.3
Moisture content after the FBD (% dry basis)	18.3	18.5	18.7
Grain temperature after the first FBD (°C)	107.5	112.5	120.6
The tempering time (min)	19	20	22
The ventilation time (min)	30.0	26.5	25.2
Moisture content after the ventilator (% dry basis)	17.2	17.0	17.3
Energy consumption			
For the FBD			
SPC (MJ/kg)	1.37	1.48	1.63
SHC (MJ/kg)	6.89	7.57	7.95
For the ventilator			
SPC (MJ/kg)	1.59	1.43	1.42
Total energy consumption			
SPC (MJ/kg)	1.40	1.47	1.61
SHC (MJ/kg)	5.91	6.67	7.32

Note: *SPC*, specific electrical energy consumption in term of primary energy (conversion factor 2.6); *SHC*, specific heat consumption; FBD, fluidised-bed drying.

Table 7
Simulation results of drying system No. 2

	Case 1	Case 2	Case 3
Initial moisture content (% dry basis)	25	30	35
Feed rate (tonnes/h)	7.9	5.0	2.3
The FBD drying condition			
Drying temperature (°C)	150	150	150
Bed height (m)	0.1	0.1	0.1
Air velocity (m/s)	2.3	2.3	2.3
Moisture content after the first FBD (% dry basis)	21.9	24.8	26.7
Grain temperature after the first FBD (% dry basis)	81.2	89.6	97.7
The first tempering time (min)	22	26	19
The first ventilation time (min)	19.5	22.5	24.0
Moisture content after the second FBD (% dry basis)	18	18.4	18.2
Grain temperature after the second FBD (% dry basis)	95.1	96.5	106.5
The second tempering time (min)	20	27	20
The second ventilation time (min)	25	27	32
Moisture content after the second ventilator (% dry basis)	16.7	17.0	16.9
Energy consumption			
For the first FBD	0.61	0.84	1.02
SPC (MJ/kg of water evap.)			
SHC (MJ/kg of water evap.)	5.36	5.07	5.55
For the second FBD			
SPC (MJ/kg of water evap.)	0.73	1.09	1.39
SHC (MJ/kg of water evap.)	5.36	6.15	6.89
For the first ventilator			
SPC (MJ/kg of water evap.)	1.37	1.45	1.57
For the second ventilator			
SPC (MJ/kg of water evap.)	1.54	1.56	1.68
Total energy consumption			
SPC (MJ/kg of water evap.)	0.92	1.10	1.36
SHC (MJ/kg of water evap.)	3.64	3.96	4.75

Note: *SPC*, specific electrical energy consumption in term of primary energy (conversion factor 2.6); *SHC*, specific heat consumption.

No. 2 is relatively economical over the range of moisture contents compared with system No. 1 whilst the electrical energy utilisation for both systems is relatively comparable.

4. Conclusions

Three paddy-drying processes were examined for energy consumption and paddy qualities in terms of head-rice yield and whiteness. Paddy dried through the system Nos. 1 and 2 yielded the highest quality. The colour of paddy had the most intense yellowness when treated with system No. 3. In system No. 2, the tempering section between two sub-drying systems was not necessary.

Heat and mass-transfer equations for each unit enabled us to estimate the moisture content and energy consumption. The simulation results have shown that the process with tempering and ventilation as important elements of each stage provided superior performance, with a high drying capacity and less energy consumption. In the first stage, paddy at initial moisture content of 25–35% dry basis should be dried to the corresponding range of 21.9–26.7% dry basis at the first fluidised-bed dryer followed by tempering for 22 down to 19 min and ventilating for 19 up to 24 min. In the second stage, the moisture content at the outlet of the second fluidised-bed dryer was approximately 18% dry basis and the required time ranged between 20 and 27 min for tempering and between 25 and 32 min for ventilation.

Acknowledgements

The authors would like to express their sincere thanks to the Thailand Research Fund for financial support and The Division of Agricultural Engineering, Department of Agriculture, Thailand for test milling.

References

Ávila, I.M.L.B., Silva, C.L.M., 1999. Modelling kinetics of thermal degradation of colour in peach puree. Journal of Food Engineering 39, 161–166.

Inprasit, C., Noomhorm, A., 2001. Effect of drying air temperature and grain temperature of different types of dryer and operation on rice quality. Drying Technology 19, 389–404.

Kunze, O.R., 1972. Moisture adsorption related to tensile strength of rice. Cereal Chemistry 49, 684–696.

Laithong, C., 1987. Study of thermo-physical properties of rough rice. Masters Thesis, King Mongkut's Institute of Technology Thonburi, Bangkok.

Nguyen, C.N., Kunze, O.R., 1984. Fissures related to post drying treatments in rough rice. Cereal Chemistry 61, 63–68.

Peplinski, A.J., Paulis, J.W., Bietz, J.A., Pratt, R.C., 1994. Drying of high-moisture corn: changes in properties and physical quality. Cereal Chemistry 71, 129–133.

Poomsa-ad, N., Soponronnarit, S., Prachayawarakorn, S., Terdyothin, A., 2002. Effect of tempering on subsequent drying of paddy using fluidisation technique. Drying Technology 20, 195–210.

Siebenmorgen, T.J., Nehus, Z.T., Archer, T.R., 1998. Milled rice breakage due to environmental conditions. Cereal Chemistry 75, 149–152.

Soponronnarit, S., Prachayawarakorn, S., 1994. Optimum strategy for fluidised bed paddy drying. Drying Technology 12, 1667–1686.

Soponronnarit, S., Prachayawarakorn, S., Sripawatakul, O., 1996. Development of cross-flow fluidised bed paddy dryer. Drying Technology 14, 2397–2410.

Soponronnarit, S., Srisubati, N., Yoovidhya, T., 1998. Effect of temperature and relative humidity on yellowing rate of paddy. Journal of Stored Products Research 34, 323–330.

Soponronnarit, S., Wetchacama, S., Swasdisevi, T., Poomsa-ad, N., 1999. Managing moist paddy by drying, tempering and ambient air ventilation. Drying Technology 17, 335–344.

Soponronnarit, S., Wetchacama, S., Trutassanawin, S., Jariyatontivait, W., 2001. Designing, testing and optimization of vibro-fluidised paddy dryer. Drying Technology 19, 1891–1908.

Steffe, J.F., Singh, R.P., 1980. Theoretical and practical aspects of rough rice tempering. Transactions of the American Society of Agricultural Engineering 23, 775–782.

Sutherland, J.W., Ghaly, T.F., 1990. Rapid fluid-bed drying of paddy rice in the humid tropics. In: Naewbanij, J.O. (Ed.), Proceedings of the Thirteenth ASEAN Seminar on Grain Post Harvest Technology, Bandar Seri Begawan, Brunei Darussalam. ASEAN Grain Postharvest Programme, Bangkok, Thailand, pp. 168–180.

Taweerattanapanish, A., Soponronnarit, S., Wetchakama, S., Kongseri, N., Wongpiyachon, S., 1999. Effects of drying in head rice yield using fluidization technique. Drying Technology 17, 345–353.

Tolaba, P., Aguerre, R.J., Suárez, C., 1999. Drying simulation of corn with tempering. Drying Technology 17, 1081–1093.

Wiset, L., Srzednicki, G., Driscoll, R., Nimmuntavin, C., Siwapornrak, P., 2000. Effects of high temperature on rice quality. Proceedings of the XIV Memorial Commission Internationale du Génie Rural World Congress, 28 November–1 December 2000, Tsukuba, Japan, pp. 794–799.

Yap, A.B., Juliano, B.O., Perez, C.M., 1988. Artificial yellowing of rice at 60 °C. In: Naewbanij, J.O. (Ed.), Proceedings of the Eleventh ASEAN Technical Seminar on Grain Postharvest Technology, 23–26 August, 1988 Kuala Lumpur, Malaysia. ASEAN Grain Postharvest Programme, Bangkok, Thailand, pp. 3–20.

Zhang, Q., Litchfield, J.B., 1991. An optimization of intermittent corn drying in laboratory scale thin layer dryer. Drying Technology 9, 233–244.

Ind. Eng. Chem. Res. 2005, *44*, 1934−1941

Drying Kinetics and Inversion Temperature in a Low-Pressure Superheated Steam-Drying System

P. Suvarnakuta,[†] S. Devahastin,*[,†] S. Soponronnarit,[‡] and A. S. Mujumdar[§]

Department of Food Engineering and School of Energy and Materials, King Mongkut's University of Technology Thonburi, Bangkok 10140, Thailand, and Department of Mechanical Engineering, National University of Singapore, Singapore 117576, Singapore

The present study aimed at investigating the drying rates and inversion temperatures of model porous particles undergoing low-pressure superheated steam and vacuum drying. Molecular sieve beads, which were used as the model material in this work, were dried as a single layer in a low-pressure superheated steam dryer. The effects of steam temperature and pressure on the drying rates of these particles were determined. The same dryer was also operated in a vacuum mode to determine the effects of the above-mentioned operating parameters as well as the variation of the inversion temperature of the processes with the operating pressure. The differences between the values of the inversion temperature calculated only from the rates of drying in the constant rate period and those calculated from the whole drying period are pointed out and discussed. Page's equations and a single-term exponential equation were found to satisfactorily describe the kinetics of low-pressure superheated steam- and vacuum-drying systems, respectively.

Introduction

Despite the many advantages of near-atmospheric pressure superheated steam drying, there still exist some limitations, especially when applying it to drying of heat-sensitive materials, e.g., foods and bioproducts.[1] Because most foods or other heat-sensitive products melt, undergo glass transition, or are damaged at the temperature of superheated steam corresponding to the atmospheric or higher pressures, one possible way to alleviate the above-mentioned problems is to operate the dryer at reduced pressure.[1−3] In addition to being able to preserve the quality of heat-sensitive products, lowering the operating pressure may enhance the drying rates as well.[1,4,5−8]

Some investigators have recently applied the concept of low-pressure (or subatmospheric pressure) superheated steam drying (LPSSD) to various heat-sensitive materials. Elustondo et al.[3] studied subatmospheric-pressure superheated steam drying of wood slabs and shrimp, banana, apple, pear, potato, and cassava slices both experimentally and theoretically. A semiempirical model was developed assuming that water removal was accomplished by evaporation in a moving boundary, allowing the vapor to flow through the dry layer built up as drying proceeds. The model proposed was found to predict the drying kinetics reasonably well. More recently, Devahastin et al.[9] studied experimentally drying of carrot cubes in both low-pressure superheated steam and vacuum dryers. They observed that the differences between the two sets of drying rate data (low-pressure superheated steam and vacuum drying) were smaller at higher drying temperatures. This suggested that raising the drying temperature further would eventually lead to equal rates of drying at the so-called inversion temperature[1,10] because of the increased temperature difference between the steam and product as well as a reduction in the initial steam condensation[11] that occurs as the wet material enters the drying chamber at a temperature lower than the saturation temperature of steam at prevailing pressure. Such information on the inversion temperature for the LPSSD system and the effect of vacuum pressure on this temperature is still missing, however. Shibata et al. (respectively in refs 4 and 12) have studied the steam-drying mechanisms of sintered spheres of glass beads under atmospheric pressure and vacuum. They reported that the drying mechanisms of the two processes were different and that superheated steam drying under vacuum gave lower critical moisture contents as well as higher drying rates in the falling rate period (FRP) than those in air drying under vacuum. However, they have not reported any information about the inversion temperature of the systems.

The present work, therefore, aimed at investigating the effect of vacuum pressure on the value of the inversion temperature by comparing the single-layer drying rates obtained in LPSSD and in vacuum drying of model porous particles, viz., molecular sieve beads. In addition, the values of the inversion temperature calculated only from the rates of drying in the constant rate period (CRP) were compared with those calculated from the whole drying period (CRPs and FRPs) in order to point out the fundamental differences between the two sets of temperatures, obtained from two different sets of drying rate information, beyond which drying rates in LPSSD are higher than those in vacuum drying. Three simple mathematical models that enable prediction of the drying behavior of molecular sieves undergoing LPSSD and vacuum drying were also proposed and compared.

* To whom correspondence should addressed. Tel.: +662 470 9246. Fax: +662 470 9240. E-mail: sakamon.dev@kmutt.ac.th.

[†] Department of Food Engineering, King Mongkut's University of Technology.

[‡] School of Energy and Materials, King Mongkut's University of Technology.

[§] National University of Singapore.

10.1021/ie049675r CCC: $30.25 © 2005 American Chemical Society
Published on Web 02/10/2005

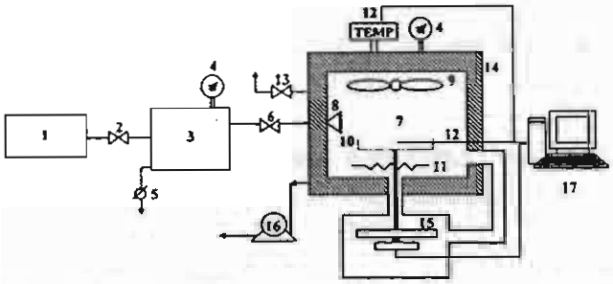


Figure 1. Schematic diagram of the low-pressure, superheated steam dryer and associated units: 1, boiler; 2, steam valve; 3, steam reservoir; 4, pressure gauge; 5, steam trap; 6, steam regulator; 7, drying chamber; 8, steam inlet and distributor; 9, electric fan; 10, sample holder; 11, electric heater; 12, online temperature sensor and logger; 13, vacuum breakup valve; 14, insulator; 15, online weight indicator and logger; 16, vacuum pump; 17, PC with installed data acquisition card.

Experimental Setup, Material, and Methods

Experimental Setup. A schematic diagram of the low-pressure superheated steam dryer and its accessories is shown in Figure 1. The dryer consists of a stainless steel drying chamber, insulated carefully with rock wool, with inner dimensions of 45 × 45 × 45 cm^3; a steam reservoir, which received steam from the boiler and maintained its pressure at around 200 kPa (gauge); and a liquid ring vacuum pump (model ET32030, Nash, Trumbull, CT), which was used to maintain a vacuum in the drying chamber. A steam trap was installed to reduce excess steam condensation in the reservoir. An electric heater, rated at 1.5 kW, controlled by a proportional−integral−derivative controller (model E5CN, Omron, Tokyo, Japan), was installed in the drying chamber to control the steam temperature and to minimize condensation of steam in the drying chamber during start-up; with the use of a heater, the initial steam condensation during the start-up period was reduced considerably. A variable-speed electric fan was used to disperse steam throughout the drying chamber. The steam inlet was made into a conical shape and was covered with a screen to help in the distribution of the steam in the chamber. The sample holder was made of a stainless steel screen with dimensions of 12 × 12 cm^2. The change of the mass of the sample was detected continuously (at 1 min intervals) using a load cell (model Ucg-3kg, Minebea, Nagano, Japan), which was installed in a smaller chamber connected to the drying chamber by a flexible hose (in order to maintain the same vacuum pressure as that in the drying chamber) and also to an indicator and recorder (model AD 4329, A&D Co., Tokyo, Japan). The temperature of the steam was also measured continuously using type K thermocouples, which were connected to an expansion board (model no. EXP-32, Omega Engineering, Stamford, CT). Thermocouple signals were then multiplexed to a data acquisition card (model no. CIO-DAS16Jr., Omega Engineering, Stamford, CT) installed in a PC. LABTECH NOTEBOOK software (version 12.1, Laboratory Technologies Corp.) was used to read and record the temperature data.

Material and Methods

Molecular sieve beads (no. 69837, Fluka, Buchs, Switzerland) that have a pore size of 0.4 nm and an average diameter of 3.02 mm with a standard deviation of 0.34 mm and a particle density of 750 kg/m^3 were used as the test material in this work. Prior to the start of each experiment, distilled water (6.7 g) was slowly sprayed onto the beads (22 g) to make the initial moisture content of the beads around 0.3 kg/kg (db), which was roughly the maximum moisture-holding capacity of the beads. The particles were then left in a tightly closed box at room temperature for about 6 h to allow them to equilibrate. The drying experiment was performed by placing roughly 28.7 g of water-saturated particles (about 1000 beads) on the sample holder as a single layer. The drying chamber was then sealed tightly, and valve 2 was opened to allow the steam from the boiler to flow into the reservoir; the steam pressure was maintained at about 200 kPa (gauge) in the reservoir. A vacuum pump was then switched on to evacuate the drying chamber to the desired operating pressure, and the steam regulator was opened to slowly flash the steam into the drying chamber. Because of the low-pressure environment in the chamber, the steam became superheated. An electric heater was used to maintain the steam temperature at the desired drying temperature. Although the ratio of the steam pressure in the steam reservoir to that in the drying chamber was rather high, the effect of the adiabatic expansion of steam introduced into the drying chamber on the steam temperature was rather small. This is because

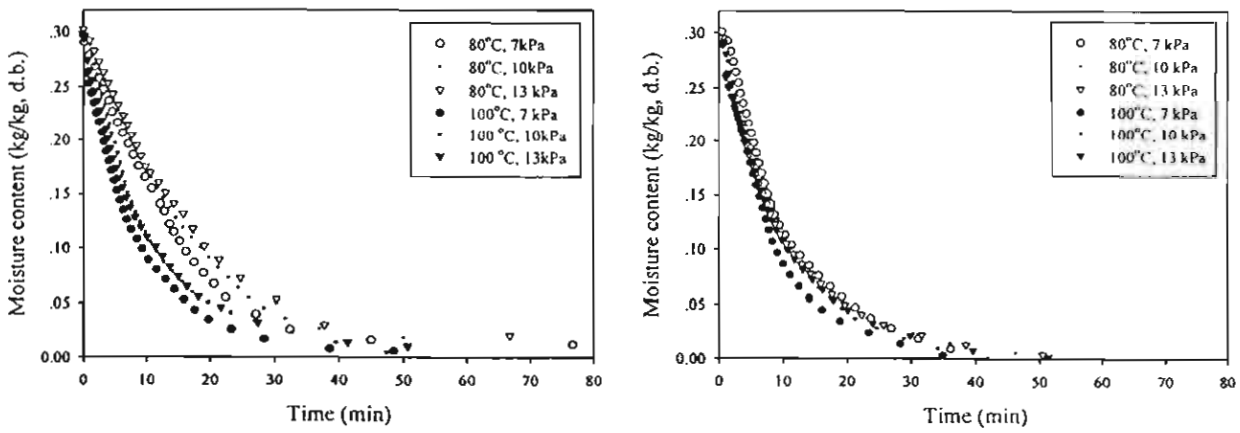


Figure 2. Drying curves of molecular sieve particles.

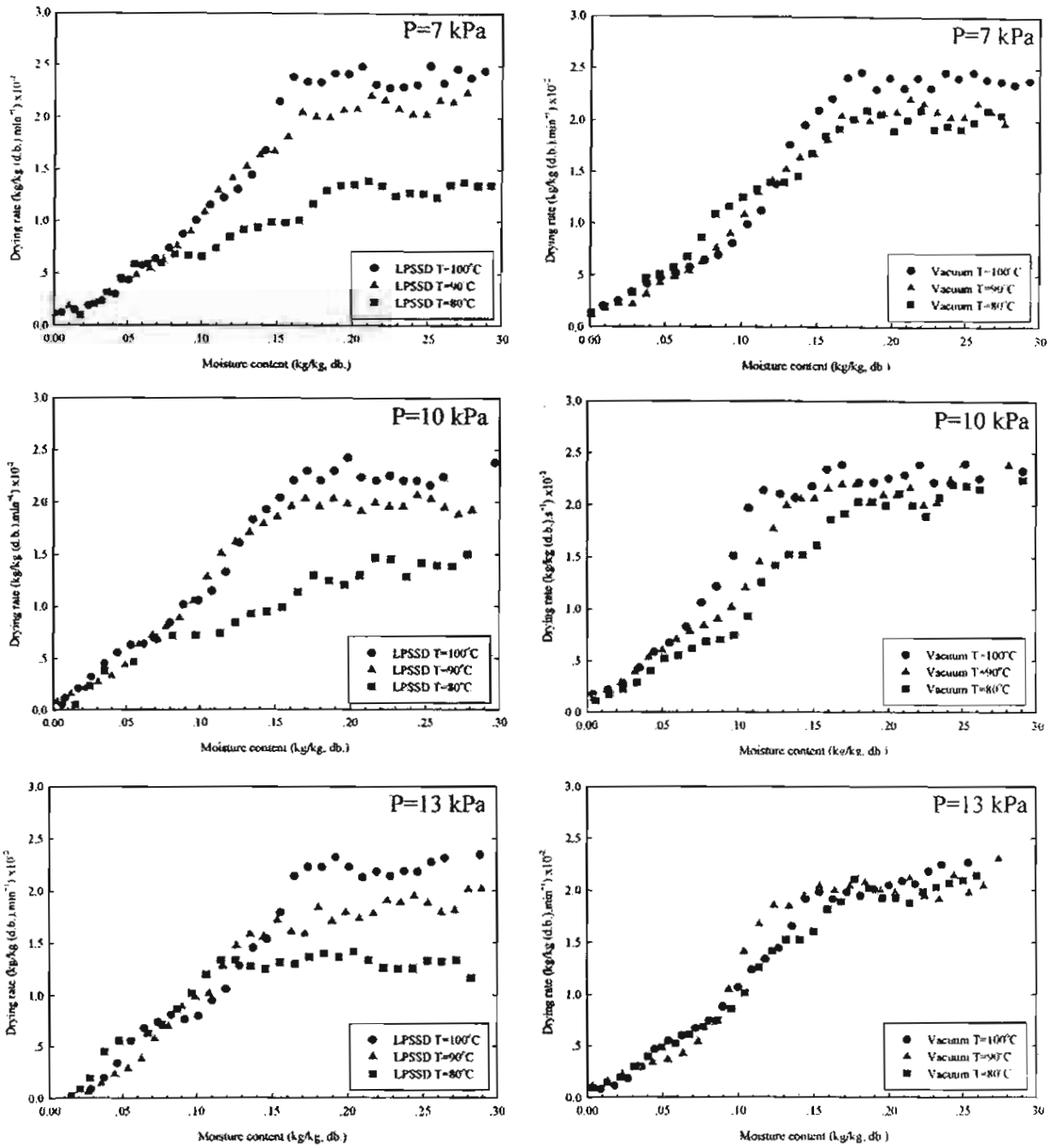


Figure 3. Drying rate curves of molecular sieve beads undergoing LPSSD and vacuum drying at various operating pressures.

an electric heater was installed in the drying chamber to help in the stabilization of the steam temperature. In addition, the temperature measurement was done carefully to ensure that the variation of the steam temperature within the drying chamber was negligible. At the end of drying, the breakup valve was opened to allow air into the drying chamber before opening up the chamber door and loading off the sample.

The experiments were performed under the following conditions: steam absolute pressures of 7, 10, and 13 kPa; steam temperatures of 80, 90, and 100 °C. The flow rate of steam into the drying chamber was maintained at about 26 kg/h, and the speed of the fan was fixed at around 2100 rpm. All experiments were performed in duplicate.

For vacuum-drying experiments, the same experimental setup was used but without the application of steam to the drying chamber. The same operating conditions as those used for LPSSD were therefore achievable.

Results and Discussion

Drying Rates of Porous Particles. Molecular sieve beads, which were saturated with water [the initial moisture content was about 0.3 kg/kg (db) or 23% (wb)], were dried to their equilibrium moisture content at each

operating condition in the dryer using both low-pressure superheated steam and vacuum conditions. During each experiment, the drying rates were calculated from the recorded weight changes, during both the CRPs and FRPs. Because, strictly speaking, the inversion temperature is defined only for surface moisture evaporation and not for internal moisture removal, the drying rates in the CRP are reported first. The overall average drying rates, based on the rates in both the CRPs and FRPs, are then calculated and compared with the rates in the CRP to point out the fundamental differences between the values of the inversion temperatures calculated using only the rates in the CRP and those obtained using the overall average drying rates in both drying periods.

First, the drying curves for the single layer of particles undergoing LPSSD and vacuum drying at some selected conditions are shown in Figure 2. While the drying curves for LPSSD at different conditions are quite different and the effect of the temperature on the drying curves is greater than the effect of the pressure, the drying curves for vacuum drying at different operating conditions are rather similar. It is seen that the drying times of LPSSD at an operating temperature of 80 °C were longer than those of vacuum drying for all operating pressures tested. However, the drying times for both processes operated at 100 °C were quite similar. This is due to the fact that an increased drying temperature led to higher drying rates, resulting from sharply increased temperature differences or gradients between the samples and the ambient steam in the case of superheated steam drying. However, the differences between the air temperature and the particle surface temperature in vacuum drying increased only slightly as the drying temperature increased. In addition, it can be observed that the equilibrium moisture contents of the beads undergoing LPSSD were much higher than those undergoing vacuum drying. For example, the equilibrium moisture contents of particles dried at 80, 90, and 100 °C using LPSSD at an operating pressure of 7 kPa were 1.5, 0.9, and 0.2% (db), respectively, while the equilibrium moisture contents of particles were 0.09, 0.05, and 0.02% (db), respectively, in the case of vacuum drying at the same pressure. This is due to a higher humidity condition in the drying chamber of LPSSD and, hence, a reduced vapor pressure gradient, which is the driving force of the drying process. Therefore, the drying times of most LPSSD were longer than those of vacuum drying.

Figure 3 shows a comparison of the observed drying rate curves in superheated steam drying with those in vacuum drying at different operating conditions. For all conditions, the drying rates fluctuated marginally but remained nearly constant as the moisture content decreased until the critical moisture content for each condition was reached. The drying rates then decreased continuously in the FRP. It can be seen from this figure that the critical moisture content was different for different conditions in the case of superheated steam drying [the critical moisture contents of particles dried, for example, at 80, 90, and 100 °C were 20, 17, and 15% (db), respectively, at an operating pressure of 7 kPa] but were quite similar in the case of vacuum drying [17% (db) over the temperature range of 80−100 °C at an operating pressure of 7 kPa]. It was also observed that the lower-pressure and higher-temperature superheated steam led to larger amounts of water evaporation and also to higher critical moisture contents.

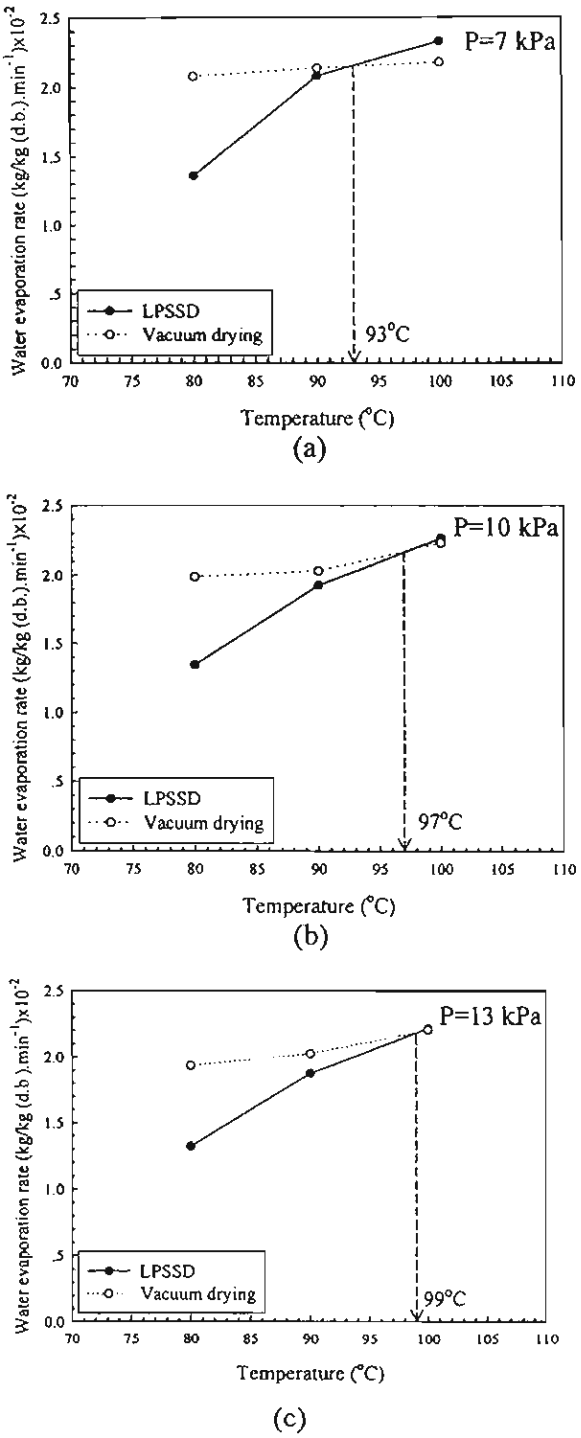


Figure 4. CRP evaporation rates of moisture from molecular sieve beads at various operating pressures.

Figure 4 gives the rates of water evaporation during the CRP at various operating temperatures and pressures. It was found, as expected, that raising the drying temperature led to higher CRP drying rates because of an increased temperature difference between the steam (or air) and the samples as well as a reduction of the initial steam condensation in the case of superheated steam drying. In the case of LPSSD, the temperature

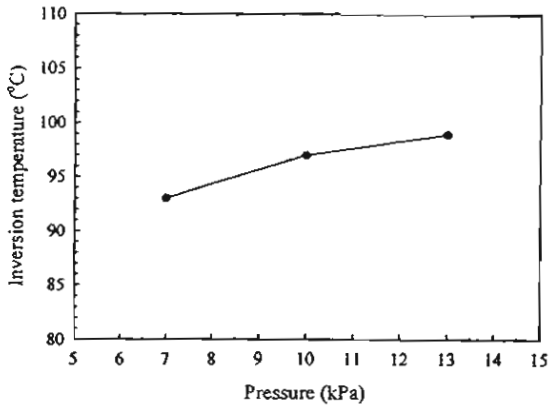


Figure 5. Effect of the operating pressure on the inversion temperature (based on CRP drying rates) of molecular sieve beads.

difference is the difference between the superheated steam temperature and the saturation temperature at the corresponding operating pressure, while for vacuum drying, the difference is between the air temperature and a temperature between the wet-bulb temperature and the saturation temperature (not saturation temperature because, in this case, the level of vacuum was not so high that the effect of convection by the fan could be negligible). While the temperature differences (or driving forces for heat transfer) in vacuum drying were higher at lower operating temperatures than those observed in LPSSD, the values of the heat-transfer coefficient of the medium in the case of vacuum drying were lower because of the inferior thermal properties of air. Raising the drying temperature, however, led to higher temperature differences and, hence, higher CRP drying rates. The counteracting effects of the heat-transfer coefficient and the temperature difference led to the inversion phenomenon, as is evident in Figure 4, where the CRP drying rates of vacuum drying and LPSSD are seen to be equal. Beyond the inversion temperature, the CRP drying rates of steam drying were higher than those of vacuum drying because of both the increased temperature difference and the higher heat-transfer coefficient.

When the operating pressure was increased (at the same operating temperature), it can be seen that the drying rate was lower. This was due to the fact that the boiling temperature of water at higher pressure is higher; this leads to a decreased temperature difference and, hence, a lower drying rate.

As mentioned earlier, the CRP drying rates depend on the rate of heat transfer and, hence, the difference between the surface temperature of the sample and the drying medium temperature. For this reason, the drying temperature had only a small effect on the rates of vacuum drying as compared with the case of LPSSD because the particle surface temperature in the case of vacuum drying (which relates somehow to the wet-bulb temperature) changes only slightly with an increased drying temperature compared with the change of the boiling temperature, especially at lower operating pressures.

Inversion Temperature. Figure 5 shows the effect of the operating pressure on the inversion temperature, which was calculated from the CRP rates (Figure 4). The inversion temperature at each operating pressure was obtained from the plots of the drying rates at the point where the rates of vacuum drying and LPSSD were equal.

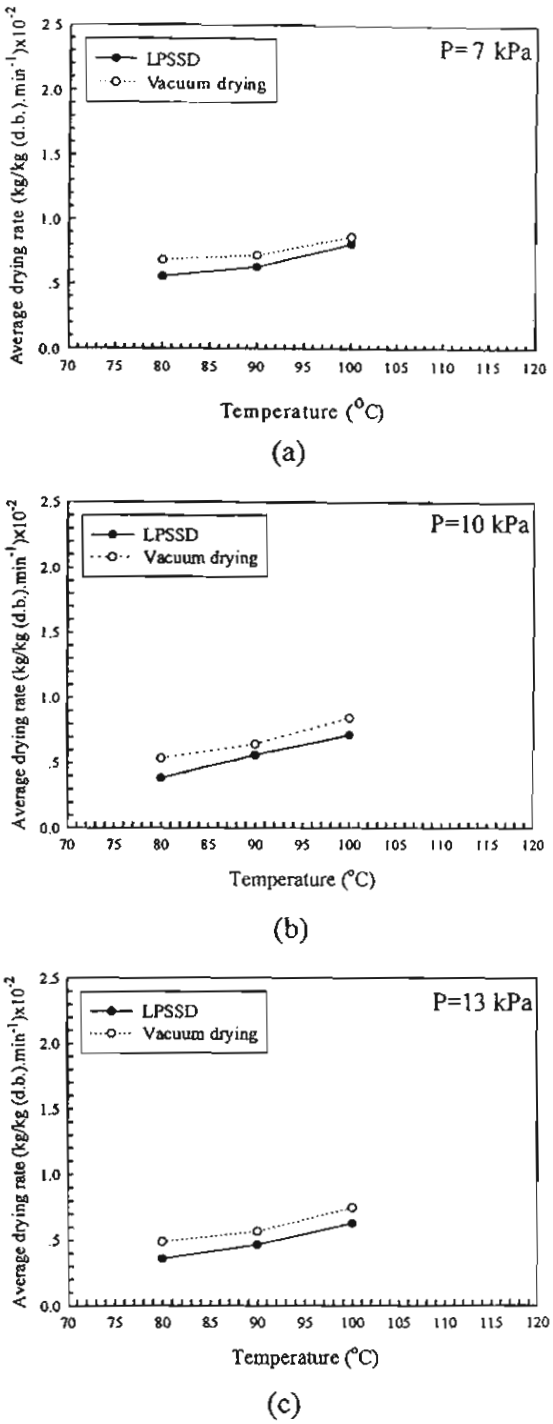


Figure 6. Average rate (CRP + FRP) of moisture removal from molecular sieve beads at various operating pressures.

Figure 6 shows the overall average drying rates calculated from combined CRP and FRP drying rates at various operating pressures. As mentioned earlier, the CRP drying rates depend only on the external heat- and mass-transfer conditions because free water is always available for evaporation at the surface of the sample. However, in the FRP, the rates depend not only on the rate of external heat transfer but more on

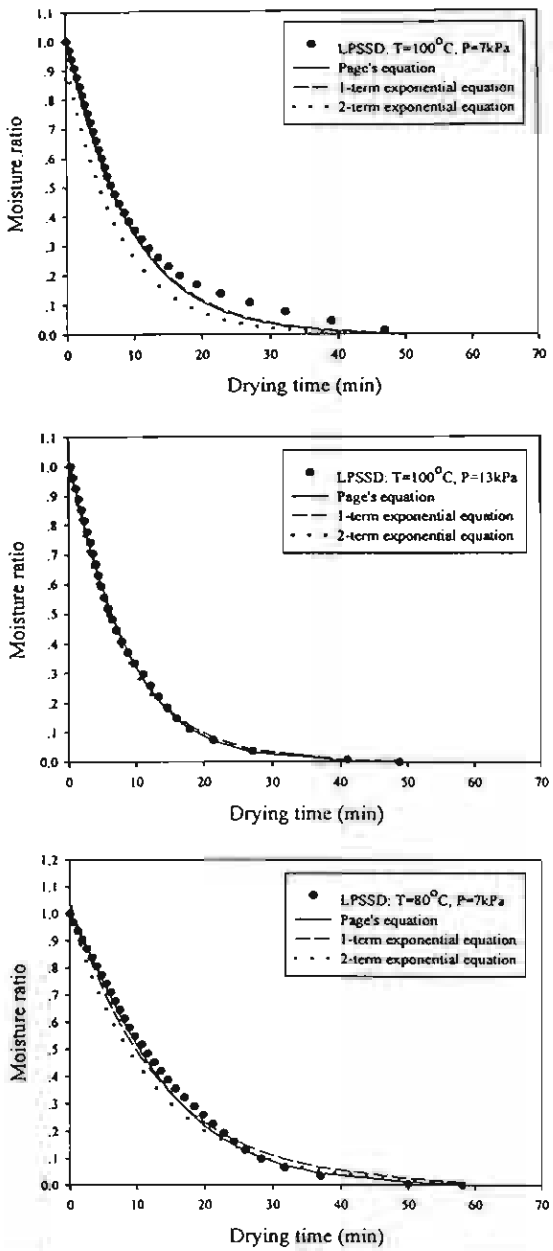


Figure 7. Comparison of fitted models with the experimental data in the case of LPSSD.

internal resistances to heat and mass transfer, which are somewhat material-dependent. Therefore, the average drying rates calculated from combined CRP and FRP rates were not the same as the CRP drying rates. It can be seen from Figures 4 and 6 that the differences between vacuum- and steam-drying CRP rates are greater than those between vacuum and steam drying calculated from combined CRP and FRP rates. This is due to the fact that in FRP the resistances to heat and mass transfer of superheated steam drying are lower than those of vacuum drying because the drying medium of steam drying is water vapor and, hence, there is no diffusional resistance of water from the sample into the drying medium. These effects of the FRP drying rates, therefore, increase the values of the combined (or overall) drying rates of superheated steam drying and, hence, lead to smaller differences between the overall drying rates of vacuum and steam drying. No inversion temperature was observed from the plots of the overall drying rates as well.

Mathematical Modeling. Simple mathematical models that enable prediction of the drying curves of molecular sieves undergoing LPSSD and vacuum drying were developed based on the well-known Page's equation,[13] single-term exponential equation, and two-term exponential equation (Arrhenius-type model). Exponential equations were listed, and their prediction abilities were compared with that of a simpler Page's equation with no real physical basis but just to illustrate that different sets of equations are suitable for different drying techniques.

Page's Equation.

$$\mathrm{MR} = \frac{X_t - X_{eq}}{X_i - X_{eq}} = \exp(-kt^n) \qquad (1)$$

The parameters k and n in the equation were determined from the experimental data and were correlated as follows:

For LPSSD

$$k = -2.39 \times 10^{-1} + 2.86 \times 10^{-3}T - 7.13 \times 10^{-3}P - 3.83 \times 10^{-6}TP + 5.42 \times 10^{-2} \ln P \qquad R^2 = 0.95$$

$$n = (1.87{-}3.91) \times 10^{-3}T + 1.11 \times 10^{-1}P - 5.44 \times 10^{-4}TP - 4.35 \times 10^{-1} \ln P \qquad R^2 = 0.86$$

For vacuum drying

$$k = -7.42 \times 10^{-2} - 7.07 \times 10^{-5}T - 1.01 \times 10^{-2}P + 1.22 \times 10^{-5}TP + 1.12 \times 10^{-1} \ln P \qquad R^2 = 0.96$$

$$n = (1.12{-}2.40) \times 10^{-3}T - 7.88 \times 10^{-2}P + 4.92 \times 10^{-4}TP + 2.21 \times 10^{-1} \ln P \qquad R^2 = 0.73$$

Single-Term Exponential Equation.

$$\mathrm{MR} = \frac{X_t - X_{eq}}{X_i - X_{eq}} = a \exp(-bt) \qquad (2)$$

For LPSSD

$$a = (1.12{-}1.41) \times 10^{-3}T + 4.53 \times 10^{-3}P - 6.87 \times 10^{-6}TP + 6.53 \times 10^{-3} \ln P \qquad R^2 = 0.75$$

$$b = -6.15 \times 10^{-2} + 1.12 \times 10^{-3}T - 9.75 \times 10^{-3}P + 7.56 \times 10^{-5}TP + 3.77 \times 10^{-2} \ln P \qquad R^2 = 0.91$$

For vacuum drying

$$a = 9.68 \times 10^{-1} + 1.22 \times 10^{-3}T + 1.59 \times 10^{-4}P - 2.73 \times 10^{-5}TP - 1.12 \times 10^{-1} \ln P \qquad R^2 = 0.94$$

$$b = 1.97 \times 10^{-2} - 3.74 \times 10^{-4}T - 2.13 \times 10^{-2}P + 1.08 \times 10^{-4}TP + 1.03 \times 10^{-1} \ln P \qquad R^2 = 0.70$$

Two-Term Exponential Equation.

$$\mathrm{MR} = \frac{X_t - X_{eq}}{X_i - X_{eq}} = a_1 \exp(-b_1 t) + c_1 \exp(-d_1 t) \qquad (3)$$

For LPSSD

$$a_1 = (0.699P^{-0.051}) \exp(-51.312/T_{abs}) \quad R^2 = 0.62$$

$$b_1 = (354.576P^{-0.0267}) \exp(-2958/T_{abs}) \quad R^2 = 0.95$$

$$c_1 = (5.63 \times 10^{-3}P^{0.408}) \exp(-1269.76/T_{abs}) \quad R^2 = 0.59$$

$$d_1 = (827.98P^{-0.132}) \exp(-3175.72/T_{abs}) \quad R^2 = 0.93$$

For vacuum drying

$$a_1 = (3.709P^{0.554}) \exp(-1056.055/T_{abs}) \quad R^2 = 0.53$$

$$b_1 = (0.164P^{0.059}) \exp(-185.677/T_{abs}) \quad R^2 = 0.49$$

$$c_1 = (1.63 \times 10^{-3}P^{-1.082}) \exp(2773.12/T_{abs}) \quad R^2 = 0.75$$

$$d_1 = (4.73 \times 10^{-2}P^{-0.903}) \exp(871.105/T_{abs}) \quad R^2 = 0.95$$

The equations were fitted with the experimental data; the fitted equations were evaluated based on their R^2 and standard error of estimation. When the three drying models are compared, the results show that Page's equation fits the experimental data better than the single-term exponential equation and the two-term exponential equation in the case of LPSSD, while the single-term exponential equation fits the experimental data well in the case of vacuum drying at operating temperatures in the range of 80−100 °C and pressures of 7−13 kPa as exemplified in Figures 7 and 8. The minimum R^2 of Page's equation was 0.997 and its maximum standard error of estimation was 0.0181 in the case of LPSSD, while the minimum R^2 of the single-term exponential equation was 0.998 and its maximum standard error was 0.0233 in the case of vacuum drying. Drying constants of Page's equation (k and n) and of the single-term exponential equation (a and b) are found to depend on the operating temperature as well as pressure.

Concluding Remarks

The effects of operating parameters, i.e., drying temperature and pressure, on the rates of vacuum drying and LPSSD of model porous particles were investigated experimentally. In addition, the values of the inversion temperature calculated only from the rates of drying in the CRP were compared with those calculated from the whole drying period (CRP and FRP) in order to point out the fundamental differences between the two sets of temperatures beyond which the drying rates in LPSSD were higher than those in vacuum drying. It was found that the inversion temperatures calculated from combined CRP and FRP rates were not the same as the inversion temperatures calculated from only CRP rates; in the former case, no inversion temperature was indeed observed within the ranges of study. Empirical models that describe the experimental drying curves are also proposed. It is found that Page's equation and the single-term exponential equation can fit well the experimental data for LPSSD and vacuum drying, respectively, over the ranges of operating temperature of 80−100 °C and pressure of 7−10 kPa.

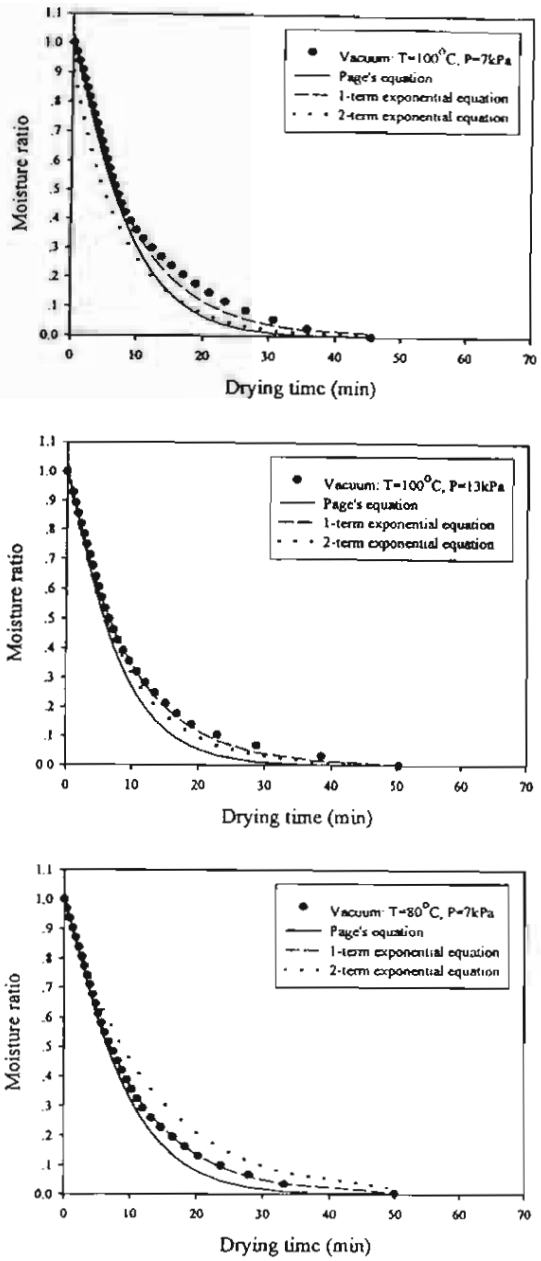


Figure 8. Comparison of fitted models with the experimental data in the case of vacuum drying.

Acknowledgment

The authors express their sincere appreciation to the Thailand Research Fund (TRF), National Science and Technology Development Agency (NSTDA), and the International Foundation for Science (Sweden) for supporting this study financially.

Nomenclature

a = constant of the single-term exponential model
a_1 = constant of the two-term exponential model
b = constant of the single-term exponential model
b_1 = constant of the two-term exponential model

c_1 = constant of the two-term exponential model
d_1 = constant of the two-term exponential model
k = constant of Page's equation
MR = moisture ratio
n = constant of Page's equation
P = absolute pressure, kPa
t = drying time, min
T = temperature of the drying medium, °C
T_{abs} = temperature of the drying medium, K
X_{eq} = equilibrium moisture content, kg/kg (db)
X_i = initial moisture content, kg/kg (db)
X_t = moisture content at any time, kg/kg (db)

Literature Cited

(1) Mujumdar, A. S. Superheated steam drying—Technology of the future. In *Mujumdar's Practical Guide to Industrial Drying*; Devahastin, S., Ed.; Exergex: Brossard, Canada, 2000; pp 115–138.

(2) Kumar, P.; Mujumdar, A. S. Superheated-steam drying: A bibliography. *Drying Technol.* **1990**, *8*, 195.

(3) Elustondo, D.; Elustondo, M. P.; Urbicain, M. J. Mathematical modeling of moisture evaporation from foodstuffs exposed to subatmospheric pressure superheated steam. *J. Food Eng.* **2001**, *49*, 15.

(4) Shibata, H.; Mada, J.; Shinohara, H. Drying mechanism of sintered spheres of glass beads in superheated steam. *Ind. Eng. Chem. Res.* **1988**, *27*, 2353.

(5) Shibata, H.; Mada, J.; Funatsu, K. Prediction of drying curves on sintered spheres of glass beads in superheated steam under vacuum. *Ind. Eng. Chem. Res.* **1990**, *29*, 614.

(6) Senda, Y.; Bando, Y.; Yasuda, K.; Nakamura, M.; Sugimura, Y.; Shibata M. Development of superheated steam dryer at reduced pressure. *Proceedings of the 1st Asia–Pacific Drying Conference*, Bali, Indonesia, 2001; p 247.

(7) Elustondo, D. M.; Mujumdar, A. S.; Urbicain, M. J. Optimum operating conditions in drying foodstuffs with superheated steam. *Drying Technol.* **2002**, *20*, 381.

(8) Elustondo, D.; Elustondo, M. P.; Urbicain, M. J. Drying with superheated steam: Maximum drying rate as a linear function of pressure. *Chem. Eng. J.* **2002**, *86*, 69.

(9) Devahastin, S.; Suvarnakuta, P.; Soponronnarit, S.; Mujumdar, A. S. A comparative study of low-pressure superheated steam and vacuum drying of a heat-sensitive material. *Drying Technol.* **2004**, *22*, 1845.

(10) Iyota, H.; Nishimura, N.; Onuma, T.; Nomura, T. Drying of sliced raw potatoes in superheated steam and hot air. *Drying Technol.* **2001**, *19*, 1411.

(11) Iyota, H.; Nishimura, N.; Onuma, T.; Nomura, T. Simulation of superheated steam drying considering initial steam condensation. *Drying Technol.* **2001**, *19*, 1425.

(12) Shibata, H.; Mada, J.; Shinohara, H. Steam drying of sintered glass bead spheres under vacuum. *Ind. Eng. Chem. Res.* **1988**, *27*, 2385.

(13) Page, G. Factors influencing the maximum rates of air drying shelled corn in thin layers. Master's Thesis, Purdue University, West Lafayette, IN, 1949.

Received for review April 21, 2004
Revised manuscript received November 10, 2004
Accepted January 5, 2005

IE049675R

Available online at www.sciencedirect.com
SCIENCE DIRECT
ELSEVIER
Journal of Stored Products Research 41 (2005) 387–400
Journal of STORED PRODUCTS RESEARCH
www.elsevier.com/locate/jspr

Investigations on head-rice yield and operating time in the fluidised-bed drying process: experiment and simulation

Nattapol Poomsa-ad[a], Apichit Terdyothin[b], Somkiat Prachayawarakorn[c,*], Somchart Soponronnarit[b]

[a]*Faculty of Engineering and Computer Science, Mahasarakham University, Mahasarakham 44150, Thailand*
[b]*School of Energy and Materials, King Mongkut's University of Technology Thonburi, Suksawat 48 Road, Bangkok 10140, Thailand*
[c]*Faculty of Engineering, King Mongkut's University of Technology Thonburi, Suksawat 48 Road Tongkru, Bangkok 10140, Thailand*

Accepted 7 June 2004

Abstract

This analysis of the drying process is based on experiments and simulations of the influence of temperature in the fluidised-bed dryer, moisture content and tempering period on head-rice yield, and operating time. A mathematical model incorporating the head-rice yield equation for predictions of the moisture content and the grain temperature in each drying stage and the final head-rice yield, is in good agreement with experimental data. The moisture content after first-stage drying and tempering have a dominant effect on head-rice yield and operating time in reducing high-moisture contents to a safe level. The simulation results recommend that the allowable temperature should be not higher than 150 °C for the first stage and the moisture content after first-stage drying should be not lower than 22.5% dry basis, with subsequent tempering for at least 25 min.
© 2004 Elsevier Ltd. All rights reserved.

Keywords: Dehydration; Head rice; Fluidised bed; Grain; Modelling

*Corresponding author. Tel.: +662-4270-9221; fax: +662-428-3534.
E-mail address: somkiat.pra@kmutt.ac.th (S. Prachayawarakorn).

0022-474X/$ - see front matter © 2004 Elsevier Ltd. All rights reserved.
doi:10.1016/j.jspr.2004.06.002

Nomenclature

C_a	specific heat of dry air, kJ/kg °C
C_v	specific heat of water vapour, kJ/kg °C
C_{pw}	specific heat of moist paddy, kJ/kg °C
D	effective diffusivity, m^2/s
$h_{f\theta}$	latent heat of water, kJ/kg
I_c	tempering index, decimal
M	moisture content, decimal or per cent dry basis
M_{eq}	equilibrium moisture content, decimal dry basis
M_{av}	average inlet moisture content at time t, decimal dry basis
M_f	average moisture content at time $= t + \Delta t$, decimal dry basis
M_i	average moisture content at time $= t$, decimal dry basis
M_{in}	initial moisture content, decimal dry basis
$M_{s,t}$	surface moisture content at time t, decimal dry basis
$\dot{m}_a$	mass flow rate of dry fresh air, kg/s
m_p	mass of dry matter, kg
l	half height of cylinder axis, m
R	ratio of dry mass of grain to mass of air, kg dry matter /kg dry air
RHY	relative head-rice yield
r	co-ordinate along the radius of cylinder, m
r_o	radius of paddy, m
T_{abs}	absolute temperature, K
T_f	exhaust-air temperature, °C
T_{in}	inlet-air temperature, °C
t	drying time or tempering time, minute or s
V_p	particle volume, m^3
W_f	exhaust-humidity ratio of air, kg water/kg dry air
W_{in}	inlet-humidity ratio of air, kg water/kg dry air
z	length of cylinder, m
θ	grain temperature, °C
θ_{in}	inlet-grain temperature, °C

1. Introduction

High-moisture paddy grains must be dried rapidly to prevent deterioration, and in this study the fluidised-bed drying system is considered. The paddy drying process is traditionally divided into three steps in order to reduce the moisture content to a safe level of 16.5% dry basis. Paddy is first dried for a few minutes at a temperature above 130 °C, then the grain is tempered for a certain period and, as the last step, the tempered paddy is dried again with ambient air or slightly heated air until its moisture content reaches the safe storage level.

The tempering period is the stage in which paddy is kept in a closed bin without airflow. After a sufficiently long period of tempering, the moisture profile throughout the paddy becomes uniform. This uniformity provides a decrease of tensile stress occurring inside the grains from the first drying stage, thus maintaining high head-rice yield after subsequent drying (Steffe et al., 1979; Zhang and Litchfield, 1991; Li et al., 1999; Soponronnarit et al., 1999). In addition, tempering also reduces the drying time in the final stage, resulting in more effective energy utilisation. The parameters determining head-rice yield are tempering period, moisture contents at the start and at the end of the first stage, and grain temperature after the first stage (tempering temperature). The tempering temperature is related to drying-air temperature and drying time. In practice, these parameters vary widely across the industry, depending upon the owners' experiences. Hence, operating times longer than necessary for obtaining optimum grain quality may be used. A thorough investigation of these factors in paddy processing is needed.

Therefore, the objectives of the present work were: (1) to study the effect of initial moisture content, inlet-air temperature and tempering period on head-rice yield, and to establish a head-rice yield equation: (2) to determine suitable operating conditions which provide a superior quality head-rice yield and optimum operating time. To achieve the second objective, a mathematical model has been formulated that is capable of predicting moisture content, grain temperature and relative head-rice yield (RHY).

2. Mathematical model of drying system

The paddy drying process consists of a drying unit, a tempering unit and an ambient-air ventilation unit (Fig. 1). A mathematical model for each stage was developed.

The formulation of the mathematical model was based on the following assumptions:

- The paddy kernel were of uniform size and a finite cylindrical shape.
- The grains in the bed were perfectly mixed such that every individual grain had the same moisture content at any drying time.
- Internal diffusion was the dominant mechanism for moisture transport in the grains.
- The drying air was in thermal equilibrium with the exiting grain kernels, so that the grain temperature was equivalent to the exhaust air temperature.
- The temperature gradient inside the kernels and grain shrinkage were negligible.

The model of a drying process with the above assumptions must comprise three governing equations, mass balance, energy balance between air and grain bed, and the drying-rate equation.

2.1. Heat and mass balances

In a small interval of time Δt, a certain amount of moisture evaporates from the grain bed into the air, resulting in a change in the humidity ratio. This moisture balance can be written as

$$W_f = R(M_i - M_f) + W_{in}, \tag{1}$$

where W_f is the exhaust-humidity ratio of air (kg water/kg dry air), W_{in} the inlet-humidity ratio of air(kg water/kg dry air), M_i the average moisture content at time $= t$, decimal dry basis, M_f the average moisture content at time $= t + \Delta t$, decimal dry basis and R the ratio of dry mass of grain to mass of air $(m_p/(\dot{m}_a \times \Delta t))$, decimal.

The exhaust-air temperature from the fluidised-bed dryer can be determined by Eq. (2),

$$T_f = (C_a T_{in} + W_{in}(h_{fg} + C_v T_{in}) - W_i h_{fg} + RC_{pw}\theta_{in})/(C_a + W_f C_v + RC_{pw}), \quad (2)$$

where T_f is the exhaust-air temperature (°C), T_{in} the inlet-air temperature (°C), θ_{in} the inlet-grain temperature (°C), C_a the specific heat of dry air (kJ/kg °C), C_v the specific heat of water vapour (kJ/kg °C), C_{pw} the specific heat of moist grain (kJ/kg °C), and h_{fg} the latent heat of moisture evaporation (kJ/kg).

At the inlet, the grain temperature is equal to the ambient air temperature.

2.2. Drying kinetics for a single kernel

Moisture migration within a kernel is described by mass diffusion during the drying and tempering stages. For a finite cylinder, the partial differential equation for moisture diffusion in a single paddy kernel can be written as

$$\frac{\partial M}{\partial t} = D\left[\frac{\partial^2 M}{\partial r^2} + \left(\frac{1}{r}\right)\frac{\partial M}{\partial r} + \frac{\partial^2 M}{\partial z^2}\right], \quad (3)$$

where D is the effective moisture diffusion (m^2/s), M the moisture content, decimal dry basis, r the co-ordinate along the radius of cylinder (m), t the time (min or s), and z the length of cylinder (m).

The expression for D obtained by Poomsa-ad et al. (2002) is given by

$$D = 5.41141 \times 10^{-6} \exp\left(-\frac{28436.4}{T_{abs}}\right), \quad (4)$$

where T_{abs} is the absolute air temperature (K). Eq. (4) is valid over the temperature range from 373.15 to 443.15 K. The average air temperature between the inlet and exhaust conditions was used to calculate the effective diffusion coefficient.

2.3. Initial and boundary conditions

Moisture content within the grain at the inlet can be assumed to be spatially uniform and the gas-film resistance around the grain surface is presumed negligible, allowing the moisture content at the surface to equilibrate with the drying air

$$\begin{aligned}
&t = 0, \quad 0 \leqslant r \leqslant r_o, && M = M_{in},\\
&-l \leqslant z \leqslant +l, && M = M_{in},\\
&t > 0, \quad r = r_o, && M = M_{eq},\\
&z = \pm l, && M = M_{eq},\\
&t > 0, \quad r = 0, && \frac{\partial M}{\partial r} = 0,
\end{aligned}$$

where M_{in} is the initial moisture content, decimal dry basis, M_{eq} the moisture content at the equilibrium, decimal dry basis, and l the half height of cylinder representing grain (m).

The moisture equilibrium equation of Laithong (1987) used in the present study is given by

$$1 - \Phi = \exp\{(-4.584 \times 10^{-6}) T_{abs} (100 M_{eq})^{2.397}\}. \quad (5)$$

The solution of Eq. (3) can be found by the finite difference method. In calculation, the grain shape was divided into 80 nodes in length and 10 nodes in radius. The average moisture content for a single kernel can be determined by

$$M_{av} = \frac{1}{V_p} \iint 2\pi M(r, z, t)\, dr\, dz, \quad (6)$$

where M_{av} is the average moisture content at time t, decimal dry basis, and V_p the volume of a single kernel (m^3).

Eqs. (1)–(4) can be solved by iteration. Assuming the exhaust air temperature, the amount of water evaporation from the grains into the air can be determined by Eqs. (3)–(6). The value of W_f from Eq. (1) allows recalculation of T_f by Eq. (2). Iteration leads to final values of M_f and T_f at time t.

2.4. Initial and boundary conditions for tempering stage

During this period, moisture inside a paddy kernel moves to the exterior surface, but does not evaporate to the environment due to the limited volume in tempering storage and consequent lack of air movement. The validity of this behaviour has been noted by Sabbath (1970) and Steffe (1979). The boundary and initial conditions for the tempering period are as follows:

$$\begin{aligned} &t = 0, && M = M(r, z), \\ &t > 0, \quad r = r_o, && \frac{\partial M}{\partial r} = 0, \\ &z = \pm l, && \frac{\partial M}{\partial z} = 0, \\ &t > 0, \quad r = 0, && \frac{\partial M}{\partial r} = 0. \end{aligned}$$

2.5. Head-rice yield

RHY can be written in the general function as

$$RHY = f(\theta, M, t), \quad (7)$$

where RHY is the RHY yield, M the preset moisture content, per cent dry basis, t the tempering time (min), and θ the grain temperature (°C).

RHY is defined as the ratio of head rice obtained from the drying process to that from ambient-air drying. Details of this equation will be discussed in the section on results and discussion. After determining the required tempering time, head rice can then be calculated. In calculating moisture content, we assume that drying at the second stage using ambient air does not affect the quality due to the low drying rate.

2.6. Ambient-air ventilation

The analogous equations of heat and mass balances throughout the thin bed as previously represented are used again for the ventilation stage by replacing θ_{in} in Eq. (2) by the tempering temperature or grain temperature after the first stage, and then solving for moisture content with Eq. (3). At this stage, the grain temperature is much higher than the ambient air temperature so the grain temperature is used as an input parameter in calculating the effective diffusion coefficient. The grain temperature and the inlet-air humidity are used to calculate the equilibrium moisture content with Eq. (5). Initial and boundary conditions for the single grain kernel during this step are given by

$$
\begin{aligned}
&t = 0, && M = M(r, z),\\
&t > 0, \quad r = r_o, && M = M_{eq},\\
&z = \pm l, && M = M_{eq},\\
&t > 0, \quad r = 0, && \frac{\partial M}{\partial r} = 0.
\end{aligned}
$$

3. Materials and methods

The freshly harvested paddy was rewetted, mixed and kept in cool storage at 3–5 °C for 5–7 days. Before starting the experiment, the cooled paddy was kept in ambient air until the grain temperature was close to ambient temperature. A schematic drying system is shown in Fig. 1. The drying system comprised a cylinder-shaped drying chamber of 20 cm diameter and 140 cm height, a 12 kW electrical heater and a backward curved-blade centrifugal fan driven by a 1.5 kW motor. Drying-air temperature was controlled by a proportional integral derivative controller with an accuracy of ±1 °C. A mechanical variable speed unit regulated airflow rate. Moist paddy was dried initially by a batch-type fluidised-bed dryer. After the moisture content of the paddy was reduced to a preset value, the paddy was collected in a glass bottle with a diameter of 12 cm and a height of 10 cm and kept in an oven at a temperature equal to the grain temperature after drying. Finally, it was ventilated immediately by an ambient airflow until its moisture content was close to 16.5% dry basis. A 300 g sample was kept in a sealed plastic bag for 2 weeks before testing the head-rice yield.

Paddy prepared at three moisture levels, 35%, 30% and 25% dry basis, was dried at drying-air temperatures of 110, 130, 150 and 170 °C and drying times of 1, 2, 3 and 4 min. Such conditions were performed at a fixed-bed air velocity of 2.2 m/s and a bed thickness of 10 cm. Tempering times studied in the present work were 0, 15, 30 and 45 min. Temperatures at different positions were measured with an accuracy of ±1 °C by K-type thermocouples connected to a data logger. The moisture content of the paddy was determined in an air oven at a temperature of 103 °C for 72 h. For head-rice yield, a 125 g paddy sample was dehusked with a two-rubber roller machine and the bran removed with a SATAKE milling machine. Head rice was separated from the broken rice by a sieving screen. Head rice is defined in this study as the ratio of the head-rice mass to the original paddy mass.

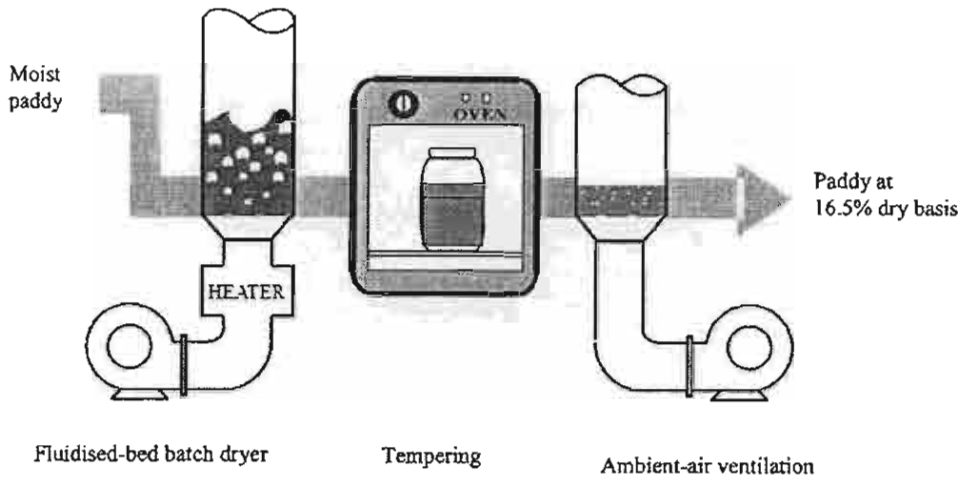


Fig. 1. Schematic diagram of a paddy drying system.

4. Results and discussion

4.1. Effect of drying conditions on RHY without tempering

Fig. 2 shows the effect of final moisture content and grain temperature on RHY at different initial moisture contents. Both final moisture content and grain temperature showed a strong influence on head-rice yield reduction. Most of the data show the RHYs lower than 40% if there was no tempering treatment between stages. Corresponding grain temperatures varied widely between 80 and 115 °C depending upon initial moisture content, inlet-air temperature and drying time.

High values of RHY (>90%) can be obtained for the initial moisture contents of 30 and 35% dry basis when final moisture content after the first stage is higher than 25% dry basis, corresponding to grain temperatures between 60 and 95 °C. For an initial moisture content of 25% dry basis, however, moisture content should not be reduced below 20% dry basis.

Broken rice exists after milling as a result of the steep moisture gradient in the grain produced by the rapid drying (Kunze, 1996). This causes the development of compressive stresses at the grain surface and tensile stresses at the centre. When the compressive stresses exceed the tensile stresses of grain at its centre, grain cracking develops, leading to less mechanical resistance during milling.

4.2. Effect of tempering time on RHY

The RHY from a set of tempering times is shown in Fig. 3. The percentage of RHY became higher with increased tempering time. The head-rice yield showed a small improvement with the 15-min tempering time as represented in Fig. 3a and increased to a moderate level with a longer tempering time. The improved quality was mainly in paddy dried to moisture contents lower than 24% dry basis at the first stage, which previously represented poor head-rice yield as shown

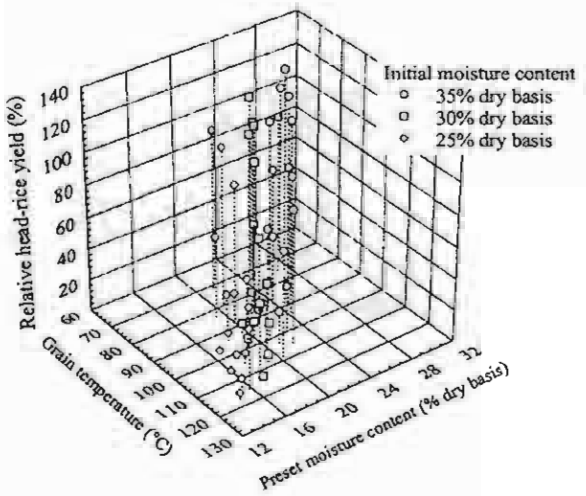


Fig. 2. Effects of preset moisture content and grain temperature after fluidised-bed drying on RHY (without tempering).

in Fig. 2. Values of RHY were now greater than 60% for a 30-min tempering time, as presented in Fig. 3b, with a few results at lower levels. For the case of 45 min as shown in Fig. 3c, results showed a similar trend to that in Fig. 3b. The better quality of the head-rice yield may be due to the combined effects of partially gelatinised grain and relaxing of the moisture gradient inside the grains.

4.3. The prediction equation for RHY

Multiple-linear regression was used to fit experimental data to a polynomial equation. The form of the prediction equation for RHY chosen was

$$RHY = A + Bt + Ct,^2 \quad R^2 = 0.82, \tag{8}$$

where

$$A = -39.232 + 8.4227\,M - 0.34060\,T - 0.029105\,TM,$$
$$B = 25.945 - 1.1878\,M - 0.24443\,T + 0.012302\,TM,$$
$$C = -0.33610 + 0.015028\,M + 0.0032590\,T - 0.00015762\,TM,$$

t, M and T were tempering time in minutes, moisture content in per cent dry basis and tempering temperature in °C, respectively. The correlation coefficient between model and data was 0.82. This equation was valid in the following range:

15.5% dry basis $< M < 30\%$ dry basis,

$65\,^{\circ}\mathrm{C} < T < 115\,^{\circ}\mathrm{C}$,

$0\,\mathrm{min} < t < 60\,\mathrm{min}$.

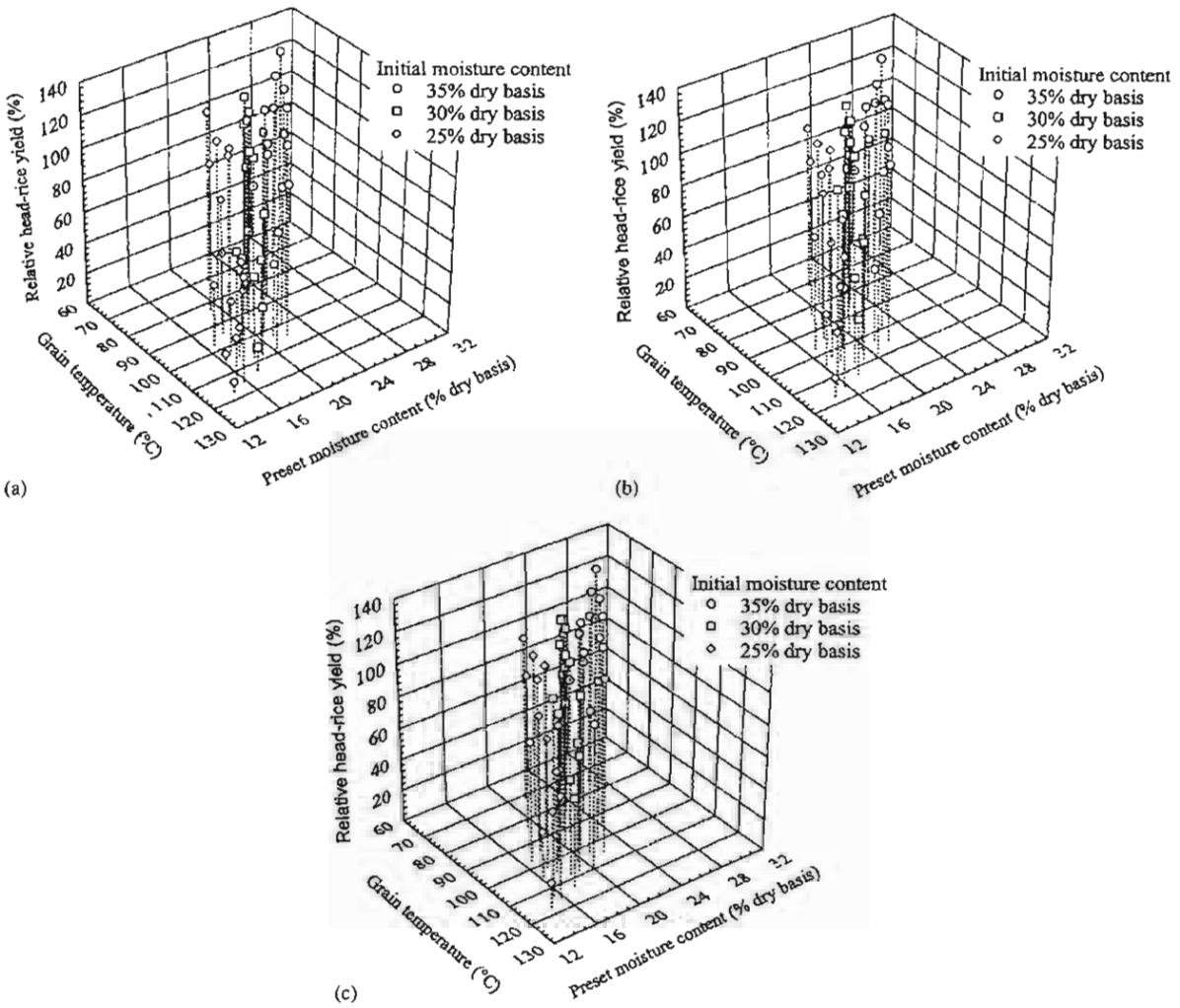


Fig. 3. Effects of preset moisture content and grain temperature after fluidised-bed drying (tempering temperature) on RHY at different tempering times. (a) Tempering time of 15 min, (b) tempering time of 30 min, and (c) tempering time of 45 min.

4.4. Mathematical model validation

Experimental data for grain temperature and moisture content obtained from Soponronnarit et al. (1999) were used in comparison with the model. Fig. 4 shows moisture content, grain temperature and head-rice yield during the drying, tempering and ambient air ventilation stages obtained from the experiments and the predictions, indicating that the predictions are in agreement with the experimental results. As seen in Fig. 4b, the temperature dropped steeply during the small interval of ventilation, thus causing great reduction of head-rice yield if the grain was not passed through the tempering section first even though the outlet moisture content of

paddy was not too low at the first stage. This effect can be seen clearly in Fig. 4c for the case (B) where the initial moisture content of paddy was 30% dry basis. However, such an effect is unimportant for case (A) where the initial moisture content was relatively higher than in case (B). This might be because the high moisture content, along with the high temperature, encouraged the development of a polymeric network of starch in the paddy structure, thus making the kernel more strengthened.

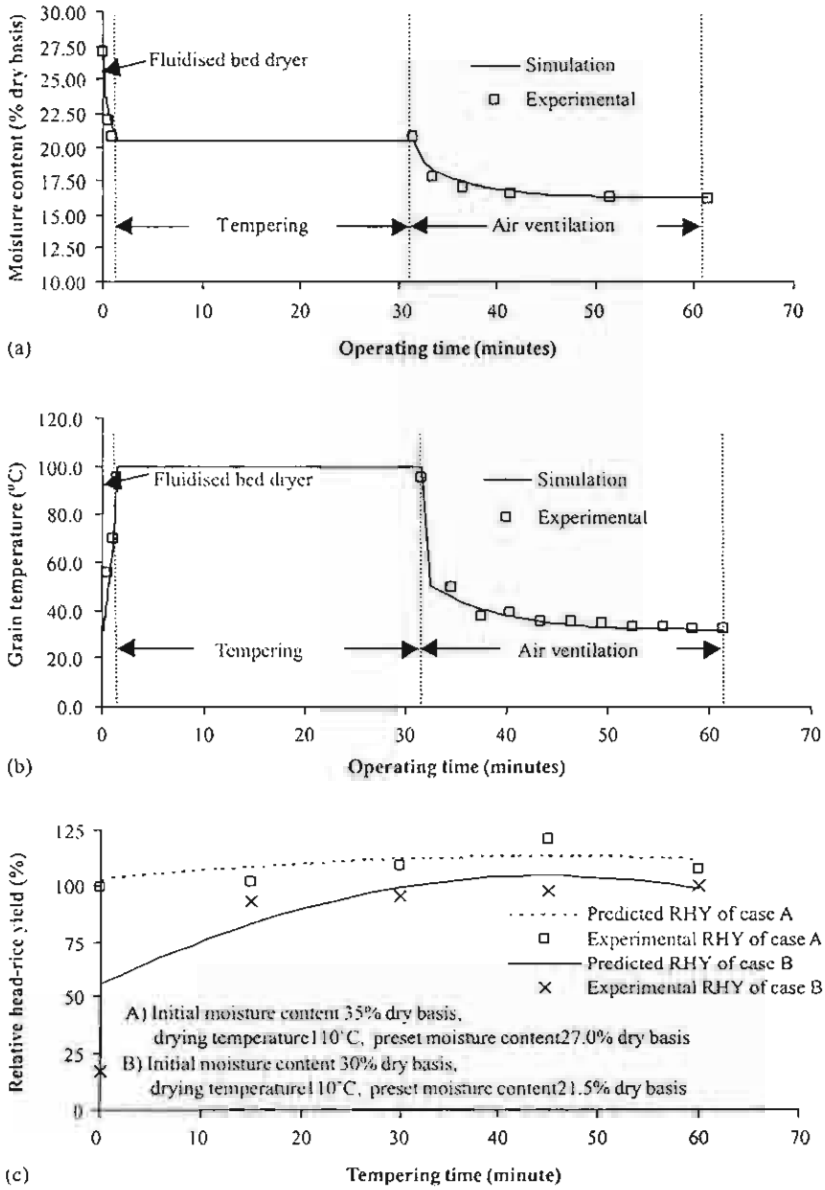


Fig. 4. Comparison of moisture content, grain temperature and RHY between experiments and simulations. (a) Moisture content, (b) grain temperature, and (c) RHY.

The results for head-rice yield indicate that the change in head-rice yield is rather complicated and depends on a number of parameters i.e. moisture content, tempering time and grain temperature. Such parameters ultimately relate to drying temperature. To obtain the appropriate drying conditions, that provide least drying time and maximise drying capacity and head-rice yield, the equations for heat and mass with incorporation of the head-rice equation need to be solved together.

4.5. *Effects of operating parameters on the operating time and the head-rice yield*

Even though drying time in the fluidised-bed dryer was only a small fraction of total operating time, it strongly affected the time required for the subsequent processes, i.e., tempering and ventilation, and head-rice yield. Thus, moisture content after first-stage drying, initial moisture content and drying temperature must be considered in this study.

The developed mathematical model was employed to determine the total operating time to achieve both a final moisture content of 16.5% dry basis and a grain temperature of 35 °C. Criteria for these simulations were as follows: (1) the fluidised-bed dryer was operated at a superficial air velocity of 2.2 m/s and a static bed thickness of 10 cm; (2) the ambient air was ventilated through a thin layer bed of 3 cm with a superficial air velocity of 0.075 m/s; (3) ambient conditions were 30 °C and 60% relative humidity, a normal range for tropical countries.

Tempering index is an important guideline to indicate how far the moisture content at the surface deviates from the equilibrium value at a finite time in the tempering stage. Several researchers (Steffe and Singh, 1980; Zhang and Litchfield, 1991; Tolaba et al., 1999) defined this index as

$$I_c = \frac{(M_{s,t} - M_{s,t=0})}{(M_{s,t=\infty} - M_{s,t=0})}, \tag{9}$$

where I_c is the tempering index and $M_{s,t}$ refers to the moisture content at the kernel surface at time t. Average moisture content of the kernel surface can be determined by the following equation:

$$M_{s,av} = \frac{\sum M_i V_i + \sum M_j V_j}{\sum V_i + \sum V_j}, \tag{10}$$

where i, j and V refer to the curved surface, the plane surfaces and the volume of the cylinder, respectively. Complete tempering (tempering index = 1.0) results in the most efficient drying performance when compared with the case of incomplete tempering (tempering index < 1.0). The required time for this is infinite. Steffe and Singh (1980) and Zhang and Litchfield (1991) found that a tempering index of 0.95 is an appropriate value which provides local moisture contents inside the grain similar to those obtained from the complete tempering. This value was thus used as a base line throughout these simulations.

The effects of preset moisture content and initial moisture content on RHY and operating time are shown in Figs. 5 and 6, respectively. Operating time increased linearly with increase in the preset moisture content but was independent of the initial moisture content. The increase in operating time resulted from the last stage requiring prolonged ventilation time. In considering the quality of paddy, it indicates that high RHY may be achieved when the preset moisture content of paddy is not too low.

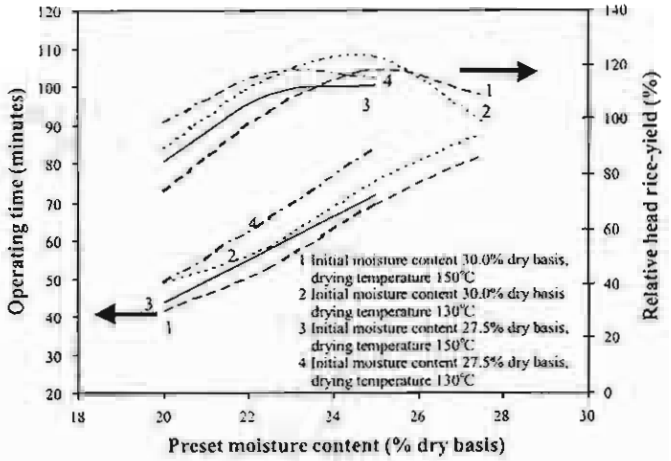


Fig. 5. Effect of preset moisture contents on total process time and RHY.

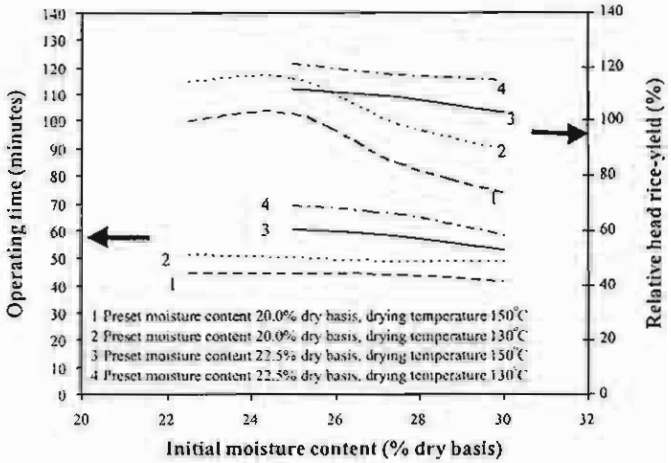


Fig. 6. Effect of initial moisture contents on total process time and RHY.

Some of the conditions which provided superior quality (as shown in Figs. 5 and 6) were selected to determine the effect of temperature on operating time and head-rice yield. In these simulations, we limited preset moisture contents at first-stage exit to 20 and 22.5% dry basis. The results demonstrate in Fig. 7 that operating time decreased moderately with increased temperature, as expected. RHY increased slightly with temperature until 130 °C and then decreased. These results suggest that inlet temperature should not be higher than 150 °C and preset moisture content should not be lower than 22.5% dry basis for high-temperature fluidised-bed drying.

Plots of tempering time versus RHY and operating time for drying temperatures of 130 and 150 °C are shown in Fig. 8. This figure shows that air ventilation through the paddy bed immediately after drying gave a very low quality of head rice in spite of relatively high values of

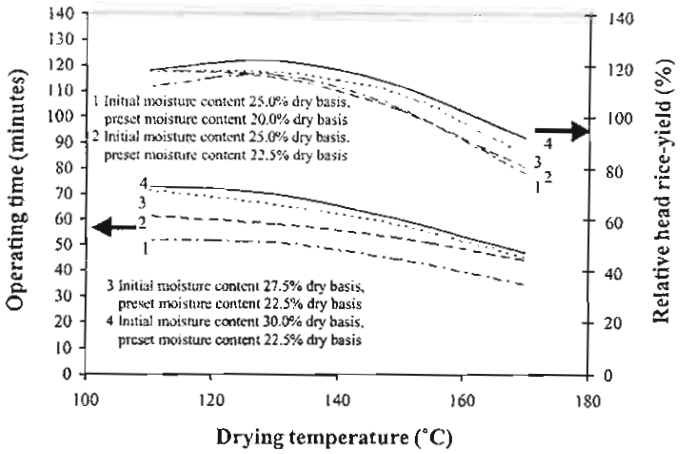


Fig. 7. Effect of drying temperatures on total process time and RHY.

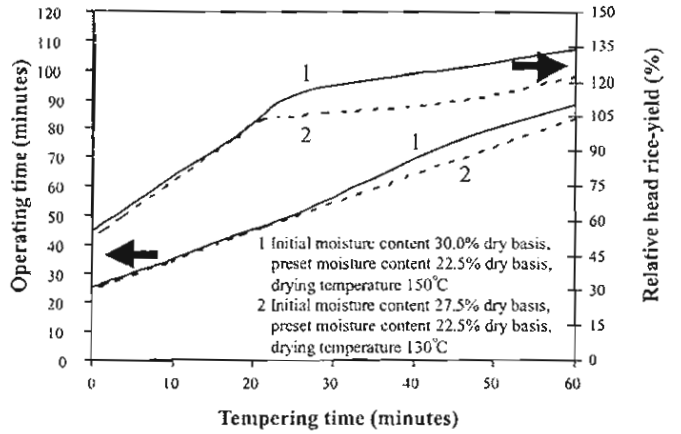


Fig. 8. Effect of tempering times on total process time and RHY.

preset moisture contents. Head-rice yield increased rapidly with tempering time. But after 25 min, the head-rice yield appeared to reach a limit, beyond which improvement was insignificant. Under such conditions, the colour of white rice is still acceptable as reported by Soponronnarit et al. (1999).

5. Conclusions

The experimental and simulation results for drying using the fluidised-bed dryer, tempering and ambient air ventilation can be summarised as follows:

1. A drying process with no tempering between stages causes low head-rice yield. The reduction in head-rice yield can be improved by the tempering technique.

2. A second-order polynomial equation can be fitted to experimental values of head-rice yield with the tempering time in which their coefficients are related to preset moisture content and grain temperature.
3. As a compromise between operating time and high head-rice yield, the maximum temperature to be used for the first-stage is 150 °C and the moisture content at any level should not be reduced to lower than 22.5% dry basis in the fluidized bed. The tempering time for such conditions must be at least 25 min.

Acknowledgements

The authors would like to express their sincere thanks to the Thailand Research Fund for financial support and The Division of Agricultural Engineering, Department of Agriculture, Thailand, for milling tests.

References

Kunze, O.R., 1996. Effect of drying on grain quality. In: Champ, B.R., Highley, E., Johnson, G.I. (Eds.), Grain Drying in Asia. Proceedings of an International Conference held at the FAO Regional Office for Asia and the Pacific, Bangkok, Thailand, 17–20 October 1995, ACIAR Proceedings No. 71, pp. 178–185.

Laithong, C., 1987. Study of thermo-physical properties of rough rice. Master's Thesis, King Mongkut's Institute of Technology Thonburi, Bangkok.

Li, Y.B., Cao, C.W., Yu, Q.L., Zhong, Q.X., 1999. Study on rough rice fissuring during intermittent drying. Drying Technology 7, 1779 -1793.

Poomsa-ad, N., Soponronnarit, S., Prachayawarakorn, S., Terdyothin, A., 2002. Effect of tempering on subsequent drying of paddy using fluidisation technique. Drying Technology 20, 195–210.

Sabbath, M.A., 1970. Convective heat transfer coefficient and tempering effects on cooling rate of shelled corn. Ph.D. Thesis, Purdue University, Lafayette, IN.

Soponronnarit, S., Wetchacama, S., Swasdisevi, T., Poomsa-ad, N., 1999. Managing moist paddy by drying, tempering and ambient-air ventilation. Drying Technology 17, 335 -344.

Steffe, J.F., 1979. Moisture diffusion and tempering in the drying of rough rice. Ph.D.Thesis, Department of Agricultural Engineering, University of California, Davis. Unpublished.

Steffe, J.F., Singh, R.P., 1980. Theoretical and practical aspects of rough rice tempering. Transactions of the American Society of Agricultural Engineering 23, 775 -782.

Steffe, J.F., Singh, R.P., Bakshi, A.S., 1979. Influence of tempering time and cooling on rice milling yields and moisture removal. Transactions of the American Society of Agricultural Engineering 22, 1214–1218 1224.

Tolaba, P., Aguerre, R.J., Suárez, C., 1999. Drying simulation of corn with tempering. Drying Technology 17, 1081–1093.

Zhang, Q., Litchfield, J.B., 1991. An optimization of intermittent corn drying in a laboratory scale thin layer dryer Drying Technology 9, 233–244.

Drying Technology, 23: 205–223, 2005
Copyright © 2005 Taylor & Francis, Inc.
ISSN: 0737-3937 print/1532-2300 online
DOI: 10.1081/DRT-200047892

Taylor & Francis
Taylor & Francis Group

Simultaneous Momentum, Heat, and Mass Transfer with Color Change during Paddy Storage in Silo

Somkiat Prachayawarakorn*
Faculty of Engineering, King Mongkut's University of Technology Thonburi, Bangkok, Thailand

Chate Choteboon and Somchart Soponronnarit
School of Energy and Materials, King Mongkut's University of Technology Thonburi, Bangkok, Thailand

Abstract: A theoretical model has been developed to describe heat, mass, and momentum phenomena in cylinder-shaped silos where paddy is stored. Calculation based on the model predicts local temperature and moisture within the silo as a function of time and space. This information is then coupled with known kinetics of color change to predict yellowness or whiteness generated during storage. The model is evaluated using the published data. Natural air currents and the corresponding moisture migration are small for short storage periods and more extensive for long-term storage. The calculated result shows the similar trend to the published data in that moisture migrates from the central region, where the grains experience high temperature, to the outer regions, where the grains have lower temperatures. Paddy near the wall and on the top of the silo has relatively lower whiteness than at inner areas for storing it at 15% wet basis, this low luminosity is in part motivated by relative humidity, which is relatively high at such areas. At elevated initial moisture contents, paddy at the inner areas has lower whiteness due to large accumulation of heat from grain respiration, hence, it is a predominant effect on the color change, while the humidity plays a minor role.

Keywords: Mixed convection; Paddy; Storage; Yellowness

*Correspondence: Somkiat Prachayawarakorn, Faculty of Engineering, King Mongkut's University of Technology Thonburi, Suksawat 48 Road, Bangkok 10140, Thailand; E-mail: somkiat.pra@kmutt.ac.th

INTRODUCTION

Freshly harvested paddy contains moisture content higher than 25% dry basis. At this moisture level, paddy cannot be kept for a long time. In common practice, water content inside the kernel is removed by convective dryers; i.e., mixed flow, fluidized bed, and circulating dryer. The safe moisture level is between 14 and 16% dry basis. After processing, paddy is stored in silos, at least 6 months before milling. This storage period is a typical condition used in rice industries for domestic consumption.

During storage period, heat generated from respiration of grains and insects increases the temperature in grain bulk. The gradient of temperature subsequently encourages the air currents to circulate within the bulk. The natural air currents lead to water vapor in warm regions of the grain stores escaping to cooler areas.[1,2] In the warm regions, vapor pressure in gas phase is high and moisture content in grains is loosed. As the air reaches the cooler regions, its relative humidity escalates, thereby gaining moisture content of grains. The moisture migration produces nonuniformity of moisture content of paddy. The areas where the moisture content of grains is increased may lead to deterioration of their qualities, i.e., grain agglomeration and loss of native color and head-rice yield. The grain agglomeration is found near the walls of silos where the vapor pressure is low and the temperature gradient is relatively large,[3] and the discoloration is found inside of the bulk where temperature is high.

Another factor affecting the natural convection in silos is the solar radiation. The amount of heat absorbed by silos due to radiation mode is difficult to predict due to many factors, including silo position, geographical area, absorptivity/reflectivity properties of material, and cloudiness.[2] However, the radiative heat transfer effect is insignificant compared to the heat from the respiration. With radiation effect, temperature variation in the bulk was present only at a depth not far from the periphery.[4]

In the present work, the transport models of heat, mass, and momentum in conjunction with the kinetics of rice yellowing are developed to describe phenomenological and color changes that occur when the grains are stored under tropical weather conditions.

MATHEMATICAL MODEL

The paddy is supposed to be stored in a perfectly sealed silo that has a cylindrical geometry with a dimension of 6 m height and 3 m diameter as shown in Fig. 1. This simple geometry is rather modified to make the calculation easily. In fact, silos that are used in the rice industry have a cylindrical shape with a conical base. The conical base is designed for effectively unloading paddy from the bin, without a dead zone. In addition to the simple geometry, the moisture migration and temperature

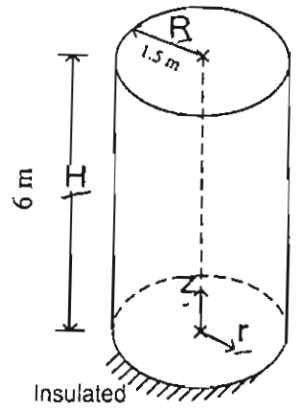


Figure 1. Idealized geometry of grain storage.

gradient presumably occur in two-dimensional systems, both radial and axial directions. However, this simplified approach can be extended to grain storages that are three-dimensional systems or that have arbitrary shapes. The method involves using a mathematical transformation of the grain storage into a computational domain that has the simple geometry of a cube.[5,6] The fundamental equations of heat, mass, and momentum, including the kinetics of rice yellowing, apply to storages, regardless of their shape, and the initial and boundary conditions must be given to solve the problems of convective flow and quality change.

Heat Transport Model

The stored grains release the energy from their respiration, resulting in an increase of temperature in the bulk. The increased temperature produces the natural convective air flow that carries not only moisture but also heat from one region to others. To describe such change, the energy balance was made for a small element in the grain bulk and the energy equation is written as:

$$\rho_s \varepsilon_s (C_s + WC_l)\frac{\partial T}{\partial t} + \rho_a \varepsilon_a (C_a + \omega C_l)\frac{\partial T}{\partial t} + \rho_a (C_a + C_v)\left[v_r \frac{\partial T}{\partial r} + v_z \frac{\partial T}{\partial z}\right]$$

$$= k_{\text{eff}}\left[\frac{\partial^2 T}{\partial r^2} + \frac{1}{r}\frac{\partial T}{\partial r} + \frac{\partial^2 T}{\partial z^2}\right] + \rho_s \varepsilon_s (Q_r - 0.6 h_v)\text{DML} \qquad (1)$$

In writing Eq. (1), the energy source from solar radiation is negligible since grain is a good insulator. The first two terms on the left-hand side of Eq. (1) account for the change of temperatures of grain and air with time, assuming temperature in phases of solid and gas to be equal.

The last term on the left-hand side of Eq. (1) represents the bulk heat flow, carried by the natural convective currents. The net change of internal energy, plus the heat flow term, is equal to the energy conducted through the grain bulk, presented by the first term on the right-hand side of Eq. (1), and the generation energy released from paddy, presented by the second term on the right-hand side of Eq. (1). The generation energy is obtained from the respiration energy minus the energy used for vaporizingthe water, which is produced from grain respiration.

The temperature distribution in the bulk can be known when the initial and boundary conditions are specified. In this work, we suppose the temperatures at the wall and on the top of silo equal to weather temperature, and average ambient temperature on the day and night times are used as boundary condition. In addition, it is usual to assume that the floor of the silo is thermally insulated. Along the periphery of grain bulk, the following boundary conditions are:

$$T(R,z,t) = T(t) \quad \text{at } r = R \quad 0 \le z \le H \text{ for } t \ge 0 \tag{2}$$

$$T(r,H,t) = T(t) \quad \text{at } z = H \quad 0 \le r \le R \text{ for } t \ge 0 \tag{3}$$

$$\frac{\partial T(r,0,t)}{\partial z} = 0 \quad \text{at } z = 0 \quad 0 \le r \le R \text{ for } t \ge 0 \tag{4}$$

The last boundary condition assumed is the maximum temperature at the center as given by

$$\frac{\partial T(0,z,t)}{\partial z} = 0 \quad \text{at } r = 0 \quad 0 \le z \le H \text{ for } t \ge 0 \tag{5}$$

Rate of dry matter loss, $\dot{DML}$, can be readily determined if the moisture content of paddy is known. Respiration is the process of oxidizing carbohydrates and producing carbon dioxide and water vapor, as well as energy. Respiration therefore consumes the amount of dry matter of paddy. Teter[7] reported that the rate of dry matter loss was higher with higher moisture content. His data were statistically fitted with two empirical equations proposed in the present study, each of which is suitably described for each moisture range. A power equation was applied to low moisture content of 13 to 16% wet basis and a polynomial equation with a third degree was used for a higher range of moisture content. The empirical equations of dry matter loss for such moisture ranges are expressed by:

$$\dot{DML} = 7 \times 10^{-11}(100 \times W)^{8.531} \quad 0.13 \le W \le 0.16 \text{ wet basis} \tag{6}$$

$$\dot{DML} = -0.0636(100 \times W)^3 + 4.0827(100 \times W)^2 - 80.608(100 \times W) + 505.38 \quad 0.16 \le W \le 0.28 \text{ wet basis} \tag{7}$$

To obtain the temperature distribution, Eq. (1) is written as the discretized form, in which the first derivatives are written using backward differences and the second derivatives with central differences, and then solved by alternating direction implicit method.[8] This method treats the problem as being implicit in the direction of one coordinate, the r coordinate given by the present work, during the first half of a time increment and the temperatures in the z-direction are carried out explicitly. During the second half, the temperature in z component is advanced implicitly, while temperatures in the r-direction are treated explicitly. Temperature distribution in the bulk is known by simply solving a set of Eq. (1)–(7) using the tridiagonal method algorithm.[8]

Moisture Transport Model

Moisture migration in silos is caused by two possible mechanisms, natural convection and diffusive transport, with the first mechanism in the majority. The moisture movements in the bulk can accordingly be described by:

$$\rho_s \varepsilon_s \frac{\partial W}{\partial t} + \rho_a \varepsilon_a \left(v_r \frac{\partial \omega}{\partial r} + v_z \frac{\partial \omega}{\partial z} \right) = D_{\text{eff}} \varepsilon_a \rho_a \left(\frac{\partial^2 \omega}{\partial r^2} + \frac{1}{r}\frac{\partial \omega}{\partial r} + \frac{\partial^2 \omega}{\partial z^2} \right) + 0.6 \rho_s \varepsilon_s \dot{DML} \tag{8}$$

The first term on the left-hand side of Eq. (8) presents the moisture content of paddy that will decrease or increase depending upon the local relative humidity and temperature surrounded the existing kernels, and the second term describes the water vapor flow in bulk. On the right-hand side, the first term shows the water vapor diffusion through the void spaces of bulk grain; the last term accounts for the water vapor produced by the respiration.

In this study, we assume that the water vapor cannot diffuse through the wall of the silo and the moisture content of stored grains initially has uniform moisture content. Hence, the boundary conditions may be written as

$$\frac{\partial \omega(R,z)}{\partial r} = 0 \quad \text{at } r = R \text{ and } 0 \le z \le H \tag{9}$$

$$\frac{\partial \omega(r,H)}{\partial z} = 0 \quad \text{at } z = H \text{ and } 0 \le r \le R \tag{10}$$

$$\frac{\partial \omega(0,z)}{\partial r} = 0 \quad \text{at } r = 0 \text{ and } 0 \le z \le H \tag{11}$$

$$\frac{\partial \omega(r,0)}{\partial z} = 0 \quad \text{at } z = 0 \text{ and } 0 \le r \le R \tag{12}$$

Except for the other boundaries, the boundary in Eq. (9) implies the lowest moisture content at the central bulk. Before solving Eq. (8) to detemine the moisture content, it is essential to know the humidity ratio of air surrounding the kernels. The air humidity is calculated by using a psychometric equation given elsewhere.[3] Due to very low natural convective currents, the moisture content of the grains changes very slowly, and the explicit method is used to calculate the moisture content at the internal nodes for the advanced time step.

Momentum Model

Darcy's equation, where the pressure gradient is directly proportional to the velocity gradient and the hydrostatic head, is applied to describe the buoyancy-driven flows in silo, and is mathematically expressed as

$$\nabla p = \frac{\mu}{\kappa}\vec{v} - \rho_a \vec{g} \tag{13}$$

Rearrangement of Eq. (13) and writing in terms of velocity components yields:

$$v_r = -\frac{\kappa}{\mu}\frac{\partial p}{\partial r} \tag{14}$$

$$v_z = -\frac{\kappa}{\mu}\left(\frac{\partial p}{\partial z} + \rho_a g_z\right) \tag{15}$$

Differentiation of Eq. (14) with respect to z is minus with the r derivative of velocity component in Eq. (15), giving

$$\frac{\partial v_r}{\partial z} - \frac{\partial v_z}{\partial r} = \frac{\kappa g_z}{\mu}\frac{\partial \rho_a}{\partial r} \tag{16}$$

To account for the buoyancy force effect, the air density varying with temperature is approximated by Boussinesq's equation,

$$\rho_a = (\rho_a)_o[1 - \beta(T - T_o)] \tag{17}$$

White[9] defined the velocity components in the form of stream functions as follows:

$$v_r = \frac{1}{r}\frac{\partial \psi}{\partial z} \tag{18}$$

$$v_z = -\frac{1}{r}\frac{\partial \psi}{\partial r} \tag{19}$$

Differentiation of Eqs. (17) and (19) with respect to r, and Eq. (18) with respect to z, is replaced into Eq. (16), yields the expression for behavior of stream function:

$$\frac{\partial^2 \psi}{\partial^2 z} + \frac{\partial^2 \psi}{\partial^2 r} = -\frac{r\kappa g_z (\rho_a)_o \beta}{\mu}\frac{\partial T}{\partial r} + \frac{1}{r}\frac{\partial \psi}{\partial r} \tag{20}$$

Because of the impermeable surfaces at the wall, bottom, and top, the following boundary conditions on stream function are

$$\psi(R, z) = 0 \quad \text{at } r = R \quad 0 \le z \le H \tag{21}$$

$$\psi(r, H) = 0 \quad \text{at } z = H \quad 0 \le r \le R \tag{22}$$

$$\psi(r, 0) = 0 \quad \text{at } z = 0 \quad 0 \le r \le R \tag{23}$$

In addition to the impermeable boundaries, the necessary boundary condition for central region of the bulk, which presents no flow across the line of symmetry, is

$$\psi(0, z) = 0 \quad \text{at } r = 0 \quad 0 \le z \le H \tag{24}$$

The stream function expression, along with the boundary conditions, was solved explicitly using temperature field calculated from Eq. (1). The calculation procedure was repeated until the temperature difference between two subsequent calculations was less than 10^{-3}.

Kinetics of Rice Yellowing

During grain storage, the environmental conditions in the bulk, i.e., relative humidity and temperature, stimulate the color of paddy to be changed from white to yellow. The color change, measured by the h-value, was explained accordingly by zero-order reaction:[10]

$$\frac{dh}{dt} = k \tag{25}$$

where

$$k = \exp\left(71.87 - 25.32\mathrm{RH} - \frac{25{,}919.3}{T + 273.15} + \frac{10{,}712.78\mathrm{RH}}{T + 273.15}\right) \tag{26}$$

The relationship between the whiteness and h-value was given by[11],

$$W = 85.1 - 3.36h \tag{27}$$

Table 1. Some physical and thermal properties used in the model

Specific heat $C_s = 1.292 + 4.2\,W$*
Effective thermal conductivity $k_{eff} = 0.319 + 0.479\,\frac{W}{1+W}$*
Permeability of grain bulk $\kappa = 9.27 \times 10^{-9}$**
Porosity $\varepsilon_s = 0.623 - 0.25\,W$*
Bulk density $\rho_s = 552 + 282\,W$*

*See Soponronnarit[16] and **Thorpe.[3]

RESULTS AND DISCUSSION

The result from calculation should be independent of the grid sizes and the time steps. In general, as the grid sizes and time steps are made smaller, the errors resulting from the discretization of the governing equations become smaller. In the present study, many grid sizes, together with the time steps, were tried and it was found that a grid size of 16 points in the radial direction and 61 points in the axial direction, and a time step of 50 seconds, were fine enough to represent the simultaneous transport of heat, mass, and momentum. Some physical and thermal properties used in the model are presented in Table 1. Figure 2 illustrates the cyclic change of ambient air temperature during storage and it is used as boundary condition in Eqs. (2) and (3) for solving the thermal transport equation.

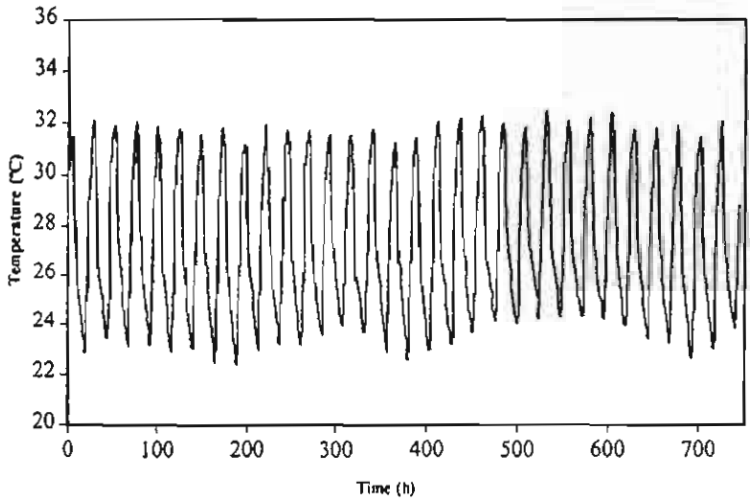


Figure 2. Illustration of ambient air temperature during storage.

The mathematical model was validated with the experimental data as reported by Naupanich et al.[12] In their work, paddy with an initial moisture content of 14 to 15% wet basis was stored in steel silos, with a dimension of 6 m height and 3 m diameter for which a 20-ton paddy was kept. Paddy was collected in two silos, one with the inside wall layered with bamboo sheet and another silo without bamboo sheet. The grain temperature at the beginning was 30°C. The experiments were started in March and finished in October, covering the critical period when paddy is easily deteriorated.

Validation of the Model

Figure 3 shows the change of temperature in the bulk when paddy was stored in the silos with the inside wall covered with bamboo sheet and without bamboo sheet. The temperature difference for both silos throughout the storage period is very small, presenting the grains acting as a good insulator so that a bamboo sheet lining does not assist heat prevention from the outside. The average temperatures within bulk for both silos are increased by approximately 2°C for 4-month storage and 5°C for 7-month storage. A comparison between experimental and predicted results is also shown in Fig. 3. Both experiment and calculation show the same tendency, with temperature being highest at the middle and declining toward the exterior surface. The variation in temperature of the paddy bulk is probably due to the combined effect of natural air flow and respiration reaction that is usually higher with higher moisture content.

Figure 4 illustrates the experimental and calculated moisture profiles of paddy in silo the period of 6-month storage. After long-term storage, moisture content of paddy stored in the silo changes such that the moisture content of paddy at the inner positions of bulk is lower than at the outer positions, with the highest moisture content near the silo wall. For the 6-month storage, the moisture content of paddy, measured at 3 m height from the silo base, was 13.5% w.b. at the center and 15.8% w.b. near the wall. This change, which is opposite to the result of measured temperature, confirms that moisture migrates from warm regions to cooler regions. The moisture migration is due to the combined effects of water vapor diffusion, which transports through interglanular spaces, as a result of vapor pressure difference and convective airflow as a result of temperature difference.

Temperature Distribution

Figure 5 shows the simulation results of temperature distribution in the bulk at different storage periods. In calculation, we supposed that paddy

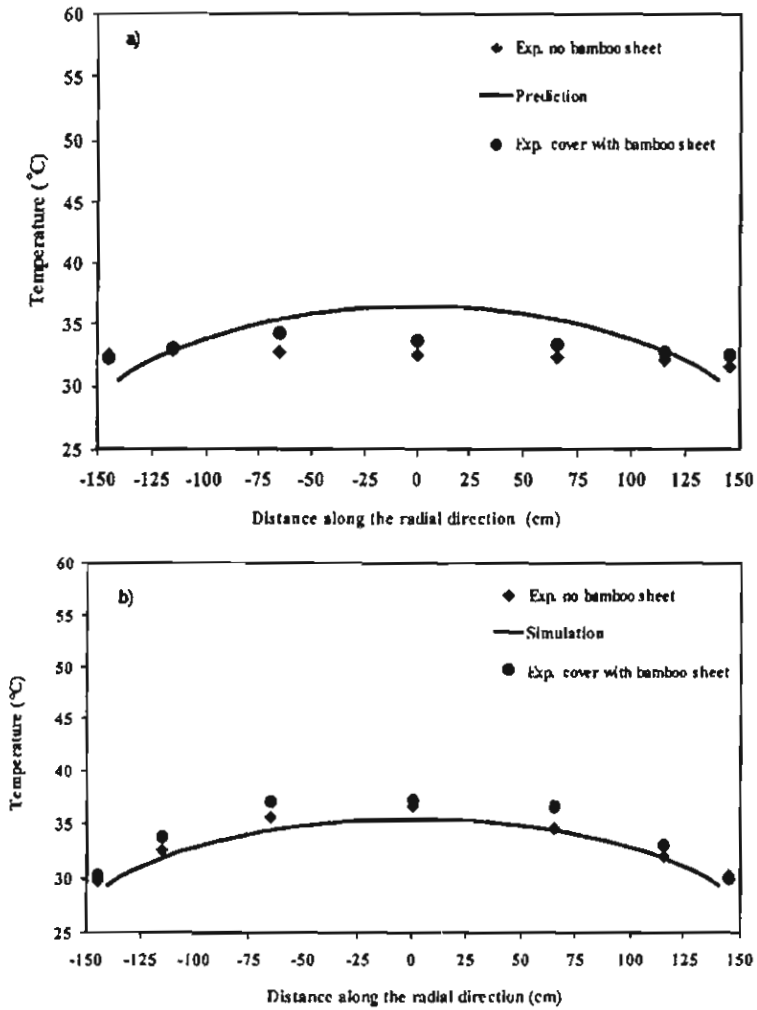


Figure 3. Temperature distribution in steel silos covered with and without bamboo sheet and prediction from the model (at positions of 3 m height from base): a) 4 months storage, and b) 7 months storage.

kept in the silo had an initial moisture content of 15% wet basis. After one month, a small creation of temperature gradient is obvious, as indicated by a small number of isothermal lines, and when the grains are stored for longer than 4 months a larger temperature gradient is evident. Note that at 8-months storage, temperatures inside the bulk are reduced

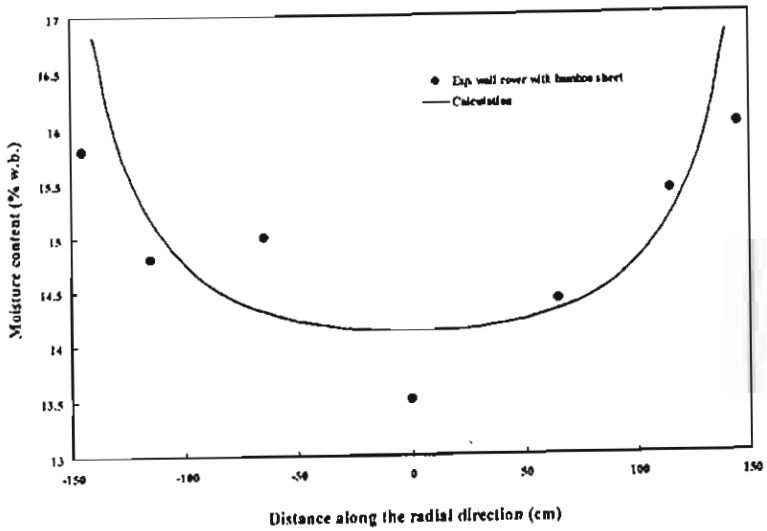


Figure 4. Moisture profile in silo at the period of 6 months storage and prediction from the model (measured at 3 m height from base).

to be relatively lower than that at 4-months storage (average ambient air temperature of 32°C at 4th month storage). This result is affected by the change of weather condition: the ambient temperature at 8-months storage was relatively cooler (average ambient air temperature of 29°C), resulting in more heat transferring from paddy bulk to the environment.

From this figure it also can be seen that the high temperature zone is moved to the upper level. If the storage period is extended further, we expect the higher temperature to be taken place above the middle region of the grain bulk. This part is reflected by the high-temperature air currents that move up to the higher level.

Streamlines and Velocity Components

Figure 6 presents the stream lines at different storage periods. The buoyancy-driven air flow transports within the grain bulk in a way that it moves vertically up to the top part at the center region and then moves down near the inside wall. The natural convection flows that occur are very low for short storage periods and become higher for a longer period, similar to the behavior of temperature distribution. The stream lines presented in Fig. 6 were used to calculate the velocity components of radial and axial directions by Eqs. (18) and (19), respectively, and the calculated results are shown in Fig. 7. It is clear that the radial velocity is very high

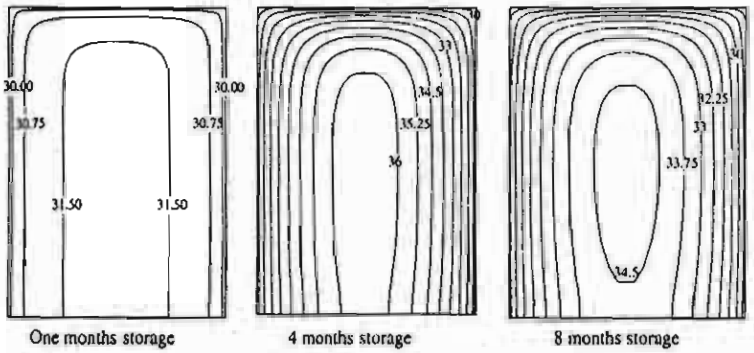


Figure 5. Temperature distribution in grain bulk.

at the bottom and on the top of the grain bulk and almost zero for the region far from the edges, indicating that any flow within the bulk exists only in the axial direction as shown in Fig. 7b. The radial velocity on the top moves in the direction from the inside to the outside, whereas it moves in the opposite direction for the bottom region, as indicated by the arrow.

Moisture Distribution

Figure 8 shows the moisture migration in silo where it is absent at the 1 month storage, although there is a small temperature gradient and

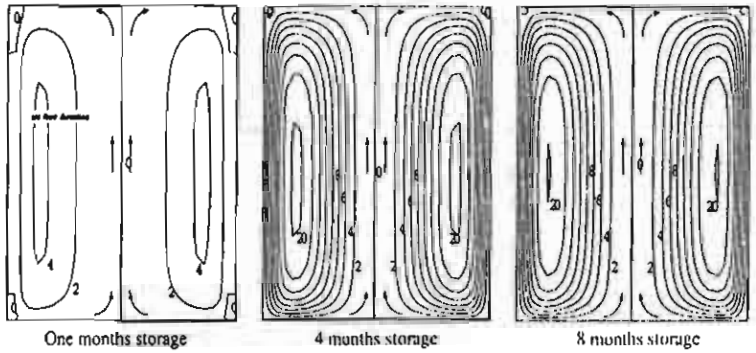


Figure 6. Stream lines at different periods of storage ($\times 10^{-6}$ m^3/s).

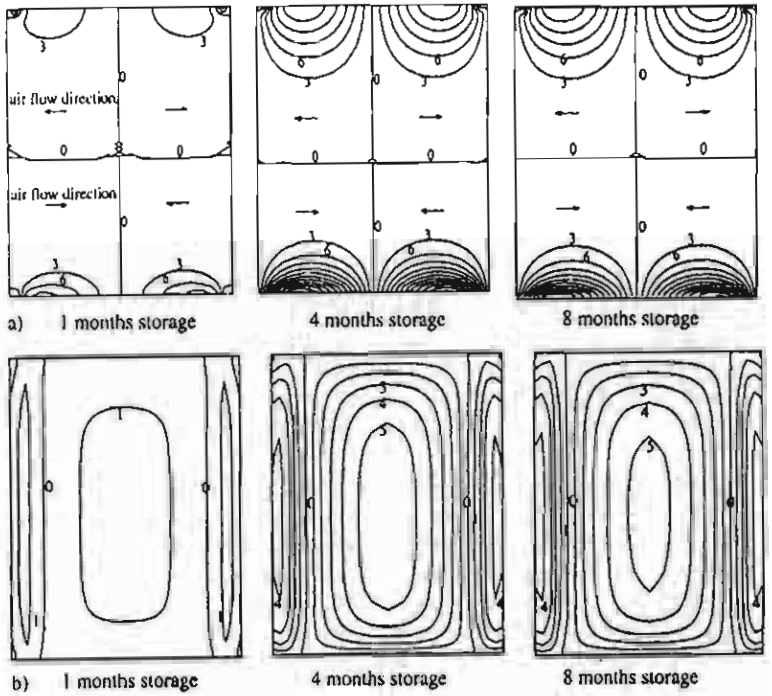


Figure 7. Change of velocity components at different storage periods ($\times 10^{-6}$ m/s): a) velocity component in radial direction, and b) velocity component in axial direction.

natural convective air flow. As the storage period is longer than 4 months, the moisture movement is shown up near the inside of the wall and at the top of silo where the moisture content of paddy increases to 15.6% wet basis. This reflects the effects of the temperature field and the flow field where the air rises from the warm central region to the upper surfaces. At 8 months storage, the moisture content of paddy changes to 16.1% wet basis at the periphery, whereas the moisture content of paddy at the central region becomes lower than the initial value. This moisture content is highest compared to that at the other regions, and it corresponds to the region where the vertically downward velocities are high, as evidence of many stream lines close together. The calculated results agree with several findings,[1,3] in which the grains near the wall and at the top of the bin gained in moisture content, resulting in the agglomeration of grains.

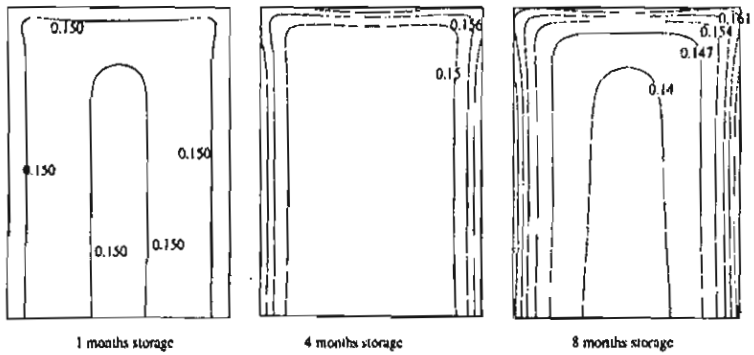


Figure 8. Moisture distribution in silo at different storage periods (decimal wet basis).

Whiteness Distribution

Color of product reflects a sensation to human eye and the visual examination is common method of evaluating product quality. In view of commercial, the white color for paddy is favorably preferred and is accepted for premium price. The change of color, due to browning reactions, is caused by the reactive components in paddy activated under suitable storage condition.

As reported by several researchers for agricultural materials, the maximum browning rate occurs under the range of relative humidity of 70 to 80%.[13,14] In simulation, we assumed that the color of stored paddy had an initial *b*-value of 11.5, corresponding to value of rice whiteness of 46.4. The combined effects of natural convective flow and temperature gradient produce the color change, from white to yellow color, and its change is relatively more complicated than the moisture migration behavior since the development of yellow pigment is stimulated by the temperature and relative humidity, the first being the most important factor. The natural air currents carrying the water vapor evaporated from the grains generate the different levels of relative humidity at the positions within the bulk. The complex behavior is elucidated in Fig. 9. The value of whiteness is inversely related with *b*-value, according to Eq. (27). In general, higher temperature and relative humidity result in lower whiteness. At the first month storage, the value of whiteness around the exterior surface of the grain bulk is slightly lower than that at the interior, indicating the dominant effect of relative humidity on lowering of whiteness value, while the temperature effect is insignificant because the temperature difference between inner and outer is small, as previously shown in Fig. 4.

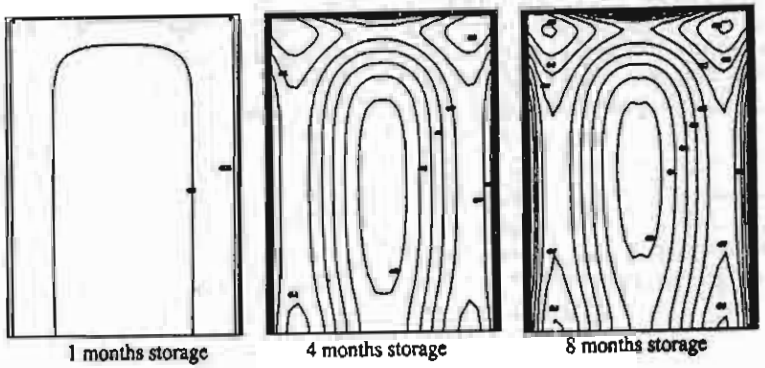


Figure 9. Whiteness distribution in the bulk during storage (initial moisture content of 15% wet basis).

When the difference of temperature is larger for a longer period, i.e., 3 months storage, the change of whiteness within the bulk is, in turn, different from that found for shorter storage periods. In this case, the values of whiteness at the inner part of the grain bulk are almost lower than at the outer part, except for the color of paddy near the wall and on the top of silo, which shows a value of 43.5. The lower whiteness at the inner areas, compared to the outer areas, is caused by the higher temperature within bulk, which plays an important role in forming yellow pigment.

In contrast, for the paddy near the wall and on the top of the bulk where the radial and axial velocities are very high, the temperature is less influential to the color development compared with the relative humidity effect. The prevalent contribution of relative humidity stimulates the reactive components existing inside the kernel and thus leads to relatively lower value of rice whiteness at such areas than at the inner part. The similar result is also found in 8 months storage.

Effect of Initial Moisture Content

This section draws attention to the applicable developed models to explore how long the moist paddy can be kept, without deterioration of color, when the paddy at different initial moisture contents is stored. This information is very useful for related industries to ensure that the paddy is still safe. In harvesting season a large amount of paddy is directly transported to the industries and it may not be dried immediately due to limitation of drying equipment, so that the remaining portion in

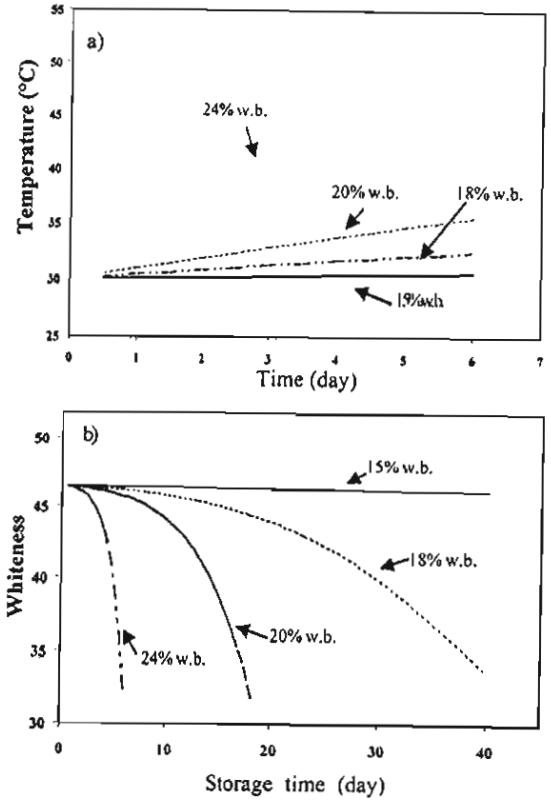


Figure 10. Changes of temperature and color of paddy with storage time at different initial moisture contents: a) average temperature, and b) whiteness.

practice is placed on a concrete pad under shade. In the simulation, we supposed that paddy was kept in a silo.

The simulated results shown in Fig. 10 are presented in a form of the average value. The average values of temperature and whiteness are respectively calculated by:

$$\overline{T} = \frac{\iint T(r,z)2\pi r dr dz}{\iint 2\pi r dr dz} \tag{28}$$

$$\overline{W} = \frac{\iint W(r,z)2\pi r dr dz}{\iint 2\pi r dr dz} \tag{29}$$

The increase in temperature in the bulk strongly depends on initial moisture content and the storage period. The rapid rise in temperature, due to high respiration rate of paddy, is obvious with high initial moisture content. This is clearly illustrated in Figure 9a by the case of initial moisture content of 24% wet basis at which temperature linearly strikes from 30°C at the beginning to 45°C on the fourth day of storage. As the initial moisture content becomes lower, the increasing rate of temperature is obviously lower. Similarly, Raj and Singaravadivel[15] reported that a temperature rise of 2, 6, and 19°C over the ambient temperature was observed in moisture contents of 17.9%, 22.8%, and 25.7% wet basis, respectively, after seven days for storing paddy without drying.

According to the result of temperature change, the limitation of storage period for storing paddy at high moisture level, i.e., 18, 20, and 24% wet basis, is governed only by the temperature, since the high temperature promotes the components inside the kernel to be more reactive. In this circumstance, the whiteness of paddy goes from highest value at the periphery of silo to the lowest value at the center. However, the relative humidity is somewhat more important for the paddy at low moisture content, due to low respiration rate, and this effect is shown in Fig. 9.

As shown in Fig. 10b, the drop of whiteness value is very fast for initial moisture content of 24% wet basis and the yellowing rate declines with lowering of initial moisture content. To obtain the acceptable white color, the paddy at initial moisture contents of 24, 20, and 18% wet basis should not be kept longer than 4, 9, and 18 days, respectively; otherwise, the color of paddy in some places within bulk becomes lower than 35, which is not acceptable for producing white rice.

CONCLUSIONS

The temperature gradient is a main cause of the natural convective air currents and the corresponding moisture migration in the paddy bulk. Mathematical models for the heat, mass, and momentum transfers, with incorporation of yellowing kinetics, are used to describe their changing behaviors in the cylinder-shaped silo and the computational results reasonably agree with the published data. The amount of air currents and water migration is very small for short storage periods and becomes larger for a longer period, thereby gaining in moisture content of paddy at the outer region of the bulk. In contrast to water movement behavior, the paddy located at the inner part of the bulk has a relatively lower whiteness than at the outer part, except for the sample near the wall and at the top of the bulk where the whiteness is lowest. The simulation has been made further to investigate the initial moisture content effect and the results

show a shorter storage period with higher initial moisture content if the color of paddy is to be maintained as an acceptable white color.

NOMENCLATURE

C	specific heat, kJ/kg°C
D_{eff}	effective diffusivity of water vapor through grains, m^2/s
DML	rate of dry matter loss, kg/s
g	gravity vector, m^2/s
H	height of silo, m
h_v	heat of vaporisation, J/kg
k_{eff}	effective thermal conductivity of paddy, $W/m^{2o}C$
Q_r	heat from respiration, J/kg of dry matter
P	pressure, Pa
R	radius of silo, m
RH	relative humidity of air, decimal
r	distance in radial direction, m
T	temperature, °C
t	time, s
v	velocity vector, m/s
W	moisture content of paddy, decimal dry basis, or whiteness
z	distance in axial direction, m
ψ	stream function, m^3/s
ε	porosity
ρ	density, kg/m^3
ω	humidity ratio, kg water/kg dry air
κ	permeability of grain bulk, m
μ	viscosity of air, Pa s/m
β	volume expansivity of air, 1/K

Subscripts

a	dry air
l	water
O	reference state
r	radial direction
s	dry matter of paddy
v	water vapour
z	axial direction

ACKNOWLEDGEMENT

The authors thank the Thailand Research Fund for supporting this work.

REFERENCES

1. Griffith, H.J. Bulk storage of grain: a summary of factors governing control of deterioration. Melbourne, Australia, CSIRO Division of Mechanical Engineering, Report ED8, 1964.
2. Freer, M.W.; Siebenmorgen, T.J.; Couvillion, R.J.; Loewer, O.J. Modeling temperature and moisture content changes in bunker-stored rice. American Society of Agricultural Engineers **1990**, *33*, 211–220.
3. Thorpe, G.R. Modelling moisture migration in stored grains. In *Grain Drying in Asia: Proceedings of an International Conference*, Bangkok: Thailand, October 17–20, 1995; Champ, B.R., Highly, E., Johnson, G.I., Eds.; 1995; 99–122.
4. Babbit, J.D. Thermal properties of wheat in bulk. Canadian Journal Res. **1945**, *23*, 388–401.
5. Singh, A.K.; Thorpe, G.R. A solution procedure for three-dimensional free convective flow in peaked bulks of grain. Journal of Stored Products Research **1993**, *29*, 221–235.
6. Shih, T.I.P.; Bailey, R.T.; Nguyen, H.L.; Roelke, R.J. Algebraic grid generation for complex geometries. International Journal of Mechanical Fluids **1991**, *13*, 1–31.
7. Teter, N.C. *Grain Storage*. Published by SouthEast Asia Post-Harvest Research and Development Programme, Searca College: Philippines, 1981, 1–86.
8. Hoffman, J.D. *Numerical Methods for Engineers and Scientists*, McGraw-Hill, Inc. 1992, 42–50.
9. White, F.M. *Fluid Mechanics*, 3rd Ed.; McGraw-Hill, Inc. 1994.
10. Soponronnarit, S.; Srisubati, S.; Yoovidhya, T. Effect of temperature and relative humidity on yellowing rate of paddy. Journal of Stored Products Research **1998**, *34*, 323–330.
11. Tirawanichakul, Y.; Prachayawarakorn, S.; Tungtrakul, P.; Chaiwatpongskorn, W.; Soponronnarit, S. Experiments on in-store paddy drying under tropical climate: Simulation and product quality. Drying Technology **2003**, *21*, 1049–1064.
12. Naupanich, M.; Tapan, V.; Tungpinijkul, V.; Wuthisin, P.; Songsermpong, S.; Noosawad, S. Report on development of steel silo for stored paddy. Department of Agricultural Farm Machinery, 1993, 1–20.
13. Prachayawarakorn, S.; Sawangduanpen, S.; Saynampheung, S.; Poolpatarachewin, T.; Soponronnarit, S.; Nathakarakule, A. Kinetics of colour change during storage of garlic slices as affected by relative humidity and temperature. Journal of Food Engineering **2004**, *62*, 1–7.
14. Rapusas, R.S.; Driscoll, R.H. Kinetics of non-enzymatic browning in onion slices during isothermal heating. Journal of Food Engineering **1995**, *24*, 417–429.
15. Raj, S.A.; Singaravadivel, K. Biodeterioration in rice (*Oryza sativa* L.) due to low, medium and high moisture. International Biodeterioration **1990**, *27*, 237–248.
16. Soponronnarit, S. (in Thai) Grain drying, 7th Ed., King Mongkut's University of Technology Thonburi: Bangkok Thailand, 1997.

Drying Technology, 23: 225–248, 2005
Copyright © 2005 Taylor & Francis, Inc.
ISSN: 0737-3937 print/1532-2300 online
DOI: 10.1081/DRT-200047883

Taylor & Francis
Taylor & Francis Group

Simulation of a Mixed Air and Superheated Steam Drying System

Yuvanaree Namsanguan*, Sumran Tichangtong, Warunee Tia, and Somchart Soponronnarit
School of Energy and Materials, King Mongkut's University of Technology, Bangkok, Thailand

Sakamon Devahastin
Department of Food Engineering, King Mongkut's University of Technology, Bangkok, Thailand

Abstract: Numerical simulation of a cabinet-type superheated steam drying system was conducted and validated experimentally using shrimp as the test material. The experimental and simulated drying temperatures used were in the range of 140–160°C while the volume flow rate of steam of 1.04 m^3/s was used throughout. The initial masses of the drying product were 50.7 and 31.2 kg, with initial moisture contents of 4.0 kg/kg and 3.61 kg/kg dry basis, respectively; the final moisture content of the dried product was 0.25 kg/kg dry basis. The simulated moisture content of shrimp, the drying medium temperature at the outlet of the dryer, and the performance of the dryer in terms of drying time, drying rate, specific energy consumption, and drying efficiency, were verified using available experimental data. The results showed that the simulated results agreed well with the experimental results. Based on the present study, the desirable operating conditions were also evaluated for the dryer for shrimp by considering the optimized performance and good product quality.

Keywords: Dryer performance; Drying efficiency; Drying rate; Shrimp drying; Specific energy consumption

*Correspondence: Yuvanaree Namsanguan, School of Energy Materials, King Mongkut's University of Technology Thonburi, 91 Pracha U-tid Road, Bangkok 10140, Thailand. Tel.: 662-470-8663; Fax: 662-470-8663; E-mail: yuvanaree@yahoo.com

INTRODUCTION

In the superheated steam drying (SSD) process superheated steam acts both as the heat source and as the drying medium to take away the evaporated water from the drying product. Since SSD necessarily produces steam (albeit at lower specific enthalpy) equal in amount to the water evaporated from the product, it would be possible to recover all of the latent heat supplied to the SSD by condensing the exhaust steam or by mechanical or thermal compression for re-use in the dryer or elsewhere.[1-3] Energy recovery, which leads to the lower net energy consumption of the dryer, is therefore possible. The closed steam drying process is clean (better pollution control), absent of the risk of explosion and burning, and also able to enhance the drying rate due to high heat transfer coefficient.[4-7]

Superheated steam drying has recently received considerable attention for drying food and other heat-sensitive products due to its several advantages; e.g., absence of oxidative reactions due to lack of oxygen and its ability to yield products that have lower degree of shrinkage and good color;[8-11] a number of food products have recently been dried successfully in SSD of various designs.[12-15] For shrimp, SSD has been found to be an attractive drying process. Prachayawarakorn et al.[16] investigated the drying of shrimp using superheated steam and found that the use of SSD was very beneficial, since boiling and drying, which are the two main steps of the production of dried shrimp, can be performed in a single step with superheated steam as the drying medium. The color and shrinkage of the dried product were also found to be better than shrimp dried in a conventional hot air dryer. However, the system used was relatively inefficient and had large footprint and included several such units as a steam generator, a steam superheater, a drying chamber, and a blower to deliver the steam to the drying chamber. This bulkiness also resulted in excessive energy usage. For the successful development of the commercial scale dryer, the system should be more compact, available at lower cost, and able to save more energy.

Soponronnarit et al.[17] designed and constructed the prototype of a superheated steam cabinet dryer, which used steam evaporating from the drying product as the drying medium. As reported by several investigators, when superheated steam drying is performed in a closed system, the vapor evaporating from the drying material itself can be utilized as the drying medium;[18,19] when a dryer is operated in a completely closed circuit, air inside the dryer changed to humid air, then highly humid air (or an air–steam mixture), and superheated steam would almost completely replace the air. Similarly, for this dryer, during the first period of drying, the drying medium was treated as the mixture of air and superheated steam. As drying proceeded, the amount of steam evaporated from the product gradually increased while the air was released from the dryer through a small venting hole. The ratio of superheated steam to air increased until the mixture became mostly superheated steam. Steam was forced to flow parallel to a series of wire screens where the samples sat upon in the dryer. Due to the use of vapor evaporated from the drying product as the drying medium, energy consumption was minimized.

Another notable advantage of this dryer prototype is that it can be operated without a steam generator; steam is recirculated and reheated by a burner. To make the energy recovery more efficient, the exhaust gas from the combustion chamber is used to supply heat to the steam at the heat exchanger before being released to the environment. This process saves a significant amount of capital and operating cost of the dryer. However, one of the most important problems experienced in this dryer is the nonuniformity of the flow of drying medium in the dryer, especially at the entrance of the drying chamber. This causes variation of the product's final moisture content. As recommended by Nijdam and Keey[20] and Kiranoudis and Markatos,[21] a uniform flow distribution can be attained by using flow guides or baffles in the drying chamber entrance. Three guide vanes were then installed at appropriate locations in the dryer to help distributing the steam.

Although there are numerous works, both experimental and numerical, that reported results on superheated steam drying of various products, no published work is available on modeling of a complete drying system including the dryer, burner, heat exchanger, and blower, especially for a system similar to that studied in the present work. Such information is necessary if the system is to be used successfully in industry. The objective of this study was therefore to simulate a cabinet-type superheated steam drying system using shrimp as the drying material; the simulation was validated with available experimental results. Variables considered in the model were the drying temperature, the amount of the wet product, and the initial moisture content of the product; the volume flow rate of the drying medium was fixed in this work. Criteria for validation of the model were the moisture content of shrimp, the drying, medium temperature at the outlet of the dryer and the dryer performance. In addition, the suitable drying conditions for optimum performance of the dryer in terms of the specific energy consumption (SEC), drying efficiency (DE), and acceptable product quality were determined.

MATHEMATICAL MODEL

Figure 1 shows the drying system simulated in the present study, and a diagram of the drying system is shown in Fig. 2. The system is very

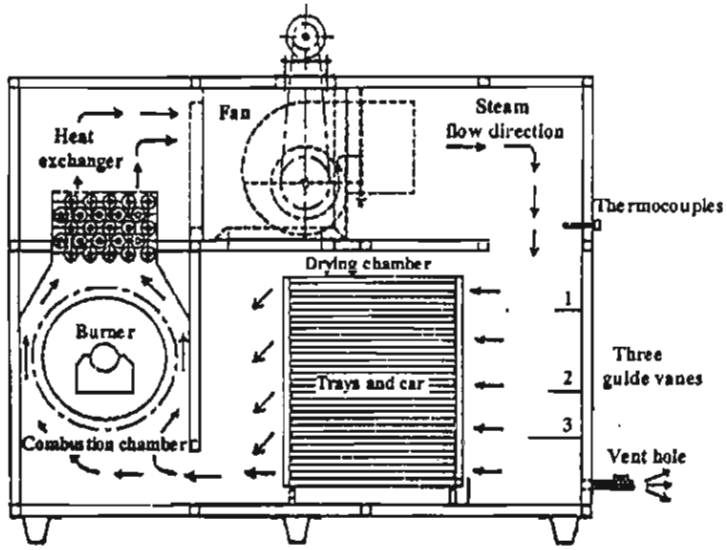


Figure 1. Simulated drying system.

compact, *viz.* 1.27 × 2.24 × 1.675 m^3. The wall of the drying system is insulated with asbestos. The unit consists of a 0.95 × 0.8 × 0.98 m^3 drying chamber, an oil burner rated between 35.5 and 71 kW, a cylindrical combustion chamber of 0.4 m in diameter and 1.1 m in length with surrounding fins providing a total heat transfer area of 4.59 m^2, a compact heat exchanger with 24 finned tubes providing a total heat transfer area of 16.8 m^2, and a 0.75 kW forward-curved blade centrifugal fan, which is used to circulate the drying steam through the dryer. The dryer has a maximum capacity of 50 kg.

In this case, steam, which was generated from evaporation of water in the product, was used as the drying medium. The vapor was circulated in the drying chamber (CV.1) and reheated by a burner, which generated heat through a combustion chamber (CV.2). Before being released to the environment, the flue gas exhausting (m_g) from the combustion chamber was reused to supply heat to the drying medium (m_3) at the heat exchanger (CV.3). Drying was performed at a pressure slightly above atmospheric pressure; thus, the evaporated moisture of the product became superheated steam only after passing through the combustion chamber and heat exchanger. However, during the first period of drying, steam generated from the product was not enough to fill the whole dryer and there was still some air in the drying chamber; the dryer had a small vent

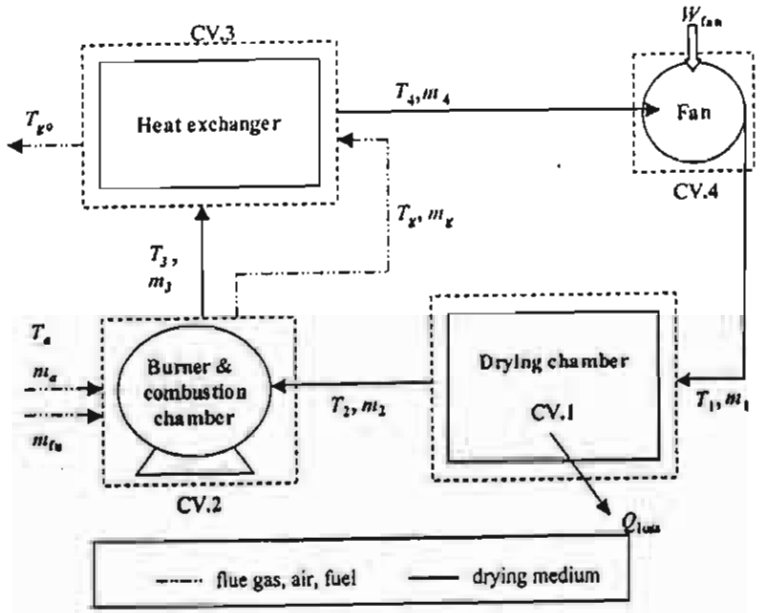


Figure 2. Diagram of the simulated drying system (CV = control volume).

hole to release air to the atmosphere until the drying medium became purely superheated steam. Unfortunately, from the experimental characteristic curve of the fan power requirement, it was found that air was still present and mixed with superheated steam for the whole drying process. Consequently, the drying medium was treated as a mixture of air and superheated steam in the model developed similarly to the studies of Costa and Silva,[22] Schwartze and Brocker,[23] and Chu et al.;[24] properties of the drying medium were calculated as properties of a fluid mixture according to the methods of Avallone and Baumeister[25] and Chow and Chung[26] by using the ratio of steam and air estimated from the experimental data of the fan power requirement versus the drying time.

The mathematical model of the drying system consists of a drying model, a burner and combustion chamber model, a heat exchanger model, and a performance model. The assumptions made in the development of these models are as follows: drying medium was a mixture of air and superheated steam, thermal equilibrium existed between the drying medium and the product, the change in internal energy of the dryer and product was negligible, and the effect of product shrinkage during drying was negligible.

Drying Model

First of all, the moisture content of the drying product (shrimp) was calculated using the analytical solution of a simple liquid diffusion equation. It was assumed that the initial moisture content of the product was uniform and the moisture content at the surface of the product was in equilibrium with the surrounding drying medium immediately after the start of the drying process. By considering shrimp as a spherical body, the diffusion equation is written as Eq. (1).[27] The choice of the spherical geometry of shrimp was due to the fact that the only correlations for the effective moisture diffusivity of shrimp available in the literature are based on a spherical geometry.[16]

$$MR = \frac{M(t) - M_{eq}}{M_{in} - M_{eq}} = \frac{6}{\pi^2}\sum_{n=1}^{\infty}\frac{1}{n^2}\exp\frac{n^2\pi^2 D_{eff}t}{a^2} \tag{1}$$

The correlations for the effective diffusion coefficients were those of Prachayawarakorn et al.[16] who dried shrimp using both superheated steam and hot air.

$$\text{Superheated steam:}\quad D_{eff} = 0.00253\ \exp\left(\frac{-32,714.9}{RT_{abs}}\right) \tag{2a}$$

$$\text{Hot air:}\quad D_{eff} = 0.00034\ \exp\left(\frac{-25,578.0}{RT_{abs}}\right) \tag{2b}$$

where T_{abs} is the absolute temperature of the drying medium used. The effective diffusion coefficient of shrimp dried in a mixture of air and superheated steam is weighed as follows:

$$D_{eff,m} = \frac{\sum(m_i D_{eff,i})}{m} \tag{2c}$$

where $m = m_s + m_d$ denotes the total mass of the mixture; m_s and m_d denote the masses of the constituent gases; and the subscripts $i = s$ and $i = d$ denote superheated steam and air, respectively.

The properties of the air and superheated steam mixture leaving the drying chamber were calculated by performing mass and energy balances in control volume 1 (CV.1) of Fig. 2. Both air and superheated steam were individually assumed to be an ideal gas because their Z factors are very close to unity[28] in the ranges of drying temperature and pressure used in the present study. An ideal gas behavior could be assumed in this case as the level of pressure was in an atmospheric range. The drying medium was therefore treated as an ideal gas mixture. Then, mass and energy balances in CV.1 can be written as follows:

$$\text{Mass balance:}\quad m_2 = m_1 + \Delta m \tag{3}$$

where $\Delta m = m_p(M_i - M_o)/\Delta t$

$$\text{Energy balance:}\quad (m_{d,1}c_{pa} + m_{s,1}c_{ps})T_1 = (m_{d,2}c_{pa} + m_{s,2}c_{ps})T_2 + \Delta m h_{fg} + Q_{loss} \tag{4}$$

where m_1 and m_2 are the total mass flow rates of the mixture entering and leaving the drying chamber, respectively; $m_1 = m_{d,1} + m_{s,1}$ and $m_2 = m_{d,2} + m_{s,2}$.

Burner and Combustion Chamber Model

In this system, the energy needed to heat up the drying medium to the desired temperature was supplied by a burner instead of an electric heater. Diesel oil was used as the fuel in the burner and energy was generated from the burner and transferred to the drying medium through the combustion chamber. From CV.2, two parts of mass balance, one of which belongs to the drying medium and another belongs to the fuel, are written in Eqs. (5) and (6), respectively. For combustion, 20% excess air and 14.5 air/fuel ratio (A/F) were used in the model.

$$m_3 = m_2 \tag{5}$$

$$m_g = [1 + 1.2(A/F)]m_{fu} \tag{6}$$

Energy balance equations are given in Eqs. (7), (8), and (9). For an energy balance in Eq. (9), since the flue gas temperature was high (≈1000°C) and the wall of the combustion chamber was very thin, it was assumed that the wall resistance was negligible. This implies that there was no difference in temperature between inside and outside surfaces of the combustion chamber wall. Eq. (9) can also be decomposed into Eqs. (9a) and (9b):[29]

$$m_{fu}\,\text{LHV} = m_g c_{pg}(T_g - T_a) + Q_{tr} \tag{7}$$

$$Q_{tr} = (m_{d,2}c_{pa} + m_{s,2}c_{ps})(T_3 - T_2) \tag{8}$$

$$Q_{tr} = Q_{conv,i} + Q_{radia,i} = Q_{conv,o} + Q_{radia,o} \tag{9}$$

$$Q_{tr} = h_{c,i}A_i(T_g - T_w) + \sigma A_i(\varepsilon_g T_g^4 - \alpha_g T_w^4) \tag{9a}$$

$$h_{c,i}A_i(T_g - T_w) + \sigma A_i(\varepsilon_g T_g^4 - \alpha_g T_w^4) = \eta_o h_{c,o} A_o(T_w - T_{ar}) + \varepsilon_s \sigma A_o(T_w^4 - T_{ar}^4) \tag{9b}$$

where T_{av} is the average drying medium temperature passing through the combustion chamber, which is defined as $T_{av} = (T_2 + T_3)/2$.

Heat Exchanger Model

Based on CV.3, the equations for mass and energy balances can be written as follows:

$$m_4 = m_3 = m_2 \tag{10}$$

$$Q_{he} = (m_{d,2}c_{pa} + m_{s,2}c_{ps})(T_4 - T_3) = m_g c_{pg}(T_g - T_{go}) \tag{11}$$

$$Q_{he} = \varepsilon C_{\min}(T_g - T_3) \tag{12}$$

where ε is the effectiveness of the heat exchanger and $C_{\min}$ is the minimum heat capacity rate corresponding to the hot fluid (flue gas).

$$\varepsilon = 1 - \exp\left((\mathrm{NTU})^{0.22}/C_r\left\{\exp\left[-Cr(\mathrm{NTU})^{0.78}\right] - 1\right\}\right) \tag{12a}$$

$$\text{and } \mathrm{NTU} = \frac{U_o A_o}{C_{\min}} \tag{12b}$$

$$C_{\min} = C_h = m_g c_{pg} \tag{12c}$$

$$\text{and } C_{\max} = C_c = m_{d,2}c_{pa} + m_{s,2}c_{ps} \tag{12d}$$

$$C_r = C_{\min}/C_{\max} \tag{12e}$$

Energy Consumption of Fan

The rate of electricity consumption (W_{fan}) for driving the fan (CV.4) can be calculated by the following equation:

$$W_{\text{fan}} = \frac{Q\Delta P}{\eta_f \eta_m} \tag{13}$$

Performance Model

The performance of the dryer is defined in terms of the specific energy consumption (SEC), average drying rate (DR), and drying efficiency (DE). They can be calculated from:

$$\mathrm{SEC} = (2.6\mathrm{E} + Q_h)/[(M_{\text{in}} - M_f)m_p] \tag{14}$$

$$\mathrm{DR} = m_w/\mathrm{DT} \tag{15}$$

$$\mathrm{DE} = Q_{\text{evap}}/Q_{\text{in}} \tag{16}$$

where 2.6 is the energy conversion factor.[17]

Solution Procedure

As mentioned earlier, the simulation was performed to study the drying characteristics of shrimp as well as the performance of the mixed air and superheated steam drying system. The inputs for the model are the initial moisture content and initial mass of the product, the volume flow rate of the drying medium, the drying temperature, the fuel flow rate in the burner, and other constants listed in the previous section. The temperature of the drying medium at the entrance of the drying chamber (T_1) was set equal to the drying temperature, and the humidity ratio of air at the beginning of the process was estimated initially from the experimental fan power requirement. The ratio of air and superheated steam along the drying process was estimated from the experimental data of the fan power requirement versus the drying time as mentioned earlier; Fig. 3 presents the experimental fan power data and the fraction of steam evaluated. The temperature of the mixture leaving the combustion

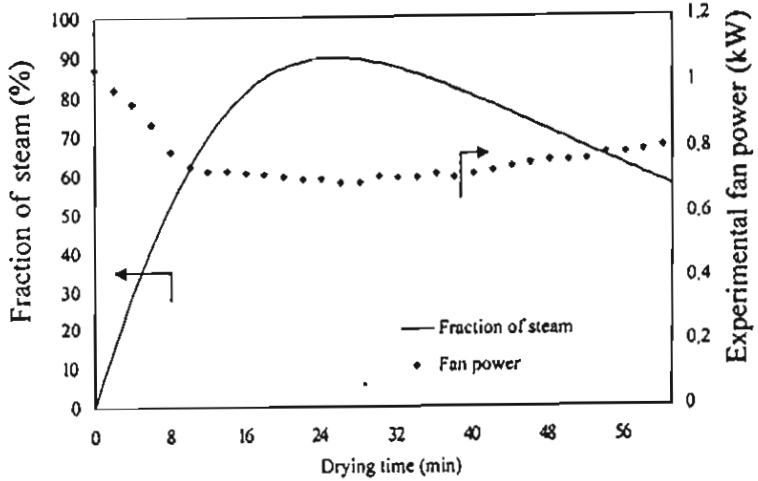


Figure 3. Evolution of fraction of steam estimated from experimental fan power requirement.

chamber (T_3), the temperature of flue gas exiting the combustion chamber (T_g), the average temperature of mixture passing through the combustion chamber (T_{av}), the temperature of the wall of the combustion chamber (T_w), the rate of heat transfer from the combustion chamber to the drying medium (Q_{tr}), and the rate of heat exchanged at the heat exchanger (Q_{hc}) were initially guessed values. The steps of the simulation are as follows: the drying model, the burner and combustion chamber model, and the heat exchanger model were simulated, and the temperature of the mixture leaving the drying chamber (T_2), all other guessed values, and the final moisture content of the product were checked. The relative humidity of the mixture, however, was not checked except at the beginning of the process because the mixture of air and superheated steam behaved like moist air during the beginning of the drying process. Thus, the model also included a subroutine to check for moisture condensation (relative humidity < 1) in the case when the temperature of the drying medium at the outlet of the drying chamber (T_2) was less than 100°C, which occurred only at the beginning of the drying process. Newton-Raphson technique was used for checking the guessed values and determining the acceptable ones. Next, an energy consumption of the fan and the burner were computed and then moisture content of product after drying was checked. To calculate the final moisture content of the product at each time step, Eq. (1) was differentiated with respect to time and solved numerically using fourth-order Runge-Kutta algorithm. In this case, M_{eq} was assumed to be zero.[16] Regarding the moisture content of the product after drying, if the final moisture content of the product was higher than the desired value, the moisture content of the product before drying was replaced by the moisture content after drying, and the time step was advanced. Since the moisture of the product evaporated and became superheated steam, the mass flow rate of superheated steam leaving the drying chamber during this time step would be that of superheated steam entering the drying chamber during the next time step ($m_{s,1}^{k+1} = m_{s,2}^{k}$). The calculation continued until the moisture content of the product was less than or equal to the desired value. Finally, the performance of the dryer was determined.

RESULTS AND DISCUSSION

Validation of Model

The experimental shrimp drying data that were used to verify the present model were conducted by Soponronnarit et al.[17] The experimental and simulated drying conditions were as follows: the drying temperatures in the range of 140–160°C, the volume flow rate of the drying medium of

1.04 m^3/s, the initial masses of product of 50.7 and 31.2 kg, the initial moisture contents of 4.0 kg/kg and 3.61 kg/kg dry basis (80% and 78.3% wet basis, respectively), and the final moisture content of 0.25 kg/kg dry basis (20% wet basis). Drying was performed at a pressure slightly above the atmospheric pressure.

Evolution of Product Moisture Content

The simulated moisture content of shrimp is shown in Fig. 4 where drying conditions employed were the drying temperatures of 140–160°C, the initial masses of product of 50.7 kg, and the initial moisture content of 4.0 kg/kg dry basis. The other drying conditions were fixed as described above. As the drying temperature increased, the moisture reduction rate was higher and the drying time was reduced, as expected, because a higher drying temperature led to a higher effective diffusion coefficient of shrimp; the existence of an inversion temperature of 140°C has indeed been found by Prachayawarakorn et al.[16] The experimental moisture content evolution of shrimp is not shown here since there is no such data available. However, the experimental and simulated total drying times and drying rates are compared as shown in Table 1 (Test nos. 1–6). It is seen that the drying times (DT) obtained from the model and those obtained from the experiments are relatively close. The results indicate that the drying model is able to predict the drying rate (DR) accurately.

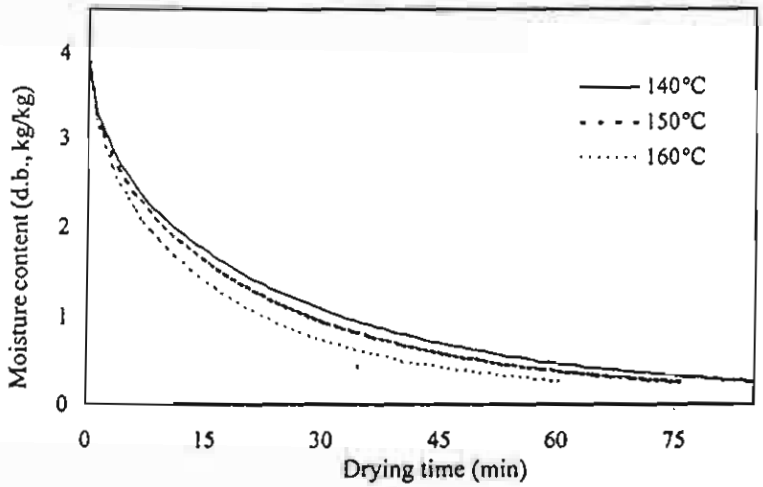


Figure 4. Evolution of simulated moisture content (Test nos. 4, 5, and 6).

Table 1. Comparison between experimental and simulated results of shrimp drying

	Test no.											
	1		2		3		4		5		6	
Description	Exp.	Sim.	Exp.	Sim.	Exp.	Sim.	Exp.	Sim.	Exp.	Sim.	Exp.	Sim.
Product conditions												
Initial moisture content (kg/kg d.b.)	3.61	3.61	3.61	3.61	4.0	4.0	4.0	4.0	4.0	4.0	4.0	4.0
Final moisture content (kg/kg d.b.)	0.27	0.25	0.27	0.25	0.25	0.25	0.22	0.25	0.21	0.25	0.23	0.25
Initial weight (kg)	31.2	31.2	31.2	31.2	31.2	31.2	50.7	50.7	50.7	50.7	50.7	50.7
Final weight (kg)	8.4	8.5	8.4	8.5	7.9	7.8	12.4	12.7	12.3	12.7	12.1	12.7
Drying conditions												
Drying temperature (°C)	142.7	140	150.3	150	158.3	160	142.3	140	150.4	150	159.9	160
Volume flow rate (m^3/s)	1.04	1.04	1.04	1.04	1.04	1.04	1.04	1.04	1.04	1.04	1.04	1.04
Dryer performance												
Drying time (min)	76	82	64	72	44	48	86	87	70	76.5	60	61
Drying rate (kg water evap./h)	18.1	16.6	21.4	19.0	31.8	29.2	26.7	26.2	32.9	29.8	38.6	37.4
Energy consumption												
Diesel fuel (kg)	2.8	3.04	2.9	3.26	2.8	3.06	3.25	3.29	3.9	4.26	3.55	3.61
Electricity (kW-h)	1.5	1.58	1.35	1.33	0.95	0.93	1.7	1.68	1.38	1.42	1.2	1.07
Specific primary energy consumption												
Diesel fuel (MJ/kg water evap.)	5.48	5.95	5.7	6.42	5.38	5.85	3.25	3.29	3.9	4.26	3.55	3.61
Electricity (MJ/kg water evap.)	0.61	0.65	0.55	0.548	0.38	0.37	0.42	0.41	0.34	0.35	0.29	0.26
Total (MJ/kg water evap.)	6.09	6.6	6.25	6.97	5.77	6.22	4.22	4.28	4.89	5.37	4.41	4.51
Drying efficiency (%)	42.7	39.4	41.6	37.3	45.1	41.7	61.7	60.6	53.2	48.4	58.9	57.6

The differences between the experimental and simulated results are less than 10%.

Drying Medium Temperature

The evolution of the experimental and simulated mean drying medium temperature at the inlet and outlet of the dryer (drying chamber, CV.1) are presented in Figs. 5–8 for various inlet drying temperatures (T_1), initial shrimp weights, and initial moisture contents. The results indicate that the drying model is capable of predicting the drying medium temperature evolution reasonably well. The outlet drying temperature (T_2) increased suddenly at the beginning of the process and then slowly increased and finally approached the inlet drying temperature. The simulated temperatures were generally slightly lower than the experimental ones during the first period of drying. This is possibly due to the fact that there was some amount of heat stored in the heat exchanging equipment during the warm-up period before the sample was placed in the drying chamber. During the warm-up period, the temperature at the drying chamber entrance was set at higher values than the desired drying temperature by about 20–40°C (shifting temperature) to help recover the heat loss during the loading of the sample; it was then reset down to the drying temperature and fixed at that value along the whole drying process. Thus,

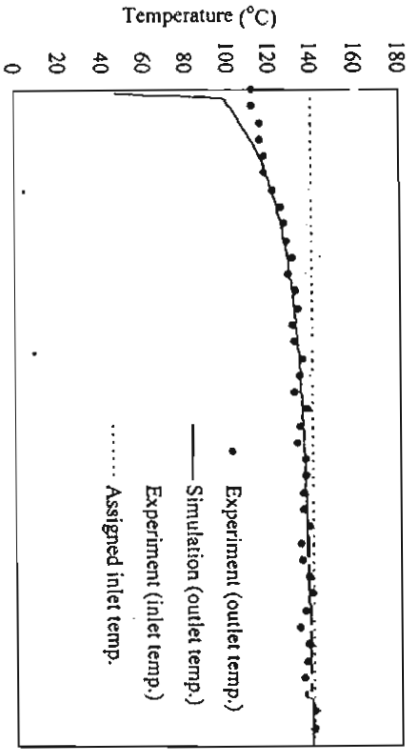


Figure 5. Evolution of simulated and experimental drying medium temperatures (Test no. 1).

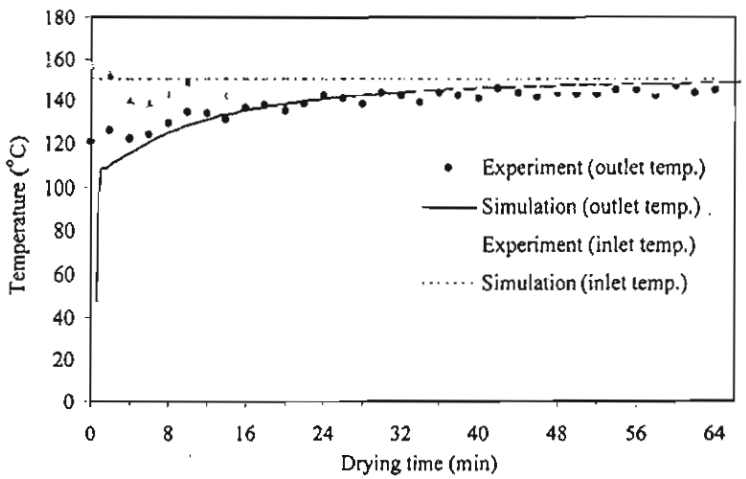


Figure 6. Evolution of simulated and experimental drying medium temperatures (Test no. 2).

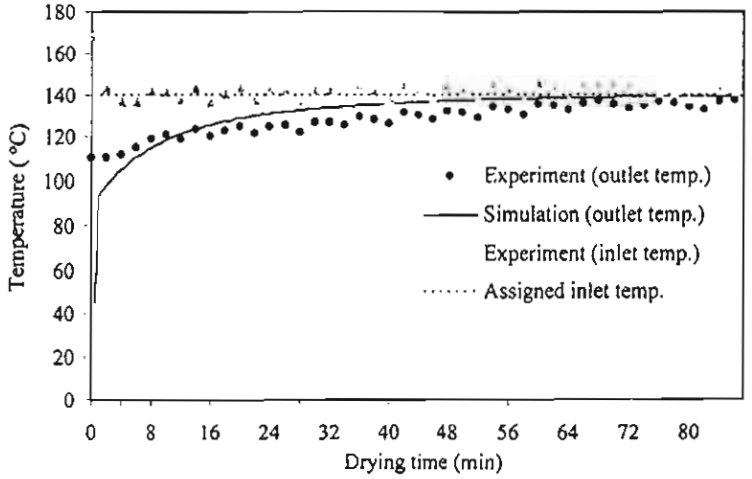


Figure 7. Evolution of simulated and experimental drying medium temperatures (Test no. 4).

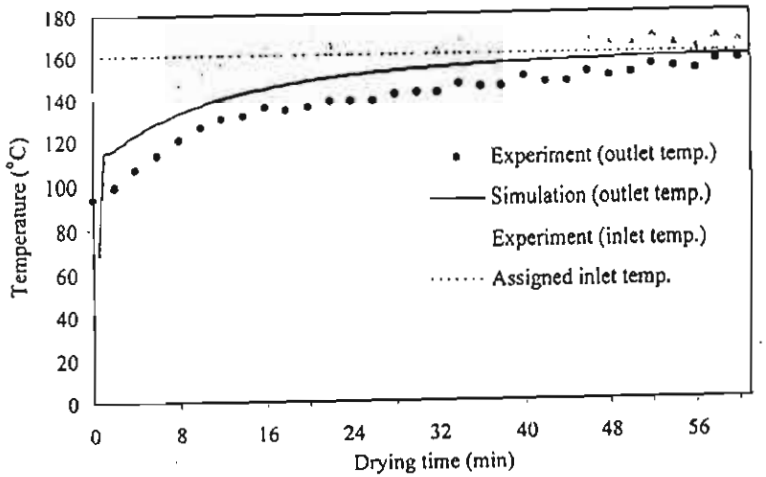


Figure 8. Evolution of simulated and experimental drying medium temperatures (Test no. 6).

the experimental outlet drying temperature was found to be slightly higher than the simulated value during the first period of drying.

Considering the drying temperature and initial mass of shrimp, it was found that the simulated results agreed very well with the experimental data when using low drying temperatures of 140–150°C and low initial shrimp weight of 31.2 kg. The difference between the experimental data and simulated results at higher drying temperatures was due to the fact that the change of the internal energy of the dryer and the product was assumed to be negligible in this study. However, it is known that the higher the drying temperature and the larger the initial weight of the product, the more change of internal energy of the dryer and the product would be observed. This is why the experimental and simulated results only agreed well when the drying medium temperature and the initial weight of the product were reduced. In addition, poorer agreements at higher drying medium temperatures also may be due to physical or chemical changes, e.g., shrinkage; the effect of product shrinkage during drying was not considered in this study.

However, as illustrated in Fig. 8, the experimental and simulated results for the case where the drying conditions were the drying temperature of 160°C and the initial weight of product of 50.7 kg (Test no. 6) seemed to be more deviated from each other than for other cases. In this test, the inlet drying temperature dropped significantly at the beginning of the drying process because of the smaller shifting temperature during

the warm-up period (only 20°C above the inlet drying temperature) than in the case of other experiments. Therefore, it took a longer time for the temperature to reach the desired value during the first period of drying.

Energy Consumption And Dryer Performance

The experimental shrimp drying results that were used to verify the model and the simulated results are shown in Table 1. Specific energy consumption, drying time, drying rate, and drying efficiency were used for the verification of the mathematical model. It can be seen in this table that the simulated results agreed well with the experimental data; the differences were less than 10%. Furthermore, for clearer understanding of the data, the results of the energy consumption and the dryer performance are presented in Figs. 9–12.

The relationship between the energy consumption and the drying time is demonstrated in Fig. 9. It can be observed that the specific energy consumption increased with drying time. At low moisture content, the rate of moisture diffusion was low resulting in slow drying and high energy consumption. Since the energy consumption included two main types of energy mode, the fuel energy consumption, which was around 90–93%, and electricity consumption, which was another 7–10% of the total energy consumption, the former was the main part of the energy

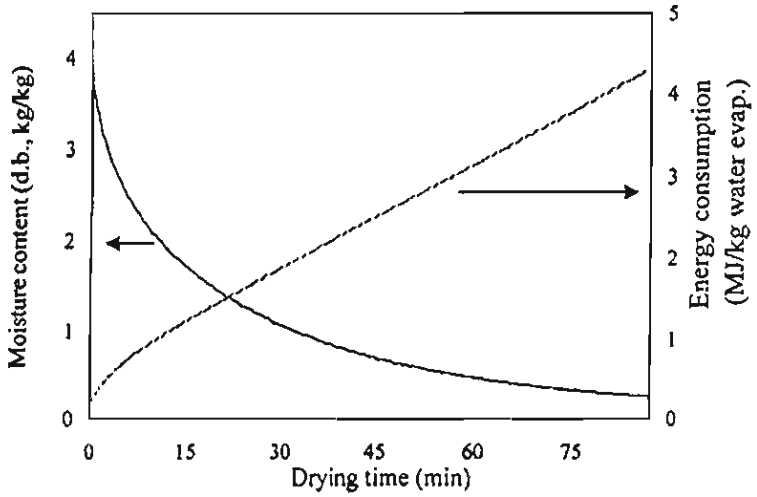


Figure 9. Evolution of simulated moisture content and specific energy consumption.

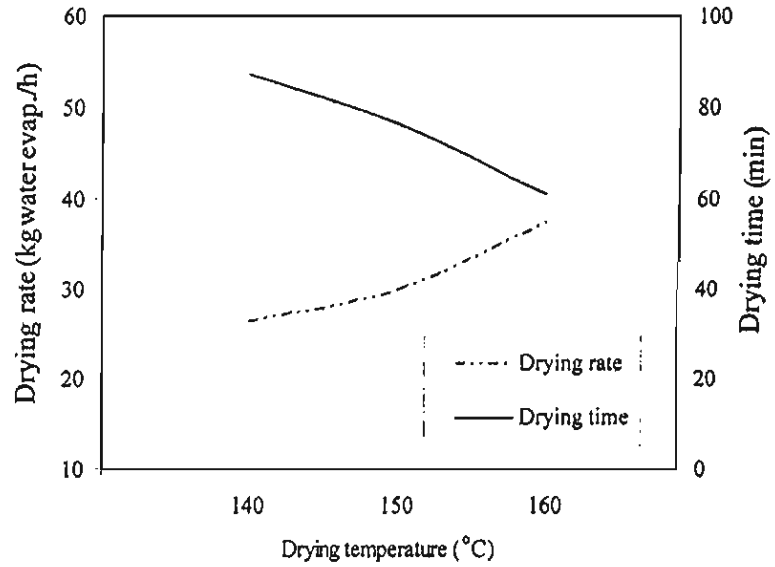


Figure 10. Evolution of simulated drying rate and drying time.

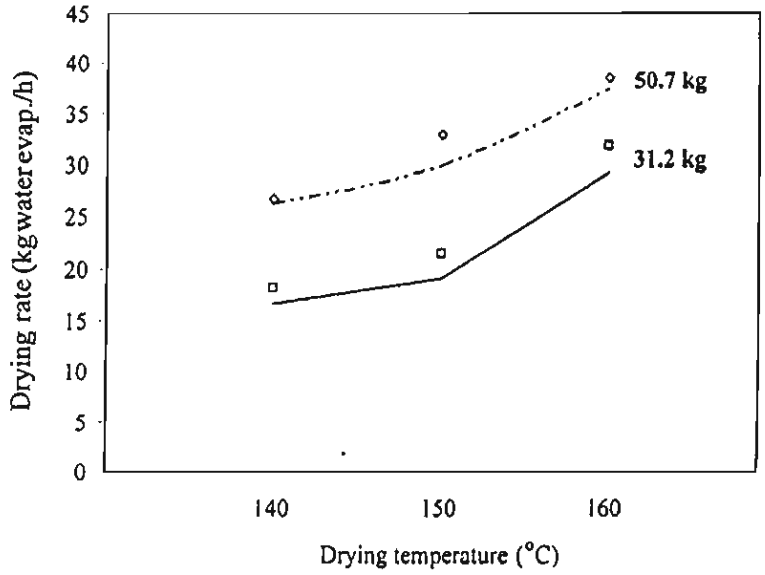


Figure 11. Evolution of simulated and experimental drying rates at different initial weights of product.

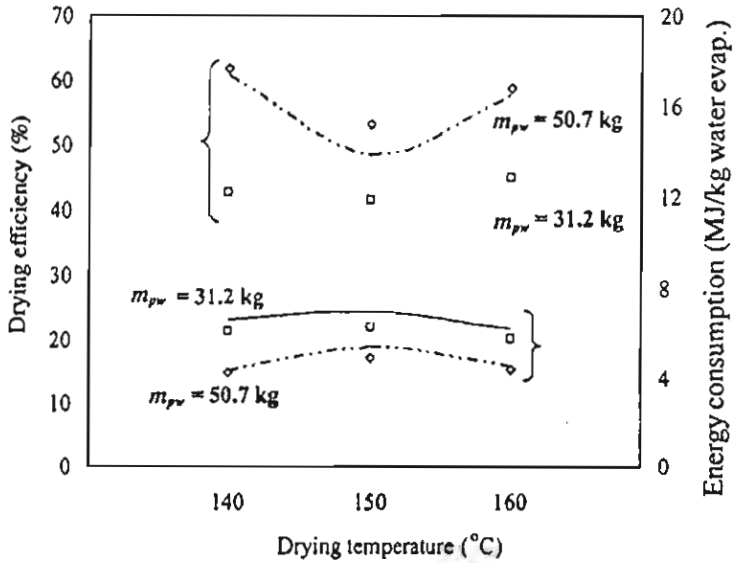


Figure 12. Evolution of simulated and experimental drying efficiencies and specific energy consumption.

usage for this dryer. It can be seen that the overall energy consumption of the system was very low compared to a conventional hot air dryer. Furthermore, using fuel as a source of energy was more economical than using an electric heater.

Figure 10 shows the evolution of the simulated drying rate and drying time when the initial weight of the product was 50.7 kg and the initial moisture content was 4.0 kg/kg dry basis. From simulation results the total drying time (DT) decreased and drying rate (DR) increased with increasing drying medium temperature. This is consistent with the fundamental drying theory since the heat transfer from the drying medium to the product increases with increased medium temperature. These trends were also similar for the case of decreasing initial weight and initial moisture content of the drying product.

Figure 11 shows the effect of drying temperature on the drying rate (DR) at different initial weights of the product. The agreement between the simulated drying rates and the experimental results is observed. It was found that the drying temperature had a significant effect on the drying rate. By considering the initial weight of the product, it was found that a lower initial weight of the product led to a slower drying rate since using a lower initial weight provided the less amount of water evaporated

from the product (m_w). As shown in Eq. (15), the drying rate is the function of the water evaporated from the product (m_w) and the drying time (DT); the simulated drying time was slightly different at the same initial weight of the product. In the case where the initial weights of the product were 50.7 kg and 31.2 kg, an increase in the drying temperature from 140 to 160°C caused the drying rate to increase from 26.2 to 37.4 kg water evap./h and from 16.6 to 29.2 kg water evap./h (simulation result), respectively.

Figure 12 shows the effect of drying temperature on the drying efficiency (DE) and the specific energy consumption (SEC). It was observed that the drying temperature affected SEC; SEC increased with increased drying temperature to the maximum point, and then decreased. This is due to the fact that drying at a higher temperature requires a higher capacity of the burner to combust the fuel (main energy part), resulting in a higher energy consumption rate than drying at a lower temperature. However, drying at this higher temperature resulted in a shorter drying time, as expected. Since the energy consumption is the product of the energy consumption rate and drying time, there possibly existed a maximum value of SEC in this range of drying temperature. An inverse relationship was also found between DE and SEC. Finally, as a result of the high initial shrimp weight, SEC could be reduced and this resulted in a higher DE since higher initial weight of the product yielded a higher drying rate. Consequently, specific energy consumption was lower when using higher initial weight of the product.

Based on the assumptions and results of this study, a maximum capacity of the raw product of 50 kg and drying temperatures between 140 and 160°C are recommended for the operation of the dryer. The drying temperature should not exceed 160°C due to the limitation of product quality (very poor color, high degree of shrinkage, and the difficulty of removing the shell from the shrimp body) as suggested by Prachayawarakorn et al.[16] From the experiments, it was also found that the desired red-orange color of dried shrimp was obtained at the drying temperature of 140°C.[8] It is possible to scale up the dryer by dividing the drying chamber into several thin sections, assuming the plug flow of the drying medium, and assuming that the temperature gradient exists only in the direction of the flow of the drying medium in the model.

CONCLUSION

Numerical simulation of a mixed air and superheated steam cabinet drying system was conducted and validated with experimental shrimp drying results. The model was found to predict the moisture reduction rates of shrimp as well as the outlet drying medium temperature relatively well.

It was also found that the simulated results agreed well with the experimental data in terms of the drying time, drying rate, energy consumption, and dryer performance. The drying temperature and the initial load of the raw product were found to affect the specific energy consumption (SEC) and the drying efficiency (DE) of the dryer; SEC decreased with an increase in the initial load of the raw product, while it increased with an increase of the drying temperature to the maximum point, and then decreased again in the range of drying temperature studied. Based on the present study, it was found that the desirable operating conditions for the dryer for shrimp would be as follows: the drying temperature of 140°C and the initial shrimp weight of 50.7 kg (for optimized performance and good product quality).

NOMENCLATURE

A_i	internal area of combustion chamber or heat exchanger (m^2)
A_o	external area of combustion chamber or heat exchanger (m^2)
A/F	air/fuel ratio (kg of air/kg of fuel)
a	particle radius (m)
C_c	cold fluid heat capacity rate (kW/K)
C_h	hot fluid heat capacity rate (kW/K)
C_{max}	maximum heat capacity rate corresponding to the cold fluid (kW/K)
C_{min}	minimum heat capacity rate corresponding to the hot fluid (kW/K)
C_r	heat capacity ratio (decimal)
c_{pa}	specific heat capacity of dry air (kJ/kg K)
c_{pg}	specific heat capacity of flue gas (kJ/kg K)
c_{ps}	specific heat capacity of superheated steam (kJ/kg K)
D_{eff}	effective diffusion coefficient (m^2/min)
DE	drying efficiency (%)
DR	drying rate (kg water evap./h)
DT	drying time (min)
E	electricity consumption (kJ)
h	convective heat transfer coefficient (W/m^2K)
h_{fg}	heat of evaporation (kJ/kg)
LHV	lower heating value (kJ/kg)
M	moisture content (decimal, dry-basis)
MR	moisture ratio, dimensionless
M_i	moisture content before drying at each time step (decimal, dry-basis)
M_o	moisture content after drying at each time step (decimal, dry-basis)
m	total mass flow rate or total mass (kg/s or kg)
m_{pw}	initial mass of wet product (kg)
m_w	water evaporated from product (kg)
Δm	rate of water evaporated from product (kg/s)

NTU	number of transfer units
ΔP	pressure drop (kPa)
Q	volume flow rate of drying medium (m^3/s)
$Q_{conv,i}$	convective heat transfer rate inside the wall of combustion chamber (kW)
$Q_{conv,o}$	convective heat transfer rate outside the wall of combustion chamber (kW)
$Q_{evap.}$	energy used for water evaporation of product (kJ)
Q_h	energy consumption provided by fuel (kJ)
Q_{he}	rate of heat exchanged at the heat exchanger (kW)
Q_{in}	energy input to system (kJ)
Q_{loss}	heat loss from control volume to surroundings (kW)
$Q_{radia,i}$	radiation heat transfer rate inside the wall of combustion chamber (kW)
$Q_{radia,o}$	radiation heat transfer rate outside the wall of combustion chamber (kW)
Q_{tr}	rate of heat transfer from the combustion chamber to the drying medium (kW)
R	universal gas constant (8.314 kJ/mole-K)
SEC	specific energy consumption (MJ/kg water evap.)
T	temperature (°C or K)
t	drying time (min)
Δt	time step (min)
U_o	overall heat transfer coefficient (W/m^2K)
W_{fan}	power of fan (kW)

Greek Letters

α_g	absorptivity of flue gas at the inside surface of combustion chamber (0.1695 decimal)
ε	effectiveness of heat exchanger (decimal)
ε_g	emissivity of flue gas at the inside surface of combustion chamber (0.1126 decimal)
ε_s	emissivity of mixture at the outside surface of combustion chamber (0.56 decimal)
η_f	efficiency of fan (0.575 decimal)
η_m	efficiency of motor (0.5 decimal)
η_o	overall surface efficiency of finned combustion chamber surface (0.94 decimal)
σ	Stefan–Boltzmann constant (5.669 10^{-8} W/m^2K^4)

Subscripts

a	air
abs	absolute
av	average
d	dry air
c,i	inner combustion chamber surface

c,o	outer combustion chamber surface
eq	equilibrium
f	final
fu	fuel
g	flue gas
go	exhaust gas
in	initial
m	mixture
p	dry product
s	superheated steam
w	wall of combustion chamber
1	entering the drying chamber
2	leaving the drying chamber
3	leaving the combustion chamber
4	leaving the heat exchanger

ACKNOWLEDGEMENTS

The authors express their sincere appreciation to the Thailand Research Fund (TRF) for supporting this study financially.

REFERENCES

1. Kudra, T.; Mujumdar, A.S. *Advanced Drying Technologies;* Marcel Dekker: New York, 2002.
2. Mujumdar, A.S. Superheated steam drying. *Handbook of Industrial Drying*, 2nd Ed., Marcel Dekker: New York, 1995; 1071–1086.
3. Shibata, H.; Mujumdar, A.S. Steam drying technologies: Japanese R&D. Drying Technology **1994**, *12*, 1485–1524.
4. Pronyk, C.; Cenkowski, S.; Muir, W.E. Drying foodstuffs with superheated steam. Drying Technology **2004**, *22* (5), 899–916.
5. Elustondo, D. Drying foodstuff with superheated steam. Drying Technology **2002**, *20* (1), 235–237.
6. van Deventer, H.C.; Hejimans, R.M.H. Drying with superheated steam. Drying Technology **2001**, *19* (8), 2003–2045.
7. Mujumdar, A.S. Superheated steam drying—Technology of the future. In *Mujumdar's Practical Guide to Industrial Drying;* Devahastin, S. Ed.; Exergex: Brossard, Canada, 2000; 115–138.
8. Namsanguan, Y.; Tia, W.; Devahastin, S.; Soponronnarit, S. Drying kinetics and quality of shrimp undergoing different two-stage drying processes. Drying Technology **2004**, *22* (4), 759–778.
9. Uengkimbuan, N.; Soponronnarit, S.; Prachayawarakorn, S.; Nathakaranakule, A. *Comparative study of pork dried using superheated steam and hot air.* In *Proceedings of the 3rd Asia-Pacific Drying Conference (ADC'03)*, Bangkok, Thailand, September 1–3, 2003; 679–691, 2003.

10. Tang, Z.; Cenkowski, S. Equilibrium moisture content of spent grains in superheated steam under atmospheric pressure. Transactions of the ASAE **2001**, *44*, 1261–1264.
11. Chen, S.-R.; Chen, J.-Y.; Mujumdar, A.S. A preliminary study of steam drying of silkworm cocoons. Drying Technology **1992**, *10* (1), 251–260.
12. Elustondo, D.; Mujumdar, A.S.; Urbicain, M.J. Optimum operating conditions in drying foodstuffs with superheated steam. Drying Technology **2002**, *20* (2), 381–402.
13. Iyota, H.; Nishimura, N.; Onuma, T.; Nomura, T. Drying of sliced raw potatoes in superheated steam and hot air. Drying Technology **2001**, *19* (7), 1411–1424.
14. Moreira, R.G. Impingement drying of foods using hot air and superheated steam. Journal of Food Engineering **2001**, *49*, 291–295.
15. Li, Y.B.; Seyed-Yagoobi, J.; Moreira, R.G.; Yamsaengsung, R. Superheated steam impingement drying of tortilla chips. Drying Technology **1999**, *17* (1–2), 191–213.
16. Prachayawarakorn, S.; Soponronnarit, S.; Wetchacama, S.; Jaisut, D. Desorption isotherms and drying characteristics of shrimp in superheated steam and hot air. Drying Technology **2002**, *20* (3), 669–684.
17. Soponronnarit, S.; Tichangtong, S.; Prachayawarakorn, S. Prototype of superheated-steam cabinet dryer. The Journal of the Royal Institute of Thailand **2002**, *27* (4), 1079–1090.
18. Tatemoto, Y.; Bando, Y.; Oyama, K.; Yasuda, K.; Nakamura, M; Sugimura, Y.; Shibata, M. Effects of operational conditions on drying characteristics in closed superheated steam drying. Drying Technology **2001**, *19* (7), 1287–1303.
19. Yoshida, T.; Hyodo, T. Evaporation of water in air, humid air and superheated steam. Industrial and Engineering Chemistry, Process Design and Development **1970**, *9* (2), 207–214.
20. Nijdam, J.J.; Keey, R.B. Airflow behavior in timber (lumber) kilns. Drying Technology **1999**, *17* (7–8), 1511–1522.
21. Kiranoudis, C.T.; Markatos, N.C. Computer analysis of industrial batch dryer aerodynamics. Drying Technology **1998**, *16* (7), 1283–1303.
22. Costa, V.A.F, da Silva, F.N. On the rate of evaporation of water into a stream of dry air, humidified air and superheated steam, and the inversion temperature. International Journal of Heat and Mass Transfer **2003**, *46*, 3717–3726.
23. Schwartze, J.P.; Brocker, S. The evaporation of water into air of different humidities and the inversion temperature phenomenon. International Journal of Heat and Mass Transfer **2000**, *43*, 1791–1800.
24. Chu, J.C.; Finelt, S.; Hoerrner, W; Lin, M.S. Drying with superheated steam-air mixtures. Industrial and Engineering Chemistry **1959**, *51* (3), 275–280.
25. Avallone, E.A.; Baumeister, T, III. Ideal gas mixtures. In *Handbook for Mechanical Engineers*, 10th Ed.; McGraw-Hill: New York, 1997; 4–8.
26. Chow, L.C.; Chung, J.N. Evaporation of water into a laminar stream of air and superheated steam. International Journal of Heat and Mass Transfer **1983**, *26* (3), 373–383.

27. Crank, J. Diffusion in sphere. In *The Mathematics of Diffusion*, 2nd Ed.; Oxford University Press: England, 1975; 89–103.
28. Wark, K. Jr. Equations of state. In *Advanced Thermodynamics for Engineers.*, McGraw-Hill: New York, 1995; 159–188.
29. Incropera, F.P.; Dewitt, D.P. *Introduction to Heat Transfer;* 3rd Ed.; John Wiley & Sons: New York, 1996.

Drying Technology, 23: 473–495, 2005
Copyright © 2005 Taylor & Francis, Inc.
ISSN: 0737-3937 print/1532-2300 online
DOI: 10.1080/DRT-200054121

Taylor & Francis
Taylor & Francis Group

High Temperature Spouted Bed Paddy Drying with Varied Downcomer Air Flows and Moisture Contents: Effects on Drying Kinetics, Critical Moisture Content, and Milling Quality

Thanid Madhiyanon*
Department of Mechanical Engineering, Mahanakorn University of Technology, Nong Chok, Bangkok, Thailand

Somchart Soponronnarit
School of Energy and Materials, King Mongkut's University of Technology, Thonburi, Bangkok, Thailand

Abstract: This research is an experimental study on paddy drying conducted in a two-dimensional spouted bed batch dryer to investigate the effects of downcomer airflow, drying temperature, and initial moisture content on drying kinetics, milling quality, and thermal energy consumption. The system of spouted bed drying and a comparison of spouted bed drying in the present study, and fluidized bed drying in the related literature, are also discussed. Downcomer air flows of 0, 20, and 30% ([defined as mass flow rate of downcomer air/total mass flow rate of air] × 100%), inlet air temperatures of 110, 130, and 150°C, and initial moisture contents of 18–35% d.b. were used. It was found that moisture transfer did not only occur in the spout region but also took place in the downcomer region. The moisture content and temperature of the paddy dropped as grain moved downward in the downcomer, which resulted from the presence of an evaporative cooling phenomenon. The characterization of drying curves regardless of any drying condition could be described by nearly linear relationships between moisture content and time. Although high downcomer air flow and drying temperature could enhance effective moisture reduction, they caused an adverse decrease in critical moisture content and HRY (head rice yield). Critical moisture content and HRY could also increase with an increase in initial moisture content. The difference in moisture content between the initial and critical moisture contents varied between 4.5 and 8.0%d.b., depending upon drying conditions. No significant

*Correspondence: Thanid Madhiyanon, Ph.D., Department of Mechanical Engineering, Mahanakorn University of Technology, 51 Cheum-Sampan Rd., Nong Chok, Bangkok 10350, Thailand. E-mail: thanid_m@yahoo.com, thanid_m@mut.ac.th

effect on color was evident. From the point of view of HRY, the correct management of a two-stage spouted bed drying system could be a suitable and attractive alternative for rice mills. Finally, a comparison between the spouted bed drying and fluidized bed drying showed that the spouted bed had advantages over the fluidized bed in terms of product quality. The specific drying rates (kg water evaporated $h^{-1}m^{-3}$) of both techniques were comparable. With respect to energy consumption, spouted bed drying was not as efficient as fluidized bed drying for intermediate initial moisture content, but a contrary result was obtained for low initial moisture content.

Keywords: Dehydration; Dryer; Fluidized bed; Head rice yield; Product quality; Rice mill; Rough rice; Spouting; Thermal energy consumption; Whiteness

INTRODUCTION

The combination of two hydrodynamic features, i.e., pneumatic transport, which is accompanied by intensive heat and mass transfers, and moving bed transport, which gives a chance for moisture relaxation as a tempering process, is a major feature of the spouted bed technique. The spouted bed technique was reviewed by Pallai et al.[1] The design principle was proposed by Passos et al.[2] A two-dimensional spouted bed dryer was first proposed by Mujumdar[3] in order to overcome the scaling-up limitations of the conventional cylindrical-conical spouted bed. Kalwar et al.[4] and Kalwar and Raghavan[5,6] later modified it with draft plates to study the drying of soybean, wheat, corn, and shelled corn. They found that the drying kinetics of these cereal grains during the constant drying rate period did not clearly exist. But the phenomenon could be represented by Page's equation. On the contrary, the experimental results found by Wetchakama et al.,[7] Nguyen,[8] Nguyen et al.,[9] and the recent work of Wiriyaumpaiwong et al.[10] showed nearly linear moisture and time relationships. A similar result was confirmed by a mathematical simulation performed by Madhiyanon et al.[11] Tulasidas et al.[12] found that effective moisture diffusion coefficient and drying rate increased as bed height decreased. This resulted from the shorter cycle time, which increased the intensive heat transfer period in the spout region. Drying characteristics were reported elsewhere in the literature.[13–18] However, the product quality after drying has received less attention in the literature, although it is very important and usually employed in appraising the success or failure of a grain drying system.

Recently, there was an attempt to introduce the two-dimensional spouted bed drying technique into a rice mill (Madhiyanon et al.[19]). The prototype displayed a maximum capacity of 3550 kg h^{-1} and a thermal energy consumption of 3.5–7.0 MJ (kg water evaporated)$^{-1}$, using

140–160°C drying temperatures and 0.6–0.7 fraction of air recycled. No serious loss in milling quality was observed. However, the prototype had limited success in moisture reduction due to insufficient dryer length. Madhiyanon et al.[20] developed a mathematical model for the prototype of continuous spouted bed dryer and found very good agreement between the simulated and experimental results.

However, after evaluating the experimental results of Madhiyanon et al.[19] it was believed that the continuous spouted bed paddy dryer had not been ready for positioning itself among other conventional dryers or fluidized bed paddy dryers that are now popular in Thai rice mills. Three main questions about spouted bed paddy drying have as yet not been answered, i.e., 1) how to maximize drying capacity in terms of drying rate per unit volume of dryer and related quality in terms of head rice yield; 2) if dryer length is extended in order to increase mean residence time, which results in more moisture reduction than that achieved by the prototype, are there any adverse effects on milling quality; and, finally 3) what strategies would be suitable for managing moist paddy with a variety of moisture contents. Information on the milling quality of paddy dried by spouted bed technique was rarely found. Only Nguyen et al.[9] reported that their triangular spouted bed dryer could continuously reduce paddy moisture content to around 18%d.b. with a satisfactory head rice yield regardless of drying temperature reaching up to 160°C.

The main objectives of this study are 1) to investigate the effects of introducing air through downcomer regions on drying kinetics, which is expected to promote intensive drying without any change of dryer volume; 2) to study the impact of drying conditions, i.e., drying temperatures, downcomer air flow, and initial moisture content, on the physical properties of rice after the milling process; 3) to determine a suitable system for drying paddy by spouted bed technique through analysis of the experimental results for drying kinetics and milling quality; and, finally, 4) to compare the present work and the work involved in fluidized bed paddy drying (Tirawanichakul et al.,[21] Poomsa-ad et al.[22]). We anticipate that this research will provide valuable outcomes for the rice mill industry and lead to further development of an industrial-scale continuous spouted bed paddy dryer that is acceptable for the rice mill industry.

MATERIALS AND METHODS

Materials

This experiment with paddy drying was conducted using a two-dimensional spouted bed batch dryer, as shown in Fig. 1. The dryer included

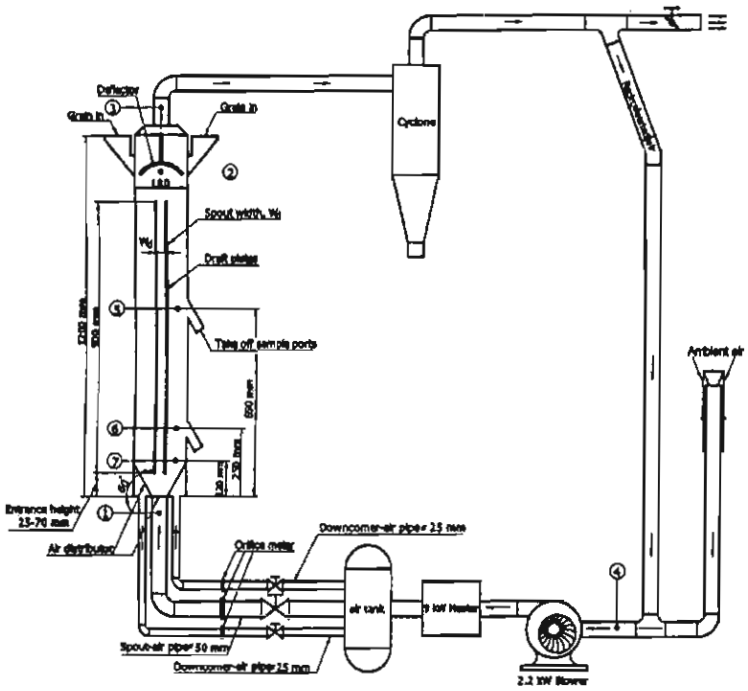


Figure 1. Schematic diagram of the two-dimensional spouted bed dryer with various downcomer air flow and temperature measurement positions.

a vertical rectangular chamber with a tempered glass window fitted to the front to permit visualization of the grain flow pattern, and a slant base chamber with an angle of 60°. Two draft plates, 90 cm in height, were installed centrally, such that each draft plate was 3.7 cm apart from the other. The overall dimensions were 80 cm in width, 8.4 cm in depth, and 120 cm in height. To investigate the drying kinetics and milling quality in terms of head rice yield and whiteness when air was introduced through the downcomer regions, hot air was distributed at the bottom of the slant base chamber through three air inlets, namely a central rectangular air inlet serving for the spout region with 3 cm in width and 8.4 cm in depth, and two round air inlets for the downcomer regions, each being 2.5 cm in diameter.

Air was heated by six electric heaters with a capacity of 1.5 kW each. The inlet air temperature was automatically controlled by a PID temperature controller with an accuracy of ±1°C. Temperatures were measured by a data logger and a temperature indicator with an accuracy

of ±1°C connected to a type K thermocouple. Air flow rates at high temperature were regulated by three orifice meters incorporating manual valves. For air recycled with temperatures under 90°C, air velocity was measured by hot wire anemometer with an accuracy of ±0.3 m/s and for temperatures of 90°C or more, a Pitot-static tube with U-tube manometer was used. A 2.2 kW variable speed drive was used to regulate blower motor speed to attain the desired air flow rate that could sustain the stability of spouting behavior, even when sharing much of the hot air for the downcomer regions. A three-phase kilowatt-hour meter was used to measure heater energy usage. One variety of long-grain rough rice, i.e., Suphanburi-1, which contains a high amylose content (27%) (Tirawanichakul et al.[21]) provided by the National Rice Research Center, Thailand, was selected as the test material.

Experiment Setup

Paddy moisture content was prepared by rewetting and keeping it in cold storage in a temperature range of 4–6°C for 7 days. During the cold storage period, paddy was mixed thoroughly once each day to ensure moisture uniformity. A preliminary study found that grain velocity was impacted upon and varied according to different fractions of downcomer air flow to total air flow, which could have either positive or negative effects on drying kinetics. Therefore, to eliminate the influence of different grain velocities accompanied by different airflows through the downcomer regions, the entrance height (see Fig. 1) was adjusted from one experiment to another to minimize any variations in grain velocity. Measurement of grain velocity was done by flow visualization and a stop watch. However, the finding in our experiments was that the maximum deviation in grain velocity did not exceed 15%. By visualizing paddy velocities, it was found that the lowest paddy velocity was 0.7 cm/s for 0% downcomer air flow, whereas it was nearly 1.0 cm/s for the remaining downcomer air flows (20 and 30%). By visualization, it could be seen that if air were allowed to flow upward through the downcomer, it would facilitate the circulation of grains at the bottom and hence grains stacked above could move downward easily to replace the ones below. In all experiments, the total mass flow rate of air was held constant at $0.053\,kg\,s^{-1}$.

The paddy samples for each set of conditions were collected at intervals of 2–3 mins for moisture content evaluation, milling quality, and energy consumption. Particularly for determining moisture variations in the downcomer region, samples were taken at distances of 23 and 63 cm above the air distributor. The total amount of sample taken from a dryer for each experiment was restricted to not more than 5% of the

initial holdup (6 kg) to ensure that the process mechanism was not deviated or disturbed. Therefore, several experiments were done to complete each set of conditions and more than 280 experiments were done for this study.

Experimental Conditions

Six kilograms of paddy, which created a bed height of 72 cm, were loaded into the drying chamber for each experiment. The inlet air temperatures were set at 110, 130, and 150°C. The total air mass flow rate for all experiments was held constant at around 0.053 kg/s, and some of it was divided and sent to the downcomer regions. The percentages of downcomer air flow ([mass flow rate of downcomer air/total mass flow rate of air] × 100%) were controlled at 0 (no downcomer air), 20, and 30%, respectively. Fractions of air recycled were varied within the range 0.75 to 0.80. Besides studying the effects of downcomer air flow and drying temperature, the effect of initial moisture content on critical moisture content (considered as the lowest that moisture content could be reduced before significant grain damage) and energy consumption were also studied. Thus, paddy was rewetted until reaching desirable moisture levels in the range of 18–35%d.b.

Physical Properties

In order to determine the moisture content of the paddy, 20 g samples of paddy were weighed with an electronic balance with an accuracy of 0.0001 g and were dried in a hot air oven at 103°C for 72 h. Before determining the quality of the paddy in terms of head rice yield and whiteness, paddy samples taken at each time step were dried under room conditions for 2 weeks or until the moisture content had been reduced to around 16%d.b. Then, each 125 g paddy sample was shelled by Satake rubber roll dehusker, polished by Satake rice polisher, and graded by a Satake grader, respectively. Finally, its color was measured by a Kett digital whiteness meter, which was calibrated with a white color reference.

RESULTS AND DISCUSSION

Variation of Air and Grain Temperatures

All temperatures within the dryer were measured at the positions shown in Fig. 1. The experimental results showed that even using the varied drying temperatures with the same downcomer air flow, air and grain temperature variations showed a similar trend. The experiments carried

out at 130°C drying temperature were chosen as an example to show the influence of downcomer air flow on temperature change within the dryer, as shown in Figs. 2a–c. It was apparent that the temperature difference between the inlet and exit air temperatures (curves 1 and 3), which represented the amount of heat consumed for moisture removal, was nearly constant throughout the drying period, which did not generally occur in other batch drying techniques. This was also found in related literatures.[7–10,11] In additional, the temperature difference increased with higher downcomer air flow.

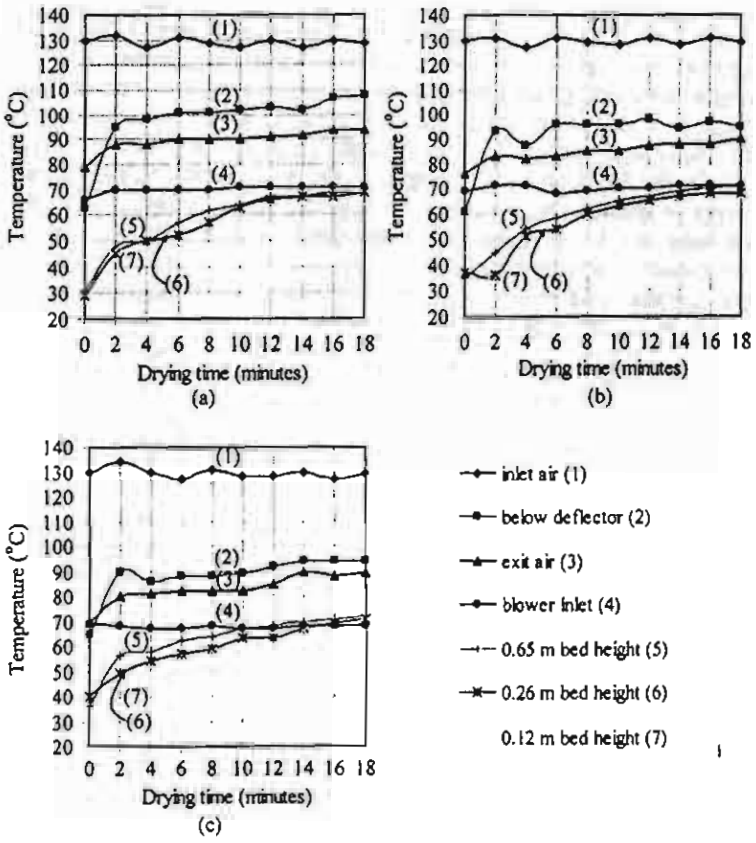


Figure 2. Variation of air and grain temperatures within the dryer according to different percentages of downcomer air flow (inlet temperature 130°C). (a) 0% Downcomer air flow. (b) 20% Downcomer air flow. (c) 30% Downcomer air flow.

According to the simulated results obtained from Madhiyanon et al.,[11] grain and air temperatures approached equilibrium within a few centimeters upstream from the air inlet. Thus, temperatures measured in the downcomer should represent the grain temperatures in the following text. Figs. 2a–c show that paddy temperatures decreased around 2–5°C during downstream movement, from 0.65 m (curve 5) to 0.12 m (curve 7). An explanatory hypothesis for this was the presence of an evaporative cooling phenomenon (instead of conventional drying process) while the paddy was traveling in the downcomer. This would be confirmed by the experimental results of moisture reduction inside the downcomer region. Finally, the effect of downcomer air flow on grain temperature was observed. When additional downcomer air flow was introduced, the paddy at the bottom had higher temperatures (curve 7) and would approximate the temperatures of the paddy in the near proximity above (curve 6). However, they were still lower than the temperatures of the paddy at the top (curve 5). Furthermore, it was also demonstrated that high grain temperature, accompanied by high downcomer air flow, was directly related to the drying rate and will be discussed later.

Moisture Reduction in the Downcomer Region

Madhiyanon et al.[11] presented simulation results that indicated that moisture reduction of grains did not only occur in the spout region, but also occurred in the downcomer region due to air leakage from the central inlet to the downcomer. This was proven experimentally by the present study. As shown in Figs. 3a–f, corresponding to experiments allowing air penetration to the downcomer (0, 20, and 30% downcomer air flow), moisture content of the paddy in the downcomer had been reduced around 0.2 to 0.7%d.b. from the moisture content at the beginning of the downcomer period for each 0.4 m trip of downstream movement (see Fig. 1 for positions of sample taking). The results also revealed that 20 and 30% downcomer air flows offered greater moisture reduction than no downcomer air flow (0%) (comparing Figs. 3a and 3f; 3b and 3d). However, in summary, it was found that operating the dryer at 20 and 30% downcomer air flows yielded no significant differences in moisture reduction. This was attributed to the moisture transfer mechanism, with internal control by moisture diffusion rather than external surface convective mass transfer. It was interesting to note that moisture reduction in the downcomer largely took place by "evaporative cooling phenomena," not conventional drying. Since the downcomer air flow had a low mass compared with that of the grain, it did not have enough energy to evaporate the moisture from the paddy. Specifically, it approached thermal equilibrium conditions with the paddy[11] and,

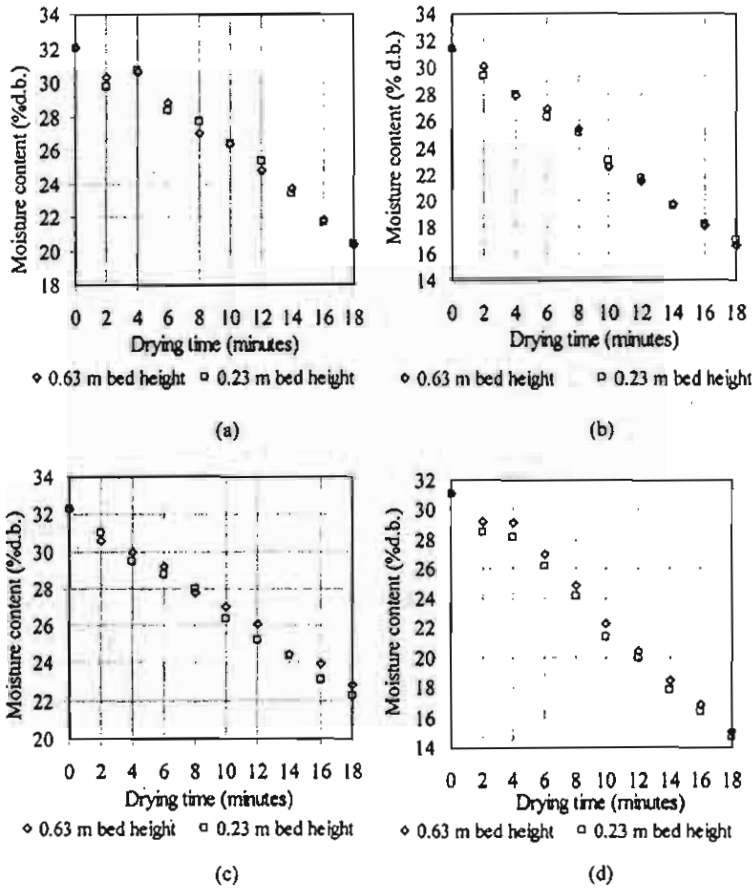


Figure 3. Moisture reduction along with the bed height in the downcomer region. (a) Inlet air temperature 130°C; 0% of downcomer air flow. (b) Inlet air temperature 150°C; 0% of downcomer air flow. (c) Inlet air temperature 110°C; 20% of downcomer air flow. (d) Inlet air temperature 150°C; 20% of downcomer air flow. (e) Inlet air temperature 110°C; 30% of downcomer air flow. (f) Inlet air temperature 130°C; 30% of downcomer air flow.

therefore, decreased moisture in the downcomer should result from heat accumulating inside the paddy, which performed as an internal heat generator to evaporate the water at the paddy surface. Then the water was picked up by the air uniformly distributed through the downcomer, which consequently causing the paddy to cool down while moving downward in the downcomer, as previously described.

Drying Curve Characteristics and Effective Moisture Reduction

Figures 4a–c exhibits the drying characteristics and the effects of drying temperatures on effective moisture reduction, which represent a combination of moisture reduction in the spout and downcomer regions. All experiments, regardless of varieties of drying temperatures and downcomer air flow conditions, found that most of the drying curves had similar drying characteristics, in which the correlations between moisture content and time were nearly linear relationships, as can be seen in

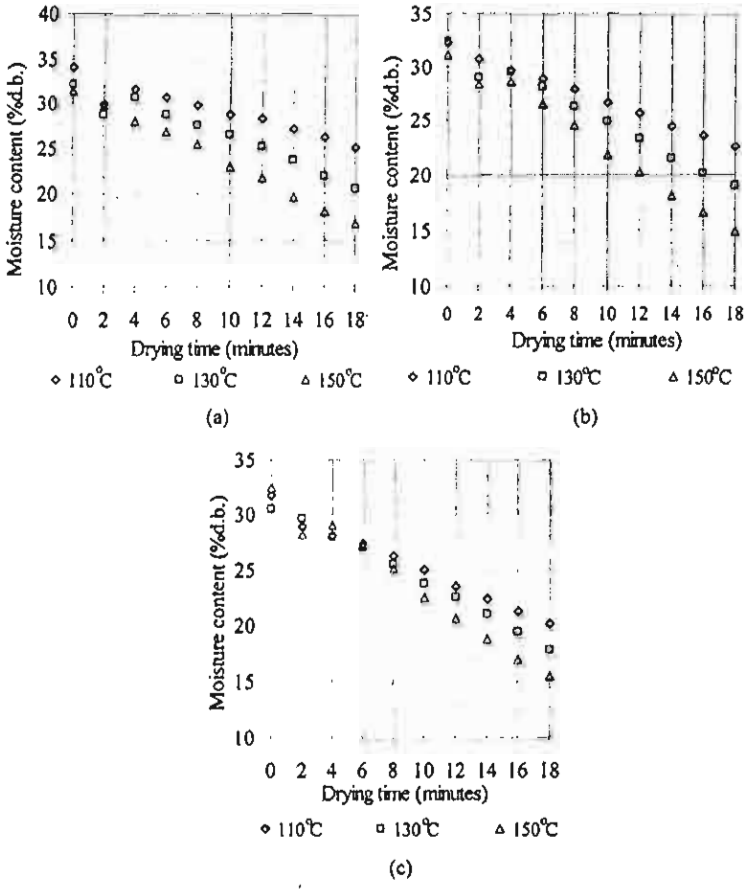


Figure 4. Nearly linear characteristic of spouted bed drying regardless of drying conditions of temperature and percentage of downcomer air flow. (a) 0% of downcomer air flow. (b) 20% of downcomer air flow.

previous studies.[7–11] This resulted from the assistance of moisture relaxation in the downcomer motion period, i.e., causing water to migrate from the inside to the outside of the grain kernel. This should facilitate water vaporization when grains transit to the spout region, where the grain is exposed to relatively high temperatures and air velocity. The drying kinetics of spouted bed are very different from the fluidized bed technique, in which the correlation between moisture content and drying time is exponential.[23,24] It was evident that the drying temperature significantly influenced the drying rate as the drying rate increased with increased drying temperature. Furthermore, in comparing Figs. 4a–c, it was clear that the drying rate was directly related to the drying temperature, since rapid decreases in moisture were achieved by applying high temperatures.

Figures 5a–c show the effect of downcomer airflow on effective moisture reduction. It was found that effective moisture reduction increased with increased downcomer airflow. However, moisture reduction in the downcomer was nearly the same, using either high or low downcomer air flow. Therefore, the difference of moisture reduction between using 0, 20, and 30% downcomer air flow should be gained from the drying mechanism in the spout region. This resulted from the grain being hotter with higher downcomer air flow, as seen in curve 7, in Figs. 2a–c.

Milling Quality

Figures 6–8 show the experimental results of milling quality, with relative head rice yield (HRY) variations with decreased moisture content at drying temperatures of 110, 130, and 150°C. At the beginning of drying, relative HRY increased and thereafter decreased along with decreasing moisture content. At the beginning, paddy drying under sufficiently high temperature and moisture content was quite suitable for initiating the gelatinization process. Therefore, the kernel became more resistant to cracking due to partial gelatinization that occurred at the surface of the rice kernel. However, as moisture was further continuously reduced, more stresses developed with a steep moisture gradient dominating the gelatinization effect, resulting in grain breakage during the milling process. In this study, initial moisture contents were classified into three levels, low (17–21%d.b.), medium (24–28%d.b.), and high (31–35%d.b.).

The Effects of Drying Temperatures, Downcomer Air Flows, and Initial Moisture Content on Critical Moisture Content

For drying paddy at a temperature of 110°C, paddy with a low initial moisture content of 21%d.b. could be safely dried to 14%d.b., which

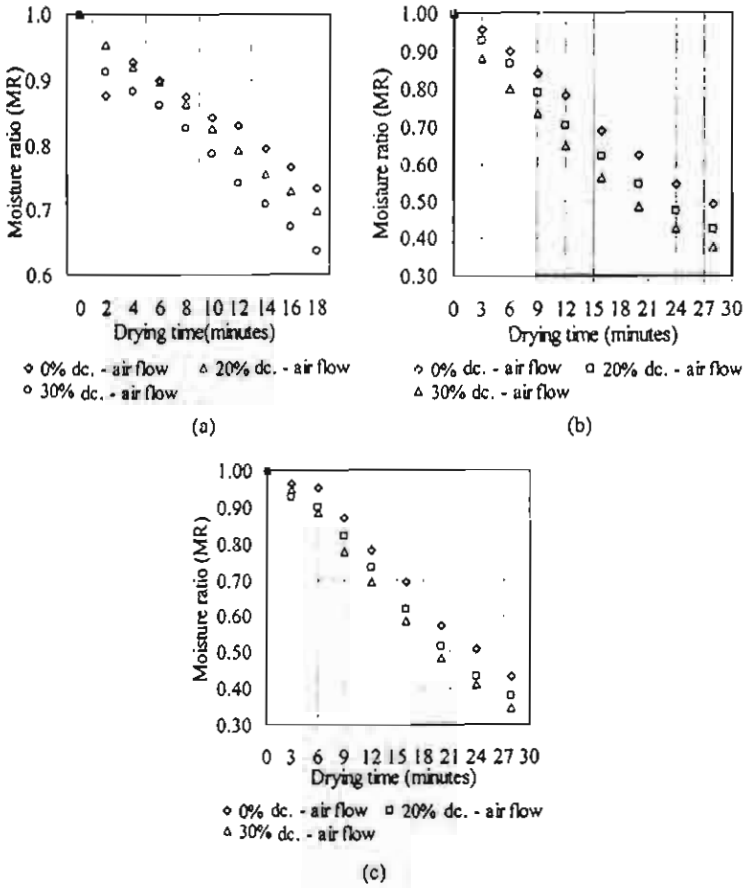


Figure 5. The effect of downcomer air flow on effective moisture reduction (dc. = downcomer). (a) Inlet air temperature 110°C. (b) Inlet air temperature 130°C.

was quite safe for storage (Fig. 6a). In the case of medium initial moisture contents of 27–28%d.b. (Fig. 6b), it was found that, in order to preserve paddy quality, paddy should not be continuously dried to a moisture level lower than the critical moisture content (defined as moisture content with 100 ± 5% relative HRY) of 21%d.b. These results are presented numerically in Table 1.

For a drying temperature of 130°C, moisture content could be reduced from 18%d.b. (low moisture content) to 13%d.b. without any

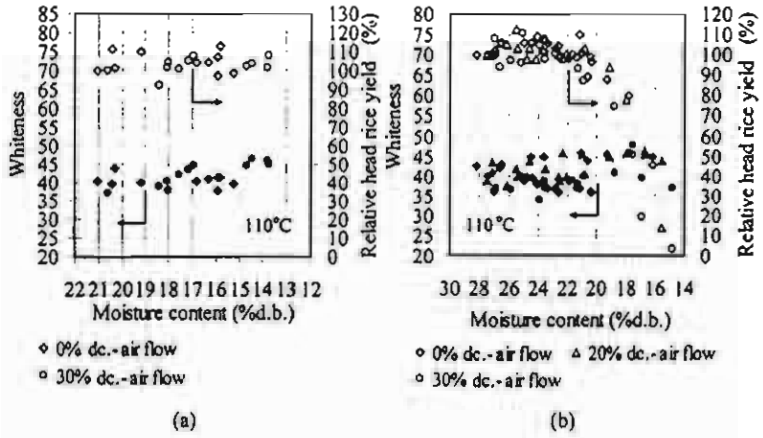


Figure 6. Variation of relative head rice yield and whiteness in relation to moisture content and initial moisture content at 110°C drying temperature (dc. = downcomer). (a) Low initial moisture content, 20.5 and 21%d.b. (whiteness reference, 37 and 40). (b) Medium initial moisture content, 27 and 28%d.b. (whiteness reference, 38 and 43).

loss of milling quality, as shown in Fig. 7a. However, as shown in Fig. 7b, paddy with a medium initial moisture content of 27–28%d.b. could not be dried below a critical moisture content of 22%d.b. in the case of 0% downcomer air flow, and the critical moisture content increased in the case of 20 and 30% downcomer air flows. In the case of a high initial moisture of 35%d.b., paddy could be dried to a critical moisture of 27–28%d.b. Table 1 gives more numeric details.

Fig. 8a shows the results of HRY under the highest drying temperature (150°C) and medium initial moisture contents of 24–25%d.b. The results show that the critical moisture content was about 19.5–20.5%d.b. and the critical moisture content for 30% downcomer air flow was less than that for 0% downcomer air flow, of around 1%d.b. For drying paddy with high initial moisture contents of 31–32%d.b., as shown in Fig. 8b, the critical moisture content was around 25–26%d.b.

In summary, a higher drying temperature was responsible for a higher critical moisture content, as seen by comparing Figs. 6b and 7b. Data in Figs. 6–8 and Table 1 show the influence of downcomer air flow on HRY, in that 0% downcomer air flow gave the best relative HRY results, while 30% downcomer air flow gave the worst. It was found that critical moisture content increased with initial moisture content. Finally, the differences between the initial and critical moisture

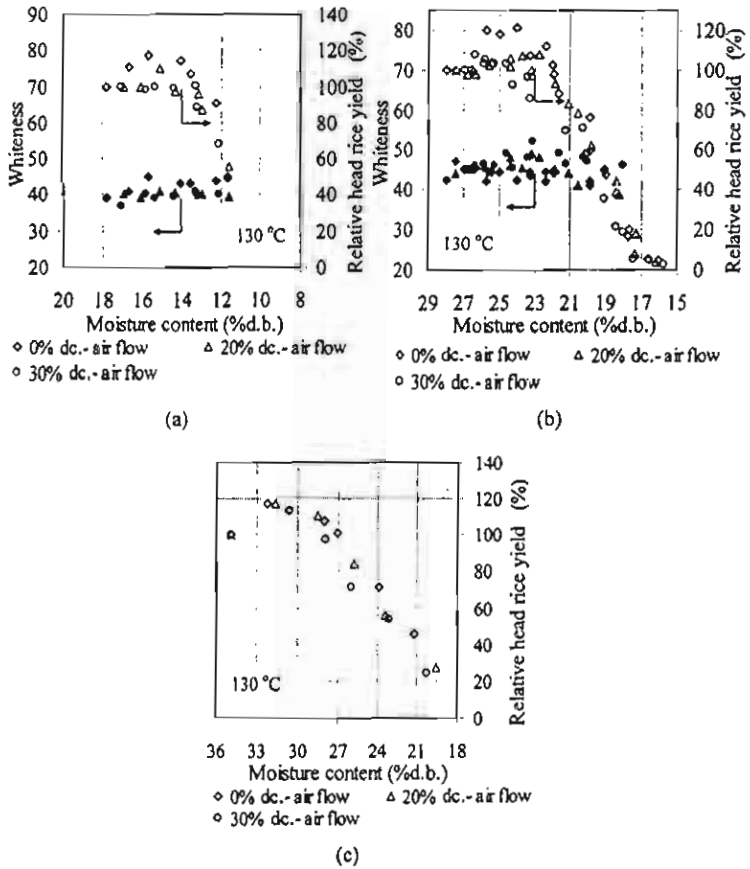


Figure 7. Variation of relative head rice yield and whiteness in relation to moisture content and initial moisture content at 130°C drying temperature (dc. = downcomer). (a) Low initial moisture content, 17%d.b. (whiteness reference, 39). (b) Medium initial moisture content, 26 and 27.5%d.b. (whiteness reference, 41 and 44. (c). High initial moisture content, 35%d.b.

contents varied between 4.5 to 8.0%d.b., depending upon the drying conditions.

Whiteness

Besides HRY, whiteness was also an important issue for judging paddy quality. The experimental results indicated no serious loss in whiteness, as shown in Figs. 6–8 and Table 1.

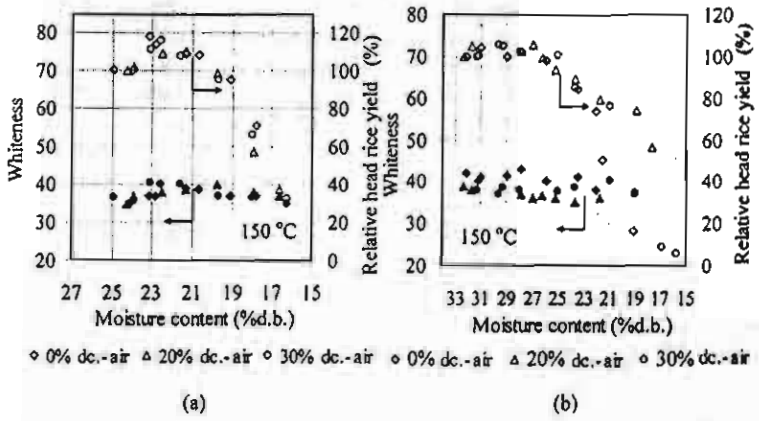


Figure 8. Variation of relative head rice yield and whiteness in relation to moisture content and initial moisture content at 150°C drying temperature (dc. = downcomer). (a) Medium initial moisture content, 24 and 25%d.b. (whiteness reference, 35 and 37). (b) High initial moisture content, 32%d.b. (whiteness reference, 38 and 42).

Thermal Energy Consumption

The experimental results (Table 2) indicated that the specific thermal energy consumption (SEC_{th}) slightly differed for any downcomer air flow and drying temperature. Using temperatures of 110, 130, and 150°C, with 75–80% recirculated air flow for drying paddy from a moisture content of 31%d.b. to approximately 15–20%d.b., consumed 5–6 MJ(kg water evaporated)$^{-1}$. These values of SEC_{th} were in line with 3.5–7.0 MJ(kg water evaporated)$^{-1}$ obtained from an industrial-scale continuous spouted bed paddy dryer prototype.[19] They were reasonable and relatively comparable with other conventional commercial dryers. Moreover, due to the almost constant drying rate characteristic of the spouted bed technique, the SEC_{th} remains almost unchanged throughout the entire drying period. Therefore, in respect to energy utilization, the spouted bed dryer would be competitive with other commercial dryers, especially for the intermediate moisture level.

Strategy for the Spouted Bed Drying Technique

The results of the paddy quality evaluation indicated that drying paddy from a high moisture content level to a level that was considered safe for storage in one stage was not recommended, and this is also true for

Table 1. Summary of the experimental results in accordance with Figures 6–8

Drying temp. (°C)	Fig. Nos.	%DC[a] air flow (%)	Initial MC (%d.b.)	Critical MC (moisture content at 100 ± 5% relative HRY, %d.b.)	Diff.[b] (%d.b.)	Reference whiteness	Average whiteness after drying
110	Fig. 6a	0	21.0	< 15.0	5.5	41	41
		20		—	—	—	—
		30	21.0	< 15.0	7.0	37	43
	Fig. 6b	0	27.0–28.0	20.5–21.0	6.5–7.0	42	41
		20	27.0	20.5–21.0	6.0–6.5	41	42
		30	27.0–27.4	21.5	6.0	39	39
130	Fig. 7a	0	17.8	13.0	4.8	39	43
		20	17.0	13.0	4.0	40	40
		30	17.0	13.0	4.0	37	40
	Fig. 7b	0	27.2–28.0	22.0	5.5–6.5	45	43
		20	26.7–27.4	22.0–23.5	3.5–5.5	45	45
		30	26.4–27.0	24.0–24.5	3.0–3.5	45	47
	Fig. 7c	0	35.0	27.0	8.0	—	—
		20	35.0	27.0	8.0	—	—
		30	35.0	28.0	7.0	—	—
150	Fig. 8a	0	24.0	19.5	4.5	36	38
		20	24.2	20.0	4.2	35	38
		30	25.0	20.5	4.5	37	38
	Fig. 8b	0	32.0	25.0	7.0	42	41
		20	32.3	25.0	7.3	39	36
		30	31.3	25.0	6.3	38	38

[a]DC = downcomer.
[b]Difference in moisture content between initial and critical moisture contents.

Table 2. The specific thermal energy consumption (SEC_{th}) of the spouted bed dryer.[a]

Drying temp. (°C)	Downcomer air (%)	Initial moisture content (%d.b.)	Final moisture content (%d.b.)	SEC_{th}[b] (MJ/kg water evap.)
110	0	34.0	24.9	4.9
	20	32.3	22.5	5.7
	30	31.6	20.1	5.5
130	0	32.0	20.4	5.8
	20	32.8	20.2	5.7
	30	30.5	17.8	5.6
150	0	31.4	16.8	5.9
	20	32.2	16.6	5.2
	30	32.5	15.5	5.6

[a]Air recycled fraction ranged between 0.7 and 0.8.
[b]Using diesel oil with 97% combustion efficiency instead of electrical heaters was an assumption for these SEC_{th} calculations.

fluidized bed drying or other conventional hot air drying. Therefore, two-stage drying (coupled with an intermediate tempering process) should be quite suitable for the spouted bed paddy drying. For moist paddy with a high moisture content, such as 30%d.b., which is within the moisture content range at harvest, temperatures of 130 or 150°C without downcomer air flow can be used for first-stage drying with a consequent approximate moisture content of 24%d.b. at the end of the first stage (interpreted with the assistance of Table 1). For the second stage, a temperature of 110°C with 0–30% downcomer air flows would give a final moisture content around 17–18%d.b. which is close to safe storage level. Before storage, paddy will be cooled by ambient air and the moisture content will further drop to 16–17%d.b. Therefore, properly managed spouted bed paddy drying could be an attractive alternative for rice mills.

Comparison of Spouted Bed and Fluidized Bed Techniques

Milling Quality Comparison

Comparing the drying capacity and milling quality of the spouted bed and fluidized bed techniques should be synchronized, since high drying capacity has no meaning if the product quality after drying is unacceptable. Regarding milling quality after the drying of paddy, Poomsa-ad et al.[22] reported that while drying paddy with a high initial moisture content of 30–35%d.b. with high drying temperatures of 110, 130, 150,

and 170°C in a single stage of a lab-scale fluidized bed dryer, more than 80% relative HRY, if final moisture content was above 25%d.b., could be achieved. The grain temperatures were in the range of 70–90°C. Under similar drying conditions to the present study, spouted bed dryer was able to reduce moisture content from 31 to 35%d.b. to 25 to 27%d.b. producing 100 ± 5% relative HRY (Figs. 7c, 8b, and Table 1).

For drying paddy with a medium moisture content, the study by Poomsa-ad et al.[22] found that continuous drying of paddy from 25 to 20%d.b. would have resulted in low relative HRY, which was lower than 40%, unless incorporating a subsequent tempering for 30 mins, which could raise relative HRY to more than 60%. Meanwhile, spouted bed drying could produce100 ± 5% relative HRY while reducing moisture content from 24 to 19.5%d.b. and 20 to 14%d.b. without tempering process (Figs. 6a, 8a, and Table 1). Poomsa-ad et al.[22] also noted that, to achieve high HRY under a high drying temperature in one pass of fluidized drying, corresponding to a grain temperature not above 100°C, the moisture content of paddy should not be reduced below 22.5%d.b., and a subsequent tempering for 30 mins was strongly recommended to preserve HRY.

As the above discussion has indicated, it was clear that, if starting drying with a high initial moisture content (30–35%d.b.), spouted bed drying was able to reach a lower critical moisture content compared with fluidized bed drying. In the other words, spouted bed drying could reach the same final moisture content in a single drying stage as fluidized bed drying, but achieve a higher HRY. For an initial moisture content no greater than 25%d.b., spouted bed drying offered greater moisture content decrease from the beginning, and better HRY.

Drying Capacity Comparison

The specific drying rate, defined as the drying rate per unit volume of drying chamber (kg water evaporated $h^{-1}m^{-3}$), was used as an index to measure the drying capacity of the dryer. A comparison of the specific drying rates of both techniques is shown in Table 3. The calculation of dryer volume according to spouted bed drying was based on dimensions, as shown in Fig. 1, while that of fluidized bed drying was based on the fluidized bed dryer studied by Tirawanichakul et al.[21] In that study, the dryer was of a cylindrical shape, 20 cm in diameter and 140 cm in height, and 1.9 kg of paddy corresponding to 10 cm static bed height was maintained constant. However, a drying chamber height of 100 cm, which largely matches the desired height of a fluidized bed paddy dryer was used in the present calculations. As Table 3 shows, if drying time was the only factor considered an indicator of drying capacity, it would appear that fluidized bed drying could reduce moisture substantially faster than

Table 3. Comparison of fluidized bed and spouted bed drying performance

Drying temp. (°C)	Initial moisture content (%d.b.)	Final moisture content (%d.b.)	Drying time (min)	Specific drying rate (kg water $h^{-1}m^{-3}$)
The fluidized bed drying[21]				
110	25.0	22.0	1.3	67
	28.2	21.5	2.4	78
130	28.2	22.7	1.4	110
	32.5	21.5	2.5	120
150	28.2	22.3	1.1	150
	32.5	22.0	2.0	144
The spouted bed drying (present study)				
110	21.0	14.0	15.0	80
	27.5	23.5	9.0	72
	27.5	20.9	15.0	72
130	26.9	21.2	10.0	93
	26.9	18.4	16.0	87
	35.0	27.0	12.0	103
150	25.0	18.0	10.0	116
	31.3	25.0	8.0	125
	31.3	20.9	12.0	137

spouted bed drying. However, the volume of the dryer and its holdup (capability of holding an amount of paddy for one batch of an experiment) should be taken into account for a fair comparison, and thus the specific drying rate was introduced as an indicator for this purpose.

Data in Table 3 show that the specific drying rates of spouted bed drying were comparable with those of fluidized bed drying at all drying temperatures. For fluidized bed drying, with an intermediate temperature of 110°C, the advantage of aggressive heat and mass transfer, due to the continuous contact of the grain and the air and good mixing characteristic, was counteracted by lesser driving force due to a lower temperature gradient between grain and air. Despite continuous exposure of grain to air, spouted bed drying allowed relaxation time (approximate 110 s for one cycle) in the downcomer period, which should help substantially in equalizing temperatures within the grain kernel. Thus, the surface temperature of the paddy at the end of downcomer period was not as high as when it was just emerging from the spout region, which led to enhanced heat transfer between the paddy surface and the air in the spout region.

For a high temperature of 150°C, spouted bed drying could also compete with fluidized bed drying, which could be explained by the observation that the drying characteristics of the fluidized bed were in

Arrhenius, or exponential, form, while an almost linear relationship represented the spouted bed drying characteristics. The fluidized bed conferred a steep decrease in moisture at the start of the drying process (accelerating drying speed), and thereafter moisture gradually decreased (decelerating drying speed), while a special feature of spouted bed drying was that it gave an almost constant drying rate, regardless of any moisture decrease from the initial moisture content. This made the specific drying rate of the spouted bed lag behind that of the fluidized bed at the start, while in the remaining period it could catch up with that of the fluidized bed.

Thermal Energy Consumption Comparison

Finally, the thermal energy consumption of both techniques was compared. Since experimental results of the energy consumption of a lab-scale fluidized bed were not available, records of thermal energy consumption of commercial fluidized bed dryers, as reported by Soponronnnarit et al.[25] (dryers with capacities of 2.5–5 tons/h and 5–10 tons/h), were used for this comparison. That study concluded that when drying paddy with initial moisture contents between 26.0–30.6%d.b., down to 21.0–23.0%d.b., SECsth (specific thermal energy consumption) were in the range 2.5–4.0 MJ(kg water evaporated)$^{-1}$, which was quite low compared with a conventional hot air dryer. However, in the case of drying paddy with low initial moisture content, such as 22.0%d.b. down to 20.1%d.b., SECth rose steeply to 7.8 MJ(kg water evaporated)$^{-1}$. Table 2 shows that the spouted bed could dry paddy from a high initial moisture content, i.e., 31.6–32.3%d.b. down to around 20.1–22.5%d.b. with SECsth of 5.5–5.7 MJ(kg water evaporated)$^{-1}$. Moreover, due to the almost constant drying rate characteristic of the spouted bed technique, the SECth should be almost the same for any level of moisture content. Table 2 indicates that it could reduce moisture content from 30.5 to 32.5%d.b. to 15.5 to 17.8%d.b. with nearly the same SECth of 5.6 MJ(kg water evaporated)$^{-1}$. In addition, referring to the data in Table 1 and the work done by Poomsa-ad et al.[22] it was necessary to divide the drying process into two stages to reduce moisture almost to safe storage level, while simultaneously maintaining acceptable milling qualities for both drying techniques. Therefore, the fluidized bed should consume less energy than the spouted bed for first-stage drying, but the opposite result would be obtained for second-stage drying, which normally starts with moisture contents around 20.0–22.0%d.b.

CONCLUSIONS

This experimental study of paddy drying in a two-dimensional spouted bed batch dryer was conducted to investigate the effects of drying temperature, downcomer air flow, and initial moisture content on drying kinetics, critical moisture content, and product quality. A comparison of spouted bed and fluidized bed drying and an appropriate system for spouted bed paddy drying were also discussed. The conclusions of this study follow.

1. Moisture decrease in spouted bed drying was a combination of moisture reduction in both the spout and downcomer regions. The evaporative cooling phenomenon was believed to be the main cause of moisture and bed temperature reduction, along with the downward movement of the paddy within the downcomer. It was demonstrated that downcomer air flows played an important role in effective moisture reduction, in that it increased with increasing downcomer air flow.
2. Drying curves, regardless of variations in drying temperature and downcomer air flow, were characterized by almost linear relationships between moisture content and time.
3. Drying conditions, such as drying temperature, amount of downcomer air flow, and initial moisture content, also significantly influenced critical moisture content and HRY. Using a high drying temperature and introducing downcomer air flow enhanced moisture reduction, but they had adverse effects on critical moisture content and HRY. The differences between initial and critical moisture contents were in the range of 4.5–8.0%d.b. and increasing with increases in initial moisture content.
4. From a product quality viewpoint, two-stage drying incorporating an intermediate tempering process appears suitable for a spouted bed paddy drying system. The commencement of drying with temperatures of 130 or 150°C for the first stage, followed by a drying temperature of 110°C for the second stage, is feasible.
5. A comparison of spouted bed paddy drying in the present study and fluidized bed paddy drying in the literature shows that for single-stage drying, the spouted bed provided significantly better product quality in terms of HRY than fluidized bed drying. The specific drying rates (kg water evaporated h^{-1} m^{-3}) of both techniques were comparable. Finally, the spouted bed consumed more energy than the fluidized bed when drying paddy with an intermediate initial moisture content, but the result was opposite with low initial moisture content. The SECsth of the spouted bed were almost the same at any level of moisture content and were in the range 5.5–5.7 MJ(kg water evaporated)$^{-1}$.

ACKNOWLEDGMENTS

This research was supported by a grant from Thailand Research Fund (TRF). We would like to gratefully acknowledge the contribution of Viboon Thepent (Post Harvest Engineering Research Group,

Agricultural Engineering Institute, Department of Agricultural) for milling quality test equipments. Thanks also are due to graduate students of mechanical engineering program (Mahanakorn University of Technology): Karn Karnjanabat, Siam Buntaowong, Arnut Suksa-add, Niwat Yimyoo, Arrun Maneenun, Arkom Siamol, Vacharapong Rukthongloh, Ubol Somjai, Apisit Prasertvit, Pakpoom Srilian, Itipon Yatoonkroh, and Nipol Chaitui for their assistance in experiments.

REFERENCES

1. Pallai, E.; Szentmarjay, T.; Mujumdar, A.S. Spouted bed drying. In *Handbook of Industrial Drying, Vol. 1*; 2nd Ed.; Mujumdar, A.S., Ed.; Marcel Dekker, Inc.; New York, 1995; 753–773.
2. Passos, M.L.; Mujumdar, A.S.; Raghavan, G.S.V. Spouted bed drying. In *Principles and Design Consideration in Drying, Vol. 4*; Mujumdar, A.S., Ed.; Hemisphere: New York, 1987; 359–398.
3. Mujumdar, A.S. *Spouted Bed Technology: A Brief Review, Drying'84*; Hemisphere: Washington, 1984; 151–157.
4. Kalwar, M.I.; Kudra T.; Raghavan, G.S.V.; Mujumdar A.S. Drying of grains in a drafted two dimensional spouted bed. Journal of Food Process Engineering **1991**, *13*, 321–332.
5. Kalwar, M.I.; Raghavan, G.S.V. Batch drying of shelled corn in two-dimensional spouted beds with draft plates. Drying Technology—An International Journal **1993**, *11* (2), 339–354.
6. Kalwar, M.I.; Raghavan, G.S.V. Circulation of particles in two-dimensional spouted beds with draft plates. Powder Technology **1993**, *77*, 233–242.
7. Wetchacama, S.; Soponronnarit, S.; Swasdisevi, T.; Panich-ing-orn, J.; Suthicharoenpanich, S. *Drying of high moisture paddy by two-dimensional spouted bed technique*. In Proceedings of the First Asian-Australian Drying Conference (ADC '99), Bali: Indonesia, October 24–27, 1999, 300–307.
8. Nguyen, L.H. *Evaluation of a Modified Spouted Bed Dryer for High Moisture Grain Drying*. Ph.D. Thesis, University of New South Wales: Australia, 2000.
9. Nguyen, L.H.; Driscoll, R.H.; Srzednicki, G. Drying of high moisture content paddy in a pilot scale triangular spouted bed dryer. Drying Technology—An International Journal **2001**, *19* (2), 375–387.
10. Wiriyaumpaiwong, S.; Soponronnarit, S.; Prachayawarakorn, S. Soybean drying by two-dimensional spouted bed. Drying Technology—An International Journal **2003**, *21* (9), 1735–1757.
11. Madhiyanon, T.; Soponronnarit, S.; Tia, W. A two-region mathematical model for batch drying of grains in a two-dimensional spouted bed. Drying Technology—An International Journal **2001**, *19* (5), 1045–1064.
12. Tulasidas, T.N.; Kudra, T.; Raghavan, G.S.V. Effect of bed height on simultaneous heat and mass transfer in a two-dimensional spouted bed dryer. Heat Mass Transfer **1993**, *20*, 79–88.
13. Becker, H.A.; Sallans, H.R. Drying wheat in a spouted bed. Chemical Engineering Science **1960**, *13*, 97–112.

14. Zuritz, C.A.; Singh, R.P. In *Simulation of Rough Rice Drying in a Spouted Bed, Drying'82*; Mujumdar, A.S., Ed.; McGraw-Hill Hemisphere: New York, 1982; 239–247.
15. Zahed, A.H.; Epstein, N. Batch and continuous spouted bed drying of cereal grains: The thermal equilibrium model. Canadian Journal of Chemical Engineering **1992**, *70*, 945–953.
16. Zahed, A.H.; Epstein, N. On the diffusion mechanism during spouted bed drying of cereal grains. Drying Technology—An International Journal **1993**, *11* (2), 339–354.
17. Jumah, R.Y.; Mujumdar, A.S.; Raghavan, G.S.V. A mathematical model for constant and intermittent batch drying of grains in a novel rotating jet spouted bed. Drying Technology—An International Journal **1996**, *14* (3–4), 765–802.
18. Jumah, R.Y.; Mujumdar, A.S.; Raghavan, G.S.V. A mathematical model for constant and intermittent batch drying of grains in a novel rotating jet spouted bed. In *Mathematical Modeling and Numerical Techniques in Drying Technology;* Mujumdar, A.S., Turner, I., Eds.; Marcel Dekker, Inc.: New York, 1997; 339–380.
19. Madhiyanon, T.; Soponronnarit, S.; Tia, W. Industrial-scale prototype of continuous spouted bed paddy dryer. Drying Technology—An International Journal **2001**, *19* (1), 207–216.
20. Madhiyanon, T.; Soponronnarit, S.; Tia, W. A mathematical model for continuous drying of grains in a spouted bed dryer. Drying Technology—An International Journal **2002**, *20* (3), 587–614.
21. Tirawanichakul, S.; Prachayawarakorn, S.; Tungtrakul, P.; Warunyanond, W.; Soponronnarit, S. *Effect of drying temperature on physical property of high and low amylose content paddy*. In Proceedings of the International Conference on Innovation in Food Processing Technology and Engineering, AIT, Bangkok, Thailand, December 11–13, 2002; Jindal et al., Eds.; Asian Institute of Technology: Bangkok, Thailand, 2002, 467–480.
22. Poomsa-ad, N.; Soponronnarit, S.; Prachayawarakorn, S.; Terdyothin, A. *Head rice yield after drying by fluidization technique and tempering*. In Proceedings of 2nd Asian-Oceania Drying Conference (ADC), Batu Feringhi, Pulau Pinang, Malaysia, August 20–22, 2001; Daud et al., Eds.; The Institute of Chemical Engineers: Malaysia, 2001, 717–726.
23. Prachayawarakorn, S.; Soponronnarit, S. Mathematical model of fluidised bed paddy drying. Engineering Journal: Research and Development **1993**, *4*, 101–109 (in Thai).
24. Tumambing, J.A.; Driscoll, R.H. *Modelling the performance of a continuous fluidised bed dryer for rapid pre-drying of paddy*. In Proceedings of the 14th ASEAN Seminar on Grain Post-Harvest Technology; Naewbanij, J.O.; Manilay, A.A., Eds.; Manila, Philippines. AGGP, Bangkok, Thailand, 1991, 193–213.
25. Soponronnarit, S.; Prachayawarakorn, S.; Wangji, M. *Commercial fluidised bed paddy dryer*. In Proceedings of the 10th International Drying Symposium, Krakow, Poland, 1996; Strumillo, C.; Pakowski, Z., Eds.; Poland. Lodz Technical University: Poland, 1996, Vol. A, 638–644.

Available online at www.sciencedirect.com
SCIENCE DIRECT®
Applied Energy 81 (2005) 198–208
APPLIED ENERGY
www.elsevier.com/locate/apenergy

Closed-ended oscillating heat-pipe (CEOHP) air-preheater for energy thrift in a dryer

S. Rittidech *, W. Dangeton, S. Soponronnarit

Faculty of Engineering, Mahasarakham University, Thailand

Accepted 2 June 2004
Available online 5 January 2005

Abstract

The CEOHP air-preheater consisted of two main parts, i.e. the rectangular house casing and the CEOHP. The house casing was designed to be suitable for the CEOHP. The inside house casing divided the CEOHP into three parts, i.e. the evaporator, the adiabatic section and condenser section. The CEOHP air-preheater design employed copper tubes: thirty-two sets of capillary tubes with an inner diameter of 0.002 m, an evaporator and a condenser length of 0.19 m, and each of which has eight meandering turns. The evaporator section was heated by hot-gas, while the condenser section was cooled by fresh air. In the experiment, the hot-gas temperature was 60, 70 or 80 °C with the hot-gas velocity of 3.3 m/s. The fresh-air temperature was 30 °C. Water and R123 was used as the working fluid with a filling ratio of 50%. It was found that, as the hot-gas temperature increases from 60 to 80 °C, the thermal effectiveness slightly increases. If the working fluid changes from water to R123, the thermal effectiveness slightly increases. The designed CEOHP air-preheater achieves energy thrift.
© 2004 Elsevier Ltd. All rights reserved.

Keywords: Closed-ended oscillating heat-pipe air-preheater; Energy thrift dryer

* Corresponding author. Tel.: +66-43-754316; fax: +66-43-754316.
E-mail address: s_rittidej@hotmail.com (S. Rittidech).

0306-2619/$ - see front matter © 2004 Elsevier Ltd. All rights reserved.
doi:10.1016/j.apenergy.2004.06.003

Nomenclature

A	area (m^2)
C_p	specific heat at constant pressure (J/kg K)
D	diameter (m)
g	gravitational acceleration (m/s^2)
h_{fg}	latent heat of vaporization (kJ/kg)
Ku	Kutateladze number $\left(\frac{q}{h_{fg}\rho_v\left(\sigma g(\rho_l-\rho_v)/\rho_v^2\right)^{1/4}}\right)$ (–)
k	thermal conductivity (W/mK)
L	length (m)
n	number of the capillary tube (–)
Pr_v	Prandtl number of vapor $\left(\frac{C_{pv}\mu_v}{k_v}\right)$ (–)
Q	heat-transfer rate (W)
q	heat flux (W/m^2)
T	temperature (°C)
V	velocity (m/s)

Greek symbols

μ	viscosity (Pa s)
ρ	density (kg/m^3)
σ	surface tension (N/m)

Subscripts

c	cold
e	evaporator
i	inside, inlet
l	liquid
o	outet
t	total
v	vapor

1. Introduction

1.1. Target

The effort to reduce energy consumption is a main goal for the dryer. Traditionally the dryer is unable to use its waste heat. Compared with other conventional heat-exchangers, the closed-ended oscillating heat-pipe (CEOHP) heat-exchanger has many advantages, e.g. large quantities of heat are transported through a small cross-section area. The CEOHP is a very effective heat-transfer device [1]: it has a simple structure and a fast thermal-response. The CEOHP consists of a long capil-

lary tube bent into many turns and the evaporator, adiabatic section and condenser section are located at these turns. However, there is no wick structure to return the condensate liquid from the condenser to the evaporator section. Heat is transported from the evaporator section to the condenser section by the pulsation of the working fluid moving in an axial direction in the tube. The inner diameter of the pipe is important. It must be small enough so that, under operational conditions, liquid slugs and vapor plugs can be formed. If the diameter is too large, the liquid and vapor inside the tube will become stratified and operation cannot be established. Rittidech et al. [3] investigated the effect of inclination angles, evaporator lengths and working-fluid properties on the heat-transfer characteristics of the CEOHP under normal operating condition. Rittidech et al. [4] devised a correlation to predict the heat-transfer characteristics of a CEOHP. Yang et al. [5] studied a water heat-pipe heat-exchanger using automotive-exhaust gas. The experimental results indicate it is worthwhile using a heat-pipe heat-exchanger employing the exhaust gas.

The application of CEOHPs, in order to save energy, is considered. The CEOHP can have many applications such as, economizers or air preheaters, electronic-cooling devices and solar collectors to name just a few. The new type of heat-pipe or CEOHP, shown in Fig. 1, can help in energy saving, specifically for air preheating in a dryer. The objective of the present study is to design, construct and test the CEOHP air-preheater for a dryer that can recover the waste heat from the drying process.

1.2. Conventional-drying process (see Fig. 2)

First, the air is heated by fuel combustion. Then the hot air moves through the layers of the product. The heat is transferred to the product and evaporation occurs.

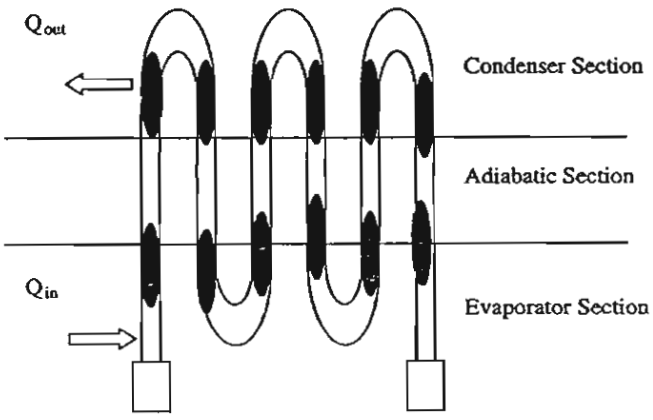


Fig. 1. Closed-end oscillating heat-pipe (CEOHP).

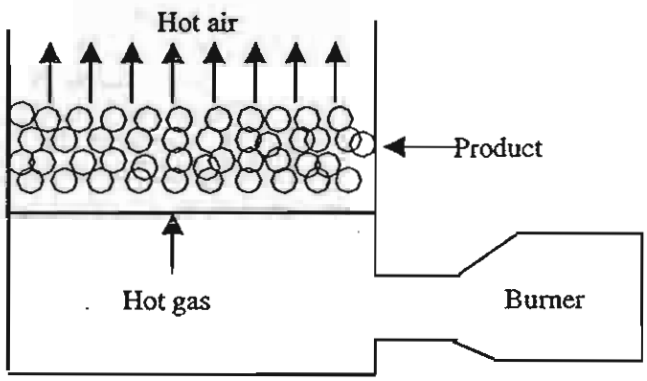


Fig. 2. Conventional drying-process.

2. CEOHP air-preheater system – design concept and calculation

Some fundamental design parameters e.g. the maximum heat-transfer rate of the drying system (Q_{max}, W) and the installation site depending on the available space have to be considered. Hence for the counterflow air-preheater heat-exchanger, the following set of equations applies [6]:

$$Q_{max} = C_{min}(T_{hi} - T_{ci}),$$
$$C_{min} = \rho V A C_p. \tag{1}$$

2.1. CEOHP air-preheater design

When considering the design of the CEOHP air-preheater, the size and position of the air-preheater are taken into consideration, as well as the maintenance and budget costs. In addition, insulating the ducts and air-preheater also decreases the heat loss. The CEOHP air-preheater heat-transfer design was solved in six steps as follows:

- The hot-gas temperature of initial and fresh air temperature from drying process is obtained.
- The working temperature is calculated and the tube material is selected.
- The type of working fluid that is appropriate to the operational temperature.
- The inner diameter of the CEOHP is calculated from Maezawa et al. [2].

$$D_{max} \leqslant \sqrt{\frac{\sigma}{\rho_l g}}. \tag{2}$$

- L_e, L_a, L_c, L_t, and n are defined corresponding to the duct size of the dryer and the installation area.

- Pr_v, ρ_v, ρ_l, h_{fg} and the oscillation phenomena of the working fluid at working temperature are described and the heat flux of CEOHP air-preheater is solved by the correlation from [4]. The standard deviation of this equation is ±30%.

$$Ku_{90} = 0.0067\left[\left(\frac{D_i^{3.1}L_t^{0.1}}{L_c^{3.2}}\right)n^{0.9}Pr_v^{-12}\left(\frac{\rho_v}{\rho_l}\right)^{-0.1}\left(\frac{\omega\mu_v^3}{\sigma^2\rho_v}\right)^{0.01}\right]^{0.175}. \quad (3)$$

It was necessary to change from the heat flux (q) from to the heat-transfer (Q)

$$Q_{90} = (Aq_{90}). \quad (4)$$

From this correlation, the meaning of each parameter can be discussed as follows:

Ku_{90} indicates the ratio of heat flux to critical heat flux for the vertical orientation.

$D_i^{3.1}L_t^{0.1}/L_c^{3.2}$ defines the size of the CEOHP. For example, if the value of $D_i^{3.1}L_t^{0.1}/L_c^{3.2}$ was very high, then the tube would be large and the evaporator section would be short. Because of the boiling phenomenon, the value of Ku_{90} or heat flux would be high. If the value of $D_i^{3.1}L_t^{0.1}/L_c^{3.2}$ was very low, then the tube would be small and the evaporator section would be long. Because the boiling phenomenon within this type of tube will be akin to the boiling phenomenon in a confined channel, the values of Ku_{90} or heat flux will be low.

The number n indicates that of the capillary tubes which connect the evaporator and the condenser section of a CEOHP or represents the number of turns of a CEOHP; Pr_v indicates the ratio of momentum diffusivity to the thermal diffusivity of vapor slug. If the value is very low, the vapor slug will be able to transfer the thermal energy to the condenser section relatively efficient. Therefore, the vaule of Ku_{90} or heat flux will be high.

The ratio ρ_v/ρ_l indicates the vapor phase density to liquid phase density of the working fluid that represents the working pressure the working fluid within the CEOHP.

The oscillation phenomena within the CEOHP, can be described by $\omega\mu_v^3/\sigma^2\rho_v$, i.e.

$$\frac{\omega\mu_v^3}{\sigma^2\rho_v} = \left(\frac{g\mu_v^4/\rho_v\sigma^3}{\rho_v L_v\sigma/\mu_v^2}\right)^{0.5}\left(\frac{\rho_l}{\rho_v}\right)^{0.5},$$

where the capillary buoyancy number is $(g\mu_v^4/\rho_v\sigma^3)$ and the Suratman number $(\rho_v L_v\sigma/\mu_v^2)$.

The capillary bouyancy and Suratman numbers are the ratios of surface tension force and the viscous force. The frequency ω of the oscillating motion of the vapor slug in a tube is defined as the frequency of simple harmonic motion, i.e. $\omega = \sqrt{\rho_l g/\rho_v L_v}$.

Values of some of these parameters are shown in Table 1.

The effectiveness of CEOHP air-preheater, ε, is defined as the ratio of the actual heat-transfer rate for an air-preheater heat-exchanger to the maximum possible heat-transfer rate, i.e.,

Table 1
The parameters used in the correlation for predicting the heat-transfer rate

Characteristic and parameter	Description
Material of tube	Copper
Internal diameter of tube from criterion (2) (m)	0.002
Length of CEOHP	
Total length (m)	6
Evaporator length (m)	0.19
Condenser length (m)	0.19
Number of turns	8
Working fluid	Water
T_{hi}, T_{Ci} (°C)	80,30
Working temperature (°C)	55

Table 2
The results of calculation

Heat-transfer from correlation [3] (W)	111
Number of CEOHP (set)	32
Total heat-transfer from correlation [3] (W)	3552

$$\varepsilon = \frac{Q_{\text{Actual}}}{Q_{\text{Max}}}, \tag{5}$$

where

$$Q_{\text{Actual}} = \rho V A C_p (T_{co} - T_{ci}). \tag{6}$$

The results of the calculation are shown in Table 2.

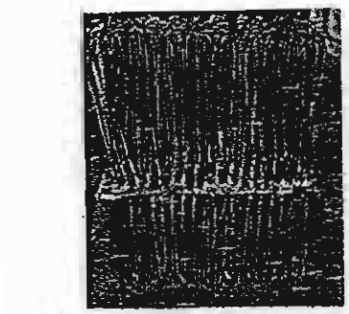
3. Experimental set-up

3.1. Prototype

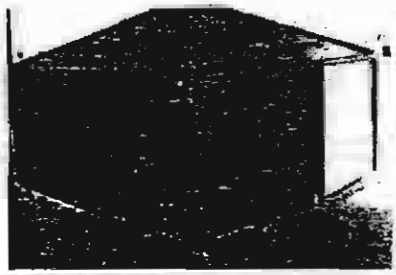
The CEOHP air-preheater for the drying process, see Fig. 3, was divided into two parts, i.e. the evaporator and condenser section with the length of 0.19 m. The tube arrangement was aligned in the direction of the hot-gas flow. The condenser section was connected to the fresh-air section and the evaporator section was in contact with the heat source from the gas burner. The dryer-bath type was selected to be appropriate to the CEOHP air-preheater. The prototype has a duct size area of 200 mm × 200 mm including the fibre insulation.

3.2. Test rig

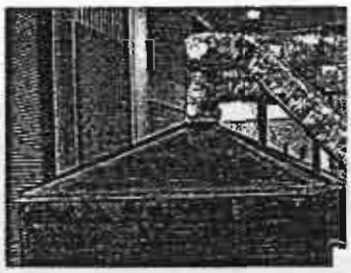
This prototype was installed in a test rig, as shown in Fig. 4. The hot-gas coming from the gas burner flows through the CEOHP air-preheater. The initial and final temperatures are measured with thermocouples. Twelve thermocouples type K were



(a) CEOHP air-preheater



(b) Batch-type dryer



(c) Dryer with CEOHP air-preheater

Fig. 3. The prototype: (a) CEOHP air-preheater; (b) batch-type dryer; (c) dryer with CEOHP air-preheater.

installed on the evaporator section and twelve more on the condenser. These thermocouples were connected to a Yokogawa-MX100 acquisition data-system. When a steady state was achieved, the temperatures at the inlet and outlet of the evaporator and the condenser section were recorded. The heat-transfer rate and effectiveness were determined and compared with the predicted values.

The controlled parameter was the hot-gas velocity of 3.3 m/s

The variable parameters were:

- working-fluid water or R123,
- hot-gas temperature of 60, 70 or 80 °C.

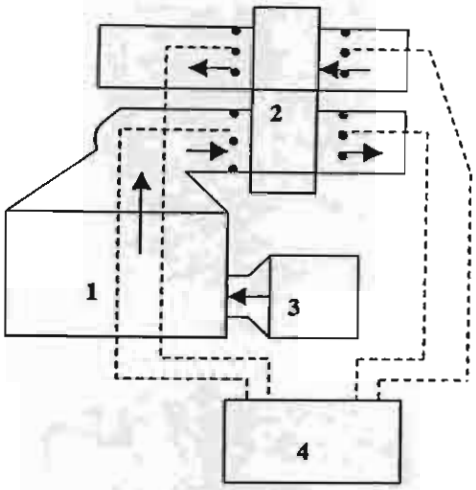


Fig. 4. Test rig: 1, dryer; 2, CEOHP air-preheater; 3, gas burner; 4, data logger; •, thermojunction.

4. Results and discussion

Table 3 shows the results of the experiment.

4.1. Effect of hot-gas temperature on heat-transfer rate

In this experiment, the CEOHP air-preheater had eight turns, 32 columns, and a hot-gas velocity of 3.3 m/s. The experimental results present the effect of the hot-gas temperature on the heat-transfer rate – see Fig. 5. This figure compares the experimental results with the predictions from the correlation [3]. It can be seen that, when the hot-gas inlet temperature increases, the heat-transfer rate also rises. This is because when the hot-gas inlet-temperature increases, the fresh-air outlet-temperature also increases. Thus, the temperature difference between the inlet and outlet air temperature also increases and the actual heat-transfer rate will be high. The heat-transfer rate as measured was lower than that predicted via the correlation [3]. However,

Table 3
The results of experiment

W	T_{hi}	T_{ci}	T_{co}	Q_{ac}	Q_{pred}	Q_{max}	ε
Water	80	30	48	2628	3552	373	0.41
	70	30	44	2044	3265	5356	0.38
	60	30	40	1460	2970	4288	0.34
R123	80	30	54	3504	3554	6373	0.54
	70	30	47	2482	3390	5356	0.46
	60	30	43	1898	3129	4288	0.44

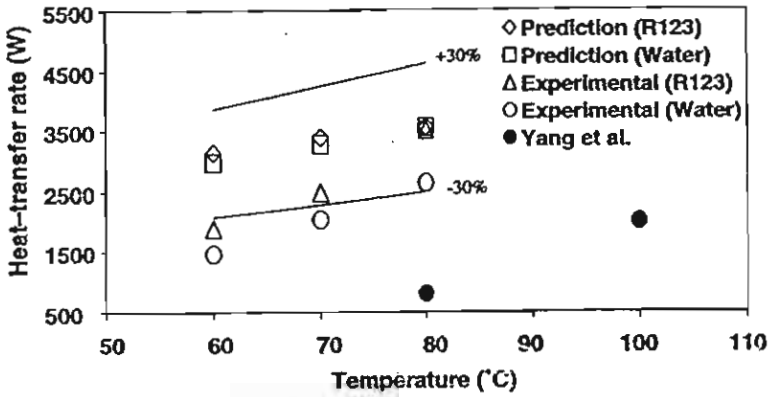


Fig. 5. Effect of temperature and working fluid on heat-transfer rate.

the predictions compare well with experimental data for the 80 °C run. In addition, when the hot-gas temperature increased from 70 to 80 °C the experimental data were within the standard deviation of ±30% from the correlation predictions. It can be concluded that, if the hot-gas temperature increases, the heat-transfer rate increases.

4.2. Effect of working fluid on heat-transfer rate (see Fig. 5)

In this experiment, the effect was measured for the CEOHP air-preheater with eight turns and 32 columns, and a hot-gas velocity of 3.3 m/s. Fig. 5 compares the heat-transfer rate experimental data to the heat-transfer rate predicted from the correlation [3] and the data [5]. If the working fluid changes from water to R123, the heat-transfer rate also increases, because the R123 has a lower latent heat of vaporization. It can be concluded that, if the working fluid is changed from water to R123, the heat-transfer rate increases.

4.3. Effect of hot-gas temperature on thermal effectiveness (see Fig. 6)

In this experiment, the CEOHP air-preheater has eight turns and 32 columns, and a hot-gas velocity of 3.3 m/s. Fig. 6 shows the effect of the hot-gas inlet-temperature on the effectiveness of the CEOHP air-preheater. It can be seen that, when the hot-gas inlet-temperature increases, the effectiveness also rises because the fresh-air outlet temperature also increases. Thus, the temperature difference between the inlet and outlet air also increases and the actual heat-transfer rate will be high. It can be concluded that, if the hot-gas inlet temperature increases, the effectiveness increases.

4.4. Effect of working fluid on thermal effectiveness (see Fig. 6)

In this experiment, the CEOHP air-preheater has eight turns and 32 columns, and a hot-gas velocity of 3.3 m/s. It can be seen in Fig. 6 that, if the working fluid changes

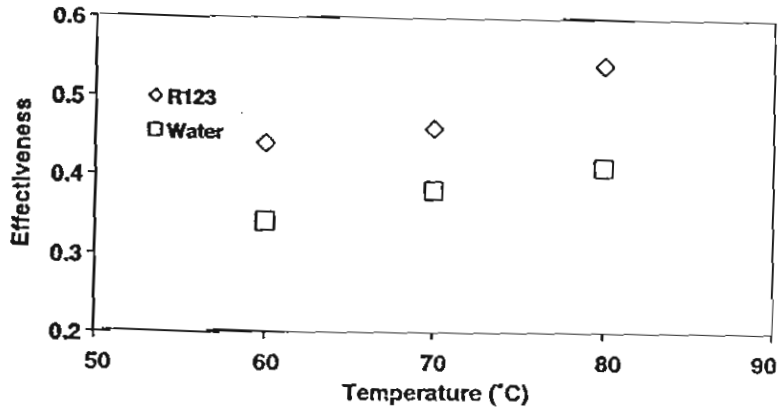


Fig. 6. Effect of temperature and working fluid on effectiveness.

from water to R123, the effectiveness also increases because the R123 has a lower latent heat of vaporization.

5. Conclusion

In this study, we designed and built an experimental prototype to investigate the applicability of a CEOHP air-preheater as a waste-heat recovery device for a drying process. It can be concluded that:

- As the hot-gas temperature increases from 60 to 80 °C, the heat-transfer rate slightly rises.
- If the working fluid changes from water to R123, the heat-transfer rate slightly increases.
- The designed CEOHP air-preheater can achieve energy thrift.

Acknowledgements

The research has been supported generously by the Thailand Research Fund (Under Contract No. MRG4680023). The authors express their sincere appreciation for all of the support provided.

References

[1] Akachi H, Polasek F, Stulc P. Pulsating heat-pipe. In: Proceedings of the fifth international heat-pipe symposium. Melbourne, Australia; 1996. p. 208–17.

[2] Maezawa S, Gi KY, Minimisawa A, Akachi H. Thermal performance of capillary-tube thermosyphon. In: Proceedings of the ninth international heat-pipe conference, vol. 2, Albuquerque, USA; 1996. p. 791–5.
[3] Rittidech S, Terdtoon P, Murakami M, Kamonpet P, Jompakdee W. Effect of inclination angles, evaporator-section lengths and working-fluid properties on the heat-transfer characteristics of a closed-ended osciilating heat-pipe, In: Proceedings of the sixth international heat-pipe symposium, Chiang Mai, Thailand; 2000. p. 413–21.
[4] Rittidech S, Terdtoon P, Murakami M, Kamonpet P, Jompakdee W. Correlation to predict the heat-transfer characteristics of a closed-ended oscillating heat-pipe under normal operating conditions. Appl Therm Eng 2003;23:497–510.
[5] Yang F, Yuan X, Lin G. Waste-heat recovery using a heat-pipe heat-exchanger for heating an automobile using its exhaust gas. Appl Therm Eng 2003;23:367–72.
[6] Incropera Frank P, Dewitt David P. Fundamentals of heat and mass transfer. 4th ed. New York: Wiley; 1976.

Available online at www.sciencedirect.com
SCIENCE DIRECT®
Journal of Stored Products Research 41 (2005) 479–497
Journal of STORED PRODUCTS RESEARCH
www.elsevier.com/locate/jspr

Comparison of performances of pulsed and conventional fluidised-bed dryers

Somkiat Prachayawarakorn[a,*], Warunee Tia[b], Korakot Poopaiboon[b], Somchart Soponronnarit[b]

[a]*Faculty of Engineering, King Mongkut's University of Technology Thonburi, Suksawat 48 Road, Tongkru, Bangkok 10140, Thailand*
[b]*School of Energy and Materials, King Mongkut's University of Technology Thonburi, Suksawat 48 Road, Tongkru, Bangkok 10140, Thailand*

Accepted 7 June 2004

Abstract

Consumption of energy, outlet moisture content and quality of the dried commodity are important parameters of paddy-dryer performance. The fluidised-bed paddy-dryer has been commercialised for several years and in this paper, paddy drying by pulsed and conventional fluidised-bed dryers are compared. Experimental results have shown that the variation of moisture content at the exits of both dryer types in test runs was very small. Heat utilisation was more effective when such dryers were used to dry paddy at moisture contents above 24% dry basis and up to 50% of the thermal energy was saved by recycling 70–80% of the air. Paddy qualities i.e. head-rice yield and colour of the dried white rice were similar with both dryers and almost the same as the original undried values, or slightly higher in the case of head-rice yield, depending upon the drying conditions. Below 28% dry basis, it is recommended that inlet-air temperature should be lower than 145 °C in order to maintain white colour. The cooked rice obtained from paddy dried at a temperature of 145 °C was harder than naturally dried control samples. A mathematical model based on energy and mass balance predicted values in good agreement with experimental results for both the pulsed and conventional fluidised-bed dryers. Calculated thermal and electrical energy consumptions indicated that the pulsed flow dryer was more economical than the conventional dryer.
© 2004 Elsevier Ltd. All rights reserved.

Keywords: Modelling; Paddy drying; Quality; Pulsed fluidised beds

*Corresponding author. Tel.: +662-4270-9221; fax: +662-428-3534.
E-mail address: somkiat.pra@kmutt.ac.th (S. Prachayawarakorn).

0022-474X/$ - see front matter © 2004 Elsevier Ltd. All rights reserved.
doi:10.1016/j.jspr.2004.06.003

Nomenclature

C_a	specific heat of dry air, kJ/kg °C
C_v	specific heat of water vapour, kJ/kg °C
C_{pw}	specific heat of moist paddy, kJ/kg °C
h_{fg}	latent heat of water, kJ/kg
$M(t)$	moisture content of paddy at time t, decimal dry basis
M_{eq}	equilibrium moisture content of paddy, decimal dry basis
M_{in}	initial moisture content of paddy, decimal dry basis
M_f	outlet moisture content, decimal dry basis
$M_{i,n}$	moisture content of paddy at the inlet of the nth element, dry basis decimal
$M_{f,n}$	moisture content of paddy at the outlet of the nth element, dry basis decimal
$\dot{M}_p$	grain mass flow rate, kg/s
$\dot{m}_{inlet}$	total mass of dry air at drying chamber inlet, kg/s
m_s	total mass of paddy at drying chamber, kg
P	pressure drop, Pa
Q	specific thermal energy, kJ/kg water evaporated
R	ratio of mass of dry paddy to mass of dry air, kg dry paddy/kg dry air
SEC	specific electrical energy, kJ/kg water evaporated
T_i	temperature of ambient air, °C
$T_{f,avg}$	exhaust air temperature, °C
$T_{f,n}$	outlet-air temperature at the nth element, °C
T_{inlet}	inlet-air temperature at drying chamber, °C
T	drying time, s
$W_{f,avg}$	humidity ratio of air at the dryer outlet, kg H_2O/kg dry air
$W_{f,n}$	outlet-humidity ratio of air at the nth element, kg H_2O/kg dry air
W_{inlet}	inlet-humidity ratio of air, kg H_2O/kg dry air
θ_{in}	grain temperature, °C
η	combustion efficiency, decimal
η_{fan}	fan efficiency, decimal
ρ_{air}	air density, kg/m^3

1. Introduction

Fluidisation is a technique in which a bed of solid particles is transformed to a liquid-like condition by passing a stream of fluid through the solid bed, at a sufficiently high velocity that frictional forces between the particles and flowing fluid counterbalance the weight of particles. Above this velocity, the pressure drop across the bed is always constant even though fluid velocity increases. This velocity is referred to as the minimum fluidisation velocity. In the operation of a conventional fluidised bed, the air velocity used is at least 1.5 times the minimum fluidisation velocity, in order to obtain good gas–solid contact performance and sustain stable solid particle movement.

Whenever the fluidised-bed technique is applied to solid particles that have strong cohesive forces, fluidisation may not behave as well. Paddy kernels at high moisture content are easily agglomerated and their agglomerations result in poor heat and mass transfer rates. Use of high velocities to prevent agglomeration may not be appropriate for drying grains in which moisture transport inside grains is dominated by internal diffusion, resulting in wastage of energy. To solve this problem, different approaches are employed. Application of mechanical vibrations or pulsations to improve the fluidisation quality is an interesting technique (Gawrzynski and Glaser, 1996; Nie and Liu, 1998; Soponronnarit et al., 2001). Work on drying using the pulsation technique has shown that the pulsed gas stream can improve the drying rate, especially for solids that have a high moisture content.

Pulsed fluidised beds seem to be more fashionable than conventional fluidised beds requiring high velocity, because of lower power requirements in the air unit (Gawrzynski et al., 1996). Furthermore, pulsing the air influences the dynamics of the bubbles, which improves gas–solid contact performance. A bubble can break up into two small bubbles (Moussa and Fowle, 1985).

The objective of this work was to study the performance of industrial-scale pulsed and non-pulsed fluidised-bed paddy dryers, and to propose a mathematical model to predict the paddy moisture change and the energy consumption for both dryer types. The physical quality of the paddy, in terms of head-rice yield and whiteness, was also determined. In the pulsed fluidised bed, the airflow was relocated by rotating two metal sheets. Air was supplied to the dryer at the required flow rate and the metal sheet distributed the air to the respective sections of the plenum without stopping the flow. This redistribution did not affect the external design of the rigid-frame dryer because pulsation forces were directly conveyed to bed particles.

2. Material and methods

A pulsed fluidised-bed dryer (PFBD), of 20 tonnes/h capacity (Fig. 1), was operated in a continuous mode in which paddy was moved in cross-flow to the pulsed air. Air was transported through the main duct, containing two metal sheets rotating continuously at a particular angular velocity, as presented in Fig. 1b. The pulsed airflow was then passed through a particular section of the paddy bed (along the left or right of the drying chamber), thereby fluidising the paddy kernels. Paddy in the remaining part of the bed behaved as a packed bed. Operation of the conventional fluidised bed was similar to that of the pulsed fluidised bed, except that airflow in the conventional type was uniform throughout the bed.

The total exhaust air was cleaned by a cyclone separator before escaping to atmosphere. In the present work, a backward-curved blade centrifugal fan, with a 37 kW motor, was used to generate the required airflow, and a rice-husk furnace was used to heat the air to the specified temperature. The desired fan power was relatively lower in the pulsed fluidised bed than in the conventional fluidised-bed dryer (FBD), at least 25% less for the same capacity. Frequency of rotation for the plates was fixed at 25 cycles/min and grain residence time was 1.5 min.

Experiments were carried out at private rice mills, located in the northeast of Thailand. Initial moisture contents from harvest varied between 28% and 30% dry basis. Foreign materials present in the paddy bulk were removed before the paddy kernels were passed through the drying section. Superficial velocity in the drying chamber, measured by a static pitot tube, was 1.85 m/s. The

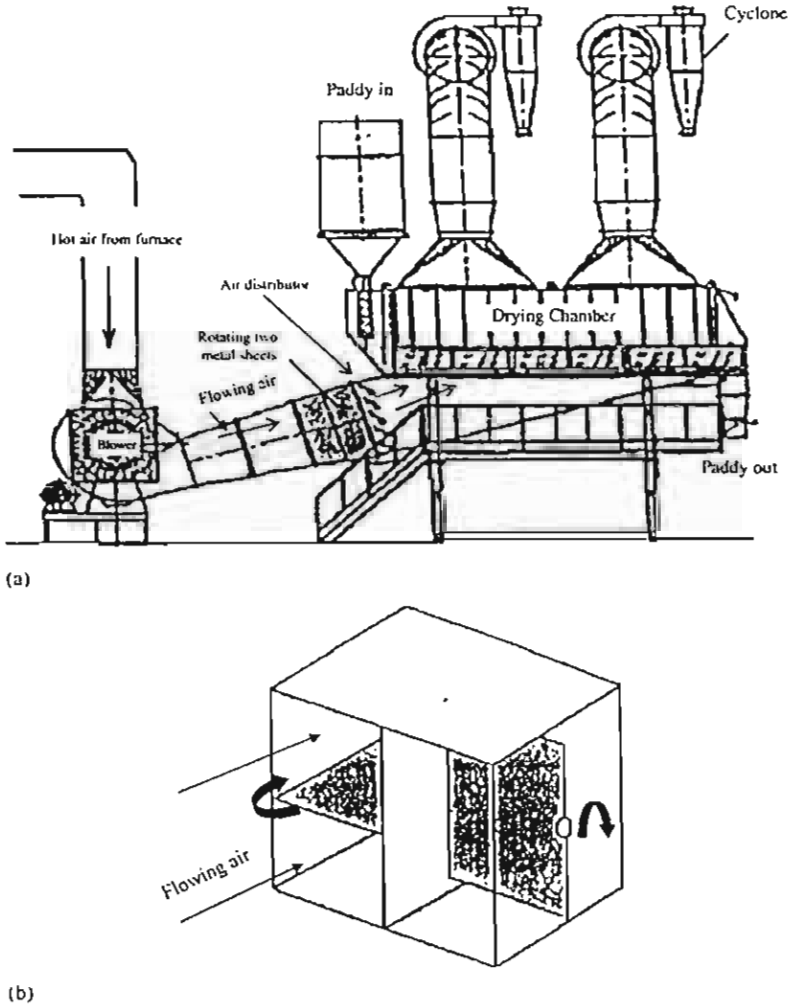


Fig. 1. Schematic diagram of pulsed fluidised bed with relocated air. (a) Pulsed fluidised-bed dryer. (b) Direction of rotating two metal sheets.

drying temperature used was dependent on initial moisture content; a high temperature was preferred at high moisture contents. For the present study, drying temperature was in the range of 144–154 °C. When conditions, i.e. drying air temperature and feed rate, reached steady state, outlet moisture content, temperature and paddy quality were examined. Inlet- and outlet-air temperatures were monitored by a data logger, with an accuracy of ±1 °C. Power consumed by the fan was measured by a clamp-on power meter, with an accuracy of ±3%.

Samples taken from the dryer outlet at various operating times were used to determine the moisture content, head-rice yield and rice whiteness. Moisture content was determined in a fan-forced oven at a temperature of 103 °C for 72 h. White rice colour was measured with a SATAKE whiteness meter. For head-rice yield, a 125 g paddy sample was dehusked with a two-rubber roller machine and the bran was removed with a SATAKE milling machine. Head-rice was separated

from brokens by a sieving screen. Head-rice yield was defined in this study as the ratio of head-rice mass to original paddy mass.

Hardness of cooked rice was measured with an Instron Universal Testing Machine (model TA-XT2i). A 30 g sample was placed in an aluminium cylindrical cup and the sample rinsed and strained to remove excess water. Distilled water was added at a ratio of 1:1.5 of rice to water by weight and the samples presoaked at room temperature for 10 min and then cooked in an automatic rice cooker. After completion of the cooking cycle, samples were held for a further 10–15 min in the cooker and then cooled to room temperature. A sample of 50 g of the cooked rice was taken from the middle cup. The test speed for compressing the sample was 0.5 mm/s and the post-test speed was 10 mm/s. The hardness of cooked rice was defined as the minimum force required to compress it to 90% of its initial height.

3. Mathematical model

In the pulsed fluidised bed, transport of kernels and air is at right angles with grains moving from one side of the dryer to the other while air flows upward. Under such movement, there exists a simultaneous heat and mass transfer and the product moisture content is reduced along the direction of grain movement. To describe the change in moisture content mathematically, the dryer is divided into N small elements as shown in Fig. 2. The mass balance equation for a single element is written as

$$W_{f,n} = R(M_{i,n} - M_{f,n}) + W_{inlet}, \tag{1}$$

where $W_{f,n}$ is outlet-humidity ratio of air at the nth element (kg H_2O/kg dry air), W_{inlet} is inlet-humidity ratio of the air, R is ratio of mass of dry paddy to mass of dry air (kg dry paddy/kg dry air), $M_{i,n}$ is paddy moisture content at the inlet of the nth element (dry basis decimal) and $M_{f,n}$ is paddy moisture content of paddy at the outlet of the nth element. From the heat balance equation for a single element, the outlet-air temperature, $T_{f,n}$, at the nth element is

$$T_{f,n} = (C_a T_{inlet} + W_{inlet}(h_{fg} + C_v T_{inlet}) - W_{inlet} h_{fg} + RC_{pw}\theta_{in})/(C_a + W_{f,n}C_v + RC_{pw}), \tag{2}$$

where C_a is specific heat of dry air (kJ/kg °C), C_v is specific heat of water vapour, C_{pw} is specific heat of moist paddy, h_{fg} is latent heat of water (kJ/kg), T_{inlet} is air temperature at drying chamber inlet and θ_{in} is grain temperature.

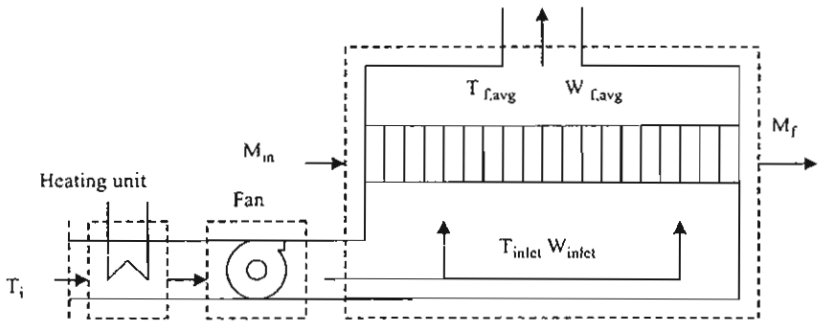


Fig. 2. Control volumes of fluidised bed.

Eqs. (1) and (2) describe the change in humidity and temperature in the gas phase. In writing Eq. (2), we make several simplifying assumptions. First, grain temperature is in thermal equilibrium with outlet-air temperature, implying a high transfer rate of heat between air and the grain bed. It will also be assumed that grain movement and pulsing air may be described by a plug flow model although grain dispersion may occur while the bed of particles is fluidised. This effect is small, however, based on observations during experiments. The proposed model is similar to the previous work reported by Soponronnarit et al. (1996a).

Average temperature and absolute humidity at the dryer outlet are calculated by the arithmetic means

$$T_{f,avg} = \frac{\sum_{i=1}^{n} \rho_{air} C_a T_{f,n}}{\sum_{i=1}^{n} \rho_{air} C_a} \tag{3}$$

and

$$W_{f,avg} = \frac{\sum_{i=1}^{n} W_{f,n}}{n}, \tag{4}$$

where $T_{f,avg}$ is exhaust air temperature, $W_{f,avg}$ is humidity ratio of air at the dryer outlet, ρ_{air} is air density (kg/m^3) and n is number of elements.

Change in moisture content of paddy during drying is modelled by the following empirical form:

$$\frac{M(t) - M_{eq}}{M_{in} - M_{eq}} = \exp(-xt^y), \tag{5}$$

where

$$\begin{aligned} x = {} & 0.00163100 T_{inlet} - 1.16202(\dot{m}_{inlet}/m_s) \\ & + 0.00415300(\dot{m}_{inlet}/m_s) T_{inlet} \\ & + 0.147383 \ln(\dot{m}_{inlet}/m_s) + 0.474743, \end{aligned}$$

$$\begin{aligned} y = {} & -0.00322000 T_{mix} - 0.835960(\dot{m}_{inlet}/m_s) \\ & + 0.0203190(\dot{m}_{inlet}/m_s) T_{inlet} \\ & - 0.143150 \ln(\dot{m}_{inlet}/m_s) + 0.548493, \end{aligned}$$

where M_{in} and M_{eq} are, respectively, moisture content of paddy at the beginning and at equilibrium, t is drying time (s), $\dot{m}_{inlet}$ is total mass flow rate at the drying chamber inlet (kg/s) and m_s is total mass of paddy in the drying chamber (kg).

Eq. (5) was developed by Sripawatakul (1994) and was valid for temperatures ranging from 90 to 150 °C and specific airflow rates of 0.03–0.16 kg/s/kg dry matter of paddy. Eq. (5) showed that faster drying rates were achieved with both higher temperatures and specific air flow rates, the first being the more significant effect. For calculating moisture content at any time t, Eq. (5) is differentiated with respect to t and the finite difference technique is then applied. Moisture content

of paddy in the next layer can be determined by substituting the known values of both moisture content in the previous layer and time step into the differentiated equation (5). By repeating the calculation procedure, outlet moisture content is eventually estimated.

Specific thermal energy used for evaporating water is calculated using

$$Q = \frac{\dot{m}_{inlet}(C_a + C_v W_i(T_i - T_{f,avg})}{\eta \dot{M}_P(M_{in} - M_f)}, \tag{6}$$

where Q is specific thermal consumption (kJ/kg water evaporated), $\dot{M}_p$ is grain mass flow rate (kg/s), M_f is moisture content at the dryer outlet and η is the combustion efficiency (decimal).

Electrical energy consumption can be determined using

$$SEC = P\left(\frac{\dot{m}_{inlet}/\rho_{air}\eta_{fan}}{\dot{M}_p(M_{in} - M_f) \times 1000}\right), \tag{7}$$

where SEC is electrical energy consumption (kJ/kg water evaporated), P is the pressure drop of the system (Pa) and η_{fan} is fan efficiency. The fan efficiency is about 0.8.

4. Results and discussion

4.1. Moisture content and grain temperature

Paddy quality, in particular head-rice yield, rice whiteness and cooking quality is usually affected by drying conditions: temperature and grain exposure time or moisture content from the dryer outlet. Poor head-rice yield is normally observed with non-uniform grain moisture at the outlet. In evaluation of dryer performance, it is thus necessary to consider all relevant parameters. Fig. 3 shows the variation in outlet moisture content (Fig. 3a) and outlet grain temperature (Fig. 3b) in the fluidised bed with no pulsation. The inlet moisture content was $33.0 \pm 0.3\%$ dry basis and when passed through the conventional dryer, the outlet moisture content was 25.3% dry basis with a standard deviation of 0.7% dry basis, indicating a small variation in outlet moisture content. This result also implied only limited dispersion of grains in the dryer. The outlet grain temperature was $77 \pm 1\,^{\circ}C$. Effect of pulsation on variation in grain temperature and moisture content, as shown in Fig. 4 (corresponding to Experiment 1 in Table 1), was not remarkable, as indicated by the standard deviation in outlet moisture content and grain temperature being 0.7% dry basis and $2\,^{\circ}C$, respectively. Such variations are still small and similar to those found in the conventional FBD. The other tests presented in Table 1 showed similar standard deviations of temperature and moisture content at the outlet.

As shown in Table 1, the moisture content at the dryer outlet was still relatively higher than the level appropriate for storage and the grain needed to be further dried. Reducing moisture content from 22.2% to 16% dry basis is a very difficult step since the remaining water, which exists in the interior of the grain, moves slowly through the diversity of components and chaotic void space to reach the exterior surface and eventually evaporates into the air stream. Hence, drying rate is low, although heat transfer and contact between solid particles and air are good. Application of fluidised-bed technology at this drying stage is not effective, since the energy is largely wasted, as

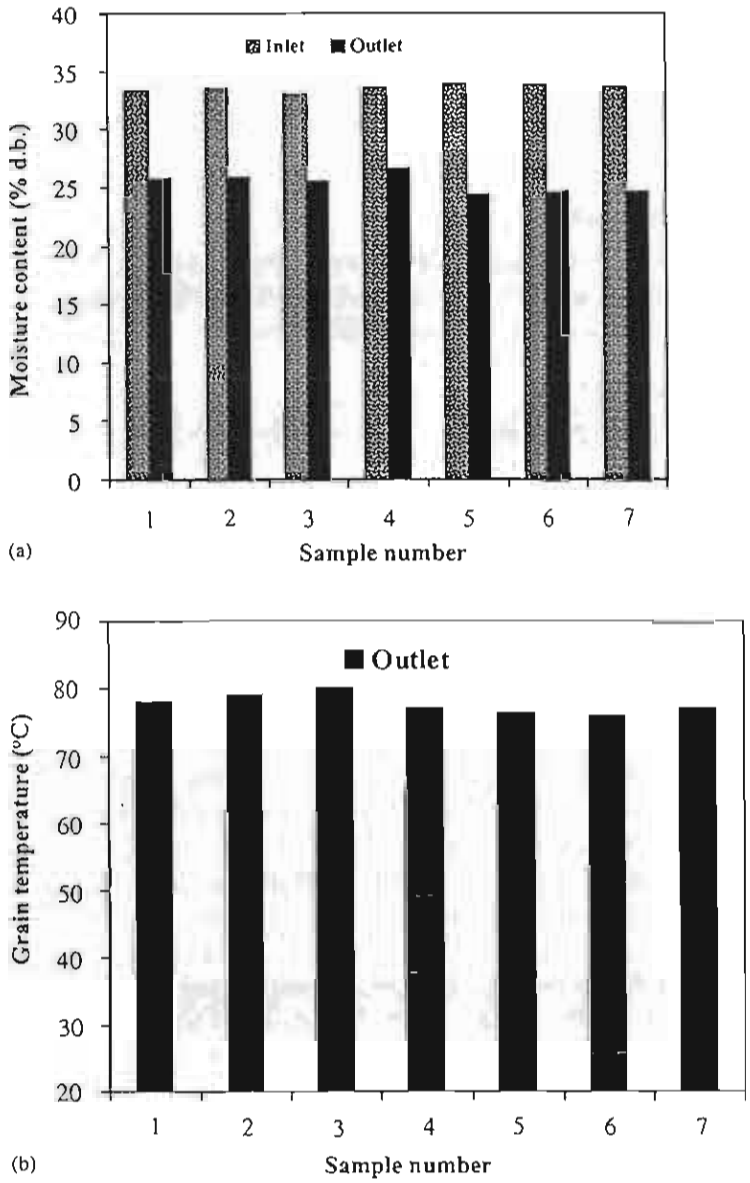


Fig. 3. Changes in moisture content and grain temperature in a conventional fluidised bed (feed rate of 3.8 tonnes/h, inlet-air temperature of 145 °C, superficial velocity of 2.8 m/s and residence time of 1.4 min, Soponronnarit et al., 1998). (a) Moisture content of paddy taken from dryer inlet and outlet. (b) Grain temperature taken from dryer outlet.

discussed in the following section, and the percentages of broken kernels are enormous. As is common practice at the rice mills, a fixed-bed or mixed-flow dryer should be applied for the slow-drying stage (Srzednicki and Driscoll, 1995; Soponronnarit et al., 1997; Giner et al., 1998).

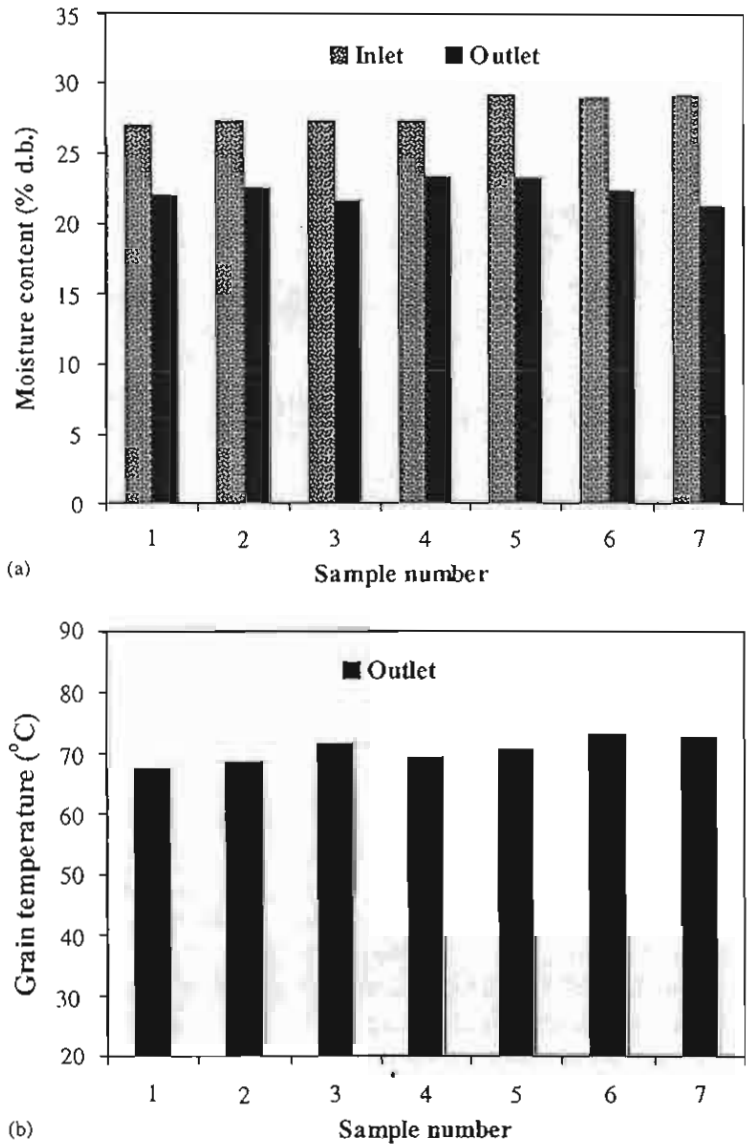


Fig. 4. Changes in moisture content and grain temperature in a pulsed fluidised bed (feed rate of 16.13 tonnes/h, inlet-air temperature of 145 °C and rotation speed of 25 cycles/min). (a) Moisture content of paddy taken from dryer inlet and outlet. (b) Grain temperature taken from dryer outlet.

4.2. *Energy consumption*

The thermal energy used for drying paddy in the rice industry is produced from two main energy sources, rice husk combustion in a cyclonic furnace and diesel oil in a burner. Gases resulting from combustion are used directly to dry paddy. When diesel oil is used as raw material for heating, a certain portion of the exhaust air is reused by mixing it with fresh air and the

Table 1
Experimental results: pulsed fluidised-bed paddy drying (no air recycling)

Experiment No.	1	2	3
Feed rate (tonnes/h)	16.13	15.87	15.18
Inlet-air temperature (°C)	145	144	154
Rotation speed of two metal sheets (cycle/min)	25	25	25
Grain temperature (°C)			
Inlet	40 ± 1[a]	40 ± 0.7	38 ± 0.5
Outlet	70 ± 2	71 ± 2	73 ± 1.8
Moisture content (% d.b.)			
Inlet	27.9 ± 0.9	28.4 ± 0.34	30.2 ± 0.9
Outlet	22.2 ± 0.7	23.1 ± 0.8	23.8 ± 0.4
Thermal energy (MJ/kg water evap.)	6.3	6.5	7.8
Hardness (kg)			
Before drying	29.4	29.4	NA
After drying	31.9	30.1	NA

[a]Mean ± standard deviation ($n = 7$ replicates).

remainder released to environment. By contrast, for a rice husk-type energy source, all exhaust air is vented to atmosphere. Specific data on conventional fluidised beds with/without air recirculation, presented in Fig. 5, were obtained from various workers (Soponronnarit et al., 1995, 1998; Meeso et al., 2000; Sungareeyakul et al., 2002). The amount of thermal energy consumed was calculated from Eq. (5), assuming a combustion efficiency of 70% for the rice husk (Swasdisevi et al., 1997) and complete combustion of diesel oil.

As shown in Fig. 5, for the FBD with no air recirculation, the energy consumption curve has an exponential decay characteristic when plotted against initial moisture content, showing the rapid reduction in energy consumption when the initial moisture content increases from low levels to 24% dry basis. The corresponding energy consumption drops from 14 MJ/kg water evaporated to approximately 7.2 MJ/kg water evaporated. At moisture contents higher than 24% dry basis, energy consumption changes only slightly with the initial moisture content. This result emphasises the powerful potential of a fluidised bed to remove water in the high moisture range, since the drying medium surrounds individual particles and comes into direct contact with water concentrated near the particle surface, thus allowing the water to evaporate easily without the interference of the physical structure of the paddy kernel. This performance, however, is not observed when a FBD is applied at relatively low moisture contents, where the particle surfaces are rather dry, although the convective heat transfer coefficient is high and has almost the same magnitude as for high moisture contents under similar drying conditions. Hence, high consumption is a consequence of reduced availability of surface moisture.

As observed from Fig. 4, the reduction in moisture transfer rate in the PFBD, calculated by ΔM% dry basis divided by the residence time, was 4.1% dry basis/min, slightly lower than in the

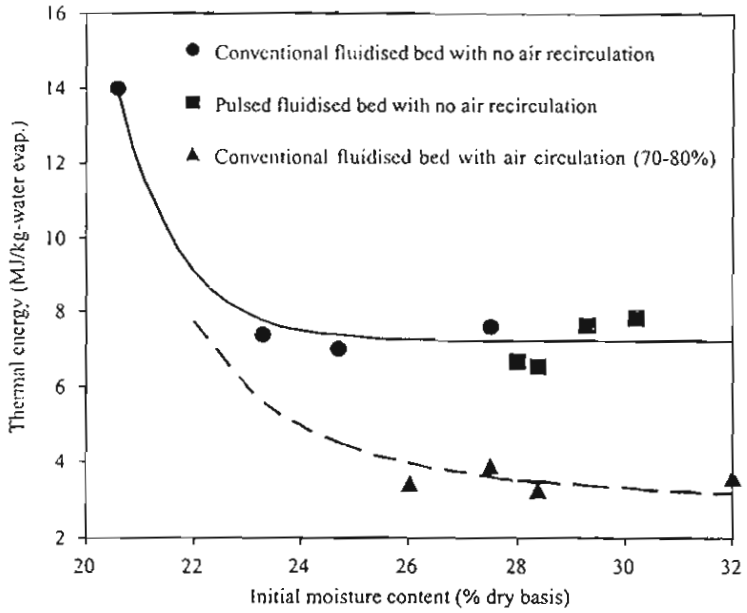


Fig. 5. Thermal energy consumption at different initial moisture contents (inlet-air temperature of 140–150 °C and final moisture content of 18–22% dry basis).

conventional dryer at 5.1% dry basis/min as shown in Fig. 3. The reduced drying rate for the PFBD does not imply poor performance, since in this case the amount of thermal energy consumption was also reduced with drying rate. Therefore, when energy consumption is plotted in terms of amount of consumed energy per kilogram water evaporated as shown in Fig. 5, the PFBD at a frequency of 25 cycles/min did not show much difference from the conventional dryer. According to these results, it would be difficult to indicate which technique is more efficient, and thus more investigation into the theory is needed as shown in a later section.

Fig. 5 also shows that thermal energy efficiency can be improved remarkably by recirculating exhaust air. Energy saved may be up to 50% at an air recycling ratio between 70% and 80%, at which the amount of consumed energy lies between 3 and 4 MJ/kg evaporated water if the initial moisture content is higher than 25% dry basis.

Table 2 presents electrical energy consumption for PFBD and conventional FBD systems. Data were recorded from a system having similar main components, such as a rice-husk cyclonic furnace and non-recirculating air. As illustrated in the conventional FBD, the larger amounts of electrical energy consumed were closely related to the lower initial moisture content, with values being 0.27, 0.33 and 0.65 MJ/kg evaporated water at initial moisture contents of 27.5%, 23.3% and 20.6% dry basis, respectively.

The beneficial effect of pulsation flow over a conventional FBD is in the reduced electrical energy consumption; the amount of electrical energy consumed under similar drying conditions is 0.19 MJ/kg evaporated water for the PFBD at 25 cycles/min, and 0.27 MJ/kg evaporated water for the FBD (Experiment No. 2).

Table 2
Electrical energy consumption for fluidised-bed dryer with no air recirculation

	Pulsed fluidised-bed dryer	Conventional fluidised-bed dryer		
		1	2	3
Feed rate (tonnes/h)	16.13	11.8	9.3	10.5
Inlet-air temperature (°C)	145	140	145	149
Moisture content (% d.b.)				
Inlet	28.0	27.5	23.3	20.6
Outlet	22.2	22.5	18.5	18.4
Evaporation rate (kg water evap/h)	731	461	362	192
Electrical energy consumption (MJ/kg water evap.)	0.19	0.27	0.33	0.65

4.3. Head-rice yield

Since the head-rice yield of freshly harvested paddy was different in each test depending upon harvest history and season, relative head-rice yield, defined as the value of head-rice yield of paddy dried by the hot-air drying divided by that dried by natural air, was presented in Fig. 6. Throughout the experiments, the initial moisture content of samples covering the range between 24% and 30% dry basis was reduced to 21–24% dry basis, depending upon the inlet-air temperature. The influence of inlet-air temperature and drying technique on the head-rice yield of paddy is shown in Fig. 6, indicating that head-rice yield was not related to airflow characteristics (whether uniform or pulsating), but was related negatively or positively with temperature. Drying at temperatures below 145 °C reflected a small reduction in head-rice yield, values varying between 95% and 98%. Breaking of kernels in milling is caused by the high moisture gradient of paddy during drying, enabling development of internal stresses causing fissures as a consequence (Kunze and Choudhury, 1972; Kobayashi et al., 1972). Head-rice yield for paddy dried at temperatures beyond 150 °C was improved and higher than that of the paddy dried naturally, relative head-rice yield at high-temperature drying being between 103% and 110%. The improved head-rice yield indicates that drying at this temperature directly affects the conformational structure of starch granules improving their ability to withstand milling forces. Swelling of starch granules along with subsequent leaching of amylose from the granules to outer space generates stronger intermolecular binding forces between granules, implying the gelatinisation of starch granules. Inprasit and Noomhorm (2001) reported that starch gelatinisation was occurring partially in this moisture range for paddy and some starch granules fused themselves to form composite clusters with a smooth interior.

4.4. Hardness

In testing the performance of a PFBD, paddy samples were taken from different seasons, the dry season in Experiments 1 and 2 as shown in Table 1. The hardness of cooked rice without heat treatment was 29.4 kg for Experiments 1 and 2. The hardness of cooked-rice samples for these

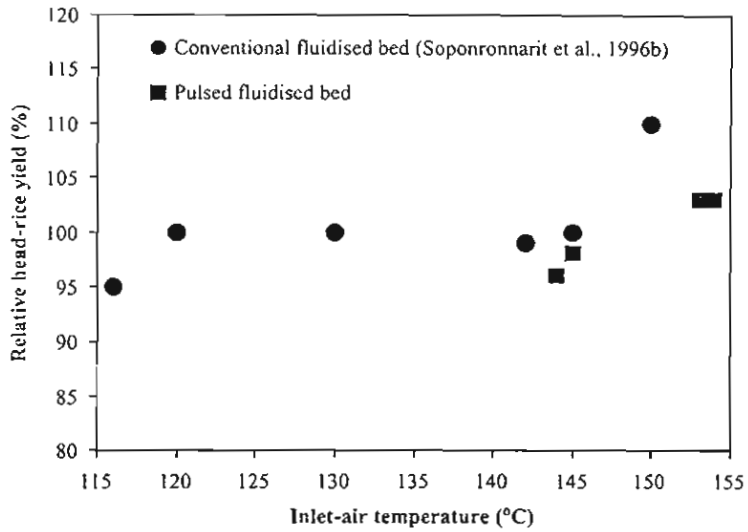


Fig. 6. Relative head-rice yield obtained from the pulsed and conventional fluidised-bed dryers (Soponronnarit et al., 1996b) operated at various temperatures (initial moisture content of 26–30% dry basis and final moisture content of 21–24% dry basis).

experiments tended to increase by 5.7–8.5% relative to the gently dried sample. Increased hardness is probably due to partial gelatinisation of the starch. Such an increase in hardness of cooked rice, after the paddy was thermally treated at high temperature, has also been reported by Gujral and Kumar (2003) and Inprasit and Noomhorm (2001).

It should be noted that the stronger inter-molecular binding forces resulting from the formation of partial gelatinisation may not always improve head-rice quality. This can be noticed easily in the case of paddy dried at 145 °C, as presented earlier in Fig. 6. This might be because the degree of gelatinisation produced is so small that binding forces between granules are weaker, compared with forces generated by moisture stresses, thereby reducing the proportion of whole kernels after milling.

4.5. Whiteness

As for head-rice yield, colour of milled rice was defined as relative whiteness. Colour of the paddy dried by conventional and pulsed FBD at different inlet-air temperatures is shown in Fig. 7. At an inlet temperature below 145 °C, colour of milled rice samples, with an initial moisture range of 24% to 30% dry basis, was slightly degraded by heat, as indicated by most data indicating the value of relative whiteness between 98% and 100%. Similarly, colour of milled rice from the paddy at the higher moisture content of 29% dry basis dried at a temperature higher than 150 °C was also slightly inferior. At a moisture content of 27% dry basis, however, it appeared to darken and yellow when a higher temperature of 150 °C was used. Consequently, colour of the white rice showed a relatively large drop to a value of 91% (see Fig. 7). Such a

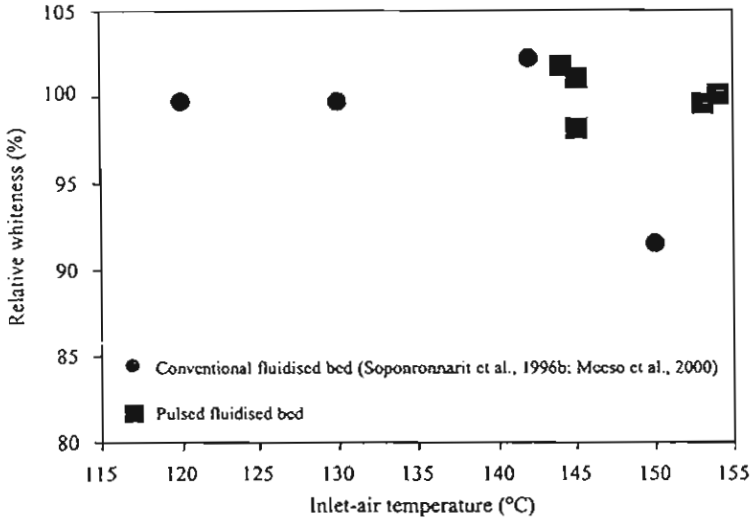


Fig. 7. Relative whiteness obtained from the pulsed and conventional fluidised-bed dryers (Soponronnarit et al., 1996b) operated at various temperatures (initial moisture content of 26–30% dry basis and final moisture content of 21–24% dry basis).

negative change in colour is induced by the more rapid increase in grain temperature for samples at lower moisture content, leading towards faster non-enzymatic browning.

To maintain colour at its original value, paddy at a lower moisture content of 27–28% dry basis should be in contact with drying air at a lower temperature, 145 °C being the maximum allowable temperature. Under these drying conditions, however, head-rice recovery falls slightly due to moisture stresses.

The experimental results previously presented on energy consumption and paddy quality, showed the PFBD as a possible alternative method for drying paddy. Paddy quality, in terms of head-rice yield and colour obtained from the pulsed and conventional FBD, was comparable. Drying at a temperature of 150 °C or slightly above should be applied only to a higher initial moisture content of 29% dry basis. High quality dried paddy can be achieved, particularly with head-rice yield being slightly higher than that of the original sample.

4.6. Validation of a mathematical model

To predict outlet moisture content, average absolute humidity of air leaving the dryer was calculated and a finite difference approach used to solve the resulting set of equations. Knowing T_{inlet} enabled determination of the moisture content of paddy leaving the first control volume, using Eq. (5). From Eqs. (1) and (2), humidity and temperature at the outlet of the first control volume were readily calculated. The same calculation procedure was repeated with successive control volumes until the dryer exit. Average outlet temperature and humidity were eventually determined by Eqs. (3) and (4). In addition, the thermal and electrical energy consumptions were determined by Eqs. (6) and (7), respectively.

Fig. 8 presents the results of calculated outlet moisture content compared with the experimental values taken from the conventional and pulsed FBD. Inlet moisture content of paddy in the experiments varied between 25.5% and 26.5% dry basis and inlet-air temperature was fixed at a temperature of 116 °C for the conventional dryer. For the PFBD, drying conditions were as shown in Table 1. The proposed model predicted outlet moisture content from the conventional FBD as lower than the experimental value, with a maximum error of prediction being 2.5% as shown in Fig. 8a.

When applying the same model to predict outlet moisture content from the PFBD, the pulsed airflow needed to be modified by taking the average velocity, determined by total airflow rate divided by the cross-sectional area of the drying chamber. It can be seen that the model described well the change in moisture content, in agreement with the experiment, as indicated by the estimated error lines of $\pm 2.7\%$ in Fig. 8b. The accuracy of the prediction of a simplified analysis clearly points out the negligible effect of pulsing the flow on diffusional mass transfer inside the kernel, although the convective heat transfer rate estimated by this approach was rather high due to the increase in local velocity.

The proposed model also reasonably quantified the amount of thermal energy consumed in the pulsed dryer, with a prediction error of $\pm 3.0\%$ of the measured quantity which ranged from 6.3 to 7.8 MJ/kg water evaporated. These calculated results are not presented here.

The simulation was then used to compare pulsed and conventional FBD. Inlet moisture content was set at 28% d.b., bed depth was fixed at 12 cm and all exhaust air was conveyed to atmosphere. Pulsation frequency was fixed at 25 cycles/min and maximum pulse velocity in the PFBD was limited to 3.0 m/s, equivalent to an average superficial velocity of 1.5 m/s throughout the bed, since kernels had a chance of being entrained out of the chamber at pulse speeds higher than 3.0 m/s. For the conventional FBD, air speed was fixed at 2–2.5 m/s. Other drying conditions were identical for both dryer types. Simulation results (Fig. 9) show that the PFBD used slightly less energy, in terms of heat and electricity, than the conventional dryer, whilst its ability to remove water was less (due to the lower average airflow rate). Lower water removal rate in the pulsed-flow dryer can be attributed to higher humidity inside the environmental drying chamber. The corresponding moisture content at the paddy surface became higher, reducing the driving force of moisture concentration difference between the centre and surface. The resulting water movement inside the kernel decreased.

Experimental and simulation results indicated that the pulsed-flow dryer had a great potential for drying paddy. Since the total airflow rate used was relatively lower in the pulsed-flow dryer than the conventional FBD, electrical energy consumption was reduced by at least 30%. In addition, transfer of heat from air to the grain bed was more effective, reducing thermal energy consumption and thus increasing drying efficiency. The main drawback of this dryer was the slightly lower drying capacity, which may not be favoured by the grain industry which strives for high capacity. The general situation found in industry, however, indicated that the initial moisture content in grain obtained from fields varied from 21% to 33% dry basis, depending upon harvesting season. The pulsed-dryer type is suitable for this wide range of moisture content since at lower moisture contents, heat utilisation in the PFBD is more efficient than the conventional FBD because using a higher air volume does not increase drying rate for the low moisture range.

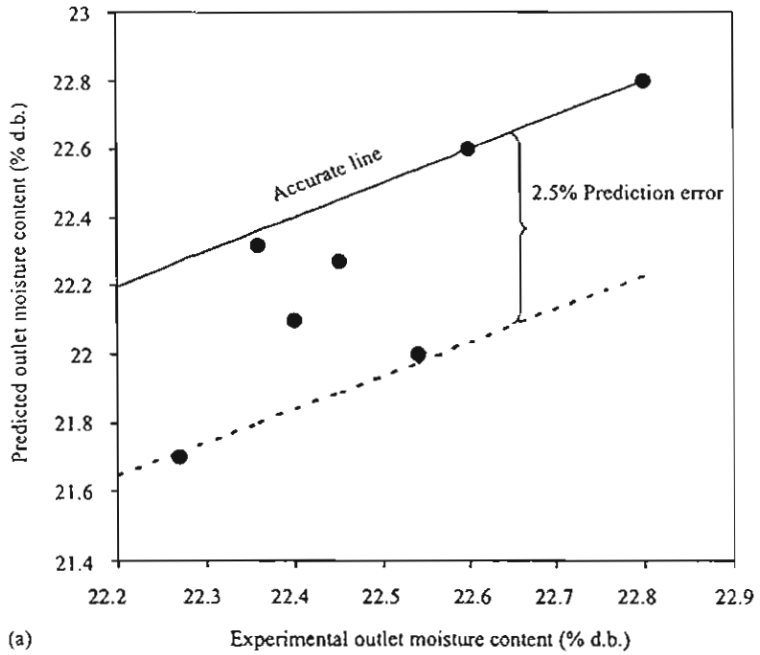


Fig. 8. Experimental and predicted values of outlet moisture content. (a) Conventional fluidised bed with a capacity of 9.5 tonnes/h (inlet-air temperature of 116 °C and superficial velocity of 2.2 m/s, Wangji, 1996). (b) Pulsed fluidised bed with a capacity of 15–16 tonnes/h (inlet-air temperature of 145–154 °C and superficial velocity of 1.5 m/s and frequency of 25 cycles/min).

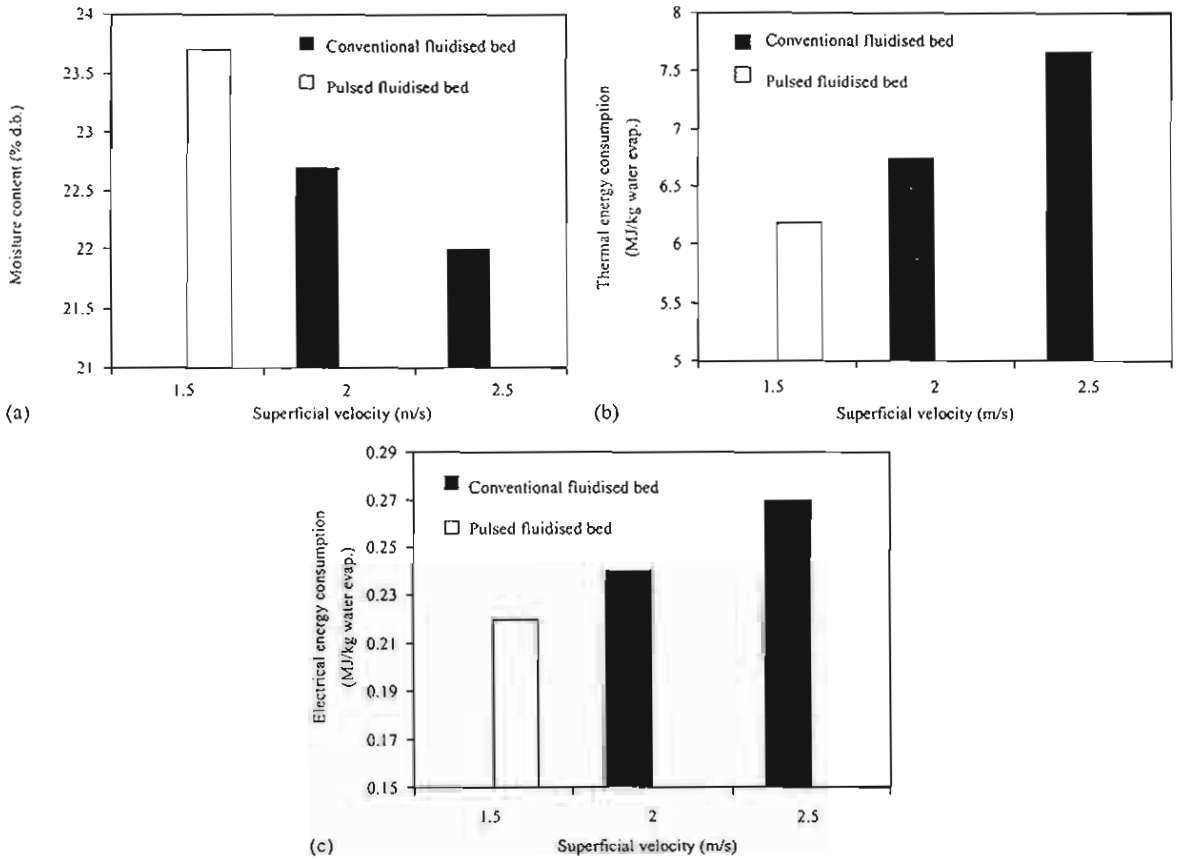


Fig. 9. Simulated performance of pulsed and conventional fluidised-bed dryers (inlet temperature of 145 °C, drying capacity of 20 tonnes/h and initial moisture content of 28% dry basis).

5. Conclusions

The moisture content of grain leaving pulsed and conventional fluidised-bed dryers did not differ greatly. Thermal energy consumed was between 6.5 and 7.8 MJ/kg water evaporated at moisture contents higher than 24% dry basis for both dryer types, without air recirculation. Below 24% dry basis, where internal water transport was restricted by diffusion, the thermal energy requirement was rapidly increased. When exhaust air was recycled, heat utilisation became more effective, with a 50% thermal energy reduction at 70–80% of recycled air. Electrical energy consumed by the pulsed fluidised bed was at least 30% lower than conventional FBD, and drying efficiency was higher. The mathematical model reasonably predicted the moisture change observed in the experiments. Simulation results showed better performance, in terms of energy consumption per unit moisture extracted, for the pulsed flow dryer than for the conventional FBD, whilst its ability to remove moisture was reduced. Head-rice yield and colour of white rice samples after drying were almost identical to those which were dried gently as a control over the whole range of moisture reduction from 24–30% dry basis down to 21–24% dry basis At an initial

moisture content lower than 28% dry basis, it was shown that inlet-air temperature should not be higher than 145 °C in order to avoid unacceptable change in colour of white rice. Hardness of cooked rice for samples dried at high temperature increased by about 8–12%, relative to the gently dried control sample.

Acknowledgements

The authors would like to thank The Thailand Research Fund for their financial support.

References

Gawrzynski, Z., Glaser, R., 1996. Drying in pulsed–fluid bed with relocated gas stream. Drying Technology 14, 1121–1172.

Gawrzynski, Z., Glaser, R., Zgorzalewicz, J., Pelech, Z., Stanislawski, J., Rogula, G., Pieczaba, B., 1996. Operational tests of a pulsed fluid bed dryer/cooler for granulated sugar. In: Strumillo, C., Pakowski, Z. (Eds), Proceedings of the 10th International Drying Symposium, Krakow, Poland, 30 July–2 August 1996, pp. 771–777.

Giner, S.A., Bruce, D.M., Mortimore, S., 1998. Two-dimensional simulation model of steady-state mixed-flow grain drying, part 1: the model. Journal of Agricultural Engineering Research 71, 37–50.

Gujral, H.S., Kumar, V., 2003. Effect of accelerated aging on the physicochemical and textural properties of brown and milled rice. Journal of Food Engineering 59, 117–121.

Inprasit, C., Noomhorm, A., 2001. Effect of drying air temperature and grain temperature of different types of dryer and operation on rice quality. Drying Technology 19, 389–404.

Kobayashi, H., Miwa, Y., Ishikowa, M., 1972. On the mechanism of cracking in rice kernels during drying of paddies; particularly moisture distribution and drying strain in one kernel. Research Bulletin of the Faculty of Agriculture of Gifu University 33, 279–293.

Kunze, O.R., Choudhury, M.S.U., 1972. Moisture adsorption related to the tensile strength of rice. Cereal Chemistry 49, 684–696.

Meeso, N., Soponronnarit, S., Wetchacama, S., 2000. Evaluation of drying system performance of rice mills in the central part of Thailand. Engineering Journal Kasetsart 14, 81–93 (in Thai).

Moussa, N.A., Fowle, A.A., 1985. Exploratory study of pulsed atmospheric fluidized-bed combustion. Proceedings of Eighth International Conference on Fluidized-Bed Combustion, vol. III, Texas, USA, pp. 1300–1310.

Nie, Y., Liu, D., 1998. Dynamics of collapsing fluidised beds and its application in the simulation of pulsed fluidised beds. Powder Technology 99, 132–139.

Soponronnarit, S., Yapha, M., Prachayawarakorn, S., 1995. Cross-flow fluidised bed paddy dryer: prototype and commercialization. Drying Technology 3, 2207–2216.

Soponronnarit, S., Prachayawarakorn, S., Sripawatakul, O., 1996a. Development of cross-flow fluidized bed paddy dryer. Drying Technology 14, 2397–2410.

Soponronnarit, S., Prachayawarakorn, S., Wangji, M., 1996b. Commercial fluidised-bed paddy dryer. In: Strumillo, C., Pakowski, Z. (Eds), Proceedings of the 10th International Drying Symposium, vol. (A), Krakow, Poland, 30 July–2 August 1996, pp. 638–644.

Soponronnarit, S., Amatachaya, P., Prachayawarakorn, S., Nathakaranakule, A., Inchan, S., 1997. Field trial of in-store drying and storage. The Kasetsart Journal 18, 86–100.

Soponronnarit, S., Rordprapat, W., Wetchacama, S., 1998. Mobile fluidised bed paddy dryer. Drying Technology 16, 1501–1513.

Soponronnarit, S., Wetchacama, S., Trutassanawin, S., Jariyatontivait, W., 2001. Designing, testing and optimization of vibro-fluidised paddy dryer. Drying Technology 19, 1891–1908.

Sripawatakul, O., 1994. Study of drying paddy by cross-flow fluidization technique. Master's Thesis, King Mongkut's University of Technology Thonburi, Bangkok, Thailand, 108pp.

Srzednicki, G.S., Driscoll, R.H., 1995. Adoption of in-store drying technology in Southeast Asia. Proceedings of the 17th ASEAN Technical Seminar on Grain Postharvest Technology, Lumut, Malaysia, 25–27 July 1995, 8pp.

Sungareeyakul, K., Wetchacama, S., Pongpullponsak, A., Soponronnarit, S., 2002. Evaluation of status of paddy dryers in Thailand. Thai Society of Agricultural Engineering Journal 9, 32–41 (in Thai).

Swasdisevi, T., Soponronnarit, S., Chujinda, A., Wetchacama, S., Thepent, V., 1997. Rice husk furnace for fluidised bed paddy dryer. Proceedings of the Second Asean Renewable Energy Conference, Phuket, Thailand, 6–9 November 1997, pp. 603–612.

Wangji, M., 1996. Development of industrial scale fluidised bed paddy dryer. Master's Thesis, King Mongkut's University of Technology Thonburi, Bangkok, Thailand, 197pp.

Available online at www.sciencedirect.com
SCIENCE DIRECT®
Journal of Food Engineering 71 (2005) 28–36
JOURNAL OF FOOD ENGINEERING
www.elsevier.com/locate/jfoodeng

Comparative study of fluidized bed paddy drying using hot air and superheated steam

Wathanyoo Rordprapat *, Adisak Nathakaranakule, Warunee Tia, Somchart Soponronnarit

School of Energy and Materials, King Mongkut's University of Technology Thonburi, 91 Pracha u-tid Road, Bangkok 10140, Thailand

Received 18 February 2004; accepted 7 October 2004
Available online 7 December 2004

Abstract

This research investigated the physical properties of paddy, i.e., head rice yield, whiteness, white belly, viscosity of rice flour and change of microstructure of rice kernel. The experimental results showed that, for the same duration of drying, drying rates of paddy dried by superheated steam were lower than those dried by hot air due to an initial steam condensation during the first few minutes of superheated steam drying. This initial condition, however, promoted starch gelatinization making head rice yield of paddy dried by superheated steam higher than that dried by hot air. However, the values of whiteness of paddy dried by superheated steam were lower than those dried by hot air, especially during the first few minutes of drying due to a higher degree of Maillard reaction. Nevertheless, no obvious difference between the percentage of white belly of paddy dried by superheated steam and hot air was noted. Measured pasting properties indicated that gelatinization occurred more in paddy dried by superheated steam than that dried by hot air.
© 2004 Elsevier Ltd. All rights reserved.

Keywords: Condensation; Gelatinization; Physical properties; SEM

1. Introduction

Recently, it has been shown by various investigators that paddy dried by a high-temperature fluidized bed drying technique (140–150 °C) has high-head rice yield (Soponronnarit & Prachayawarakorn, 1994; Taweerattanapanish, Soponronnarit, Wetchacama, Kongseri, & Wongpiyachon, 1999); the technique has thus become an increasingly more popular technique for paddy drying. In addition, it is reported that higher drying air temperature results in a higher grain temperature and longer tempering time leads to partial gelatinization of starch granules inside paddy affecting the grain qualities in a similar way to parboiled rice (Inprarsit & Noomhorm, 2001). Fluidized bed drying parameters affecting the various properties of paddy are moisture content, drying air temperature and bed thickness (Sutherland & Ghaly, 1992; Tumambing & Driscoll, 1993). Moreover, changing the medium in paddy drying from hot air to superheated steam affects the various qualities of paddy including the head rice yield and color. In addition, paddy dried by superheated steam has cooking and eating qualities similar to those of parboiled rice as well (Taechapairoj, Dhuchakallaya, Soponronnarit, Wetchacama, & Prachayawarakorn, 2003).

From the above reasons, a comparative study of paddy drying with hot air and superheated steam is interesting and was performed in this study. The qualitative indicators used for comparing the paddy quality

* Corresponding author. Tel./fax: +662 470 8663.
E-mail address: r_wathanyoo23@yahoo.com (W. Rordprapat).

0260-8774/$ - see front matter © 2004 Elsevier Ltd. All rights reserved.
doi:10.1016/j.jfoodeng.2004.10.014

from both drying methods are head rice yield, whiteness, percentage of white belly, viscosity of rice flour and microstructure of the starch granules.

2. Materials and methods

A schematic diagram of a hot air fluidized bed dryer and its accessories is shown in Fig. 1. The system consists of three major components: a cylindrical drying chamber with an inner diameter of 20 cm and a height of 140 cm, a 12 kW electrical heater with a temperature controller, and a backward-curved-blade centrifugal fan, which was driven by a 1.5 kW motor. Exhaust air could be recycled, if needed, by means of two butterfly valves.

A batch superheated steam fluidized bed dryer is shown in Fig. 2. It consists of five major components: a cylindrical drying chamber with an inner diameter of 15 cm and a height of 100 cm, a 13.5 kW steam superheater, which was used to heat up saturated steam to become superheated steam, a backward-curved blade centrifugal fan driven by a 2.2 kW motor, a cyclone, and a small boiler capable of generating steam at a rate of 31 kg/h. A perforated sheet, with 10 holes per cm^2, was used for distributing the drying medium in the dryer. Superheated steam temperature was controlled by a PID controller with an accuracy of ±1 °C. To minimize the initial steam condensation inside the superheated steam dryer, hot air was first used to warm up the system until the temperature in all parts of the system reached the desired level (higher than 100 °C). Then, hot air was replaced by superheated steam. The steam generator generated saturated steam at 106 kPa (absolute) corresponding to a saturation temperature of around 100 °C.

Long grain rough rice (Supanburi 1 variety) from Pathum Thani Rice Research Center in Pathumthani Province, Thailand was used in all experiments. Rice

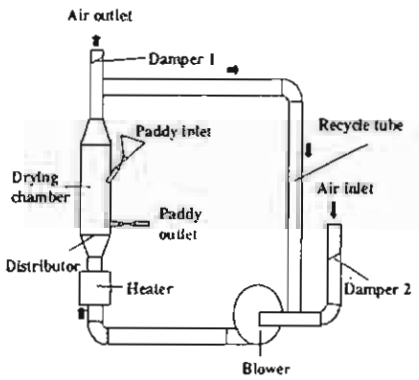


Fig. 1. A schematic diagram of a batch hot air fluidized bed dryer.

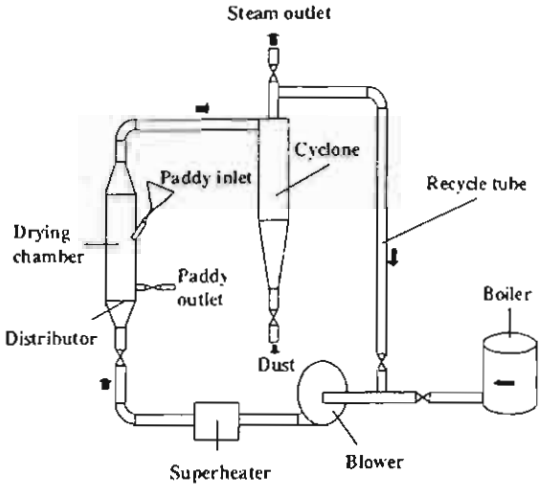


Fig. 2. A schematic diagram of a batch superheated steam fluidized bed dryer.

was cleaned and soaked in water with an initial temperature of 80 °C for 3 or 4 h, before being tempered for another hour. The experiments were conducted within the following ranges: initial bed depth of paddy of 10 cm medium temperature of 150 °C, superficial medium velocities of $1.3U_{mf}$ and $1.5U_{mf}$ (U_{mf} of hot air = 1.65 m/s, as reported by Soponronnarit & Prachayawarakorn (1994) and U_{mf} of superheated steam = 2.6 m/s, as reported by Taechapairoj et al. (2003)). Grain and drying medium temperatures were measured by type K thermocouples connected to a data logger having an accuracy of ±1 °C (COMARK Model 8510, England).

Dried paddy kernels were gently ventilated by ambient air until their temperatures become ambient and their moisture content reached 16% (d.b.). Finally, two samples, weighed 300 and 250 g, were taken from the bulk of dried kernels. The first 300 g sample was kept in a seal plastic bag for two weeks before testing for its head rice yield, whiteness and percentage of white belly. Another 250 g sample was shelled by a rubber roll husk (THU, Japan), polished by a Satake rice polisher (TM05, Japan) and graded by a rice grader (TRG, Japan) to measure the head rice yield. In this case, head rice yield is defined as milled rice having kernel length of at least 75% of its original length. The color of polished rice was measured by Kett digital whiteness meter (Model C-300, Japan), which was calibrated with a white reference color. The individual head rice kernels after milling were graded manually to check for the white belly. Kernels which had an opaque white area of more than 50% of the total area were deemed to be in the white belly category, according to the Thai Standard Rice (Ministry of Commerce Thailand, 1997).

The moisture content of paddy was determined by drying paddy in a hot air oven at a temperature of 103 °C for 72 h, according to the approved method of

the American Association of Cereal Chemists (AACC, 1995).

The changes in the microstructure of sample dried by hot air and superheated steam were observed by using a scanning electron microscope (SEM) (JSM-5600LV/ JSM-5600, Japan). The sampled rice kernel was cut along its cross-sectional axis, attached to an SEM stub, coated with a gold layer using a sputter-coater and photographed at an accelerator potential of 10 kV. The inspected location was between the kernel surface and its endosperm center.

Pasting properties of rice flour were determined by using a Rapid Visco Analyzer, RVA (Newport Scientific, Model RVA-4, Australia) and the approved method 61-02 (AACC, 1995). Rice flour (3 g on dry basis) was poured into distilled water (25 mL) in a canister and mixed thoroughly. The mixture was stirred at 960 rpm for 10 s and then changed to 160 rpm. Its temperature was first maintained at 50 °C for 1.5 min and then raised to 95 °C at a rate of 12 °C/min. After that the temperature was maintained at 95 °C for 2.5 min, followed by a cooling down to 50 °C at 12 °C/min and was maintained at 50 °C for 2.1 min. These tests were done in duplicate. A plot of pasting viscosity in an arbitrary RVA unit (RVU) versus time was used to determine the peak viscosity, temperature at peak viscosity, trough final viscosity, breakdown viscosity and setback viscosity. Peak viscosity indicates the water-biding capacity of the mixture. It is often correlated with the final product quality, and also provides an indication of the viscous load likely to be encountered by cooking. Breakdown viscosity measures the degree of disintegration of the granules or paste stability. Setback viscosity is a measure of gelling or retrogradation tendency of rice flour (Dengete, 1984).

3. Results and discussion

Drying behavior and physical properties of paddy, i.e., drying rate, grain temperature, head rice yield, whiteness, percentage of white belly, pasting properties and microstructure of rice kernel dried by superheated steam and hot air are discussed in the following sections.

3.1. Drying kinetics and grain temperature

Fig. 3 shows the evolutions of moisture content and temperature of paddy (soaked for 3 h) dried by superheated steam and hot air at 150 °C; an initial bed height was set at 10 cm and the superficial velocities of the drying medium were set at $1.3U_{mf}$ (Fig. 3a) and $1.5U_{mf}$ (Fig. 3b).

Fig. 3a indicates that during the first five minutes of drying moisture content of paddy dried by superheated steam decreased slower than that dried by hot air. This

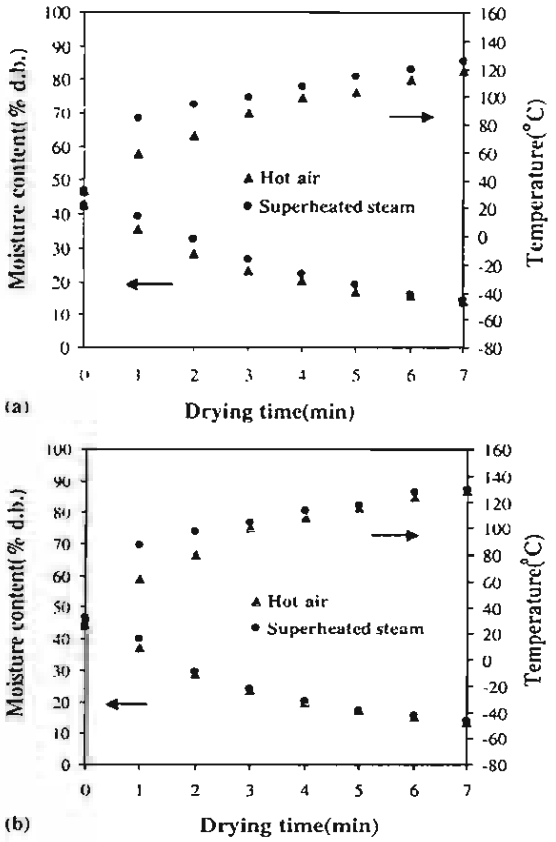


Fig. 3. Drying curves and temperature of paddy dried by superheated steam and hot air (drying temperature of 150 °C; bed depth of paddy of 10 cm; soaking time of 3 h). (a) superficial velocity of $1.3U_{mf}$, (b) superficial velocity of $1.5U_{mf}$.

is because paddy dried by superheated steam gained some moisture due to an initial steam condensation, which noticably occurred during the first few minutes of drying. This early stage condensation was also reported by Iyota, Nishimura, Onuma, and Nomura (2001) and Taechapairoj et al. (2003). After 5 min, the drying curves of both drying methods were almost the same. Temperature of paddy dried by superheated steam, however, increased faster than that dried by hot air during the first few minutes of drying. This phenomenon was due to the latent heat released to paddy from steam during an initial condensation mentioned earlier as well as due to the superior heat transfer properties of superheated steam compared with hot air (Mujumdar, 1995). The trends of moisture content evolution of paddy dried by superheated steam and hot air when using a superficial velocity of $1.5U_{mf}$ (Fig. 3b) were almost similar to those in the case of using a superficial velocity of $1.3U_{mf}$. Slightly higher rate of increase of temperature and decrease of paddy moisture content when using a superficial velocity of $1.5U_{mf}$ was a consequence of the higher heat transfer rate at higher

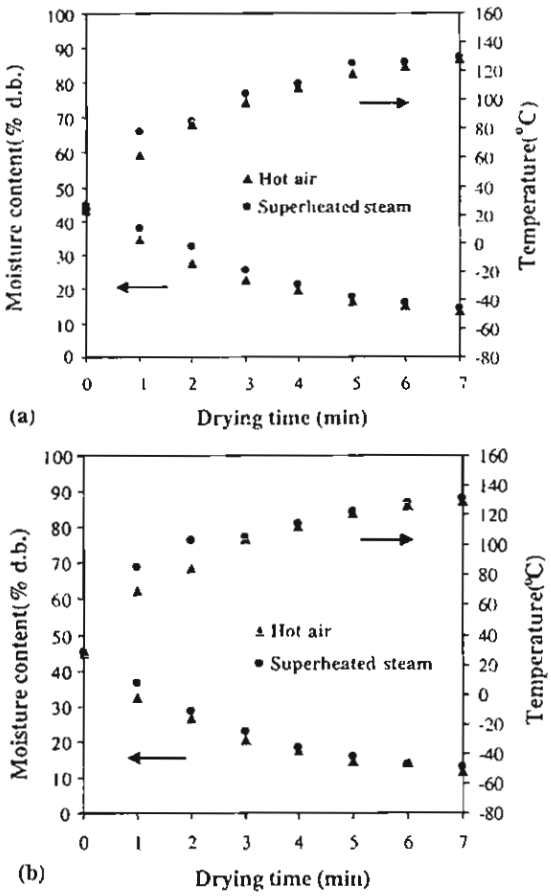


Fig. 4. Drying curves and temperature of paddy dried by superheated steam and hot air. (Drying temperature of 150 °C; bed depth of paddy of 10 cm; soaking time of 4 h). (a) Superficial velocity of $1.3U_{mf}$, (b) superficial velocity of $1.5U_{mf}$.

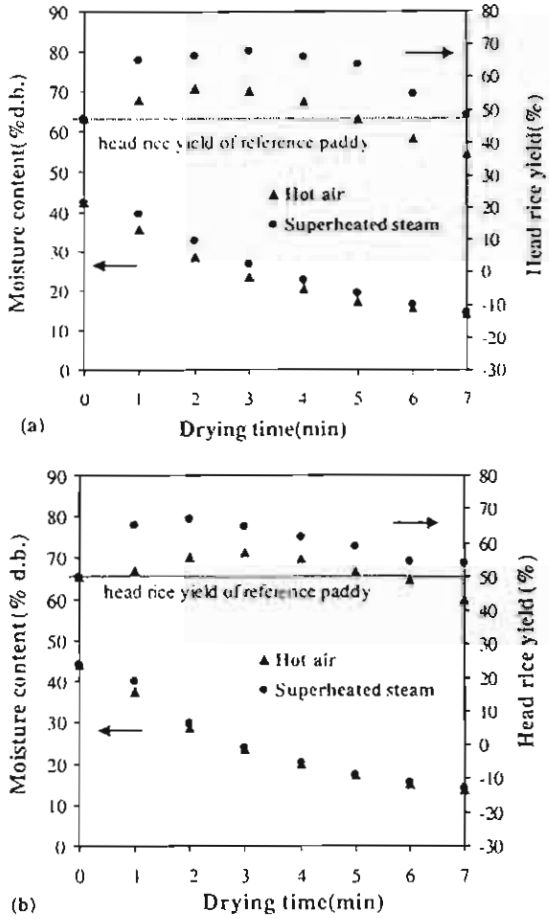


Fig. 5. Drying curves and head rice yield of paddy dried by superheated steam and hot air (soaking time of 3 h). (a) Superficial velocity of $1.3U_{mf}$, (b) superficial velocity of $1.5U_{mf}$.

superficial medium velocity (Looi, Mao, & Rhodes, 2002). The drying and temperature curves of paddy dried by both drying methods were almost the same after 3 min of drying.

Fig. 4 shows the evolutions of moisture content and temperature of paddy (soaked for 4 h) dried by superheated steam and hot air at the drying temperature of 150 °C, a paddy bed depth of 10 cm, and superficial velocities of $1.3U_{mf}$ (Fig. 4a) and $1.5U_{mf}$ (Fig. 4b). The experimental results were found to be similar to the case of 3-h soaking time (Fig. 3), and could be explained by the same reasons. Different soaking times, therefore, had no significant effect on the drying rate and the rate of change of temperature of paddy dried by both media in the ranges of our study.

3.2. Head rice yield

The evolutions of head rice yield and moisture content of paddy dried by superheated steam and hot air are presented in Figs. 5 and 6 for 3 and 4-h soaking conditions, respectively. The reference head rice yield of paddy dried by ambient air is also shown in these figures for comparison.

Head rice yields of paddy dried by both drying media (Fig. 5a) increased beyond that of the reference sample within the first few minutes of drying because starch granules inside the paddy kernels were partially gelatinized (Inprarsit & Noomhorm, 2001; Taweerattanapanish et al., 1999). The gelatinization process of starch inside the paddy kernels helped joining cracks inside the kernels and, consequently, led to an increase in the head rice yield. The gelatinization process is activated at different temperatures and moisture contents depending on the type of material dried. For paddy the proper temperature and moisture content for the gel formation are approximately 73–86 °C and 24–25% w.b., respectively (Taweerattanapanish et al., 1999; Zhou, Robards, Helliwell, & Blanchard, 2002). In the case of paddy dried with superheated steam, paddy temperature increased rapidly to the gelatinization temperature at an early stage of drying, while the moisture content of paddy was still in a suitable range for the gel formation.

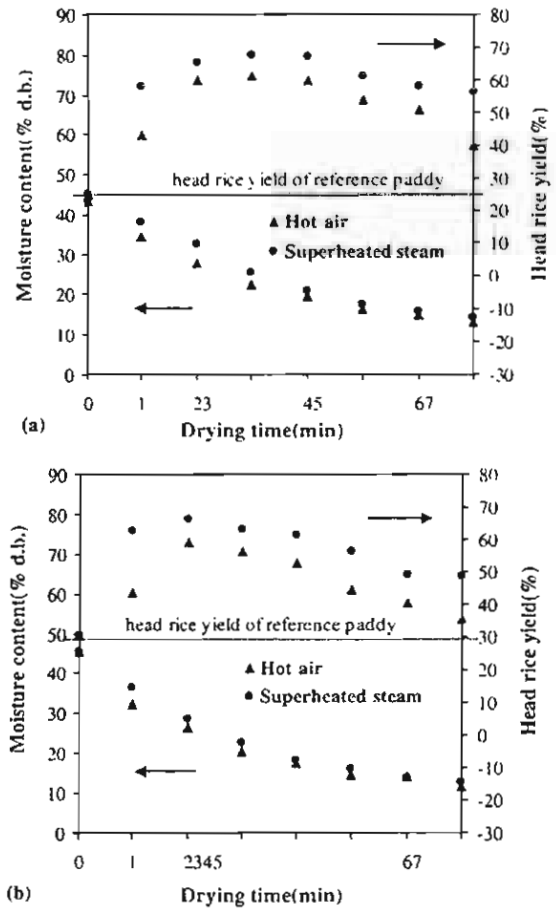


Fig. 6. Drying curves and head rice yield of paddy dried by superheated steam and hot air (soaking time of 4 h). (a) Superficial velocity of $1.3U_{mf}$, (b) superficial velocity of $1.5U_{mf}$.

This allowed the gel forming process to be longer in the case of superheated steam drying than in the case of hot air drying, which had lower rate of temperature rise but higher initial rate of drying. Therefore, head rice yield of paddy dried by superheated steam was higher than that dried by hot air. The slower gelatinization process in hot air drying compared to that in superheated steam drying was also reported by Iyota et al. (2001).

After 2 min of drying, head rice yield of paddy dried by superheated steam was almost constant and started to drop after 5 min of drying because paddy kernels had higher temperature and moisture gradients; these gradients led to the development of stress inside the kernels, which damaged the kernels. Head rice yield of hot air dried paddy was similar to that of superheated steam dried samples except that its value increased slower and decreased faster than in the case of superheated steam drying. The fast drop in head rice yield was due to the fast development of moisture gradient inside paddy kernel in hot air drying.

It can also be seen in these figures that a higher superficial velocity ($1.5U_{mf}$) resulted in a higher heat transfer from both media to the kernels. Paddy temperature in the case of using a superficial velocity of $1.5U_{mf}$ therefore rose to the gelatinization temperature faster than in the case of using a lower superficial velocity. Paddy moisture content, however, dropped below the suitable value for gelatinization faster than in the case of using a superficial velocity of $1.3U_{mf}$. The trade-off between the two parameters resulted in similar head rice yields of paddy dried at both drying medium velocities. The higher heat transfer rate also resulted in a rapid drop of head rice yield due to a rapid increase of the paddy temperature and moisture gradient inside the kernels.

3.3. Whiteness

Color changes of polished rice dried by superheated steam and hot air at superficial velocities of $1.3U_{mf}$ and $1.5U_{mf}$ (soaking time of 3 h) are shown in Fig. 7a and b, respectively. The whiteness of rice during the first few minutes of superheated steam drying decreased much faster than that of hot air drying, which slightly

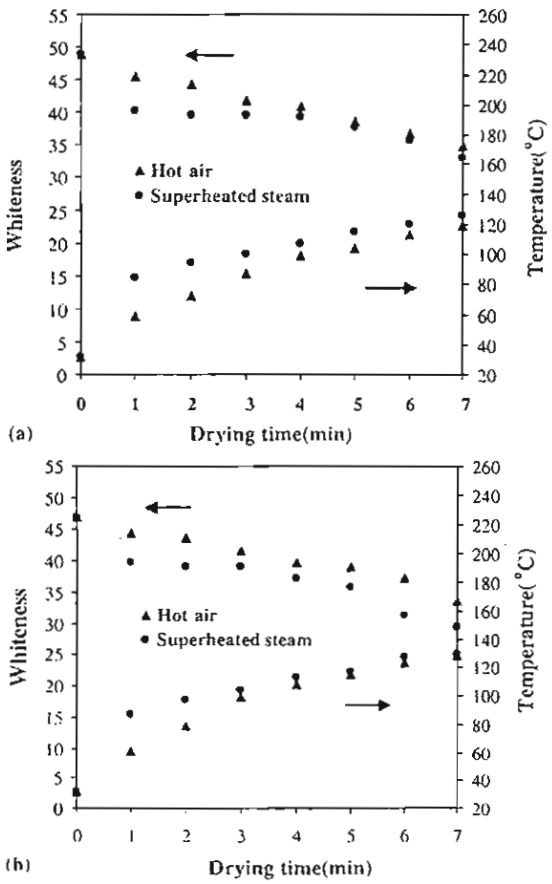


Fig. 7. Whiteness and temperature of paddy dried by superheated steam and hot air (soaking time of 3 h). (a) Superficial velocity of $1.3U_{mf}$, (b) superficial velocity of $1.5U_{mf}$.

but continuously dropped throughout the whole drying period. Such rapid drop in whiteness was a result of three phenomena, i.e., an initial steam condensation, which led to an increase in amount of free amino acid (Iyota, Nishimura, Komoshi, & Yoshida, 2002), a sharp increase in paddy temperature, which accelerated Maillard reaction and the transition of color substances from rice husk and rice bran into endosperm (Inprarsit & Noomhorm, 2001; Khan, Amilhussin, Arbolida, Manolo, & Chancellor, 1974; Yap, Juliano, & Pereze, 1988). After 1 min, the whiteness of rice dried by superheated steam was almost constant and started to drop after 3–4 min of drying. Paddy temperature increased with drying time in both drying methods; this induced Maillard reaction and caused whiteness of rice to drop slightly. The superficial velocity of the drying medium had no effect on the whiteness of rice.

The experimental results in the case of 4 h soaking time (Fig. 8a and b) were similar to those in the case of 3 h soaking time (Fig. 7a and b) and could be explained by the same reasons. Interestingly, it can be seen that in the case of using a superficial velocity of $1.5U_{mf}$ the whiteness slightly increased after 2 min of superheated steam drying (Fig. 8b). This phenomenon might be the consequence of the high-moisture diffusion rate, which moved the color substances out of the paddy kernels.

3.4. White belly

Paddy kernels having an opaque white area of more than 50% of the total area are categorized into the white-belly paddy category, according to the Thai rice standard (Ministry of Commerce Thailand, 1997). The changes of white belly of superheated steam and hot air dried paddy are shown in Fig. 9a and b, respectively. White belly was found to decrease with drying time in all experiments. The reduction of white belly was resulted from the gelatinization process. The trends of decreasing white belly of paddy dried by superheated steam were similar to those dried by hot air. At the end of drying, white belly was less than 2% for all drying conditions, which is an acceptable level for commercial parboiled rice.

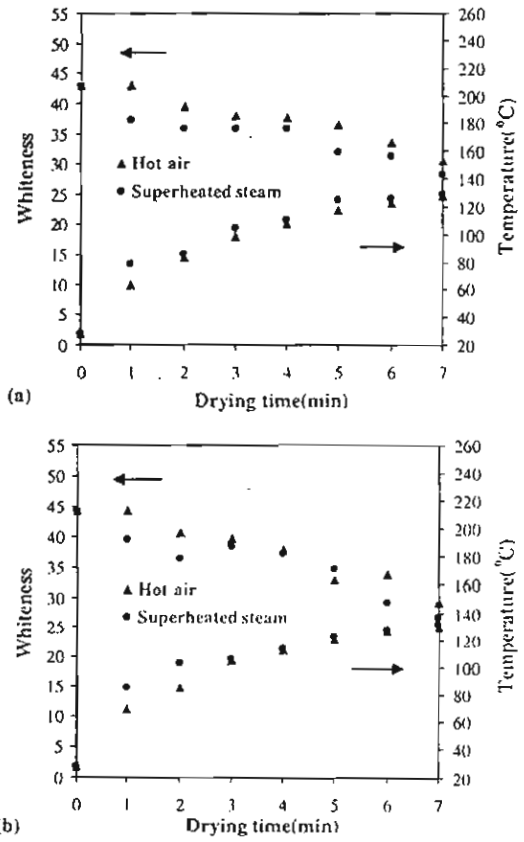


Fig. 8. Whiteness and temperature of paddy dried by superheated steam and hot air (soaking time of 4 h). (a) Superficial velocity of $1.3U_{mf}$, (b) superficial velocity of $1.5U_{mf}$.

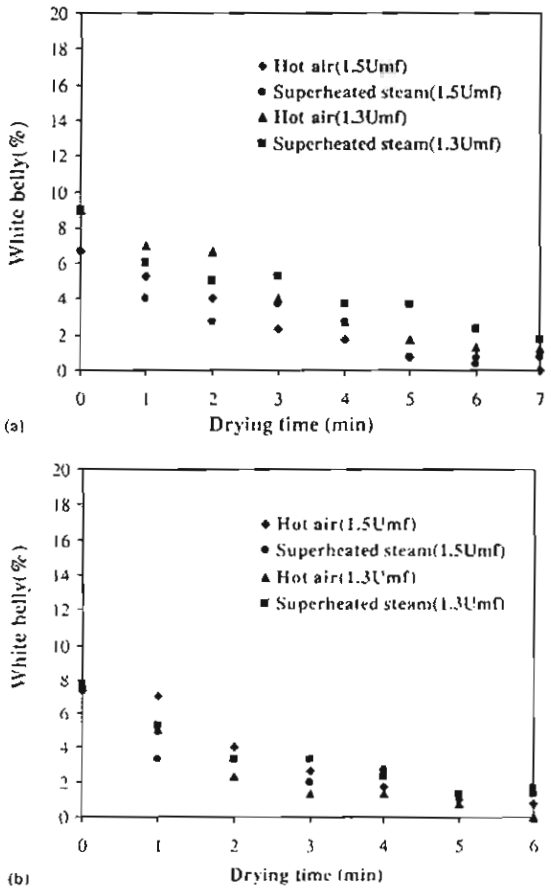


Fig. 9. White belly curves of paddy dried by superheated steam and hot air (soaking time of 3 and 4 h). (a) Paddy soaked of 3 h, (b) paddy soaked of 4 h.

3.5. Pasting properties

High-head rice yield of paddy dried either by superheated steam and hot air compared with that of the reference sample could be confirmed by the pasting properties of rice flour of the dried paddy measured by a Rapid Visco Analyzer (RVA). The measurement results are shown as RVA pasting curves in Figs. 10 and 11. It can be seen from Fig. 10a for the 1.3-U_{mf} and 3-h soaking condition that the pasting temperatures of paddy dried by both techniques were higher than those of the reference paddy, but the peak viscosities of paddy dried by both techniques were lower. In addition, it was observed that the pasting temperature of paddy dried by superheated steam was higher than that dried by hot air, but the peak viscosity was lower. Higher pasting temperature and lower peak viscosity indicated that more gelatinization occurred during both drying processes and this led to higher head rice yields of the processed paddy.

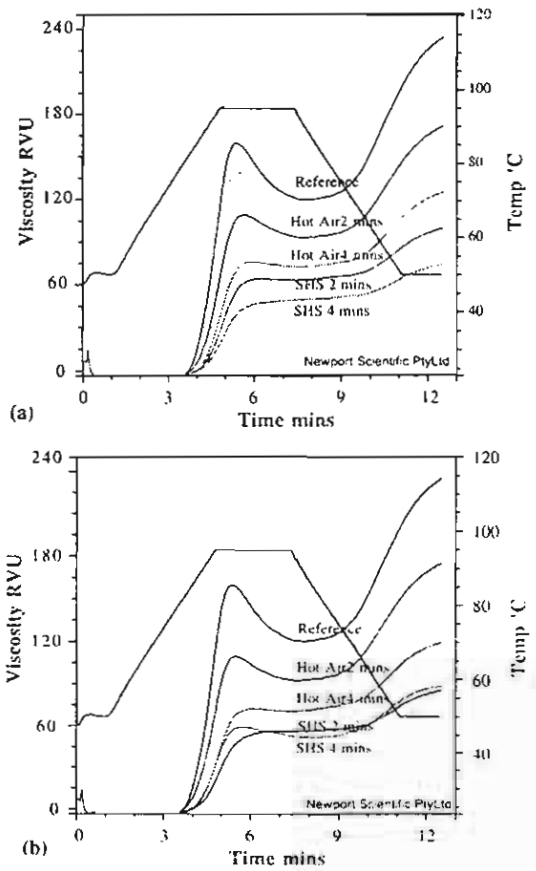


Fig. 10. Viscograph of rice flour dried by superheated steam and hot air (soaking time of 3 h). (a) Superficial velocity of 1.3U_{mf}, (b) superficial velocity 1.5U_{mf}.

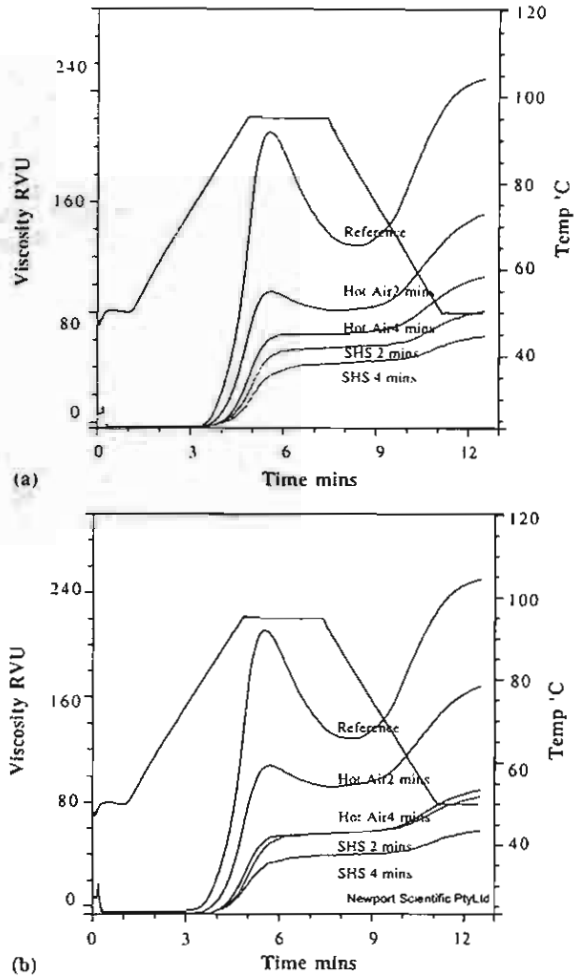


Fig. 11. Viscograph of rice flour dried by superheated steam and hot air (soaking of 4 h). (a) Superficial velocity of 1.3U_{mf}, (b) superficial velocity 1.5U_{mf}.

The final and setback viscosities of paddy dried by superheated steam and hot air were lower than those of the reference paddy and decreased with the drying time. When comparing with hot air, these properties

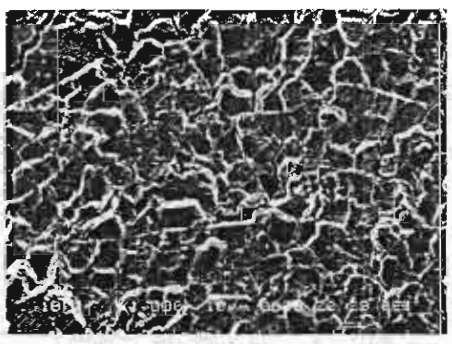


Fig. 12. SEM of cross-section of reference paddy.

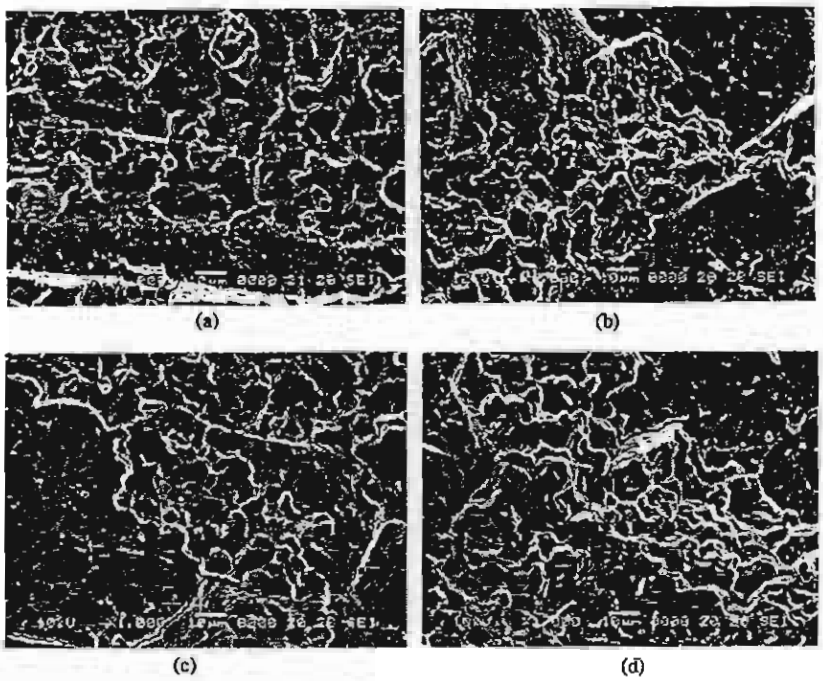


Fig. 13. SEM of cross-section of paddy dried by hot air and superheated steam for 4 min. (a) Hot air at $1.3U_{mf}$, (b) superheated steam at $1.3U_{mf}$, (c) hot air at $1.5U_{mf}$, (d) superheated steam at $1.5U_{mf}$.

of paddy dried by superheated steam were lower than that dried by hot air.

All pasting properties of paddy soaked for 3 h, dried at $1.5\text{-}U_{mf}$ condition, as shown in Fig. 10b, were similar to those at the $1.3\text{-}U_{mf}$ condition. This means that the medium velocity had no effect on the pasting properties of dried paddy. The same trends were observed for paddy soaked for 4 h, as can be seen in Fig. 10a and b.

3.6. Scanning electron microscopy (SEM)

SEM results of the reference paddy (soaked for 3 h and dried by ambient air) and paddy dried by superheated steam and hot air are shown in Figs. 12 and 13. Starch granules of the reference paddy (Fig. 12) spreaded throughout the cross-section of paddy with a loose crystal-like structure. On the other hand, starch granules of paddy dried by superheated steam and hot air (Fig. 13) were tightly packed. Comparing with the reference, starch granules of dried paddy obtained from both drying methods swelled and changed from crystallize to amorphous form due to the gelatinization effect. This structure transition made head rice yield of paddy dried by both media increased.

4. Conclusion

The superior heat transfer properties of superheated steam and the initial condensation occurred during an early stage of superheated steam drying increased the paddy temperature and maintained its moisture content at the level suitable for gelatinization, which changed the starch granules of rice kernels from the crystal-like structure to the amorphous form as revealed by SEM. As a result, head rice yield of paddy dried by superheated steam was found to be higher than that dried by hot air drying, which resulted in no condensation and slower increasing rate of paddy temperature. Measured pasting properties indicated that partial gelatinization occurred more in paddy dried by superheated steam than that dried by hot air and the reference paddy. Whiteness of paddy dried by superheated steam was lower than that of paddy dried by hot air due to an early stage condensation, which also resulted in a faster increase of the grain temperature. Percentage of white belly was reduced with the drying time; the value was less than 2% after 5 min of drying.

Acknowledgement

The authors would like to express their sincere appreciation to the Thailand Research Fund for financial support. Thanks are also due to the Pathum Thani Rice Research Center for testing physical qualities of rice and to the Institute of Food Research and Product Development, Kasetsart University for allowing the use of an RVA.

References

AACC (1995). *Approved method of the American association of cereal chemists* (9th ed.). MN: American Association of Cereal Chemists St. Paul.

Dengete, H. N. (1984). *Swelling pasting, and gelling of wheat starch. Advances in cereal science and technology* (vol. 6). MN: American Associated Cereal Chemistry, St. Paul (pp. 49–82).

Inprarsit, C., & Noomhorm, A. (2001). Effect of drying air temperature and grain temperature of different type of dryer and operation on rice quality. *Drying Technology, 19*(2), 389–404.

Iyota, H., Nishimura, N., Onuma, T., & Nomura, T. (2001). Drying of sliced raw potatoes in superheated steam and hot air. *Drying Technology, 19*(7), 1411–1424.

Iyota, H., Nishimura, T., Komoshi, Y., & Yoshida, K. (2002). Effect of initial steam condensation on color changes of potatoes during drying in superheated steam. In *Proceedings of the 13th International Drying Symposium* (pp. 1352–1359), Beijing China, B.

Khan, A. V., Amilhussin, A., Arbolida, J. R., Manolo, A. S., & Chancellor, W. J. (1974). Accelerated drying of rice using heat-conduction media. *Transactions of the ASAE, 17*, 949–955.

Looi, Y. A., Mao, Q. M., & Rhodes, M. (2002). Experimental study of pressurized gas-fluidized bed heated transfer. *International Journal of Heat and Mass Transfer, 45*, 255–265.

Ministry of Commerce, Thailand, Thai Standard Rice. Available from http://203.151.17.19/document/grain/english/standard.htm 1997, last revised on 20 June 2002.

Mujumdar, A. S. (1995). Superheated steam drying. In A. S. Mujumdar (Ed.), *Handbook of industrial drying* (2nd ed., pp. 1071–1086). New York: Marcel Dekker.

Soponronnarit, S., & Prachayawarakorn, S. (1994). Optimum strategy for fluidized bed paddy drying. *Drying Technology, 12*(7), 1667–1686.

Sutherland, J. W., & Ghaly, T. F. (1992). Rapid fluid-bed drying of paddy rice in the humid tropics. In *Proceedings of the 13th ASEAN Conference on Grain Post-harvest Technology*, Bruei Darussalam.

Taechapairoj, C., Dhuchakallaya, I., Soponronnarit, S., Wetchacama, S., & Prachayawarakorn, S. (2003). Superheated steam fluidized bed paddy drying. *Journal of Food Engineering, 58*, 67–73.

Taweerattanapanish, A., Soponronnarit, S., Wetchacama, S., Kongseri, N., & Wongpiyachon, S. (1999). Effect of drying on rice yield using fludization technique. *Drying Technology, 17*(1&2), 345–353.

Tumambing, J. A., & Driscoll, R. H. (1993). Modeling the performance of continuous fluidized bed paddy dryer for rapid pre-drying of paddy. In *Proceedings of the 14th ASEAN seminar on Grain Post-harvest Technology* (pp. 193–213), Manila, Philippines.

Yap, A., Juliano, O. B., & Pereze, C. M. (1988). Artificial yellow of rice at 60 °C. In *Proceedings of the 11th ASEAN Technical Seminar on Grain Post harvest Technology*, Kuala Lumpur, Malaysia, ASEAN Grain Post harvest Program, Bangkok, Thailand.

Zhou, Z. K., Robards, K., Helliwell, S., & Blanchard, C. (2002). Aging of stored rice: Changes in chemical and physical attributes. *Journal of Cereal Science, 35*, 65–78.

Biosystems Engineering (2006) **93** (2), 213–219
doi:10.1016/j.biosystemseng.2005.12.003
SE—Structures and Environment

Available online at www.sciencedirect.com
SCIENCE DIRECT®



Field Experiments and Economic Evaluation of an Evaporative Cooling System in a Silkworm Rearing House

C. Lertsatitthanakorn; S. Rerngwongwitaya; S. Soponronnarit

Faculty of Engineering, Mahasarakham University, Khantarawichai, Mahasarakham 44150, Thailand; e-mail of corresponding author: freeconvect@hotmail.com

(Received 10 November 2004; accepted in revised form 5 December 2005; published by 30 January 2006)

High ambient temperature has a negative effect on silk production. During heat stress, penalties to the efficient performance, production, reproduction, feed conversion, health and welfare of the animals can be severe. This research was aimed at investigating the feasibility of using direct evaporative cooling to improve the indoor air conditions in a silkworm rearing house. To this end, a silkworm rearing house of 32 m^2 floor area was fabricated and tested at Mahasarakham University. A cooling pad measuring 1·8 m by 3·6 m was placed on the north wall and a fan on the south wall. Experiments were performed through two seasons, namely: winter (November–December 2003) and summer (March–April 2004). Various operating airflow rates were considered to assess cooling performance and energy efficiency ratio (EER) of the evaporative cooling system. The results showed indoor dry bulb temperature drops of 6–13 °C could be achieved parallel with a 30–40% rise in relative humidity. The EER tends to be very high because the system consumes only fan and water pumping power. The economic analysis indicates that the payback period of the evaporative cooling system is about 2·5 years. Therefore, the direct evaporative cooling method demonstrates significant potential for silkworm rearing house cooling.
© 2006 Silsoe Research Institute. All rights reserved
Published by Elsevier Ltd

1. Introduction

Thailand is one of the countries well known for its silk fabrics and other fine silk products. During the period 1997–2001, the average annual value of the export of silk products was 1038·8 million Baht (40 Baht = 1 US$), compared to the average value of imports of 629·3 million Baht, or 54% of exports (Sericulture Extension Center No.1–9, 2002). It has been shown that Thai silk production is not sufficient to meet local demands. This situation has greatly obstructed the development of Thai silk industry. Among the strategies for silk production development during the Nine National Economic and Social Development Plan (2002–2006), was a plan to increase the silk yarn about 42% by the year 2006 (Chuprayoon *et al.*, 2002).

The ability of silkworms to produce is affected by seasonal factors such as temperature and humidity. It has been well established that efficiency in silkworm production is often lower during and after the hot season. One reason for the reduction in their productive performance might be elevated ambient temperatures, which induce heat stress. This is especially true in tropical areas such as Thailand where the temperature exceeds 30 °C for several months of the year (Suriyasomboon *et al.*, 2004) and, consequently, is not appropriate for rearing silkworms. Temperatures in the range of 21–27 °C with relative humidity (RH) of 70–85% (Tazima, 1978) are required. Most silkworm production in Thailand is performed in conventional stables which have an open air system with no walls. In recent years, a new housing system with a direct evaporative cooling system has been introduced to improve the microclimate for livestock in Thailand such as pigs (Boonyawattana *et al.*, 2003) and poultry (Ketjoy, 1999). Various other works on evaporative cooling systems applied to greenhouses had already been published such as Willits (2003), who presented a

 © 2006 Silsoe Research Institute. All rights reserved
Published by Elsevier Ltd

cooling model that predicts axial gradients of temperature and humidity of a greenhouse evaporative cooling system. Kittas *et al.* (2003) reported on a large commercial greenhouse cooled with evaporative pads and partially shaded. Evaporative cooling is an adiabatic humidification process (Wiersma & Short, 1983) that does not involve heat gain or loss. Sensible heat from the air is used to evaporate the water that comes in contact with the air. This sensible heat is then converted into latent heat, resulting in a reduction of the dry bulb temperature with a complementary increase of the RH and water vapour content of the air. An evaporative cooling system might be one alternative way of reducing the impact of a harsh climate on silkworm production.

This paper presents an investigation of the feasibility of using evaporative cooling in a silkworm rearing house.

2. Analysis

2.1. *Cooling efficiency and enthalpy change in air*

Cooling efficiency η is an index used to assess the performance of a direct evaporative cooler. Cooling efficiency in percentage can be defined as follows (Koca *et al.*, 1994):

$$\eta = \frac{T_d - T_c}{T_d - T_w} \times 100 \qquad (1)$$

where: T_d and T_w are the dry and web bulb temperatures of the ambient air and T_c is the dry bulb of the cooled air in °C.

The enthalpy change in air ΔH, which can be calculated as follows:

$$\Delta H = MC_{pa}(T_d - T_c) \qquad (2)$$

where: C_{pa} is the specific heat of moist air in $kJ\,kg^{-1}\,K^{-1}$; and M is the air mass flow rate in $kg\,s^{-1}$.

2.2. *Energy efficiency ratio*

Energy efficiency ratio (EER) was developed by the industry to evaluate the rate of energy consumption for air conditioning units (El-Dessouky *et al.*, 2000). The EER represents a measure for rating air conditioning units. The energy efficiency ratio E_{ER} is defined as the net thermal energy removed from air for cooling purposes per watt of energy expended. That is

$$E_{ER} = \frac{\Delta H}{P}$$

where P is input electrical power in kW of the exhaust fan and water pump.

The value of EER is calculated by determining the difference in the enthalpy of the inlet and outlet air streams through the cooling pad and the input power.

3. Experimental silk worm rearing house and measurements

3.1. *Silk worm rearing house*

A roof type even span house with an effective floor area of 8 m by 4 m and a height of 2·5 m, with one access door and no windows has been considered for experimental purposes as shown in *Fig. 1*. The walls are made

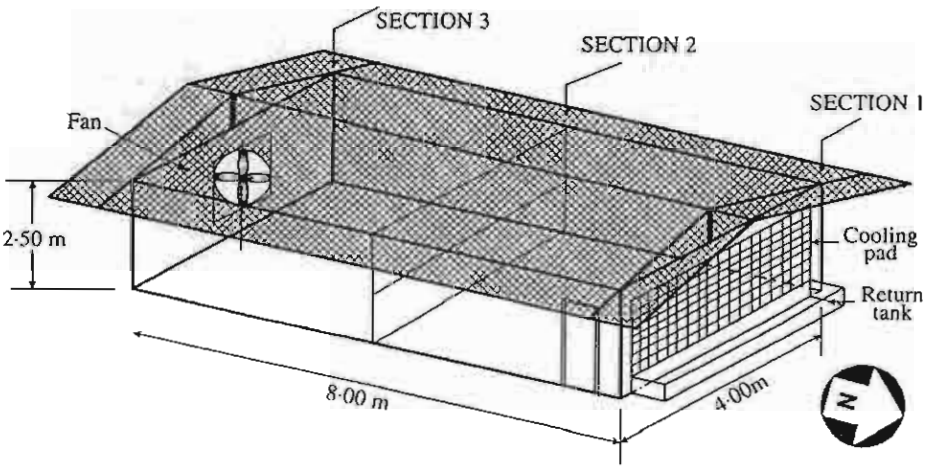


Fig. 1. Isometric view of silkworm rearing house

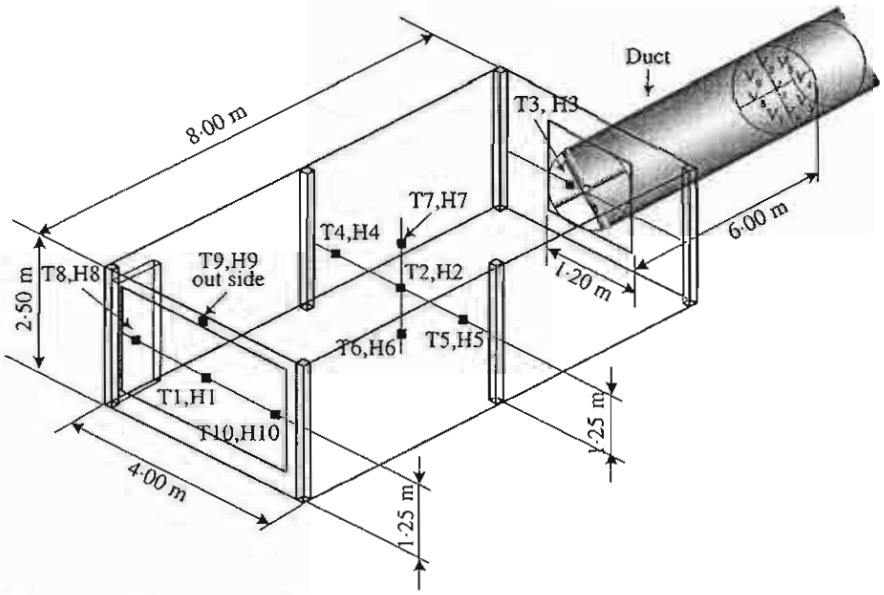


Fig. 2. Locations of temperature (T), humidity (H) and velocity (V) sensors in the experimental house

of asbestos-cement flat sheet. The roof gable, tilted at a 20°, is covered by Roman tiles. The horizontal ceiling is made of gypsum with 36 cm attic height. A cooling pad sized of 1·8 m by 3·6 m is located on the north wall and a 746 W exhaust fan is fitted at the south wall. The cooling pad is made of corrugated cellulose of 15 cm thickness has been impregnated with wetting agents. It was used to provide maximum surface area for evaporation. A water inlet is fitted on the top of the cooling pad. Several small holes of different diameters are made in the top solid part of the cooling pad to insure uniform distribution of the water throughout the cooling pad. A 373 W pump with water tank was attached to cooling pad for continuous water trickling.

3.2. *Measurements*

The silkworm rearing house temperature and humidity were measured at nine positions using nine calibrated temperature and humidity sensors (Testo model 175-H2, Germany, accuracy ±0·5 °C and ±3% RH) as shown in *Fig. 2*. The ambient temperature and humidity were also measured by Testo model 175-H2. A hot wire anemometer (Testo model 445, Germany, accuracy ±0·03 m s^{-1}) was used to measure air velocity (average of nine points as shown in *Fig. 2*). A variable voltage was used to drive the exhaust fan. A clamp on power meter [Hioki model 3286, Japan, accuracy ±2·3% reading (rdg) ±5 digit (dgt)] was used to measure the power consumption of the exhaust fan and water pump. The experiment started at 10 a.m. and ended at 5 p.m. with data recording at 15 min intervals.

4. Results and discussion

4.1. *Indoor temperature and humidity fluctuation*

Figure 3 shows that when the evaporative cooling system was not operating, the room temperature (average of nine points) was nearly the same as the ambient (before 14:00 h) because outdoor air infiltrates through the channels of the cooling pad. After 14:00 h, the room temperature was higher than ambient. This was due to the heat accumulated in the room. The maximum indoor temperature was about 33·1 °C. When the evaporative cooling system was turned on, the room temperature decreased from 32 to 22 °C while RH increased from 33% to 82% RH, which is appropriate for rearing the silkworm [suggest temperature in the range of 21–27 °C with RH of 70–85% (Tazima, 1978)] as shown in *Fig. 4*. The results in this study indicate that silkworms in the conventional system were exposed to higher temperatures than silkworms in the evaporative cooling system.

4.2. *Effect of seasonal variation*

In general, three different seasons in Thailand can be recognised as follows: the summer season is about 3

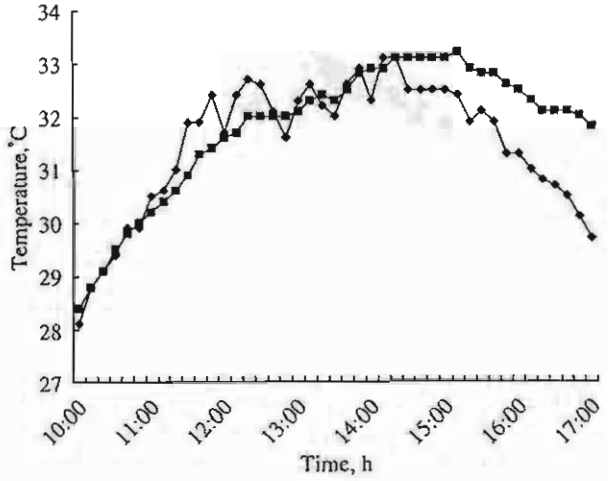


Fig. 3. Hourly variation of ambient and room temperatures when the evaporative cooling system was not operating (23/11/2003); –◆–, ambient temperature; –■– room temperature

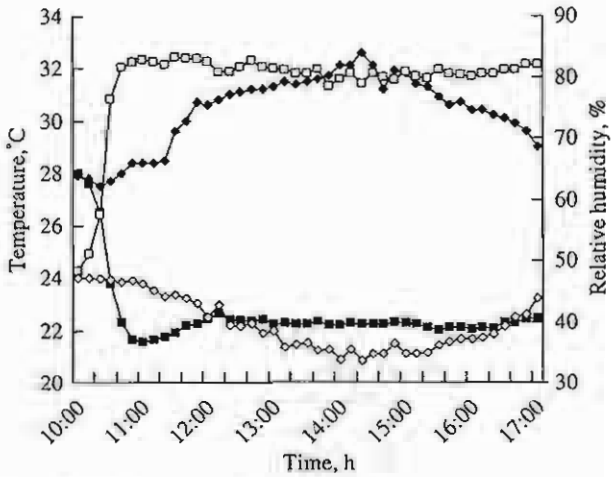


Fig. 4. Hourly variation of ambient and room temperatures and humidities of the open evaporative cooling system (4/12/2003); –◆–, ambient temperature; –■– room temperature; –◇–, ambient relative humidity; –□–, room relative humidity

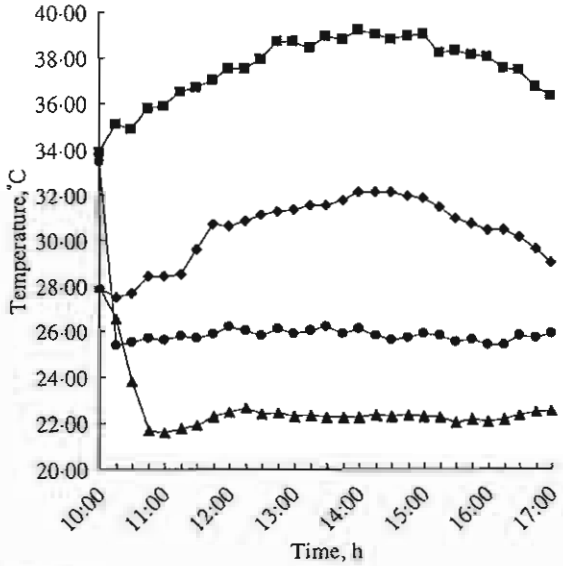


Fig. 5. Effect of seasons on room temperature (air mass flow rate = 6·3 kg s^{-1}); –◆–, outside temperature (4/12/2003); –■– outside temperature (25/3/2004); –▲–, room temperature (4/12/2003); –●–, room temperature (25/3/2004)

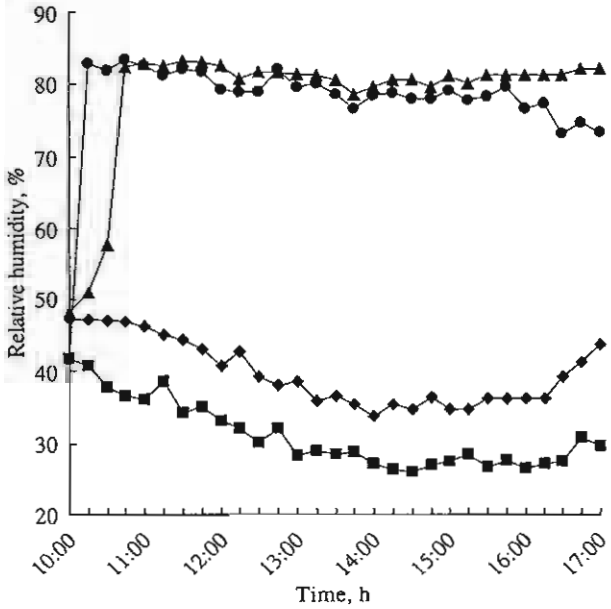


Fig. 6. Effect of seasons on room humidity (air mass flow rate = 6·3 kg s^{-1}); –◆–, outside relative humidity (4/12/2003); –■– outside relative humidity (25/3/2004); –▲–, room relative humidity (4/12/2003); –●–, room relative humidity (25/3/2004)

months long: from mid-February to mid-May. The rainy season occurs from mid-May to mid-October, and the winter season occurs from mid-October to mid-February (Khedari *et al.*, 2002). A comparison of ambient air inlet/outlet temperatures and humidity during different seasons of the year was undertaken during the winter season (4/12/2003) and the summer season (25/3/2004). It was seen that a lower outlet temperature of the processed air can be realised if the temperature and RH of the air is lower at the inlet. In the summer, the maximum outside air temperature was 39·2 °C at 14:00 h. The system reduced the air temperature by 13 °C and increased the RH by about 51·2%. In the winter the air temperature drops by about 10 °C as shown in *Figs 5* and *6*. This drop is because the ambient humidity in summer is lower than in the winter. In

summer there is a greater potential to absorb the moisture of the evaporative water. It is clear that evaporative cooling systems are efficient for dry conditions, but not as effective for humid conditions.

4.3. *Effect of air mass flow rate*

Testing of the effects of air mass flow rate on room temperature and humidity was undertaken on different days. Thus, it was not easy to draw a comparison amongst the results because of the various climatic conditions as presented in the above section. Nevertheless, general and subjective conclusions could be formulated. Tests were conducted at three different air mass flow rates: 4·4 kg s^{-1} (8/12/2003), 6·3 kg s^{-1} (4/12/2003) and 9·2 kg s^{-1} (3/12/2003). There is a little variation of RH with increase of air mass flow rate from 4·4 to 9·2 kg s^{-1} as shown in *Fig. 7*, whereas the temperatures are reduced with increase of air mass flow rate as shown in *Fig. 8*. The cooling efficiency is affected by several factors, such as pad design, thickness of pad, airflow rates and outside air temperature and RH. Using a fixed 15 cm thickness of pad, the cooling efficiency varies between 66% and 80·2%. This result agreed well with that presented in Watt (1986).

The power consumption in kWh and EER for the three air mass flow rates is shown in Table 1. The EER range of 24·4 to 59·9 at air mass flow rates increased from 4·4 to 9·2 kg s^{-1}. This is due to the cooling effect, which prevails over power consumption. However, in order to reduce the power consumption of the fan, an alternative scenario could be proposed by varying the airflow rate between summer and winter seasons. An example of temperature and humidity of the system are also shown in *Figs 5* and *6*. Where two airflow rates were considered, the air mass flow rate of 6·3 kg s^{-1} for summer and 4·4 kg s^{-1} for winter are shown.

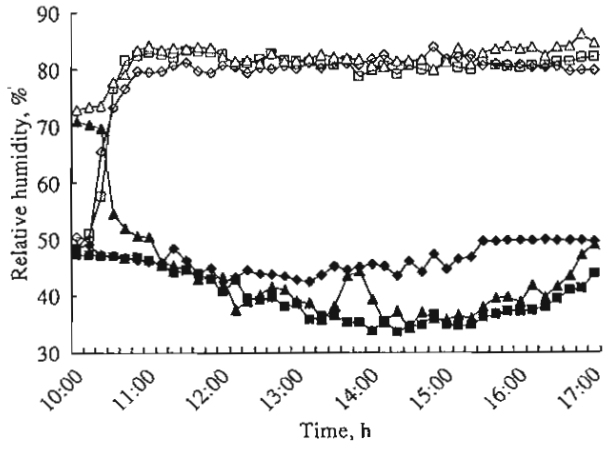


Fig. 7. Effect of ambient relative humidity and air mass flow rates on room humidity; –◆–, ambient relative humidity (4·4 kg s^{-1}); –■– ambient relative humidity (6·3 kg s^{-1}); –▲–, ambient relative humidity (9·2 kg s^{-1}); –◇–, room relative humidity (4·4 kg s^{-1}); –□–, room relative humidity (6·3 kg s^{-1}); –△–, room relative humidity (9·2 kg s^{-1})

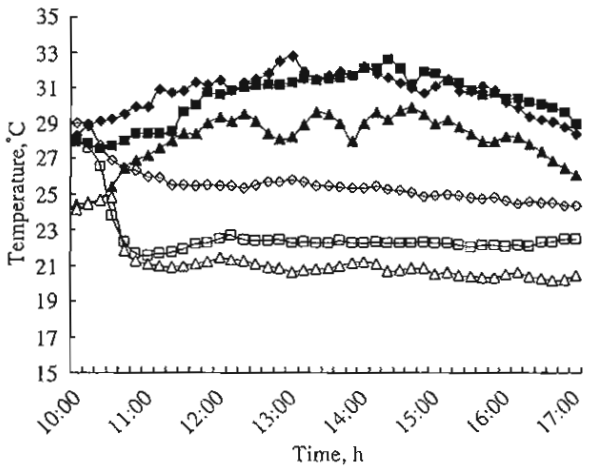


Fig. 8. Effect of ambient temperature and air mass flow rates on room temperature; –◆–, ambient temperature (4·4 kg s^{-1}); –■– ambient temperature (6·3 kg s^{-1}); –▲–, ambient temperature (9·2 kg s^{-1}); –◇–, room temperature (4·4 kg s^{-1}); –□–, room temperature (6·3 kg s^{-1}); –△–, room temperature (9·2 kg s^{-1})

Table 1
Input power and energy efficiency ratio at different airflow rate

Air flow rate, kg s^{-1}	*Input power, kW*	*Energy efficiency ratio*
4·4	1·14	24·4
6·3	1·15	51·2
9·2	1·23	59·9

4.4. *Rearing of silkworms—a demonstrative application*

The general question of the feasibility of a given application is not being addressed in this study. Instead, an experiment performed on the evaporative cooling system for rearing silkworms is used to illustrate a possible application. At this stage, two generations of Multi-voltine Thai silkworm 'Nanglai' (*Bombyx mori*) with 5000 larvae per generation were reared in the evaporative cooling house. The first and second generations were reared during November to December 2003 and March to April 2004, respectively. An interesting observation here is that, the percentage of survival of silkworms was 91% for the first generation and 93% for the second generation. Comparable conventional system percentage survival rates of silkworms were separated by

Table 2
Summary of economic evaluation of evaporative cooling system

Item	*Value, Baht*
Fixed cost	70 000
Variable cost	22 000
Income	49 420·8

season as follows: 46·5% for summer, 82·4% for rainy and 83% for winter (Attathom *et al.*, 2002). Obviously, the percentage of survival of the silkworms reared in the evaporative cooling system was higher than that obtained with the conventional rearing system, especially in summer. It could be concluded that the evaporative cooling system application could be an alternative in the silkworm rearing process.

4.5. *Economic evaluation*

In this section, a cost analysis of the evaporative cooling is evaluated. A payback period is employed to determine the period of time required for a profit that could be attributed to using the evaporative cooling. The payback period is defined as the investment of time required for the profit of an investment to equal the cost of the investment (Newnan, 1980). The life cycle of the Thai silkworm is approximately 25 days. Thus, 12 generations of silkworm can be raised per year with 44 000 larvae per generation. Assuming the percentage survival of silkworms was 90%, silkworm survival would be 39 600 larvae per generation. The average weight of a Thai silkworm cocoon was 1·3 g per larvae. The total weight for a survival of 39 600 larvae would be 51·48 kg per generation. During 2003, the purchase price of cocoon in the local market was 80 Baht per kg. The resulting annual income would have been 49 420·8 Baht. Fixed costs for the evaporative cooling house, including those for construction cost, suction fan, pump, piping and cooling pad, were 70 000 Baht. Variable costs, mainly the power cost, silkworm eggs and feed, were 22 000 Baht. These costs divided by the annual income of 49 420·8 Baht give a payback period of approximately 2·5 years. The summary of economic evaluation is given in Table 2. Therefore, the evaporative cooling system in a silkworm rearing house should be promoted as an alternative technology for the household farmer. Additional cost savings could be recognised in larger scale operations.

5. Conclusions

The feasibility of improving the indoor condition of a silkworm rearing house by using direct evaporative cooling was investigated experimentally. An experimental silkworm rearing house was built. The study was conducted during the summer and winter seasons in Mahasarakham, Thailand. It was found that the evaporative cooling system was capable of reducing the temperature and increasing the relative humidity as required for rearing the silkworm. An alternative scenario was also proposed that involved varying the air mass flow rate between summer and winter seasons to reduce operating costs. Consequently, as the experiment revealed, the evaporative cooling system should be recommended.

Acknowledgements

The authors would like to thank the Thailand Research Fund (TRF) for providing financial support to this study. Thanks are also due to Mr. N. On-uthai, Mr. M. Chinda, Mr. C. Sawasdee and Ms. S. Worrakhot for their assistance extended during data collection.

References

Attathom T; Saksirirat S; Pattanasethanon V (2002). Eri silkworm: potential culture on cassava leaf, factors affecting culturing and production cost analysis. Proceedings of XIXth Congress of the International Sericultural Commission, pp 274–278, Bangkok, Thailand

Boonyawattana K; Promwungkwa A; Terdtoon P; Rerkkriangkrai P (2003). The study of evaporative cooling pads performance and simulation of a swine house. Proceedings of the 17th Conference on Mechanical Engineering Network of Thailand

Chuprayoon S; Boonchoo S; Chuprayoon S (2002). Sericulture in Thailand. Proceedings of XIXth Congress of the International Sericultural Commission, pp 493–504, Bangkok, Thailand

El-Dessouky H T; Ettouney H M; Bouhamra W (2000). A novel air conditioning system membrane air drying and evaporative cooling. Transactions of the Institution of Chemical Engineering, 78(A), 999–1009

Ketjoy N (1999). Development of a mathematical model of changing temperature and relative humidity in the poultry house. Master Thesis 1999, Energy Technology Division, King Mongkut's University of Technology Thonburi, Bangkok, Thailand

Khedari J; Sangprajak A; Hirunlabh J (2002). Thailand climatic zones. Renewable Energy, 25(2), 267–280

Kittas C; Bartzanas T; Jaffrin A (2003). Temperature gradients in a partially shaded large greenhouse equipped with evaporative cooling pads. Biosystems Engineering, 85(1), 87–94

Koca R; Hughes W; Christiason L (1994). Evaporative cooling pads—test procedures and evaluation. Applied Engineering in Agriculture, 7(4), 485–490

Newnan D G (1980). Engineering Economic Analysis. Engineering Press Inc., California

Sericulture Extension Center No. 1-9 and Sericulture Sub-Division (2002). Silk yarn quality development by farmer groups in Thailand. Proceedings of XIXth Congress of the International Sericultural Commission, pp 568–574, Bangkok, Thailand

Suriyasomboon A; Lundeheim N; Kunavongkrit A; Einarsson S (2004). Effect of temperature and humidity on sperm production in Durco boars under different housing in Thailand. Livestock Production Science, **89**(1), 19–31

Tazima Y (1978). The Silkworm an Important Laboratory Tool. Kodansha Ltd., Tokyo, Japan

Watt J R (1986). Evaporative Air Conditioning Handbook, 2nd Edn. Chapman Hall, London, UK

Wiersma F; Short T (1983). Evaporative cooling. In: Ventilation of Agricultural Structures (Hellickson M A ed), pp 101–118. ASAE, St. Joseph, MI, USA

Willits D H (2003). Cooling fan-ventilated greenhouse: a modelling study. Biosystems Engineering, **84**(3), 315–329

Available online at www.sciencedirect.com
SCIENCE DIRECT®
Journal of Food Engineering 75 (2006) 423–432
JOURNAL OF FOOD ENGINEERING
www.elsevier.com/locate/jfoodeng

Parboiling brown rice using super heated steam fluidization technique

Somchart Soponronnarit [a], Adisak Nathakaranakule [a], Athikom Jirajindalert [a], Chaiyong Taechapairoj [b,*]

[a] *School of Energy and Materials, King Mongkut's University of Technology Thonburi, Suksawat 48 Road, Bangkok 10140, Thailand*
[b] *Faculty of Engineering and Industrial Technology, Silpakorn University, Sanamchandra Palace Campus, Nakorn Pathom 73000, Thailand*

Received 15 November 2004; accepted 27 April 2005
Available online 7 July 2005

Abstract

This research is a study of parboiling of brown rice using superheated steam fluidization technique. The influence of soaking temperature and time, steaming temperature, and bed depth on qualities of product: head rice yield, white belly, whiteness, and viscosity of rice flour were focused. The experiments were set up at the material initial moisture content of 12.8% dry basis (d.b.), soaking temperatures of 70–90 °C, soaking times of 0.5–2.0 h., steaming temperatures of 120–160 °C, velocity of 3.9 m/s and bed depths of 8–12 cm. The experimental result showed that gelatinization occurred while product moisture content decreased and final moisture content about 28% d.b. gave the acceptable levels of the whiteness and white belly. The final moisture content lower than 28% and 18% d.b. resulted in the lower percent of head rice yield and whiteness, respectively. Considering white belly, it was found that the white belly decreased with increasing drying time. Additionally, peak viscosity, breakdown viscosity and setback viscosity of rice flour were found lower than those of raw rice.
© 2005 Elsevier Ltd. All rights reserved.

Keywords: Drying; Gelatinization; Grain; Head rice; Quality

1. Introduction

Parboiling of paddy is a hydro-thermal process aimed at improving milling, nutritional and organoleptic attributes of rice. It is an alternative method for prolonging rice storage. In addition, it reduces broken grain, increases head rice yield and reduces nutritional loss during polishing process (Bhattacharya, 1985). There are three steps of parboiling process consisting of soaking, steaming and drying. Paddy is moistened during the soaking process in which hot water is usually applied to enhance water diffusion into rice grain. Soaking process in warm water was found enhancing the effective cooking stage when the grain became saturated (Velupillai & Verma, 1982) because water makes starch granule sufficiently swell to be gelatinized. After soaking in hot water, paddy is left to cool down to environmental temperature for 2 h to allow water to enter the core part of rice grain.

The drying method is the key factor influencing the milling quality of rice (Bhattacharya & Indudhara Swamy, 1967). Several drying methods have been used for drying parboiled rice such as sun drying, hot air drying, vacuum drying and superheated steam drying (Bhattacharya, 1985; Soponronarit, Taechapairoj, & Prachayawarakorn, 2004; Taechapairoj, Prachayawarakorn, & Soponronarit, 2004).

Fluidization technique is an effective drying method, in which air and solid particles are rigorously mixed. It has been suggested that high moisture paddy should be dried quickly to approximate 23% d.b. to prevent the yellowing of rice kernels which is easily occurred at high moisture level and then subjected to ambient air

* Corresponding author. Fax: +66 34219360.
E-mail address: chaiyong_t@yahoo.com (C. Taechapairoj).

0260-8774/$ - see front matter © 2005 Elsevier Ltd. All rights reserved.
doi:10.1016/j.jfoodeng.2005.04.058

drying in a storage bin until its moisture content is down to 16% d.b. (Soponronnarit & Prachayawarakorn, 1994). Sutherland and Ghaly (1990) undertook an intensive investigation into the feasibility of using a hot air fluidized-bed drying technique for paddy. Their experiments showed that the head rice yield related to the final moisture content: the head rice yield was 58–61% when paddy was dried from 28.2% to 20.5% d.b. but was 15–24% for final moisture content lower than 20% d.b.

The drying medium which is used for carrying the evaporated water and fluidizing solid particles could be hot air or superheated steam. Superheated steam drying offers many important advantages over hot air drying. Firstly, the energy supplied to the dryer can be reduced economically by recycling the exhaust steam in a closed loop. Secondly, the energy from the exhaust steam resulting from the evaporation of moisture inside the solids can be recovered and used in the other sections. Lastly, environmental pollution or odour emission to the atmosphere can be eliminated since drying occurs in a closed chamber without air.

Parboiling of brown rice can save 40% of energy consumption compared to that of parboiled rice paddy. In addition, it prevents foreign matters and unsatisfied smell from rice paddy during soaking process. The cooking time is also reduced (Kar, Jain, & Srivastav, 1999).

The aim of this study is to determine the optimum parboiling process of brown rice using superheated steam fluidized bed. The physical properties of rice grain in terms of head rice yield, whiteness and white belly, rice flour viscosity and starch granule microstructure were compared with those of products dried in hot air under the same condition.

2. Materials and methods

Two fluidized-bed drying systems were used in the experiment. These are superheated steam and hot air systems (Fig. 1). The system of the superheated steam fluidized-bed dryer consists of five main components (Fig. 1a): a cylindrical chamber with a 15 cm inner diameter and a 100 cm height, a 13.5 kW electrical heater for converting saturated steam to the superheated steam, a backward-curved blade centrifugal fan driven by a 2.2 kW motor, a reverse flow cyclone and a small boiler with a 31 kg/h capacity of generated steam. A PID controller with an accuracy of ±1 °C was used to control steam temperature. Before using steam for drying, hot air was used for warming up the system until the temperature in every part reached the desired temperature. Then, the steam was replaced accordingly. The steam generator was generated the saturated steam at 106 kPa (absolute pressure) with the corresponding temperature of 100 °C. When the saturated steam was flowed through the electrical heaters, the additional heat

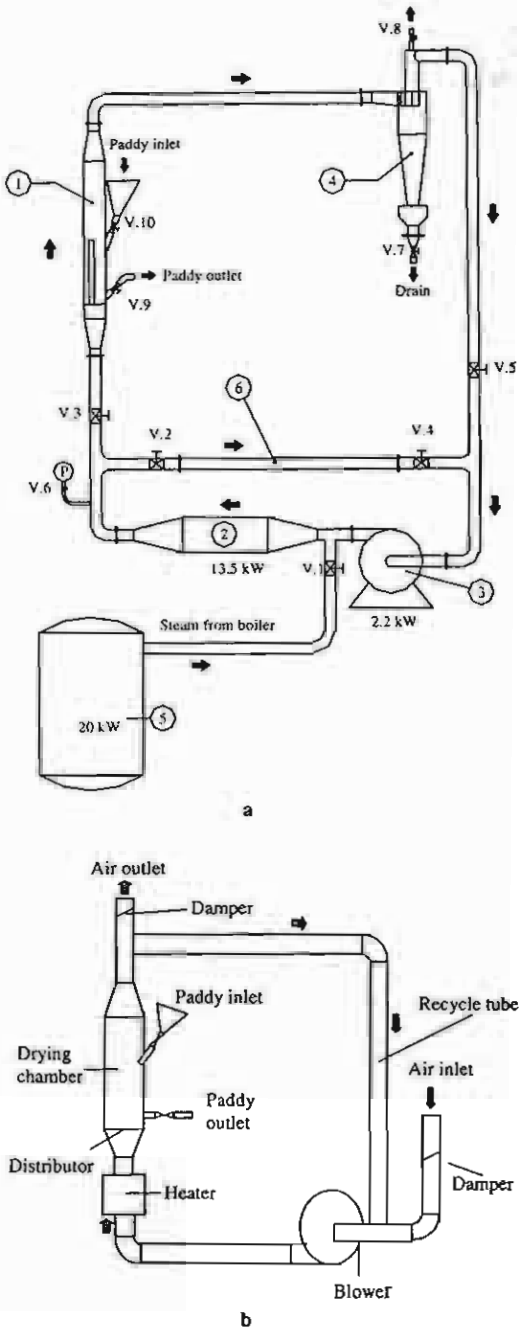


Fig. 1. Schematic diagrams of drying system. (a) Superheated steam fluidized-bed dryer. (b) Hot air fluidized-bed dryer.

was supplied to rise the steam temperature up to the required level. It was subsequently flowed through the fluidized-bed dryer. The dust particles and the immature grains being suspended in the exhaust steam were collected at the cyclone. Finally, the cleaning exhaust steam was reused again.

The hot air fluidized-bed dryer (Fig. 1b) consists of stainless steel cylindrical drying chamber of 20 cm

diameter and 140 cm height, a 12 kW heater with a PID controller with an accuracy of ±1 °C, a backward-curved blade centrifugal fan driven by a 1.5 kW motor.

Brown rice was prepared from long grain paddy of Chainat1 (CNT1) variety from Pathum Thani Rice Research Center, Pathum Thani Province, Thailand. The initial moisture of rice grain was 12.8% d.b. Brown rice was then soaked in hot water temperature of 70 °C for 0.5–2 h before draining and tempering to ambient temperature for 30 min. The drying condition was set at temperatures of 120, 140 and 160 °C, bed height of 8–12 cm at superficial velocity of 3.9 m/s under 106.1 kPa absolute pressure. The dried samples were then tempered to ambient temperature until the grain final moisture content was 16% d.b. before its quality was inspected.

The moisture content of paddy was determined by an electrical air oven at a temperature of 103 °C for 72 h. Paddy qualities in terms of head rice yield and whiteness were quantitatively determined and compared to the reference sample (paddy dried by the ambient air). The methods were followed with the guideline of the Ministry of Agriculture and Cooperatives, Thailand. Head rice is defined as milled rice having kernel length at least three-fourths of its original length. The head rice yield was calculated from the mass of white rice that remains as head rice after milling divided by the mass of paddy sample.

The colour of rice samples was measured by a Kett digital whiteness meter (Model C–300). Before measuring the colour of sample, the whiteness meter was calibrated with a white coloured reference, presenting a standard value of 86.3.

2.1. Scanning electron microscopy

Structural changes of kernels were investigated by scanning electron microscopy (SEM) (JSM-5600LV, Japan). The rice kernel was broken along the cross-sectional axis. Samples were placed on adhesive tape attached to a circular aluminum specimen stub, coated with gold layer using a sputter-coater and photographed at an accelerator potential of 10 kV.

2.2. RVA measurement

Pasting properties of rice flour were determined by a Rapid Visco Analyser model-4 (Newport Scientific Pty Ltd., Warriewood, Australia) utilizing thermocline. Following AACC Method 61-02 (AACC, 1995), the sample (3 g, 14% moisture basis) was mixed with distilled water in a RVA aluminum canister to make the total weight of slurry 28 g. The mixture was stirred at 900 rpm for 10 s and then changed to 160 rpm. The mixture was held at 50 °C for 1 min and then heated to 95 °C at 12 °C/min. After that, holding at 95 °C was 2.5 min, followed by cooling down to 50 °C at 12 °C/min and kept for 2.1 min. These tests were done in triplication. A plot of paste viscosity in arbitrary RVA unit (RVU) versus time was used to determine the peak viscosity (PV), temperature at peak viscosity (P_{Temp}), trough, final viscosity (FV), breakdown viscosity (BKV = PV − trough) and setback viscosity (SBV = FV − trough). The first point at which the viscosity increases to 1 RVU/s or faster is defined as the onset gelatinization temperature of rice flour (P_{Temp}). Peak viscosity (PV) indicates the water-binding capacity of mixture. It is often correlated with the final product quality, and also provides an indication of the viscous load likely to be encountered by a cook. Breakdown viscosity measures the degree of disintegration of the granules or paste stability. Setback viscosity is a measure of gelling or retrogradation tendency (Dengate, 1984).

3. Results and discussions

3.1. Drying curve

3.1.1. Effect of superheated steam temperature and bed depth

Fig. 2a shows the relationship between brown rice grain moisture content and temperature, and drying

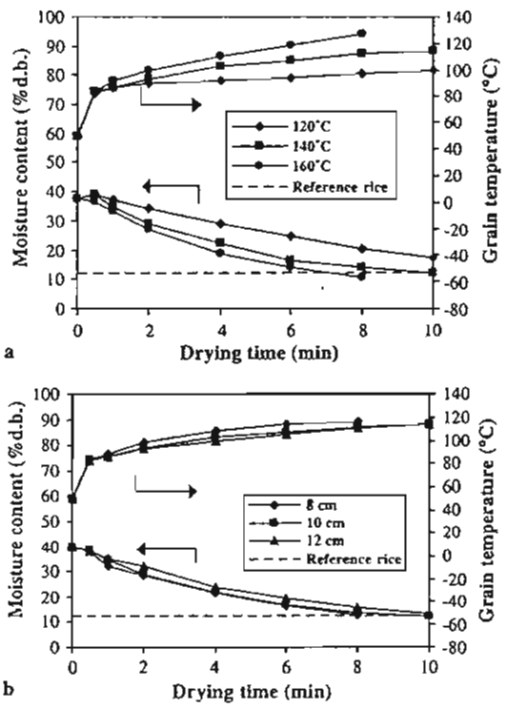


Fig. 2. Effect of superheated steam temperature and bed depth on moisture content and grain temperature at soaking temperature of 70 °C and soaking time of 1 h. (a) Bed depth 10 cm and (b) superheated steam temperature 140 °C.

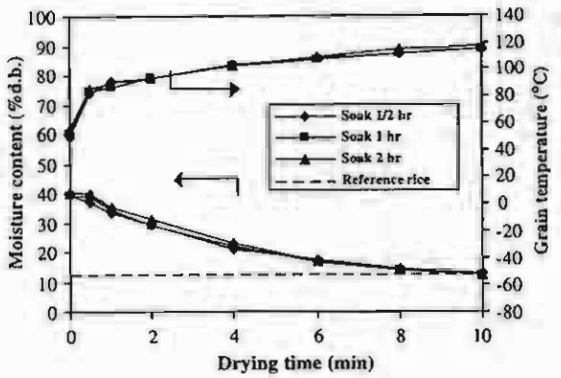


Fig. 3. Effect of soaking time on moisture content and grain temperature at superheated steam temperature of 140 °C and bed depth of 10 cm.

time. During the initial stage of drying, flowing water vapor was condensed due to its sudden contact with a low initial temperature of brown rice grain. This rapid release of heat vaporisation by condensation resulted in rapid increase in grain temperature. As shown in Fig. 2a, the grain temperature is slightly above 80 °C in the first minute of drying time and then relatively rises to 100 °C in 3 or 4 min. The grain temperature rapidly increases and higher grain temperatures follow with higher steam temperatures, resulting in the relative difference of moisture content.

The effect of bed depth on drying rate and grain temperature were of less significant than that of superheated steam temperature (Fig. 2b).

3.1.2. The effect of soaking time

Fig. 3 shows the relationship between soaking and drying rate. It was found that moisture content of grain increased with increasing soaking time due to water uptake of rice grain. However, its impact on drying rate of rice grain was not significant.

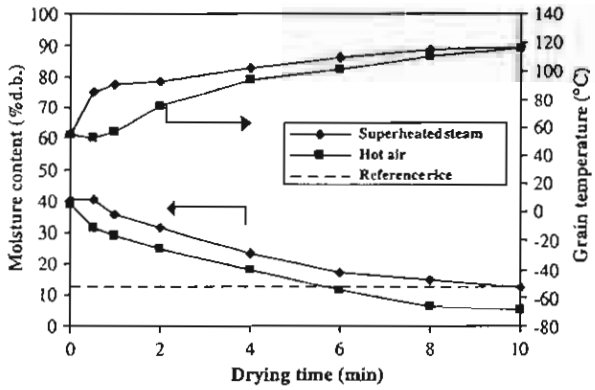


Fig. 4. Effect of heating media on moisture content and grain temperature at drying temperature of 140 °C, bed depth of 10 cm and soaking time of 2 h.

3.1.3. Comparison between superheated steam and hot air drying

Fig. 4 indicated that moisture content of rice grain dried by hot air dropped more rapidly and kept lower through the drying period. In contrast, the temperature of rice grain dried by superheated steam during the first minutes of drying increased faster than that dried by hot air. This phenomenon was due to latent heat from steam condensation added to rice grain during the initial stage of drying and superior heat transfer properties of superheated steam over hot air (Mujumdar & Menon, 1995).

3.2. Mathematical model of superheated steam drying

Fig. 5 shows drying curve predicted by the mathematical model in comparison with that from experimental data at various superheated steam temperatures and bed depths. It was found that the predicted curve was in accordant with experimental data. There were two drying periods in the predicted mathematical model as following.

3.2.1. Constant drying rate period

At the initial stage of drying, the drying rate of rice grain was constant due to the vaporization of water at grain surface. This period is indicated by the linear curve

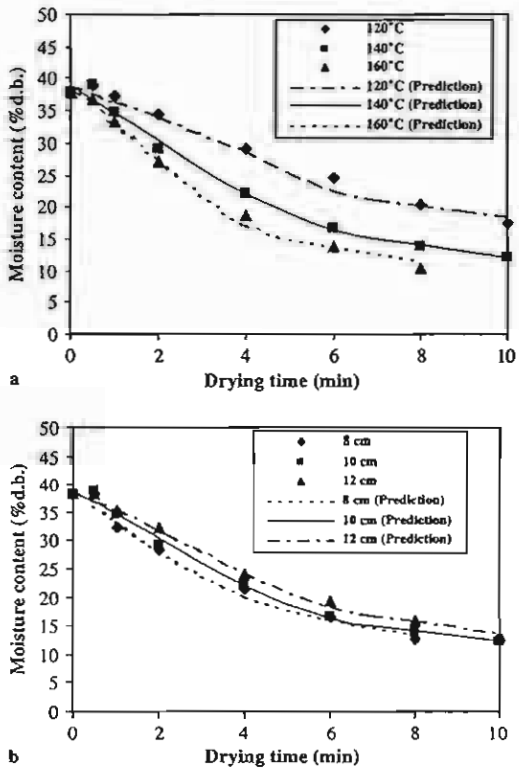


Fig. 5. Experimental data and the predicted drying curve under superheated steam. (a) Bed depth 10 cm and (b) superheated steam temperature 140 °C.

of grain moisture versus drying time. The drying rate is explained by the following equation:

$$MR = (-1.9594 \times 10^{-3} VT + 0.7586V + 4.004 \times 10^{-5} T - 0.016268)t + 1.030765 \ (R^2 = 0.92) \quad (1)$$

where V is specific mass velocity ($kg_{steam}/s\ kg_{drymatter}$), T is the inlet steam temperature (K) and t is drying time (s).

This equation is applicable in the range of temperature of 120–160 °C and specific mass velocity of 0.035–0.053 $kg_{steam}/s\ kg_{drymatter}$, and until the grain moisture reaches the critical moisture content of brown rice (about 25.5–26% d.b.) at which the falling drying rate period begins.

3.2.2. Falling drying rate period

After rice grain reaches its critical moisture content, the loss of moisture was at an exponential rate due to internal water diffusion to the grain surface at which the vaporization occurs. The effective diffusion coefficient of spherical shape brown rice grain was determined by analytical solution as Eq. (2).

$$\frac{M_t - M_{eq}}{M_{cr} - M_{eq}} = \frac{6}{\pi^2} \sum_{n=1}^{\infty} \frac{1}{n^2} \exp\left[\left(\frac{n\pi}{R}\right)^2 D_{eff}(t - t_{cr})\right] \quad (2)$$

where D_{eff} is the effective diffusion coefficient (m^2/s), R is the radius of brown rice (m) and t_{cr} is the drying time at the critical point (s)

Fig. 6 shows the relationship between the effective diffusion coefficient and bed depths, and superheated steam temperature. At drying temperature of 120–160 °C, the effective diffusion coefficient was between 1.0497×10^{-10}–2.4672×10^{-10} m^2/s. The effective diffusion coefficient increased with increasing drying temperature as indicated in the following Arrhenius equation.

$$D_{eff} = 9.95289 \times 10^{-7} \exp\left(\frac{-32915.126}{RT}\right) \ (R^2 = 0.86) \quad (3)$$

where T is the inlet steam temperature (K) and R is universal gas constant.

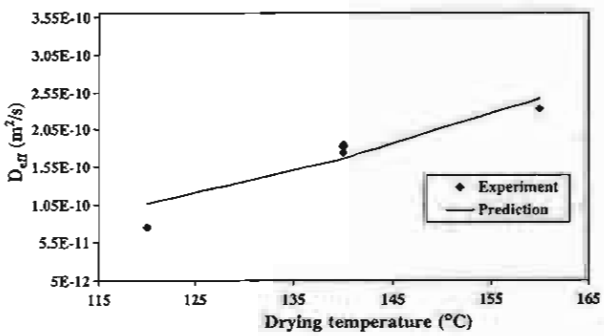


Fig. 6. Experimental and the predicted values of effective diffusivity (superheated steam).

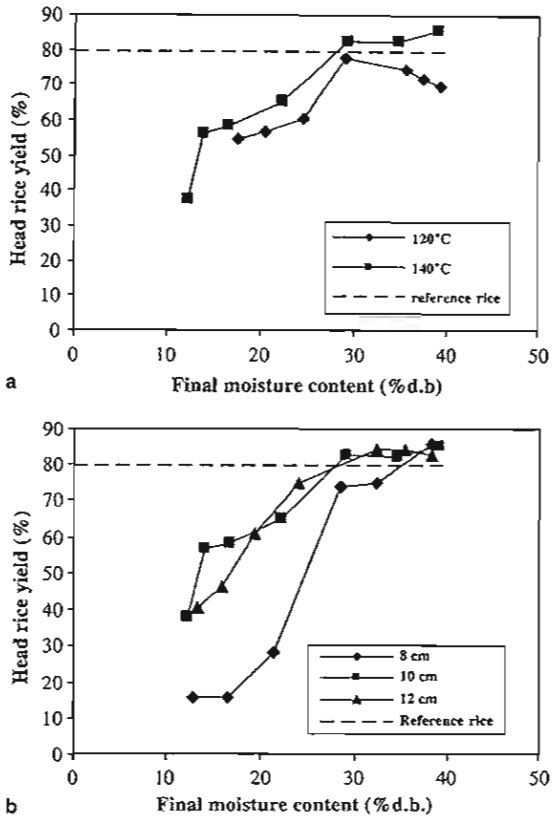


Fig. 7. Relationship between head rice yield and final moisture content during drying in superheated steam at different bed depths and superheated steam temperatures. (a) Bed depth 10 cm and (b) superheated steam temperature 140 °C.

3.3. Head rice yield

The relationship between head rice yield and final moisture content of brown rice grain at various

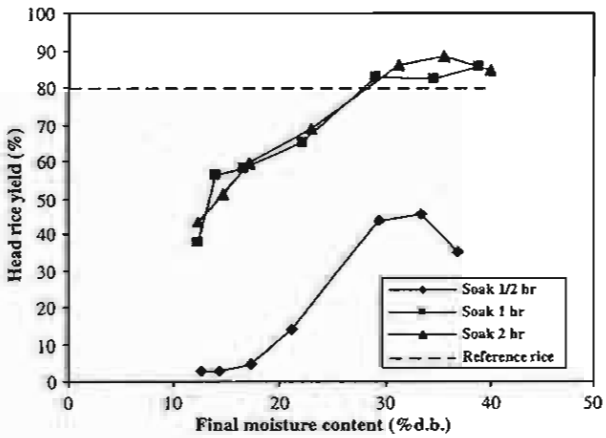


Fig. 8. Relationship between head rice yield and final moisture content at superheated steam temperature of 140 °C and bed depth of 10 cm.

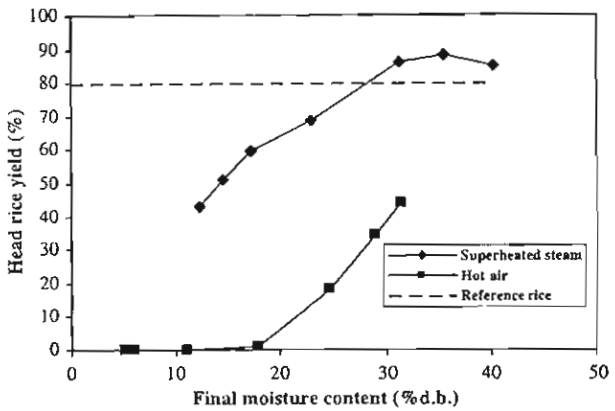


Fig. 9. Relationship between head rice yield and final moisture content of brown rice dried by superheated steam and hot air at drying temperature of 140 °C and bed depth of 10 cm.

superheated steam temperatures and bed depths are presented in Fig. 7.

Drying brown rice with superheated steam at an initial stage provided higher head rice yield compared to that of reference sample. An increase in head rice yield closed to that of reference rice was apparent at the final rice moisture content of 28–29% d.b. This improvement was caused by stronger structure of rice starch as a result of gelatinization process (Fig. 10c). Furthermore, the denaturation of protein and diffused into inter-granular space of starch increase the binding effect. With higher moisture content, rice starch dried by superheated steam was more rapidly gelatinized, thus, stronger structure was obtained. When rice grain with moisture content of lower than 28% d.b. was exposed to longer heat, rice grain temperature will be increased resulting in more porosities within rice starch, high moisture and temperature gradient causing stress development inside the kernels. As a result, rice kernel are more susceptible to physical damage during milling process leading to lower head rice yield. At given final moisture content, head rice yield increased with increasing superheated steam temperature and bed depth.

The relationship between head rice yield and final moisture content of rice grain at different soaking times is presented in Fig. 8. It was found that an increase in soaking time prompted an increase in head rice yield because of higher initial moisture content of rice grain. Soaking rice for less than 1 h is insufficient for rice to uptake water for gelatinization process resulting in lower head rice yield with white belly appearance.

Fig. 9 shows the relationship between head rice yield and final moisture content of brown rice grain comparing superheated steam drying and hot air drying. It was

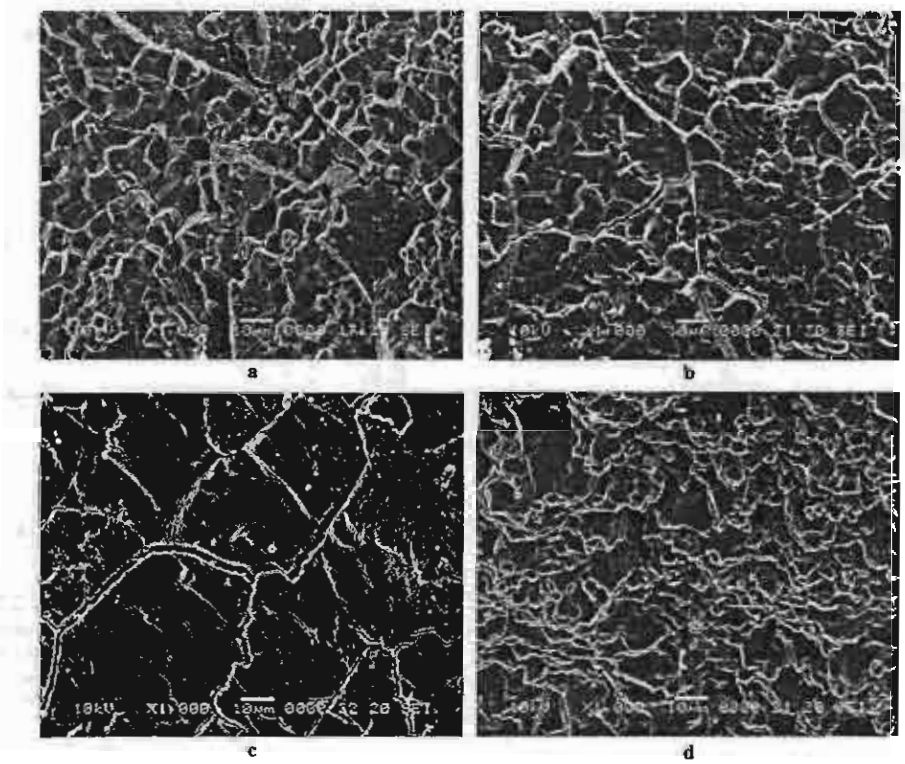


Fig. 10. Scanning electron micrographs of rice at different processes. (a) Raw rice, (b) soaked rice dried by ambient air, (c) soaked rice dried by superheated steam at temperature of 140 °C and (d) soaked rice dried by hot air at temperature of 140 °C.

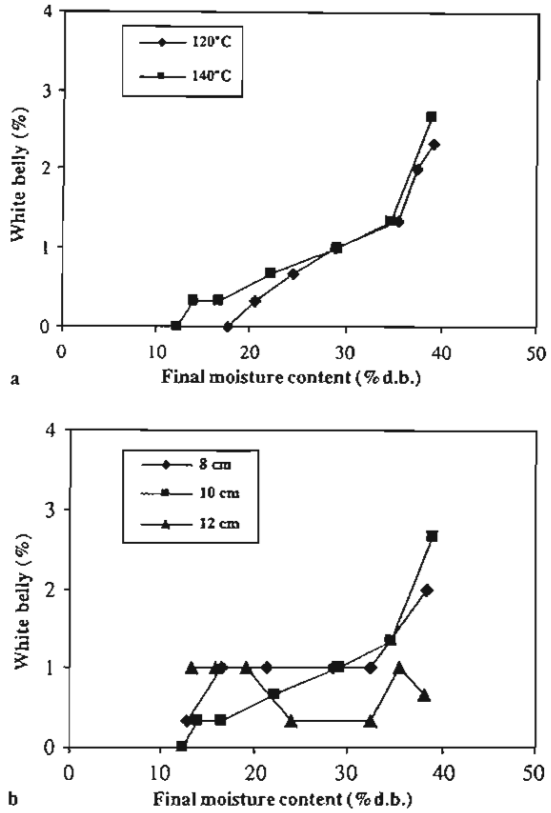


Fig. 11. Relationship between white belly percentage and final moisture content during drying in superheated steam at different drying temperatures and bed depths (white belly percentage of reference rice = 20%). (a) Bed depth 10 cm and (b) superheated steam temperature 140 °C.

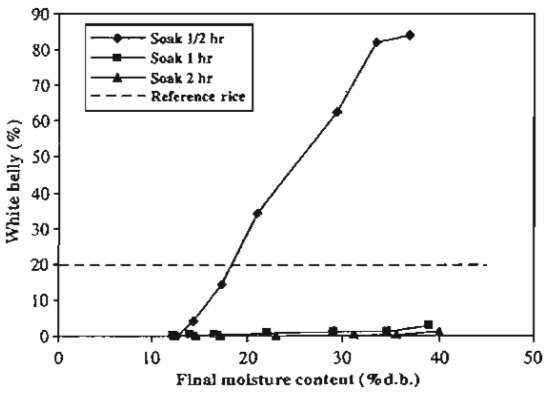


Fig. 12. Relationship between white belly percentage and final moisture content during drying in superheated steam temperature of 140 °C and bed depth of 10 cm at different soaking times.

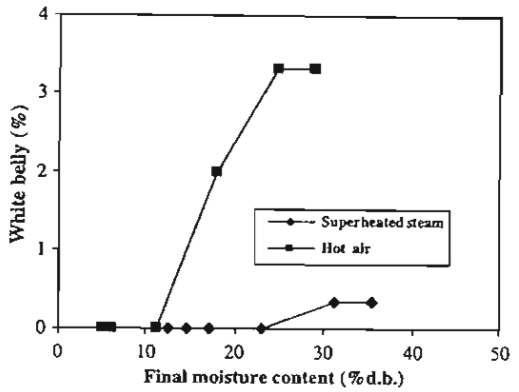


Fig. 13. Relationship between white belly percentage and final moisture content of brown rice dried by superheated steam and hot air at drying temperature of 140 °C and bed depth of 10 cm (white belly percentage of reference rice = 20%).

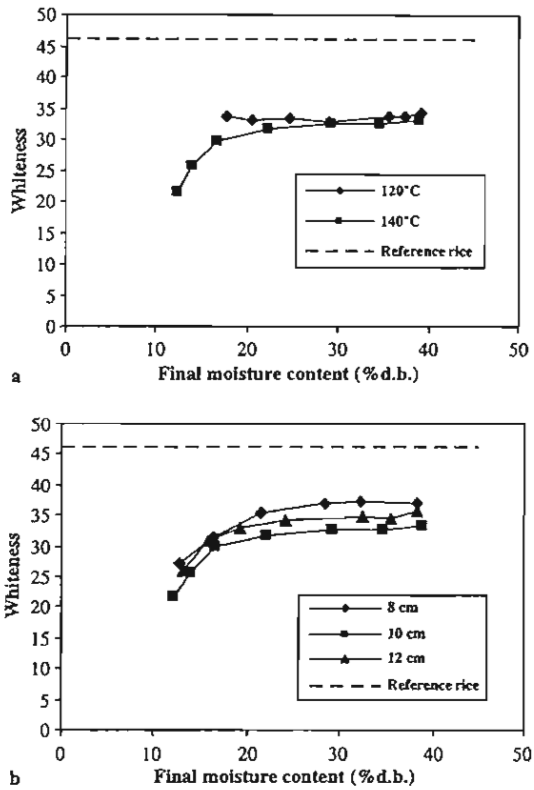


Fig. 14. Relationship between whiteness and final moisture content during drying in superheated steam at different drying temperatures and bed depths (whiteness of reference rice = 44.6). (a) Bed depth 10 cm and (b) superheated steam temperature 140 °C.

found that brown rice dried by superheated steam provided higher head rice yield than that dried by hot air. High head rice yield was still found at final moisture content of rice grain at 28% d.b. An improvement of head rice yield at initial stage of drying with superheated steam could be explained by suitable condition for gelatinization. Slow gelatinization process in hot air compared with superheated steam (Iyota, Nishimura,

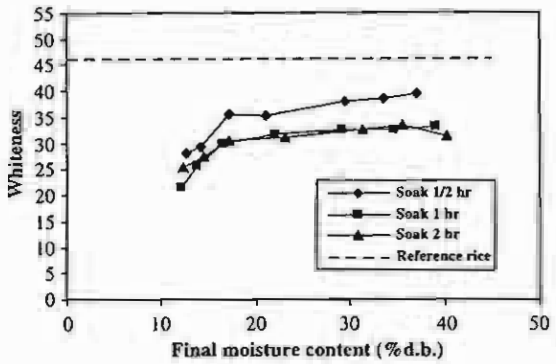


Fig. 15. Relationship between whiteness and final moisture content during drying in superheated steam temperature of 140 °C and bed depth 10 cm at different soaking times (whiteness of reference rice = 44.6).

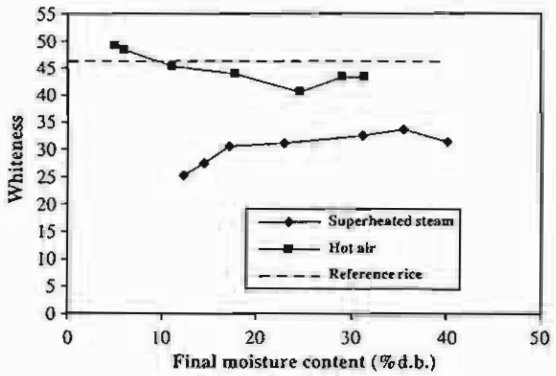


Fig. 16. Relationship between whiteness and final moisture content of brown rice dried by superheated steam and hot air at drying temperature of 140 °C and bed depth of 10 cm (whiteness of reference rice = 44.6).

Onuma, & Nomura, 2001) causes susceptible grain to damage during milling process; thus, lower head rice yield. Fig. 10c shows the completed gelatinization of rice starch obtained from superheated steam compared with incomplete gelatinized structure as indicated in Fig. 10d.

3.4. White belly

White belly is considered a poor characteristic of parboiled rice caused by incomplete gelatinization of rice starch. It is described as dully white spot with porosities between the starch granules. White belly is usually found at the core of rice kernel. Figs. 11 and 12 show the relationship between white belly and final moisture content of brown rice at various temperatures, bed depths and soaking times. The results indicated that soaking time influenced the white belly intensity. The longer soaking period, the less extent of white belly was the rice kernel. However, this association was obvious only at the soaking period of 0.5 h. When the soaking period was over half an hour, final moisture was not related to white belly. This could be explained that at soaking period of 0.5 h, the water uptake was found only at the surface of rice kernel resulting in uneven gelatinization of starch with the rice kernel.

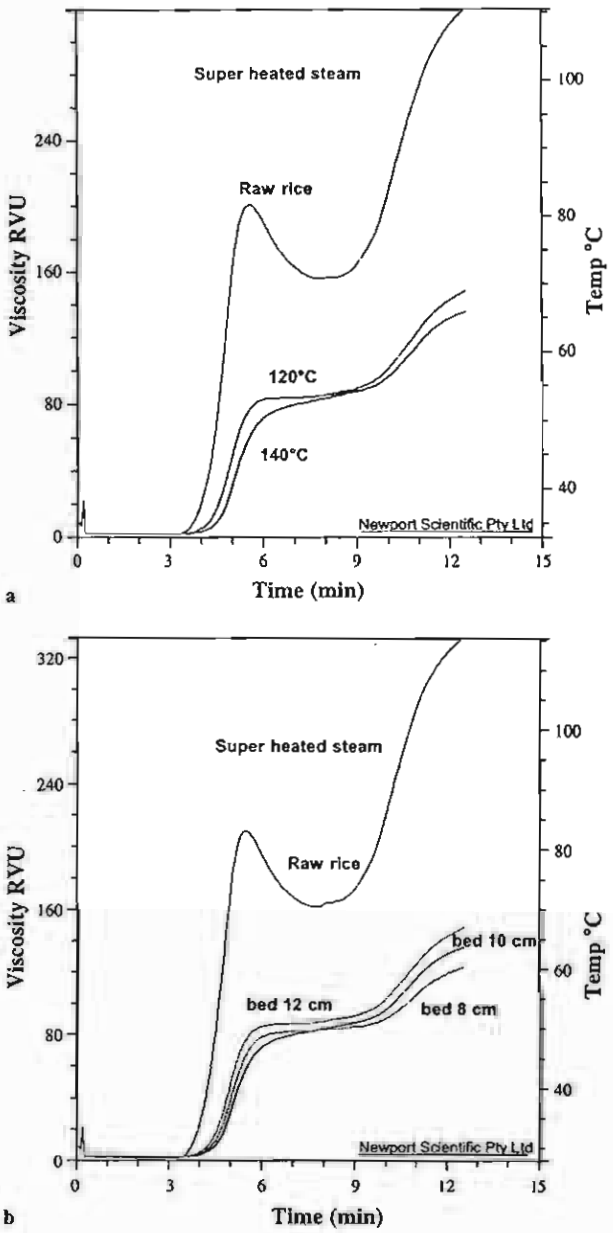


Fig. 17. Viscograph of raw rice flour and rice flour dried by superheated steam (soaking time 1 h). (a) Bed depth 10 cm and (b) superheated steam temperature 140 °C.

Fig. 13 shows the relationship between white belly and final moisture content of brown rice grain during drying with superheated steam and hot air. It was found that drying brown rice grain with superheated steam

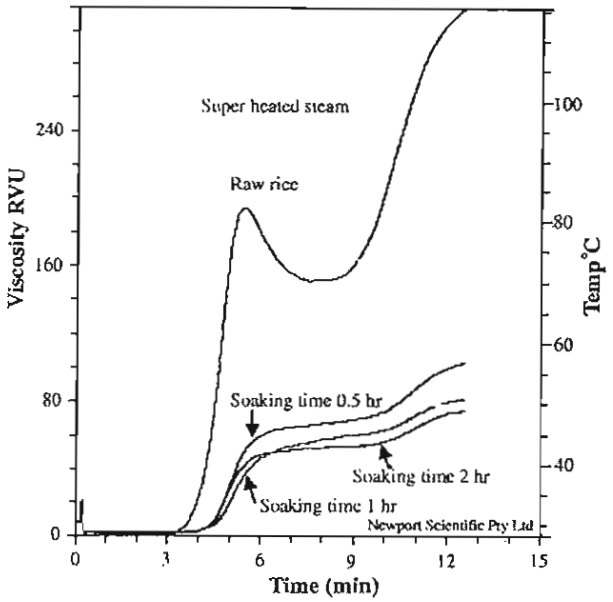


Fig. 18. Viscograph of raw rice flour and rice flour dried by superheated steam at drying temperature of 140 °C and bed depth of 10 cm.

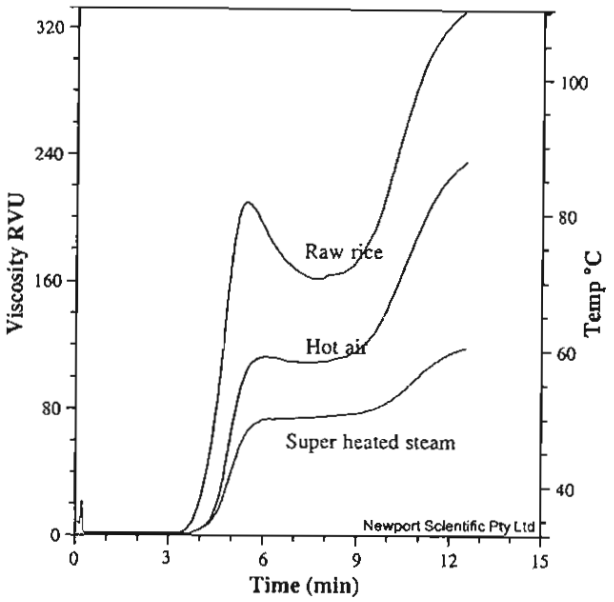


Fig. 19. Viscograph of raw rice flour and rice flour dried by superheated steam and hot air at drying temperature of 140 °C and bed depth of 10 cm.

gave less white belly kernel than that with hot air. This improvement was due to more complete gelatinization resulted from water condensation from superheated steam while no condensation was found in hot air drying.

3.5. Whiteness

Compared with reference rice, dried brown rice gave lower whiteness value (Figs. 14–16). The dark colour of dried grain was caused by maillard browning reaction between reducing sugar and amino acid activated by heat. Fig. 14 shows the relationship between the whiteness and final moisture content of brown rice at various temperatures and bed depths. It was found that whiteness of brown rice dried by superheated steam was higher in value compared to that of reference rice. Superheated steam temperature did not show significant effect on the whiteness. The decrease in whiteness was found only when the final moisture content of brown rice was lower than 20% d.b.

Whiteness of brown rice is associated bed depth. At bed depth of 8 cm, the whiteness of brown rice was highest in value. Soaking time was also related to whiteness of brown rice. However, there was significant effect only at soaking time of 0.5 h (Fig. 15). This was due to the short period of soaking allowing less moisture uptake into rice grain; thus, it was insufficient for complete

Table 1
Pasting properties of raw and dried rice flour

	Peak viscosity (rvu)	Trough 1 (rvu)	Breakdown viscosity (rvu)	Final viscosity (rvu)	Setback viscosity (rvu)	Pasting temperature (°C)
Raw rice	209.67	161.92	47.75	332.67	123.00	79
Hot air 140 °C, soaking time 2 h and bed depth 10 cm	112.92	109.33	3.58	236.67	123.75	89
Superheated steam 120 °C, soaking time 1 h and bed depth 10 cm	84.33	84.42	−0.08	148.58	64.25	89
Superheated steam 140 °C, soaking time 1/2 h and bed depth 10 cm	84.92	84.83	0.08	139.42	54.50	89
Superheated steam 140 °C, soaking time 1 h and bed depth 10 cm	80.08	80.50	−0.42	135.92	55.83	89
Superheated steam 140 °C, soaking time 2 h and bed depth 10 cm	77.75	77.58	0.17	125.08	47.33	89.9
Superheated steam 140 °C, soaking time 1 h and bed depth 8 cm	82.17	82.17	0.00	123.00	40.83	89
Superheated steam 140 °C, soaking time 1 h and bed depth 12 cm	87.17	87.17	0.00	148.58	61.42	89

gelatinization. This appearance was in accordant with white belly characteristic.

As shown in Fig. 16, the result indicated more whiteness of brown rice dried by hot air than that by superheated steam. The whiteness of brown rice dried by hot air increased when final moisture content of grain decreased. On the contrary, the whiteness of brown rice started to decrease at final moisture content of rice kernel lower than 20% d.b.

3.6. Pasting properties

Pasting properties of rice starch dried by superheated steam and hot air, and reference rice (not dried) are shown in Figs. 17–19 and Table 1. The result shows that pasting temperature of rice starch dried by superheated steam and hot air was higher than that of reference rice. On the other hand, PV, BKV and FV of rice starch dried by superheated steam and hot air was lower than that of reference rice (Figs. 17 and 18). Decrease in PV of dried rice was due to its loss of water-binding capacity as a result of partial gelatinization. Since rice dried by superheated steam gave more complete gelatinization, its PV was lower than that dried by hot air. FV and SBK indicate cooked rice hardness (Ali & Bhattacharya, 1980; Priestley, 1976; Ranghavendra & Juliano, 1970). Brown rice dried by superheated steam gave lower FV and SBK compared to those of hot air dried grain. Therefore, cooked rice obtained from superheated steam drying provided higher hardness than that of hot air dried rice and reference rice when cooked.

4. Conclusion

From the study of superheated steam fluidized-bed drying of parboiled brown rice, it was found that superheated steam temperature was the most significant effect on drying rate while bed depth and rice soaking period were of minor importance. The head rice yield considerately decreased when final moisture content of rice grain was lower than 28% d.b. When final moisture content of brown rice was lower than 18% d.b. the whiteness of rice decreased. Increasing soaking time improved head rice yield and reduced white belly due to increasing gelatinization. According to the viscosity properties of rice starch, superheated steam drying provided lower PV, BKV and SBV compared with hot air.

Acknowledgements

The authors would like to express their profound thanks to Thailand Research Fund for financial support and Institute of Food Research and Product Development, Kasetsart University for physical properties testing machine.

References

AACC. (1995). *Approved method of the American Association of Cereal Chemists*, 9th ed. St. Paul, MN: American Association of Cereal Chemists, AACC.

Ali, S. Z., & Bhattacharya, K. R. (1980). Pasting behaviour of parboiled rice. *Journal of Texture Studies, 11*, 239–245.

Bhattacharya, K. R. (1985). Parboiling of rice. In B. O. Juliano (Ed.), *Rice: Chemistry and technology* (pp. 289–348). St. Paul, MN, USA: American Association of Cereal Chemists.

Bhattacharya, K. R., & Indudhara Swamy, Y. M. (1967). Conditions of drying parboiled Paddy for optimum milling quality. *Cereal Chemistry, 44*, 592–600.

Dengate, H. N. (1984). Swelling pasting and gelling of wheat starch. In Y. Pomeranz (Ed.). *Advances in cereal science and technology* (vol. 6, pp. 49–82). St. Paul, MN, USA: American Associated Cereal Chemistry.

Iyota, H., Nishimura, N., Onuma, T., & Nomura, T. (2001). Drying of sliced raw potatoes in superheated steam and hot air. *Drying Technology, 19*(7), 1411–1424.

Kar, N., Jain, R. K., & Srivastav, P. P. (1999). Parboiling of dehusked rice. *Journal of Food Engineering, 39*(1), 17–22.

Mujumdar, A. S., & Menon, A. S. (1995). Drying of solids. In A. S. Mujumdar (Ed.), *Handbook of industrial drying* (2nd ed., pp. 1–46). New York: Marcel Dekker.

Priestley, R. J. (1976). Studies on parboiled rice. I. Comparison of the characteristics of raw and parboiled rice. *Food Chemistry, 1*, 5–14.

Ranghavendra, R. S. N., & Juliano, B. O. (1970). Effect of parboiling on some physicochemical properties of rice. *Journal Agricultural Food Chemistry, 18*, 289–294.

Soponronnarit, S., & Prachayawarakorn, S. (1994). Optimum strategy for fluidised bed paddy drying. *Drying Technology, 12*(7), 1667–1686.

Soponronarit, S., Taechapairoj, C., & Prachayawarakorn, S. (2004). New technique producing parboiled rice. *The Journal of the Royal Institute of Thailand, 29*(1), 78–86.

Sutherland, J. W., & Ghaly, T. F. (1990). Rapid fluid-bed drying of paddy rice in the humid tropics. Presented the 13th ASEAN seminar on grain postharvest technology, Bandar Seri Begawan, Brunei Darussalam (pp. 1–12).

Taechapairoj, C., Prachayawarakorn, S., & Soponronarit, S. (2004). Characteristics of rice dried in superheated steam fluidised bed. *Drying Technology, 22*(4), 719–743.

Velupillai, L., & Verma, L. R. (1982). Parboiled rice quality as affected by the level and distribution of moisture after the soaking process. *Transactions of the American Society of Agricultural Engineering*, 1450–1456.

Available online at www.sciencedirect.com
SCIENCE DIRECT®
Journal of Food Engineering 76 (2006) 411–419
JOURNAL OF FOOD ENGINEERING
www.elsevier.com/locate/jfoodeng

Modelling of parboiled rice in superheated-steam fluidized bed

Chaiyong Taechapairoj [a,*], Somkiat Prachayawarakorn [b], Somchart Soponronnarit [c]

[a] Faculty of Engineering and Industrial Technology, Silpakorn University, Sanamchandra Palace Campus, Rajamankha Nai Road, Amphoe Muang, Nakhon Phathom 73000, Thailand
[b] Faculty of Engineering, King Mongkut's University of Technology Thonburi, Suksawat 48 Road, Bangkok 10140, Thailand
[c] School of Energy and Materials, King Mongkut's University of Technology Thonburi, Suksawat 48 Road, Bangkok 10140, Thailand

Received 8 July 2004; accepted 21 May 2005
Available online 21 July 2005

Abstract

Mathematical model of paddy drying in superheated-steam fluidized bed has been developed to predict moisture content and temperature. The model was written based on mass and energy balance. The kinetics of gelatinization of paddy at fluidizing condition described by zero-order reaction was also included in the model. The operating parameters set in the model development included superheated-steam temperature, bed depth and superficial superheated-steam velocity. The numeric calculations from the model were in agreement with experimental investigations for different operating conditions. The model was then used to examine the effect of the operating conditions on the drying behavior and gelatinization of paddy.
© 2005 Elsevier Ltd. All rights reserved.

Keywords: Fluidized bed; Gelatinization; Mathematical model; Superheated steam

1. Introduction

Traditional parboiling process consists of many steps. In the process, paddy is steeped in water overnight or longer until attaining the moisture content between 42% and 54% dry basis. Boiling or steaming the steeped rice at 100 °C is proceeded in order to gelatinize the starch. The parboiled rice is then cooled down to ambient environment and then dried before storage and milling. In the modern parboiling process, hot water is applied during steeping stage in order to eliminate the enzymatic activity that produces the sour odor and accelerate transport of water into the kernels. However, these processes are still not very convenient in practice since they still consist of many steps and take a long time. With the advent of using superheated steam for dehydrating foods (Blasco & Alvarez, 1995; Makowski, Cenkowski, Hatcher, Dexter, & Edwards, 2003; Tang & Cenkowski, 2000), it shows great potential to replace the hot air, particularly when used with starch-based materials. Recent studies have also reported on advantages of superheated-steam drying such as high drying rate and deodorization of products (Iyota, Nishimura, Nomura, Konishi, & Yoshida, 2002; Tatemoto, Mawatari, Sakurai, Noda, & Komatsu, 2002). Therefore, an attempt to use this medium for producing the parboiled rice is of particular interest in the present investigation. When using this medium type, both steaming and drying stages, required for the traditional method, are incorporated into a single stage.

In producing the parboiled rice, the translucent kernel, implying the starch available in the raw material to be gelatinized, is the most important feature that is concerned by the producer, in addition to the colour. The quality of parboiled rice is downed from the premium grade when the white belly, which is in part of ungelatinized starch, appears. The white belly problem is not very serious for the conventional method since the paddy is closely contacted with steam in a closed

* Corresponding author. Fax: +66 34219360.
E-mail address: chaiyong_t@yahoo.com (C. Taechapairoj).

0260-8774/$ - see front matter © 2005 Elsevier Ltd. All rights reserved.
doi:10.1016/j.jfoodeng.2005.05.040

bin for a sufficient long time and there is no moisture loss from the grains during steaming so that the starch is almost gelatinized completely. The gelatinization behaviour may be changed when the parboiled rice is made with superheated-steam drying where three stages i.e. heat, moisture transfer and gelatinization, are simultaneously occurred in the drying chamber. The gelatinization may not complete if the temperature is not adequately high and the grains held in the drying chamber too short. To obtain a good quality of parboiled rice, a mathematical model with incorporation of gelatinization kinetics is thus needed to simulate the drying of paddy in bed fluidized with superheated steam. This investigation is directed towards understanding the dehydration process associated with gelatinization of paddy occurring in the superheated-steam fluidized bed.

2. Mathematical model of drying system

As a model for the fluidized-bed dryer, the designation presented in Fig. 1 is used. To produce the parboiled rice, dry paddy is soaked in water until its moisture content reach 44–45% dry basis, at which it is almost uppermost holding capacity of kernel. When the soaked paddy is come into contact with steam, the corresponding steam condenses onto the paddy surface, thereby gaining moisture content. The increased moisture content may be present in the area near the exterior surface. Under such state together with the existing high initial moisture content, the evaporation rate is very fast, as evident from the experiment, and the moisture transport is governed by heat transfer control. As drying further proceeds, the surface dries and the available moisture in part of interior area is transported to the exterior by the Fick's law of diffusion. To predict the moisture content over the entire drying period, three distinct phases with different heat and mass transfer mechanisms are therefore identified and the energy balance for the components of steam, solid and water evaporated or contained in the grains are set up. To develop a mathematical model, it requires the following assumptions:

- Uniform moisture content throughout the bed.
- A plug flow of steam.
- Negligible heat loss of drying system.
- The temperature gradient inside single kernel and the grain shrinkage are negligible.
- Small Biot number, presenting unimportant heat conduction in paddy kernel.
- During period of condensation, the amount of steam flowing through the bed is totally condensed.

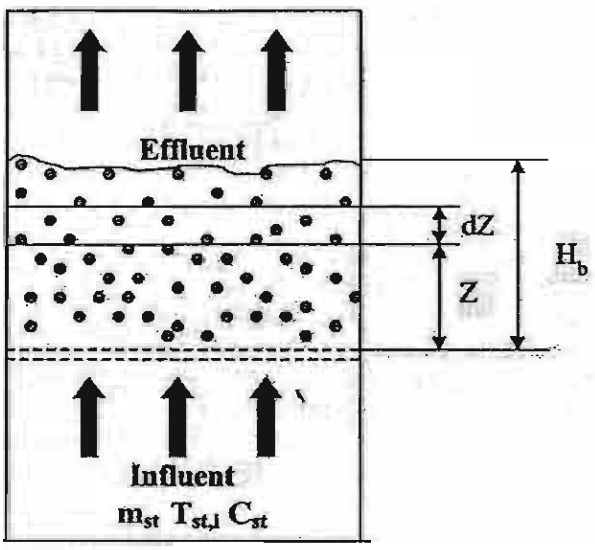


Fig. 1. Control volume of fluidised bed chamber.

2.1. Heating up period

At initial heating phase, superheated steam will thoroughly contact with cold surface of grain. As a result, the steam condensation will obviously occur onto the grain surface and the subsequent grain temperature rapidly increases from the initial temperature (room temperature) to the steam saturation temperature. The steam condensation is stopped when the grain temperature arrives at the saturation temperature which is 100 °C at the corresponding pressure of 106 kPa. To account for such change, the energy balance was made and the first term on the left side of Eq. (1) stands for the heat released by superheated steam, the second term represents heat of condensation and the last term characterizes the heat released from the saturated water to the temperature T_p, which is lower than the saturation temperature:

$$\dot{m}_{st}C_{st}(T_{st,i}-T_{sat})+\dot{m}_{st}h_{fg}+\dot{m}C_{fl}(T_{sat}-T_p) = m_{ds}(M_iC_{fl}+C_p)\frac{dT_p}{dt} \quad (1)$$

where $\dot{m}_{st}$ is the mass flow rate of steam (kg s^{-1}), m_{ds} is the dry mass of solid particles in the bed (kg), C_{st} is the specific heat of steam (J kg^{-1} K^{-1}), C_{fl} is the specific heat of water (J kg^{-1} K^{-1}), C_p is the specific heat of solid particle (J kg^{-1} K^{-1}), h_{fg} is the latent heat of vaporization (J kg^{-1}), $T_{st,i}$ is the temperature of steam at the inlet of drying chamber (K), T_{sat} is the saturated steam (K) and T_p is the temperature of particles (K), M_i is the initial moisture content and t is the drying time. To solve Eq. (1), it requires the initial condition which is the grain temperature equal to the room temperature.

While steam condenses in the bed of particles, paddy immediately adsorbs the condensing water and the resulting its moisture content is changed. The varying

quantities of moisture content of paddy can be can be calculated by the following equation:

$$\left(\frac{dM}{dt}\right)_{heat-up} = \frac{\dot{m}_{st}}{m_{ds}} \quad (2)$$

2.2. Constant rate period

Drying of paddy, with an initial moisture content of 41–42.5% dry basis, using superheated-steam fluidized bed existed the constant drying rate period, in addition to the falling rate period (Taechapairoj, Prachayawarakorn, & Soponronnarit, 2004). At the constant rate period, temperature of moist paddy keeps a constant value at the saturation temperature (T_{sat}) when using superheated steam as drying medium, whereas it is equal to the wet-bulb temperature for the hot air drying. The heat transfer rate from superheated steam to the grains, imposed by difference between steam temperature, T_{st}, and sample temperature, T_p, must be equal to the enthalpy change of superheated steam and it can thus be written for a small control volume in the fluidized-bed as

$$-\dot{m}_{st}C_{st}dT_{st} = h_p(T_{st} - T_p)dA \quad (3)$$

let

$$A = A_p\frac{Z}{H_b}$$

where h_p is the heat transfer coefficient (W m^{-2} K^{-1}), A_p is the surface area of a single kernel (m^2), Z is the distance along the bed height (m) at any time and H_b is the total solid bed height (m). Substitution of A into Eq. (3) yields

$$-\dot{m}_{st}C_{st}dT_{st} = h_p(T_{st} - T_p)d\left(A_p\frac{Z}{H_b}\right)$$

The above equation is rewritten as

$$\int_{T_{st,i}}^{T_{st}}\frac{dT_{st}}{T_{st} - T_p} = -\int_0^Z \frac{h_pA_p}{\dot{m}_{st}C_{st}H_b}dZ \quad (4)$$

Upon integrating Eq. (4) and then rearranging it, we obtain

$$T_{st} = (T_{st,i} - T_p)\exp\left(-\frac{h_pA_p}{\dot{m}_{st}C_{st}H_b}Z\right) + T_p \quad (5)$$

The average temperature of superheated steam in drying chamber can be determined by

$$T_{st,avg} = \frac{1}{H_b}\int_0^{H_b} T_{st}dZ \quad (6)$$

Substituting T_{st} in Eq. (5) into Eq. (6), the average steam temperature is thus

$$T_{st,avg} = \frac{\dot{m}_{st}C_{st}}{h_pA_p}(T_{st,i} - T_p)\left(1 - \exp\left(-\frac{h_pA_p}{\dot{m}_{st}C_{st}}\right)\right) + T_p \quad (7)$$

where $T_{st,avg}$ is the average steam temperature (K).

To determine the kernel moisture content, the energy balance is applied again by which the heat transferred from medium to the grains is equal to the heat of vaporization, plus sensible heat of the evaporated water, yielding

$$\{h_{fg} + C_{st}(T_{st,avg} - T_{sat})\}m_{ds}\left(\frac{dM}{dt}\right)_{cons} = -h_pA_p(T_{st,avg} - T_p)$$

and reporting:

$$\left(\frac{dM}{dt}\right)_{cons} = \frac{-h_pA_p(T_{st,avg} - T_p)}{m_{ds}\{h_{fg} + C_{st}(T_{st,avg} - T_p)\}} \quad (8)$$

2.3. Falling rate period

Drying rate starts reducing when moisture content of paddy is lower than the critical moisture content. Below the critical level, the paddy surface is rather dried and the moisture existing inside kernel will transport to the surface via chaotically void spaces by moisture diffusion mechanism and this mechanism is a main controlling step in dehydration process.

Similar to the energy balance as mentioned in the constant drying rate period, the average steam temperature is

$$T_{st,avg} = \frac{\dot{m}_{st}C_{st}}{h_pA_p}(T_{st,i} - T_p)\left(1 - \exp\left(-\frac{h_pA_p}{\dot{m}_{st}C_{st}}\right)\right) + T_p \quad (9)$$

where T_p is the grain temperature (K) and it is equivalent to the steam saturation temperature at the beginning of falling rate period. In the solid phase, the heat is transferred from steam and this provides energy to increase grain temperature and evaporate some amounts moisture from the grain. Hence, the grain temperature can then be calculated by

$$\frac{dT_p}{dt} - \frac{1}{m_{ds}C_p}\left[\{h_{fg} + C_{st}(T_{st,avg} - T_p)\}m_{ds}\left(\frac{dM}{dt}\right)_{fall} + h_pA_p(T_{st,avg} - T_p)\right] \quad (10)$$

where m_{ds} is the total dry matter of grains in the dryer. Eqs. (9) and (10) are solved using the iterative technique. The initial condition for Eq. (10) is the particle temperature equal to the temperature of saturated steam. Convective heat transfer coefficient (h_p) can be determined by the equation proposed by Shi-Jan-Fou, Romankov & Rashkovska and this equation is appeared in the article written by Ciesielczyk (1996) as follows:

$$Nu = 0.25Re\frac{d_s}{H_b(1 - \varepsilon_0)} \quad (11)$$

where d_s is the particle diameter, ε_0 is the void and Re is the Reynold number, $\frac{d_s u \rho_s}{\mu}$ (u is the superficial velocity of superheated steam (m s^{-1}), μ is the superheated steam viscosity (kg/m s)). Using Eq. (11), we assume that the void in the fluidized bed was equivalent to the void at the minimum fluidizing condition. The rate of water removal, $\frac{dM}{dt}$ in Eq. (10), can be determined from the theoretical diffusion equation, Eq. (12).

$$\mathrm{MR} = \frac{6}{\pi^2}\sum_{n=1}^{\infty}\frac{1}{n^2}\exp\left[-\frac{n^2\pi^2}{r}\left(\frac{D_{\mathrm{eff}}t}{r}\right)\right] \tag{12}$$

where MR is the dimensionless ratio of $\frac{M(t)-M_{eq}}{M_{cr}-M_{eq}}$, r is the radius of sphere (m), t is the time (s), M_{cr} is the critical moisture content, with a value of 25% d.b. (Taechapairoj et al., 2004) and M_{eq} is assumed to be zero since the high steam temperature is used.

The effective diffusion of paddy in superheated-steam fluidized-bed dryer (Taechapairoj et al., 2004) is given by

$$D_{\mathrm{eff}} = 2.4243\times10^{-6}\exp\left(-\frac{29100}{RT_p}\right) \tag{13}$$

where R is the universal gas constant (J/mol K) and D_{eff} is the effective diffusion coefficient (m/s^2). Eq. (13) is valid in the grain temperature range between 112 and 126 °C.

2.4. Gelatinization kinetics

During gelatinization, starch granules undergo hydration, formation of ghost remnants, swelling, exudation of amylose and amylopectin, loss of birefringence, loss of crystallinity and changes in viscosity. To develop mechanisms for starch gelatinization, Taechapairoj et al. (2004) measured the degree of gelatinization of samples, dried by superheated-steam fluidized-bed dryer at different temperatures, using a differential scanning calorimeter. The change in gelatinized starch was described by the zero-order reaction (Taechapairoj et al., 2004):

$$\frac{\mathrm{d}(\%\mathrm{USG})}{\mathrm{d}t} = k \tag{14}$$

and

$$k = 75.93504 - (933.9536 - (97.5594 * H_b) + (3.3496 * H_b^2))\exp\left(\frac{-21944.38}{RT_p}\right) \tag{15}$$

where H_b is the bed depth, USG is the ungelatinization (%) and t is the time (s). Eq. (15) is valid in the bed depth 10–15 cm and the grain temperature range between 112 and 126 °C.

2.5. Solution algorithm

The calculation procedure of moisture change and gelatinization development during simultaneous heat and mass transfer in superheated-steam fluidized-bed dryer is shown in Fig. 2. The input variables are an initial moisture content of paddy, a bed depth, a superficial superheated-steam velocity and a superheated-steam temperature. The calculation steps are as follows: the change of grain temperature in the heating up period is determined. If the grain temperature is lower than the boiling point temperature, the calculation procedure

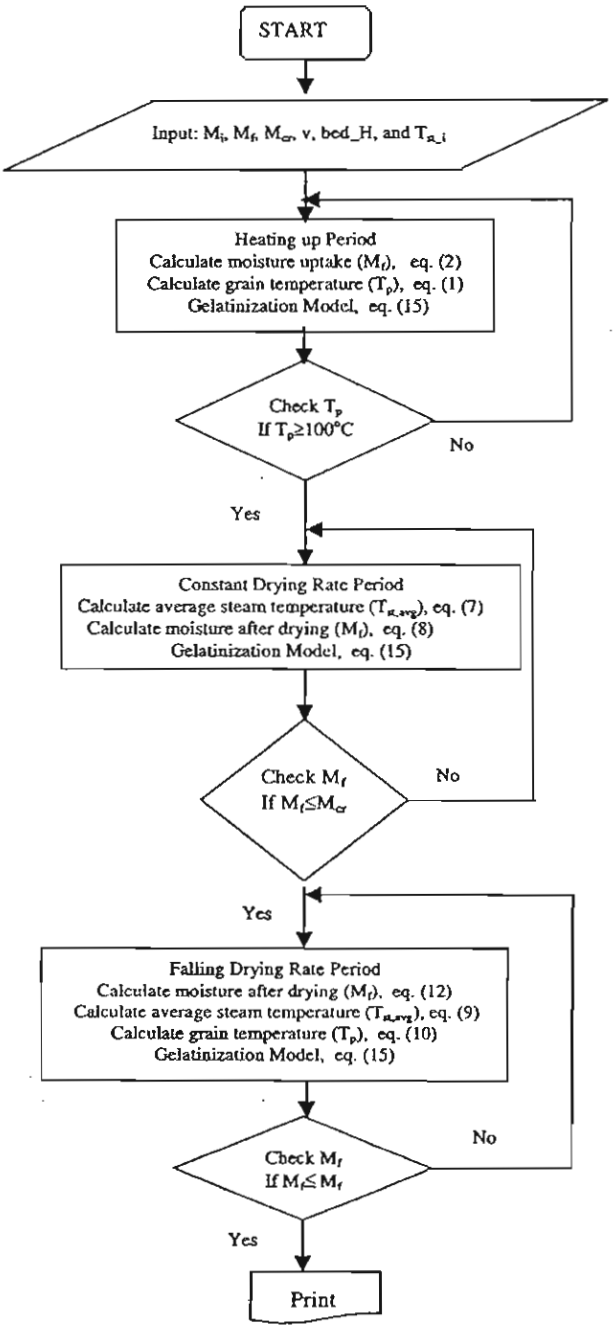


Fig. 2. Simulation flow chart of superheated-steam fluidized-bed dryer.

in this section is repeated until the grain temperature is higher or equal to the boiling point temperature. Next, the constant drying rate period is computed and then the moisture content is determined. If grain moisture content is higher than the critical moisture content, it will be used as an initial moisture content for the next calculation in this loop and the calculation continues until the moisture of paddy is lower or equal to the critical moisture content. Finally, the falling drying rate is calculated. The time step used in the calculation was set at 10 s and in each step, the degree of ungelatinization is determined by Eq. (14).

3. Material and methods

3.1. Sample preparation

Long grain paddy of Chainat1 (CNT1) variety from the Rice Experiment Station at Ayutthaya Province, Thailand, was used in the present investigation. In preparation, it was followed by a traditional method where paddy was cleaned and soaked at a temperature of 80 °C for 3.5 h. Then, water was drained out and the paddy was tempered at the same tank for 1 h prior to drying.

3.2. Drying

After soaking, paddy samples were dried with a batch superheated steam fluidized bed dryer as shown in Fig. 3. The system of the fluidized-bed dryer consists of five main components: a cylindrical chamber with an 15 cm inner diameter and a 100 cm height, a 13.5 kW electrical heater for converting saturated steam to the superheated steam, a backward-curved blade centrifugal fan driven by a 2.2 kW motor, a reverse flow cyclone and a small boiler with a 31 kg/h capacity of generated steam. A PID controller with an accuracy of ±1 °C was used to control steam temperature. Before using steam for drying, hot air was used for warming up the system until the temperature in every part reached the desired temperature. Then, the steam was replaced accordingly. The steam generator generated the saturated steam at 106 kPa (absolute pressure), a pressure slightly above the atmospheric pressure. When the saturated steam flew through the electrical heaters, the additional heat was supplied to raise the steam temperature up to the desired level. It was subsequently flowed through the fluidized-bed dryer. Paddy was loaded into the dryer by opening valve no. 10 and while loading the sample, valves no. 3 and 5 were closed and valves nos. 2 and 4 were opened. After loading the material, valve nos. 10, 2, and 4 were closed whereas valve nos. 3 and 5 were opened. During operation, all valves were manually controlled. The dust particles and the immature grains being suspended in the exhaust steam were collected at the cyclone. Finally, the cleanning exhaust steam was reused again.

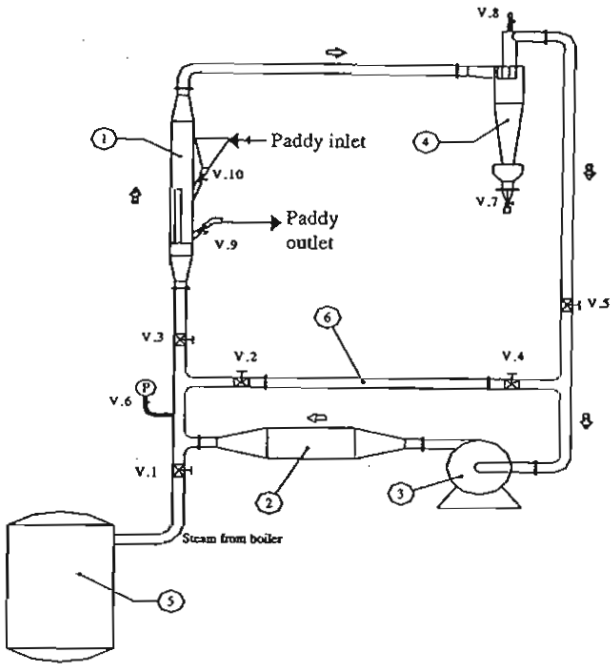


Fig. 3. A schematic diagram of the superheated-steam fluidized bed dryer: (1) fluidised bed dryer, (2) heater, (3) fan, (4) cyclone, (5) boiler, (6) bypass line, (V) = valve, and (P) = pressure gauge.

All drying conditions were performed at a superficial velocity of 3 m/s and static bed depths of 10–15 cm. To determine the moisture content and grain temperature, samples were taken out from the drying chamber at valve no. 9. For measuring grain temperature, the sample was collected in a well-insulated container. Grain temperature and drying superheated steam temperature were measured by Chromel-Alumel thermocouples (Type K) connected to a data logger with an accuracy of ±1 °C. The moisture content of paddy was determined by an electrical air oven at temperature of 103 °C for 72 h. Error of measurement was approximately ±0.1% dry basis. In the experiments, two experiments were carried out under each set of conditions, so as to confirm the reproducibility of the experiments. Good reproducibility was found as shown by moisture content in Fig. 4, grain temperature in Fig. 5 and degree of starch gelatinization in Fig. 6.

Gelatinization properties of parboiled rice flours were analyzed using a differential scanning calorimeter (DSC Pyris-I, Perkin–Elmer, Norwalk, CT, USA). The calibration was periodically performed using indium (heat of fusion of 28.41 J/g and 156.66 °C of melting temperature). Flour samples (~3 mg each) were weighed in sample pans, mixed with distilled water (~9 μL). The sample pan was sealed and allowed to stand for 1 h at

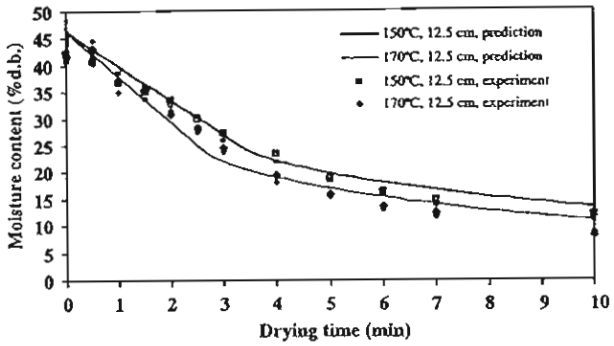


Fig. 4. Comparison between simulated moisture profile and experimental data of paddy at two temperatures and initial moisture content of 42% dry basis (superheated-steam velocity of 3 m/s).

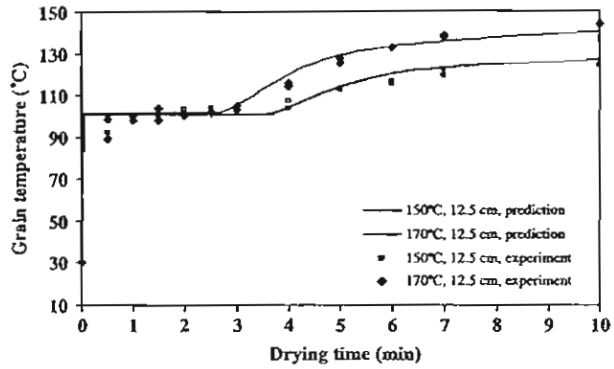


Fig. 5. Variation in grain temperature at different inlet temperature superheated-steam temperatures and initial moisture content 42% dry basis (superheated-steam velocity of 3 m/s).

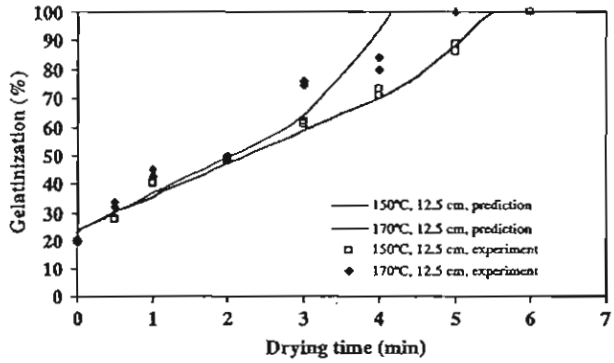


Fig. 6. Gelatinization of rice at different inlet temperatures (superheated-steam velocity of 3 m/s and initial moisture content 42% dry basis).

room temperature (Normand & Mashall, 1989). The sample was held isothermally at 30 °C for 1 min, and then scanned at a heating rate of 5 °C/min until the temperature raise to 100 °C. The calorimetric measures were made by duplications. The enthalpy change (ΔH) was evaluated using Thermal Analyzer (TA) Instruments analysis software program. The degree of gelatinization (SG) of rice flour was calculated by the following equation (Marshall, Wadsworth, Verma, & Velupillai, 1993):

$$SG(\%) = [1 - (\Delta H_{pg}/\Delta H_{raw})] \times 100 \quad (16)$$

where ΔH_{pg} and raw ΔH_{raw} are the enthalpies of gelatinized and raw rice grains, respectively.

4. Results and discussion

4.1. Validation of the model

4.1.1. Moisture content and grain temperature

The experimental data on moisture content and grain temperature are compared with those obtained from the simulations. In Fig. 4, the comparison between calculation and experiment for the moisture content is presented, indicating that the prediction from the model proposed is relatively consistent to the experimental data for a wide range of drying conditions. After the experiments are started, the superheated steam comes into contact with kernels that have a lower temperature. Hence, the steam is condensed and the condensed water is correspondingly adsorbed by grains, leading towards the increase in moisture content of paddy at the early drying stage as evident in Fig. 4, and this condensation results in a rapid rise in grain temperature as shown in Fig. 5. This temperature and the amount of water containing in kernels are sufficiently high enough to promote the starch granules to be gelatinized.

From the calculation, the water adsorption process of paddy together with the increase of grain temperature occurs rapidly: its moisture content is increased to a value higher than 45% dry basis, corresponding to the saturated steam temperature, in a few seconds (Fig. 4). The grain temperature prediction at this period slightly overestimates, as compared to the measured grain temperatures in Fig. 5 that shows the grain temperatures of 93 and 97 °C at the drying time of 30 s for the inlet steam temperatures of 150 and 170 °C, respectively. The over prediction of temperature is probably due to the steam flow entering into the bed of grains to be partly condensed whilst the total condensation is assumed for the calculations throughout which the grain temperature is below the saturation temperature. However, the partial condensation may probably occur when the grain temperature is nearing the saturation point.

After the elapsed time of 1 min, as observed from Fig. 5, the grain temperatures reach the saturation temperature at the operating pressure and stay at that temperature for a certain time. At the saturation temperature, the moisture content of paddy linearly decreases with drying time, representing the constant dry-

ing rate. When the drying rate is reduced, the grain temperature is increased. As shown in Fig. 5, the higher grain temperature is found with a higher steam inlet temperature because of a greater heat transfer rate from the superheated steam to the grains.

4.1.2. Gelatinization

Fig. 6 shows the progression of paddy gelatinization over time for two superheated steam temperatures. Before drying paddy kernels with superheated steam, some starch granules previously soaked with hot water were gelatinized, to a certain degree of 20%. The prediction from the kinetic model in conjunction with heat and mass transfer equations generally agrees with the experimental data for a wide range of experimental conditions. The rate of gelatinization was increased with increased temperature. As shown in Fig. 6, the complete gelatinization is accomplished in 6 min at 150 °C and 5 min at 170 °C.

4.2. Simulation results

The model was employed to predict moisture change, temperature and degree of gelatinization when paddy was dried at different operating conditions. The operating conditions we were interested in this study were the bed depth, drying temperature and superficial velocity. Throughout the simulations, the operating pressure was fixed at the atmospheric pressure and the operating conditions simulated were limited at the bed depth between 10 and 15 cm, and superficial velocity between 2.5 and 3.5 m/s. This is because if the bed depth is too thick and superficial velocity is too high, the quality of fluidization will become very poor, characterizing the large bubble sizes in the bed. This behaviour accordingly impedes the transfer of heat from medium to the kernels, and hence, the kernels throughout the bed do not uniformly receive the heat, leading to the subsequent non-uniformity of starch gelatinization for each kernel.

4.3. Effect of variables on drying rate and grain temperature

4.3.1. Effect of bed depth

Fig. 7 shows the effect of bed depth on the changes of moisture content and grain temperature. In the heating up period, because of steam condensation, the moisture content of paddy is increased from the initial moisture content of 42% dry to approximately 46% dry basis, for all bed depths. When the grain temperature arrives the saturation temperature, the evaporation period starts with a rate depending upon the bed depth. The calculated results present a faster drying rate following with a decrease of bed depth. The faster evaporation rate at thinner bed may possibly be related

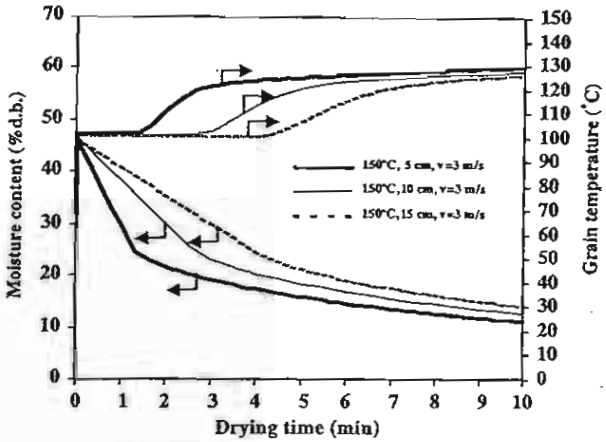


Fig. 7. Simulated results of effect of bed depth on moisture content and grain temperature (initial moisture content 42% dry basis).

to particle collision where the impaction amongst solid particles is very intensive for thin bed, thus reducing the laminar boundary layer near the heated particle surface. This effect is remarkable during which surface water is eliminated, and becomes less important when proportion of water inside the kernel is removed as indicated by moisture reduction, in which the drying curves at different bed depths are relatively closer at the later drying time than at the early drying time. For example, at the elapsed time of 1.5 min which still appeared the available surface moisture, the moisture content of paddy was reduced from the peak to approximately 25% dry basis for the bed depth of 5 cm and to 37% dry basis for 15 cm while the moisture content at the elapsed time of 5 min (no available surface moisture) was 18% for 5 cm bed depth and 23% for 15 cm bed depth.

As observed from the experiment, the falling rate period started when the surface water was completely evaporated, corresponding to the critical moisture content of ~25% dry basis, so that this critical value was used as input parameter for determining the moisture reduction in the falling rate period. During the falling rate period, the temperature starts increasing due to limitation of water transport. After the drying time of about 7 min, the grain temperature is slightly increased and seems to be slightly affected by bed depth.

4.3.2. Effect of superficial superheated-steam velocity

Fig. 8 shows the effect of superficial velocity on the changes of moisture content and grain temperature at bed depth of 15 cm and superheated temperature of 150 °C. Rate of moisture removal is accelerated by increasing the superficial velocity. In this case, the moisture transfer rate is governed by the heat transfer characteristics between solid surface and bulk stream. The steam velocity also influences on grain temperature, with

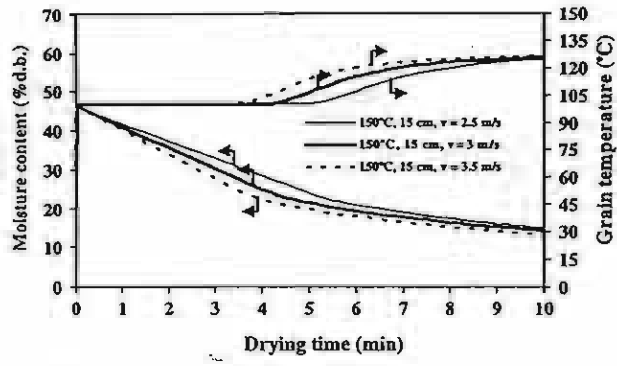


Fig. 8. Simulated results of effect of superficial superheated-steam velocity on moisture content and grain temperature (initial moisture content 42% dry basis).

more rapid rise in grain temperature in relation to higher steam velocity.

4.3.3. Effect of superheated steam temperature

As shown in Fig. 9, when the superheated steam temperature changes from 140 to 180 °C, the rate of moisture reduction, along with the progression of grain temperature, is increased with increased steam temperature, because of a greater difference of temperature between grain and superheated steam. Reducing the moisture content from 42% dry basis to approximately 19% dry basis requires drying times of 3.7, 4.5 and 5 min for the corresponding steam temperatures of 180, 160 and 150 °C. These calculated drying times included the initial condensation period.

It is note that paddy should not be dried below 19% dry basis by using superheated steam otherwise the drop in head rice yield is enormous (Taechapairoj, Prachayawarakorn, & Soponronnarit, 2003). To maintain high head-rice yield, the slow-drying technique is necessary for reducing the moisture content from the critical level.

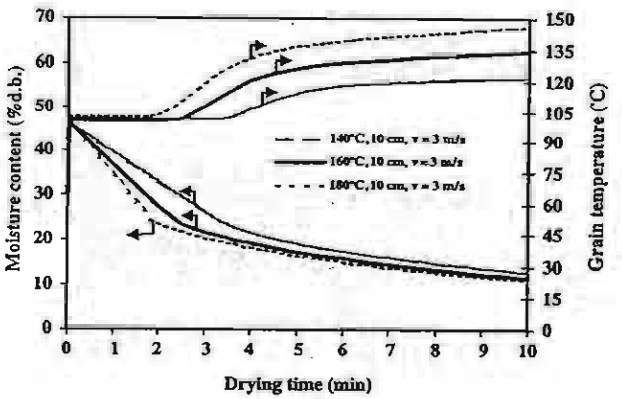


Fig. 9. Simulated results of effect of superheated-steam temperature on moisture content and grain temperature (initial moisture content 42% dry basis).

4.4. Effects of operating parameters on grain gelatinization

Good quality of parboiled rice should have a characteristic of translucent kernel or less amount of white belly. The appearance of white belly in kernel, which is usually found at the central area of kernel, intrinsically implies some starch granules inside kernel to be not fully gelatinized. This is in part affected by insufficient time for gelatinization. According to this, it is important to know the time required for complete gelatinization under different operating conditions i.e. temperature, bed depth and velocity. This useful information provides us to choose the suitable condition for producing high-quality parboiled rice, along with a high production capacity.

4.4.1. Bed depth

Fig. 10, on the left axis, shows the calculated time of complete gelatinization by plotting against the superheated–steam temperature at different bed depths, indicating that the processing time is shorter using higher temperature and thinner bed depth. This is because paddy experiences a higher heat transfer rate, resulting in more rapid rise in grain temperature and hence stimulating the starch to be gelatinized with a higher rate.

Although the gelatinization time at higher bed depth is apparently increased, this is not disadvantageous since the holding capacity is increased and it is more compensated than the increase of spent time for complete gelatinization. When the productivity, defined as the ratio of holding capacity to the reaction time, were consequently plotted against the steam temperature as shown in Fig. 10 on the right axis, the result represents the higher production at higher bed depth.

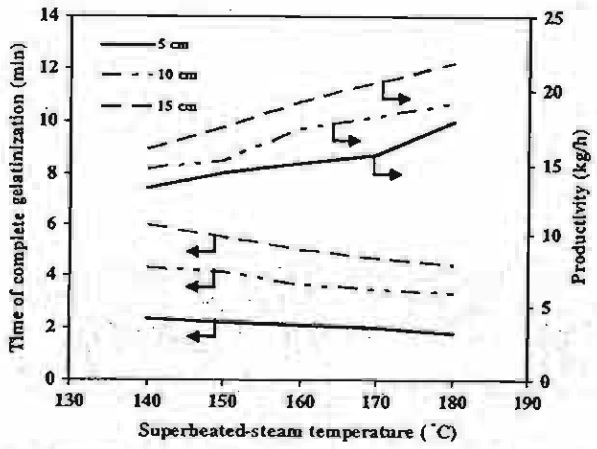


Fig. 10. Simulated results of effect of bed depth on the time of complete gelatinization and productivity of paddy during drying (initial moisture content 42% dry basis, final moisture content 19.9 ± 0.7% dry basis and superficial superheated-steam velocity = 2.5 m/s).

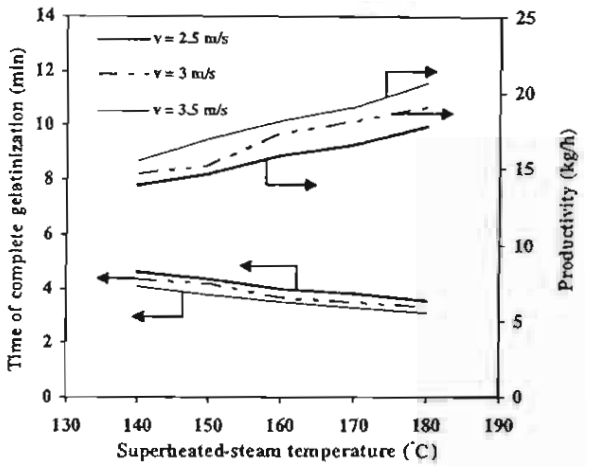


Fig. 11. Simulated results of effect of superficial superheated-steam velocity on the time of complete gelatinization and productivity of paddy during drying (initial moisture content 42% dry basis, final moisture content 19.9 ± 0.7% dry basis and bed depth 10 cm).

4.4.2. Superficial superheated-steam velocity

Fig. 11 shows the time of complete gelatinization as affected by superficial superheated-steam velocity at different superheated-steam temperatures. At a given temperature, increasing superficial velocity leads to shorter time to complete gelatinization due to higher convective heat transfer from heating medium to the grains. However, the effect of superficial superheated-steam velocity on the reaction time is relatively less important than the effects of bed depth and temperature.

According to these simulated results, they suggest that an efficient way to improve the productivity can be made by increasing the bed thickness and temperature.

5. Conclsions

Superheated-steam showed a high possibility of producing parboiled rice. A mathematical model for the drying of paddy in superheated steam had been developed and tested against the experimental results. The validation showed that the developed model had the capability to predict moisture content, temperature and degree of gelatinization. The validated model was then used to explore the suitable operating condition for producing parboiled rice and the simulated results showed that the times for complete gelatinization and evaporating water were shorten by increasing superficial superheated-steam velocity and temperature as well as decreasing bed depth, the first factor being least important. To obtain high productivity of parboiled rice, it was recommended from the simulations that the superheated-steam fluidized bed dryer should be operated at the bed depth of 15 cm and temperature of 180 °C.

Acknowledgement

The authors would like to express their sincere thanks to the Thailand Research Fund for financial support.

References

Blasco, R., & Alvarez, P. I. (1995). Flash drying of fish meals with superheated steam: isothermal process. *Drying Technology, 17*, 775–790.

Ciesielczyk, W. (1996). Analogy of heat and mass transfer during constant rate period in fluidized bed drying. *Drying Technology, 14*(2), 217–230.

Iyota, H., Nishimura, N., Nomura, T., Konishi, Y. & Yoshida, K. (2002). Effect of initial steam condensation on color changes of potatoes during drying in superheated steam. In *Proceedings of the 13th international drying symposium* (Vol. B, pp. 1352–1359). Beijing, China.

Makowski, M., Cenkowski, S., Hatcher, D. W., Dexter, J. E., & Edwards, N. M. (2003). The effect of superheated-steam dehydration kinetics on textural properties of Asian noodles. *Transactions of the American Society of Agricultural Engineers, 46*, 389–395.

Marshall, W. E., Wadsworth, J. I., Verma, L. R., & Velupillai, L. (1993). Determining the degree of gelatinization in parboiled rice: comparison of a subjective and an objective method. *Cereal Chemistry, 70*, 226–230.

Normand, F. L., & Mashall, W. E. (1989). Differential scanning calorimetry of whole grain milled rice and milled rice and milled rice flour. *Cereal Chemistry, 66*(4), 317–320.

Taechapairoj, C., Prachayawarakorn, S., & Soponronnarit, S. (2003). Superheated steam fluidized bed paddy drying. *Journal of Food Engineering, 58*, 67–73.

Taechapairoj, C., Prachayawarakorn, S., & Soponronnarit, S. (2004). Characteristics of rice dried in superheated-steam fluidized-bed. *Drying Technology, 22*(4), 719–743.

Tang, Z., & Cenkowski, S. (2000). Dehydration dynamics of potatoes in superheated steam and hot air. *Canadian Agricultural Engineering, 42*, 43–49.

Tatermoto, Y., Mawatari, Y., Sakurai, K., Noda, K. & Komatsu, N. (2002). Drying characteristics of pours material in superheated steam fluidized bed. In *Proceedings of the 13th international drying symposium* (Vol. A, pp. 624–633), Beijing, China.

Drying Technology, 24: 65–75, 2006
Copyright © 2006 Taylor & Francis Group, LLC
ISSN: 0737-3937 print/1532-2300 online
DOI: 10.1080/07373930500538717

Taylor & Francis
Taylor & Francis Group

Effects of Peeled and Unpeeled Garlic Cloves on the Changes of Drying Rate and Quality

Somkiat Prachayawarakorn[1], Narongsak Kaewnin[2], Adisak Nathakaranakule[2], and Somchart Soponronnarit[2]

[1]*Faculty of Engineering, Thonburi, Bangkok, Thailand*
[2]*School of Energy and Materials, King Mongkut's University of Technology, Thonburi, Bangkok, Thailand*

Reducing moisture content as fast as possible, together with minimizing loss of quality, is important to food processing. To reach these objectives, experimental investigations were conducted to examine the effects of both peeled and unpeeled garlic cloves as well as operating parameters such as temperature and superficial velocity on the drying rate and quality of dried product. Peel resistance to moisture diffusion is considerably dominated and yields the longer drying time. Drying at high temperature shows the shrinkage of garlic clove to be lower than that at low temperature, whereas the product color is browner and the sizes of produced pores as revealed by scanning electron microscope are larger. The loss of volatile oil is insignificantly different among low- and high-temperature drying. The peel effect exhibits negative results on the product color, giving lower luminosity than the peeled sample, in particular at low temperature, because of longer drying time.

Keywords Dehydration; Garlic; Shrinkage; Volatile oil

INTRODUCTION

Garlic (*Allium sativum* L.), one of the most important *Allium* species, is well known in folk medicine for prevention of stroke and coronary thrombosis[1] and is commonly used as a primary ingredient in food formulations and a flavoring agent. The flavor, mainly containing sulphur aromatic volatiles, is produced when garlic cloves are disrupted, enabling alliinase enzyme to come in contact with alliin.[2,3] With this enzymatic reaction, the alliin is converted to 2-propenyl-2-propenethiol-sulphinate and eventually decompose to disulfides and thiosulfinates. The diallyl disulfide has been identified as the main component in garlic oil.[4]

Garlic after harvesting contains a large amount of water with an approximately 1.8–2.0 g water/g dry matter and the considerable loss in quantity, due to infection of microorganisms, is unavoidable. The garlic, with high moisture, will also quickly sprout if the environmental condition is suitable. When this event takes place, the nutritional qualities of garlic become degradable, besides the loss of commercial value. To eradicate such problems, drying is therefore needed. Drying is an important food process that causes the physical and chemical changes of products, such as in the physical properties, i.e., color, shrinkage, microstructure, and the quality of products.[5–7] Garlic is a biological material that is very sensitive to heat, and when dried, the volatile oil in the garlic is lost, consequently reducing the flavor intensity.[8,9] This may degrade the quality of dried garlic. Therefore, choice of drying condition to obtain high-end product quality is an important issue to investigate in the present work. In addition, the physical pretreatment of garlic clove by eliminating peel before drying is another matter to explore to find how it affects the moisture diffusion rate and the subsequent qualities compared to no pretreatment, which is commonly practiced in factory. The quality parameters of dried garlic cloves are characterized by color, volatile oil, and shrinkage. The microstructure of the dried garlic tissue is also examined. In addition, the series diffusion model, describing the transport of water through two composite layers, garlic tissue and peel, is developed to determine their effective diffusion coefficients.

Correspondence: Somkiat Prachayawarakorn, Faculty of Engineering, King Mongkut's University of Technology Thonburi, Suksawat 48 Road, Bangkok 10140, Thailand; E-mail: somkiat.pra@kmutt.ac.th

MATERIALS AND METHODS

Equipment

The experimental setup is schematically shown in Fig. 1. Ambient air, which is heated by electrical heater, flows with a constant mass flow rate through samples lying on a screen metal sheet within the drying chamber. The air speed could be changed by setting a frequency inverter connected with a 1/2 hp motor to drive a forward curved blade centrifugal

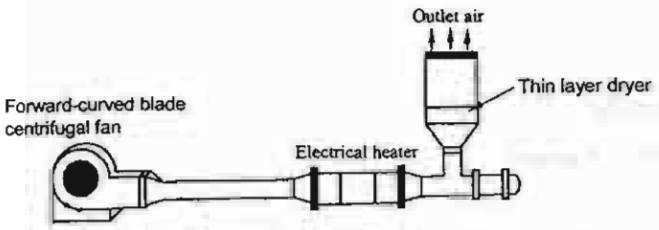


FIG. 1. Experimental thin-layer drying equipment.

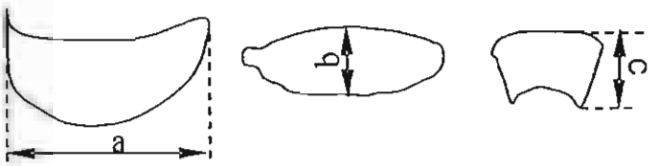


FIG. 2. Garlic clove dimension.

fan. A hot-wire anemometer, with a precision of ±0.1 m/s of reading, was used to measure the velocity. A PID-type controller was chosen for controlling heating system and the variation of inlet air temperature was in the range of ±1°C from the setting temperature. In the experiment, the temperature at different positions, i.e., dryer inlet, outlet, and grain, was measured by a K-type thermocouple connected with a Yogokawa data logger with an accuracy of ±1°C. To measure garlic temperature while being dried, the thermocouple was inserted into the middle position of the sample.

Drying

The dryer was operated at the three temperatures, 50, 60, and 70°C, and two air velocities, 0.7 and 1.7 m/s. The relative humidity of inlet air was not controlled in this study. Garlic bulbs obtained from local markets had a moisture content of 181–203% (dry basis). Before drying, the bulbs were manually cracked and the subsequent garlic cloves including the thin peel were obtained and divided into two groups in order to study the drying kinetics. The garlic cloves with peel were taken to dry immediately and another group was physically treated by peeling the shell before drying. Since the garlic clove was not a well-defined geometrical shape, the equivalent sphere diameter, calculated from its volume, was employed. The original size of the garlic cloves was given as a range of 12.9 to 13.6 mm. The moisture curve was determined by weighing the sample every hour during the early drying period, where the moisture content loosed rapidly, and every 5 h afterwards. In addition to moisture, shrinkage of garlic was measured. At the drying end, the samples were taken to determine moisture content using a hot air oven at temperature of 103°C,[10] volatile oil, and color, and also to characterize the microstructure of garlic tissue.

Shrinkage

To investigate the behavior of material shrinkage, the experiment was conducted separately from the drying experiment and the material shrinkage in this work was defined as the volume of material at time t divided by the volume at the beginning. The solid volume was obtained by measuring each garlic clove dimension, shown in Fig. 2, and then calculated by the following equation:

$$V = \frac{\pi}{6}(a \cdot b \cdot c) \tag{1}$$

where a is the longest intercept, b is the longest intercept normal to a, and c is the longest intercept normal to a and b. Five samples were measured and the average value was represented.

Color

A tristimulous colorimeter (Juki model JP-700), which could be specified by three coordinates in the color space, i.e., L-value, a-value, and b-value, was used to measure the product color. The L-value is a measure of lightness with a scale of 0 to 100, the a-value indicates the change of the color from green to red, and the b-value the change from blue to yellow, both latter indicators being in the scale of −60 to +60. Before measuring the sample, the colorimeter was examined with a standard pure white having Hunter values of 97.76 for L-value, −0.06 for a-value, and −0.31 for b-value.

Volatile Oil

The volatile oil content of garlic mainly consisting of sulphur compounds was determined by chloramine-T method.[11] Five grams of the finely ground sample (fresh and dried) was homogenized with water for 5 min, with a wait period of 30 min for fresh garlic and 60 min for dried garlic, in order to completely release the flavor. An aliquot of the slurry was distilled and oxidised by chloramine-T. The amount of excess chloramine-T in the experiment and the blank were determined. The volatile oil content in the samples was expressed as mg oil/g dry matter.

Microstructure

Samples of garlic cloves dried at different temperatures were taken to examine the microstructure. The samples were cut in cross section with sieve tubes using a sharp razor blade. The samples were then placed on adhesive tape attached to a circular aluminum specimen stub, followed by gold coating using a sputter-coater. The samples were finally viewed in a transmission electron microscope (Leica Cambridge Tld, model Stereosoan 206) at an accelerating voltage of 10 kV.

Mathematical Model of Drying Kinetics

Drying of porous media is a simultaneous process of heat and mass transfer and the models are written, based on energy and mass balance, to describe the transport process.[12,13] Under certain conditions, drying can be approximately treated as an isothermal process. In this case, the problem is reduced to a single differential equation, describing specifically the water transport inside porous solid. The transport of water in most agricultural products is governed by the diffusion and its change is simply described by Fick's second law of diffusion, where the expression for spherical shape is given by

$$\frac{\partial M}{\partial t} = D\left(\frac{\partial^2 M}{\partial r^2} + \frac{2}{r}\frac{\partial M}{\partial r}\right) \tag{2}$$

where the moisture content, M (dry basis decimal), is a function of both the radial coordinate, r (m), and drying time, t (s). The effective diffusivity, D (m^2/s), as a transport property of material, is a lumped parameter that is taken into account the several transport mechanisms, i.e., capillary, film flow, and vapor diffusion.

While material is being dehydrated, the physical change such as shrinkage causes the transport of water inside the porous solid to be changed, hence, the diffusivity.[14,15] To determine the effective diffusivity of the shrinkable material, the shrinkage effect must be included in the diffusion model and Eq. (2) is discretized by the finite difference method. In this work, the explicit method was used. Throughout the calculation, the volume of peeled garlic clove is divided into a constant number of elements, while the size of each element volume is changed following the shrinkage expression.

Since the garlic clove is a heterogeneous material consisting of peel and tissue, both of which are connected in series, the moisture transporting through each particular part may exhibit different characteristics of diffusion property, and the components of garlic are modeled as concentric layers of materials as shown in Fig. 3. Equation (2) is applied for predicting the moisture change in the tissue ($0 < r < R_1$) and the peel ($R_1 < r < R_2$) where the corresponding D_t and D_p present the effective moisture diffusion in the tissue and peel, respectively.

First Falling Rate Period

Kinetics of the garlic drying can be divided into two drying periods, namely first and second falling rate periods. At the first falling rate period, the evaporation of water always occurs near the material surface and the moisture removal rate depends on air velocity, temperature, and water concentration between the surface and air stream. At this period, the drying rate of garlic clove at any time t is decreased and can simply be calculated from the mass flux at the surface, which is expressed by

$$D_p \left.\frac{\partial M}{\partial r}\right|_{r=R_2} = k(M|_{r=R_2} - M_{eq}) \qquad t > 0 \tag{3}$$

where k is the experimentally determined drying constant (m/s), R_2 is the radius of garlic clove (m), and M_{eq} is the equilibrium moisture content. The thickness of peel measured by a digital micrometer was approximately 96 μm. To predict the moisture change from Eq. (2), it is also

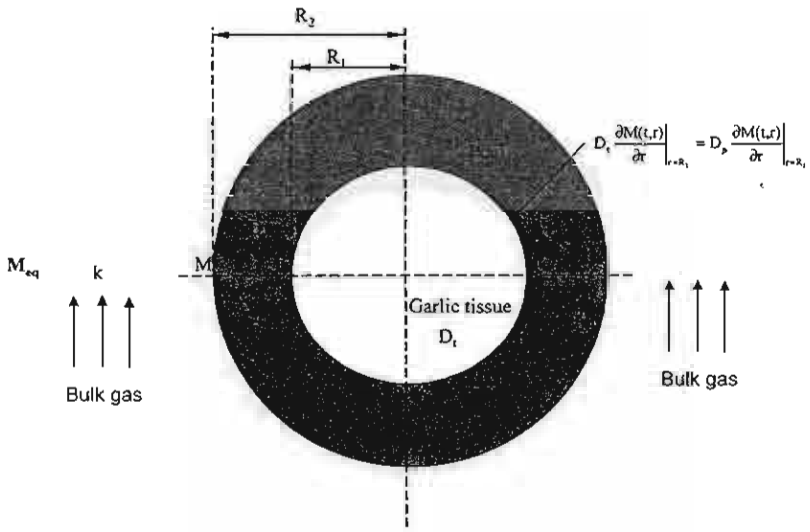


FIG. 3. Schematic diagram of idealized model of garlic clove with peel surrounded with gaseous film.

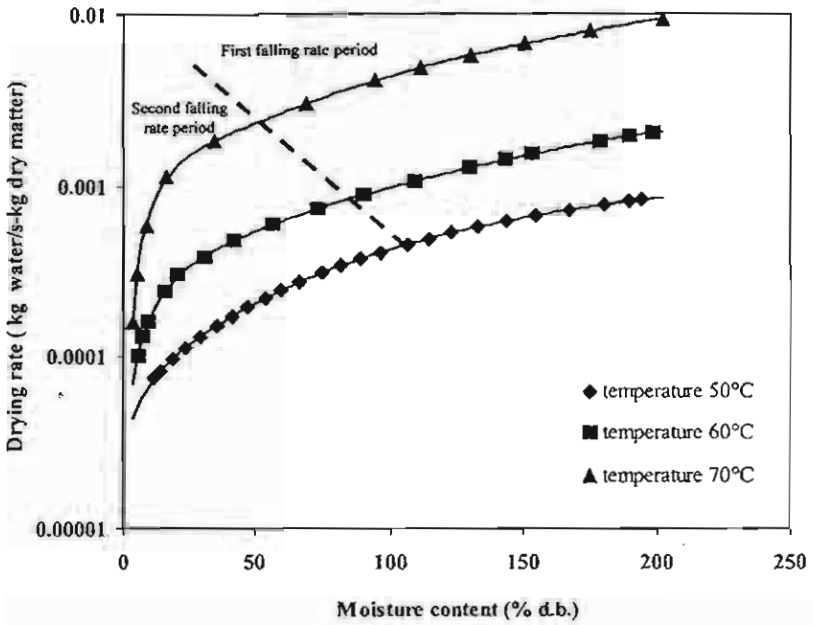


FIG. 4. Drying rate of peeled garlic clove as functions of moisture content and drying temperature (superficial velocity of 0.7 m/s).

assumed that the moisture content throughout the size range is spatially uniform at the beginning and the moisture gradient at the center is zero at $t > 0$.

Second Falling Rate Period

When moisture content reaches a certain level, the drying kinetics fall to the second falling rate period, characterizing the nonlinear drop of rate with moisture content, as will be shown in Fig. 4. At this period, we assume that the surface moisture equilibrates with the environmental drying condition and the moisture transport is governed by pure diffusion mechanism[16] and the following boundary condition is given by

$$M(R_2, t) = M_{eq} \qquad t > 0 \tag{4}$$

In addition to above-mentioned boundary conditions, another boundary is given at the interface between the innermost peel and outermost tissue by equating the mass flux of water diffusing through the tissue at any time to that diffusing through the peel.

$$D_t \left.\frac{\partial M(t,r)}{\partial r}\right|_{r=R_1} = D_p \left.\frac{\partial M(t,r)}{\partial r}\right|_{r=R_1} \qquad t > 0 \tag{5}$$

From the known moisture profile, the average moisture content of garlic clove is calculated by

$$\overline{M} = \frac{\int_0^{R_2} 4\pi r^2 M(r,t)dr}{V_p} \tag{6}$$

where $\overline{M}$ is the average moisture content and V_p is the particle volume (m^3).

The behaviour of garlic clove shrinkage during dehydration is explained by the following exponential equation:

$$\frac{V}{V_0} = a \exp\left(-b\frac{\overline{M}}{M_{in}}\right) \tag{7}$$

where V is the particle volume (m^3) at moisture M, with subscript 0 presenting the volume at the beginning. The constant parameters of a and b are obtained by the statistical fit with experimental data using a linear regression method.

When garlic clove is peeled, its drying process can be mathematically described by accounting for the moisture diffusion in the garlic tissue and the water vapor in gaseous film surrounding the garlic clove. Equation (2), together with the boundary conditions (Eqs. (3–4)), were used to determine the effective diffusivity of garlic tissue, D_t, and drying constant, k. A trial-and-error approach was used to estimate the transport parameters, and the estimated parameters were supposed to be correct when the mean residual square of moisture content, MRS_M, was less than 0.002. MRS is generally defined as

$$\text{MRS} = \frac{\sum_{i=1}^{n} (\text{observed data} - \text{calculated data})^2}{n} \tag{8}$$

where n is the number of experimental data.

To determine D_p and k for drying garlic clove with peel, the aforementioned calculation procedure, with an

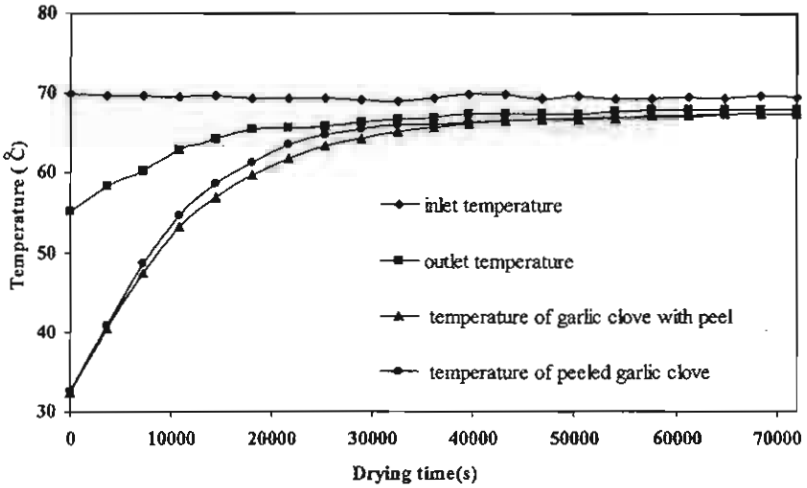


FIG. 5. Evolution of temperatures in thin-layer drying system (inlet air temperature of 70°C and superficial velocity of 0.7 m/s).

additional Eq. (5), was used. In this calculation step, D_t was already known.

RESULTS AND DISCUSSION

Temperature Change in Drying System

Temperature at several positions in the thin-layer dryer was recorded during the experiments and their changes are illustrated in Fig. 5, in which the operating parameters were controlled at the inlet-air temperature of 70°C and the superficial velocity of 0.7 m/s. The temperatures of the garlic cloves with and without peels were initially at 32°C and were increased by a different rate; the increase of the peeled garlic temperature was slightly faster. When the time was elapsed for 8 h, the change of both product temperatures was not very sensitive as well as the product temperatures appeared closer together. The temperature of the materials kept constantly at the temperature of 66°C for the inlet temperature of 70°C. This clearly indicates that the heat transfer rate approaches the equilibrium state faster than the moisture transfer rate.

Moisture Change

Some experimental results of moisture change of garlic clove at temperatures of 50, 60, and 70°C are shown in Fig. 6, indicating that increasing the drying temperature

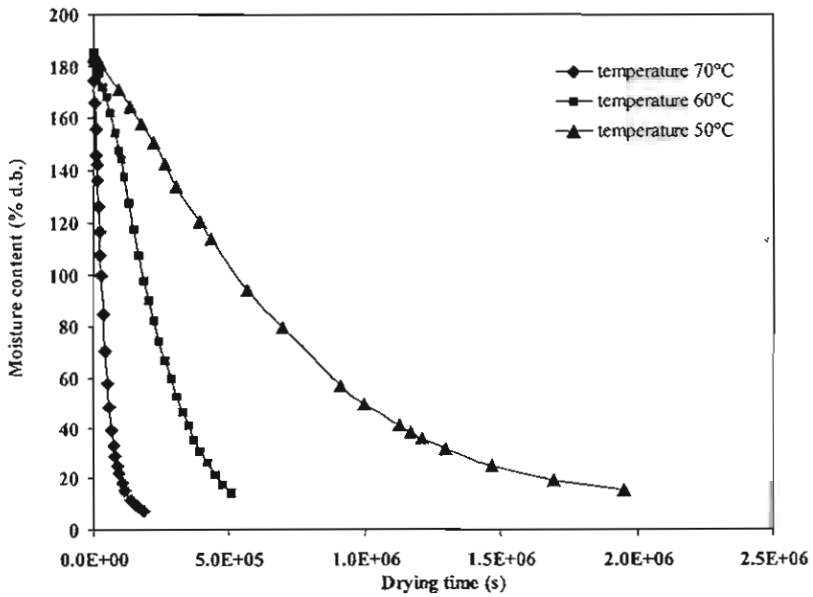


FIG. 6. Moisture change of garlic clove with peel at different temperatures (superficial velocity of 0.7 m/s).

causes an important increase in the drying rate. Drying garlic clove at a temperature of 50°C can not obtain the moisture content of finished product required at 5% dry basis. At this drying temperature, the moisture content of dried garlic, as observed from the drying curve, equilibrates with the flowing air at 19.2% dry basis. To reach the required moisture content of product, the higher temperature of 60°C is needed.

Figure 4 illustrates the drying rates as functions of moisture content and temperature. Each drying rate curve presented was obtained by differentiating the suitable empirical equation with respect to time. The suitable form that predicted the moisture change was in exponential relation as indicated by R^2, of which the value obtained from fitting was given above 0.98 for each experiment. As can be seen in Fig. 4, it appears that two well-defined drying zones where the linear decrease of drying rate followed with nonlinearity behavior with moisture content are found. These drying rate curves also suggest that drying at high temperature provides more potential capability to remove moisture than that at low temperature and the drying efficiency is possibly improved because the enhanced removal rate is more compensated than the energy consumed: drying rate at 70°C increases approximately 10 times of that at 50°C at the remaining moisture content above 50% dry basis, whereas the drying temperature used increases only 1.4 times. At the lower moisture content, however, the use of high temperature may not get potential benefit since the drying rate is not largely different among low and high temperature.

TABLE 1
Pseudo-critical moisture content of garlic at different operating parameters

Temperature (°C)	Air velocity (m/s)	Pseudo-critical moisture content (% dry basis)	
		Unpeeled garlic clove	Peeled garlic clove
50	0.7	123	120
	1.7	121	118
60	0.7	109	98
	1.7	107	95
70	0.7	69	58
	1.7	67	58

It is also shown in Fig. 4 that the moisture content at which the drying rate changes from linear to nonlinear is pseudo-critical moisture content in this work and this value is relied on the drying condition. Table 1 presents the pseudo-critical moisture content of unpeeled and peeled garlic cloves, indicating the dependence of pseudo-critical moisture content upon the drying temperature and characteristics of garlic clove, the first factor playing more important role, whereas it is independent on velocity.

Drying Constant

The drying constants estimated from the first falling rate period for the peeled and unpeeled garlic cloves are shown in Fig. 7 and the result indicates that the drying constant

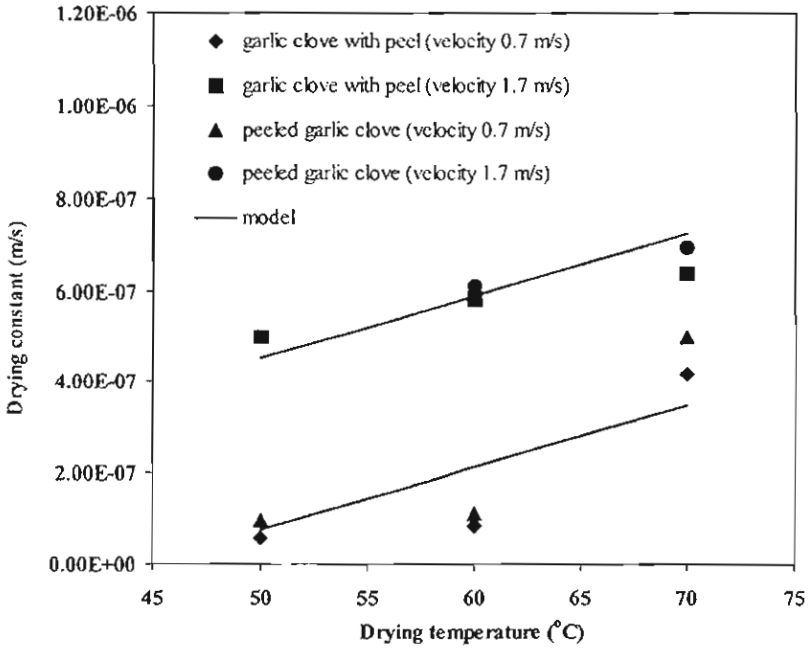


FIG. 7. Change of drying constants as functions of drying temperature and air velocity.

increases as the superficial velocity and temperature increase, whereas it is not affected by surface characteristics (peeled and unpeeled garlic cloves). Correlation of the drying constant to the involved parameters is thus given by

$$k = -2.87 \times 10^{-5} + 4.20 \times 10^{-6} V^{0.100} + 8.65 \times 10^{-6} T^{0.182} \quad (9)$$

where V is the superficial velocity (m/s) and T is the drying temperature (K). R^2 and MRS_k of the drying constant obtained from the statistical fitting of Eq. (9) are 0.90 and 5.2×10^{-15}, respectively, implying the suitability of proposed equation in predicting the drying constant at condition studied. The constant parameters in Eq. (9) indicate that the drying constant is rather more influenced by temperature than by the air velocity.

Effective Diffusivity

The effective diffusivity of moisture moving through the garlic tissue and the peel are shown in Fig. 8 and the values presented were estimated from the drying characteristic curve. The temperature renders a strong contribution to the effective diffusivity, where the higher effective moisture diffusivity is shown up as temperature is increased. As shown in Fig. 8, transport of water through the garlic clove with peel is governed by the peel resistance, of which the value of effective diffusivity is remarkably lower than that found in the garlic tissue. The dependence of moisture diffusivity on temperature is explained by a well-known Arrhenius relationship and the results from statistical fitting for the effective diffusivities of the garlic tissue and peel is expressed by

$$\text{Garlic tissue: } D_t = 6.97 \times 10^9 \exp\left(-\frac{131,221}{RT}\right) \quad (10)$$
$$R^2 = 0.99, \quad \mathrm{MRS}_{D_t} = 3.6 \times 10^{-24}$$

$$\text{Peel: } D_p = 1.47 \times 10^9 \exp\left(-\frac{133,671}{RT}\right) \quad (11)$$
$$R^2 = 0.98, \quad \mathrm{MRS}_{D_p} = 3.3 \times 10^{-25}$$

where R is the universal gas constant (kJ/kmol) and T is the absolute temperature (K). The calculations of effective diffusivities of moisture transporting through the garlic tissue and the subsequent garlic peel using the respective Eqs. (10) and (11) agree well with the experiments, as shown by solid lines against the experimental data in Fig. 8. From the Arrhenius equation, it is also seen that the energy required for driving the moisture through the peel is slightly larger than through the tissue.

Shrinkage

When foods undergo volumetric changes during water loss, this is referred as shrinkage, which has a negative result for the quality of dehydrated product. These physical modifications, taking place continuously while material is being dried, influence the physical properties of the solids and the diffusive transport properties. The shrinkage of material is generated from a pressure unbalance between the inner material and the external pressure that leads to material shrinkage or collapse. Figure 9 shows the relation of shrinkage of garlic tissue to the remaining moisture content at temperatures, indicating that the size of garlic is rapidly and almost linearly reduced with moisture content at early period drying period and then followed with a slow

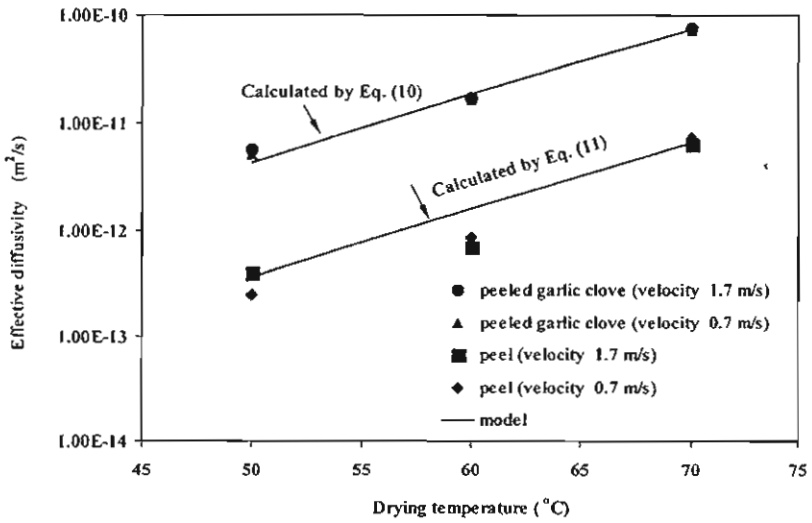


FIG. 8. Effective moisture diffusivities of garlic tissue and peel at temperatures.

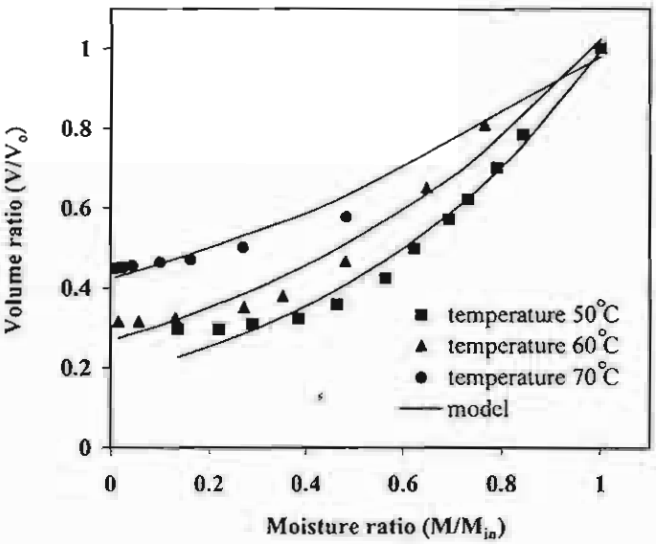


FIG. 9. Shrinkage behavior of garlic tissue during drying at different temperatures.

shrinking rate. The rapid decrease of size occurs while garlic has high moisture content, and tissue characteristics at this moisture level are rather soft. As the moisture content is decreased, the surface of garlic becomes more rigid, allowing the slower decrease of its size until no further shrinkage occurs, although the drying continues. This phenomenon was also found in some foods, i.e., potato and apple.[17,18]

It was found that the garlic dried at temperatures of 60 and 70°C possessed a rigid crust at the outer surface, whereas the outer surface was rather softer for drying garlic at temperature of 50°C. The difference of physical characteristics of dried garlic clove may produce different shrinkage rates, in which the shrinkage is relatively lower for drying garlic at high temperature than one dried at low temperature, as presented in Fig. 9. The lower shrinkage at higher temperature may possibly be attributed to the rigid crust formation at external garlic surface that fixes the volume of garlic.

The constant parameters in Eq. (7), a and b, were correlated with the temperature in the empirical forms, which are given by

$$a = 684171.98 \exp\left(-\frac{4907.86}{T}\right) \qquad (12)$$
$$R^2 = 0.99,\ \mathrm{MRS}_a = 0.0000225$$

$$b = 0.043884\mathrm{T} - 15.92 \quad R^2 = 0.99, \mathrm{MRS}_b = 0.000868 \qquad (13)$$

Equations (12) and (13) are limited to the temperature range of 50 to 70°C. The predictions from the proposed shrinkage model presented by solid lines in Fig. 9 show good agreements with the experimental ones. It is noted that the value of volume shrinkage ratio at the ratio of M/M_{in} equal to unity is, in fact, always unity, but the calculated values under the studied temperature range are slightly different from unity, with a maximum difference being 2.0% for a temperature of 70°C.

Validation of Moisture Content

The constant parameters for diffusive Eqs. (9), (10), and (11), together with shrinkage Eqs. (12) and (13), were used to calculate the moisture changes of the peeled and unpeeled garlic cloves at temperatures and the calculated results are shown in Fig. 10, indicating that the agreement between the experiments and simulations is good for a wide range of experimental conditions and the difference of moisture content between experiment and prediction at

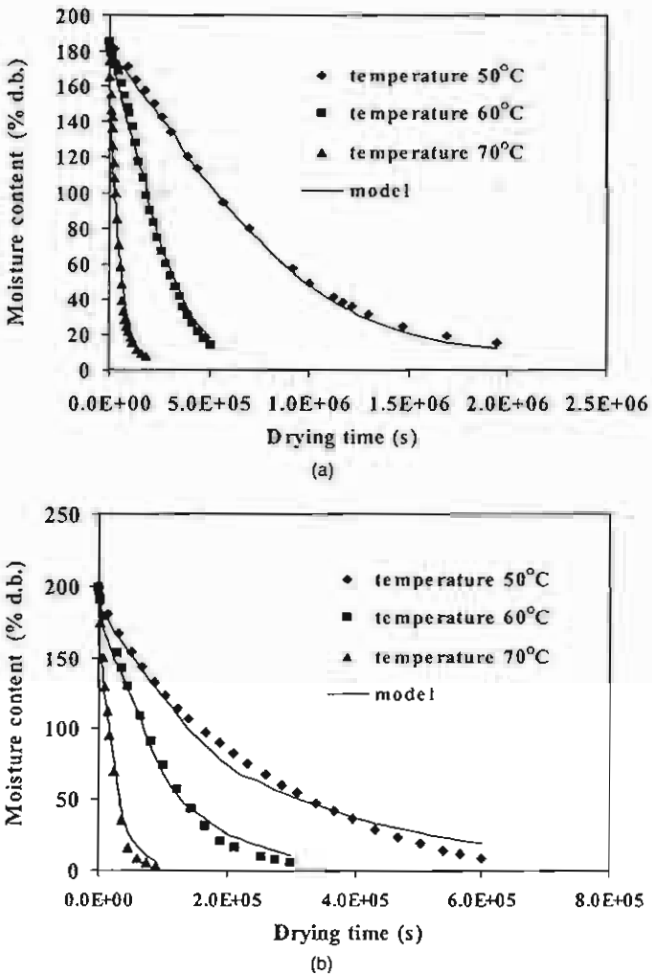


FIG. 10. Comparison of moisture content obtained from the experiments and prediction. (a) Garlic clove with peel and (b) peeled garlic clove.

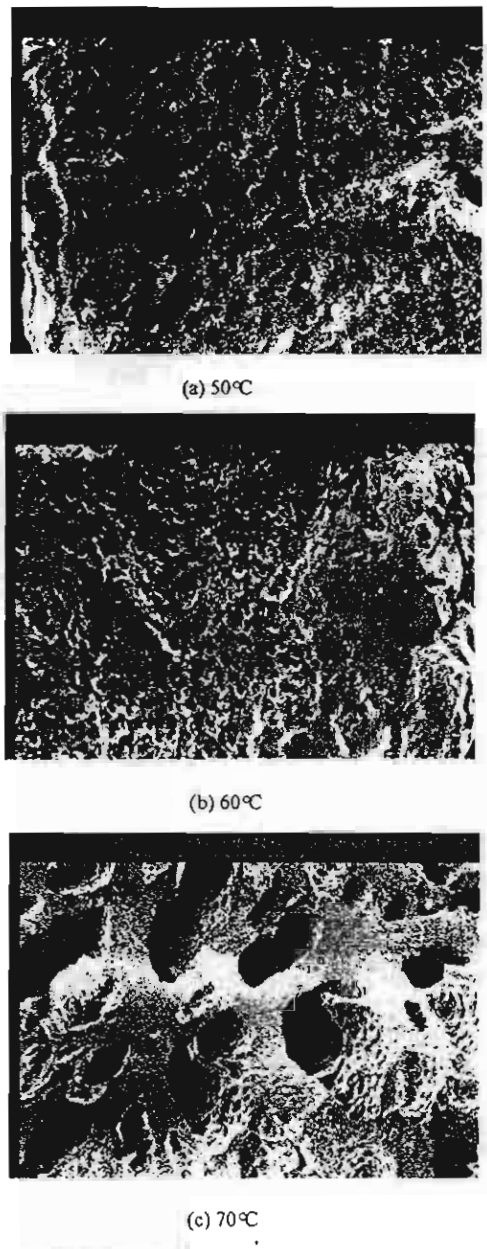
the drying end for each drying condition was less than 4%, except only for the peeled garlic clove dried at 50°C with the difference being up to 10%. Compared to the effect of peel on temperature development as illustrated in Fig. 5, the effect of peel on retarding the moisture movement is considerably more dominant. Particularly, when the garlic was dried at temperature of 50°C, the time employed for drying garlic clove takes much longer than the peeled one: for example, requiring the drying time of 470 min for the unpeeled garlic clove and of 167 min for the peeled garlic clove in reducing moisture content from 180–200% dry basis to 19.2% dry basis.

Morphology of Dried Garlic

Different drying conditions may produce diverse structures of material. Figure 11 shows modifications of garlic tissue in the course of drying at temperatures of 50, 60, and 70°C. A small number of pores, with small sizes, are formed at the temperature of 50°C and the pore sizes, along with degree of porosity, are increased as temperature is increased. According to the SEM photographs, such pore formation is possibly induced by moisture stresses developed during drying, with larger moisture stresses as the rate of drying is accelerated. The larger stresses generally result in larger decrease of pasta size.[19] For the garlic drying, however, the smaller decrease of the size, when the moisture removal rate became faster, was found. This is because at higher temperature, the rigidity of the external surface exists and the volume of the sample becomes fixed, and it can thus withstand the moisture-induced stress forces, yielding a reduced degree of shrinkage.

Color

Figure 12 shows L-, a-, and b-values of garlic cloves with and without peels dried at different temperatures and the samples taken to examine the color had final moisture content of 19% dry basis for garlic dried at 50°C and 5% dry basis for the drying temperatures of 60 and 70°C. Garlic initially possesses creamy white color as interpreted by L-value ranging from 67.5 to 67.6, a-value ranging from -3.3 to -3.4, and b-value ranging from 11.3 to 11.7. As the garlic was thermally dried, the L-, a-, and b-values changed dissimilar ways, in which the L-value was decreased while the a- and b-values were increased. The change in their values in such direction implies the color of garlic becoming brown, with least degree of browning being at 50°C and increasing with higher temperature. At a temperature of 60 or 70°C, however, the dried garlic color is insignificantly different as indicated by the L-, a-, and b-values in which the value of each Hunter parameter of the finished product is almost equal. In addition, the color of product obtained by drying garlic with and without peels is not different. On the contrary, the effect of peel on the color of garlic is evident for drying at temperature of 50°C, especially for the L-value,



(a) 50°C

(b) 60°C

(c) 70°C

FIG. 11. Morphology of peeled garlic clove dried at different temperatures.

which shows 61 for the garlic clove and 52 for the peeled one, the lower value presenting the darker color. The darker color of unpeeled garlic clove is due to slower drying rate compared to that of the peeled sample, resulting in longer drying time. From Fig. 12 it can be seen that because of the wrinkles and roughness on the shrunken surface, there is a deviation of measuring the color of samples, indicated by the error bar, and the deviation becomes smaller when the powdered garlic is employed.[5]

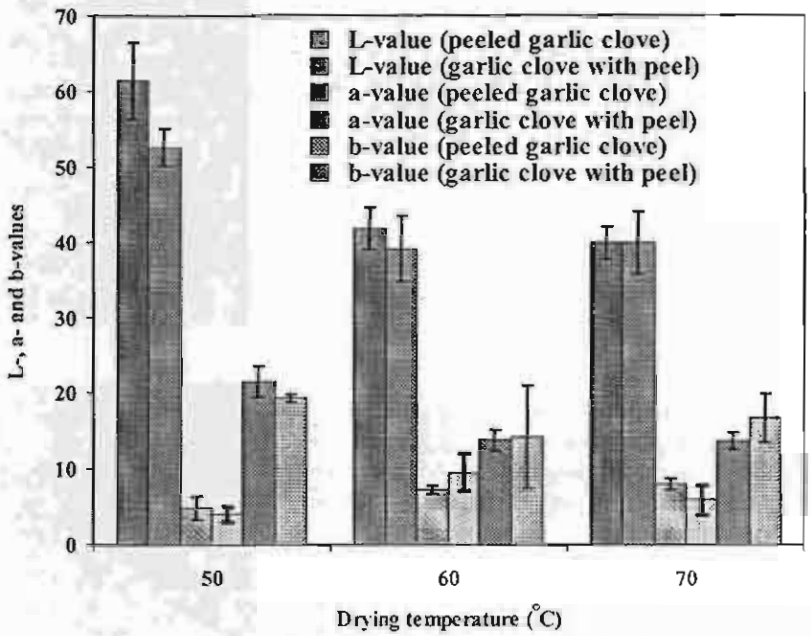


FIG. 12. Comparison of color of garlic with and without peel dried at different temperatures.

Volatile Oil

From the view points of color quality of the finished product and moisture reduction, garlic clove should be peeled before drying. Further examination was made with the peeled garlic clove by evaluating the loss of volatile oil content. Total volatile oil content of raw garlic ranges between 7.2 and 10.8 mg oil/g dry matter and the loss of volatile oil content after drying at different conditions is summarized in Table 2. The loss of volatile oil is not very different for samples dried at low or high temperature.

TABLE 2
Volatile oil content of peeled garlic cloves dried at different operating conditions

Temperature (°C)	Superficial velocity (m/s)	Volatile oil (mg oil/g dry matter) Before drying	After drying	% Loss
50	0.7	10.8	2.7	75
	1.7	7.2	1.5	79
60	0.7	9.6	3.3	65
	1.7	10.7	3.4	68
70	0.7	9.6	2.8	71
	1.7	10.6	3.2	70

CONCLUSIONS

Drying of unpeeled and peeled garlic cloves exhibited a linear reduction in water removal rate to moisture content at the early period of drying, followed by a nonlinear decrease. The effective diffusivity of garlic tissue and peel showed the drying rate of garlic clove to be limited by the peel resistance, giving lower drying rate of garlic clove with peel than that of the peeled one. Drying at high temperature provides the advantage of lower shrinkage compared to low-temperature drying, while disadvantageously producing browner and larger damage of garlic tissue, which is characterized by large pore sizes. It is recommended that garlic cloves should be peeled before drying and further tests indicated that the loss of volatile oil of peeled samples was not different among the samples dried at low or high temperature.

ACKNOWLEDGEMENTS

The authors thank King Mongkut's University of Technology Thonburi and The Thailand Research Fund for their financial support.

REFERENCES

1. Block, E.; Ahmad, S.; Catalfamo, J.L.; Jain, M.K.; Apitz-Castro, R. Antithrombotic organosulfur compounds from garlic: Structure, mechanic and synthetic studies. Journal of the American Chemical Society **1986**, *108*, 7045–7055.

2. Schwimmer, S.; Weston, W.J. Enzymatic development of pyruvic in onion as measure of pungency. Journal of Agricultural Food Chemistry **1961**, *9*, 301–304.
3. Brodnitz, M.H.; Pascale, J.V.; van Derslice, L. Flavour components of garlic extract. Journal of Agricultural Food Chemistry **1971**, *19*, 273–275.
4. Teleky-Vamossy, G.; Petro-Turza, M. Evaluation of odour intensity versus concentration of natural garlic oil and some of its individual aroma compounds. Die nahrung **1986**, *30*, 775–782.
5. Cui, Z.W.; Xu, S.Y.; Sun, D.W. Dehydration of garlic slices by combined microwave-vacuum and air drying. Drying Technology **2003**, *21*, 1173–1184.
6. Lewicki, P.P.; Pawlak, G. Effect of drying on microstructure of plant tissue. Drying Technology **2003**, *21*, 657–683.
7. Senadeera, W.; Bhandari, B.R.; Young, G.; Wijesinghe, B. Influence of shapes of selected vegetable materials on drying kinetics during fluidized bed drying. Journal of Food Engineering **2003**, *58*, 277–283.
8. Pezzutti, A.; Crapiste, G.H. Sorptional equilibrium and drying characteristics of garlic. Journal of Food Engineering **1997**, *31*, 113–123.
9. Sharma, G.P.; Prasad, S. Drying of garlic (*Allium sativum*) cloves by microwave-hot air combination. Journal of Food Engineering **2001**, *50*, 99–105.
10. AOAC. *AOAC Official Methods of Analysis: Association of Official Analytical Chemists*. 15th Ed; Washington, DC. 1995.
11. Shankaranarayana, M.L.; Abraham, K.O.; Raghavan, B.; Natarajan, C.P. Determination of flavour strength in alliums (onion and garlic). Indian Food Packer **1981**, *35*, 3–8.
12. Rovedo, C.O.; Suarez, C.; Viollaz, P. Analysis of moisture profiles, mass Biot number and driving forces during drying of potato slabs. Journal of Food Engineering **1998**, *36*, 211–231.
13. Dufour, P.; Blanc, D.; Tiure, Y.; Laurent, P. Infrared drying process of an experimental water painting: Model predictive control. Drying Technology **2004**, *22*, 269–284.
14. Hernández, J.A.; Pavón, G.; García, M.A. Analytical solution of mass transfer equation considering shrinkage for modelling food-drying kinetics. Journal of Food Engineering **2000**, *45*, 1–10.
15. Báez-González, J.G.; Pérez-Alonso, C.; Beristain, C.I.; Vernon-Carter, E.J.; Vizcarra-Mendoza, M.G. Effective moisture diffusivity in biopolymer drops by regular regime theory. Food Hydrocolloids **2004**, *18*, 325–333.
16. Belhamri, A. Characterization of the first falling rate period during drying of a porous material. Drying Technology **2003**, *21*, 1235–1252.
17. Lozano, J.E.; Rotstein, E.; Urbicain, M.J. Shrinkage, porosity and bulk density of foodstuffs at changing moisture contents. Journal of Food Science **1983**, *48*, 1497–1502, 1553.
18. Ratti, C. Shrinkage during drying of Food stuffs. Journal of Food Engineering **1994**, *23*, 91–105.
19. Willis, B.; Okos, M.; Campanella, O. Effects of glass transition on stress development during drying of a shrinking food system. In *Proceedings of the Sixth Conference of Food Engineering (CoFE'99)* Dallas, TX, 1999: 496–

Available online at www.sciencedirect.com
SCIENCE DIRECT
LWT 39 (2006) 770–778
LWT
www.elsevier.com/locate/lwt

Heating process of soybean using hot-air and superheated-steam fluidized-bed dryers

Somkiat Prachayawarakorn[a,*], Paveena Prachayawasin[a], Somchart Soponronnarit[b]

[a]Department of Chemical Engineering, King Mongkut's University of Technology Thonburi, Suksawat 48 Road, Bangkok 10140, Thailand
[b]School of Energy and Materials, King Mongkut's University of Technology Thonburi, Suksawat 48 Road, Bangkok 10140, Thailand

Received 7 December 2004; received in revised form 24 May 2005; accepted 24 May 2005

Abstract

The present work investigated drying characteristics and inactivation of urease in soybean dried by superheated-steam and hot-air fluidized beds. The value of effective diffusion coefficient, which was determined by a method of slopes, was increased with increased drying temperature and increased moisture content. Furthermore, it depended on the type of heating medium, with higher moisture diffusion for soybean dried by hot air. Inactivation of the urease enzyme in both media showed difference in rate, in which the enzymatic inactivation was faster for soybean dried in superheated steam than in hot air. For the individual heating medium, the modified first-order reaction was adequately fitted to experimental data. The rate of inactivation was found to increase as the temperature and moisture content were increased. The urease enzyme was inactivated, along with maintaining protein solubility and lysine content being in standard range, as soybean was treated at a temperature between 135 and 150 °C for the hot air and the treatment temperature could be reduced to be lower than 135 °C by using superheated steam.
© 2005 Swiss Society of Food Science and Technology. Published by Elsevier Ltd. All rights reserved.

Keywords: Antinutritional factor; Drying; Fluidized bed; Superheated steam

1. Introduction

Full fat soybean, referred as soybean prior to oil extraction, is used as a feedstuff because of its high oil and high-quality protein contents. However, the presence of biologically active compounds in raw full fat soybean, such as trypsin inhibitors, haemagglutinins, lectins and saponins, limits the utilization of their nutritive values (Hensen, Flores, Tanksley, & Knabe, 1987; Liener, 1994), resulting in the compromised health and performance of nonruminants and immature ruminants. To eliminate or reduce antinutritional factors, heat treatment is needed. Different technological processes have been developed but all are based upon heating for a certain amount of time. Heat treatment methods frequently used are for example cooking, microwave treatment and roasting treatments (Hensen et al., 1987; Raghavan & Harper, 1974; Stewart, Raghavan, Orsat, & Golden, 2003). The present research is concentrating on roasting treatments. Roasting methods involve the treatment of soybean with a temperature varying between 110 and 170 °C (Cheong, 1997). There are many types of roasting technique such as rotary drum dryer, salt-bed roasting and conventional grain dryer. Most of these methods provide nonuniform cooking of soybean with uneven temperature distributions.

To improve temperature uniformity, fluidization is an alternative approach. With this technique, the heating fluid is forced through a bed of particles, with a sufficiently high flow rate that the lift force is counterbalanced with the weight of particles. This accordingly induces particles to suspend and simultaneously rotate in fluid stream, so that each particle in the bed intimately contacts with almost the same fluid temperature. While soybean kernels are being suspended, drying and inactivation of trypsin inhibitors

*Corresponding author. Tel.: +662427 0221; fax: +662428 3534.
E-mail address: somkiat.pra@kmutt.ac.th (S. Prachayawarakorn).

0023-6438/$30.00 © 2005 Swiss Society of Food Science and Technology. Published by Elsevier Ltd. All rights reserved.
doi:10.1016/j.lwt.2005.05.013

can take place simultaneously in the bed. Control of the fluidized-bed roasting for eliminating antinutritional factors in soybean is difficult since different variables, i.e. temperature, moisture content and time influence each other and are therefore difficult to separate independently (Osella, Gordo, González, Tosi, & Ré, 1997; Soponronnarit, Swasdisevi, Wetchacama, & Wutiwiwatchai, 2001). Thus, it is necessary to understand the involved parameters and their relationships in order to be able to control the roasting process effectively.

Air is commonly used as a drying medium. With hot air, the energy is largely consumed. There is a strong incentive to make the process more efficient. Superheated steam as drying medium is easier to get high energy efficiency than the hot air due to the possibility of reuse of the latent heat of evaporation (Berghel & Renström, 2002; Fitzpatrick, 1998). Fixed bed, fluidized bed, flash and impinging steam driers have been applied to dehydrate a variety of products including paddy, shrimp, sugar beet pulp and potato (Prachayawarakorn, Soponronnarit, Wetchagama, & Jaisut, 2002; Taechapairoj, Prachayawarakorn, & Soponronnarit, 2004; Tang & Cenkowski, 2000; Topin & Tadrist, 1997). Some of the agricultural products dried by superheated steam show better quality than ones dried by hot air, for example, paddy and shrimp, with higher head rice quality and less shrinkage, respectively.

This study is aimed at studying the drying rate and inactivation of antinutritional factors while soybean is treated by hot air and superheated steam. In addition, protein solubility of treated samples was determined.

2. Materials and methods

Raw soybean, with an initial moisture content of 135 g/kg dry matter was purchased from local market. The dry soybean was rewetted by adding the required amount of water to get the initial moisture contents of 19.5% and 135 g/kg dry matter. After rewetting, samples were kept in cold room at a temperature range between 8 and 10 °C for a week to allow water to penetrate into kernels. Before processing, the soybean samples were taken out of cold storage and left under environmental condition until grain temperature reached ambient temperature. It was noted that the use of the rewetted soybean in this study might be limited to its application for real drying situation since the diffusivity obtained from the drying curve of the rewetted soybean and of the freshly harvested soybean was different.

2.1. Equipments

Fig. 1 schematically shows a system of superheated-steam fluidized-bed dryer. The system consists of four main components, i.e. a boiler, a drying chamber with a dimension of 15 cm diameter and 100 cm height, an electrical fan and heaters. The designed system can alternatively use either hot air or superheated steam. Before treating soybean with superheated steam, the hot air at the same temperature as the desired level of superheated steam was initially employed for warming up the components until their temperatures reached the desired level. Hot air was initially used to prevent possible condensation of steam in the system. The saturated steam, generated from a small boiler at 106 kPa absolute pressure, was then entered into the system by opening a valve V1 and at the same time, the air was exhausted to atmosphere at valve V8. The saturated vapour was reheated at unit No. 2 containing 13.5 kW electrical heaters to change its state to superheated vapour. The velocity required for fluidizing kernels in the bed was accelerated by the backward curve blade electrical fan, with a 2.2 kW motor connected to a frequency inverter to precisely adjust the flow rate.

The superficial velocity flowing through particle bed was approximately 3.2 m/s. Upon exiting the drying chamber, the fluid was conveyed to a reverse flow cyclone where the superheated steam was conditioned fully reused, whereas the hot air was partially exhausted to the atmosphere while a portion was mixed with fresh air and reheated.

Soybean, with an amount of 1 kg corresponding to a 10 cm bed height, was treated with hot air and superheated steam at temperatures of 120, 135 and 150 °C. A

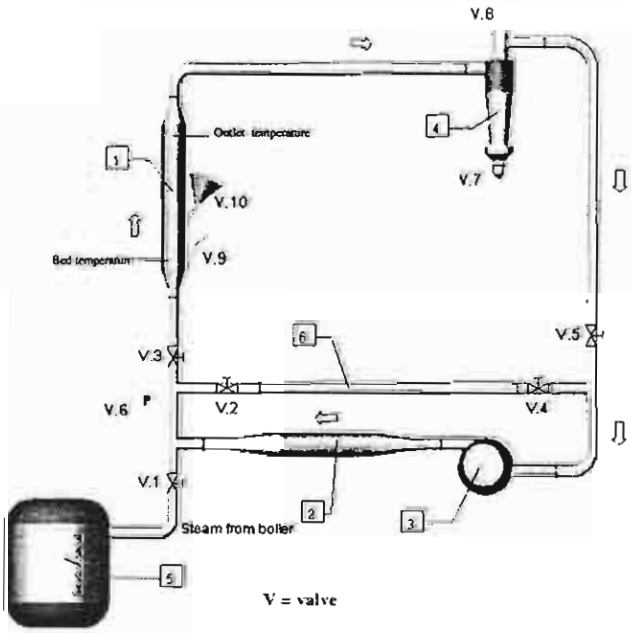


Fig. 1. Schematic diagram of superheated-steam fluidized-bed system: (1) fluidized-bed dryer, (2) heater unit, (3) fan, (4) cyclone, (5) boiler, (6) bypass line.

PID controller, with an accuracy of ±1 °C, was used to control the inlet temperature at desired level. The temperature at other two positions viz within bed and outlet of drying chamber was also monitored by inserting K-type thermocouples connected to a data logger (COMARK C8510), with an accuracy of reading ±1 °C. The temperature at positions in the system was measured every 30 s. Samples at the drying times of 2, 5, 7, 10 and 15 min were withdrawn from drying chamber at valve V9 to determine quantitatively the moisture content, urease activity, protein solubility and lysine content. After the sample was taken out of dryer at predetermined time, the new one was put into the dryer. The moisture content of soybean was determined by drying in an electrical oven at 103 °C for 72 h (ASA, 1990). An error in measuring moisture content by this method was less than 5%. Experiment for each drying condition was taken in replications and the average value was presented.

2.2. Urease activity measurement

Urease enzyme can be inactivated by heat treatment of soybean and its inactivation rate is similar to that of trypsin inhibitors (Baker & Mustakas, 1973; Osella et al., 1997). Hence, urease activity is practically used as a criterion for quality control of soybean meal. In this study, it was determined by Rasmussen's method (Rasmussen, 2002). The residual urease activity is expressed as the ratio of milliequivalents of ammonia produced from urea per gram of thermally treated soybean to that obtained from raw soybean. In uncooked soybean, ammonia was produced with an approximate value of 5 milliequivalents/g. The residual urease activity for adequately treated soybean is in the range of 10% and 20%. Below 10% indicates overheating.

2.3. Protein solubility measurement

Protein solubility is an important parameter of the feed meal industry which is used to characterize the quality of soybean after passing the heating process, in addition to determining trypsin inhibitors. Protein solubility was determined according to the AOCS method BA 10-63 (AOCS, 1979). This method involves the dispersion of proteins in 0.2% KOH solution. The protein solubility is defined as the ratio of nitrogen content in the supernatant after extraction with 0.2% KOH to total nitrogen content of the material. The total nitrogen content and the nitrogen content in the supernatant were determined by Kjeldahl method. The protein solubility required for feed meal should be in the range of 73–85% (ASA, 1990).

2.4. Lysine measurement

Lysine content in soybean was analysed by AccQ-Tag method (1993). The grounded soybean was hydrolysed by HCl solution at 110 °C for 22 h and was then derivatized with 6-aminoquinolyl-N-hydroxysuccinimidyl carbamate (AccQ-Flour reagent). The lysine content was determined by high-performance liquid chromatography.

2.5. Drying kinetics

Solid materials, when dried with superheated steam and hot air under the same inlet temperature, exhibit different phenomenological changes in rate of moisture removal. Difference in the moisture transport rate amongst both drying media is mostly explained by the temperature difference between the drying surface and drying medium (Schwartze & Bröcker, 2000; Sheikholeslami & Watkinson, 1992). This leads to different heat transfer rates, which may then influence the diffusivity as a parameter characterizing the internal structure and the nature of the solid.

In determining the effective diffusivity, it was assumed that soybean had a spherical shape and that Fick's equation for transient state, along with the initial and boundary conditions, can be solved analytically and expressed the solution as (Crank, 1975)

$$\frac{M(t)-M_{eq}}{M_{in}-M_{eq}}=\frac{6}{\pi^2}\sum_{n=1}^{\infty}\frac{1}{n^2}\exp\left(-\frac{n^2\pi^2D_{eff}t}{r^2}\right), \quad (1)$$

where D_{eff} is the effective diffusion coefficient (m^2/s), r is the particle radius (m), $M(t)$ is the moisture content of soybean at time t (decimal dry basis.), M_{in} is the initial moisture content, t is the drying time (s) and M_{eq} is the equilibrium moisture content. To obtain Eq. (1), it was assumed that gas-phase mass transfer resistance was negligible and the initial moisture content of soybean was uniform. At the present work, it was assumed that the equilibrium moisture content was nil since the kernel was contacted with a fluid at a temperature above 100 °C.

Several authors (Babalis & Belessiotis, 2004; Hebbar & Rastogi, 2001; Prachayawarakorn et al., 2002) used Eq. (1) to describe the diffusional flow of moisture inside the agricultural materials dried with various methods, i.e. infrared radiation, superheated steam and hot air. In their work, the effective diffusivity was determined by correlating the moisture data with Eq. (1) and then applying a nonlinear regression technique to estimate the diffusive parameter.

Because of nonlinearity of drying curves, a method of slopes was used to determine the effective diffusivity through which the moisture content of material was reduced under a given condition. Differentiation

of Eq. (1) with respect to time yields

$$\frac{dM(t)}{dt} = -\frac{6(M_{in} - M_{eq})D_{eff}}{r^2}\sum_{n=1}^{\infty}\exp\left(-\frac{n^2\pi^2 D_{eff}t}{r^2}\right). \quad (2)$$

The drying slope was established experimentally and replaced into Eq. (2) on the left-hand side. Accordingly, its effective value was estimated using the method of trial and error. Ten terms in Eq. (2) were sufficiently used for calculating the drying rate. A diameter of soybean in the experiments was approximately 6.4×10^{-3} m.

2.6. Thermal inactivation of urease enzyme

The apparent kinetics of urease inactivation in raw soybean were studied in a series of experiments by means of thermal treatment in the fluidized bed using superheated steam and hot air as described in Section 2.1. The thermal inactivation of urease follows the modified first-order reaction which is expressed by

$$\frac{C(t) - C_{eq}}{C_{in} - C_{eq}} = \exp(-kt), \quad (3)$$

where $C(t)$ is the residual urease activity at time t, C_{in} is the urease activity at the beginning, C_{eq} is the residual urease activity at infinite time, k is the apparent rate constant, min^{-1}, and t is the drying time, minute. Rewriting Eq. (3), it thus becomes

$$C(t) = (C_{in} - C_{eq})\exp(-kt) + C_{eq}, \quad (4)$$

where k and C_{eq} are obtained by the method of nonlinear regression when the residual urease activity is plotted against the treatment time and their values depend on both drying condition and drying medium. Relationships of k and C_{eq} with temperature and initial moisture content are explained by an empirical equation with constants determined by a nonlinear regression technique. The validity of the proposed equation is dictated by the coefficient of determination, R^2, and residual sum of square, RSS.

3. Results and discussions

3.1. Moisture reduction in superheated steam and hot air

Fig. 2 shows the changes of moisture content of soybean in superheated steam and hot air. In the experiments, soybean at initial moisture content of 135 g/kg dry matter were dried at a temperature of 135 °C and the experimental results show that the curve of moisture change in superheated-steam drying follows the same trend as found in hot air, except for the early period of drying at which soybean kernel gains in moisture content from the steam condensation. As found from the experiments, soybean adsorbed more moisture in low-temperature superheated steam than high-temperature superheated steam. The moisture contents of soybean in superheated steam at temperatures of 120, 135 and 150 °C were increased by 30, 19 and 6 g/kg dry matter, respectively, for the samples at initial moisture content of 13.5%. Tang and Cenkowski (2000) also found a similar result in which quantity of adsorbing condensed steam by potatoes was larger with lower temperature of superheated steam. These results may possibly suggest that the amount of condensed steam is reduced when using superheated steam at elevated temperatures.

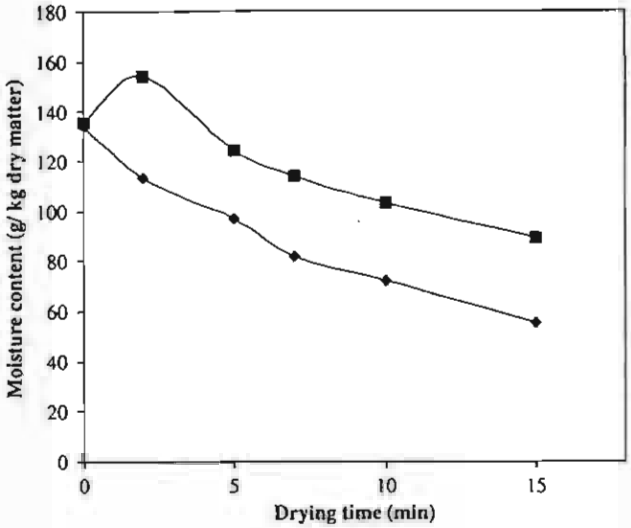


Fig. 2. Drying curves of soybean superheated-steam and hot-air fluidized bed (◆ Hot air_135 g/kg dry matter and 135 °C; ■ Superheated steam_135 g/kg dry matter and 135 °C).

During period of steam condensation, the superficial velocity flowing through the particle bed was dropped, and this caused insufficient speed to lift the particles. Consequently, bed of particles likely acted as a packed bed. This behaviour occurred for a very short period, approximately a half of minute of total drying time. After that, the bed of particles could be moved freely although the condensation period still existed, indicating decrease in the amount of condensed steam.

Difference in the behaviours between superheated steam and hot air reflects on the temperature within bed of particles where the bed temperature from the superheated-steam drying rapidly increased from room temperature to above 100 °C in a very short period, as shown in Fig. 3 for the temperature of 135 °C, whilst the bed temperature from the hot-air drying rose at a slower rate. However, when the drying extended for a longer period, the bed temperatures amongst superheated steam and hot air were not largely different.

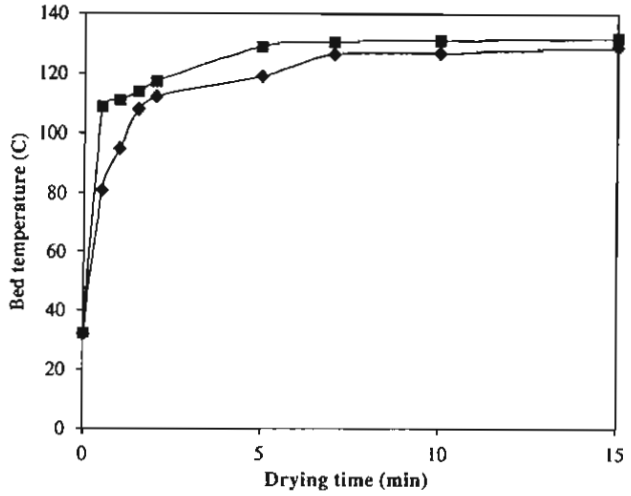


Fig. 3. Change of temperature within bed of soybean being fluidized by superheated steam and hot air (+ Hot air_135 g/kg dry matter and 135 °C; ● Superheated steam_135 g/kg dry matter and 135 °C).

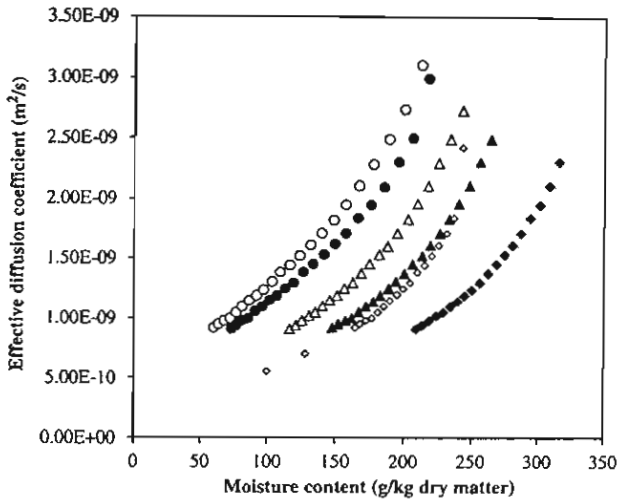


Fig. 4. Variation of effective diffusion coefficient with moisture content for soybean dried by superheated steam and hot air at temperatures (◆ Steam 120 °C; ▲ Steam 135 °C; ● Steam 150 °C; ◇ Air 120 °C; △ Air 135 °C; ○ Air 150 °C).

3.2. *Effective diffusion coefficient*

By applying Eq. (2) to the experimental drying curve, one notices that the effective diffusion coefficient varies with moisture content in a way that their values decrease with decrease in moisture content as illustrated in Fig. 4. The dependence of effective diffusion coefficient with moisture content was also reported by several workers (Azzous, Guizani, Jomaa, & Belghith, 2002; Koptyug et al., 2000; Pel, Brocken, & Kopinga, 1996).

In addition, the value of effective diffusion coefficient also relies upon the drying media in which soybean drying using hot air has higher moisture diffusion than one dried with superheated steam. As seen from this figure, difference of the value of effective diffusion coefficient obtained from superheated steam and hot air, throughout the reduced moisture range, is very large at temperature of 120 °C and the difference becomes smaller at elevated temperatures, the smallest one being at 150 °C.

The lower effective diffusion in the superheated steam was also found by several workers (Prachayawarakorn et al., 2002; Taechapairoj et al., 2004; Tang & Cenkowski, 2000). However, Tang and Cenkowski (2000) reported that under certain conditions, drying in the falling rate period is faster in superheated steam than in hot air.

3.3. *Inactivation of urease enzyme*

Soybean treated by superheated steam and hot air was withdrawn from the fluidized bed at different treatment times to determine the urease activity and the results are illustrated in Fig. 5, showing the variation of residual urease activity, for initial moisture contents of 135 and 195 g/kg dry matter, and soybean thermally treated by superheated steam and hot air at temperature of 120 °C. Insufficient inactivation is obvious with hot air for soybean at the initial moisture content of 135 g/kg dry matter for which the residual urease activity, shown in Fig. 5, remains steadily 40% although an extended period of drying time is applied. As the initial moisture content is increased to 195 g/kg dry matter, however, the sufficient inactivation is detected at a drying time of over 25 min.

In contrast to hot air, inactivation of urease enzyme can be achieved with superheated-steam temperature at 120 °C, to a level of residual activity below 20% for soybean with moisture contents of 135 and 195 g/kg dry matter heated for 7 and 5 min, respectively. The appearance of steam condensation on the kernel surfaces makes the bed temperature to be strikingly increased because of releasing heat from the steam condensation, which is more powerful than the heat from the hot-air convection, in particular at early period of time for the superheated steam and correspondingly stimulating the faster inactivation of urease enzyme.

Fig. 6 shows the apparent rate constant of urease inactivation, determined by fitting the experimental data to Eq. (4), under conditions of different initial moisture contents and inlet-steam temperatures. At each of the initial moisture content, the apparent rate constant in the superheated steam is higher than is in the hot air and the difference in their apparent rates becomes larger when the higher level of moisture is employed. As observed for these results, it can be seen that the temperature shows a strong contribution to inactivate the urease enzyme, as indicated by the steep slope of plotting the residual urease activity against the bed temperature, when soybean at any moisture level are treated with superheated steam or hot air. However, the temperature effect seems to be less pronounced for sample

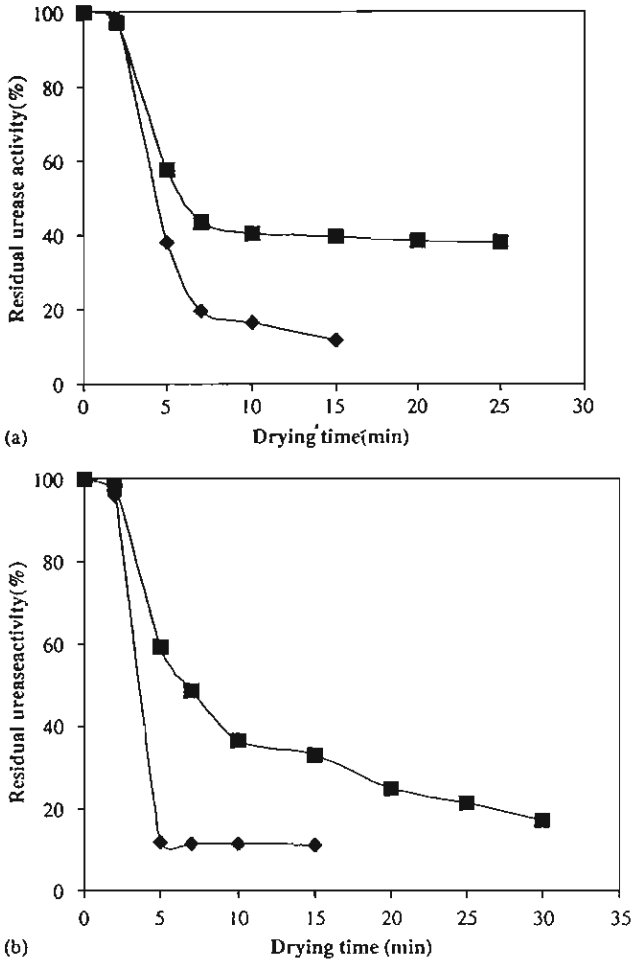


Fig. 5. Apparent kinetics of urease inactivation present in soybean during thermal treatments with superheated steam and hot air. (a) Min = 135 g/kg dry matter and (b) Min = 195 g/kg dry matter (← Superheated steam_120 °C; ● Hot air_120 °C).

at 360 g/kg dry matter treated with superheated steam: the value of inactivation rate constant increases slightly with temperature. This is perhaps because the prevalent contribution of moisture initially present in soybean induces the rapid inactivation in the first 2 min of drying, at which the residual urease activity lies between 15% and 17% for the temperature range studied.

The relationships of the apparent rate constant and equilibrium value with the relevant parameters i.e. bed temperature and initial moisture content, are given separately for each heating medium by the following empirical equations:

Hot air:

$$k = \left(-7.92 \times 10^{9} + 3.54 \times 10^{8} M_{in} + 2.086 \times 10^{7} T - \frac{1.224 \times 10^{8} M_{in}}{T} \right)$$

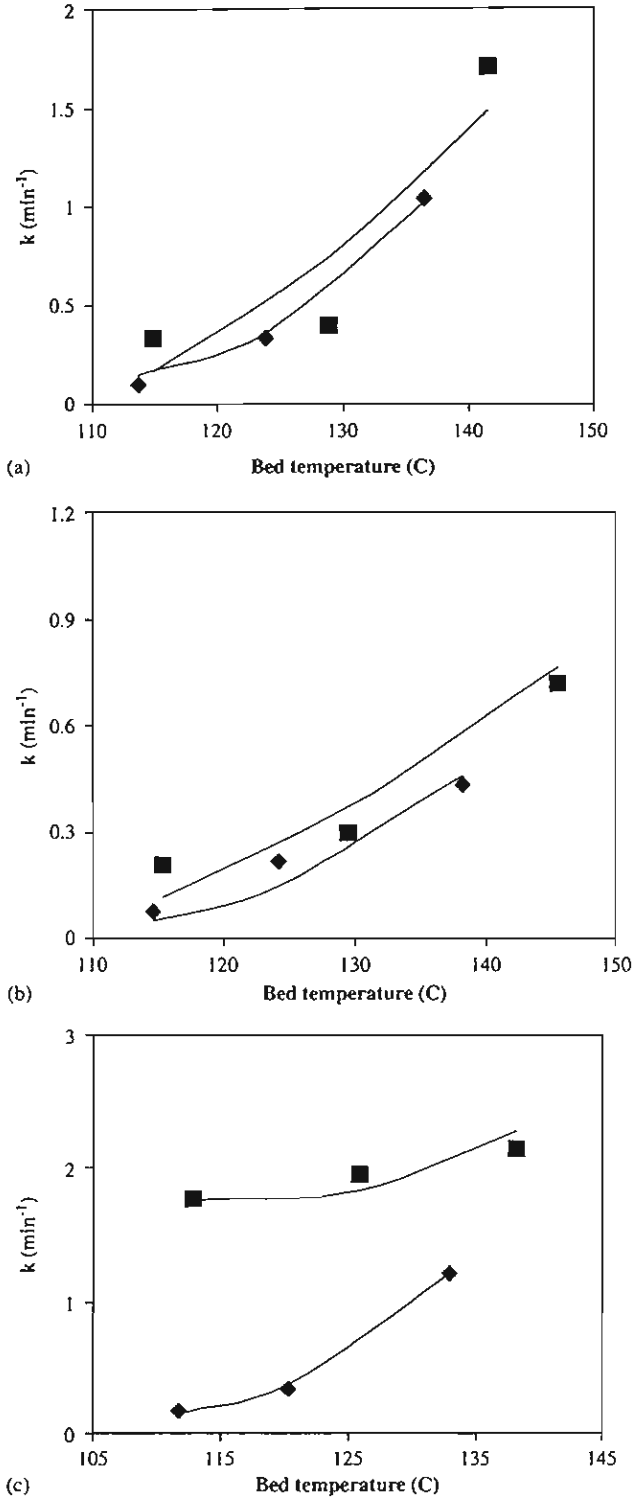


Fig. 6. Variation of apparent rate constant of urease inactivation with bed temperature for initial moisture content of (a) 135 g/kg dry matter, (b) 195 g/kg dry matter and (c) 360 g/kg dry matter (◆ Hot air; ■ Superheated steam; – Calculated).

$$\times\exp\left(-\frac{0.5526}{M_{in}}-\frac{6697.61}{T}-\frac{2392.2M_{in}}{T}\right),$$

$R^2 = 0.99$ and RSS = 0.079, (5)

$$C_{eq} = \left(6.67\times10^{-8}+5.0\times10^{-6}M_{in}^2+1.80\times10^{-11}T - 2.69\times10^{-11}M_{in}T\exp\left(\frac{0.740}{M_{in}}+\frac{5960.5}{T}\right)\right),$$

$R^2 = 0.85$ and RSS = 10.4. (6)

Superheated steam:

$$k = \left(-1.014\times10^{4}+0.075T^2-7.66\times10^{4}M_{in} +1.89\times10^{4}M_{in}^2+\frac{2.62\times10^{7}M_{in}}{T}\right) \times\exp\left(-\frac{0.5348}{M_{in}}-\frac{1507.5}{T}\right),$$

$R^2 = 0.95$ and RSS = 0.347, (7)

$$C_{eq} = (-0.047523+0.071742M_{in}^2+1.22\times10^{-4}T) \times\exp\left(-\frac{978.15M_{in}}{T}+\frac{3227.286}{T}\right),$$

$R^2 = 0.95$ and RSS = 1.47, (8)

where T is the bed temperature (K). The adequacy of the fitted models to predict the apparent rate constants throughout the operating conditions, for both steam and hot air, is presented in Fig. 6 by solid lines.

3.4. Protein solubility and amino lysine

In addition to antinutritional factors considered by feed meal industries, protein solubility and lysine content are also important because both qualities are detrimentally affected by thermal process. Overcooking of soybean can denature and insolubilize the protein, resulting in poor performance of poultry when the overcooked soybean are fed (Marsman Gruppen, van Zuilichem, Resink, & Voragen, 1995; Osella et al., 1997; Zhu, Riaz, & Lusas, 1996). Treated soybean samples that contained a urease activity below 20% were taken to examine the protein solubility and lysine content. Changes in protein solubility of soybean thermally treated by superheated steam and hot air at different temperatures are shown in Table 1. Raw soybean contains the lysine in the range of 2.9–3.1 mg/g soybean. When the soybean are thermally treated, quality parameters in terms of protein solubility and lysine content depend upon the treatment time, temperature and type of heating medium.

Soybean with an initial moisture content of 135 g/kg dry matter dried at the hot-air temperatures above 120 °C can have the urease enzyme inactivated within 5 min. At this temperature range, the protein solubility

Table 1
Protein solubility and lysine content of soybean treated with superheated steam and hot air at various temperatures

Temperature (°C)		M_{in} (g/kg dry matter)	Time(min)	$M(t)$ (g/kg dry matter)	Urease activity (%)	Protein solubility (%)	Lysine content (mg/g soybean)
		Raw soybean			100	94.28	2.9–3.1
Hot air	120	135	50	39.3	37	71.10	N/A
		195	30	69.8	19	70.98	3.0
		360	30	100.6	17	63.28	3.0
	135	135	5	97.2	15	78.68	3.1
		195	5	144.2	13	84.33	N/A
		360	5	237.2	12	85.19	N/A
			15	126.8	0	66.64	N/A
	150	135	5	82.1	10	74.17	2.8
		195	2	155.2	16	87.86	N/A
		360	5	207.4	10	76.83	N/A
			10	103.2	0	57.90	N/A
Superheated steam	120	135	7	139.5	16	85.66	2.8
		195	5	183.4	12	85.20	2.7
		360	2	389.5	13	80.59	N/A
	135	135	5	124.4	11	71.76	2.7
		195	5	165.2	9	82.25	2.7
		360	2	341.4	12	81.38	N/A
			15	147.0	0	59.51	N/A
	150	135	5	106.7	12	54.94	N/A
		195	2	189.4	11	83.84	N/A
			5	140.6	10	72.90	2.8
		360	2	316.1	11	75.13	N/A
			10	114.1	0	53.59	N/A

was in a range of 71–78%. Below 73%, protein solubility was unacceptable for the feed meal. The lysine was in the range of 2.8–3 mg/g soybean, which is above the standard requirement of 2.4 mg/g soybean.

For the superheated steam, the urease can be inactivated within the same period of time as the hot air. Under these treatment times, the protein solubility and the lysine fall to the respective ranges of 54.9–85% and 2.7–2.8 mg/g soybean. These results, for both superheated steam and hot air, show that the treatment temperature can be reduced when the heating medium is changed from hot air to superheated steam. The temperature of 120 °C can be effectively employed for the superheated steam whilst the temperature of 135 °C is a minimum required for hot air. Under the specified temperatures for both drying media, it is likely that soybean treated by superheated steam have a higher quality of protein solubility than those treated by hot air, due to faster heating rate and the corresponding shorter treating time.

When both drying media are introduced to treat soybean at an elevated moisture content, the results show that although the level of urease activity is in the acceptable range, using hot air at temperature of 120 °C is not recommended because of poor protein solubility whereas the protein solubility for the steam-treated soybean is beyond 80%. The increase of temperature for particular hot air shows positive results in which the higher protein solubility is clearly noticed and its quality is not very different from that obtained from treatment by superheated steam at temperature of 120 °C or higher. As can be seen in Table 1, even though the higher moisture content can eliminate the enzymatic activity in a short period of time and consequently improve the protein solubility, the moisture content of soybean does not reach an adequate level for storage. Under such situations, treatment requirements can be met at the initial moisture content up to 195 g/kg dry matter for which soybean should be treated with hot-air temperature of 135–150 °C or steam temperature of 120–135 °C. Beyond this moisture level (> 195 g/kg dry matter), two-stage drying, where the soybean is treated with superheated steam or hot air at such a temperature range for a certain time to inactivate the urease enzyme and then followed with low-temperature hot-air drying, should be applied, otherwise the soybean are over-cooked, as indicated by the lower protein solubility than the standard range which is between 73% and 85%.

According to these results, there are two practical approaches to treat the raw soybean for feed meal industries where the dry soybean is stored. The superheated-steam fluidized bed may suitably be applied to eliminate the antinutritional factors in dry soybean and the appropriate treatment temperature should be lower than 135 °C, preferably a temperature of 120 °C. To avoid the difficulty of operating the superheated steam system, hot air is an alternative method and in this case, the dry soybean should be added with a certain amount of water in order to accelerate the enzymatic inactivation before the large amount of protein insolubilization is developed. To achieve the high quality of treated soybean, the suitable initial moisture content for treating soybean with hot air should be kept below 200 g/kg dry matter and the temperature should be employed at a temperature higher than 135 °C.

4. Conclusions

Soybean when subjected to thermal treatments using different drying media exhibit different moisture transfer rate and inactivation of urease enzyme. The diffusional rate of moisture in soybean, as evaluated by effective diffusion coefficient, is relatively slower in the superheated steam than in the hot air, whereas the rate of enzymatic inactivation in the superheated steam, as evaluated by apparent inactivation rate constant of the modified first-order reaction, becomes faster. For each heating medium, the effective diffusion coefficient and inactivation rate constant are shown to be positively related to moisture content and temperature. To get rid of the urease enzyme present in soybean and simultaneously preserve its nutritional qualities, protein solubility and lysine content, fluidized-bed drying should be operated at temperature of 135–150 °C for the hot air and below 135 °C for the superheated steam. Under such temperature ranges, the superheated steam-type heating medium shows the protein solubility of treated sample to be higher than hot air when applied to the dry soybean. For the moist soybean, the types of heating medium do not impact on such quality since the urease enzyme is inactivated at a short period of time before the protein denaturation is largely formed.

Acknowledgements

The authors would like to thank the Thailand Research Fund for financially supporting this work.

References

AccQ-Tag Instruction Manual. (1993). Lysine determination. Manual no. WAT052874. Revo April.

American Oil Chemists' Society (AOCS). (1979). Protein solubility index. AOCS Official method BA 10-63: AOCS.

American Soybean Association (ASA). (1990). Fullfat Soybean *Handbook of American Soybean Association*, Singapore.

Azzous, A., Guizani, A., Jomaa, W., & Belghith, A. (2002). Moisture diffusivity and drying kinetics equation of convective drying of grapes. *Journal of Food Engineering, 55*, 323–330.

Babalis, S. T., & Belessiotis, V. G. (2004). Influence of the drying conditions on the drying constants and moisture diffusivity during

the thin-layer drying of figs. *Journal of Food Engineering, 65*, 449–458.

Baker, E. C., & Mustakas, G. C. (1973). Heat inactivation of trypsin inhibitor, lipoxgygenase and urease in soybean: Effect of acid and base additives. *Journal of The American Oil Chemists' Society, 50*, 137–141.

Berghel, J., & Renström, R. (2002). Basic design criteria and corresponding results performance of a pilot-scale fluidized superheated atmospheric condition steam dryer. *Biomass and Bioenergy, 23*, 103–112.

Cheong, Y. L. (1997). Fullfat soybean meal production and utilization. *Technical Bulletin of American Soybean Association*, Singapore. MITA (P) No. 044/11/96.

Crank, J. (1975). *The mathematics of diffusion* (2nd ed.). Oxford: Oxford University Press.

Fitzpatrick, J. (1998). Sludge processing by anaerobic digestion and superheated steam drying. *Water Research, 32*, 2897–2902.

Hebbar, U., & Rastogi, N. K. (2001). Mass transfer during infrared drying of cashew kernel. *Journal of Food Engineering, 47*, 1–5.

Hensen, B. C., Flores, E. S., Tanksley, T. D., Jr., & Knabe, D. A. (1987). Effect of different heat treatments during processing of soybean meal on nursery and growing pig performance. *Journal of Animal Science, 65*, 1283–1291.

Koptyug, I. V., Kabanikhin, S. I., Iskakov, K. T., Fenelonov, V. B., Khitrina, L. Yu., Sagdeev, R. Z., et al. (2000). A quantitative NMR imaging study of mass transport in porous solids during drying. *Chemical Engineering Science, 55*, 1559–1571.

Liener, I. E. (1994). Implications of antinutritional components in soybean foods. *Critical Reviews in Food Science and Nutrition, 34*, 31–67.

Marsman, G. J. P., Gruppen, H., van Zuilichem, D. J., Resink, J. W., & Voragen, A. G. J. (1995). The influences of screw configuration on the in vitro digestibility and protein solubility of soybean and rapeseed meals. *Journal of Food Engineering, 26*, 13–28.

Osella, C. A., Gordo, N. A., González, R. J., Tosi, E., & Ré, E. (1997). Soybean heat-treated using a fluidized bed. *Lebensmittel-Wissenschaft und-Technology, 30*, 676–680.

Pel, L., Brocken, H., & Kopinga, K. (1996). Determination of moisture diffusivity in porous media using moisture concentration profiles. *International Journal of Heat and Mass Transfer, 39*, 1273–1280.

Prachayawarakorn, S., Soponronnarit, S., Wetchagama, S., & Jaisut, D. (2002). Desorption isotherms and drying characteristics of shrimp in superheated steam and hot air. *Drying Technology, 20*, 669–684.

Raghavan, G. S. V., & Harper, J. M. (1974). Nutritive value of salt-bed roasted soybean for broiler chicks. *Poultry Science, 53*, 547–553.

Rasmussen. (2002). Determination of residual urease activity. http://www.analytichem.com/Applications/Kjeldah/.

Schwartze, J. P., & Bröcker, S. (2000). The evaporation of water into air of different humidities and the inversion temperature phenomenon. *International Journal of Heat and Mass Transfer, 43*, 1791–1800.

Sheikholeslami, R., & Watkinson, A. P. (1992). Rate of evaporation of water into superheated steam and humidified air. *International Journal of Heat and Mass Transfer, 35*, 1743–1751.

Soponronnarit, S., Swasdisevi, T., Wetchacama, S., & Wutiwiwatchai, W. (2001). Fluidised bed drying of soybean. *Journal of Stored Products Research, 37*, 133–151.

Stewart, O. J., Raghavan, G. S. V., Orsat, V., & Golden, K. D. (2003). The effect of drying on unsaturated fatty acids and trypsin inhibitor activity in soybean. *Process Biochemistry, 39*, 483–489.

Taechapairoj, C., Prachayawarakorn, S., & Soponronnarit, S. (2004). Characteristics of rice dried in superheated-steam fluidized bed. *Drying Technology, 22*, 719–743.

Tang, Z., & Cenkowski, S. (2000). Dehydration dynamics of potatoes in superheated steam and hot air. *Canadian Agricultural Engineering, 42*, 6.1–6.12.

Topin, F., & Tadrist, L. (1997). Analysis of transport phenomena during the convective drying in superheated steam. *Drying Technology, 15*, 2239–2261.

Zhu, S., Riaz, M. N., & Lusas, E. W. (1996). Effect of different extrusion temperature and moisture content on lipoxygenase inactivation and protein solubility in soybean. *Journal of Agricultural Food Chemistry, 44*, 3315–3318.

Available online at www.sciencedirect.com
SCIENCE DIRECT
ELSEVIER
International Journal of Heat and Mass Transfer 49 (2006) 2277–2290
International Journal of HEAT and MASS TRANSFER
www.elsevier.com/locate/ijhmt

Mathematical models based on heat transfer and coupled heat and mass transfers for rapid high temperature treatment in fluidized bed: Application for grain heat disinfestation

T. Madhiyanon [a,*], A. Techaprasan [b], S. Soponronnarit [b]

[a] Department of Mechanical Engineering, Mahanakorn University of Technology, Bangkok 10530, Thailand
[b] School of Energy and Materials, King Mongkut's University of Technology, Thonburi, Bangkok 10140, Thailand

Received 28 September 2004
Available online 9 March 2006

Abstract

This study sought to develop a mathematical model of rapid, high temperature heat treatment of stored grains in a fluidized bed. The model was intended to evaluate dynamic changes in temperature distributions inside grain kernel, and grain and exit air temperatures. No differences in temperature profiles within individual paddy kernels obtained from either analytical or numerical solutions for one- and two-dimensional heat diffusion models were found. Cylindrical coordinates gave clearer pictures of temperature profiles than spherical coordinates, and the former was chosen for the model. Thin-layer heat diffusion alone is inadequate for explaining transport phenomena in a fluidized bed; it must be incorporated into a deep bed model. The loss of as little as 1.0% dry basis moisture content from the grain surface during heating significantly affected the predictiveness of the model. Therefore, a model coupling heat and mass transfer performs much better in predicting grain and exit air temperatures than one that neglects the effect of moisture loss, when compared with the experimental results. The results showed agreement between the measured and predicted results, although the predicted results tended toward over-estimation. The results indicate that the model is a powerful tool for disinfestation applications, to predict the exposure time required to obtain lethal temperatures throughout grain kernel, so ensuring the total mortality of insects within it.
© 2006 Elsevier Ltd. All rights reserved.

Keywords: Disinfestation; Fluidized bed; Hot air treatment; Mortality; Numerical method; Paddy

1. Introduction

For many decades, chemical methods have been used world-wide for controlling insect pests in agricultural products, such as fruits and cereal grains. However, because of increasing consumer dissatisfaction with the presence of residues in cereals and other foodstuffs, more interest has recently been directed towards thermal treatment methods. Heat disinfestation, conventional heating comprised of convective heat transfer from a medium, usually heated air or hot water, to the product surface, after which the heat flows inward from the surface to the center of the product, as well as combinations of convective and radiation heat transfer, have been extensively studied for controlling insect pests in fruits [1–11] and grains [12–22]. Technologies for the rapid high temperature disinfestation of grain have been available for many years; among these technologies is the fluidized bed which has interested many researchers [12–17] because of its great advantages in rapidly promoting heat transfer and thorough mixing, leading to uniform product properties. High temperature disinfestation of wheat in batch fluidized beds apparently performed very well, in completely killing all stages of insect pests when grain reached maximum temperature, up to 60–90 °C [12,13,15]. Evans et al. [16] carried out

* Corresponding author. Tel.: +66 (0) 2988 3666x241; fax: +66 (0) 2988 3655x241.
E-mail addresses: thanid@mut.ac.th, thanid_m@yahoo.com (T. Madhiyanon).

0017-9310/$ - see front matter © 2006 Elsevier Ltd. All rights reserved.
doi:10.1016/j.ijheatmasstransfer.2005.11.020

Nomenclature

A_t	surface area of a single cylindrical paddy kernel (m^2)
c	specific heat (J/kg K)
D_p	equivalent diameter of paddy (m)
h	heat transfer coefficient (W/m^2 K)
h_{fg}	latent heat (J/kg)
ΔH	heat of vaporization (J/kg)
J_0	Bessel function zero order
J_1	Bessel function first order
k	thermal conductivity of paddy (W/m K)
k_a	thermal conductivity of air (W/m K)
$2L$	length of paddy (m)
m_a	mass flow rate of air (kg/s)
m_w	moisture evaporated from a single paddy (kg water evaporated/one paddy)
m_p	mass of a single paddy (kg/one paddy)
m_b	total dry mass of paddy in the bed (kg)
m_{wp}	total mass of moisture evaporated in the bed (kg water evaporated)
M	moisture content (decimal dry basis)
Nu	Nusselt number (–)
Pr	Prandtl number (–)
r	radial distance from center of paddy (m)
Δr	space step in r-direction (m)
R	radius of paddy (m)
RC	fraction of recycled air (–)
S	Biot number of heat transfer (–)
t	time (s)
Δt	time step (s)
T	temperature (°C)
T_{abs}	absolute temperature (K)
$\overline{T_p}$	average temperature of paddy (°C)
T_{mean}	arithmetic mean temperature of air across the bed (°C)
v	velocity (m/s)
V_p	volume of a single paddy (m^3/one paddy)
W	air humidity ratio (kg water/kg dry air)
Δz	space step in z-direction (m)
z	axial distance from center of paddy (m)

Subscripts

a	air
amb	ambient
in	initial
i	inlet
i	space nodal grid index (radial axis)
j	space nodal grid index (axial axis)
mix	mixing condition of air
n	time nodal grid index
o	outlet
p	paddy
s	surface
v	vapor
w	water

Greek symbols

α	thermal diffusivity (m^2/s)
β_n	root of Bessel function (–)
ε	bed void (–)
ρ_a	density of air (kg/m^3)
ρ_b	bulk density of paddy (kg/m^3)
ρ_t	true density of paddy (kg/m^3)

experiments in a 0.5 ton per hour capacity continuous-flow fluidized bed, where grain was heated to at least 65 °C to obtain complete mortality of all immature stage of heat-tolerant species. The other rapid high temperature techniques for grain disinfestation are spouted bed, studied by Claflin and Evans [18] and Beckett and Morton [19], and pneumatic conveyor, studied by Sutherland et al. [20,21].

However, different insect species and stages, physical and thermal properties of products, and product size have different susceptibilities to heat treatment and furthermore, mortality is not related only to grain temperature; the rate at which the grain is heated is also important, and an increasing rate of heating by a higher medium temperature will create thermal shock and achieve significantly higher mortality [15,19,22]. Above tests for investigating conditions to meet insect mortality, therefore, are very labor-intensive and costly, and the results are only valid for the product tested under the specified conditions investigated. Furthermore, there is difficulty in measuring temperature distribution inside small products, such as cereals. Several researchers [9–12] have endeavored to develop mathematical methods to investigate the influences of the physical properties of fruit and heating methods on the evolution of temperature profiles inside fruits, and the heat transfer rate to the fruit core, which directly relates to insect mortality.

In an effort to predict maximum wheat temperature during the heat disinfestation process, Sutherland et al. [21] developed a model for wheat heat in a pneumatic conveyor, based only upon heat transfer mechanism, without including moisture transfer from the grain to the heated air. Thorpe [17] used his model to predict wheat temperature in a continuous-flow fluidized bed disinfestor. His model was derived from a simplified assumption of thermal equilibrium conditions between air leaving the bed and grain in the bed, which led to the model not necessarily dealing with the heat transfer coefficient. The model could not present the evolution of temperature profiles regarding the time required for complete mortality, which is useful for explaining insect death.

The purpose of the present study is to develop a model to investigate the influence of thermal treatments for paddy in a fluidized bed on dynamic changes in temperature profile and moisture content, as well as maximum paddy temperature obtained at a given exposure time. A model accounting only for heat transfer mechanism and another coupling both heat mass transfer phenomena are discussed in this study. The spherical and cylindrical coordinates for grain are compared in the simulation results from the heat diffusion equation, and the results obtained from analytical and numerical methods are also investigated for both coordinates. The validity of the model is checked with the experimental results. However, while the insect mortality test is not within the scope of this study, we anticipate that this research will provide valuable outcomes for further research into heat disinfestation for paddy by fluidized bed technique.

2. Transient thin-layer heat diffusion model

The thin-layer models for heat diffusion assume that grain diffusivity remains constant throughout the grain kernel, which is isotropic and in which shrinkage is negligible. The first model is based on one-dimensional heat diffusion for spherical geometry, as follows:

$$\frac{\partial T}{\partial t} = \alpha\left(\frac{\partial^2 T}{\partial r^2} + \frac{2}{r}\frac{\partial T}{\partial r}\right) \tag{1}$$

which is the equation of conservation of energy.

The initial and boundary conditions are:

Initial condition

$$t = 0, \quad 0 \leqslant r \leqslant R : T = T_{in} \tag{2}$$

Boundary condition

$$t > 0, \quad r = 0 : \frac{\partial T}{\partial r} = 0 \tag{3}$$

$$r = R : k\frac{\partial T}{\partial r} = h(T_a - T_s) \tag{4}$$

The convection boundary equation (Eq. (4)) does not account for moisture loss from the kernel surface during the heat disinfestation process. The average grain temperature $\overline{T_P}(t)$ is obtained by integrating $T(r,t)$ over the sphere volume.

$$\overline{T_P}(t) = \frac{4\pi}{V_P}\int_0^R r^2 T(r,t)\,dr \tag{5}$$

The second model is based on cylindrical coordinates with similar assumptions to the first model, and may be expressed as follows:

$$\frac{\partial T}{\partial t} = \alpha\left(\frac{\partial^2 T}{\partial r^2} + \frac{1}{r}\frac{\partial T}{\partial r} + \frac{\partial^2 T}{\partial z^2}\right) \tag{6}$$

which is the cylindrical geometry of the grain kernel, as shown in Fig. 1. The initial and boundary conditions are described as follows:

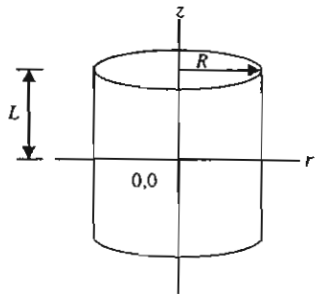


Fig. 1. The cylindrical geometry of grain kernel used for simulation.

Initial conditions

$$t = 0, \quad 0 \leqslant r \leqslant R : T = T_{in} \tag{7}$$

$$0 \leqslant z \leqslant L : T = T_{in} \tag{8}$$

Boundary conditions

$$t > 0, \quad r = 0, \ 0 \leqslant z \leqslant L : \frac{\partial T}{\partial r} = 0 \tag{9}$$

$$z = 0, \ 0 \leqslant r \leqslant R : \frac{\partial T}{\partial z} = 0 \tag{10}$$

$$r = R, \ 0 \leqslant z \leqslant L : k\frac{\partial T}{\partial r} = h(T_a - T_s) \tag{11}$$

$$z = L, \ 0 \leqslant r \leqslant R : k\frac{\partial T}{\partial z} = h(T_a - T_s) \tag{12}$$

The average temperature of grain in a cylindrical shape is defined by:

$$\overline{T_P}(t) = \frac{2\pi}{V_P}\int_0^L\int_0^R rT(r,t)\,dr\,dz \tag{13}$$

For a sphere with an aid of analogy between heat and mass diffusion problem, the solution form of mass diffusion in a sphere proposed by Vernaud [23] is used, as the solution to Eqs. (1)–(4), in which the solution is in the form containing temperature rather than the concentration of diffusing substance as a space-time dependent variable, and may be expressed as

$$\frac{T - T(r,t)}{T - T_{in}} = \frac{2SR}{r}\sum_{n=1}^{\infty}\frac{1}{(\beta_n^2 + S^2 - S)}\frac{\left(\sin\frac{\beta_n r}{R}\right)}{\sin\beta_n}\exp\left[-\frac{\beta_n^2}{R^2}\alpha t\right] \tag{14}$$

where the β_ns are roots of the following equation:

$$\beta_n\cot\beta_n + S - 1 = 0 \tag{15}$$

and the dimensionless number S is a Biot number for heat transfer, which is an indication of internal thermal resistance to external boundary layer thermal resistance, and may be expressed as

$$S = \frac{hR}{k} \tag{16}$$

For a cylinder, the solution of a two-dimensional, time-dependent heat conduction problem is equivalent to the

product of the solution of two one-dimensional transient heat conduction problems [24], thus the solution to determine the temperature profile of a finite cylinder associating to Eqs. (6)–(12) is

$$\frac{T-T(r,z,t)}{T-T_{in}} = \left[\frac{T-T(r,t)}{T-T_{in}}\right]_{\text{infinite cylinder}} \times \left[\frac{T-T(z,t)}{T-T_{in}}\right]_{\text{infinite plate}} \quad (17)$$

where the solutions for infinite cylinder and infinite plate are again adapted from the solution of Vernaud [23], as follows:

For infinite cylinder (non-steady state with finite rate of convection heat transfer)

$$\left[\frac{T-T(r,t)}{T-T_{in}}\right]_{\text{infinite cylinder}} = \sum_{n=1}^{\infty} \frac{2SJ_0(\beta_n \frac{r}{R})}{(\beta_n^2+S^2)J_0\beta_n} \exp\left[-\frac{\beta_n^2}{R^2}\alpha t\right] \quad (18)$$

where β_ns are roots of

$$\beta_n J_1(\beta_n) - SJ_0(\beta_n) = 0 \quad (19)$$

which J_0 and J_1 are Bessel function zero and first order, respectively, and may be described as [25]

$$J_0(\beta_n) = 1 - \frac{\beta_n^2}{2^2} + \frac{\beta_n^4}{2^2\cdot 4^2} - \frac{\beta_n^6}{2^2\cdot 4^2\cdot 6^2} + \ldots \quad (20)$$

$$J_1(\beta_n) = \frac{\beta_n}{2} - \frac{\beta_n^3}{2^2\cdot 4} + \frac{\beta_n^5}{2^2\cdot 4^2\cdot 6} - \frac{\beta_n^7}{2^2\cdot 4^2\cdot 6^2\cdot 8} + \ldots \quad (21)$$

where β_n can be simultaneously solved from Eqs. (19)–(21) by iteration procedure.

For infinite plate (non-steady state with finite rate of convection heat transfer)

$$\left[\frac{T-T(z,t)}{T-T_{in}}\right]_{\text{infinite plate}} = \sum_{n=1}^{\infty} \frac{2S\cos(\beta_n \frac{z}{L})}{(\beta_n^2+S^2+S)\cos\beta_n} \times \exp\left[-\frac{\beta_n^2}{L^2}\alpha t\right] \quad (22)$$

where L is half plate thickness, β_ns are positive roots of

$$\beta_n \tan\beta_n = S \quad (23)$$

Numerical solutions were also used to solve the partial differential equations with mixed boundary conditions, and the corresponding results were compared with the computed results obtained from analytical solutions (Eqs. (14) and (17)). The finite-difference approach was used to discretize the derivative in partial differential equations into a system of algebraic equations, the well-known Crank–Nicholson implicit method was chosen to solve spherical coordinate problems and an explicit method for cylindrical coordinate problems. To simulate a heat diffusion thin-layer model, it is reasonably assumed that air temperature remains unchanged when passing through a thin layer of grain; thus, the thermodynamic properties of air used for calculation can be evaluated at the inlet air temperature.

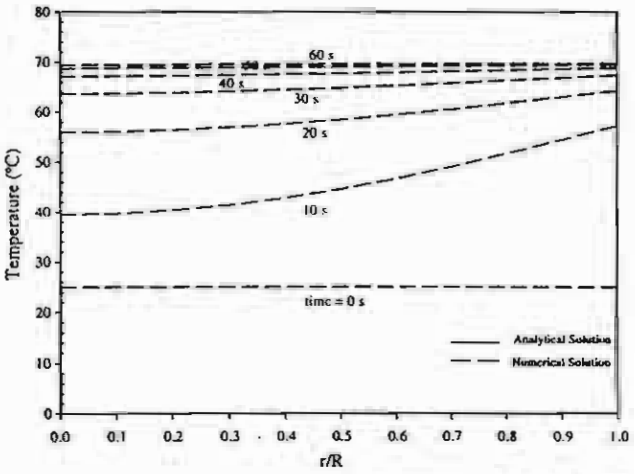


Fig. 2. Comparison of temperature profiles inside a spherical paddy kernel between obtaining from numerical and analytical solution of thin layer model.

The heat transfer coefficient correlation and the thermal properties of paddy can be found in the relevant section of this study. The moisture content of the paddy was assumed to be constant at 14% dry throughout the heating period, which is generally in the range for the moisture content of stored paddy.

Fig. 2 shows the computed temperature distribution inside a spherical paddy kernel with 3.5 mm equivalent diameter at inlet air temperature of 70 °C and air velocity of 2.5 m/s. The temperature data of both solutions, obtained from analytical and numerical methods, appeared to be indistinguishable. The intra-temperatures became uniform across the grain kernel and were elevated to inlet air temperature within 60 s of commencement.

Figs. 3 and 4 show predicted temperature profiles inside a paddy kernel assumed to be cylindrical in the air condi-

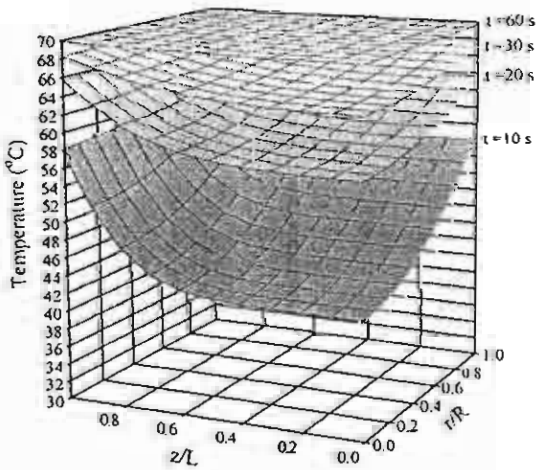


Fig. 3. Temperature profiles inside a cylindrical paddy kernel computed by analytical solution at inlet air temperature of 70 °C.

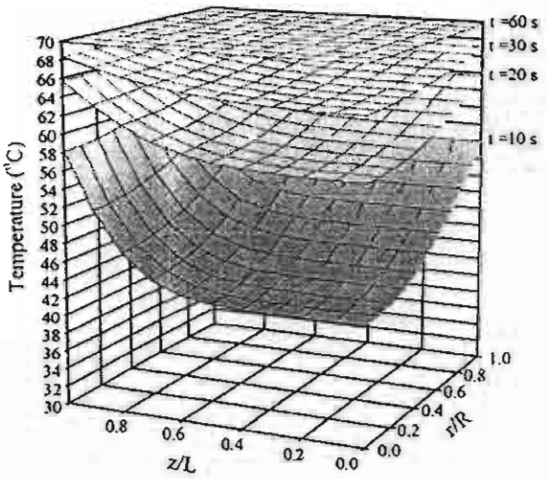


Fig. 4. Temperature profiles inside a cylindrical paddy kernel computed by numerical solution at inlet air temperature of 70 °C.

tions for an assumed spherical paddy kernel. A cylindrical paddy kernel has a diameter of 2.5 mm and length of 9.5 mm. In Fig. 3, the temperature profiles determined by analytical solution are identical with those determined by numerical solution, as shown in Fig. 4. It is clearly seen that temperature along with the radius became uniform more rapidly than along with the length, however, there is no evidence of temperature gradient within a kernel, either in the radial or axial direction, exiting after 60 s of heating. This is consistent with the computed results for a spherical paddy kernel.

Fig. 5 presents the average grain temperature of a spherical grain kernel compared with that of the cylindrical grain kernel. It is evident that there is almost no difference in the average grain temperature between both coordinates.

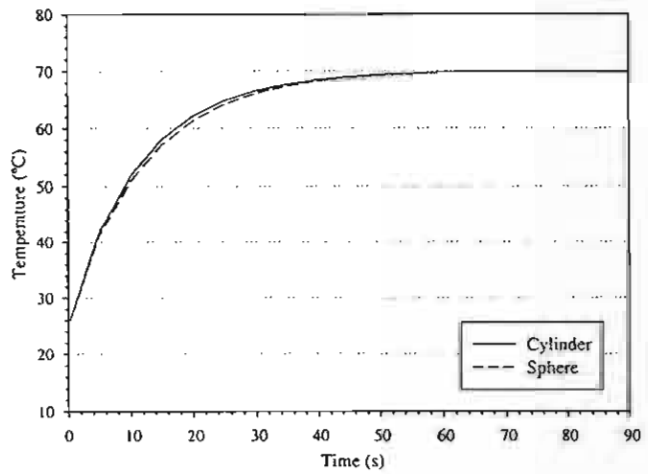


Fig. 5. Comparison between predicted average paddy temperature of a spherical and cylindrical shape at inlet air temperature of 70 °C.

3. Model development for heat disinfestation in a fluidized bed

Even though the thin-layer heat diffusion models discussed above can provide temperature profiles inside grain kernels, which is necessary for analyzing the mortality of all insects inside grain kernels, they alone cannot sufficiently describe the transport process phenomena in deep bed grain disinfestations, such as fluidized bed disinfestation. They must be incorporated into a deep bed simulation model derived from mass and energy conservation laws. Because there are differences in heat diffusion rates between axial and radial directions, a paddy kernel was assumed to be a cylindrical object, as discussed in Section 2, and a geometric cylinder should be more appropriate than a spherical shape for paddy. Thus, cylindrical coordinates of heat diffusion equation were used in the simulation.

The following assumptions were made in developing the model:

1. Paddy kernels are uniform in size and internally homogeneous.
2. In the first fluidized bed disinfestation model, assuming that any change in the moisture content of stored grain is very small and has no effect on the process, moisture loss from the grain surface was not accounted for. However, in the second model, moisture loss and the corresponding heat of evaporation were added to the convective boundary conditions and energy equation, respectively.
3. The effects of heat conduction and moisture transfer between the grains, and heat loss, were not accounted for.
4. The accumulation of thermal energy and water vapor in the air in the bed was disregarded.
5. It was assumed that the grains were well mixed and had the same temperature and moisture content at any location in the bed.
6. With respect to up-modulating high air temperature and high air flow rate, as in a fluidized bed application, it was assumed the exit air and the grains in the bed had not reached a condition of thermal equilibrium.

To simulate heat disinfestation in a fluidized bed system, in which part of the exhaust air is recycled for energy-saving reasons, the system is divided into a series of elementary control volumes, as shown in Fig. 6. The basic principles of the laws of mass and energy conservation, accounting for convective heat transfer and mass transfer based on the empirical model fitted from the experimental data, are employed to each elementary control volume, leading to a set of governing equations, as follows:

3.1. Fluidized-bed chamber (cv. 1)

The appreciable fluidization of grains accounting for a current model is characterized by assuming the well-mixed

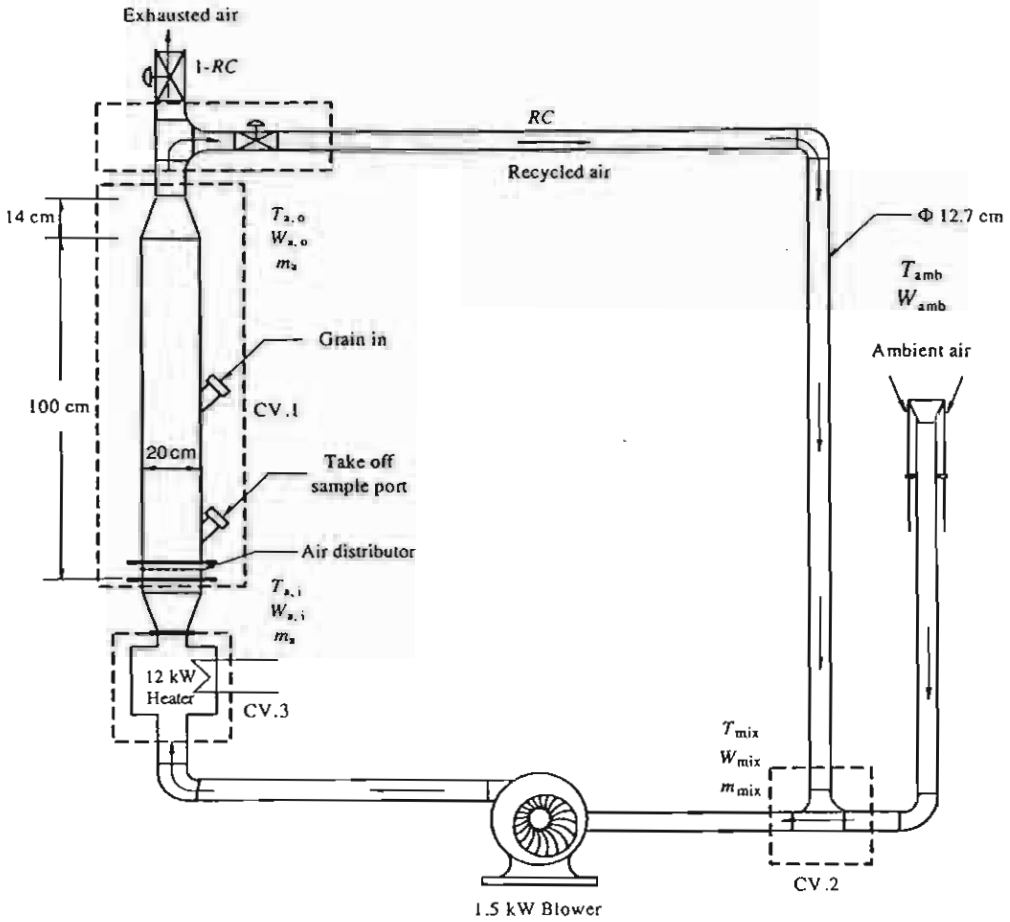


Fig. 6. Schematic diagram of batch fluidized bed disinfestor.

condition of grains (Assumption 5) so as all grains elsewhere inside the bed are in the same moisture content and temperature.

3.1.1. Macroscopic mass balance

Control volume 1 (cv. 1), as shown in Fig. 6, represents the fluidized-bed chamber. By employing Assumption 4, that the accumulation rate of water vapor in the air within the bed is not accounted for, the physical meaning of the law of mass conservation may be written as

[Mass of moisture evaporated from grain]

= [Change in moisture of grain]

= [Change in humidity of air]

which are mathematically expressed as follows:

$$m_{wb} = m_b \frac{dM}{dt} \tag{24}$$

and

$$-m_b \frac{dM}{dt} = m_a(W_{a.o} - W_{a.i}) \tag{25}$$

term $\left[\frac{dM}{dt}\right]$ can be determined by applying Eq. (31) and is not implied if moisture loss is not accounted for.

3.1.2. Macroscopic energy balance

With the Assumption 4 that the accumulation of thermal energy in the air in the bed is negligible. The exchange energy between the air across the bed and the grains gives a relationship, as follows:

[Enthalpy change of air across bed]

= [Internal change of the grain in the bed]

+ [Energy used for evaporation of moisture evaporated from the grain]

+ [Energy for increasing the temperature of the moisture evaporated to the temperature of the air]

The last term on the right-hand side of the above equation may be omitted when compared with other terms, and is mathematically expressed as

$$m_a c_a(T_{a.i} - T_{a.o}) + m_a c_v(W_{a.i}T_{a.i} - W_{a.o}T_{a.o}) = m_b(c_p + c_w M_{in})\frac{d\overline{T_p}}{dt} + m_{wb}\Delta H \tag{26}$$

which is a non-equilibrium thermal condition. The last term on the right hand side of Eq. (26) ($m_{wb}\Delta H$) is respon-

sible for the heat of evaporation and is not considered when the moisture evaporated is negligible.

3.1.3. Heat and mass transfer of a single grain

Heat transfer of a single grain is governed by a heat diffusion equation for cylindrical geometry, with appropriate initial and boundary conditions, as described by Eqs. (6)–(12). In the second fluidized bed heat disinfestation model, including accounting for moisture loss from the grain surface, boundary equations (11) and (12) are replaced by the following equations:

$$t > 0, \quad r = R, \ 0 \leqslant z \leqslant L : k\frac{\partial T}{\partial r} = h(T_a - T_s) - m_w\frac{\Delta H}{A_t} \tag{27}$$

$$z = L, \ 0 \leqslant r \leqslant R : k\frac{\partial T}{\partial z} = h(T_a - T_s) - m_w\frac{\Delta H}{A_t} \tag{28}$$

moisture loss of a single grain (m_w) can be determined from

$$m_w = m_p\frac{dM}{dt} \tag{29}$$

where

$$m_p = \rho_t V_p \tag{30}$$

Term $\left[\frac{dM}{dt}\right]$ is the rate of change in moisture content in which the relationship between the moisture content (M) and the disinfestation time (t) was evaluated by fitting corresponding data from the present experiments carried out under the various heating temperatures. A exponential form correlation performed by least square method was found to provide good agreement between the experimental data and the correlation, and can be expressed as

$$M(t) = M_{in} - \exp(a)\exp(b\ln T_{a,i})\exp(c\ln t) \tag{31}$$

where t is disinfestation time (s), and a, b, c are constant parameters for the various disinfestation temperatures, shown below:

Air temperature (<75 °C): $a = -20.3969, b = 4.3215, c = 0.4883$.
Air temperature (<110 °C): $a = -9.7093, b = 1.8136, c = 0.5778$.
Air temperature (<150 °C): $a = -6.7201, b = 1.2184, c = 0.4234$.

3.2. Mixing section (cv. 2)

Because the system employs exhaust air recycling, the ambient air temperature must be elevated to inlet air temperature and hence the mixing temperature must be determined before assessing the energy required to heat the mixed air to desirable inlet air temperature. Using the basic knowledge of energy conservation, the mixing temperature can be determined by the following equation:

$$m_{mix}c_a T_{mix} + m_{mix}W_{mix}(h_{fg} + c_v T_{mix}) - (1 - RC)m_a c_a T_{amb} - (1 - RC)m_a W_{amb}(h_{fg} + c_v T_{amb}) - RC\,m_a c_a T_{a,o} - RC\,m_a W_{a,o}(h_{fg} + c_v T_{a,o}) = 0 \tag{32}$$

The mass balance for the air phase is written as

$$m_{mix} = m_a \tag{33}$$

and the mass balance for the vapor phase is expressed as

$$W_{mix} = RC\,W_{a,o} + (1 - RC)W_{amb} \tag{34}$$

The increase in the humidity of the air leaving the bed, by moisture transferred from the surface of stored grains, which usually have a relatively low moisture content and for which it is difficult to shed moisture, is very small and can be approximately unchanged when the air leaves the bed. Thus Eqs. (25) and (34) can be simplified to

$$W_{a,o} \cong W_{a,i} \tag{35}$$

and

$$W_{mix} \cong W_{a,o} \tag{36}$$

3.3. Heating chamber (cv. 3)

The energy input to heat air before entering the fluidized-bed chamber can be calculated from

$$Q = m_{mix}(c_a + W_{mix}c_v)(T_{a,i} - T_{mix}) \tag{37}$$

3.4. Properties and thermodynamic equations

The correlation of heat transfer subjected to the fluidized bed reported by Kunii and Levenspiel [26] was selected for simulation, and may be expressed as

$$Nu = 2 + 0.6Re^{0.5}Pr^{0.33} \tag{38}$$

where $h = Nuk_a/D_p$, $Re = \rho_a v_a D_p/\mu_a$; $(0.1 < Re < 10^4)$ and $Pr = c_a\mu_a/k_a$.

In which D_p equates with the diameter of a grain. Although Eq. (38) is primary correlated for spherical particles in the fluidized bed but it is permitted for non-spherical particle as well.

Expressions for properties of product and thermodynamics equations for air–water systems (Eqs. (49)–(60)) are listed in Tables 1 and 2. Eqs. (52)–(54) are used to calculate true density of paddy ρ_t and hence the mass of one grain may be determined from Eq. (30).

4. Solution algorithm

The solution procedure for the governing equation involves the following steps:

1. Parameters, i.e. inlet air temperature ($T_{a,i}$), inlet air humidity ($W_{a,i}$), which is approximately equal to ambient air humidity (W_{amb}), initial moisture content (M_{in}), initial grain temperature, air mass flow rate (m_a), dry

Table 1
Properties of paddy used for simulation [27–29]

Equations	Property	Expression	References	Units
(49)	ΔH	$\Delta H = (2502 - 2.386\overline{T}_p)(1 + 2.496\exp(-21.733M)) \times 10^3$	[27]	J/kg H_2O
(50)	c_p	$c_p = 1.11 \times 10^3 + 44.8(M/(1+M))$	[27]	J/kg
(51)	k	$k = 0.0863 + 0.00134(M/(1+M))$	[28]	W/m K
(52)	ε	$\varepsilon = 0.62 - 0.25(M/(1+M))$	[29]	Decimal
(53)	ε	$\varepsilon = 1 - \rho_b/\rho_t$	[30]	Decimal
(54)	ρ_b	$\rho_b = 552 + 282(M/(1+M))$	[29]	kg/m^3

Table 2
Thermodynamics of air and water system [27,30]

Equations	Property	Expression	Units
(55)	c_a	$c_a = 1.00926 \times 10^3 - 4.0403 \times 10^{-2}T + 6.1759 \times 10^{-4}T^2 - 4.097 \times 10^{-7}T^3$	J/kg K
(56)	k_a	$k_a = 2.425 \times 10^{-2} + 7.889 \times 10^{-5}T - 1.790 \times 10^{-8}T^2 - 8.570 \times 10^{-12}T^3$	W/m K
(57)	ρ_a	$\rho_a = 101.325/(0.287T_{abs})$	kg/m^3
(58)	μ_a	$\mu_a = 1.691 \times 10^{-5} + 4.984 \times 10^{-8}T - 3.187 \times 10^{-11}T^2 + 1.319 \times 10^{-14}T^3$	kg/m s
(59)	c_v	$c_v = 1.883 \times 10^3 - 1.6737 \times 10^{-1}T + 8.4386 \times 10^{-4}T^2 - 2.6966 \times 10^{-7}T^3$	J/kg K
(60)	c_w	$c_w = 2.8223 \times 10^3 + 11.828T - 3.5043 \times 10^{-2}T^2 + 3.601 \times 10^{-5}T^3$	J/kg K

mass of paddy in bed (m_b), air recycling ratio (RC), and superficial air velocity, are taken as input parameters to initiate the simulation.

2. For each given time step, by applying the heat diffusion equation for cylindrical coordinates (Eq. (6)) and appropriate initial and boundary conditions (Eqs. (7)–(12)) or replacing Eqs. (11) and (12) with Eqs. (27) and (28) where accounting for moisture loss, temperature profiles inside the kernel, in respect to a given time step, can be determined. Moisture loss from one grain (m_w) appeared in the convection boundary conditions (Eqs. (27) and (28)) can be evaluated from Eqs. (29)–(31). The temperature of the air decreases as it flows throughout the bed; thus, to calculate the corresponding heat transfer coefficient, the properties of the air are evaluated at an average temperature between inlet and exit air. However, the exit temperature ($T_{a,o}$) is not yet known; therefore, in this step, an iterative solution is necessary and $T_{a,o}$ is assumed as initial estimate to determine the heat transfer coefficient and the solution of the heat diffusion equation, respectively. The implicit finite difference with the discrete grid of the cylindrical object, as shown in Fig. 7, was advanced. The finite difference representing the governing equations, including accounting for moisture loss, may be written in the following form:

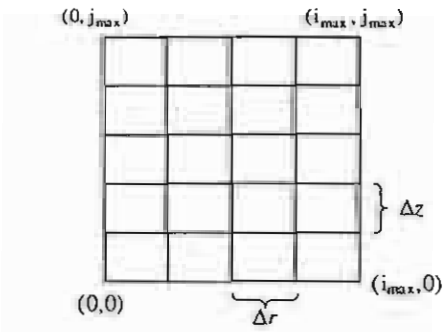


Fig. 7. Numerical grids for a one-forth cylindrical object for the governing equations.

Case 1: $i = 0, j = 0$

$$T^{n+1}_{0,0} = (1 - 4F_r - 2F_z)T^n_{0,0} + 4F_rT^n_{1,0} + 2F_zT^n_{0,1} \tag{39}$$

Case 2: $i = 0, j = j_{max}$

$$T^{n+1}_{0,j_{max}} = (1 - 4F_r - 2F_z\beta_N)T^n_{0,j_{max}} + 2F_zT^n_{0,j_{max}-1} + 4F_rT^n_{1,j_{max}} + 2F_z\gamma_N - 2F_z\left(\frac{\Delta z}{k}\right)\left(\frac{m_w\Delta H}{A_t}\right) \tag{40}$$

Case 3: $i = i_{max}, j = 0$

$$T^{n+1}_{i_{max},0} = (1 - 2F_r\beta_M - 2F_z)T^n_{i_{max},0} + 2F_r\gamma_M + 2F_rT^n_{i_{max}-1,0} + 2F_zT^n_{i_{max},1} - \left(1 + \frac{1}{2i}\right)\left(\frac{2F_r\Delta r}{k}\right)\left(\frac{m_w\Delta H}{A_t}\right) \tag{41}$$

Case 4: $i = i_{max}, j = j_{max}$

$$T^{n+1}_{i_{max},j_{max}} = (1 - 2F_r\beta_M - 2F_z\beta_N)T^n_{i_{max},j_{max}} + 2F_r\gamma_M + 2F_z\gamma_N + 2F_rT^n_{i_{max}-1,j_{max}} + 2F_zT^n_{i_{max},j_{max}-1} - 2\left(\frac{F_z\Delta z}{k}\right)\left(\frac{m_w\Delta H}{A_t}\right) - \left(1 + \frac{1}{2i}\right)\left(\frac{2F_r\Delta r}{k}\right)\left(\frac{m_w\Delta H}{A_t}\right) \tag{42}$$

Case 5: $i = i_{\max}, j = 1,2,3,\ldots,j_{\max}-1$

$$T^{n+1}_{i_{\max},j} = (1 - 2F_r\beta_M - 2F_z)T^n_{i_{\max},j} + 2F_r\gamma_M + 2F_rT^n_{i_{\max}-1,j} + F_zT^n_{i_{\max},j+1} + F_zT^n_{i_{\max},j-1} - \left(1+\frac{1}{2i}\right)\left(\frac{2F_r\Delta r}{k}\right)\left(\frac{m_w\Delta H}{A_t}\right) \quad (43)$$

Case 6: $i = 1,2,3,\ldots,i_{\max}-1, j = j_{\max}$

$$T^{n+1}_{i,j_{\max}} = (1 - 2F_r - 2F_z\beta_N)T^n_{i,j_{\max}} + \left(1+\frac{1}{2i}\right)F_rT^n_{i+1,j_{\max}} + 2F_z\gamma_N + \left(1-\frac{1}{2i}\right)F_rT^n_{i-1,j_{\max}} + 2F_zT^n_{i,j_{\max}-1} - \left(\frac{2F_z\Delta z}{k}\right)\left(\frac{m_w\Delta H}{A_t}\right) \quad (44)$$

Case 7: $i = 1,2,3,\ldots,i_{\max}-1, j = 0$

$$T^{n+1}_{i,0} = (1 - 2F_r - 2F_z)T^n_{i,0} + \left(1+\frac{1}{2i}\right)F_rT^n_{i+1,0} + \left(1-\frac{1}{2i}\right)F_rT^n_{i-1,0} + 2F_zT^n_{i,1} \quad (45)$$

Case 8: $i = 0, j = 1,2,3,\ldots,j_{\max}-1$

$$T^{n+1}_{0,j} = (1 - 4F_r - 2F_z)T^n_{0,j} + 4F_rT^n_{1,j} + F_zT^n_{0,j+1} + F_zT^n_{0,j-1} \quad (46)$$

Case 9: $i = 1,2,3,\ldots,i_{\max}-1, j = 1,2,3,\ldots j_{\max}-1$

$$T^{n+1}_{i,j} = (1 - 2F_r - 2F_z)T^n_{i,j} + \left(1+\frac{1}{2i}\right)F_rT^n_{i+1,j} + \left(1-\frac{1}{2i}\right)F_rT^n_{i-1,j} + F_zT^n_{i,j+1} + F_zT^n_{i,j-1} \quad (47)$$

The stability criterions for the above equations are

$$F_r + F_z \leqslant \frac{1}{2} \quad (48)$$

where

$$F_r = \frac{\alpha\Delta t}{\Delta r^2}; \quad \alpha = \frac{k}{\rho_t c_p}$$

$$F_z = \frac{\alpha\Delta t}{\Delta z^2}$$

$$\beta_N = 1 + \left(\Delta z\frac{h}{k_a}\right)$$

$$\beta_M = 1 + \left(\left(1+\frac{1}{2i}\right)\Delta r\frac{h}{k_a}\right)$$

$$\gamma_M = \left(1+\left(\frac{1}{2i}\right)\right)\left(\Delta r\frac{h}{k_a}\right)T_{\text{mean}}; \quad T_{\text{mean}} = \frac{T_{a,i}+T_{a,o}}{2}$$

$$\gamma_N = \left(\Delta z\frac{h}{k_a}\right)T_{\text{mean}}$$

In the above equations, terms involving evaporated moisture are neglected if not considering moisture loss during the heat disinfestation process.

3. Knowing the temperature accompanied by each node inside the grain kernel, the average temperature can be resolved by applying Simpson's method to Eq. (13).
4. From the mass and energy conservation equations (Eqs. (24)–(26)), the exit air temperature is determined and compared to the initial estimated value. If the difference in result is not within an acceptable level, the initial estimate will be changed to the update result, and the entire procedure repeated until the difference in the exit air temperature is less than 0.005 °C, which is considered insignificant based on practical considerations. Once the solution regarding the fluidized-bed chamber section has been assembled, the simulation will be continued further for subsequent sections, by solving Eq. (25) to determine the change in humidity ratio of the air leaving the bed, Eqs. (32) and (34) to calculate mixing temperature and mixing humidity ratio of the air departing from mixing section and Eq. (37) to find out heat input. In the specific event of not accounting moisture evaporated, Eqs. (25) and (34) are omitted and consequently replaced by Eqs. (35) and (36).
5. The final conditions of the air throughout the bed and the grain within the bed, accomplished by the procedure in steps 1–4, are now initialized for the condition of the next time step. The entire procedure is repeated until the end of the disinfestation period.

5. Experiments

Experiments were conducted to validate the simulation results of changes in air and grain temperatures during the heat treatment process.

5.1. Materials

Experiments with paddy heating were conducted using a fluidized bed batch disinfestor, as shown in Fig. 6. The fluidized-bed chamber was made of stainless steel and was of a cylindrical shape, 20 cm in diameter and 140 cm in height. The chamber and connected air ducts were insulated with fiberglass insulation 25 mm in thickness. Hot air was distributed to the bottom of the chamber through an air distributor plate. Air was heated by electric heaters with a total capacity of 12 kW. The inlet air temperatures were automatically controlled by PDI temperature controller, with an accuracy of ±1 °C. Temperatures were measured by a data logger and a temperature indicator with an accuracy of ±1 °C connected to a type K thermocouple. Air velocity was measured by hot wire anemometer with an accuracy of ±5%. A mechanical variable speed drive was used to regulate blower motor speed to attain the desired airflow rate.

5.2. Experimental set-up and conditions

Dried long-grain rough rice (paddy) with moisture contents in the range 12–14% (dry basis) was selected as the

test material. 0.8 kg of paddy, which created a non-fluidized bed height of 4 cm, was loaded into the fluidized chamber for each experiment. To guarantee complete fluidization of paddy is attained, the fluidization velocity of 2.5 m/s, which is equal to 1.5 times of the calculated minimum fluidization velocity (1.65 m/s), was used and held constant, and the percentage-air-recycled ratio was set at 20% for each experiment. The exit air temperatures were measured at a distance of 85 cm above the air distributor. The paddy samples were taken for determination of temperature and moisture content at intervals of 10 s. To ensure that the process mechanism was not deviated from, or disturbed by collecting the samples, the process with same desired conditions was restarted after collecting each sample until the target time was reached. The inlet air temperatures were set at 60, 80, 100 and 120 °C, respectively.

6. Result and discussion

6.1. Prediction of temperature gradient inside individual paddy kernel

Fig. 8 presents the moisture profile inside individual paddy kernels at an air temperature of 70 °C computed by the fluidized bed model, in which the moisture evaporation effect was not accounted for. Heat flow patterns similar to the thin-layer model (Fig. 4) were observed, but different times were required for temperature equalization. The temperature throughout the grain kernel, as predicted by the fluidized bed model, attained uniformity more slowly than that predicted by the thin-layer model. This is because the air temperature used for calculating heat transfer coefficient and heat transfer rate in the thin layer model was assumed unchanged and was equal to the inlet air temperature, whilst the fluidized bed model acknowledges the effects of air temperature changes within the bed. Therefore, the arithmetic mean of the air temperatures across the bed was used in calculation.

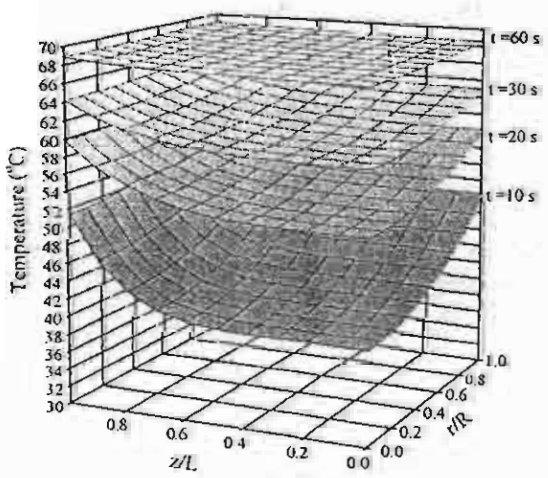


Fig. 8. Temperature profiles inside a cylindrical paddy kernel computed by fluidized bed model excluding moisture loss effect at inlet air temperature of 70 °C.

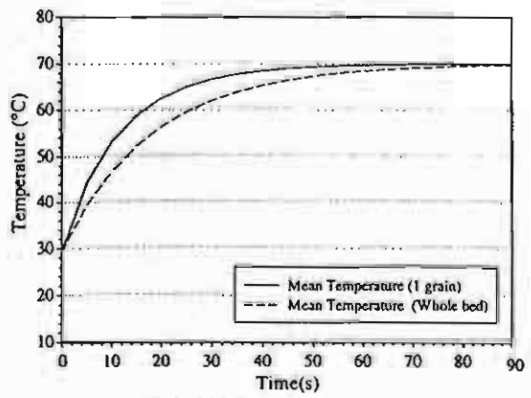


Fig. 9. Comparison of simulated average paddy temperature between computational from thin layer and fluidized bed models at inlet air temperature of 70 °C.

To provide a clearer picture, the average temperatures of grain for both the thin layer and fluidized bed models, corresponding to temperature distribution data in Figs. 4 and 8 were plotted, as shown in Fig. 9. It is indicative of more rapid changes in grain temperature in the thin layer model, leading to incorrect determination of the lethal time required for mortality of insects inside grain kernels.

6.2. Experimental validation without accounting for moisture loss

Fig. 10(a–c) shows the experimental and predicted average grain temperatures and exit air temperatures at inlet air temperatures of 60, 80, 100 and 120 °C, respectively. The model excluding moisture loss effect over-predicted experimental results where the dynamic changes in predicted values progressed more quickly than in the experimental values and resulted in predicting grain and exit air temperatures approaching inlet air temperature at the end period, whilst that did not happen in the experiments. It was also noticeable that use of a higher inlet air temperature resulted in higher discrepancies between experimental and simulation results. Over-prediction of grain and exit air temperatures was assumed to be caused by neglecting evaporation heat for moisture reduction during heat treatment, leading to over-accelerating the changes in the predicted air and grain temperatures. In an attempt to investigate the relationship between moisture reduction and changes in grain and air temperatures, the moisture content of grain versus time under several inlet air temperatures were plotted, together with air and grain temperatures, as shown in Fig. 10. It is clearly illustrated that the moisture content of the grain decreases with heating time, especially at high inlet air temperatures, and this could affect the predictiveness of the model.

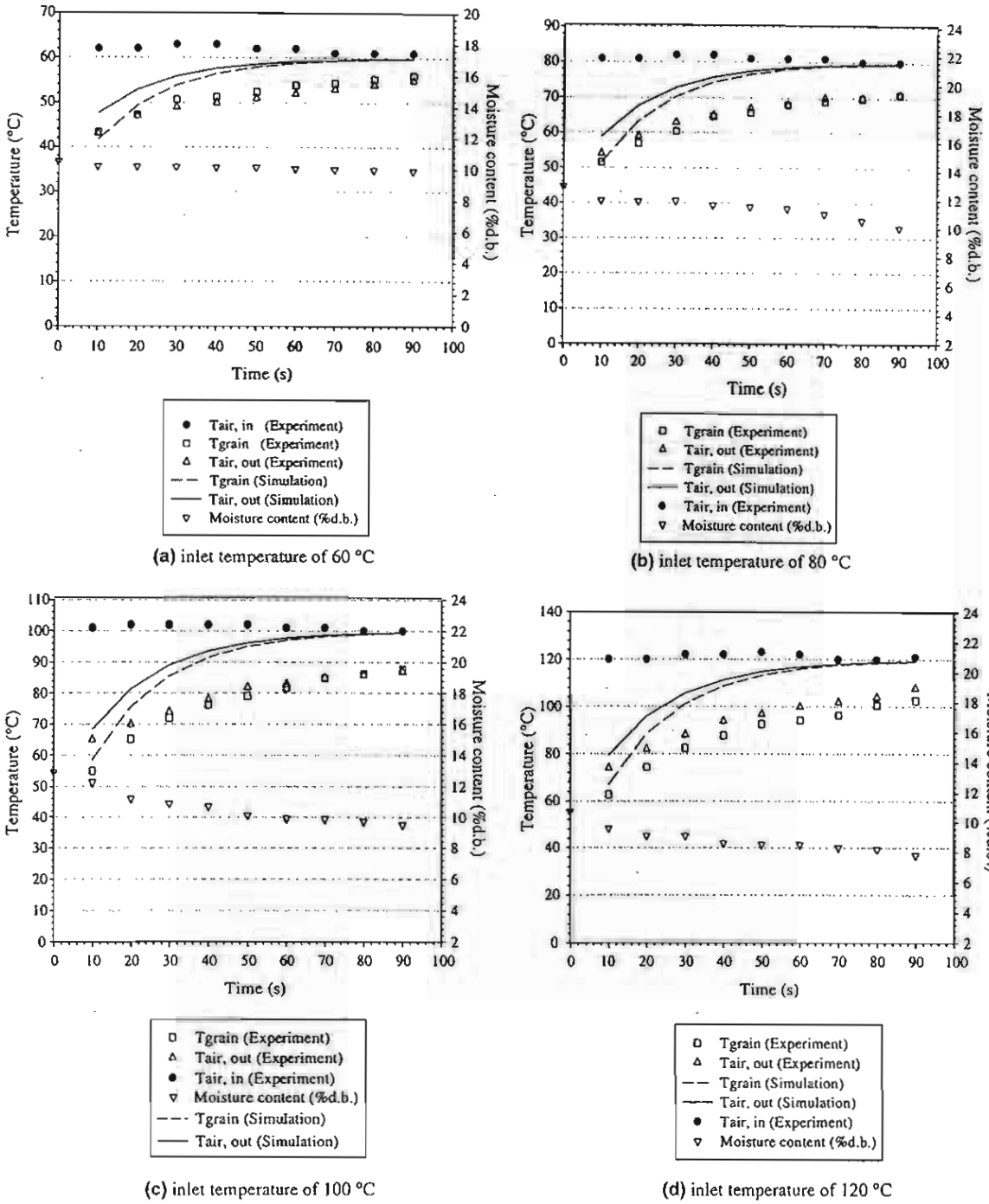


Fig. 10. Simulation and experimental results of heat disinfestation fluidized bed model excluding moisture transfer effect.

6.3. Simulation of coupled heat and mass transfer in fluidized bed disinfestor

The previous section indicated that a model in which the influence of moisture evaporation on energy exchange between air and grain was excluded did not provide a realistic prediction. Fig. 10 indicates that only 1.0% d.b. of average moisture reduction may significantly affect the predicted results. To improve the model predicting grain and exit air temperatures, moisture losses and the relative energy used for evaporation are taken into account, and then the solution is resolved by simultaneously combining the heat exchange contribution and the moisture transfer in the bed. The experimental data in Fig. 10(a–d) are duplicated in Fig. 11(a–d), but the model incorporating moisture transfer was used to predict grain and exit air temperatures

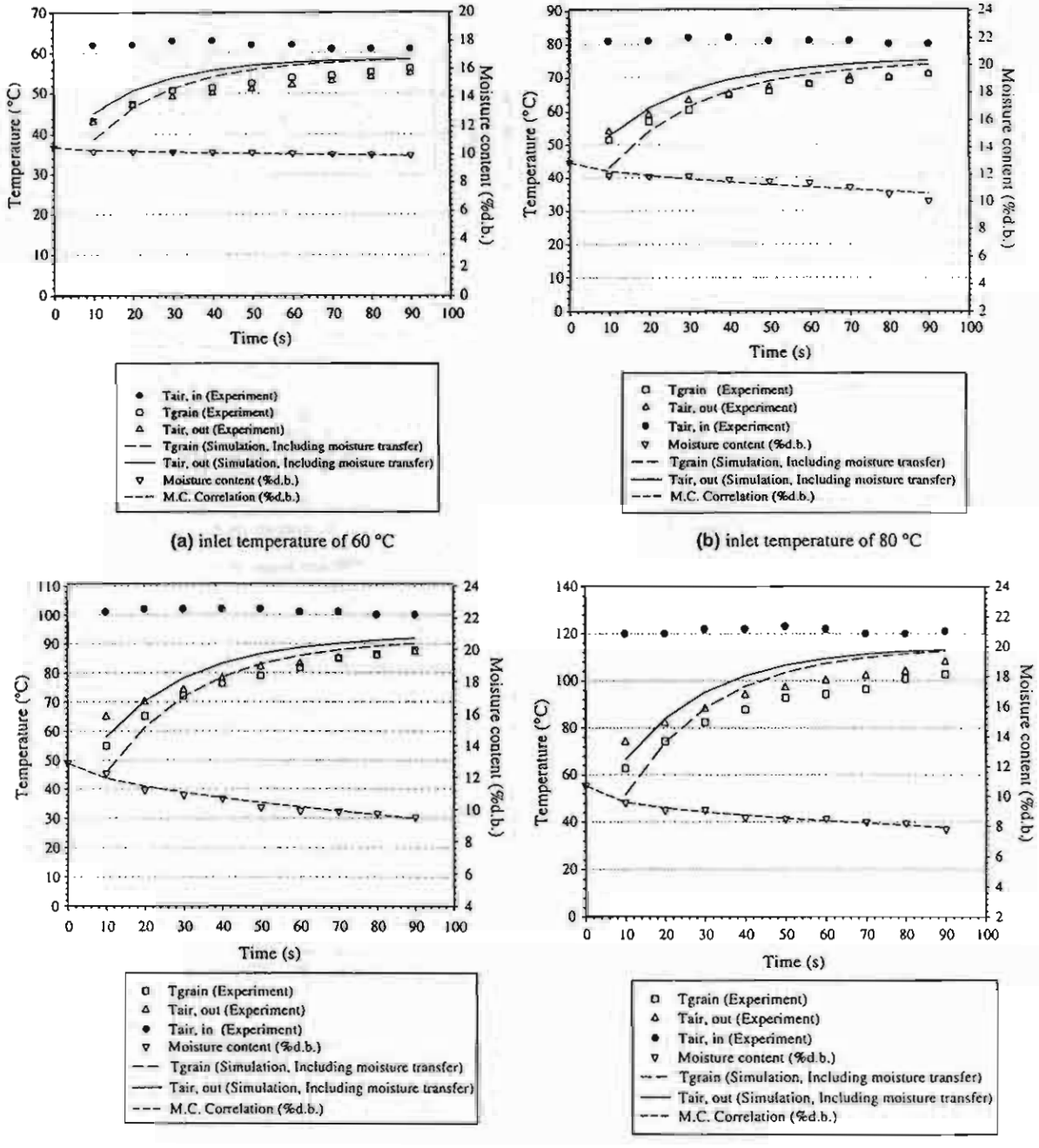


Fig. 11. Simulation and experimental results of heat disinfestation fluidized bed model coupling heat and mass transfer.

with a consequential improvement in predicted values. The model predicted grain temperature more accurately than exit air temperature, but not for the test undergoing inlet air temperature of 120 °C. The discrepancies between predicted and measured exit air temperatures are between 2 and 5 °C (except for the testing under high inlet air temperature of 120 °C) and may partly due to the effect of heat loss through the wall of the fluidized-bed chamber. The measuring point for the exit air is located 85 cm above the air distributor plate, which is quite high compared with a dynamic bed height where it is accompanied by most of the fluidized grain; hence, those temperature values represent the temperature of the air leaving the chamber rather than the temperature of the air leaving the bed.

The air temperature drop due to heat loss effect is reflected by consistently lower measured temperature of the air containing low energy, i.e. air with a low temperature of 60 °C than the measured temperature of the grain,

as presented in Fig. 11(a), which is not possible unless it is due to the heat loss effect. To investigate these errors, the hand calculations (not shown herein) were performed for heat loss calculation and found that the discrepancies may reduce to 0.5–2.5 °C instead of 2–5 °C if involving heat loss, confirming the responsibility of heat loss effect for these discrepancies, in part. The model performed reasonably well in predicting grain temperature, although the predicted values were over-estimated. The differences in predicted and measured values were less than 2–3 °C, except for conditions with high inlet air temperature of 120 °C. After thoroughly checking the model, we believed that the main factor significantly affecting grain temperature computation was the heat transfer coefficient. The heat transfer coefficient used in the model determined subject to the arithmetic mean temperature between the inlet and exit air, which may be not be an adequate representation of the temperature of the air across the bed. Some additional data were required to investigate the variation in air temperature along with the fluidized bed height. Measurements were taken and the data are shown in Fig. 12, which illustrates that the air temperature decreases sharply just above 2.5 cm from the air distributor plate and does not fall in temperature once it is about 10 cm above the air distributor plate. This means that the heat transfer coefficient, determined based on the arithmetic mean temperature of air is over-estimated, resulting in over-prediction of grain temperature. The effect of over-estimating the mean temperature of the air inside the bed will be more powerful, especially in high temperature conditions, e.g. air temperatures of 120 °C.

6.4. Model application for heat disinfestations

Although a long heat treatment time is adequate for us to be confident of destroying the insect population however, the period cannot be too long because it must be balanced with the impact on product quality. The appropriate lethal time required for the complete mortality of all insects embedded inside the product at various given operating conditions may be determined by simulating the time that all locations inside the product must attain the target temperature. Increasing the rate of mortality by allowing the product to undergo higher temperatures near the surface, and more rapidly promoting the target temperature at the center, or creating thermal shock [15,19,22], can also be simulated by the model.

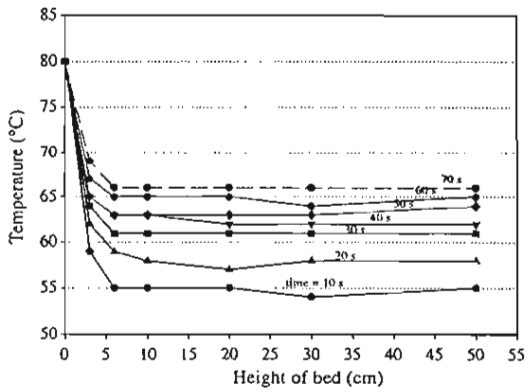


Fig. 12. Experimental results of variation of air temperature within the fluidized bed.

7. Conclusions

Cylindrical coordinates for the heat diffusion problem were chosen rather than spherical coordinates to model fluidized bed heat disinfestation because of its clearer picture of temperature profiles inside individual paddy kernels. The simulation results from the thin layer heat diffusion model, obtained from numerical methods, do not distinguish between those obtained from the analytical solution method and the numerical method was used in modeling. Coupling the thin-layer heat diffusion model with other relevant mass and energy balance equations that were developed for the relative parts of the fluidized bed system gave different results from applying the thin-layer model alone. It was quite apparent that only 1.0% d.b. of grain moisture reduction, the model which takes full account of the changes in energies due to differential changes in moisture content, significantly improve prediction of grain and exit temperatures. The model tends to over-estimate grain and exit temperatures in most cases considered, but the errors are not considered significant. The use of arithmetic mean temperature for air across the bed, to determine the heat transfer coefficient, was primarily motivated by the lack of information regarding variations in air temperature within the bed, and led to over-estimation of grain temperature, whilst the over-estimation of exit air temperature was mainly due to the heat loss effect. Finally, in applying heat disinfestations, the model is able to predict the mortality of insects inside grain kernels by knowing the lethal temperature and operating conditions, so that consequently the lethal time required for completely destroying all insects can be determined.

Acknowledgement

Thanks are due to the Thailand Research Fund (TRF) for financial support and the Japanese International Research Center for Agricultural Sciences (JIRCAS).

References

[1] J.L. Sharp, J.J. Gaffney, J.I. Moss, W.P. Gould, Hot-air treatment device for quarantine research, J. Econ. Entomol. 84 (1991) 520–527.

[2] L.G. Neven, Combined heat treatments and cold storage effects on mortality of fifth-instar codling moth (Lepidoptera: Tortricidae), J. Econ. Entomol. 87 (1994) 1262–1265.

[3] L.G. Neven, E.J. Mitcham, CATTS (controlled atmosphere/temperature treatment system): a novel tool for the development of quarantine treatments, J. Amer. Entomol. 42 (1996) 56–59.

[4] L.G. Neven, L.M. Rehfield, K.C. Shellie, Moist and vapor forced air treatment of apples and pears: effects on the mortality of fifth instar codling moth (Lepidoptera: Tortricidae), J. Econ. Entomol. 89 (1996) 700–704.
[5] S. Lurie, Postharvest heat treatments, Postharvest Biol. Technol. 14 (1998) 257–269.
[6] R.L. Mangan, K.C. Shellie, S.J. Ingle, M.J. Firko, High temperature forced-air treatments with fixed time for 'Dancy' tangerines, 'Valencia' orange and 'Rio Star' grape fruit, J. Econ. Entomol. 91 (1998) 933–939.
[7] K.K. Jacobi, L.S. Wong, J.E. Giles, Postharvest quality of zucchini (*Cucurbita pepo* L.) following high humidity hot air disinfestation treatments and cool stage, Postharvest Biol. Technol. 7 (1996) 309–316.
[8] N.W. Heather, R.J. Corcoran, R.A. Kopittke, Hot air disinfestation of Australian 'Kensington' mangoes against two fruit flies (Diptera: Tephritidae), Postharvest Biol. Technol. 10 (1997) 99–105.
[9] C.F. Hayes, H. Young, Extension of model to predict survival from heat transfer of papaya infested with oriental fruit flies (Diptera: Tephritidae), J. Econ. Entomol. 82 (1989) 1157–1160.
[10] J.D. Hansen, Heating curve models of quarantine treatments against insect pests, J. Econ. Entomol. 85 (1992) 1846–1854.
[11] S. Wang, J. Tang, R.P. Cavalieri, Modeling fruit internal heating rates for hot air and hot water treatment, Postharvest Biol. Technol. 22 (2001) 257–270.
[12] T. Dermott, D.E. Evans, An evaluation of fluidized-bed heating as a means of disinfesting wheat, J. Stored Prod. Res. 14 (1978) 1–12.
[13] D.E. Evans, T. Dermott, Dosage-mortality relationships for *Rhyzopertha dominica* (F.) (Coleoptera: Bostrychidae) exposed to heat in a fluidized bed, J. Stored Prod. Res. 17 (1981) 53–64.
[14] D.E. Evans, The influence of some biological and physical factors on the heat tolerance relationships for *Rhyzopertha dominica* (F.) and *Sitophilus oryzae* (L.) (Coleoptera: Bostrychidae and Curculionidae), J. Stored Prod. Res. 17 (1981) 65–72.
[15] D.E. Evans, The influence of rate of heating on the mortality of *Rhyzopertha dominica* (F.) (Coleoptera: Bostrychidae), J. Stored Prod. Res. 23 (1987) 73–77.
[16] D.E. Evans, G.R. Thorpe, T. Dermott, The disinfestation of wheat in a continuous-flow fluidized bed, J. Stored Prod. Res. 19 (1983) 125–137.
[17] G.R. Thorpe, The thermodynamic performance of a continuous-flow fluidized bed grain disinfestor and dryer, J. Agric. Eng. Res. 37 (1987) 27–41.
[18] J.K. Claflin, D.E. Evans, A.G. Fane, R.J. Hill, The thermal disinfestation of wheat in a spouted bed, J. Stored Prod. Res. 22 (1986) 153–161.
[19] S.J. Beckett, R. Morton, Mortality of *Rhyzopertha dominica* (F.) (Coleoptera: Bostrychidae) at grain temperatures ranging from 50 °C to 60 °C obtained at different rates of heating in a spouted bed, J. Stored Prod. Res. 39 (2003) 313–332.
[20] J.W. Sutherland, D.E. Evans, A.G. Fane, G.R. Thorpe, Disinfestation of grain with heated air, in: E. Donahaye, S. Navarro (Eds.), Proceeding of the Fourth International Working Conference on Stored-Product Protection, Tel Aviv, Israel, Maor-Wallach Press, Jerusalem, Israel, 1987, pp. 261–274.
[21] J.W. Sutherland, P.W. Fricke, R.J. Hill, The entomological and thermodynamic performance of a pneumatic conveyor wheat disinfestor using hot air, J. Agric. Eng. Res. 44 (1989) 113–124.
[22] H. Mourier, K.P. Poulsen, Control of insects and mites in grain using a high temperature/short time (HTST) technique, J. Stored Prod. Res. 36 (2000) 309–318.
[23] J.M. Vergnaud, Drying of Polymeric and Solid Materials: Modelling and Industrial Application, Springer-Verlag, London, 1992, pp. 13–70.
[24] M.N. Ozisik, Heat Transfer: A Basic Approach, McGraw-Hill, New York, 1985, pp. 124–127.
[25] F. Bowman, Introduction to Bessel Functions, Dover Publications, Inc., New York, 1958, pp. 1–3.
[26] D. Kunii, O. Levenspiel, Fluidization Engineering, second ed., Butterworth-Heinemann, Boston, 1991, Chapter 11, pp. 268–271.
[27] A.S. Mujumdar, Handbook of Industrial Drying, second ed., Marcel Dekker, Inc., New York, 1995. Appendix.
[28] D.B. Brooker, F.W. Bakker, C.W. Hall, Drying and Storage of Grain and Oilseed, AVI, New York, 1992. Appendix E.
[29] C. Laithong, Study of thermo-physical properties of rough rice, M.Sc. Thesis, King Mongkut's Institute of Technology Thonburi, Bangkok, Thailand, 1987.
[30] Z. Pakowski, Z. Bartezak, C. Strumillo, S. Stenstrom, Evaluation of equations approximating thermodynamic and transport properties of water, stream and air for use in CAD of drying processes, Drying Technol. 9 (3) (1991) 753–773.

Available online at www.sciencedirect.com
SCIENCE DIRECT®
Journal of Food Engineering 76 (2006) 327–333
JOURNAL OF FOOD ENGINEERING
www.elsevier.com/locate/jfoodeng

Characteristics of heat transfer in two-dimensional spouted bed

Somkiat Prachayawarakorn [a,*], Samart Ruengnarong [b], Somchart Soponronnarit [b]

[a] *Faculty of Engineering, King Mongkut's University of Technology, Thonburi, Suksawat 48 Road, Bangkok 10140, Thailand*
[b] *School of Energy and Materials, King Mongkut's University of Technology, Thonburi, Suksawat 48 Road, Bangkok 10140, Thailand*

Received 24 January 2005; accepted 19 May 2005
Available online 18 July 2005

Abstract

Heat transfer characteristics in a two-dimensional spouted bed with draft plates were studied using three agricultural materials, paddy, corn and soybean. Increases in inlet superficial velocity and bed porosity result in the increased superficial velocity in downcomer. Heat transfer coefficients for the spout and downcomer were founded to be a function of the superficial velocity and bed depth-to-particle diameter ratio. Two equations correlating heat transfer coefficients for both regions have been developed.
© 2005 Elsevier Ltd. All rights reserved.

Keywords: Heat transfer coefficient; Spouted bed; Draft plates

1. Introduction

Spouted bed is a fluid-particle contactor similar to fluidised bed, but it is different in the sense that fluid is moving through the core region using a nozzle rather than a porous or perforated distributor as in the fluidised bed. The inherent characteristics of spouted bed are composed of the dilute-phase spout zone with the solids moving upwards by co-current gas stream and the dense-phase downcomer zone with the solids moving downwards by counter-current gas stream. Such characteristics result in the contact time between particles and fluid stream being very short in the spout region, and relatively longer in the downcomer zone. These unique characteristics make various types of spouted bed popular for drying heat-sensitive materials (Hung-Nguyen, Driscoll, & Srzednicki, 2001; Madhiyanon, Soponronnarit, & Tia, 2001; Mathur & Epstein, 1974; Zahed & Elsayed, 1993).

To overcome the large pressure drop and instability of the operation that are usually experienced with the conventional spouted beds, the draft plates are inserted at central part of the spouted beds in order to separate the regions between spout and downcomer (Epstein & Grace, 1997; Fane, Wong, & Firek, 1985). This particular configuration takes advantage of the favourable characteristics associated with the conventional type of spouted bed and yet enables to improve the uniformity of the products resulting from the chemical or physical treatment due to the elimination of the back mixing (Eng, Svrcek, & Behie, 1989; Kalwar, Raghavan, & Mujumdar, 1992). The insertion of draft plates results in both hydrodynamic behaviour and subsequent heat transfer characteristics to be changed from those found in the conventional spouted beds. In the present work, the heat transfer characteristics in a two-dimensional spouted bed with draft plates are investigated.

The heat transfer from gas stream to solid particles in a two-dimensional spouted bed occurs in well-defined regions, namely the spout and in the downcomer regions, each of which is governed by different heat transfer mechanisms. Therefore, the heat transfer coefficient for

* Corresponding author. Tel.: +662 4270 9221; fax: +662 428 3534.
E-mail address: somkiat.pra@kmutt.ac.th (S. Prachayawarakorn).

0260-8774/$ - see front matter © 2005 Elsevier Ltd. All rights reserved.
doi:10.1016/j.jfoodeng.2005.05.028

Nomenclature

A	total heat transfer area, m^2
c_g	specific heat capacity of drying medium, J/kg K
c_w	specific heat capacity of water vapour, J/kg K
d_p	particle diameter, m
H	static bed depth, m
h	heat transfer coefficient, W/m^2 K
$\dot{m}_g$	mass flow rate of drying medium, kg/s
$q_{conduct}$	heat conduction from spout to downcomer through draft plates, W
q	heat transfer rate between drying medium and solid particles, W
$q_{loss,s}$	heat loss, W
T	temperature, °C
T_{in}	inlet air temperature, °C
T_{out}	outlet air temperature, °C
$T_{1,ps}$	particle temperature at the spout inlet, °C
$T_{2,ps}$	particle temperature at the spout outlet, °C
U	superficial velocity, m/s
U_{in}	inlet superficial velocity, m/s
V	volume of static bed occupied the solid particles, m^3
w_g	humidity ratio, kg_{H_2O}/kg_{air}
ε	porosity

Subscripts

d	downcomer region
p	particle
s	spout region

each region is determined experimentally and empirically correlated with the operating parameter in a simple form. The calculation of the heat transfer coefficients is principally based on the energy balance equation that requires the data of temperature and volumetric airflow rate in each zone. However, the data of air velocity passing through the downcomer zone was not available in the literature for this dryer type and thus the correlation was determined in the present study, in order to predict the airflow in the downcomer under different operating conditions. Products, namely soybean, paddy and corn were used.

2. Materials and methods

2.1. Spouted bed

The experiments were carried out in a two-dimensional spouted bed with draft plates as shown in Fig. 1. The dryer has a vertical rectangular shape, with an inclined base (60° angle) in order to avoid the dead zone (Passos, Mujumdar, & Raghavan, 1987). The inlet cross sectional area of 4×15 cm^2, drying chamber with a dimension of $60 \times 15 \times 50$ cm, spout width of 8 cm and entrance height of 12.5 cm were used. The selected values of spout width and entrance height could steadily maintain the transport of examined materials in the dryer. A 24 kW electric heater connected to a PID controller with an accuracy of ±1 °C was installed to heat the air up to the desired temperature. A 2.2 kW backward-curved blade centrifugal fan supplied the air and a variable speed unit controlled the air speed passing through the spouted bed. The entire drying system was insulated with the layers of glass wool to minimise heat loss of the system. The dryer front was made of heat-resistant glass to visualise the flow of solid particles.

Before starting the experiments, the system was heated until every part reached the desire temperature. To prevent the entrainment of particles, a deflector was fitted at a height of 142 cm from the dryer base. After the particles hit the deflector, they fell freely to downcomer region.

2.2. Experimental procedure

Paddy, soybean and corn obtained from local markets had the equivalent diameters of 3.7, 7.1 and 7.7 mm, respectively. The initial moisture content of these agricultural materials was in the range of 24–26% dry basis. At this moisture range, the materials did not agglomerate.

Grain samples of each of the above-mentioned crops were dried at temperatures of 130, 140 and 150 °C, inlet air velocities of 40–70 m/s and a bed height of 65 cm. The air velocity was measured with a hot-wire anemometer, with an accuracy of ±0.1 m/s. To measure the superficial air velocity at the downcomer, the equipment was inserted at above bed of particle. Temperature measurements were made with K-type thermocouple connected to a data logger, with an accuracy of ±1 °C. This thermal couple was inserted axially at 20, 40 and 60 cm from the base and at the bottom and top of spout region. The temperatures at the both sides of draft plate were recorded to calculate the heat conducted from the spout to downcomer region.

2.3. Heat-transfer calculation

Determination of heat transfer coefficient in the two-dimensional spouted bed with draft plates is divided into two regions: spout and downcomer. Their calculations are based on experimentally determined temperature

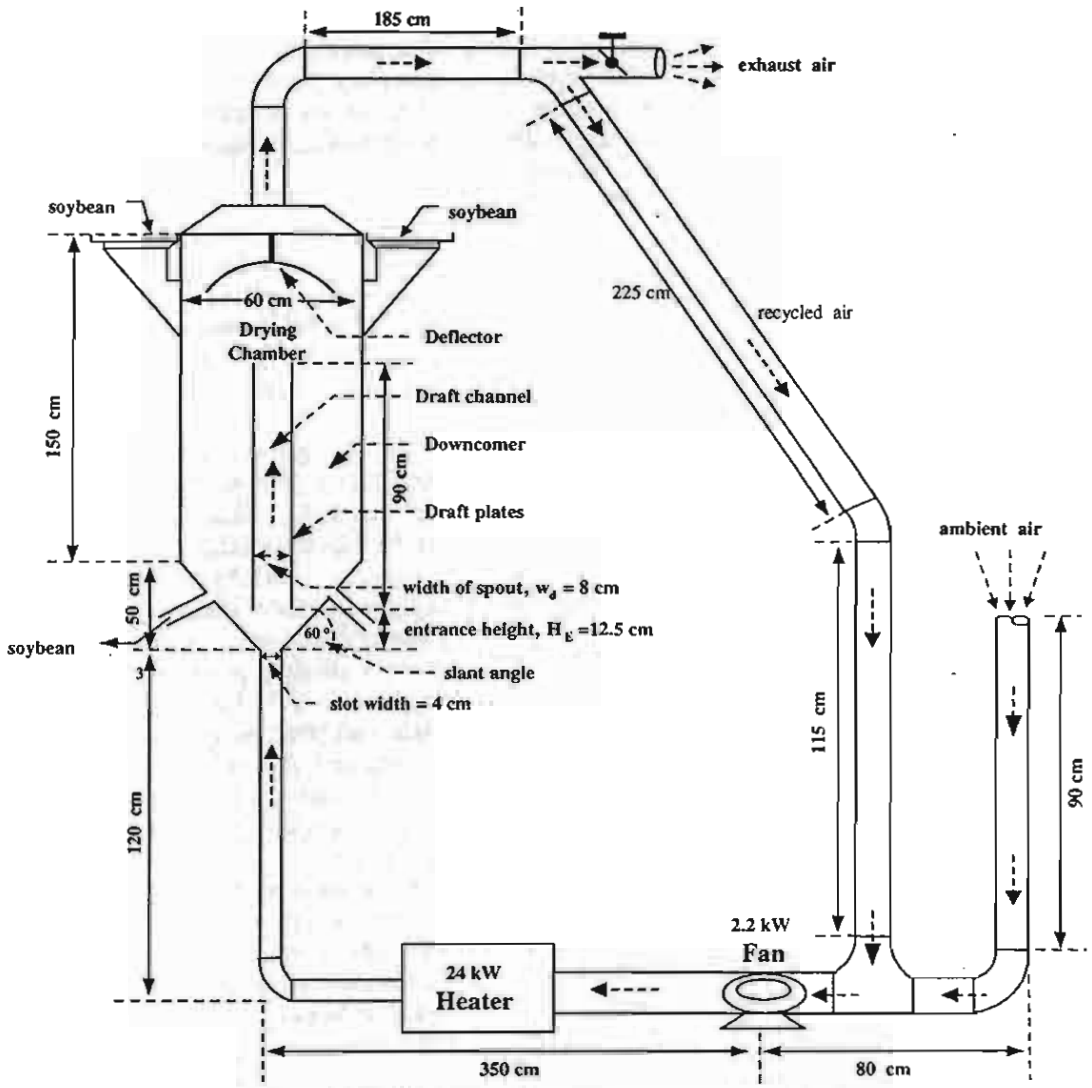


Fig. 1. Schematic diagram of a two-dimensional spouted bed.

for each region and the calculation method is described below.

Considering the transfer of heat in the spout region, the enthalpy change of drying medium is produced from the heat transferred to the solid particles, conducted through the flat plates and dissipated to the environment, yielding

$$q_s = \dot{m}_{gs}(c_g + w_{gs}c_w)(T_{in} - T_{out,s}) - q_{loss,s} - q_{conduct} \quad (1)$$

In writing Eq. (1), we assumed insignificant change of humidity ratio between inlet and outlet air for a small time interval. The heat transfer coefficient in the spout zone is determined by

$$h = \frac{q_s}{A_p \Delta T_{ln,s}} \quad (2)$$

with temperature difference between air and particles represented by logarithm mean

$$\Delta T_{ln,s} = \frac{(T_{in} - T_{1,ps}) - (T_{out,s} - T_{2,ps})}{\ln \frac{(T_{in} - T_{1,ps})}{(T_{out,s} - T_{2,ps})}} \quad (3)$$

The particle temperature at the spout inlet ($T_{1,ps}$) was measured at the bottom of downcomer zone, near the inclined plate before particles enter the spout region, and the particle temperature at the spout outlet ($T_{2,ps}$) was measured at the top of downcomer zone. The K-type thermocouples, connected to the data logger, were inserted at such both positions to record the temperatures. In this work, the total heat-transfer surface area is determined by the following equation:

$$A_s = \frac{6\,V_s}{d_p}(1 - \varepsilon) \quad (4)$$

Paddy, corn and soybean, when loosely packed in the bed, have a porosity of 0.56, 0.41 and 0.36, respectively.

In the downcomer, the particles travelling from the top to the bottom took approximately 12–18 s, depending upon the inlet velocity and material characteristics. During their travelling, the particle temperature did not drop. Eq. (1) was applied again to determine the enthalpy change of air in the downcomer zone and it is written as

$$q_d = \dot{m}_{g\,d}(c_g + w_{g\,d}c_w)(T_{in} - T_{out,d}) - q_{loss,d} + q_{constant} \quad (5)$$

Replacing q_d from Eq. (5) into Eq. (2), the heat transfer coefficient will be obtained. Hence, the mean temperature difference is expressed as

$$\Delta T_{ln,d} = \frac{(T_{in} - T_{pd}) - (T_{out,d} - T_{pd})}{\ln \frac{(T_{in} - T_{pd})}{(T_{out,d} - T_{pd})}} \quad (6)$$

The standard error in the measured values of heat transfer coefficient was in the ranges of 4–14% in the spout and of 2–11% in the downcomer.

3. Results and discussion

3.1. Effect of voids on superficial air velocity in the downcomer

Fig. 2 shows the superficial velocity in the downcomer against the inlet air velocity for three agricultural materials. The amount of air percolating through the downcomer linearly increases with increase of inlet air velocity. In addition, it depends upon the material type through which the air is passing. Thus, highest superficial air velocity occurs in the bed of paddy followed by corn and soybean. The proportion of the air in the downcomer was approximately 28% of total airflow for paddy and 21% for corn and soybean. The larger amount of air flowing through downcomer can be attributed to the larger proportion voids in the material, thus reducing the resistance to airflow and the corresponding pressure drop. The relations between velocities at the downcomer and at the inlet as well as voids can be mathematically described by

$$\frac{U_d}{U_{in}} = 0.0435\varepsilon_d^{0.3} \quad (7)$$

with R^2 of 0.93. Eq. (7) was statistically fitted with the data in the range of voids between 0.36 and 0.56 and inlet velocities between 37 and 52 m/s.

3.2. Heat transfer in spout region

Fig. 3 represents the effect of superficial velocity in the spout region on the heat transfer coefficient under different H_s/d_p ratios. The heat transfer coefficient is related to the superficial velocity in a way that the increase in superficial velocity accelerates the transfer rate of heat to the assembly of the solid particles. This effect was also apparent in some experiments reported by several authors (Freitas & Freire, 2001a; Taranto, Rocha, & Raghavan, 1997). However, the increase of heat transfer coefficient with the superficial velocity seems to be less pronounced for paddy than the other two materials, and a possible explanation can be attributed to the geometric ratio effect, which will be discussed in the following section.

In addition to the spout velocity, the geometric ratio takes the effect on the heat transfer coefficient of which the higher value is associated with the lower H_s/d_p ratio. At the inlet velocity of 22–24 m/s, the heat transfer coefficient increases from 100 to 123 W/m^2 K for corn and from 78 to 80 W/m^2 K for paddy. The higher heat transfer coefficient at the lower H/d_p ratio is due to the turbulence intensity which is related to the size of particle and the amount of particles in the bed or, in the other words, bed depth. The collision of larger particles, at a given bed depth, is stronger which makes a greater turbulence

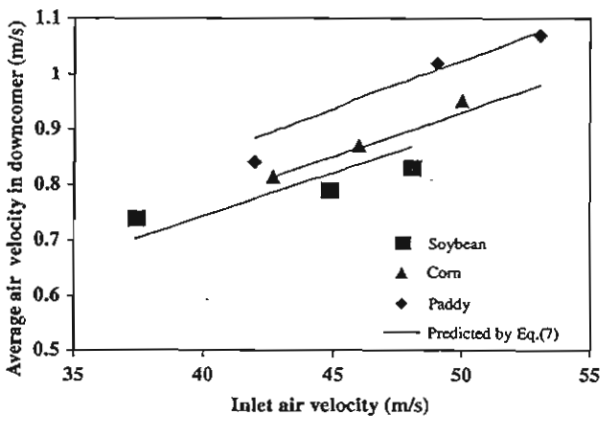


Fig. 2. Relationships between inlet superficial velocity and average velocity in downcomer for different agricultural materials.

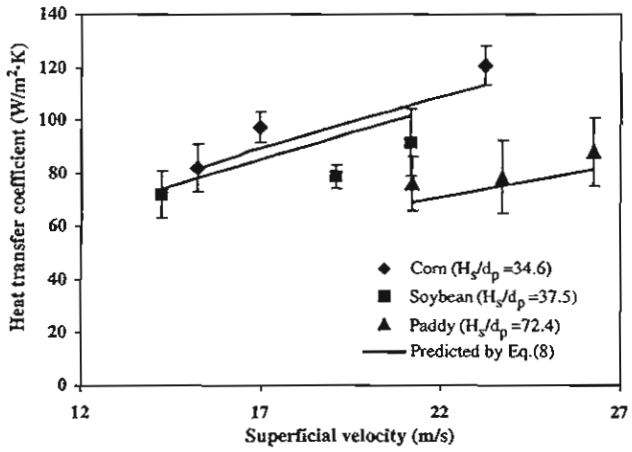


Fig. 3. Effects of superficial velocity in spout region and H_s/d_p ratio on heat transfer coefficient in spout region.

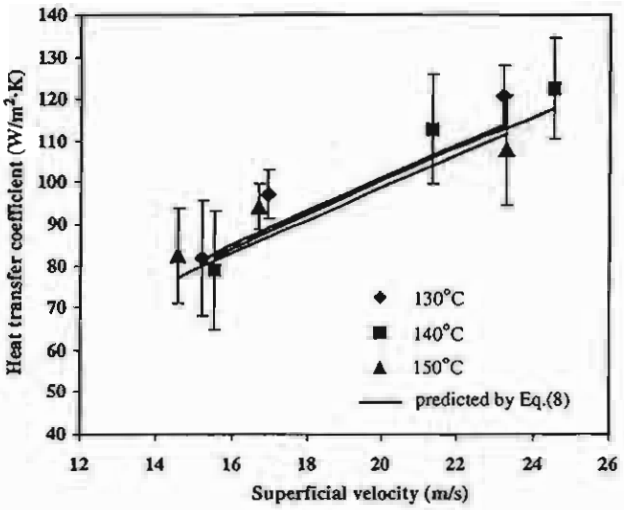


Fig. 4. Effect of inlet air temperature on heat transfer coefficient in spout region at $H_s/dp = 34.6$.

of gas stream in the spout region and reduces the gas film-thermal resistance around the particle surface, thus enhancing the heat transfer coefficient by gas convection. As bed depth is increased, however, the intensity of their impaction diminishes and this results in lower heat transfer coefficient.

In Fig. 4, the heat transfer coefficients at various inlet air temperatures are plotted versus the superficial velocity. The heat transfer coefficients obtained from the experiments at the same superficial velocity are very likely to be identical over the temperature range of 130–150 °C, indicating less important contribution of temperature to the heat transfer coefficient. The dimensional analysis was used to correlate the heat transfer coefficient represented by Nusselt number, Nu, with Reynolds number, Re, and geometric factor, H/d_p. A power form of the function was assumed

$$Nu_s = ARe_{p,s}^{B}\left[\frac{H_s}{d_p}\right]^{c} \tag{8}$$

The values of the constant A and of the power exponents B and C were determined by the method of least square. These values are equal to $A = 0.4$, $B = 0.779$ and $C = -0.81$. The coefficient of determination, R^2, for gas-to-particle heat transfer coefficients was 0.98. Eq. (8) was fitted with the experimental data in the ranges of $2600 < Re_{p,s} < 6800$ and $34.6 < H_s/d_p < 72.4$. The particle Reynolds number was calculated using the superficial velocity measured between the draft plates. The heat transfer coefficient over the range of the parameters studied varied from 57 to 123 W/m^2 K, which was relatively higher than that found in the two-dimensional spouted bed with draft plates, varying from 29 to 74.8 W/m^2 K (Kudra, Mujumdar, Raghavan, & Kalwar, 1990). The higher values in the present work are due to the different methods of determining the value of heat transfer coefficient in which non-separation zone between spout and downcomer was considered in the study described by these authors whilst each zone was taken into account separately in the present study.

The result of fitting Eq. (8) with the experimental data indicates the Reynolds number exponent found to be 0.779 whilst the Reynolds number exponents in conventional spouted beds reported in literature are given in the typical range of 0.47–0.64 (Kmiec, 1975; Kucharski & Kmiec, 1983). This implies the transfer of heat in the spout region for the two-dimensional spouted bed to be governed by the relative combined effects of lamina and turbulent boundary layers. If the laminar boundary layer controls the heat transfer, the Reynolds number exponent is equal to 0.5, which is mostly found in the packed beds. With the prevalent contribution of turbulent boundary layer, the resulting Reynolds number exponent equals 0.82 at which it fulfils with the vertical pneumatic dryer (Bandrowski & Kaczmarzyk, 1978).

Comparison of the heat transfer coefficients from the present work to those from the various kinds of turbulent dryers i.e. cylindrical spouted bed with draft tube, vertical pneumatic dryer and fluidised bed was made. In calculating the heat transfer coefficients, the heat transfer equations developed by several researchers, except for the Shi-Jan-Fous' equation, required the volumetric concentration as input parameter, in addition to the Reynolds number. The volumetric concentrations for paddy, soybean and corn, defined as the ratio of circulation rate of particle to that of flowing air in the spout region, ranged from 0.08 to 0.11. The circulation rate of particles was determined by suddenly interrupting the steadily flowing particles and then mass of particles in the spout region was quantified. The results

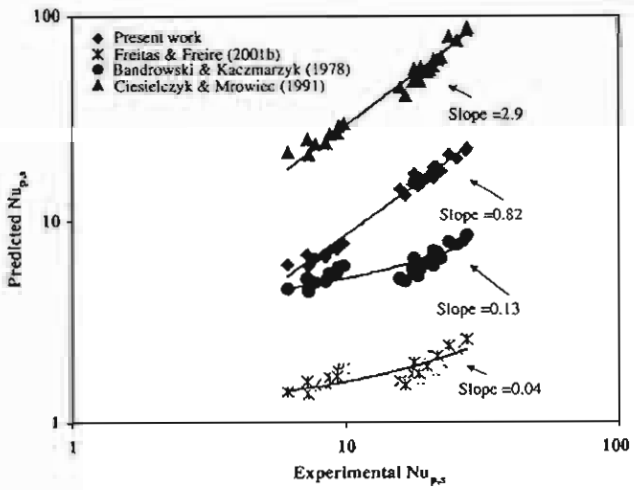


Fig. 5. Predicted and experimental Nusselt numbers in spout region in comparison with other works.

shown in Fig. 5 indicate that the discrepancy of predictions amongst the heat transfer coefficient expressions, when compared with the present results, is considerable in which Shi-Jan-Fous' expression for the fluidised bed, reviewed by Ciesielczyk and Mrowiec (1991), predicts an overestimate as indicated by the slope of 2.9 whereas the prediction by Freitas and Freire (2001b, 'correlation) for the draft-tube spouted bed is an underestimate as pointed out by the slope of 0.04. However, a good agreement is obvious with Bandrowski and Kaczmarzyk (1978, 'correlation), in particular for the low range of Nusselt number that corresponds to the smallest particle size in this study.

3.3. Heat transfer in downcomer

In downcomer, the particles at the bottom before entering the spout regime are in contact with the hottest air stream and on the top are in contact with the colder air stream. The temperatures at the inlet and outlet downcomer zones were measured, for both particles and air streams, in order to calculate the heat transfer coefficient. The effects of superficial velocity and H_d/d_p ratio on heat transfer coefficient for the three types of grain are shown in Fig. 6. The heat transfer coefficient tends to be increased with increasing superficial velocities and with decreasing H_d/d_p ratio, as was found in the spout region, but the increase is weak, in view of the standard errors (2–11%) in the heat transfer coefficient. The scatter of the data could be probably due to the unsmooth flow of the solids, which sometimes occurred during the operation. This problem leads to the error in measurement of porosity.

Fig. 7 shows the effect of inlet air temperature on the heat transfer coefficient, indicating that the temperature

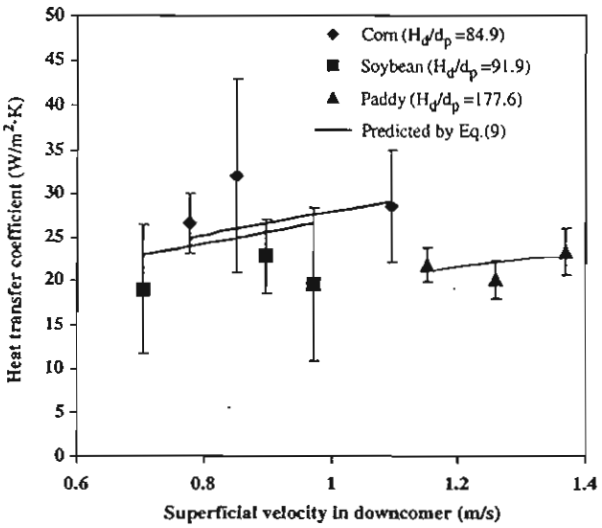


Fig. 6. Effects of superficial velocity in downcomer and H_d/d_p ratio on heat transfer coefficient in downcomer region.

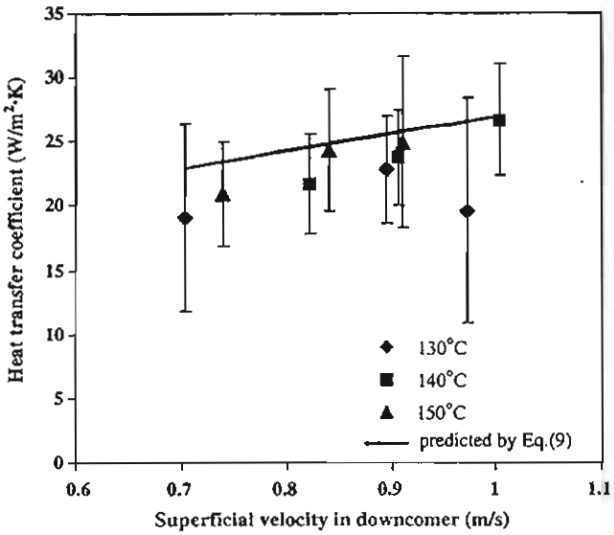


Fig. 7. Effect of inlet air temperature on heat transfer coefficient in downcomer region.

is not an important factor to improve the heat transfer coefficient between the air stream and the solid particle. The heat transfer coefficient in the downcomer is empirically correlated with the relevant parameters using the same equation as Eq. (8). Thus,

$$Nu_d = 42.07 Re_{p,d}^{0.454} \left(\frac{H_d}{d_p}\right)^{-1.006} \quad R^2 = 0.91 \tag{9}$$

The range of applicability is: $150 < Re_{p,d} < 380$; $84 < H_d/d_p < 178$. Under the examined range, the heat transfer coefficient is in between 19 and 32 W/m² K.

Fig. 8 shows the validity of equation proposed and predicted from the correlations of the heat transfer coefficients in the annulus for the classical spouted bed and in the fixed bed. The Nusselt numbers prediction by the equations from published data are prominently above

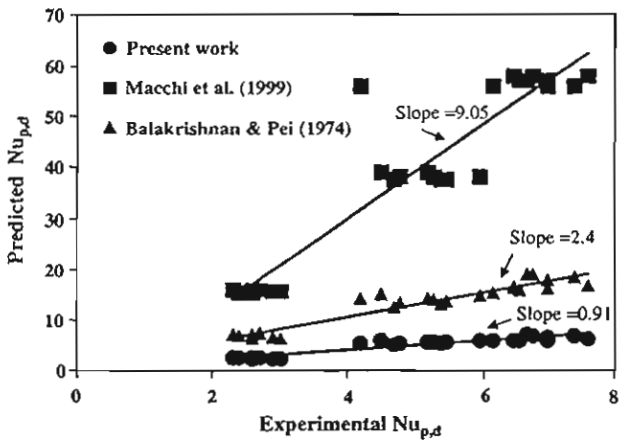


Fig. 8. Predicted and experimental Nusselt numbers in downcomer region in comparison with other works.

the experimental values in this work, as indicated by the slopes of straight line equal to 9.05 for Macchi, Bi, Legros, and Chaouki (1999) and 2.4 for Balakrishnan and Pei (1974). However, the predictable capability by the proposed equation shows a relatively good tendency, with the slope being 0.91. This difference indicates that the use of correlations from other equipment types may not reasonably be applied to predict the heat transfer coefficient in the two-dimensional spouted bed with draft plates.

4. Conclusion

During operation, the air flowing through the two-dimensional spouted bed with draft plates is divided into two directions where the main air stream flows through the draft channel and the minor one flows through the downcomer. The amount of air separated from the main stream is related with the operating parameter in a way that higher airflow rate and bed porosity encourage the larger quantity of air in the downcomer. Such airflow characteristics result in an increase of the heat transfer to the particles in the spout region in comparison with the downcomer, with the heat transfer coefficient being in between 57 and 123 $W/m^2 K$ for the spout region and between 19 and 32 $W/m^2 K$ for the downcomer. The influence of superficial velocity on the heat transfer coefficient is very important for the spout whereas it has a slight effect for the downcomer. The increase of H/d_p ratio with the decrease of heat transfer coefficient is evident whilst the change of inlet air temperature remains constant for both regions. Two equations have been developed by correlating the heat transfer coefficients of each region with the associated parameters. A comparison of heat transfer coefficient in the developed model with the earlier works has shown that the equations of heat transfer coefficient, which have been developed from other equipment types, may not reasonably describe the experimental results for the two-dimensional spouted bed with draft plates.

Acknowledgement

The authors would like to thank the Thailand Research Fund for supporting this work.

References

Balakrishnan, A. R., & Pei, D. C. T. (1974). Heat transfer in fixed beds. *Industrial and Engineering Chemistry Process Design and Development, 13*, 441–446.

Bandrowski, J., & Kaczmarzyk, G. (1978). Gas to particle heat transfer in vertical pneumatic conveying of granular materials. *Chemical Engineering Science, 33*, 1303–1310.

Ciesielczyk, W., & Mrowiec, M. (1991). The method of decreasing the number of experiments needed to design a fluidised bed drying. *Inzynieria Chemiczna I Procesowa (in Polish), 4*, 551–567.

Eng, J. H., Svrcek, W. H., & Behie, L. A. (1989). Dynamic modelling of a spouted bed reactor with a draft plate. *Industrial and Engineering Chemistry Research, 28*, 1778–1785.

Epstein, N., & Grace, J. R. (1997). Spout of particulate solids. In L. Otten (Ed.), *Handbook of Powder Science and Technology* (2nd ed., pp. 532–567). New York, NY: Chapman & Hall.

Fane, A. G., Wong, C. W. P., & Firek, A. E. (1985). Spout with a solids-laden gas stream. In Chemica' 85 (pp. 465–469). Perth, Australia.

Freitas, L. A. P., & Freire, J. T. (2001a). Heat transfer in a draft tube spouted bed with bottom solids feed. *Powder Technology, 114*, 152–162.

Freitas, L. A. P., & Freire, J. T. (2001b). Gas to particle heat transfer in the draft tube of a spouted bed. *Drying Technology, 19*, 1065–1082.

Hung-Nguyen, L., Driscoll, R. H., & Srzednicki, G. (2001). Drying of high moisture content paddy in a pilot scale triangular spouted bed dryer. *Drying Technology, 19*, 375–387.

Kalwar, M. I., Raghavan, G. S. V., & Mujumdar, A. S. (1992). Spout of two-dimensional spouted beds with draft plates. *The Canadian Journal of Chemical Engineering, 70*, 887–894.

Kmiec, A. (1975). Simultaneous heat and mass transfer in spouted beds. *The Canadian Journal of Chemical Engineering, 53*, 18–24.

Kucharski, J., & Kmiec, A. (1983). Hydrodynamics, heat and mass transfer during coating of tablets in spouted Bed. *The Canadian Journal of Chemical Engineering*, 435–439.

Kudra, T., Mujumdar, A. S., Raghavan, G. S. V., & Kalwar, M. I. (1990). Two-dimensional spouted beds for thermal processing of particulates. *Powder Handling and Processing, 2*, 347–353.

Macchi, A., Bi, H. T., Legros, R., & Chaouki, J. (1999). An investigation of heat transfer from a vertical tube in a spouted bed. *The Canadian Journal of Chemical Engineering, 77*, 45–53.

Madhiyanon, T., Soponronnarit, S., & Tia, W. (2001). Industrial-scale prototype of continuous spouted bed paddy dryer. *Drying Technology, 19*, 207–216.

Mathur, K. B., & Epstein, N. (1974). *Spouted beds*. New York: Academic Press, 304 pp.

Passos, M. L., Mujumdar, A. S., & Raghavan, G. S. V. (1987). Spouted beds for drying: principles and design considerations. *Advances in Drying, 4*, 359–397.

Taranto, O. P., Rocha, S. C. S., & Raghavan, G. S. V. (1997). Convective heat transfer during coating of particles in two-dimensional spouted beds. *Drying Technology, 15*, 1909–1918.

Zahed, A. H., & Elsayed, M. M. (1993). Performance of single and multi-stage spouted bed drying systems. *Drying Technology, 11*, 1783–1808.

Drying Technology, 24: 609–617, 2006
Copyright © 2006 Taylor & Francis Group, LLC
ISSN: 0737-3937 print/1532-2300 online
DOI: 10.1080/07373930600626503

Taylor & Francis
Taylor & Francis Group

Paddy Drying Using Adsorption Technique: Experiments and Simulation

Kittisak Witinantakit,[1] Somkiat Prachayawarakorn,[2] Adisak Nathakaranakule,[1] and Somchart Soponronnarit[1]

[1]*School of Energy and Materials, King Mongkut's University of Technology Thonburi, Bangkok, Thailand*
[2]*Faculty of Engineering, King Mongkut's University of Technology Thonburi, Bangkok, Thailand*

Quality of agricultural product can be degraded easily by heat. Heatless drying using an adsorption method may be a possible alternative to grain drying. The experiments of paddy drying using rice husk adsorbent were performed with single and multi-stages. In single stage, where high-moisture paddy were intimately mixed with rice husk in closed containers, high water concentration in the air within the container limits the moisture transfer rate and the resulting moisture content of the sample could not be decreased to the safe level for storage in spite of using low initial moisture content of the adsorbent or increasing the volumetric mixing ratio. However, the moisture content of paddy was reduced to the desire level as the multi-stage, where the adsorbent was physically separated in each stage and then replaced with the new one. The mathematical description of desorption-adsorption processes for a single kernel associated with the mass balance equation on the humidity ratio of the air surrounding the particles was formulated. The predictions of relative humidity and moisture contents of paddy and rice husk were shown to be in agreement with the experiments. The quality parameters, i.e., head-rice yield and rice whiteness obtained from multi-stage drying, were similar to those obtained by shade drying.

Keywords Dehydration; Desiccant; Quality; Rice husk

INTRODUCTION

Hot air drying, commonly used to dry agricultural materials before storage, may cause deterioration of quality for the heat-sensitive products; for example, paddy, corn, and soybean. This work is concentrating on paddy. The drying air at a high temperature can accelerate the rate of moisture evaporation, which induces stresses and consequently creates fissures inside the kernel, thus resulting in decreased head-rice yield after milling.[1–3] To minimize the loss in head-rice yield, tempering of paddy between each drying stage is used practically.[4,5] Tirawanichakul[6] investigated the pasting properties of rice dried at different temperatures by including the tempering stage in the process and found that the pasting properties of dried rice, i.e., peak, final, and setback viscosities, were changed from those of the gently dried one, whereas the head-rice yield could be maintained or improved. The change in the pasting viscosities reflects the starch degradation, and this may have an effect on cooking qualities, such as tenderness and cohesiveness.

In addition to hot air drying, drying using an adsorption technique by which adsorbent is intimately mixed with moist paddy is an alternative approach in reducing moisture content of the paddy to a certain level. In this process, moisture is removed from the grain by pressure differences between the water vapor at the grain surface and the water vapor in the surrounding. This method does not require heat for removing the moisture and the resulting grain quality may not be degraded.

There are various types of adsorbent materials, i.e., silica gel,[7,8] bentonite,[9,10] molecular sieve,[11] and ash,[12] all used to dry agricultural products. Since this method provides a very slow rate of drying, the acceleration of drying is very important. Mass ratio between desiccants and agroproducts and the initial moisture content of the adsorbents and adsorbates[7–11] are found to be affected on the final moisture content of products. The optimum value of mass ratio varies from material to material. Moreover, the particle size and temperature of adsorbent also have influence on the moisture removal.[11]

Generally, the limitation of using adsorbent in adsorption process is the high cost of the adsorbent when compared to the adsorbate. In this work, rice husk is therefore used as an adsorption medium to remove moisture from paddy because of its low cost. In addition, rice husk is a waste material that is available in plenty in the rice mills. The difference between densities of rice husk and paddy enables them to easily separate from each other. The objective of this research is to study the effects of mixing ratio between rice husk and

Correspondence: Kittisak Witinantakit, School of Energy and Materials, King Mongkut's University of Technology Thonburi, 91 Pracha U-tid Road, Bangkok 10140, Thailand; E-mail: k_yong28@hotmail.com

paddy and initial moisture content of rice husk on moisture changes in paddy and to examine qualities of dried paddy in terms of head-rice yield and whiteness. In addition, a mathematical model of paddy drying using rice husk as an adsorbent medium is developed. The predicted results of moisture content and relative humidity of air within airtight closed vessels were compared to the experimental results.

MATHEMATICAL MODEL

The moisture exchange between product and adsorbent in the intimate mixture is first mathematically described by purely or semi-empirical equations, both in the form of exponential function of which the constant parameters depend on system parameters.[10,13] The applicability of these results is, however, particularly limited in the range of experimental conditions studied. This drawback can be avoided when the equation developed from a theoretical point of view is employed. Graham and Bilanski[14] described moisture concentration in grain using the Fick's equation, with convective boundary condition as primarily required for solving the equation. In their model, only a partition parameter, a parameter linking between the equilibrium concentrations in the grain and adsorbent, is determined experimentally.

In this work, the developed mathematical model does not require any parameters from drying experiments with adsorbent material. The changes of moisture in paddy and rice husk are governed by the water content of the existing air within the bin and the Fick's equation is applied to predict their changes. Moreover, the humidity of air within the bulk also varies during mixing, and its change is taken into account on the developed model.

Desorption-adsorption processes between paddy and rice husk simultaneously occurs under isothermal condition in this study. Paddy is well mixed with rice husk. During their mixing, moisture at grain surface evaporates into surrounding air because water vapor pressure at the grain surface is higher than that of surrounding air. Rice husk, concomitantly, adsorbs moisture from surrounding air, with a lower rate than the desorption rate of paddy. To describe their phenomena, mathematical models of moisture desorption for paddy and moisture adsorption for rice husk are therefore separately considered and are described below.

Paddy

With the assumption of a spherical shape for paddy, the movement of moisture in the kernel is mathematically described by Fick's equation:

$$\frac{\partial M_p}{\partial t} = D_p\left[\frac{\partial^2 M_p}{\partial r^2} + \frac{2}{r}\frac{\partial M_p}{\partial r}\right] \tag{1}$$

where D_p is the moisture diffusion coefficient (m^2/s), M_p is the moisture content (decimal dry basis), r is the equivalent radius (m), and t is the mixing time (s).

Initially, the moisture content of paddy is assumed to be spatial uniform. When the paddy is mixed with rice husk, moisture around the grain surface evaporates into the surrounding air due to the vapor pressure difference and the moisture profile is assumed to be symmetrical at the center of the particle. Hence, the initial and the boundary conditions are as follows:

$$M_p = M_{p,i} \quad t = 0,\ 0 \le r \le a \tag{2}$$

$$-D_p\left.\frac{\partial M_p}{\partial r}\right|_{r=a} = h_{m,p}(M_{p,s} - M_{p,e}) \quad t > 0 \tag{3}$$

$$\frac{\partial M_p}{\partial r} = 0 \quad t > 0,\ r = 0 \tag{4}$$

where $h_{m,p}$ is the convective mass transfer coefficient between paddy and surrounding air (m/s), $M_{p,e}$, $M_{p,i}$, and $M_{p,s}$ are the equilibrium moisture content, initial moisture content, and moisture content at the grain surface of paddy (decimal dry basis), respectively; and a is the equivalent radius of sphere (m).

With the above-mentioned boundary conditions, Eq. (1) can be solved by analytical technique. Experimentally, however, relative humidity of the air within the paddy-rice husk mixture changed with the elapsed time, which subsequently affects on the drying rate. A finite difference method (explicit method) is therefore used in this study. A sphere is divided into N intervals, the distance between each node is given at $\Delta r = 3.57 \times 10^{-5}$ m, and the time step is $\Delta t = 1$ s. A finite approximation of Eq. (1) can be expressed by

$$M_{p,i}^{t+1} + M_{p,i}^{t}(2\alpha_p - 1) - M_{p,i+1}^{t}(\alpha_p + \beta_p) + M_{p,i-1}^{t}(\beta_p - \alpha_p) = 0 \tag{5}$$

where

$$\alpha_p = \frac{D_p \Delta t}{\Delta r^2} \tag{6}$$

$$\beta_p = \frac{D_p \Delta t}{i\Delta r^2} \tag{7}$$

Subscripts i and superscripts t refer, respectively, to the spatial nodal grid index and the nodal temporal grid index. Equation (5) is used to calculate the internal node concentrations starting from i = 1 until N − 1. The boundary conditions given by Eqs. (3) and (4) can be written in the finite different forms as:

for i = N at the grain surface

$$M_{p,N}^{t+1}(\gamma_p + 1) - M_{p,N-1}^{t+1} - \gamma_p M_{p,e}^{t+1} = 0 \tag{8}$$

for i = 0 at sphere center

$$M_{p,0}^{t+1} + M_{p,0}^{t}(6\alpha_p - 1) - 6\alpha_p M_{p,1}^{t} = 0 \tag{9}$$

where

$$\gamma_p = \frac{h_{p,m}\Delta r}{D_p} \tag{10}$$

In this study, the grain has an equivalent radius of 0.00175 m and the moisture diffusion coefficient of paddy was obtained from Tirawanichakul[6]

$$D_p = 4.33 \times 10^{-5} \exp\left(\frac{-37099}{RT}\right) \tag{11}$$

The moisture equilibrium for paddy was obtained from Laithong[15]

$$RH = \exp\left[-21803 \exp\left(\frac{-18.7 M_{p,e}}{(RT)}\right)\right] \tag{12}$$

where R is the universal gas constant (kJ/kmol·K), RH is the relative humidity of air (in decimal), and T is the air temperature (K).

The convective mass transfer coefficients between the paddy and the surrounding can be calculated by the following relationship:[16]

$$\frac{\bar{h}_p}{h_{m,p}} = \rho C_p Le^{2/3} \tag{13}$$

where $\bar{h}_p$ is the convection heat transfer coefficient of paddy ($W/m^2 \cdot K$), ρ is the density of air (kg/m^3), C_p is the specific heat capacity of air (kJ/kg·K), and Le is the Lewis number (dimensionless). The Nusselt number of paddy can be calculated by Eq. (14).[16] By assuming that there is no temperature difference between air and paddy, the Rayleigh number in Eq. (15) is thus reduced to zero and the Nusselt number is equal to 2. When Nu is known, convective mass transfer coefficient in Eq. (13) can readily be calculated.

$$\overline{Nu}_p = 2 + \frac{0.589 Ra_p^{1/4}}{\left[1 + (0.469/Pr)^{9/16}\right]^{4/9}}, \quad (Pr \geq 0.7 \text{ and } Ra \leq 10^{11}) \tag{14}$$

$$Ra_p = \frac{g\beta(T_p - T)d_p^3}{\alpha\nu} \tag{15}$$

where k is the thermal conductivity (W/m·K), $\overline{Nu}_p$ is the Nusselt number of paddy (dimensionless), d_p is the diameter of paddy (m), Ra_p is the Rayleigh number of paddy (dimensionless), Pr is the Prandtl number (dimensionless), T_p is the grain temperature (K), g is the gravitational acceleration (m/s^2), β is the volumetric thermal expansion coefficient (1/K), α is the thermal diffusivity of air (m^2/s), and ν is the kinematic viscosity of air (m^2/s).

Rice Husk

A rice husk was considered as an infinite plate with a constant effective diffusion coefficient. The movement of moisture can therefore be explained by the following equation:

$$\frac{\partial M_h}{\partial t} = D_h\left[\frac{\partial^2 M_h}{\partial x^2}\right] \tag{16}$$

where D_h is the moisture diffusion coefficient of rice husk (m^2/s), M_h is the rice husk moisture content (decimal dry basis), and x is the thickness of rice husk (m).

The initial and the boundary conditions were as follows:

$$M_h = M_{h,i} \quad t = 0,\ 0 \leq x \leq \pm L \tag{17}$$

$$\frac{\partial M_h}{\partial x} = 0 \quad t > 0,\ x = 0 \tag{18}$$

The air water vapor adsorbed by rice husk can be expressed by

$$D_h \frac{\partial M_h}{\partial x}\bigg|_{x=\pm L} = h_{m,h}(M_{h,e} - M_{h,s}) \quad t > 0 \tag{19}$$

where $h_{m,h}$ is the convective mass transfer coefficient between rice husk and surrounding (m/s) and $M_{h,e}$, $M_{h,i}$, and $M_{h,s}$ are the equilibrium moisture content, initial moisture content, and moisture content at rice husk surface (decimal dry basis), respectively.

Similar to the method used in calculating the moisture of paddy, the explicit method is applied again and it can be expressed by

for i = 1 to N − 1 at internal node concentrations of infinite plate

$$M_{h,i}^{t+1} + M_{h,i}^{t}(2\alpha_h - 1) - \alpha_h(M_{h,i+1}^{t} + M_{h,i-1}^{t}) = 0 \tag{20}$$

where

$$\alpha_h = \frac{D_h \Delta t}{\Delta x^2} \tag{21}$$

for i = 0 at middle thickness of rice husk

$$M_{h,0}^{t+1} + M_{h,0}^{t}(2\alpha_h - 1) - 2\alpha_h M_{h,1}^{t} = 0 \tag{22}$$

for i = N at the surface of rice husk

$$M_{h,N}^{t+1}(\gamma_h + 1) - M_{h,N-1}^{t+1} - \gamma_h M_{h,e}^{t+1} = 0 \tag{23}$$

where

$$\gamma_h = \frac{h_{h,m}\Delta x}{D_h} \tag{24}$$

In this study, the thickness and the length of rice husk are 0.2 and 5 mm, respectively, and the moisture diffusion

coefficient of rice husk as a function of air temperature was given by Steffe and Singh[17] as follows:

$$D_h = 0.1344 \exp\left(\frac{-7.38 \times 10^3}{T}\right) \quad (25)$$

The moisture equilibrium for rice husk can be written as the following equation:

$$RH = \exp[-5.24 \exp(-25.25 M_{p,e})] \quad (26)$$

Equation (26) was experimentally obtained in the range of 11 to 97% relative humidity at 40°C, using the salt solution.

Nusselt number of the rice husk was obtained from Churchill and Chu.[18]

$$\overline{Nu_h} = \left(0.825 + \frac{0.387 Ra_h^{1/6}}{\left[1 + (0.492/Pr)^{9/16}\right]^{8/27}}\right)^2 \quad (27)$$

where $\overline{Nu_h}$ is the Nusselt number of rice husk (dimensionless), and Ra_h is the Rayleigh number of rice husk (dimensionless). In this study, the experiments were carried out under isothermal condition, thus yielding Ra = 0. Hence, Nu of the rice husk is equal to 0.825.

After knowing the moisture profile inside paddy or rice husk, the average moisture content can then calculated by the following equation:

$$M_{ave} = \frac{1}{V}\int_0^R M(r,t)dV \quad (28)$$

where V is the volume of particle (m^3).

Mass Balance Equation

While paddy and rice husk were being mixed within a closed bin, rice husk adsorbed water vapor, with a relatively lower rate than the rate of water evaporation from paddy, and this enables the increase in the concentration of water vapor in the existing air within the bin or, in other words, the increase in the relative humidity. The change of water concentration can be calculated by making the mass balance of moisture and humidity ratio of air within the bin for a small time interval:

$$m_p(M^t_{p,ave} - M^{t+1}_{p,ave}) = m_h(M^{t+1}_{h,ave} - M^t_{h,ave}) + m_a(W^{t+1}_a - W^t_a) \quad (29)$$

where m_a, m_p, and m_h are, respectively, the dry mass of air, paddy, and rice husk (kg); $M_{p,ave}$ and $M_{h,ave}$ are, respectively, the average moisture contents of paddy and rice husk (decimal dry basis), and W is the humidity ratio (kg water/kg dry air). The humidity ratio and relative humidity are correlated with vapour pressure by the following equations:

$$W_a = \frac{0.622 P_v}{(P - P_v)} \quad (30)$$

$$RH = \frac{P_v}{P_{sat}} \quad (31)$$

where P, P_v, and P_{sat} are, respectively, the pressure of air, vapor, and saturated vapor (kPa).

Calculation Method

The calculation procedure for grain drying using an adsorption technique is shown in Fig. 1. The relative humidity of air at a time $t + \Delta t$ was assumed and the equilibrium moisture contents of paddy and rice husk were then calculated using Eqs. (12) and (26), followed by determining the moisture content at positions inside the paddy and rice husk. After obtaining their average moisture contents, the relative humidity was calculated by Eqs. (30) and (31) and compared with the assumed value. If the difference between assumed and calculated values of relative humidity is higher than 0.005, the calculation was repeated again by assuming the new relative humidity, correlated to the old value plus δ with the value being 0.00001 in this study. Choosing δ is important to solution. If the chosen δ is larger than 0.00001, the solution will be diverged. Iteration method leads to the final values for $M_{p,ave}$, $M_{h,ave}$, and RH.

MATERIALS AND METHODS

Materials

The long grain paddy (Suphanburi 1 *indica* variety) was rewetted to a calculated moisture content of 32–34% d.b. and kept in a cool storage at a temperature range of 4–6°C for a week. For the rice husk, three initial moisture contents, 10.5, 4.5, and 0.9% d.b. were prepared, the highest value being the equilibrium moisture content at ambient temperature. To obtain the desired moisture content of rice husk lower than equilibrium value, the rice husk at 10.5% d.b. was dried overnight using hot air oven at temperatures of 45 and 90°C, which then obtained the moisture content of 4.5 and 0.9% d.b., respectively.

Methods

Before conducting the experiments, the cooled paddy was placed in an ambient environment and hot rice husk was packed in a plastic bag and left in a desiccator until their temperatures were close to the ambient air

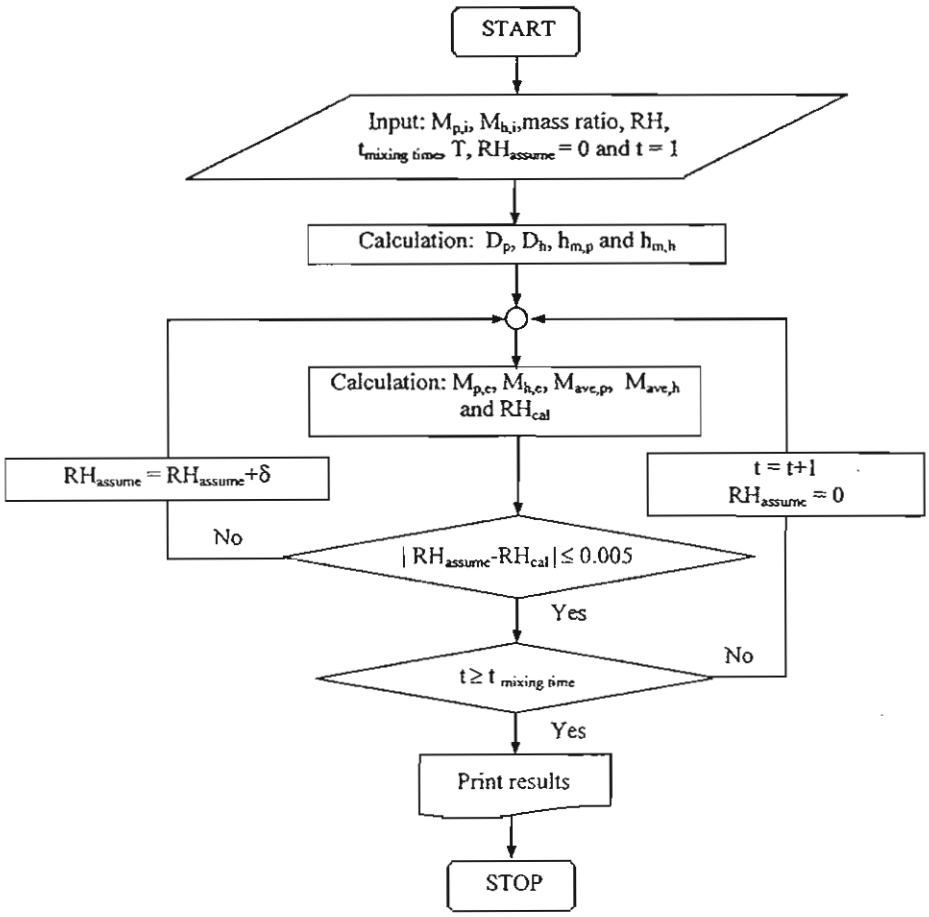


FIG. 1. Block diagram for M and RH calculation.

temperature. Paddy was then mixed with rice husk at the following conditions: the volumetric mixing ratios between rice husk and paddy of 1.0:1, 1.5:1, and 2.0:1 (corresponding to mass ratios of 0.17:1, 0.26:1, and 0.34:1). An intimate mixture of wet paddy and rice husk was packed and sealed in a closed insulated plastic vessel with an inner diameter of 18 cm and an inner height of 22 cm. Temperatures of the mixture were measured by a K-type thermocouple connected to a Yogokawa data logger with an accuracy of ±1°C. Relative humidity of the air in the airtight plastic vessels was measured by a thermo/hygrometer (Sato SK-110TRH) with an accuracy of ±4% RH. In this work, the experiments were performed in single and multi-stages. In single-stage drying, each mixing vessel was opened at drying times of 1, 3, 5, and 7 h and the mixture was separated by an electric fan.

For multi-pass drying, paddy was separated from the rice husk using an electrical fan and then mixed again with the new rice husk every 2 h. The moisture contents of paddy and rice husk were determined by the hot air oven at 103°C for 72 h, according to AOAC.[19] The final moisture content of paddy that was higher than 16.5% d.b. was then dried by ambient air ventilation. Qualities of paddy in terms of head-rice yield and whiteness were determined and compared to the reference samples, which were gently dried by shade drying. The head-rice yield was defined as the ratio of mass of head-rice obtained from milling to mass of paddy before milling. The whiteness value of rice kernel was determined by using a whiteness tester, model Kett C-300-3.

RESULTS AND DISCUSSION

Comparisons between Experiments and Calculations

After the rice husk at the initial moisture contents of 10.5% and 0.9% d.b. was mixed with the high-moisture paddy, the changes of relative humidity and moisture contents of paddy and rice husk were found. Their changes are shown in Fig. 2a for 10.5% d.b. rice husk and Fig. 2b for 0.9% d.b. In Fig. 2a, the temperature and relative humidity

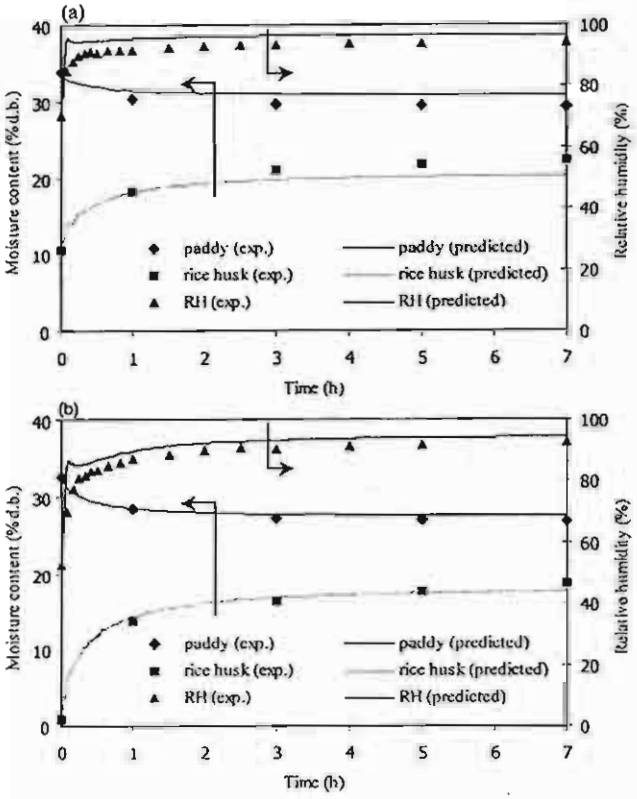


FIG. 2. Comparisons between experimental data and calculations at a volumetric ratio of rice husk to paddy of 1.5:1. (a) Rice husk with initial moisture content of 10.5% d.b.; (b) rice husk with initial moisture content of 0.9% d.b.

of the existing air within the bin at the beginning were 29°C and 70%, respectively. The loss of moisture content of paddy was very rapid in the first 2 h of mixing. This responded to a rapid increase in moisture content of rice husk, from 10.5 to 18.1% d.b., but the increased quantity of moisture of rice husk was not the same amount as the moisture evaporating from the paddy kernel, as directly indicated by the relative humidity, which shows the increasing trend. Beyond 3 h, there are no further changes in moisture contents of paddy and rice husk because the water vapor pressure at the paddy surface and rice husk surface tends toward equilibrium with the partial water vapor pressure in the surrounding air. At the end, the final moisture contents of paddy and rice husk were, respectively, 29.3 and 23.2% d.b., and the relative humidity of air was 96.1%. In addition, the temperature within the bin was increased by 2–3°C after the elapsed time of 7 h, due to the respiration effect.[20] The similar patterns of their changes, i.e., drying characteristic curves and relative humidity were also found with the 0.9% d.b. initial moisture content of rice husk.

These results clearly indicate the diffusional transfer of moisture from paddy to rice husk to be limited by the water

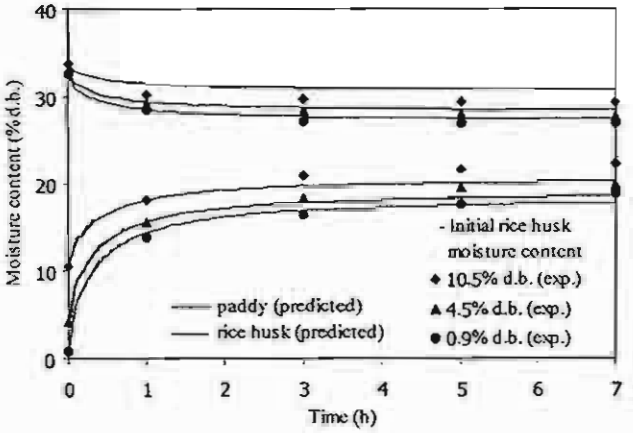


FIG. 3. Effect of initial moisture content of rice husk on drying rate of paddy at a volumetric ratio of rice husk to paddy of 1.5:1.

content in the air, where it has a low water content at the early period, speeding up the desorption-adsorption processes, and has a high water content at the later period, slowing down the processes. This evidence was taken into account in the before-mentioned mathematical model, and the predictions, shown by the solid lines in Fig. 2, reasonably agree with the experiments. The comparisons are also made with the other cases, as will be shown in Figs. 3 and 4.

Effect of Initial Moisture Content of Rice Husk on Moisture Change of Paddy

Since the moisture removal rate from paddy using an adsorption technique is controlled by the resistance in the gas phase, it is important to know how this resistance affects the drying rate when the different initial moisture contents of rice husk are employed. Figure 3 shows the effect of the initial moisture content of rice husk on removal rate of moisture from paddy, indicating that using lower

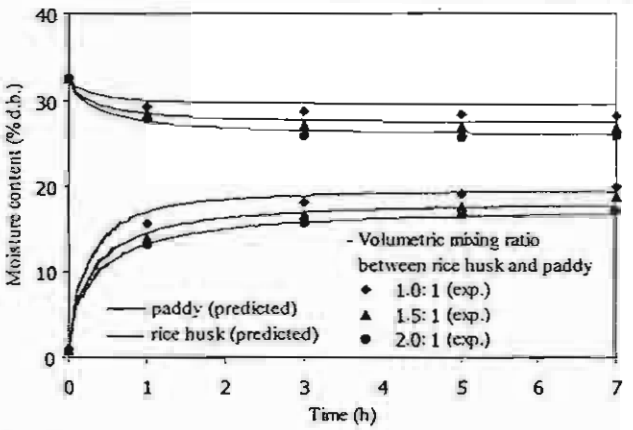


FIG. 4. Moisture changes of paddy and rice husk at various volumetric ratios of rice husk to paddy.

moisture content of adsorbent led to the faster rate of moisture removal from the grain than using higher moisture content of adsorbent. From these drying curves, it can be noticed that less drying potential is evident after 2 h whether the low or high initial moisture content of the adsorbent is applied for drying paddy. The final moisture contents of paddy were 29.3, 27.6, and 26.8% d.b. for the respective rice husk moisture contents of 10.5, 4.5, and 0.9% d.b.

Effect of Volumetric Mixing Ratio between Rice Husk and Paddy on Moisture Change of Paddy

Reducing moisture content of paddy as fast as possible, without any quality loss, is a primary objective in any drying process. One of the possibilities to increase the drying rate of the grain using the adsorption technique can be made by increasing the volumetric mixing ratio of rice husk to paddy. The mixing ratios of 1.0:1.0, 1.5:1.0, and 2.0:1.0, along with an initial moisture content of rice husk of 0.9%d.b., were chosen in this study and the experimental results are illustrated in Fig. 4, indicating that there is a small difference in final moisture content of paddy obtained from the experiments at the volumetric mixing ratios of 1.0 and 1.5 and insignificant difference beyond the mixing ratio of 1.5. The final moisture contents of paddy were 28.1, 26.8, and 25.8% d.b. for the corresponding mixing ratios of 1.0, 1.5, and 2.0. These results indicate that there is a maximum effective contact area between rice husk and paddy and the mixing ratio of 1.5 may appropriately be employed for drying paddy.

Multi-Pass Drying of Paddy

Using rice husk as an adsorbent material could not reduce the moisture content of paddy to the level for safe storage by single-stage drying even though the low initial moisture content of rice husk and the high mixing ratio were used. The remaining moisture content is still higher than 26.8% d.b., which is risk for spoilage by either microorganism infection or yellowing-induced grain respiration. To further reduce the moisture content of paddy, it is necessary to separate the rice husk from the paddy since high relative humidity of the air limits capability of rice husk to adsorb moisture. In this study, the experiments were carried out at the volumetric mixing 1.5 and two initial moisture contents of rice husk, 11.8 and 1.2% d.b.

During the experiments, the temperature within the bin was in a narrow range of 33 to 35°C. The experimental results shown in Fig. 5 indicate that after four or five times of replacement, the moisture content of paddy can be reduced from 34.0 to 25.4% d.b. for the rice husk at initial moisture content of 11.8% d.b. and to 17.8% d.b. for the initial moisture content of 1.2% d.b. Rice husk at initial moisture content of 11.8% d.b. may not be suitable for adsorbing the moisture from paddy since the relative humidity of the air within the bin at the beginning of each

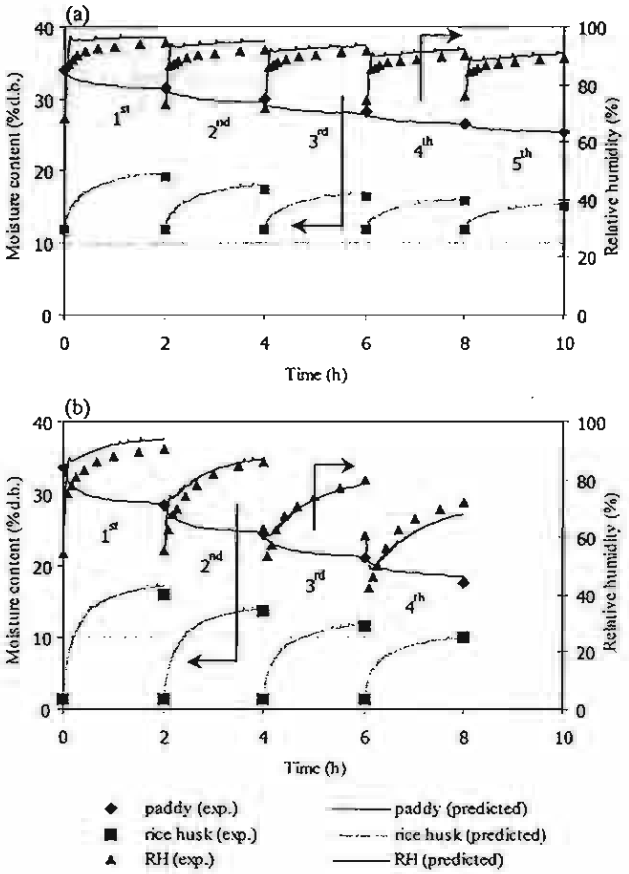


FIG. 5. Comparisons between experimental data and calculations of multi-pass drying at a volumetric ratio of rice husk to paddy of 1.5:1. (a) Initial moisture content of rice husk at 11.8% d.b.; (b) initial moisture content of rice husk at 1.2% d.b.

replacement is in the range of 68 to 76%, which is near the water concentration at the rice husk surface, thereby slowing down the adsorption of moisture from paddy, in particular, at the 4th and 5th replacement. With low initial moisture content of rice husk, on the other hand, although the adsorption rate of rice husk is reduced at the later stage of drying, it still has high potential to adsorb the moisture. This can observe from Fig. 5b where the relative humidity of the air within the bin is relatively reduced from 62 to 42–53% at the beginning of the 3rd and 4th rice husk replacements (at drying times of 6 and 8 h) before it increases again. As shown in Fig. 5b, the final moisture content of paddy at 8 h is slightly higher than the desired final moisture content. To obtain the final moisture content of 16.9% d.b., the volumetric mixing ratio of 2.0 was required; otherwise, the drying time was extended longer for the mixing ratio of 1.5, approximately 1 h from calculation.

Figure 5 also shows the predictions in relative humidity of the air and moisture contents of paddy and rice husk.

TABLE 1
Head-rice yield and rice whiteness from multi-pass drying

Volumetric ratio of rice husk to paddy	Initial rice husk moisture content (% d.b.)	Final paddy moisture content (% d.b.)	Head-rice yield	Rice whiteness
1.5:1	11.8 ± 0.5	25.4 ± 0.2	50.7 ± 0.5	51.0 ± 0.4
	6.6 ± 0.1	20.9 ± 0.3	50.6 ± 0.5	51.8 ± 0.4
	1.2 ± 0.1	17.8 ± 0.1	50.6 ± 0.6	52.4 ± 0.4
2.0:1	11.8 ± 0.5	24.7 ± 0.5	49.6 ± 0.3	52.0 ± 0.5
	6.6 ± 0.1	18.7 ± 0.3	50.8 ± 0.4	52.6 ± 0.3
	1.2 ± 0.1	16.9 ± 0.1	49.8 ± 0.5	52.4 ± 0.1
Reference	—	—	49.6 ± 0.5	51.2 ± 0.3

In calculations, the same mathematical model as mentioned before was used for multi-stages but the initial condition for moisture content inside the kernel for each drying stage was not the same. In multi-modes, the moisture gradient created inside the kernel for each drying stage can be known from the calculation and was then used as input parameter for the subsequent stage. The simulations shown by solid lines were in agreement with the experiment results.

Head-Rice Yield and Rice Whiteness

Head-rice yield and whiteness obtained from the multi-pass drying process at different conditions are shown in Table 1. The values of head-rice yield and whiteness obtained by this technique were around 50, which is insignificantly different to those obtained from the reference samples that were dried by shade drying.

CONCLUSIONS

Single and multi-pass drying of paddy using rice husk as adsorbent were investigated. The faster drying rate and the lower final moisture content of paddy could be accomplished by reducing the initial moisture content of rice husk and increasing the volumetric mixing ratio. For single-stage drying, rice husk could not adsorb the moisture content of paddy to the safe level for storage. In multi-pass drying, however, the moisture content of paddy was reduced to the desired level using the adsorbent with low initial moisture content. The mathematical model of desorption-adsorption processes developed was found to be quite capable of predicting the moisture contents of the paddy and the rice husk and the air relative humidity. Considering qualities, the head-rice yield and whiteness of rice sample produced by multi-stage adsorption processes were similar to those dried by shade drying. The adsorption process using rice husk as adsorbent is technically feasible to replace the hot air drying for reducing high-moisture paddy, with insignificant loss of the quality.

ACKNOWLEDGEMENTS

The authors express their appreciation to the Thailand Research Fund (TRF) and the Japan International Research Center for Agricultural Sciences (JIRCAS) for their financial support, and to the Institute of Food Research and Product Development (IFRPD) of Kasetsart University, Thailand, for rice whiteness testing.

REFERENCES

1. Cnossen, A.G.; Jiménez, M.J.; Siebenmorgen, T.J. Rice fissuring response to high drying and tempering temperatures. Journal of Food Engineering 2003, *59*, 61–69.
2. Bonazzi, C.; du Peuty, M.A.; Themelin, A. Influence of drying conditions on the processing quality of rough rice. Drying Technology 1997, *15* (3&4), 1141–1157.
3. Tirawanichakul, S.; Prachayawarakorn, S.; Varanyanond, W.; Tungtrakul, P.; Soponronnarit, S. Effect of fluidized bed drying temperature on various quality attributes of paddy. Drying Technology 2004, *22* (7), 1731–1754.
4. Poomsa-ad, N.; Soponronnarit, S.; Prachayawarakorn, S.; Terdyothin, A. Effect of tempering on subsequent drying of paddy using fluidisation technique. Drying Technology 2002, *20*, 195–210.
5. Steffe, J.F.; Singh, R.P.; Bakshi, A.S. Influence of tempering time and cooling on rice milling yields and moisture removal. Transactions of the American Society of Agricultural Engineering 1979, *22*, 1214–1218.
6. Tirawanichakul, S. *Influence of Fluidized-Bed Drying Temperature on Chemical and Physical Properties of Paddy*; Ph.D. thesis, King Mongkut's University of Technology Thonburi: Bangkok, 2004.
7. Danziger, M.T.; Steinberg, M.P.; Nelson, A.I. Drying of field corn with silica gel. Transactions of the ASAE 1972, *15* (6), 1071–1074.
8. Yamaguchi, S.; Kawasaki, H. Basic research for rice drying with silica gel. Drying Technology 1994, *12* (5), 1053–1067.
9. Sturton, S.L.; Bilanski, W.K.; Menzies, D.R. Drying of cereal grains with the desiccant bentonite. Canadian Agricultural Engineering 1981, *23*, 101–103.
10. Sturton, S.L.; Bilanski, W.K.; Menzies, D.R. Moisture exchange between corn and the desiccant bentonite in an intimate mixture. Canadian Agricultural Engineering 1983, *25* (1), 139–141.
11. Raghavan, G.S.V.; Alikhani, Z.; Fanous, M.; Block, E. Enhanced grain drying by conduction heating using molecular sieves. Transactions of the ASAE 1988, *31* (4), 1289–1294.
12. Akpaetok, O.I. Drying and storage of cowpeas with ashes in air-tight containers. Journal of Agricultural Engineering Research 1974, *19*, 279–287.

13. Graham, V.A.; Bilanski, W.K.; Menzies, D.R. Adsorption grain drying using bentonite. Transactions of the ASAE 1983, 1512–1515.
14. Graham, V.A.; Bilanski, W.K. Simulation of grain drying in intimate contact with adsorbents. Transactions of the ASAE 1986, *29* (6), 1776–1783.
15. Laithong, C. *Study of Thermo-Physical Properties of Rough Rice*; M.Sc. Thesis, King Mongkut's Institute of Technology Thonburi, Bangkok, 1987.
16. Incropera, F.P.; Dewitt, D.P. *Fundamentals of Heat and Mass Transfers*, 5th Ed; John Wiley & Sons: New York, 2002.
17. Steffe, J.F.; Singh, R.P. Liquid Diffusivity of rough rice components. Transactions of the ASAE 1980, 767–774.
18. Churchill, S.W.; Chu, H.H.S. Correlating equations for laminar and turbulent free convection from a vertical plate. International Journal of Heat and Mass Transfer 1975, *18*, 1323.
19. AOAC. *Official Methods of Analysis*, 16th Ed; Association of Official Analytical Chemists: Washington, DC, 1995.
20. Witinantakit, K.; Prachayawarakorn, S.; Nathakaranakule, A.; Soponronnarit, S. Drying of paddy using rice husk as adsorbent. In *Proc. of ICFPTE'04*; Asian Institute of Technology: Bangkok, Thailand, 11–13 January 2005, 312–319.

The Journal of the Royal Institute of Thailand
Vol. 28 No. 4 Oct.-Dec. 2003



ธันวาคม

การเพิ่มปริมาณต้นข้าวของข้าวคุณภาพต่ำโดยวิธีแช่ร่วมกับการอบแห้งบนฐานไหล

สุทธินี วานิชสำราญ*
พัชรี ตั้งตระกูล+
วารุณี วารัญญานนท์#
สมชาติ โสภณรณฤทธิ์**

งานวิจัยนี้ได้ศึกษาความเป็นไปได้ของการเพิ่มปริมาณต้นข้าวของข้าวคุณภาพต่ำโดยการแช่ร่วมกับการอบแห้งบนฐานไหล, โดยพิจารณาถึงอิทธิพลของระยะเวลาที่ใช้ในการแช่และการอบแห้งข้าวเปลือกต่อการเพิ่มปริมาณต้นข้าว, สี, จุดขาวขุ่นในเมล็ดข้าว, ค่าความแข็งของข้าวสุก, ค่าความเหนียวยึดเกาะตัวของข้าวสุก, ความหนืดของน้ำแป้ง และการเกิดสภาพวุ้น, จากการทดลองโดยใช้ข้าวเปลือกที่มีความชื้นเริ่มต้นร้อยละ ๑๓ ฐานแห้ง (db). แช่ในน้ำอุณหภูมิ ๘๐°ซ เป็นเวลา ๐.๕-๔ ชั่วโมง, แล้วนำมาอบแห้งด้วยเครื่องฐานไหลที่อุณหภูมิอบแห้ง ๑๕๐°ซ เป็นเวลา ๒-๔ นาที. จากนั้นนำข้าวเปลือกไปเก็บในที่อับอากาศเป็นเวลา ๓๐ นาที แล้วนำไปเป่าด้วยอากาศปรกติเป็นเวลา ๑ ชั่วโมง. ผลการศึกษาแสดงว่าการแช่และการอบแห้งบนฐานไหลสามารถเพิ่มปริมาณต้นข้าวได้สูงสุด เมื่อแช่เป็นระยะเวลา ๔ ชั่วโมง และอบแห้ง ๓ นาที, โดยคุณภาพด้านความขาวและปริมาณจุดขาวขุ่นในเมล็ดข้าวอยู่ในเกณฑ์ดี. ความขาวและปริมาณจุดขาวขุ่นในเมล็ดข้าวลดลงตามเวลาที่เพิ่มขึ้นของการแช่และการอบแห้ง. จากการทดสอบเนื้อสัมผัส พบว่าข้าวสุกแข็งและร่วนขึ้น เมื่อใช้เวลาในการอบแห้งมากขึ้น ที่ระยะเวลาการแช่เท่ากัน. นอกจากนี้ยังทำให้ค่าความหนืดสูงสุด และความหนืดสุดท้ายลดลง, แต่ค่าอุณหภูมิเกิดแป้งเปียกสูงขึ้น ในการวิเคราะห์การเกิดสภาพวุ้นด้วยเครื่อง differential scanning calorimeter (DSC) พบว่าข้าวที่แช่นาน ๔ ชั่วโมง เกิดสภาพวุ้นมากกว่าข้าวที่แช่เป็นระยะเวลา ๓ ชั่วโมง โดยมีอัตราการเกิดสภาพวุ้นเท่ากับร้อยละ ๗๔.๘ และ ๖๐.๘ ตามลำดับ

คำสำคัญ: การอบแห้งข้าวเปลือก /คุณภาพข้าว / ฐานไหล

พืชเศรษฐกิจที่สำคัญที่สุดของประเทศไทยในปัจจุบันคือ ข้าว เพราะนอกจากข้าวจะเป็นอาหารหลักของคนไทยแล้ว ข้าวยังเป็นสินค้าส่งออกที่สำคัญ โดยราคาของข้าวจะแปรผันตามคุณภาพของข้าว เช่น ร้อยละต้นข้าว, ความขาวของข้าว, โดยเฉพาะร้อยละต้นข้าวจะมีผลอย่างมากต่อราคาข้าว. ในด้านของข้าวคุณภาพต่ำนั้น เมล็ดข้าวสารที่สีออกมาจะมีสัดส่วนของข้าวหักสูง, ปริมาณต้นข้าวต่ำ.

การแช่ข้าวทำให้เมล็ดดูดน้ำเข้าไปแทนที่อากาศ ซึ่งจะทำให้เม็ดแป้งพองตัวขึ้น. อุณหภูมิของน้ำที่เหมาะสมในการแช่เมล็ดข้าวเปลือกจะอยู่ระหว่าง ๗๕-๘๐°ซ ถ้าน้ำมีอุณหภูมิประมาณ ๗๕°ซ ก็จะแช่ข้าวเปลือกประมาณ ๓-๖ ชั่วโมง หรือถ้าน้ำมีอุณหภูมิ ๘๐°ซ จะแช่ข้าวเปลือกนาน ๑-๓ ชั่วโมง จะทำให้เมล็ดข้าวเปลือกดูดความชื้นได้เพียงพอ[๑]. Ali และ Bhattacharya[๒] ทำการทดลองอบแห้งข้าวเปลือกที่แช่น้ำซึ่งข้าวนั้นมีปริมาณอมีย์โลสสูง โดยอบแห้งด้วย

*นักศึกษาปริญญาโท คณะพลังงานและวัสดุ มหาวิทยาลัยเทคโนโลยีพระจอมเกล้าธนบุรี กรุงเทพฯ
**ราชบัณฑิต สำนักวิทยาศาสตร์ ราชบัณฑิตยสถาน
#นักวิจัยชำนาญการ สถาบันค้นคว้าและพัฒนาผลิตภัณฑ์อาหาร มหาวิทยาลัยเกษตรศาสตร์ กรุงเทพฯ

อากาศร้อนที่อุณหภูมิ ๑๒๐-๒๐๐°ซ. จากการทดลองสรุปได้ว่า การอบแห้งข้าวเปลือกที่ผ่านการแช่น้ำที่อุณหภูมิสูงเป็นเวลาสั้นๆ สามารถทำให้ข้าวคล้ายข้าวนึ่งได้ และความชื้นหลังการอบแห้งควรมีค่าสูงกว่าร้อยละ ๒๐ ฐานเปียก (wb), ร้อยละการแตกของข้าวที่ได้น้อยกว่าร้อยละ ๕. Velupillai และ Verma[๓] ได้ทำการศึกษาการอบแห้งและการเทมเปอร์ ข้าวนึ่งที่มีผลต่อคุณภาพของข้าวนึ่ง ที่ช่วงอุณหภูมิอบแห้ง ๖๕-๑๔๐°ซ สรุปได้ว่าการเทมเปอร์ ช่วยให้อัตราร้อยละต้นข้าวเพิ่มขึ้น แต่จะทำให้สีของข้าวนึ่งคล้ำขึ้นเล็กน้อย. สมชาติ โสภณรณฤทธิ์ และคณะ[๔] ได้ทำการศึกษาสมรรถนะเครื่องอบแห้งข้าวเปลือกแบบฐานไหลโดยใช้อุณหภูมิในการอบแห้ง ๖๐-๑๒๐°ซ อบแห้งจนเหลือความชื้นสุดท้ายร้อยละ ๒๒ ฐานแห้ง (db). ความสูงเบดที่ใช้ ๙.๕ เซนติเมตร และพบว่าการอบแห้งที่อุณหภูมิสูงถึง ๑๔๐°ซ คุณภาพของข้าวเปลือกก็ยังอยู่ในเกณฑ์ที่ยอมรับได้. สมชาติ โสภณรณฤทธิ์ และคณะ[๕] ได้ทำการศึกษาต่อเนื่องโดยอบแห้งข้าวเปลือกที่อุณหภูมิ ๑๔๐ และ ๑๕๐°ซ พบว่า สามารถเพิ่มปริมาณต้นข้าวได้และมีค่าใกล้เคียงกัน โดยที่ปริมาณข้าวต้นจะสูงสุดเมื่อข้าวเปลือกมีความชื้นสุดท้ายอยู่ในช่วงร้อยละ ๑๙-๒๒ ฐานเปียก และได้มีการศึกษาต่อเนื่องโดยทำการอบแห้งข้าวเปลือกที่มีความชื้นเริ่มต้นร้อยละ ๔๔.๓ ฐานแห้งที่อุณหภูมิ ๑๕๐°ซ พบว่าอัตราร้อยละต้นข้าวเพิ่มขึ้น ซึ่งคล้ายกับงานของอดิเทพ ทวีรัตน-พาณิชย์ และคณะ[๖] ที่ได้ทำการอบแห้งในช่วงอุณหภูมิ ๑๔๐-๑๕๐°ซ พบว่า สามารถเพิ่มร้อยละต้นข้าวได้ เมื่อความชื้นข้าวเปลือกหลังการอบแห้งอยู่ในช่วงร้อยละ ๒๕-๒๘ ฐานแห้ง และช่วงความชื้นข้าวเปลือกเริ่มต้นที่เหมาะสมควรอยู่ระหว่างร้อยละ ๓๐-๔๕ ฐานแห้ง. สมชาติ โสภณรณฤทธิ์ และคณะ.[๗] และ Zhang และ Litchfield[๘] แนะนำว่าควรมีการเทมเปอร์ข้าวเปลือกก่อนการอบแห้งในช่วงที่ ๒ หรือเป่าด้วยอากาศแวดล้อม เพื่อเพิ่มสมรรถนะในการอบแห้งและรักษาคุณภาพข้าวเปลือก และระยะเวลาในการเทมเปอร์ข้าวเปลือกที่เหมาะสมควรมีอย่างน้อย ๓๐ นาที แต่ไม่ควรเกิน ๑ ชั่วโมง, ความเร็วของอากาศในช่วงการเป่าด้วยอากาศปรกติประมาณ ๐.๑๕ เมตร/วินาที.

จากผลงานวิจัยที่ผ่านมาอาจสรุปได้ว่า มีความเป็นไปได้ในการทำให้ร้อยละต้นข้าวเพิ่มขึ้นโดยการแช่ข้าวเปลือกในน้ำร้อน, การอบแห้งบนฐานไหลที่อุณหภูมิ ๑๕๐°ซ, การเก็บในที่อับอากาศ และการเป่าด้วยอากาศแวดล้อม. ดังนั้นงานวิจัยนี้จึงได้ศึกษาหาแนวทางที่เหมาะสมสำหรับการเพิ่มปริมาณต้นข้าวโดยการแช่ร่วมกับการอบแห้งบนฐานไหล และศึกษาระยะเวลาที่ใช้ในการแช่และการอบแห้งข้าวเปลือก รวมทั้งศึกษาถึงคุณภาพของข้าว, สมบัติการหุงต้มและการบริโภคข้าว, และลักษณะเคมีกายภาพบางประการของข้าว.

อุปกรณ์และวิธีการทดลอง

ในการทดลองอบแห้งข้าวเปลือกด้วยอากาศร้อนจะใช้เครื่องอบแห้งบนฐานไหลแบบงวด ซึ่งมีส่วนประกอบดังนี้

การทดลองอบแห้งด้วยอากาศร้อนใช้เครื่องอบแห้งฐานไหลแบบงวด (แสดงรายละเอียดในรูปที่ ๑). ห้องอบแห้งเป็นรูปทรงกระบอก มีขนาดเส้นผ่านศูนย์กลาง ๒๐ ซม. บริเวณผิวห้องอบแห้งและระบบท่อหุ้มด้วยฉนวนใยแก้วหนาประมาณ ๒.๕ มม. อุปกรณ์ให้ความร้อนใช้ขดลวดความร้อน ๑๒ กิโลวัตต์ ใช้พัดลมแบบแรงเหวี่ยงหนีศูนย์ ใบพัดโค้งหลัง, มอเตอร์ขับขนาด ๑.๕ กิโลวัตต์, สามารถปรับรอบความเร็วได้. อุปกรณ์วัดอุณหภูมิที่ทางเข้าห้องอบแห้ง ใช้เทอร์โมคัปเปิลชนิด K ต่อเข้ากับเครื่องควบคุมอุณหภูมิ เพื่อควบคุมอุณหภูมิในการอบแห้งให้ได้ ±๐.๑°ซ, ที่ช่องทางป้อนข้าวเปลือกติดตั้งด้านบนห้องอบแห้งมีขนาดเส้นผ่านศูนย์กลาง ๗.๖ ซม.

การเตรียมข้าวเปลือกชื้นใช้ข้าวเปลือกพันธุ์ กข๓๕ ซึ่งมีความชื้นเริ่มต้นก่อนแช่ประมาณร้อยละ ๑๓ ฐานแห้ง ใส่ในถังกลมขนาดประมาณ ๕๐ ลิตร หุ้มด้วยฉนวนใยแก้ว (เพื่อรักษาอุณหภูมิของน้ำในถังแช่) แล้วใส่น้ำร้อนที่มีอุณหภูมิเริ่มต้น ๘๐°ซ แช่ข้าวเปลือกทิ้งไว้นาน ๐.๕, ๑, ๒, ๓ และ ๔ ชั่วโมง แล้วจึงระบายน้ำแช่ทิ้งและปล่อยข้าวเปลือกทิ้งไว้บ่มในถังแช่ (tempering) อีก ๑ ชั่วโมงก่อนที่จะนำข้าวเปลือกชื้นไปทดลองอบแห้ง.

ในการอบแห้งข้าวเปลือกใช้เทคนิคทำให้เกิดการไหลด้วยความเร็วลมภายในฐาน ๒.๕ เมตร/วินาที (ความถูกต้อง ± ๐.๑ เมตร/วินาที), อุณหภูมิอบแห้ง ๑๕๐°ซ (ความถูกต้อง ± ๑°ซ), ความสูงของฐาน ๙.๕ ซม. และอบแห้งนาน ๒, ๓ และ ๔ นาที, แล้วนำข้าวเปลือกที่ผ่านการอบแห้งมาผ่านกระบวนการบ่ม โดยปล่อยให้ไหลเข้ามายังขวดแก้วขนาดเส้นผ่านศูนย์กลาง ๑๐ ซม. สูง ๑๐ ซม. ซึ่งสามารถปิดสนิทและทนความดันไม่ให้เกิดการรั่วได้ เพื่อป้องกันการถ่ายเทมวลสู่สิ่งแวดล้อม โดยขวดแก้วผ่านการอบให้มีอุณหภูมิเท่ากับอุณหภูมิของข้าวเปลือกขณะที่ออกจากเครื่องอบแห้ง. ต่อจากนั้นนำขวดแก้วภายในบรรจุข้าวเปลือกกลับเข้าตู้อบซึ่งควบคุมอุณหภูมิให้เท่ากับอุณหภูมิของเมล็ดข้าวเปลือกที่ออกจากเครื่องอบเพื่อป้องกันการถ่ายเทความร้อนกับสิ่งแวดล้อมเป็นระยะเวลา ๓๐ นาที. จากนั้นนำมาเป่าด้วยอากาศแวดล้อมเป็นระยะเวลา ๑ ชั่วโมง. เก็บตัวอย่างข้าวเปลือกไว้ที่อุณหภูมิแวดล้อมประมาณ ๑๔ วัน แล้วจึงนำไปทดสอบคุณภาพการสี.

ก่อนและหลังการอบแห้ง ข้าวเปลือกประมาณ ๓๐ กรัม ถูกนำมาหาความชื้นโดยการอบที่อุณหภูมิ ๑๐๓ °ซ เป็นเวลา ๗๒ ชั่วโมง สำหรับคุณภาพของข้าวทางด้านกายภาพทำการวิเคราะห์ค่าร้อยละต้นข้าว, ปริมาณจุดขาวขุ่นในเมล็ดข้าว (white belly) และความขาว.

- ร้อยละต้นข้าว คือ น้ำหนักของข้าวต้นที่ผ่านการอบแห้งหารด้วยน้ำหนักข้าวเปลือก

- ความขาววัดได้จากเครื่องวัดความขาว Kett C-300

- White belly คือ จำนวนข้าวที่มีจุดขาวขุ่นในเมล็ด โดยการสุ่มตัวอย่าง ๑๐๐ เมล็ด ทำซ้ำ ๓ครั้ง.

การวัดค่าการยึดเกาะตัวและค่าความแข็งของข้าวสุกโดยใช้เครื่อง Texture Analyzer รุ่น TA-XT๒i ใช้หัววัด Ottawa cell load cell ๕๐ กิโลกรัม นำข้าวสาร ๓๐ กรัม ใส่ถ้วยอลูมิเนียมแล้วนำไปซาวแล้วเทน้ำทิ้ง. จากนั้นใส่น้ำกลั่นด้วยอัตราส่วนข้าวต่อน้ำเป็น ๑:๑.๗ แล้วนำไปหุงรอจนข้าวสุก พักทิ้งไว้ ๑๐ นาที. จากนั้นนำข้าวสุกที่ได้จากการหุงประมาณ ๓๐ กรัม ใส่ลงในตะแกรงสำหรับใส่ข้าวเพื่อทดสอบ แล้วเกลี่ยให้หน้าเรียบเท่ากัน เครื่องจะทำการกดอัดข้าวและแสดงค่าความแข็งของข้าวสุกและค่าความเหนียวยึดเกาะตัวของข้าวสุก ในหน่วย kg.f ทำการทดลองซ้ำตัวอย่างละ ๒ ครั้ง.

การวัดสมบัติการเป็นแป้งเปียก (pasting) ของข้าวโดยใช้เครื่อง rapid visco analyzer (Newport Scientific Pty Ltd., Warriewood, Australia) โดยการนำตัวอย่างแป้งข้าว ๓ กรัม (ทศนิยม ๔ ตำแหน่ง) ที่ความชื้นร้อยละ ๑๒ ฐานแห้ง ใส่ผสมกับน้ำกลั่นในถ้วยอลูมินัม ใส่พายลงในกระป๋องและนำตัวอย่างที่เตรียมได้เข้าเครื่อง RVA. ตัวอย่างจะถูกทำให้ร้อนที่ ๕๐°ซ เป็นเวลา ๑ นาที. ต่อจากนั้นให้ความร้อนแก่ของผสมด้วยอัตรา ๑๒°ซ/นาที ไปที่อุณหภูมิ ๙๕°ซ คงไว้ที่อุณหภูมิ ๙๕°ซ เป็นเวลา ๒.๕ นาที จากนั้นถูกทำให้เย็นลงมาที่ ๕๐°ซ ด้วยอัตรา ๑๒°ซ/นาที แล้วคงไว้ที่ ๙๕°ซ เป็นเวลา ๒ นาที. ตัวอย่างดังกล่าวทดสอบซ้ำ ๖ ครั้ง, แล้วนำมาวิเคราะห์ทางสถิติ. สมบัติการเป็นแป้งเปียกต่างๆ ถูก plot เทียบกับเวลา. ค่าที่ได้จากสมบัติแป้งเปียกได้แก่ อุณหภูมิแป้งเปียก, ความหนืดสูงสุด และความหนืดสุดท้าย.

การวิเคราะห์การเกิดสภาพวุ้นของข้าวโดยใช้เครื่อง differential scanning calorimeter (DSC) โดยการเตรียมตัวอย่างแป้งข้าวที่ทราบความชื้นแน่นอน โดยทำเป็นสารละลายให้มีความเข้มข้นร้อยละ ๓๐ โดยน้ำหนักแห้ง ด้วยน้ำกลั่น ดูดสารละลายแป้งให้มีปริมาณ ๓.๕-๔ มิลลิกรัม (โดยน้ำหนักแห้ง) ใส่ในถาดอลูมิเนียมของเครื่อง DSC บ่มไว้ประมาณ ๑ ชั่วโมง. จากนั้นนำถาดใส่ในช่องตัวอย่างของเครื่อง DSC และวาง reference indium pan โดยให้ profile อุณหภูมิ ๒๕-๑๐๐°ซ ที่อัตรา ๕°ซ/นาที. บันทึกค่าต่างๆ ที่เกี่ยวข้องกับการเกิดสภาพวุ้นซึ่งได้แก่ อุณหภูมิเริ่มต้นในการเกิดสภาพวุ้น (onset temperature, T_O), อุณหภูมิสูงสุดในการเกิดสภาพวุ้น (peak temperature, T_P), อุณหภูมิสุดท้ายในการเกิดสภาพวุ้น (conclusion temperature, T_C) และพลังงานที่เปลี่ยนแปลงระหว่างการเกิดสภาพวุ้น (Enthalpy, $\triangle H$, J/g) โดยอัตราร้อยละของการเกิดสภาพวุ้นคำนวณได้จาก

Degree of gelatinization = $[1 - (\triangle H/\triangle H^{\circ})] \times 100$

$\triangle H$ คือ ค่าเอนทัลปีของแป้งที่เกิดสภาพวุ้น (J/g) และ $\triangle H^{\circ}$ คือ ค่าเอนทัลปีของแป้งที่ไม่เกิดสภาพวุ้น (J/g)

ผลการทดลองและวิจารณ์

จากผลการทดลองแช่ข้าวในน้ำอุณหภูมิเริ่มต้น ๘๐°ซ เป็นเวลานาน ๐.๕-๔ ชั่วโมง จากนั้นนำไปอบแห้งแบบฟลูอิไดซ์เบดที่อุณหภูมิอบแห้ง ๑๕๐°ซ เป็นเวลา ๒-๔ นาที แล้วทำการเก็บข้าวเปลือกในที่อับอากาศเป็นเวลา ๓๐ นาที แล้วนำไปเป่าด้วยอากาศแวดล้อมเป็นเวลา ๑ ชั่วโมง พบว่า การเปลี่ยนแปลงความชื้นและอุณหภูมิของเมล็ดข้าวเปลือก, ร้อยละต้นข้าว, ความขาวของข้าวสาร, ร้อยละของเมล็ดข้าวที่มีจุดขาวขุ่น, ค่าความแข็ง, ค่าความเหนียวยึดเกาะตัวของข้าวสุก, ความหนืดของแป้งข้าว และการเกิดสภาพวุ้นของข้าวโดยใช้เครื่อง DSC มีรายละเอียดดังแสดงในรูปที่ ๒-๖ และตารางที่ ๑-๖.

การเปลี่ยนแปลงความชื้นและอุณหภูมิของเมล็ดข้าวเปลือก

การเปลี่ยนแปลงความชื้นและอุณหภูมิของเมล็ดข้าวเปลือกแสดงดังรูปที่ ๒ จะเห็นว่าความชื้นของเมล็ดข้าวเปลือกหลังการแช่จะเพิ่มขึ้นตามระยะเวลาในการแช่ และเมื่อนำไปอบแห้งที่เวลาต่างกันพบว่า ความชื้นของข้าวเปลือกหลังอบแห้งที่แช่เป็น

ตารางที่ ๑ ผลการทดสอบความแข็งของข้าวสุก

ระยะเวลาแช่ข้าว (ชั่วโมง)	ความแข็งของข้าวสุก kg.f ข้าวที่อบแห้งระยะเวลาต่าง ๆ (นาที)			
	๐	๒	๓	๔
๐	๒๑.๙๗	-	-	-
๐.๕	-	๒๓.๘๖	๒๗.๐๔	๒๓.๘๑
๑	-	๒๓.๕๒	๒๗.๑๐	๒๗.๒๖
๒	-	๒๔.๔๔	๒๗.๐๗	๒๗.๒๔
๓	-	๒๕.๐๒	๒๕.๘๖	๓๑.๒๖
๔	-	๒๕.๒๒	๒๖.๐๕	๓๑.๒๔

ตารางที่ ๒ ผลการทดสอบความเหนียวยึดเกาะตัวของข้าวสุก

ระยะเวลาแช่ข้าว (ชั่วโมง)	การยึดเกาะตัวของข้าวสุก kg.f ข้าวที่อบแห้งระยะเวลาต่าง ๆ (นาที)			
	๐	๒	๓	๔
๐	๑.๑๕	-	-	-
๐.๕	-	๐.๙๘	๐.๘๕	๐.๓๑
๑	-	๐.๙๑	๐.๘๙	๐.๖๓
๒	-	๐.๗๒	๐.๕๙	๐.๕๒
๓	-	๐.๘๗	๐.๘๐	๐.๖๕
๔	-	๐.๘๙	๐.๗๒	๐.๕๘

ตารางที่ ๓ การเปรียบเทียบอุณหภูมิเริ่มเกิดความหนืดของแป้งข้าวที่ใช้เวลาในการแช่และการอบแห้งต่างกัน

ระยะเวลาแช่ข้าว (ชั่วโมง)	อุณหภูมิเกิดแป้งเปียก (°ซ) ข้าวที่อบแห้งระยะเวลาต่าง ๆ (นาที)			
	๐	๒	๓	๔
๐	๗๙.๙g	-	-	-
๐.๕	๘๐.๑fg	๘๑.๖efg	๘๒.๒ef	๘๖.๓ab
๑	๘๐.๒fg	๘๒.๐ef	๘๓.๕cde	๘๖.๓ab
๒	๘๐.๒fg	๘๒.๐ef	๘๔.๔bcd	๘๖.๗a
๓	๘๐.๗fg	๘๑.๙efg	๘๓.๑de	๘๕.๕ab
๔	๘๐.๖fg	๘๑.๕efg	๘๓.๒de	๘๕.๒abc

ตารางที่ ๔ การเปรียบเทียบความหนืดสูงสุดของแป้งข้าวที่ใช้เวลาในการแช่และการอบแห้งต่างกัน

ระยะเวลาแช่ข้าว (ชั่วโมง)	ความหนืดสูงสุด (RVU) ข้าวที่อบแห้งระยะเวลาต่าง ๆ (นาที)			
	๐	๒	๓	๕
๐	๒๔๗.๔a	-	-	-
๐.๕	๒๓๗.๗b	๑๘๔.๑c	๑๒๓.๕e	๘๙.๗hi
๑	๒๓๕.๕b	๑๖๖.๕d	๑๑๒.๑f	๘๘.๔i
๒	๒๔๐.๖ab	๑๖๔.๙d	๑๒๓.๘e	๘๖.๖i
๓	๒๓๘.๗b	๑๖๓.๒d	๑๒๕.๖e	๙๘.๑g
๔	๒๔๑.๖ab	๑๖๖.๕d	๑๒๕.๐e	๙๖.๙gh

หมายเหตุ : *ตัวเลขที่ตามด้วยตัวอักษรที่แตกต่างกันแสดงว่ามีความแตกต่างกันทางสถิติที่ระดับความเชื่อมั่น ๙๕%*

ตารางที่ ๕ การเปรียบเทียบความหนืดสุดท้ายของแป้งข้าวที่ใช้เวลาในการแช่และการอบแห้งต่างกัน

ระยะเวลาแช่ข้าว (ชั่วโมง)	ความหนืดสุดท้าย (RVU) ข้าวที่อบแห้งระยะเวลาต่าง ๆ (นาที)			
	๐	๒	๓	๕
๐	๓๑๙.๖a	-	-	-
๐.๕	๓๑๒.๗a	๒๗๓.๓b	๒๑๕.๙d	๑๕๑.๔g
๑	๓๐๙.๑a	๒๕๕.๐c	๑๗๔.๕f	๑๕๐.๔g
๒	๓๑๒.๑a	๒๔๗.๘c	๒๐๖.๒de	๑๔๘.๙g
๓	๓๑๔.๐a	๒๔๗.๑c	๒๐๒.๔de	๑๖๒.๗fg
๔	๓๑๖.๑a	๒๔๐.๕c	๑๙๘.๗e	๑๕๙.๘fg

หมายเหตุ : *ตัวเลขที่ตามด้วยตัวอักษรที่แตกต่างกันแสดงว่ามีความแตกต่างกันทางสถิติที่ระดับความเชื่อมั่น ๙๕%*

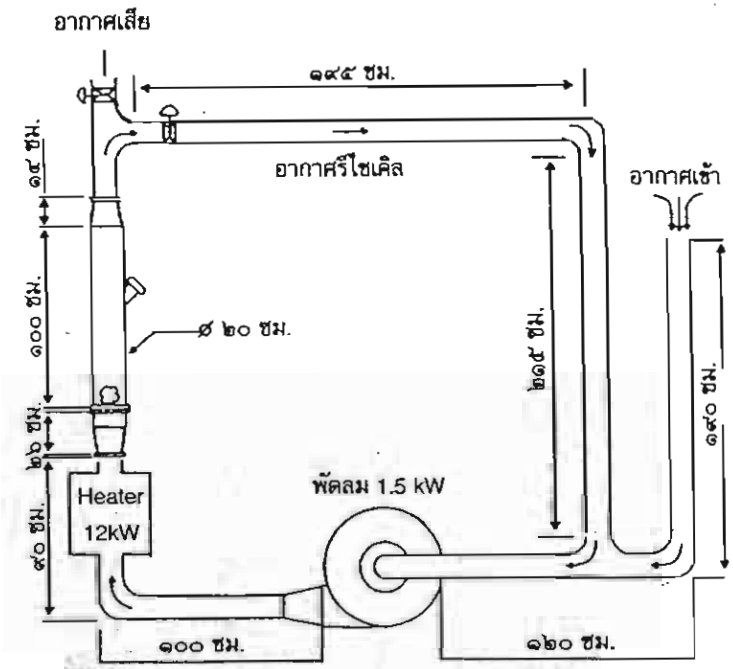
เวลาสั้น ๆ จะลดลงได้เร็วกว่าข้าวเปลือกที่แช่เป็นระยะเวลานาน ทั้งนี้เนื่องจากปริมาณความชื้นของข้าวเปลือกที่แช่เป็นระยะเวลาสั้น ๆ มีค่าต่ำกว่า จึงทำให้ความชื้นในการอบแห้งลดลงเร็วกว่า และเมื่อระยะเวลาในการอบแห้งเพิ่มมากขึ้น ความชื้นของเมล็ดข้าวเปลือกหลังอบแห้งมีแนวโน้มลดลงใกล้เคียงกัน เพราะว่าความชื้นของเมล็ดข้าวเปลือกส่วนใหญ่จะอยู่ที่ภายในเมล็ด ขณะที่อุณหภูมิของเมล็ดข้าวเปลือกมีแนวโน้มที่เพิ่มขึ้นตามเวลาในการอบแห้ง โดยอุณหภูมิของเมล็ดข้าวเปลือกที่ผ่านการแช่เป็นระยะเวลาสั้นจะเพิ่มขึ้นเร็วกว่าเมล็ดข้าวเปลือกที่ผ่านการแช่เป็นระยะเวลานาน

ร้อยละต้นข้าว

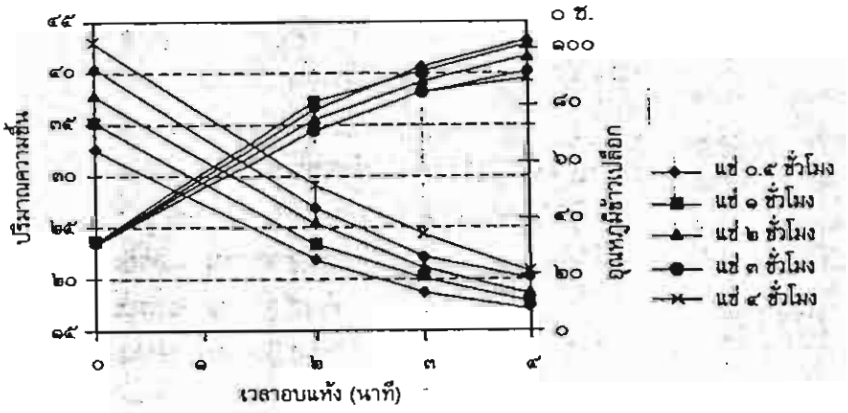
รูปที่ ๓ แสดงความสัมพันธ์ระหว่างร้อยละต้นข้าวกับระยะเวลาในการอบแห้งที่ใช้เวลาในการแช่ต่างกัน จะเห็นว่าข้าวที่ผ่านการแช่เพียงอย่างเดียว (เวลาการอบแห้ง ๐ นาที) มีร้อยละต้นข้าวสูงกว่าข้าวอ้างอิง (ข้าวที่ไม่ผ่านการแช่และการอบแห้ง) และเมื่อผ่านการอบแห้งพบว่า ข้าวที่

ตารางที่ ๖ ผลการวิเคราะห์การเกิดเจลาทิไนเซชันของข้าวโดยใช้เครื่อง Differential Scanning Calorimeter

ตัวอย่างข้าว	อุณหภูมิ (°ซ)			(H	อัตราการเกิดสภาพวุ้น
	เริ่มต้น	สูงมาก	สรุป	(J/g)	
อ้างอิง ๑๓% ฐานแห้ง	๗๓.๐	๗๖.๓	๘๐.๔	๗.๓๕	๐
แช่ ๓ ชั่วโมง อบแห้ง ๔ นาที	๗๖.๙	๘๐.๗	๘๔.๙	๒.๘๘	๖๐.๘
แช่ ๔ ชั่วโมง อบแห้ง ๔ นาที	๗๖.๖	๘๐.๔	๘๔.๗	๑.๘๕	๗๔.๘

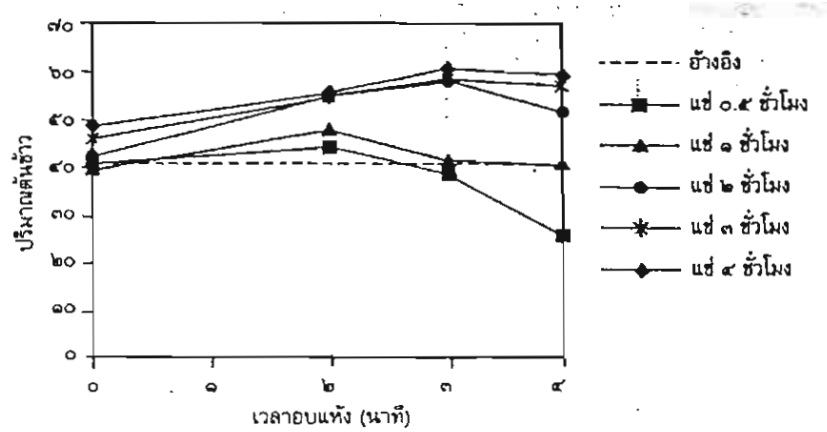


รูปที่ ๑
ไดอะแกรมของเครื่องอบแห้งฐาน ไหลแบบงวด



รูปที่ ๒
การเปลี่ยนแปลงความชื้นและอุณหภูมิของข้าวเปลือกที่ใช้เวลาในการแช่และการอบแห้งต่างกัน

ผ่านการแช่เป็นระยะเวลา ๐.๕ และ ๑ ชั่วโมง เมื่ออบแห้ง ๒ นาที ร้อยละต้นข้าวที่ได้สูงขึ้น แต่เมื่ออบแห้งที่ ๓ และ ๔ นาที ร้อยละต้นข้าวที่ได้จะลดต่ำลงตามระยะเวลาการอบแห้งที่เพิ่มขึ้น ส่วนข้าวที่ผ่านการแช่ตั้งแต่ ๒ ชั่วโมงขึ้นไป ร้อยละต้นข้าวเพิ่มขึ้นเมื่อใช้เวลาในการอบแห้ง ๒ นาที และสูงขึ้นอีกเมื่ออบแห้งที่ ๓ นาที แต่จะลดลงเล็กน้อยเมื่ออบแห้งที่ ๔ นาที ความแตกต่างของร้อยละต้นข้าวที่เกิดขึ้นนั้น เนื่องมาจากการเกิดสภาพวุ้นในเมล็ดข้าวเปลือก เพราะเมื่อข้าวที่มีความชื้นสูงได้รับความร้อนแป้งที่ถูกน้ำจะพองตัว โมเลกุลจะยึดเข้าด้วยกันทำให้โครงสร้างโมเลกุลแข็งแรงขึ้น รอยร้าวภายในเมล็ดข้าวสามารถประสานกันอย่างสนิท และเมื่อนำมาทำให้แห้งเมล็ดข้าวจะมีลักษณะแข็งใส เหนียว ทนต่อการขัดสี เมื่อนำเมล็ดข้าวไปขัดสีจึงมีร้อยละต้นข้าวสูง การเกิดสภาพวุ้นที่สมบูรณ์นั้นจะต้องประกอบด้วยอุณหภูมิและปริมาณน้ำในข้าวเปลือกที่เหมาะสม ซึ่งถ้าความชื้นเริ่มต้นสูงก็จะทำให้ช่วงเวลาในการเกิดสภาพวุ้นมากขึ้น ส่งผลให้ร้อยละต้นข้าวสูง. ด้วยเหตุนี้จึงทำให้ข้าวที่แช่นานขึ้นมีร้อยละต้นข้าวสูงขึ้น แต่ถ้าใช้เวลาในการอบแห้งนานเกินไป ทำให้ปริมาณความร้อนส่วนใหญ่ที่ใช้ในการระเหยน้ำ ถูกนำไปเพิ่มอุณหภูมิแก่ข้าวเปลือก ทำให้เมล็ดข้าวเปลือกมีอุณหภูมิสูงขึ้น และเมื่ออุณหภูมิสูงถึงอุณหภูมิสภาพวุ้นของแป้งแล้ว แต่ความชื้นภายในเมล็ดข้าวเปลือกเหลือน้อยจึงส่งผลให้ระยะเวลาในการเกิดสภาพวุ้นสั้น และในขณะที่อัตราการอบแห้งลดลง จึงเกิดความแตกต่างของความชื้นที่บริเวณผิวและแกนกลางของเมล็ดข้าวเปลือกเพิ่มขึ้น ทำให้เกิดความเค้นขึ้นภายในเมล็ดข้าวเปลือก ซึ่งนำไปสู่การเกิดรอยร้าวและแตกหัก เมื่อนำไปสีจึงได้ร้อยละต้นข้าวลดลง.



รูปที่ ๓
ความสัมพันธ์ระหว่างร้อยละต้นข้าวกับระยะเวลาในการอบแห้งที่ใช้เวลาในการแช่ต่างกัน

ความขาวของข้าวสาร

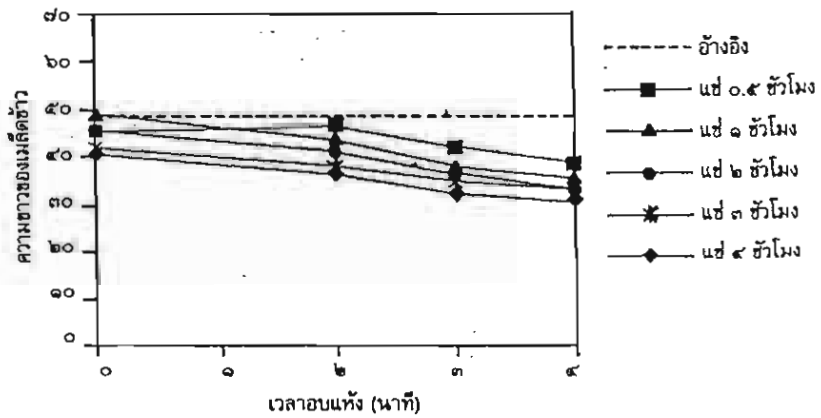
รูปที่ ๔ แสดงความสัมพันธ์ระหว่างความขาวกับระยะเวลาในการอบแห้งที่ใช้เวลาในการแช่ต่างกัน จะเห็นว่า ข้าวที่ผ่านการแช่และการอบแห้งจะมีความขาวลดลงต่ำกว่าข้าวอ้างอิง (ข้าวที่ไม่ผ่านการแช่และการอบแห้ง) ในทุกเงื่อนไขการทดลอง ระยะเวลาในการอบแห้งและการแช่ที่เพิ่มขึ้นมีผลทำให้ความขาวมีค่าลดลง ซึ่งเกิดจาก ปฏิกิริยาการเกิดสีน้ำตาล โดยมีความร้อนเป็นตัวเร่งปฏิกิริยา และสีน้ำตาลอาจมีส่วนเกิดจากสีของเปลือกข้าวแพร่เข้าสู่เนื้อเมล็ดขณะแช่และดิดแน่นขณะอบแห้ง จึงทำให้ความขาวของข้าวที่ผ่านการอบแห้งมีสีคล้ำขึ้น

ร้อยละของเมล็ดข้าวที่มีจุดขาวขุ่น

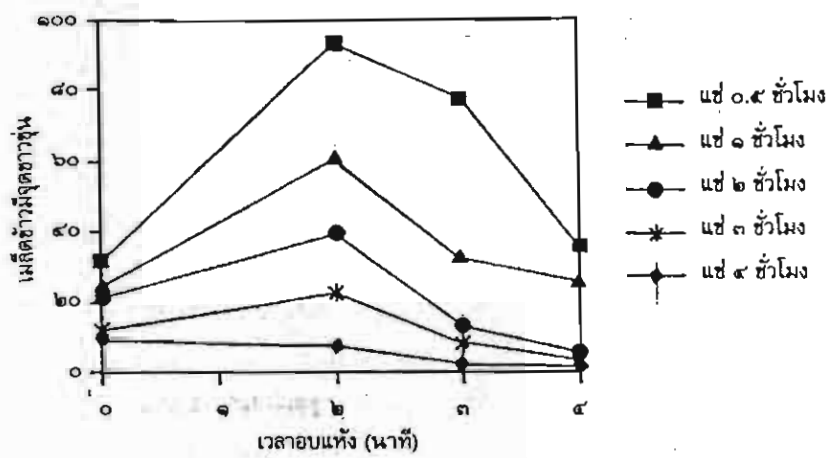
ลักษณะของข้าวที่มีจุดขุ่นขาวทึบแสง เป็นส่วนที่กลุ่มแป้งและโปรตีนมีการเกาะตัวกันอย่างหลวมๆ จึงมีส่วนที่เป็นช่องว่างอยู่มากและภายในช่องว่างนี้จะมีอากาศแทรกอยู่ ซึ่งจะเกิดขึ้นเมื่อข้าวเกิดการเป็นสภาพวุ้นไม่สมบูรณ์ทั่วทั้งเมล็ด จากรูปที่ ๕ แสดงความสัมพันธ์ระหว่างร้อยละของเมล็ดข้าวที่มีจุดขาวขุ่นกับระยะเวลาในการอบแห้งที่ใช้เวลาในการแช่ต่างกัน พบว่า เมื่อระยะเวลาในการแช่และการอบแห้งเพิ่มมากขึ้น ร้อยละของเมล็ดข้าวที่มีจุดขาวขุ่นจะลดลง เป็นผลเนื่องมาจากเวลาในการอบแห้งและปริมาณความชื้นที่เพิ่มขึ้นทำให้ช่วงเวลาในการอบแห้งคงที่มากขึ้น เกิดการสภาพวุ้นได้สมบูรณ์ทั่วทั้งเมล็ดมากขึ้น Degree of gelatinization ก็มากขึ้นด้วย ทำให้ค่าร้อยละของเมล็ดข้าวที่มีจุดขาวขุ่นที่ลดลง.

ค่าความแข็งและค่าการยึดเกาะตัวของข้าวสุก

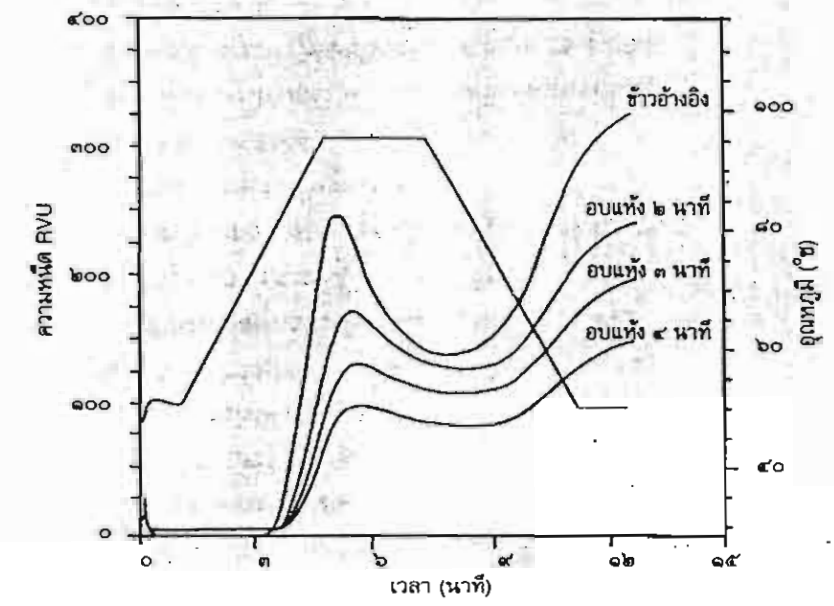
จากการทดสอบหาค่าความแข็งและค่าความเหนียวมีการยึดเกาะตัวของข้าวสุก ได้ผลดังแสดงในตารางที่ ๑ และ ๒ ข้าวที่ผ่านการแช่และอบแห้งด้วยฟลูอิไดซ์เบดนั้น ข้าวสุกที่ได้จะมีความแข็งเพิ่มขึ้นจากข้าวอ้างอิง (ข้าวที่ไม่ผ่านการแช่และการอบแห้ง) ทุกเงื่อนไขการทดลอง ที่ระยะเวลาการแช่เท่ากัน ข้าวที่แช่ตั้งแต่ ๑



รูปที่ ๔
ความสัมพันธ์ระหว่างความขาวกับระยะเวลาในการอบแห้งที่ใช้เวลาในการแช่ต่างกัน



รูปที่ ๕
ความสัมพันธ์ระหว่างร้อยละเมล็ดข้าวมีจุดขาวขุ่นกับระยะเวลาในการอบแห้งที่ใช้เวลาในการแช่ต่างกัน



รูปที่ ๖
ความหนืดของแป้งข้าวจากเครื่อง RVA เมื่อแช่เป็นระยะเวลา ๔ ชั่วโมง และอบแห้งที่เวลาต่างๆ

ชั่วโมงขึ้นไป เมื่อใช้เวลาในการอบแห้งเพิ่มขึ้นจะทำให้ความแข็งของข้าวสุกเพิ่มขึ้นด้วย แรงที่ใช้ในการยึดเกาะตัวของข้าวสุกของข้าวที่ผ่านการแช่และอบแห้งจะลดลงต่ำกว่าข้าวอ้างอิงทุกเงื่อนไขการทดลอง นั่นคือข้าวสุกมีความเหนียวลดลงหรือมีความร่วนมากขึ้น ที่ระยะเวลาการแช่เท่ากัน ความร่วนจะเพิ่มขึ้นเมื่อใช้เวลาในการอบแห้งนานขึ้น ทั้งนี้เป็นผลเนื่องมาจาก การเกิดสภาพวุ้นอะมิโลสจะละลายน้ำและดูดน้ำได้มาก ทำให้เกิดการพองตัวขึ้น และเมื่อนำมาอบแห้งจะทำให้สตาร์ชที่เป็นเจลแล้วจัดเรียงตัวกัน จับกับโปรตีนและไขมัน ทำให้เมล็ดแข็งแรงขึ้น เมื่อนำมาหุงทำให้ความสามารถในการดูดซับน้ำและละลายน้ำลดลง ส่วนระยะเวลาที่ใช้ในการแช่นั้นไม่มีอิทธิพลอย่างชัดเจนต่อความแข็ง และการยึดเกาะตัวของข้าวสุก

ความหนืดของแป้งข้าว

รูปที่ ๖ และตารางที่ ๓-๕ แสดงสมบัติการเป็นแป้งเปียกของข้าวที่ผ่านการแช่และอบแห้งด้วยฐานไหล. จากผลการทดลองและผลการวิเคราะห์ทางสถิติพบว่า ข้าวที่ผ่านการแช่และอบแห้งให้ค่าอุณหภูมิแป้งเปียกสูงกว่าข้าวอ้างอิง (ข้าวที่ไม่ผ่านการแช่และการอบแห้ง) และสูงขึ้นเมื่อใช้เวลาในการอบแห้งเพิ่มขึ้นที่ระยะเวลาการแช่เท่ากันอย่างมีนัยสำคัญ แต่ค่าความหนืดสูงสุด และความหนืดสุดท้าย มีค่าต่ำกว่าข้าวอ้างอิง และจะลดต่ำลงเมื่อใช้เวลาในการอบแห้งเพิ่มขึ้นที่ระยะเวลาการแช่เท่ากันอย่างมีนัยสำคัญ. ทั้งนี้เป็นผลเนื่องมาจากข้าวที่ผ่านการแช่และอบแห้งได้เกิดการสภาพวุ้นมาบางส่วนแล้ว โดยข้าวที่ผ่านการแช่จะมีความชื้นสูงเมื่อได้รับความร้อนจากการอบแห้งทำให้เม็ดแป้งที่ถูกน้ำเกิดการพองตัวและถูกทำให้สุก เมื่อนำมาวัดความหนืดทำให้ความสามารถในการดูดซับน้ำของแป้งนั้นลดลงเกิด

การพองตัวได้น้อยลง ส่งผลให้ค่าความหนืดสูงสุดที่วัดได้มีค่าลดลง และต้องใช้อุณหภูมิสูงขึ้นเพื่อให้เกิดการพองตัวอีก สำหรับค่าความหนืดสุดท้ายนั้นแสดงถึงสมบัติความแข็งกระด้างของข้าวสุก ถ้ามีค่าสูงแสดงว่าข้าวสุกนั้นมีความแข็งกระด้างมาก หลังจากการหุงสุกและปล่อยให้ข้าวเย็นตัวลง ส่วนระยะเวลาในการแช่ไม่มีอิทธิพลอย่างชัดเจนต่อค่าอุณหภูมิเกิดแป้งเปียก, ความเปียกสูงสุด และความหนืดสุดท้ายอย่างมีนัยสำคัญที่ระดับความเชื่อมั่นร้อยละ ๙๕.

การวิเคราะห์การเกิดสภาพวุ้นของข้าวโดยใช้เครื่อง DSC

จากการนำข้าวอ้างอิง, ข้าวที่ผ่านการแช่ ๓ และ ๔ ชั่วโมง อบแห้ง ๔ นาที มาทำการวิเคราะห์การเกิดสภาพวุ้นโดยเครื่อง DSC วิเคราะห์ค่าเอนทัลปีที่เปลี่ยนแปลง (_H) ได้ผลดังตารางที่ ๖ ซึ่งจะเห็นว่าอุณหภูมิเริ่มต้นในการเกิดสภาพวุ้นของข้าว, (อุณหภูมิสูงสุดในการเกิดสภาพวุ้น และอุณหภูมิสุดท้ายในการเกิดสภาพวุ้น ของข้าวที่ผ่านการแช่และการอบแห้งสูงขึ้นจากข้าวอ้างอิง แสดงให้เห็นว่าข้าวที่ผ่านการแช่และการอบแห้งได้เกิดการสภาพวุ้นไปบางส่วนแล้ว ค่า _H แสดงถึงการใช้พลังงานความร้อนในการทำให้ข้าวสุก ถ้ามีค่าน้อยแสดงว่าข้าวนั้นเกิดการสภาพวุ้นไปบางส่วนแล้วจึงใช้พลังงานความร้อนในการทำให้ข้าวสุกน้อยลง และจากการคำนวณอัตราการเกิดสภาพวุ้นจะเห็นว่าข้าวที่แช่ ๔ ชั่วโมง อบแห้ง ๔ นาที เกิดสภาพวุ้นมากกว่าข้าวที่แช่ ๓ ชั่วโมง อบแห้ง ๔ นาที.

สรุป

จากการทดลองแช่และอบแห้งข้าวเปลือกบนฐานไหล พบว่าเมื่ออบแห้งและแช่นานขึ้น ทำให้ช่วงเวลาการเกิดสภาพวุ้นมากขึ้นอัตราการเกิดสภาพวุ้นก็มากขึ้นด้วย จึงส่งผลให้เมล็ดข้าวเปลือกมีความแข็งและทนต่อการขัดสีทำให้ได้ร้อยละต้นข้าวสูงขึ้น และจุดขาวขุ่นในเมล็ดข้าวลดลง อย่างไรก็ตามการเพิ่มขึ้นของระยะเวลาในการอบแห้งจะเป็นตัวเร่งปฏิกิริยาการเกิดสีน้ำตาลให้มากขึ้น จึงทำให้ข้าวมีความขาวลดลง ที่ระยะเวลาการแช่เท่ากันเวลาการอบแห้งที่เพิ่มขึ้นยังมีผลทำให้ข้าวสุกมีความแข็งและร่วนมากขึ้นอีกด้วย ส่วนสมบัติการเกิดแป้งเปียกให้ค่าอุณหภูมิเกิดแป้งเปียกสูงขึ้นเมื่อใช้เวลาในการอบแห้งนานขึ้นที่ระยะเวลาการแช่เท่ากัน แต่ค่าความหนืดสูงสุดและความหนืดสุดท้ายมีค่าลดต่ำลง สำหรับการวิเคราะห์การเกิดสภาพวุ้นของข้าวด้วยเครื่อง DSC. ข้าวที่แช่นานกว่าจะเกิดสภาพวุ้นมากกว่า.

จากการศึกษาหาแนวทางที่เหมาะสมสำหรับการเพิ่มปริมาณต้นข้าวของข้าวคุณภาพต่ำโดยการแช่ร่วมกับการ อบแห้งแบบฟลูอิไดซ์เบดนี้ พบว่าควรนำข้าวเปลือกมาแช่น้ำที่อุณหภูมิ ๘๐°ซ เป็นเวลา ๔ ชั่วโมง แล้วนำมาอบแห้งด้วยเครื่องทำฐานไหลเป็นเวลา ๓ นาที แล้วนำข้าวเปลือกไปเก็บในที่อับอากาศเป็นเวลา ๓๐ นาที และนำไปเป่าด้วยอากาศปรกตินาน ๑ ชั่วโมง ทำให้ข้าวที่ได้มีร้อยละต้นข้าวสูงสุด และคุณภาพด้านความขาวและการมีจุดขาวขุ่นในเมล็ดข้าวอยู่ในเกณฑ์ดี

กิตติกรรมประกาศ

เจ้าหน้าที่สถาบันค้นคว้าและพัฒนาผลิตภัณฑ์อาหาร มหาวิทยาลัยเกษตรศาสตร์ ได้ให้ความอนุเคราะห์ในการทดสอบคุณภาพทางเคมี. สำนักงานกองทุนสนับสนุนการวิจัย และ Japan International Research Center for Agricultural Sciences ให้ทุนทำวิจัย.

เอกสารอ้างอิง

๑. อัมมาร สยามวาลา, วิโรจน์ ณ ระนอง. ประมวลความรู้เรื่องข้าว. กรุงเทพฯ: สถาบันวิจัยเพื่อการพัฒนาประเทศไทย; ๒๕๓๓, หน้า ๑๕๘-๖.

๒. Ali SZ, Bhattacharya KR. High-Temperature Drying-Cum-Parboiling of Paddy. Journal of Food Process Engineering 1980; 4:123-36.

๓. Velupillai L, Verma LR. Drying and Tempering Effects on Parboiled Rice Quality. Transaction of the American Society of Agricultural Engineering 1986; 29:312-9.

๔. สมชาติ โสภณรณฤทธิ์, Pachayawarakorn S, Wangji M. Commercial Fluidized Bed Paddy Dryer. Proceedings of the 10th International Drying Symposium 1996; A: 638-44.

๕. สมชาติ โสภณรณฤทธิ์, อดิเทพ ทวีรัตนพาณิชย์, สมบูรณ์ เวชกามา, งามชื่น คงเสรี, สุนันทา วงศ์ปิยชน. ผลพลอยได้

จากการอบแห้งข้าวเปลือกโดยใช้เทคนิคฟลูอิไดเซชัน. วารสารราชบัณฑิตยสถาน ๒๕๔๑; ๒๔: ๔๕-๖๓.
๖. อดิเทพ ทวีรัตนพาณิชย์, สมชาติ โสภณรณฤทธิ์, สมบูรณ์ เวชกามา, งามชื่น คงเสรี. Wongpiyachon S. Effect of Drying on Head Yield Using Fluidization Technique. Drying Technology 1999; 17(1&2): 345-53.
๗. สมชาติ โสภณรณฤทธิ์, สมบูรณ์ เวชกามา, ท. สวันดิเสรี, น. พุ่มสะอาด. Managing Moist Paddy by Drying Tempering and Ambient Air Ventilation. Drying Technology 1999; 17(1&2): 335-44.
๘. Zhang Q. Litchfield JB. An Optimization of Intermittent Corn Drying in a Laboratory Scale Thin Layer Dryer. Drying Technology 1991; 9(11): 233-44.
๙. Lai HM. Effects of Hydrothermal Treatment on the Physicochemical Properties of Pregelatinized Rice Flour. Food Chemistry 2001; 72:455-63.

Abstract

Increased Yield in Head Rice of Poor Quality Paddy by Combined Soaking and Fluidized Bed Drying

Suttinee Wanichsumran, Patcharee Tungtrakul+, Wanunee Waranyanon#, Somchart Soponronnarit***
**Master's Degree Student, School of Energy and Materials, King Mongkut's University of Technology Thonburi, Bangkok, **Fellow of the Royal Institute; Professor, School of Energy and Materials, King Mongkut's University of Technology Thonburi, Bangkok, +,#Researcher Specialist, Institute of Food Research and Product Development, Kasetsart University, Chatuchak, Bangkok.*

This research is a feasibility study for increasing the head rice yield of poor quality paddy by combined soaking and fluidized bed drying. The effects of soaking time and drying time on head rice yield, color, white belly, hardness of cooked rice, stickiness of cooked rice, pasting viscosity of rice flour and gelatinization are considered. In the experiments, paddy with jnitial moisture content of 13% d.b. is soaked in hot water at a temperature of 80°C for 0.5-4 hours. Next, paddy is dried by a fluidized bed dryer at 150°C for 2-4 minutes. After that, it is tempered for 30 minutes. Finally, it is ventilated in the ambient air for one hour. Experimental results find that the soaking time of four hours and drying time of three minutes can considerably increase head rice yield. Moreover, whiteness and white belly are good criteria; however, these will be reduced with an increase in soaking and drying times. In the texture test, the cooked rice is moderately hardened and flaked with an increase in drying time. In addition, the peak and the final viscosity are reduced, but the pasting temperature is increased. For the gelatinization analysis by DSC, paddy with soaking time of four hours appears to produce a degree of gelatinization more than paddy with a soaking time of three hours (degree of gelatinization of 60.8 and 74.8% for soaking times of 3 and 4 hours respectively).

Key words: fluidized bed, paddy drying, rice quality

เตาเผาไหม้จำลองวอร์เทค-ฟลูอิไดซ์เบด : การศึกษาเชิงการทดลองพฤติกรรมการไหลของอากาศ-แกลบ

The Vortexing-Fluidized Bed Combustor Cold Model : Experimental Study of Air-Rice Husk Flow Behavior

ฐานิดย์ เมธิยานนท์[1] นิวัติ พิริยะรุ่งโรจน์[1] อดิศักดิ์ นาถกรณกุล[2] และ สมชาติ โสภณรณฤทธิ์[2]

Thanid madhiyanon[1] Niwat Piriyarungroj[1] Adisak Nathakaranakule[2] Somchart Soponronnarit[2]

[1]ภาควิชาวิศวกรรมเครื่องกล มหาวิทยาลัยเทคโนโลยีมหานคร หนองจอก กรุงเทพฯ 10530

[2]คณะพลังงานและวัสดุ มหาวิทยาลัยเทคโนโลยีพระจอมเกล้าธนบุรี ถ.ประชาอุทิศ ทุ่งครุ กรุงเทพฯ 10140

โทร. 0-2988-3666 ต่อ 241 แฟกซ์ 0-2988-3666 ต่อ 241 E-mail: thanid@mut.ac.th

บทคัดย่อ

เตาเผาไหม้วอร์เทค-ฟลูอิไดซ์เบด(Vortexing-fluidized bed combustor, VFBC)จำลองได้ถูกพัฒนาขึ้นมาเพื่อศึกษาพฤติกรรมการไหลของอากาศและแกลบภายในเตาเผาไหม้จำลองซึ่งจะใช้เป็นข้อมูลพื้นฐานในการออกแบบและสร้างเตาเผาไหม้จริงต่อไป งานวิจัยนี้เป็นการศึกษาเชิงทดลองโดยการสังเกตพฤติกรรมการไหลของอากาศและแกลบตลอดจนบันทึกความเร็วอากาศภายใน VFBC จำลอง จากการทดลองพบว่าอากาศและแกลบภายใน VFBC จำลองมีพฤติกรรมการไหลทั้งแบบฟลูอิไดซ์เบดและแบบวอร์เทคโดยมีวงแหวนวอร์เทค(vortex ring)ทำหน้าที่คล้ายหัวฉีดอากาศช่วยเพิ่มความเร็วในแนวสัมผัสและก่อให้เกิด เป็นชั้นแขวนลอย (suspension layer)ของแกลบทำให้แกลบไม่สามารถลอยหนีออกไปจาก VFBC จำลองได้ การหมุนเวียนของอากาศพบได้ที่บริเวณใกล้ผนังอันเนื่องมาจากการไหลย้อนกลับของอากาศในแนวแกนซึ่งจะเป็นประโยชน์ต่อการเผาไหม้เชื้อเพลิงแข็งผลของวงแหวนวอร์เทคและการเกิดสเปาเต็ดเบดที่ด้านล่างสุดของ VFBC ช่วยเหนี่ยวนำให้เกิดพฤติกรรมการไหลแบบฟลูอิไดซ์เบดในโซนที่อยู่ถัดขึ้นไปได้โดยไม่ต้องใช้วัสดุเฉื่อยผสมลงไปในเบด

Abstract

The present work involves the experimental study to investigate the basic feature of air-rice husk flow behavior as well as the measurements of air velocity are also conducted in a vortexing-fluidized bed combustor (VFBC) cold model which is essential for proper design and operation of combustor. The results shown that a combination phenomena of vortex and fluidization flow were simultaneously developed. The vortex ring functions as an air nozzle which facilitates the swirling motion and hence enhancing tangential air velocity. This created the suspension layer of rice husk between the vortex ring which could substantially reduce the elutriation of solid. The circulation flow is aggressive at near the wall due to the reverse flow of air which is beneficial for solid combustion. The vortex ring and spouted bed feature developed at the bottom of VFBC induced the fluidization in the next above zones without using any inert materials mixed in to the bed.

1. บทนำ

การเผาไหม้โดยใช้หลักการของการไหลวนหรือการไหลแบบวอร์เทคได้เป็นที่รู้จักกันแพร่หลายมาหลายทศวรรษแล้ว เช่น เตาเผาไหม้ไซโคลน [1] และต่อมาได้มีการนำมาประยุกต์ใช้กับเชื้อเพลิงชีวมวล เช่น แกลบ [2, 3, 4] สำหรับเตาเผาไหม้ฟลูอิไดซ์เบดก็ได้มีการพัฒนามานานแล้วเช่นกัน ส่วนใหญ่จะใช้กับเชื้อเพลิงถ่านเพื่อผลิตกระแสไฟฟ้าซึ่งก็มีนำมาประยุกต์ใช้กับเชื้อเพลิงชีวมวล [5, 6, 7] แต่เนื่องจากเชื้อเพลิง ชีวมวล เช่น แกลบ การเกิดฟลูอิไดซ์เซชันเป็นได้ยากจำเป็นต้องใช้วัสดุเฉื่อย จำพวกทรายซิลิกา, อลูมินา ผสมลงในเบดในอัตราที่เหมาะสม [5, 8] และเมื่อประมาณ 10 กว่าปีมานี้ได้มีการพัฒนาเตาเผาไหม้ฟลูอิไดซ์เบดซึ่งใช้กับถ่านหินชนิดป้อนเชื้อเพลิงใต้เบด โดยการเพิ่มการฉีดอากาศในแนวสัมผัสเข้าไปในเตาเผาไหม้บริเวณ free board ทำให้ช่วยลดความสูงของเตาเผาไหม้ลงได้มาก [9, 10, 11] ต่อมาได้มีการศึกษาพฤติกรรมการไหลก๊าซ-อนุภาคภายในเตาเผาไหม้วอร์เทคพบว่ามีบริเวณที่เกิดการหมุนเวียนอนุภาคภายในเตาเผาไหม้ ซึ่งทำให้ residence time นานขึ้น[12] ซึ่งงานวิจัยนี้มีจุดประสงค์เพื่อศึกษาพฤติกรรมการไหลของอากาศ - แกลบภายในเตาเผาไหม้วอร์เทค-ฟลูอิไดซ์เบด (VFBC) ซึ่งได้ออกแบบมาเพื่อรวมลักษณะเด่นของเตาเผาไหม้วอร์เทค และเตาเผาไหม้ฟลูอิไดซ์เบดไว้ด้วยกันเพื่อใช้เป็นพื้นฐานในการออกแบบและจัดสร้างเตาเผาไหม้จริง

2. วิธีการทดลอง

2.1 การสังเกตการไหลของอากาศ-แกลบภายใน VFBC จำลอง

1. การเตรียมอุปกรณ์การทดลองและประกอบ VFBC จำลองกับวงแหวนวอร์เทค ดังแสดงในรูปที่ 1

RECEIVED 7 July, 2003

ACCEPTED 30 October, 2003

2. การปรับอัตราการไหลของแกลบและอากาศให้สอดคล้องกับเงื่อนไขที่แสดงในตารางที่ 1.(RunNo.1-No.8)

3. บันทึกผลการทดลอง

2.2 การวัดความเร็ว ณ ตำแหน่งต่างๆ ภายในเตาเผา VFBC ซึ่งมีวิธีทำการทดลองดังต่อไปนี้

1. เตรียมอุปกรณ์การทดลองและประกอบ VFBC จำลองกับวงแหวนวอร์เทค

2. ปรับอัตราการไหลของอากาศให้สอดคล้องกับ เงื่อนไขในตารางที่ 1 Run No.1 โดยไม่ต้องป้อนแกลบ

3. ทำการวัดความเร็วของอากาศในแนวสัมผัสและในแนวแกนโดยใช้ Hot wire ที่มีค่าความคลาดเคลื่อน 3% ของค่าที่วัดได้ ที่ระดับความสูงในแนวแกน(z axis)เท่ากับ 20 cm. โดยอ้างอิงเริ่มต้นจากแผ่นกระจายลม(Air distributor)และตำแหน่งในแนวรัศมี(r axis)เท่ากับ 0.5 cm. โดยอ้างอิงจากผนังเตาด้านในดังแสดงในรูปที่ 2b

4. ทำการทดลองซ้ำข้อ 3 โดยเปลี่ยนตำแหน่งวัดในแนวรัศมี (ตามแนวเส้นผ่าศูนย์กลาง)ทั้งหมด 17 ตำแหน่งซึ่งแต่ละตำแหน่งอยู่ห่างกัน 1 cm.

5. ทำการทดลองซ้ำข้อ 3 และข้อ 4 โดยเปลี่ยนตำแหน่งวัดในแนวแกน เท่ากับ 30 cm. , 40 cm. , 50 cm. และ 60 cm. ตามลำดับ

6. ทำการทดลองซ้ำข้อ 1-5 โดยไม่ประกอบวงแหวนวอร์เทคเข้ากับชุด VFBC จำลอง

3. ผลการทดลองและวิจารณ์

3.1 การศึกษาถึงพฤติกรรมการไหลของอากาศ - แกลบภายในเตาเผาไหม้วอร์เทค - ฟลูอิไดซ์เบดจำลอง

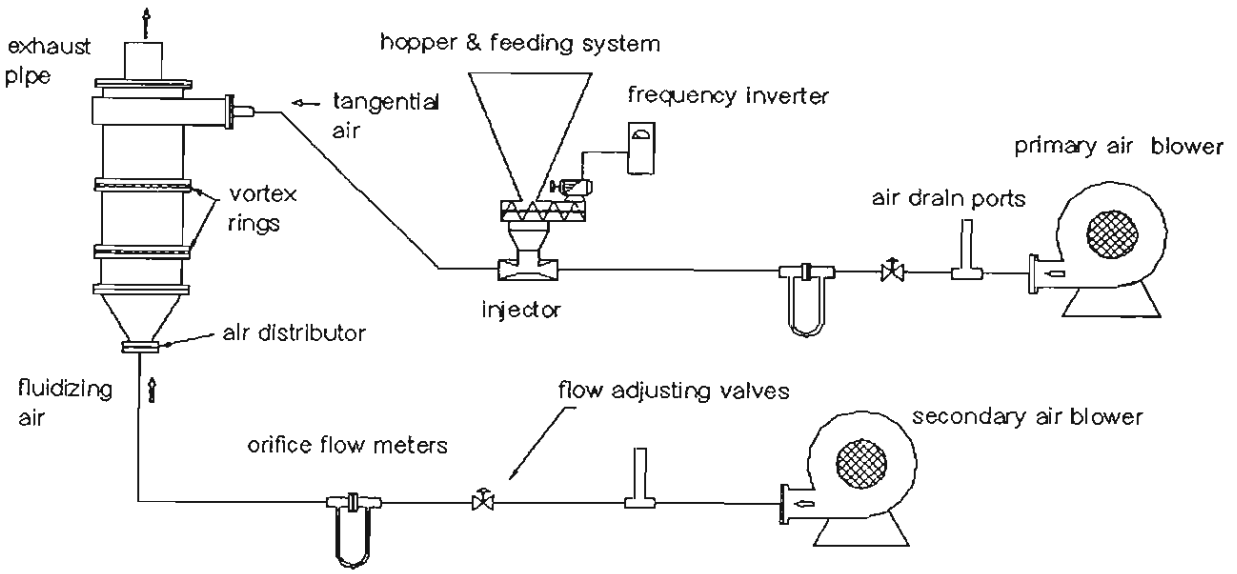
เพื่อให้เข้าใจพื้นฐานของรูปแบบลักษณะการไหลของอากาศ - แกลบภายในเตาเผาไหม้จริง จึงได้จำลองการไหลของอากาศ - แกลบในเตาเผาไหม้วอร์เทค-ฟลูอิไดซ์เบด(Vortex Fluidized Bed Combustor, VFBC) จำลอง ผลการทดลองได้แสดงด้วยภาพถ่ายดังแสดงในรูปที่ 3 และ 4 สำหรับเงื่อนไขในแต่ละการทดลองได้แสดงไว้ ในตารางที่ 1 จากการทดลองพบว่าหลังจากอากาศส่วนแรกและแกลบถูกจ่ายในแนวสัมผัส (tangential flow)ที่ทางด้านบนของ VFBC จำลอง และไหลเข้าไปใน Zone I (ตำแหน่งของแต่ละ Zone ดังแสดงในรูปที่ 2a)แกลบจะไหลเวียนเป็นเกลียวไปตามผนังของ VFBC จำลองลงสู่ด้านล่างในลักษณะการไหลแบบวอร์เทค ซึ่งเป็นผลมาจากแรงเหวี่ยง(centrifugal force) ของมวลอากาศที่ไหลในแนวสัมผัส (tangential flow) เมื่ออากาศพาแกลบไหลวนมาขังบริเวณเหนือวงแหวนวอร์เทค (vortex ring) อันแรกซึ่งทำหน้าที่เสมือนหัวฉีดอากาศ(air nozzle)จะช่วยเร่งความเร็วของอากาศให้เพิ่มขึ้นและไหลวนผ่านช่องตรงกลางของวงแหวนไปยัง Zone II

สำหรับ Zone II สังเกตพฤติกรรมได้ว่าแกลบจะยังคงไหลวนไปตามผนังของ VFBC จำลอง พร้อมๆกับที่เกิดลักษณะการไหลแบบฟลูอิไดซ์เบด (fluidized bed flow)ของแกลบจาก Zone III ซึ่งอยู่ด้านล่างและถูกพาให้ลอยขึ้นมาพร้อมกับอากาศ ซึ่งเป็นผลมาจากโมเมนตัมของแกลบในแนวแกน โดยการเกิดขึ้นของลักษณะการไหลแบบฟลูอิไดซ์เบดของแกลบจะเกิดขึ้นสม่ำเสมอทั่วทั้งบริเวณ Zone II รวมถึงบริเวณแกนกลาง(core region)ของ VFBC จำลองดังแสดงในรูป 3 และ 4 และที่สังเกตได้อย่างชัดเจนคือแกลบในบริเวณ Zone II นี้แทบจะไม่หลุดลอยเข้าไปใน Zone I ซึ่งอยู่ด้านบนเนื่องจากมีการไหลแบบวอร์เทคที่รุนแรงบริเวณเหนือและใต้วงแหวนวอร์เทคก่อให้เกิดแรงเหวี่ยงที่รุนแรงบริเวณนี้จึงมีลักษณะคล้ายม่านอากาศ (air curtain) ทำให้แกลบซึ่งเป็นอนุภาคขนาดใหญ่และมีน้ำหนักมากไม่สามารถไหลข้ามไปได้ ดังนั้นภายใน Zone II จึงมีสภาพเป็นเหมือนชั้นแขวนลอย (suspension layer) ของแกลบ และแกลบที่ไหลเวียนมาตามผนังจะสังเกตได้ว่าไม่ไหลเกาะกลุ่มกันเป็นเส้นเกลียวเหมือนกับใน Zone I แต่จะไหลตามกันมาเป็นแผงสาเหตุเนื่องจากแรงเหวี่ยงการเกิดวอร์เทคใน Zone II นี้มีกำลังอ่อนลง

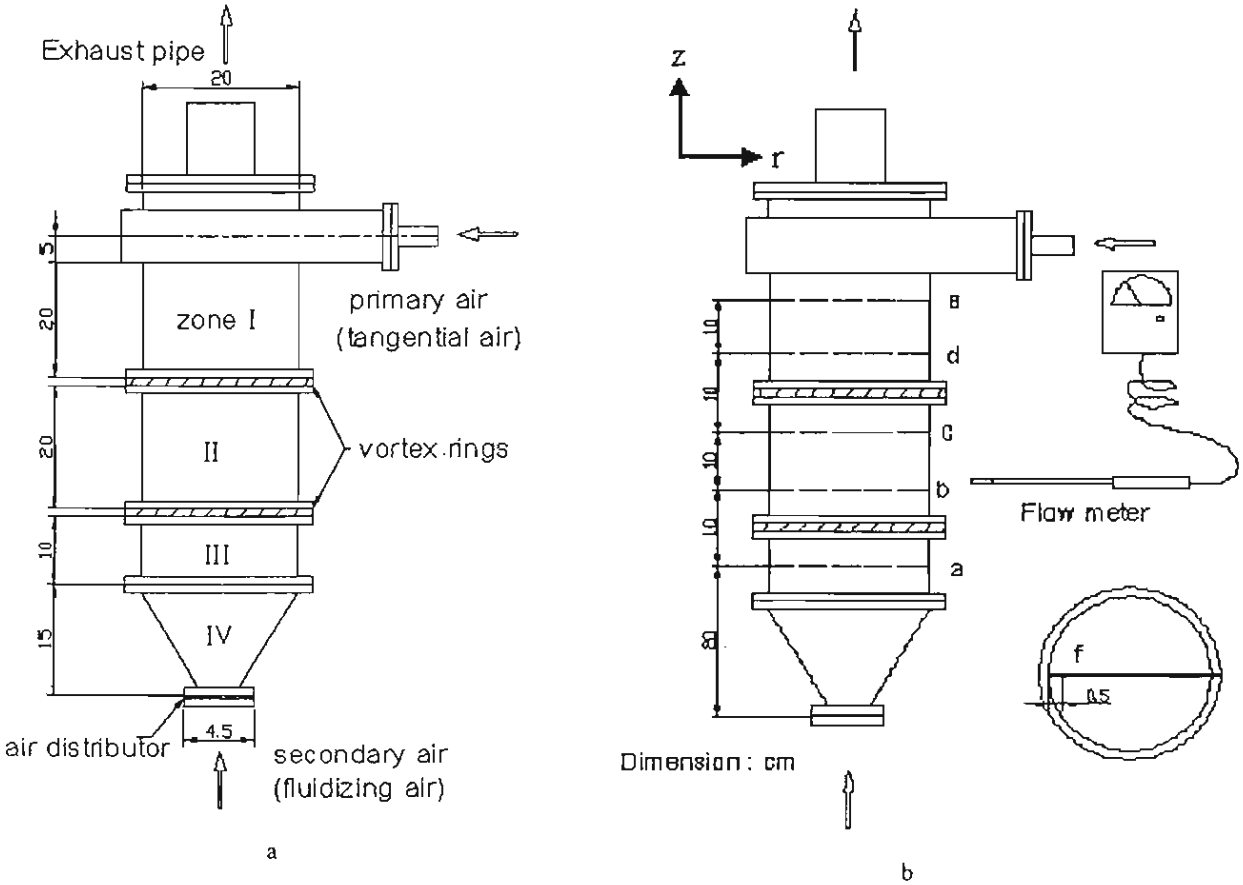
แกลบที่ไหลออกจาก Zone II จะไหลเข้าสู่ Zone III ซึ่งอยู่ด้านล่างโดยในบริเวณ Zone III จะสังเกตการไหลวนของแกลบได้ไม่ชัดเจนมีเพียงลักษณะการไหลแบบฟลูอิไดซ์เบดเท่านั้นที่เด่นชัดใน Zone นี้ สำหรับใน Zone IV ซึ่งอยู่ล่างสุดของ VFBC จำลอง แกลบจะไหลมากองรวมกันเป็นเบดโดยมีอากาศส่วนที่สอง (fluidizing air)ไหลขึ้นมาแนวแกนจากทางด้านล่างของเบดผ่านแผ่นกระจายลม (air distributor) และด้วยความเร็วอากาศที่เหมาะสมอากาศจะดันให้แกลบขยับตัวจนเกิดเป็นโพรงอากาศบริเวณตรงกลางเบดและ แกลบที่อยู่บริเวณล่างสุดของเบดจะลอยไปกับอากาศโดยแกลบที่อยู่บริเวณรอบๆ โพรงอากาศจะเคลื่อนตัวลงสู่ด้านล่างของเบดเพื่อให้ไปแทนที่แกลบด้านล่างที่ถูกพาไปกับอากาศ ซึ่งลักษณะเช่นนี้ก็คือการเกิดของสเปาท์เต็ดเบด (spouted bed)

3.1.1 วงแหวนวอร์เทคกับพฤติกรรมการไหลของแกลบใน VFBC จำลอง

ในการทดลองเบื้องต้นที่ยังไม่ได้ติดตั้งวงแหวนวอร์เทคพบว่าอากาศจะไหลวนมาจากทางเข้าด้านบน ลงมาถึงบริเวณที่เป็นเบดของแกลบใน Zone IV ก่อนที่จะหมุนวนกลับขึ้นไปในแนวแกนโดยอากาศส่วนที่สองจากทางด้านล่างของ VFBC จำลองไม่สามารถพาแกลบให้ลอยขึ้นสู่ด้านบนได้นอกเสียจากว่าจะต้องใช้ปริมาณอากาศส่วนที่สองเป็นปริมาณมากเพื่อเอาชนะความดันเหนือเบด ซึ่งอาจทำให้ต้องใช้ปริมาณอากาศส่วนเกิน(excess air)เกินความจำเป็นในการเผาไหม้จริง เพื่อแก้ปัญหานี้ จึงได้ออกแบบวงแหวนวอร์เทคและติดตั้งเข้าไปภายใน VFBC ที่ระดับความสูง H/D = 1.25 และ 2.25 ตามลำดับ ดังแสดงในรูปที่ 2a โดยผลการทดลองเป็นไปตามที่กล่าวมาแล้วในหัวข้อ 3.1



รูปที่ 1 อุปกรณ์การทดลองเตาเผาไหม้วอร์เทค-ฟลูอิไดซ์เบดจำลอง



รูปที่ 2 ขนาดและตำแหน่งการวัดความเร็วของเตาเผาไหม้วอร์เทค-ฟลูอิไดซ์เบดจำลอง

ตารางที่ 1 เงื่อนไขการทดลองสำหรับการศึกษาพฤติกรรมการไหลของอากาศ-แกลบใน VFBC จำลอง

Run No.		1	2	3	4	5	6	7	8
Rice husk feed rate	g/min	300	300	300	300	250	250	250	250
Primary (tangential) air									
Flow rate	m^3/min	2.68	2.44	2.19	2.07	2.68	2.19	2.07	1.95
Velocity	m/s	22	20	18	17	22	18	17	16
Secondary (fluidizing) air									
Flow rate	m^3/min	0.573	0.573	0.573	0.573	0.573	0.573	0.573	0.573
Velocity	m/s	6	6	6	6	6	6	6	6
Swirl number, S	-	5.25	5.07	4.86	4.74	5.25	4.86	4.74	4.61

3.1.2 การเกิดชั้นแขวนลอยของแกลบภายใน VFBC จำลองและความสามารถในการดักแกลบ

จากรูปที่ 3 (a-c) และ 4 (a-c) จะเห็นได้อย่างชัดเจนว่าแกลบจะรวมตัวกันอยู่เป็นชั้นแขวนลอย (suspension layer) ภายในบริเวณ Zone II ซึ่งอยู่ระหว่างวงแหวนวอร์เทคทั้งสอง แกลบที่เข้ามาสู่บริเวณ Zone II นี้จะมาจากสองส่วนคือแกลบส่วนแรกมาจากการไหลวนจากทางด้านบนของ VFBC จำลองซึ่งก็จะไหลออกไปสู่ Zone III ซึ่งอยู่ถัดลงไป แกลบอีกส่วนหนึ่งมาจากแกลบในเบดของ Zone IV ซึ่งลอยขึ้นมาพร้อมกับอากาศ ที่เรียกว่าเป็นชั้นแขวนลอยของแกลบก็เพราะสังเกตได้อย่างชัดเจนว่าแกลบซึ่งจัดเป็นอนุภาคขนาดใหญ่และมีน้ำหนักมาก ซึ่งโดยทั่วไปแล้วจะไม่สามารถหลุดลอยเข้าไปสู่ Zone I ซึ่งอยู่เหนือขึ้นไปได้และเมื่อปริมาณแกลบที่สะสมอยู่ในชั้นนี้มีมากขึ้น จนกระทั่งน้ำหนักของแกลบมากกว่าแรงฉุด (drag force) ที่เกิดจากการไหลของอากาศ จะทำให้แกลบบางส่วนตกลงสู่เบดด้านล่าง เพื่อรักษาสมดุลทางพลศาสตร์ของชั้นแขวนลอยนี้ไว้ ปรากฏการณ์เช่นนี้สามารถอธิบายได้ว่าเกิดจากการไหลวนของอากาศที่รุนแรงบริเวณเหนือและใต้วงแหวนวอร์เทคทำให้เกิดแรงเหวี่ยงที่มีกำลังมากและเมื่อแกลบลอยตัวขึ้นมาในบริเวณใกล้วงแหวนนี้ก็จะถูกเหวี่ยงไปชนกับผนังของ VFBC จำลองและไหลหล่นลงมาสู่ด้านล่างเนื่องจากแรงโน้มถ่วงลักษณะเช่นนี้คล้ายกับมีม่านอากาศ (air curtain) ที่บริเวณวงแหวนวอร์เทคทำหน้าที่ดักอนุภาคขนาดใหญ่ เช่น แกลบที่ยังไม่ได้เผาไหม้ไม่ให้ผ่านขึ้นไปได้ปรากฏการณ์เช่นนี้คล้ายคลึงกับที่ Yang และ Nieh [10] ค้นพบว่าการฉีดอากาศส่วนที่สองเข้าไปในแนวสัมผัสบริเวณ free board ของเตาเผาไหม้ฟลูอิไดซ์เบดจะทำให้เกิดชั้นแขวนลอยของอนุภาคในบริเวณ free board ได้

3.1.3 การกระจายตัวของแกลบภายใน VFBC จำลอง

พิจารณาจากรูปที่ 3(a-c) และ 4(a-c) จะสังเกตได้ว่าใน Zone I ซึ่งเป็นบริเวณทางเข้าของอากาศส่วนแรกและแกลบจะมีแกลบอยู่เฉพาะบริเวณผนังของ VFBC จำลองเท่านั้น บริเวณตรงกลางรอบๆแนวแกนของ VFBC จำลอง ซึ่งตรงกับแนวของท่อทางออกด้านบนสุดของ VFBC จำลอง ไม่พบว่ามีแกลบอยู่ในบริเวณนี้ซึ่งทำให้มั่นใจได้ว่าถ้าเป็นในกรณีของเตาเผาไหม้จริงแกลบซึ่งยังเผาไหม้ไม่หมดจะไม่ลอยหนีออกไปจากเตาได้

3.1.4 ผลของ Swirl number

ค่า Swirl No. (S) สำหรับ VFBC จะใช้เป็นดัชนีบอกว่าการไหลของอากาศ-แกลบเป็นผลมาจากการไหลอันเนื่องมาจากโมเมนตัมเชิงมุมหรือโมเมนตัมในแนวแกนมากกว่ากัน ซึ่งสามารถหาค่าได้ดังนี้

$$S = \sum_{i=1}^{m} f_i^2 \frac{\pi D_e D_o}{4A_{ti}} \qquad (1)$$

เมื่อ m คือ จำนวนท่อทางเข้าในแนวสัมผัส

A_t คือ พื้นที่หน้าตัดของท่อทางเข้าในแนวสัมผัส

f_i คือ สัดส่วนของปริมาณอากาศส่วนแรกต่อปริมาณอากาศทั้งหมด

D_e, D_o คือ เส้นผ่านศูนย์กลางภายในของท่อทางออกและของเตาตามลำดับ

ค่า S ของแต่ละการทดลองดูได้จากตารางที่ 1 จากผลการทดลองพบว่าการทดลองที่มีค่า S มากการเกิดวอร์เทคบริเวณวงแหวนวอร์เทคอันแรก (ที่ระยะ H/D = 2.25) จะมากพอที่จะทำให้ชั้นแขวนลอย (suspension layer) มีความเสถียรอยู่ได้และแกลบซึ่งเป็นอนุภาคขนาดใหญ่ไม่สามารถไหลข้ามชั้นนี้ไปได้ ดังเช่นการทดลองที่แสดงในรูปที่ 3 (a-c) (S = 5.25, 5.07, 4.86) ซึ่งมีอัตราการป้อนแกลบเท่ากับ 300 g/min และรูปที่ 4 (a-c) (S = 5.25, 4.86, 4.74) ซึ่งมีอัตราการป้อนแกลบเท่ากับ 250 g/min ในการทดลองที่มีค่า S ต่ำมาก จะทำให้เกิดแรงเหวี่ยงน้อยเกินไปจนกระทั่งแกลบใน Zone II จะไหลข้ามขึ้นมาใน Zone I และลอย

หลุดออกไปที่ท่อทางออก และนอกจากนี้แกลบใน Zone I ก็จะไม่เกาะกลุ่มกันเป็นเส้นเกลียว ดังแสดงในรูปที่ 3d (S = 4.74) และ 4d (S = 4.61) ผลของ Swirl Number อีกประการหนึ่งคือการไหลที่มีค่า S สูง ระยะพิทช์ของเกลียวจะสั้นลง (มุมที่แนวเกลียวทำกับแนวระดับจะน้อย)ซึ่งจะทำให้ residence time ของอนุภาคในเตาเผามากขึ้น ซึ่งดูได้จากรูปที่ 3a (S = 5.25) เปรียบเทียบกับรูปที่ 3d (S = 4.74)

3.1.5 การเหนี่ยวนำให้เกิดฟลูอิไดซ์เซชันในชั้นแขวนลอยจากสเปาเต็ดเบดในชั้นล่างสุดของ VFBC จำลอง

ในตอนเริ่มต้นของการออกแบบที่ส่วนด้านล่างสุดของ VFBC จำลองซึ่งเป็นที่อยู่ของเบดไม่ได้มีลักษณะเป็นรูปทรงกรวยอย่างที่แสดงในรูปแต่เป็นรูปทรงกระบอกเหมือนกับส่วนอื่นๆของเตาจำลอง แต่จากการทดลองในเบื้องต้นพบว่า เมื่ออากาศส่วนที่สองไหลจากด้านล่างผ่านแผ่นกระจายลมขึ้นมาไม่สามารถทำให้แกลบลอยตัวขึ้นมาแบบฟลูอิไดซ์เบดได้โดยภายในเบดของแกลบจะเกิดเป็นโพรงอากาศขึ้นในบางตำแหน่งและอากาศจากด้านล่างจะไหลผ่านโพรงอากาศนี้ขึ้นมาโดยไม่ได้พาแกลบให้ลอยตัวขึ้นมาด้วย ทำให้เบดมีลักษณะเป็นเบดนิ่ง สาเหตุเนื่องมาจากรูปทรงของแกลบและความหนาแน่นของแกลบซึ่งมีค่าน้อย ทำให้ยากต่อการเกิดฟลูอิไดซ์เซชัน Rao และคณะ [8] และ Natarajan และคณะ [5] จึงได้ใช้วัสดุเฉื่อยจำพวกทรายซิลิกา อลูมินา เป็นต้น ผสมกับเชื้อเพลิงชีวมวลเพื่อให้เกิดฟลูอิไดซ์เซชันขึ้นได้แต่สิ่งที่ตามมาคือความดันตกคร่อมเบดจะสูงมาก ในงานวิจัยนี้จึงได้มีแนวทางแก้ไขที่ต่างกันไปคือนำหลักการของสเปาเต็ดเบดมาประยุกต์ใช้กับเบดของ VFBCจำลองจึงได้ออกแบบด้านล่างของ VFBC จำลองให้มีลักษณะเป็นทรงกรวยทำให้แกลบในเบดลอยตัวขึ้นไปได้และมีลักษณะการไหลแบบภายในชั้นแขวนลอยของ Zone II แบบฟลูอิไดซ์เบด

3.1.6 อัตราส่วนความสูงต่อเส้นผ่าศูนย์กลาง (H/D) ของ VFBC จำลอง

ค่า H/D เป็นพารามิเตอร์ที่สำคัญอย่างหนึ่งในการออกแบบเตาเผาไหม้วอร์เทคและเตาเผาไหม้ฟลูอิไดซ์เบด เตาเผาไหม้ที่มีค่า H/D ต่ำโดยที่ยังมีประสิทธิเชิงความร้อนสูงจะมีค่า combustion intensity (หน่วยเป็น kg fuel/h/m^2 หรือ kg fuel/h/m^3)สูงในขณะที่ต้นทุนในการก่อสร้างต่ำ และสะดวกต่อการติดตั้งในพื้นที่จำกัด โดยทั่วไปแล้วค่า H/D ของเตาเผาไหม้จะถูกจำกัดด้วยเงื่อนไขของ residence time ที่ต้องมีระยะเวลานานพอเพียงต่อการเผาไหม้โดยสมบูรณ์ สำหรับเตาเผาไหม้ฟลูอิไดซ์เบด มีค่า H/D ประมาณ 13 และค่า combustion intensity ประมาณ 265 kg fuel/h/m^3 (530 kg fuel/h/m^2) [5,6] ในขณะที่เตาเผาไหม้ไซโคลนที่ใช้เชื้อเพลิงแกลบ ที่ผลิตใช้อยู่ภายในประเทศ มีค่า H/D เท่ากับ 2.5 และค่า combustion intensity ประมาณ 100 kg/h/m^3 [4] สำหรับในงานวิจัยนี้ ค่า H/D ของ VFBC จำลอง เท่ากับ 3.5 ซึ่งต่ำกว่าเตาเผาไหม้ฟลูอิไดซ์เบด แต่ยังสูงกว่าของเตาเผาไหม้ไซโคลนเนื่องจากมีส่วนที่เพิ่มขึ้นมาคือชั้นแขวนลอยของอนุภาคซึ่ง เป็นบริเวณที่มีลักษณะการไหลร่วมกันระหว่างวอร์เทคกับฟลูอิไดซ์เบดซึ่งเมื่อนำไปใช้งานในลักษณะของเตาเผาไหม้จริงส่วนนี้จะทำหน้าที่เป็นห้องเผาไหม้อีกส่วนหนึ่ง

3.2 การกระจายความเร็วของอากาศในแนวสัมผัสและแนวแกน

ในการทดลองที่ไม่มีการป้อนแกลบเข้าไปใน VFBC จำลอง ได้บันทึกความเร็วของอากาศทั้งในแนวสัมผัสและแนวแกนบนระนาบแนวดิ่งที่ผ่านกลาง (vertical midplane) ของ VFBC จำลอง ดังแสดงในรูปที่ 5(a-b) และ 6(a-b) ซึ่งเป็นการเปรียบเทียบความเร็วของอากาศในกรณีมีกับไม่มีวงแหวนวอร์เทคโดยทั้งสองการทดลอง อากาศทั้งสองส่วนมีเงื่อนไขการไหลตาม Run No.I ดังแสดงในตารางที่ 1

3.2.1 ความเร็วอากาศในแนวสัมผัส

จากรูปที่ 5 (a) เปรียบเทียบ รูปที่ 6 (a) เห็นได้อย่างชัดเจนว่าการเกิดวอร์เทคในกรณีมีวงแหวนวอร์เทคจะรุนแรงมากกว่าในกรณีไม่มีวงแหวนวอร์เทคโดยความเร็วสูงสุดในแนวสัมผัส ในกรณีมีวงแหวนวอร์เทคจะสูงกว่าในกรณีไม่มีวงแหวนวอร์เทคถึงประมาณ 3 เท่า ลักษณะโปรไพล์ ของความเร็วอากาศในแนวสัมผัส ในกรณีที่มีวงแหวนวอร์เทคค่อนข้างจะเป็นไปตามความสัมพันธ์ Rankine vortex ซึ่งรวมผลของการไหลแบบวอร์เทคอิสระ (free vortex flow) กับการไหลแบบวอร์เทคบังคับ (forced vortex flow) และเป็นไปตามความสัมพันธ์ดังนี้

$$W r^{n} = \text{constant} \qquad (2)$$

เมื่อ W = ความเร็วในแนวสัมผัส

R = รัศมีภายในของเตา

n = -0.8 , $0 < r < 0.65R$

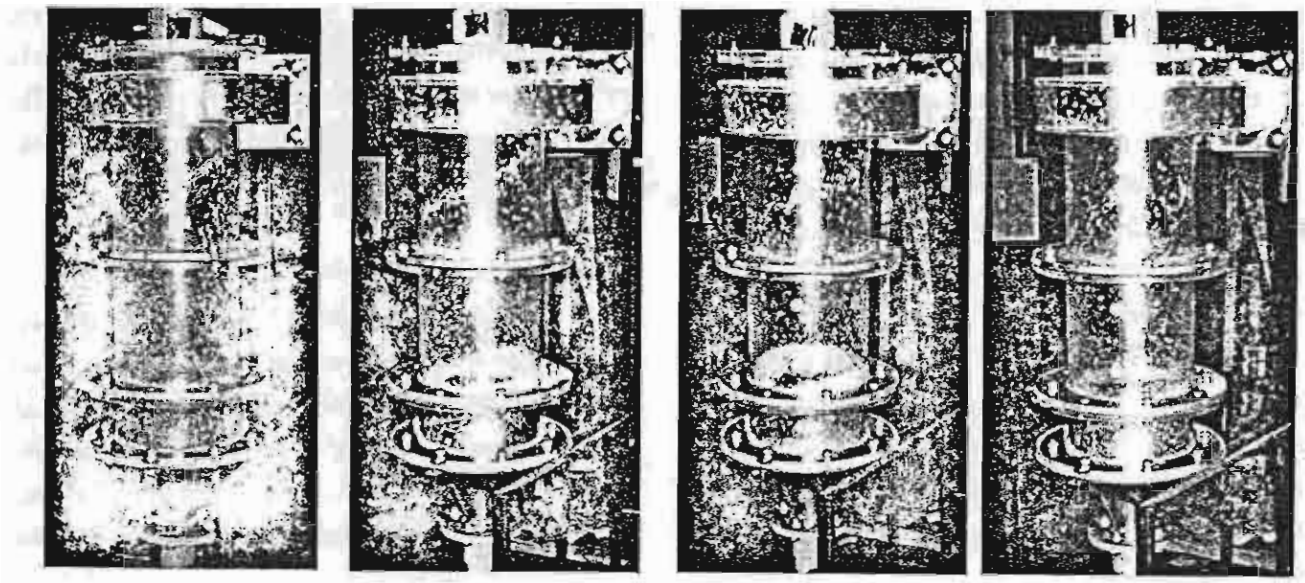
n = 0.5 , $0.65R < r < R$

r = ระยะที่วัดออกจากจุดศูนย์กลางในแนวรัศมี

สำหรับ VFBC จำลองที่ใช้งานวิจัยนี้ จากรูปที่ 5 (a) จะพบว่าการเกิดวอร์เทคแบบบังคับจะเกิดขึ้นในช่วงประมาณ $0 < r < 0.55R$ และวอร์เทคแบบอิสระจะเกิดขึ้นบริเวณช่วง $0.55R < r < R$ โดยวอร์เทคที่เกิดขึ้นเหนือวงแหวนวอร์เทคจะรุนแรงมากกว่าวอร์เทคที่เกิดขึ้นด้านล่างของวงแหวน สำหรับการทดลองกรณีที่ไม่ใช้วงแหวนวอร์เทคดังแสดงในรูปที่ 6a ดีกริการไหลแบบวอร์เทคไม่มากเมื่อเปรียบเทียบกับกรณีที่ใส่วงแหวนยกเว้น บริเวณด้านบนของ VFBC จำลองซึ่งอยู่ใกล้ท่อทางเข้าของอากาศส่วนแรก นอกจากนี้ยังพบว่าบริเวณของการเกิดวอร์เทคแบบอิสระจะแคบกว่าของวอร์เทคแบบบังคับมาก

การที่ความเร็วในแนวสัมผัสมีค่าสูงขึ้นมากเมื่อใส่วงแหวนวอร์เทคเข้าไปอธิบายได้ว่าเป็นผลมากจากความหนืดของอากาศบริเวณพื้นผิวของวงแหวนทำให้อากาศบริเวณพื้นผิวนี้ชลอความเร็วลงอย่างมาก ทำให้ความเร็วอากาศในแนวสัมผัสเหนือแผ่นวงแหวนขึ้นไปมีความเร็วเพิ่มขึ้นเพื่อให้ได้อัตราการไหลคงเดิม ดังนั้นจึงอาจกล่าวได้ว่าวงแหวนวอร์เทคจึงทำหน้าที่คล้ายหัวฉีดอากาศ (air nozzle) ตัวหนึ่งที่ช่วยเพิ่มความเร็วให้กับอากาศ จากรูปที่ 5 และ 6 จะเห็นได้ว่าโปรไฟล์ความเร็วในแนวสัมผัสค่อนข้างจะสมมาตรทั้งสองด้านของแกน VFBC จำลอง สำหรับที่บริเวณท่อทางออกและ ลักษณะโปรไฟล์ความเร็วคล้ายคลึงกันทั้งสองกรณี

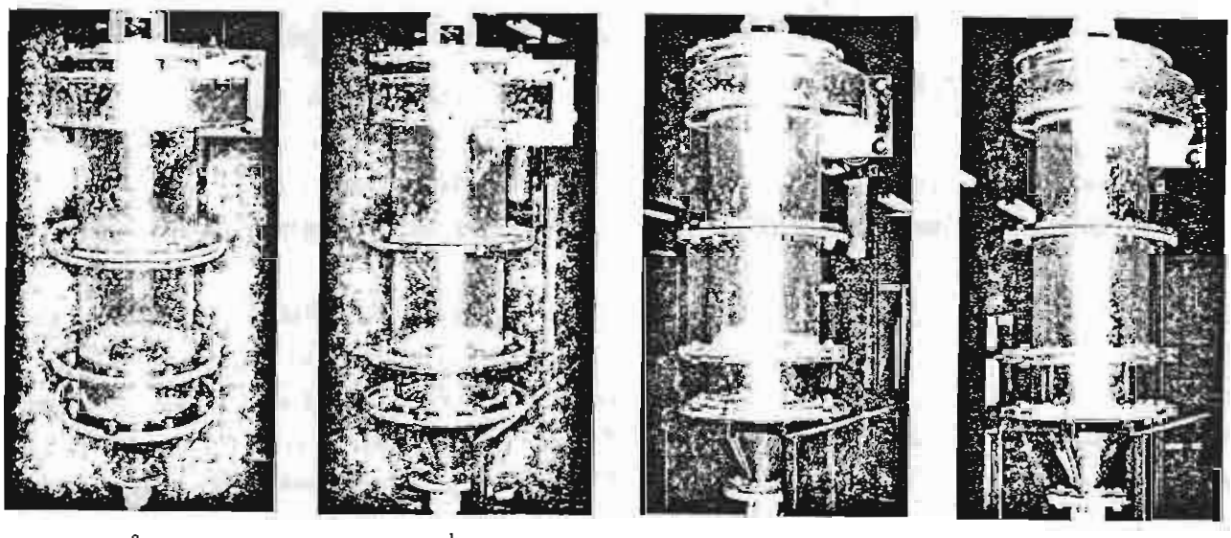
ผลประการสำคัญของการเกิดวอร์เทคที่รุนแรงใกล้บริเวณที่ติดตั้งวงแหวนวอร์เทคคือจะช่วยดักอนุภาคขนาดใหญ่ที่ยังเผาไหม้ไม่หมดไม่ให้ลอยหนีออกไปจากเตาได้



a b c d

Run No. 1 , S = 5.25 Run No. 2 , S = 5.07 Run No. 3 , S = 4.86 Run No. 4 , S = 4.74

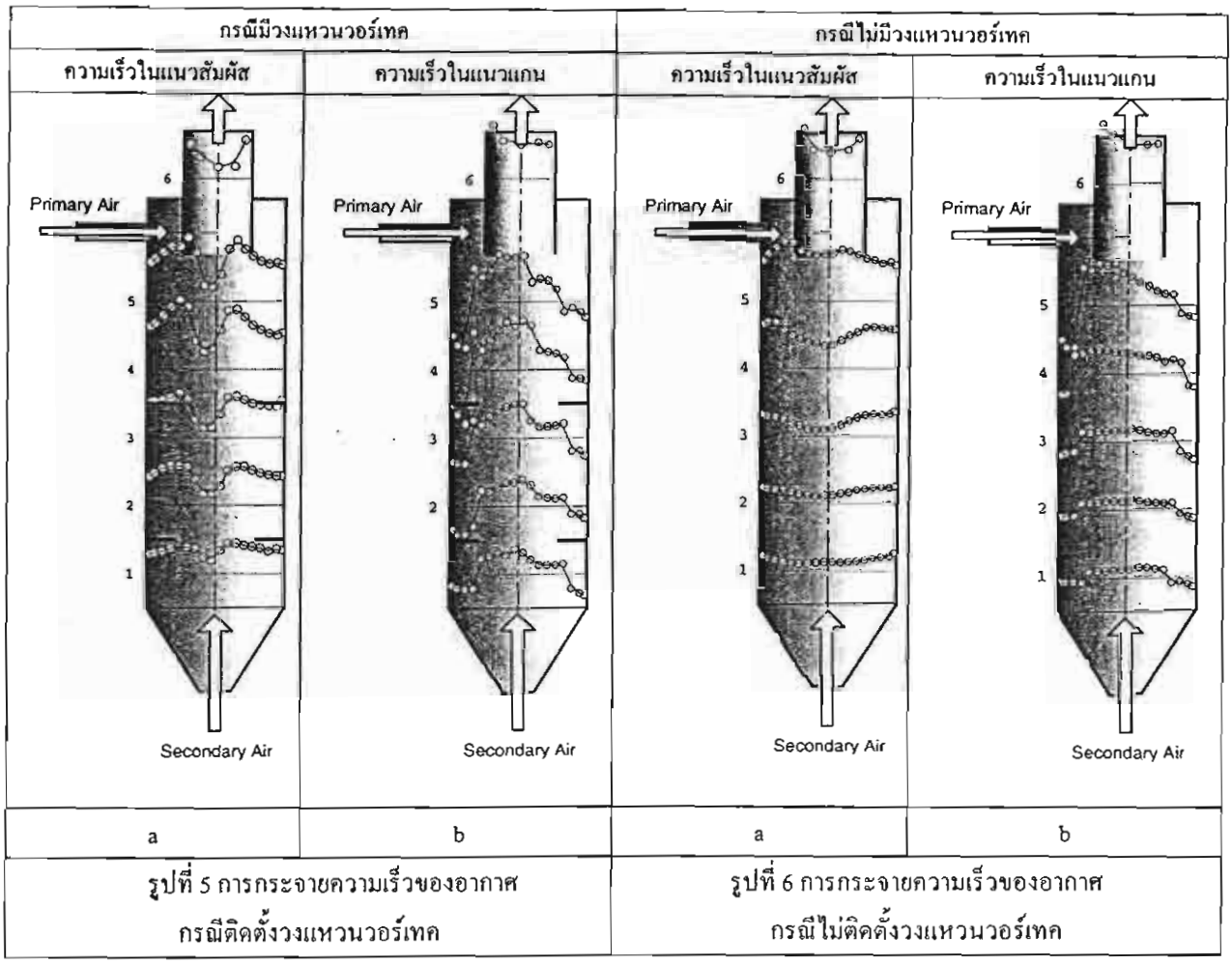
รูปที่ 3 การไหลของอากาศและแกลบใน VFBC จำลอง ในกรณีอัตราการป้อนแกลบ 250 g/min



a b c d

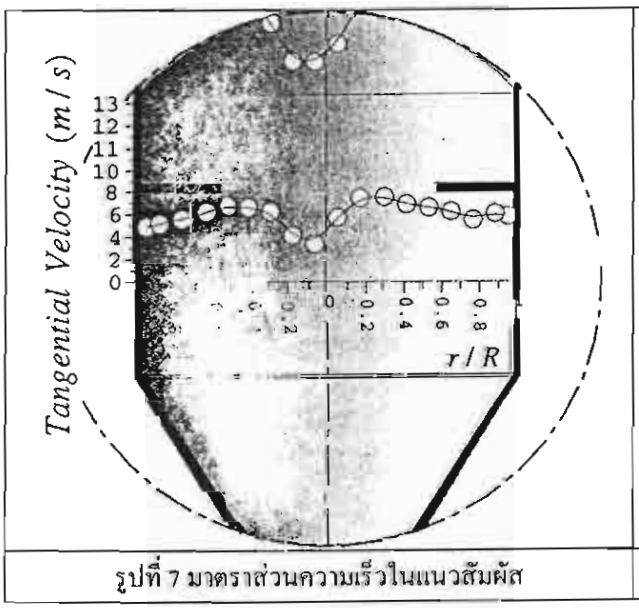
Run No. 5 , S = 5.25 Run No. 6 , S = 4.86 Run No. 7 , S = 4.74 Run No. 8 , S = 4.61

รูปที่ 4 การไหลของอากาศและแกลบใน VFBC จำลอง ในกรณีอัตราการป้อนแกลบ 300 g/min

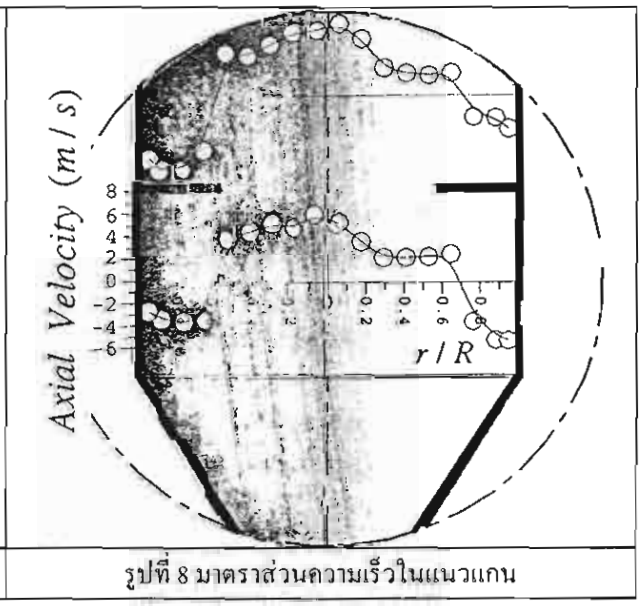


รูปที่ 5 การกระจายความเร็วของอากาศ
กรณีติดตั้งวงแหวนวอร์เทค

รูปที่ 6 การกระจายความเร็วของอากาศ
กรณีไม่ติดตั้งวงแหวนวอร์เทค



รูปที่ 7 มาตราส่วนความเร็วในแนวสัมผัส



รูปที่ 8 มาตราส่วนความเร็วในแนวแกน

3.2.2 ความเร็วอากาศในแนวแกน

ความเร็วอากาศในแนวแกน (axial velocity)ในทิศขึ้นในกรณีที่ใส่วงแหวนวอร์เทคจะมีค่าสูงกว่ากรณีที่ไม่ใส่วงแหวนวอร์เทคหลายเท่าดังแสดงในรูป 5b กับ 6b โดยเฉพาะที่ด้านล่างของ VFBC จำลองทำให้อากาศสามารถพาแกลบลอยตัวสูงขึ้นไหลเข้าไปสู่ที่แขวนลอยใน Zone II ได้ซึ่งจะตรงข้ามกับในกรณีที่ไม่ใส่วงแหวนวอร์เทคที่ความเร็วในแนวแกนไม่สูงพอที่จะยกแกลบให้ลอยสูงขึ้นได้ ซึ่งอาจเกิดจากสาเหตุสองประการ ประการแรก แรงเหวี่ยงซึ่งมีมากในกรณีที่ใส่วงแหวนวอร์เทคทำให้บริเวณตรงกลาง (Core region) มีความดันที่ต่ำจนทำให้เกิดผลต่างความดัน (pressure gradient) ระหว่างความดันที่ตำแหน่งทางเข้าของอากาศส่วนที่สอง(ด้านล่างของเตา)กับความดันภายใน VFBC จำลองมีค่ามากจึงทำให้อากาศไหลขึ้นในแนวแกนด้วยความเร็วสูงหรือประการที่สองอาจเกิดจากการที่พื้นที่ของการไหลวอร์เทคแบบบังคับซึ่งอยู่บริเวณกลางเตาถูกบีบให้พื้นที่เล็กลง จึงทำให้อากาศไหลขึ้นด้วยความเร็วสูงได้

จากรูปที่ 5b กับ 6b จะเห็นได้ว่า ความเร็วอากาศในแนวแกนทิศลงจะเกิดขึ้นในช่วง $0.65R < r < 1$ และมีความสมมาตรทั้งสองด้าน โดยกรณีที่ใส่วงแหวนวอร์เทคความเร็วในแนวแกนทิศทางลงจะมีมากกว่ากรณีที่ไม่ใส่วงแหวนวอร์เทคมากซึ่งการไหลกลับทาง (reverse flow) ของอากาศภายในเตา VFBC จำลองเช่นนี้จะช่วยทำให้แกลบหรืออนุภาคภายในเตาผาไหม้จริงมีการไหลหมุนเวียน (recirculating flow) โดยแกลบหรืออนุภาคที่มีขนาดใหญ่ และน้ำหนักมากที่ยังเผาไหม้ไม่หมด เมื่อลอยตัวขึ้นมาก็จะถูกเหวี่ยงไปปะทะผนังเตาด้วยแรงเหวี่ยงที่เกิดจากวอร์เทค และจะถูกอากาศบริเวณใกล้ผนังพาให้ไหลลงไปสู่เบดด้านล่างอีกครั้ง ซึ่งเท่ากับเป็นการเพิ่ม residence time และการคลุกเคล้ากันของอากาศกับอนุภาค (mixing)

4. สรุปผลการทดลอง

ในงานวิจัยนี้ได้ศึกษาพฤติกรรมการไหลของอากาศ-แกลบภายใน VFBC จำลองและได้วัดความเร็วของอากาศภายใน VFBC จำลองในขณะที่ไม่มีการป้อนแกลบ ซึ่งผลการทดลองสรุปได้ดังนี้

1. การไหลของอากาศ-แกลบภายใน VFBC จำลอง แสดงให้เห็นถึงการรวมคุณลักษณะเด่นของการไหลแบบฟลูอิไดซ์เบดและการไหลแบบวอร์เทคเข้าไว้ด้วยกันโดยการไหลแบบฟลูอิไดซ์เบดเกิดขึ้นบริเวณเหนือเบดและภายในชั้นแขวนลอยส่วนการไหลแบบวอร์เทคเกิดขึ้นที่บริเวณผนัง ตั้งแต่ด้านบนจนถึงด้านล่างของ VFBC

2. เกิดชั้นแขวนลอยของแกลบขึ้นภายใน VFBC จำลอง ระหว่างวงแหวนวอร์เทคทั้งสองโดยวงแหวนวอร์เทค ทำหน้าที่คล้ายหัวฉีดอากาศก่อให้เกิดการหมุนวนอย่างรุนแรงทำให้บริเวณวงแหวนจะมีสภาพคล้ายกับม่านอากาศทำหน้าที่ดักแกลบไม่ให้ลอยหนีออกไปจาก VFBC จำลองได้

3. การออกแบบด้านล่างสุดของ VFBC ให้มีลักษณะรูปทรงกรวยทำให้เกิดลักษณะของสเปาเต็ดเบดซึ่งจะช่วยให้แกลบลอยตัวขึ้นมาได้ง่าย และอนุภาคในเบดมีการหมุนเวียนทั่วถึงโดยไม่ต้องใช้วัตถุเฉื่อยซึ่งมีน้ำหนักมากมาผสมลงในเบด

4. พฤติกรรมการไหลของอากาศในแนวสัมผัสยังคงเป็นไปตามความสัมพันธ์ของ Rankine vortex

5. วงแหวนวอร์เทคนอกจากจะช่วยเพิ่มความรุนแรงในการเกิดวอร์เทคแล้วยังช่วยเพิ่มความเร็วอากาศในแนวแกน ทำให้แกลบลอยตัวได้ง่ายขึ้น

6. เกิดการไหลสวนทางของอากาศในแนวแกนขึ้นบริเวณผนัง VFBC ทำให้เกิดการหมุนเวียนของแกลบและเป็นการเพิ่ม residence time

กิตติกรรมประกาศ

ขอแสดงความขอบคุณสำนักงานกองทุนสนับสนุนการวิจัยที่ให้การสนับสนุนทุนวิจัย และ คุณวิบูลย์ เทเพนทร์ สถาบันวิจัยเกษตรวิศวกรรม กลุ่มงานวิจัยวิศวกรรมหลังการเก็บเกี่ยว ที่กรุณาให้คำแนะนำที่เป็นประโยชน์ต่องานวิจัยนี้อย่างมาก

เอกสารอ้างอิง

[1] A.k.Gupta, D.G.Lilley and N.Syred, "Swirl Flows", AbacusPress, Tunbridge Wells England, 1984.

[2] R.Singh, R.C.Maheshwari and T.P.Ojha, "Development of a Husk Fired Furnace", Journal of Agricultural Engineering Research, 1980, Vol.25, pp.119-120.

[3] J.A.Tumambig, "Testing and Evaluation of Rice Hull-Fed Furnace for Grain Drying", National Post Harvest Institute for Research and Extension, 1984, pp.197-214.

[4] S.Soponronnarit, T.Swasdisevi, S.Wetchacama, A.Shujinda, and B.Srisawat, "Cyclone Rice Husk Furnace and Its Application on Paddy Drying", International Energy Journal, 2000, Vol.1, No.2, pp.67-75.

[5] E.Natarajan, A.Nordin and A.N.Rao, "Overview of Combustion and Gasification of Rice Husk in Fluidized Bed Reactor", Biomass and Bioenergy, 1998, Vol.14, No.5/6. pp.533-546.

[6] J.Werther, M.Saenger, E.U.Hartge, T.Ogada, and Z.Siagi, "Combustion of Agricaltural residues. Progress in Energy and Combustion Science", 2000, Vol.26, No.1, pp.1-27.

[7] L.Armesto, A.Bahillo, K.Veijonen, A.Cabanillas, and J.Otero, "Combustion Behavior of Rice Husk in a Bubbling Fluidized

Bed. Biomass and Bioenergy", 2002, Vol.23, No.3, pp.171-179.

[8] T.R.Rao and J.V.Ram.Bheemarasetti, "Minimum Fluidization Velocities of Mixtures of Biomass and Sands", Energy, 2000, Vol.26, No.6, pp.633-644.

[9] G.Yang and S.Nieh, "Particle Flow Pattern in the Freeboard of a Vortexing Fluidized Bed", Powder Technology, 1987, Vol.50, pp.121-131.

[10] G.Yang and S.Nieh, "On the Suspension Layers in the Freeboard of Vortexing Fluidized Beds", Powder Technology, 1989, Vol.57, pp.171-179.

[11] S.Nigh, G.Yang, A.Q.Zhu and C.S.Zhao, "Measurements of Gas-Particle Flows and Elutriation of an 18 i.d. Cold Vortexing Fluidized-Bed Combustor Model", Powder Technology, 1992, Vol.69, pp.139-146.

[12] S.Nieh and J.Zhang, Swirling, Reacting, "Turbulent Gas-Particle Flow in a Vortex Combustor", Powder Technology, 2000, Vol.122, pp.70-78.

ıe Journal of the Royal Institute of Thailand
ıl. 29 No. 1 Jan.-Mar. 2004

การพัฒนาแบบจำลองทางคณิตศาสตร์ของระบบการทำความเย็นข้าวเปลือก

ปกรณ์ เหลืองมาลาวัฒน์
นักศึกษาปริญญาโท คณะพลังงานและวัสดุ
มหาวิทยาลัยเทคโนโลยีพระจอมเกล้าธนบุรี
อดิศักดิ์ นาถกรณกุล
ผู้ช่วยศาสตราจารย์ คณะพลังงานและวัสดุ
มหาวิทยาลัยเทคโนโลยีพระจอมเกล้าธนบุรี
สมชาติ โสภณรณฤทธิ์
ศาสตราจารย์ คณะพลังงานและวัสดุ
มหาวิทยาลัยเทคโนโลยีพระจอมเกล้าธนบุรี
ราชบัณฑิต สำนักวิทยาศาสตร์
ราชบัณฑิตยสถาน

บทคัดย่อ

งานวิจัยนี้มีวัตถุประสงค์เพื่อที่จะพัฒนาแบบจำลองทางคณิตศาสตร์ของระบบการทำความเย็นข้าวเปลือก และตรวจสอบความถูกต้องของแบบจำลอง โดยเปรียบเทียบกับการทำความเย็นข้าวเปลือกในไซโลขนาด ๒๕๐ ตัน แบบจำลองแบ่งเป็น ๒ ส่วน คือ แบบจำลองการทำความเย็นอากาศ และแบบจำลองการทำความเย็นข้าวเปลือก แบบจำลองการทำความเย็นอากาศใช้วิธีแก้สมการแบบแทนค่าต่อเนื่องในการแก้สมการที่ได้จากการสมดุลมวลและพลังงาน และสมการถ่ายเทความร้อนที่เครื่องแลกเปลี่ยนความร้อนระหว่างอากาศกับสารทำความเย็น และสมการสมรรถนะของเครื่องอัดไอ เพื่อหาภาวะอากาศหลังจากทำความเย็น แล้วนำไปแทนค่าในแบบจำลองการทำความเย็นข้าวเปลือก การจำลองการทำความเย็นข้าวเปลือกแบ่งเป็น ๒ ช่วง คือ ช่วงการทำความเย็นและช่วงการทำความเย็นซ้ำ ในช่วงทำความเย็นได้ลดอุณหภูมิข้าวเปลือกจากจุดเริ่มต้นจนถึง ๒๐ องศาเซลเซียส หลังจากนั้นได้ทำความเย็นข้าวเปลือกซ้ำเมื่อข้าวเปลือกที่ทำความเย็นไว้มีอุณหภูมิเพิ่มจาก ๒๐ องศาเซลเซียส ไปเป็น ๒๒ องศาเซลเซียส จากผลการเปรียบเทียบแบบจำลองกับการทดลองพบว่า แบบจำลองสามารถทำนายสภาวะของอากาศก่อนเข้าเครื่องทำความเย็นได้ใกล้เคียงกับผลการทดลอง ± ๒ องศาเซลเซียส อุณหภูมิของข้าวเปลือกในแต่ละชั้นได้ค่าความถูกต้องอยู่ในช่วง ± ๓ องศาเซลเซียส การทำนายเวลาในการทำความเย็นใกล้เคียงกับการทดลอง และแบบจำลองสามารถทำนายพลังงานในการทำความเย็นได้ความถูกต้องในช่วงไม่เกินร้อยละ ๑๘

คำสำคัญ : การทำความเย็น, เมล็ดพืช, แบบจำลองทางคณิตศาสตร์

๑. บทนำ

ปัจจุบันผู้บริโภคหันมาให้ความสนใจในด้านคุณภาพและความปลอดภัยของอาหารมากขึ้น ด้วยเหตุนี้ผู้ค้าข้าวหรือเจ้าของโรงสีจึงต้องปรับตัวให้เข้ากับความต้องการของตลาด โดยการรักษาคุณภาพข้าวของตนเพื่อให้เป็นที่ต้องการของผู้บริโภค โดยทั่วไปการเก็บรักษาข้าวเปลือกให้มีคุณภาพดีมีปัจจัยหลายอย่างที่จะต้องพิจารณา เช่น ความชื้นของข้าวเปลือก อุณหภูมิในกองข้าวเปลือกต้องไม่สูงเกินไป และต้องปลอดจากแมลง รา และหนู การเก็บกองข้าวด้วยอากาศแวดล้อมนั้นไม่สามารถลดอุณหภูมิของกองข้าวให้อยู่ในระดับต่ำกว่าอุณหภูมิบรรยากาศได้ ดังนั้น เพื่อให้ข้าวเปลือกปลอดจากการรบกวนจากแมลง การทำความเย็นข้าวเปลือกจึงเป็นทางเลือกที่ดีที่จะสามารถยืดระยะเวลาการเก็บรักษาข้าวเปลือกและยังสามารถลดการสูญเสียมวลแห้งอันเนื่องมาจากการหายใจของเมล็ดพืช ในการที่จะทำนาย

ภาวะต่าง ๆ เช่น อุณหภูมิและความชื้นของข้าวเปลือก ระยะเวลาและพลังงานที่ใช้ในการทำความเย็น จำเป็นต้องพัฒนาแบบจำลองทางคณิตศาสตร์ขึ้นมาเพื่อทำนายผลต่าง ๆ เหล่านี้

แบบจำลองการทำความเย็นข้าวเปลือกประกอบด้วยส่วนหลัก ๒ ส่วน คือ การทำความเย็นอากาศและการทำความเย็นข้าวเปลือก จากงานวิจัยที่ผ่านมาพบว่า การคำนวณการทำความเย็นอากาศสามารถทำได้โดยการใช้สมการเอมพิริคัลที่ได้จากการกราฟข้อมูลผู้ผลิต เพื่อมาทำนายกำลังของเครื่องอัดไอและความสามารถในการทำความเย็นของเครื่องทำระเหย โดยสมการอยู่ในรูปของอุณหภูมิของสารทำความเย็นที่เครื่องควบแน่นและเครื่องทำระเหย

วราภรณ์ รัตดนงพิสัตย์[๓] คำนวณการถ่ายเทความร้อนโดยใช้วิธีการคำนวณหาความแตกต่างอุณหภูมิเฉลี่ยเชิงลอการิทึม การหาคำตอบของสมการสามารถทำได้หลายวิธี เช่น วิธีของ Newton Raphson หรือวิธีการแทนค่าต่อเนื่อง โดยทั่วไปวิธีหลังจะเหมาะสมกว่าวิธีแรก เพราะไม่ซับซ้อน แต่มีข้อเสียคือ ใช้เวลาคำนวณมากกว่าวิธีแรก Khan and Zubair[๒] ได้ใช้วิธีการคำนวณแบบแทนค่าต่อเนื่องนี้ ศึกษาการจำลองการทำงานของระบบทำความเย็นแบบอัดไอ เพื่อคำนวณขนาดของการทำความเย็นและกำลังงานของเครื่องอัดไอ และวราภรณ์ รัตดนงพิสัตย์[๓] ใช้วิธีการนี้คำนวณแบบจำลองการอบแห้งมะละกอแช่อิ่มโดยใช้ปั๊มความร้อน ได้ผลใกล้เคียงกับผลการทดลอง ทั้งในส่วนของความชื้นสุดท้าย อุณหภูมิอากาศที่ตำแหน่งต่าง ๆ ในระบบ และอุณหภูมิของสารทำความเย็น

แบบจำลองทางคณิตศาสตร์ของการอบแห้งเมล็ดพืชที่มีผู้ศึกษากันอย่างกว้างขวางและมีอยู่หลายแบบ เช่น *แบบจำลองแบบสมดุล* คือ มีสมดุลความร้อนและความชื้นระหว่างเมล็ดพืชกับอากาศ แบบจำลองนี้มีการคำนวณที่ง่าย ไม่ต้องใช้สมการอบแห้งชั้นบาง แต่มีข้อจำกัดในการใช้ คือ สามารถใช้ได้ดีกับการอบแห้งด้วยอัตราการไหลของอากาศต่ำ แบบจำลองลอการิทึม (logarithemic model) เป็นแบบจำลองที่สามารถทำนายการอบแห้งได้ถูกต้องพอสมควร แต่แบบจำลองนี้ไม่ได้คำนึงผลของอุณหภูมิของเมล็ดพืชขณะอบแห้ง นอกจากนี้ภาวะอากาศที่ใช้จะต้องคงที่ และความชื้นของเมล็ดต้องเท่ากันทุกชั้น *แบบจำลองแบบไม่สมดุล* คือ แบบจำลองที่สมมติว่าไม่มีสมดุลความร้อนและความชื้นระหว่างเมล็ดพืชกับอากาศ แบบจำลองนี้สามารถทำนายการอบแห้งได้ดี แต่มีการคำนวณที่ยุ่งยากซับซ้อน และใช้เวลาในการคำนวณนาน จึงไม่เหมาะที่จะนำไปใช้ แบบจำลองที่มีการศึกษากันมาก คือ *แบบจำลองแบบใกล้สมดุล* ซึ่งสมดุลความร้อนแต่ไม่มีสมดุลความชื้นระหว่างเมล็ดพืชกับอากาศ แบบจำลองนี้มีข้อดี คือ เวลาที่ใช้ในการคำนวณน้อยกว่าแบบจำลองแบบไม่สมดุลและมีความถูกต้องใกล้เคียงกับแบบจำลองแบบไม่สมดุล โดยเฉพาะที่อัตราการไหลของอากาศสูง จากข้อดีของแบบจำลองแบบใกล้สมดุลในงานวิจัยนี้จึงใช้แบบจำลองแบบใกล้สมดุลของ Soponronnarit[๗] ในการทำแบบจำลอง

Maier et al.[๔] ได้ศึกษาการระบายอากาศในกองข้าวเปลือก โดยใช้อากาศเย็นและอากาศแวดล้อม โดยใช้ข้าวเปลือกความชื้นร้อยละ ๑๓ มาตรฐานเปียก บรรจุในไซโลขนาดเส้นผ่านศูนย์กลาง ๑๕ เมตร สูง ๑๐ เมตร อัตราการไหลของอากาศ ๐.๐๕-๐.๕ ลูกบาศก์เมตร/นาที/ตันข้าวเปลือก และใช้แบบจำลองทางคณิตศาสตร์แบบสมดุลที่พัฒนามาจากแบบจำลองของ Thompson[๕] มาทำนายการเปลี่ยนแปลงอุณหภูมิและความชื้นของข้าวเปลือก จากการศึกษาพบว่า การระบายอากาศอย่างต่อเนื่องโดยใช้อากาศเย็นสามารถทำให้อุณหภูมิของกองข้าวเปลือกลดลงเหลือ ๑๕ องศาเซลเซียส ใช้เวลา ๑๑๐-๑๔๔ ชั่วโมง ความชื้นของข้าวเปลือกลดลงเล็กน้อย การระบายอากาศอย่างต่อเนื่องโดยใช้อากาศแวดล้อมไม่สามารถทำให้อุณหภูมิข้าวเปลือกลดลงถึงค่า ๒๕ องศาเซลเซียส ได้ทั้งในฤดูฝนและฤดูร้อน (ใช้ภาวะอากาศภาคกลางประเทศไทย พ.ศ. ๒๕๓๑-๒๕๓๒) และได้ศึกษาการระบายอากาศโดยการเป่าด้วยอากาศแวดล้อมเป็นช่วง ๆ โดยวิธีควบคุมความชื้นสัมพัทธ์ พบว่าวิธีระบายอากาศแบบนี้ทำให้อุณหภูมิของกองข้าวเปลือกสูงกว่า ๒๖ องศาเซลเซียส ความชื้นลดลงร้อยละ ๐.๘ จากความชื้นเริ่มต้น แต่ใช้พลังงานน้อยกว่าวิธีระบายอากาศอย่างต่อเนื่องถึงร้อยละ ๓๘-๖๔

เอกภูมิ บุญธรรม[๖] สร้างเครื่องต้นแบบทำความเย็นข้าวเปลือกและทดลอง

ทำความเย็นข้าวเปลือกที่บรรจุในไซโลขนาด ๒๕๐ ตัน แบ่งการทดลองเป็น ๒ ช่วง คือ ช่วงทำความเย็นและช่วงทำความเย็นซ้ำ ในช่วงทำความเย็นจะลดอุณหภูมิข้าวเปลือกจากอุณหภูมิเริ่มต้น ๓๗-๔๐ องศาเซลเซียส จนถึง ๒๐ องศาเซลเซียส หลังจากนั้นจะทำความเย็นซ้ำเมื่ออุณหภูมิข้าวเปลือกเพิ่มจาก ๒๐ องศาเซลเซียส เป็น ๒๒ องศาเซลเซียส จากการทดลองช่วงความเย็น พบว่าใช้เวลา ๑๒๐-๑๔๔ ชั่วโมง ข้าวเปลือกในไซโลจะมีอุณหภูมิเพิ่มขึ้นจนถึงอุณหภูมิที่ต้องทำความเย็นซ้ำภายใน ๔๒ วันและช่วงทำความเย็นซ้ำใช้เวลา ๓๖ ชั่วโมง

งานวิจัยนี้มีวัตถุประสงค์เพื่อพัฒนาแบบจำลองทางคณิตศาสตร์ของระบบทำความเย็นข้าวเปลือก และตรวจสอบความถูกต้องของแบบจำลองกับผลการทดลองทำความเย็นข้าวเปลือกในไซโลขนาด ๒๕๐ ตัน (ขนาดเส้นผ่านศูนย์กลาง ๖.๔ เมตร สูง ๑๗ เมตร) ของเอกภูมิ บุญธรรม[๖] ซึ่งแบ่งการทำความเย็นข้าวเปลือกเป็น ๒ ช่วง คือ ช่วงทำความเย็นลดอุณหภูมิข้าวเปลือกจาก ๓๗-๔๐ องศาเซลเซียส ลงเหลือ ๒๐ องศาเซลเซียส และช่วงทำความเย็นซ้ำเมื่อข้าวเปลือกมีอุณหภูมิเพิ่มจาก ๒๐ องศาเซลเซียส เป็น ๒๒ องศาเซลเซียส

๒. วิธีการ

แบบจำลองการทำความเย็นข้าวเปลือกในงานวิจัยประกอบด้วย แบบจำลองทำความเย็นอากาศและแบบจำลองทำความเย็นข้าวเปลือก แบบจำลองการทำความเย็นอากาศใช้ในการคำนวณภาวะของอากาศเย็นที่ใช้ในแบบจำลองการทำความเย็นข้าวเปลือก แบบจำลองทั้งสองมีรายละเอียดดังนี้

๑. แบบจำลองการทำความเย็นอากาศ

๑.๑ การคำนวณอุณหภูมิและอัตราส่วนความชื้นของอากาศที่ทางออกเครื่องทำระเหย

การจำลองภาวะอากาศที่ทางเข้าไซโลนั้นประกอบไปด้วยสมการดังต่อไปนี้ คือ สมการในการคำนวณกำลังงานที่ให้กับเครื่องอัดไอ

$$P = A_1+A_2T_e+A_3T_e^2+A_4T_c+A_5T_c^2+A_6T_eT_c+A_7T_e^2T_c+A_8T_eT_c^2+A_9T_e^2T_c^2 \qquad (๑)$$

โดยที่ A1 = 4216.4694, A2 = 120.05706, A3 = 0.88326514, A4 = 117.71113
A5 = -0.026719114, A6 = -4.3301458, A7 = -0.033485281, A8 = 0.093942676
A9 = 0.00055950600

สมการคำนวณภาระความร้อนที่เครื่องทำระเหย :

$$Q_e = B_1+B_2T_e+B_3T_e^2+B_4T_c+B_5T_c^2+B_6T_eT_c+B_7T_e^2T_c+B_8T_eT_c^2+B_9T_e^2T_c^2 \qquad (๒)$$

โดยที่ A1 = 49539.545, A2 = 1536.5762, A3 = 14.595157, A4 = -344.00485
A5 = -0.96297989, A6 = 1.5698803, A7 = 0.12180095, A8 = -0.13283189
A9 = -0.0021689060

ภาระความร้อนที่เครื่องควบแน่นคำนวณได้จาก ผลรวมของภาระความร้อนที่เครื่องทำระเหยกับกำลังงานที่ป้อนให้กับเครื่องอัดไอ เมื่อทราบอุณหภูมิที่เครื่องควบแน่นและที่เครื่องทำระเหย

$$Q_c = Q_e + P \qquad (๓)$$

อุณหภูมิของสารทำความเย็นที่เครื่องทำระเหยคำนวณได้จากสมการ

$$Q_c = UA_c[(T_{ci}-T_c) - (T_{co}-T_c)]/[\ln((T_{ci}-T_c)/(T_{co}-T_c))]$$

จัดรูปได้

$$T_c = [T_{ci}-T_{co}\exp((T_{ci}-T_{co})UA_c/Q_c)]/[1-\exp((T_{ci}-T_{co})UA_c/Q_c \qquad (๔)$$

เมื่อพิจารณาให้ค่า heat transfer effectiveness ให้มีค่าคงตัว อุณหภูมิของสารทำความเย็นที่เครื่องควบแน่นคำนวณได้จากสมการ

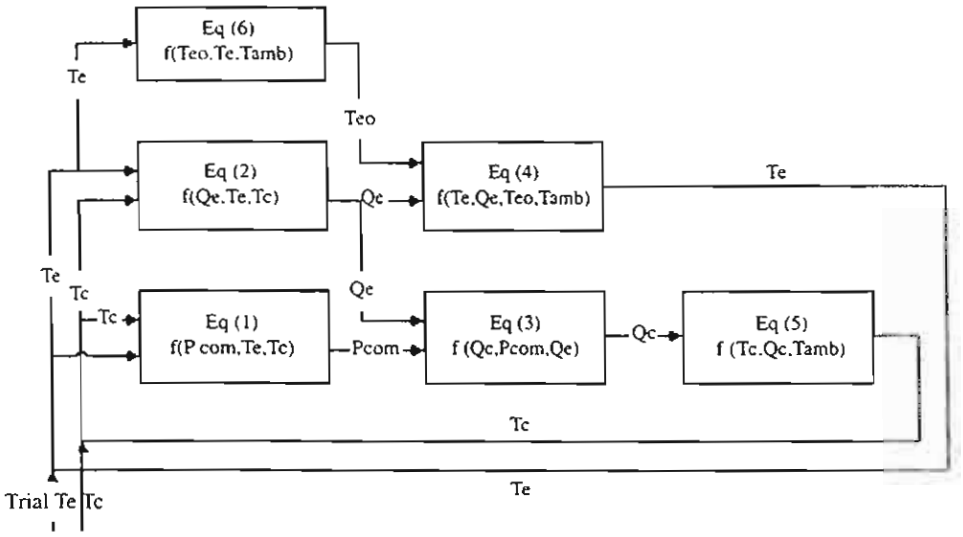
$$Q_c = \varepsilon C_{min}(T_c - T_{amb})$$
$$T_c = Q_c/(\varepsilon C_{min}) + T_{amb} \qquad (๕)$$

เมื่อ C_{min} คือ ผลคูณของอัตราการไหลกับความร้อนจำเพาะที่มีค่าต่ำสุด

เมื่อกำหนดอัตราส่วนอากาศที่ไม่สัมผัสเครื่องทำระเหยมีค่าเท่ากับ Bypass factor (BF) จากกฎทรงมวลสามารถคำนวณอุณหภูมิอากาศขาออกเครื่องทำระเหยได้ดังนี้

$$T_{eo} = (1-BF)T_e + (BF)T_{amb} \qquad (๖)$$

กลุ่มของสมการข้างต้น (สมการ ๑-๖) สามารถแก้ได้ด้วยวิธีการแทนค่าต่อเนื่อง โดยการกำหนดค่า T_e และ T_c เริ่มต้นให้แก่สมการ แล้วคำนวณตามลำดับขั้นตอนดังแสดงใน Information flow diagram (รูปที่ ๑)



รูปที่ ๑
Information flow diagram

อัตราส่วนความชื้นของอากาศคำนวณจากสมการ

$$W_{eo} = (1-BF)W_{con} + (BF)W_{ei} \qquad (๗)$$

โดยที่ W_{con} คือ อัตราส่วนความชื้นของอากาศอิ่มตัวอุณหภูมิเครื่องทำระเหย

เงื่อนไขของอากาศที่คำนวณได้จากสมการที่ ๗ ต้องนำไปตรวจสอบความเป็นไปได้โดยนำไปหาค่าความชื้นสัมพัทธ์ของอากาศ ถ้าความชื้นสัมพัทธ์ของอากาศน้อยกว่าหรือเท่ากับ ๑ แสดงว่าเป็นไปได้ ให้ข้ามไปคำนวณขั้นตอนถัดไป แต่ถ้ามากกว่า ๑ จะต้องปรับค่าอุณหภูมิและอัตราส่วนความชื้นใหม่ โดยใช้หลักการอนุรักษ์มวลและพลังงาน

๑.๒ อุณหภูมิอากาศที่ออกจากขดลวดความร้อนและพัดลมหลัก อุณหภูมิของอากาศที่ออกจากขดลวดความร้อนหาได้จากสมการอนุรักษ์พลังงาน ดังสมการ

$$Q_{Heater} = m_a(C_a+WC_v)(T_{ho}-T_{hi})$$

จัดรูปสมการ

$$T_{ho} = T_{hi} + \frac{Q_{Heater}}{m_a(C_a + WC_v)} \qquad (๘)$$

เมื่อสมมติว่าค่าการสูญเสียความร้อนระหว่างระบบและสิ่งแวดล้อมมีค่าน้อยมาก อุณหภูมิอากาศที่ทางออกพัดลมหลักคำนวณได้จากสมการ

$$m_a(C_a+WC_v)(T_{fo}-T_{ho}) = W_s$$

จัดรูปสมการ

$$T_{fo}= T_{ho}- \frac{W_s}{m_a(C_a + W.C_v)} \qquad (๙)$$

โดยที่กำลังงานเพลาสำหรับขับเคลื่อนพัดลมหลักหาได้จากสมการ

$$W_s = \frac{P_t.m_a}{\rho_a \eta_t} \qquad (๑๐)$$

๑.๓ อุณหภูมิของอากาศที่เพิ่มขึ้นจากการถ่ายเทความร้อนที่ท่อส่งลมเย็น เนื่องจากอากาศบริเวณรอบ ๆ ท่อส่งลมเย็นมีอุณหภูมิสูงกว่าอุณหภูมิของอากาศเย็น ทำให้เกิดการถ่ายเทความร้อนเข้ามาสู่ลมเย็นภายในท่อ ส่งผลให้อุณหภูมิของลมเย็นมีค่าสูงขึ้น จากสมการอนุรักษ์พลังงาน

$$m_a(C_a+WC_v)(T_{od}-T_{id}) = UA(T_{amb}-(T_{od}+T_{id})/2)$$

จัดรูปสมการใหม่เพื่อหาค่าอุหภูมิที่ทางออกลมเย็น (T_{od}) ได้

$$T_{od}= (UAT_{amb}-(UA/2-m_a(C_a+WC_v))T_{id})/(UA/2+m_a(C_a+WC_v)) \qquad (๑๑)$$

อุณหภูมิของอากาศ และอัตราส่วนความชื้นที่คำนวณได้จากขั้นตอนต่าง ๆ นี้จะนำไปใช้เป็นข้อมูลในการคำนวณในแบบจำลองการทำความเย็นข้าวเปลือกต่อไป

๒. แบบจำลองการทำความเย็นข้าวเปลือก

แบบจำลองทางคณิตศาสตร์ที่ใช้งานวิจัยนี้เป็นแบบจำลองแบบไกล้สมดุลของ Soponronnarit[๓] เนื่องจากไซโลที่เก็บข้าวเปลือกเป็นชนิดฐานกรวย ต้องปรับรูปทรงกรวยให้อยู่ในรูปของทรงกระบอกโดยใช้ความสัมพันธ์ทางปริมาตร แล้วแบ่งข้าวเปลือกที่ต้องการทำความเย็นออกเป็นชั้นบางย่อย ๆ หลาย ๆ ชั้น แล้วจึงคำนวณทีละชั้นบางโดยมีขั้นตอนในการคำนวณดังนี้

๒.๑ การคำนวณหาความชื้นของเมล็ดพืชภายหลังการทำความเย็น

ความชื้นของเมล็ดพืชหลังการทำความเย็นของแต่ละชั้นบาง คำนวณได้จากสมการการเปลี่ยนแปลงความชื้นของ Bannaszek and Sibenmorgen[๗] ซึ่งเขียนได้ดังนี้

$$(M-M_{eq})/(M_{in}-M_{eq}) = \exp(-kt^n) \qquad (๑๒)$$

การคำนวณอัตราการเปลี่ยนแปลงความชื้น ทำได้โดยการหาอนุพันธ์สมการอบแห้งชั้นบางสมการ (๑๒) เทียบกับเวลา แล้วใช้เทคนิควิธี Finite Difference เพื่อคำนวณหาความชื้นของข้าวเปลือกภายหลังการทำความเย็น

โดยที่ $k = 0.0038177105\ M_{in} + 0.0081804980T - 0.038923141$ และ $n = 0.67924731$
และความชื้นสมดุล (M_{eq}) หาได้จากสมการความชื้นสมดุลของ Bannaszek and Sibenmorgen[๗] ซึ่งเขียนได้ดังนี้

$$M_{eq} = 0.12669489M_{in} + 20.633281RH_{bd} - 0.029797360T_{bd} - 2.5887973 \qquad (๑๓)$$

M_{eq} และ M_{in} ในสมการที่ ๑๒ และ ๑๓ มีหน่วยเป็นร้อยละมาตรฐานเปียก แต่ความชื้นของข้าวเปลือกในสมการอื่น ๆ ในบทความนี้มีหน่วยเป็นเศษส่วนมาตรฐานแห้ง

๒.๒ การคำนวณภาวะอากาศภายหลังการทำความเย็น

ภาวะของอากาศที่เปลี่ยนไปหลังจากการทำความเย็น หาได้จากสมการอนุรักษ์มวลและพลังงาน จากหลักการอนุรักษ์มวล ความชื้นของอากาศที่เปลี่ยนไปเมื่อผ่านชั้นบางของเมล็ดพืชเท่ากับปริมาณน้ำที่ระเหยออกจากเมล็ดพืช ดังนั้น อัตราส่วนความชื้นของอากาศหลังการทำความเย็น (W_f) คำนวณได้จากสมการ

$$W_f - W_{bd} = (M_{bd} - M_f)R \qquad (๑๔)$$

จากหลักการอนุรักษ์พลังงาน ผลรวมของความแตกต่างของเอนทัลปีของกระแสอากาศชื้นที่ไหลเข้าและออกจากปริมาตรบังคับและการเปลี่ยนแปลงของพลังงานภายในของปริมาตรบังคับเท่ากับศูนย์

$$C_a T_{bd} + W_{bd}(2502 + C_v T_{bd}) + RC_{pw}\theta_{bd} = C_a T_f + W_f(2502 + C_v T_f) + RC_{pw}T_f \qquad (๑๕)$$

ภาวะของอากาศหลังการทำความเย็น (W_r และ T_r) ที่คำนวณได้จากสมการ ๑๔ และ ๑๕ ต้องตรวจสอบความเป็นไปได้ ของความชื้นสัมพัทธ์ของอากาศ

ขั้นตอนการคำนวณที่กล่าวทั้งหมดเป็นการคำนวณที่ชั้นบางชั้นเดียวเท่านั้น อากาศที่ทางออกชั้นบางนี้จะเป็นอากาศที่ทางเข้าของชั้นบางถัดไป การคำนวณจะดำเนินไปในลักษณะเดียวกันสำหรับชั้นบางทีละชั้น ตั้งแต่ชั้นล่างจนถึงชั้นบนสุดก็จะสิ้นสุดในช่วงเวลาที่พิจารณา หลังจากนั้นก็คำนวณในช่วงเวลาถัดไปจนกระทั่งครบตามเวลาที่กำหนดไว้

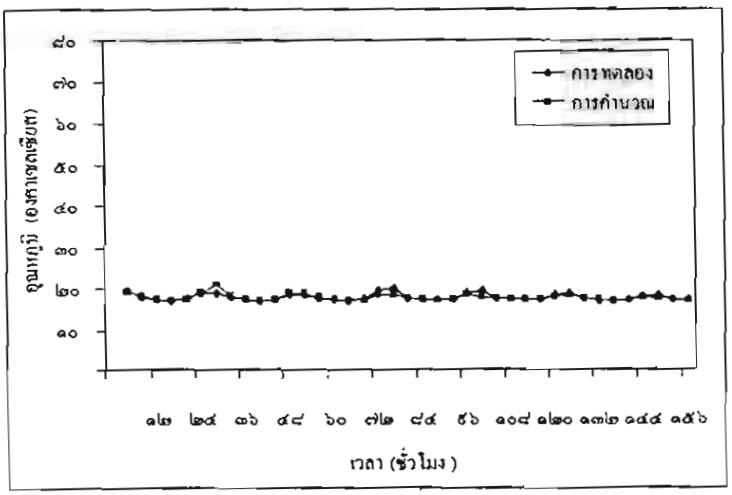
การจำลองการทำความเย็นข้าวเปลือกมีเงื่อนไขในการทำแบบจำลองตามการทดลองของเอกภูมิ บุญธรรม[๖] โดยแบ่งการคำนวณเป็น ๒ ช่วงคือ ช่วงทำความเย็นและช่วงทำความเย็นซ้ำ ช่วงทำความเย็นใช้อัตราการไหลของอากาศ ๑,๕๙๒ ลูกบาศก์เมตร/ชั่วโมง อุณหภูมิเริ่มต้นของข้าวเปลือกอยู่ในช่วง ๓๗-๔๐ องศาเซลเซียส ความชื้นเริ่มต้นร้อยละ ๑๔ มาตรฐานเปียก ทำความเย็นจนกระทั่งข้าวเปลือกมีอุณหภูมิเท่ากับ ๒๐ องศาเซลเซียส ในช่วงทำความเย็นซ้ำใช้อัตราการไหล ๑,๔๒๘ ลูกบาศก์เมตร/ชั่วโมง อุณหภูมิเริ่มต้นของข้าวเปลือกอยู่ในช่วง ๒๒ องศาเซลเซียส ความชื้นเริ่มต้นร้อยละ ๑๔ มาตรฐานเปียก ทำความเย็นจนกระทั่งอุณหภูมิข้าวเปลือกลดลงจนถึง ๒๐ องศาเซลเซียส

๓. ผลการศึกษาและวิจารณ์

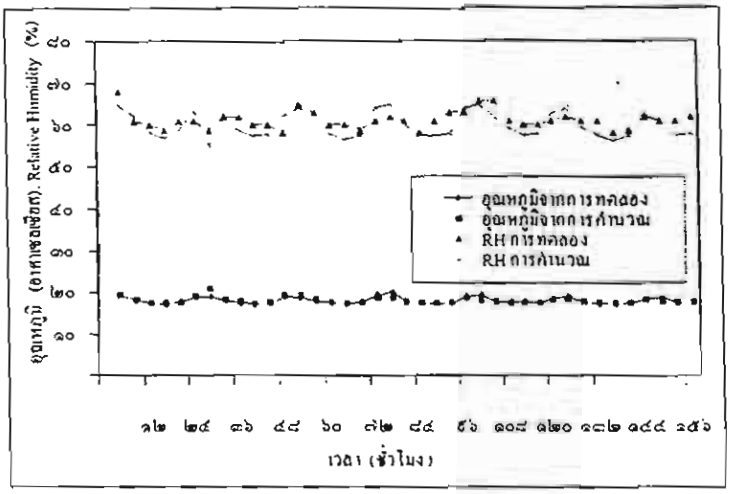
การตรวจสอบความถูกต้องของแบบจำลองการทำความเย็นข้าวเปลือกที่พัฒนาขึ้นมา ทำได้โดยเปรียบเทียบผลจากการคำนวณกับผลการทดลองของ เอกภูมิ บุญธรรม[๖] และแบ่งการเปรียบเทียบออกเป็น ๒ ส่วน คือ ส่วนของการทำความเย็นอากาศ และส่วนของการทำความเย็นข้าวเปลือก โดยจะเปรียบเทียบเฉพาะอุณหภูมิของอากาศเย็นและข้าวเปลือก เนื่องจากในการทดลองของเอกภูมิ บุญธรรม[๖] ไม่สามารถหาความชื้นของข้าวเปลือกในไซโลในช่วงเวลาทำความเย็นได้

๓.๑ แบบจำลองการทำความเย็นอากาศ

แบบจำลองการทำความเย็นอากาศ ใช้ข้อมูลภาวะของอากาศที่ทำการทดลองมาคำนวณหาอุณหภูมิและความชื้นสัมพัทธ์ของอากาศก่อนเข้าเครื่องทำความเย็น จากการจำลองในช่วงทำความเย็นอัตราการไหลของอากาศ ๑,๕๙๒ ลูกบาศก์เมตร/ชั่วโมง ได้ผลการเปรียบเทียบระหว่างอุณหภูมิและความชื้นสัมพัทธ์ของอากาศที่ทางออกเครื่องทำระเหยกับที่ทางเข้าไซโลกับการทดลองแสดงดังรูปที่ ๒ และ ๓ ตามลำดับ



รูปที่ ๒ อุณหภูมิของอากาศที่ทางออกของเครื่องทำระเหย



รูปที่ ๓ อุณหภูมิและความชื้นสัมพัทธ์ของอากาศที่ทางเข้าไซโล

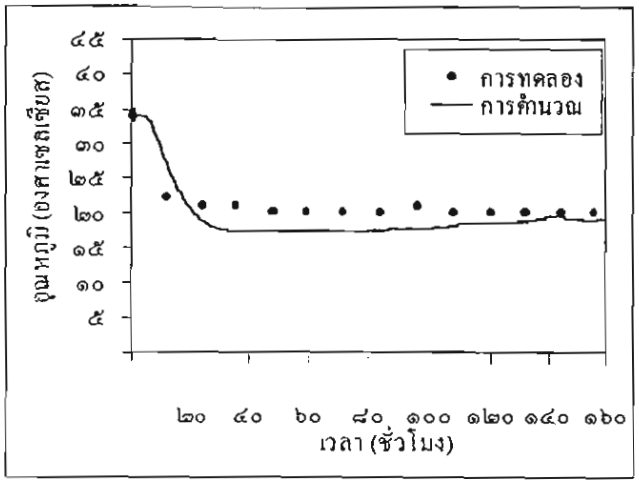
จากการเปรียบเทียบพบว่าแบบจำลองสามารถทำนายอุณหภูมิที่ทางออกเครื่องทำระเหย(รูปที่ ๒) และทางเข้าไซโล (รูปที่ ๓)ใกล้เคียงกับผลการทดลอง โดยมีความผิดพลาดในช่วง ±๒ องศาเซลเซียส

สำหรับความชื้นสัมพัทธ์ของอากาศนั้น แบบจำลองทำนายได้ค่าความแตกต่างในช่วงร้อยละ ๔-๕ ซึ่งอยู่ในช่วงค่าความถูกต้องของการวัดความชื้นสัมพัทธ์โดยวิธีวัดค่าอุณหภูมิกระเปาะเปียกและอุณหภูมิกระเปาะแห้ง (±๕%)

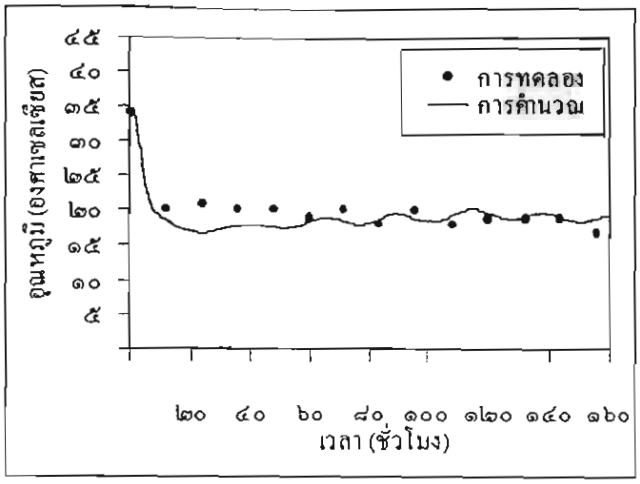
ส่วนพลังงานที่ใช้ในการทำความเย็นอากาศ ซึ่งประกอบไปด้วยพลังงานที่เครื่องอัดไอ พัดลมหลัก และขดลวดความร้อนนั้น แบบจำลองสามารถทำนายพลังงานนี้ได้ค่าใกล้เคียงกับพลังงานที่ใช้จริงในการทดลอง คือ ในการทดลองการทำความเย็นข้าวเปลือกใช้พลังงานเท่ากับ ๑,๔๑๘.๖ กิโลวัตต์ชั่วโมง แต่จากแบบจำลองคำนวณได้ ๑,๖๕๖.๐๙ กิโลวัตต์ชั่วโมง และช่วงทำความเย็นซ้ำใช้พลังงาน ๔๐๖.๓ กิโลวัตต์ชั่วโมง แบบจำลองคำนวณได้ ๔๖๑.๖๙ กิโลวัตต์ชั่วโมง ซึ่งจากการเปรียบเทียบจะพบว่าการทำนายพลังงานนั้นมีความผิดพลาดอยู่ในช่วงร้อยละ ๑๘ เมื่อเทียบกับผลการทดลองทั้ง ๒ ช่วง

๓.๒ แบบจำลองการทำความเย็นข้าวเปลือก

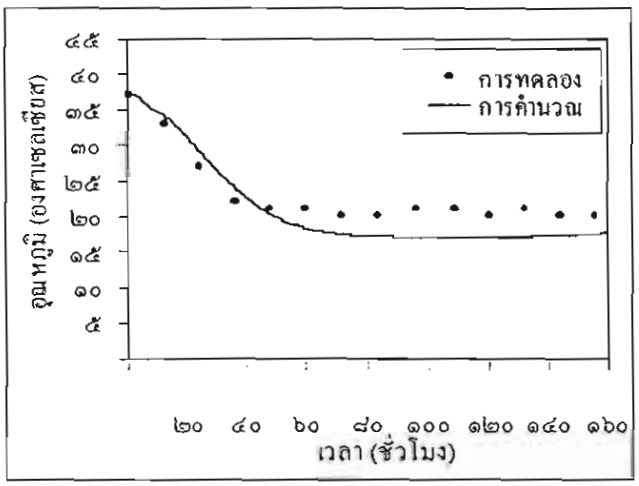
จากการเปรียบเทียบอุณหภูมิของข้าวเปลือกในไซโลตามจุดวัดที่วัดได้จากการทดลองจำนวน ๗ จุดตามระดับความสูงกับแบบจำลองโดยใช้อัตราการไหลของอากาศ ๑,๕๙๒ ลูกบาศก์เมตร/ชั่วโมง อุณหภูมิเริ่มต้นของข้าวเปลือกในช่วง ๓๗-๔๐ องศาเซลเซียส ความชื้นข้าวเปลือกเริ่มต้นร้อยละ ๑๔ มาตรฐานเปียก ใช้ผลการคำนวณอุณหภูมิและความชื้นสัมพัทธ์ที่ทางเข้าไซโลจากแบบจำลองการทำความเย็นอากาศเป็นอุณหภูมิและความชื้นสัมพัทธ์ของอากาศที่ใช้ทำความเย็นข้าวเปลือก พบว่าอุณหภูมิข้าวเปลือกที่คำนวณได้มีค่าใกล้เคียงกับผลการทดลองในทุกระดับความสูงที่วัด โดยมีค่าความแตกต่าง ± ๓ องศาเซลเซียส (แสดงในรูปที่ ๔ ถึงรูปที่ ๑๐) การทำนายผลที่ใกล้เคียงนี้แสดงให้เห็นโดยนัยว่า สมการอบแห้งชั้นบางและสมการสมดุลของข้าวเปลือกที่ใช้ในแบบจำลอง สามารถใช้ได้ดีกับการทำความเย็นข้าวเปลือก



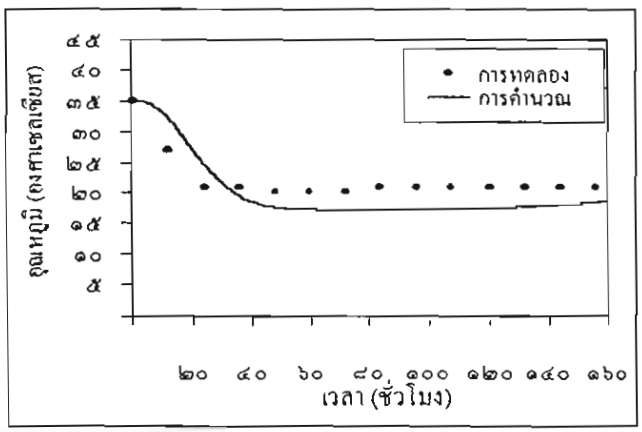
รูปที่ ๔
อุณหภูมิของข้าวเปลือกขณะทำความเย็นในระดับที่ ๑
(๒ เมตรจากฐานไซโล)



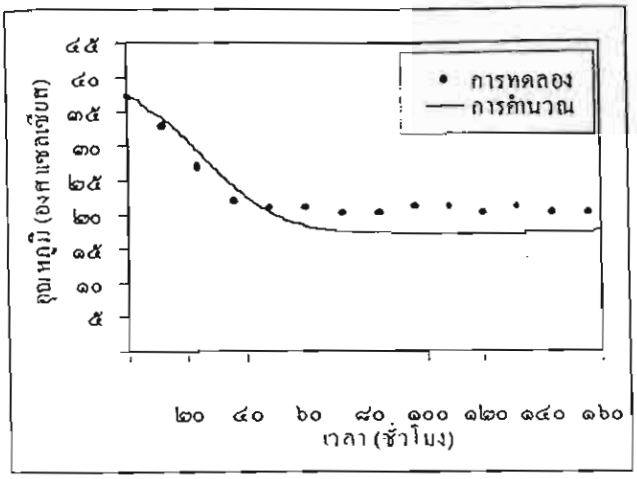
รูปที่ ๕
อุณหภูมิของข้าวเปลือกขณะทำความเย็นในระดับที่ ๒
(๔ เมตรจากฐานไซโล)



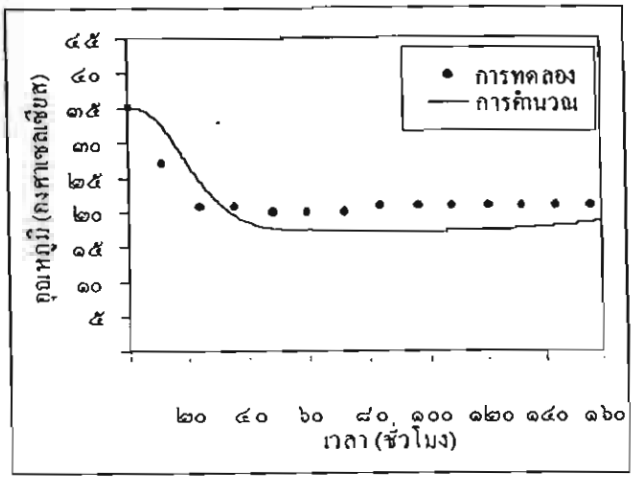
รูปที่ ๖
อุณหภูมิของข้าวเปลือกขณะทำความเย็นในระดับที่ ๓
(๖ เมตรจากฐานไซโล)



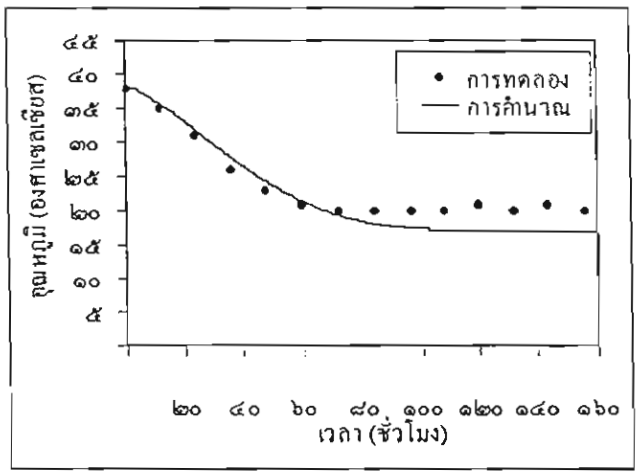
รูปที่ ๗
อุณหภูมิของข้าวเปลือกขณะทำความเย็นในระดับที่ ๔
(๘ เมตรจากฐานไซโล)



รูปที่ ๘
อุณหภูมิของข้าวเปลือกขณะทำความเย็นในระดับที่ ๕ (๑๐ เมตรจากฐานไซโล)

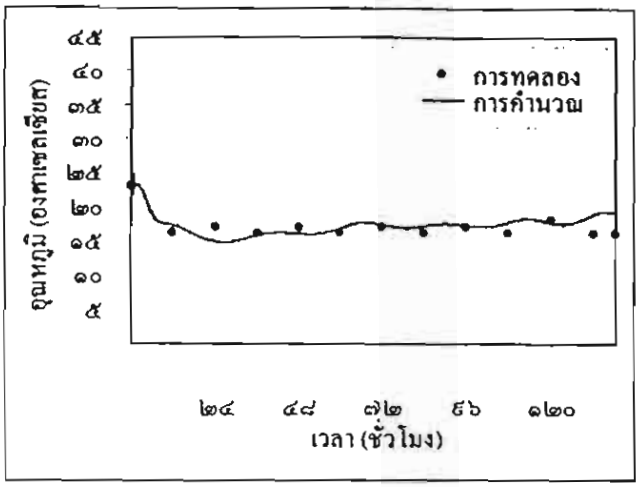


รูปที่ ๙
อุณหภูมิของข้าวเปลือกขณะทำความเย็นในระดับที่ ๖ (๑๒ เมตรจากฐานไซโล)

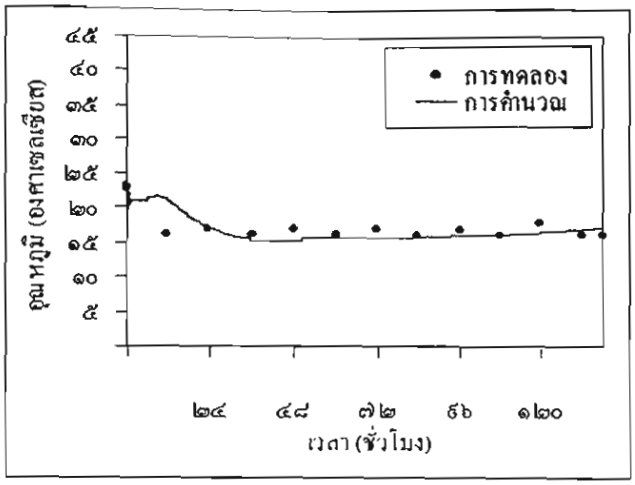


รูปที่ ๑๐ อุณหภูมิของข้าวเปลือกขณะทำความเย็นในระดับที่ ๗ (๑๔ เมตรจากฐานไซโล)

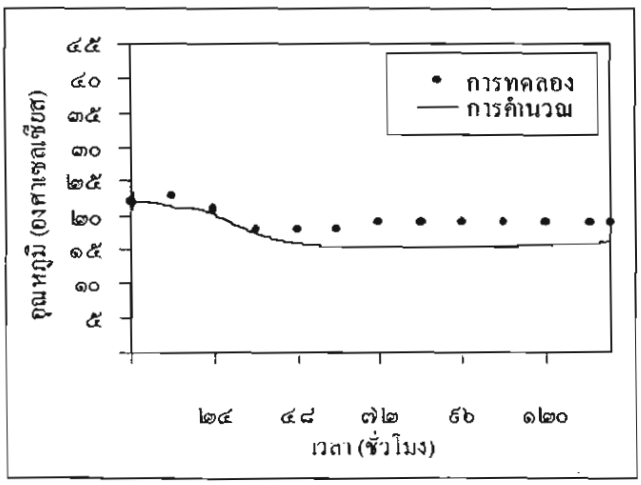
เมื่อเปรียบเทียบผลการคำนวณจากแบบจำลองกับผลการทดลองในช่วงทำความเย็นซ้ำ (แสดงการเปรียบเทียบในรูปที่ ๑๑ ถึงรูปที่ ๑๗) โดยใช้อุณหภูมิและความชื้นสัมพัทธ์ที่ทางเข้าไซโลที่ได้จากการคำนวณจากแบบจำลองการทำความเย็นอากาศในช่วงทำความเย็นซ้ำเป็นอุณหภูมิที่ใช้ทำความเย็นซ้ำ อัตราการไหลของอากาศ ๑.๔๒๘ ลูกบาศก์เมตร/ชั่วโมง ใช้อุณหภูมเริ่มต้นของข้าวเปลือก ๒๒ องศาเซลเซียส และความชื้นเริ่มต้นของข้าวเปลือกร้อยละ ๑๔ มาตรฐานเปียก พบว่า แบบจำลองสามารถทำนายอุณหภูมิของข้าวเปลือกในแต่ละชั้นที่เก็บในไซโลได้ใกล้เคียงกับผลการทดลอง โดยมีความผิดพลาด ± ๓ องศาเซลเซียส เช่นเดียวกับในช่วงทำความเย็น



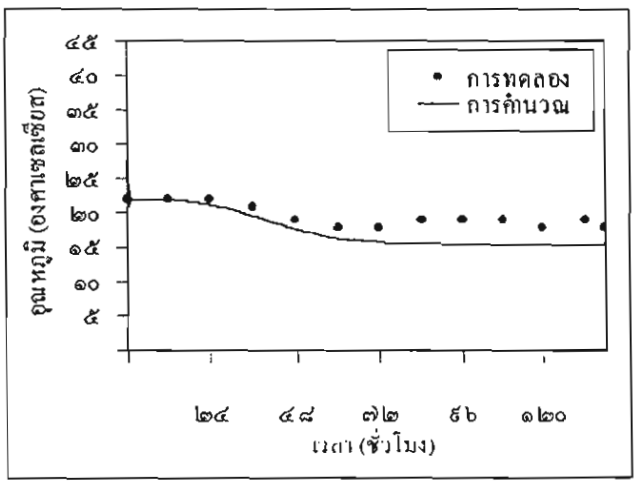
รูปที่ ๑๑
อุณหภูมิของข้าวเปลือกขณะทำความเย็นชั้นในระดับที่ ๑
(๒ เมตรจากฐานไซโล)



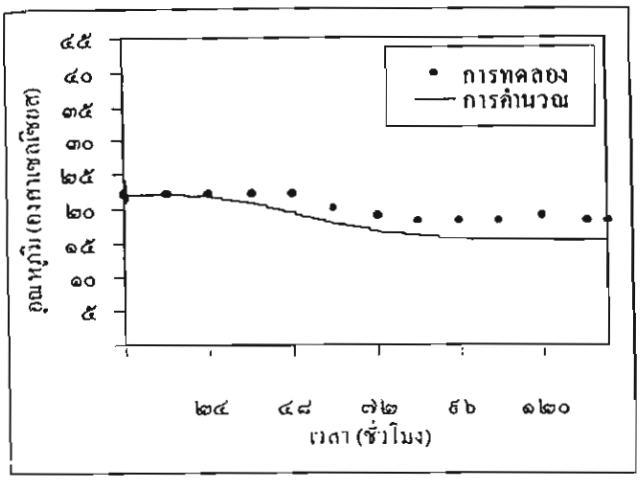
รูปที่ ๑๒
อุณหภูมิของข้าวเปลือกขณะทำความเย็นชั้นในระดับที่ ๒
(๔ เมตรจากฐานไซโล)



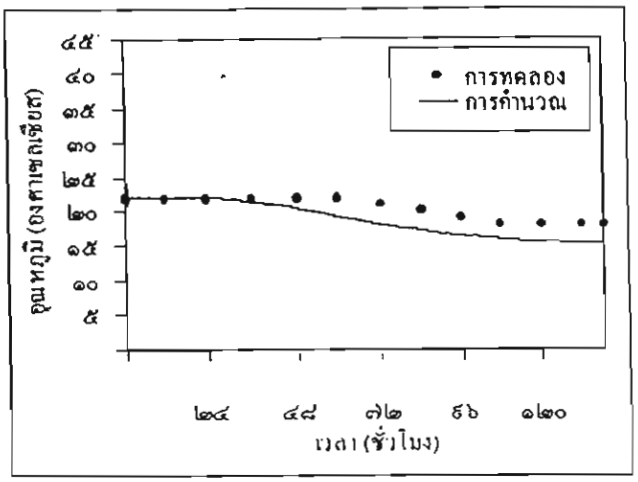
รูปที่ ๑๓
อุณหภูมิของข้าวเปลือกขณะทำความเย็นชั้นในระดับที่ ๓
(๖ เมตรจากฐานไซโล)



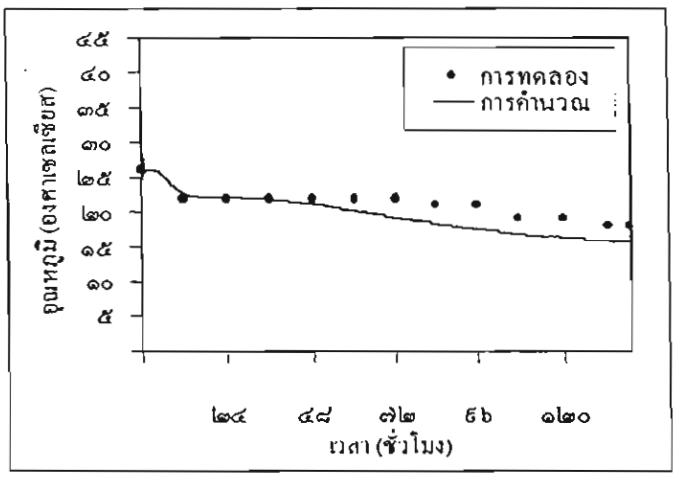
รูปที่ ๑๔
อุณหภูมิของข้าวเปลือกขณะทำความเย็นชั้นในระดับที่ ๔
(๘ เมตรจากฐานไซโล)



รูปที่ ๑๕
อุณหภูมิของข้าวเปลือกขณะทำความเย็นชั้นที่ ๕ (๑๐ เมตรจากฐานไซโล)



รูปที่ ๑๖
อุณหภูมิของข้าวเปลือกขณะทำความเย็นชั้นที่ ๖ (๑๒ เมตรจากฐานไซโล)



รูปที่ ๑๗ อุณหภูมิของข้าวเปลือกขณะทำความเย็นชั้นที่ ๙ (๑๔ เมตรจากฐานไซโล)

เวลาที่ใช้ในการทำความเย็นจากการเปรียบเทียบนั้นพบว่าการทดลองการทำความเย็นข้าวเปลือกใช้เวลา ๑๒๐ ชั่วโมง แบบจำลองใช้เวลา ๑๑๕ ชั่วโมง และในช่วงทำความเย็นชั้นการทดลองใช้เวลา ๓๖ ชั่วโมง แบบจำลองใช้เวลา ๓๒ ชั่วโมง

ผลการเปรียบเทียบแสดงให้เห็นว่าแบบจำลองสามารถประมาณเวลาที่ใช้ในการทำความเย็นและการทำความเย็นชั้นข้าวเปลือกได้ใกล้เคียง โดยมีค่าความผิดพลาดประมาณร้อยละ ๔ ในช่วงการทำความเย็น และประมาณร้อยละ ๑๑ ในช่วงการทำความเย็นชั้น

๔. สรุปผลการศึกษา

จากการเปรียบเทียบผลการคำนวณแบบจำลองทางคณิตศาสตร์ในการทำความเย็นข้าวเปลือกกับผลการทดลองของเอกภูมิ บุญธรรม[๖] สามารถสรุปได้ดังนี้

๑. แบบจำลองการทำความเย็น

อากาศที่อาศัยการหาคำตอบของระบบสมการ โดยวิธีการแทนค่าต่อเนื่อง สามารถทำนายอุณหภูมิที่ตำแหน่งต่าง ๆ ในระบบทำความเย็น เช่น ทางออกเครื่องทำระเหย ที่ทางเข้าไซโล ได้ใกล้เคียงกับผลการทดลองซึ่งมีความผิดพลาดในช่วง ± ๒ องศาเซลเซียส

๒. แบบจำลองการทำความเย็นข้าวเปลือกที่พัฒนามาจากแบบจำลองทางคณิตศาสตร์แบบใกล้สมดุลสามารถทำนายอุณหภูมิของข้าวเปลือกในแต่ละชั้นในไซโลใกล้เคียงกับข้อมูลจากการทดลอง มีความถูกต้องในช่วง ± ๓ องศาเซลเซียส

๓. แบบจำลองการทำความเย็นข้าวเปลือกสามารถทำนายพลังงานที่ใช้ในการทำความเย็นโดยมีค่าผิดพลาดน้อยกว่าร้อยละ ๑๘

๔. แบบจำลองการทำความเย็นข้าวเปลือกสามารถทำนายเวลาที่ใช้ทำความเย็นและทำความเย็นซ้ำได้ใกล้เคียงกับเวลาที่ใช้จริงในการทดลองทั้ง ๒ ช่วง

กิตติกรรมประกาศ

สำนักงานกองทุนสนับสนุนงานวิจัยสนับสนุนด้านการเงิน, บริษัทไรซ์เอ็นจิเนียริ่งซัพพลาย จำกัด, บริษัทนวกิจกรุ๊ป จำกัด, โรงสีบ้านหลวง, โรงสีคุงหลีจั่น, โรงสีปฐมวิวัฒน์, โรงสีเทพมงคล ให้ข้อมูลสำหรับการจำลองปัญหาทางคณิตศาสตร์

รายการสัญลักษณ์และสัญลักษณ์กำกับล่าง

A	พื้นที่หน้าตัด, m^2	a	อากาศ
BF	Bypass factor	amb	ภาวะที่อากาศแวดล้อม
C	ความร้อนจำเพาะ, kj/kg.K	bd	ภาวะหลังสมดุลทางความร้อน
m	อัตราการไหลเชิงมวล, kg/s	c	ภาวะที่เครื่องควบแน่น
M	ความชื้นของเมล็ดพืช, เศษส่วนมาตรฐานแห้ง	con	อากาศอิ่มตัว
P	กำลังงานของเครื่องอัดไอ, Watt	e	ภาวะที่เครื่องทำระเหย
P_t	ความดันลดที่พัดลมหลัก, Pa	ei	ภาวะที่ทางเข้าเครื่องทำระเหย
Q	ภาระความร้อน, Watt	eo	ภาวะที่ทางออกเครื่องทำระเหย
R	อัตราส่วนมวลเมล็ดพืชแห้งต่อมวลอากาศแห้ง	eq	ภาวะสมดุล
RH	ความชื้นสัมพัทธ์, decimal	f	ภาวะสุดท้าย
t	เวลา, ชั่วโมง	fo	ทางออกพัดลมหลัก
T_e	อุณหภูมิของสารทำความเย็นที่เครื่องทำระเหย,°ซ	hi	ทางเข้าขดลวดความร้อน
T_c	อุณหภูมิของสารทำความเย็นที่เครื่องควบแน่น,°ซ	ho	ทางออกขดลวดความร้อน
T	อุณหภูมิของอากาศ, °ซ	id	ทางเข้าท่อลม
U	สัมประสิทธิ์การถ่ายเทความร้อนรวม kW/m^2-°C	in	ภาวะเริ่มต้นก่อนคำนวณ
W	อัตราส่วนความชื้นของอากาศ, kg น้ำ/kg อากาศแห้ง	od	ทางออกท่อลม
θ	อุณหภูมิของเมล็ดพืช,°ซ	pw	เมล็ดพืชชื้น
W_s	งานที่พัดลม, วัตต์	v	ไอน้ำ
Ɛ	Heat exchanger effectiveness		
ρ	ความหนาแน่น kg/m^3		
η_f	ประสิทธิภาพของพัดลม		

เอกสารอ้างอิง

๑. วรากรณ์ รัตนนงพิสัยย์. การพัฒนาแบบจำลองทางคณิตศาสตร์สำหรับการอบแห้งผลไม้โดยใช้ปั๊มความร้อน. วิทยานิพนธ์ปริญญาวิทยาศาสตรมหาบัณฑิต สาขาวิชาเทคโนโลยีพลังงาน สถาบันเทคโนโลยีพระจอมเกล้าธนบุรี. ๒๕๔๐.

๒. เอกภูมิ บุญธรรม, อดิศักดิ์ นาถกรณกุล, สมชาติ โสภณรณฤทธิ์. การพัฒนาเครื่องต้นแบบทำความเย็นข้าวเปลือก. วารสารราชบัณฑิตยสถาน ๒๕๔๖; ๒: ๔๖๕-๗๖.

๓. Banaszek MM, Sibenmorgen TJ. Moisture adsorption rate of rough rice. Trans. ASAE 1990; 33(4): 1257-62.

๔. Khan JR, Zubair SM. Design and Performance of Reciprocating Refrigeration Systems. International Journal of Refrigeration 1999; 22 : 235-43.

๕. Maier DE, Baker-Arkema FW, Ilangantileke SG. Ambient and Chilled Paddy Aeration under Thai Condition. Agricultural Engineering J 1993; 2(1&2) : 15-33.

๖. Soponronnarit S.Energy Model of Grain Drying System. ASEAN Journal for Science and Technology for Development 1988; 5(2) : 43-68.

๗. Thompson TL. Temporary Storage of High-Moisture Shelled Corn Using Continuous Aeration. Trans. ASAE 1972; 15 : 333-7.

Abstract **Developing a mathematical model of paddy cooling system.**

The purpose of this paper is to develop a mathematical model of paddy cooling system. The model is verified by comparing with experimental results of paddy cooling in a 250 ton-silo. It comprises two parts, i.e. a mathematical model for air cooling and a mathematical model for paddy cooling. The air cooling model uses successive substitution method to solve the equations which are obtained from mass and energy balance and heat transfer between air and refrigerant at heat exchanger, and performance equations for reciprocation compressor. The results of this air cooling model are temperature and relative humidity of cooling air which are used as inputs into the paddy cooling model. The simulation of paddy cooling was divided into two parts: cooling and re-cooling. Paddy was cooled from its initial temperature to 20°C and was re-cooled when its temperature rose from 20°C to 22°C. The comparison results showed that the model predicted conditions of cooled air in good agreement with experimental data within ±2°C, temperature of paddy in each layer within an accuracy of ±3°C, cooling time nearly equal to that of the experiments, and cooling energy within 18% accuracy.

Key words : **Cooling/Grain/Mathematical model**

e Journal of the Royal Institute of Thailand
Vol. 29 No. 1 Jan.-Mar. 2004

เทคนิคใหม่ในการผลิตข้าวนึ่ง*

สมชาติ โสภณรณฤทธิ์*
ราชบัณฑิต สำนักวิทยาศาสตร์
ชัยยงค์ เตชะไพโรจน์*,
สมเกียรติ ปรัชญาวรากร[๒]
*คณะพลังงานและวัสดุ
[๒]คณะวิศวกรรมศาสตร์ มหาวิทยาลัยเทคโนโลยีพระจอมเกล้าธนบุรี*

บทคัดย่อ

การผลิตข้าวนึ่งด้วยวิธีปัจจุบันต้องใช้เวลายาวนาน ดังนั้น งานวิจัยนี้จึงมีวัตถุประสงค์เพื่อศึกษาเทคนิคใหม่ในการผลิตข้าวนึ่งด้วยเครื่องอบแห้งฟลูอิไดซ์เบด โดยใช้ไอน้ำร้อนยวดยิ่งในการลดความชื้นของข้าวเปลือกจากร้อยละ ๔๑-๔๒.๕ มาตรฐานแห้ง จนเหลือความชื้นสุดท้ายร้อยละ ๑๖-๒๘ มาตรฐานแห้ง เงื่อนไขของการทดลองที่ศึกษามีดังนี้ ความสูงเบดของข้าวเปลือก ๑๐-๑๕ เซนติเมตร อุณหภูมิไอน้ำร้อนยวดยิ่ง ๑๕๐-๑๗๐ องศาเซลเซียส ความดันไอน้ำในระบบอบแห้ง ๑๐๖.๑ กิโลพาสคัล ความเร็วในห้องอบ ๓.๑ เมตร/วินาที จากการทดลองพบว่าอุณหภูมิไอน้ำร้อนยวดยิ่งมีอิทธิพลต่ออัตราการอบแห้งมากกว่าความสูงเบดข้าวเปลือก การอบแห้งด้วยไอน้ำร้อนยวดยิ่งสามารถลดความชื้นได้ต่ำถึงร้อยละ ๑๘ มาตรฐานแห้ง โดยที่ต้นข้าว มีค่ามากกว่าร้อยละ ๖๐ ถ้าลดความชื้นต่ำกว่านี้ร้อยละต้นข้าวจะลดลงอย่างรวดเร็วในขณะที่อุณหภูมิของการอบแห้งมีผลต่อความขาวและ white belly จากการวิเคราะห์สมบัติความหนืดของแป้งข้าวเป็น peak viscosity, breakdown viscosity และ setback viscosity พบว่ามีค่าต่ำ**

คำสำคัญ : การอบแห้ง, ต้นข้าว, ความขาว

บทนำ

ประเทศไทยเป็นแหล่งกสิกรรมที่สำคัญแห่งหนึ่ง พืชเศรษฐกิจที่สำคัญได้แก่ ข้าวและผลิตภัณฑ์จากข้าว ผลผลิตข้าวนอกจากใช้สำหรับบริโภคภายในประเทศแล้ว ยังสามารถส่งออกเป็นอันดับ ๑ ของโลกมาแล้วหลายปี ข้าวนึ่งเป็นผลิตภัณฑ์ที่แปรรูปจากข้าวเปลือก โดยผ่านกระบวนการต่าง ๆ ดังนี้ ๑. การแช่ (soaking) เพื่อทำให้ข้าวเปลือกมีความชื้นเพิ่มขึ้นเป็นร้อยละ ๔๒-๕๔ มาตรฐานแห้ง โดยทั่วไปแช่ในน้ำร้อนอุณหภูมิประมาณ ๖๐-๘๐ องศาเซลเซียส ๒. การนึ่ง (steaming) เพื่อทำเมล็ดสตาร์ชของข้าวที่แช่มาแล้วเกิดเจล ๓. การอบแห้งเพื่อลดความชื้นที่มีอยู่ในข้าวเปลือกนึ่งลงต่ำกว่าร้อยละ ๑๖ มาตรฐานแห้ง ก่อนจะนำไปเก็บรักษาหรือขัดสีให้เป็นข้าวนึ่ง ผลจากกระบวนการดังกล่าวข้างต้นทำให้ข้าวนึ่งที่ได้มีคุณค่าทางโภชนาการสูงกว่าข้าวขาว"

กระบวนการผลิตข้าวนึ่งดังกล่าวข้างต้น อาจรวมขั้นตอนการนึ่งและการอบแห้งเข้าเป็นขั้นตอนเดียวกัน โดยการประยุกต์ใช้ไอน้ำร้อนยวดยิ่งเป็นตัวกลางในการนึ่งและอบแห้งในฟลูอิไดซ์เบด จากการศึกษางานวิจัยที่ผ่านมาพบว่าการอบแห้งโดยใช้ไอน้ำร้อนยวดยิ่งมีข้อดีบางประการ เช่น มี

* บรรยายในการประชุมสำนักวิทยาศาสตร์ ราชบัณฑิตยสถาน เมื่อวันพุธที่ ๑ ตุลาคม พ.ศ. ๒๕๔๖
**ต้นข้าว หมายถึง เมล็ดข้าวสาร (หลังจากกระเทาะเปลือกและขัดขาวแล้ว) ที่มีขนาดความยาว $\geq \frac{8}{10}$ ของเมล็ดข้าวสารเต็มเมล็ด

อัตราการอบแห้งสูงและสามารถกำจัดกลิ่นของผลิตภัณฑ์ได้[๔,๕]

จุดประสงค์ของงานวิจัยนี้เพื่อศึกษาลักษณะและสมบัติบางประการของข้าวที่ผ่านการอบแห้งโดยเทคนิคฟลูอิไดซ์เบดด้วยไอน้ำร้อนยวดยิ่งที่เงื่อนไขต่างๆ ได้แก่ โครงสร้างระดับจุลภาค, สมบัติทาง pasting ตลอดจนสมบัติทางกายภาพ ซึ่งประกอบด้วยปริมาณต้นข้าว, ความขาว และ white belly

อุปกรณ์และวิธีการ

เครื่องอบแห้งที่ใช้ในการทดลองศึกษาในงานวิจัยนี้เป็นเครื่องอบแห้งฟลูอิไดซ์เบดแบบงวด รูปทรงกระบอกทำด้วยเหล็กกล้าไม่เป็นสนิม ขนาดเส้นผ่านศูนย์กลาง ๑๕ เซนติเมตร และสูง ๑๐๐ เซนติเมตร อุปกรณ์ให้ความร้อนมีขนาด ๑๓.๕ กิโลวัตต์ ใช้เพื่อเปลี่ยนสถานะของไอน้ำอิ่มตัวเป็นไอน้ำร้อนยวดยิ่งตามอุณหภูมิที่ต้องการซึ่งควบคุมโดย PID ± ๑ องศาเซลเซียส พัดลมเป็นแบบเหวี่ยงหนีศูนย์กลางใบพัดโค้งหลัง (backward-curved centrifugal blower) ขับด้วยมอเตอร์ขนาด ๒.๒ กิโลวัตต์ อัตราการไหลของไอน้ำสามารถปรับเปลี่ยนได้โดยการปรับความเร็วรอบของพัดลม เครื่องดักฝุ่นแบบไซโคลนทำด้วยเหล็กกล้าไม่เป็นสนิม เครื่องกำเนิดไอน้ำความดันสามารถผลิตไอน้ำอิ่มตัว ๓.๑ กิโลกรัม/ชั่วโมง ภายใต้ความดันบรรยากาศ ดังรายละเอียดในรูปที่ ๑

ลักษณะการทำงานของระบบอบแห้ง เริ่มต้นจากการอุ่นระบบให้ร้อนด้วยอากาศ โดยเปิดวาล์ว V.3 และ V.5 ส่วนวาล์วที่เหลือปิดหมด แล้วเปิดพัดลมและอุปกรณ์ให้ความร้อนเพื่อให้ระบบร้อนขึ้นจนได้อุณหภูมิตามที่ต้องการ ทั้งนี้เพื่อป้องกันการควบแน่นของไอน้ำที่จะป้อนเข้าระบบ เมื่ออุณหภูมิภายในระบบสูงเท่ากับค่าที่ต้องการแล้วจึงเริ่มป้อนไอน้ำจากเครื่องกำเนิดไอน้ำเข้าในระบบโดยเปิดวาล์ว V.1 เนื่องจากในระบบมีอากาศอยู่จึงต้องไล่อากาศออกโดยเปิดวาล์ว V.8 และ V.9 ไอน้ำจะปนออกมากับอากาศ รอจนกระทั่งแน่ใจว่าไม่มีอากาศแล้วจึงปิดวาล์ว V.8 และ V.9 ปรับความดันเกจในระบบจากวาล์ว V.1 ให้ได้ประมาณ ๕,๐๐๐ พาสคัล ปรับอุณหภูมิอบแห้งจากเครื่องควบคุมอุณหภูมิและปรับความเร็วของไอน้ำในระบบจากความเร็วรอบของพัดลมให้ได้ตามต้องการ ก่อนป้อนข้าวเปลือกเข้าห้องอบแห้งต้องสลับเส้นทางการไหลของไอน้ำ เพื่อความปลอดภัย โดยปิดวาล์ว V.3 และ V.5 ขณะเดียวกันก็เปิดวาล์ว V.2 และ V.4 แล้วจึงป้อนข้าวเปลือกเข้าทางวาล์ว V.10 หลังจากนั้นก็สลับเส้นทางการไหลของไอน้ำกลับสู่ตำแหน่งเดิม คือเปิดวาล์ว V.3 และ V.5 แล้วปิดวาล์ว V.2 และ V.4 เมื่อได้เวลาอบแห้งตามที่ต้องการแล้วจึงนำข้าวเปลือกออกโดยเปิดวาล์ว V.9 แล้วนำข้าวเปลือกที่ได้ไปทดสอบต่อไป ลักษณะรายละเอียดของเครื่องอบแห้งด้วยไอน้ำร้อนยวดยิ่งที่แสดงในรูปที่ ๑

งานวิจัยนี้ผู้วิจัยอบแห้งข้าวเปลือกโดยการนำข้าวเปลือกแช่น้ำร้อนที่อุณหภูมิ ๘๐ องศาเซลเซียส เป็นเวลาประมาณ ๓.๕ ชั่วโมง จากนั้นรินน้ำที่ใช้แช่ออก แล้วเก็บไว้ในที่อับอากาศประมาณ ๑ ชั่วโมง ซึ่งทำให้ได้ความชื้นเริ่มต้นของข้าวเปลือกประมาณร้อยละ ๔๒ มาตรฐานแห้ง จากนั้นนำตัวอย่างมาอบแห้งภายใต้เงื่อนไขดังต่อไปนี้ ความสูงเบดข้าวเปลือก ๑๐-๑๕ เซนติเมตร อุณหภูมิไอน้ำร้อนยวดยิ่งอยู่ในช่วง ๑๕๐-๑๗๐ องศาเซลเซียส ความเร็วของไอน้ำร้อนยวดยิ่งมีค่า ๓.๑ เมตร/วินาที และความดันไอน้ำในระบบอบแห้งประมาณ ๑๐๖.๑ กิโลพาสคัล ซึ่งเป็นความดันเหนือบรรยากาศเล็กน้อย ทั้งนี้เพื่อป้องกันการรั่วเข้าของอากาศ จากนั้นนำข้าวที่ผ่านการอบแห้งแล้วมาปล่อยไว้ให้เย็นตัวลงที่อุณหภูมิห้องภายในถุงปิดสนิทเพื่อป้องกันการสูญเสียความชื้น แล้วนำไปเป่าด้วยอากาศแวดล้อมจนมีความชื้นเหลือร้อยละ ๑๖ มาตรฐานแห้ง สุดท้ายนำข้าวไปทดสอบคุณภาพต่อไป

การหาความชื้นของข้าวเปลือกใช้ตู้อบไฟฟ้า โดยอบแห้งข้าวเปลือกตัวอย่างที่อุณหภูมิ ๑๐๓ องศาเซลเซียส เป็นเวลา ๗๒ ชั่วโมง การวัดอุณหภูมิใช้เทอร์โมคัปเปิล ชนิด K ค่าความถูกต้อง ± ๑ องศาเซลเซียส และการวัดความเร็วไอน้ำใช้ inclined manometer และ pitot static tube

สำหรับคุณภาพของผลิตภัณฑ์มีวิธีการวิเคราะห์ดังนี้

- ร้อยละต้นข้าว

คือน้ำหนักของต้นข้าวที่ผ่านการอบแห้งหารด้วยน้ำหนักข้าวเปลือกแล้วคูณด้วย ๑๐๐

- ความขาว

วัดได้จากเครื่องวัดความขาว (Kett model C-300) โดยใช้ความขาวอ้างอิงเท่ากับ ๘๖.๓

- **ร้อยละ white belly**

คือจำนวนของข้าวที่เป็นจุดขาวขุ่นเกินร้อยละ ๕๐ ของเมล็ด จากการสุ่มตัวอย่างของข้าวจำนวน ๑๐๐ เมล็ด

- **โครงสร้างระดับจุลภาค**

นำตัวอย่างเมล็ดข้าวที่ผ่านการอบแห้งมาหักครึ่งและเคลือบทองด้วยเครื่องเคลือบทอง (Hitachi E-1010 10N, Tokyo, Japan) แล้วส่องด้วยกล้องอิเล็กตรอนแบบส่องกราด (SEM, S-4500, Hitachi, Tokyo, Japan) ที่กำลังขยาย ๕๐๐ เท่า

- **ความหนืดของแป้ง**

ในการวัดสมบัติทาง pasting ของข้าวนึ่งโดยใช้เครื่อง Rapid Visco Analyser, RVA model-4 (Newport Scientific Pty Ltd., Warriewood, Australia)ทำตามวิธีการของ AACC method ๖๑-๐๒[๙] โดยการนำตัวอย่างแป้งข้าวปริมาณ ๓ กรัม (ความชื้นร้อยละ ๑๔) ผสมกับน้ำกลั่น ในถ้วยอะลูมิเนียมโดยน้ำหนักรวม ๒๘ กรัม จากนั้นนำตัวอย่างที่เตรียมได้เข้าเครื่อง RVA อุ่นให้ร้อนที่ ๕๐ องศาเซลเซียส คงไว้ ณ อุณหภูมิดังกล่าวเป็นเวลา ๑ นาที ต่อจากนั้นให้ความร้อนแก่ของผสมด้วยอัตรา ๑๒ องศาเซลเซียส/นาที จนถึงอุณหภูมิ ๙๕ องศาเซลเซียส คงไว้ที่อุณหภูมิ ๙๕ องศาเซลเซียส เป็นเวลา ๒.๕ นาที จากนั้นทำให้เย็นลงมาที่ ๕๐ องศาเซลเซียส ด้วยอัตราการทำให้เย็น ๑๒ องศาเซลเซียส/นาที แล้วคงไว้ที่ ๕๐ องศาเซลเซียส เป็นเวลา ๒.๑ นาที ทำการทดสอบสองซ้ำ พล็อตสมบัติ pasting ต่าง ๆ เทียบกับเวลา ค่าต่าง ๆ ที่ได้จาก pasting properties ได้แก่ peak viscosity (PV), trough, final viscosity (FV), breakdown viscosity (BKV = PV- trough) and setback viscosity (SBV = FV- trough)

- **ไขมัน (lipid)**

ปริมาณไขมันทั้งหมดในข้าวดัดแปลงตามวิธีของ Folch และคณะ[๙] โดยการชั่งแป้งข้าว ๑ กรัม ใส่ในหลอดทดลองแล้วเติมด้วยสารละลาย chloroform : methanol ในอัตราส่วน ๒ : ๑ (ปริมาตร : ปริมาตร) ปริมาณ ๑๐ มิลลิลิตร เขย่าหลอดทดลองเป็นเวลา ๕ นาที ตั้งทิ้งไว้ ๓๐ นาที จนกระทั่งสารละลายตกตะกอน ดูดเฉพาะส่วนใส แล้วเติมน้ำ ๐.๒๕ เท่าของสารละลายที่ดูดได้ เขย่าให้เข้ากัน สารละลายจะแยกเป็นสองชั้น ไขมันละลายในชั้นล่าง แยกเอาเฉพาะสารละลายชั้นล่างแล้วนำมาเป่าให้ตัวทำละลายระเหยจนแห้งด้วยแก๊สไนโตรเจน ชั่งน้ำหนักไขมันที่ได้ ปริมาณไขมันที่ได้คิดเป็นร้อยละของไขมันต่อน้ำหนักแห้งของแป้ง

ผลและวิจารณ์

- อิทธิพลของอุณหภูมิไอน้ำร้อนยวดยิ่งและความสูงเบดที่มีต่ออัตราการอบแห้งข้าวเปลือกด้วยไอน้ำร้อนยวดยิ่ง

รูปที่ ๒ แสดงความสัมพันธ์ระหว่างอุณหภูมิของเมล็ดข้าวเปลือก ความชื้น และเวลาในการอบแห้ง เนื่องจากช่วงแรกของการอบแห้งเกิดการควบแน่นของไอน้ำเกิดขึ้น กล่าวคือ ทันทีที่ไอน้ำร้อนยวดยิ่งไหลผ่านเบดของข้าวเปลือก ไอน้ำจะเริ่มเกิดการควบแน่นที่เบดข้าวเปลือกซึ่งเกิดในช่วงแรกเป็นเวลาสั้น ๆ เป็นผลให้อุณหภูมิของข้าวเปลือกเพิ่มขึ้นอย่างรวดเร็วจากอุณหภูมิแวดล้อมจนถึงอุณหภูมิจุดเดือดของน้ำ ต่อจากนั้นอุณหภูมิของข้าวเปลือกจะเพิ่มขึ้นอย่างช้าๆ ตามความชื้นข้าวเปลือกที่ลดลง

ความสูงเบดมีอิทธิพลต่ออุณหภูมิและความชื้นของข้าวเปลือกน้อยกว่าอุณหภูมิไอน้ำร้อนยวดยิ่ง เมื่ออุณหภูมิสูงขึ้นเป็น ๑๗๐ องศาเซลเซียส อุณหภูมิของข้าวเปลือกจะเพิ่มสูงขึ้นและความชื้นจะลดลงรวดเร็วขึ้นกว่าเดิม (ที่ ๑๕๐ องศาเซลเซียส)

- ข้าวต้นทาง

รูปที่ ๓ แสดงความสัมพันธ์ระหว่างร้อยละต้นข้าวกับความชื้นสุดท้ายของข้าวเปลือกที่อุณหภูมิและความสูงเบดต่าง ๆ จากการทดลองพบว่า ร้อยละต้นข้าวมีค่าค่อนข้างคงตัว (ร้อยละ ๖๕-๗๐) ในช่วงความชื้นสุดท้ายสูงกว่าร้อยละ ๑๘ มาตรฐานแห้ง เนื่องจากเกิด gelatinisation ซึ่งสามารถอธิบายได้ดังนี้ เมื่อข้าวที่มีความชื้นสูงได้รับความร้อนสูงแป้งที่ถูกน้ำเกิดการพองตัวและถูกทำให้สุก นอกจากนี้ ยังทำให้โปรตีนแตกตัวและเกิดการแทรกเข้าไปภายในช่องว่างระหว่างเม็ดแป้ง (รูปที่ ๔) ทำให้ช่องว่างหรือรอยร้าวและรอยแตกภายในเมล็ดข้าวประสานกันอย่างสนิทเมื่อนำไป

ทำให้แห้ง เมล็ดข้าวจะมีลักษณะแข็งใส เหนียวและทนทานต่อการขัดสี จึงทำให้ได้ร้อยละต้นข้าวสูง เมื่อความชื้นสุดท้ายต่ำกว่าร้อยละ ๑๘ มาตรฐานแห้ง พบว่าร้อยละต้นข้าวลดลงอย่างรวดเร็วเนื่องจากความแตกต่างของความชื้นภายในเมล็ดที่มีมากเกินไป ทำให้เกิดแรงเค้นขึ้น เป็นผลให้เกิดรอยร้าวภายในเมล็ด เมื่อนำไปขัดสีจึงได้ร้อยละต้นข้าวลดลง

- White belly

White belly คือ ข้าวที่เป็นจุดขุ่นขาวทึบแสงภายในเมล็ดข้าว ซึ่งเกิดจากข้าวผ่านการนึ่งแล้วเกิดกระบวนการเจลาทิไนซ์ในเมล็ดข้าวไม่สมบูรณ์ โดยส่วนมากจะปรากฏจุดขุ่นขาวบริเวณแกนกลางในเมล็ดข้าวสาร รูปที่ ๕ แสดงความสัมพันธ์ระหว่างร้อยละ white belly กับความชื้นสุดท้ายของข้าวเปลือกที่อุณหภูมิและความสูงเบดต่าง ๆ จากการทดลองพบว่า อุณหภูมิที่ใช้ในการอบแห้งมีอิทธิพลต่อร้อยละ white belly โดยที่อุณหภูมิไอน้ำร้อนยวดยิ่งสูงขึ้นทำให้ร้อยละ white belly ลดลง แต่ความสูงเบดไม่มีผลต่อร้อยละ white belly

- ความขาว

รูปที่ ๖ แสดงความสัมพันธ์ระหว่างร้อยละความขาวกับความชื้นสุดท้ายของข้าวเปลือกที่อุณหภูมิและความสูงเบดต่าง ๆ โดยความชื้นเริ่มต้นของข้าวเปลือกร้อยละ ๔๒ มาตรฐานแห้ง จากการทดลองพบว่าช่วงเวลาการอบแห้ง ๒ นาทีแรก ความขาวของข้าวลดลงอย่างรวดเร็ว (ความขาวเริ่มต้น ๔๑-๔๓) และมีค่าค่อนข้างคงตัว (๓๐-๓๕) ที่ความชื้นสุดท้ายในช่วงร้อยละ ๑๘-๓๐ มาตรฐานแห้ง การเปลี่ยนแปลงสีของข้าวอันเนื่องจากกระบวนการเกิดสีน้ำตาลแบบเมลลาร์ด โดยสภาพที่เหมาะสมของน้ำตาลรีดิวซ์กับกรดแอมิโนที่มีความร้อนเป็นตัวเร่งปฏิกิริยาสีน้ำตาล และอีกสาเหตุอันเนื่องมาจากช่วงที่เกิดการควบแน่นของไอน้ำที่ผิวของข้าวเปลือกอาจทำให้สีของเปลือกที่หุ้มเมล็ดข้าวอยู่นั้นซึมเข้าสู่เนื้อเมล็ดข้าว มีผลให้ข้าวที่ผ่านการอบแห้งมีสีคล้ำขึ้น ปริมาณรำที่ได้หลังการขัดสี พบว่ามีค่าร้อยละ ๕.๓-๗.๑ ซึ่งน้อยกว่าตัวอย่างอ้างอิงครึ่งหนึ่ง นอกจากนี้จากตารางที่ ๑ พบว่าปริมาณไขมันในข้าวที่ผ่านการอบแห้งมีสูงกว่าข้าวตัวอย่างที่ไม่ได้ผ่านการอบแห้ง สาเหตุเนื่องจากเอนโดสเปิร์ม (endosperm) ของเมล็ดข้าวเปลือกได้ดูดซึมไขมันที่แพร่จากชั้นของรำในระหว่างการอบแห้งเอาไว้

- Pasting behaviour

รูปที่ ๗ และตารางที่ ๒ แสดงสมบัติ pasting ของข้าวที่ผ่านการอบแห้งด้วยไอน้ำร้อนยวดยิ่งและข้าวที่ไม่ผ่านการอบแห้ง ผลการทดลองพบว่าข้าวที่ผ่านการอบแห้งภายใต้อุณหภูมิ ๑๕๐-๑๗๐ องศาเซลเซียส ให้ค่า PV, BKV และ SBV ต่ำกว่าข้าวที่ไม่ได้ผ่านการอบแห้ง การที่ค่า PV สูงเกิดจากการที่เมล็ดสตาร์ชมีความสามารถในการจับกับน้ำได้ปริมาณมากกว่าข้าวที่ผ่านกระบวนการอบแห้ง ทำให้เมล็ดสตาร์ชเกิดการพองตัวเป็นผลทำให้ค่าความหนืดสูงขึ้น ส่วนข้าวผ่านการอบแห้งค่า PV ลดลงตามอุณหภูมิการอบแห้งที่สูงขึ้น ในช่วงเวลา ๓ นาทีแรกระหว่างการอบแห้งข้าวที่มีความชื้นสูงได้รับความร้อนสูง เมล็ดสตาร์ชที่ถูกน้ำจะพองตัวและกลายเป็นเจล และทำให้โปรตีนแตกตัวและแทรกเข้าไปภายในช่องว่างระหว่างเมล็ดสตาร์ช เมื่อนำไปวัดสมบัติ pasting มีผลทำให้ความสามารถในการจับน้ำของเมล็ดสตาร์ชลดลง ซึ่งทำให้เมล็ดสตาร์ชพองตัวได้น้อยลงด้วย มีผลทำให้ค่า PV ลดลง สำหรับค่า FV และ SBK แสดงถึงสมบัติความแข็งกระด้างของข้าวสุก[๖,๗] ข้าวที่ผ่านการอบแห้งที่อุณหภูมิสูงให้ค่า FV และ SBK ต่ำกว่าข้าวที่ผ่านการอบแห้งที่อุณหภูมิต่ำและที่ไม่ผ่านการอบแห้งตามลำดับ ข้าวที่ผ่านการอบแห้งด้วยไอน้ำร้อนยวดยิ่งมีลักษณะความแข็งกระด้างต่ำกว่าข้าวที่ไม่ผ่านการอบแห้ง หลังจากการหุงสุกและปล่อยให้ข้าวเย็นตัวลง

สรุป

จากกระบวนการผลิตข้าวนึ่งโดยการนำข้าวเปลือกที่มีความชื้นเริ่มต้นร้อยละ ๔๒ มาตรฐานแห้ง มาผ่านการอบแห้งโดยเทคนิคฟลูอิไดซ์เบดภายใต้อุณหภูมิ ๑๕๐-๑๗๐ องศาเซลเซียส ด้วยไอน้ำร้อนยวดยิ่ง และความสูงเบด ๑๐-๑๕ เซนติเมตร พบว่าอุณหภูมิที่ใช้ในการอบแห้งมีผลต่ออัตราการอบแห้งมากกว่าความสูงเบด ความขาวของข้าวที่ผ่านการอบแห้งที่อุณหภูมิสูงมีสีที่คล้ำขึ้นมากกว่าที่อุณหภูมิต่ำ ร้อยละ white belly ลดลงเมื่ออุณหภูมิ

ที่ใช้ในการอบแห้งสูงขึ้น หากต้องการให้ได้ร้อยละต้นข้าวสูงควรอบแห้งโดยการลดความชื้นไม่ต่ำกว่าร้อยละ ๑๘ มาตรฐานแห้ง ส่วนสมบัติทาง pasting ให้ค่า PV, BKV และ SBV ลดต่ำลงเมื่อเทียบกับข้าวที่ไม่ได้ผ่านการอบแห้งด้วยไอน้ำร้อนยวดยิ่ง และเมื่อดูลักษณะของโครงสร้างภายในเมล็ดข้าวด้วยกล้องอิเล็กตรอนแบบส่องกราด พบว่าไม่ปรากฏโครงสร้างของเมล็ดสตาร์ชหลังจากผ่านการอบแห้งแล้ว ซึ่งข้าวสารที่หลังจากการอบแห้งด้วยเทคนิคนี้มีลักษณะเป็นข้าวนึ่ง

กิตติกรรมประกาศ

ผู้เขียนใคร่ขอขอบคุณ สำนักงานกองทุนสนับสนุนการวิจัยที่ให้ทุนสนับสนุนการวิจัย ขอขอบคุณคณะวิศวกรรมศาสตร์และเทคโนโลยีอุตสาหกรรม มหาวิทยาลัยศิลปากร ที่ให้ความอนุเคราะห์ในการทดสอบสมบัติ pasting ของข้าว ขอขอบคุณศูนย์วิจัยข้าวปทุมธานี กลุ่มงานวิจัยวิศวกรรมหลังการเก็บเกี่ยว ที่ให้ความอนุเคราะห์ในการทดสอบคุณภาพข้าว และขอขอบคุณบริษัทฟิลิปส์เซมิคอนดักเตอร์ จำกัด ที่ให้ความอนุเคราะห์ใช้กล้องอิเล็กตรอนแบบส่องกราด

เอกสารอ้างอิง

AACC. Approved method of the American Association of Cereal Chemist 9th ed., 1995; St. Paul, MN : AACC.

Ali SZ, Bhattacharya KR, Pasting behaviour of parboiled rice, J. Texture Stud., 1980; 11 : 239-245.

Dimopoulos JS, Muller HG. Effect of processing conditions on protein extraction and composition and on some other physicochemical characteristics of parboiled rice, Cereal Chemistry, 1972; 49 : 54-62.

Folch J, Lees M, Sloane-Stanley GH. A simple method for isolation and purification of total lipids from animal tissues. *J. Bio. Chem.* 1957; 226 : 497-509.

Iyota H, Nishimura N, Onuma T, Nomura T. Drying of sliced raw potatoes in superheated steam and hot air, Drying Technology, 2001; 19 (7) : 1411-1424.

Priestley RJ. Studies on parboiled rice. I. Comparison of the characteristics of raw and parboiled rice, Food Chemistry, 1976; 1, 5-14.

Ranghavendra RSN, Juliano BO. Effect of parboiling on some physicochemical properties of rice, Journal Agricultural Food Chemistry, 1970; 18 : 289-294.

Tang Z, Cenkowski S, Muir WE. Dehydration of sugar-beet pulp in superheated steam and hot air, Trans. of the ASAE, 2000; 43(3) : 685-689.

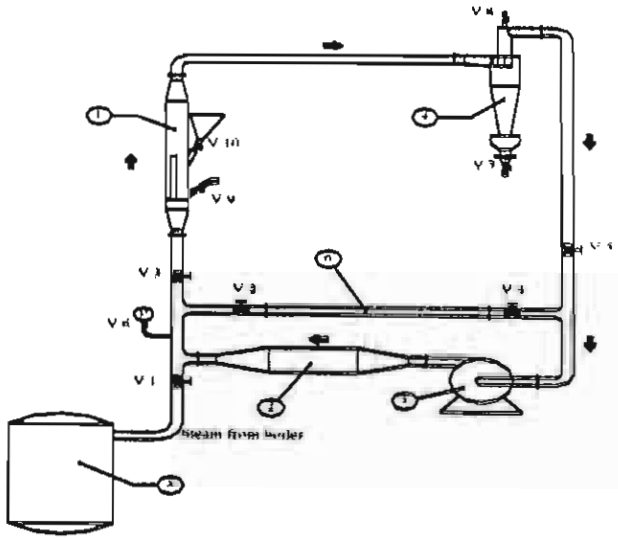
Tatemoto Y, Mawatari Y, Sakurai K, Noda K, Komatsu N. Drying characteristics of porous material in superheated steam fluidized bed, Proceedings of the 13th International Drying Symposium. Beijing, China, 27-30 August 2002, Vol. A, 624-633.

ตารางที่ ๑ ปริมาณไขมันของข้าวที่ผ่านการอบแห้งที่อุณหภูมิและความสูงต่าง ๆ

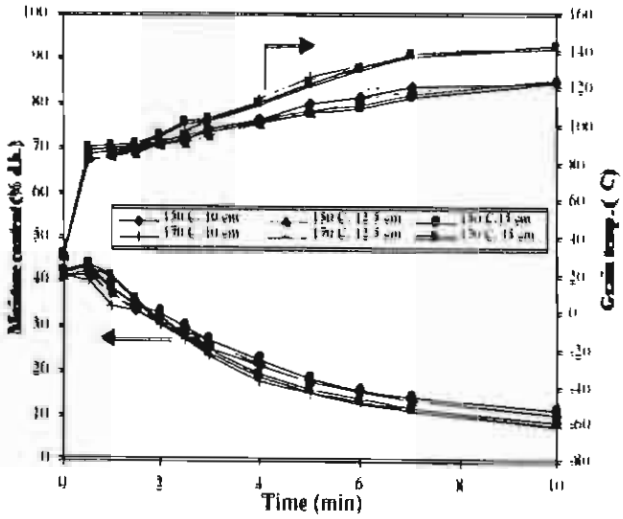
			Lipid content (%g/$g_{dry\ matter\ flour}$)
Raw white rice			0.2 ± 0.02
Rice	150°C	10 cm	0.4 ± 0.03
		12.5 cm	0.23 ± 0.04
		15 cm	0.23 ± 0.04
	160°C	10 cm	0.43 ± 0.03
		12.5 cm	0.3 ± 0.04
		15 cm	0.21 ± 0.03
	170°C	10 cm	0.65 ± 0.02
		12.5 cm	0.35 ± 0.02
		15 cm	0.21 ± 0.03

ตารางที่ ๒ สมบัติ pasting ของข้าวที่ไม่ผ่านและผ่านกระบวนการอบแห้งด้วยไอน้ำร้อนยวดยิ่ง

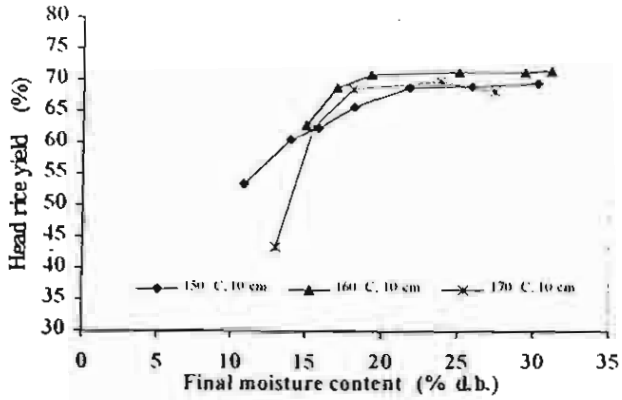
	Pv	Trough	BKV	FV	SBV	P_{Temp}
	rvu	rvu	rvu	rvu	rvu	°C
Raw rice	296	218	78	399	181	79.9
150°C 15 cm	120	113	7	205	92	89.7
160°C 15 cm	57	47	10	81	34	88
170°C 15 cm	25	20	5	35	15	89.7
170°C 12.5 cm	23	19	4	32	13	89.7
170°C 10 cm	14	12	2	21	9	89.7



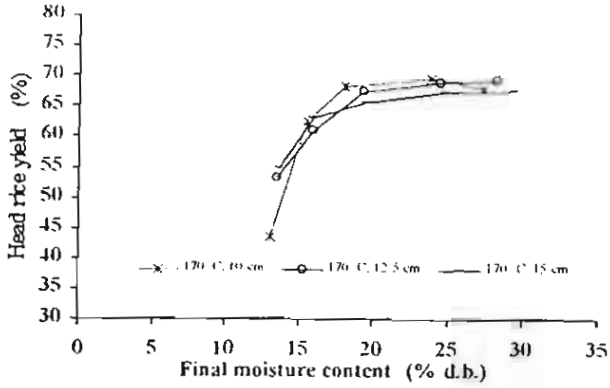
รูปที่ ๑ แผนภาพระบบอบแห้งด้วยไอน้ำร้อนยวดยิ่ง : (๑) ห้องอบแห้งแบบฟลูอิไดซ์เบด; (๒) อุปกรณ์ให้ความร้อน; (๓) พัดลม; (๔) เครื่องดักฝุ่น; (๕) เครื่องกำเนิดไอน้ำ; (๖) Bypass line, (V) วาล์ว; (P) มาตรความดัน



รูปที่ ๒ อิทธิพลของความสูงและอุณหภูมิของไอน้ำร้อนยวดยิ่งต่อการอบแห้งข้าวเปลือกและอุณหภูมิของเมล็ดข้าว

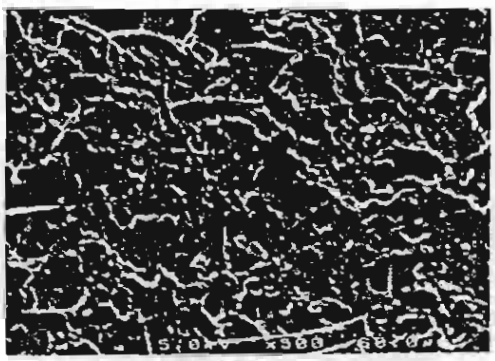


ก) ความสูง ๑๐ เซนติเมตร

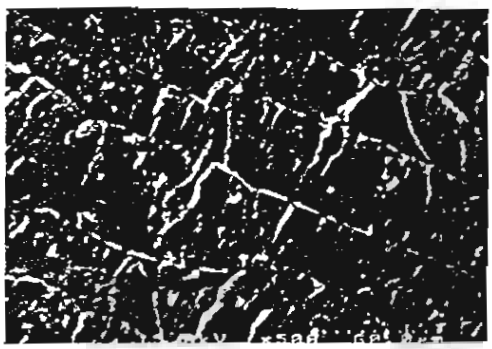


ข) อุณหภูมิไอน้ำร้อนยวดยิ่ง ๑๗๐ องศาเซลเซียส

รูปที่ ๓ ความสัมพันธ์ระหว่างร้อยละข้าวต้นทางกับความชื้นสุดท้ายของข้าวเปลือกที่อุณหภูมิของไอน้ำร้อนยวดยิ่งและความสูงเบดต่าง ๆ (ความชื้นเริ่มต้นร้อยละ ๔๒ มาตรฐานแห้ง)



ก) ตัวอย่างข้าวที่ไม่ได้ผ่านการอบแห้ง



ข) ข้าวที่ผ่านการอบที่อุณหภูมิ ๑๕๐ องศาเซลเซียส (ความชื้นสุดท้ายร้อยละ ๑๔.๘ มาตรฐานแห้ง)

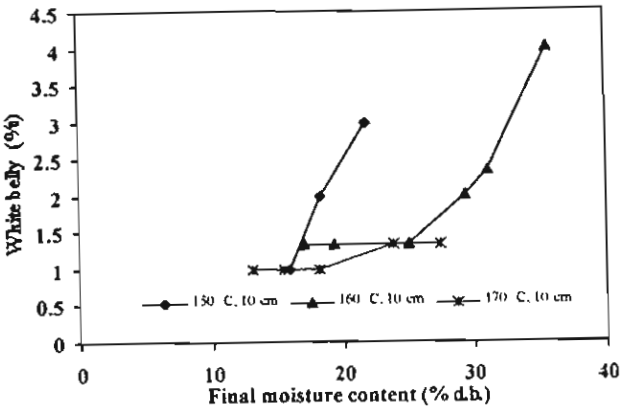


ค) ข้าวที่ผ่านการอบที่อุณหภูมิ ๑๖๐ องศาเซลเซียส (ความชื้นสุดท้ายร้อยละ ๑๓.๘ มาตรฐานแห้ง)

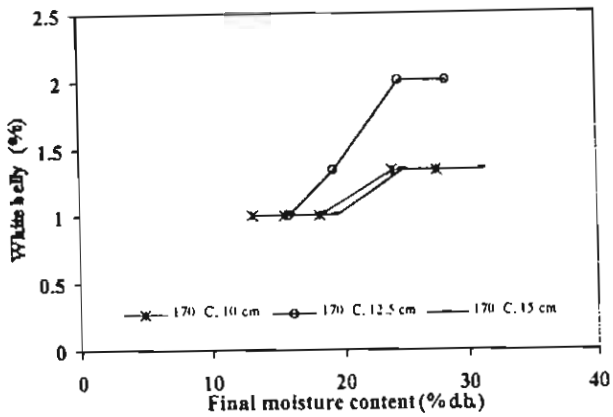


ง) ข้าวที่ผ่านการอบที่อุณหภูมิ ๑๗๐ องศาเซลเซียส (ความชื้นสุดท้ายร้อยละ ๑๙.๕ มาตรฐานแห้ง)

รูปที่ ๔ อิทธิพลของอุณหภูมิที่ใช้อบแห้งต่อโครงสร้างระดับจุลภาค

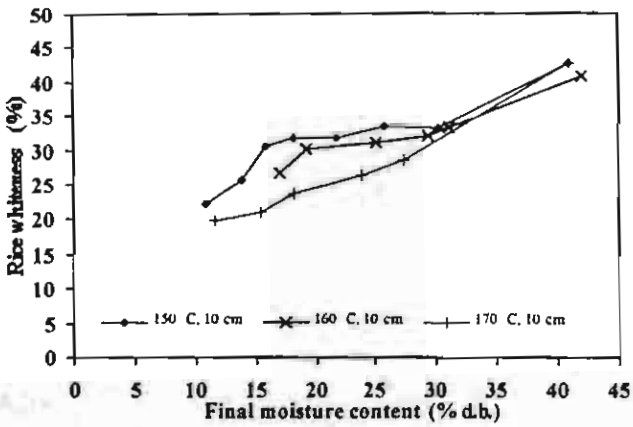


ก) ความสูง ๑๐ เซนติเมตร

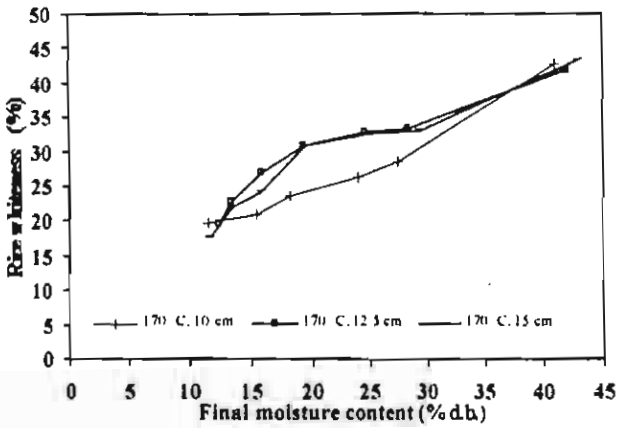


ข) อุณหภูมิไอน้ำร้อนยวดยิ่ง ๑๗๐ องศาเซลเซียส

รูปที่ ๕ ความสัมพันธ์ระหว่างร้อยละ white belly กับความชื้นสุดท้ายของข้าวเปลือก ที่อุณหภูมิของไอน้ำร้อนยวดยิ่งและความสูงเบดต่าง ๆ (ความชื้นเริ่มต้นร้อยละ ๔๒ มาตรฐานแห้ง)

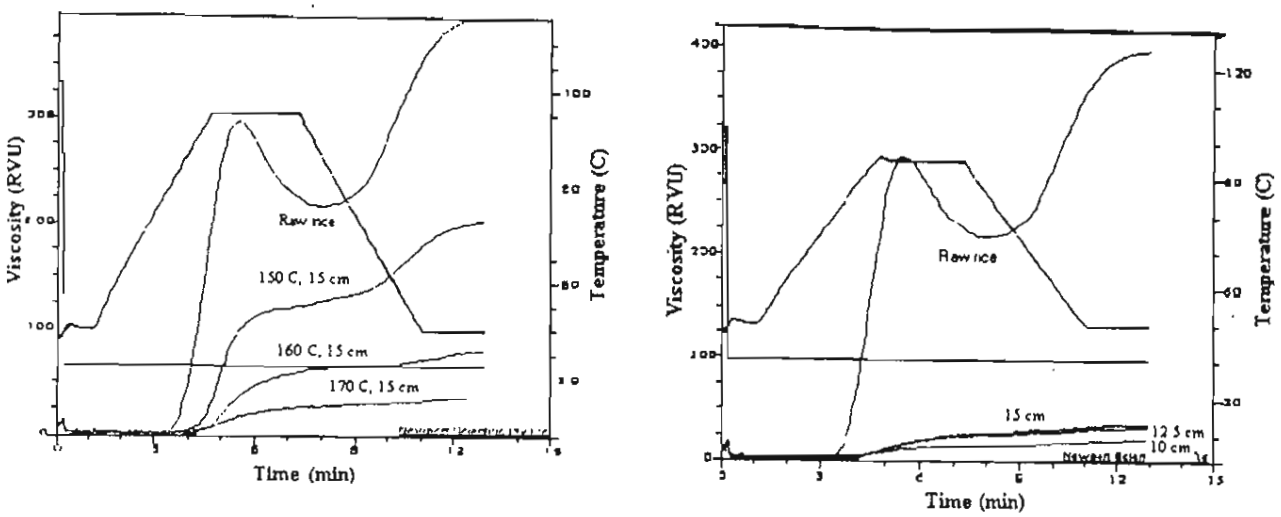


ก) ความสูง ๑๐ เซนติเมตร



ข) อุณหภูมิไอน้ำร้อนยวดยิ่ง ๑๗๐ องศาเซลเซียส

รูปที่ ๖ ความสัมพันธ์ระหว่างความขาวกับความชื้นสุดท้ายของข้าวเปลือกที่อุณหภูมิของไอน้ำร้อนยวดยิ่งและความสูงเบดต่าง ๆ (ความชื้นเริ่มต้นร้อยละ ๔๒ มาตรฐานแห้ง ความขาว = ๔๑-๔๓)



ก) ความสูงเบด ๑๕ เซนติเมตร ข) อุณหภูมิไอน้ำร้อนยวดยิ่ง ๑๗๐ องศาเซลเซียส

รูปที่ ๗ ความหนืดของข้าวที่ไม่ผ่านและผ่านกระบวนการอบแห้งด้วยไอน้ำร้อนยวดยิ่ง

Abstract

The present method of production of parboiled rice takes time. Therefore, the objective of this work is to investigate a new technique for producing parboiled rice by superheated-steam fluidised-bed drying. The operating conditions were carried out at the initial moisture contents of 41-42.5% dry basis, three bed heights of 10, 12.5 and 15 cm, superheated steam temperatures of 150-170°C with a constant pressure of 106.1 kPa and a fixed superficial velocity of 3.1 m/s. The experimental results showed that the inlet temperature had much more effect on removal of moisture content than the bed height. For the paddy quality, the head rice yield after reducing moisture content to 18% dry basis was higher than 60% (average reference value of 52%) whereas the colour indicating rice whiteness became darker and white belly was significantly affected by the inlet temperature. In addition, the lower values of peak viscosity, breakdown viscosity and setback viscosity were found under high temperatures.

Keywords : drying, head rice yield, whiteness

การทำน้ำร้อนด้วยปั๊มความร้อน

Water Heating Using Heat Pump

อาทิตย์ ไชยอรนันทน์ สมชาติ ไสภณรณฤทธิ์ และวารุณี เตีย
คณะพลังงานและวัสดุ มหาวิทยาลัยเทคโนโลยีพระจอมเกล้าธนบุรี
91 ถนนประชาอุทิศ บางมด ทุ่งครุ กรุงเทพฯ 10140
โทร 02 470-8632-3 โทรสาร 02 470-8635
E-Mail: warunee.tia@kmutt.ac.th

บทคัดย่อ

งานวิจัยนี้เป็นการออกแบบ สร้างและประเมินสมรรถนะของเครื่องทำน้ำร้อนด้วยปั๊มความร้อน สำหรับบ้านพักอาศัยขนาด 4 คน เครื่องทำน้ำร้อนด้วยปั๊มความร้อนประกอบด้วยถังเก็บน้ำร้อนขนาด 100 ลิตร เครื่องอัดไอขนาด 1.4 kW เครื่องทำระเหยขนาด 3.5 kW และเครื่องควบแน่นขนาด 4.5 kW ระบบปั๊มความร้อนใช้ R22 เป็นสารทำงาน จากการประเมินสมรรถนะของเครื่องทำน้ำร้อน โดยผลิตน้ำร้อนที่อุณหภูมิ 50.5°C สำหรับ อาบน้ำครั้งละ 150 ลิตร ที่อัตราการไหล 2.5 ลิตร/นาที เป็นจำนวน 2 ครั้งต่อวัน ใช้ไฟฟ้า 3.89 kWh/วัน สัมประสิทธิสมรรถนะเฉลี่ยของระบบปั๊มความร้อนเท่ากับ 3.25 อัตราส่วนประสิทธิภาพพลังงานเฉลี่ยใน 1 วันของเครื่องทำน้ำร้อนเท่ากับ 2.02 kW_{th}/kW_{elec} สามารถประหยัดไฟฟ้าได้ประมาณ 50% ของเครื่องทำน้ำร้อนด้วยไฟฟ้า ในกรณีพิจารณาที่อายุการใช้งาน 10 ปี อัตราค่าไฟฟ้าเฉลี่ย 3 บาท/kWh ต้นทุนรวมของน้ำร้อนที่ผลิตได้เท่ากับ 3.50 บาท/kWh_{th} ซึ่งคิดเป็นค่าเครื่อง 43 % ค่าไฟฟ้า 42 % และค่าบำรุงรักษา 15 % ตามลำดับ

คำสำคัญ(keywords):การทำน้ำร้อน / ปั๊มความร้อน/ การอนุรักษ์พลังงาน

ABSTRACT

In this paper, the design, construction and performance evaluation of a residential heat pump water heater (HPWH) for a family of 4 persons were conducted. The HPWH unit consists of a 100-liter storage tank integrated with a heat pump having 1.4 kW compressor, 3.5 kW evaporator, and 4.5 kW condenser. The performance of HPWH had been evaluated by using hot water of 150 liters at water flow rate of 2.5 liters/min with temperature of 50.5°C in the morning and by the same conditions in the evening. It was found that the electricity consumption was 3.89 kWh/d. The average coefficient of performance (COP_{hp}) and energy efficiency ratio (EER) were 3.25 and 2.02 kW_{th}/kW_{elec}, respectively. However the energy saving was approximately 50% when it was compared with the conventional electric water heater. In case of 10-year life time and 3 Baht/kWh electricity rate, the total cost of hot water was 3.50 Baht/kWh_{th}, of which capital cost, electricity cost and maintenance cost were 43%, 42%, and 15%, respectively.

Keywords: Water Heating/ Heat Pump/ Energy Conservation

1. บทนำ

เครื่องทำน้ำร้อนด้วยไฟฟ้าเป็นเครื่องใช้ไฟฟ้าชนิดหนึ่งที่นิยมใช้ในที่พักอาศัย เนื่องจากมีขนาดกระทัดรัด การใช้งานสะดวกอีกทั้งราคาเครื่องไม่สูงมากนัก แต่การทำน้ำร้อนด้วยไฟฟ้าต้องเสียค่าใช้จ่ายไฟฟ้าสูง และมีแนวโน้มที่ค่าไฟฟ้าจะเพิ่มขึ้นเรื่อยๆ ตามอัตราค่าไฟฟ้าที่การไฟฟ้าจัดเก็บ แนวทางหนึ่งในการลดความต้องการใช้ไฟฟ้าหรือลดค่าไฟฟ้าในที่พักอาศัย คือ การใช้อุปกรณ์ที่มีประสิทธิภาพสูงขึ้น [1] การทำน้ำร้อนด้วยปั๊มความร้อนเป็นแนวทางหนึ่งที่จะสามารถเพิ่มประสิทธิภาพของระบบทำน้ำร้อนด้วยไฟฟ้าได้ ซึ่งสามารถประหยัดพลังงานได้ถึง 50 % [2], [3] เนื่องจากสามารถนำความร้อนจากอากาศแวดล้อมมาใช้ ได้มีการทดลองใช้ระบบปั๊มความร้อนในการทำน้ำร้อนสำหรับที่พักอาศัยสามารถประหยัดค่าใช้จ่ายพลังงาน และประหยัดพลังงานได้โดยใช้พลังงานเพียง 80% ของการใช้ก๊าซทำน้ำร้อน และ 75% ของการใช้ไฟฟ้าทำน้ำร้อน [4] และได้มีการใช้ระบบปั๊มความร้อนสำหรับอุ่นน้ำเพื่อผลิตน้ำร้อนในร้านซักรีด[5] พบว่ามีค่าใช้จ่ายในการทำน้ำร้อนลดลงเหลือเพียง 1/3 ถึง 1/2 เท่าของการทำน้ำร้อนด้วยหม้อไอน้ำโดยใช้ก๊าซธรรมชาติเป็นเชื้อเพลิง ดังนั้นเพื่อให้มีการใช้เครื่องทำน้ำร้อนที่มีประสิทธิภาพสำหรับที่พักอาศัยในประเทศไทย งานวิจัยนี้จึงมีวัตถุประสงค์ที่จะออกแบบและสร้าง รวมถึงประเมินสมรรถนะและวิเคราะห์ต้นทุนของเครื่องทำน้ำร้อนด้วยปั๊มความร้อนเพื่อใช้ในบ้านพักอาศัยสำหรับครอบครัวขนาด 4 คน

RECEIVED 7 March, 2003
ACCEPTED 21 May, 2004

2. การออกแบบเครื่องทำน้ำร้อนด้วยปั๊มความร้อน

เครื่องทำน้ำร้อนด้วยปั๊มความร้อนนี้ได้ออกแบบเพื่อใช้งานในบ้านพักอาศัยสำหรับครอบครัวขนาด 4 คน เพื่อทำน้ำอุ่นสำหรับการอาบน้ำ การออกแบบเครื่องทำน้ำร้อนแบ่งออกเป็น 2 ส่วนได้แก่ การออกแบบถังเก็บน้ำร้อน และ การออกแบบระบบปั๊มความร้อน

2.1 การออกแบบถังเก็บน้ำร้อน

เนื่องจากระบบปั๊มความร้อนทำน้ำอุ่นได้ช้ากว่าเครื่องทำน้ำอุ่นทั่วไปที่ใช้ไฟฟ้า ดังนั้นจึงต้องมีถังเก็บน้ำร้อนเพื่อให้เพียงพอต่อการใช้งานได้อย่างต่อเนื่องสำหรับ 4 คน

การหาขนาดถังเก็บน้ำร้อน ได้พิจารณาตามสมมติฐานดังนี้

- อุณหภูมิน้ำอุ่นที่ใช้ในการอาบน้ำเท่ากับ 40 °C
- การอาบน้ำเป็นไปในลักษณะแบบใช้ฝักบัว ซึ่งปริมาณน้ำอุ่นที่ใช้ในการอาบน้ำประมาณ 40 ลิตร/คน/ครั้ง [6]
- อุณหภูมิน้ำร้อนจากเครื่องทำน้ำร้อนมีค่าประมาณ 50 °C
- อุณหภูมิน้ำจากท่อประปา 25 °C

จากข้อสมมติฐานนี้ หาปริมาณน้ำร้อน (50 °C) ที่ต้องการใช้แต่ละครั้งสำหรับ 4 คนได้ 96 ลิตร/ครั้ง ดังนั้นจึงเลือกถังเก็บน้ำร้อนขนาด 100 ลิตร การหาความหนาของถังเก็บน้ำร้อน ถังน้ำร้อนที่ออกแบบมีลักษณะเป็นแบบปิดซึ่งตัวถังจะต้องทนความดันของน้ำในระบบได้ ดังนั้นในการพิจารณาเลือกวัสดุที่ใช้ทำถังเก็บน้ำร้อน จะต้องเป็นวัสดุที่ทนการกัดกร่อนและแรงดันเนื่องจากการขยายตัวของน้ำเมื่ออุณหภูมิสูงขึ้นได้ ถังเก็บน้ำร้อนแบบปิดนี้จะต้องมีวาล์วนิรภัย ซึ่งเลือกใช้วาล์วที่สามารถทนความดันได้ 8 บาร์ จากมาตรฐานของ ASME Boiler and Pressure Vessel [7] การออกแบบถังเก็บน้ำร้อนจะต้องทนความดันได้ 16 บาร์ และกำหนดค่าแฟคเตอร์เพิ่มที่ใช้ในการออกแบบ (safety factor) เท่ากับ 1.5 ดังนั้นจึงเลือกใช้สแตนเลสสตีล เบอร์ 304 ซึ่งสามารถรับแรงดันได้ 207 Mpa ที่มีขายท้องตลาดมีขนาด 1.2 ม.x2.4 ม. หนา 3 มม ซึ่งนำมาม้วนเป็นรูปทรงกระบอกขนาดเส้นผ่าศูนย์กลาง 0.382 ม. สูง 0.873 ม. และความสูงของส่วนหัวของถังทรงกระบอกเท่ากับ 0.0175 ม.

2.2 การออกแบบระบบปั๊มความร้อน

สมมติฐานและข้อมูลที่ใช้

- น้ำเข้าเครื่องทำน้ำร้อนมีอุณหภูมิ 25 °C
- น้ำออกจากเครื่องทำน้ำร้อนอุณหภูมิ 50 °C
- อัตราการไหลของน้ำในถังเก็บน้ำร้อน 0.042 kg/s หรือ 2.5 ลิตร/นาที
- การอาบน้ำแบบฝักบัวมีอัตราการไหลของน้ำอุ่น 4 ลิตร/นาที
- ระบบปั๊มความร้อนใช้สารทำงาน R22
- อุณหภูมิสารทำงานที่เครื่องควบแน่น 55 °C
- อุณหภูมิสารทำงานที่เครื่องทำระเหย 10 °C
- ประสิทธิภาพทางกลของเครื่องอัดไอเท่ากับ 0.8 และประสิทธิภาพมอเตอร์ไฟฟ้าเท่ากับ 0.85 เป็นข้อมูลที่ได้จากผู้ผลิตเครื่องอัดไอ

ในการออกแบบเริ่มจากการคำนวณหาอัตราความร้อนที่ใช้ทำน้ำร้อนจากน้ำอุณหภูมิ 25 °C ถึง 50 °C ได้จาก

$$Q_w = m_w c_{p,w} \Delta T_w \qquad (1)$$

เมื่อ m_w คือค่าอัตราการไหลของน้ำร้อนออกจากถัง, $c_{p,w}$ คือค่าความจุความร้อนของน้ำ, ΔT_w คือค่าผลต่างอุณหภูมิน้ำร้อนที่ออกจากถังและน้ำที่เข้าถัง จากนั้นคำนวณหาขนาดของเครื่องอัดไอ โดยหาอัตราการไหลของสารทำงาน (m_r) ก่อน ซึ่งคำนวณจากอัตราความร้อนที่ต้องการใช้ในการทำน้ำร้อนได้จากสมการดังนี้

$$Q_{con} = m_r(h_{com,o} - h_{con,o}) \qquad (2)$$

เมื่อ Q_{con} คืออัตราความร้อนที่ถ่ายเทออกจากเครื่องควบแน่น, $h_{com,o}$ และ $h_{con,o}$ คือค่าเอนทัลปีของสารทำงานที่ออกจากเครื่องอัดไอและที่ออกจากเครื่องควบแน่นตามลำดับ จากนั้นคำนวณหากำลังงานที่ใช้ในการอัดไอ (W_{com}) ได้จากสมการ

$$W_{com} = m_r(h_{com,o} - h_{com,i}) \qquad (3)$$

เมื่อ $h_{com,i}$ คือค่าเอนทัลปีของสารทำงานที่เข้าเครื่องอัดไอ จากนั้นหากำลังไฟฟ้าที่ให้แก่เครื่องอัดไอ (P_{com}) ได้จาก

$$P_{com} = \frac{W_{com}}{\eta_m \eta_e} \qquad (4)$$

เมื่อ η_m และ η_e คือประสิทธิภาพทางกลของเครื่องอัดไอ และมอเตอร์ไฟฟ้า นำค่าที่คำนวณได้ไปเลือกขนาดของเครื่องอัดไอที่มีขายตามท้องตลาดที่มีค่า

ใกล้เคียงกับที่คำนวณได้ ถ้าไม่มีก็ให้เลือกขนาดที่ใหญ่กว่า จากนั้นคำนวณหาขนาดของเครื่องควบแน่นจากขนาดของเครื่องอัดไอที่เลือกใช้ โดยคำนวณย้อนกลับโดยใช้สมการ (4), (3), (2) แล้วคำนวณหาขนาดของเครื่องทำระเหย ($\dot{Q}_e$) ได้จาก

$$\dot{Q}_e = \dot{m}_r(h_{com,i} - h_{e,i}) \qquad (5)$$

เมื่อ $h_{e,i}$ คือค่าเอนทัลปีของสารทำงานที่เข้าเครื่องทำระเหย

ผลการออกแบบเครื่องทำน้ำร้อนด้วยปั๊มความร้อนสำหรับบ้านพักอาศัยขนาด 4 คน แสดงดังรูปที่ 1 ซึ่งสรุปได้ดังนี้

1. ถังเก็บน้ำร้อนเป็นรูปทรงกระบอกขนาด 100 ลิตร ทำด้วยสแตนเลสสตีล เบอร์ 304 หนา 3 มิลิเมตร ขนาดเส้นผ่าศูนย์กลางของถัง 0.382 ม. สูง 0.873 ม. และความสูงของส่วนหัวของถังทรงกระบอกเท่ากับ 0.0175 ม.
2. เครื่องอัดไอแบบถูกสูบของบริษัท TECUMSEH รุ่น AW 5515EK ขนาดกำลังไฟฟ้า 1.39 kW ใช้ R-22 เป็นสารทำงาน
3. เครื่องทำระเหยขนาดภาระการทำความเย็น 3.51 kW
4. เครื่องควบแน่นขนาดภาระการทำความร้อน 4.46 kW มีลักษณะเป็นท่อทองแดงขดอยู่ภายในถังเก็บน้ำร้อน

3. การทดสอบสมรรถนะของเครื่องทำน้ำร้อน

ในการทดสอบสมรรถนะของเครื่องทำน้ำร้อน ได้ประเมินหาค่าสัมประสิทธิ์สมรรถนะระบบปั๊มความร้อน (COP_{HP}) อัตราส่วนประสิทธิภาพทางพลังงานของเครื่องทำน้ำร้อน (EER) ได้จาก

$$COP_{HP} = \frac{\dot{Q}_{con}}{\dot{W}_{com}} \qquad (6)$$

$$EER = \frac{\dot{m}_w c_{p,w}(\Delta T_w)}{P_T} \qquad (7)$$

เมื่อ P_T คือ ค่ากำลังไฟฟ้ารวมที่ให้แก่เครื่องทำน้ำร้อน

วิธีการทดลอง

1. หาสมรรถนะของเครื่องทำน้ำร้อนตามสภาพการใช้งานจริงสำหรับ 4 คนที่อาบน้ำอย่างต่อเนื่อง ที่อัตราการไหลของน้ำร้อน 2.5 ลิตร/นาที โดยตั้งค่าอุณหภูมิควบคุมน้ำในถังเก็บน้ำร้อนไว้ที่ 50 °C ในแต่ละวันอาบน้ำ 2 ครั้ง คือ ช่วงเช้า และช่วงเย็น ในแต่ละช่วงเปิดน้ำร้อนอย่างต่อเนื่องครั้งละ 150 ลิตร ขณะที่ปล่อยน้ำร้อนออกจากถังจะมีน้ำเย็นไหลเข้าถังตลอดเวลา บันทึกค่าอุณหภูมิและความดันของสารทำงาน อุณหภูมิน้ำที่เข้าและออกจากถังเก็บน้ำร้อน ตำแหน่งที่ทำการวัดแสดงดังรูปที่ 1 วัดกำลังไฟฟ้าของเครื่องอัดไอและพัดลมของเครื่องทำระเหย ทุก 2 นาทีในช่วงที่ใช้น้ำร้อนและวัดค่าพลังงานไฟฟ้าที่ให้แก่เครื่องทำน้ำร้อนตลอดทั้งวัน
2. หาอุณหภูมิของน้ำร้อนที่ออกจากถังในกรณีที่มีการใช้น้ำอย่างต่อเนื่องที่อัตราการไหล 2, 3, 4, 5 ลิตร/นาที

อุปกรณ์ที่ใช้ในการทดลองได้แก่

- เทอร์โมคัปเปิลชนิดเคต่อเข้ากับเครื่องบันทึกอุณหภูมิ มีค่าความถูกต้อง ± 1%
- บรูดองเกจแบบวัดความดันต่ำ มีค่าความถูกต้อง ± 6.9 kPa และแบบวัดความดันสูง มีค่าความถูกต้อง ± 34.5 kPa
- มาตรวัดกำลังไฟฟ้า (clip-on-meter) มีค่าความถูกต้อง ± 0.1 kW
- มาตรวัดกิโลวัตต์ชั่วโมง มีค่าความถูกต้อง ± 0.1 kWh

4. ผลการทดสอบ

ผลการทดสอบสมรรถนะของเครื่องทำน้ำร้อนด้วยปั๊มความร้อน พบว่าที่อัตราการไหลของน้ำร้อน 2.5 ลิตร/นาที อัตราการใช้น้ำอุ่น 4 ลิตร/นาที ได้อุณหภูมิเฉลี่ยของน้ำร้อนที่ออกจากถังเท่ากับ 50.5 °C พลังงานไฟฟ้ารวมที่ใช้ตลอดวันเท่ากับ 3.89 kWh ค่า COP_{HP} เฉลี่ยเท่ากับ 3.25 และอัตราส่วนประสิทธิภาพของเครื่องทำน้ำร้อนเฉลี่ยใน 1 วัน (EER_{avg}) เท่ากับ 2.02 kW_{th}/kW_{elec} ซึ่งค่านี้ได้รวมผลการสูญเสียความร้อนทั้งวันซึ่งปั๊มความร้อนจะต้องทำงานเพื่อรักษาระดับอุณหภูมิน้ำให้ได้ตามที่ตั้งไว้ จากการทดลองสังเกตุได้ว่าตลอด 24 ชั่วโมงในช่วงที่ไม่มีการใช้น้ำปั๊มความร้อนจะทำงานประมาณ 3 ครั้ง รวมเป็นพลังงานไฟฟ้าใช้ 1.04 kWh คิดเป็น 27%ของไฟฟ้าที่เครื่องทำน้ำร้อนใช้ตลอด 24 ชั่วโมง

ผลการทดสอบอุณหภูมิน้ำร้อนที่ผลิตได้ ในกรณีที่มีการใช้น้ำร้อนอย่างต่อเนื่องที่อัตราการไหลน้ำร้อน 2, 3, 4, 5 ลิตร/นาที ซึ่งมีความสัมพันธ์ระหว่างอุณหภูมิและอัตราการไหลของน้ำร้อนดังแสดงในรูปที่ 2 - 5 จากรูปจะสังเกตุเห็นได้ว่าในช่วงแรกจะได้น้ำร้อนอุณหภูมิค่อนข้างสูงแล้วลดต่ำลงเรื่อยๆจนอุณหภูมิคงที่ที่ค่าค่าหนึ่ง เนื่องจากเครื่องควบแน่นมีอัตราการถ่ายเทความร้อนคงที่ ค่าอัตราการไหลของน้ำร้อนและอุณหภูมิของน้ำร้อนที่คงที่สรุปได้ดังตารางที่ 1 จะเห็นได้ว่ายังคงผลิตน้ำร้อนได้อุณหภูมิสูงกว่า 40°C และค่าอุณหภูมิคงที่ของน้ำร้อนที่ออกจากถังลดลงเมื่อเพิ่มอัตราการไหลของน้ำ ส่วนค่า COP_{HP} มีค่าเพิ่มขึ้น เนื่องจากอุณหภูมิที่ใช้ในการควบแน่นต่ำลง

ตารางที่ 1 ค่า COP_{HP} และอุณหภูมิคงที่ของน้ำร้อนเมื่อมีการใช้งานอย่างต่อเนื่องที่อัตราการไหลค่าต่างๆ

อัตราการไหลของน้ำร้อน (ลิตร/นาที)	อุณหภูมิคงที่ของน้ำร้อนเมื่อมีการใช้งานอย่างต่อเนื่อง (^{o}C)	COP_{HP}
2	52.5	3.65
3	47.0	3.79
4	43.0	3.85
5	41.0	3.93

5. การประเมินต้นทุนในการทำน้ำร้อนด้วยปั๊มความร้อน

ข้อมูลทางด้านเทคนิคของเครื่องทำน้ำร้อนด้วยปั๊มความร้อน ได้แก่ ปริมาณการใช้น้ำร้อน 300 ลิตร/วัน วันละ 2 ครั้ง คือ ตอนเช้า และตอนเย็น ครั้งละ 150 ลิตร ที่อัตราการไหล 2.5 ลิตร/นาที จากผลการทดลองได้อุณหภูมิเฉลี่ยของน้ำร้อน 50.5 ^{o}C อุณหภูมิน้ำเข้าถังน้ำร้อน 28 ^{o}C ปริมาณการใช้ไฟฟ้า 3.89 kWh/วัน

สมมติฐานและข้อมูลทางการเงินที่ใช้ในการประเมิน ได้แก่

- ต้นทุนในการสร้างเครื่องทำน้ำร้อน 30,060 บาท
- มูลค่าซากคิด 10% ของต้นทุนเครื่องทำน้ำร้อน
- ค่าบำรุงรักษารายปีคิดเป็น 5% ของต้นทุนสร้างเครื่องทำน้ำร้อน
- ค่าอัตราส่วนลด (discount rate) 8%
- อายุการใช้งาน 5 ปี
- อัตราค่าไฟฟ้าเฉลี่ย 3 บาท/kWh
- จำนวนชั่วโมงการทำงาน 365 วัน/ปี

ผลการประเมินหาต้นทุนรวมของน้ำร้อน(ไม่คิดค่าน้ำ)สรุปได้ดังนี้ ต้นทุนรวมของน้ำร้อน(ไม่คิดค่าน้ำ)ต่อหน่วยความร้อนที่ผลิตได้ เท่ากับ 1.24 บาท/MJ_{th} หรือ 4.46 บาท/kWh_{th} ซึ่งคิดเป็นต้นทุนค่าเครื่องทำน้ำร้อน 55%, ค่าไฟฟ้า 33%, และค่าบำรุงรักษา 12%

เนื่องจากชั่วโมงการทำงานต่อวันของเครื่องทำน้ำร้อนด้วยปั๊มความร้อนมีค่าต่ำมาก ดังนั้นอายุการใช้งานน่าจะสูงกว่า 10 ปี กรณีที่พิจารณาอายุการใช้งานเพิ่มขึ้นเป็น 10 ปี ต้นทุนรวมของน้ำร้อนลดลงเหลือ 0.97 บาท/MJ_{th} หรือ 3.50 บาท/kWh_{th} ซึ่งคิดเป็นต้นทุนค่าเครื่องทำน้ำร้อน 43%, ค่าไฟฟ้า 42%, และค่าบำรุงรักษา 15% จะเห็นได้ว่าถึงแม้จะสามารถลดค่าใช้จ่ายไฟฟ้าได้ประมาณ 50 % แต่เงินลงทุนค่าเครื่องปั๊มความร้อนค่อนข้างสูงเมื่อเทียบกับเครื่องทำน้ำร้อนด้วยไฟฟ้าที่ใช้กันทั่วไปประมาณ 5 เท่า (เป็นกรณีที่ไม่มีถังเก็บน้ำร้อน หากมีถังเก็บน้ำร้อนด้วยจะต่ำกว่านี้) ซึ่งณ.อัตราค่าไฟฟ้าปัจจุบันจึงทำให้ระบบปั๊มความร้อนมีต้นทุนใกล้เคียงกับเครื่องทำน้ำร้อนด้วยไฟฟ้า อย่างไรก็ดีอัตราค่าไฟฟ้ามีแนวโน้มสูงขึ้นเรื่อยซึ่งทำให้เครื่องทำน้ำร้อนด้วยปั๊มความร้อนมีแนวโน้มที่จะสามารถนำมาใช้ทดแทนเครื่องทำน้ำร้อนด้วยไฟฟ้าได้คุ้มค่ามากขึ้น

6. สรุป

เครื่องทำน้ำร้อนขนาดถังเก็บน้ำร้อน 100 ลิตร ซึ่งมีระบบปั๊มความร้อนประกอบด้วยเครื่องอัดไอแบบลูกสูบขนาดกำลังไฟฟ้า 1.39 kW ใช้ R-22 เป็นสารทำงาน เครื่องทำระเหยขนาดภาระการทำความเย็น 3.51 kW และ เครื่องควบแน่นขนาดภาระการทำความร้อน 4.46 kW มีลักษณะเป็นท่อทองแดงขดอยู่ภายในถังเก็บน้ำร้อน เหมาะสำหรับบ้านพักอาศัยขนาด 4 คน สามารถผลิตน้ำร้อนได้อุณหภูมิเฉลี่ย 50.5 ^{o}C ที่อัตราการไหล 2.5 ลิตร/นาที เพื่อใช้ทำน้ำอุ่นสำหรับอาบน้ำ ใช้พลังงานไฟฟ้ารวมตลอดวันเท่ากับ 3.89 kWh ได้ค่า COP_{HP} เฉลี่ยเท่ากับ 3.25 และอัตราส่วนประสิทธิภาพของเครื่องทำน้ำร้อนเฉลี่ยใน 1 วัน (EER_{d}) เท่ากับ 2.02 kW_{th}/kW_{elec} สามารถประหยัดค่าไฟฟ้าได้ประมาณ 50% เมื่อพิจารณาเทียบกับเครื่องทำน้ำอุ่นด้วยไฟฟ้าทั่วไป ที่อัตราค่าไฟฟ้าค่า 3 บาท/kWh และอายุการใช้งาน 10 ปี ต้นทุนรวมของน้ำร้อน(ไม่คิดค่าน้ำ)ต่อหน่วยความร้อนที่ผลิตได้ เท่ากับ 0.97 บาท/MJ_{th} หรือ 3.50 บาท/kWh_{th} ซึ่งคิดเป็นต้นทุนค่าเครื่องทำน้ำร้อน 43%, ค่าไฟฟ้า 42%, และค่าบำรุงรักษา 15%

7. เอกสารอ้างอิง

[1] http://www.nepo.go.th, 2002.

[2] http://www.chilipepperapp.com/hpwh.htm, 2002.

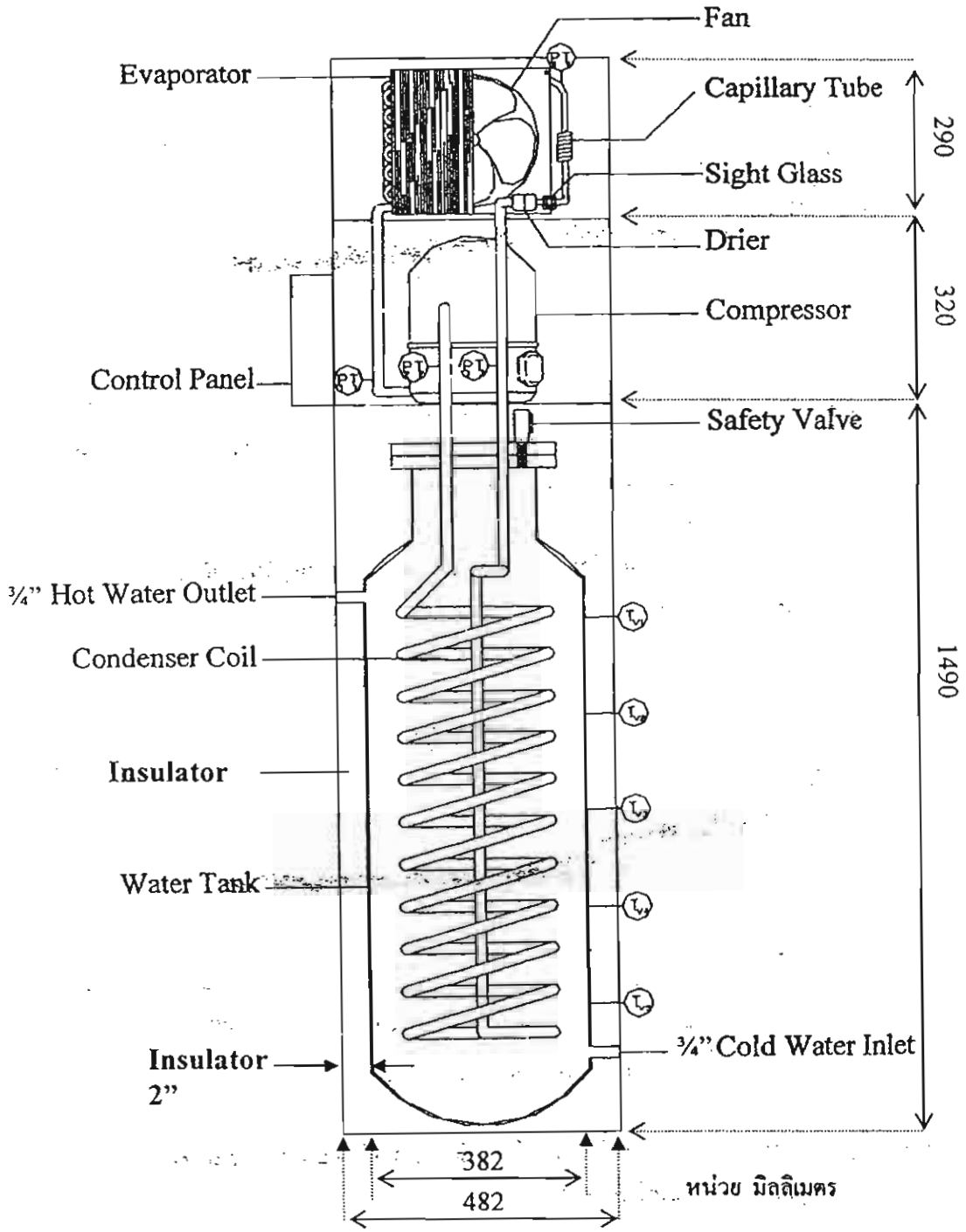
[3] http://www.pnl.gov/fta/3_res.htm, 2002.

[4] Wiebusch,B., "Pump Efficiently Heat Water", Design News, Boston, Vol.56, 2001.

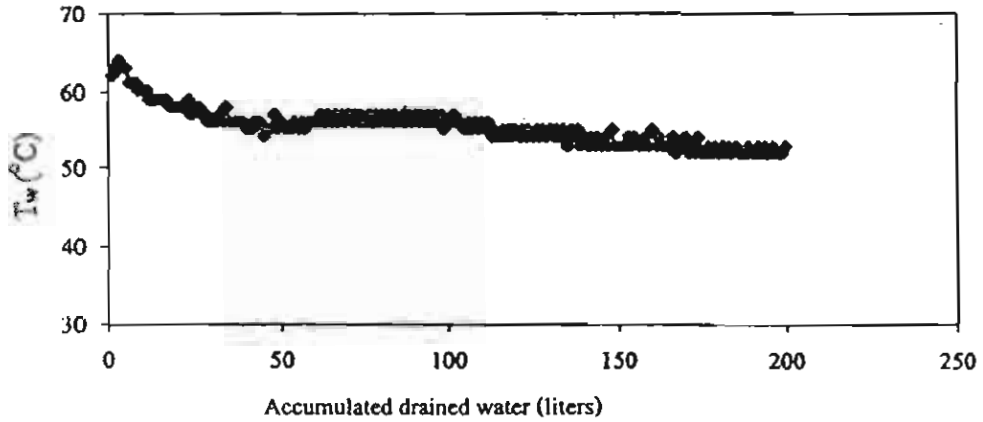
[5] Robert,O. and Schowalter,P.E., 1997, "Heat Pump Water for Laundry", ASHRAE Journal, Vol.39, No.7, pp 77-79.

[6] วริทธิ์ อึ้งภากรณ์, 2526, การออกแบบระบบท่อภายในอาคาร, วิศวกรรมสถานแห่งประเทศไทย, หน้า 145-191.

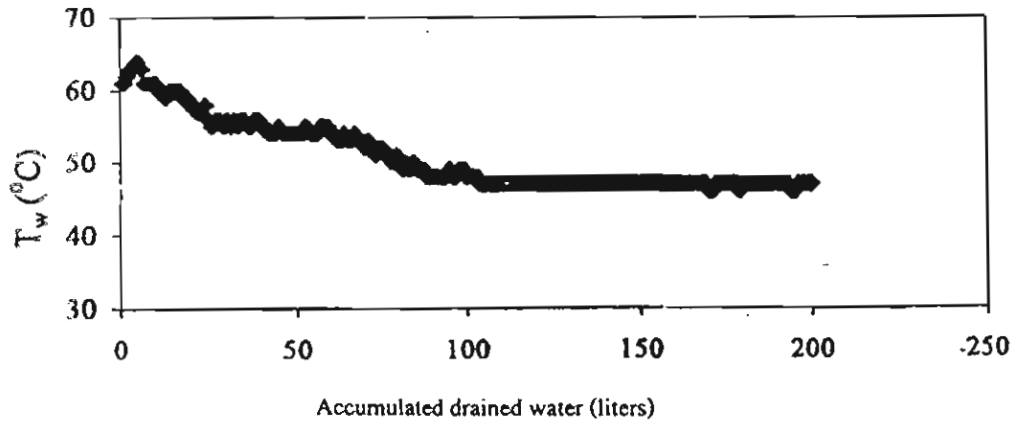
[7] American Society of Mechanical Engineers, 1977, ASME Boiler and Pressure Vessel Code: An American National Standard ANSI/ASME BPV-VIII-1, Section VIII; Rules for Construction of Pressure Vessels, Division 1, New York, ASME, pp.245-280.



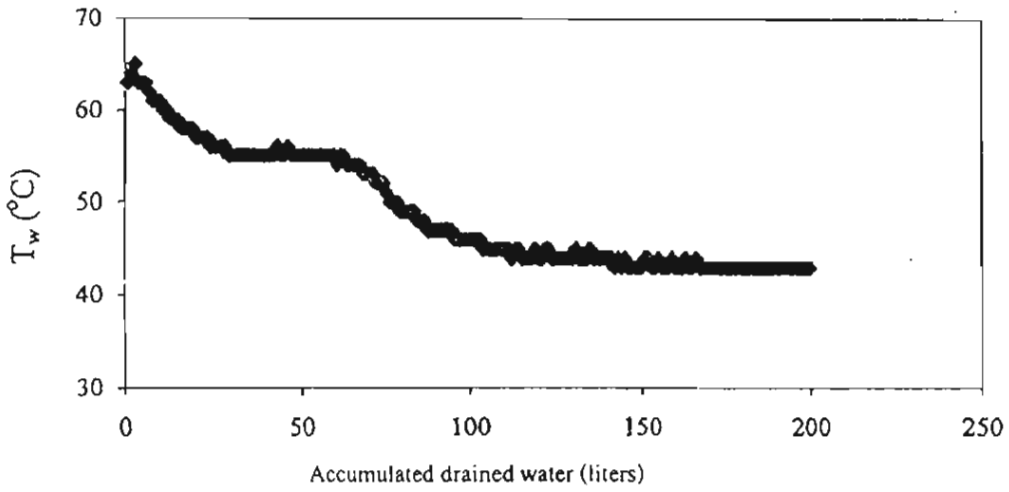
รูปที่ 1 แผนภาพเครื่องทำน้ำร้อนด้วยปั๊มความร้อน และตำแหน่งที่วัดอุณหภูมิและความดัน



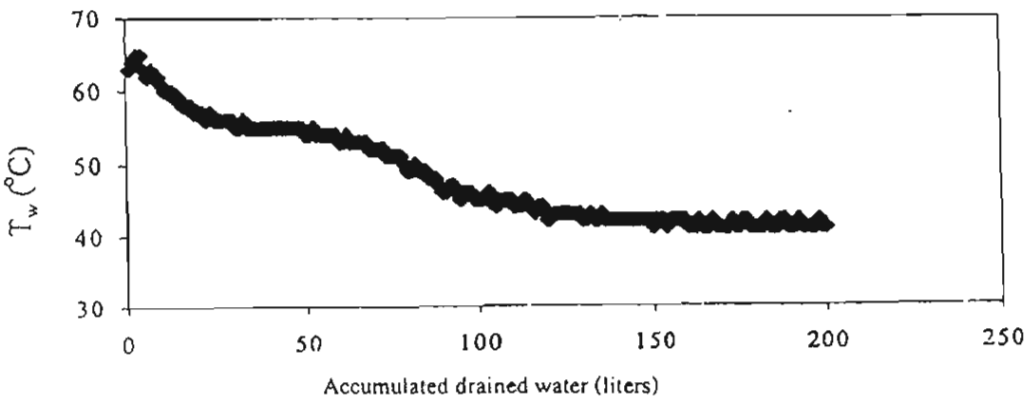
รูปที่ 2 อุณหภูมิน้ำร้อนปล่อยจากถังที่อัตราการไหล 2 ลิตร/นาที เมื่ออุณหภูมิน้ำเข้าถัง 28°C และ อุณหภูมิอากาศแวดล้อม 30°C



รูปที่ 3 อุณหภูมิน้ำร้อนปล่อยจากถังที่อัตราการไหล 3 ลิตร/นาที เมื่ออุณหภูมิน้ำเข้าถัง 28°C และ อุณหภูมิอากาศแวดล้อม 30°C



รูปที่ 4 อุณหภูมิน้ำร้อนปล่อยจากถังที่อัตราการไหล 4 ลิตร/นาที เมื่ออุณหภูมิน้ำเข้าถัง 28°C และ อุณหภูมิอากาศแวดล้อม 30°C



รูปที่ 5 อุณหภูมิน้ำร้อนปล่อยจากถังที่อัตราการไหล 5 ลิตร/นาที เมื่ออุณหภูมิน้ำเข้าถัง 28°C และ อุณหภูมิอากาศแวดล้อม 30°C

บทความ

วารสารวิชาการ
ปีที่ ๒๙ ฉบับที่ ๓ ก.ค.-ก.ย. ๒๕๔๗

สถานภาพและแนวทางการวิจัยพลังงานมวลชีวภาพในประเทศไทย

วารุณี เตีย*
พิมพร แจ้งพลอย*
กังสดาล สกุลพงษ์มาลี**
สมชาติ โสภณรณฤทธิ์***
ราชบัณฑิต สำนักวิทยาศาสตร์
ราชบัณฑิตยสถาน

บทคัดย่อ

มวลชีวภาพเป็นแหล่งพลังงานหมุนเวียนที่มีศักยภาพสูงสำหรับประเทศไทย รัฐบาลได้มีการวางแผนและกำหนดนโยบายในการส่งเสริมเพื่อพัฒนาและใช้ประโยชน์จากมวลชีวภาพ บทความนี้นำเสนอสถานภาพและแนวโน้มงานวิจัยด้านมวลชีวภาพ โดยได้ศึกษามวลชีวภาพ ๔ รูปแบบ ได้แก่ เชื้อเพลิงมวลชีวภาพ เอทานอล ไบโอดีเซล และแก๊สชีวภาพ ข้อจำกัดโดยทั่วไปของการใช้มวลชีวภาพ คือ แหล่งมวลชีวภาพที่นำมาใช้ได้มักเปลี่ยนแปลงตามฤดูกาล โดยเฉพาะอย่างยิ่งแหล่งมวลชีวภาพจากอุตสาหกรรมเกษตร เพื่อขยายประโยชน์จากการใช้มวลชีวภาพให้มากขึ้นจึงควรทำการวิจัยทางด้านการจัดการแหล่งมวลชีวภาพ การปรับปรุงประสิทธิภาพของระบบหรืออุปกรณ์ การลดต้นทุน นอกจากนี้ ควรมีงานวิจัยเกี่ยวกับการใช้เชื้อเพลิงชนิดอื่นร่วมกันในการเผาไหม้ และการศึกษาความเป็นไปได้ของการผลิตไฟฟ้าด้วยมวลชีวภาพสำหรับไบโอเอทานอลและไบโอดีเซล ควรมีการศึกษาสมรรถนะของเครื่องยนต์ระยะยาว รวมถึงการกำหนดมาตรฐานลักษณะเฉพาะของน้ำมันไบโอดีเซล นอกจากนี้ควรมีการศึกษาการใช้ประโยชน์และเทคโนโลยีที่เหมาะสมสำหรับแก๊สชีวภาพด้วย

คำสำคัญ : มวลชีวภาพ, พลังงานหมุนเวียน, แนวทางการวิจัย

บทนำ

พลังงานเป็นปัจจัยที่สำคัญต่อการพัฒนาเศรษฐกิจและสังคมของประเทศ ประเทศไทยเป็นประเทศที่ต้องนำเข้าพลังงานเชิงพาณิชย์ เนื่องจากแหล่งพลังงานเชิงพาณิชย์ที่ผลิตได้ภายในประเทศไม่เพียงพอต่อความต้องการ จึงต้องนำเข้าพลังงานมากกว่าร้อยละ ๖๐ ของความต้องการใช้พลังงานเชิงพาณิชย์ของประเทศ[๑] ใน พ.ศ. ๒๕๔๕ มูลค่าการนำเข้าพลังงาน เชิงพาณิชย์สุทธิรวมทั้งสิ้นสูงถึง ๒๖๖, ๕๘๖ ล้านบาท[๒] รัฐจึงได้กำหนดนโยบายให้ส่งเสริม จัดหา พัฒนา และใช้พลังงานทดแทนอย่างมีประสิทธิภาพ เพื่อลดการพึ่งพาแหล่งพลังงานจากต่างประเทศ เนื่องจากประเทศไทยมีผลผลิตทางการเกษตรมาก จึงมีของเหลือทางการเกษตรที่สามารถนำมาใช้เป็นแหล่งพลังงานทดแทนได้ ถึงแม้ปัจจุบันได้มีการใช้มวลชีวภาพเป็นแหล่งเชื้อเพลิงทั้งในภาคอุตสาหกรรมและครัวเรือนแล้วบางส่วน แต่ก็ยังมีมวลชีวภาพเหลืออีกมากที่สามารถพัฒนามาใช้เป็นแหล่งพลังงานได้ และบางส่วนยังมีการใช้อย่างไม่มีประสิทธิภาพ ดังนั้น ในบทความนี้จะกล่าวถึงสถานการณ์และแนวทางการวิจัยเพื่อพัฒนาและส่งเสริมให้มีการใช้มวลชีวภาพมากขึ้นและเป็นไปอย่างมีประสิทธิภาพ

* รองศาสตราจารย์ คณะพลังงานและวัสดุ มหาวิทยาลัยเทคโนโลยีพระจอมเกล้าธนบุรี
**นักศึกษาปริญญาโท คณะพลังงานและวัสดุ มหาวิทยาลัยเทคโนโลยีพระจอมเกล้าธนบุรี
*** ศาสตราจารย์ คณะพลังงานและวัสดุ มหาวิทยาลัยเทคโนโลยีพระจอมเกล้าธนบุรี

วิธีดำเนินงานวิจัย

มวลชีวภาพที่ทำการศึกษามี ๔ รูปแบบ ได้แก่ เชื้อเพลิงมวลชีวภาพ เอทานอล ไบโอดีเซล และแก๊สชีวภาพ การดำเนิน งานวิจัยได้รวบรวมข้อมูลจากแหล่งต่าง ๆ ได้แก่ รายงานและบทความวิจัย ด้านพลังงานมวลชีวภาพ เพื่อนำมาศึกษาและเสนอแนวทางวิจัย ซึ่งมีรายละเอียดดังนี้

ก. ศึกษาศักยภาพของแหล่งพลังงานมวลชีวภาพ ได้แก่

- มวลชีวภาพจากการเกษตร ซึ่งเป็นส่วนที่เหลือทิ้งจากอุตสาหกรรม เช่น แกลบ ชานอ้อย ฯลฯ และมวลชีวภาพที่เป็นผลผลิตทางการเกษตรที่สามารถนำมาเป็นวัตถุดิบในการแปรรูปเป็นเชื้อเพลิง เช่น มันสำปะหลัง พืชน้ำมัน ฯลฯ
- มวลชีวภาพจากปศุสัตว์ เช่น ของเสียจากการขับถ่ายของสัตว์
- มวลชีวภาพจากน้ำเสียจากอุตสาหกรรมและขยะ

ข. ศึกษาสถานภาพการใช้และงานวิจัยด้านพลังงานมวลชีวภาพของประเทศไทย

ค. วิเคราะห์ข้อมูลศักยภาพของแหล่งพลังงานมวลชีวภาพ สถานภาพการใช้และงานวิจัยที่ผ่านมา นำมาสรุปเสนอเป็นแนวทางงานวิจัยที่ควรดำเนินการต่อไปพลังมวลชีวภาพ

ผลการศึกษาและวิจารณ์ศักยภาพมวลชีวภาพของประเทศไทย

ปริมาณมวลชีวภาพจากวัสดุเหลือใช้ทางการเกษตรขึ้นอยู่กับผลผลิตทางการเกษตรและการใช้ในแต่ละปี ใน พ.ศ. ๒๕๔๓ ได้มีการประเมินศักยภาพมวลชีวภาพจากวัสดุเหลือใช้ทางการเกษตร[๓] ๑๐ ชนิด ดังแสดงในตารางที่ ๑ จะเห็นได้ว่ามีปริมาณมวลชีวภาพเหลือใช้ทางเกษตรที่ยังไม่ได้นำมาใช้เป็นเชื้อเพลิงยังมีอยู่อีกมาก คิดเป็นพลังงานรวมทั้งสิ้น ๖๐๔,๘๒๒ × $๑๐^{๖}$ จูล

มูลสัตว์น้ำเสียจากโรงงานอุตสาหกรรม และขยะ สามารถนำมาผลิตเป็นแก๊สชีวภาพได้ ใน พ.ศ. ๒๕๔๓ ได้มีการประเมินศักยภาพศักยภาพการผลิตแก๊สชีวภาพจากมูลสัตว์ ๖ ชนิด ดังแสดงในตารางที่ ๒ มีศักยภาพรวมทั้งสิ้น ๑๑,๗๕๐ × $๑๐^{๖}$จูล (คิดที่ค่าความร้อนแก๊สชีวภาพผลิตจากมูลสัตว์เท่ากับ ๒๑ เมกะจูลต่อลบ.ม.) ซึ่งนับว่าเป็นพลังงานที่มาก สำหรับน้ำเสียในโรงงานอุตสาหกรรม ๑๑ ประเภท ดังแสดงในตารางที่ ๓ มีศักยภาพรวมทั้งสิ้น ๑๐,๔๔๖ × $๑๐^{๖}$จูล (คิดที่ค่าความร้อนแก๊สชีวภาพผลิตจากน้ำเสียเท่ากับ ๒๔ เมกะจูลต่อลบ.ม.) จะเห็นได้ว่าโรงงานแป้งมันและโรงงานน้ำตาลมีศักยภาพสูงมากในส่วนของการผลิตแก๊สชีวภาพจากการฝังกลบขยะมีศักยภาพรวมทั้งสิ้น ๒๓,๐๙๒×$๑๐^{๖}$ จูล (คิดที่ค่าความร้อนแก๊สชีวภาพผลิตจากขยะเท่ากับ ๑๙.๕ เมกะจูลต่อลบ.ม.) ดังแสดงในตารางที่ ๔ ศักยภาพรวมของการผลิตแก๊สชีวภาพจากมูลสัตว์ น้ำเสียจากโรงงานอุตสาหกรรม และขยะที่ได้จากการฝังกลบรวมทั้งหมดเท่ากับ ๔๕,๒๘๘×$๑๐^{๖}$ เมกะจูลต่อปี ถึงแม้ว่าศักยภาพที่ได้จากการฝังกลบจะมีค่ามาก แต่ในปัจจุบันการรวบรวมทำได้ยาก ดังนั้นจึงจะพิจารณาการผลิตแก๊สชีวภาพจากมูลสัตว์ น้ำเสียจากโรงงานอุตสาหกรรม เป็นสำคัญ

มวลชีวภาพสำหรับการผลิตไบโอดีเซล ประเทศไทยมีพืชน้ำมันที่ทำการเกษตรอย่างเป็นระบบและเชิงพาณิชย์ ได้แก่ ถั่วเหลือง ถั่วลิสง ปาล์มน้ำมัน งา มะพร้าว ละหุ่ง ซึ่งมีผลผลิตดังแสดงในตารางที่ ๕ จะเห็นได้ว่าปาล์มน้ำมันมีศักยภาพสูงที่สุด การนำน้ำมันพืชมาใช้มีปัญหาหลักคือ ความหนืด การนำน้ำมันพืชมาสังเคราะห์เป็นเอสเตอร์ หรือไบโอดีเซลจะทำให้น้ำมันปาล์มมีความหนืดลดลงและมีความคงตัวมากขึ้นเมื่ออุณหภูมิเปลี่ยนและจุดวาบไฟของไบโอดีเซลสูงกว่าน้ำมันดีเซลจึงมีความปลอดภัยในการใช้และการขนส่ง[๔]

ตารางที่ ๑ ศักยภาพพลังงานจากวัสดุเหลือใช้ทางการเกษตร พ.ศ. ๒๕๔๓

ชนิด	ผลผลิต/ปี (พันตัน)	วัสดุเหลือใช้	ปริมาณวัสดุเหลือใช้ (พันตัน)	แฟกเตอร์วัสดุเหลือใช้ที่ยังไม่มีการใช้	ปริมาณวัสดุเหลือใช้ที่ยังไม่มีการใช้ (พันตัน)	ค่าพลังงานความร้อน (MJ/kg)	ศักยภาพพลังงาน (*10^6 MJ)
อ้อย	๕๓,๔๖๔	ชานอ้อย	๑๕,๕๖๗	๐.๒๐๗	๓,๒๒๒	๑๔.๔๐	๔๖,๔๐๑
		ส่วนยอดและใบ	๑๖,๑๕๕	๐.๙๕๖	๑๕,๙๒๙	๑๗.๓๙	๒๗๗,๐๐๖
ข้าว	๒๔,๑๗๒	แกลบ	๕,๕๖๐	๐.๔๙๓	๒,๗๔๑	๑๔.๒๗	๓๙,๑๑๒
		ฟาง (ส่วนบน)	๑๐,๘๐๕	๐.๖๘๔	๗,๓๙๑	๑๐.๒๔	๗๕,๖๗๙
ปาล์มน้ำมัน	๓,๒๕๖	ทะลายเปล่า	๑,๓๙๔	๐.๕๘๔	๘๑๔	๑๗.๘๖	๑๔,๕๓๕
		ลันใยปาล์ม	๔๗๙	๐.๑๓๔	๖๔	๑๗.๖๒	๑,๑๓๐
		กะลาปาล์ม	๑๖๐	๐.๐๓๗	๖	๑๘.๔๖	๑๐๙
		ก้าน	๘,๔๗๙	๑.๐๐๐	๘,๔๗๙	๙.๘๓	๘๓,๓๔๕
	ทะลายตัวผู้		๗๕๙	๑.๐๐๐	๗๕๙	๑๒,๓๘๙	
มันสำปะหลัง	๑๙,๐๖๔	ลำต้น	๑,๖๗๘	๐.๔๐๗	๖๘๓	๑๘.๔๒	๑๒,๕๗๗
ข้าวโพด	๔,๒๘๖	ซังข้าวโพด	๑,๑๗๐	๐.๖๗๐	๗๘๔	๑๘.๐๔	๑๔,๑๔๒
มะพร้าว	๑,๔๐๐	เปลือก	๕๐๗	๐.๕๙๕	๓๐๒	๑๖.๒๓	๔,๘๙๔
	กะลา	๒๒๗	๐.๓๗๘	๘๕	๑๗.๙๓	๑,๕๑๘	
		ทะลาย	๖๙	๐.๘๔๓	๕๘	๑๕.๔๐	๘๙๑
		ทางมะพร้าว	๓๑๕	๐.๘๐๙	๒๕๕	๑๖.๐๐	๓,๐๗๗
ถั่วเหลือง	๓๑๙	ลำต้น,ใบ, เปลือก	๘๔๙	๐.๗๖๐	๖๔๖	๑๙.๔๔	๑๒,๕๕๑
ข้าวฟ่าง	๑๔๒	ใบ,ต้น	๑๗๘	๐.๖๔๘	๑๑๕	๙.๒๓	๒,๒๑๕
ฝ้าย	๓๖	ลำต้น	๑๑๖	๑.๐๐๐	๑๑๖	๑๔.๔๙	๑,๖๘๖
ถั่วลิสง	๑๓๘	เปลือก	๔๕	๑.๐๐๐	๔๕	๑๒.๖๖	๕๖๔
รวม							๖๐๔,๘๒๒

ที่มา : กรมพัฒนาและส่งเสริมพลังงาน"

ตารางที่ ๒ ศักยภาพการผลิตแก๊สชีวภาพจากมูลสัตว์ พ.ศ. ๒๕๔๓

ชนิดสัตว์	จำนวน (ตัว)	ปริมาณมูลสัตว์ (กก./ตัว/วัน)	อัตราส่วนมูลที่เก็บได้	อัตราส่วนของแข็งระเหย (ร้อยละ)	อัตราส่วนแก๊สชีวภาพที่ผลิตได้ (ลบ.ม./กก. ของแข็งระเหย)	ปริมาณแก๊สชีวภาพ (10^6 ลบ.ม./ปี)	ศักยภาพพลังงาน ($*10^6$MJ)
สุกร	๗,๗๖๑,๐๕๖	๒.๐	๐.๘	๒๔.๘๔	๐.๒๑๗	๑๓๔.๖๗	๒,๘๒๘
โคเนื้อ	๔,๙๐๐,๖๑๔	๕.๐	๐.๕	๑๓.๓๗	๐.๓๐๗	๑๘๓.๕๕	๓,๘๕๕
โคนม	๓๐๗,๙๒๗	๑๕	๐.๘	๑๓.๓๗	๐.๓๐๗	๕๕.๓๖	๑,๑๖๓
กระบือ	๑,๗๐๒,๒๒๓	๘.๐	๐.๕	๑๓.๖๔	๐.๒๘๖	๙๖.๙๕	๒,๐๓๖
ไก่	๑๗๒,๒๔๗,๕๖๑	๐.๐๓	๐.๘	๒๒.๓๔	๐.๒๔๒	๘๑.๕๗	๑,๗๑๓
เป็ด	๒๗,๘๘๔,๐๔๑	๐.๐๓	๐.๔	๑๗.๔๔	๐.๓๑๐	๖.๖๐	๑๓๙
ช้าง	๒,๑๗๘	๔๐	๐.๕	๒๑.๖๑	๐.๒๔๑	๐.๘๓	๑๗
รวม						๕๕๙.๕๔	๑๑,๗๕๐

ที่มา : กรมพัฒนาและส่งเสริมพลังงาน[๓]

และไบโอดีเซลยังมีค่าซีเทนสูงกว่าน้ำมันดีเซลอีกด้วย กล้าณรงค์ ศรีรอดและคณะ[๖] ได้ศึกษาพื้นที่ที่เหมาะสมและพื้นที่ปลูกจริงของปาล์มน้ำมัน พบว่าสามารถขยายพื้นที่เพาะปลูกได้อีก ๑๑,๙๙๓,๒๑๔ ไร่ ต้นทุนการผลิตไบโอดีเซลอยู่ในช่วง ๘.๐๐-๑๙.๕๐ บาทต่อลิตร ขึ้นกับราคาวัตถุดิบ ต้นทุนสำหรับกระบวนการ transesterification อยู่ในช่วง ๒.๕๐- ๓.๐๐ บาทต่อลิตร[๖]

สำหรับเอทานอลสามารถผลิตได้จากผลผลิตทางเกษตรและวัสดุเหลือใช้ทางการเกษตร[๗] ได้แก่ วัตถุดิบประเภทแป้ง เช่น มันสำปะหลัง วัตถุดิบประเภทน้ำตาล เช่น อ้อย กากน้ำตาล และเศษวัสดุที่เป็นเซลลูโลส เช่น ฟางข้าว ขี้เลื่อย ฯลฯ สำหรับประเทศไทยวัตถุดิบที่เหมาะสมและสามารถนำมาผลิตเอทานอล ได้แก่ มันสำปะหลัง กากน้ำตาล และอ้อย พื้นที่เพาะปลูกมันสำปะหลังของประเทศไทยประมาณ ๖.๕ ล้านไร่ จะผลิตมันสำปะหลังได้ ๒๐ ล้านตันต่อปี (เมื่อคิดที่ปริมาณผลผลิต ๓ ตันต่อไร่) หัวมันสำปะหลังได้นำมาใช้ในภาคอุตสาหกรรมผลิตแป้งมันสำปะหลังประมาณ ๘ ล้านตันต่อปี ผลิตมันเส้น/มันอัดเม็ดอีกประมาณ ๘ ล้านตันต่อปี จะทำให้มีหัวมันสำปะหลังเหลืออยู่ประมาณ ๔ ล้านตันต่อปี สามารถนำไปผลิตเป็นเอทานอลได้ ๑.๘๓ ล้านลิตรต่อวัน[๖] การใช้มันสำปะหลังควรใช้ในรูปของมันเส้นเพราะสามารถแปรรูปได้ง่าย และสามารถเก็บไว้ใช้ได้ตลอดปี ต้นทุนการผลิตเอทานอลจากมันสดอยู่ในช่วง ๑๑.๙ - ๑๔.๓ บาทต่อลิตร (ที่ราคามันสำปะหลังอยู่ในช่วง ๑,๐๐๐ - ๑,๔๐๐ บาท/ตัน) และจากมันเส้น ๑๑.๕๕-๑๒.๕๕ บาทต่อลิตร[๖]

ตารางที่ ๓ ศักยภาพการผลิตแก๊สชีวภาพจากน้ำเสียอุตสาหกรรม พ.ศ. ๒๕๔๓

ประเภทอุตสาหกรรม	หน่วย	ผลผลิต (หน่วย/ปี)	น้ำเสีย/ผลผลิต (ลบ.ม./ตัน)	ปริมาณน้ำเสีย (ลบ.ม./ปี)	แก๊สชีวภาพ (ลบ.ม./ปี)	ศักยภาพพลังงาน ($*10^6$ MJ)
โรงฆ่าสัตว์	ตัน	๒๒๕,๘๔๖	๗๔.๕๔	๑๖,๘๓๔,๕๖๑	๑๕,๓๙๐,๐๕๕	๓๖๙
โรงงานน้ำตาล	ตัน	๖,๔๔๗,๐๐๐	๑๑.๘๒	๗๖,๒๐๓,๕๔๐	๘๙,๓๗๑,๕๑๒	๒,๑๔๕
โรงงานสุรา	ลิตร	๗๕,๓๘๐,๐๐๐	๓.๔๐	๒๕๖,๒๙๒	๒,๕๙๓,๖๗๕	๖๒
โรงงานเบียร์	ลิตร	๑,๑๖๕,๐๐๐,๐๐๐	๔.๑๒	๔,๗๙๙,๘๐๐	๕,๕๔๖,๓๗๑	๑๐๙
โรงงานน้ำนมดิบ	ตัน	๔๙๑,๓๗๐	๔.๐๕	๑,๙๙๐,๐๔๙	๑,๐๑๔,๗๒๕	๒๔
โรงงานสับปะรดกระป๋อง	ตัน	๓๙๑,๒๘๒	๔.๙๘	๑,๙๕๘,๕๘๔	๑๒,๘๔๙,๗๔๕	๓๐๘
โรงงานอาหารทะเลแช่แข็ง	ตัน	๔๙๕,๑๗๔	๓๑.๑๔	๑๕,๔๑๙,๗๑๘	๑๖,๐๓๖,๕๐๗	๓๘๕
โรงงานอาหารทะเลกระป๋อง	ตัน	๕๕๘,๒๙๗	๓๑.๑๔	๑๗,๓๘๕,๓๖๙	๔๗,๒๙๕,๑๕๗	๑,๑๓๕
โรงงานน้ำอัดลม	ตัน	๑,๓๘๑,๐๐๐	๙.๓๐	๑๒,๘๔๓,๓๐๐	๑๒,๒๔๗,๓๗๑	๒๙๔
โรงงานแป้งมัน	ตัน	๒,๒๒๕,๑๒๕	๒๔.๗๒	๕๕,๐๐๕,๐๙๐	๑๖๖,๒๖๙,๓๘๖	๓,๙๙๐
โรงงานน้ำมันปาล์ม	ตัน	๓,๒๕๖,๐๐๐	๑.๐๐	๓,๒๕๖,๐๐๐	๖๗,๗๒๔,๘๐๐	๑,๖๒๕
รวม					๔๓๕,๓๒๙,๕๐๒	๑๐,๔๔๖

ที่มา : กรมพัฒนาและส่งเสริมพลังงาน[๗]

(ที่ราคามันสำปะหลังเส้นอยู่ในช่วง ๒,๕๐๐-๒,๙๐๐ บาท/ตัน)[๘] ปัจจุบันสามารถใช้เทคโนโลยีการผลิตเอทานอลโดยวิธี Simultaneous Saccharification and Fermentation (SSF) สามารถลดต้นทุนการผลิตเอทานอลลงได้ร้อยละ ๒๕ ในส่วนของต้นทุนการหมักปรกติ

ตารางที่ ๔ ศักยภาพการผลิตแก๊สชีวภาพจากขยะที่ได้จากการฝังกลบ พ.ศ. ๒๕๔๓

ภูมิภาค	ปริมาณขยะ (ตัน/ปี)	สัดส่วนขยะที่ฝังกลบ (ร้อยละ)	ปริมาณขยะที่ฝังกลบ (ตัน/ปี)	ปริมาณแก๊สชีวภาพจากการฝังกลบ (*10^6ลบ.ม.)	พลังงานจากแก๊สชีวภาพจากการฝังกลบ (*10^6 MJ)
กรุงเทพและปริมณฑล	๓,๓๓๒,๔๕๐	๘๕	๒,๘๓๒,๕๘๓	๒๘๓.๒๖	๕,๕๒๓.๓๙
เขตเทศบาลและเมืองพัทยา					
-ภาคกลางและตะวันออก	๑,๘๖๘,๘๐๐	๘๕	๑,๕๘๘,๔๘๐	๑๕๘.๘๕	๓,๐๙๗.๕๙
-ภาคเหนือ	๗๓๗,๖๖๕	๘๕	๖๒๗,๐๑๕	๖๒.๗๐	๑,๒๒๒.๖๘
-ภาคตะวันออกเฉียงเหนือ	๙๘๙,๑๕๐	๘๕	๘๔๐,๗๗๘	๘๔.๐๘	๑,๖๓๙.๕๒
-ภาคใต้	๗๐๕,๙๑๐	๘๕	๖๐๐,๐๒๔	๖๐.๐๐	๑,๑๗๐.๐๕
นอกเขตเทศบาล	๖,๒๙๘,๐๗๕	๘๕	๕,๓๕๓,๓๖๔	๕๓๕.๓๔	๑๐,๔๓๙.๐๖
รวม	๑๓,๙๓๒,๐๕๐		๑๑,๘๔๒,๓๖๔	๑,๑๘๔	๒๓,๐๙๒.๓๗

ที่มา : กรมพัฒนาและส่งเสริมพลังงาน[๓]

ตารางที่ ๕ พื้นที่และผลผลิตของพืชน้ำมันที่สำคัญของไทย ปีเพาะปลูก ๒๕๔๔/๒๕๔๕

พืชน้ำมัน	พื้นที่เพาะปลูก (*พันไร่)	ผลผลิต (พันตัน)	ผลผลิต/ไร่ (กก./ไร่)
ปาล์มน้ำมัน	๑,๔๕๗	๔,๐๘๙	๒,๘๐๗
มะพร้าว	๒,๐๓๗	๑,๓๙๖	๖๘๕
ถั่วเหลือง	๑,๓๒๔	๒๙๒	๒๒๗
ถั่วลิสง	๕๒๑	๑๒๙	๒๔๒
งา	๓๙๔	๓๙	๙๙
ละหุ่ง	๘๔	๙	๑๐๗

ที่มา : สำนักงานเศรษฐกิจการเกษตร[๔]

การใช้อ้อยเป็นวัตถุดิบในการผลิตเอทานอลนั้นไม่เหมาะสม เนื่องจากปริมาณอ้อยไม่เพียงพอต่อความต้องการของอุตสาหกรรมน้ำตาล กากน้ำตาลเป็นผลพลอยได้จากการผลิตน้ำตาล ในการผลิตน้ำตาลจากอ้อยประมาณ ๕๐ ล้านตันต่อปี จะได้กากน้ำตาลประมาณร้อยละ ๕ หรือประมาณ ๒.๕ ล้านตันต่อปี กากน้ำตาลนำไปใช้ในอุตสาหกรรมอาหารภายในประเทศประมาณ ๑.๕ ล้านตัน และส่งออกประมาณ ๑ ล้านตัน เนื่องจากราคาการส่งออกของกากน้ำตาลต่ำกว่าราคาของเอทานอลมาก การนำกากน้ำตาลในส่วนของการส่งออกมาเพิ่มมูลค่าโดยการผลิตเป็นเอทานอล ถ้าสามารถส่งออกเอทานอลแทนกากน้ำตาลได้จะเป็นการเพิ่มรายได้ให้แก่ประเทศ โดยกากน้ำตาล ๑ ล้านตัน จะสามารถนำมาผลิตเอทานอลได้ประมาณ ๘๐๐,๐๐๐ ลิตรต่อวัน ต้นทุนการผลิตเอทธานอลจากกากน้ำตาลอยู่ในช่วง ๑๑.๓ - ๑๕.๓ บาทต่อลิตร[๖] (ที่ราคากากน้ำตาลอยู่ในช่วง ๑,๕๐๐ - ๒,๕๐๐ บาทต่อตัน)

สถานภาพการใช้พลังงานมวลชีวภาพของประเทศไทย

ในพ.ศ. ๒๕๔๕ ประเทศไทยได้จัดหามวลชีวภาพมาใช้ในพลังงานขั้นต้นรวมทั้งสิ้น ๔๕,๑๖๗ พันตัน หรือเท่ากับ ๑๓,๘๒๑ พันตันเทียบเท่าน้ำมันดิบ[๖] คิดเป็นร้อยละ ๑๖.๑ ของการจัดหาพลังงานขั้นต้นทั้งหมดของประเทศ ซึ่งส่วนใหญ่ผลิตได้ภายในประเทศ รวมทั้งสิ้น ๑๓,๘๑๔ พันตันเทียบเท่าน้ำมันดิบ[๖] ได้แก่ ไม้ฟืนร้อยละ ๗๐.๙ ที่เหลือเป็นชานอ้อย และแกลบ คิดเป็นสัดส่วนร้อยละ ๒๐.๒ และ ๘.๘ ตามลำดับ ประมาณร้อยละ ๖๕ ของไม้ฟืนนำไปใช้ในการแปรรูปเป็นถ่านไม้[๖] มีการนำเข้าถ่านไม้เล็กน้อยรวมทั้งสิ้น ๑๐ พันตันเทียบเท่าน้ำมันดิบ[๖] คิดเป็นมูลค่าประมาณ ๓๔ ล้านบาท และมีการส่งออกถ่านไม้รวมทั้งสิ้น ๓ พันตันเทียบเท่าน้ำมันดิบ[๖] คิดเป็นมูลค่า ๖๙,๘๐๒ ล้านบาท รัฐบาลได้สนับสนุนให้มีการใช้มวลชีวภาพเป็นเชื้อเพลิงในการผลิตไฟฟ้า โดยรับซื้อไฟฟ้าจากผู้ผลิตรายเล็กและเล็กมากที่ใช้พลังงานนอกรูปแบบเป็นเชื้อเพลิง ใน พ.ศ. ๒๕๔๕ มีการใช้แกลบ ชานอ้อยและไม้ฟืนและวัสดุเหลือทิ้งทางการเกษตรอื่น ๆ เป็นเชื้อเพลิงในการผลิตไฟฟ้ารวมทั้งสิ้น ๒,๒๔๘ พันตัน[๗] ซึ่งส่วนใหญ่ผลิตจากโรงงานน้ำตาลประมาณร้อยละ ๗๕ นอกจากนี้ ยังมีการใช้แบล็กลิเคอร์และแก๊สเหลือใช้จากกระบวนการผลิตอีกประมาณ ๒,๓๑๘ x ๑๐[๑๖] จูล[๗] มาใช้เป็นเชื้อเพลิงในการผลิตไฟฟ้าซึ่งส่วนใหญ่ผลิตจากโรงงานกระดาษประมาณร้อยละ ๗๕ ที่เหลือผลิตจากโรงงานผลิตเม็ดพลาสติก

สำหรับการใช้มวลชีวภาพในพลังงานขั้นสุดท้ายในสาขาเศรษฐกิจต่าง ๆ รวมทั้งสิ้น ๙,๐๔๓ พันตันเทียบเท่าน้ำมันดิบ[๖] ได้แก่ ไม้ (ร้อยละ ๓๗.๐) ถ่านไม้ (ร้อยละ ๒๕.๔) ชานอ้อย (ร้อยละ ๒๗.๖) และแกลบ (ร้อยละ ๙.๙) ซึ่งใช้ในครัวเรือนประมาณร้อยละ ๕๕.๗ ส่วนใหญ่ใช้ไม้และถ่านไม้ ส่วนที่เหลืออีกร้อยละ ๔๔.๓ ใช้ในภาคอุตสาหกรรม ซึ่งส่วนใหญ่ใช้ชานอ้อยและแกลบ

ไบโอดีเซล ปัจจุบันยังมีปริมาณวัตถุดิบไม่เพียงพอที่จะนำมาผลิตไบโอดีเซล ในพ.ศ. ๒๕๔๓ ประเทศไทยสามารถผลิตน้ำมันปาล์มดิบภายในประเทศได้ทั้งหมด ๕๙๗,๒๘๑ ตัน ในขณะที่มีความต้องการใช้ในอุตสาหกรรมต้องการถึง ๕๗๖,๘๕๘ ตัน[๙] ซึ่งเกือบทั้งหมดถูกใช้ไปเพื่อการบริโภค

เอทานอล จากความเป็นไปได้ของการผลิตเอทานอลในเชิงพาณิชย์ รัฐบาลจึงมีนโยบายในการสนับสนุนส่งเสริมการผลิตเอทานอลจากพืชเป็นเชื้อเพลิง ส่งผลให้มีการจัดตั้งโรงงานผลิตเอทานอลเพื่อเป็นเชื้อเพลิงแล้วจำนวน ๘ ราย มีกำลังการผลิตรวม ๑,๕๐๒,๐๐๐ ลิตรต่อวัน[๑๐]

แก๊สชีวภาพ ในพ.ศ.๒๕๔๖ ประเทศไทยมีระบบผลิตแก๊สชีวภาพรวมทั้งสิ้น ๑๒๒,๘๕๔ ลบ.ม จากการเลี้ยงสัตว์มีทั้งประเภทครัวเรือนและเพื่อการค้า ส่วนน้ำเสียในโรงงานอุตสาหกรรมจากข้อมูลของกรมพัฒนาพลังงานทดแทนและอนุรักษ์พลังงานสามารถผลิตแก๊สชีวภาพได้ประมาณ ๖๑,๓๒๐ ลบ.ม. ต่อวัน[๑๑] ที่ค่าความร้อนของแก๊สชีวภาพจากน้ำเสียมีค่าเท่ากับ ๒๔ เมกะจูลต่อลบ.ม. จะได้เป็นพลังงานรวมประมาณ ๑,๔๗๑,๖๘๐ เมกะจูลต่อวัน

สถานภาพงานวิจัยด้านพลังงานมวลชีวภาพของประเทศไทย

งานวิจัยด้านเชื้อเพลิงมวลชีวภาพได้มีการปรับปรุงเตาเผาไหม้มวลชีวภาพเพื่อให้มีประสิทธิภาพสูงขึ้น เช่น เตา

ถ่านไม้[๖] เตาเผาแกลบแบบไซโคลน[๗] เตาฟลูอิไดซ์เบด[๘] เนื่องจากมวลชีวภาพเป็นเชื้อเพลิงแข็งจึงได้มีการวิจัยเพื่อเปลี่ยนให้เป็นเชื้อเพลิงแก๊สก่อนที่จะมีการเผาไหม้เพื่อให้ใช้ประโยชน์ได้กว้างมากขึ้น[๙] สำหรับการนำมวลชีวภาพเป็นเชื้อเพลิงในการผลิตไฟฟ้าได้มีงานวิจัยที่ประเมินศักยภาพด้านเทคนิคและเศรษฐศาสตร์ของการใช้ระบบผลิตไฟฟ้าและความร้อนร่วมของโรงงานสกัดน้ำมันปาล์ม[๖] โรงสีข้าว[๗] โรงงานน้ำตาล[๘] โรงงานไม้ยางพารา[๙] ถ้าพบว่าเดิมโรงงานบางแห่งได้มีการผลิตกำลังงานจากมวลชีวภาพอยู่แล้วแต่ใช้ไอน้ำที่ความดันไม่สูงมากนักก็จะพิจารณาปรับปรุงระบบให้ใช้ไอน้ำที่ความดันสูงขึ้นเพื่อจะผลิตกำลังงาน/ไฟฟ้าได้มากขึ้น นอกจากนี้ ยังมีงานวิจัยเพื่อนำความร้อนจากการเผาไหม้ไปใช้ประโยชน์ เช่น การอบแห้งข้าวเปลือก[๑๐]

งานวิจัยด้านไบโอดีเซล มีการวิจัยด้านกระบวนการผลิตไบโอดีเซลจากน้ำมันพืชชนิดต่าง ๆ เช่น น้ำมันปาล์ม[๑๑] น้ำมันพืชใช้แล้ว[๑๒] พบว่าไบโอดีเซลมีสมบัติสามารถใช้กับเครื่องยนต์ดีเซลได้ และมีงานวิจัยที่ทดสอบการใช้งานน้ำมันไบโอดีเซลกับเครื่องยนต์เพื่อดูสมรรถนะและปัญหาต่าง ๆ ที่อาจจะเกิดได้ นอกจากนี้ มีการทดลองนำน้ำมันดีเซลไปผสมกับน้ำมันพืชชนิดต่าง ๆ โดยตรงในสัดส่วนต่าง ๆ [๑๓, ๑๔] แล้วไปทดสอบเดินเครื่องยนต์ พบว่าปริมาณควันดำขึ้นอยู่กับสัดส่วนน้ำมันพืชที่ผสม อย่างไรก็ดี การทดสอบกับเครื่องยนต์ส่วนใหญ่เป็นการทดสอบระยะสั้น

งานวิจัยด้านเอทานอล มีการวิจัยหาแนวทางลดต้นทุนในกระบวนการผลิตในการกลั่นโดยใช้พลังงานแสงอาทิตย์มาเสริม[๑๕] และการหมัก[๑๖] การประเมินความเป็นไปได้ในการผลิตเอทานอลจากผลผลิตทางเกษตร[๑๗, ๑๘] และนำเอทานอลไปใช้เป็นเชื้อเพลิงในเครื่องยนต์แก๊สโซลีนเพื่อทดสอบสมรรถนะและการสึกหรอของเครื่องยนต์ นอกจากนี้ ยังมีงานวิจัยด้านบูรณาการกระบวนการผลิตเอทานอลกับโรงน้ำตาล และโรงงานแป้งมันสำปะหลัง[๑๙] สามารถลดต้นทุนค่าขนส่งวัตถุดิบ ส่วนการบูรณาการด้านพลังงานสามารถลดต้นทุนด้านพลังงานได้

งานวิจัยด้านแก๊สชีวภาพ ได้มีการวิจัยระบบผลิตแก๊สชีวภาพจากมูลสัตว์ และน้ำเสียจากอุตสาหกรรมทั้งระบบเดี่ยว ๆ ของแต่ละแห่ง และระบบบำบัดรวมขนาดใหญ่[๒๐, ๒๑] รวมถึงการใช้ประโยชน์จากแก๊สชีวภาพ และการวิเคราะห์ความคุ้มค่าทางการเงินของการลงทุน

แนวทางวิจัยพลังงานมวลชีวภาพของประเทศไทย

ปัญหาโดยทั่วไปของการใช้มวลชีวภาพ คือ แหล่งมวลชีวภาพที่นำมาใช้ได้มีไม่สม่ำเสมอ เปลี่ยนแปลงตามฤดูกาล โดยเฉพาะจากอุตสาหกรรมเกษตร โดยส่วนใหญ่มวลชีวภาพแต่ละชนิดจะปลูกและมีผลผลิตตามฤดูกาล และยังขึ้นอยู่กับสภาพอากาศ นอกจากนี้ ยังขึ้นอยู่กับราคา และความต้องการของตลาดซึ่งส่งผลให้เกษตรกรเปลี่ยนชนิดของพืชที่เพาะปลูก และการเปลี่ยนแปลงพื้นที่การเกษตรไปใช้ประโยชน์ด้านอื่นอีกด้วย เนื่องจากมวลชีวภาพมีอยู่อย่างกระจัดกระจาย ทำให้รวบรวมได้ยาก และมีปริมาตรมากทำให้ค่าขนส่งสูง ดังนั้น การพัฒนาเพื่อนำมวลชีวภาพที่ยังไม่ได้ใช้มาผลิตพลังงานได้เพิ่มขึ้น จึงควรมีการวิจัยด้านการจัดการมวลชีวภาพที่ใช้เป็นวัตถุดิบ เช่น การจัดหารวบรวม และจัดเก็บ เพื่อสามารถนำมาผลิตพลังงานได้ต่อเนื่องไม่ขาดช่วง และมีต้นทุนวัตถุดิบต่ำ นอกจากนี้ ควรมีการวิจัยเชิงนโยบายหามาตรการส่งเสริมเพื่อจูงใจให้มีการใช้มวลชีวภาพเป็นพลังงานทดแทนมากขึ้น

ในการใช้มวลชีวภาพเป็นเชื้อเพลิง ควรทำการวิจัยเพื่อเพิ่มประสิทธิภาพเตาหรือห้องเผาไหม้มวลชีวภาพด้วย และควรใช้กับเชื้อเพลิงมวลชีวภาพได้หลาย ๆ ประเภท เนื่องจากเตาเผามวลชีวภาพแต่ละเตาจะออกแบบมาเพื่อใช้กับมวลชีวภาพแต่ละชนิด ดังนั้นถ้ามวลชีวภาพชนิดดังกล่าวมีปริมาณไม่เพียงพอจำเป็นต้องพึ่งพามวลชีวภาพประเภทอื่น ก็จะทำให้ได้ประสิทธิภาพในการเผาไหม้ต่ำ นอกจากนี้ ควรมีการศึกษาการเผาไหม้มวลชีวภาพร่วมกับเชื้อเพลิงเชิงพาณิชย์บางชนิด เช่น ถ่านหิน เพื่อหาแนวทางเสริมการให้ใช้เชื้อเพลิงมวลชีวภาพทดแทนถึงแม้จะมีเชื้อเพลิงมวลชีวภาพไม่เพียงพออย่างต่อเนื่องตลอดช่วงความต้องการใช้งานและควรมีการศึกษาความเป็นไปได้ของการ ผลิตไฟฟ้าจากเชื้อเพลิงมวลชีวภาพอื่นที่ยังไม่ได้นำมาใช้ให้มากขึ้น

สำหรับไบโอดีเซล จากการศึกษาพบว่า ปาล์มน้ำมันมีศักยภาพมากที่สุดประเทศไทยถึงแม้จะมีพื้นที่ที่เหมาะสมในการปลูกปาล์มน้ำมันหลายพื้นที่ แต่มีข้อจำกัดบางประการทำให้ไม่ได้ใช้พื้นที่เหล่านั้นในการเพาะปลูก และเมื่อเปรียบเทียบกับต่างประเทศ ประเทศไทยยังมีผลผลิตต่อไร่ต่ำ ทำให้ต้นทุนการผลิตมีค่าสูง เนื่องจากการจัดการหลังการเก็บเกี่ยวยังไม่ดีพอจึงทำให้คุณภาพปาล์มน้ำมันที่สกัดได้ยังไม่ดีเท่าที่ควร ดังนั้น ควรมีงานวิจัยด้านการเกษตรเพื่อใช้พื้นที่ในการเพาะปลูกที่เหมาะสม การคัดเลือกและปรับปรุงพันธุ์ปาล์ม เพื่อหาวิธีขยายพันธุ์ที่ดี การถ่ายทอดเทคโนโลยีสู่ชาวไร่ เทคโนโลยีการเก็บเกี่ยวและหลังการเก็บเกี่ยวเพื่อควบคุมคุณภาพของปาล์มน้ำมัน ทั้งหมดนี้เพื่อเพิ่มผลผลิตต่อไร่ให้มีค่าสูงขึ้น ลดต้นทุนของวัตถุดิบ และให้ได้ผลผลิตที่มีคุณภาพ นอกจากนี้ ควรมีการศึกษาวิจัยเพื่อลดค่าใช้จ่ายในกระบวน การผลิตไบโอดีเซล เนื่องจากไบโอดีเซลที่ผลิตมาจากวัตถุดิบหลายชนิดที่มีคุณภาพและต้นทุนการผลิตแตกต่างกัน จึงควรมีการศึกษาเพื่อกำหนดมาตรฐานคุณภาพของไบโอดีเซล และควรมีการศึกษาผลระยะยาวของเครื่องยนต์ที่ใช้ไบโอดีเซลเป็นเชื้อเพลิง

การวิจัยด้านเอทานอล จากการศึกษาข้อมูลพบว่าวัตถุดิบที่เหมาะสมจะนำมาผลิตเอทานอล ได้แก่ มันสำปะหลัง และกากน้ำตาล เพราะไม่มีผลกระทบต่อการบริโภค สำหรับมันสำปะหลังควรศึกษาวิธีการวางแผนการกำหนด พื้นที่เพาะปลูกเพื่อให้เก็บเกี่ยวผลผลิตได้อย่างต่อเนื่อง และควรมีการวิจัยเพื่อกำหนดมาตรฐานอัตราส่วนผสมระหว่างเอทานอลกับน้ำมันเบนซิน และควรมีการศึกษาผลระยะยาวเครื่องยนต์ที่ใช้น้ำมันเบนซินผสมนี้ด้วย

สำหรับแก๊สชีวภาพ ยังมีโรงงานและฟาร์มเป็นจำนวนมากที่มีศักยภาพแต่ยังไม่มีระบบการผลิตแก๊สชีวภาพ จึงควรมีงานวิจัยด้านการศึกษาความเป็นไปได้ของการผลิตและประยุกต์ใช้แก๊สชีวภาพในรูปแบบต่าง ๆ เพื่อให้ได้รูปแบบ ขนาดระบบ และการนำไปใช้ประโยชน์ได้อย่างเหมาะสม ในฟาร์มเลี้ยงสัตว์บางแห่งยังพบว่ามีปัญหาในด้านความเสียหายของอุปกรณ์ที่ใช้เนื่องจากเกิดการกัดกร่อนที่เกิดจากไฮโดรเจนซัลไฟด์ (H_2S) เมื่อรวมกับน้ำจะเป็นกรดซัลฟิวริกมีฤทธิ์กัดกร่อนโลหะได้ ซึ่งขึ้นอยู่กับองค์ประกอบทางเคมีของแก๊สชีวภาพที่ได้จากมูลสัตว์หรือน้ำเสียจากโรงงานอุตสาหกรรม จึงควรมีแนวทางวิจัยของระบบกำจัดแก๊สไฮโดรเจนซัลไฟด์ในแก๊สชีวภาพด้วย

สรุป

การศึกษาศักยภาพของแหล่งพลังงานมวลชีวภาพ สถานภาพของการใช้และงานวิจัยที่ผ่านมาเพื่อเสนอแนวทางวิจัยเพื่อพัฒนาการผลิต และใช้พลังงานจากมวลชีวภาพให้มากขึ้น มวลชีวภาพที่ศึกษามี ๕ รูปแบบ ได้แก่ เชื้อเพลิงมวลชีวภาพ ไบโอดีเซล เอ-ทานอล และแก๊สชีวภาพ พบว่ายังมีแหล่งมวลชีวภาพอีกมากที่ยังไม่ได้นำมาใช้เป็นเชื้อเพลิง และข้อจำกัดโดยทั่วไปของการใช้มวลชีวภาพ คือ แหล่งวัตถุดิบที่นำมาใช้มีปริมาณเปลี่ยนแปลงตามฤดูกาล เก็บรวมยาก และมีต้นทุนสูง ดังนั้นเพื่อลดข้อจำกัดของแหล่งพลังงานมวลชีวภาพ ควรมีแนวทาง วิจัยด้านการจัดการแหล่งวัตถุดิบ และการลดต้นทุนวัตถุดิบที่นำมาใช้ผลิตพลังงาน การเพิ่มประสิทธิภาพการเปลี่ยนรูปพลังงานมวลชีวภาพ รวมทั้งหาแนวทางเพิ่มการใช้มวลชีวภาพที่ยังไม่มีการพัฒนานำมาใช้มาผลิตพลังงาน เช่น ซังข้าวโพด ฟางข้าว ทะลายปาล์มเปล่า ด้านเอทานอลและไบโอดีเซล ควรมีงานวิจัยด้านการศึกษาสมรรถนะและผลกระทบระยะยาวของเครื่องยนต์ และการกำหนดมาตรฐานคุณภาพของเชื้อเพลิง สำหรับแก๊สชีวภาพควรมีงานวิจัยในการศึกษาการใช้ประโยชน์ และศึกษาความเป็นไปได้ของเทคโนโลยีที่เหมาะสมสำหรับการผลิตและใช้ประโยชน์จากแก๊สชีวภาพ

กิตติกรรมประกาศ

ผู้เขียนใคร่ขอบคุณสำนักงานกองทุนสนับสนุนการวิจัยที่ให้การสนับสนุนทุนวิจัย

เอกสารอ้างอิง

๑. คณะทำงานวารสารนโยบายพลังงาน, สถานการณ์พลังงานของไทยปี ๒๕๔๕, *วารสารนโยบายพลังงาน*, ๒๕๔๖, ฉบับที่ ๕๕, หน้า ๓๔-๕๐.

๒. รายงานพลังงานของประเทศไทยปี ๒๕๔๕, กรมพัฒนาพลังงานทดแทนและอนุรักษ์พลังงาน, กรุงเทพฯ, ๒๕๔๖.

๓. กรมพัฒนาพลังงานทดแทนและอนุรักษ์พลังงาน, *ศักยภาพพลังงานชีวมวล*, http://๒๐๓.๑๕๐.๒๔.๔/dede/renew/bio_p.htm, เมษายน ๒๕๔๗.

๔. สำนักงานเศรษฐกิจการเกษตร, สถิติการเกษตรของประเทศไทยปีเพาะปลูก พ.ศ. ๒๕๔๔-๒๕๔๕, http://oae.go.th/statistic/yearbook/๒๐๐๑-๐๒/, เมษายน ๒๕๔๗.

๕. สุรกิตติ ศรีกุล, สุนีย์ นิเทศพัตรพงศ์ และชาย โรจวิส., เอกสารประกอบการประชุมระดมความคิด เรื่อง แนวทางการวิจัยและพัฒนาไบโอดีเซลสู่เชิงพาณิชย์, สำนักงานคณะกรรมการวิจัยแห่งชาติ, ๒๕๔๔, หน้า B-1-B-18.

๖. กล้าฉรงค์ ศรีรอต , พูนศุข ประเสริฐสรรพ์ , สมพร อิศวิลานนท์ และเกื้อกูล ปิยะจอมขวัญ, *รายงานการวิจัยการศึกษาสถานภาพวัตถุดิบที่จะนำมาใช้ในอุตสาหกรรมการผลิตไบโอดีเซล*, สำนักงานคณะกรรมการวิจัยแห่งชาติ, กรุงเทพฯ, ๒๕๔๔, ๑๑๒ หน้า.

๗. คณะกรรมาธิการพลังงาน สภาผู้แทนราษฎร, วัตถุดิบสำหรับผลิตเอทานอล, พลังงานทดแทน เอทานอล และไบโอดีเซล, กรุงเทพฯ, ๒๕๔๕, หน้า ๑๓๗-๑๓๙.

๘. กล้าฉรงค์ ศรีรอต, เจริญศักดิ์ โรจนฤทธิ์พิเชษฐ์, เอ็ช ฮไรบล, พิพัฒน์ วีระถาวร และเกื้อกูล ปิยะจอมขวัญ, *รายงานการวิจัยการศึกษาสถานภาพวัตถุดิบที่จะนำมาใช้ในอุตสาหกรรมการผลิตแก๊สโซฮอล์*, สำนักงานคณะกรรมการวิจัยแห่งชาติ, กรุงเทพฯ, ๒๕๔๔, ๑๐๔ หน้า.

๙. รายงานไฟฟ้าของประเทศปี ๒๕๔๕, กรมพัฒนาพลังงานทดแทนและอนุรักษ์พลังงาน, กรุงเทพ, ๒๕๔๖.

๑๐. ธนาคารกรุงเทพ : Bangkok Bank, ความคืบหน้าการผลิตเอทานอลเป็นเชื้อเพลิง, เมษายน ๒๕๔๖, http://www.bangkokbank.com/download/speacial_Ethanol.pdf,๒๐๐๓.

๑๑. กรมพัฒนาพลังงานทดแทนและอนุรักษ์พลังงาน, สถานภาพการใช้พลังงานชีวมวล: น้ำเสียในโรงงานอุตสาหกรรม, มกราคม ๒๕๔๖, http://๒๐๓.๑๕๐.๒๔.๔/renew/status.asp.

๑๒. ภาณุวัฒน์ คล้ายวงศ์วาจย์, วิทยานิพนธ์ปริญญาวิทยาศาสตรมหาบัณฑิต, มหาวิทยาลัยเทคโนโลยีพระจอมเกล้าธนบุรี, กรุงเทพฯ, ๒๕๔๖.

๑๓. บุญเรือง ศรีสวัสดิ์, การปรับปรุงสมรรถนะเตาเผาแกลบ, วิทยานิพนธ์ปริญญาวิทยาศาสตรมหาบัณฑิต, *มหาวิทยาลัยเทคโนโลยีพระจอมเกล้าธนบุรี*, กรุงเทพฯ ๒๕๔๑.

๑๔. สุวิทย์ เตีย, ภัทวุฒิ พุกอมรพันธ์, พรเทพ จิควุฒิไกร, แสง แซ่เล้า และ ทนงค์ ฉายาวัฒนะ, "การเผาไหม้เชื้อเพลิงในเตาฟลูอิดไดซ์เบด", วารสารวิจัยและพัฒนา มจธ., ๒๕๔๒, ปีที่ ๒๒,ฉบับที่ ๒, หน้า ๔๗-๖๓.

๑๕. นิรมล ชุลีเฉิศวิทยาภรณ์ และคณะ, ๒๕๓๗, การหาสภาวะที่ผลิตก๊าซคาร์บอนมอนนอกไซด์ที่ดีที่สุดของเครื่องผลิตก๊าซชีวมวลแบบไหลขึ้นโดยวิธีการค้นหาแบบ Simplex, รายงานการประชุมทางวิชาการ คณะวิศวกรรมศาสตร์, มหาวิทยาลัยเทคโนโลยีพระจอมเกล้าธนบุรี, ๙-๑๑ พฤษภาคม ๒๕๓๗, หน้า๙๗.

๑๖. สุรศักดิ์ สุรนันท, การวิเคราะห์ระบบผลิตพลังงานร่วมในโรงงานปาล์มน้ำมัน, วิทยานิพนธ์ปริญญาวิศวกรรมศาสตรมหาบัณฑิต, *สถาบันเทคโนโลยีพระจอมเกล้าธนบุรี*, กรุงเทพฯ, ๒๕๓๕.

๑๗. วารุณี เตีย, สมชาติ โสภณรณฤทธิ์ และ ชุวดี เรืองเดช, "ศักยภาพการผลิตไฟฟ้าและความร้อนร่วมในโรงสีข้าวขาวของประเทศไทย", *วิศวกรรมสาร ฉบับวิจัยและพัฒนา*, ๒๕๔๕, ปีที่ ๑๑, ฉบับที่ ๒, หน้า ๕๐-๕๗.

๑๘. จิระพันธุ์ เนื่องจากนิล, บูรณาการระบบพลังงานความร้อนและไฟฟ้าในโรงงานน้ำตาล, วิทยานิพนธ์ปริญญาวิศวกรรมศาสตรมหาบัณฑิต, *มหาวิทยาลัยเทคโนโลยีพระจอมเกล้าธนบุรี*, กรุงเทพฯ, ๒๕๔๒.

๑๙. สุธีระ ประเสริฐสรรพ์, การจำลองโรงจักรผลิตพลังงานร่วมความร้อนและไฟฟ้าโดยชีวมวล, สำนักงานคณะกรรมการนโยบายแห่งชาติ, ๒๕๔๒, ๑๕๑ หน้า.

๒๐. เอกรินทร์ โบษกรนัฏ, สมชาติโสภณรณฤทธิ์, และ วารุณี เตีย, การอบแห้งข้าวนึ่งด้วยเครื่องอบแห้งฟลูอิดไดซ์เบด, รายงานการประชุมวิชาการสมาคมวิศวกรรมเกษตรแห่งประเทศไทย ครั้งที่ ๔, ๒๕๔๖, หน้า ๒๕๗-๓๐๕.

๒๑. กนกอร รจนากิจ , พงษ์ศักดิ์ คำมูล และ จินดา เจริญพรพาณิชย์, การทำไบโอดีเซลจากไขมันปาล์มบริสุทธิ์เป็นเชื้อเพลิงในเครื่องยนต์จุดระเบิดด้วยการอัด, รายงานการประชุมวิชาการเครือข่ายวิศวกรรมเครื่องกลแห่งประเทศไทย ครั้งที่ ๑๖, ๒๕๔๕, หน้า ๖๖-๗๑.

๒๒. วัชระ ถอยสนุทร, อุทารวิศว์ ครองยุทธ, สุรชัย ฝั่นแก้ว และ ศิริกุล จันทร์สว่าง, การปรับปรุงน้ำมันพืชใช้แล้วเป็นเชื้อเพลิงในเครื่องยนต์ดีเซล, RSU JET, ๒๕๔๒, ฉบับที่ ๓, เล่มที่ ๓, หน้า ๓๔-๓๗.

๒๓. สุพัฒน์ หวังวงศ์วัฒนา, "ผลกระทบของการใช้น้ำมันดีเซลผสมน้ำมันพืช ต่อเครื่องยนต์และมลพิษทางอากาศ", เอกสารประกอบการสัมมนาเรื่องแนวทางการวิจัยและพัฒนาไบโอดีเซลไปสู่เชิงพาณิชย์, สำนักงานคณะกรรมการวิจัยแห่งชาติ, ๒๕๔๔, หน้า F-๑-F-๗.

๒๔. อภิชิต เสมศรี, มณฑล ใจกุศล และ จินดา เจริญพรพาณิชย์, การใช้น้ำมันพืชผสมสำหรับเครื่องยนต์ดีเซลขนาดเล็กแบบฉีดตรงเข้าห้องเผาไหม้, รายงานการประชุมวิชาการเครือข่ายวิศวกรรมเครื่องกลแห่งประเทศไทย ครั้งที่ ๑๖, ๒๕๔๕, หน้า ๑๓๕-๑๔๓.

๒๕. ธีระพงษ์ ว่องรัตนไพศาล , ทนงเกียรติ เกียรติศิริโรจน์ และ ผัฐ วรยศ, เอกสารประกอบการสัมมนาเผยแพร่ผลงานวิจัยด้านพลังงานทดแทน เรื่อง การผลิตเอทานอลโดยใช้พลังงานแสงอาทิตย์ในรูปความร้อน, สำนักงานคณะกรรมการวิจัยแห่งชาติ, ๒๕๔๖, หน้า B-1-B-13.

๒๖. เจริญศักดิ์ โรจนฤทธิ์พิเชษฐ์, กล้าฉรงค์ ศรีรอต, สุวิทย์ เตีย, มณเฑียร นิติวรรัตน์, เกื้อกูล ปิยะจอมขวัญ , สุทธิพันธ์ แก้วสมพงษ์ และ สิทธิโชค วัลลภาทิตย์., เอกสารประกอบการสัมมนาเผยแพร่ผลงานวิจัยด้านพลังงานทดแทน เรื่อง โครงการศึกษาต้นแบบโรงงานเอทานอลโดยการพัฒนาเทคโนโลยีการผลิตจากมันเส้น, สำนักงานคณะกรรมการวิจัยแห่งชาติ, ๒๕๔๖, หน้า A-๑-A-๕

๒๗. สุวิทย์ เตีย, บุณยพัต สุภานิช และ สุทธิดา สาย, แบบสรุปผลการวิจัย เรื่อง โครงการประเมินความเป็นไปได้ของการผลิตเชื้อเพลิงเอทานอลจากผลผลิตทางการเกษตรของประเทศไทย, สำนักงานคณะกรรมการวิจัยแห่งชาติ, ๒๕๔๔, ๖ หน้า.

๒๘. สุวิทย์ เตีย, การสัมมนาเรื่องศักยภาพของประเทศไทยในการผลิตเอทานอลเพื่อทดแทนการนำเข้า, กลุ่มงานเกษตรและอุตสาหกรรมเกษตร, กองโครงการและประสานงานวิจัย สำนักงานคณะกรรมการวิจัยแห่งชาติ,๒๕๔๔, หน้า D-1 - D-19.

๒๙. บุญชพัคร สุภานิช , สุวิทย์ เตีย และปนัดดา ภูอากาศ, เอกสารประกอบการสัมมนาเผยแพร่ผลงานวิจัยด้านพลังงานทดแทน เรื่อง การบูรณาการกระบวนการผลิตเอทานอลกับโรงงานน้ำตาลและโรงงานแป้งมันสำปะหลัง และการประเมินเทคโนโลยีในการทำเอทานอลให้บริสุทธิ์, สำนักงานคณะกรรมการวิจัยแห่งชาติ, ๒๕๔๖, หน้า C-๑-C-๑๓

๓๐. อาณัติ มีป้อม, การศึกษาความเป็นไปได้ในการจัดตั้งระบบบำบัดน้ำเสียรวมเพื่อการผลิตก๊าซชีวภาพในจังหวัดนครปฐม ๑) ของเสียที่เกิดจากฟาร์มเลี้ยงสุกรและโรงงาน อุตสาหกรรมอาหารขนาดกลางและเล็ก, วิทยานิพนธ์ปริญญาโทวิทยาศาสตรมหาบัณฑิต, *มหาวิทยาลัยเทคโนโลยีพระจอมเกล้าธนบุรี*, กรุงเทพฯ, ๒๕๔๔.

๓๑. นันทนิตย์ ทัศน์เอี่ยม, การเปรียบเทียบการผลิตก๊าซชีวภาพจากน้ำบีบเปลือกสับปะรดในอังปฏิกรณ์แบบชั้นกรองระหว่างกระบวนการหมักแบบขั้นตอนเดียวและสองขั้นตอน, วิทยานิพนธ์ปริญญาวิทยาศาสตรมหาบัณฑิต, *มหาวิทยาลัยเทคโนโลยีพระจอมเกล้าธนบุรี*, กรุงเทพฯ, ๒๕๓๑.

Abstract **Status and Research Trends on Biomass Energy in Thailand**

Warunee Tia
Pimporn Jangploy
Kangsadan Sakunpongmalce
Somchart Soponronnarit

Biomass, which is a high potential renewable energy resource for Thailand, has been planned and set up the policy by the government to promote the biomass development and utilization. This paper presents the status and research trends on biomass. Four types of biomass applications, namely biomass fuel, bio-ethanol, bio-diesel and biogas, were studied. The common limitation of using biomass was their resources availability, which showed seasonal variation especially those from agro-industries. To extend the utilization of biomass the research management, system-efficiency improvement and cost reduction should be conducted. Additional research on the co-combustion system and project feasibility should be considered for power generation. For bio-ethanol and bio-diesel, the long-term performance of the engine and standard specification of bio-fuel should be studied. The study on appropriate technology and utilization should be carried out as well on biogas.

Key words : **biomass, renewable energy, research trend**

นิพนธ์ต้นฉบับ

เตาเผาไหม้วอร์เทค-ฟลูอิไดซ์เบดแบบสองห้องเผาไหม้สำหรับเชื้อเพลิงแกลบ

ฐานิตย์ เมธิยานนท์[1] นิวัติ พิริยะรุ่งโรจน์[2] และ สมชาติ โสภณรณฤทธิ์[3]

Abstract

Madhiyanon, T.[1], Piriyarungroj, N.[1] and Soponronnarit, S.[2]

A novel vortex-fluidized bed combustor with two combustion chambers for rice-husk fuel

Songklanakarin J. Sci. Technol., 2004, 26(6) : 875-893

A novel vortexing-fluidized bed combustor (VFBC) using rice-husk as fuel was developed and presented. The combined characteristics of vortex combustion and fluidized bed combustion are the main features of the VFBC, which was designed to achieve high thermal capacity (MW_{th} m^{-3}), high thermal efficiency and low diameter to height ratio. The VFBC comprises a vertical cylinder chamber and a conical base, which provides a bed for incompletely combusted fuel. The overall dimensions are 1.10 m in height and 0.40 m in diameter. To evaluate combustor performance, the specific feed rate of fuel and mass flow rates of the primary, secondary, and tertiary air were varied independently of one another. The combustion appeared into two zones characterized by different combustion behaviors, i.e. 1) vortext combustion above the vortex ring and 2) fluidized bed combustion below the vortex ring. The fluidized bed zone has uniform

[1]Department of Mechanical Engineering, Mahanakorn University, 51 Cheum-Sampan Road, Nong Chok, Bangkok 10530 Thailand. [2]School of Energy and Materials, King Mongkut's University of Technology Thonburi, 91 Prachauthit Road (Suksawad 48), Bangmod Thung Kharu District, Bangkok 10140 Thailand.

[1]Ph.D.(Energy Technology), [2]M.Sc.(Mechanical Engineering), ภาควิชาวิศวกรรมเครื่องกล คณะวิศวกรรมศาสตร์ มหาวิทยาลัยเทคโนโลยีมหานคร 51 ถนนเชื่อมสัมพันธ์ เขตหนองจอก กรุงเทพฯ 10530 [3]Ph.D.(Production and Processing of Vegetable Raw Materials), ศาสตราจารย์, คณะพลังงานและวัสดุ มหาวิทยาลัยเทคโนโลยีพระจอมเกล้าธนบุรี 91 ถ.ประชาอุทิศ แขวงบางมด เขตทุ่งครุ กรุงเทพฯ 10400

Corresponding e-mail: thanid_m@yahoo.com

รับต้นฉบับ 6 กุมภาพันธ์ 2547 รับลงพิมพ์ 27 มิถุนายน 2547

temperature distributions across the cross-section of the combustor. The swirling of air above the vortex ring and the vortex ring itself played important roles in preventing the escape of combustion particulates. Bottom ash appeared as fine black and grey particles of ash, which ranged in size from 200 to 600 μm. Fluidization could be initiated without the assistance of any inert material mixed into the bed. The experimental results indicated that thermal efficiency did not depend on the secondary or tertiary airflows, but was significantly influenced by the excess air resulting from the combined total of the three airflows. The introduction of the tertiary airflow helped maintaining the temperature inside the combustor within acceptable levels. According to experimental conditions, i.e. a specific feed rate of 240 kg $h^{-1}m^{-3}$ and excess air (157%), it was found that the VFBC could achieve an exit gas temperature of 1060°C, thermal efficiency of 95%, and thermal capacity of 0.91 MW_{th} m^{-3}. The amounts of CO_2, CO, and O_2 gases emitted were directly related to thermal efficiency, and the amounts of CO and NO_x were 50 and 380 ppm, respectively.

Key words : biomass, combustor, cyclone, fluidization, solid fuel, vortex ring

บทคัดย่อ

ฐานิดย์ เมธิยานนท์ นิวัติ พิริยะรุ่งโรจน์ และ สมชาติ โสภณรณฤทธิ์

เตาเผาไหม้วอร์เทค-ฟลูอิไดซ์เบดแบบสองห้องเผาไหม้สำหรับเชื้อเพลิงแกลบ

ว. สงขลานครินทร์ วทท. 2547 26(6) : 875-893

ในงานวิจัยนี้ได้มีการพัฒนาเตาเผาไหม้วอร์เทค-ฟลูอิไดซ์เบด (Vortexing-Fluidized bed Combustor, VFBC) ที่ใช้แกลบเป็นเชื้อเพลิงโดยออกแบบให้มีการร่วมลักษณะเด่นของการเผาไหม้แบบวอร์เทคและฟลูอิไดซ์เบดไว้ด้วยกัน โดยมีจุดประสงค์เพื่อต้องการเตาเผาไหม้แบบใหม่ที่ให้ค่าพิกัดความร้อน (MW_{th} m^{-3}) และประสิทธิภาพเชิงความร้อนสูง แต่ในขณะเดียวกันมีค่าสัดส่วนความสูงต่อเส้นผ่านศูนย์กลางต่ำ เตาเผาที่ใช้ในการทดลองมีเส้นผ่านศูนย์กลางภายในและความสูงเท่ากับ 0.4 และ 1.10 เมตร ตามลำดับ และมีฐานเป็นรูปกรวยสำหรับรองรับอนุภาคที่ยังเผาไหม้ไม่หมด ในการทดสอบสมรรถนะของเตาได้มีการแปรเปลี่ยนอัตราการป้อนเชื้อเพลิงจำเพาะและอัตราการไหลของอากาศส่วนที่หนึ่ง สอง และสาม ในแต่ละการทดลอง จากผลการทดลองพบว่าภายในเตาเผาไหม้จะถูกแบ่งออกเป็นห้องเผาไหม้สองส่วนตามลักษณะการเผาไหม้คือ 1) บริเวณที่อยู่เหนือวงแหวนวอร์เทคขึ้นไปซึ่งมีลักษณะการเผาไหม้แบบวอร์เทค และ 2) บริเวณห้องเผาไหม้ที่อยู่ด้านล่างวงแหวนวอร์เทคลงมาเกิดการเผาไหม้แบบฟลูอิไดซ์เบด ซึ่งสอดคล้องกับผลของการกระจายอุณหภูมิภายในเตาที่มีการกระจายอุณหภูมิสม่ำเสมอตลอดทั้งหน้าตัดเตาในส่วนนี้ นอกจากนี้การหมุนวนของอากาศเหนือวงแหวนและตัววงแหวนเองมีส่วนสำคัญในการดักจับอนุภาคขนาดใหญ่ที่ยังเผาไหม้ไม่หมดไม่ให้หนีออกไปจากเตาทำให้เถ้าที่ออกมามีลักษณะละเอียดสีดำปนเทาโดยมีขนาดอยู่ในช่วง 200 ถึง 600 μm. การเกิดฟลูอิไดซ์เซชันภายในเตาไม่จำเป็นต้องผสมวัสดุเฉื่อยลงในเบด ประสิทธิภาพเชิงความร้อนไม่ขึ้นกับปริมาณอากาศส่วนที่สองหรือสาม แต่จะขึ้นกับปริมาณอากาศส่วนเกินทั้งหมดซึ่งเป็นผลมาจากปริมาณอากาศทั้งสามส่วน ผลของการจ่ายอากาศส่วนที่สามจะช่วยควบคุมอุณหภูมิภายในเตาไม่ให้สูงเกินไป จากการทดลองพบว่าที่อัตราการป้อนแกลบ 240 kg $h^{-1}m^{-3}$ ปริมาณอากาศส่วนเกิน 157% จะได้แก๊สร้อนตรงทางออกเตามีอุณหภูมิ 1,060°C ประสิทธิภาพเชิงความร้อน 95% และพิกัดความร้อนเตาที่ทำได้เท่ากับ 0.91 MW_{th} m^{-3} โดยปริมาณ CO_2, CO และ O_2 เป็นไปในแนวทางที่สอดคล้องกับค่าประสิทธิภาพเชิงความร้อนโดยปริมาณ CO และ NO_x ที่ปล่อยออกมาจากเตามีค่า 50 และ 380 ppm ตามลำดับ

เนื่องจากในแต่ละปี อุตสาหกรรมโรงสีข้าว อุตสาหกรรมแปรรูปอาหารสัตว์ มีความต้องการพลังงานความร้อนไปใช้ในกระบวนการผลิตเป็นจำนวนมาก เช่น ใช้ในการอบแห้ง ผลิตไอน้ำ เป็นต้น ซึ่งทำให้มีค่าใช้จ่ายในการดำเนินการสูงและประเทศต้องนำเข้าน้ำมันจากต่างประเทศเข้ามาปีละจำนวนมาก จึงได้มีผู้ประกอบการหลาย

รายภายในประเทศผลิตเตาเผาไหม้ที่ใช้เชื้อเพลิงจากชีวมวล เช่น แกลบ ซังข้าวโพด เป็นต้น เพื่อใช้กับอุตสาหกรรม ดังกล่าวโดยเตาที่ผลิตขึ้นภายในประเทศ ได้แก่ เตาเผาไหม้แบบปล่องควันและตะแกรงเอียง และเตาเผาไหม้ไซโคลน ซึ่งในกรณีเตาเผาไหม้ไซโคลน (Gupta *et al.*, 1984) มีการเผาไหม้จะใช้หลักการของการไหลวนหรือการไหลแบบวอร์เทคได้เป็นที่รู้จักกันแพร่หลายมาหลายทศวรรษแล้ว ซึ่งนอกจากทำหน้าที่ผลิตความร้อนแล้วยังทำหน้าที่ดักเถ้าไม่ให้หลุดลอยออกไปพร้อมกับแก๊สเผาไหม้ด้วย ต่อมาได้มีการนำมาประยุกต์ใช้กับเชื้อเพลิงชีวมวล เช่น แกลบ (Singh *et al.*, 1980; Soponronnarit *et al.*, 2000 and Tumambig, 1984) สำหรับเตาเผาไหม้ฟลูอิไดซ์เบดก็ได้มีการพัฒนามานานแล้วเช่นกัน ส่วนใหญ่จะใช้กับเชื้อเพลิงถ่านหินเพื่อผลิตกระแสไฟฟ้าแต่ก็มีการนำมาประยุกต์ใช้กับเชื้อเพลิงชีวมวลเช่นกัน (Armesto *et al.*, 2002; Natarajan *et al.*, 1998 and Werther *et al.*, 2000) แต่เนื่องจากเชื้อเพลิงชีวมวลส่วนใหญ่จะมีรูปร่างที่ไม่เป็นทรงกลมและมีความหนาแน่นต่ำ เช่น แกลบ ขี้เลื่อย เป็นต้น ทำให้ยากต่อการทำให้เกิดฟลูอิไดซ์เซชัน จึงมีความจำเป็นต้องผสมวัสดุเฉื่อยที่ไม่ทำปฏิกิริยาออกซิเดชันจำพวกทรายซิลิกา อลูมินา ผสมลงในเบดในอัตราส่วนที่เหมาะสม (Natarajan *et al.*, 1998 and Rao *et al.*, 2000) อย่างไรก็ตาม การผสมวัสดุเฉื่อยเหล่านี้ลงไปจะทำให้ความดันตกคร่อมห้องเผาไหม้มีค่าสูงมากจำเป็นต้องใช้พัดลมที่มีขนาดใหญ่ทำให้สิ้นเปลืองพลังงานไฟฟ้าในส่วนนี้สูง และเมื่อประมาณ 10 กว่าปีมานี้ได้มีการพัฒนาเตาเผาไหม้ฟลูอิไดซ์เบดซึ่งใช้กับถ่านหินบดและเป็นเตาชนิดที่ป้อนเชื้อเพลิงเข้าทางด้านล่างของเบด (Nieh *et al.*, 1992; Yang *et al.*, 1987 and Yang *et al.*, 1989) และได้มีการพัฒนาขึ้นโดยมีการเพิ่มอากาศส่วนที่สอง ซึ่งถูกฉีดเข้าไปในแนวสัมผัสในบริเวณ free board โดยจะทำให้เกิดการหมุนวนของแก๊สเผาไหม้และอนุภาคขึ้นในบริเวณ free board การฉีดอากาศส่วนที่สองสามารถทำได้ที่ระดับความสูงต่างๆ ของตัวเตา ผลของการเกิดวอร์เทคจากการฉีดอากาศเข้าไปในแนวสัมผัสนี้จะทำให้สามารถดักอนุภาคที่ยังเผาไหม้ไม่หมดไม่ให้หลุดลอยออกไปจากเตาและยังทำให้เกิดการหมุนเวียนของอนุภาคเชื้อเพลิง ระหว่างบริเวณเบดด้านล่างกับบริเวณที่เกิดวอร์เทคใน free board ส่งผลให้สามารถลดความสูงของเตาฟลูอิไดซ์เบดลงได้ งานวิจัยเหล่านี้ (Nieh *et al.*, 1992; Yang *et al.*, 1987 and Yang *et al.*, 1989) คล้ายคลึงกับ U.S. Patent no. 4,867,079 (Sang *et al.*) ดังที่ได้กล่าวมาแล้ว ซึ่งเตาเผาไหม้ฟลูอิไดซ์เบดที่ใช้เชื้อเพลิงชีวมวลในประเทศไทยยังไม่มีการผลิตขายแต่ในต่างประเทศได้มีการทำวิจัยในห้องปฏิบัติการ พบว่ามีจุดเด่นที่น่าสนใจอยู่หลายประการ ซึ่งสามารถนำข้อมูลมาเปรียบเทียบกับเตาเผาไหม้ไซโคลนได้ดังแสดงใน Table 1 และเมื่อไม่นานมานี้ได้มีการศึกษาพฤติกรรมการไหลของแก๊ส-อนุภาค ภายในเตาเผาไหม้วอร์เทคพบว่าบริเวณใกล้ผนังเตาอากาศที่จะมีการไหลในทิศทางลง (สู่ด้านล่างเตา) ซึ่งจะทำให้เกิดการหมุนเวียนของอนุภาคภายในเตา และมีส่วนสำคัญให้ residence time นานขึ้น (Nieh *et al.*, 2000)

ขั้นตอนการออกแบบเตาเผาเตาเผาไหม้วอร์เทค-ฟลูอิไดซ์-เบด (Vortex-Fluidized Bed Combustor, VFBC)

จากผลการศึกษาพฤติกรรมของอากาศ-แกลบภายใน

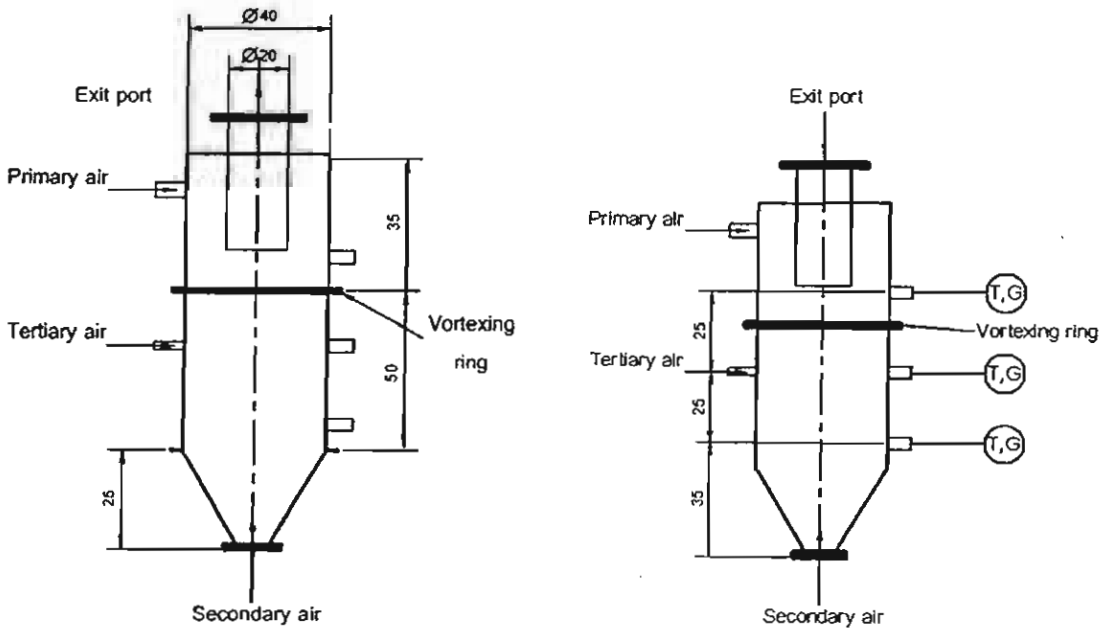
Table 1. Comparative characteristic of cyclone and the fluidized bed combustor (Natarajan, *et al.*, 1998 and Soponronnarit *et al.*, 2000)

Fluidized bed Combustor	Cyclone Combustor
1. Thermal capacity approximately 1 MW/m^3	1. Thermal capacity approximately 0.34 MW/m^3
2. Height to inside diameter (H/D, approximately 13	2. Height to inside diameter (H/D) approximately 2.5
3. Thermal efficiency 80-95%	3. Thermal efficiency 60-80%
4. Need insert materials such as silica or alumina mixed into the bed	4. No need inert materials
5. Ash is conveyed from combustor through exhaust pipe	5. Require mechanical transportation for ash conveying

เตาเผาไหม้จำลอง (Madhiyanon *et al*, 2003(a) and Madhiyanon *et al.*, 2003(b)) แสดงให้เห็นถึงแนวโน้มที่สามารถจะนำหลักการดังกล่าวไปใช้กับเตาเผาไหม้วอร์เทค-ฟลูอิไดซ์เบด (Vortexing-fluidized bed combustion, VFBC) จริงได้จึงได้นำข้อมูลจากการศึกษาในข้างต้นมาใช้เป็นแนวทางในการออกแบบเตาเผา VFBC ในระดับห้องปฏิบัติการ ซึ่งเตาเผา VFBC เป็นเตาเผาที่ถูกออกแบบมาเพื่อรวมเอาลักษณะเด่นของเตาเผาแบบไซโคลนและเตาเผาแบบฟลูอิไดซ์เบดเข้าด้วยกันโดยเตาเผา VFBC มีขนาดของเส้นผ่านศูนย์กลางภายในเตาเผาเท่ากับ 40 ซม. สูง 110 ซม. ดังแสดงใน Figure 1a และสามารถแบ่งเตาเผาออกเป็น 2 ส่วน ส่วนที่หนึ่งรูปร่างของเตาเผาแบบทรงกระบอก และส่วนที่สองรูปร่างของเตาเผาแบบทรงกรวยหงายโดยบริเวณปลายกรวยถูกตัดเพื่อติดตั้งแผ่นกระจายอากาศ (Air Distributor) สำหรับอากาศส่วนที่สอง ซึ่งอากาศที่ถูกใช้ในการเผาไหม้แกลบภายในเตาเผา VFBC สามารถแบ่งออกได้เป็น 3 ส่วน ดังแสดงใน Figure 1b คือ อากาศส่วนที่หนึ่ง (primary air) คือ อากาศที่นำแกลบเข้าสู่เตาเผาซึ่งจะถูกป้อนในแนวสัมผัสทางด้านบนของห้องเผาไหม้แบบทรงกระบอก เพื่อทำให้เกิดการหมุนวนของอากาศและแกลบแบบวอร์เทค อากาศส่วนที่สอง (secondary air) จะถูกจ่ายผ่านแผ่นกระจายลมเข้าสู่เตาเผา VFBC ที่บริเวณด้านล่างของห้องเผาไหม้ที่มีลักษณะเป็นทรงกรวยหงายทำให้เกิดพฤติกรรมแบบฟลูอิไดซ์เบดทั่วในบริเวณของห้องเผาไหม้ที่อยู่ถัดจากวงแหวนวอร์เทคลงมา โดยรูปร่างของเตาเผาแบบทรงกรวยหงายจะช่วยทำให้แกลบลอยตัวได้ง่ายและอนุภาคในเบดมีการหมุนเวียนทั่วถึงโดยไม่ต้องใช้วัสดุเฉื่อยมาผสมลงในเบด และอากาศส่วนที่สาม (tertiary air) จะเป็นอากาศที่ถูกจ่ายในแนวสัมผัสที่ตำแหน่งด้านข้างเตาเผาแบบทรงกระบอกในระดับความสูงเท่ากับ 60 ซม. เพื่อลดอุณหภูมิในห้องเตาเผา

วิธีการทดลอง

แบ่งออกเป็น 2 ส่วนหลักๆ คือ



(a) Dimensions of VFBC

(b) Temperature (T) and combustion gas component (G) measure positions

Figure1. Dimensions and Temperature measure positions of VFBC. (unit : cm.)

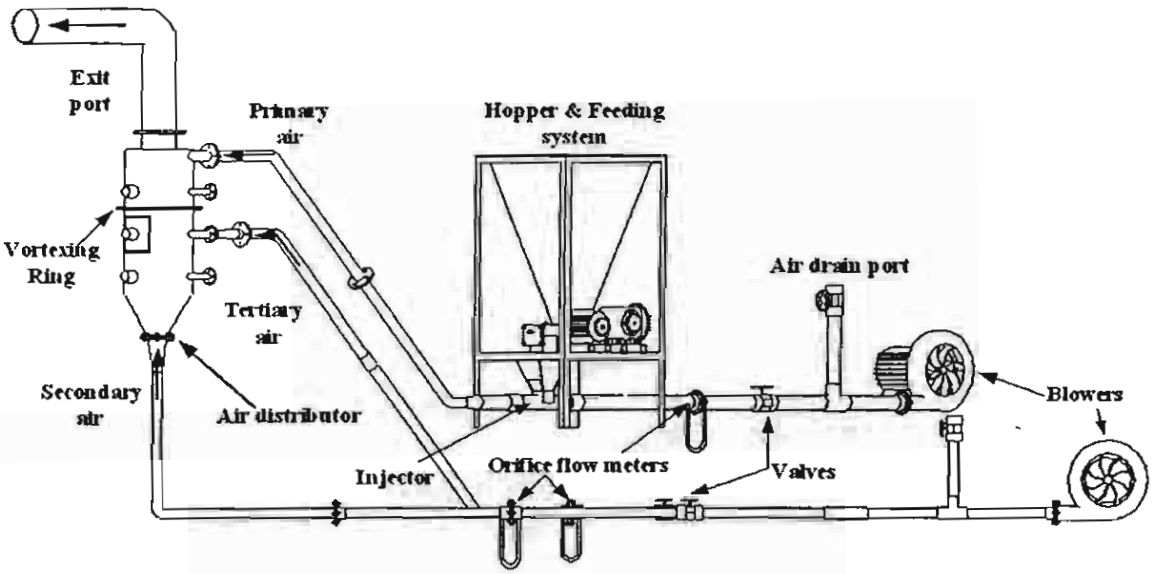


Figure 2. Schematic diagram of the overall experimental set-up of VFBC.

1. การทดลองเบื้องต้นเพื่อให้รู้ถึงเงื่อนไขการทำงานของเตาเผา VFBC

เตรียมอุปกรณ์การทดลองดังแสดงใน Figure 2 ทำการติดเตาเผาโดยใช้แกลบเป็นเชื้อเพลิงและอุ่นเตาจนอุณหภูมิภายในห้องเผาไหม้ประมาณ 600°C จึงเริ่มทำการทดลอง

1. ปรับอัตราการไหลของอากาศและแกลบให้สอดคล้องกับเงื่อนการทดลองที่ 1-6 ใน Table 2 ในการทดลอง

Table 2. The operating conditions of VFBC

	Run No.	Specific Rice husk feed rate (kg/h-m³)	Primary air Flow rate (m³/min)	Primary air Velocity (m/s)	Secondary air Flow rate (m³/min)	Secondary air Velocity (m/s)	Tertiary air Flow rate (m³/min)	Tertiary air Velocity (m/s)	Excess air (%)
The preliminary study of VFBC operation condition	1	160	2.75	22.7	0.97	2	-	-	288
	2	187	2.75	22.7	0.97	2	-	-	233
	3	213	2.75	22.7	0.97	2	-	-	192
	4	240	2.2	18.2	0.97	2	-	-	117
	5	240	2.33	19.2	0.97	2	-	-	125
	6	240	2.75	22.7	0.97	2	-	-	157
The study of the effects of tertiary airflow on performance of VFBC	7	240	2.06	17	0.85	1.75	-	-	108
	8	240	2.06	17	0.85	1.75	0.37	12.3	133
	9	240	2.06	17	0.85	1.75	0.76	25.0	157
	10	240	2.06	17	0.85	1.75	1.12	37.0	182
The study of the effects of secondary airflow on performance of VFBC	11	240	2.06	17	0.66	1.35	0.75	25.0	145
	12	240	2.06	17	0.93	1.92	0.75	25.0	163
	13	240	2.06	17	1.22	2.5	0.75	25.0	182

จะใช้พัดลมอัดอากาศ 2 ตัว ตัวละ 2.2 kW ในการวัดอัตราการไหลของอากาศใช้ออริฟิสมิเตอร์ซึ่งถูกปรับเทียบจาก Hot wire anemometer ที่มีค่าความคลาดเคลื่อน 3% ของค่าที่วัดได้ และสามารถควบคุมอัตราการป้อนของแกลบโดยใช้อินเวอเตอร์ในการควบคุมความเร็วรอบของมอร์เตอร์ป้อนแกลบ

2. เริ่มบันทึกอุณหภูมิที่ตำแหน่งท่อทางออกเตาเผา VFBC ทุก 5 นาที จนครบ 120 นาที โดยใช้ Thermo-couple type K และใช้ตัวชี้บอก ซึ่งมีความละเอียด ±1℃

2. การศึกษาผลของอากาศส่วนที่สองและสามต่อสมรรถนะของ VFBC

(อุปกรณ์การทดลองเป็นชุดเดียวกับชุดศึกษาการทดลองเบื้องต้น เพื่อให้รู้ถึงเงื่อนไขการทำงานของเตาเผา VFBC)

1. การปรับอัตราการไหลของแกลบและอากาศให้สอดคล้องกับเงื่อนที่การทดลองที่ 7-13 ใน Table 2

2. เริ่มบันทึกอุณหภูมิที่ตำแหน่ง Y = 0.35 เมตร โดยอ้างอิงตำแหน่งความสูงจากแผ่นกระจายลม (Air distributor) ที่ตำแหน่ง r/R = 0.05, 0.1, 0.15, 0.2, 0.25, 0.3, 0.35, 0.4, 0.45, 0.5, 0.55, 0.6, 0.65, 0.7, 0.75, 0.8, 0.85, 0.9, 0.95 และ 1.0 หลังจากนั้นทำการเก็บขี้เถ้าที่ได้จากการเผาไหม้ (เมื่อ r คือ ตำแหน่งที่วัดอุณหภูมิในแนวรัศมีของเตาเผาไหม้ VFBC และ R คือ รัศมีของเตาเผาไหม้ VFBC ซึ่งเท่ากับ 20 ซม.)

3. บันทึกอุณหภูมิที่ตำแหน่งทางออกและตรวจวัดองค์ประกอบของแก๊สที่เกิดจากการเผาไหม้โดยใช้เครื่อง Gas analyzer รุ่น Testo 350 XL

4. ทำการทดลองซ้ำข้อ 2-3 โดยบันทึกอุณหภูมิที่ตำแหน่ง Y = 0.60 เมตร และ 0.85 เมตร ตามลำดับ

ประสิทธิภาพเชิงความร้อน (η_{th}) ของเตานิยามได้ด้วยสมการดังนี้

$$\eta_{th} = \frac{\dot{m}_a (c_{p,g} T_e - c_{p,a} T_i)}{\dot{m}_f HHV} \qquad (1)$$

เมื่อ

$\dot{m}_a$ = อัตราการไหลของอากาศ, kg/s

$\dot{m}_f$ = อัตราการป้อนเชื้อเพลิงแกลบ, kg/s

$c_{p,g}, c_{p,a}$ = ค่าความจุความร้อนของแก๊สเสียและอากาศที่เข้าเผาไหม้

HHV = ค่าความร้อนสูงของแกลบ 14.5 MJ/kg

T_e = อุณหภูมิแก๊สเสียที่ตำแหน่งทางออกของ VFBC

T_i = อุณหภูมิอากาศที่ตำแหน่งทางเข้าของ VFBC

โดยกำหนดให้ $c_{p,g}$ ที่ตำแหน่งทางออกเท่ากับ $c_{p,a}$ ที่มีอุณหภูมิแก๊สเสีย

สมการที่ (1) อยู่บนสมมติฐานที่ว่า $\dot{m}_f << \dot{m}_a$ ดังนั้นมวลของแก๊สเสียจึงประมาณเท่ากับมวลของอากาศที่เข้าเผาไหม้

ผลการทดลอง

เนื่องจากงานวิจัยนี้เป็นงานวิจัยเบื้องต้น ดังนั้นเพื่อให้รู้ถึงเงื่อนไขการทำงานที่เหมาะสมของเตาเผา VFBC จึงได้กำหนดเงื่อนไขทดลองออกเป็น 6 เงื่อนไขโดยเปลี่ยนอัตราการไหลของแกลบและอากาศต่างๆ กันดังแสดงใน Table 2 เงื่อนการทดลองที่ 1-6

1. การทดลองเบื้องต้นเพื่อให้รู้ถึงเงื่อนไขการทำงานของเตาเผา VFBC

จากผลการทดลองสามารถสรุปในประเด็นสำคัญได้ดังนี้

1.1 จากการสังเกตการเผาไหม้ผ่านช่องมองของเตาเผา VFBC พบว่าการเกิดฟลูอิไดซ์เซชันจะครอบคลุมบริเวณตั้งแต่ด้านล่างของเตาเผา VFBC จนถึงบริเวณที่เป็นที่ตั้งของวงแหวนวอร์เทค (Vortexing ring) ทุกเงื่อนไขการทดลองดังแสดงใน Table 2 ซึ่งการเกิดฟลูอิไดซ์เซชันของแก๊สเผาไหม้กับอนุภาคภายในของเตาเผาจะสอดคล้องกับการเกิดฟลูอิไดเซชันของอากาศ-แกลบในกรณีเตาเผาไหม้จำลอง (Madhiyanon *et al.*, 2003(a) and Madhiyanon *et al.*, 2003(b))

1.2 การเกิดฟลูอิไดซ์เซชันภายในเตาเผา VFBC ไม่จำเป็นต้องผสมวัสดุเฉื่อยจำพวกทรายซิลิกาหรืออลูมินาลงในเบดเหมือนเช่นในเตาเผาไหม้ฟลูอิไดซ์เบดโดยทั่วไป

1.3 เตาเผา VFBC สามารถทำอัตราการป้อนเชื้อเพลิงจำเพาะ (Specific rice husk feed rate = SFR) ได้ 240 kg/h/m³ ที่ปริมาณอากาศส่วนเกิน 157% เมื่อคำนวณเป็นค่าพิกัดความร้อนของเตา (โดยกำหนดให้ HHV ของแกลบ = 14.5 MJ/kg) ที่ η_{th} เท่ากับ 95% จะมีพิกัดความร้อนเท่ากับ 0.91 MW_{th}/m^3 ซึ่งความจริงอาจสามารถป้อนเชื้อเพลิงด้วยอัตราที่มากกว่านี้ได้ ถ้าเพิ่มปริมาณอากาศส่วนเกินให้มากขึ้นโดยการจ่ายอากาศส่วนที่สามเข้าไปในเตา จากการทดลองจะได้ว่า SFR ที่เตาเผา VFBC ทำได้มีค่าใกล้เคียงกับของเตาเผาไหม้ฟลูอิไดซ์เบดสำหรับเชื้อเพลิงชีวมวลซึ่ง SFR มีค่าประมาณ 265 kg/h/m³ (Natarajan *et al.*, 1998) และสูงกว่าที่เตาเผาไหม้ไซโคลนที่ผลิตขายอยู่ภายในประเทศทำได้ ซึ่ง SFR มีค่าสูงสุดประมาณ 110 kg/h/m³ สำหรับในงานวิจัยนี้เนื่องจากมีข้อจำกัดของพัดลมอัดอากาศที่ใช้ในการทดลองจึงได้กำหนดอัตราการป้อนเชื้อเพลิงไว้สูงสุดเท่ากับ 240 kg/h/m³

1.4 ประสิทธิภาพเชิงความร้อนของเตา (η_{th}) ในกรณีที่ค่า SFR เท่ากับ 240 kg/h/m³ เมื่อใช้ปริมาณอากาศส่วนเกินเท่ากับ 157% ดังแสดงใน Figure 3 (เส้นกราฟ F) พบว่าค่า η_{th} จะเพิ่มขึ้นไปตามเวลาที่เตาทำงานโดยจะเริ่มคงที่เมื่อเวลาผ่านไปประมาณ 90 นาที (และเป็นจริงสำหรับในกรณีอื่นๆ ด้วย) โดย η_{th} จะมีค่าประมาณ 95% ซึ่งเท่ากับในกรณีของเตาเผาไหม้ฟลูอิไดซ์เบดซึ่ง η_{th}

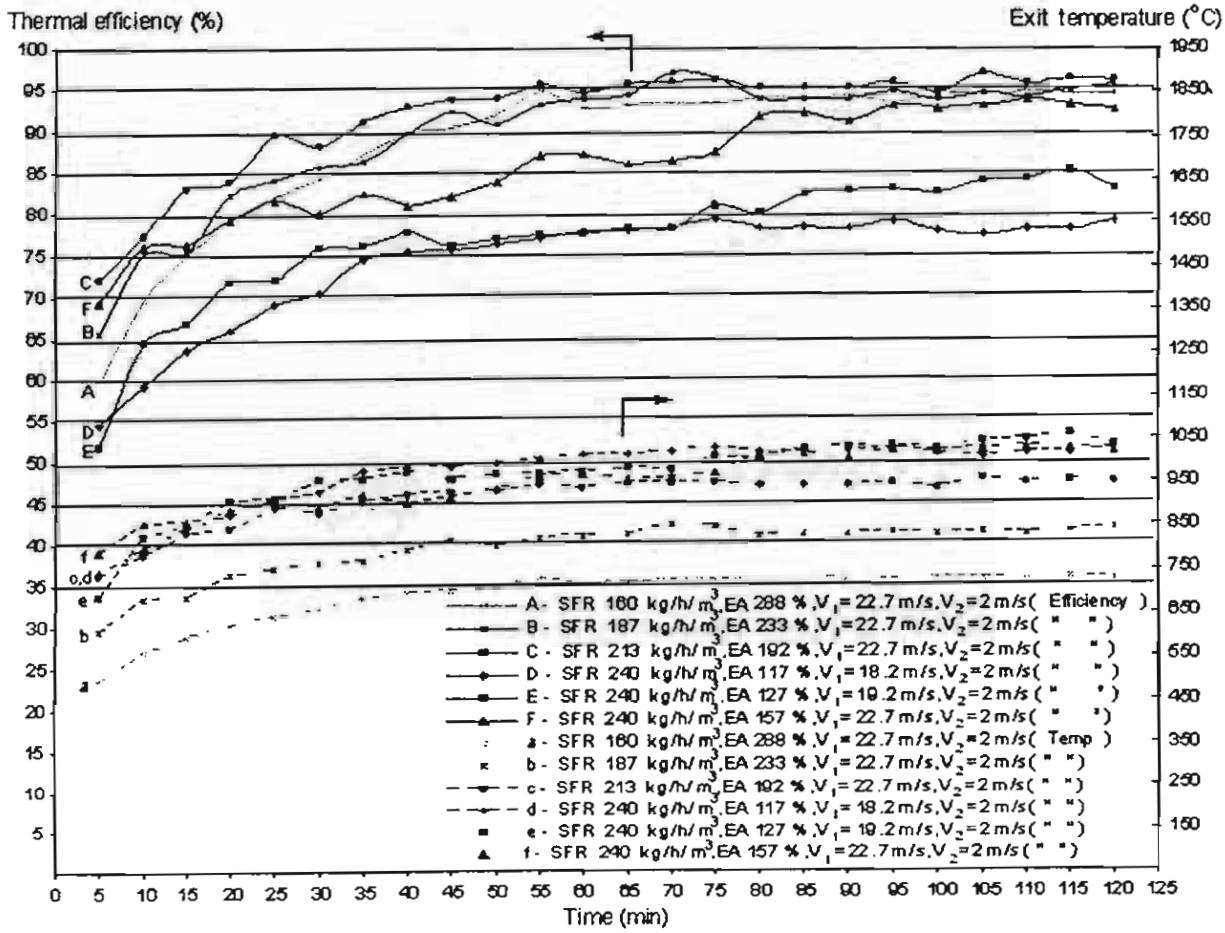
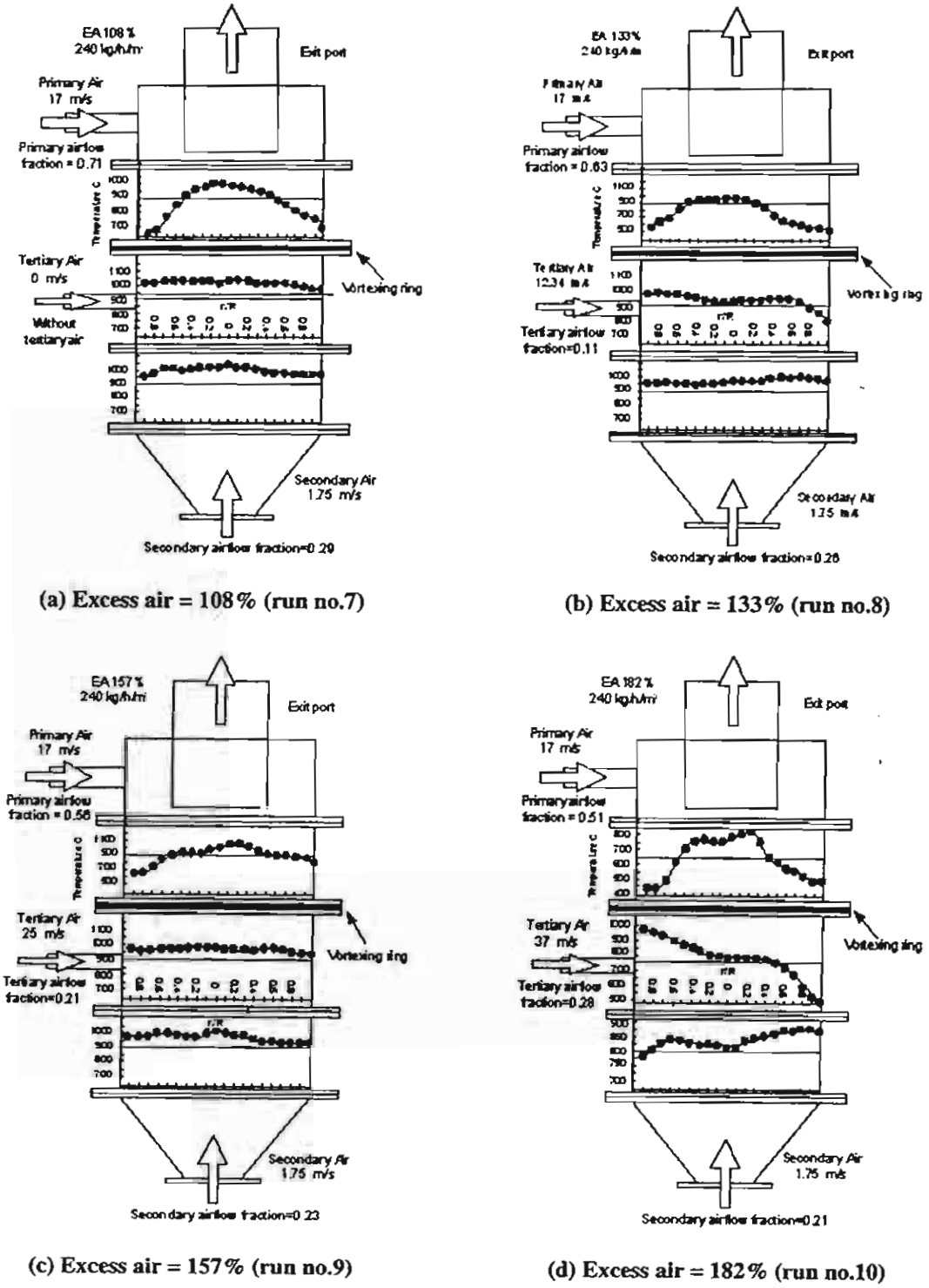


Figure 3. The variation of thermal efficiency of VFBC and exhaust gas temperature with a variety of specific rice husk feed rate(SFR) and primary air velocities (v_1). (Secondary air velocity (v_2)= 2 m/s; EA = Excess air)



(a) Excess air = 108% (run no.7)

(b) Excess air = 133% (run no.8)

(c) Excess air = 157% (run no.9)

(d) Excess air = 182% (run no.10)

Figure 4. Temperature distributions inside VFBC at distance of 0.35, 0.6 and 0.8 M. above air distributor according to run nos. 7-10

มีค่าในช่วง 90-95% และสูงกว่าของเตาไซโคลนมาก ซึ่ง η_{ig} มีค่าประมาณ 65-80%

1.5 อุณหภูมิแก๊สเผาไหม้ที่ทางออกของเตาจะเพิ่มขึ้นอย่างรวดเร็วในช่วงเวลา 30 นาทีแรกของการทดลอง และจากนั้นอัตราการเปลี่ยนแปลงอุณหภูมิก็จะเริ่มลดน้อยลงจนกระทั่งเข้าสู่สภาวะคงตัว โดยอุณหภูมิแก๊สเผาไหม้จะมีอุณหภูมิประมาณ 900°C ในเวลาเพียง 20 นาที และถึง 1,000°C ในเวลาประมาณ 80 นาที ดังแสดงใน Figure 3 (เส้นกราฟ f)

1.6 ในกรณีที่ค่า SFR 240 kg/h/m^3 ที่ปริมาณอากาศส่วนเกิน 157% ขี้เถ้าที่ออกจากเตาเผามีลักษณะเป็นเถ้าป่นขนาดประมาณ 200-600 μm. มีสีดำปนเทา ซึ่งแสดงให้เห็นถึงประสิทธิภาพในการเปลี่ยนคาร์บอนในเชื้อเพลิงไปเป็นแก๊สเผาไหม้ (carbon conversion efficiency) ได้ดี ซึ่งมีสาเหตุจากการหมุนวนแบบวอร์เทคที่รุนแรงในบริเวณห้องเผาไหม้ที่อยู่เหนือวงแหวนและตัววงแหวนเองทำหน้าที่ดักอนุภาคที่มีขนาดใหญ่ทำให้ไม่หลุดออกจากเตาเผา VFBC ได้ซึ่งสอดคล้องกับพฤติกรรมการเกิดม่านอากาศที่ใช้ดักอนุภาคภายในเตาเผาไหม้วอร์เทค-ฟลูอิไดซ์เบดแบบจำลอง (Madhiyanon *et al.*, 2003(a) and Madhiyanon *et al.*, 2003(b))

จากผลการทดลองข้างต้นจึงได้เลือกเงื่อนไขที่ทำให้เตาเผา VFBC ประสิทธิภาพเชิงความร้อนของเตาสูงสุด คือที่อัตราการป้อนเชื้อเพลิงจำเพาะสูงสุด (SFR) เท่ากับ 240 kg/h/m^3 ดังแสดงใน Figure 3 (เส้นกราฟ F) โดยใช้เป็นเงื่อนไขที่มีการใช้อากาศส่วนที่สาม

2. การศึกษาผลของปริมาณอากาศส่วนที่สามต่อสมรรถนะของ VFBC

2.1 การกระจายอุณหภูมิภายในเตาเผา VFBC

ในการทดลองนี้กำหนดอัตราการไหลของเชื้อเพลิงจำเพาะ 240 kg/h/m^3 และทำการเปลี่ยนอัตราการไหลของอากาศส่วนที่สามดังแสดงในเงื่อนไขการทดลองที่ 7-10 ใน Table 2 การกระจายอุณหภูมิภายใน VFBC สามารถแบ่งออกเป็นสองบริเวณคือ 1) บริเวณห้องเผาไหม้ที่อยู่เหนือวงแหวนวอร์เทค พบว่าการกระจายอุณหภูมิของทั้งสี่การทดลองดังแสดงใน Figure 4(a-d) กระจายอุณหภูมิที่คล้ายคลึงกันเป็นรูปพาราโบลาคว่ำ โดยบริเวณขอบผนังจะมีอุณหภูมิต่ำเนื่องจากใกล้ตำแหน่งที่จ่ายอากาศส่วนที่หนึ่งและส่วนบริเวณแกนกลางของเตาเผาจะมีอุณหภูมิสูงเนื่องจากเป็นบริเวณที่แก๊สร้อนที่ได้จากการเผาไหม้ไหลผ่านเพื่อเข้าสู่ท่อทิ้งเถ้าที่อยู่ด้านบนของเตาเผา 2) คือบริเวณห้องเผาไหม้ที่อยู่ต่ำกว่าวงแหวนวอร์เทค พบว่าที่ปริมาณอากาศส่วนเกินเท่ากับ 108, 133 และ 157% มีการกระจายอุณหภูมิของแก๊สเผาไหม้เกิดขึ้นอย่างความสม่ำเสมอตลอดพื้นที่หน้าตัดเตาที่ความสูงเท่ากับ 0.35 เมตร และ 0.60 เมตร ดังแสดงใน Figure 4(a-c) ซึ่งสะท้อนให้เห็นการเผาไหม้แบบฟลูอิไดซ์เบดขึ้นภายในเตาที่ระดับความสูงดังกล่าวโดยทั้งอากาศและอนุภาคมีการเคลื่อนที่แบบไม่มีทิศทางแน่นอน (Random movement) ซึ่งสอดคล้องกับพฤติกรรมการเคลื่อนที่ของอากาศภายในเตาเผาไหม้วอร์เทค-ฟลูอิไดซ์เบดในแบบจำลอง (Madhiyanon *et al.*, 2003(a) and Madhiyanon *et al.*, 2003 (b)) ส่งผลให้สามารถเผาไหม้เชื้อเพลิงที่อัตราการป้อนเชื้อเพลิงจำเพาะ (SFR) 240 kg/h/m^3 สำหรับที่ปริมาณอากาศส่วนเกิน 182% ดังแสดงใน Figure 4(d) อุณหภูมิบริเวณผนังจะต่ำกว่าที่บริเวณอื่นภายในเตาเผาค่อนข้างมาก สาเหตุมาจากการจ่ายอากาศส่วนที่สามในบริเวณนี้มากเกินความจำเป็นทำให้มีการสูญเสียความร้อนที่ได้จากการเผาไหม้ไปกับการทำให้ไนโตรเจนในอากาศมีอุณหภูมิสูงขึ้น สำหรับอุณหภูมิเฉลี่ยภายในเตานับจากบริเวณที่ถัดจากวงแหวนวอร์เทคลงมา พบว่าที่ปริมาณอากาศส่วนเกิน 108% จะมีอุณหภูมิเฉลี่ยสูงสุดอยู่ในช่วง 990-1,025°C และเมื่อเพิ่มปริมาณอากาศส่วนเกินเป็น 133 และ 157% จะมีอุณหภูมิเฉลี่ยต่ำกว่า 1,000°C โดยมีค่าในช่วง 930-975°C โดยที่ปริมาณอากาศส่วนเกิน 157% จะให้ประสิทธิภาพเชิงความร้อน (η_{ib}) สูงสุดเท่ากับ 95% (กรณี C Figure 5) และพบว่าอุณหภูมิแก๊สเผาไหม้ตรงทางออกของเตามีอุณหภูมิเฉลี่ยเท่ากับ 1,060°C

2.2 สมรรถนะของเตา VFBC

ประสิทธิภาพเชิงความร้อนและพิกัดความร้อนของเตาเป็นค่าดัชนีที่ใช้บอกสมรรถนะของเตา โดยค่าประสิทธิภาพเชิงความร้อนเป็นดัชนีที่ใช้ บอกความคุ้มค่าของการใช้พลังงานจากเชื้อเพลิง ส่วนพิกัดความร้อนของเตาซึ่งมีหน่วยเป็น MW$_{th}$/m^3 เป็นตัวบ่งบอกถึงความคุ้มค่าในการใช้พื้นที่ภายในเตาโดยในทางเศรษฐศาสตร์แล้ว

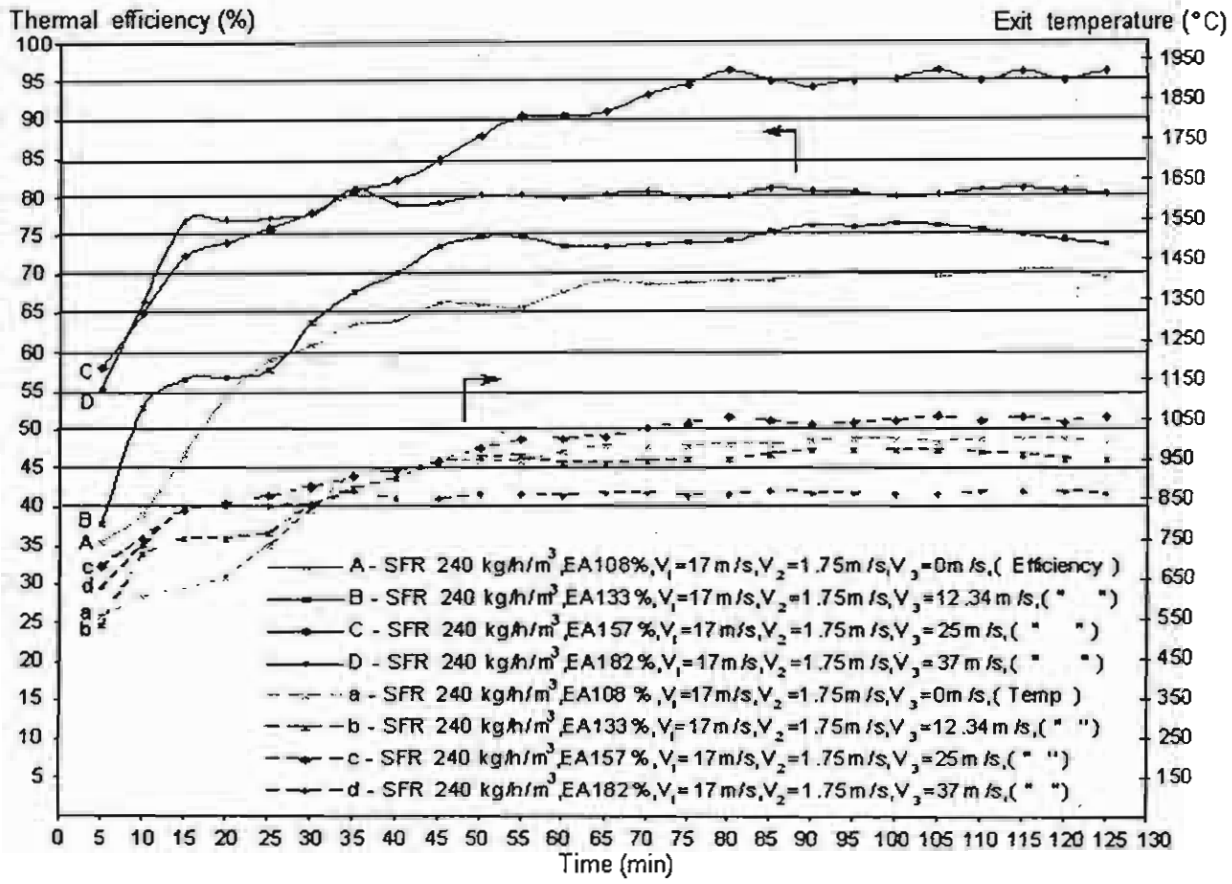


Figure 5. The variation of thermal efficiency of VFBC and exhaust gas temperature with a variety of tertiary air velocity (v_3). (Specific rice husk feed rate(SFR) = 240 kg/h/m³; Primary air velocities (v_1) = 17 m/s; Secondary air velocity (v_2) = 1.75 m/s; EA = Excess air)

ค่าพิกัดความร้อนของเตาจะแปรผกผันกับเงินทุนในการก่อสร้าง ดังนั้นในการประเมินสมรรถนะของเตาต้องพิจารณาจากดัชนีทั้งสองตัวไปพร้อมๆ กัน จาก Figure 3 และ 5 พบว่าที่ปริมาณอากาศส่วนเกิน 157% η_{th} จะมีค่าสูงสุดประมาณ 95% โดยมีค่าพิกัดความร้อนเตาเท่ากับ 0.91 MW_{th}/m^3 (คำนวณโดยใช้ค่า HHV ของแกลบเท่ากับ 14.5 MJ/kg) ซึ่งทั้งค่า η_{th} และพิกัดความร้อนของเตาเผา VFBC ใกล้เคียงกับของเตาเผาไหม้ฟลูอิไดซ์เบด (Natarajan *et al.*, 1998) แต่สูงกว่าเตาเผาไซโคลน (Soponronnarit *et al.*, 2000) จากการทดลองเบื้องต้นที่ไม่มีการใช้อากาศส่วนที่สาม (เงื่อนไขการทดลองที่ 1-6 ใน Table 2) และการทดลองที่มีการเพิ่มอากาศส่วนที่สามเข้าไป (เงื่อนไขการทดลองที่ 7-10) พบว่า η_{th} จะแปรผันตรงกับปริมาณอากาศส่วนเกิน ซึ่งจากการทดลองพบว่าการใช้หรือไม่ใช้อากาศส่วนที่สามจะไม่มีผลต่อค่า η_{th} ซึ่งดูได้จากกราฟ Figure 6 แต่การใช้อากาศส่วนที่สามจะมีผลต่อการควบคุมอุณหภูมิสูงสุดที่เกิดขึ้นภายในเตาไม่ให้เกิน 1,000°C ความสัมพันธ์ระหว่างปริมาณอากาศส่วนเกินและ η_{th} ที่อัตราการป้อนเชื้อเพลิงจำเพาะเท่ากับ 240 kg/h/m³ แสดงใน Figure 6 ซึ่งจะพบว่าในช่วงแรก η_{th} จะเพิ่มขึ้นตามปริมาณอากาศส่วนเกินและหลังจากปริมาณอากาศส่วนเกินมากกว่า 157% ค่า η_{th} จะลดลง ซึ่งอธิบายได้ว่าในช่วงแรกที่มีการใช้ปริมาณอากาศส่วนเกินน้อย ความปั่นป่วน (Turbulent) ที่เกิดจากความเร็วของอากาศ

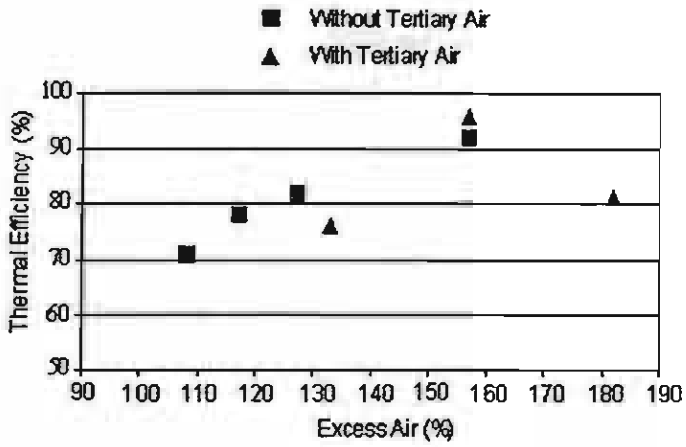


Figure 6. The effect of excess air on thermal efficiency.(run nos. 4-10; SFR = 240 kg/h-m^3)

ภายในเตาไม่มากพอที่จะทำลายชั้นฟิล์มของเถ้าที่ปกคลุมพื้นผิวอนุภาคของแข็งที่ยังเผาไหม้ไม่หมดทำให้ O_2 แพร่ไปทำปฏิกิริยากับคาร์บอนที่พื้นผิวอนุภาคได้น้อยการเผาไหม้จึงไม่ค่อยสมบูรณ์และเมื่อความเร็วของอากาศเพิ่มมากขึ้นการเผาไหม้ก็จะสมบูรณ์ขึ้นจนกระทั่งได้ประสิทธิภาพสูงสุดประมาณ 95% ที่ปริมาณอากาศส่วนเกิน 157% และจากนั้นถ้าเพิ่มปริมาณอากาศส่วนเกินเพิ่มขึ้นไปอีกจะทำให้ต้องสูญเสียความร้อนส่วนหนึ่งกับการทำให้อากาศส่วนเกินมีอุณหภูมิสูงขึ้นเท่ากับอุณหภูมิในเตาเผา ผลก็คืออุณหภูมิในเตาจะต่ำลงดังแสดงใน Figure 5 (เส้นกราฟ d) ทำให้เกิดปฏิกิริยาออกซิเดชันไม่ดีพอจึงทำให้ η_{th} ต่ำลง

2.3 องค์ประกอบของแก๊สเสีย

จากการทดลองพบว่า CO_2 และ CO ที่เกิดขึ้นจะสัมพันธ์โดยตรงกับปริมาณอากาศส่วนเกินและประสิทธิภาพเชิงความร้อนของเตาดังแสดงใน Figure 7 (a,b) โดยถ้าใช้ปริมาณอากาศส่วนเกินที่เหมาะสมเท่ากับ 157% จะทำให้การเผาไหม้เกิดขึ้นสมบูรณ์และส่งผลให้ประสิทธิภาพเชิงความร้อนของเตาสูง (η_{th} = 95 %) และเกิดปริมาณ CO_2 ในสัดส่วนที่สูงในขณะที่สัดส่วนปริมาณของ CO จะมีค่าน้อยที่ประสิทธิภาพเชิงความร้อนของเตาสูงสุด ปริมาณ CO จะมีค่าน้อยที่สุดเท่ากับ 50 ppm และปริมาณ O_2 ส่วนเกินในแก๊สเสียที่ออกมาจากเตาดังแสดงใน Figure 8(a) จะแปรผันตรงกับ η_{th} โดยที่ปริมาณอากาศส่วนส่วนเกิน 87% จะมีค่า η_{th} ต่ำที่สุด จึงมีปริมาณ O_2 ส่วนเกินเหลืออยู่ในแก๊สเสียมากที่สุดประมาณ 9.5% ในขณะที่ถ้าใช้ปริมาณอากาศส่วนเกิน 157% ค่า η_{th} จะมี

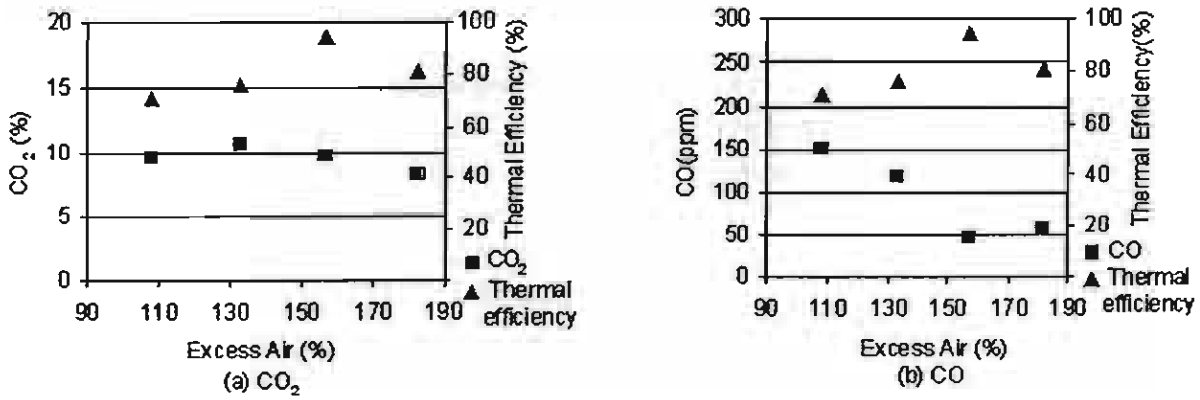


Figure 7. The effect of excess air on emitted gases and thermal efficiency. (run nos. 7-10)

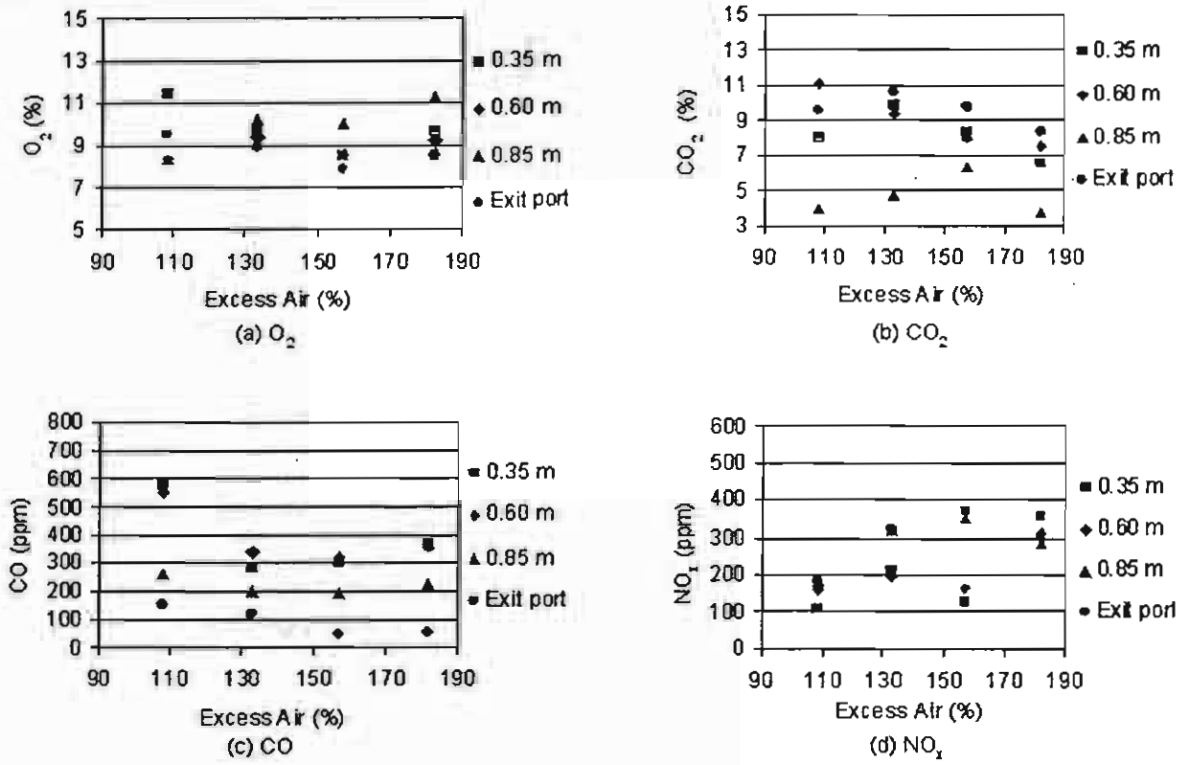


Figure 8. The variation of emitted gases with excess air at different heights of combustor. (run nos. 7-10)

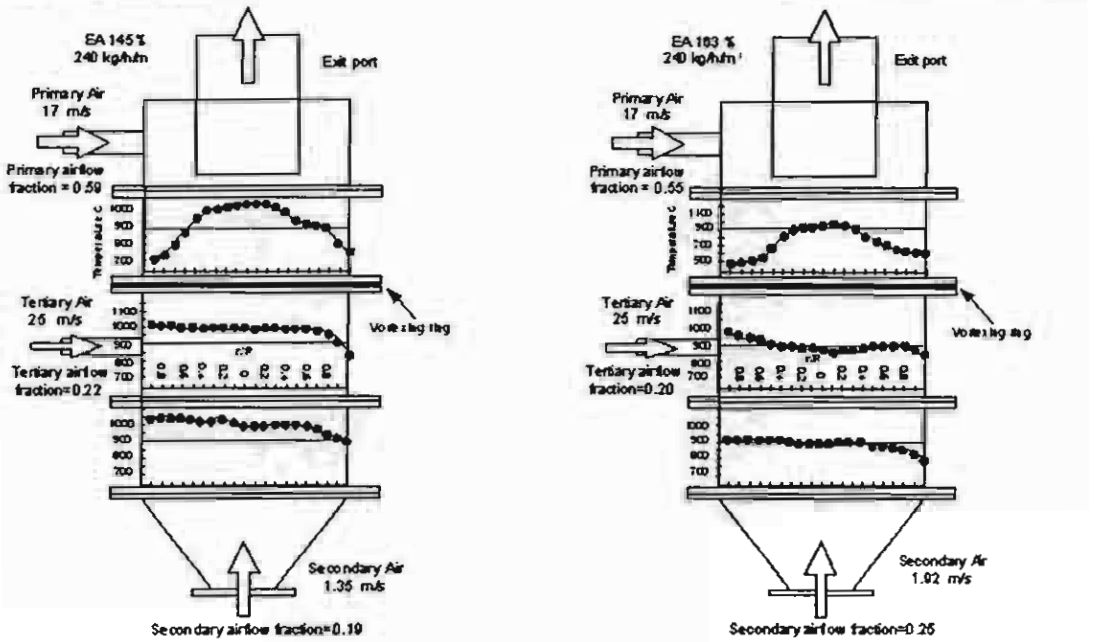
ค่าสูงสุดทำให้ O_2 ถูกใช้ไปในการเผาไหม้มาก ปริมาณ O_2 ที่ออกมากับแก๊สเสียตรงทางออกจึงเหลือน้อยที่สุดประมาณ 7.8% การเปลี่ยนแปลงปริมาณแก๊ส CO_2, CO, O_2 และ NO_x ตามระดับความสูงของเตาแสดงใน Figure 8(a-d) โดยพบว่าปริมาณ CO_2, O_2 และ NO_x ยังไม่สามารถสรุปได้ว่ามีความสัมพันธ์อย่างไรกับความสูงของเตา มีเฉพาะ CO เท่านั้นที่พบว่าที่ทุกปริมาณอากาศส่วนเกินค่า CO จะเกิดขึ้นมากที่สุดที่ระดับความสูง 0.35 เมตร เพราะปริมาณอนุภาคที่ยังเผาไหม้ไม่หมดซึ่งมากองรวมกันเป็นเบดที่บริเวณด้านล่างเตาซึ่งมีปริมาณมากเมื่อเทียบกับปริมาณอากาศส่วนที่สองที่จ่ายจากด้านล่างทำให้การเผาไหม้ยังไม่สมบูรณ์หรืออาจเกิดจากปฏิกิริยา reduction

3. การศึกษาผลของปริมาณอากาศส่วนที่สองต่อสมรรถนะของ VFBC

ในการทดลองนี้ได้กำหนดอัตราการไหลของเชื้อเพลิงจำเพาะ 240 kg/h/m^3 อัตราการไหลของอากาศส่วนที่หนึ่งและส่วนที่สามเท่ากับ 2.06 m^3/min และ 0.75 m^3/min ตามลำดับ และปรับเปลี่ยนอัตราการไหลของอากาศที่สอง ดังแสดงใน Table 2 เงื่อนไขการทดลองที่ 11-13

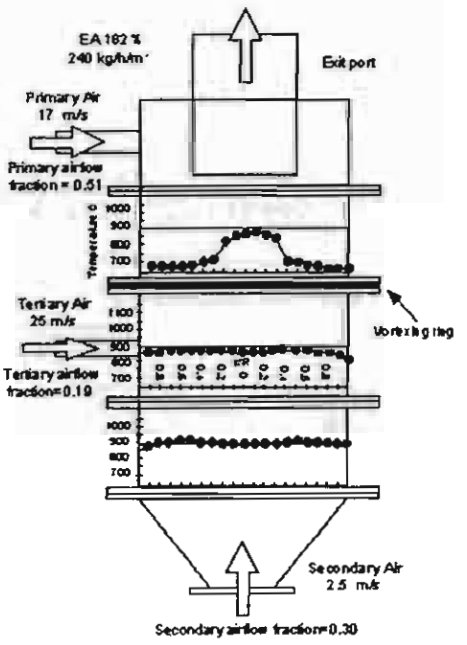
3.1 การกระจายอุณหภูมิภายในเตาเผา VFBC

Figure 9(a-c) แสดงให้เห็นว่าอัตราการไหลของอากาศส่วนที่สองเท่ากับ 0.66 m^3/min และ 1.22 m^3/min (V_2 = 1.35 m/s และ 2.5 m/s) ซึ่งเป็นอัตราการไหลที่ต่ำที่สุดและสูงที่สุดในการทดลองของทั้ง 13 การทดลอง พบว่ายังคงก่อให้เกิดพฤติกรรมการเผาไหม้แบบวอร์เทคและฟลูอิไดซ์เบด โดยการกระจายอุณหภูมิภายใน VFBC แบ่งออกเป็น 2 ส่วน คือ 1) บริเวณห้องเผาไหม้ที่อยู่เหนือวงแหวนวอร์เทค ลักษณะการกระจายอุณหภูมิมีลักษณะคล้ายพาราโบลาคว่ำ 2) บริเวณห้องเผาไหม้ที่อยู่ต่ำกว่าวงแหวนวอร์เทค พบว่าที่ระดับความสูงของเตาเท่ากับ



(a) Excess air = 145% (run no.11)

(b) Excess air = 163% (run no.12)



(c) Excess air = 182% (run no.13)

Figure 9. Temperature distributions inside VFBC at distance of 0.35, 0.6 and 0.8 M. above air distributor according to run nos. 11-13

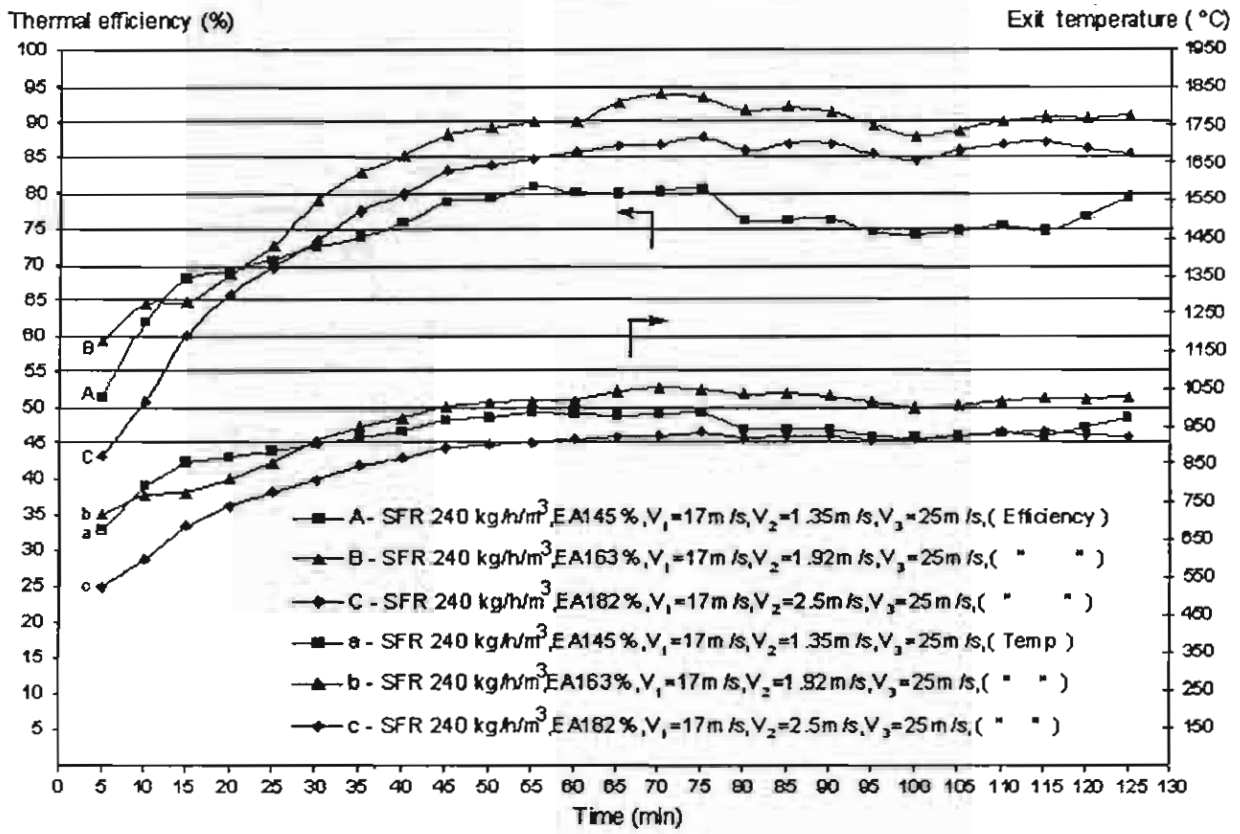


Figure 10. The variation of thermal efficiency of VFBC and exhaust gas temperature with a variety of secondary air velocity (v_2). (Specific rice husk feed rate (SFR) = 240 kg/h/m^3; Primary air velocities (v_1) = 17 m/s; tertiary air velocity (v_3) = 25 m/s; EA = Excess air)

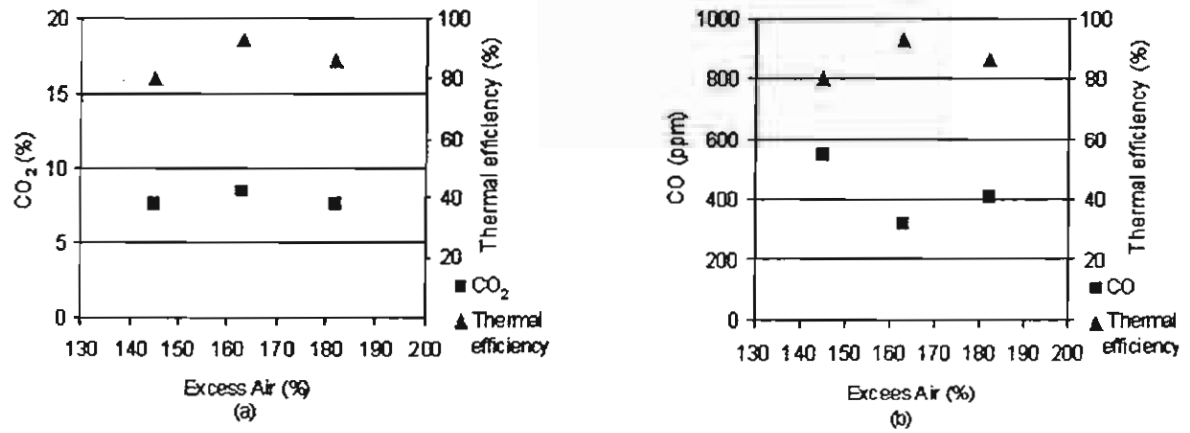


Figure 11. The effect of excess air on emitted gases and thermal efficiency. (run nos. 11-13)

0.35 เมตร, 0.6 เมตร มีการกระจายอุณหภูมิสม่ำเสมอตลอดพื้นที่ ซึ่งลักษณะการกระจายอุณหภูมิทั้ง 2 ส่วน คล้ายกับลักษณะการกระจายอุณหภูมิในหัวข้อ 2.1

3.2 สมรรถนะของเตา VFBC

จากการทดลอง เมื่อปรับเปลี่ยนอัตราการไหลของอากาศส่วนที่สองซึ่งมีผลทำให้ได้ค่าปริมาณอากาศส่วนเกิน 145% (V_2 = 1.35 m/s) และ 182% (V_2 = 2.5 m/s) ตามลำดับ พบว่าแนวโน้มของประสิทธิภาพเชิงความร้อนดังแสดงใน Figure 10 และ 11 เป็นไปในลักษณะคล้ายคลึงกับของกรณีการศึกษาเบื้องต้นที่ไม่มีการจ่ายอากาศส่วนที่สาม (หัวข้อ 1 Figure 3) และการศึกษาผลของอากาศส่วนที่สาม (หัวข้อ 2.2 Figure 5) กล่าวคือ ถ้าผลของการปั่นป่วนไม่มากพอ (กรณีนี้คือปริมาณอากาศส่วนที่สองน้อย) ทำให้ η_{th} ต่ำ ซึ่งเท่ากับ 78% และเมื่อเพิ่มดีกรีความปั่นป่วน (กรณีเพิ่มปริมาณอากาศส่วนที่สอง) จะทำให้ η_{th} สูงขึ้น ซึ่งเท่ากับ 92% (คือกรณีอากาศส่วนเกิน 163% ตาม Figure 10 เส้นกราฟ B) แต่เมื่อเพิ่มปริมาณอากาศส่วนเกินมากเกินไปจะทำให้อุณหภูมิในห้องเผาไหม้ตกลง ประกอบกับการที่ความเร็วในการทำให้เกิดฟลูอิไดซ์เซชันสูงทำให้อนุภาคที่ยังเผาไหม้ไม่หมดหลุดออกจากเตาเผาได้ จึงจะทำให้ η_{th} ลดลง เหลือเท่ากับ 87% (คือกรณีอากาศส่วนเกิน 182% ตาม Figure 10 เส้นกราฟ C) นอกจากนี้ที่สำคัญจะเห็นได้จากผลการทดลองทั้งหมดตั้งแต่ต้น (หัวข้อ 1 เป็นต้นมา) จะพบว่าถึงแม้ว่าปริมาณอากาศในแต่ละส่วนจะแตกต่างกันไปแต่ถ้ารวมกันแล้วได้ปริมาณอากาศส่วนเกินใกล้เคียงกันจะให้ประสิทธิภาพเชิงความร้อนที่ไม่แตกต่างกันดังจะเห็นได้จากผลการทดลองดังต่อไปนี้

ในกรณีศึกษาผลของอากาศส่วนที่สองในหัวข้อนี้พบว่าเมื่อใช้อากาศส่วนเกิน 145% (V_2 = 1.35 m/s) ในการเผาไหม้ ทำให้มีอุณหภูมิทางออกเฉลี่ยเท่ากับ 950°C และ η_{th} เท่ากับ 78% ดังแสดงใน Figure 10 (เส้นกราฟ a และ A) เมื่อนำมาคำนวณจะมีพิกัดความร้อนเท่ากับ 0.76 MW_{th}/m^3 ซึ่งค่า η_{th} ดังกล่าวมีค่ามากกว่า η_{th} ที่ได้จากการใช้อากาศส่วนเกิน 108% และ 133% ของกรณีการศึกษาผลของอากาศส่วนที่สามในหัวข้อ 2.2 ซึ่งมีค่า η_{th} เท่ากับ 70% และ 75% ตามลำดับ ดังแสดงใน Figure 5 (เส้นกราฟ A และ B) ดังนั้นอาจกล่าวได้ว่าค่า η_{th} ที่เพิ่มขึ้นหรือลดลงเป็นผลมาจากความปั่นป่วนของปริมาณอากาศทั้งหมดที่ใช้มากกว่าที่จะขึ้นกับปริมาณอากาศที่ใช้ในแต่ละส่วน (อากาศส่วนที่สองหรือสาม) และเมื่อใช้อากาศส่วนเกินเพิ่มขึ้นเท่ากับ 163% (V_2 = 1.92 m/s) ของกรณีศึกษาผลของอากาศส่วนที่สองทำให้มีอุณหภูมิทางออกเฉลี่ยเท่ากับ 1,025°C และ η_{th} เท่ากับ 92% ดังแสดงใน Figure 10 (เส้นกราฟ b และ B) ทำให้ได้พิกัดความร้อนของเตาเท่ากับ 0.9 MW_{th}/m^3 ซึ่งทั้งค่า η_{th} และพิกัดความร้อนเตาจะใกล้เคียงกับของกรณีอื่น ๆ ที่มีปริมาณอากาศส่วนเกินใกล้กันคือ 1) กรณีใช้อากาศส่วนเกิน 157% (กรณีมีการจ่ายอากาศส่วนที่สามเข้าสู่เตาเผา VFBC, run no.9 หัวข้อ 2) ทำให้อุณหภูมิทางออกสูงสุดเท่ากับ 1,060°C และ η_{th} สูงสุดเท่ากับ 95% ดังแสดงใน Figure 5 (เส้นกราฟ c และ C) โดยให้พิกัดความร้อนของเตาเท่ากับ 0.92 MW_{th}/m^3 3) กรณีใช้อากาศส่วนเกิน 157% (กรณีไม่มีการจ่ายอากาศส่วนที่ 3 เข้าสู่เตาผา VFBC, run no.6 หัวข้อ 1) ทำให้มีอุณหภูมิทางออกเท่ากับ 1,020°C และ η_{th} เท่ากับ 92% ดังแสดงใน Figure 3 (เส้นกราฟ f และ F) นอกจากนี้พบว่าถ้าเพิ่มปริมาณอากาศส่วนเกินให้มากขึ้นเท่ากับ 182% (V_2 = 2.5 m/s) ในการเผาไหม้จะทำให้มีอุณหภูมิทางออกลดลงเหลือเท่ากับ 924°C และ η_{th} ลดลงเหลือเท่ากับ 87% ดังแสดงใน Figure 10 (เส้นกราฟ c และ C) ทำให้พิกัดความร้อนของเตาลดลงเหลือเท่ากับ 0.85 MW_{th}/m^3 ซึ่งเป็นผลมาจากการใช้ปริมาณอากาศส่วนเกินที่มากเกินปริมาณที่เหมาะสมจะทำให้ความร้อนที่ได้จากการเผาไหม้ส่วนหนึ่งต้องสูญเสียให้กับไนโตรเจนในอากาศให้มีอุณหภูมิสูงขึ้นจึงทำให้อุณหภูมิภายในห้องเผาไหม้ลดลง ซึ่งคล้ายกับกรณีใช้อากาศส่วนเกินเท่ากับ 182% ที่กล่าวมาแล้วในหัวข้อ 2.2

3.3 องค์ประกอบแก๊สไอเสีย

ในการวิเคราะห์ถึงปริมาณแก๊ส CO_2, CO และ O_2 ที่ตำแหน่งทางออกของเตาเผา VFBC เมื่อทำการปรับเปลี่ยนปริมาณอากาศส่วนเกินที่ใช้ในการเผาไหม้ พบว่าทุกเงื่อนไขของการทดลองปริมาณแก๊ส CO_2, CO และ O_2 ที่เกิดขึ้นให้ผลที่สอดคล้องกับค่า η_{th} ที่ได้จากการเผาไหม้ในทิศทางที่เมื่อค่า η_{th} สูงขึ้น ปริมาณ CO_2 จะเพิ่มขึ้น แต่ปริมาณ CO และ O_2 จะลดลง

จาก Figure 11(a) แสดงให้เห็นว่า CO_2 ที่

ตำแหน่งทางออกจะแปรผันโดยตรงกับปริมาณอากาศส่วนเกินที่ใช้ในการไหม้ โดยเมื่อใช้อากาศส่วนเกินเท่ากับ 145% ทำให้ η_{th} ต่ำ ซึ่งเท่ากับ 78% เนื่องจากเป็นการเผาไหม้ที่ไม่สมบูรณ์ (ซึ่งได้กล่าวไว้แล้วในหัวข้อ 3.2) จึงทำให้มี CO_2 ที่เกิดจากการเผาไหม้มีปริมาณน้อย ซึ่งเท่ากับ 7.5% แต่เมื่อใช้ปริมาณอากาศส่วนเกินในการไหม้ให้มากขึ้น ซึ่งเท่ากับ 163% พบว่า η_{th} เพิ่มขึ้นเป็น 92% เนื่องจากการเกิดการปั่นป่วนในการเผาไหม้เพิ่มขึ้น ทำให้เกิดการเผาไหม้ที่สมบูรณ์มากขึ้น ดังนั้นจึงทำให้ปริมาณ CO_2 เพิ่มมากขึ้น ซึ่งเท่ากับ 8.5% อย่างไรก็ตามเมื่อใช้ปริมาณอากาศส่วนเกินเท่ากับ 182% ทำให้ปริมาณ CO_2 ลดลงเหลือเท่ากับ 7.5% เนื่องจากการใช้ปริมาณอากาศส่วนเกินที่เพิ่มมากขึ้นทำให้ 1) เกิดการเผาไหม้ที่ไม่สมบูรณ์ ซึ่งสอดคล้องกับ η_{th} ที่ลดลงต่ำลง ซึ่งเท่ากับ 87% (ดังได้กล่าวไว้แล้วในหัวข้อ 2.2) และ 2) สัดส่วนของปริมาณ CO_2 ลดลงเพราะสัดส่วนของอากาศทั้งหมดที่นำมาใช้ในการเผาไหม้เพิ่มมากขึ้น ส่วนการพิจารณาปริมาณ CO ที่เกิดจากการเผาไหม้พบว่า จาก Figure 11(b) แสดงให้เห็นว่า CO ที่ตำแหน่งทางออกจะแปรผกผันกับปริมาณอากาศส่วนเกินที่ใช้ในการไหม้ เมื่อใช้อากาศส่วนเกินเท่ากับ 145% ในการเผาไหม้พบว่าเกิด CO ออกมาปริมาณมาก มีค่าเท่ากับ 547 ppm แสดงให้เห็นว่าเป็นเงื่อนไขที่ทำให้เกิดการเผาไหม้ที่ไม่สมบูรณ์ ทำให้ได้ η_{th} ต่ำเท่ากับ 78% แต่เมื่อใช้ปริมาณอากาศส่วนเกินเท่ากับ 163% พบว่าปริมาณ CO ลดลงเหลือเท่ากับ 315 ppm เนื่องจาก 1) ปริมาณอากาศที่เพิ่มขึ้นทำให้เกิดการเผาไหม้ที่สมบูรณ์มากขึ้น ซึ่งสอดคล้องกับ η_{th} ที่เพิ่มขึ้นเป็น 92% และ 2) การที่ใช้อากาศส่วนเกินมากขึ้นทำให้สัดส่วนของ CO ลดลง (เช่นเดียวกับกรณีของ CO_2 ที่ EA = 182%) แต่เมื่อเพิ่มปริมาณอากาศส่วนเกินขึ้นไปอีกเป็น 182% ทำให้ CO กลับมาเพิ่มขึ้นเป็นเท่ากับ 404 ppm เนื่องจากเกิดการเผาไหม้ที่ไม่สมบูรณ์ ซึ่งสอดคล้องกับค่า η_{th} ที่ลดลงเหลือเท่ากับ 87% (ซึ่งความสัมพันธ์ระหว่างปริมาณอากาศส่วนเกินกับ η_{th} ที่ได้จากการเผาไหม้ ได้กล่าวไว้แล้ว

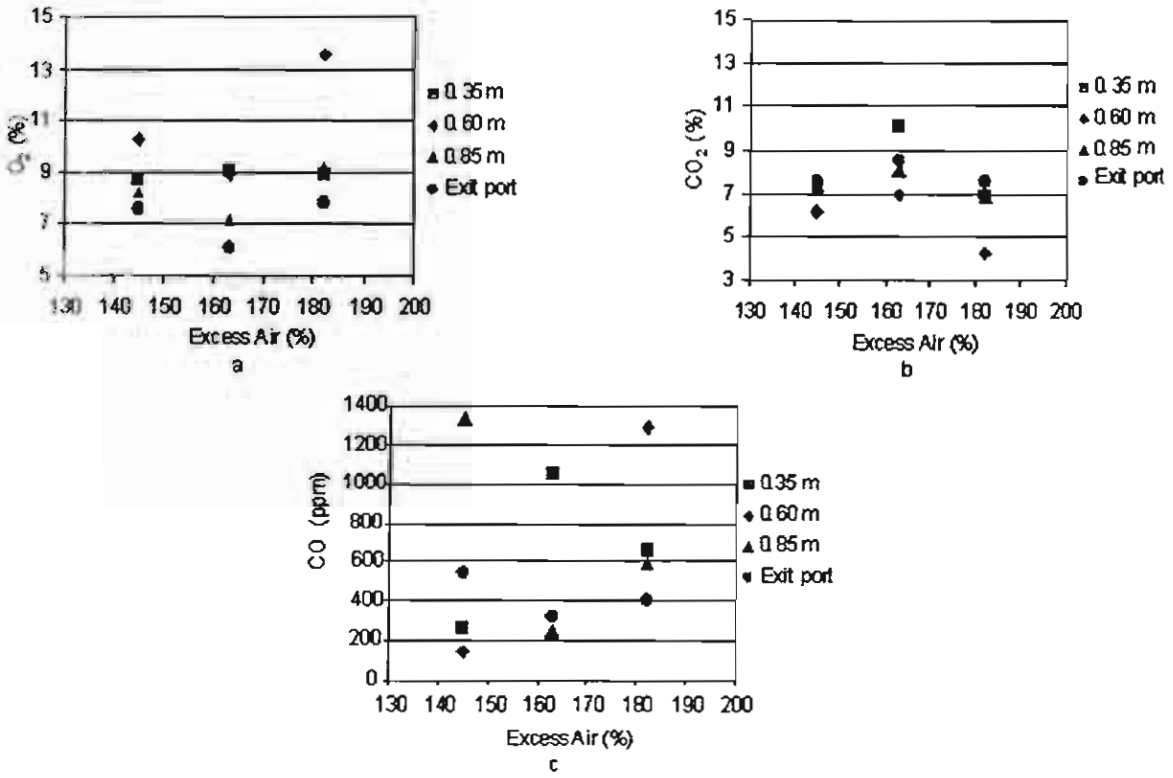


Figure 12. The variation of emitted gases with excess air at different heights of combustor. (run nos. 11-13)

Table 3. The specification of Gas analyzer model Testo 350 XL

GAS	Range
O_2	0-25%
CO	0-10,000 ppm
NO	0-3,000 ppm
SO_2	0-5,000 ppm

ในหัวข้อ 2.2) และในการพิจารณาปริมาณ O_2 ที่เกิดจากการเผาไหม้ จาก Figure 12(a) แสดงให้เห็นว่า O_2 ที่ตำแหน่งทางออก จะแปรผันโดยตรงกับปริมาณอากาศส่วนเกินที่ใช้ในการไหม้ โดยเมื่อใช้อากาศส่วนเกินเท่ากับ 145% ทำให้ η_{th} ที่ต่ำ ซึ่งเท่ากับ 78% ทำให้เหลือ O_2 ที่ไม่ได้ใช้ในการเผาไหม้จำนวนมาก ซึ่งเท่ากับ 7.6% แต่เมื่อใช้ปริมาณอากาศส่วนเกินในการไหม้เท่ากับ 163% ทำให้ η_{th} เพิ่มมากขึ้น ซึ่งเท่ากับ 92% ซึ่งทำให้ O_2 ถูกนำไปใช้ในการเผาไหม้มากขึ้น จึงทำให้เหลือ O_2 ออกมาน้อย ซึ่งเท่ากับ 6.1% และเมื่อปริมาณอากาศส่วนเกินใช้ในการไหม้เท่ากับ 182% ทำให้ O_2 เพิ่มขึ้นเป็นเท่ากับ 7.8% เนื่องจาก 1) ปริมาณอากาศส่วนเกินที่เพิ่มขึ้นทำให้เกิดการเผาไหม้ที่ไม่สมบูรณ์ เหลือ O_2 ที่ไม่ได้ใช้ในการเผาไหม้จำนวนมากขึ้น ซึ่งสอดคล้องกับ η_{th} ที่ลดลงเหลือเท่ากับ 87% และ 2) การเพิ่มอากาศส่วนเกินมากขึ้น เป็นการทำให้สัดส่วนของปริมาณ O_2 ในแก๊สเสียที่ได้จากการเผาไหม้เพิ่มมากขึ้นตาม และจากผลการทดลองนี้ทำให้พบว่าการเปลี่ยนแปลงปริมาณแก๊ส CO_2, CO และ O_2 ที่เกิดขึ้นสอดคล้องกับประสิทธิภาพเชิงความร้อนที่ได้จากการเผาไหม้ดังที่ได้กล่าวมาแล้วตั้งแต่ต้น ส่วนในการวิเคราะห์ถึงการเปลี่ยนแปลงปริมาณแก๊ส CO_2, CO และ O_2 ตามระดับความสูงของเตาแสดงใน Figure 12(a-c) โดยพบว่าปริมาณ CO_2, CO และ O_2 ยังไม่สามารถสรุปได้ว่ามีความสัมพันธ์อย่างไรกับความสูงของเตาซึ่งคล้ายกับผลการทดลองที่กล่าวมาแล้วในหัวข้อ 2.3

สรุปผลการทดลอง

ในการวิจัยนี้ได้มุ่งเน้นการพัฒนาเตาเผาไหม้วอร์เทค-ฟลูอิไดซ์เบดสำหรับเชื้อเพลิงแกลบซึ่งสามารถสรุปผลการทดลองได้ดังนี้

1. เตาเผา VFBC ที่มีสัดส่วนของเส้นผ่านศูนย์กลางต่อความสูงมีค่าต่ำเพียง 2.75 สามารถรวมพฤติกรรมการไหลของอากาศและแกลบแบบวอร์เทคและฟลูอิไดซ์เบดขณะที่เกิดการเผาไหม้ได้ซึ่งสังเกตได้จากการกระจายอุณหภูมิภายในเตาที่สามารถแบ่งออกเป็นสองบริเวณคือ 1) บริเวณห้องเผาไหม้ที่อยู่เหนือวงแหวนวอร์เทคโดยมีลักษณะการกระจายอุณหภูมิคล้ายรูปพาราโบลาคว่ำแสดงให้เห็นถึงพฤติกรรมการไหลแบบวอร์เทค และ 2) บริเวณห้องเผาไหม้ที่อยู่ต่ำกว่าวงแหวนวอร์เทคการกระจายอุณหภูมิของแก๊สเผาไหม้เกิดขึ้นอย่างความสม่ำเสมอตลอดพื้นที่หน้าตัดเตาแสดงให้เห็นถึงพฤติกรรมการเผาไหม้แบบฟลูอิไดซ์เบด

2. จากการรวมพฤติกรรมการเผาไหม้แบบวอร์เทคและฟลูอิไดซ์เบดขณะที่เกิดการเผาไหม้จะทำให้เกิดการเผาไหม้ตลอดทั่วทั้งพื้นที่หน้าตัดของเตาเผา VFBC ทำให้เตาสามารถผลิตพิกัดความร้อนจำเพาะได้สูงสุด 0.91 MW_{th}/m^3 ที่ประสิทธิภาพเชิงความร้อนเท่ากับ 95% และปริมาณอากาศส่วนเกิน 157% โดยอุณหภูมิแก๊สเผาไหม้ที่ทางออกประมาณ 1,060°C

3. การเกิดฟลูอิไดซ์เซชันภายในเตาไม่จำเป็นต้องผสมวัสดุเฉื่อยจำพวกทรายซิลิกาหรืออลูมินา ลงไปในเบด

4. การติดตั้งวงแหวนวอร์เทคจะช่วยเพิ่มการเคลื่อนที่หมุนวนอย่างรุนแรงบริเวณห้องเผาไหม้ที่อยู่เหนือวงแหวนวอร์เทค โดยอนุภาคที่มีน้ำหนักมากจะไม่สามารถเคลื่อนที่ออกจากเตาเผาได้ ขี้เถ้าที่ออกจากเตาเผา VFBC จึงมีขนาดเล็กละเอียดประมาณ 200-600 μm. และมีสีดำปนเทา

5. ประสิทธิภาพเชิงความร้อนจะแปรผันตรงกับปริมาณอากาศส่วนเกิน ในลักษณะที่เมื่อเพิ่มปริมาณอากาศ

ส่วนเกินประสิทธิภาพเชิงความร้อนจะเพิ่มขึ้น แต่ถ้าปริมาณอากาศส่วนเกินมีค่ามากเกินไปประสิทธิภาพเชิงความร้อนก็จะลดต่ำลง โดยปริมาณอากาศส่วนที่สองและสามจะไม่ส่งผลต่อประสิทธิภาพของเตา แต่ถ้าความเร็วอากาศส่วนที่สองที่ทำให้เกิดฟลูอิไดซ์เซชันมากไปก็จะทำให้อนุภาคเชื้อเพลิงที่ยังเผาไหม้ไม่หมดมีโอกาสหลุดออกมาจากเตาได้ และอากาศส่วนที่สามจะมีผลต่อการควบคุมอุณหภูมิสูงสุดภายในเตาไม่ให้เกิน 1,000°C

6. ปริมาณ CO_2, CO และ O_2 สอดคล้องกับปริมาณอากาศส่วนเกินและประสิทธิภาพของเตาโดยที่ประสิทธิภาพเชิงความร้อนเท่ากับ 95% จะให้ปริมาณ CO และ NO_x ที่ปล่อยออกมาจากเตาค่าไม่เกิน 50 ppm และ 380 ppm ตามลำดับ

กิตติกรรมประกาศ

ขอขอบคุณสำนักงานกองทุนสนับสนุนการวิจัย (สกว.) ที่ให้การสนับสนุนทุนวิจัย คุณวิบูรณ์ เทเพนทร์ สถาบันวิจัยเกษตรวิศวกรรมกลุ่มงานวิจัยวิศวกรรมหลังการเก็บเกี่ยวที่กรุณาให้คำแนะนำต่องานวิจัยนี้ และนักศึกษาภาควิชาวิศวกรรมเครื่องกล มหาวิทยาลัยเทคโนโลยีมหานคร ที่ช่วยเหลือในการทดลอง โดยมีรายชื่อดังต่อไปนี้ นายอำนาจ มากกลาง นายสิงห์ชัย ทรัพย์อุดมมาก นายวสันต์ ศรีคำมูล นายธีระวัช อ่อนดี นายไกรสร ล้อสุวรรณ นายสุรสิตร์ ภู่เมือง นายอนุชา ใจกล้า นายสุรัตน์ จตุรสุขสกุล นายอดิเรก ไสส่อง นายวีระ ศรีอริยะกุล นายเสรี อรวัฒนานนท์ นายวรรโณ วุ่นแป้น นายคำนวน เพ็ญรักษา และ นายสิทธิโชค นพคุณขจร

เอกสารอ้างอิง

Armesto, L., Bahillo, A., Veijonen, k., Cabanillas, A. and Otero, J. 2002. Combustion Behavior of Rice Husk in a Bubbling Fluidized Bed, B Bioenergy, 23(3): 171-179.

Becker *et al.*, Patent Number: 4,881,476. Cyclone Reactor with Internal Separation and Axial Recirculation.

Gupta, A.k., Lilley, D.G and Syred, N. 1984. Swirl Flows. Abacus Press, Tunbridge Wells, England.

Madhiyanon, T., Piriyarungroj, N., Nathakarannakule, A. and Soponronnarit, S. 2003(a). A Study on Air-Rice Husk Flow Behavior Cold Model, In Proc 4th the Technical Conference of the Thai Society of Agricultural Engineering., Kasetsart University, Bangkok,Thailand, Much. 13-14, 2003: 332-343.

Madhiyanon, T., Piriyarungroj, N., Nathakarannakule, A. and Soponronnarit, 2003(b). The Vortexing-Fluidized bed Combustor Cold Model: Experiment Study of Air-Rice Husk Flow Behavior, K & D Journal of EIT., 14(4): 59-67.

Natarajan, E., Nordin A and Rao A.N. 1998. Overview of Combustion and Gasification of Rice Husk in Fluidized Bed Reactor, B Bioenergy, 14(5/6): 533-546.

Nieh, S. and Zhang, J. 2000. Swirling, Reacting, Turbulent Gas-Particle Flow in a Vortex Combustor, Powder Technol., 122: 70-78.

Nigh, S., Yang, G., Zhu, A.Q. and Zhao, C.S. 1992. Measurements of Gas-Particle Flows and Elutriation of an 18 i.d. Cold Vortexing Fluidized-Bed Combustor Model, Powder Technol., 69: 139-146.

Patent Number: 4,867,079. Combustor with Multistage Internal Vortices.

Patent Number: 4,881,476. Cyclone Reactor with Internal Separation and Axial Recirculation.

Rao, T.R., and Bheemarasetti, J.V. Ram. 2000. Minimum Fluidization Velocities of Mixtures of Biomass and Sands, Energy., 26(6): 633-644.

Shang *et al.*, Patent Number: 4,867,079. Combustor with Multistage Internal Vortices.

Singh, R., Maheshwari, R.C and Ojha, T.P. 1980. Development of a Husk Fired Furnace. J. agric Engng Res., 25: 119-120.

Soponronnarit, S., Swasdisevi, T., Wetchacama, S, Shujinda, A. and Srisawat, B. 2000. Cyclone Rice Husk Furnace and Its Application on Paddy Drying, Int. Energy J., 1(2): 67-75.

Tumambig, J.A. 1984. Testing and Evaluation of Rice Hull-Fed Furnace for Grain Drying, National Post Harvest Institute for Research and Extension., pp. 197-214.

Werther, J., Saenger, M., Hartge, E.U., Ogada, T. and Siagi, Z. 2000. Combustion of Agricaltural residues, Prog. Energy Combus. Sci, 26(1): 1-27.

Yang, G. and Nieh, S. 1987. Particle Flow Pattern in the Freeboard of a Vortexing Fluidized Bed, Powder Technol., 50: 121-131.

Yang, G. and Nieh, S. 1989. On the Suspension Layers in the Freeboard of Vortexing Fluidized Beds, Powder Technol., 57: 171-179.

บทความพิเศษ

วิศวกรรมสาร มข. ปีที่ 32 ฉบับที่ 1 (1-14) มกราคม - กุมภาพันธ์ 2548
KKU Engineering Journal Vol. 32 No. 1 (1-14) January – February 2005

การจำลองแบบปัญหาทางคณิตศาสตร์ของการอบแห้งข้าวเปลือกด้วยเทคนิคผสมผสาน

สมชาติ โสภณรณฤทธิ์[1] และสมเกียรติ ปรัชญาวรากร[2]

[1] คณะพลังงานและวัสดุ มหาวิทยาลัยเทคโนโลยีพระจอมเกล้าธนบุรี ถนนสุขสวัสดิ์ 48 กรุงเทพ 10140 ประเทศไทย
[2] คณะวิศวกรรมศาสตร์ มหาวิทยาลัยเทคโนโลยีพระจอมเกล้าธนบุรี ถนนสุขสวัสดิ์ 48 กรุงเทพ 10140 ประเทศไทย

บทคัดย่อ

ในปัจจุบันได้มีการผลิตเครื่องอบแห้งฟลูอิไดซ์เบดเป็นเชิงการค้า และส่งออกไปยังหลายประเทศ ศักยภาพของเครื่องอบแห้งชนิดนี้ค่อนข้างสูงโดยเฉพาะเมื่อนำมาอบแห้งเมล็ดพืชที่มีความชื้นสูง เช่น ข้าว ข้าวนึ่ง ข้าวโพด และถั่วเหลือง อัตราการลดความชื้นของเครื่องอบแห้งชนิดนี้สูงกว่าเครื่องอบแห้งเมล็ดพืชที่ใช้กันทั่วไปในอุตสาหกรรม จากข้อดีดังกล่าวดังกล่าวทำให้เครื่องอบแห้งมีขนาดกะทัดรัดเมื่อเทียบกับความสามารถในการอบแห้งของเครื่อง ความสิ้นเปลืองพลังงานในการอบแห้งต่ำ คุณภาพของเมล็ดพืชหลังการอบแห้งด้วยเทคนิคนี้อยู่ในเกณฑ์ดี ในบทความนี้เป็นการบรรยายถึงงานวิจัยและพัฒนาการอบแห้งเมล็ดพืชด้วยเทคนิคฟลูอิไดซ์เบด โดยเริ่มตั้งแต่การศึกษาการอบแห้งแบบเป็นงวดในระดับห้องปฏิบัติการ จนมาถึงการพัฒนาเครื่องอบแห้งชนิดต่อเนื่องเพื่อผลิตเป็นเชิงการค้า นอกจากนี้ยังกล่าวถึงแบบจำลองทางคณิตศาสตร์ของระบบอบแห้งด้วยเทคนิคฟลูอิไดซ์เบดซึ่งประกอบไปด้วยขั้นตอนการอบแห้ง การพัก และการเป่าลมเย็น ในแบบจำลองดังกล่าวนี้ยังได้รวมสมการของข้าวเต็มเมล็ดซึ่งจะทำให้แบบจำลองที่พัฒนาขึ้นนี้มีประโยชน์สำหรับงานออกแบบหาเงื่อนไขในการอบแห้ง เพื่อให้ได้อัตราการผลิตและคุณภาพอยู่ในเกณฑ์ดี

คำสำคัญ: ข้าวเปลือก คุณภาพ ระบบอบแห้ง

MATHEMATICAL MODELLING AND SIMULATION OF FLUIDISED-BED DRYING, TEMPERING AND VENTILATION OF GRAINS

Somehart Soponronnarit [1] and Somkiat Prachayawarakorn [2]

[1] School of Energy and Materials King Mongkut's University of Technology Thonburi Suksawat 48 Road, Bangkok 10140, Thailand

[2] Faculty of Engineering King Mongkut's University of Technology Thonburi Suksawat 48 Road, Bangkok 10140, Thailand

ABSTRACT

The fluidized-bed grain dryer is now fully commercialized and exported to several countries. Its potential is great especially for high moisture grains such as paddy, parboiled rice, maize and soybean. Its drying rate is very fast as compared to conventional grain dryers. Consequently, the size of drying unit is very compact relative to its capacity. Its energy consumption is relatively low while grain quality is maintained. In this paper, the research and development effort on fluidised bed grain drying is described, starting with an experimental batch dryer and culminating with a commercial continuous-flow dryer. A mathematical model of the fluidised bed grain drying system including a series of drying, tempering, ambient air ventilation and head-rice equation is derived. The model provides the useful information about designing and operating condition for the drying system in order to optimize the drying capacity and quality, both of which show the contradict results.

Keywords: Drying system, paddy, quality

Introduction

It has been suggested that high moisture paddy should be dried quickly to approximately 23% moisture content (dry basis[1]) then subjected to ambient air drying in storage (Soponronnarit et al. 1994; Driscoll and Srzednicki 1991). Following two-stage drying, cost and product quality appear to be optimised. During the first stage, fluidised bed drying is an alternative to conventional hot-air drying. Its advantages are: (1) uniform product moisture content, and thus high drying air temperature can be employed but with less overdried grain; (2) high drying capacity due to better heat and mass transfer; (3) a much smaller drying chamber and thus a significantly lower initial cost; and (4) significant spin-off in terms of increasing head rice yield and potential for producing aging rice.

Sutherland and Ghaly (1992) were probably the first research group who investigated feasibility of using fluidisation technique for paddy drying. Japanese researcher may have conducted similar research work before. Experimental results reported by Sutherland and Ghaly (1992) showed that head yield was 58-61% when paddy was dried from 28.2 to 20.5% but was 15-24% when the final moisture content was 19%. Tumambing and Driscoll (1993) found that drying rate was affected by drying air temperature and bed thickness under experimental conditions as follows: drying air temperature of 40-100°C; bed thickness of 5-20 cm and air velocity of 1.5-2.5 m/s. They also developed a mathematical model for continuous fluidised bed paddy dryer.

Soponronnarit and Prachayawarakorn (1994) have reviewed the research and development work on fluidised bed drying of grain, and conducted both experimental and simulation studies on batch fluidised bed drying of paddy. Soponronnarit et al. (1996) described the development of a cross-flow fluidised bed paddy dryer with a capacity of 200 kg/hour (Fig.1). Experimental results showed that final moisture content of paddy should not be lower than 23% if quality in terms of both whiteness and head yield were to be maintained. Drying air temperature was 115°C. Simulation results indicated that the appropriate operating parameters should be as follows: air speed, 2.3 m/s; bed thickness, 10 cm; and fraction of air recycled of 0.8. With these conditions, energy consumption was close to the minimum, while drying capacity was near maximal. In this study, moisture of paddy was reduced from 30 to 24%.

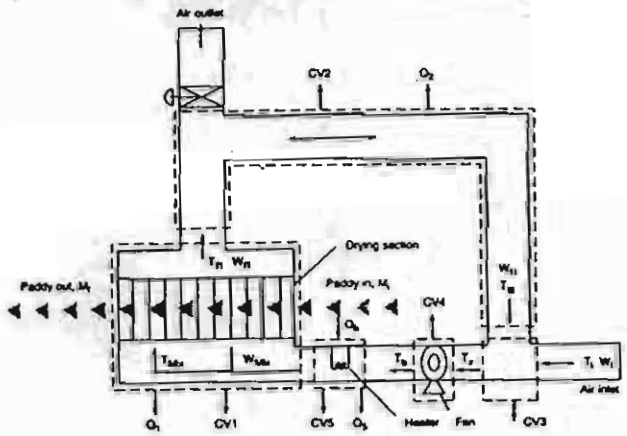


Figure 1 *Control volumes of continuous cross-flow fluidised bed drying system: ↓ grain flow; ← air flow; T, temperature; W, humidity ratio; M, grain moisture content; Q, heat; CV, control volume.*

[1] Unless otherwise stated, the moisture contents (m.c.) quoted in this paper are dry basis.

Following the success of the development of the cross-flow fluidised bed paddy dryer, Rice Engineering Supply Co. Ltd., a private company in Thailand, showed interest in collaborating in the development of a prototype with a capacity of approximately 1 t/hour as shown in Figure 2 (Soponronnarit et al. 1995). It comprises a drying section, a 7.5 kW backward curved blade centrifugal fan, a diesel fuel-oil burner, and a cyclone. The bed length, width and height of the drying section are 1.7, 0.3 and 1.2 m, respectively. The depth of the paddy bed is controlled by a weir. Paddy is fed in and out by rotary feeders. In operation, hot air (temperature controlled by thermostat) is blown into the drying section through a perforated steel sheet floor. The air and grain flows are perpendicular to each other. A small portion of the air leaving the drying chamber is vented to the atmosphere, while the remainder, after cleaning in a cyclone, is recycled to the dryer, mixed with ambient air and reheating to the desired temperature, respectively. The feed rate of paddy can be varied from less than 1 t/hour to more than 1.5 t/hour. More detail is given in Yapha (1994). Experimental results showed that the unit operated efficiently and yielded high product quality in terms of head yield and whiteness. In reducing the moisture content from 45 to 24% using air temperature of 100-120°C, fraction of air recycled of 0.66, specific airflow rate of 0.05 kg/s-kg dry matter, superficial air velocity of 3.2 m/s, and bed depth of 0.1 m, total primary energy consumption was 2.32 MJ/kg of water evaporated, of which 0.35 was primary energy from electricity (electrical energy multiplied by 2.6) and 1.79 was primary energy in terms of heat energy.

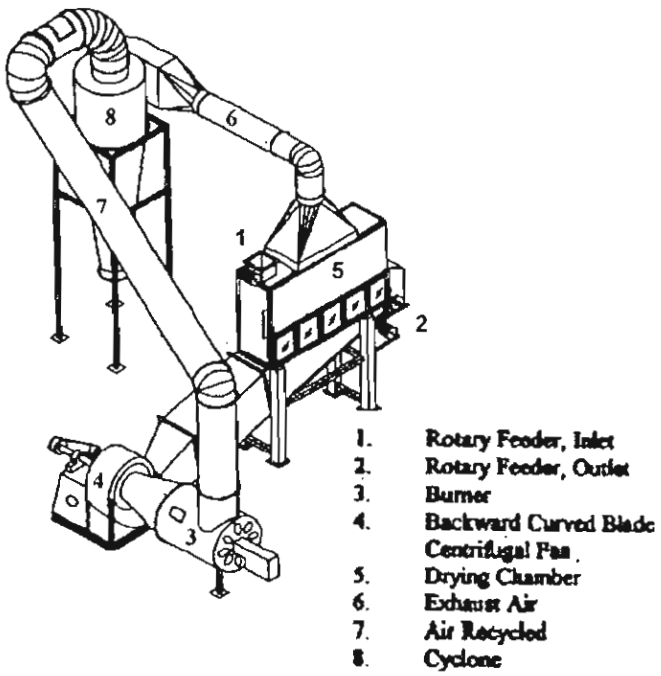


Figure 2 *Commercial fluidised-bed paddy dryer*

As a result of the success of the prototype, commercial fluidised bed paddy dryers with capacities of 5, 10 and 20 t/hour are now available. More than 200 units have been sold since the beginning of 1995. The fluidised bed dryer is mainly composed of a drying chamber, a backward curved blade centrifugal fan, a burner using diesel oil or fuel oil for heating air, and a cyclone or a cyclo-fan. Commercial cyclonic rice husk furnace is now available commercially. More than

200 units have been sold since the beginning of 1999.

Operation of the commercial fluidised bed paddy dryer is similar to the prototype except that a small portion of exhaust air is vented to the atmosphere after being cleaned by the cyclone.

DEVELOPMENT OF MATHEMATICAL MODEL

It was assumed that there is thermal equilibrium between the drying air and the product, and that the air and grain flow were in plug type. Experimental results reported by Sripawatakul (1994) indicated that the flow regime of paddy was between near plug flow and high dispersion flow. Though dispersion was a known factor in the fluidised bed, the mathematical model assumed plug flow in order to simplify calculation. The model is similar to that presented by Soponronnarit and Prachayawarakorn (1994). Figure 1 shows control volumes (CVs) for the derivation of energy and mass balance equations.

Equation of mean residence time

The empirical equation of mean residence time of paddy developed by Sripawatakul (1994) was used. It is written as follows:

$$\tau = hu/F \qquad (1)$$

where τ = mean residence time, second (s)
hu = hold up, kg
F = feed rate, kg/s

and $hu = [\{-0.0095000 + 0.59870\ F - (0.00020000 + 0.17360\ F)\ V\} + \{1.1728 - 0.082300\ V + (2.2093 - 0.15050\ V)\ F\}\ h]\ \rho_p A$

where A = paddy bed area, m^2
V = air velocity, m/s
ρ_p = average product density, kg/m^3
h = weir height, m

It is valid for weir heights in the range 0.04 - 0.10 m, air velocities in the range 1.7 - 2.3 m/s, and paddy feed rates in the range 0.025 - 0.058 kg/s. For a rough calculation, hu is approximately equal to $hA\rho_p$ and can be applied to other grains.

Dividing the paddy bulk into n layers, changes in moisture content of paddy, temperature, and the humidity ratio of air were calculated for each layer. The following basic equations were employed.

Equation for the drying rate

The empirical equation for fluidised bed paddy drying in the form of the equation of Page (1949), developed by Sripawatakul (1994), was used. It is written as follows:

$$MR = \exp\{-x(t/60)^y\} \quad (2)$$

where $MR = (M - M_{eq})/(M_{in} - M_{eq})$

t = drying time, s

$x = 0.00163100\ T_{mix} - 1.16202\ (m_{mix}/hu) + 0.00415300\ (m_{mix}/hu)\ T_{mix} + 0.147383\ \ln(m_{mix}/hu) + 0.474743$

$y = -0.00322000\ T_{mix} - 0.835960\ (m_{mix}/hu) + 0.0203190\ (m_{mix}/hu)\ T_{mix} - 0.143150\ \ln(m_{mix}/hu) + 0.548493$

Equation (2) is similar to that developed by Soponronnarit and Prachayawarakorn (1994) for higher specific airflow rate (m_{mix}/hu). It is valid for temperatures of 90 - 140°C and specific airflow rates of 0.03 - 0.16 kg/s/kg dry matter of paddy. The symbols are defined as follows:

M = moisture content of paddy at time t, decimal dry basis
M_{in} =moisture content of paddy at the inlet of drying section, decimal dry basis
M_{eq} =equilibrium moisture content, decimal dry basis
T_{mix} =air temperature at the inlet of drying section, °C
m_{mix} =airflow rate at the inlet of drying section, kg/s

During calculation, Equation (2) was differentiated with time, and finite difference was employed to obtain the solution. Equilibrium moisture content was determined using the equation developed by Laithong (1987).

For the drying rates of maize and soybean, they are available in Soponronnarit et al. (1997) and Soponronnarit et al. (2001), respectively.

Equation of mass conservation

$$W_{fl,i} = R_t(M_i - M_f) + W_{mix} \quad (3)$$

where $W_{fl,i}$ = humidity ratio of outlet air at the i^{th} layer, kg water/kg dry air
W_{mix} = humidity ratio of inlet air at the i^{th} layer, kg water/kg dry air
M_i = moisture content of paddy at the inlet of i^{th} layer, decimal dry basis
M_f = moisture content of paddy at the outlet of i^{th} layer, decimal dry basis
R_t = ratio of dry mass of paddy to mass of dry air.

Equation of energy conservation

$$T_{fl,i} = [Q_l/m_{mix} + C_a T_{mix} + W_{mix}(h_{fg} + C_v T_{mix}) - W_{fl,i} h_{fg} + R_t C_{pw} \theta_g]/(C_a + W_{fl,i} C_v + R_t C_{pw}) \quad (4)$$

where $T_{fl,i}$ = temperature of outlet air at the i^{th} layer, °C
θ_g = grain temperature, °C
Q_l = heat loss, kW
C_a = specific heat of dry air, kJ/kg °C
C_v = specific heat of vapour, kJ/kg °C
C_{pw} = specific heat of moist paddy, kJ/kg °C

h_{fg} = latent heat of moisture vaporisation, kJ/kg

Average temperature and humidity ratio of the outlet air from n layers were determined by arithmetic mean.

For other calculations such as mixing of air streams, and consumption of energy at the fan and the heater, solutions can be achieved by the application of first law of thermodynamics [see Soponronnarit and Prachayawarakorn (1994) for details].

The equations were solved by iteration. Firstly, the value of exit humidity ratio of air was assumed. The equations presented by Wilhelm (1976) were used to determine properties of moist air.

The accuracy of the mathematical model was tested and found to be in good agreement with the experimental results. The model was employed to investigate optimum operating parameters such as air temperature, specific airflow rate, and fraction of air recycled. Details for paddy drying and maize drying are available in Soponronnarit et al. (1996) and Soponronnarit et al. (1997), respectively.

Further development of the mathematical model

In simulation of multi-stage drying including the tempering between each stage, the moisture profile in a grain kernel at the end of each drying stage must be known. Unfortunately, the moisture profile in a grain kernel cannot be predicted by the empirical drying equations such as Equation (2). But, it can be determined only by using a theoretical equation, mostly described by the Fick's unsteady state diffusion equation in which an effective moisture diffusion coefficient is taken into account.

Poomsa-ad et al. (2002) developed the mathematical model for the simulation of multi-stage drying including the tempering between each stage. It was assumed that water moves in the combined radial and axial direction and paddy is an isotropic solid. The partial differential equation of moisture diffusion for a single paddy kernel considered geometrically to be a finite cylindrical shape can be written as follows:

$$\frac{\partial M}{\partial t} = D\left[\frac{\partial^2 M}{\partial r^2} + \left(\frac{1}{r}\right)\frac{\partial M}{\partial r} + \frac{\partial^2 M}{\partial z^2}\right] \qquad (5)$$

where D = effective moisture diffusion coefficient, m/s^2
r = coordinate along the radius of cylinder, m
z = coordinate along the length of cylinder, m

The initial and boundary conditions for paddy drying are given by

$t = 0,\ 0 \le r \le r_o \quad M = M_{in}$ or $M = M(r,z)$
$-\ell \le z \le +\ell \quad M = M_{in}$ or $M = M(r,z)$
$t > 0,\ r = r_o \quad M = M_{eq}$
$z = \pm\ell \quad M = M_{eq}$
$t > 0,\ r = 0 \quad \frac{\partial M}{\partial r} = 0$

where ℓ = half length of cylinder, m
r_o = radius of cylinder, m

The effective moisture diffusion coefficient described by the Arrhenius type equation is given as follows:

$$D = 5.41141\times10^{-6}\exp\left(\frac{-28436.4}{R(273.15+T)}\right) \qquad (6)$$

where R = universal gas constant, kJ/kmol-K

For tempering process, moisture profile at the end of the first stage drying is used as the initial condition. During this period, the moisture inside a paddy kernel transports to the exterior surface, but it does not evaporate to the environment. The redistribution of moisture inside the kernel can be described again by Equation (5) with the new boundary and initial conditions as follows:

$$t = 0, \qquad M = M(r,z)$$

$$t > 0, \ r = r_o \qquad \frac{\partial M}{\partial r} = 0$$

$$z = \pm\ell \qquad \frac{\partial M}{\partial z} = 0$$

$$t > 0, \ r = 0 \qquad \frac{\partial M}{\partial r} = 0$$

The degree of uniformity of moisture content in this stage is described by the tempering index, I_c,

$$I_c = \frac{(M_{s,t} - M_{s,t=0})}{(M_{s,t=\infty} - M_{s,t=0})} \qquad (7)$$

where M_s is the surface moisture content, decimal dry basis. Theoretically, the uniform distribution of moisture, corresponding to the tempering index of unity, required infinite time.

After tempering stage, the grains are cooled to room temperature, using ambient air temperature, to stop formation of yellow pigment. Yellowing can be a severe problem in rice drying because temperature stimulates the development of rice yellowness, a non-enzymatic browning reaction (Taweerattanapanish et al., 1999; Soponronnarit et al., 1998a; Yap et al., 1988). Ventilation was stopped when the grain temperature approached or was slightly above ambient air temperature. While the air ventilated through the heated grains, there was the simultaneous heat and mass transfer from the grain to air, making the air slightly warmer and more humid. The heat-transfer phenomenon in this unit was opposite to that occurring in the dryer section. Assuming that the air flowed through a thin bed in the cross-flow dryer, the outlet-air temperature, T_{fl}, is thus given by

$$T_{fl} = \frac{(C_a T_i + W_i(h_{fg} + C_v T_i) - W_i h_{fg} + R_t C_{pw}\theta_{in})}{(C_a + W_{fl} C_v + R_t C_{pw})} \qquad (8)$$

where θ is the grain temperature (°C) and W_{fl} is the outlet humidity ratio at the ventilation unit. Using such a simplified assumption, the properties of air change insignificantly along the bed height, thereby providing economic computation by a single-step approach. For the moisture transport in the ventilation, it is calculated by using Equation (5) again, with the following initial and boundary conditions:

$t = 0, \quad M = M(r,z) \quad t > 0, \; r = r_o \quad M = M_{eq}$

$z = \pm l \quad M = M_{eq}$

In the determination of moisture reduction, the grain temperature is replaced in Equation (6), instead of the inlet-air temperature, because the grain temperature at the beginning of ventilation was approximately 50°C higher than the ambient-air temperature.

Head-rice yield equation

Poomsa-ad et al. (2001) reported that the amount of head rice yield related with tempering time, grain temperature or tempering temperature and the moisture content after fluidised-bed drying. A head rice equation was simply described by

$$RHY = A + Bt + Ct^2 \qquad (9)$$

where $A = -39.232+8.4227M_f-0.34060T-0.029105TM_f$

$B = 25.945-1.1878M_f-0.2443T+0.012302TM_f$

$C = -0.33610+0.015028M_f+0.003259T$
$-0.00015762TM_f$

t is the tempering time (minute), M_f is the moisture content (%d.b.) after drying and T is the tempering temperature (°C).

SIMULATION RESULTS

Figure 3 shows the change of moisture content and grain temperature after passing through the units i.e. drying, tempering and ventilation in the process of paddy drying. This experiment was carried out with a batch fluidized-bed drying and the details were given in Poomsa-ad et al. (accepted to be published). As shown in this Figure, the moisture content is reduced from 27.5% d.b. to 22.5% d.b. in the fluidised-bed dryer followed the unchanged value of moisture content in the tempering stage. In the last stage, the moisture content is decreased to 17.5% d.b. The model proposed reasonably predicts the changes of moisture content and grain temperature at various units of the paddy drying process. As seen in Figure 3b, the temperature steeply drops during a small interval of ventilation, thus causing a high reduction of head rice yield, due to the thermal and moisture gradients, if the grains are not tempered. The poor head-rice yield can be seen in Figure 4 for zero tempering time, with a relative head-rice yield of 20% for the case of B. The relative head-rice yield is defined as the ratio of head-rice yield obtained by drying paddy at high temperature to that at ambient temperature. For the case of A, on the other hand, the head-rice yield quality does not drop although the sample is not subjected to temper.

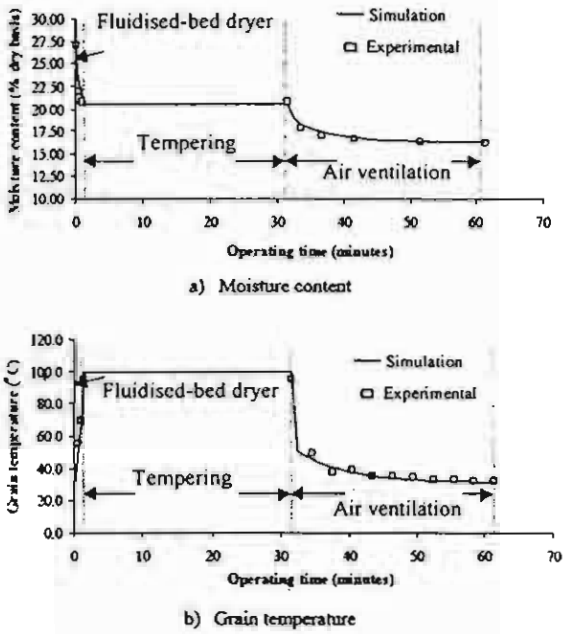


Figure 3 Comparisons of moisture content and grain temperature obtained from the experiment and prediction. (Poomsa-ad et al. (accepted to be published))

The insignificant reduction of head-rice yield for the case of 35% d.b. moisture content is probably attributed to the gelatinization effect, making paddy to withstand the milling forces. When the tempering time increases, the head-rice yield is improved and higher than that at zero tempering time. According to this result, it is questionable whether the paddy should be tempered for how long after drying with fluidised-bed dryer. To answer such a question, the proposed model is used to estimate the suitable tempering time. The criterion indicating the appropriate tempering time is related to the tempering index. Poomsa-ad et al. (2002) recommended the tempering index of 0.95, corresponding to the calculated tempering time of 35 minutes for high-temperature drying. This agrees with the experiment results shown in Figure 4, indicating insignificant change of head-rice yield after tempering for 30 minutes. In addition to the aforementioned quality, the fastest drying rate at the subsequent stage is achieved, giving the benefit of effective energy utilisation. From this figure, it also shows that the head-rice yield equation when included in the heat and mass transfer equations reasonably explains the quality change with the tempering time.

The similar result was also reported by several workers (Steffe et al., 1979; Soponronnarit et al., 1998b; Soponronnarit et al., 1999), showing a higher head-rice yield when the tempering was included between drying stages.

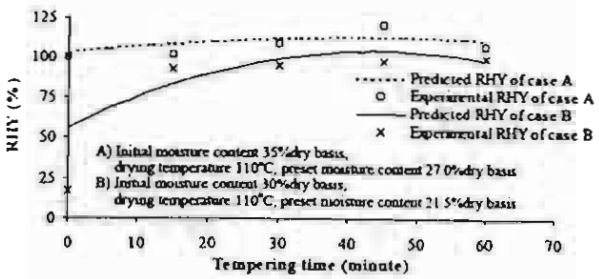


Figure 4 Effect of tempering time on relative head-rice yield (Poomsa-ad et al. (accepted to be published))

SIGNIFICANCE OF SIMULATION RESULTS

Reducing moisture content of paddy by using only fluidised-bed dryer seems an inappropriate method since the transport of water is controlled by internal resistances, resulting in wastage of energy. Besides, the amount of broken rice is enormous, due to excessive stresses produced inside the kernel, and the colour of white rice changes from white to yellow, causing by the non-enzymatic browning reaction (Soponronnarit and Prachayawarakorn, 1994; Sutherland and Ghaly, 1992). To optimise the drying time and energy consumption, along with high head-rice yield, moist paddy should be followed with three stages in series i.e. fluidised bed, tempering and ambient air ventilation to remove its moisture content to a certain level for safe storage. Both experiments and simulations agree well that fluidised-bed dryer, with inlet air temperature of 150°C, is used to decrease the moisture content of paddy to 19.5% d.b. followed with tempering for 30 minutes. In the last stage, the paddy is cooled by ambient air (temperature and relative humidity of 30°C and 55-60%, respectively with air velocity of 0.15 m/s) for 20 minutes. Quality of paddy in terms of head-rice yield and whiteness is acceptable. Under the specified conditions, the thermal and electrical energy consumptions were in the respective ranges of 5-7 MJ/kg-water evaporated and 0.54-0.61 MJ/kg-water evaporated. For drying paddy within high moisture range using fluidized bed technique only, it was reported by Soponronnarit (2000) that energy consumption was lower, i.e. 2.2-3.9 MJ/kg-water evaporated in terms of thermal energy and 0.15-0.43 MJ/kg-water evaporated in terms of electrical energy. Under proper conditions such as high initial moisture content of paddy (higher than 30%) and high air temperature (140 - 150°C), head yield can be increased up to 50% compared to ambient-air drying. For consumer acceptance, tested rice with fluidised bed drying is insignificantly different from that dried by ambient air.

Conclusion

Fluidised bed grain drying has been developed for almost 10 years in Thailand. The first fluidised bed paddy dryer was first commercialized in Thailand in 1995. It is probably the first commercial continuous fluidised bed dryer for paddy drying. Since then, more than 200 commercial units with capacities of 5, 10 and 20 tons/hour have been sold in Thailand, Cambodia, Indonesia, Laos, Malaysia, Mexico, Myanmar, the Philippines, Taiwan and Venezuela.

A basic study including drying kinetics and factors affecting grain quality, moisture reduction rate and energy consumption was conducted for paddy, maize and soybean. Important results are presented in this paper. Finally, a complete mathematical model for the fluidised bed grain drying system including a series of drying, tempering and subsequent ventilation was derived.

In conclusion, the fluidised bed paddy dryer is competitive with conventional hot air dryers especially at high moisture level, i.e. low energy consumption, low cost and acceptable paddy quality. Important operating parameters are: drying air temperature of 140 - 150°C, fraction of air recycled of 0.8, air velocity around 2.0 - 2.3 m/s and bed thickness of 10 - 15 cm. Under proper conditions such as high initial moisture content of paddy (higher than 30%) and high air temperature (140 - 150°C), head yield can be increased up to 50% compared to ambient-air drying. For consumer acceptance, tested rice with fluidised bed drying is not significantly different from that dried by ambient air.

Acknowledgment

Thanks are due to the Thailand Research Fund for financial support to the Research Group on Drying Technology, King Mongkut's University of Technology Thonburi, Bangkok, Thailand.

References

Driscoll, R.H. and Srzednicki, G.S., 1991. **Design for a complete grain drying system under Southeast Asian climates**. Proceedings of the 12th ASEAN Technical Seminar on Grain Post-harvest Technolog; 29-31 August 1989; Surabaya; Indonesia.

Laithong, C., 1987. **Study of physico-thermal properties of rough rice**. [Master's thesis]. Bangkok. Thailand: King Mongkut's Institute of Technology Thonburi.

Page, G.E., 1949. **Factors influencing the maximum rate of drying shelled corn in layers**. [Master of Science]: Purdue University.

Poomsa-ad, N., Soponronnarit, S., Prachayawarakorn, S. and Terdyothin, A. 2002. Effect of tempering on subsequent drying of paddy using flidisation technique. **Drying Technology** 20: 195-210.

Poomsa-ad, N, Soponronnarit, S., Terdyothin, A. and Prachayawarakorn, S., 2001. **Head rice yield after drying by fluidization technique and tempering. Proc**. the 2nd Asian-Oceana Drying Conference;20-23 August 2001; Penang, Malaysia.

Poomsa-ad, N., Soponronnarit, S. and Prachayawarakorn, S. Investigation on head-rice yield and operating time in drying process: Experiment and Simulation. **Journal of Stored Product Research**. (Accepted to be published)

Soponronnarit, S., 2000. Fluidised bed grain drying. In: Mujumdar, A. **and Suvachittanont, S. (Eds.), Developments in Drying Vol. II. Drying of Food and Agro-Products** : 135-148

Soponronnarit, S. and Prachayawarakorn, S. 1994. Optimum strategy for fluidized bed paddy drying. **Drying Technology** 12: 1667-1686.

Soponronnarit, S., Kittiporn, K. and Prachayawarakorn, S. 1997. Appropriate operating parameters for fluidized bed corn drying. **RERIC International Energy Journal** 19: 1-13.

Soponronnarit, S., Prachayawarakorn, S. and Sripawatakul, O., 1996. Development of cross-flow fluidized bed paddy dryer. **Drying Technology** 14: 2397-2410.

Soponronnarit, S., Srisubati, N., Yoovidhya, T., 1998a, Effect of temperature and relative humidity on yellowing rate of paddy. **Journal of Stored Products Research**. 34: 323-330.

Soponronnarit, S., Swasdisevi, T., Wetchacama, S. and Wutiwatchai, W., 2001, Fluidised bed drying of soybeans. **Journal of Stored Product Research**. 37: 133-151.

Soponronnarit, S., Taweerattanapanish, A., Wetchacama, S., Kongseri, N. and Wongpiyachon, S. 1998b. **Spin-off from paddy drying by fluidization technique**. Keynote paper in

Proc. at the 7th International Working Conference on Stored-Product Protection;14-19 October 1998; Beijing, China.

Soponronnarit, S., Wetchacama, S., Swasdisevi, T. and Poomsa-ad, N., 1999, Managing moist paddy by drying, tempering and ambient air ventilation. **Drying Technology** 17: 335-344.

Soponronnarit, S., Wongvirojtana, P., Nathakaranakule, A. and Prachayawarakorn, S., 1994. **Maintaining paddy quality by appropriate ventilation under tropical climate**. Proceedings of the 9th International Drying Symposium; 1-4 August 1994; Gold Coast; Australia.

Soponronnarit, S., Yapha, M. and Prachayawarakorn, S., 1995, Cross-flow fluidized bed paddy dryer: prototype and commercialization. **Drying Technology** 13: 2207-2216.

Sripawatakul, O., 1994. **Study of drying paddy by cross-flow fluidization technique**.[Master's thesis Faculty of Engineering]. Bangkok. Thailand: King Mongkut's Institute of Technology Thonburi.

Steffe, J.F., Singh, R.P. and Bakshi, A.S., 1979, Influence of tempering time and cooling on rice milling yields and moisture removal. **Trans.of the ASAE**. 17: 1214-1218.

Sutherland, J.W. and Ghaly, T.F., 1992. **Rapid fluid bed drying of paddy rice in the humid tropics**. Proceedings of the 13th ASEAN Conference on Grain Post-harvest Technology. 4-7; September 1990; Brunei Darussalam.

Taweerattanapanish, A., Soponronnarit, S., Wetchacama, S., Kongseri, N., Wongpiyachon, S., 1999. Effects of drying in head rice yield using fluidization technique. **Drying Technology** 17: 345-353.

Tumambing, J.A. and Driscoll, R.H. 1993. **Modeling the performance of continuous fluidized bed paddy dryer for rapid pre-drying of paddy**. *Proceedings of the 14th ASEAN seminar on Grain Post-harvest Technology*; 5-8 November 1991; Manila, Philippines.

Wilhelm, L.R. 1976. Numerical calculation on psychrometric properties in SI units. **Transactions of the American Society of Agricultural Engineers** 19: 318-321, 325

Yapha, M., 1994. **Design and testing of pilot continuous fluidized bed paddy dryer**. [Master's thesis, School of Energy and Materials]. Bangkok. Thailand; King Mongkut's Institute of Technology Thonburi.

Yap, A.B., Juliano., B.O., Perez. C.M. 1988. **Artificial yellowing of rice at 60°C. In: Naewbanij**. J.O. (Ed).Proceedings of the Eleventh ASEAN Technical Seminar on Grain Postharvest Technology; 23-26 August, 1988; Kuala Lumpur, Malaysia. ASEAN Grain Postharvest Programme. Bangkok. Thailand.



ประวัติส่วนตัว

ศาสตราจารย์ ดร.สมชาติ โสภณรณฤทธิ์ เกิดเมื่อวันที่ 27 พฤษภาคม พ.ศ. 2495 ที่กรุงเทพมหานคร สำเร็จการศึกษาระดับปริญญาตรีเกียรตินิยมอันดับ 1 จากมหาวิทยาลัยขอนแก่นด้านวิศวกรรมศาสตร์ สาขาวิศวกรรมเกษตร ปริญญาโทจาก Asian Institute of Technology และระดับปริญญาเอกด้าน Agricultural Process Engineering จาก Ecole National Superieur Agronomique de Toulouse สมรสกับนางเจิมใจ (อัศวเสนา) โสภณรณฤทธิ์ มีบุตร 3 คน คือนางสาวกุลยา นางสาวกชพร และนายกานต์ โสภณรณฤทธิ์ ปัจจุบันดำรงตำแหน่งศาสตราจารย์ระดับ 11 คณะพลังงานและพัสดุ มหาวิทยาลัยเทคโนโลยีพระจอมเกล้าธนบุรี และรักษาการคณบดีคณะวิศวกรรมศาสตร์ มหาวิทยาลัยมหาสารคาม ปี พ.ศ. 2539 ได้รับรางวัลนักวิจัยดีเด่นแห่งชาติ สาขาวิศวกรรมศาสตร์และอุตสาหกรรมวิจัย จากสำนักงานคณะกรรมการวิจัยแห่งชาติ และได้รับทุนเมธีวิจัยอาวุโส สกว.รุ่นที่ 2 พ.ศ. 2539-2542 ปี พ.ศ. 2543 ได้รับรางวัลนักวิทยาศาสตร์ดีเด่น และได้รับทุนทุนเมธีวิจัยอาวุโส สกว.รุ่นที่ 5 พ.ศ. 2543-2546 ในปี 2546 ได้รับรางวัลนักวิทยาศาสตร์ขององค์การยูเนสโก (2003 UNESCO SCIENCE PRIZE) และในปี พ.ศ. 2547 ได้รับพระราชทานเครื่องราชอิสริยาภรณ์ ม.ป.ช. มหาปรมาภรณ์ช้างเผือก

ผลงานเด่นได้แก่ การร่วมมือกับภาคเอกชนพัฒนาเครื่องต้นแบบสำหรับอบแห้งข้าวเปลือกและเตาเผาแกลบ จนนำไปสู่การจดสิทธิบัตร ผลิตขาย และส่งออกอย่างแพร่หลาย ปฏิบัติการหลังการเก็บเกี่ยวเป็นขั้นตอนที่สำคัญต่อคุณภาพของผลผลิต โดยเฉพาะขั้นตอนการลดความชื้นซึ่งสำคัญต่อการรักษาคุณภาพ และลดการสูญเสีย ผลผลิตรวมของข้าวเปลือกมีมูลค่ากว่า 80,000 ล้านบาทต่อปี หากสามารถลดการสูญเสียเพียง 1% ก็สามารถลดความเสียหายได้ถึง 800 ล้านบาท การอบแห้งโดยเทคนิคฟลูอิไดเซชัน (fluidization) เป็นวิธีการใหม่ที่นำมาใช้ลดความชื้นของข้าวเปลือก สามารถลดทั้งระยะเวลาและค่าใช้จ่ายในการผลิต นอกจากนี้เตาเผาแกลบไซโคลน (cyclone) ที่พัฒนาขึ้น สามารถลดการใช้น้ำมันเชื้อเพลิงได้อย่างน้อยปีละ 200-300 ล้านบาท และได้มีเอกชนหลายบริษัทนำต้นแบบเครื่องอบแห้งฟลูอิไดซ์เบดและเตาเผาแกลบไซโคลนไปผลิตขายเชิงการค้าทั้งในประเทศและต่างประเทศแล้วไม่ต่ำกว่า 500 เครื่อง เป็นมูลค่าไม่ต่ำกว่า 500 ล้านบาท

การรวมกระบวนการผลิตของการนึ่งและการอบแห้งข้าวนึ่งสำหรับข้าวหอม

Combination Process of Steaming and Drying for Parboiling Aromatic Rice

เฉลิมพร เอี่ยมมิ[1], พัชรี ตั้งตระกูล[2], ชัยยงค์ เตชะไพโรจน์[3], สมชาติ โสภณรณฤทธิ์[4]

Chalermporn Eiammi[1], Pacharee Tangtrakul[2], Chaiyong Tachapairoj[3], Somchart Sophonronnarit[4]

Abstract

This research is the feasible study for the combination process of steaming and drying for parboiling aromatic rice using superheated steam fluidized bed drying. The effects of soaking times and drying times on the head rice yield, color, white belly, cooking quality, pasting viscosity of rice flour and gelatinization are considered. In the experiments, paddy with initial moisture content of 15.7% d.b. was soaked by hot water at temperature of 80 °C for 0.5 - 3 hours. Next, paddy was dried at 150 °C for 0.5 - 7 minutes, superheated steam velocity of 3.0 m/s and bed height of 10 cm. Experimental results foud the soaking time of 3 hour and drying time of 2 minutes provide considerable increase in head rice yields which lines in the rang of 67.9%. Moreover, whiteness are the good criteria; however, it will be reduced with increase in soaking and drying time. White belly of all condition are increased more than rice reference. In the texture test, the cooked rice is moderately hardened and flaked with increase in drying time. Besides, the peak and the final viscosity are reduced, but the pasting temperature will be increased. For the gelatinization analysis by DSC, paddy with soaking time of 3 hours and drying 2 minutes appears to have the gelatinization more than paddy of soaking time of 2 hours and drying 2 minutes (degree of gelatinization of 88.5 and 78% for soaking time of 3 and 2 hours respectively).
Keywords: Parboiling aromatic rice, Fluidized bed, Paddy drying, Rice quality, Superheated steam

บทคัดย่อ

งานวิจัยนี้ได้ศึกษาการรวมกระบวนการผลิตของการนึ่งและการอบแห้งข้าวนึ่งสำหรับข้าวหอม โดยการอบแห้งด้วยเครื่องฟลูอิไดซ์เบดมีไอน้ำร้อนยวดยิ่งเป็นตัวกลาง ซึ่งพิจารณาถึงอิทธิพลของระยะเวลาที่ใช้ในการแช่ข้าวเปลือกและระยะเวลาที่ใช้ในการอบแห้ง ที่มีต่อการเพิ่มปริมาณต้นข้าว สี White belly คุณภาพการหุงต้ม ความหนืดของน้ำแป้ง และการเกิดเจลาติไนเซชัน (Gelatinization) ทำการทดลองโดยใช้ข้าวเปลือกที่มีความชื้นเริ่มต้นก่อนแช่ 15.7% มาตรฐานแห้ง แช่ในน้ำอุณหภูมิ 80 °ซ. เป็นเวลา 0.5 - 3 ชั่วโมง จากนั้นนำมาอบแห้ง ที่อุณหภูมิอบแห้ง 150 °ซ. เป็นเวลา 0.5-7 นาที ความเร็วของไอน้ำร้อนยวดยิ่งเท่ากับ 3.0 ม./วินาที และความสูงของเบด 10 ซม. จากผลการศึกษาพบว่า การแช่และการอบแห้งสามารถเพิ่มปริมาณต้นข้าวได้สูงสุด 67.9% เมื่อแช่เป็นระยะเวลา 3 ชั่วโมง และอบแห้ง 2 นาที โดยความขาวของข้าวจะลดลงตามเวลาที่เพิ่มขึ้นของการแช่และการอบแห้ง ส่วน White belly จะเพิ่มสูงขึ้นกว่าข้าวอ้างอิงทุกเงื่อนไขการทดลอง จากการทดสอบเนื้อสัมผัสพบว่า ข้าวสุกจะแข็งและร่วนขึ้น เมื่อใช้เวลาในการอบแห้งมากขึ้นที่ระยะเวลาการแช่เท่ากัน นอกจากนี้เวลาในการอบแห้งที่มากขึ้น ยังทำให้ค่าความหนืดสูงสุด (Peak viscosity) และความหนืดสุดท้าย (Final viscosity) มีค่าลดลง แต่ค่าอุณหภูมิที่แป้งเริ่มพองตัว (Pasting temperature) สูงขึ้น การวิเคราะห์การเกิดเจลาติไนเซชันด้วยเครื่อง DSC ข้าวที่แช่นาน 3 ชั่วโมงและอบแห้ง 2 นาที เกิดการเจลาทิไนเซชันมากกว่าข้าวที่แช่เป็นระยะเวลา 2 ชั่วโมงและอบแห้ง 2 นาทีโดยมี ระดับของเจลาทิไนเซชัน (Degree of gelatinization) เท่ากับ 88.5% และ78% ตามลำดับ

บทนำ

ประเทศไทยเป็นประเทศที่ผลิตข้าวหอมที่สำคัญ ผลผลิตข้าวหอมนอกจากใช้บริโภคในประเทศ ยังสามารถส่งออกในปีหนึ่งๆ นั้นมีมูลค่าหลายพันล้านบาท ข้าวนึ่งเป็นส่วน

1) นักศึกษาปริญญาโท, 4) ศาสตราจารย์ คณะพลังงานและวัสดุ , มหาวิทยาลัยเทคโนโลยีพระจอมเกล้าธนบุรี เขตทุ่งครุ, กรุงเทพฯ

2) นักวิจัยชำนาญการ สถาบันค้นคว้าและพัฒนาผลิตภัณฑ์อาหาร , มหาวิทยาลัยเกษตรศาสตร์ เขตจตุจักร, กรุงเทพฯ

3) อาจารย์ คณะวิศวกรรมศาสตร์และเทคโนโลยีอุตสาหกรรม, มหาวิทยาลัยศิลปากร สนามจันทร์, นครปฐม

หนึ่งของมูลค่าข้าวที่ประเทศไทยส่งออกในแต่ละปี การผลิตข้าวนึ่งแบ่งออกได้เป็น 3 ขั้นตอนหลักๆ คือ การแช่ (Soaking) การนึ่ง (Steaming) และการอบแห้ง (Drying) ถ้าสามารถลดขั้นตอนการผลิตโดยการรวมกระบวนการในการผลิตซึ่งจะสามารถลดต้นทุนและประหยัดพลังงานในขั้นตอนเหล่านั้นด้วย ก็จะทำให้ประเทศไทยสามารถแข่งขันและมีความได้เปรียบทางด้านการค้ามากขึ้น

Kar และคณะ (1999) พบว่าความร้อนจะทำให้น้ำแพร่เข้าไปในเมล็ดได้อย่างรวดเร็ว ทำให้สามารถลดระยะเวลาในกระบวนการผลิตข้าวนึ่งลงได้มาก แต่ระยะเวลาและอุณหภูมิตลอดจนน้ำที่ใช้ในการแช่มีอิทธิพลต่อคุณภาพข้าวนึ่งที่ได้ Bhattacharya (1996) ได้นำข้าวเปลือกไปทำการแช่น้ำอุณหภูมิ 70 °ซ. เป็นระยะเวลา 3 ชั่วโมง จากนั้นจึงนำไปนึ่งด้วยไอน้ำภายใต้ความดันต่างๆ คือ 101-304 กิโลปาสคาล (ระบบปิด) ระยะเวลา 0-60 นาที พบว่าการเปลี่ยนสีของข้าวนึ่งทั้งหมดเป็นไปตามจลนศาสตร์อันดับศูนย์ ถ้าระยะเวลาที่ใช้ในกระบวนการผลิตนานและความดันที่ใช้เพิ่มมากขึ้น จะมีผลทำให้ข้าวสารที่ได้มีความเหลืองเพิ่มขึ้น

Toshinori และคณะ (1993) ได้ศึกษาถึงผลกระทบของอุณหภูมิและระยะเวลาในการนึ่ง พบว่าเมื่ออุณหภูมินึ่งสูงความขาวของเมล็ดข้าวจะลดลง และเมื่อระยะเวลาในการนึ่งมากขึ้นความขาวของเมล็ดข้าวมีแนวโน้มลดลง Taechapairoj และคณะ (2003) ได้ศึกษาการอบแห้งข้าวเปลือกโดยเทคนิคฟลูอิไดซ์เบดด้วยไอน้ำร้อนยวดยิ่งที่ความชื้นเริ่มต้น 44.4% มาตรฐานแห้ง ให้เหลือความชื้นสุดท้าย 16-28% มาตรฐานแห้ง โดยใช้อุณหภูมิไอน้ำร้อนยวดยิ่ง 150-170 °ซ. ความสูงของเบด 10-15 ซม. และความดันสมบูรณ์ของไอน้ำในระบบเหนือบรรยากาศเล็กน้อย พบว่าอุณหภูมิของไอน้ำมีผลต่อการอบแห้งมากกว่าความสูงของเบด และความชื้นเริ่มต้นของข้าวเปลือกมีอิทธิพลต่อร้อยละและได้เสนอแนะว่าควรใช้อุณหภูมิในการแช่ข้าวเปลือกประมาณ 80 °ซ. เพื่อให้ข้าวเปลือกเกิดเจลาติไนเซชัน (Gelatinization) ได้ดีขึ้นซึ่งเป็นการลดปริมาณ White belly นอกจากนี้ พบว่าทำให้ได้ปริมาณต้นข้าวเพิ่มขึ้น แต่สีของข้าวสารที่ขัดสีแล้วมีสีที่เข้มขึ้นเมื่ออุณหภูมิอบแห้งสูงขึ้น และเมื่อนำไปทดสอบคุณภาพจะมีลักษณะคล้ายข้าวนึ่งมาก

Rordprapat และคณะ (2002) ได้ศึกษาเปรียบเทียบการอบแห้งข้าวเปลือกด้วยไอน้ำร้อนยวดยิ่งกับการอบแห้งด้วยอากาศร้อนโดยใช้เทคนิคฟลูอิไดซ์เบด ที่อุณหภูมิอบแห้ง 150 °ซ. ความสูงเบด 10 ซม. ความเร็วที่ใช้อบแห้งเท่ากับ 1.5 เท่าของความเร็วต่ำสุดในการเกิดฟลูอิไดเซชัน พบว่าข้าวเปลือกที่ผ่านการอบแห้งด้วยไอน้ำร้อนยวดยิ่งมีร้อยละต้นข้าวสูงกว่าการอบแห้งด้วยอากาศร้อน แต่ความขาวของข้าวสารต่ำกว่าการอบแห้งด้วยอากาศร้อน ซึ่งมีสีน้ำตาลอ่อน จากงานวิจัยต่างๆ ที่ผ่านมาจึงสามารถรวมกระบวนการนึ่งและการอบแห้งเข้าด้วยกันได้โดยวิธีการเทคนิคฟลูอิไดซ์เบดที่มีไอน้ำร้อนยวดยิ่งเป็นตัวกลาง

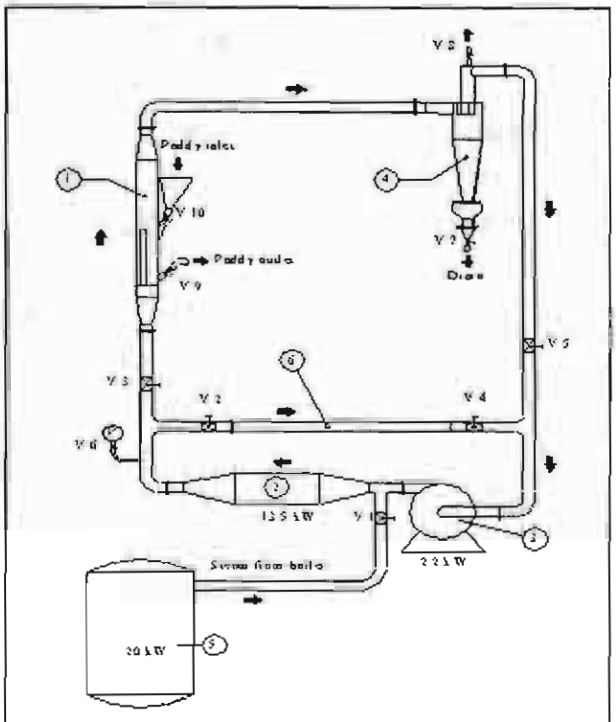
จุดประสงค์ของงานวิจัยนี้จึงได้ศึกษาผลของการผลิตข้าวนึ่งโดยการรวมกระบวนการนึ่งและการอบแห้งข้าวนึ่งข้าวหอมไว้ด้วยกัน ตลอดจนสมบัติของข้าวทางด้านกายภาพและเคมีกายภาพของข้าวหอมที่ได้หลังจากผ่านกระบวนการอบแห้งข้าวนึ่งโดยเทคนิคฟลูอิไดซ์เบดที่ใช้ไอน้ำร้อนยวดยิ่งเป็นตัวกลาง

อุปกรณ์และวิธีการทดลอง

อุปกรณ์

1. เครื่องอบแห้งแบบฟลูอิไดซ์เบด โดยมีไอน้ำร้อนยวดยิ่งเป็นตัวกลางชนิดอบแห้งเป็นงวด แสดงดังรูปที่ 1 มีส่วนประกอบคือ

- ห้องอบแห้ง (Drying chamber) เป็นรูปทรงกระบอก



1) Drying chamber
2) Superheater
3) Blower
4) Cyclone
5) Boiler
6) Bypass line
V= Valve,
P = Pressure gauge

รูปที่ 1 แผนภาพระบบอบแห้งด้วยไอน้ำร้อนยวดยิ่งที่ใช้ในการทดลอง

ทำด้วยสแตนเลส ขนาดเส้นผ่านศูนย์กลาง 15 ซม. และสูง 100 ซม.

- อุปกรณ์ให้ความร้อน (Superheater) มีขนาด 13.5 กิโลวัตต์ โดยมีเครื่องควบคุมอุณหภูมิแบบ PID มีค่าความถูกต้อง ±1 °ซ.

- พัดลม (Blower) เป็นแบบแรงเหวี่ยงใบพัดโค้งหลัง (Backward - curved centrifugal blower)

- มอเตอร์ขนาด 2.2 กิโลวัตต์ สามารถปรับความเร็วรอบของพัดลมได้

- เครื่องดักฝุ่น (Cyclone) เป็นแบบ Reverse flow ทำด้วยสแตนเลส

- เครื่องกำเนิดไอน้ำ (Boiler) ออกแบบความดันใช้งานสูงสุด 3.5 บาร์ โดยมีวาล์วระบายไอน้ำเพื่อระบายไอน้ำเมื่อความดันเกินพิกัด ตั้งที่ค่าความดัน 3.5 บาร์ ความสามารถผลิตไอน้ำได้ 31 กก./ชม. ที่อุณหภูมิ 100 °ซ. ความดันบรรยากาศ หรือเทียบได้กับพลังงานความร้อน 20 กิโลวัตต์ ใช้ไฟฟ้า 380 V, 3 phase, 50 Hz

2) เครื่องมือวัดที่ใช้ในการทดลอง

- เครื่องวัดอุณหภูมิ ใช้เทอร์โมคัปเปิล ชนิด K ต่อเข้ากับเครื่องอ่านและบันทึกอุณหภูมิ (Data logger) มีความละเอียด ±1 °ซ.

- เครื่องมือวัดความเร็วของไอน้ำร้อนยวดยิ่ง ใช้ Pitot static tube ต่อเข้ากับมานอมิเตอร์

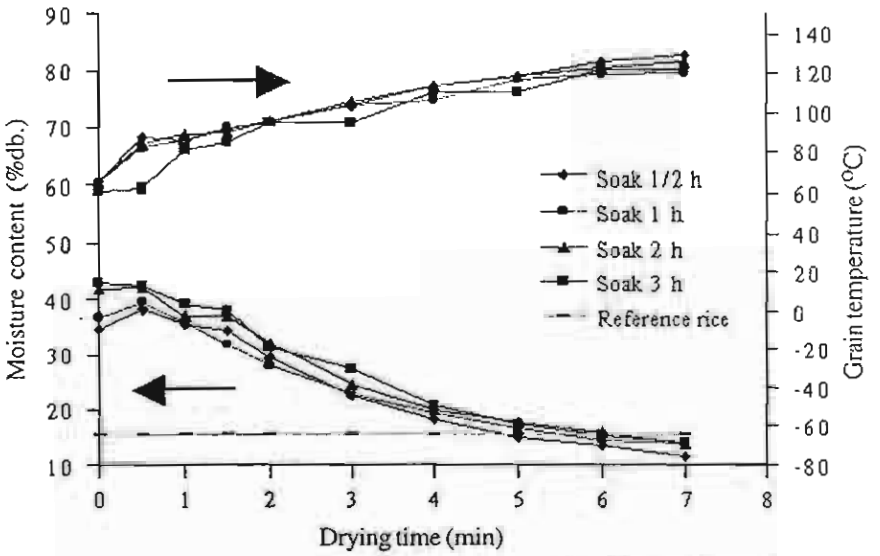
- เครื่องชั่งน้ำหนักเพื่อหาความชื้น ใช้เครื่องชั่งแบบดิจิตอลที่มีความละเอียด ± 0.01 กรัม ชั่งน้ำหนักได้สูงสุด 500 กรัม

- เครื่องชั่งน้ำหนักเพื่อหาคุณภาพ ใช้เครื่องชั่งแบบดิจิตอลที่มีความละเอียด ± 0.1 กรัม ชั่งน้ำหนักได้สูงสุด 500 กรัม

วิธีการ

แช่ข้าวเปลือกที่อุณหภูมิน้ำแช่ 80 °ซ. เวลาในการแช่ 0.5 - 3 ชั่วโมง นำไปอบแห้งที่อุณหภูมิไอน้ำร้อนยวดยิ่ง 150 °ซ. เวลาในการอบแห้ง 0.5 - 7 นาที ความสูงเบดของข้าวเปลือก 10 ซม. ความเร็วของไอน้ำร้อนยวดยิ่ง 3.0 ม./วินาที ความดันของระบบเหนือบรรยากาศเล็กน้อยเพื่อป้องกันการรั่วเข้าของอากาศ

คุณภาพทางกายภาพของข้าวที่ทำการวิเคราะห์ในงานวิจัยนี้ได้แก่ ร้อยละต้นข้าว ความขาวใช้อุปกรณ์วัดความขาวแบบอิเล็คทรอนิค (Kett C-300) ร้อยละ White belly โดยการนับจำนวนของข้าวที่เป็นจุดขาวขุ่นในเมล็ดข้าวใน 100 เมล็ดจากการสุ่มตัวอย่าง และคุณภาพการหุงต้ม คุณภาพทางเคมีกายภาพของข้าวที่ทำการวิเคราะห์ในงานวิจัยนี้ได้แก่ ความหนืดของน้ำแป้งหาโดยเครื่อง Rapid Visco Analyser model-4 (Newport Scientific Pty Ltd., Warriewood, Australia) ตามวิธีการของ AACC method 61-02 (AACC, 1995) ความแข็งและการยึดเกาะตัวของข้าวสุกโดยเครื่อง Texture Analyzer (TA.XT2, UK) การเกิดเจลาติไนเซชันหาโดยใช้เครื่อง Differential Scanning Calorimetry (DSC) (Pyris-I, Perkin) และ Scanning Electron Micrographs (JSM-5600LV/JSM5600 Japan)



รูปที่ 2 ความสัมพันธ์ของร้อยละความชื้นและอุณหภูมิของเมล็ดข้าวเปลือกที่เวลาในการแช่และการอบแห้งต่าง ๆ

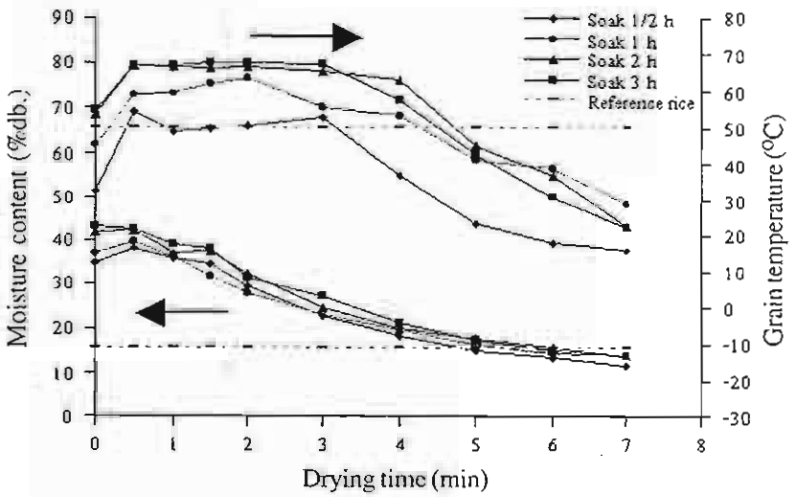
ผลและวิจารณ์

1. การเปลี่ยนแปลงความชื้นและอุณหภูมิเมล็ดข้าวเปลือก

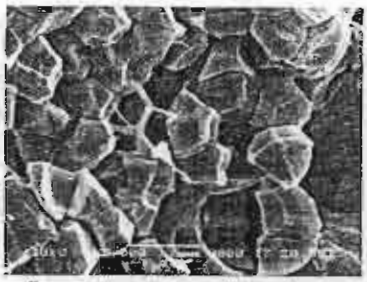
จากผลการทดลองการเปลี่ยนแปลงความชื้นและอุณหภูมิเมล็ดข้าวเปลือกโดยทำการทดลอง 2 ซ้ำได้ผลการทดลองคล้ายกัน แสดงผลดังรูปที่ 2 พบว่าความชื้นของเมล็ดข้าวเปลือกที่ความชื้นเริ่มต้นเดียวกัน (15.7% มาตรฐานแห้ง) เพิ่มขึ้นตามระยะเวลาในการแช่ และเมื่อนำไปอบแห้งที่เวลาการอบแห้งต่างกัน พบว่าในช่วงเวลาการอบแห้ง 0.5 นาที ความชื้นของเมล็ดข้าวเปลือกเพิ่มขึ้นเนื่องจากไอน้ำร้อนยวดยิ่งมีอุณหภูมิสูงกว่าอุณหภูมิเมล็ดข้าวเปลือก จึงทำให้ไอน้ำเกิดการควบแน่นและเกิดชั้นฟิล์มของของเหลวขวางทิศทางการไหลของไอน้ำร้อนยวดยิ่ง ส่งผลให้เมล็ดข้าวเปลือกมีความชื้นเพิ่มมากขึ้นซึ่งเปรียบเทียบได้กับช่วงการนึ่ง (Steaming) ของการผลิตข้าวนึ่ง และเมื่อระยะเวลาการอบแห้งเพิ่มมากขึ้นความชื้นของเมล็ดข้าวเปลือกลดลงมีแนวโน้มใกล้เคียงกันเป็นไปตามจลนศาสตร์ของการอบแห้ง เพราะว่าความชื้นของเมล็ดส่วนใหญ่จะอยู่ที่ภายในเมล็ด อุณหภูมิเมล็ดข้าวเปลือกจึงเพิ่มมากขึ้นตามระยะเวลาการอบแห้งโดยอุณหภูมิเมล็ดข้าวเปลือกที่ผ่านการแช่ระยะเวลาสั้นเพิ่มขึ้นเร็วกว่าเมล็ดข้าวเปลือกที่ผ่านระยะเวลาการแช่นาน เนื่องจากเมล็ดข้าวเปลือกที่ผ่านการแช่ระยะเวลาสั้นมีความชื้นน้อยกว่าทำให้เกิดช่วงระยะเวลาการอบแห้งลดลงเร็วกว่า ส่งผลให้ผิวของเมล็ดข้าวเปลือกมีอุณหภูมิเพิ่มขึ้นอย่างรวดเร็วเมื่อเปรียบเทียบกับข้าวเปลือกที่ผ่านการแช่เป็นระยะเวลานาน เมล็ดข้าวเปลือกยังมีความชื้นสูง จึงมีช่วงอัตราการอบแห้งคงที่นาน อุณหภูมิเมล็ดจึงเพิ่มขึ้นช้ากว่า

2. ปริมาณต้นข้าว

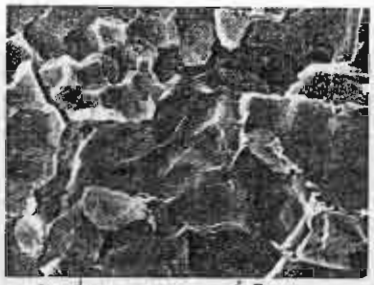
ปริมาณต้นข้าวทำการทดลอง 2 ซ้ำได้ผลการทดลองคล้ายกันแสดงผลดังรูปที่ 3 พบว่าเมื่อความชื้นของเมล็ดข้าวเปลือกเริ่มต้นที่ผ่านการแช่อย่างเดียว (เวลาการอบแห้ง 0 นาที) มีค่าต่ำ จะได้ร้อยละต้นข้าวลดลงต่ำกว่าข้าวอ้างอิง (50.2%) และถ้าความชื้นเมล็ดข้าวเปลือกสูงขึ้นตามระยะเวลาการแช่ที่นานขึ้น ร้อยละต้นข้าวจะเพิ่มสูงขึ้นตามไปด้วย ร้อยละต้นข้าวของข้าวเปลือกที่ผ่าน การอบแห้งตามระยะเวลาต่าง ๆ จะสูงขึ้นและค่อนข้างคงที่ (66-68% มาตรฐานแห้ง) ที่ความชื้นสุดท้ายของเมล็ดข้าวเปลือกสูงและจะลดลงอย่างรวดเร็วที่ความชื้นสุดท้ายต่ำกว่า 18-20% มาตรฐานแห้ง เนื่องจากการเกิดเจลาติไนเซชัน สามารถอธิบายได้ดังนี้ ภายในเมล็ดข้าวนั้นประกอบด้วยกลุ่มแป้งและโปรตีนเกาะตัวกันส่วนที่เป็นอมิโลสจะละลายและดูดซับน้ำทำให้เกิดการพองตัวของเม็ดแป้งเมื่อได้รับอุณหภูมิสูงขึ้นและทำให้โครงสร้างของเม็ดแป้งเกิดการเปลี่ยนแปลงแบบผันกลับไม่ได้ เช่นส่วนผลึกหายไป (Crystalline melting) ไม่เห็นลักษณะกากบาท (Loss of birefringence) โดยโมเลกุลจะยึดเกาะเข้าด้วยกันทำให้โครงสร้างแข็งแรงขึ้นสอดคล้องกับงานวิจัยของ Lai, H (2000) รอยร้าวหรือรอยแตกภายในเมล็ดสามารถประสานกันมากขึ้นดังรูปที่ 4 และเมื่อนำมาทำให้แห้งเมล็ดข้าวจะมีลักษณะแข็งใสเหนียวทนต่อการขัด เมื่อนำเมล็ดไปขัดสีจะได้ร้อยละต้นข้าวสูง การเกิดเจลาติไนเซชันมากหรือน้อยขึ้นกับอุณหภูมิ ปริมาณความชื้นในเมล็ดข้าวเปลือก และระยะเวลาที่เหมาะสม ถ้าความชื้นเริ่มต้นสูงจะทำให้ช่วงเวลาการเกิดเจลาทิไนเซชันมากขึ้นส่งผลให้ร้อยละต้นข้าวสูง ซึ่งสอดคล้องกับผลการวิเคราะห์การเกิดเจลาติไนเซชันของข้าวที่



รูปที่ 3 ความสัมพันธ์ของร้อยละความชื้นและร้อยละต้นข้าว ที่เวลาในการแช่และการอบแห้งที่เวลาต่าง ๆ



ก) โครงสร้างของเม็ดสตาร์ชข้าวอ้างอิง



ข) ข้าวที่ผ่านการแช่ 0.5 ชั่วโมง และอบแห้ง 2 นาที

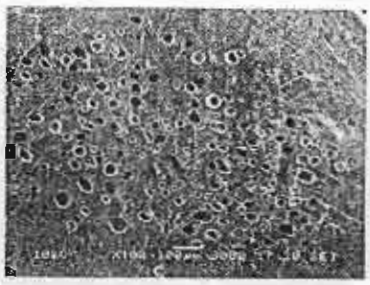


ค) ข้าวที่ผ่านการแช่ 1 ชั่วโมง และอบแห้ง 2 นาที

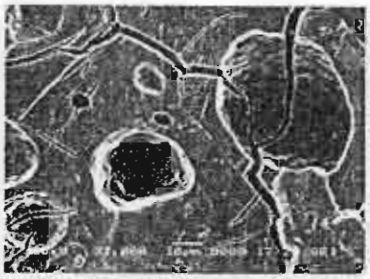


ง) ข้าวที่ผ่านการแช่ 2 ชั่วโมง และอบแห้ง 2 นาที

รูปที่ 4 ลักษณะการเกิดเจลาติไนเซชันของข้าวโดยเครื่อง Scanning electron micrographs



ก) ภาพขยาย X100



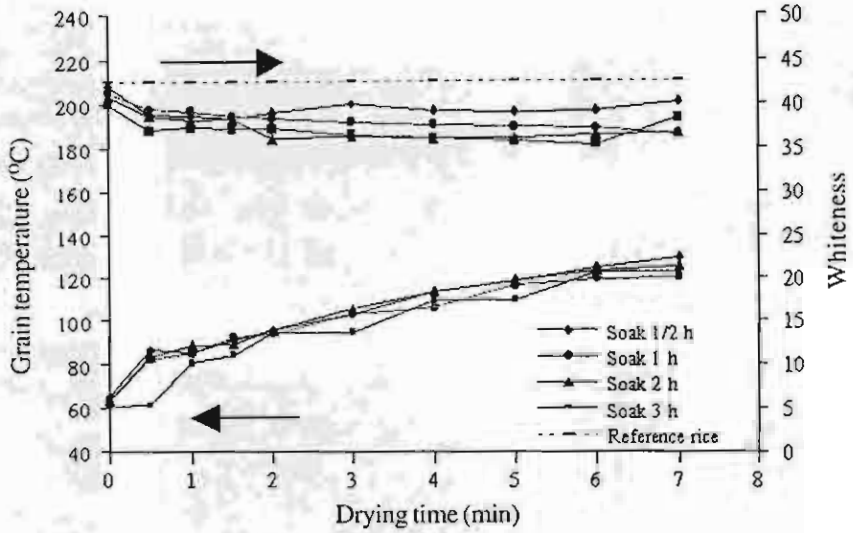
ข) ภาพขยาย X 1000

รูปที่ 5 ลักษณะการเกิดเจลาติไนเซชันของข้าวที่ผ่านการแช่เป็นระยะเวลา 0.5 ชั่วโมง และอบแห้ง 7 นาที โดยเครื่อง Scanning electron micrographs

ตารางที่ 1 ผลการวิเคราะห์การเกิดเจลาติไนเซชันของข้าวโดยใช้เครื่อง DSC

ตัวอย่างข้าว	อุณหภูมิ (°ซ.)			ΔH	Degree of gelatinization
	T_{onset}	T_{peak}	$T_{conclusion}$	(J/g)	
อ้างอิง 15.7% มาตรฐานแห้ง	63.8	69.0	72.3	3.32	0
แช่ 0.5 ชั่วโมง	63.7	68.8	70.9	3.27	1.5
แช่ 1 ชั่วโมง	63.9	68.7	72.2	3.11	6.3
แช่ 2 ชั่วโมง	63.6	68.7	72.3	2.9	12.6
แช่ 3 ชั่วโมง	63.7	68.7	72.0	2.62	21.1
แช่ 0.5 ชั่วโมง อบแห้ง 2 นาที	63.8	68.8	71.9	2.28	31.3
แช่ 1 ชั่วโมง อบแห้ง 2 นาที	63.9	68.8	72.0	1.29	61.1
แช่ 2 ชั่วโมง อบแห้ง 2 นาที	68.2	68.8	71.7	0.73	78.0
แช่ 3 ชั่วโมง อบแห้ง 2 นาที	68.2	68.8	71.7	0.38	88.5

ผ่านกระบวนการโดยเครื่อง DSC ดังตารางที่ 1 ด้วยเหตุนี้จึงทำให้ข้าวที่แช่ระยะเวลานานขึ้นมีร้อยละต้นข้าวสูงขึ้น จากการทดลองใช้อุณหภูมิน้ำแช่เริ่มต้น 80 °ซ. ซึ่งสูงกว่าอุณหภูมิการเกิดเจลาติไนเซชันของข้าวขาวดอกมะลิ 105 ซึ่งมีอุณหภูมิการเกิดเจลาติไนเซชันประมาณ 64-68 °ซ. (ศูนย์วิจัยข้าวปทุมธานี, 2542) ในกรณีที่ร้อยละต้นข้าวที่เวลาการแช่ 0.5 และ 1 ชั่วโมง ต่ำกว่าข้าวอ้างอิง เนื่องจากช่วงเวลาในการเกิดเจลาติไนซ์สั้นทำให้ได้ร้อยละต้นข้าวลดลง และสาเหตุที่ความชื้นสุดท้ายต่ำที่เวลาการอบแห้งต่างๆ ได้ร้อยละต้นข้าวลดลงต่ำมาก เนื่องจากใช้เวลาการอบแห้งนานเกินไปทำให้ปริมาณความร้อนส่วนใหญ่ที่ใช้ในการระเหยน้ำถูกนำไปเพิ่มอุณหภูมิแก่เมล็ดข้าวเปลือก เมล็ดข้าวจึงมีอุณหภูมิสูงขึ้นมากเกิน โครงสร้างเม็ดแป้งเกิดการเปลี่ยนแปลงถึงขั้นเกิดเป็นโพรงอากาศลักษณะคล้ายการเดือดของน้ำแป้งขึ้นภายในเมล็ดข้าวดังรูปที่ 5 ทำให้เกิดการแตกหักได้ง่าย และอีกประการหนึ่งเมื่อนำเมล็ดข้าวเปลือกออกจากห้องอบแห้ง เมล็ดข้าวเปลือกมีอุณหภูมิสูงและเกิดการเย็นตัวอย่างรวดเร็ว จึงเกิดความแตกต่างของอุณหภูมิและความชื้นที่

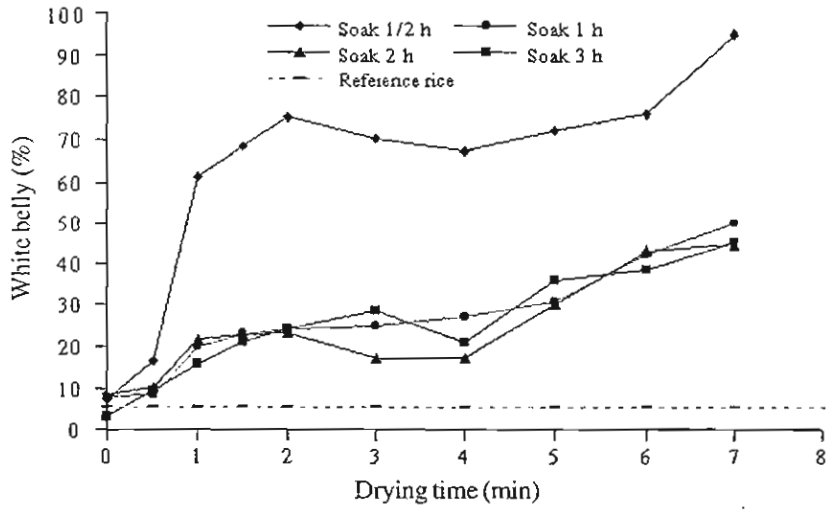


รูปที่ 6 ความสัมพันธ์ของอุณหภูมิเมล็ดข้าวเปลือกและความขาวของข้าวสาร ที่เวลาในการแช่และการอบแห้งที่เวลาต่าง ๆ

บริเวณผิวและแกนกลางของเมล็ด ทำให้เกิดความเค้นขึ้นภายในเมล็ดนำไปสู่การเกิดรอยร้าว เมื่อนำไปขัดสีจึงได้ร้อยละต้นข้าวลดลง

3. ความขาวของข้าวสาร

ความขาวของข้าวสารโดยทำการทดลอง 2 ซ้ำได้ผลการทดลองคล้ายกันแสดงผลดังรูปที่ 6 พบว่าข้าวที่ผ่านการแช่และการอบแห้งจะมีความขาวลดลงต่ำกว่าข้าวอ้างอิงในทุกเงื่อนไขการทดลอง การเปลี่ยนแปลงความขาวของข้าวดังกล่าวเป็นผลเนื่องมาจากสารประกอบที่อยู่ในเมล็ดข้าวเปลือกเกิดการเปลี่ยนแปลงทางเคมีโดยเกิดปฏิกิริยาสีน้ำตาล (Browning reaction) แบบเมลลาร์ด โดยมีความร้อนเป็นตัวเร่งปฏิกิริยา เมื่อน้ำตาลที่มีอยู่ในข้าวได้รับความร้อน ซึ่งความร้อนจะไปทำให้พันธะระหว่างโมเลกุลภายในน้ำตาลหลุดออกจากกันกลายเป็นน้ำตาลโมเลกุลต่ำและเมื่อให้ความร้อนต่อไป พันธะภายในน้ำตาลโมเลกุลต่ำจะหลุดออกจากกันและเกิดเป็นสารประกอบคีโตนขึ้นมา ซึ่งสารดังกล่าวเป็นสารที่ทำให้เกิดสีคล้ำในเมล็ดข้าว และสีน้ำตาลอาจมีส่วนเกิดจากสีของเปลือกข้าวซึมแพร่เข้าสู่เนื้อเมล็ดขณะแช่และติดแน่นขณะอบแห้ง ระหว่างการอบแห้งด้วยไอน้ำร้อนยวดยิ่งจะมีช่วงการเกิดการควบแน่นของไอน้ำอุณหภูมิของเมล็ดต่ำกว่าจุดเดือดของน้ำ และอุณหภูมิของเมล็ดข้าวเปลือกจะเพิ่มขึ้นอย่างรวดเร็ว ทำให้เกิดความแตกต่างของ



รูปที่ 7 ความสัมพันธ์ของปริมาณ White belly ของข้าวสาร ที่เวลาในการแช่และการอบแห้งที่เวลาต่าง ๆ

ความดันไอภายในเมล็ดข้าวเปลือก ความดันไอภายนอกเมล็ดจะสูงกว่าภายในเมล็ด จึงเกิดการแพร่ความชื้นเข้าภายในเมล็ดและพาเอาสารประกอบและสารสีของข้าวเปลือกและข้าวกล้องที่อยู่บริเวณผิวซึมแพร่เข้าไปภายในเมล็ด ด้วยเหตุดังกล่าวจึงทำให้ข้าวมีความขาวลดต่ำลง หรือมีสีเหลืองเพิ่มขึ้นตามระยะเวลาที่ใช้ในการแช่และอบแห้ง

4. ร้อยละ White belly

ร้อยละ White belly โดยทำการทดลอง 2 ซ้ำได้ผลการทดลองคล้ายกัน แสดงผลดังรูปที่ 7 พบว่าปริมาณ White belly ของข้าวสารเพิ่มขึ้นมากกว่าข้าวอ้างอิงในทุกเงื่อนไขการทดลอง ข้าวที่ผ่านการแช่ระยะเวลาสั้นและอบแห้งระยะเวลานานจะมีแนวโน้มการเพิ่มในปริมาณที่สูงขึ้นกว่าข้าวที่แช่ระยะเวลาการแช่มากขึ้นและระยะเวลาการอบแห้งน้อยลง

จากคุณสมบัติของข้าวที่ใช้ในการทดลองคือ ข้าวขาวดอกมะลิ 105 เป็นพันธุ์ข้าวที่มีปริมาณอมิโลสต่ำ จากการทดลองพบว่าปริมาณ White belly เพิ่มขึ้น สามารถอธิบายได้คือ White belly เกิดจากการหักเหของแสงที่ส่องผ่านเมล็ดข้าวทำให้มองเห็นมีลักษณะขาวขุ่นตรงกลางเมล็ดข้าวสาร (Kim et al., 2000) เนื่องจากอมิโลเพกตินมีโครงสร้างของโมเลกุลเป็นกิ่งก้านสาขา เมื่อเกิดการพองตัวเป็นเจลโมเลกุลซ้อนทับกันแสงที่สองผ่านจึงเกิดการหักเหทำให้มองเห็นเมล็ดข้าวมีลักษณะขาวขุ่น ส่วนอมิโลสโครงสร้างของโมเลกุลเป็นเส้นตรงการหักเหของแสงจึงน้อยกว่า ดังนั้นในช่วงที่ใช้ระยะเวลาการอบแห้งที่มากขึ้น ข้าวที่มีปริมาณอมิโลสต่ำเมื่อเกิดเจลาติไนเซชันภายในเมล็ดขึ้น ปริมาณอมิโลสไม่สามารถไปแทรกอุดตามโครงสร้างของอมิโลเพกตินภายในเมล็ดได้ทั่วถึง และนอกจากนี้โครงสร้างของเม็ดแป้งเปลี่ยนแปลงมีลักษณะเกิดเป็นโพรงอากาศคล้ายการเดือดของน้ำแป้ง (รูปที่ 5) ทำให้เกิดการหักเหของแสงมากขึ้น จึงมีปริมาณ White belly เพิ่มมากขึ้นตามไปด้วย

ตารางที่ 2 ผลการทดสอบความแข็งของข้าวสุก (Hardness) ของข้าวขาวดอกมะลิ 105 ที่ใช้เวลาในการแช่ข้าว และระยะเวลาในการอบแห้งต่าง ๆ

ระยะเวลาการอบแห้ง (นาที)	ความแข็งของข้าวสุก (Hardness), (นิวตัน) ข้าวที่แช่ระยะเวลาต่าง ๆ				
	0 ชั่วโมง	0.5 ชั่วโมง	1 ชั่วโมง	2 ชั่วโมง	3 ชั่วโมง
0	108.38 a	104.7 a	102.7 a	112.8 a	107.0 a
0.5	-	106.9 a	105.2 a	117.1 a	106.6 a
2	-	112.8 a	107.3 a	119.3 a	117.0 a
3	-	115.6 a	115.4 a	119.1 a	117.8 a
4	-	117.8 a	114.7 a	122.1 a	114.1 a

หมายเหตุ: ตัวเลขที่ตามด้วยอักษรที่เหมือนกันแสดงว่าไม่มีความแตกต่างกันทางสถิติที่ระดับความเชื่อมั่น 95%

ตารางที่ 3 ผลการทดสอบการยึดเกาะตัวของข้าวสุก (Stickiness) ของข้าวขาวดอกมะลิ 105 ที่ใช้วลาในการแช่ข้าว และระยะเวลาในการอบแห้งต่าง ๆ

ระยะเวลาการอบแห้ง (นาที)	ความแข็งของข้าวสุก (Hardness), (นิวตัน) ข้าวที่แช่ระยะเวลาต่าง ๆ				
	0 ชั่วโมง	0.5 ชั่วโมง	1 ชั่วโมง	2 ชั่วโมง	3 ชั่วโมง
0	18.8 fdec	26.1 a	22.0 bac	24.0 ba	25.1 ba
0.5	-	13.2 b	20.0 bdac	16.6 gfdeh	21.0 bdac
2	-	18.5 gfdec	14.5 gfh	15.9 gfeh	16.5 gfdeh
3	-	14.0 gfh	14.4 gfh	14.9 gfh	13.9 gfh
4	-	13.1 gh	16.4 gfdeh	14.6 gfh	12.6 h

หมายเหตุ: ตัวเลขที่ตามด้วยอักษรที่เหมือนกันแสดงว่าไม่มีความแตกต่างกันทางสถิติที่ระดับความเชื่อมั่น 95%

5. ความแข็งของข้าวสุก และการยึดเกาะตัวของข้าวสุก

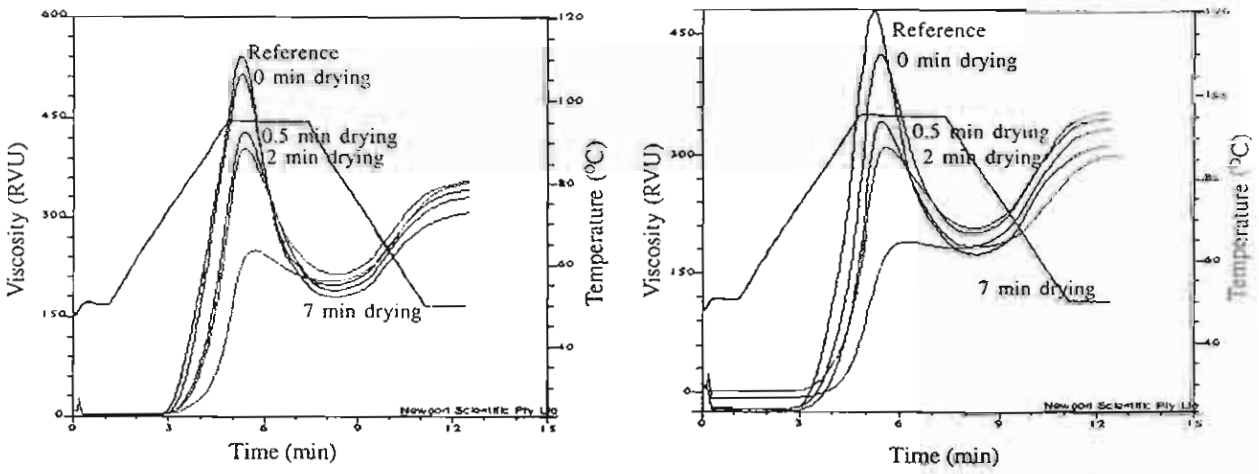
จากการทดสอบหาค่าความแข็ง (Hardness) และค่าการยึดเกาะตัว (Stickiness) ของข้าวสุก โดยใช้ข้าวสารที่ได้จากการทดลองมาหุงและทำการวัดโดยใช้เครื่อง Texture Analyzer โดยทำการทดลอง 2 ซ้ำ ได้ผลการทดลองคล้ายกันแสดงผลดังตารางที่ 2 และ 3 จากการทดสอบพบว่า ความแข็งของข้าวสุก (Hardness) ที่ผ่านการแช่และอบแห้งไม่มีความแข็งเพิ่มขึ้นจากข้าวอ้างอิง อย่างมีนัยสำคัญ (ที่ระดับความเชื่อมั่น 95%) แรงที่ใช้ในการยึดเกาะตัวของข้าวสุก (Stickiness) ที่ผ่านการแช่และอบแห้งจะลดลงอย่างมีนัยสำคัญ (ที่ระดับความเชื่อมั่น 95%) เมื่อเทียบกับข้าวอ้างอิง นั่นแสดงว่าข้าวสุกมีความเหนียวลดลงหรือมีความร่วนมากขึ้น ความร่วนจะเพิ่มขึ้นเมื่อใช้ระยะเวลาในการอบแห้งนานขึ้น ส่วนระยะเวลาที่ใช้ในการแช่ไม่มีอิทธิพลอย่างชัดเจนต่อการยึดเกาะตัวของข้าวสุก

การแช่และอบแห้งด้วยเทคนิคฟลูอิไดซ์เบดโดยมีไอน้ำร้อนยวดยิ่งเป็นตัวกลาง จะมีผลทำให้ข้าวสุกแข็งขึ้น และมีความร่วนมากขึ้นเมื่อใช้เวลาในการอบแห้งนานขึ้น ทั้งนี้เป็นผลเนื่องมาจากการเกิดเจลาติไนเซชัน อมิโลสจะละลายน้ำและดูดน้ำได้มาก ทำให้เกิดการพองตัวขึ้น และเมื่อนำมาอบแห้งจะทำให้สตาร์ชที่เป็นเจลแล้วจัดเรียงตัวกันจับกับโปรตีนและไขมัน ทำให้เมล็ดแข็งแรงขึ้น เมื่อนำมาหุงทำให้ความสามารถในการดูดซับน้ำและละลายน้ำลดลง มีผลทำให้ข้าวสุกที่ได้มีความแข็งและความร่วนมากขึ้น

6. ค่าความหนืดเมื่อวิเคราะห์ด้วยเครื่อง Rapid Visco Analyzer (RVA)

จากการศึกษาความหนืดของน้ำแป้งของข้าวขาวดอกมะลิ 105 โดยเครื่อง RVA ของข้าวที่ผ่านการแช่และอบแห้งที่ระยะเวลาต่างๆ จะให้กราฟที่มีค่าอุณหภูมิที่แป้งเริ่มพองตัว (Pasting temperature), ความหนืดสูงสุด (Peak viscosity), ความหนืดสุดท้าย (Final viscosity) และค่าความคงตัวของแป้งสุก (Setback) แตกต่างกันโดยทำการทดลอง 2 ซ้ำ ได้ผลการทดลองคล้ายกัน แสดงผลดังรูปที่ 8 ในช่วงแรกเม็ดแป้งกระจายตัวในน้ำที่อุณหภูมิ 50 °ซ. อุณหภูมิยังไม่เพียงพอที่ทำให้เม็ดแป้งพองตัว ความหนืดจึงต่ำ เมื่อให้ความร้อนถึงอุณหภูมิที่แป้งเริ่มพองตัว เม็ดแป้งดูดซับน้ำแล้วพองตัวขึ้น ทำให้ความหนืดเพิ่มขึ้น ค่าอุณหภูมิที่แป้งเริ่มพองตัวของข้าวที่ผ่านการแช่และการอบแห้ง มีค่าสูงกว่าข้าวอ้างอิง และสูงขึ้นเมื่อใช้เวลาในการอบแห้งเพิ่มขึ้น ในขณะที่ระยะเวลาในการแช่ไม่มีอิทธิพลอย่างชัดเจนต่ออุณหภูมิที่แป้งเริ่มพองตัว

ความหนืดสูงสุด เป็นจุดที่เม็ดแป้งพองตัวเต็มที่ ถ้ามีค่าสูงแสดงว่าเม็ดแป้งมีความสามารถในการดูดซับน้ำได้ดี ทำให้แป้งเกิดการพองตัวเป็นผลให้ค่าความหนืดสูงขึ้น ความหนืดสูงสุดของข้าวที่ผ่านการแช่และอบแห้งมีค่าต่ำกว่าข้าวอ้างอิง และลดต่ำลงเมื่อใช้เวลาในการอบแห้งเพิ่มขึ้น ที่เป็นเช่นนี้เนื่องมาจากข้าวที่ผ่านการแช่และอบแห้งได้เกิดการเจลาติไนซ์มาบางส่วนแล้ว (ดังตารางที่ 1) โดยข้าวที่ผ่านการแช่จะมีความชื้นสูงเมื่อได้รับความร้อนจากการอบแห้งทำให้เม็ดแป้งที่ถูกน้ำเกิดการพองตัวและถูกทำให้สุก เมื่อนำมาวัดความหนืดทำให้ความสามารถในการดูดซับน้ำของแป้งนั้นลดลงเกิดการพองตัวได้น้อยลง ส่งผลให้ค่าความหนืดสูงสุดที่วัดได้มีค่าลดลง และต้องใช้อุณหภูมิสูงขึ้นเพื่อให้เกิดการพองตัวอีก



ก) แช่เป็นระยะเวลา 0.5 ชั่วโมงและอบแห้งที่เวลาต่างๆ

ข) แช่เป็นระยะเวลา 3 ชั่วโมงและอบแห้งที่เวลาต่างๆ

รูปที่ 8 ความหนืดของแป้งจากเครื่อง RVA

ความหนืดสุดท้าย ที่เกิดขึ้นคือ ความหนืดเมื่อแป้งถูกทำให้เย็นหลังการเกิดเจลาติไนซ์ ส่วนของอมิโลสจะเกิดโครงสร้างขึ้นใหม่ในลักษณะโครงร่างสามมิติ ทำให้ความหนืดเพิ่มขึ้น เจลแข็งขึ้น ค่าความหนืดสุดท้าย ของข้าวที่ผ่านการแช่และอบแห้งมีค่าสูงกว่าข้าวอ้างอิง และมีแนวโน้มสูงขึ้นเมื่อใช้เวลาในการอบแห้งเพิ่มขึ้น

ค่าความคงตัวของแป้งสุก เป็นผลต่างระหว่างความหนืดสุดท้าย กับ ความหนืดต่ำสุด (Trough) ซึ่งมีความสัมพันธ์กับลักษณะเนื้อสัมผัสของอาหารที่มีสตาร์ชเป็นองค์ประกอบหลัก เป็นตัวบ่งชี้ลักษณะของผลิตภัณฑ์ที่ความหนืดหรือ เจลซึ่งเกิดขึ้นหลังจากการหุงต้มและทำให้เย็นลง ถ้าค่าความคงตัวของแป้งสุกที่ได้มีค่าต่ำแสดงว่าข้าวสุกนั้นมีความแข็งกระด้างต่ำหลังจากการหุงสุกและปล่อยให้ข้าวเย็นตัวลง จากการทดลองพบว่าข้าวที่ผ่านการแช่และการอบแห้งมีค่าความคงตัวของแป้งสุกลดลงตามระยะเวลาการอบแห้ง

7. การเกิดเจลาติไนเซชันของข้าวโดยใช้เครื่อง Differential Scanning Calorimeter (DSC)

การวิเคราะห์ค่าเอนทัลปีที่เปลี่ยนแปลง (ΔH) แสดงผลดังตารางที่ 1 จะเห็นว่า T_{onset} หรืออุณหภูมิเริ่มต้นในการเกิดเจลาติไนซ์ของข้าว, T_{peak} หรืออุณหภูมิสูงสุดในการเกิดเจลาติไนซ์ และ $T_{conclusion}$ หรืออุณหภูมิสุดท้ายในการเกิดเจลาติไนซ์ของข้าวที่ผ่านการแช่และอบแห้งสูงขึ้นจากข้าวอ้างอิง ซึ่งให้ผลสอดคล้องกับผลที่ได้จากการวัดความหนืดด้วยเครื่อง RVA แสดงให้เห็นว่าข้าวที่ผ่านการแช่และอบแห้งได้เกิดการเจลาติไนซ์ไปบางส่วนแล้ว ค่า ΔH หรือพลังงานที่เปลี่ยนแปลงระหว่างการเกิดเจลาติไนซ์ จะแสดงถึงการใช้พลังงานความร้อนในการทำให้ข้าวสุก จากตารางที่ 1 จะเห็นว่าข้าวอ้างอิงมีค่า ΔH มากกว่าข้าวที่ผ่านการแช่และเมื่อนำข้าวที่ผ่านการแช่ที่เวลาต่างๆไปผ่านการอบแห้งที่เวลา 2 นาที ค่า ΔH จะลดลงตามระยะเวลาการแช่เช่นกันนั่น แสดงถึงว่าข้าวที่ผ่านการแช่ ได้เกิดการเจลาติไนซ์ไปบางส่วนแล้ว จึงใช้พลังงานความร้อนในการทำให้ข้าวสุกน้อยลง ข้าวที่ผ่านการแช่เป็นระยะเวลา 3 ชั่วโมง มีค่า ΔH น้อยกว่าข้าวที่ผ่านการแช่เป็นระยะเวลา 0.5 ชั่วโมง แสดงให้เห็นว่าข้าวที่ผ่านการแช่เป็นระยะเวลายาวนานจะเกิดการเจลาติไนซ์มากกว่าข้าวที่ผ่านการแช่เป็นระยะเวลาสั้นซึ่งเมื่อนำมาคิดเป็นระดับของเจลาติไนเซชัน (Degree of gelatinization) ข้าวที่แช่ 0.5 ชั่วโมงจะมีค่า 1.5% และข้าวที่แช่ 3 ชั่วโมงจะมีค่า 21% และเมื่อผ่านการอบแห้งที่ระยะเวลา 2 นาที ข้าวที่แช่ 0.5 ชั่วโมงจะมีค่า 31.3% และข้าวที่แช่ 3 ชั่วโมงจะมีค่า 88.5% จากการวิเคราะห์การเกิดเจลาติไนเซชันของข้าวโดยใช้เครื่อง DSC นี้เป็นการยืนยันว่าข้าวที่แช่นานกว่า (แช่ 3 ชั่วโมง) เกิดการเจลาติไนเซชันมากกว่าข้าวที่ผ่านการแช่เป็นระยะเวลาน้อยกว่า (แช่ 0.5 ชั่วโมง) ที่ระยะเวลาในการอบแห้งค่าเดียวกัน

สรุปผลการทดลอง

จากการศึกษาการรวมกระบวนการผลิตของการนึ่งและการอบแห้งข้าวนึ่งสำหรับข้าวหอมโดยการอบแห้งด้วยเครื่องฟลูอิไดซ์เบดมีไอน้ำร้อนยวดยิ่งเป็นตัวกลาง ร้อยละต้นข้าวเพิ่มมากขึ้นเมื่อใช้ระยะเวลาการแช่และอบแห้งนานขึ้น ซึ่งได้ต้นข้าวสูง 65-67% ที่เวลาการอบแห้ง 1.5-3 นาที และลดลงเมื่อใช้เวลาการอบแห้งมากกว่า 3 นาทีขึ้นไป เมื่อใช้เวลาในการอบแห้งนานความร้อนที่เพิ่มขึ้นเป็นตัวเร่งปฏิกิริยาการเกิดสีน้ำตาลของข้าวจึงส่งผลให้ความขาวของข้าวลดลงตามการเพิ่มขึ้นของระยะเวลาการแช่และการอบแห้ง เมื่อเวลาในการอบแห้งนานขึ้นทำให้ช่วงเวลาการเกิดเจลาติไนเซชันมากขึ้น แต่เนื่องจากพันธุ์ข้าวที่ใช้ทดลองเป็นพันธุ์ข้าวที่มีอมิโลสต่ำ ทำให้อมิโลสไม่สามารถอุดตามรอยแตกร้าวได้ทั่วถึงส่งผลทำให้ปริมาณ White belly เพิ่มมากขึ้นในทุกเงื่อนไขการทดลอง การทดสอบเนื้อสัมผัสของข้าวสุก เวลาอบแห้งที่เพิ่มขึ้นมีผลทำให้ข้าวสุกมีความแข็งและร่วนมากขึ้น เนื่องจากการเกิด เจลาติไนเซชัน ทำให้ความสามารถในการดูดซับน้ำและละลายน้ำลดลง จากการศึกษาความหนืดของแป้งโดยเครื่อง RVA เวลาอบแห้งที่เพิ่มขึ้นทำให้อุณหภูมิที่แป้งเริ่มพองตัว (Pasting temperature) มีค่าสูงขึ้น แต่ความหนืดสูงสุด (Peak viscosity) ลดต่ำลงเนื่องจากการเกิดเจลาติไนเซชันที่เพิ่มขึ้น ความหนืดสุดท้าย (Final viscosity) มีค่าลดลงตามเวลาอบแห้งที่เพิ่มขึ้นและค่าค่าความคงตัวของแป้งสุก (Setback) ต่ำลงตามเวลาการอบแห้งด้วย และจากการวิเคราะห์การเกิดเจลาติไนเซชันของข้าวด้วยเครื่อง DSC เป็นการยืนยันว่าข้าวที่แช่และอบแห้งที่ระยะเวลานานกว่าจะเกิดการเจลาทิไนเซชันมากกว่า โดยมีระดับของเจลาติไนเซชัน (Degree of gelatinization) สูงสุดเท่ากับ 88.5% ที่ระยะเวลาการแช่ 3 ชั่วโมงและอบแห้ง 2 นาที

คำขอบคุณ

ขอขอบคุณสำนักงานกองทุนสนับสนุนการวิจัยที่ให้การสนับสนุนอย่างต่อเนื่อง

เอกสารอ้างอิง

ศูนย์วิจัยข้าวปทุมธานี, กรมวิชาการเกษตร, 2542, การวิเคราะห์คุณภาพข้าวหอมมะลิทางเคมี, ศูนย์วิจัยข้าวปทุมธานี สถาบันวิจัยข้าว กรมวิชาการเกษตร, 70 หน้า

Bhattacharya, S., 1996, Kinetics on Colour Changes in Rice due to Parboiling , J. of Food Engineering, Vol. 29 pp. 99-106.

Kar, N., Jain, R.K., Srivastav. P.P., 1999, Parboiling of Dehusked Rice, J. of Food Engineering, Vol. 9, pp.17-22.

Kim, S.S., Lee, S.E., Kim, O.W., Kim, D.C., 2000, Physicochemical Characteristics of Chalky Kernels of Cook

Rice, Cereal Chem., Vol.77, pp. 376-379.

Lai, H., 2000, Effects of Hydrothermal Treatment on the Physicochemical Properties of Pregelatinized Rice

Flour, Food Chemistry, Vol. 72, pp. 455-463.

Rordprapat, W., Soponronnarit, S., Nathakaranakule, A., Tia, W., 2002, Comparative Study of Fluidised Bed

Paddy Drying Using Hot Air and Superheated Steam, Proceeding of International Conference on

Innovations in Food processing Technology and Engineering, 11-13 December 2002, AIT Bangkok,Thailand, pp. 453-466.

Taechapairoj, C., Dhuchakallaya, I., Soponronarit, S., Wetchacama, S., and Prachayawarakorn, S., 2003, Superheated Steam Fluidised Bed Paddy Drying , Journal of food Engineering , pp 67-73.

Toshinori, K., Bhattacharya, K.R., and Ali, S.Z., 1993, Effect of Processing Conditions on the Color Intensity of Parboiled Rice, J. of Soc of Agri. Struc. Japan, Vol. 20, No. 1, pp, 153-160.

he Journal of the Royal Institute of Thailand
Vol. 30 No. 1 Jan.-Mar. 2005

การผลิตข้าวกล้องนึ่งด้วยเทคนิคฟลูอิไดเซชันโดยใช้ไอน้ำร้อนยวดยิ่ง

สมชาติ โสภณรณฤทธิ์[๑]
ราชบัณฑิต สำนักวิทยาศาสตร์
ราชบัณฑิตยสถาน
อธิคม จิรจินดาเลิศ[๒]
อดิศักดิ์ นาถกรณกุล[๓]
ชัยยงค์ เตชะไพโรจน์[๔]

บทคัดย่อ

กระบวนการผลิตข้าวนึ่งในปัจจุบันใช้ข้าวเปลือกเป็นวัตถุดิบในการผลิตซึ่งใช้ระยะเวลานานและสิ้นเปลืองพลังงาน ดังนั้น งานวิจัยนี้จึงมีแนวคิดที่จะลดระยะเวลาในการผลิตข้าวนึ่งโดยการนึ่งข้าวกล้องด้วยเทคนิคฟลูอิไดเซชันโดยใช้ไอน้ำร้อนยวดยิ่ง ผู้วิจัยได้ศึกษาอิทธิพลของระยะเวลาในการแช่ อุณหภูมิไอน้ำร้อนยวดยิ่ง และความสูงเบดที่มีผลต่อคุณภาพข้าวในด้านปริมาณต้นข้าว ความขาวของข้าวสาร white belly และความหนืดของแป้งข้าว และได้ทดลองโดยใช้ข้าวกล้องที่มีความชื้นเริ่มต้นก่อนแช่ร้อยละ ๑๒.๘ มาตรฐานแห้ง แช่ในน้ำที่อุณหภูมิ ๗๐ องศาเซลเซียส เป็นระยะเวลา ๐.๕ - ๒ ชั่วโมง นำมาอบแห้งที่อุณหภูมิไอน้ำร้อนยวดยิ่ง ๑๒๐ - ๑๖๐ องศาเซลเซียส ความเร็วของไอน้ำร้อนยวดยิ่งเท่ากับ ๓.๙ เมตรต่อวินาที และความสูงเบด ๘ - ๑๒ เซนติเมตร ผลการศึกษาแสดงว่า สามารถนึ่งข้าวกล้องที่ผ่านการแช่ ๑ ชั่วโมงด้วยไอน้ำร้อนยวดยิ่งที่อุณหภูมิ ๑๔๐ องศาเซลเซียส เจลเกิดขึ้นพร้อม ๆ กับความชื้นของข้าวกล้องที่ลดลง ความชื้นหลังการนึ่งข้าวกล้องด้วยไอน้ำร้อนยวดยิ่งที่เหมาะสมมีค่าประมาณร้อยละ ๒๘ มาตรฐานแห้ง โดยที่ร้อยละต้นข้าวยังสูงอยู่ คุณภาพด้านความขาวและ white belly อยู่ในเกณฑ์ที่ยอมรับได้ ถ้าลดความชื้นต่ำกว่านี้ร้อยละต้นข้าวจะลดลงอย่างรวดเร็ว ในขณะที่ความขาวของข้าวสารจะลดลงอย่างรวดเร็วเมื่อความชื้นต่ำกว่าร้อยละ ๑๘ มาตรฐานแห้ง สำหรับ white belly จะลดลงเมื่อเวลาการอบแห้งเพิ่มขึ้น จากการวิเคราะห์สมบัติความหนืดของแป้งเป็น peak viscosity, breakdown viscosity และ setback viscosity พบว่ามีค่าต่ำกว่าข้าวก่อนนึ่ง

คำสำคัญ : **ข้าวนึ่ง, คุณภาพ, ฟลูอิไดซ์เบด, อบแห้ง**

๑. บทนำ

ประเทศไทยเป็นประเทศผลิตข้าวที่สำคัญ ข้าวจึงถือเป็นสินค้าผลผลิตทางการเกษตรที่มีมูลค่าการส่งออกทางเศรษฐกิจเป็นอันดับแรก ๆ ของประเทศ เนื่องจากความก้าวหน้าทางด้านเทคโนโลยี ทำให้ประเทศผู้ส่งออกข้าวต่าง ๆ พยายามที่จะใช้เทคโนโลยีมาพัฒนาคุณภาพของข้าวให้มีคุณภาพสูงกว่าคู่แข่ง ในขณะที่ใช้ต้นทุนการผลิตต่อตันต่ำที่สุด ดังนั้น การพัฒนาผลิตภัณฑ์ข้าว เช่น ข้าวนึ่ง ที่กำลังเป็นที่ต้องการของผู้บริโภคมากขึ้นในขณะนี้ จะช่วยให้มีส่วนแบ่งทางการตลาดประเภทข้าวมากขึ้น ข้าวนึ่ง

[๑] ศาสตราจารย์ประจำคณะพลังงานและวัสดุ มหาวิทยาลัยเทคโนโลยีพระจอมเกล้าธนบุรี กรุงเทพฯ
[๒] บัณฑิตปริญญาโท คณะพลังงานและวัสดุ มหาวิทยาลัยเทคโนโลยีพระจอมเกล้าธนบุรี กรุงเทพฯ
[๓] ผู้ช่วยศาสตราจารย์ประจำคณะพลังงานและวัสดุ มหาวิทยาลัยเทคโนโลยีพระจอมเกล้าธนบุรี กรุงเทพฯ
[๔] อาจารย์ประจำคณะวิศวกรรมศาสตร์และเทคโนโลยีอุตสาหกรรม มหาวิทยาลัยศิลปากร สนามจันทร์ นครปฐม

คุณภาพดีของไทยยังมีโอกาสพัฒนาได้อีกมาก เพราะต้นทุนข้าวเปลือกไทยราคาถูกกว่าต่างประเทศ ข้าวนึ่งจึงนับเป็นผลิตภัณฑ์ที่ควรได้รับการส่งเสริมและพัฒนาอย่างยิ่ง การทำข้าวนึ่ง (parboiling) เป็นแนวทางหนึ่งที่จะช่วยให้เก็บรักษาข้าวได้นานขึ้น ลดปริมาณข้าวหักระหว่างการขัดสี ทำให้มีปริมาณต้นข้าวสูง ลดการสูญเสียแร่ธาตุอาหารในบางส่วนของเมล็ดข้าวระหว่างการขัดสี

ในปัจจุบัน ผู้บริโภคนิยมรับประทานข้าวกล้องมากขึ้น เพราะให้คุณค่าอาหารทางโภชนาการสูงกว่าข้าวขาว แต่ปัญหาที่สำคัญของข้าวกล้องนั้นคืออายุการเก็บรักษาสั้น คือมีระยะเวลาประมาณ ๓ - ๖ เดือน เกิดกลิ่นหืนได้เร็วกว่าข้าวสารเนื่องจากข้าวกล้องมีปริมาณน้ำมันสูงกว่าข้าวสาร การนึ่งข้าวกล้อง (parboiling of dehusked rice) จึงเป็นการพัฒนาผลิตภัณฑ์ข้าวกล้องให้ดียิ่งขึ้น ช่วยเก็บรักษาข้าวกล้องได้นานขึ้น การผลิตข้าวนึ่งมีขั้นตอนที่สำคัญอยู่ ๓ ขั้นตอน คือ การแช่ (soaking) การนึ่ง (steaming) และการอบแห้ง (drying) โดยเฉพาะการแช่เป็นขั้นตอนที่ใช้เพิ่มความชื้นให้แก่เมล็ดข้าว ในปัจจุบันนิยมแช่ข้าวด้วยน้ำร้อน จะทำให้ความชื้นเข้าไปในเมล็ดข้าว ความร้อนจะทำให้น้ำแพร่เข้าไปในเมล็ดได้อย่างรวดเร็ว ความชื้นนี้ทำให้เม็ดแป้งเกิดการพองตัวจนเพียงพอที่ทำให้เกิดเจลาทิไนเซชันได้ การแช่ข้าวกล้องในน้ำร้อนแล้วปล่อยให้เย็นตัวลงที่อุณหภูมิแวดล้อมเป็นเวลาอย่างน้อย ๒ ชั่วโมง ทำให้น้ำสามารถแพร่ผ่านเข้าไปในแกนของเมล็ดข้าวได้ การนึ่งข้าวกล้องประหยัดพลังงานกว่าการนึ่งข้าวเปลือกถึงร้อยละ ๔๐ เนื่องจากเปลือกข้าวมีค่าการนำความร้อนที่ต่ำ จึงทำให้การถ่ายเทความร้อนเข้าไปในเมล็ดข้าวเปลือกช้ากว่าข้าวกล้อง นอกจากนี้ ยังช่วยลดปัญหาสิ่งสกปรกที่มากับเปลือกข้าวขณะแช่ ลดกลิ่นที่ติดมากับเปลือกข้าว และใช้เวลาในการหุงข้าวเร็วขึ้น[๑] สำหรับการแช่ข้าวเปลือกควรแช่ข้าวที่อุณหภูมิสูงกว่าอุณหภูมิเจลาทิไนเซชันของข้าว เพื่อมิให้เมล็ดข้าวปริแตกและทำให้แป้งบางส่วนละลายไปกับน้ำแช่[๒,๓]

อุณหภูมิและระยะเวลาในการนึ่งมีผลต่อความขาวของข้าว เมื่ออุณหภูมิการนึ่งสูงขึ้นจะได้ร้อยละความขาวของข้าวลดลงและเมื่อระยะเวลาในการนึ่งมากขึ้นทำให้ได้ค่าความขาวของข้าวมีแนวโน้มลดลง[๔,๕] การอบแห้งข้าวเปลือกด้วยไอน้ำร้อนยวดยิ่งโดยเทคนิคฟลูอิไดซ์เบด พบว่าความเร็วต่ำสุดของการเกิดฟลูอิไดเซชันมีค่าเท่ากับ ๒.๖ เมตร/วินาที อุณหภูมิของไอน้ำร้อนยวดยิ่งมีผลต่ออัตราการอบแห้งมากกว่าความสูงเบด และปริมาณต้นข้าวจะขึ้นกับความชื้นสุดท้ายของข้าวเปลือก โดยความชื้นสุดท้ายไม่ควรต่ำกว่าร้อยละ ๑๘ มาตรฐานแห้ง[๖]

ในการเปรียบเทียบการอบแห้งข้าวเปลือกด้วยไอน้ำร้อนยวดยิ่งกับการอบแห้งด้วยอากาศร้อนโดยเทคนิคฟลูอิไดซ์เบด พบว่าร้อยละต้นข้าวของการอบแห้งด้วยไอน้ำร้อนยวดยิ่งมีค่าสูงกว่าการอบแห้งด้วยอากาศร้อน เพราะการอบแห้งด้วยอากาศร้อนนั้นอุณหภูมิของข้าวเปลือกจะเพิ่มขึ้นในขณะเดียวกันก็จะมีการระเหยของน้ำที่เมล็ดข้าวเปลือกด้วย ทำให้ความชื้นในเมล็ดข้าวเปลือกไม่สม่ำเสมอ การเกิดเจลาทิไนเซชันของการอบแห้งด้วยอากาศร้อนจึงไม่สมบูรณ์ทั่วทั้งเมล็ด ข้าวเปลือกที่อบแห้งด้วยไอน้ำร้อนยวดยิ่งจะเกิดเจลาทิไนเซชันได้สมบูรณ์กว่าการอบแห้งด้วยอากาศร้อน นอกจากนี้ การอบแห้งข้าวเปลือกด้วยไอน้ำร้อนยวดยิ่งโดยใช้เทคนิคฟลูอิไดซ์เบดจะได้ค่าความขาวของข้าวต่ำกว่าอบแห้งด้วยอากาศร้อน เนื่องจากการควบแน่นของไอน้ำที่บริเวณผิวของข้าวเปลือก ทำให้สีของรำถูกดูดซึมเข้าไปในเมล็ดข้าวและพบว่าปริมาณ white belly ขึ้นกับความชื้นเริ่มต้นของข้าวเปลือก โดยปริมาณ white belly จะน้อยเมื่อความชื้นเริ่มต้นของข้าวเปลือกสูงและยังพบว่าข้าวเปลือกที่ผ่านการอบแห้งด้วยไอน้ำร้อนยวดยิ่งจะมีลักษณะคล้ายข้าวนึ่ง[๖,๗,๘]

วัตถุประสงค์ของงานวิจัยนี้เพื่อศึกษาแนวทางที่เหมาะสมของการทำข้าวนึ่งจากข้าวกล้องด้วยไอน้ำร้อนยวดยิ่งโดยเทคนิคฟลูอิไดซ์เบดและสมบัติของข้าวทางด้านกายภาพ ซึ่งประกอบด้วย ปริมาณต้นข้าว ความขาว และ white belly ตลอดจนสมบัติทางด้านเคมีกายภาพ โดยการวัดสมบัติความหนืดของแป้งข้าว โครงสร้างระดับจุลภาค และเปรียบเทียบกับการอบแห้งด้วยอากาศร้อนที่ภาวะเดียวกัน

๒. อุปกรณ์และวิธีการทดลอง

เครื่องอบแห้งที่ใช้ในการทดลอง

ศึกษาในงานวิจัยนี้เป็นเครื่องอบแห้งฟลูอิไดซ์เบดแบบงวด โดยมีไอน้ำร้อนยวดยิ่งเป็นตัวกลาง แสดงดังรูปที่ ๑ก ประกอบด้วยห้องอบแห้ง เป็นรูปที่ทรงกระบอก ทำด้วยสเตนเลส ขนาดเส้นผ่านศูนย์กลาง ๑๕ เซนติเมตร สูง ๑๐๐ เซนติเมตร อุปกรณ์ให้ความร้อน (heater) ขนาด ๑๓.๕ กิโลวัตต์ โดยมีเครื่องควบคุมอุณหภูมิแบบ PID มีความถูกต้อง ±๑ องศาเซลเซียส พัดลม (blower) เป็นแบบเหวี่ยงใบพัดโค้งหลัง (backward-curved centrifugal blower) มีมอเตอร์ขนาด ๒.๒ กิโลวัตต์ สามารถปรับความเร็วรอบของพัดลมได้ เครื่องดักฝุ่น (cyclone) เป็นแบบ reverse flow ทำด้วยสเตนเลส เครื่องกำเนิดไอน้ำ (boiler) ออกแบบความดันใช้งานสูงสุด 3.5 bars สามารถผลิตไอน้ำได้ ๓๑ กิโลกรัมต่อชั่วโมง ที่อุณหภูมิ ๑๐๐ องศาเซลเซียส ความดันบรรยากาศ และเครื่องอบแห้งฟลูอิไดซ์เบดแบบงวดโดยมีอากาศร้อนเป็นตัวกลางแสดงดังรูปที่ ๑ข ประกอบด้วยห้องอบแห้งรูปที่ทรงกระบอก ทำด้วยสเตนเลส ขนาดเส้นผ่านศูนย์กลาง ๒๐ เซนติเมตร และสูง ๑๔๐ เซนติเมตร อุปกรณ์ให้ความร้อน ขนาด ๑๒ กิโลวัตต์ โดยมีเครื่องควบคุมอุณหภูมิมีความถูกต้อง ±๑ องศาเซลเซียส พัดลมเป็นแบบเหวี่ยงใบพัดโค้งหลัง มีมอเตอร์ขนาด ๑.๕ กิโลวัตต์ เป็นตัวขับเคลื่อนพัดลม มีลิ้นปีกผีเสื้อที่ทางออกของเครื่องอบแห้งและที่ท่ออากาศเวียนกลับสำหรับใช้ปรับอากาศไหลเวียนกลับ

การเตรียมข้าวกล้องใช้ข้าวเจ้าพันธุ์ชัยนาท ๑ มากะเทาะเปลือกออกจนได้ข้าวกล้อง (เฉพาะต้นข้าวเท่านั้น) ซึ่งมีความชื้นเริ่มต้นร้อยละ ๑๒.๘ มาตรฐานแห้ง เนื่องจากได้มีการทดลองศึกษาอุณหภูมิในการแช่ข้าวที่ ๗๐, ๘๐ และ ๙๐ องศาเซลเซียสด้วย พบว่าข้าวกล้องที่แช่น้ำอุณหภูมิ ๙๐ องศาเซลเซียส มีลักษณะโครงสร้างของเมล็ดข้าวเปลี่ยนไป เกิดการแตกปริของเยื่อหุ้มเมล็ด (pericarp) ส่วนที่แช่น้ำอุณหภูมิ ๘๐ องศาเซลเซียส ให้ผลที่ได้ค่อนข้างใกล้เคียงกับที่อุณหภูมิ ๗๐ องศาเซลเซียส ดังนั้น ใช้อุณหภูมิของน้ำที่ใช้แช่ข้าวกล้อง ๗๐ องศาเซลเซียส ระยะเวลาในการแช่ ๑/๒ - ๒ ชั่วโมง แล้วจึงระบายน้ำแช่ทิ้งและปล่อยให้ถังแช่ข้าวกล้องเย็นตัวลงที่อุณหภูมิแวดล้อม (tempering) เป็นเวลา ๑/๒ ชั่วโมง ก่อนจะนำข้าวกล้องไปทดลองอบแห้ง ในการอบแห้งได้ใช้อุณหภูมิไอน้ำร้อนยวดยิ่ง ๑๒๐, ๑๔๐ และ ๑๖๐ องศาเซลเซียส ความสูงเบด ๘ - ๑๒ เซนติเมตร เวลาในการอบแห้ง ๐.๕ - ๑๐ นาที และความเร็วของไอน้ำร้อนยวดยิ่งเท่ากับ ๓.๙ เมตรต่อนาที ความดันของระบบเหนือบรรยากาศเล็กน้อย เพื่อป้องกันการรั่วเข้าของอากาศ และเปรียบเทียบกับการอบแห้งด้วยอากาศร้อนที่สภาวะเดียวกัน จากนั้นนำข้าวที่ผ่านการอบแห้งมาปล่อยให้เย็นตัวลงโดยการเป่าด้วยอากาศแวดล้อมจนมีความชื้นสุดท้ายร้อยละ ๑๖ มาตรฐานแห้ง แล้วจึงนำข้าวไปทดสอบคุณภาพต่อไป

การวัดความชื้นได้สุ่มเก็บตัวอย่างข้าวกล้องก่อนและหลังการอบแห้ง นำไปเข้าตู้อบไฟฟ้าที่อุณหภูมิ ๑๐๓ องศาเซลเซียส เป็นเวลา ๗๒ ชั่วโมง ส่วนคุณภาพของข้าวทางกายภาพได้แก่ ร้อยละต้นข้าว ความขาว และร้อยละ white belly ตลอดจนสมบัติทางด้านเคมีกายภาพได้วัดสมบัติความหนืดของแป้งข้าวและโครงสร้างระดับจุลภาคด้วยกล้องจุลทรรศน์อิเล็กตรอนแบบส่องกราด (Scanning Electron Micrographs; SEM, JSM-5600LV/JSM5600 Japan)

- ร้อยละต้นข้าว คือน้ำหนักของต้นข้าวที่ผ่านการอบแห้งหารด้วยน้ำหนักของข้าวกล้อง
- ความขาว วัดได้จากเครื่องวัดความขาวของ Kett model C-300
- ร้อยละ white belly คือ จำนวนข้าวที่เป็นจุดขาวขุ่นทึบแสงเกินกว่าร้อยละ ๕๐ ของเมล็ด จากการสุ่มตัวอย่างของข้าวจำนวน ๑๐๐ เมล็ด
- การวัดสมบัติความหนืดของแป้งข้าว (pasting property) โดยใช้เครื่อง Rapid Visco Analyzer, RVA (Newport Scientific Pty Ltd., Warriewood, Australia) ทำตามวิธีการของ AACC method 61-02[10] โดยนำตัวอย่างแป้งข้าว ๓ กรัม ที่ความชื้นร้อยละ ๑๔ มาตรฐานแห้ง ใส่ผสมกับน้ำกลั่นในถ้วยอะลูมิเนียม ใส่พายลงในกระป๋อง จากนั้นนำตัวอย่างที่เตรียมได้เข้าเครื่อง RVA ตัวอย่างจะถูกทำให้ร้อนที่ ๕๐ องศาเซลเซียส เป็นเวลา ๑ นาที ต่อจากนั้นให้ความร้อนแก่ของผสมด้วยอัตรา ๑๒ องศาเซลเซียสต่อนาที จนถึงอุณหภูมิ ๙๕ องศาเซลเซียส คงไว้ที่อุณหภูมิ ๙๕ องศาเซลเซียส เป็นเวลา ๒.๕ นาที จากนั้นทำให้เย็นลงที่ ๕๐ องศาเซลเซียส ด้วยอัตรา ๑๒ องศาเซลเซียสต่อนาที แล้วคงที่ไว้ ๕๐

องศาเซลเซียส เป็นเวลา ๒ นาที ทดสอบซ้ำ ๓ ครั้ง นำสมบัติความหนืดของแป้งต่าง ๆ มาพล็อตเทียบกับเวลา ค่าต่าง ๆ ที่ได้จากสมบัติความหนืดของแป้งได้แก่ pasting temperature (PT), peak viscosity (PV), final viscosity (FV), breakdown viscosity (BKV = PV-trough) และ setback viscosity (SBV = FV-trough)

๓. ผลและวิจารณ์

๓.๑ การเปลี่ยนแปลงความชื้นและอุณหภูมิของเมล็ดข้าวกล้อง

๓.๑.๑ อิทธิพลของอุณหภูมิไอน้ำร้อนยวดยิ่งและความสูงเบดที่มีต่ออัตราการอบแห้งข้าวกล้องด้วยไอน้ำร้อนยวดยิ่ง

รูปที่ ๒ก แสดงความสัมพันธ์ระหว่างความชื้น อุณหภูมิของเมล็ดข้าวกล้องและเวลา ในช่วงแรกของการอบแห้งของข้าวกล้องเกิดการควบแน่นของไอน้ำ เนื่องจากทันทีที่ไอน้ำร้อนยวดยิ่งไหลผ่านเบดของข้าวกล้อง ไอน้ำจะเกิดการควบแน่นที่เบดของข้าวกล้องซึ่งเกิดในช่วงแรก ๆ ของการอบแห้งในระยะเวลาสั้นเป็นผลทำให้อุณหภูมิของข้าวกล้องเพิ่มขึ้นอย่างรวดเร็ว (อุณหภูมิเริ่มต้นประมาณ ๖๐ องศาเซลเซียส) จนถึงอุณหภูมิของจุดเดือดของน้ำ ต่อจากนั้นอุณหภูมิของข้าวกล้องจะเพิ่มขึ้นอย่างช้า ๆ ตามความชื้นที่ลดลง และจากรูปที่ ๒ ความสูงเบดมีอิทธิพลต่ออัตราการอบแห้งและอุณหภูมิเมล็ดของข้าวกล้องน้อยกว่าอุณหภูมิไอน้ำร้อนยวดยิ่ง เมื่ออุณหภูมิของไอน้ำร้อนยวดยิ่งสูงขึ้นเป็น ๑๖๐ องศาเซลเซียส อุณหภูมิของข้าวเปลือกจะเพิ่มขึ้นอย่างรวดเร็ว ในขณะที่ความชื้นลดลงอย่างรวดเร็วกว่ากรณีที่ใช้อุณหภูมิ ๑๒๐ องศาเซลเซียส

๓.๑.๒ อิทธิพลของระยะเวลาในการแช่ที่มีต่ออัตราการอบแห้ง

รูปที่ ๓ แสดงความสัมพันธ์ของระยะเวลาในการแช่ที่มีผลต่ออัตราการอบแห้ง พบว่าความชื้นของเมล็ดข้าวกล้องหลังการแช่จะเพิ่มขึ้นตามระยะเวลาในการแช่ เนื่องจากระยะเวลาในการแช่นานขึ้น ทำให้เมล็ดข้าวสามารถดูดซับน้ำได้มากขึ้น ระยะเวลาในการแช่ที่เหมาะสมนั้น ต้องให้ข้าวกล้องมีความชื้นเพียงพอต่อการเจลาทิไนเซชันที่สมบูรณ์ของเม็ดสตาร์ชในเมล็ดข้าว เมื่อนำข้าวกล้องไปอบแห้งที่เวลาต่าง ๆ พบว่าความชื้นของข้าวกล้องที่ผ่านการอบแห้งที่แช่เป็นระยะเวลาสั้นจะลดลงได้เร็วกว่าข้าวกล้องที่แช่เป็นระยะเวลานาน เนื่องจากข้าวกล้องที่แช่เป็นระยะเวลาสั้นจะมีความชื้นต่ำ ทำให้ความชื้นลดลงได้เร็วกว่า เมื่อระยะเวลาในการอบแห้งนานขึ้นความชื้นในเมล็ดข้าวมีแนวโน้มลดลงใกล้เคียงกัน เพราะว่าความชื้นส่วนใหญ่จะอยู่ที่เยื่อหุ้มเมล็ด (รำข้าว) และอุณหภูมิของเมล็ดข้าวกล้องที่ผ่านการแช่ระยะเวลาสั้นมีค่าใกล้เคียงกับอุณหภูมิเมล็ดข้าวกล้องที่ผ่านการแช่เป็นระยะนาน

๓.๑.๓ ผลการเปรียบเทียบอัตราการอบแห้งข้าวกล้องด้วยไอน้ำร้อนยวดยิ่งและอากาศร้อน

รูปที่ ๔ แสดงการเปรียบเทียบอัตราการอบแห้งข้าวกล้องด้วยไอน้ำร้อนยวดยิ่งและอากาศร้อน พบว่า เมื่อเวลาในการอบแห้งเพิ่มขึ้น ความชื้นของข้าวกล้องที่อบแห้งด้วยอากาศร้อนลดลงได้เร็วกว่าข้าวกล้องที่อบแห้งด้วยไอน้ำร้อนยวดยิ่ง เนื่องจากการอบแห้งด้วยอากาศร้อนไม่มีการควบแน่นของไอน้ำและใช้อุณหภูมิในการอบแห้งสูง ส่งผลทำให้ความชื้นของข้าวกล้องที่ผ่านการอบแห้งด้วยอากาศร้อนลดลงอย่างรวดเร็ว อุณหภูมิของเมล็ดข้าวกล้องที่ผ่านการอบแห้งด้วยไอน้ำร้อนยวดยิ่งมีค่าสูงกว่าอุณหภูมิของเมล็ดข้าวกล้องที่ผ่านการอบแห้งด้วยอากาศร้อน โดยเฉพาะในช่วงเริ่มการอบแห้งเกิดการควบแน่นของไอน้ำเป็นผลทำให้อุณหภูมิของข้าวกล้องเพิ่มขึ้นอย่างรวดเร็วจากอุณหภูมิเมล็ดข้าวเริ่มต้นถึงอุณหภูมิจุดเดือดของน้ำ ทำให้ความร้อนแฝงจากการควบแน่นของไอน้ำบนผิวของเมล็ดข้าวกล้องถ่ายเทไปยังภายในเมล็ดข้าวกล้อง

๓.๒ แบบจำลองทางคณิตศาสตร์ของการอบแห้งข้าวกล้องด้วยไอน้ำร้อนยวดยิ่ง

รูปที่ ๕ เปรียบเทียบการทำนายอัตราการอบแห้งข้าวกล้องระหว่างแบบจำลองทางคณิตศาสตร์กับผลการทดลองที่อุณหภูมิไอน้ำร้อนยวดยิ่งและความสูงเบดต่าง ๆ ที่อุณหภูมิการแช่ ๗๐ องศาเซลเซียส เวลาในการแช่ ๑ ชั่วโมง พบว่าผลการทำนายจากแบบจำลองทางคณิตศาสตร์มีค่าใกล้เคียงกันกับการทดลอง โดยในแบบจำลองทางคณิตศาสตร์ได้แบ่งอัตราอบแห้ง เป็น ๒ ช่วง ดังนี้

-ช่วงอัตราการอบแห้งคงตัว

ช่วงเริ่มต้นของอัตราการอบแห้งคงตัว เป็นช่วงที่ข้าวกล้องยังมีความชื้นสูงอยู่และเกิดการควบแน่นของไอน้ำที่ผิวของข้าวกล้อง เมื่อข้าวกล้องได้รับความร้อนจะเกิดการถ่ายเทความชื้นที่ผิวด้านนอกเท่านั้น ไม่ได้เกิดจากการแพร่ของความชื้นขึ้นในอัตราการอบแห้งช่วงนี้ส่งผลทำให้ความชื้นของข้าวกล้องลดลงอย่างคงที่เป็นเส้นตรงในช่วงแรกๆ ของการอบแห้งเมื่อเทียบกับเวลา ซึ่งอัตราการอบแห้งช่วงนี้สามารถเขียนความสัมพันธ์ของอุณหภูมิไอน้ำร้อนยวดยิ่ง ความเร็วเชิงมวล และเวลากับอัตราส่วนความชื้นสามารถอธิบายโดยใช้สมการที่ ๑

$$MR = (-1.9594 \times 10^{-3}VT + 0.7586V + 4.004 \times 10^{-5}T - 0.016268)t + 1.030765 \quad (R^2 = 0.92) \quad (๑)$$

เมื่อ
- MR คือ อัตราส่วนความชื้น
- T คือ อุณหภูมิไอน้ำร้อนยวดยิ่ง, K
- V คือ ความเร็วเชิงมวลจำเพาะ, $kg_{steam}/s{\cdot}kg_{drymatter}$
- t คือ เวลาอบแห้ง, s

ในอัตราการอบแห้งช่วงนี้พบว่าอุณหภูมิไอน้ำยวดยิ่งและความเร็วเชิงมวลมีผลต่ออัตราส่วนความชื้น โดยสมการที่ (๑) ใช้ได้ในช่วงความเร็วเชิงมวลจำเพาะในช่วง 0035 - 0053 $kg_{steam}/s{\cdot}kg_{drymatter}$ และอุณหภูมิไอน้ำร้อนยวดยิ่ง ๑๒๐ - ๑๖๐ องศาเซลเซียส จนความชื้นลดลงถึงความชื้นวิกฤติ (ความชื้นวิกฤติของข้าวกล้องประมาณร้อยละ ๒๕.๕ - ๒๖ มาตรฐานแห้ง) จะเข้าสู่ช่วงอัตราการอบแห้งลดลง

-ช่วงอัตราการอบแห้งลดลง

หลังจากความชื้นลดลงจนถึงความชื้นวิกฤติ ความชื้นของข้าวกล้องเริ่มลดลงแบบ exponential จึงเป็นช่วงที่ความชื้นภายในวัสดุจะแพร่ออกมาที่ผิวนอกแล้วระเหย ค่าสัมประสิทธิ์การแพร่ประสิทธิผลหาได้จากผลเฉลยวิเคราะห์ (analytical solution) ของเมล็ดข้าวกล้องรูปทรงกลม ดังสมการที่ (๒)

$$\frac{M_t - M_{eq}}{M_{cr} - M_{eq}} = \frac{6}{\pi^2}\sum_{n=1}^{\infty}\frac{1}{2}\exp\left(\frac{n\pi}{R}\right)^2 D_{eff}(t - t_{cr}) \quad (๒)$$

เมื่อ M_t คือความชื้น ณ เวลาใดๆ M_{eq} คือความชื้นสมดุล R คือรัศมีของเมล็ดข้าวกล้อง (เมตร) t_{cr} คือเวลาของการอบแห้ง ณ จุดความชื้นวิกฤติ (วินาที)

รูปที่ ๖ แสดงความสัมพันธ์ค่าสัมประสิทธิ์การแพร่ประสิทธิผลกับความสูงเบดและอุณหภูมิของไอน้ำร้อนยวดยิ่ง โดยค่าสัมประสิทธิ์การแพร่ประสิทธิผลอยู่ในช่วง 1.0497×10^{-10} - 2.4672×10^{-10} m^2/s สำหรับอุณหภูมิอบแห้ง ๑๒๐-๑๖๐ องศาเซลเซียส และค่าสัมประสิทธิ์การแพร่ประสิทธิผลมีค่าเพิ่มขึ้นเมื่ออุณหภูมิอบแห้งเพิ่มขึ้น การหาความสัมพันธ์ระหว่างสัมประสิทธิ์การแพร่ประสิทธิผลกับอุณหภูมิไอน้ำร้อนยวดยิ่งนั้นใช้สมการ Arrhenius สมการที่ ๓

$$D_{eff} = 9.95289 \times 10^{-7} \exp\left(\frac{-32915.126}{RT}\right) \quad (R^2 = 0.86) \quad (๓)$$

๓.๓ ปริมาณต้นข้าว

รูปที่ ๗ แสดงความสัมพันธ์ระหว่างร้อยละต้นข้าวกับความชื้นสุดท้ายของข้าวกล้องที่อุณหภูมิของไอน้ำร้อนยวดยิ่งและความสูงเบดต่าง ๆ จากการทดลองพบว่า ช่วงแรกของการอบแห้งมีร้อยละต้นข้าวเพิ่มขึ้นเมื่อเทียบกับข้าวสารอ้างอิง (ร้อยละ ๗๙.๙) โดยร้อยละต้นข้าวมีค่าสูงขึ้นในช่วงความชื้นสุดท้ายหลังการอบแห้งประมาณร้อยละ ๒๘ - ๒๙ มาตรฐานแห้ง เนื่องจากการเกิดเจลาทิไนเซชันซึ่งสามารถอธิบายได้ดังนี้ เมื่อข้าวกล้องที่มีความชื้นสูงนั้นได้รับความร้อนสูง แป้งที่ถูกน้ำเกิดการพองตัวและถูกทำให้สุก นอกจากนี้ ยังทำให้โปรตีนแตกตัวและแทรกเข้าไปภายในโครงสร้างภายในช่องว่างของเม็ดแป้งทำให้เกิดการยึดตัวเข้าด้วยกันและเกาะกันแข็งแรงขึ้น และทำให้รอยร้าวภายในเมล็ดข้าวสามารถผสานกันอย่างสนิท (ดังรูปที่ ๑๐ค) เมล็ดข้าวมีลักษณะแข็งใสเหนียวและทนต่อการขัดสี เมื่อนำไปขัดสีจึงได้ร้อยละต้นข้าวสูง ถ้าข้าวกล้องได้รับความร้อนสูงเป็นเวลานานเกินไปในช่วงความชื้นสุดท้ายต่ำกว่าร้อยละ ๒๘ มาตรฐานแห้ง จะทำให้ปริมาณความร้อนส่วนใหญ่ที่ใช้ในการระเหยน้ำถูกนำไปเพิ่มอุณหภูมิให้แก่เมล็ดข้าว ส่งผลให้เมล็ดข้าวกล้องมีอุณหภูมิสูงมากเกินไปจนโครงสร้างของเม็ดสตาร์ชเปลี่ยนแปลงเกิดเป็นโพรงช่องว่างขึ้น มีผลทำให้เกิดการแตกหัก และในช่วงขณะที่อัตราการอบแห้งลดลงนี้จะเกิดความแตกต่างของความชื้นที่บริเวณผิวและแกนกลางของเมล็ดข้าวกล้อง ถ้าความแตกต่างของความชื้นนี้เพิ่มขึ้น จะทำให้เกิดความเค้นขึ้นภายในเมล็ดมากขึ้นด้วย ซึ่งนำไปสู่การร้าวของเมล็ดขึ้นได้และเมื่อนำข้าวกล้องไปขัดสีจะได้ร้อยละต้นข้าวลดลง

รูปที่ ๘ แสดงความสัมพันธ์ระหว่างร้อยละต้นข้าวกับความชื้นสุดท้ายของข้าวกล้องที่เป็นผลมาจากการเปลี่ยนแปลงระยะเวลาในการแช่ จากการทดลองพบว่าความชื้นในเมล็ดข้าวกล้องสูงขึ้นตามระยะเวลาในการแช่ที่เพิ่มขึ้น ส่งผลให้ร้อยละต้นข้าวสูงขึ้น ถ้าความชื้นเริ่มต้นของข้าวกล้องสูงจะทำให้ช่วงเวลาการเกิดเจลาทิไนเซชันนานขึ้น ถ้าระยะเวลาในการแช่ข้าวกล้องน้อยกว่า ๑ ชั่วโมง ทำให้ความชื้นในเมล็ดข้าวน้อยไม่สม่ำเสมอทั้งเมล็ด และไม่เพียงพอต่อการเกิดเจลาทิไนเซชันภายในเมล็ดข้าว ทำให้ข้าวกล้องที่ผ่านการอบแห้งแล้วมีลักษณะขาวขุ่นที่เมล็ดข้าวเมื่อขัดสีจะได้ร้อยละข้าวลดลง

รูปที่ ๙ แสดงความสัมพันธ์ระหว่างร้อยละต้นข้าวกับความชื้นสุดท้ายของข้าวกล้อง เปรียบเทียบระหว่างการอบแห้งด้วยไอน้ำร้อนยวดยิ่งและอากาศร้อน พบว่าร้อยละต้นข้าวของการอบแห้งด้วยไอน้ำร้อนยวดยิ่งมีค่าสูงกว่าการอบแห้งด้วยอากาศร้อน โดยในช่วงแรกของการอบแห้งด้วยไอน้ำร้อนยวดยิ่ง จะมีค่าร้อยละต้นข้าวเพิ่มขึ้นเมื่อเทียบกับข้าวสารอ้างอิง หลังจากนั้นร้อยละต้นข้าวจะลดลงอย่างรวดเร็วเมื่อความชื้นลดลงต่ำกว่าร้อยละ ๒๘ มาตรฐานแห้ง ขณะที่การอบแห้งด้วยอากาศร้อนจะมีค่าร้อยละต้นข้าวลดลงเมื่อเทียบกับข้าวสารอ้างอิง เนื่องจากการอบแห้งข้าวกล้องด้วยไอน้ำร้อนยวดยิ่งจะเกิดการควบแน่นของไอน้ำในช่วงแรกของการอบแห้งซึ่งเทียบได้กับการนึ่งของกระบวนการผลิตข้าวนึ่ง ทำให้ช่วงเวลาในการเกิดเจลาทิไนเซชันภายในเมล็ดนานขึ้น (ดังรูปที่ ๑๐ค) จึงมีผลทำให้ร้อยละต้นข้าวที่ได้สูงกว่าการอบแห้งด้วยอากาศร้อน ซึ่งการเกิดเจลาทิไนเซชันไม่สมบูรณ์ตลอดทั่วเมล็ด และทำให้การยึดเกาะตัวของกลุ่มแป้งและโปรตีนไม่สามารถประสานกันอย่างสนิท (ดังรูปที่ ๑๐ง) เกิดช่องว่างมากขึ้นภายในเมล็ดข้าว ทำให้เมล็ดข้าวที่ได้จึงมีลักษณะขาวขุ่นมากขึ้น เมื่อนำไปขัดสีทำให้ร้อยละต้นข้าวลดลงต่ำกว่าการอบแห้งด้วยไอน้ำร้อนยวดยิ่ง

๓.๔ White belly

ปริมาณ white belly แสดงถึงคุณภาพที่ไม่ดีของข้าวนึ่ง เพราะลักษณะข้าวมีจุดขุ่นขาวทึบแสงและเกิดช่องว่างขึ้นภายในเมล็ดข้าว ซึ่งเกิดจากกระบวนการเจลาทิไนเซชันของแป้งในเมล็ดข้าวที่ไม่สมบูรณ์ โดยส่วนใหญ่จะปรากฏบริเวณแกนกลางในเมล็ดข้าว รูปที่ ๑๑, ๑๒ แสดงความสัมพันธ์ระหว่าง white belly กับความชื้นสุดท้ายของข้าวกล้องที่อุณหภูมิ ความสูงเบดและระยะเวลาการแช่ต่าง ๆ จากการทดลองพบว่า ระยะเวลาการแช่มีอิทธิพลต่อร้อยละ white belly โดยที่ระยะเวลาการแช่นานขึ้นทำให้ร้อยละ white belly ลดลง เนื่องจากข้าวกล้องที่ผ่านการแช่ระยะเวลาต่ำกว่า ๑ ชั่วโมง ปริมาณน้ำจะซึมเข้าภายในเมล็ดข้าว

ได้น้อย โดยจะเกิดที่บริเวณผิวเท่านั้น ส่งผลให้ความชื้นเพียงพอต่อการเกิดเจลไม่สม่ำเสมอทั่วทั้งเมล็ด แต่อุณหภูมิของไอน้ำร้อนยวดยิ่งและความสูงเบด (ข้าวกล้องที่แช่ ๑ ชั่วโมง) ไม่มีผลต่อร้อยละ white belly โดยที่ร้อยละ white belly ที่ได้อยู่ในเกณฑ์ที่ดี[๑๑]

รูปที่๑๓ ความสัมพันธ์ระหว่าง white belly กับความชื้นสุดท้ายของข้าวกล้องระหว่างการอบแห้งด้วยไอน้ำร้อนยวดยิ่งกับอากาศร้อน พบว่า การอบแห้งข้าวกล้องด้วยไอน้ำร้อนยวดยิ่งมีร้อยละ white belly น้อยกว่าการอบแห้งข้าวกล้องด้วยอากาศร้อนมาก เนื่องจากการอบแห้งด้วยไอน้ำร้อนยวดยิ่งมีช่วงการควบแน่นของไอน้ำเกิดขึ้น จึงทำให้เมล็ดข้าวกล้องเกิดเจลาทิไนเซชันได้สมบูรณ์กว่าการอบแห้งด้วยอากาศร้อนที่ไม่มีการควบแน่นของไอน้ำ (รูปที่ ๑๐ค และ ๑๐ง) เนื่องจากการควบแน่นของไอน้ำนั้นเทียบได้กับช่วงการนึ่ง ทำให้ช่วงเวลาในการเกิดเจลาทิไนซ์นานขึ้น จึงทำให้ได้ปริมาณ white belly ต่ำ

๓.๕ ความขาว

รูปที่ ๑๔ แสดงความสัมพันธ์ระหว่างความขาวกับความชื้นสุดท้ายของข้าวกล้องที่อุณหภูมิและความสูงเบดต่าง ๆ จากการทดลองพบว่าข้าวกล้องที่ผ่านการอบแห้งด้วยไอน้ำร้อนยวดยิ่งจะมีค่าความขาวของข้าวสารลดลงเมื่อเทียบกับข้าวสารอ้างอิง(๔๖.๔) ผลของอุณหภูมิของไอน้ำร้อนยวดยิ่งไม่มีผลต่อค่าความขาวของข้าวสารมากนัก โดยความขาวของข้าวจะมีค่าคงที่ตลอดช่วงความชื้นค่าหนึ่ง ๆ และจะมีค่าความขาวลดลงเมื่อความชื้นลดลงต่ำกว่าร้อยละ ๑๘-๒๐ มาตรฐานแห้ง ผลของความสูงเบดที่มีต่อความขาวของข้าวสาร พบว่าที่ความสูงเบด ๑๒ เซนติเมตร จะมีความขาวของข้าวสารมากกว่าที่ความสูงเบด ๑๐ เซนติเมตร แต่ที่ความสูงเบด ๘ เซนติเมตร มีความขาวของข้าวสารมากกว่าที่ความสูงเบด ๑๒ และ ๑๐ เซนติเมตร ตามลำดับ เนื่องจากข้าวกล้องที่ผ่านการอบแห้งที่ความสูงเบด ๘ เซนติเมตร เกิดช่องว่างภายในเมล็ดข้าว จึงทำให้เกิดการร้าวขึ้น ซึ่งทำให้การวัดค่าความขาวของข้าวสารผิดพลาดได้ เนื่องจากเครื่องที่ใช้วัดความขาวได้ใช้หลักการของการหักเหของแสง นอกจากนี้ ระยะเวลาการแช่ก็มีผลต่อความขาวของข้าวสารเช่นเดียวกัน (รูปที่ ๑๕) พบว่าระยะเวลาในการแช่ ๒ ชั่วโมง และ ๑ ชั่วโมง ค่าความขาวของข้าวสารใกล้เคียงกัน แต่ถ้าระยะเวลาในการแช่น้อยกว่า ๑ ชั่วโมง ค่าความขาวของข้าวสารจะเพิ่มขึ้น เนื่องจากทำให้ความชื้นในเมล็ดข้าวน้อยและไม่เพียงพอแก่การเกิดเจลาทิไนเซชันภายในเมล็ดข้าว ทำให้ข้าวกล้องที่ผ่านการอบแห้งแล้วมีลักษณะขาวขุ่นที่เมล็ดข้าว เมื่อนำข้าวสารไปวัดความขาวทำให้ความขาวของข้าวสารเพิ่มขึ้น เมื่อเปรียบเทียบความขาวของข้าวที่ผ่านการอบแห้งด้วยไอน้ำร้อนยวดยิ่งและอากาศร้อน (รูปที่ ๑๖) จากการทดลองพบว่าความขาวของข้าวที่ผ่านการอบแห้งด้วยอากาศร้อนมีค่าสูงมากกว่าข้าวที่ผ่านการอบแห้งด้วยไอน้ำร้อนยวดยิ่ง เนื่องจากข้าวกล้องที่ผ่านการอบแห้งด้วยอากาศร้อน มีลักษณะขาวขุ่นคล้ายข้าวเหนียว ซึ่งเป็นผลจากเกิดเจลาทิไนเซชันไม่สมบูรณ์ตลอดทั่วเมล็ด เกิดช่องว่างขึ้นภายในเมล็ดข้าว และค่าความขาวจะเพิ่มขึ้นเมื่อความชื้นสุดท้ายของข้าวกล้องต่ำลง ดังนั้น การเปลี่ยนแปลงความขาวของข้าวสารสามารถอธิบายได้ดังนี้ การเปลี่ยนแปลงความขาวเป็นผลมาจากการเปลี่ยนแปลงทางเคมีของสารประกอบที่อยู่ภายในเมล็ดข้าว ซึ่งเกิดปฏิกิริยาสีน้ำตาลแบบเมลลาร์ด โดยสภาพที่เหมาะสมของน้ำตาลรีดิวซ์กับกรดแอมิโนโดยมีความร้อนเป็นตัวเร่งปฏิกิริยาสีน้ำตาล จึงส่งผลทำให้ค่าความขาวของข้าวที่ผ่านการอบแห้งจะมีสีคล้ำขึ้น

๓.๖ สมบัติความหนืดของแป้งข้าว (pasting properties)

รูปที่ ๑๗, ๑๘ และ ๑๙ ตารางที่ ๑ แสดงสมบัติความหนืดของแป้งข้าวที่ผ่านการอบแห้งด้วยไอน้ำร้อนยวดยิ่ง อากาศร้อน และข้าวที่ไม่ผ่านกระบวนการอบแห้ง (ข้าวอ้างอิง) ผลการทดลองพบว่าข้าวที่ผ่านกระบวนการอบแห้งด้วยไอน้ำร้อนยวดยิ่งและอากาศร้อนมีค่า pasting temperature สูงกว่าข้าวอ้างอิง และค่า PV, BKV และ FV ต่ำกว่าข้าวอ้างอิง (รูปที่ ๑๗ และ ๑๘) การที่ค่า PV สูงเกิดจากการที่เม็ดสตาร์ชมีความสามารถในการจับกับน้ำได้ปริมาณมากกว่าข้าวที่ผ่านกระบวนการอบแห้ง ทำให้เม็ดสตาร์ชเกิดการพองตัวเป็นผลทำให้ค่าความหนืดสูงขึ้น ส่วนข้าวผ่านการอบแห้งค่า PV ลดลงในช่วงเวลา ๒ นาทีแรกระหว่างการอบแห้งด้วยไอน้ำร้อนยวดยิ่ง ข้าวที่มี

ความชื้นสูงได้รับความร้อนสูง เม็ดสตาร์ชที่ถูกน้ำจะพองตัวและกลายเป็นเจลและทำให้โปรตีนแตกตัวและแทรกเข้าไปภายในช่องว่างระหว่างเม็ดสตาร์ช เมื่อนำไปวัดสมบัติความหนืดของแป้งจะมีผลทำให้ความสามารถในการจับน้ำของเม็ดสตาร์ชลดลง ทำให้เม็ดสตาร์ชพองตัวได้น้อยลงด้วย มีผลทำให้ค่า PV ลดลง สำหรับค่า FV และ SBK แสดงถึงสมบัติความแข็งกระด้างของข้าวสุก[๑๒, ๑๓, ๑๔] ข้าวที่ผ่านการอบแห้งด้วยไอน้ำร้อนยวดยิ่งให้ค่า FV และ SBK ต่ำกว่าข้าวที่ผ่านการอบแห้งด้วยอากาศร้อนและที่ไม่ผ่านการอบแห้งตามลำดับ ดังนั้น ข้าวที่ผ่านการอบแห้งด้วยไอน้ำร้อนยวดยิ่งมีลักษณะความแข็งกระด้างต่ำกว่าข้าวที่ผ่านการอบแห้งด้วยอากาศร้อนและข้าวที่ไม่ผ่านการอบแห้ง หลังจากการหุงสุกและปล่อยให้ข้าวเย็นตัวลง

๔. สรุปผลการทดลอง

จากการศึกษาการนึ่งข้าวกล้องด้วยไอน้ำร้อนยวดยิ่งโดยเทคนิคฟลูอิ-ไดซ์เบด พบว่า อุณหภูมิของไอน้ำร้อนยวดยิ่งมีผลต่ออัตราการอบแห้งมากที่สุด ความสูงเบดและระยะเวลาในการแช่มีผลต่ออัตราการอบแห้งน้อย เมื่อความชื้นสุดท้ายของข้าวกล้องหลังการอบแห้งต่ำกว่าร้อยละ ๒๘ มาตรฐานแห้ง พบว่าร้อยละต้นข้าวจะลดลงอย่างรวดเร็ว อุณหภูมิไอน้ำร้อนยวดยิ่งไม่มีอิทธิพลอย่างชัดเจนต่อความขาวของข้าว เมื่อความชื้นสุดท้ายต่ำกว่าร้อยละ ๑๘ มาตรฐานแห้ง ความขาวจะลดลง การเพิ่มระยะเวลาในการแช่ให้นานขึ้นส่งผลให้ร้อยละต้นข้าวเพิ่มขึ้น ช่วยลดการร้าวของข้าว และการเกิด white belly ลดลง เนื่องจากทำให้ช่วงเวลาในการเกิดเจลาทิไนเซชันนานขึ้น จากการวัดสมบัติความหนืดของแป้ง ข้าวที่ผ่านการอบแห้งด้วยไอน้ำร้อนยวดยิ่งให้ค่า PV, BKV และ SBV ลดต่ำลงเมื่อเทียบกับข้าวที่อบด้วยอากาศร้อนและข้าวที่ไม่ได้ผ่านกระบวนการอบแห้งด้วยไอน้ำร้อนยวดยิ่งและอากาศร้อน นอกจากนี้เมื่อดูลักษณะโครงสร้างภายในเมล็ดข้าวด้วยกล้องจุลทรรศน์อิเล็กตรอนแบบส่องกราดพบว่าไม่ปรากฏโครงสร้างของเม็ดสตาร์ชหลังจากการอบแห้งด้วยไอน้ำร้อนยวดยิ่ง

๕. กิตติกรรมประกาศ

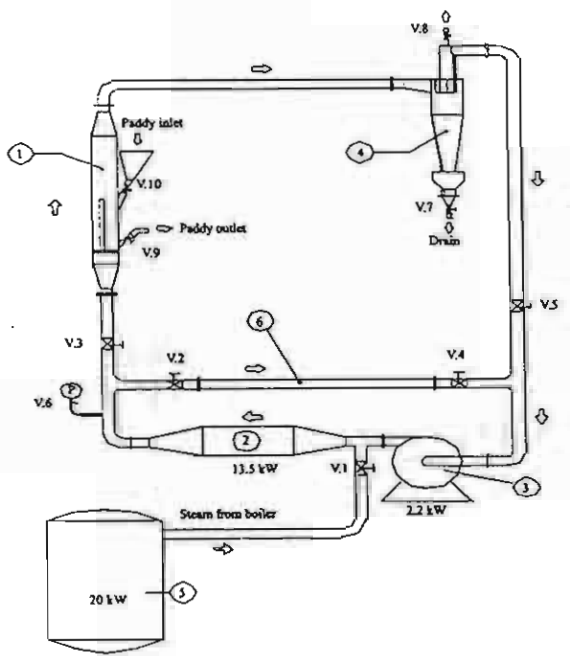
ผู้เขียนใคร่ขอขอบคุณสำนักงานกองทุนสนับสนุนการวิจัยที่ให้ทุนสนับสนุนงานวิจัย ขอขอบพระคุณสถาบันค้นคว้าและพัฒนาผลิตภัณฑ์อาหาร มหาวิทยาลัยเกษตรศาสตร์ที่ให้ความอนุเคราะห์ในการทดสอบสมบัติทางเคมีกายภาพ

เอกสารอ้างอิง

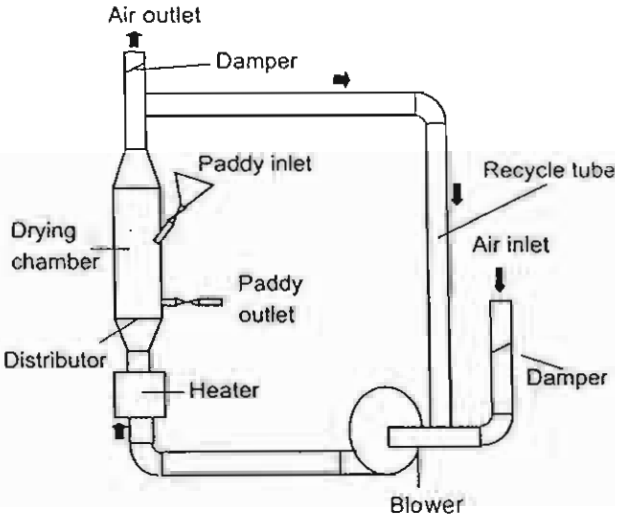
1. Kar N, Jain RK, Srivastav PP. Parboiling of Dehusked Rice, Journal of Food Engineering. 1999; 39 (1) : 17 - 22.
2. Ali, SZ, Bhattacharya, KR. High-Temperrature Drying-Cum-Parboiling of Paddy, Journal of Food Process Engineering. 1980; 4 : 123 - 136.
3. Unnikrishnan, KR, Viraktamath, CS, Krishnamurthy, H, Bhattacharya, KR. Parboiling of Paddy by Simple Soaking in Hot Water, Journal Food Tech., 1982; 17 : 499 - 506.
4. Toshinari, K, Bhattacharya, KR, Ali, SZ., Effect of Processing Conditions on the Color Intensity of Parboiled Rice, Journal of Soc of Agri Struc. Japan, 1993. 20(1) : pp. 153 - 160.
5. Elbert, G, Marcela, P, Suarez, C. Effect of Drying Condition on Head Rice Yield and Browning Index of Parboiled Rice, Journal of Food Engineering. 2001; 47 : 37 - 41.
6. Taechapairoj, C, Dhuchakallaya, I, Soponronnarit, S, Wetchcama, S, Prachayawarakorn, S. Superheated Steam Fluidised Bed Paddy Drying, Journal of Food Engineering, 2003; 58 : 67 - 73.
7. Taweerattanapanish, A, Soponronnarit, S, Wetchcama, S, Kongseri, N, Wongpiyachon, S. Effects of Drying on Head Yield Using Fluidization Technique, Drying Technology, 1999; 17(1&2) : 345 - 353.
8. Taechapairoj, C, Prachayawarakorn, S, Soponronarit, S. Characteristics of Rice Dried in Superheated Steam Fluidised Bed, Drying Technology, 2004; 22(4) : 719 - 743.
9. Soponronarit, S, Taechapairoj, C, Prachayawarakorn, S, New Technique Producing Parboiled Rice, The Journal of the Royal Institute of Thailand, 2004; 29(1) : 78 - 86.
10. AACC. Approved method of the American Association of Cereal Chemists, 8th ed. American Association of Cereal Chemists, St. Paul, MN, 1995.
11. Department of Foreign Trade, Available: http://www.dft.moc.go.th/document/grain/rice_standard.pdf [08/30/04].
12. Ali SZ, Bhattacharya KR. Pasting behaviour of parboiled rice, J. Texture Stud., 1980; 11 : 239 - 245.
13. Priestley RJ. Studies on parboiled rice. I. Comparison of the characteristics of raw and parboiled rice, Food Chemistry, 1976; 1, 5 - 14.
14. Ranghavendra RSN, Juliano BO. Effect of parboiling on some physicochemical properties of rice, Journal Agricultural Food Chemistry, 1970; 18 : 289 - 294.

ตารางที่ ๑ สมบัติความหนืดของแป้งข้าวที่ไม่ผ่านและผ่านกระบวนการต่าง ๆ

	Peak viscosity (rvu)	Trough 1 (rvu)	Breakdown viscosity (rvu)	Final viscosity (rvu)	Setback visosity (rvu)	Pasting Temp (C)
ข้าวสารอ้างอิง	209.67	161.92	47.75	332.67	123.00	79
อากาศร้อน 140°C แช่ 2 ชั่วโมง เบด 10 cm	112.92	109.33	3.58	236.67	123.75	89
ไอน้ำร้อนยวดยิ่ง 120°C แช่ 1 ชั่วโมง เบด 10 cm	84.33	84.42	-0.08	148.58	64.25	89
ไอน้ำร้อนยวดยิ่ง 140°C แช่ 1/2 ชั่วโมง เบด 10 cm	84.92	84.83	0.08	139.42	54.50	89
ไอน้ำร้อนยวดยิ่ง 140°C แช่ 1 ชั่วโมง เบด 10 cm	80.08	80.50	-0.42	135.92	55.83	89
ไอน้ำร้อนยวดยิ่ง 140°C แช่ 2 ชั่วโมง เบด 10 cm	77.75	77.58	0.17	125.08	47.33	89.9
ไอน้ำร้อนยวดยิ่ง 140°C แช่ 1 ชั่วโมง เบด 8 cm	82.17	82.17	0.00	123.00	40.83	89
ไอน้ำร้อนยวดยิ่ง 140°C แช่ 1 ชั่วโมง เบด 12 cm	87.17	87.17	0.00	148.58	61.42	89

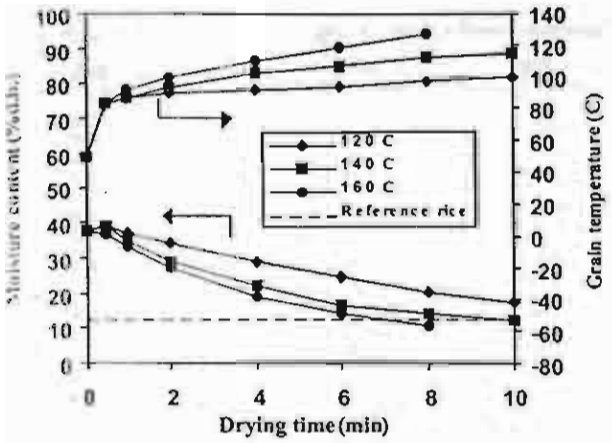


ก) เครื่องอบแห้งด้วยไอน้ำร้อนยวดยิ่ง

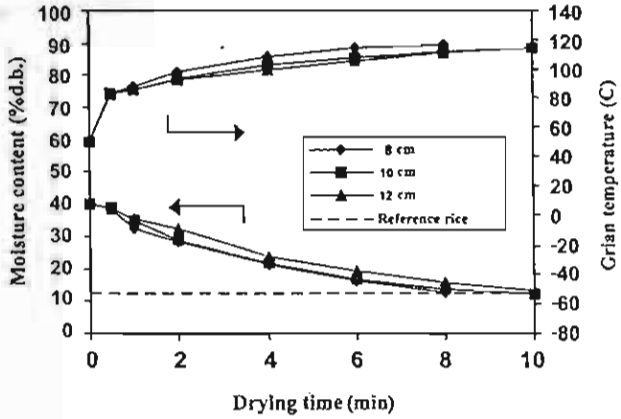


ข) เครื่องอบแห้งด้วยอากาศร้อน

รูปที่ ๑ แผนภาพระบบการอบแห้ง

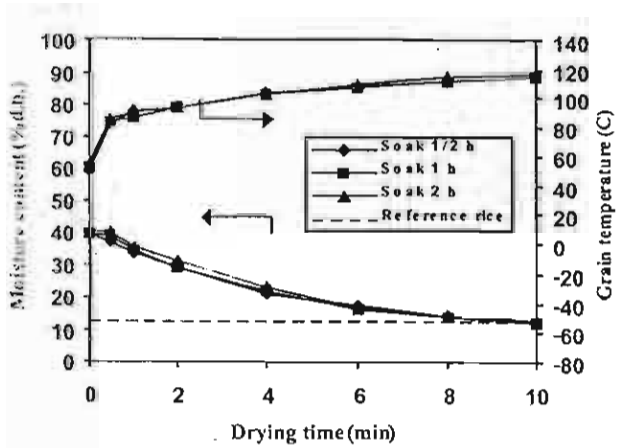


ก) ความสูงเบด ๑๐ เซนติเมตร

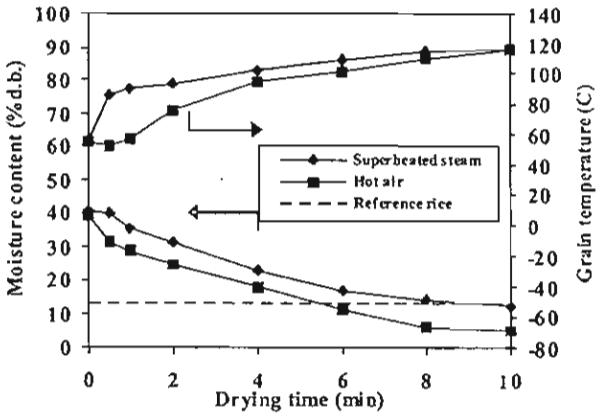


ข) อุณหภูมิไอน้ำร้อนยวดยิ่ง ๑๔๐ องศาเซลเซียส

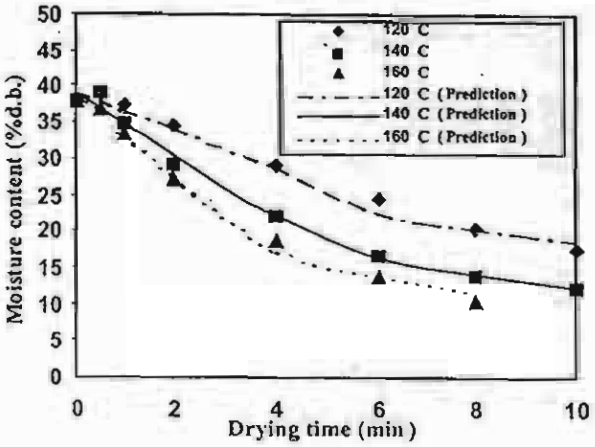
รูปที่ ๒ อิทธิพลของอุณหภูมิไอน้ำร้อนยวดยิ่งและความสูงเบดต่ออัตราการอบแห้งและอุณหภูมิของเมล็ดข้าวกล้องที่อุณหภูมิในการแช่ ๗๐ เซนติเมตร และเวลาในการแช่ ๑ ชั่วโมง



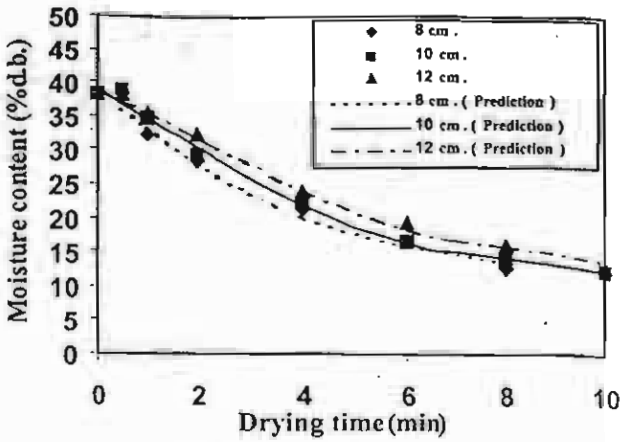
รูปที่ ๓ อิทธิพลของระยะเวลาการแช่ข้าวกล้องต่ออัตราการอบแห้งและอุณหภูมิของเมล็ดข้าวกล้องที่อุณหภูมิอบแห้ง ๑๔๐ องศาเซลเซียส ความสูงเบด ๑๐ เซนติเมตร และเวลาในการแช่ ๑ ชั่วโมง



รูปที่ ๔ อิทธิพลของการอบแห้งด้วยไอน้ำร้อนยวดยิ่งกับอากาศร้อนที่มีต่อการอบแห้งที่อุณหภูมิอบแห้ง ๑๔๐ องศาเซลเซียส ที่ความสูงเบด ๑๐ เซนติเมตร อุณหภูมิในการแช่ ๗๐ องศาเซลเซียส และเวลาในการแช่ ๒ ชั่วโมง

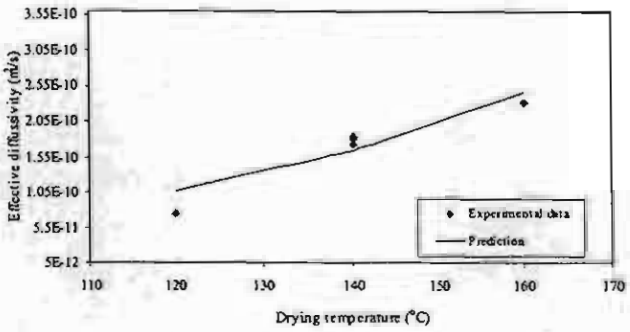


ก) ความสูงเบด ๑๐ เซนติเมตร

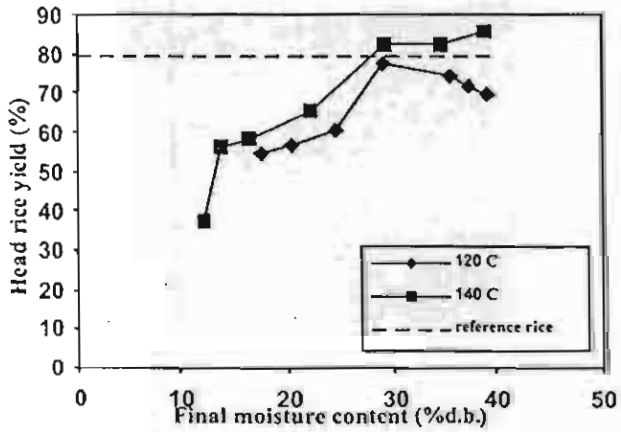


ข) อุณหภูมิไอน้ำร้อนยวดยิ่ง ๑๔๐ องศาเซลเซียส

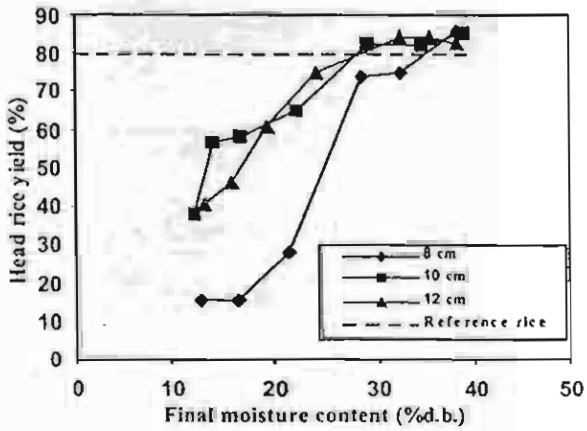
รูปที่ ๕ เปรียบเทียบผลการทำนายความชื้นของข้าวกล้องจากแบบจำลองทางคณิตศาสตร์กับผลการทดลอง ณ เวลาต่าง ๆ



รูปที่ ๖ ค่าสัมประสิทธิ์การแพร่ประสิทธิผลของการทดลองและค่าทำนาย

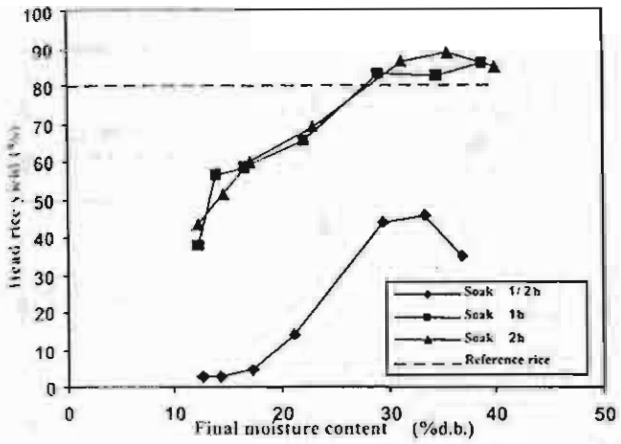


ก) ความสูงเบด ๑๐ เซนติเมตร

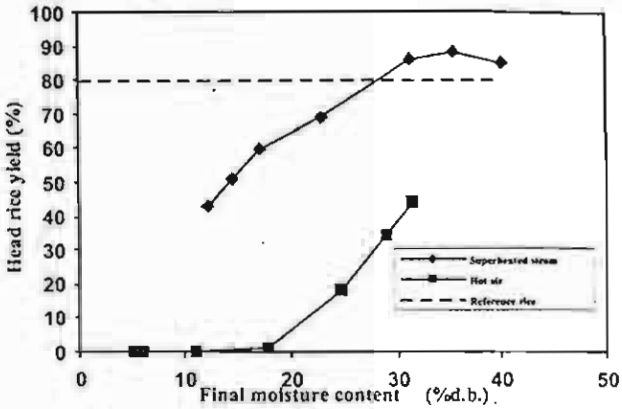


ข) อุณหภูมิไอน้ำร้อนยวดยิ่ง ๑๔๐ องศาเซลเซียส

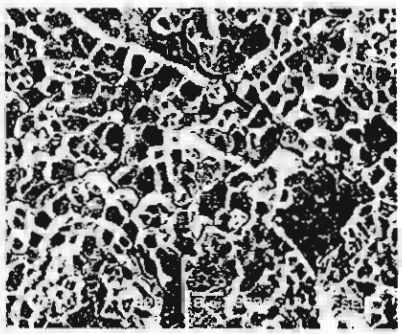
รูปที่๗ ความสัมพันธ์ระหว่างร้อยละต้นข้าวกับความชื้นสุดท้ายของข้าวกล้องที่อุณหภูมิไอน้ำร้อนยวดยิ่งและความสูงเบดต่าง ๆ ระยะเวลาในการแช่ ๑ ชั่วโมง



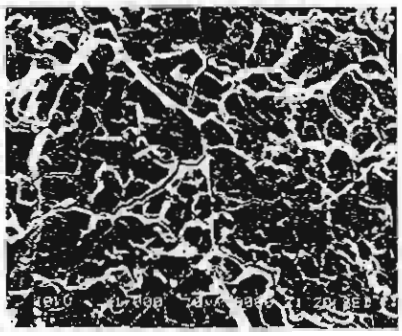
รูปที่ ๘ ความสัมพันธ์ระหว่างร้อยละต้นข้าวกับความชื้นสุดท้ายของข้าวกล่องที่ระยะเวลาในการแช่ต่าง ๆ อุณหภูมิอบแห้ง ๑๔๐ องศาเซลเซียส และความสูงเบด ๑๐ เซนติเมตร



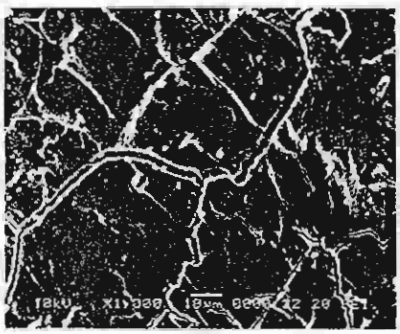
รูปที่ ๙ ความสัมพันธ์ระหว่างร้อยละต้นข้าวกับความชื้นสุดท้ายของข้าวกล่องที่อบแห้งด้วยไอน้ำร้อนยวดยิ่งกับอากาศร้อนที่ระยะเวลาในการแช่ ๒ ชั่วโมง อุณหภูมิในการอบแห้ง ๑๔๐ องศาเซลเซียส



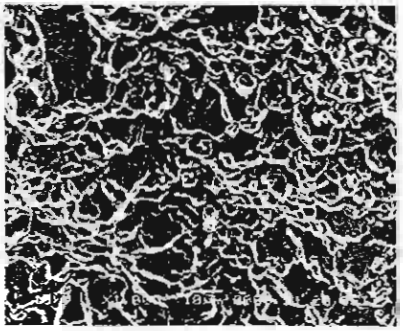
(ก)



(ข)

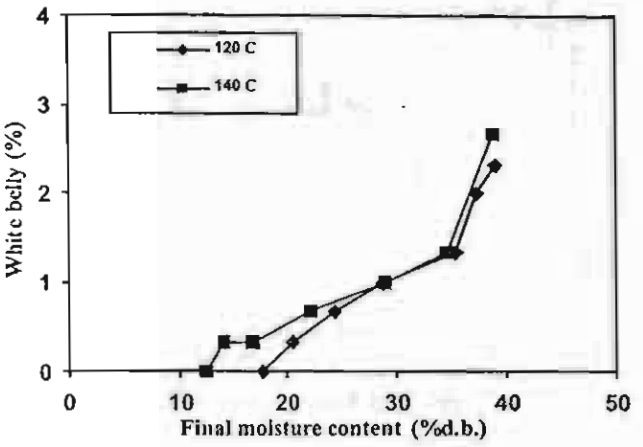


(ค)

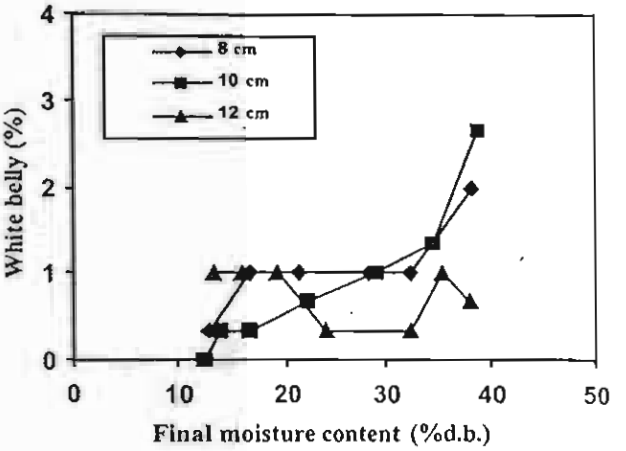


(ง)

รูปที่ ๑๐ ลักษณะการเกิดเจลาทีไนเซชันของข้าวที่ผ่านการแช่เป็นระยะเวลา ๒ ชั่วโมง ด้วยกล้องจุลทรรศน์อิเล็กตรอนแบบส่องกราด (กำลังขยาย ๑,๐๐๐ เท่า)
(ก) ข้าวที่ไม่ได้ผ่านการแช่และการอบแห้ง
(ข) ข้าวที่ผ่านการแช่และไม่ผ่านการอบแห้ง
(ค) ข้าวที่ผ่านการอบแห้งด้วยไอน้ำร้อนยวดยิ่ง
(ง) ข้าวที่ผ่านการอบแห้งด้วยอากาศร้อน

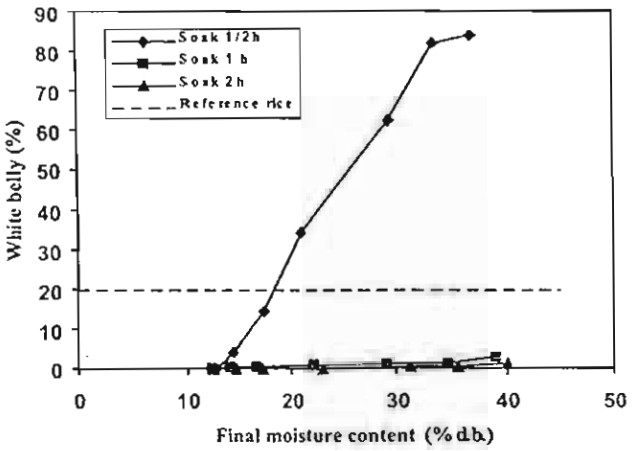


ก) ความสูงเบด ๑๐ เซนติเมตร

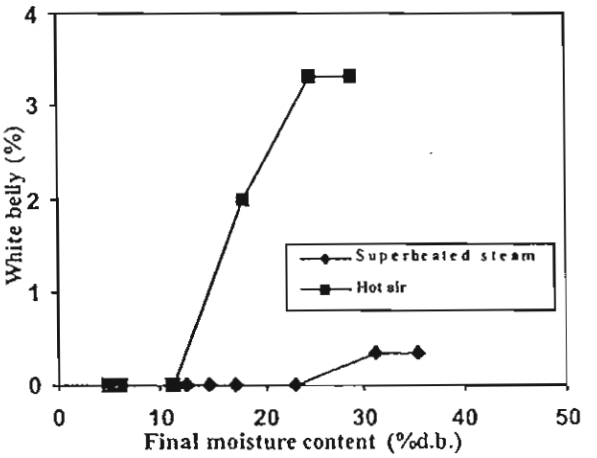


ข) อุณหภูมิไอน้ำร้อนยวดยิ่ง ๑๔๐ องศาเซลเซียส

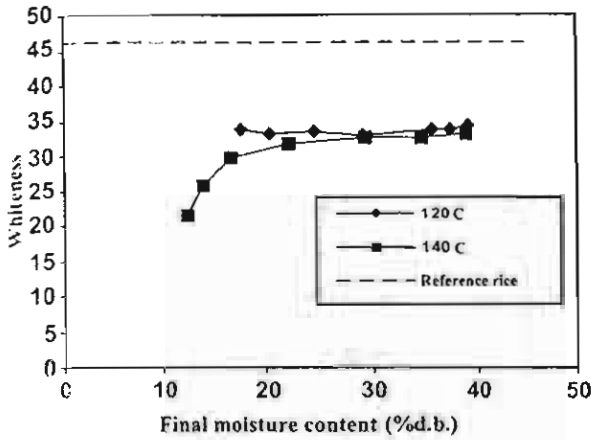
รูปที่ ๑๑ ความสัมพันธ์ระหว่าง white belly กับความชื้นสุดท้ายของข้าวกล้องที่อุณหภูมิไอน้ำร้อนยวดยิ่งและความสูงเบดต่าง ๆ ระยะเวลาในการแช่ ๑ ชั่วโมง (ร้อยละ white belly ของข้าวอ้างอิง = ร้อยละ ๒๐)



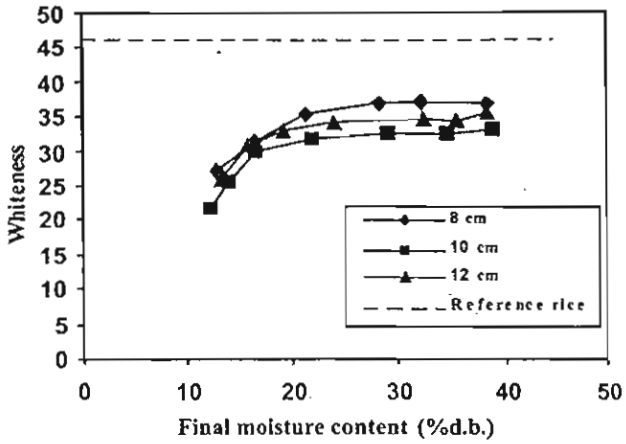
รูปที่ ๑๒ ความสัมพันธ์ระหว่าง white belly กับความชื้นสุดท้ายของข้าวกล้องที่ระยะเวลาในการแช่ต่าง ๆ อุณหภูมิไอน้ำร้อนยวดยิ่ง ๑๔๐ องศาเซลเซียสและความสูงเบด ๑๐ เซนติเมตร



รูปที่ ๑๓ ความสัมพันธ์ระหว่าง white belly กับความชื้นสุดท้าย ของข้าวกล้องที่อบแห้งด้วยไอน้ำร้อนยวดยิ่งกับอากาศร้อน ที่ระยะเวลาในการแช่ ๒ ชั่วโมง อุณหภูมิในการอบแห้ง ๑๔๐ องศาเซลเซียส

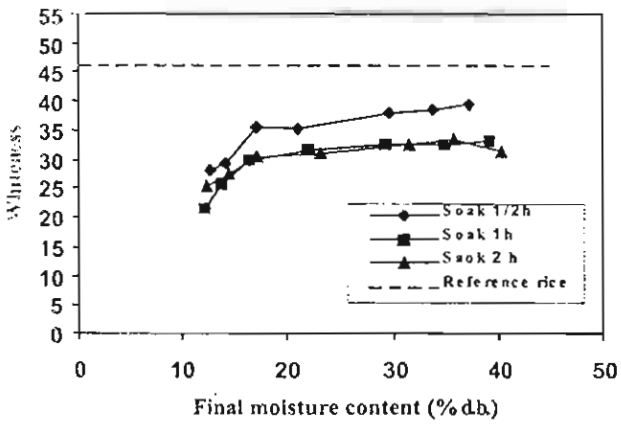


ก) ความสูงเบด ๑๐ เซนติเมตร

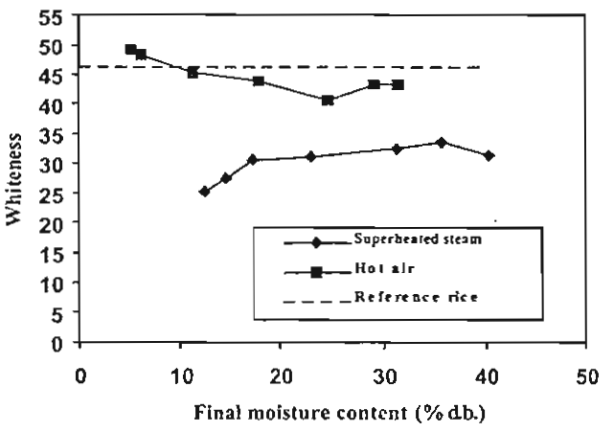


ข) อุณหภูมิไอน้ำร้อนยวดยิ่ง ๑๔๐ องศาเซลเซียส

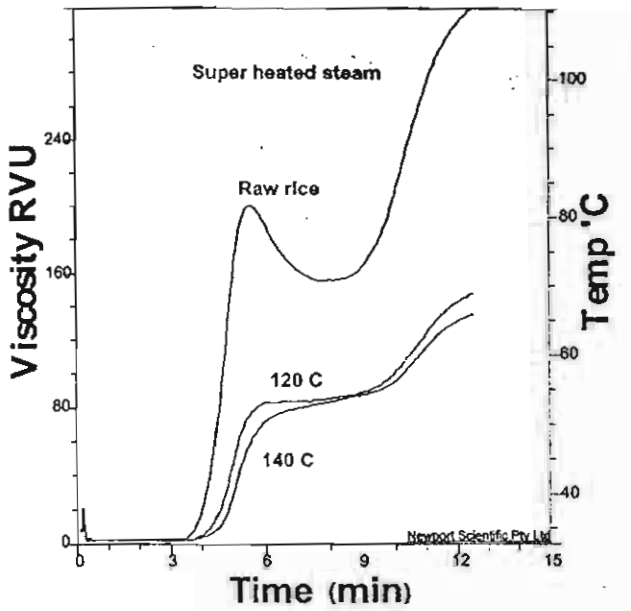
รูปที่ ๑๕ ความสัมพันธ์ระหว่างความขาวกับความชื้นสุดท้ายของข้าวกล้องที่อุณหภูมิไอน้ำร้อนยวดยิ่งและความสูงเบดต่าง ๆ ระยะเวลาในการแช่ ๑ ชั่วโมง (ความขาวของข้าวสารอ้างอิง ๔๔.๖)



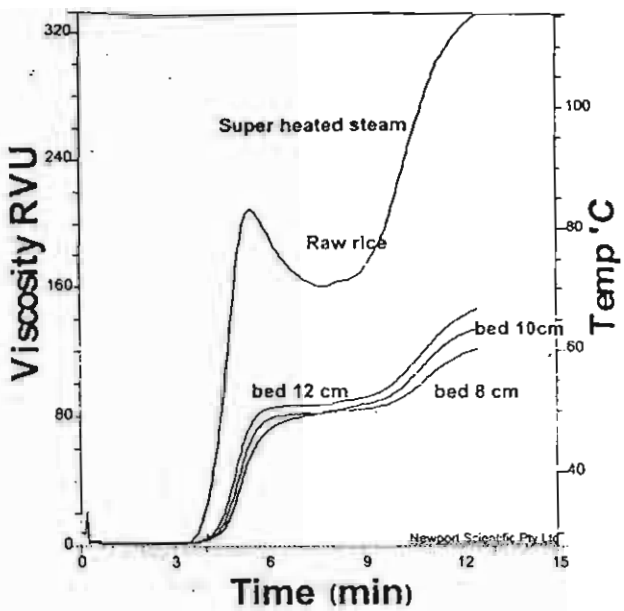
รูปที่ ๑๔ ความสัมพันธ์ระหว่างความขาวกับความชื้นสุดท้ายของข้าวกล้องที่ระยะเวลาในการแช่ต่าง ๆ อุณหภูมิไอน้ำร้อนยวดยิ่ง ๑๔๐ องศาเซลเซียส และความสูงเบด ๑๐ เซนติเมตร (ความขาวของข้าวสารอ้างอิง ๔๔.๖)



รูปที่ ๑๖ ความสัมพันธ์ระหว่างความขาวกับความชื้นสุดท้ายของข้าวกล้องที่อบแห้งด้วยไอน้ำร้อนยวดยิ่งกับอากาศร้อนที่ระยะเวลาในการแช่ ๒ ชั่วโมง อุณหภูมิในการอบแห้ง ๑๔๐ องศาเซลเซียส (ความขาวของข้าวสารอ้างอิง ๔๔.๖)

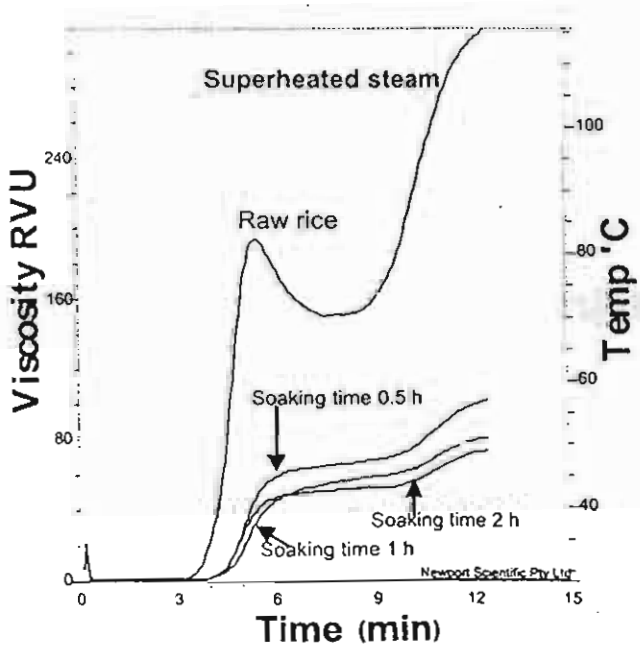


ก) ความสูงเบด ๑๐ เซนติเมตร

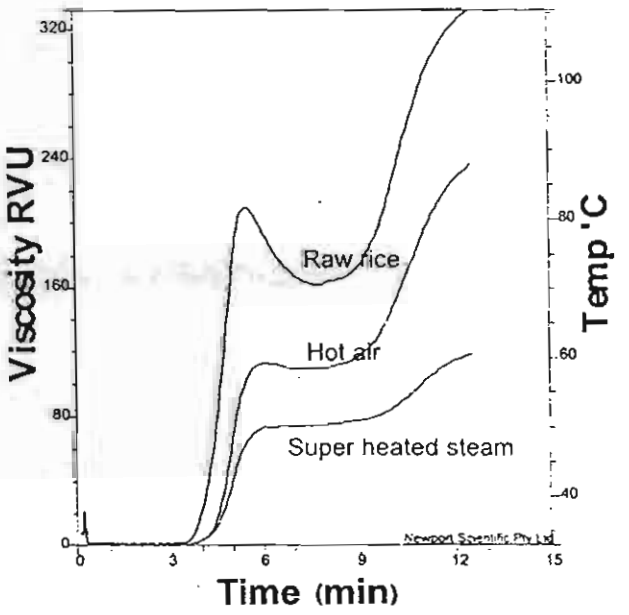


ข) อุณหภูมิไอน้ำร้อนยวดยิ่ง ๑๔๐ องศาเซลเซียส

รูปที่ ๑๗ ความเหนียวของแป้งข้าวที่อุณหภูมิของไอน้ำร้อนยวดยิ่งและความสูงเบดต่าง ๆ ที่ระยะเวลาในการแช่ ๑ ชั่วโมง



รูปที่ ๑๘ ความเหนียวของแป้งข้าวที่ผ่านการแช่ในระยะเวลาต่าง ๆ อุณหภูมิอบแห้ง ๑๔๐ องศาเซลเซียส และความสูงเบด ๑๐ เซนติเมตร



รูปที่ ๑๙ ความเหนียวของแป้งข้าวที่ผ่านกระบวนการอบแห้งด้วยไอน้ำร้อนยวดยิ่งกับอากาศร้อนที่ระยะเวลาในการแช่ ๒ ชั่วโมง อุณหภูมิอบแห้ง ๑๔๐ องศาเซลเซียสและความสูงเบด ๑๐ เซนติเมตร

Abstract

Parboiling Brown Rice Using Superheated Steam Fluidization Technique

Somchart Soponronnarit
Fellow of the Academy of Science, The Royal Institute, Thailand
Athikom Jirajindalert
Adisak Nathakaranakule
Chaiyong Taechapairoj

Conventional parboiled rice is produced from paddy as raw material which results in long process time as well as energy consumption. In order to reduce process time, this research aims to study parboiling of brown rice using superheated steam fluidization technique. The influence of soaking temperature and time, steaming temperature, and bed depth on qualities of product: head rice yield, white belly, whiteness, and viscosity of rice flour were focused. The experiments were set up at the material initial moisture content of 12.8% d.b., soaking temperatures of 70 - 90°C, soaking times of 0.5 - 2.0 h, steaming temperatures of 120 - 160°C, velocity of 3.9 m/s and bed depths of 8 - 12 cm. The experimental result showed that gelatinization occurred while product moisture content was decreasing, and final moisture content about 28% d.b. gave the acceptable levels of the whiteness and white belly. The final moisture content lower than 28% and 18% d.b. resulted in the lower percentage of head rice yield and whiteness, respectively. Considering white belly, it was found that the white belly decreased with increasing drying time. Additionally, peak viscosity, breakdown viscosity and setback viscosity of rice flour were found lower than those of raw rice.

Key words : drying, fluidized bed, parboiled rice, quality

นิพนธ์

วารสารราชบัณฑิตยสถาน
ปีที่ ๓๐ ฉบับที่ ๒ เม.ย.-มิ.ย. ๒๕๔๘

การพัฒนาเครื่องต้นแบบอบแห้งข้าวนึ่งแบบฟลูอิไดซ์เบดโดยใช้ไอน้ำร้อนยวดยิ่ง

วทัญญู รอดประพัฒน์[๑]
อดิศักดิ์ นาถกรณกุล[๒]
วารุณี เตีย[๓]
สมชาติ โสภณรณฤทธิ์[๔]
ราชบัณฑิต สำนักวิทยาศาสตร์
ราชบัณฑิตยสถาน

บทคัดย่อ

กรรมวิธีการผลิตข้าวนึ่งในปัจจุบันมีเครื่องจักรอุปกรณ์จำนวนมาก และใช้เวลาในการผลิตยาวนาน ดังนั้น งานวิจัยนี้จึงมีวัตถุประสงค์ที่จะพัฒนาการอบแห้งข้าวเปลือกด้วยเครื่องต้นแบบฟลูอิไดซ์เบดโดยใช้ไอน้ำร้อนยวดยิ่ง ขนาดกำลังผลิต ๑๐๐ กิโลกรัมต่อชั่วโมง ข้าวเปลือกที่ผ่านการแช่น้ำที่อุณหภูมิเริ่มต้น ๘๐ และ ๗๐ องศาเซลเซียส เป็นเวลา ๓ และ ๗-๘ ชั่วโมง ซึ่งจะได้ความชื้นประมาณร้อยละ ๒๘.๗ และ ๓๑.๓ มาตรฐานเปียก ตามลำดับ เมื่อผ่านการอบแห้งที่อุณหภูมิ ๑๒๘-๑๖๔ องศาเซลเซียส และใช้ความสูงเบดข้าวเปลือก ๘ เซนติเมตร ความเร็วของไอน้ำร้อนยวดยิ่ง ๓.๘ เมตรต่อวินาที เวลาในการอบแห้งประมาณ ๔-๕ นาที พบว่าสามารถลดความชื้นของข้าวเปลือกลงเหลือร้อยละ ๑๗.๙-๒๒.๘ มาตรฐานเปียก โดยที่ข้าวเปลือกที่ผ่านการอบแห้งจะมีลักษณะเป็นข้าวนึ่ง ความชื้นของข้าวเปลือกลดลงตามอุณหภูมิและระยะเวลาในการอบแห้งที่เพิ่มขึ้น ร้อยละต้นข้าวจะเพิ่มขึ้นเมื่อเทียบกับข้าวอ้างอิง ความขาวของข้าวสารจะลดลงตามอุณหภูมิอบแห้งที่เพิ่มขึ้น ส่วนสมบัติความหนืดของแป้ง มีค่า peak viscosity และค่า final viscosity ลดต่ำลง เมื่อเทียบกับข้าวอ้างอิง และมีแนวโน้มลดลงตามอุณหภูมิอบแห้งที่เพิ่มขึ้น จากผลการทดลองอบแห้งข้าวเปลือกด้วยเครื่องอบแห้งต้นแบบฟลูอิไดซ์เบดด้วยไอน้ำร้อนยวดยิ่ง พบว่านอกจากจะลดความชื้นข้าวเปลือกลงได้แล้วยังทำให้แป้งภายในเมล็ดข้าวเปลือกสุกหรือเกิดเจลาทิไนเซชันได้ในขั้นตอนเดียวกันด้วย จึงเป็นการรวมการนึ่งและอบแห้งไว้ในขั้นตอนเดียวกัน ซึ่งมีผลทำให้ลดต้นทุนและระยะเวลาในการผลิตข้าวนึ่งลง เมื่อเปรียบเทียบกับระบบการผลิตข้าวนึ่งในเชิงพาณิชย์

คำสำคัญ : การแช่, ข้าวนึ่ง, เจลาทิไนเซชัน, ฟลูอิไดเซชัน, สมบัติทางกายภาพ, ไอน้ำร้อนยวดยิ่ง

[๑] นักศึกษาปริญญาเอก คณะพลังงานและวัสดุ มหาวิทยาลัยเทคโนโลยีพระจอมเกล้าธนบุรี
[๒] ผู้ช่วยศาสตราจารย์ คณะพลังงานและวัสดุ มหาวิทยาลัยเทคโนโลยีพระจอมเกล้าธนบุรี
[๓] รองศาสตราจารย์ คณะพลังงานและวัสดุ มหาวิทยาลัยเทคโนโลยีพระจอมเกล้าธนบุรี
[๔] ศาสตราจารย์ คณะพลังงานและวัสดุ มหาวิทยาลัยเทคโนโลยีพระจอมเกล้าธนบุรี

๑. บทนำ

ประเทศไทยสามารถส่งออกข้าวเป็นอันดับหนึ่งของโลกติดต่อกันมาหลายปี แต่ต้นทุนในการผลิตข้าวในประเทศพบว่ายังคงสูงอยู่ โดยเฉพาะข้าวนึ่งที่กระบวนการผลิตมีหลายขั้นตอน คือ ๑) การแช่ (soaking) เพื่อทำให้ข้าวเปลือกนั้นมีความชื้นเพิ่มขึ้นระหว่างร้อยละ ๓๐-๔๕ มาตรฐานแห้ง โดยแช่ข้าวเปลือกในน้ำร้อนอุณหภูมิประมาณ ๖๐-๘๐ องศาเซลเซียส เป็นเวลาประมาณ ๓-๘ ชั่วโมง ๒) การนึ่ง (steaming) ด้วยไอน้ำอิ่มตัว ขั้นตอนนี้จะทำให้เม็ดแป้งเกิดเจลาทิไนซ์ ๓) การอบแห้งเพื่อลดความชื้นข้าวเปลือกที่เพิ่มขึ้นเมื่อผ่าน ๒ ขั้นตอนแรก ในการอบแห้งจะแบ่งออกเป็น ๒ ช่วง คือ ช่วงความชื้นสูงร้อยละ ๑๙ มาตรฐานเปียกขึ้นไป และช่วงความชื้นต่ำกว่าร้อยละ ๑๘ มาตรฐานเปียก

Taweerattanapanish และคณะ[๕] ได้ศึกษาความเป็นไปได้ของการอบแห้งข้าวเปลือกด้วยเทคนิคฟลูอิไดซ์เบด โดยใช้อากาศร้อน พบว่าความชื้นสุดท้ายของข้าวเปลือกมีผลต่อร้อยละต้นข้าว ถ้าความชื้นสุดท้ายของข้าวเปลือกต่ำกว่าร้อยละ ๑๘ มาตรฐานเปียก เมื่อนำไปสีจะได้ร้อยละต้นข้าวลดลง[๖] ได้ศึกษาและออกแบบเครื่องอบแห้งข้าวเปลือกแบบฟลูอิไดซ์เบด โดยใช้ไอน้ำร้อนยวดยิ่งเป็นตัวกลางในการถ่ายเทความร้อน (แบบงวด) ที่อุณหภูมิอบแห้ง ๑๕๐ และ ๑๗๐ องศาเซลเซียส ความสูงของเบด ๑๐-๑๕ เซนติเมตร พบว่าความเร็วต่ำสุดในการเกิดฟลูอิไดเซชันเท่ากับ ๒.๖ เมตรต่อวินาที อุณหภูมิอบแห้งมีผลต่ออัตราการอบแห้งมากกว่าความสูงของเบด และยังพบอีกว่าข้าวเปลือกที่ผ่านการอบแห้งด้วยไอน้ำร้อนยวดยิ่งแล้วจะมีร้อยละต้นข้าวเพิ่มสูงขึ้น แต่ความขาวของข้าวสารจะลดลง (สีคล้ายกับข้าวนึ่ง) และเมื่อนำไปทดสอบการหุง ข้าวมีลักษณะคล้ายกับข้าวนึ่ง Rordprapat และคณะ[๗] ได้ศึกษาเปรียบเทียบกับการอบแห้งด้วยอากาศร้อน พบว่าได้ร้อยละต้นข้าวที่สูงกว่าอย่างเห็นได้ชัด และจากงานวิจัยยังพบว่าการอบแห้งโดยใช้ไอน้ำร้อนยวดยิ่งมีข้อดีบางประการ เช่น มีอัตราการอบแห้งสูงและสามารถกำจัดกลิ่นของผลิตภัณฑ์ได้อีกด้วย

จากงานวิจัยที่ผ่านมาพบว่า การอบแห้งข้าวเปลือกที่มีความชื้นสูงด้วยไอน้ำร้อนยวดยิ่งด้วยเทคนิคฟลูอิไดซ์เบดสามารถลดขั้นตอนการผลิตข้าวนึ่งดังกล่าวข้างต้นได้ โดยสามารถรวมขั้นตอนการนึ่งและการอบแห้งช่วงแรกเข้าเป็นขั้นตอนเดียว ดังนั้น จุดประสงค์ของงานวิจัยนี้เพื่อออกแบบ สร้างและทดสอบสมรรถนะเครื่องอบแห้งต้นแบบฟลูอิไดซ์เบดโดยใช้ไอน้ำร้อนยวดยิ่ง สำหรับนึ่งและอบแห้งข้าวเปลือก โดยศึกษาเฉพาะสมบัติของข้าวที่ผ่านการอบแห้ง เช่น ร้อยละต้นข้าว ความขาว และร้อยละข้าวท้องไข่ โครงสร้างระดับจุลภาค (micro-structure) สมบัติทาง pasting และเปรียบเทียบกับการผลิตข้าวนึ่งในโรงสีข้าวจริง

๒. อุปกรณ์และวิธีการ

เครื่องอบแห้งที่ใช้ในการทดลองในงานวิจัยนี้เป็นเครื่องอบแห้งข้าวเปลือกแบบฟลูอิไดซ์เบดอย่างต่อเนื่อง (รูปที่ ๑) ประกอบด้วย (๑) เครื่องกำเนิดไอน้ำ (boiler) ความสามารถผลิตไอน้ำได้ประมาณ ๑๖๐ กิโลกรัมต่อชั่วโมง ความดันไอน้ำสูงสุด ๘ บาร์ ใช้สำหรับผลิตไอน้ำอิ่มตัวเพื่อป้อนเข้าระบบเครื่องอบแห้ง (๒) อุปกรณ์ให้ความร้อนขนาด ๓๐ กิโลวัตต์ มีหน้าที่เปลี่ยนสถานะของไอน้ำอิ่มตัวเป็นไอน้ำร้อนยวดยิ่ง (superheated steam) อุณหภูมิของไอน้ำร้อนยวดยิ่งก่อนเข้าห้องอบแห้งควบคุมด้วย PID ซึ่งมีค่าความถูกต้อง ± ๑ องศาเซลเซียส (๓) พัดลม (blower) เป็นแบบเหวี่ยงใบพัดโค้งหลัง (backward-curved centrifugal blower) ขับด้วยมอเตอร์ขนาด ๕.๕ แรงม้า ใช้สำหรับเวียนอากาศและไอน้ำร้อนยวดยิ่งภายในระบบเครื่องอบแห้ง (๔) ห้องอบแห้ง (drying chamber) ขนาดพื้นที่หน้าตัดตะแกรง ๒๐ × ๐.๔๕ ตารางเมตร (๕) เครื่องดักฝุ่น (cyclone) ทำหน้าที่ดักฝุ่นและข้าวลีบที่ปนมากับข้าวเปลือก (๖) โรทารีวาล์ว (rotary valve) ติดตั้งใต้เครื่องดักฝุ่นเพื่อทำหน้าที่ลำเลียงฝุ่นออกและป้องกันการรั่วของไอน้ำร้อนยวดยิ่งออกจากระบบอบแห้ง ส่วนการป้อนและปล่อยข้าวเปลือกใช้ความหนาของข้าวเปลือกเป็นตัวป้องกันการรั่วของไอน้ำร้อนยวดยิ่ง ซึ่งอุปกรณ์ทุกชิ้นทำด้วยเหล็กกล้าไม่เป็นสนิม (stainless steel) หุ้มด้วยฉนวนใยแก้วหนา ๒.๕ เซนติเมตร

๒.๑ การอบแห้งข้าวเปลือกด้วยไอน้ำร้อนยวดยิ่ง

นำข้าวเปลือกที่มีความชื้นสูง ที่ผ่านการแช่ (soaking) เพื่อเพิ่มความชื้น มาทดลองอบแห้งด้วยเครื่องอบแห้งต้นแบบฟลูอิไดซ์เบดโดยใช้ไอน้ำร้อนยวดยิ่ง มีขั้นตอนการทดลองดังนี้

๑. เริ่มเดินเครื่องอบแห้งต้นแบบ ตั้งอุณหภูมิอบแห้งไว้ที่ ๑๓๐ องศาเซลเซียส เมื่อเครื่องอบแห้งทำงานเข้าสู่ภาวะคงตัว จึงเริ่มปล่อยข้าวเปลือกเข้าไปในห้องอบแห้ง ปรับปริมาณของไอน้ำร้อนยวดยิ่งให้กระจายทั่วห้องอบแห้ง ปรับระดับความสูงของแผ่นกั้น (weir) ประมาณ ๘ เซนติเมตร วัดความเร็วของไอน้ำร้อนยวดยิ่ง

๒. ปล่อยให้เครื่องอบแห้งทำงานในภาวะคงตัว วัดอัตราการป้อนข้าวเปลือกทุก ๆ ๑๕ นาที และเก็บตัวอย่างข้าวเปลือกประมาณ ๕๐๐ กรัม ใส่ถุงพลาสติกร้อนมัดปากถุงให้สนิท ก่อนเข้าและออกจากเครื่องอบแห้งทุก ๆ ๑๐ นาที และจะทำงานต่อเนื่องประมาณ ๒-๓ ชั่วโมง

๓. นำตัวอย่างของข้าวเปลือกที่ผ่านการอบแห้งแล้ว ไปหาความชื้นด้วยตู้อบไฟฟ้า

๔. นำตัวอย่างข้าวเปลือกที่เหลือไปลดความชื้นให้เหลือประมาณร้อยละ ๑๔ มาตรฐานเปียก แล้วจึงนำไปทดสอบคุณภาพ

๕. ปรับตั้งอุณหภูมิอบแห้งของไอน้ำร้อนยวดยิ่งไว้ที่ ๑๓๐, ๑๕๐ และ ๑๗๐ องศาเซลเซียส และดำเนินการตามข้อที่ ๒-๔ ตามลำดับ

๒.๒ ข้าวเปลือกที่ใช้ในการทดลอง

ข้าวเปลือกที่นำมาใช้ในการอบแห้งแบ่งออกเป็น ๒ ส่วน คือ

๑. ข้าวเปลือกพันธุ์สุพรรณบุรี ๑ แช่ที่อุณหภูมิน้ำเริ่มต้น ๘๐ องศาเซลเซียส เป็นเวลาประมาณ ๓ ชั่วโมง แล้วรินน้ำที่ใช้แช่ข้าวเปลือกออก และเก็บข้าวเปลือกไว้ในที่อับอากาศเป็นเวลา ๑ ชั่วโมง[๕] ก่อนนำข้าวเปลือกไปอบแห้ง

๒. ข้าวเปลือกที่แช่จากโรงสีข้าวนึ่งที่ผลิตในเชิงพาณิชย์ พันธุ์ชัยนาท ๑ โดยแช่น้ำอุณหภูมิเฉลี่ยประมาณ ๗๐ องศาเซลเซียส เป็นเวลาประมาณ ๗-๘ ชั่วโมง แล้วเก็บไว้ในที่อับอากาศประมาณ ๒ ชั่วโมง ก่อนนำข้าวเปลือกไปอบแห้ง

๒.๓ หาความชื้นของเมล็ดข้าวเปลือก

การหาความชื้นของข้าวเปลือกที่ผ่านการอบแห้ง ใช้ตู้อบไฟฟ้า (hot air oven) ด้วยวิธีการของ American Association of Cereal Chemists (AACC)[๕] โดยอบแห้งข้าวเปลือกตัวอย่างที่อุณหภูมิ ๑๐๓ องศาเซลเซียส เป็นเวลา ๗๒ ชั่วโมง เครื่องชั่งน้ำหนักสำหรับหาความชื้นเป็นแบบดิจิทัลมีความละเอียด ± ๐.๐๑ กรัม ชั่งน้ำหนักสูงสุด ๕๐๐ กรัม

๒.๔ คุณภาพการสี

นำข้าวเปลือกที่ผ่านการอบแห้งตามเงื่อนไขต่าง ๆ อบแห้งด้วยอากาศแวดล้อมเพื่อให้มีความชื้นเหลือประมาณร้อยละ ๑๔ มาตรฐานเปียก แล้วจึงนำไปทดสอบคุณภาพการสี โดยใช้เครื่องกะเทาะเปลือกแบบลูกยางยี่ห้อ Satake และขัดขาวด้วยเครื่อง McGill Miller ข้าวที่ผ่านการขัดขาวแล้วนำไปคัดแยกข้าวหักด้วยตะแกรงกลม และวัดความขาวด้วยเครื่องวัดความขาวยี่ห้อ Kett model C-300 เครื่องชั่งน้ำหนักสำหรับหาคุณภาพการสีเป็นแบบดิจิทัล มีความละเอียด ± ๐.๑ กรัม ชั่งน้ำหนักสูงสุดได้ ๕๐๐ กรัม

๒.๕ วิธีการหาร้อยละข้าวท้องไข่ (white belly)

นำต้นข้าวที่ได้จากการทดสอบคุณภาพการสี จำนวน ๑๐๐ เมล็ด มาแยกข้าวที่เป็น white belly คือเมล็ดข้าวที่มีพื้นที่ขาวขุ่น ทึบแสงเกินร้อยละ ๕๐ ของพื้นที่ทั้งเมล็ดออกจากกลุ่ม โดยใช้แสงไฟส่องจากด้านล่างของเมล็ด ทำซ้ำกันจำนวน ๓ ครั้ง แล้วนำค่าที่ได้ไปหาค่าเฉลี่ยทางสถิติ

๒.๖ ตรวจสอบโครงสร้างระดับจุลภาค (micro-structure)

การหาโครงสร้างภายในของเมล็ดข้าวสารที่ผ่านกระบวนการอบแห้ง หาได้โดยนำไปส่องด้วยกล้องอิเล็กตรอนแบบส่องกราด (scanning electron microscopes) รุ่น JSM-5600 LV/JSM-5600 Japan ที่มีกำลังขยาย ๑,๐๐๐ เท่า

๒.๗ ความหนืดของแป้ง (viscosity)

ความหนืดของแป้งหาได้จากการวัดสมบัติทาง pasting ของข้าวนึ่งโดยใช้เครื่อง Rapid Visco

Analyzer model-4 (Newport Scientific Pty Ltd., Warier wood, Australia) ดำเนินตามวิธีการของ AACC (1995) Method 61-02[๔] โดยการนำตัวอย่างแป้งข้าวที่ผ่านการบดละเอียดด้วยเครื่อง Ultra centrifugal mill ตะแกรงขนาด ๐.๒๕ มิลลิเมตร ใช้แป้งในการทดสอบจำนวน ๓ ± ๐.๐๐๐๑ กรัม ผสมกับน้ำกลั่น ๒๕ ± ๐.๑ มิลลิลิตร ก่อนนำไปเข้าทดสอบใช้ใบพายคนแป้งกับน้ำให้ละลายเป็นเนื้อเดียวกัน แล้วนำตัวอย่างที่เตรียมได้เข้าเครื่อง RVA ความเร็วรอบของใบกวน ๑๐ วินาทีแรกเท่ากับ ๙๖๐ รอบต่อนาที หลังจากนั้นลดความเร็วรอบเท่ากับ ๑๖๐ รอบต่อนาที จนสิ้นสุดการทดสอบ การเปลี่ยนแปลงอุณหภูมิของเครื่องทดสอบจะเริ่มจาก ๕๐ องศาเซลเซียส เป็นเวลา ๑ นาที ต่อจากนั้นอุณหภูมิจะเพิ่มเป็น ๙๕ องศาเซลเซียส ด้วยอัตรา ๑๒ องศาเซลเซียสต่อนาที และคงไว้ที่อุณหภูมิ ๙๕ องศาเซลเซียสเป็นเวลา ๒.๕ นาที จากนั้นทำให้เย็นลงกลับมาที่อุณหภูมิ ๕๐ องศาเซลเซียส ด้วยอัตราการทำให้เย็น ๑๒ องศาเซลเซียสต่อนาที แล้วรักษาอุณหภูมิไว้ที่ ๕๐ องศาเซลเซียส เป็นเวลา ๒ นาที การทดสอบแต่ละตัวอย่างจะใช้เวลา ๑๒ นาที ๓๐ วินาที โดยจะทดสอบแต่ละตัวอย่างซ้ำ ๒ ครั้ง สมบัติ pasting ต่าง ๆ ถูก plot เทียบกับเวลา ค่าที่ได้จากกราฟ pasting properties ได้แก่ ค่าอุณหภูมิเริ่มเกิดเจลาทิไนเซชัน (pasting temperature) ค่าความหนืดสูงสุด (peak viscosity) ค่าความคงทนต่อการกวน (trough) และค่าความหนืดสุดท้าย (final viscosity)

๒.๘ ปริมาณการดูดซับน้ำ (water absorption)

กระบวนการทดสอบค่าการดูดซับน้ำของเมล็ดข้าวใช้วิธีการของ Sabularse และคณะ[๖] โดยนำข้าวสาร ๑๐ กรัม ใส่ในน้ำ ๒๐ ± ๐.๐๑ มิลลิลิตร ในหลอดทดลองแล้วต้มใน water bath ที่อุณหภูมิ ๙๕ องศาเซลเซียส เป็นเวลาเท่ากับเวลาของ cooking time หลังจากนั้นคำนวณปริมาณของน้ำหนักที่เพิ่มขึ้น ชั่งน้ำหนักโดยใช้เครื่องชั่งน้ำหนักแบบดิจิทัล มีค่าความละเอียด ± ๐.๐๐๑ กรัม

๒.๙ การหาค่าความแข็ง (hardness)

วัดค่าความแข็งโดยเครื่องมือที่เรียกว่า texture analyzer ซึ่งในการวัดค่าความแข็งนั้นต้องใช้ข้าวที่ผ่านการหุงสุกแล้ว และข้าวแต่ละชนิดจะใช้ปริมาณในการหุงที่แตกต่างกัน วิธีการหุงข้าวในงานวิจัยนี้ใช้ของ Banjong[๗]

๓. ผลการทดลองและวิจารณ์ (results and discussion)

การอบแห้งข้าวเปลือกด้วยเครื่องต้นแบบอบแห้งข้าวเปลือกแบบฟลูอิไดซ์เบดด้วยไอน้ำร้อนยวดยิ่ง ในงานวิจัยนี้แบ่งออกเป็น ๒ ส่วน คือ ทดลองที่เงื่อนไขต่าง ๆ เพื่อหาเงื่อนไขที่เหมาะสมในการอบแห้ง และทดลองร่วมกับโรงสีข้าวนึ่งที่ผลิตในเชิงพาณิชย์เพื่อเปรียบเทียบกับระบบการผลิตข้าวนึ่งแบบเดิมที่ใช้อยู่ในปัจจุบัน โดยตรวจสอบคุณภาพข้าวหลังการอบแห้งในรูปของร้อยละต้นข้าว ความขาว ร้อยละข้าวท้องไข่ ความหนืดของแป้ง และโครงสร้างระดับจุลภาค ผลการทดลองมีรายละเอียด ดังนี้

๓.๑ หลักการทำงานและลักษณะการเกิดฟลูอิไดเซชัน

ในการอบแห้งข้าวเปลือกด้วยเครื่องต้นแบบฟลูอิไดซ์เบดด้วยไอน้ำร้อนยวดยิ่ง ก่อนเริ่มอบแห้งข้าวเปลือกด้วยไอน้ำร้อนยวดยิ่ง ต้องอุ่นอุปกรณ์ในระบบด้วยอากาศร้อนเพื่อให้อุณหภูมิของอุปกรณ์สูงกว่าอุณหภูมิที่เกิดการควบแน่นของไอน้ำ (มากกว่า ๑๐๐ องศาเซลเซียส) เพื่อป้องกันการควบแน่นของไอน้ำเมื่อถูกปล่อยเข้ามาในระบบอบแห้ง ซึ่งอาจมีผลกระทบต่อการทำงานของเครื่องอบแห้ง แล้วจึงเปิดวาล์วเพื่อปล่อยไอน้ำจากเครื่องกำเนิดไอน้ำเข้ามาแทนที่อากาศร้อนที่อยู่ภายในระบบอบแห้ง โดยที่ไอน้ำอิ่มตัวจะไหลผ่านอุปกรณ์ให้ความร้อน (superheater) กลายเป็นไอน้ำร้อนยวดยิ่ง ไหลผ่านพัดลม (blower) ห้องอบแห้ง (drying chamber) เครื่องแยกฝุ่น (cyclone) ส่วนอากาศจะถูกระบายออกทางช่องระบายอากาศทิ้ง เพื่อระบบจะถูกแทนที่ด้วยไอน้ำร้อนยวดยิ่งทั้งหมด โดยสังเกตได้จากควันที่ระบายออกจากท่อระบายอากาศและกระแสไฟฟ้าที่ใช้จะลดลง จะปิดช่องระบายอากาศ เพื่อให้ภายในระบบมีเฉพาะไอน้ำร้อนยวดยิ่งเพียงอย่างเดียว เมื่ออุณหภูมิของไอน้ำร้อนยวดยิ่งใน

ระบบเท่ากับอุณหภูมิอบแห้งที่ตั้งไว้ตามเงื่อนไขการอบแห้ง ข้าวเปลือกจะถูกปล่อยจากถังพักเข้ามาในห้องอบแห้ง ในช่วงแรกของการอบแห้งเกิดการควบแน่นของไอน้ำขึ้นในเบดข้าวเปลือก เบดข้าวเปลือกในช่วงนี้จะนิ่ง และเริ่มเกิด channeling ตามมา เมื่อไอน้ำที่ควบแน่นระเหยกลายเป็นไอน้ำร้อนยวดยิ่งหมดแล้ว เมล็ดข้าวเปลือกในเบดจะเริ่มเปลี่ยนเป็น bubbling bed และจะเริ่มลอยตัวอย่างสม่ำเสมอทั่วทั้งเบดในเวลาต่อมา การอบแห้งข้าวเปลือกด้วยไอน้ำร้อนยวดยิ่งจะดำเนินไปอย่างต่อเนื่อง ในงานวิจัยนี้ควบคุมให้เมล็ดข้าวเปลือกมีเวลาอยู่ในห้องอบแห้ง (residence time) ประมาณ ๔-๕ นาที เพื่อให้ได้ความชื้นสุดท้ายประมาณร้อยละ ๑๘ มาตรฐานแห้ง ข้าวเปลือกที่ความชื้นนี้เมื่อนำไปทดสอบการสีจะได้ร้อยละต้นข้าวสูง[๖] ระยะเวลาที่ข้าวเปลือกอยู่ในห้องอบแห้งสามารถควบคุมได้โดยการควบคุมอัตราการป้อนข้าวเปลือกเข้าสู่เครื่องอบแห้ง ในการทดลองแต่ละครั้งจะใช้เวลาทั้งหมด ๒-๓ ชั่วโมง

๓.๒ การเปลี่ยนแปลงความชื้นและคุณภาพทางด้านกายภาพของข้าวที่อบแห้งแบบฟลูอิไดซ์เบดด้วยไอน้ำร้อนยวดยิ่ง

ผลการทดลองอบแห้งข้าวเปลือกพันธุ์สุพรรณบุรี ๑ ที่เพิ่มความชื้นโดยการแช่น้ำที่อุณหภูมิเริ่มต้น ๘๐ องศาเซลเซียส เป็นเวลา ๓ ชั่วโมง (ตารางที่ ๑) ข้าวเปลือกหลังการแช่มีความชื้นร้อยละ ๒๘.๗ ± ๐.๖ มาตรฐานเปียก เมื่อผ่านการอบแห้งด้วยไอน้ำร้อนยวดยิ่งอุณหภูมิ ๑๒๘, ๑๔๗ และ ๑๖๔ องศาเซลเซียส เป็นระยะเวลา ๔.๕-๔.๘ นาที พบว่าความชื้นของเมล็ดข้าวเปลือกจะลดลงตามอุณหภูมิอบแห้งที่เพิ่มขึ้น ซึ่งมีความชื้นร้อยละ ๑๘.๘ ± ๐.๖, ๑๗.๙ ± ๐.๗ และ ๑๕ ± ๐.๖ มาตรฐานเปียก ตามลำดับ เมล็ดข้าวเปลือกที่อบแห้งด้วยไอน้ำร้อนยวดยิ่งจะได้ร้อยละต้นข้าวสูงกว่าเมื่อเทียบกับข้าวเปลือกก่อนอบแห้ง (ร้อยละ ๕๓.๗) เพราะว่าแป้งภายในเมล็ดข้าวเปลือกที่ผ่านการอบแห้งด้วยไอน้ำร้อนยวดยิ่งเกิดเจลาทิไนเซชันได้อย่างเหมาะสม[๗, ๘] เมื่อนำไปสี จึงทำให้ได้ร้อยละต้นข้าวที่สูง ที่อุณหภูมิอบแห้งเฉลี่ย ๑๒๘ และ ๑๔๗ องศาเซลเซียส ร้อยละต้นข้าวมีค่าไม่แตกต่างกันมากนัก (ร้อยละ ๖๕.๙ ± ๑.๐ และ ๖๖.๘ ± ๐.๖ ตามลำดับ) เมื่ออบแห้งด้วยอุณหภูมิ ๑๖๔ องศาเซลเซียส ร้อยละต้นข้าวจะลดลง (ร้อยละ ๕๙ ± ๒.๕) เนื่องจากความชื้นข้าวเปลือกหลังการอบแห้งต่ำมาก จึงทำให้เมล็ดข้าวเปลือกเกิดความแตกต่างของความชื้นระหว่างภายนอกกับภายในเมล็ดข้าวเปลือก ทำให้เกิดความเค้นขึ้นภายในเมล็ดข้าวเปลือก ซึ่งสอดคล้องกับงานวิจัยของ Taechapiroj และคณะ[๖] ที่พบว่าถ้าความชื้นสุดท้ายของข้าวเปลือกที่อบแห้งด้วยไอน้ำร้อนยวดยิ่งต่ำกว่า ๑๕.๓ มาตรฐานเปียก จะทำให้ร้อยละต้นข้าวลดลง

ความขาวของข้าวสารที่อบแห้งด้วยไอน้ำร้อนยวดยิ่งจะลดลงเมื่อเทียบกับข้าวอ้างอิง (๔๒.๒ ± ๐.๖ จุด) โดยมีความแตกต่างกันอย่างชัดเจนตามอุณหภูมิของการอบแห้ง ๑๒๘, ๑๔๗ และ ๑๖๔ องศาเซลเซียส คือ ๓๖.๑ ± ๐.๓, ๓๓.๘ ± ๐.๗ และ ๒๙.๘ ± ๐.๘ ตามลำดับ ทั้งนี้ เพราะว่าช่วงแรกของการอบแห้งด้วยไอน้ำร้อนยวดยิ่งจะเกิดการควบแน่นของไอน้ำที่บริเวณผิว ทำให้ข้าวเปลือกมีความชื้นเพิ่มขึ้น อาจจะมีผลทำให้สีของเปลือกข้าวและสีของรำบางส่วนแพร่เข้าสู่ภายในเนื้อเมล็ดข้าวเปลือก จึงมีผลทำให้ความขาวของข้าวสารลดลง เมื่ออบแห้งข้าวเปลือกที่อุณหภูมิสูงขึ้น จะทำให้เมล็ดข้าวเปลือกมีอุณหภูมิสูงขึ้นตามอุณหภูมิเมล็ดข้าวเปลือกที่สูงนี้จะช่วยเร่งการเกิดปฏิกิริยาสีน้ำตาล (browning reaction) แบบเมลลาร์ด ซึ่งมีผลทำให้ข้าวสารที่ได้จากข้าวเปลือกที่อบแห้งที่อุณหภูมิสูงมีสีเข้มกว่าข้าวสารที่ได้จากข้าวเปลือกที่อบแห้งที่อุณหภูมิต่ำกว่า

ร้อยละข้าวท้องไข่ของข้าวเปลือกก่อนการอบแห้งเท่ากับร้อยละ ๕.๔ ± ๐.๖ เมื่อผ่านการอบแห้งด้วยไอน้ำร้อนยวดยิ่ง ร้อยละข้าวท้องไข่จะลดลงทุก ๆ เงื่อนไขการทดลอง (ร้อยละ ๑.๗ ± ๐.๖, ๑.๘ ± ๐.๖ และ ๑.๔ ± ๐.๖) ซึ่งอุณหภูมิอบแห้งของไอน้ำร้อนยวดยิ่งไม่มีอิทธิพลต่อการลดลงของร้อยละข้าวท้องไข่ เมื่อนำข้าวที่หุงสุกแล้วไปทดสอบความแข็ง (hardness) พบว่าข้าวที่อบแห้งด้วยไอน้ำร้อนยวดยิ่งจะมีความแข็งเพิ่มขึ้นเมื่อเทียบกับข้าวอ้างอิง โดยข้าวเปลือกที่ผ่านการอบแห้งที่อุณหภูมิเฉลี่ย ๑๒๘ และ ๑๔๗ องศา

เซลเซียส มีความแข็งไม่แตกต่างกัน (๔๘.๒ ± ๐.๗ N และ ๔๙.๒ ± ๑.๗ N) ส่วนข้าวเปลือกที่อบแห้งที่อุณหภูมิเฉลี่ย ๑๖๔ องศาเซลเซียส มีความแข็งเพิ่มขึ้นอย่างเห็นได้ชัด (๕๘.๙ ± ๐.๒ N) ขณะที่การดูดซับน้ำ (water absorption) ของข้าวเปลือกที่ผ่านการอบแห้งด้วยไอน้ำร้อนยวดยิ่งจะลดลงเมื่อเทียบกับข้าวเปลือกอ้างอิง (๓.๓ ± ๐.๐๓) จากการทดลองนี้พบว่าอุณหภูมิอบแห้งของไอน้ำร้อนยวดยิ่งที่สูงขึ้นไม่มีอิทธิพลต่อการดูดซับน้ำ (๒.๔ ± ๐.๐๓, ๒.๔ ± ๐.๑ และ ๒.๓ ± ๐.๑)

ผลการทดลองการอบแห้งข้าวเปลือกที่ผ่านการแช่จากโรงสีข้าวนึ่งที่ผลิตเชิงพาณิชย์ แสดงในตารางที่ ๑ และ ๒ โดยข้าวเปลือกที่ผ่านการแช่มีความชื้นร้อยละ ๓๑.๓ ± ๐.๔ มาตรฐานเปียก เมื่อผ่านการอบแห้งด้วยไอน้ำร้อนยวดยิ่ง ที่อุณหภูมิเฉลี่ย ๑๒๘ องศาเซลเซียส เป็นเวลาในการอบแห้ง ๔.๗ นาที ความชื้นลดลงเหลือร้อยละ ๒๒.๕ ± ๐.๔ มาตรฐานเปียก ถ้าอบแห้งที่อุณหภูมิอบแห้ง ๑๔๔ องศาเซลเซียส เป็นเวลาในการอบแห้ง ๔.๙ นาที ความชื้นลดลงเหลือร้อยละ ๑๘.๗ ± ๐.๓ มาตรฐานเปียก และที่อุณหภูมิอบแห้ง ๑๖๐ องศาเซลเซียส ระยะเวลาในการอบแห้ง ๔.๑ นาที ความชื้นลดลงเหลือร้อยละ ๑๗.๙ ± ๐.๓ มาตรฐานเปียก เมื่อนำข้าวเปลือกที่อบแห้งด้วยไอน้ำร้อนยวดยิ่งที่อุณหภูมิต่าง ๆ ไปผ่านกระบวนการสี พบว่าข้าวเปลือกที่อบแห้งด้วยไอน้ำร้อนยวดยิ่งมีร้อยละต้นข้าวเพิ่มขึ้นเมื่อเทียบกับข้าวเปลือกอ้างอิง หรือข้าวเปลือกที่ไม่ผ่านการอบแห้ง (ร้อยละ ๕๖.๖ ± ๑.๑) โดยข้าวเปลือกที่อบแห้งที่อุณหภูมิเฉลี่ย ๑๒๘ องศาเซลเซียส ให้ร้อยละต้นข้าว (ร้อยละ ๖๓.๕ ± ๐.๖) ต่ำกว่าข้าวเปลือกที่อบแห้งที่อุณหภูมิ ๑๔๔ และ ๑๖๐ องศาเซลเซียส (ร้อยละ ๖๖.๙ ± ๐.๖ และ ๖๗.๙ ± ๐.๖) ทั้งนี้ อาจเป็นเพราะว่าการเกิดเจลาทิไนซ์ของแป้งภายในเมล็ดข้าวเปลือกที่อุณหภูมิอบแห้งเฉลี่ย ๑๒๘ องศาเซลเซียส ยังไม่สมบูรณ์พอ

ความขาวของข้าวสารที่ได้จากข้าวเปลือกที่ผ่านการแช่จากโรงสีข้าวนึ่งมีค่าลดลง เมื่ออบแห้งด้วยไอน้ำร้อนยวดยิ่ง เมื่อเทียบกับข้าวอ้างอิง (๓๙ ± ๐.๒ จุด) ข้าวเปลือกที่อบแห้งที่อุณหภูมิ ๑๔๔ และ ๑๖๐ องศาเซลเซียส มีความขาวไม่แตกต่างกัน (๒๙.๔ ± ๐.๕ และ ๒๘ ± ๐.๖ จุด) เพราะว่าข้าวที่ผ่านการอบแห้งมีความชื้นสุดท้ายไม่แตกต่างกันมากนัก ซึ่งอาจมีผลทำให้การเกิดปฏิกิริยาสีน้ำตาลแบบเมลลาร์ดใกล้เคียงกัน แต่ความขาวข้าวสารที่ได้จากข้าวเปลือกที่อบแห้งด้วยอุณหภูมิเฉลี่ย ๑๒๘ องศาเซลเซียส (๓๒.๒ ± ๐.๘ จุด) มีค่าสูงที่สุดเพราะว่าอุณหภูมิของเมล็ดข้าวเปลือกต่ำ ดังนั้น การเกิดปฏิกิริยาสีน้ำตาลจึงน้อยกว่า

ข้าวเปลือกที่ผ่านการแช่จากโรงสีข้าวนึ่งที่มีข้าวท้องไข่เริ่มต้นร้อยละ ๕.๗ ± ๐.๖ เมื่อผ่านการอบแห้งด้วยไอน้ำร้อนยวดยิ่งแล้วไม่ปรากฏข้าวท้องไข่เหลืออยู่เลย แสดงว่าแป้งภายในเมล็ดข้าวเปลือกที่ผ่านการอบแห้งด้วยไอน้ำร้อนยวดยิ่งเกิดเจลาทิไนซ์ได้อย่างสมบูรณ์ ทั้งนี้ อาจเนื่องมาจากระยะเวลาการแช่ข้าวเปลือกที่นานกว่าทำให้น้ำสามารถแพร่เข้าสู่ภายในเมล็ดข้าวเปลือกได้มากกว่ากรณีที่แช่ ๓ ชั่วโมง ทำให้การเกิดเจลาทิไนซ์ของแป้ง ซึ่งเกิดได้ดีในช่วงอุณหภูมิและความชื้นสูง มีสภาวะที่เหมาะสมมากกว่า ความแข็งของข้าวเปลือกที่ผ่านการแช่จากโรงสีข้าวนึ่งที่อบแห้งด้วยไอน้ำร้อนยวดยิ่งจะมีค่าเพิ่มขึ้นเมื่อเทียบกับข้าวอ้างอิง และความแข็งของข้าวจะเพิ่มขึ้นตามอุณหภูมิอบแห้งที่สูงขึ้น ซึ่งตรงข้ามกับค่าการดูดซับน้ำของข้าวที่อบแห้งด้วยไอน้ำร้อนยวดยิ่งจะลดลงและลดลงตามอุณหภูมิการอบแห้งที่สูงขึ้น

๓.๓ สมบัติความหนืดของแป้ง (pasting properties)

เมื่อนำข้าวเปลือกหลังการแช่ (ข้าวอ้างอิง) และข้าวเปลือกที่ผ่านการอบแห้งด้วยเครื่องต้นแบบฟลูอิไดซ์เบดด้วยไอน้ำร้อนยวดยิ่ง ไปทดสอบสมบัติความหนืดของแป้ง ดังแสดงในรูปที่ ๒ และ ๓ พบว่า ข้าวที่ผ่านการแช่ ๓ ชั่วโมง และผ่านการอบแห้งที่อุณหภูมิต่าง ๆ ให้ค่าความหนืดสูงสุด (peak viscosity) ค่าความหนืดสุดท้าย (final viscosity) ต่ำกว่าข้าวอ้างอิง และมีแนวโน้มลดลงตามอุณหภูมิการอบแห้งที่สูงขึ้นและเมื่อเทียบข้าวนึ่งที่อบแห้งด้วยเครื่องต้นแบบฟลูอิไดซ์เบดด้วยไอน้ำร้อนยวดยิ่งกับข้าวนึ่งที่ผลิตในเชิงพาณิชย์ (parboiled rice) พบว่า ข้าวนึ่งที่ผลิตในเชิงพาณิชย์

มีค่า peak viscosity สูงกว่าข้าวที่ผ่านการอบแห้งด้วยเครื่องต้นแบบ ทุกเงื่อนไขการอบแห้ง แสดงว่าข้าวเปลือกที่ผ่านการอบแห้งด้วยเครื่องต้นแบบมีการเกิดเจลาทิไนซ์มากกว่าข้าวที่ผลิตในเชิงพาณิชย์ ซึ่งสอดคล้องกับงานวิจัยของ น้ำฝน ศีตะจิตต์ และอรอนงค์ นัยวิกุล[๙] โดยการเกิดเจลาทิไนเซชันดูได้จากค่าของความหนืดสูงสุด (peak viscosity) กล่าวคือ ข้าวอ้างอิงมีค่า peak viscosity สูง เพราะว่าเม็ดแป้งมีความสามารถในการดูดซับน้ำได้ปริมาณมากกว่าข้าวที่ผ่านกระบวนการอบแห้งด้วยไอน้ำร้อนยวดยิ่ง ทำให้เม็ดแป้งเกิดการพองตัวมากขึ้น เป็นผลทำให้แป้งมีค่าความหนืดสูง ส่วนข้าวผ่านการอบแห้งด้วยไอน้ำร้อนยวดยิ่งเมื่อได้รับความร้อนเม็ดแป้งที่ถูกน้ำจะพองตัวและถูกทำให้สุก และทำให้โปรตีนแตกตัวและแทรกเข้าไปอยู่ภายในช่องว่างระหว่างเม็ดแป้ง ซึ่งมีผลทำให้ข้าวมีการเกาะตัวกันแน่นและมีความแข็งมากขึ้น เมื่อนำไปวัดค่าความหนืด จึงทำให้ความสามารถในการดูดซับน้ำของเม็ดแป้งลดลง ซึ่งสอดคล้องกับค่าการดูดซับน้ำลดลงในตารางที่ ๑ และ ๒ นั้นแสดงว่าข้าวที่อบแห้งด้วยไอน้ำร้อนยวดยิ่งได้ผ่านการเกิดเจลาทิไนซ์มาแล้ว ซึ่งทำให้เม็ดแป้งพองตัวได้น้อยลงด้วย และค่า peak viscosity จะลดลงเมื่ออุณหภูมิอบแห้งสูงขึ้น สำหรับค่า final viscosity แสดงถึงสมบัติความแข็งกระด้างของข้าวสุก กล่าวคือข้าวที่มีค่า final viscosity ต่ำจะมีความแข็งกระด้างมากขึ้น จากผลการทดลองพบว่าข้าวที่ผ่านการอบแห้งที่อุณหภูมิสูงให้ค่า final viscosity ต่ำกว่าข้าวที่ผ่านการอบแห้งที่อุณหภูมิต่ำและที่ไม่ผ่านการอบแห้ง ตามลำดับ ดังนั้น แสดงว่าข้าวที่ผ่านการอบแห้งด้วยไอน้ำร้อนยวดยิ่งมีความแข็งกระด้างมากกว่าข้าวอ้างอิง และข้าวนึ่งที่ผลิตในเชิงพาณิชย์

๓.๔ โครงสร้างระดับจุลภาค (micro-structure)

ลักษณะโครงสร้างภายในเมล็ดข้าวที่ดูด้วยกล้องจุลทรรศน์แบบส่องกราดของข้าวอ้างอิงยังมีเม็ดแป้งเป็นส่วนใหญ่ จะสังเกตเห็นผลึกของเม็ดแป้งเหลืออยู่จำนวนมาก (รูปที่ ๔ ก) เมื่อข้าวเปลือกผ่านการอบแห้งด้วยไอน้ำร้อนยวดยิ่งที่อุณหภูมิเฉลี่ย ๑๒๘, ๑๔๗ และ ๑๖๔ องศาเซลเซียส (รูปที่ ๔ ข, ๔ ค และ ๔ ง) เม็ดแป้งจะเกิดการเจลาทิไนซ์ทำให้โครงสร้างเปลี่ยนไปเป็นเจล ผลึกที่เคยมองเห็นจากข้าวอ้างอิงจึงกลายเป็นพื้นผิวเรียบ ซึ่งผลของการเกิดเจลนี้เป็นสาเหตุของการเพิ่มขึ้นของร้อยละต้นข้าวและการลดลงของร้อยละข้าวท้องไข่ได้เมื่อเทียบกับข้าวอ้างอิง

เมื่อพิจารณาโครงสร้างของข้าวอ้างอิงที่ผ่านการแช่จากโรงสีข้าวนึ่งที่ผลิตในเชิงพาณิชย์ (รูปที่ ๕ ก) พบว่าโครงสร้างของข้าวเม็ดแป้งเหลืออยู่น้อย แสดงว่าเม็ดแป้งภายในเมล็ดข้าวเปลือกส่วนใหญ่ได้เกิดการเจลาทิไนซ์จากการแช่ เมื่อนำข้าวเปลือกดังกล่าวไปอบแห้งด้วยไอน้ำร้อนยวดยิ่ง ที่อุณหภูมิเฉลี่ย ๑๒๘, ๑๔๔ และ ๑๖๐ องศาเซลเซียส (รูปที่ ๕ ข, ๕ ค และ ๕ ง) จึงไม่ปรากฏโครงสร้างผลึกของเม็ดแป้งเหลืออยู่ ซึ่งสอดคล้องกับผลของร้อยละข้าวท้องไข่ที่ไม่พบเลย เมื่อนำข้าวเปลือกที่ผ่านการแช่จากโรงสีข้าวนึ่งที่ผลิตในเชิงพาณิชย์ไปอบแห้งด้วยไอน้ำร้อนยวดยิ่งนั้นแสดงว่าข้าวเปลือกที่ผ่านการแช่จากโรงสีข้าวนึ่ง (ที่อุณหภูมิน้ำเฉลี่ย ๗๐ องศาเซลเซียส เป็นเวลา ๗-๘ ชั่วโมง) มีการเกิดเจลที่สมบูรณ์มากกว่าข้าวเปลือกที่ผ่านการแช่ที่อุณหภูมิน้ำเริ่มต้น ๘๐ องศาเซลเซียส ระยะเวลานาน ๓ ชั่วโมง

เมื่อเปรียบเทียบโครงสร้างข้าวนึ่งที่ผ่านการอบแห้งด้วยเครื่องต้นแบบฟลูอิไดซ์เบดด้วยไอน้ำร้อนยวดยิ่งกับข้าวนึ่งที่ผลิตในเชิงพาณิชย์ ๒ โรง (ดังรูปที่ ๖ ก และ ๖ ข) พบว่าข้าวที่ผ่านการอบแห้งด้วยเครื่องต้นแบบนี้มีลักษณะคล้ายข้าวนึ่งที่ผลิตในเชิงพาณิชย์

๓.๕ ระบบการผลิตข้าวนึ่งที่ผลิตในเชิงพาณิชย์ที่ใช้อยู่ในปัจจุบัน

จากการพิจารณาระบบการผลิตข้าวนึ่งที่ผลิตในเชิงพาณิชย์ที่ใช้อยู่ในปัจจุบัน ขนาดกำลังผลิต ๒๐๐ ตันต่อวัน (ดูรูปที่ ๗ ประกอบ) ซึ่งมีขั้นตอนการทำงาน คือขั้นตอนการแช่ (soaking) นำข้าวเปลือกนาปีพันธุ์พลายงาม ความชื้นร้อยละ ๑๗.๙ มาตรฐานเปียก แช่น้ำเริ่มต้นที่อุณหภูมิ ๗๐ องศาเซลเซียส เป็นเวลาประมาณ ๗-๘ ชั่วโมง แล้วจึงระบายน้ำที่แช่ออก หลังจากนั้นปล่อยทิ้งไว้ (tempering) ประมาณ ๑ ชั่วโมง พบว่าความชื้น

ข้าวเปลือกจะเพิ่มขึ้นเป็นร้อยละ ๓๒.๖ มาตรฐานเปียก ก่อนจะลำเลียงเข้าสู่ขั้นตอนการนึ่ง (steaming) ซึ่งใช้ไอน้ำอิ่มตัวเป็นตัวกลางในการให้ความร้อน (แบบต่อเนื่อง) เป็นเวลาประมาณ ๑๕ นาที ข้าวเปลือกที่ผ่านขั้นตอนการนึ่งมามีบางส่วนเกิดการปริแตกเนื่องจากการพองและขยายตัวของเม็ดแป้งมากเกินไป ดังนั้น ก่อนการอบแห้งจึงต้องเป่าด้วยลมธรรมชาติเพื่อหุบเปลือกก่อน เพื่อป้องกันไม่ให้ฝุ่นละอองหรือลมร้อนที่ไม่สะอาดเข้าไปสัมผัสกับเนื้อข้าวสารโดยตรง หลังจากนั้นข้าวเปลือกจะเข้าสู่ขั้นตอนการอบแห้ง (drying) ด้วยเครื่องอบแห้งแบบฟลูอิไดซ์เบดโดยใช้อากาศร้อนที่อุณหภูมิ ๑๓๕ องศาเซลเซียส เพื่อลดความชื้นข้าวเปลือกลงเหลือร้อยละ ๒๘.๕ มาตรฐานเปียก ก่อนนำไปเก็บในที่อับอากาศและเป่าด้วยลมธรรมชาติให้ความชื้นลดลงเหลือร้อยละ ๒๔.๒ มาตรฐานเปียก แล้วจึงนำข้าวเปลือกไปอบแห้งต่อด้วยเครื่องอบแห้งฟลูอิไดซ์-เบดตัวที่ ๒ ที่อุณหภูมิอบแห้ง ๑๑๘ องศาเซลเซียส เพื่อลดความชื้นลงเหลือร้อยละ ๒๑.๔ มาตรฐานเปียก หลังจากนั้นนำข้าวเปลือกไปเก็บในที่อับอากาศและเป่าด้วยลมธรรมชาติอีกครั้งหนึ่งให้ความชื้นลดลงเหลือร้อยละ ๑๘.๔ มาตรฐานเปียก แล้วจึงนำไปอบแห้งด้วยเครื่องอบแห้งแบบ LSU ที่อุณหภูมิอบแห้ง ๑๒๐ องศาเซลเซียส ให้ความชื้นลดลงเหลือร้อยละ ๑๒.๔ มาตรฐานเปียก แล้วจึงนำไปเก็บไว้เพื่อรอการสีต่อไป

จะเห็นได้ว่าการผลิตข้าวนึ่งมีหลายขั้นตอนและใช้เครื่องจักรจำนวนมาก ทำให้ระยะเวลาที่ใช้ในการผลิตนาน ส่งผลต่อต้นทุนที่ใช้ในการผลิตข้าวนึ่งสูงตามไปด้วย ขณะที่การอบแห้งด้วยเครื่องอบแห้งต้นแบบฟลูอิไดซ์เบดด้วยไอน้ำร้อนยวดยิ่ง (แบบต่อเนื่อง) สามารถรวมการนึ่งและอบแห้งข้าวเปลือกไว้ในขั้นตอนเดียวกันได้ โดยที่เครื่องอบแห้งแบบใหม่นี้สามารถลดความชื้นจากร้อยละ ๓๑-๓๒ มาตรฐานเปียก เหลือความชื้นร้อยละ ๑๘-๑๙ มาตรฐานเปียก ขณะที่คุณภาพข้าวสารอยู่ในเกณฑ์ดีมากเมื่อเทียบกับข้าวนึ่งที่ผลิตในเชิงพาณิชย์ ดังนั้น การนำเครื่องต้นแบบนี้มาปรับใช้กับระบบการผลิตข้าวนึ่งที่ผลิตในเชิงพาณิชย์ในปัจจุบัน จะสามารถลดขั้นตอนการผลิตข้าวนึ่งและเครื่องจักรลง (ในกรอบเส้นประในรูปที่ ๗) คือ ขั้นตอนการนึ่ง การหุบเปลือก การอบแห้งด้วยเครื่องฟลูอิไดซ์เบด การเก็บในที่อับอากาศและการเป่าด้วยอากาศแวดล้อม และลดเครื่องอบแห้งแบบฟลูอิไดซ์เบดโดยใช้อากาศร้อนได้ ๒ เครื่อง เตาเผาแกลบแบบไซโคลน ๑ เครื่อง จะเห็นได้ว่าสามารถลดต้นทุนในการผลิตข้าวนึ่งลงได้มาก รวมทั้งสามารถลดเวลาในการผลิตข้าวนึ่งลงได้อย่างน้อย ๓-๔ ชั่วโมง ระบบการผลิตข้าวนึ่งแบบใหม่ใช้เครื่องอบแห้งฟลูอิไดซ์เบดด้วยไอน้ำร้อนยวดยิ่ง (รูปที่ ๘) มีขั้นตอนการผลิตข้าวนึ่งแบบใหม่ คือ การแช่ การอบแห้งแบบฟลูอิไดซ์เบดด้วยไอน้ำร้อนยวดยิ่ง การเก็บในที่อับอากาศและเป่าด้วยลมธรรมชาติ และการอบแห้งด้วยเครื่องอบแห้งแบบ LSU ซึ่งข้าวเปลือกที่ผ่านการอบแห้งในขั้นตอนสุดท้ายนี้จะมีความชื้นเหมาะสมแก่การแปรรูปและเก็บรักษาพอดี

๔. สรุปผลการทดลอง

จากการทดสอบอบแห้งข้าวเปลือกโดยใช้เครื่องอบแห้งต้นแบบฟลูอิไดซ์เบดด้วยไอน้ำร้อนยวดยิ่ง ขนาดกำลังผลิต ๑๐๐ กิโลกรัมต่อชั่วโมง โดยใช้ข้าวเปลือกที่ผ่านการแช่น้ำที่อุณหภูมิเริ่มต้น ๘๐ องศาเซลเซียส เป็นเวลา ๓ ชั่วโมง และข้าวเปลือกที่ผ่านการแช่ในโรงสีข้าวนึ่ง ซึ่งใช้อุณหภูมิในการแช่ต่ำกว่า (ประมาณ ๗๐ องศาเซลเซียส) แต่ใช้เวลาในการแช่นาน (ประมาณ ๗-๘ ชั่วโมง) พบว่า โครงสร้างของเม็ดแป้งภายในเมล็ดข้าวเปลือกที่ผ่านการแช่น้ำอุ่น ๓ ชั่วโมง เกิดการเจลาทิไนซ์ได้น้อยกว่าข้าวเปลือกที่ผ่านการแช่จากโรงสีข้าวนึ่ง และเมื่อนำไปอบแห้งด้วยไอน้ำร้อนยวดยิ่งที่อุณหภูมิเฉลี่ย ๑๒๘-๑๖๔ องศาเซลเซียส และความสูงของเบดข้าวเปลือก ๘ เซนติเมตร ความเร็วของไอน้ำร้อนยวดยิ่ง ๓.๘ เมตรต่อวินาที เวลาในการอบแห้ง (residence time) ๔.๑-๔.๙ นาที พบว่าความชื้นของข้าวเปลือกจะลดลงตามอุณหภูมิอบแห้งที่เพิ่มขึ้น เมื่อเทียบกับข้าวอ้างอิงร้อยละต้นข้าวจะเพิ่มขึ้น และจะมีร้อยละต้นข้าวลดลงเมื่อความชื้นสุดท้ายต่ำกว่าร้อยละ ๑๗ มาตรฐานเปียก ความขาวของข้าวสารจะลดลง

ตามอุณหภูมิอบแห้งที่เพิ่มขึ้น ส่วนสมบัติความหนืดของแป้ง มีค่า peak viscosity และค่า final viscosity ลดต่ำลง เมื่อเทียบกับข้าวอ้างอิง และมีแนวโน้มลดลงตามอุณหภูมิอบแห้งที่เพิ่มขึ้น เพราะว่าข้าวที่ผ่านการอบแห้งด้วยไอน้ำร้อนยวดยิ่งเกิดการเจลาทิไนซ์มาแล้ว การอบแห้งข้าวเปลือกแบบฟลูอิไดซ์เบดด้วยไอน้ำร้อนยวดยิ่งสามารถลดความชื้นข้าวเปลือกจากร้อยละ ๓๑.๓ มาตรฐานเปียก เหลือร้อยละ ๑๗.๙ มาตรฐานเปียก ในขั้นตอนการอบแห้งนี้นอกจากจะลดความชื้นข้าวเปลือกลงได้แล้ว ยังทำให้แป้งในเมล็ดข้าวเปลือกเกิดการเจลาทิไนซ์ได้ด้วย ดังนั้น จึงสามารถรวมการนึ่งและอบแห้งให้อยู่ในขั้นตอนเดียวกันได้ การรวมขั้นตอนดังกล่าวนี้มีผลทำให้ลดต้นทุนและระยะเวลาในการผลิตข้าวนึ่งลงได้มาก เมื่อเปรียบเทียบกับระบบการผลิตข้าวนึ่งในเชิงพาณิชย์จะสามารถลดขั้นตอนในระบบการผลิตข้าวนึ่งลงได้หลายขั้นตอน คือ การนึ่ง การหุบเปลือก เครื่องอบแห้งฟลูอิไดซ์เบดโดยใช้อากาศร้อน ๒ เครื่อง การเก็บในที่อับอากาศและการเป่าด้วยอากาศแวดล้อม และเตาเผาแกลบแบบไซโคลน คาดว่าระบบใหม่ที่ใช้เครื่องอบแห้งฟลูอิไดซ์เบดด้วยไอน้ำร้อนยวดยิ่งที่นำเสนอจะสามารถลดต้นทุนในการผลิตข้าวนึ่งลงได้มาก และลดเวลาในการผลิตข้าวนึ่งลงได้อย่างต่ำ ๓-๔ ชั่วโมง

๕. กิตติกรรมประกาศ

ผู้เขียนใคร่ขอขอบคุณ สำนักงานกองทุนสนับสนุนการวิจัยที่ให้ทุนสนับสนุนการวิจัย สถาบันเทคโนโลยีราชมงคลคลองหกให้ความอนุเคราะห์ในการทดสอบความแข็ง (hardness) ของข้าว ศูนย์วิจัยข้าวปทุมธานีให้ความอนุเคราะห์ในการทดสอบความขาว บริษัทไร้ซ์ เอ็นจิเนียริ่ง ซัพพลาย จำกัด ให้ความช่วยเหลือเรื่องค่าใช้จ่ายและอำนวยความสะดวกในการสร้างและทดสอบเครื่องอบแห้งต้นแบบ สถาบันค้นคว้าและพัฒนาผลิตภัณฑ์อาหาร และศูนย์เครื่องมือกลาง มหาวิทยาลัยเกษตรศาสตร์ให้ความอนุเคราะห์ใช้เครื่องวัดความหนืด (RVA) กล้องอิเล็กตรอนแบบส่องกราด (SEM) โรงสีข้าวเตียใจ้ฮง โรงสีข้าวนครหลวง และโรงสีข้าวทองอนันต์ ให้ความช่วยเหลือในด้านข้าวเปลือกที่ผ่านการแช่แล้ว และให้ความรู้และคำแนะนำที่เป็นประโยชน์ยิ่งเกี่ยวกับการผลิตข้าวนึ่ง ตลอดจนให้ความช่วยเหลือในการติดตั้งเครื่องอบแห้งต้นแบบอบแห้งข้าวนึ่งแบบฟลูอิไดซ์เบดโดยใช้ไอน้ำร้อนยวดยิ่ง

เอกสารอ้างอิง

1. Taweerattanapanish A, Soponronnarit S, Wetchacama S, Kongseri N, Wongpiyachon S. Effect of Drying on Rice Yield Using Fluidization Technique. Drying Technology. 1999; 17 (1&2) : 345-353.
2. Taechapairoj C, Dhuchakallaya I, Soponronnarit S, Wetchacama S, Prachayawarakom S. Superheated Steam Fluidized Bed Paddy Drying. Journal of Food Engineering. 2003; 58 : 67-73.
3. Rordprapat W, Soponronarit S, Nathakaranakule A, Tia W. Comparative Study of Fluidized Bed Paddy Drying Using Hot Air and Superheated Steam. Proceeding of the International Conference on Innovations in Food Processing Technology and Engineering. AIT, Bangkok Thailand, 2002: 453-466.
4. AACC. Approved method of the American Association of Cereal Chemist 9th ed., 1995; St. Paul, MN : AACC.
5. Rordprapat W, Nathakaranakule A, Tia W, Soponronarit S. Effect of Soaking Time and Drying Media on Qualities of Paddy Dried by Fluidization Technique. Proceeding of the 3rd Asia-Pacific Drying Conference, AIT, Bangkok Thailand, 2003: 453-466.
6. Sabularse V C, Luizzo JA, Rao RM, Groder RM. Cooking Quality Brown Rice as Influenced by Gramma Irradiation, Variety and Storage, Journal Food Science, 1991.
7. Banjong K. A Back Extrusion Tester for Evaluation Cooked Rice Texture. Asian Institute of Technology. Thesis. No. AE 86-20. Bangkok Thailand. 1986.
8. Taechapairoj C, Soponronnarit S, Prachayawarakorn S. Characteristics of Parboiled Rice in Superheated Steam Fluidized Bed Dryer. Proceeding of the International Conference on Innovations in Food Processing Technology and Engineering, AIT, Bangkok Thailand, 2002; 453-466.
9. น้ำฝน ศีตะจิตต์ และอรอนงค์ นัยวิกุล. กระบวนการผลิตข้าวนึ่งระดับห้องปฏิบัติการ. การประชุมวิชาการมหาวิทยาลัยเกษตรศาสตร์ ครั้งที่ ๔๑ มหาวิทยาลัยเกษตรศาสตร์ วิทยาเขตบางเขน. ๒๕๔๖; ๓๖-๔๔.

ตารางที่ ๑ คุณภาพข้าวเปลือกที่แช่ด้วยอุณหภูมิน้ำเริ่มต้น ๘๐ องศาเซลเซียส เป็นเวลา ๓ ชั่วโมง และข้าวที่อบแห้งด้วยไอน้ำร้อนยวดยิ่งที่อุณหภูมิต่าง ๆ

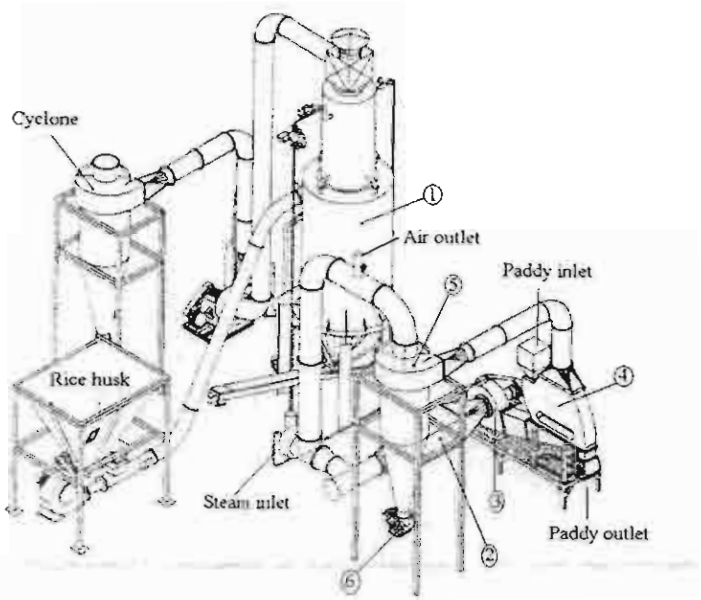
Drying Conditions	Moisture content (% w.b.)	Head rice yield (%)	Whiteness	White belly (%)	Hardness (N)	Water absorption (g water/g rice)
After soaking	28.7 ± 0.6a	53.7 ± 1.6a	42.2 ± 0.6a	5.4 ± 1.3a	36.0 ± 0.9a	3.29 ± 0.03a
128 °C	18.8 ± 0.6b	65.9 ± 1.0b	36.1 ± 0.3b	1.7 ± 0.6b	48.2 ± 0.9b	2.43 ± 0.03b
147 °C	17.9 ± 0.7b	66.8 ± 0.6b	33.8 ± 0.7c	1.8 ± 0.6b	49.2 ± 1.7b	2.35 ± 0.10b
164 °C	15.0 ± 0.6c	59.0 ± 2.5c	29.8 ± 0.8d	1.4 ± 0.6b	58.9 ± 0.2c	2.34 ± 0.05b

Note : The same letter at the same column indicated no significant difference in value at $p < 0.05$

ตารางที่ ๒ คุณภาพข้าวเปลือกที่แช่จากโรงสีข้าวนึ่งที่ผลิตในเชิงพาณิชย์ และข้าวที่อบแห้งด้วยไอน้ำร้อนยวดยิ่งที่อุณหภูมิต่าง ๆ

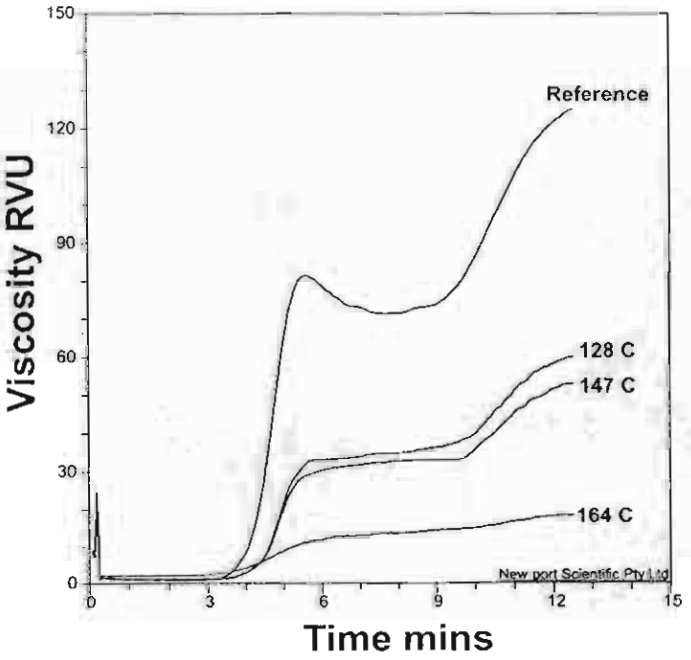
Drying Conditions	Moisture content (% w.b.)	Head rice yield (%)	Whiteness	White belly (%)	Hardness (N)	Water absorption (g water/g rice)
After soaking	31.3 ± 0.4a	56.6 ± 1.1a	39.0 ± 0.2a	5.7 ± 0.6a	37.9 ± 1.3a	3.51 ± 0.07a
128 °C	22.5 ± 0.4b	63.5 ± 0.6b	32.2 ± 0.8b	0b	48.6 ± 0.9b	2.82 ± 0.05b
144 °C	18.7 ± 0.3c	66.9 ± 0.6c	29.4 ± 0.5c	0b	51.9 ± 0.6c	2.19 ± 0.01c
160 °C	17.9 ± 0.3d	67.9 ± 0.6c	28.0 ± 0.6c	0b	55.0 ± 1.3d	1.99 ± 0.05d

Note : The same letter at the same column indicated no significant difference in value at $p < 0.05$

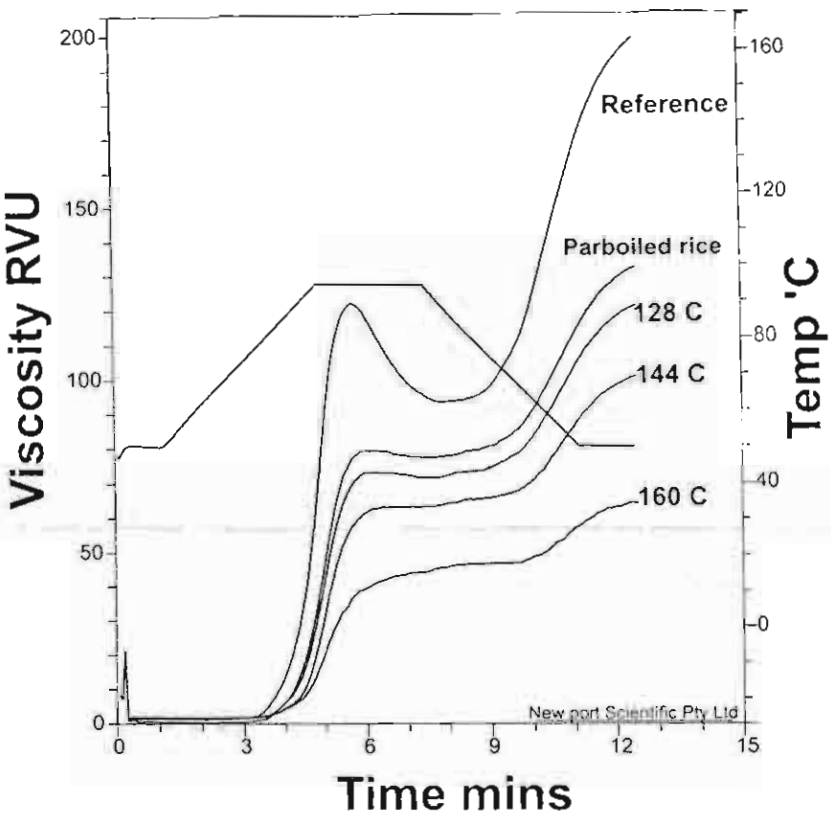


(1) Boiler (2) Superheater (3) Blower (4) Drying chamber (5) Cyclone (6) Rotary valve

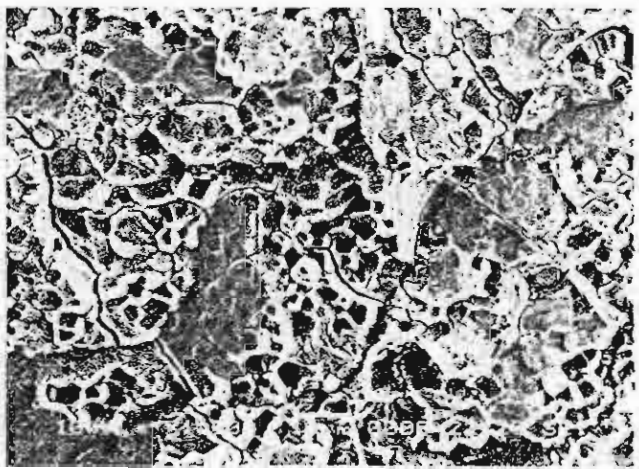
รูปที่ ๑ ส่วนประกอบของระบบอบแห้งแบบฟลูอิไดซ์เบดโดยใช้ไอน้ำร้อนยวดยิ่ง



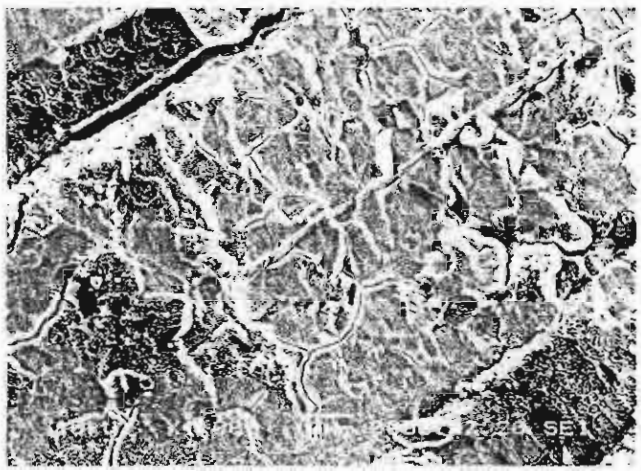
รูปที่ ๒ ความหนืดของแป้งข้าว แช่ที่อุณหภูมิน้ำเริ่มต้น ๘๐ องศาเซลเซียส เป็นเวลา ๓ ชั่วโมง และข้าวปลอกที่อบแห้งด้วยไอน้ำร้อนยวดยิ่งที่อุณหภูมิต่าง ๆ



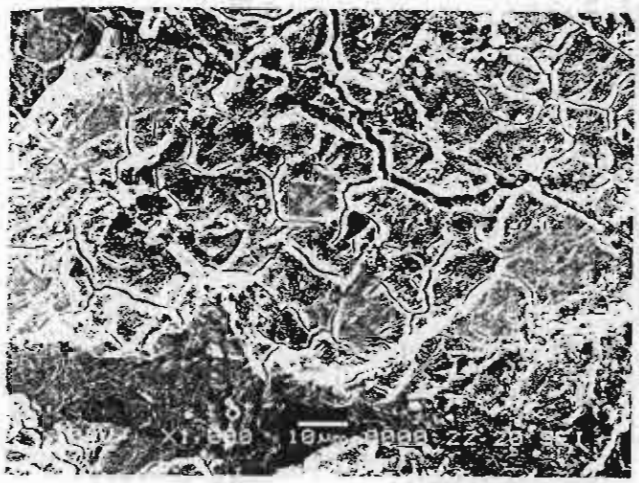
รูปที่ ๓ ความหนืดของแป้งข้าวที่แช่จากโรงสีข้าวนึ่งที่ผลิตในเชิงพาณิชย์ และข้าวเปลือกที่อบแห้งด้วยไอน้ำร้อนยวดยิ่งที่อุณหภูมิต่าง ๆ



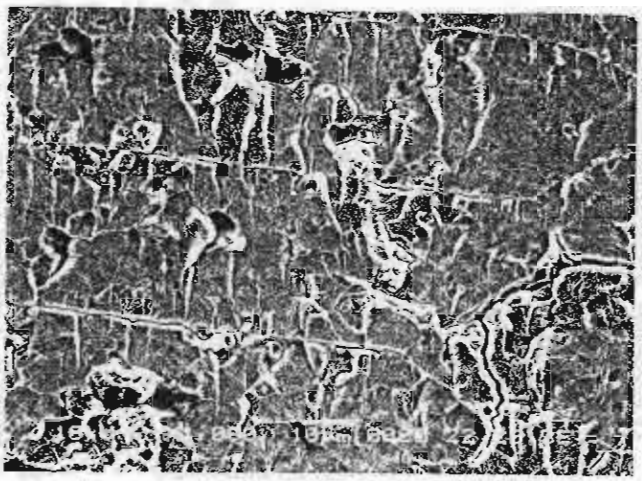
ก) ข้าวอ้างอิง (ก่อนการอบแห้ง)



ข) อุณหภูมิอบแห้ง ๑๒๘ องศาเซลเซียส

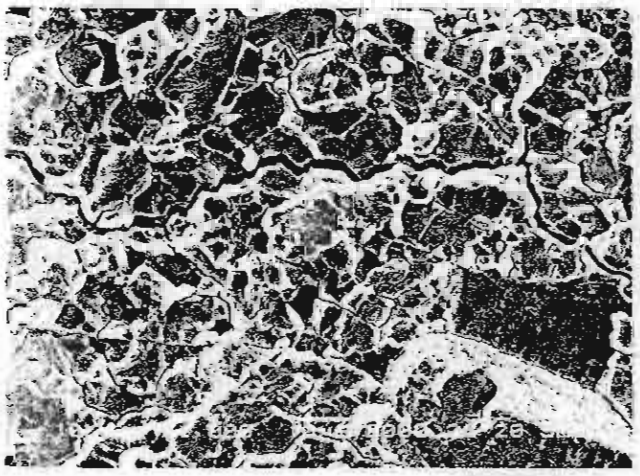


ค) อุณหภูมิอบแห้ง ๑๔๗ องศาเซลเซียส

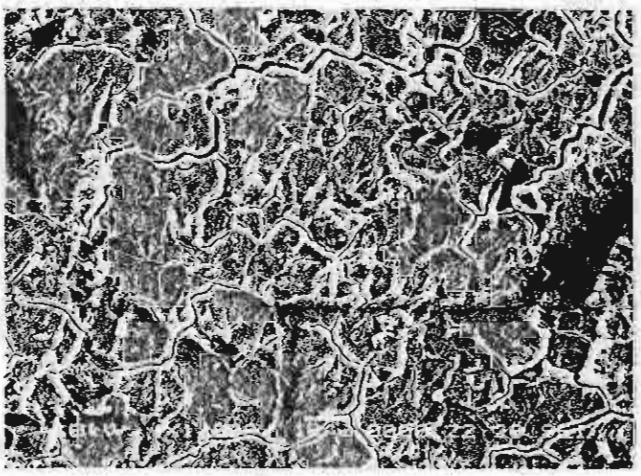


ง) อุณหภูมิอบแห้ง ๑๖๔ องศาเซลเซียส

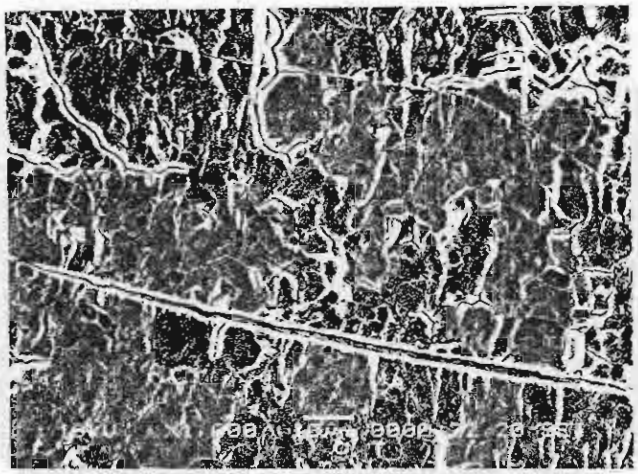
รูปที่ ๔ โครงสร้างของข้าวแช่ที่อุณหภูมิน้ำเริ่มต้น ๔๐ องศาเซลเซียส เป็นเวลา ๓ ชั่วโมง และข้าวเปลือกที่ผ่านการอบแห้งด้วยไอน้ำร้อนยวดยิ่งที่อุณหภูมิต่าง ๆ



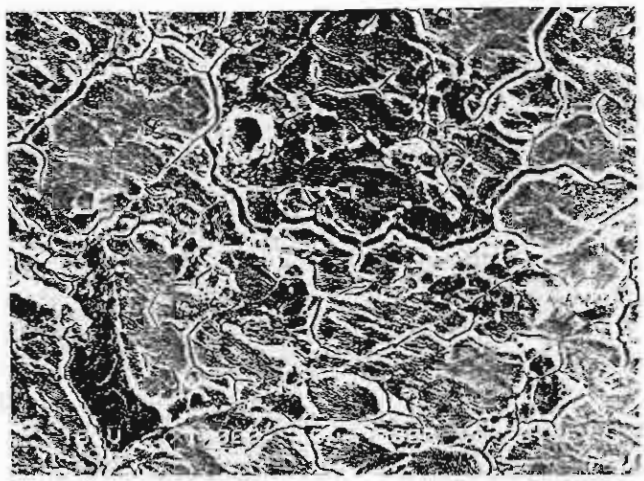
ก) ข้าวอ้างอิง (ก่อนการอบแห้ง)



ข) อุณหภูมิอบแห้ง ๑๒๘ องศาเซลเซียส

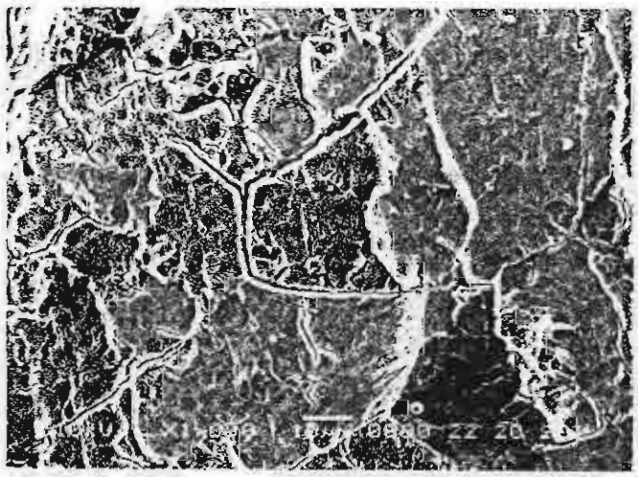


ค) อุณหภูมิอบแห้ง ๑๔๔ องศาเซลเซียส

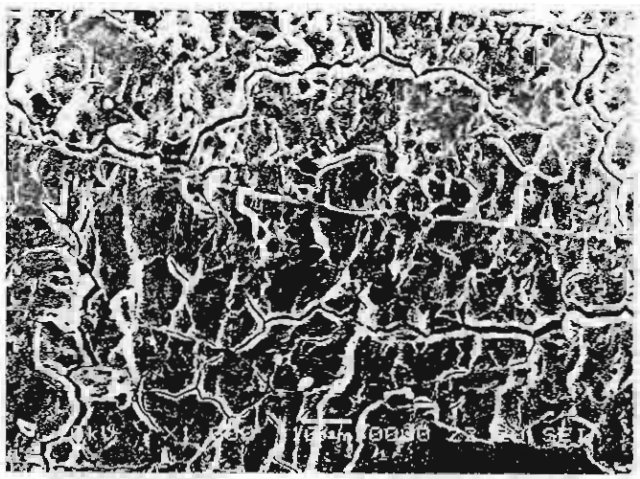


ง) อุณหภูมิอบแห้ง ๑๖๐ องศาเซลเซียส

รูปที่ ๕ โครงสร้างของข้าวที่แช่จากโรงสีข้าวนึ่งที่ผลิตในเชิงพาณิชย์ และข้าวเปลือกที่อบแห้งด้วยไอน้ำร้อนยวดยิ่งที่อุณหภูมิต่าง ๆ

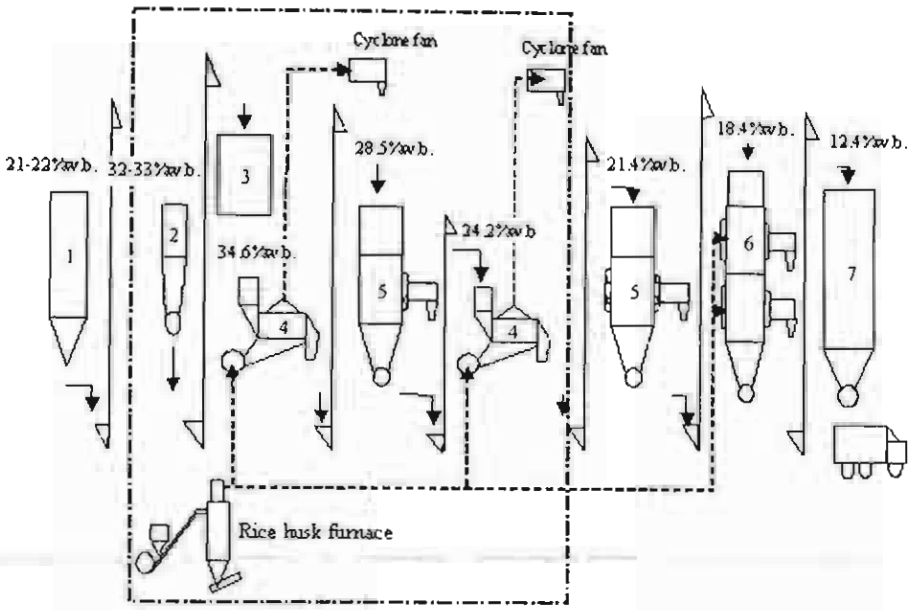


ก) ข้าวนึ่งที่ผลิตในเชิงพาณิชย์ (โรงที่ ๑)



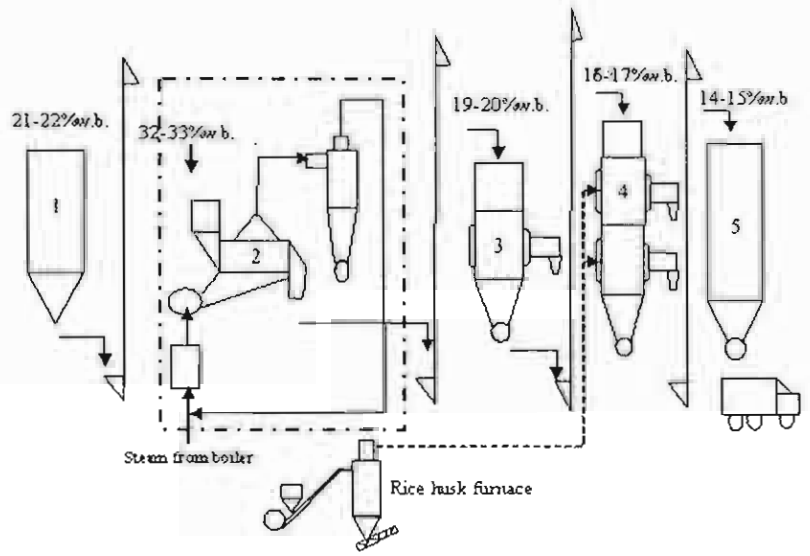
ข) ข้าวนึ่งที่ผลิตในเชิงพาณิชย์ (โรงที่ ๒)

รูปที่ ๖ โครงสร้างของข้าวนึ่งที่ผลิตในเชิงพาณิชย์ของโรงสีข้าวนึ่ง ๒ โรง



1 Soaking tank 2 Steamer 3 Ambient air ventilation 4 Fluidized bed dryer
5 Tempering and air ventilation 6 LUS dryer 7 Storage bin

รูปที่ ๗ ระบบการผลิตข้าวนึ่งของโรงสีที่ผลิตในเชิงพาณิชย์ที่ใช้อยู่ในปัจจุบัน



1 Soaking tank 2 Superheated steam fluidized bed dryer
3 Tempering and air ventilation 4 LUS dryer 5 Storage bin

รูปที่ ๘ ระบบการผลิตข้าวนึ่งแบบใหม่ที่ใช้เครื่องอบแห้งฟลูอิไดซ์เบดด้วยไอน้ำร้อนยวดยิ่งที่นำเสนอ

The Journal of the Royal Institute of Thailand
Vol. 30 No. 2 Apr.-Jun. 2005

Abstract

Development of a Superheated-steam-fluidized-bed Dryer for Parboiled Rice

Wathanyoo Rordprapat
Adisak Nathakaranakule
Warunee Tia
Somchart Soponronnarit
Fellow of the Academy of Science, The Royal Institute, Thailand

Due to possessing a large number of componential machines and long operating time, the present procedure for producing parboiled rice requires much investment and operating costs. This research is therefore aimed at developing a 100 kg/h prototype for fluidized bed paddy drying using superheated steam. The experiments were set up by pre-soaking paddy in hot water with the initial temperatures of 80 and 70°C for 3 and 4 hours to obtain the moisture contents of 28.7 and 31.7% w.b. respectively. The paddy was then dried at the temperatures in the range 128 - 164°C, with the bed height of 8 cm, the superficial velocity of 3.8 m/s, and the residence times of 4 - 5 minutes. After drying, the moisture contents were reduced to 17.9 - 22.8% w.b. and the finished rice was characterized as parboiled rice. When compared to the reference rice, the head rice yield was higher while rice whiteness was lower and decreased with increasing temperature. For pasting properties, peak and final viscosities were lower than those of the reference rice. With the above mentioned process, decreased moisture content and a gelatinized paddy starch simultaneously occurs. Consequently, steaming and drying processes can be merged into a single stage; resulting in the reduced investment cost and operating time when compared with the production system of the commercial parboiled rice.

Key words : soaking, parboiled rice, gelatinization, fluidization, physical properties, superheated steam

สถานภาพและแนวทางการวิจัยพลังงานหมุนเวียนในประเทศไทย

วารุณี เตีย[๑]
พิมพร แจ้งพลอย[๒]
กังสดาล สกุลพงษ์มาลี[๒]
สมชาติ โสภณรณฤทธิ์[๓]
ราชบัณฑิต สำนักวิทยาศาสตร์
ราชบัณฑิตยสถาน

บทคัดย่อ

การพัฒนาและขยายการใช้พลังงานหมุนเวียนเป็นแนวทางพัฒนาพลังงานที่ยั่งยืนสำหรับประเทศที่ต้องนำเข้าน้ำมันดังเช่นประเทศไทย ดังนั้น ในบทความนี้จะกล่าวถึง ศักยภาพ สถานภาพ และแนวทางงานวิจัยด้านพลังงานหมุนเวียนของประเทศไทย ได้แก่ พลังงานแสงอาทิตย์ พลังงานลม พลังน้ำขนาดเล็ก พลังงานความร้อนใต้พิภพ และพลังงานจากมหาสมุทร ยกเว้นมวลชีวภาพซึ่งได้นำเสนอในบทความที่ผ่านมาแล้ว ข้อจำกัดหลักของการใช้พลังงานหมุนเวียน คือ ความไม่แน่นอน ความไม่สม่ำเสมอของพลังงานหมุนเวียนที่จะนำมาใช้ประโยชน์ได้ และระบบการเปลี่ยนรูปพลังงานมีประสิทธิภาพต่ำ ทำให้ผลการประเมินทางเศรษฐศาสตร์ของโครงการส่วนใหญ่ไม่น่าสนใจเมื่อเทียบกับการใช้พลังงานเชิงพาณิชย์ ดังนั้น จึงควรมีงานวิจัยทางด้านการเพิ่มประสิทธิภาพ และการใช้งานได้อย่างสม่ำเสมอของระบบที่ใช้พลังงานหมุนเวียน รวมทั้งการลดต้นทุน และงานวิจัยเชิงนโยบาย เช่น โครงสร้างการกำหนดราคาเชื้อเพลิงที่รวมภาษีด้านสิ่งแวดล้อมด้วย

คำสำคัญ **: แนวทางการวิจัย, พลังงานแสงอาทิตย์, พลังงานลม, พลังน้ำขนาดเล็ก, พลังงานความร้อนใต้พิภพ, พลังงานจากมหาสมุทร, ประเทศไทย**

บทนำ

ปัจจุบันแนวโน้มของราคาน้ำมันดิบเพิ่มขึ้นอย่างต่อเนื่อง ทำให้ประเทศที่ต้องนำเข้าน้ำมันต้องประสบกับภาวะเศรษฐกิจอย่างหลีกเลี่ยงไม่ได้ รัฐจึงมีนโยบายส่งเสริมให้มีการจัดหา และใช้พลังงานทดแทนอย่างมีประสิทธิภาพ การใช้แหล่งพลังงานหมุนเวียนที่มีอยู่ภายในประเทศเพื่อมาทดแทนการนำเข้าพลังงานปิโตรเลียมจึงเป็นแนวทางการพัฒนาพลังงานที่สำคัญและยั่งยืน

นอกจากนี้ พิธีสารเกียวโตซึ่งเริ่มมีผลบังคับใช้ตั้งแต่เดือนกุมภาพันธ์พ.ศ. ๒๕๔๘ ชี้ให้เห็นว่าพลังงานหมุนเวียนจะเริ่มมีบทบาทสำคัญมากขึ้นในอนาคต แม้ว่าประเทศไทยจะยังไม่มีพันธกรณีที่จะต้องลดปริมาณการปล่อยแก๊สเรือนกระจก แต่การใช้พลังงานหมุนเวียนน้อย และการใช้พลังงานฟอสซิลซึ่งส่วนใหญ่นำเข้า เพิ่มขึ้นมากอย่างไม่มีประสิทธิภาพ จะทำให้การปล่อยแก๊สเรือนกระจกต่อประชากรของไทยสูงกว่าค่าเฉลี่ยของโลกในปัจจุบัน (พ.ศ. ๒๕๓๓) คือ ๓.๙ ตันคาร์บอนไดออกไซด์เทียบเท่าต่อคน

[๑] รองศาสตราจารย์ คณะพลังงานและวัสดุ มหาวิทยาลัยเทคโนโลยีพระจอมเกล้าธนบุรี
[๒] นักศึกษาปริญญาโท คณะพลังงานและวัสดุ มหาวิทยาลัยเทคโนโลยีพระจอมเกล้าธนบุรี
[๓] ศาสตราจารย์ คณะพลังงานและวัสดุ มหาวิทยาลัยเทคโนโลยีพระจอมเกล้าธนบุรี

ก่อน พ.ศ. ๒๕๕๓ ซึ่งจะทำให้เสี่ยงต่อการถูกจัดให้อยู่ในกลุ่มประเทศที่มีพันธกรณี*

บทความที่แล้ว (วารุณี เตีย และคณะ ๒๙, ๓ กรกฎาคม-กันยายน ๒๕๔๗ : ๕๕๗-๕๖๗) ได้กล่าวถึงศักยภาพการใช้และแนวทางวิจัยพลังงานจากมวลชีวภาพ ซึ่งเป็นแหล่งพลังงานหมุนเวียนที่มีศักยภาพสูงไปแล้ว ดังนั้น เพื่อพิจารณาพลังงานหมุนเวียนให้ครบทุกแหล่ง บทความนี้จะกล่าวถึงแหล่งพลังงานหมุนเวียนอื่น ๆ ที่เหลือ ซึ่งได้แก่ พลังงานแสงอาทิตย์ พลังงานลม พลังน้ำขนาดเล็ก พลังงานความร้อนใต้พิภพ และพลังงานจากมหาสมุทร

วิธีดำเนินงานวิจัย

แหล่งพลังงานหมุนเวียนที่กล่าวถึงในบทความนี้ ได้แก่ พลังงานแสงอาทิตย์ พลังงานลม พลังน้ำขนาดเล็ก พลังงานความร้อนใต้พิภพ พลังงานจากมหาสมุทร และพลังงานจากน้ำขึ้น-น้ำลง ยกเว้นพลังงานจากมวลชีวภาพ ซึ่งได้แยกนำเสนอเฉพาะเรื่องนี้ในบทความที่ผ่านมาแล้ว

งานวิจัยนี้ได้เก็บรวบรวมข้อมูลจากแหล่งต่าง ๆ ได้แก่ รายงาน และบทความวิจัยด้านพลังงานหมุนเวียนอื่น ๆ ยกเว้นพลังงานจากมวลชีวภาพ เพื่อนำมาศึกษาและเสนอแนวทางวิจัย ซึ่งมีรายละเอียดดังนี้

ก. ศึกษาศักยภาพของแหล่งพลังงานหมุนเวียนอื่น ๆ ในประเทศไทย

ข. ศึกษาสถานภาพการใช้พลังงานหมุนเวียนของประเทศไทย

ค. ศึกษาสถานภาพงานวิจัยที่ผ่านมา

ง. วิเคราะห์ข้อมูล ศักยภาพของแหล่งพลังงาน สถานภาพการใช้และงานวิจัยพลังงานที่ผ่านมา นำมาสรุปเสนอเป็นแนวทางงานวิจัยที่ควรดำเนินการต่อไป

ผลการศึกษาและวิจารณ์

๑. พลังงานแสงอาทิตย์ในประเทศไทย

๑.๑ ศักยภาพพลังงานแสงอาทิตย์

พื้นที่ส่วนใหญ่ของประเทศไทยมีความเข้มแสงอาทิตย์สูงสุด อยู่ในช่วงเดือนเมษายนและพฤษภาคม โดยมีค่าอยู่ช่วง ๒๐-๒๔ เมกะจูล/ตารางเมตร-วัน[๖] พื้นที่ที่ได้รับความเข้มแสงอาทิตย์สูงสุดเฉลี่ยทั้งปี ได้แก่ ภาคตะวันออกเฉียงเหนือ และภาคกลางบางส่วน ความเข้มแสงอาทิตย์เฉลี่ยต่อปีของพื้นที่ทั่วประเทศมีค่าเท่ากับ ๑๘.๕ เมกะจูล/ตารางเมตร-วัน ศักยภาพพลังงานแสงอาทิตย์เมื่อคิดจากพื้นที่ร้อยละ ๑ ของพื้นที่ทั้งหมด คิดเป็น ๕๕๔,๐๗๑ พันตันเทียบเท่าน้ำมันดิบ* ศักยภาพพลังงานแสงอาทิตย์ในพื้นที่แต่ละแห่งของประเทศแสดงได้ดังตารางที่ ๑

ตารางที่ ๑ ความเข้มแสงและศักยภาพเชิงพลังงานแสงอาทิตย์ตามแหล่งภูมิศาสตร์*

แหล่งภูมิศาสตร์	ความเข้มแสงอาทิตย์เฉลี่ยรายปี (เมกะจูล/ตารางเมตร-วัน)	ศักยภาพเชิงพลังงาน (พันตันเทียบเท่าน้ำมันดิบ)
ทั่วประเทศ	๑๘.๕	๕๕๔,๐๗๐.๖
ภาคเหนือ	๑๘.๐	๑๒๐,๓๔๕.๒
ภาคตะวันออกเฉียงเหนือ	๑๘.๗	๒๒๙,๐๘๓.๐
ภาคกลาง	๑๘.๗	๑๑๙,๘๑๔.๓
ภาคใต้	๑๘.๘	๘๔,๘๒๘.๑

๑.๒ การใช้พลังงานแสงอาทิตย์ในประเทศไทย

ใน พ.ศ. ๒๕๔๖ ประเทศไทยมีการใช้พลังงานแสงอาทิตย์ในรูปความร้อนรวมทั้งสิ้น ๕,๗๙๙,๑๒๕ เมกะจูล และไฟฟ้า ๕,๙๑๘.๒ เมกะวัตต์ชั่วโมง[๓] ดังรายละเอียดในตารางที่ ๒ ส่วนใหญ่ใช้ทางภาคเหนือ ในสาขาเศรษฐกิจบ้านอยู่อาศัยและธุรกิจการค้า

การใช้พลังงานแสงอาทิตย์ด้านความร้อน

เครื่องทำน้ำร้อนพลังงานแสงอาทิตย์เป็นที่ยอมรับในเชิงพาณิชย์แล้ว มีใช้ในบ้านเรือน โรงแรม โรงพยาบาล มียอดจำหน่ายประมาณ ๕,๐๐๐-๑๐,๐๐๐ ตารางเมตรต่อปี รวมพื้นที่ติดตั้งตัวรับรังสีอาทิตย์ชนิดแผ่นราบประมาณ ๕๐,๐๐๐ ตารางเมตร[๔] ซึ่งมีทั้งนำเข้าจากต่างประเทศและผลิตเองในท้องถิ่น แต่จำนวนยอดจำหน่ายในแต่ละปียังเพิ่มขึ้นไม่มากนัก แสดงว่าการยอมรับมีจำกัดและยังไม่แพร่หลายเท่าที่ควร เนื่องจากสาเหตุหลายประการ เช่น มีราคาสูงกว่าเครื่องทำน้ำร้อนจากไฟฟ้าและแก๊สปิโตรเลียมเหลว ความไม่สม่ำเสมอของการทำน้ำร้อนต้องใช้งานควบคู่กับพลังงานชนิดอื่น เครื่องที่ผลิตในประเทศของบางบริษัทมีคุณภาพต่ำทำให้ขาดความเชื่อถือในระยะยาว บริการหลังการขายไม่ดี รวมทั้งมาตรการสนับสนุนจากภาครัฐยังจูงใจไม่เพียงพอ

ตารางที่ ๒ การใช้พลังงานแสงอาทิตย์ตามแหล่งทางภูมิศาสตร์[๓]

แหล่งทางภูมิศาสตร์	รูปแบบพลังงานที่ใช้	
	ความร้อน (เมกะจูล)	ไฟฟ้า (เมกะวัตต์ชั่วโมง)
ทั่วประเทศ	๕,๗๙๙,๑๒๕.๒	๕,๙๑๘.๒
ภาคเหนือ	๔,๖๒๗,๖๓๒.๙	๓,๓๗๗.๗
ภาคตะวันออกเฉียงเหนือ	-	๓๒๖.๑
ภาคกลาง	๑,๑๗๑,๔๙๒.๒	๑,๒๕๘.๔
ภาคใต้	-	๙๕๖

เครื่องอบแห้งพลังงานแสงอาทิตย์ยังไม่เป็นที่ยอมรับในเชิงพาณิชย์ในประเทศไทยแต่มีการใช้งานสำหรับการอบแห้งพืชผลทางการเกษตรเป็นส่วนใหญ่ มีขนาดเล็กและการยอมรับยังอยู่ในวงจำกัด และยังไม่สามารถใช้ในเชิงอุตสาหกรรมได้ การอบแห้งผลิตภัณฑ์แต่ละครั้งทำได้ในปริมาณที่ไม่มากนัก และระยะเวลาที่ใช้ใกล้เคียงกับวิธีตากกลางแจ้งแต่มีการลงทุนสูงกว่า

สำหรับเครื่องกลั่นน้ำพลังงานแสงอาทิตย์นั้น ยังไม่มีข้อมูลการนำไปใช้งาน ประสิทธิภาพยังไม่สูงเพียงพอที่จะนำไปใช้งานได้จริงและไม่คุ้มค่าในเชิงพาณิชย์ รวมถึงยังไม่มีความต้องการและความจำเป็นในการนำมาใช้งานสำหรับประเทศไทย และมีปัญหาด้านคุณภาพของน้ำกลั่นที่ผลิตได้ว่าจะเหมาะสมสำหรับการนำไปใช้ประโยชน์ด้านใด

เครื่องทำความเย็นด้วยพลังงานแสงอาทิตย์ในประเทศไทยยังอยู่ในขั้นตอนของการวิจัยเพื่อศึกษาสมรรถนะเท่านั้น ยังไม่มีข้อมูลสำหรับการนำมาใช้งานจริง เนื่องจากหลักการทำงานของระบบจะค่อนข้างซับซ้อน ต้องใช้อุปกรณ์ที่ได้มาตรฐานและทันสมัย รวมถึงความก้าวหน้าของเทคโนโลยีที่ยังไม่ได้รับการพัฒนาเท่าที่ควร จึงทำให้เครื่องทำความเย็นพลังงานแสงอาทิตย์ยังมีประสิทธิภาพต่ำ มีราคาค่อนข้างสูงกว่าเครื่องทำความเย็นในระบบเดิมอยู่มาก

การใช้พลังงานแสงอาทิตย์ด้านไฟฟ้า

การนำเซลล์แสงอาทิตย์มาใช้ในประเทศไทย ส่วนใหญ่นำไปใช้ในพื้นที่ห่างไกลที่ระบบสายส่งไปไม่ถึงเนื่องจากต้นทุนในการผลิตไฟฟ้ายังคงสูงกว่าที่ซื้อจากสายส่งอยู่มาก มีการผลิตไฟฟ้าจากเซลล์แสงอาทิตย์สำหรับงานในระบบโทรคมนาคม ระบบประจุแบตเตอรี่หมู่บ้านห่างไกล ระบบสูบน้ำในหมู่บ้านห่างไกล ระบบสอนหนังสือทางไกล ระบบผลิตไฟฟ้าผสมผสานในพื้นที่ห่างไกล เช่น ที่จังหวัดภูเก็ตมีระบบผลิตไฟฟ้าร่วมเซลล์แสงอาทิตย์กำลังผลิต ๑๑.๓๔ กิโลวัตต์ และกังหันลมกำลังการผลิต ๑๗๐ กิโลวัตต์[๔] ปัจจุบันโรงไฟฟ้าเซลล์แสงอาทิตย์ขนาดใหญ่ที่สุดในประเทศ คือ โรงไฟฟ้าเซลล์แสงอาทิตย์ผาบ่องซึ่งมีขนาด ๒,๔๐๐ กิโลวัตต์ ผลิตไฟฟ้าจำหน่ายไฟฟ้าให้จังหวัดแม่ฮ่องสอน[๖] นอกจากนี้ ยังมีการใช้เซลล์แสงอาทิตย์ในงานอื่น ๆ เช่น ไฟสัญญาณ สถานีอนามัย

สำหรับเทคโนโลยีการติดตั้งเซลล์แสงอาทิตย์ในประเทศไทยนั้นมีอยู่ด้วยกัน ๓ แบบ คือ Solar Home System (SHM), Roof-top PV และ Centralised PV โดยที่ Solar Home System จะเป็นการติดตั้งที่ไม่ต่อเข้าระบบสายส่งของการไฟฟ้า (stand alone) ซึ่งมักจะติดตั้งในชนบทห่างไกลที่สายส่งเข้าไปไม่ถึง หรือหน่วยงานสาธิตต่าง ๆ ส่วน Roof-top PV และ Centralised PV จะเป็นการติดตั้งที่ต่อเข้าระบบสายส่ง โดยที่ Centralised PV จะเป็นการติดตั้งเพื่อผลิตกระแสไฟฟ้าเข้าระบบของการไฟฟ้าฝ่ายผลิตแห่งประเทศไทยและการไฟฟ้าส่วนภูมิภาคซึ่งจะมีขนาดใหญ่กว่า Roof-top PV ซึ่งจะติดตั้งตามหน่วยงานต่าง ๆ ที่ได้รับการคัดเลือก

รัฐได้มีนโยบายสนับสนุนให้มีการติดตั้งระบบผลิตไฟฟ้าด้วยเซลล์แสงอาทิตย์โดยได้ออกระเบียบให้การไฟฟ้าฝ่ายผลิตแห่งประเทศไทยรับซื้อไฟฟ้าจากผู้ผลิตไฟฟ้าพลังงานหมุนเวียนขนาดเล็กมาก ดังนั้น บ้านพักอาศัย หน่วยงาน หรือสถานประกอบการที่มีการติดตั้งระบบผลิตไฟฟ้าด้วยเซลล์แสงอาทิตย์ สามารถขายไฟฟ้ากลับเข้าระบบสายส่งไฟฟ้าได้ ใน พ.ศ. ๒๕๔๖ มีการผลิตไฟฟ้าด้วยพลังงานแสงอาทิตย์รวมทั้งสิ้น ๕,๙๑๘.๒ เมกะวัตต์ชั่วโมง ประมาณร้อยละ ๕๗ ผลิตในภาคเหนือรองลงมา คือ ภาคกลาง ภาคใต้ และภาคตะวันออกเฉียงเหนือ ร้อยละ ๒๑.๓, ๑๖.๒ และ ๕.๕ ตามลำดับ[๗]

๑.๓ สถานภาพงานวิจัยด้านพลังงานแสงอาทิตย์ของประเทศไทย

ประเทศไทยได้มีการส่งเสริมให้มีการวิจัย พัฒนาและสาธิตการนำพลังงานแสงอาทิตย์มาใช้ในการผลิตไฟฟ้า การผลิตน้ำร้อน การอบแห้ง การกลั่น และการทำความเย็น ซึ่งสามารถสรุปได้ดังนี้

งานวิจัยการใช้พลังงานแสงอาทิตย์ในรูปความร้อน ประเทศไทยได้มีการวิจัยและพัฒนาระบบทำน้ำร้อนด้วยแสงอาทิตย์มาเป็นเวลานาน และทำงานวิจัยในหน่วยงานหลายหน่วยด้วยกัน ปัจจุบันสามารถพัฒนามาใช้งานในเชิงพาณิชย์ได้แล้ว งานวิจัยที่ผ่านมาส่วนใหญ่จะเป็นการพัฒนาและทดสอบสมรรถนะของตัวรับรังสี[๘-๑๐] นอกจากนี้ยังมีงานวิจัยที่ศึกษาระบบทำน้ำร้อนด้วยแสงอาทิตย์ การศึกษาปัญหาและอุปสรรคของระบบทำน้ำร้อนด้วยแสงอาทิตย์ภายในประเทศ

ด้านการอบแห้งด้วยพลังงานแสงอาทิตย์นั้น งานวิจัยส่วนใหญ่จะเป็นการศึกษาสมรรถนะของเครื่องอบแห้งชนิดต่าง ๆ ให้เหมาะสมกับผลิตภัณฑ์ที่นำมาทำการอบแห้ง[๑๑-๑๔] เช่น กล้วยน้ำว้า เนื้อสัตว์ ปลา กระเทียม นอกจากนี้ ยังมีงานวิจัยด้านการใช้พลังงานแสงอาทิตย์ร่วมกับแหล่งพลังงานอื่นในการให้ความร้อน เช่น ไอน้ำ แก๊สปิโตรเลียมเหลว แก๊สชีวภาพ และมีงานวิจัยเกี่ยวกับตัวรับรังสีอาทิตย์ที่ใช้ร่วมกับห้องอบแห้ง และการใช้หินเป็นตัวกักเก็บความร้อน ถึงแม้จะมีงานวิจัยเกี่ยวกับเครื่องอบแห้งแสงอาทิตย์มากมาย แต่ยังไม่มีการนำมาใช้ประโยชน์อย่างแพร่หลาย โดยเฉพาะในระดับอุตสาหกรรม เนื่องจากความไม่สม่ำเสมอของพลังงานแสงอาทิตย์ ดังนั้น ถ้าต้องการควบคุมอุณหภูมิห้องอบแห้งให้ได้ตามต้องการ จะต้องใช้ควบคู่กับพลังงานจากแหล่งอื่น ทำให้มีการลงทุนสูงขึ้น

ด้านการกลั่นด้วยพลังงานแสงอาทิตย์ มีงานวิจัยด้านสมรรถนะของเครื่องกลั่นพลังงานแสงอาทิตย์ในรูปแบบต่าง ๆ[๑๖-๑๙] เช่น แบบผิวตั้งฝาครอบอะคริลิก แบบกระจกเอียง และใช้ผิวดูดความร้อนชนิดต่าง ๆ นอกจากนี้

ยังมีงานวิจัยที่ศึกษาตัวรับรังสีอาทิตย์แบบต่าง ๆ ที่นำมาใช้ร่วมกับเครื่องกลั่นน้ำ เพื่อเพิ่มสมรรถนะของเครื่องกลั่นน้ำ[๒๐] และมีงานวิจัยที่พัฒนาเครื่องกลั่นด้วยแสงอาทิตย์สำหรับผลิตภัณฑ์อื่น เช่น เอทานอล[๒๑-๒๓]

ในการทำความเย็นด้วยแสงอาทิตย์ งานวิจัยด้านเครื่องทำความเย็นด้วยแสงอาทิตย์ส่วนใหญ่จะเป็นการศึกษาสมรรถนะ และความเป็นไปได้ของระบบ เช่น การศึกษาเครื่องทำความเย็นแบบดูดซึม การศึกษาสมรรถนะของระบบทำความเย็นแบบดูดซับด้วยแสงอาทิตย์ที่ใช้ถ่านกัมมันต์-เมทานอลเป็นสารคู่ทำงาน[๒๔-๒๖] พบว่าสามารถทำความเย็นได้อุณหภูมิต่ำถึง -๙.๖ องศาเซลเซียส แต่สัมประสิทธิ์สมรรถนะการทำความเย็นของระบบยังมีค่าต่ำอยู่มากคือ ๐.๐๘๓๐ นอกจากนี้ ยังมีงานวิจัยด้านการพัฒนาและปรับปรุงเครื่องทำความเย็นโดยใช้พลังงานแสงอาทิตย์ระบบทำความเย็นแบบดูดเกาะชนิดต่อเนื่อง การทำความเย็นแบบดูดซึม การพัฒนาตู้เย็นพลังงานแสงอาทิตย์ และการทำความเย็นด้วยน้ำแข็งหลายแบบ เช่น แบบ Intermittent[๒๗]

ด้านการผลิตไฟฟ้าด้วยแสงอาทิตย์ เนื่องจากประเทศไทยไม่ใช่ผู้นำในการผลิตเซลล์แสงอาทิตย์ ประกอบกับการวิจัยในการพัฒนาเซลล์แสงอาทิตย์มีระบบที่ยุ่งยากและซับซ้อนและต้องใช้อุปกรณ์ที่ได้มาตรฐานและทันสมัยมาก จึงทำให้งานวิจัยส่วนใหญ่เน้นการศึกษาพารามิเตอร์ คุณภาพ สมรรถนะของการนำไปใช้ในงานต่าง ๆ เช่น การศึกษาพารามิเตอร์ของระบบผลิตไฟฟ้าแบบผสมผสานที่ประกอบด้วย เซลล์แสงอาทิตย์ พลังงานลม และเครื่องยนต์ดีเซลเพื่อใช้งานในพื้นที่ห่างไกล[๒๗] การศึกษาคุณภาพของกำลังไฟฟ้าที่ผลิตได้จากระบบผลิตไฟฟ้าแบบผสมผสาน[๒๘] การจัดการระบบผลิตสูบน้ำด้วยเซลล์แสงอาทิตย์[๒๙] ศึกษาระบบที่เชื่อมโยงกับสายส่ง[๓๐] การประจุแบตเตอรี่[๓๑] อย่างไรก็ดี สำนักงานพัฒนาวิทยาศาสตร์และเทคโนโลยีแห่งชาติ (สวทช.) ได้รับเงินสนับสนุนให้ทำวิจัยและผลิตเซลล์แสงอาทิตย์ขึ้นในประเทศไทย โดยคาดว่าจะสามารถผลิตเซลล์ให้มีประสิทธิภาพได้ถึงร้อยละ ๑๐[๓๒] โดยจะพัฒนาเซลล์แบบผลึกควบคู่กันไป

จากการศึกษาสถานภาพการใช้สถานภาพด้านงานวิจัยพลังงานแสงอาทิตย์ และการวิเคราะห์ความเป็นไปได้ทางเศรษฐศาสตร์ของเครื่องทำน้ำร้อนพลังงานแสงอาทิตย์ เครื่องอบแห้งพลังงานแสงอาทิตย์ เครื่องกลั่นน้ำพลังงานแสงอาทิตย์ เครื่องทำความเย็นพลังงานแสงอาทิตย์และเซลล์แสงอาทิตย์ สามารถสรุปตามสถานภาพต่าง ๆ ได้ดัง ตารางที่ ๓

ตารางที่ ๓ สรุปสถานภาพของพลังงานแสงอาทิตย์ของประเทศไทย

ลักษณะการใช้	สถานภาพ						
	งานวิจัยพื้นฐาน	งานวิจัยและพัฒนา	การออกแบบทางวิศวกรรมและงานสาธิต	คุ้มค่าทางเศรษฐ-ศาสตร์	มีจำหน่ายแบบตามใบสั่ง	ไม่เป็นเชิงพาณิชย์	มีการใช้ในเชิงพาณิชย์
เครื่องทำน้ำร้อน		X	X	X			X
เครื่องอบแห้ง		X	X	X	X		
เครื่องกลั่นน้ำ		X		X	X		
เครื่องทำความเย็น		X				X	
เซลล์แสงอาทิตย์		X	X	X (เฉพาะพื้นที่)			X

หมายเหตุ : X หมายถึง มีสถานภาพตามหัวข้อในแนวตั้ง

๑.๔ ข้อจำกัดและปัญหาการใช้พลังงานแสงอาทิตย์ของประเทศไทย

จากการศึกษาพลังงานแสงอาทิตย์ของประเทศไทย พบว่า ถึงแม้ว่าประเทศไทยจะมีศักยภาพของพลังงานแสงอาทิตย์เพียงพอสำหรับการนำไปใช้ประโยชน์ในด้านต่าง ๆ แต่ยังมีการนำไปใช้งานไม่มากเท่าที่ควร โดยสามารถสรุปปัญหาของงานวิจัยด้านพลังงานแสงอาทิตย์มีทั้งที่เป็นภาพรวมของประเทศและตามสถานภาพการใช้งานของอุปกรณ์แต่ละอย่างได้ดังนี้

ด้านการใช้พลังงานแสงอาทิตย์เพื่อทำความร้อน เนื่องจากความไม่สม่ำเสมอและความไม่แน่นอนของแหล่งพลังงานแสงอาทิตย์ ทำให้เกิดปัญหาในการใช้งานและข้อจำกัดต่าง ๆ ดังนี้ ไม่สามารถใช้งานได้อย่างต่อเนื่อง ไม่สามารถควบคุมอุณหภูมิได้ตามต้องการซึ่งจะส่งผลกระทบโดยตรงต่อคุณภาพผลิตภัณฑ์ สำหรับกรณีเครื่องอบแห้ง และเครื่องทำความเย็น ดังนั้น ถ้าจะแก้ไขปัญหาเหล่านี้จะต้องติดอุปกรณ์เพิ่มเพื่อใช้แหล่งพลังงานอื่นเสริม ซึ่งจะทำให้ระบบมีต้นทุนสูงขึ้น นอกจากนี้สมรรถนะของบางอุปกรณ์ยังต่ำอยู่มาก เช่น เครื่องกลั่นน้ำ และเครื่องทำความเย็น ทำให้ไม่น่าสนใจที่จะนำมาใช้งาน

สำหรับการนำแสงอาทิตย์มาผลิตไฟฟ้าด้วยเซลล์แสงอาทิตย์นั้น มีปัญหาด้านราคาแผงเซลล์และระบบที่มีค่าสูง และประสิทธิภาพเซลล์แสงอาทิตย์ต่ำ ประกอบกับความไม่สม่ำเสมอและความไม่แน่นอนของแหล่งพลังงานแสงอาทิตย์ ทำให้ต้นทุนไฟฟ้าที่ผลิตได้ยังสูงกว่าราคาไฟฟ้าที่ซื้อจากการไฟฟ้ามาก ดังนั้น จึงทำให้เกิดข้อจำกัดของการนำไปใช้งาน ซึ่งส่วนใหญ่จะนำไปใช้ในพื้นที่ที่ห่างไกลระบบสายส่งไปไม่ถึง จึงใช้งานได้ไม่แพร่หลาย

๑.๕ แนวทางงานวิจัยพลังงานแสงอาทิตย์ในประเทศไทย

จากการศึกษาสถานภาพงานวิจัยด้านพลังงานแสงอาทิตย์ พบว่า ประเทศไทยได้มีความพยายามในการทำการวิจัยด้านนี้มาเป็นเวลานาน แต่ถ้าพิจารณาถึงปัญหาและข้อจำกัดของการใช้งาน ความเป็นไปได้ทางเทคนิคและเศรษฐศาสตร์แล้ว พบว่าควรมีวิจัยด้านเพิ่มประสิทธิภาพ สมรรถนะ และหาแนวทางลดต้นทุนของระบบ/อุปกรณ์ที่ใช้พลังงานแสงอาทิตย์ และควรพัฒนาหาวัสดุที่ผลิตได้ในประเทศมาใช้เพื่อลดต้นทุน ควรมีงานวิจัยหาแนวทางพัฒนาระบบที่จะสามารถเก็บความร้อนและไฟฟ้าที่ผลิตได้จากพลังงานแสงอาทิตย์เพื่อให้มีการใช้งานได้อย่างต่อเนื่องอย่างสม่ำเสมอ และการวิจัยที่จะหาแหล่งพลังงานอื่นที่ราคาถูกมาใช้ผสมผสานเพื่อให้การใช้งานของระบบเป็นไปได้อย่างเสถียร และควรมีงานวิจัยทั้งทางด้านเทคนิคและเศรษฐศาสตร์เพื่อขยายโอกาสที่จะพัฒนาอุปกรณ์และการประยุกต์ใช้ในงานใหม่ ๆ ต่าง ๆ ได้อย่างเหมาะสมให้ได้กว้างขวางมากยิ่งขึ้น โดยเฉพาะเงื่อนไขที่เหมาะสมและความคุ้มค่าของการใช้เซลล์แสงอาทิตย์ นอกจากนี้ ควรมีงานวิจัยเชิงนโยบายและมาตรการต่าง ๆ ของประเทศที่ประสบความสำเร็จในการใช้พลังงานแสงอาทิตย์ เช่น มาตรการด้านภาษีสิ่งแวดล้อมต่าง ๆ โดยเฉพาะภาษีแก๊สคาร์บอนไดออกไซด์

๒. พลังน้ำ

๒.๑ สถานการณ์ และการใช้พลังน้ำในประเทศไทย

การผลิตไฟฟ้าจากพลังน้ำเป็นการเปลี่ยนสภาพของน้ำจากสถานะพลังงานศักย์ (potential energy) เป็นพลังงานไฟฟ้าโดยอาศัยความแตกต่างของระดับน้ำ การเปลี่ยนพลังน้ำให้เป็นพลังงานไฟฟ้า ใช้กังหันน้ำและเครื่องกำเนิดไฟฟ้า

ศักยภาพพลังน้ำประเมินจากเขื่อนที่ผลิตไฟฟ้าที่ดำเนินการแล้วในปัจจุบันมีกำลังผลิตติดตั้งรวมทั้งสิ้น ๒,๙๗๓ เมกะวัตต์[๓๓] คิดเป็นสัดส่วนร้อยละ ๑๒ ของกำลังผลิตติดตั้งโรงไฟฟ้าของภาครัฐ[๓๔] ส่วนใหญ่กว่าร้อยละ ๘๐ อยู่ทางภาคเหนือและภาคกลางของประเทศ ใน พ.ศ. ๒๕๔๖ สามารถผลิตไฟฟ้าได้รวมทั้งสิ้น ๗,๒๙๙ ล้านกิโลวัตต์ชั่วโมง คิดเทียบเท่าพลังงานปฐมภูมิ ๑,๖๑๖ พันตันเทียบเท่าน้ำมันดิบ[๓๕] ในจำนวนนี้เป็นโรงไฟฟ้าพลังน้ำที่มีขนาดเล็กกว่า ๑๒ เมกะวัตต์อยู่ ๖๙ เมกะวัตต์ สามารถผลิตไฟฟ้าได้ ๑๙๐ ล้านกิโลวัตต์ชั่วโมง

ปัจจุบันการหาแหล่งเพื่อพัฒนาเขื่อนขนาดใหญ่ในประเทศคง

เป็นไปได้ยาก ที่มีศักยภาพมากเป็นลุ่มน้ำระหว่างประเทศ ซึ่งในการพัฒนาเพื่อผลิตไฟฟ้าจะต้องเป็นไปในลักษณะความร่วมมือและถือกรรมสิทธิ์ร่วมระหว่างประเทศ

ดังนั้น การพัฒนาแหล่งพลังน้ำขนาดเล็กในประเทศไทยเพื่อผลิตไฟฟ้าจึงเป็นการสร้างแหล่งพลังงานหมุนเวียนที่สำคัญอย่างหนึ่ง กังหันพลังน้ำขนาดเล็กจะใช้น้ำในลำน้ำธรรมชาติเป็นแหล่งพลังงานโดยสร้างเขื่อนปิดกั้นแม่น้ำไว้ให้มีระดับสูงจนมีปริมาณน้ำ และแรงดันเพียงพอที่จะหมุนกังหันน้ำ และเครื่องกำเนิดไฟฟ้าที่อยู่ท้ายน้ำที่มีระดับต่ำกว่า วิธีนี้เหมาะสมกับพื้นที่แถบชนบทที่สายไฟฟ้าส่งเข้าไปไม่ถึง โรงไฟฟ้าพลังน้ำขนาดเล็กแบ่งตามปริมาณน้ำได้เป็น ๓ ประเภท[๙๕] ได้แก่ โรงไฟฟ้าแบบมีน้ำไหลผ่านตลอดปี (run-of-river hydro plant) โรงไฟฟ้าแบบนี้ไม่มีอ่างเก็บน้ำ ส่วนใหญ่จะติดตั้งอยู่กับเขื่อนผันน้ำชลประทานซึ่งมีน้ำไหลผ่านตลอดปี โรงไฟฟ้าแบบมีอ่างเก็บน้ำขนาดเล็ก (regulating pond hydro plant) และโรงไฟฟ้าแบบสูบกลับ (pumped storage plant) ส่วนใหญ่โครงการไฟฟ้าพลังน้ำขนาดเล็กจะเป็นโรงไฟฟ้าแบบมีน้ำไหลผ่านตลอดปี โรงไฟฟ้าแบบนี้ไม่มีอ่างเก็บน้ำ และมีผลกระทบต่อสิ่งแวดล้อมน้อย

จากการศึกษาเบื้องต้นด้วยแผนที่และการสำรวจภาคสนามในบางพื้นที่ รวมทั้งพิจารณาจากการศึกษาโครงการไฟฟ้าพลังน้ำของหน่วยงานอื่น ๆ ซึ่งในการศึกษาได้พิจารณาโรงไฟฟ้า ๓ รูปแบบ พบว่าทั่วประเทศไทยมีที่ตั้งโครงการไฟฟ้าพลังน้ำที่น่าจะเป็นไปได้ ๑,๑๓๖ แห่ง[๙๖] ปัจจุบันกรมพัฒนาพลังงานทดแทนและอนุรักษ์พลังงานได้คัดเลือกเพื่อพัฒนาโครงการโรงไฟฟ้าพลังน้ำขนาดเล็กเพื่อที่จะสร้างในอนาคต ๒๔ โครงการ รวมกำลังการผลิตติดตั้งทั้งหมด ๖๖.๑๓ เมกะวัตต์ คาดว่าจะผลิตไฟฟ้าได้ ๒๙๑ ล้านกิโลวัตต์ชั่วโมง ประมาณการเงินลงทุนรวมทั้งสิ้น ๔,๒๙๓ ล้านบาท[๙๗] ซึ่งมีรายละเอียดดังแสดงในตารางที่ ๔

๒.๒ สถานภาพงานวิจัยด้านพลังน้ำขนาดเล็กของประเทศไทย

การวิจัยด้านพลังน้ำขนาดเล็กของประเทศไทย มีงานวิจัยเกี่ยวกับการประเมินเชิงเทคนิคของโครงการพัฒนาพลังน้ำขนาดเล็กในประเทศที่กำลังพัฒนาและในประเทศที่พัฒนาแล้ว พบว่า มีแนวโน้มที่จะเพิ่มศักยภาพมากขึ้น[๙๖] ส่วนการศึกษาทางด้านโยธามีการศึกษาในเรื่องของวัสดุที่นำมาใช้และมาตรฐาน ปัจจัยสำคัญในการเลือกใช้วัสดุอุปกรณ์นั้น ๆ ขึ้นอยู่กับงบประมาณการลงทุน สภาพภูมิอากาศ ความยากง่ายในการสรรหาวัสดุอุปกรณ์มาใช้ในโครงการ การขนย้ายและการติดตั้ง มีการวิจัยด้านการจัดสรรน้ำเพื่อประโยชน์สูงสุดในการจัดการอ่างเก็บน้ำ ทั้งนี้เพื่อวางแผนและจัดการน้ำที่เหมาะสมเพื่อให้มีการใช้น้ำที่มีอยู่ตามธรรมชาติให้มีประสิทธิภาพและเกิดประโยชน์สูงสุด[๙๗]

๒.๓ แนวทางงานวิจัยพลังน้ำขนาดเล็กในประเทศไทย

เนื่องจากโรงไฟฟ้าพลังน้ำขนาดเล็กส่วนใหญ่เป็นแบบมีน้ำไหลผ่านตลอดปี จึงควรมีการวิจัยเพื่อเพิ่มประสิทธิภาพของกังหันที่มีความสูงของหัวน้ำที่ต่ำ ส่วนด้านวัสดุ อุปกรณ์ ควรตั้งมาตรฐานของวัสดุอุปกรณ์ต่าง ๆ ของโรงไฟฟ้าพลังน้ำขนาดเล็กเพื่อให้เหมาะสมกับความสูงของหัวน้ำที่มีความแตกต่างกันในโครงการแต่ละโครงการ ซึ่งจะทำให้ผลิตพลังงานได้ประสิทธิภาพสูงสุด จากตารางที่ ๔ จะเห็นได้ว่าโครงการก่อสร้างโรงไฟฟ้าพลังน้ำใช้เงินลงทุนสูงมาก ดังนั้น ควรมีการศึกษาวิจัยเพื่อหาแนวทางลดต้นทุน นอกจากนี้ ควรมีการวิจัยเกี่ยวกับการจัดสรรน้ำมาใช้ประโยชน์ให้ได้มากที่สุด และควรศึกษาความเป็นไปได้ของการผลิตไฟฟ้าจากเขื่อนหรือฝายน้ำขนาดเล็กที่ก่อสร้างใช้งานอยู่แล้วที่สร้างขึ้นเพื่อการชลประทานและการเกษตร ทั้งนี้เพื่อเพิ่มประโยชน์การใช้ทรัพยากรให้ได้หลายวัตถุประสงค์ เช่น เขื่อนป่าสักชลสิทธิ์ ในโครงการพระราชดำริ ที่เริ่มสร้างขึ้นเพื่อการอุปโภค การเกษตร อุตสาหกรรม คมนาคม บรรเทาอุทกภัย ปัจจุบันกำลังดำเนินการติดตั้งกังหันน้ำ และเครื่องกำเนิดไฟฟ้าขนาดกำลังผลิตสูงสุด ๖.๗ เมกะวัตต์ และคาดว่าจะเริ่มผลิตไฟฟ้าจำหน่ายได้ใน พ.ศ. ๒๕๔๘

ตารางที่ ๔ โครงการโรงไฟฟ้าพลังน้ำขนาดเล็ก จำนวน ๒๔ โครงการ ของ พพ.[๓๓]

ชื่อโครงการ	ที่ตั้ง (จังหวัด)	กำลังการผลิตติดตั้ง (กิโลวัตต์)	พลังงานที่ผลิตได้ (ล้านกิโลวัตต์ชั่วโมงต่อปี)	ประมาณการต้นทุนในการก่อสร้าง (ล้านบาท)
ห้วยตองก้อ	แม่ฮ่องสอน	๙๐๐	๔	๘๗
ห้วยผาปู่	ตาก	๒,๗๔๖	๗	๑๖๙
คลองฉวาง	สุราษฎร์ธานี	๖๕๕	๓	๑๓๐
แควน้อย	พิษณุโลก	๓,๕๒๐	๑๒	๒๔๖
ห้วยน้ำร้อง	พิษณุโลก	๒,๕๗๐	๙	๑๔๓
คลองเต่าดำ	กำแพงเพชร	๗,๑๖๐	๕๐	๓๖๓
คลองกรุงชิง	นครศรีธรรมราช	๖,๐๐๐	๒๕	๒๘๔
ห้วยแดนหมี	ตรัง	๒,๖๓๕	๑๓	๑๕๕
น้ำแม่ลาน้อย	แม่ฮ่องสอน	๒,๐๑๒	๗	๑๑๓
ห้วยคลิตี้	กาญจนบุรี	๒,๖๐๐	๑๓	๒๗๓
ห้วยแม่สงิน	เชียงใหม่	๖๕๕	๔	๙๒
ห้วยยองเผาะ	กาญจนบุรี	๑,๒๘๐	๗	๑๑๕
ห้วยแม่อุสุ	ตาก	๗,๕๒๖	๓๓	๓๔๔
ห้วยน้ำพาง	เพชรบูรณ์	๑,๗๐๐	๖	๙๘
คลองละอุ่น	ระนอง	๔,๐๐๐	๑๕	๒๒๑
น้ำฟ้า	น่าน	๖,๕๐๐	๑๓	๒๗๑
คลองแอ	สุราษฎร์ธานี	๑,๙๒๐	๒๑	๑๙๐
ห้วยน้ำร้อง	พิษณุโลก	๒,๕๗๐	๙	๑๔๓
น้ำแม่วาง (แม่เตียน)	เชียงใหม่	๑,๖๐๐	๘	๑๐๑
แม่แปะ	เชียงใหม่	๖๒๘	๔	๗๒
น้ำแม่ละป๊อก	เชียงใหม่	๗๙๐	๔	๗๘
น้ำแม่หลวง	เชียงใหม่	๙๓๐	๗	๒๑๙
น้ำปัว	น่าน	๔,๓๐๐	๑๓	๒๕๘
น้ำแม่หวาน	เชียงใหม่	๙๓๐	๔	๑๒๘

ที่มา : กรมพัฒนาพลังงานทดแทนและอนุรักษ์พลังงาน

๓. พลังงานลม

๓.๑ ศักยภาพพลังงานลมของประเทศไทย

กรมพัฒนาพลังงานทดแทนและอนุรักษ์พลังงาน ได้จัดทำแผนที่ศักยภาพพลังงานลมมา ตั้งแต่ พ.ศ. ๒๕๑๘ และได้มีการจัดทำใหม่ใน พ.ศ. ๒๕๔๔[๙] ซึ่งสรุปได้ว่า ประเทศไทยได้รับอิทธิพลลมมรสุมตะวันออกเฉียงเหนือที่พัดผ่านประเทศไทยจากทะเลจีนใต้ในเดือนพฤศจิกายนถึงมีนาคม และอิทธิพลลมมรสุมตะวันตกเฉียงใต้พัดผ่านประเทศไทยในเดือนพฤษภาคมถึงตุลาคม พื้นที่ที่ได้รับอิทธิพลทั้งลมมรสุมตะวันออกเฉียงเหนือและลมมรสุมตะวันตกเฉียงใต้เป็นบริเวณเทือกเขาทอดยาวขวางทิศทางลม ทำให้เป็นพื้นที่ที่มีลมพัดแรงเกือบตลอดทั้งปี ที่ยอดเขามีความเร็วลมประมาณ ๗.๐ เมตร/วินาทีขึ้นไป ได้แก่ จังหวัดสุราษฎร์ธานี พังงา กระบี่ นครศรีธรรมราช

พื้นที่ที่ได้รับอิทธิพลลมมรสุมตะวันออกเฉียงเหนือ โดยมีทิศทางลมพัดจากทะเลเข้าสู่ฝั่งความเร็วลมเฉลี่ยทั้งปี ๖.๔ เมตร/วินาที (ที่ความสูง ๕๐ เมตรจากพื้นดิน) ขึ้นไป ในพื้นที่ภาคใต้บริเวณชายฝั่งทะเลตะวันออก ได้แก่ จังหวัดนครศรีธรรมราช สงขลา และปัตตานี ส่วนพื้นที่ที่ได้รับอิทธิพลลมมรสุมตะวันตกเฉียงใต้ กำลังลมแรงบนยอดเขามีความเร็วลมประมาณ ๖.๔ เมตร/วินาที ขึ้นไป ได้แก่ พื้นที่บนเทือกเขาด้านทิศตะวันตก ตั้งแต่จังหวัดเพชรบุรี กาญจนบุรี และจังหวัดตาก ส่วนอุทยานแห่งชาติดอยอินทนนท์ จังหวัดเชียงใหม่ ก็ได้รับอิทธิพลจากความกดอากาศสูงจากสาธารณรัฐประชาชนจีนและลมมรสุมตะวันตกเฉียงใต้ทำให้มีความเร็วลมประมาณ ๖.๔ เมตร/วินาทีขึ้นไป

ส่วนแหล่งที่มีศักยภาพพลังงานลมรองลงมา ได้แก่ ความเร็วลมเฉลี่ย ๔.๔ เมตร/วินาทีขึ้นไป (ที่ความสูง ๕๐ เมตรจากพื้นดิน) ซึ่งเกิดจากอิทธิพลลมมรสุมตะวันออกเฉียงเหนือพบว่า อยู่ที่อ่าวไทยฝั่งตะวันตก ตั้งแต่จังหวัดสุราษฎร์ธานี ชุมพร ประจวบคีรีขันธ์ เพชรบุรี และบริเวณที่สูงบนยอดเขาในภาคเหนือ จังหวัดเชียงใหม่ และภาคตะวันออกเฉียงเหนือ จังหวัดเพชรบูรณ์ และเลย และแหล่งที่มีศักยภาพรองลงมาซึ่งได้รับอิทธิพลจากลมมรสุมตะวันตกเฉียงใต้ ได้แก่ ภาคใต้ฝั่งตะวันตกตั้งแต่จังหวัดสตูล ตรัง กระบี่ ภูเก็ต พังงา และอ่าวไทยฝั่งตะวันออกจังหวัดชลบุรี และระยอง

๓.๒ การใช้พลังงานลมในประเทศไทย

เนื่องจากพลังงานลมขึ้นอยู่กับความเร็วและมวลของอากาศ ดังนั้นการนำพลังงานลมมาใช้ประโยชน์จะต้องเลือกพื้นที่ที่มีศักยภาพความเร็วลมสูงจึงจะได้พลังงานมาก พลังงานลมสามารถเปลี่ยนเป็นพลังงานกลหรือพลังงานไฟฟ้าได้ โดยใช้กังหันลมเป็นอุปกรณ์เปลี่ยนพลังงาน ทั้งนี้ สามารถจำแนกตามลักษณะการใช้ประโยชน์ได้เป็น ๒ ประเภทหลัก ๆ ได้แก่ กังหันลมเพื่อการสูบน้ำ และกังหันลมเพื่อการผลิตไฟฟ้า

กังหันลมเพื่อการสูบน้ำ ประเทศไทยมีการใช้กังหันลม ๓ แบบ[๙] ได้แก่ กังหันลมใบเรือ กังหันลมใบพัด และกังหันลมหลายใบ กังหันลม ๒ ชนิดแรกเป็นแบบดั้งเดิมที่ใบพัดของกังหันทำด้วยเสื่อลำแพน ผ้าใบ ไม้ และสังกะสี กังหันลมชนิดใบเรือส่วนใหญ่ใช้ในนาเกลือ ส่วนกังหันลมชนิดใบพัดส่วนใหญ่ใช้ในนาข้าว กังหันลมทั้ง ๒ ชนิดนี้มีความสามารถในการยกระดับน้ำไม่เกิน ๒ เมตร สามารถสร้างเองได้ สำหรับกังหันลมชนิดหลายใบส่วนใหญ่ใช้ในการสูบน้ำเพื่อการอุปโภคและบริโภค มีความสามารถในการยกระดับน้ำได้สูงกว่า ๒ ชนิดแรก ราคากังหันลมชนิดนี้ขึ้นอยู่กับขนาดและจำนวนใบกังหันลม และจะมีราคาสูงกว่ากังหันลม ๒ แบบแรก สำหรับเครื่องสูบน้ำที่ใช้คู่กับกังหันลมมีใช้อยู่ ๒ แบบ คือ แบบระหัดและแบบสูบชัก โดยเครื่องสูบน้ำแบบระหัดจะทำจากไม้ ใช้ร่วมกับกังหันลมชนิดใบเรือและใบพัด เพื่อวิดน้ำเข้านาเกลือและนาข้าว ส่วนเครื่องสูบน้ำแบบสูบชักทำจากโลหะใช้ร่วมกับกังหันลมชนิดหลายใบ กรรมวิธีการผลิตใช้เทคนิคค่อนข้างซับซ้อนและยุ่งยากกว่าแบบระหัด ส่วนใหญ่บริษัทจำหน่ายกังหันลมคู่กับเครื่องสูบน้ำ

กังหันลมเพื่อการผลิตไฟฟ้า ใน พ.ศ. ๒๕๔๖ ประเทศไทยมีกำลังผลิตติดตั้งกังหันลมเพื่อผลิตไฟฟ้ารวมทั้งสิ้น ๑๙๕.๗ กิโลวัตต์[๑๐] ซึ่งส่วน

ใหญ่อยู่ในภาคใต้ (๑๙๒.๓ กิโลวัตต์) มีส่วนน้อยอยู่ในภาคตะวันออกเฉียงเหนือ (๒.๕ กิโลวัตต์) และภาคใต้ (๐.๙ กิโลวัตต์) การไฟฟ้าฝ่ายผลิตได้สร้างสถานีสาธิตพลังงานทดแทนที่แหลมพรหมเทพ จังหวัดภูเก็ต ซึ่งผลิตไฟฟ้าร่วมระหว่างพลังงานลม ๑๙๒ กิโลวัตต์ กับเซลล์แสงอาทิตย์ขนาด ๑๑.๓๔ กิโลวัตต์

๓.๓ สถานภาพงานวิจัยด้านพลังงานลมของประเทศไทย

จากการศึกษาข้อมูลงานวิจัยด้านพลังงานลมของประเทศไทย สามารถแบ่งงานวิจัยออกเป็น ๒ ประเภท ได้แก่ งานวิจัยด้านสมรรถนะของกังหันลมเพื่อการสูบน้ำ และงานวิจัยด้านสมรรถนะของการผลิตพลังงานไฟฟ้าจากพลังงานลม

ด้านงานวิจัยด้านสมรรถนะของกังหันลมเพื่อการสูบน้ำ มีการทดสอบกังหันลม ๘ ใบ ศึกษาสมรรถนะกังหันลมหลายใบ การศึกษาความเค้นในใบของกังหันลมแกนหมุนแนวดิ่ง การศึกษาแบบจำลองไฟไนท์เอเลเมนต์ของใบพัดกังหันลมแบบดาร์เรียส และการศึกษา Laminar Separation Bubble บนใบพัดของกังหันลม[๔๐-๔๓] การทดสอบสมรรถนะของโรเตอร์กังหันลมที่มีใช้อยู่ในประเทศไทย ๖ แบบ ได้แก่ กังหันลมหลายใบ กังหันลมล้อจักรยาน กังหันลมนาข้าว ๒ ใบ กังหันลมนาข้าว ๔ ใบ กังหันลมนาเกลือ ๖ ใบ และกังหันลมปัตตานี ๒ ใบ โดยแบบจำลองทางคณิตศาสตร์ เพื่อหาอัตราส่วนความเร็วปลายใบที่ให้ค่าสัมประสิทธิ์กำลังงานสูงสุดของกังหันแต่ละแบบ จากผลการทดสอบที่ได้ทำให้สามารถเลือกใช้กังหันลมแต่ละแบบให้เหมาะสมกับศักยภาพลมของพื้นที่แต่ละแห่ง

ด้านงานวิจัยด้านสมรรถนะการผลิตพลังงานไฟฟ้าจากพลังงานลม มีการทดสอบแบบจำลองกังหันลมแบบไจโร-โรเตอร์ชนิดใบตรง[๔๔] ศึกษาสมรรถนะของกังหันลมแบบดาร์เรียส[๔๕] ซึ่งเป็นกังหันลมแบบแนวดิ่ง

การพัฒนาเครื่องกำเนิดไฟฟ้าจากพลังงานลม[๔๖] เป็นการพัฒนางานวิจัยที่อาศัยหลักการเปลี่ยนแปลงพลังงานลมเป็นพลังงานไฟฟ้าโดยใช้กังหันลมเป็นตัวขับเคลื่อนเครื่องกำเนิดไฟฟ้า ซึ่งจากการทดสอบใช้เครื่องกำเนิดไฟฟ้าในรถยนต์เนื่องจากหาง่ายและมีราคาถูก ทนทานต่อสภาพการใช้งานในภาวะต่าง ๆ นอกจากนี้ ยังมีการศึกษาพารามิเตอร์ของระบบผลิตไฟฟ้าแบบผสมผสานที่ประกอบด้วย พลังงานลม เซลล์แสงอาทิตย์ และเครื่องยนต์ดีเซลเพื่อใช้งานในพื้นที่ห่างไกล[๖๗]

ระบบผลิตและสำรองไฟฟ้าด้วยพลังงานลม[๔๗] งานวิจัยนี้เป็นการดัดแปลงกังหันนาเกลือแบบหมุนรับลมตามทิศทางมาใช้สำหรับผลิตพลังงานไฟฟ้า ศึกษาความสัมพันธ์ระหว่างความเร็วลมกับรอบการหมุนของกังหันลม

กังหันลมเป็นเทคโนโลยีที่มีการใช้มานานอย่างแพร่หลายและคุ้มค่าทางเศรษฐศาสตร์สำหรับพื้นที่ที่มีศักยภาพความเร็วลมเพียงพอ เนื่องจากเป็นเทคโนโลยีที่แปลงพลังงานลมมาเป็นพลังงานกลแล้วนำพลังงานกลไปขับเครื่องสูบน้ำ ดังนั้น ค่าการลงทุนจึงขึ้นกับราคากังหันลมกับราคาเครื่องสูบน้ำ และไม่มีค่าเชื้อเพลิง

ประเทศไทยมีการใช้กังหันลมเพื่อผลิตพลังงานไฟฟ้าโดยการนำเข้าจากต่างประเทศ เนื่องจากประเทศไทยยังไม่มีโรงงานผลิตกังหันลมเพื่อผลิตกระแสไฟฟ้าภายในประเทศ ดังนั้น ราคาพลังงานไฟฟ้าที่ผลิตจากพลังงานลม จึงสามารถอ้างอิงราคาพลังงานของต่างประเทศได้ แต่จะมีราคาสูงกว่าเพราะต้องรวมค่าขนส่ง ค่าติดตั้ง อัตราแลกเปลี่ยนเงินตรา ภาษีนำเข้าอุปกรณ์ของประเทศไทย รวมถึงค่าอะไหล่ที่ต้องนำเข้าและการซ่อมแซมบำรุงรักษา จากข้อมูลของการไฟฟ้าฝ่ายผลิตแห่งประเทศไทย[๕๘]

จากการศึกษาศักยภาพสถานภาพการใช้ สถานภาพงานวิจัย และการวิเคราะห์ทางเศรษฐศาสตร์ของพลังงานลมที่นำมาใช้สำหรับเพื่อการสูบน้ำและผลิตไฟฟ้า สามารถสรุปสถานภาพได้ตารางที่ ๕

ตารางที่ ๕ สรุปสถานภาพของพลังงานลมของประเทศไทย

ลักษณะการใช้งาน	สถานภาพ			
	ศักยภาพทางเทคนิค	มีการใช้งานอย่างแพร่หลาย	โครงการสาธิต	มีจำหน่ายเชิงพาณิชย์
กังหันลมเพื่อการสูบน้ำ	X	X		X
กังหันลมเพื่อผลิตไฟฟ้า	X		X	

หมายเหตุ : X หมายถึง มีสถานภาพตามหัวข้อในแนวตั้ง

๓.๔ แนวทางงานวิจัยด้านพลังงานลมในประเทศไทย

ข้อจำกัดสำคัญของการใช้ประโยชน์จากพลังงานลม คือ ค่าความเร็วลม สำหรับการใช้พลังลมเพื่อการสูบน้ำ ถึงแม้จะต้องการความเร็วลมไม่สูงมากนัก แต่ในพื้นที่ที่มีความเร็วลมต่ำมาก ก็ไม่สามารถทำได้เช่นกัน และที่สำคัญจะต้องเป็นพื้นที่ที่ไม่มีสิ่งกีดขวางเส้นทางลมและห่างจากชุมชนพอสมควร ส่วนกังหันลมเพื่อการผลิตพลังงานไฟฟ้าจำเป็นต้องใช้พื้นที่ที่มีศักยภาพความเร็วลมสูง เช่น ชายฝั่งทะเล จึงทำให้สามารถติดตั้งได้เฉพาะบางพื้นที่เท่านั้น

จากการศึกษาข้างต้นพบว่า สิ่งสำคัญของการนำพลังงานลมมาใช้ประโยชน์ด้านพลังงาน ได้แก่ ค่าความเร็วลมของพื้นที่นั้น ๆ ต้องเหมาะสมกับการใช้งาน เนื่องจากกังหันลมแต่ละชนิดแต่ละแบบจะมีค่าความเร็วเริ่มต้นของการทำงานต่างกัน ดังนั้น การติดตั้งกังหันลมในพื้นที่แต่ละแห่งจะต้องศึกษาศักยภาพความเร็วลมก่อนเป็นอันดับแรก และจากการศึกษาข้อมูลด้านศักยภาพพลังงานของประเทศไทย

พบว่า ประเทศไทยมีการใช้กังหันลมเพื่อการสูบน้ำเพื่อการเกษตรทั้งในนาข้าวและนาเกลือมาเป็นเวลานาน กังหันลมเพื่อการสูบน้ำนี้ต้องการความเร็วลมไม่มากนักก็สามารถทำงานได้ จึงมีพื้นที่หลายแห่งของประเทศไทยที่มีการใช้กังหันลมเพื่อการสูบน้ำ การติดตั้งกังหันลมจะเหมาะสมกับงานและพื้นที่ที่มีค่าความเร็วลมตรงกับช่วงทำงานซึ่งอาจมีปัญหาในช่วงลมสงบทำให้ไม่สามารถทำงานได้ พื้นที่ที่มีการใช้กังหันส่วนใหญ่จะเป็นทุ่งกว้างมีสิ่งกีดขวางทางลมน้อย สำหรับสถานภาพของงานวิจัยด้านพลังงานลมเพื่อการสูบน้ำของประเทศไทย ส่วนใหญ่จะเน้นไปในด้านงานวิจัยเพื่อทดสอบสมรรถนะของกังหันลม เนื่องจากกังหันลมมีหลายแบบซึ่งเหมาะสมกับการทำงานแต่ละแบบไม่เหมือนกัน ดังนั้น แนวทางงานวิจัยพลังงานลมเพื่อการสูบน้ำควรมีงานวิจัยด้านการประยุกต์ใช้กังหันลมกับอุปกรณ์ที่ใช้พลังงานกล การเก็บรวบรวมข้อมูลสถานภาพการใช้กังหันลมเพื่อการสูบน้ำ ณ ภาวะปัจจุบัน เนื่องจากงานวิจัยนี้เป็นเพียงการศึกษาสถานภาพซึ่งใช้ข้อมูลจากหน่วยงานที่เคยทำการสำรวจไว้แล้ว จึงอาจจะคลาดเคลื่อนจากสภาพปัจจุบัน ข้อมูลสถานภาพการใช้งานจริงในปัจจุบันจะมีประโยชน์อย่างมากต่อการกำหนดแผนพัฒนาและส่งเสริมการใช้กังหันลมเพื่อการสูบน้ำต่อไป

ควรมีงานวิจัยเชิงนโยบายด้านมาตรการส่งเสริมการนำกังหันลมมาใช้ประโยชน์ให้มากขึ้นกว่าในปัจจุบัน โดยเฉพาะในพื้นที่เกษตรกรรม เนื่องจากเป็นพื้นที่ที่เหมาะสำหรับการติดตั้งและการนำพลังงานจากกังหันลมไปใช้ประโยชน์ และควรจะอนุรักษ์การใช้กังหันลมเพื่อการสูบน้ำในนาข้าวเดิมให้มีการใช้งานต่อไปและเพิ่มปริมาณจำนวนกังหันลมให้มากขึ้น

แนวทางด้านงานวิจัยพลังงานลมเพื่อผลิตไฟฟ้าของประเทศไทย จากการศึกษาการใช้กังหันลมสำหรับการผลิตไฟฟ้า พบว่า ต้องใช้ความเร็วลมสูงมากกว่า ๔ เมตร/วินาที กังหันลมจึงจะเริ่มทำงานได้ ดังนั้น การเลือกพื้นที่ที่มีความเร็วลมสูงจะมีความสำคัญ

มากสำหรับการติดตั้งกังหันลมเพื่อผลิตไฟฟ้า จากการศึกษาศักยภาพพลังงานลมของประเทศไทยพบว่า หลายจังหวัดทางภาคใต้ของประเทศไทยมีศักยภาพความเร็วลมสูงสามารถติดตั้งกังหันลมเพื่อผลิตไฟฟ้าได้ แต่ปัจจุบันประเทศไทยมีการติดตั้งกังหันลมผลิตพลังงานไฟฟ้าที่มีขนาดกำลังผลิตน้อยมาก

ดังนั้น จึงควรมีงานวิจัยด้านการศึกษาความเป็นไปได้ทางเทคนิคและเศรษฐศาสตร์สำหรับการติดตั้งกังหันลมในพื้นที่ที่มีความเร็วลมสูง โดยใช้แบบจำลองทางคณิตศาสตร์เพื่อศึกษาตัวแปรต่าง ๆ ที่มีผลต่อทางเทคนิคและเศรษฐศาสตร์ของกังหันลม เนื่องจากประเทศไทยไม่ใช้ผู้ผลิตกังหันลมเพื่อผลิตไฟฟ้าจึงต้องนำเข้าจากต่างประเทศ ทำให้ยังคงมีปัญหาทางด้านเศรษฐศาสตร์ในการนำมาใช้งาน จึงควรมีการศึกษาความเป็นไปได้ที่จะพัฒนาอุตสาหกรรมการผลิตกังหันลมเพื่อผลิตไฟฟ้าภายในประเทศในอนาคต

นอกจากนี้ ควรมีงานวิจัยเชิงนโยบายด้านมาตรการจูงใจและส่งเสริมการผลิต และติดตั้งกังหันเพื่อการสูบน้ำและเพื่อการผลิตไฟฟ้า เช่น การให้คำปรึกษาด้านเทคนิคและอุปกรณ์ที่เกี่ยวข้องกับกังหันลม การลดภาษีนำเข้าวัสดุอุปกรณ์ การกำหนดพื้นที่ที่มีศักยภาพเพื่อให้มีการลงทุนของภาคเอกชนในการผลิตไฟฟ้าจำหน่ายเข้าระบบการส่งเสริมการลงทุนสำหรับอุตสาหกรรมการผลิตกังหันลมเพื่อการสูบน้ำและเพื่อผลิตไฟฟ้า

๔. พลังงานความร้อนใต้พิภพ

พลังงานความร้อนใต้พิภพ หมายถึง พลังงานธรรมชาติที่เกิดจากความร้อนที่ถูกกักเก็บอยู่ภายใต้ผิวโลก สามารถนำไปใช้ประโยชน์ได้โดยอุณหภูมิใต้ผิวโลกจะเพิ่มขึ้นตามความลึก ตามปรกติแหล่งพลังงานนี้จะอยู่ในรูปของน้ำพุร้อน หรือน้ำร้อนจากใต้ดิน แหล่งพลังงานความร้อนใต้พิภพที่พบในโลกแบ่งตามลักษณะการเกิดได้ ๓ ลักษณะ[๙๙] คือ

- แหล่งที่เป็นไอน้ำส่วนใหญ่ (steam dominated) เป็นแหล่งกักเก็บความร้อนที่ประกอบด้วยไอน้ำมากกว่าร้อยละ ๙๕ โดยทั่วไปมักเป็นแหล่งที่มีความสัมพันธ์ใกล้ชิดกับหินหลอมเหลวร้อนที่แทรกดันขึ้นมาอยู่ในระดับตื้น ๆ โดยอุณหภูมิของไอน้ำร้อนสูงกว่า ๒๔๐ องศาเซลเซียส แหล่งที่เป็นไอน้ำส่วนใหญ่พบน้อยมาก แต่สามารถนำมาใช้ผลิตกระแสไฟฟ้าได้มากที่สุด เช่น The Geyser Field ในมลรัฐแคลิฟอร์เนีย สหรัฐอเมริกา และ Larderello ประเทศอิตาลี

- แหล่งที่เป็นน้ำร้อนส่วนใหญ่ (hot water dominated) เป็นแหล่งกักเก็บสะสมความร้อนที่ประกอบไปด้วยน้ำร้อนเป็นส่วนใหญ่ อุณหภูมิน้ำร้อนจะมีตั้งแต่ ๑๐๐ องศาเซลเซียสขึ้นไป ระบบนี้จะพบมากที่สุด เช่น Cerro prieto ประเทศเม็กซิโก Hatchobaru ประเทศญี่ปุ่น และ Wairakei ในประเทศนิวซีแลนด์

- แหล่งหินร้อนแห้ง (hot dry rock) เป็นแหล่งสะสมความร้อนที่เป็นหินเนื้อแน่น แต่ไม่มีน้ำร้อนหรือไอน้ำไหลหมุนเวียนอยู่ ดังนั้น ถ้าจะนำมาใช้จำเป็นต้องทำชั้นหินร้อนให้มีรอยแตกแล้วจึงอัดน้ำเย็นลงไปทางหลุมเจาะให้น้ำได้รับความร้อนจากหินร้อน โดยไหลหมุนเวียนภายในรอยแตกที่กระทำขึ้น จากนั้นก็สูบน้ำนี้ขึ้นมาทางหลุมเจาะอีกหลุมหนึ่ง

๔.๑ ศักยภาพของพลังงานความร้อนใต้พิภพที่พบในประเทศไทย

แหล่งพลังงานความร้อนใต้พิภพของประเทศไทย จัดอยู่ในแหล่งกักเก็บอุณหภูมิต่ำ คือ มีอุณหภูมิน้อยกว่า ๑๒๕ องศาเซลเซียส โดยแหล่งเก็บสะสมความร้อนจะประกอบไปด้วยน้ำร้อนเป็นส่วนใหญ่ อุณหภูมิน้ำร้อนจะมีค่ามากกว่า ๘๐ องศาเซลเซียส สรุปผลจากการสำรวจแหล่งพลังงานความร้อนใต้พิภพของประเทศไทย[๙๐] พบว่ามีแหล่งส่วนใหญ่อยู่ทางภาคเหนือและอุณหภูมิต่ำกว่า ๑๐๐ องศาเซลเซียส และประเทศไทยมีศักยภาพเชิงความร้อนรวมทั้งสิ้น ๕๒๗ พันตันเทียบเท่าน้ำมันดิบ ซึ่งมีรายละเอียดดังแสดงในตารางที่ ๖ เกณฑ์การพิจารณาศักยภาพพลังงานความร้อนใต้พิภพในประเทศไทยที่สามารถนำมาผลิตไฟฟ้า ได้แก่

- อุณหภูมิ อยู่ในช่วง ๑๐๐-๑๕๐ องศาเซลเซียส

- ขนาดของแหล่งกักเก็บจะต้องมีความลึกไม่เกิน ๐-๒๐๐ เมตร จากพื้นดิน

- ความดันของไอน้ำ
- ลักษณะของแหล่งประกอบไปด้วยน้ำร้อนเป็นส่วนใหญ่หรือไอน้ำเป็นส่วนใหญ่

๔.๒ การนำความร้อนใต้พิภพมาใช้ประโยชน์ในประเทศไทย

ด้านการผลิตไฟฟ้า มีการผลิตไฟฟ้าจากแหล่งพลังงานความร้อนใต้พิภพ มีอยู่เพียงที่เดียวซึ่งเป็นโครงการสาธิตของการไฟฟ้าฝ่ายผลิต คือ ที่อำเภอฝาง จังหวัดเชียงใหม่ มีกำลังการผลิตคือ ๓๐๐ กิโลวัตต์ ซึ่งเป็นโรงไฟฟ้าระบบ ๒ วงจร[๑๐] ที่ใช้แหล่งพลังงานความร้อนที่มีอุณหภูมิต่ำ ใช้น้ำร้อนจากหลุมเจาะระดับตื้นที่มีอุณหภูมิ ๑๓๐ องศาเซลเซียส ผลิตได้ประมาณปีละ ๑.๒ ล้านกิโลวัตต์ชั่วโมง จะถูกส่งเข้าสู่ระบบของการไฟฟ้าส่วนภูมิภาคเพื่อจ่ายให้ผู้ใช้ไฟฟ้าต่อไป และได้นำน้ำร้อนที่ผ่านการใช้งานในระบบผลิตไฟฟ้าแล้วไปใช้ให้ความร้อนในการอบแห้งห้องเย็น กิจการกายภาพบำบัด และเป็นสถานที่ท่องเที่ยว

ส่วนแหล่งพลังงานความร้อนใต้พิภพอื่น ๆ ที่มีศักยภาพ เช่นที่สันกำแพงนั้น ได้มีการเจาะสำรวจแต่ยังไม่มีการติดตั้งกำลังการผลิต ส่วนแหล่งพลังงานความร้อนใต้พิภพที่อำเภอป่าแป๋และเทพพนม ยังพบปัญหาหลายอย่างคือ อยู่ในเขตอุทยานแห่งชาติ ดังนั้น การพัฒนาแหล่งความร้อนใต้พิภพจะเป็นไปได้ยาก ส่วนที่อำเภอแม่จันนั้น อยู่ในพื้นที่ที่มีการจ่ายไฟฟ้าถึงอยู่แล้ว ต้นทุนของการผลิตไฟฟ้าด้วยพลังงานความร้อนใต้พิภพจะมีค่าสูงกว่า ดังนั้นจึงยังไม่มีการพัฒนา

ตารางที่ ๖ ศักยภาพเชิงพลังงานความร้อนใต้พิภพ ตามแหล่งทางภูมิศาสตร์

แหล่งทางภูมิศาสตร์	ศักยภาพเชิงพลังงาน (พันตันเทียบเท่าน้ำมันดิบ)
ทั้งประเทศ	๕๒๗.๐
ภาคเหนือ	๕๐๖.๓
ภาคตะวันออกเฉียงเหนือ	-
ภาคกลาง	๓.๑
ภาคใต้	๑๗.๖

ด้านความร้อน แหล่งความร้อนใต้พิภพในประเทศไทยส่วนใหญ่เป็นแหล่งกักเก็บที่มีอุณหภูมิต่ำ ดังนั้นควรพิจารณานำมาใช้ประโยชน์ เป็นแหล่งให้ความร้อนโดยตรง ความร้อนที่ใช้อยู่ในช่วงประมาณไม่เกิน ๑๕๐ องศาเซลเซียส[๙] สามารถนำมาใช้ประโยชน์ต่าง ๆ ได้ เช่น สามารถนำไปใช้ในการอบแห้ง และเป็นแหล่งให้พลังงานแก่ห้องเย็นสำหรับเก็บรักษาพืชผลทางการเกษตรได้ นำไปใช้ในกิจการเพื่อกายบำบัด

ปัญหาที่สำคัญอีกอย่างหนึ่งของการใช้งานคือ น้ำพุร้อนที่โผล่ขึ้นมาให้เห็นตามผิวดิน อาจไม่ได้อยู่เหนือแหล่งที่กำเนิดและกักเก็บพลังงาน ดังนั้น จึงไม่สามารถประเมินถึงศักยภาพของแหล่งพลังงานความร้อนใต้พิภพได้อย่างแน่ชัดว่ามีปริมาณเท่าไร และจะหมดเมื่อไร จึงอยากที่จะประเมินว่าเหมาะสม คุ้มค่าที่จะนำมาใช้หรือไม่

๔.๓ แนวทางวิจัยพลังงานความร้อนใต้พิภพในประเทศไทย

ข้อจำกัดของการใช้พลังงานความร้อนใต้พิภพ คือ จะมีการปล่อยแก๊สคาร์บอนไดออกไซด์ ซัลเฟอร์ไดออกไซด์และมีเทน และในน้ำแร่ร้อนยังประกอบด้วยสารละลายซิลิกา โลหะหนัก (heavy metal) โซเดียมและโพแทสเซียมคลอไรด์ บางครั้งอาจมีคาร์บอเนตด้วย ซึ่งอาจมีผลกระทบต่อสิ่งแวดล้อม และอาจมีการทรุดตัวของพื้นดินในแหล่งพลังงานความร้อนใต้

พิภพที่มีน้ำเป็นส่วนใหญ่ จากศักยภาพแหล่งพลังงานความร้อนใต้พิภพในประเทศไทย จะเห็นได้ว่า เป็นแหล่งกักเก็บที่มีอุณหภูมิต่ำ ดังนั้น ควรมีแนวทางวิจัยในการศึกษาความเป็นไปได้ในการนำความร้อนจากน้ำร้อน ไปใช้ประโยชน์โดยตรงแทน โดยพัฒนาแหล่งพลังงานและศึกษาผลกระทบทางด้านสิ่งแวดล้อมด้วย

๕. พลังงานจากมหาสมุทร

มหาสมุทรสามารถผลิตพลังงานได้ ๒ รูปแบบ คือ พลังงานความร้อนที่ได้จากแสงอาทิตย์ และพลังงานกลที่ได้จากน้ำขึ้นน้ำลง และคลื่น

๕.๑ ศักยภาพการผลิตไฟฟ้าด้วยความร้อนจากมหาสมุทรในประเทศไทย (OTEC)[๕๓]

พื้นผิวโลกกว่าร้อย ๗๐ เป็นมหาสมุทร ดังนั้น มหาสมุทรจึงเป็นเสมือนตัวเก็บรังสีอาทิตย์ (solar collector) ขนาดใหญ่ การผลิตไฟฟ้าด้วยความร้อนจากมหาสมุทร จะอาศัยความแตกต่างระหว่างอุณหภูมิน้ำทะเลส่วนบนที่มีความลึกไม่เกิน ๕๐ เมตร ซึ่งเป็นส่วนที่สะสมพลังงานจากแสงอาทิตย์มีอุณหภูมิประมาณ ๒๕-๓๐ องศาเซลเซียส กับอุณหภูมิของน้ำทะเลส่วนล่างที่มีความลึกประมาณ ๑,๐๐๐ เมตร มีอุณหภูมิประมาณ ๕ องศาเซลเซียส

บริเวณที่เหมาะสม ในการพัฒนาระบบ OTEC[๕๔] ได้แก่

๑. ชายฝั่งที่มีความลาดชันสูง

๒. ท้องมหาสมุทรลึกมากกว่า ๑,๐๐๐ เมตร และอยู่ใกล้ชายฝั่ง

๓. ระยะห่างจากที่ตั้งชายฝั่งถึงที่ตั้งโรงไฟฟ้าแบบลอยน้ำ ไม่ควรเกิน ๔๐ กิโลเมตร

นอกจากนี้ กระแสลมและกระแสน้ำก็มีอิทธิพลต่อการพัฒนาด้วย กล่าวคือ กระแสน้ำที่มีความเร็วมากกว่า ๑.๘๒ กิโลเมตรต่อชั่วโมง หรือบริเวณที่มีกระแสลมที่มีความเร็วสูงกว่า ๔๖.๔ กิโลเมตรต่อชั่วโมง จะไม่เหมาะสมต่อการติดตั้งโรงไฟฟ้า OTEC

การผลิตไฟฟ้าจากพลังงานความร้อนจากมหาสมุทร (OTEC) มีวัฏจักรการทำงาน แบ่งออกได้เป็น ๓ ระบบ คือ[๕๕] ระบบวัฏจักรเปิด (open cycle) ระบบวัฏจักรปิด (closed cycle) และแบบลูกผสม (hybrid system) ซึ่งทั้ง ๓ ระบบจะมีส่วนประกอบที่สำคัญอยู่ ๓ ส่วน คือ เครื่องระเหย (evaporator) เครื่องควบแน่น (condenser) กังหันไอน้ำและเครื่องกำเนิดไฟฟ้า (turbine and generator)

การทำงานของระบบผลิตไฟฟ้าด้วยความร้อนจากมหาสมุทร (OTEC) จะคล้ายคลึงกับโรงไฟฟ้าทั่วไป แต่ต่างกันที่ไม่มีการเผาไหม้เชื้อเพลิง เนื่องจากใช้ความร้อนจากน้ำมหาสมุทรส่วนบนเป็นต้นกำเนิดพลังงาน จึงไม่มีต้นทุนของค่าเชื้อเพลิง โรงไฟฟ้าแบบนี้จะใช้ผลิตไฟฟ้าในช่วงภาระฐาน (base load) แต่ประสิทธิภาพของระบบการผลิตจะต่ำ ประมาณร้อยละ ๖.๘-๙.๐ ซึ่งขึ้นกับค่าความแตกต่างของอุณหภูมิของน้ำที่ใช้ในระบบ ปัจจุบันการออกแบบโรงไฟฟ้ามี ๒ ลักษณะ คือ แบบที่ตั้งบนชายฝั่ง (shore base type) และแบบลอยน้ำ (floating type of ship type)

จากข้อมูลของกรมอุทกศาสตร์ กองทัพเรือ ในด้านของอุณหภูมิของน้ำทะเลที่ระดับผิวน้ำ และที่ความลึกในระดับต่าง ๆ สามารถสรุปได้ดังตารางที่ ๗

ตารางที่ ๗ อุณหภูมิของน้ำทะเลในบริเวณอ่าวไทย

ช่วงเวลา	อุณหภูมิ (องศาเซลเซียส)		
	ผิว	ลึก ๓๐ ม.	ลึก ๕๐ ม.
มีนาคม - เมษายน	๒๙.๐๐	๒๘.๑๗	๒๗.๙๔
พฤษภาคม - กันยายน	๓๐.๐๔	๒๙.๔๘	๒๘.๕๔
พฤศจิกายน - กุมภาพันธ์	๒๘.๓๕	๒๘.๒๔	๒๗.๙๖

ที่มา : โครงการศึกษาเบื้องต้นศักยภาพและความเหมาะสมในการพัฒนาพลังงานจากทะเล[๕๔]

พื้นท้องทะเลอ่าวไทยมีลักษณะคล้ายแอ่งน้ำ ส่วนที่ลึกสุดอยู่ตรงกลางและมีความลึกประมาณ ๘๓ เมตร เมื่อน้ำลงต่ำสุด ความลึกเฉลี่ยของอ่าวตอนกลางและตอนล่าง ประมาณ ๕๐ เมตร บริเวณปากอ่าวไทยที่ต่อกับทะเลจีนใต้ลึกประมาณ ๔๐ เมตร[๖] และด้านฝั่งทะเลอันดามัน พบว่าในระดับความลึก ๑,๐๐๐ เมตร อยู่ห่างชายฝั่ง ๒๒๐-๓๒๐ กิโลเมตร ซึ่งอยู่ในเขตน่านน้ำสากลและอยู่ห่างจากชายฝั่งมาก

เมื่อพิจารณาข้อมูลด้านพลังงานความร้อนจากมหาสมุทรดังแสดงในตารางที่ ๗ จะพบว่าประเทศไทยไม่มีศักยภาพเพียงพอในการพัฒนาระบบพลังงานความร้อนจากมหาสมุทร ทั้งในด้านความเหมาะสมของอุณหภูมิระหว่างผิวน้ำ และอุณหภูมิใต้ผิวน้ำที่ความลึกของท้องมหาสมุทร รวมถึงลักษณะชายฝั่งของประเทศไทยที่ไม่มีความลาดชันที่เพียงพอที่จะทำให้ท้องมหาสมุทรมีความลึกในระดับที่สามารถนำมาใช้ประโยชน์ได้

๕.๒ พลังงานจากน้ำขึ้น-น้ำลง (Tidal Energy)

น้ำขึ้น-น้ำลง (tides) เป็นปรากฏการณ์ธรรมชาติอย่างหนึ่งของโลก ซึ่งการเกิดจากการเพิ่มขึ้นและลดลงของระดับน้ำ[๙] เป็นผลมาจากการเปลี่ยนแปลงโดยแรงดึงดูด (gravitational force) และแรงจลน์ (kinetic force) ของดวงอาทิตย์ ดวงจันทร์และโลกเปลี่ยนไปเมื่อโคจรมาอยู่ในตำแหน่งต่าง ๆ กัน โดยเมื่อดวงอาทิตย์และดวงจันทร์เข้าใกล้โลกและโคจรอยู่ในแนวเดียวกันจะทำให้เกิดน้ำขึ้น และเมื่อแรงดึงดูดของดวงอาทิตย์และดวงจันทร์ทำมุม ๙๐ องศา เมื่อเปรียบเทียบกับโลกจะทำให้เกิดน้ำลง

การประเมินค่าพลังงานที่ได้จากพลังงานน้ำขึ้น-น้ำลง

การผลิตไฟฟ้าจากความสูงของระดับน้ำที่แตกต่างกันโดยอาศัยลักษณะธรรมชาติของชายฝั่ง พบว่าบริเวณที่เหมาะสมในการพัฒนาระบบพลังงานน้ำขึ้น-น้ำลง[๑๑] คือ

- ลักษณะของภูมิประเทศที่เหมาะสมกับการผลิตพลังงานไฟฟ้าจากการขึ้นและลงของน้ำทะเลนั้น จะอยู่ที่แนวเส้นรุ้งที่ ๕๐-๖๐ องศา
- ลักษณะของชายฝั่งทะเลบริเวณปากอ่าว ควรมีความลาดชันสูงเพื่อสามารถสร้างเป็นอ่างเก็บน้ำได้
- ความแตกต่างของระดับน้ำขึ้น-น้ำลง มีค่า ๕-๑๑ เมตร
- พื้นที่ของอ่างเก็บน้ำประมาณ ๒๕ ตารางเมตร

จากข้อมูลของกรมอุทกศาสตร์ ใน พ.ศ. ๒๕๒๕-๒๕๓๖ สามารถสรุปเป็นข้อมูลของระดับน้ำขึ้น-น้ำลงสูงสุดและข้อมูลของระดับน้ำขึ้น-ลงต่ำสุดได้ดังตารางที่ ๘

ตารางที่ ๘ ความแตกต่างของระดับน้ำขึ้น-น้ำลงของทะเล

ช่วงเวลา	ความแตกต่างของระดับน้ำขึ้น-น้ำลง สูงสุด		ความแตกต่างของระดับน้ำขึ้น-น้ำลง ต่ำสุด	
	สถานี	ความแตกต่าง (เมตร)	สถานี	ความแตกต่าง (เมตร)
อ่าวไทย				
มีนาคม - เมษายน	มหาชัย	๒.๕๘	สงขลา	๐.๘๔
พฤษภาคม - กันยายน	มหาชัย	๒.๗๖	สงขลา	๐.๘๕
พฤศจิกายน- กุมภาพันธ์	หัวหิน	๒.๗๔	สงขลา	๑.๐๒
ทะเลอันดามัน				
มีนาคม - เมษายน	เกาะตะเภาน้อย	๒.๙๗	ทับละมุ	๒.๗๗
พฤษภาคม -กันยายน	เกาะตะรุเตา	๒.๙๑	ทับละมุ	๒.๖๕
พฤศจิกายน- กุมภาพันธ์	กาะตะรุเตา	๒.๙๓	เกาะตะเภาน้อย	๒.๔๑

ที่มา : โครงการศึกษาเบื้องต้นศักยภาพและความเหมาะสมในการพัฒนาพลังงานจากทะเล[๑๑]

เมื่อพิจารณาข้อมูลระดับน้ำขึ้น-น้ำลง จะเห็นได้ว่าค่าความแตกต่างของระดับน้ำขึ้น-น้ำลง ยังไม่อยู่ในเกณฑ์ที่เหมาะสม โดยค่าของความแตกต่างของระดับน้ำขึ้น-น้ำลง ทั้งในบริเวณอ่าวไทย และฝั่งทะเลอันดามันนั้นอยู่ในเกณฑ์ต่ำและสภาพภูมิประเทศของไทยในบริเวณปากแม่น้ำจะมีลักษณะราบเรียบ ไม่เอื้ออำนวยในการสร้างอ่างเก็บน้ำได้ ดังนั้น จึงสรุปได้ว่าประเทศไทยไม่มีศักยภาพเพียงพอในการพัฒนาระบบพลังงานน้ำขึ้น-น้ำลง

๕.๓ พลังงานจากคลื่น

คลื่น เป็นปรากฏการณ์ธรรมชาติในทะเลที่เกิดขึ้นตลอดเวลา โดยคลื่นเกิดจากลมที่พัดผ่านผิวมหาสมุทรและทะเล ขนาดของคลื่นจะใหญ่หรือเล็ก จะขึ้นอยู่กับความเร็วลม และระยะทางของลมที่พัดผ่านเหนือผิวน้ำ

การประเมินค่าพลังงานที่ได้จากพลังงานคลื่นทะเล

เทคโนโลยีการแปลงพลังงานจากคลื่นทะเลเพื่อผลิตพลังงานนั้น ใช้หลักการแปลงพลังงานจลน์ (kinetic energy) ของคลื่นทะเลเพื่อผลิตพลังงาน[๔๔] พลังงานที่อยู่ในคลื่นทะเลจะประกอบไปด้วยพลังงาน ๒ ส่วน ได้แก่ พลังงานศักย์ และพลังงานจลน์ พลังงานศักย์จะเป็นพลังงานเกี่ยวข้องกับรูปแบบของคลื่น หรือความสูงของคลื่น ส่วนพลังงานจลน์จะเป็นพลังงานที่เกี่ยวข้องกับการเคลื่อนที่ของคลื่น หรือความเร็วของน้ำทะเลที่ประกอบกันเป็นคลื่น

จากข้อมูลของกรมอุทกศาสตร์ในพ.ศ. ๒๕๒๕-๒๕๓๖ สามารถสรุปเป็นข้อมูลของระดับความสูงของคลื่น และคาบคลื่นของฝั่งอ่าวไทย และฝั่งทะเลอันดามันได้ดังตารางที่ ๙

ตารางที่ ๙ ระดับความสูงของคลื่นและคาบคลื่น

ช่วงเวลา	ความสูงคลื่น (เมตร)	คาบคลื่น (วินาที)
อ่าวไทย		
มีนาคม - เมษายน	๐.๑ - ๐.๗	๒-๔
พฤษภาคม - กันยายน	๐.๑ - ๑.๒	๒-๖
พฤศจิกายน - กุมภาพันธ์	๐.๑ - ๑.๗	๒-๖
ทะเลอันดามัน		
พฤษภาคม - กันยายน	๐.๑ - ๐.๓	๒-๕
พฤศจิกายน - กุมภาพันธ์	๐.๕ - ๔.๕	๔-๗

ที่มา : โครงการศึกษาเบื้องต้นศักยภาพและความเหมาะสมในการพัฒนาพลังงานจากทะเล[๔๕]

จากการพิจารณาความสูงของคลื่นและคาบคลื่น รวมถึงเทคโนโลยีที่จะนำมาผลิตพลังงานจากคลื่น โดยฝั่งอ่าวไทยมีความสูงของคลื่นไม่เกิน ๒ เมตร และฝั่งทะเลอันดามันมีความสูงของคลื่นไม่เกิน ๕ เมตร ซึ่งไม่เพียงพอแก่การนำมาใช้ประโยชน์ และจากสถานภาพของเทคโนโลยีในการนำพลังงานคลื่นมาผลิตเป็นไฟฟ้า ยังไม่มีเทคโนโลยีที่รองรับการผลิตพลังงานจากความสูงคลื่นเพียง ๒-๕ เมตร

สรุป

ด้านพลังงานแสงอาทิตย์ พบว่ามีการทำงานวิจัยด้านนี้มาเป็นเวลานาน แต่มีข้อจำกัดของการใช้งาน เนื่องจากมีประสิทธิภาพต่ำและความไม่แน่นอนความไม่สม่ำเสมอของพลังงานหมุนเวียนที่จะนำมาใช้ประโยชน์ได้ ดังนั้น ควรมีวิจัยด้านเพิ่มประสิทธิภาพ สมรรถนะการใช้งานได้อย่างสม่ำเสมอและหาแนวทางลดต้นทุนของระบบ/อุปกรณ์ที่ใช้พลังงานแสงอาทิตย์ ควรมีงานวิจัยทั้งทางด้านเทคนิคและเศรษฐศาสตร์ เพื่อขยายโอกาสที่จะพัฒนาอุปกรณ์และการประยุกต์ใช้ในงานใหม่ ๆ ต่าง ๆ ได้อย่างเหมาะสมให้ได้กว้างขวางมากยิ่งขึ้น

โดยเฉพาะเงื่อนไขที่เหมาะสมและความคุ้มค่าของการใช้เซลล์แสงอาทิตย์ นอกจากนี้ ควรมีงานวิจัยเชิงนโยบายและมาตรการต่าง ๆ ของประเทศที่ประสบความสำเร็จในการใช้พลังงานแสงอาทิตย์ เช่น มาตรการภาษีสิ่งแวดล้อมด้านต่าง ๆ โดยเฉพาะภาษีแก๊สคาร์บอน-ไดออกไซด์

ด้านไฟฟ้าพลังน้ำ พบว่า การสร้างเขื่อนขนาดใหญ่เป็นไปได้ยาก ควรเน้นพลังน้ำขนาดเล็ก นอกจากนี้ ควรมีงานวิจัยเชิงนโยบายในความร่วมมือกับประเทศเพื่อนบ้าน

ด้านพลังงานลม พบว่า ข้อมูลด้านความเร็วลมที่ระดับความสูงมากกว่า ๕๐ เมตรจากพื้นดินยังไม่มี ดังนั้น จึงควรสนับสนุนให้มีการศึกษาที่ระดับความสูงนี้ รวมถึงการศึกษาความเป็นไปได้ทางเทคนิคและเศรษฐศาสตร์ สำหรับการติดตั้งกังหันลมในพื้นที่ที่มีความเร็วลมสูง รวมทั้งหาแนวทางลดต้นทุนของระบบ/อุปกรณ์ นอกจากนี้ ควรมีงานวิจัยเชิงนโยบายด้านมาตรการจูงใจและส่งเสริมการผลิตและติดตั้งกังหันเพื่อการสูบน้ำและเพื่อการผลิตไฟฟ้า

พลังงานความร้อนใต้พิภพในประเทศไทยมีศักยภาพต่ำ ส่วนพลังงานจากมหาสมุทรไม่น่าจะมีศักยภาพ

กิตติกรรมประกาศ

ผู้เขียนใคร่ขอบคุณสำนักงานกองทุนสนับสนุนการวิจัยที่ให้การสนับสนุนทุนวิจัย

เอกสารอ้างอิง

๑. นิรนาม ๒๕๔๗ สถานภาพปัจจุบันและข้อเสนอสู่อนาคต ด้านเชื้อเพลิงและเทคโนโลยีเชื้อเพลิง หน้า ๔.

๒. เสริม จันทร์ฉาย และจรุงแสง ลักษณบุญส่ง. แผนที่ศักยภาพพลังงานแสงอาทิตย์จากข้อมูลดาวเทียมสำหรับประเทศไทย. กรมพัฒนาและส่งเสริมพลังงานร่วมกับภาควิชาฟิสิกส์ คณะวิทยาศาสตร์ มหาวิทยาลัยศิลปากร. หน้า ๘๒-๘๕.

๓. รายงานพลังงานทดแทนของประเทศไทย ๒๕๔๖. กรมพัฒนาพลังงานทดแทน และอนุรักษ์พลังงาน กระทรวงพลังงาน. กรุงเทพฯ.

๔. http://www.nepo.go.th/vrs/VRS44-07-Solar.html. 2001

๕. http://www.egat.or.th/rdo/energy/phuket.html, 2005.

๖. http://www.egat.co.th/information/powerplant/solarcell.htm, 2005.

๗. คณะทำงานพลังงานแสงอาทิตย์ในรูปความร้อน. ๒๕๔๐. รายงานการประชุมคณะทำงานพลังงานแสงอาทิตย์ในรูปความร้อน. คณะอนุกรรมการประสานงานการวิจัยและพัฒนาพลังงานทดแทน. สำนักงานคณะกรรมการวิจัยแห่งชาติ. หน้า ๒-๔.

๘. สุรสิทธิ์ ประสารปราน, ๒๕๓๐, ระบบทำน้ำร้อนด้วยแสงอาทิตย์ที่มีตัวรับรังสีแบบยีทไปป์-เธอร์มัลไคโอด, วิทยานิพนธ์ปริญญาวิทยาศาสตรมหาบัณฑิต สาขาวิชาเทคโนโลยีพลังงาน คณะพลังงานและวัสดุ สถาบันเทคโนโลยีพระจอมเกล้าธนบุรี

๙. สุคนธ์ อาจฤทธิ์, ๒๕๒๔, ตัวรับแสงอาทิตย์แผ่นราบแบบเพิ่มผิวโค้งสะท้อนแสง, วิทยานิพนธ์ปริญญาวิทยาศาสตรมหาบัณฑิต สาขาเทคโนโลยีพลังงาน คณะพลังงานและวัสดุ, สถาบันเทคโนโลยีพระจอมเกล้าธนบุรี, ๙๓ หน้า.

๑๐. ประวิทย์ ถีถะแก้ว, ๒๕๒๕, สมรรถภาพของระบบทำน้ำร้อนด้วยแสงอาทิตย์ที่ใช้ชุดรับรังสีแผ่นราบกระจก ๒ ชั้น, วิทยานิพนธ์ปริญญาวิทยาศาสตรมหาบัณฑิต สาขาเทคโนโลยีพลังงาน คณะพลังงานและวัสดุ, สถาบันเทคโนโลยีพระจอมเกล้าธนบุรี, ๑๐๔ หน้า.

๑๑. สมนึก บุญญศาสตร์พันธุ์, ๒๕๒๗, ระบบทำน้ำร้อนด้วยแสงอาทิตย์ที่อุณหภูมิสูงด้วยตัวรับรังสีแบบแผ่นเรียบ, วิทยานิพนธ์ปริญญาวิศวกรรมศาสตรมหาบัณฑิต สาขาเทคโนโลยีพลังงาน คณะพลังงานและวัสดุ, สถาบันเทคโนโลยีพระจอมเกล้าธนบุรี, ๗๔ หน้า.

๑๒. สุขฤดี สุขใจ, ๒๕๓๕, สมรรถนะของเครื่องอบแห้งกล้วยน้ำว้าด้วยแสงอาทิตย์แบบหมุนเวียนและแบบต่อเนื่อง, วิทยานิพนธ์ปริญญาวิศวกรรมศาสตรมหาบัณฑิต สาขาเทคโนโลยีพลังงาน คณะพลังงานและวัสดุ, สถาบันเทคโนโลยีพระจอมเกล้าธนบุรี, ๑๔๔ หน้า.

๑๓. วรวิทย์ รุ่งจิวารักษ์, ๒๕๓๘, การศึกษาระบบอบแห้งกล้วยน้ำว้าด้วยแสงอาทิตย์ขนาดอุตสาหกรรม, วิทยานิพนธ์ปริญญาวิศวกรรมศาสตรมหาบัณฑิต สาขาวิชาเทคโนโลยีพลังงาน คณะพลังงานและวัสดุ สถาบันเทคโนโลยีพระจอมเกล้าธนบุรี, ๑๔๔ หน้า.

๑๔. ฉัฐวุฒิ คุษฎี, ๒๕๓๔, การพัฒนาระบบอบแห้งผลไม้โดยใช้พลังงานแสงอาทิตย์เป็นพลังงานเสริม, วิทยานิพนธ์ปริญญาวิศวกรรมศาสตรมหาบัณฑิต สาขาวิชาเทคโนโลยีพลังงาน คณะพลังงานและวัสดุ สถาบันเทคโนโลยีพระจอมเกล้าธนบุรี, ๑๐๗ หน้า.

๑๕. พจนา วงษ์ศิริ, ๒๕๒๘, การอบแห้งผลิตภัณฑ์อาหารโดยใช้เครื่องอบแห้งแสงอาทิตย์แบบมีตัวรับรังสี, วิทยานิพนธ์ปริญญาวิศวกรรมศาสตรมหาบัณฑิต สาขาวิชาเทคโนโลยีพลังงาน คณะพลังงานและวัสดุ สถาบันเทคโนโลยีพระจอมเกล้าธนบุรี, ๗๙ หน้า.

๑๖. อานนท์ โพธิ์หอม, ๒๕๒๐, เครื่องกลั่นน้ำด้วยแสงอาทิตย์, โครงการปริญญาวิศวกรรมศาสตรมหาบัณฑิต ภาควิชาวิศวกรรมเครื่องกล คณะวิศวกรรมศาสตร์ สถาบันเทคโนโลยีพระจอมเกล้าธนบุรี, ๘๔ หน้า.

๑๗. ทนงเกียรติ เกียรติศิริโรจน์, ๒๕๒๓, การศึกษาเครื่องกลั่นน้ำแสงอาทิตย์แบบรีเจนเนเรทิฟ, วารสารวิจัยและพัฒนา สจธ., ฉบับที่ ๔, เล่มที่ ๒, หน้า ๑-๘.

๑๘. ศิริชัย เทพา, ๒๕๓๒, เครื่องกลั่นน้ำผิวตั้งฝาครอบอคริลิค, วารสารวิจัยและพัฒนา สจธ., ฉบับที่ ๑๒, เล่มที่ ๑, หน้า ๑๖-๓๔.

๑๙. อานนท์ โพธิ์หอม, ๒๕๒๑, เครื่องกลั่นน้ำด้วยแสงอาทิตย์แบบอยู่กับที่, Seminar on Solar Energy and Applications, Technological Promotion Association (Thai-Japan) and King Mongkut's Institute of Technology, Thailand, หน้า ๗.

๒๐. สมชาย โสภณศิริกุล. ๒๕๔๓. การปรับปรุงสมรรถนะของเครื่องกลั่นน้ำ. วิทยานิพนธ์ปริญญาวิทยาศาสตรมหาบัณฑิต สาขาวิชาเทคโนโลยีพลังงาน คณะพลังงานและวัสดุ สถาบันเทคโนโลยีพระจอมเกล้าธนบุรี. ๑๐๕ หน้า.

๒๑. มานะ คงคีจันทร์. ๒๕๓๔. การกลั่นเอธานอลจากวัตถุดิบการเกษตรโดยพลังงานแสงอาทิตย์. วิทยานิพนธ์ปริญญาวิศวกรรมศาสตรมหาบัณฑิต สาขาวิชาเทคโนโลยีพลังงาน คณะพลังงานและวัสดุ สถาบันเทคโนโลยีพระจอมเกล้าธนบุรี. ๑๑๐ หน้า.

๒๒. จีรศักดิ์ จิระวารี และวีระชัย แก่นทรัพย์. ๒๕๒๓. การกลั่นเอธิลแอลกอฮอล์ด้วยตัวรับรังสีแผ่นราบ. โครงงานปริญญาวิศวกรรมศาสตรบัณฑิต ภาควิชาวิศวกรรมเครื่องกล คณะวิศวกรรมศาสตร์ สถาบันเทคโนโลยีพระจอมเกล้าธนบุรี. ๘๔ หน้า.

๒๓. ณัฐ วรยศ. ๒๕๔๔. การศึกษาความเป็นไปได้ในการกลั่นเอทธานอลด้วยพลังงานแสงอาทิตย์. เอกสารประกอบการสัมมนาเรื่องศักยภาพของประเทศไทยในการผลิตเอทธานอลเพื่อทดแทนการนำเข้า, กลุ่มงานเกษตรและอุตสาหกรรมเกษตร กองโครงการและประสานงานวิจัย สำนักงานคณะกรรมการวิจัยแห่งชาติ. หน้า E-1-E-6.

๒๔. ทวีศักดิ์ ศรีภูสิตโต และคณะ. ๒๕๓๑. Solar Adsorption Refrigeration. โครงงานปริญญาวิศวกรรมศาสตรบัณฑิต ภาควิชาวิศวกรรมเครื่องกล คณะวิศวกรรมศาสตร์ สถาบันเทคโนโลยีพระจอมเกล้าธนบุรี. ๗๕ หน้า.

๒๕. พิทยา กิ่งชม และคณะ. ๒๕๓๒. การศึกษาเครื่องทำความชื้นแบบดูดเกาะ. โครงงานปริญญาวิศากรรมศาสตรมหาบัณฑิต สาขาวิชาวิศวกรรมเครื่องกล คณะวิศวกรรมศาสตร์ สถาบันเทคโนโลยีพระจอมเกล้าธนบุรี. ๖๖ หน้า.

๒๖. ทนงเกียรติ เกียรติศิริโรจน์. ๒๕๓๕. การศึกษาสมรรถนะของระบบทำความเย็นแสงอาทิตย์ที่ใช้ถ่านกัมมันต์-เมธานอลเป็นสารคู่ทำงาน. วิศวกรรมสารฉบับวิจัยและพัฒนา. ฉบับที่ ๓, เล่มที่ ๑. หน้า ๖๑-๖๕.

๒๗. Boonbumroong, U., et al., Suwannakum, T., Pongchawee, D., Pengma, S., Kitikara, K., and Sripadungtum, P., 2004. Parametric Study of a PV/Wind/Diesel Hybrid System for Kohjik Island. 14th International Photovoltaic Science and Engineering Conference, 26-30 January, Chulalongkorn University, Bangkok, pp.841, 842.

๒๘. Somsak, T., Boonbumroong, U., Tanchareon, S., Jeenkaokam, N., and Jivacate, C., 2004. PV-Diesel Stand Alone Hybrid System at Royal Project Research Station : Observations on Power Quality. 14th International Photovoltaic Science and Engineering Conference, 26-30 January, Chulalongkorn University, Bangkok, pp.843, 846.

๒๙. Thianphu, A., 2004. Management of PV Water Pumping system. 14th International Photovoltaic Science and Engineering Conference, 26-30 January, Chulalongkorn University, Bangkok, pp.889, 890.

๓๐. Sangpanich, U., Thongpron, J., Kitikara, K., and Jivacate, C., 2004. Power Quality of Four Rooftop Grid-Connected Photovoltaic System in Thailand. 14th International Photovoltaic Science and Engineering Conference, 26-30 January, Chulalongkorn University, Bangkok, pp.139, 140.

๓๑. Buranasajja, S. and Seingsanor, S., 2004. Photovoltaic Battery Charging System in Thailand : a Case Study of Ban Bon Khao Kangriang. 14th International Photovoltaic Science and Engineering Conference, 26-30 January, Chulalongkorn University, Bangkok, pp.945, 946.

๓๒. คณะอนุกรรมการส่งเสริมการใช้พลังงานหมุนเวียน. ๒๕๔๔. เอกสารประกอบการประชุม เรื่องแผนพัฒนาพลังงานหมุนเวียนในช่วงปี ๒๕๔๕-๒๕๔๙. สำนักงานคณะกรรมการนโยบายแห่งชาติ.

๓๓. รายงานไฟฟ้าของประเทศไทย ๒๕๔๖. กรมพัฒนาพลังงานทดแทนและอนุรักษ์พลังงาน กระทรวงพลังงาน. กรุงเทพฯ.

๓๔. รายงานการใช้พลังงานของประเทศไทย ๒๕๔๖. กรมพัฒนาพลังงานทดแทน และอนุรักษ์พลังงาน กระทรวงพลังงาน. กรุงเทพฯ.

๓๕. แผนปฏิบัติการเทคโนโลยีไฟฟ้าพลังน้ำขนาดเล็ก ๕ ปี (๒๕๔๕-๒๕๔๙) กรมพัฒนาพลังงานทดแทนและอนุรักษ์พลังงาน.

๓๖. ทวีป ชัยสมภพ และจักรี คุปต์อัครภิญโญ. ๒๕๔๖. "การประเมินเชิงเทคโนโลยีของโครงการพัฒนาพลังน้ำขนาดเล็กในประเทศที่กำลังพัฒนาและในประเทศที่พัฒนาแล้ว", การสัมมนาเผยแพร่ผลงานวิจัยด้านพลังงานทดแทน, วันที่ ๒๕ กันยายน ๒๕๔๖. โรงแรมราชาการ์เดนส์. หน้า ๑๓๘-๑๔๗.

๓๗. ธนะ บุญญสิริกุล. ๒๕๔๔. "การออกแบบนโยบายจัดสรรน้ำเพื่อประโยชน์สูงสุดในการจัดการอ่างเก็บน้ำ", การประชุมสัมมนาวิชาการและนิทรรศการด้านพลังน้ำ, ครั้งที่ ๑, วันที่ ๖-๗ กุมภาพันธ์ ๒๕๔๔. การไฟฟ้าฝ่ายผลิตแห่งประเทศไทย. หน้า ๓-๑๓, ๓-๑๕.

๓๘. กรมพัฒนาส่งเสริมพลังงาน. ๒๕๔๔. เอกสารโครงการจัดทำแผนที่ศักยภาพพลังงานลมในประเทศ.

๓๙. คณะทำงานพลังงานลม. ๒๕๔๑. นโยบายแผนและแนวทางการวิจัยและพัฒนาพลังงานทดแทน : พลังงานลม. คณะอนุกรรมการประสานงานการวิจัยและพัฒนาพลังงานทดแทน, สำนักงานคณะกรรมการวิจัยแห่งชาติ. ๑๕ หน้า.

๔๐. องอาจ คงฤทธิ์ และคณะ. ๒๕๒๕. การนำอุโมงค์มาทดสอบกังหันลม ๔ ใบ. โครงงานปริญญาวิศวกรรมศาสตรบัณฑิต ภาควิชาวิศวกรรมเครื่องกล คณะวิศวกรรมศาสตร์ สถาบันเทคโนโลยีพระจอมเกล้าธนบุรี. ๔๒ หน้า.

๔๑. ประจัญ เพชรไวฑูรย์. ๒๕๓๐. การศึกษาความเค้นในใบของกังหันลมแกนหมุนแนวดิ่ง. วิทยานิพนธ์ปริญญาวิศวกรรมศาสตรมหาบัณฑิต สาขาวิชาเทคโนโลยีพลังงาน คณะพลังงานและวัสดุ สถาบันเทคโนโลยีพระจอมเกล้าธนบุรี. ๑๓๖ หน้า.

๔๒. สมชาย ชูชีพกุล. ๒๕๓๓. แบบจำลองไฟไนท์เอเลเมนท์ของใบพัดกังหันลมแบบดาร์เรียส. "วารสารวิจัยและพัฒนา สจธ.," ฉบับที่ ๑๓, เล่มที่ ๒. หน้า ๑-๑๖.

๔๓. สุกฤษณ์ โรจนวิไลกุล สุทธิชัย ศิริพรอดุลศิลป์ และอดิภพ จันทร์ศุภมงคล. ๒๕๔๒. การศึกษา Laminar Separation Brbble บนใบพัดของกังหันลม. โครงงานปริญญาวิศวกรรมศาสตรมหาบัณฑิต ภาควิชาวิศวกรรมเครื่องกล คณะวิศวกรรมศาสตร์ มหาวิทยาลัยเทคโนโลยีพระจอมเกล้าธนบุรี. ๑๕๑ หน้า.

๔๔. เกรียงศักดิ์ ขุนไชย. ๒๕๒๗. ระบบผลิตไฟฟ้าจากกังหันลมแบบไซโร-โรเตอร์ (ระยะ ๒). วิทยานิพนธ์ปริญญาวิทยาศาสตรมหาบัณฑิต สาขาวิชาเทคโนโลยีพลังงาน คณะพลังงานและวัสดุ สถาบัน

เทคโนโลยี พระจอมเกล้าธนบุรี, ๑๕๒ หน้า.
๔๕. มนชัย เหลืองวัฒนวิโล และคณะ, ๒๕๓๔, กังหันลมผลิตกระแสไฟฟ้าแบบดาร์เรียส, โครงงานปริญญาวิศวกรรมศาสตรบัณฑิต ภาควิชาวิศวกรรมเครื่องกล คณะวิศวกรรมศาสตร์ สถาบันเทคโนโลยีพระจอมเกล้าธนบุรี, ๕๔ หน้า.
๔๖. อนุวัตน์ จางวนิชเลิศ และประภาษ ไพรสุวรรณ, ๒๕๓๘, การพัฒนาเครื่องกำเนิดกระแสไฟฟ้าด้วยพลังงานลม, พลังงานลม เครื่องกำเนิดกระแสไฟฟ้า ไฟฟ้ารถยนต์ Electric generators, การประชุมวิชาการทางวิศวกรรมไฟฟ้า ครั้งที่ ๒๐ เล่ม ๓, หน้า ๓๘๖-๓๖๑.
๔๗. อนุวัตน์ จางวนิชเลิศ และประภาษ ไพรสุวรรณ, ๒๕๔๑, "ระบบผลิตและสำรองกระแสไฟฟ้าด้วยพลังงานลม", วิศวสาร
ลาดกระบัง, ปีที่ ๑๔, ฉบับที่ ๑, หน้า ๑-๘.
๔๘. กองพัฒนาพลังงานทดแทน, สำนักงานวิจัยและพัฒนา การไฟฟ้าฝ่ายผลิต, ๒๕๔๒, การผลิตไฟฟ้าจากกังหันลม, "วารสารประสิทธิภาพพลังงาน," ฉบับที่ ๔๖, หน้า ๓๓, ๓๔.
๔๙. กองพัฒนาพลังงานทดแทน, ๒๕๔๒, "พลังงานความร้อนใต้พิภพ", พลังงานความร้อนใต้พิภพ, การไฟฟ้าฝ่ายผลิตแห่งประเทศไทย.
๕๐. http://www.dmr.go.th/HOTSPING/THAIHOTSP.htm, 2002.
๕๑. http://www.egat.or.th/rdo/energy/gerothermal_plant.htm, 2002.
๕๒. นานพ รักษาสกุลวงศ์และศิริพร สูงปานเขา, ๒๕๔๕, "พลังงานความร้อนใต้พิภพ", ข่าวสารการธรณี, ปีที่ ๔๗, ฉบับที่ ๒, หน้า ๔๑-๔๕.
๕๓. http://www.nrel.gov/clean_energy/ocean.html, 2005
๕๔. สุรชัย ประเสริฐวิกัย, ๒๕๔๐, "พลังงานความร้อนจากมหาสมุทร...สำคัญที่ผลพลอยได้", วารสารการไฟฟ้าฝ่ายผลิต, ปีที่ ๖, เล่มที่ ๓, หน้า ๓๘-๔๔.
๕๕. คณะวิศวกรรมศาสตร์ มหาวิทยาลัยเชียงใหม่, ๒๕๔๑, รายงานฉบับสมบูรณ์ โครงการศึกษาเบื้องต้น ศักยภาพและความเหมาะสมในการพัฒนาพลังงานจากทะเล, กรมพัฒนาพลังงานทดแทนและอนุรักษ์พลังงาน, ๖๒ หน้า.
๕๖. มนูวศี ทังสพฤกษ์, ๒๕๔๓, "สมุทรศาสตร์กายภาพของอ่าวไทย", วารสารราชบัณฑิตยสถาน, ปีที่ ๒๕, หน้า ๑๖๘-๑๗๕.
๕๗. ประวิทย์ ธีระแก้ว, ๒๕๒๓, "พลังงานน้ำขึ้นน้ำลง", พลังงาน, หน้า ๒๕๓-๒๖๑.

Abstract

Status and Research Trends on Renewable Energy in Thailand

Warunee Tia
Pimporn Jangploy
Kangsadan Sakunpongmalee
Somchart Soponronnarit
Fellow of the Academy of Science, The Royal Institute, Thailand

The development and expansion of the utilization on renewable energy are the sustainable way of energy development of oil imported country as Thailand. Thus this paper presents the potential, status and research trends on renewable energy in Thailand, namely solar, wind, small-hydro, geothermal, and ocean energy, except biomass which had already been reported in the our previous publication. The main limitations of using renewable energy were unreliable of resource and inefficient conversion. These appeared to be perceived poor economics of renewable energy compared to commercial energy. The research on system-efficiency and reliability improvement, cost reduction, and policy research such as pricing structure of fuel with environmental taxes should be conducted.

Key words : research trend, solar energy, wind energy, small-hydro power, geothermal energy, ocean energy, Thailand

The Journal of the Royal Institute of Thailand
Vol. 30 No. 4 Oct.-Dec. 2005

อิทธิพลของชนิดตัวกลางในการอบแห้งที่มีต่อจลนพลศาสตร์ของการลดความชื้นและคุณภาพของเนื้อวัว

ชัยยงค์ เตชะไพโรจน์[๑]
ศิริวัฒ สินประเสริฐ[๒]
สมเกียรติ ปรัชญาวรากร[๓]
สมชาติ โสภณรณฤทธิ์[๔]
ราชบัณฑิต สำนักวิทยาศาสตร์
ราชบัณฑิตยสถาน

บทคัดย่อ

วิธีการอบแห้งมีผลกระทบอย่างมากต่อจลนพลศาสตร์ของการอบแห้งและคุณภาพของอาหาร เพื่อให้ได้คุณภาพเนื้อลบแห้งตามที่ต้องการสำหรับเป็นของกินเล่น จึงได้มีการศึกษาการอบแห้งขั้นตอนเดียวด้วยไอน้ำร้อนยวดยิ่งและอากาศร้อน และการอบแห้ง ๒ ขั้นตอน เพื่อศึกษาผลของวิธีการอบแห้งดังกล่าวที่มีต่อจลนพลศาสตร์ของการอบแห้งและคุณภาพของเนื้อวัวแผ่นที่มีการทั่นชิ้นตัวอย่างแบบตัดขวางและตัดตามเส้นใยกล้ามเนื้อ เงื่อนไขการทดลองมีดังนี้ อบแห้งเนื้อวัวที่มีความชื้นเริ่มต้น ๒๔๕-๒๕๕% dry basis (d.b.) จนกระทั่งความชื้นสุดท้ายเท่ากับ ๑๑% d.b. อุณหภูมิของไอน้ำร้อนยวดยิ่งและอากาศร้อนที่ใช้อยู่ในช่วง ๑๓๐-๑๕๐ องศาเซลเซียส จากการทดลองพบว่า การอบแห้งที่อุณหภูมิสูง สามารถลดความชื้นได้เร็วกว่าการอบแห้งที่อุณหภูมิต่ำ ขณะที่คุณภาพของสีโดยวัดการเปลี่ยนแปลงสีของตัวแปร L, a และ b การหดตัว การคืนตัว และความแข็ง มีค่าไม่แตกต่างกันอย่างมีนัยสำคัญ ($p > 0.05$) เมื่อพิจารณาชนิดของตัวกลางในการอบแห้ง พบว่าสัมประสิทธิ์การแพร่ของเนื้อวัวที่อบแห้งด้วยไอน้ำร้อนยวดยิ่งจะมีค่าสูงกว่ากรณีอบแห้งด้วยอากาศร้อน และสีของเนื้อวัวหลังการอบแห้งด้วยไอน้ำร้อนยวดยิ่งมีความสม่ำเสมอกว่า การหดตัวมากกว่า ส่วนการคืนตัวและความแข็งไม่แตกต่างกันอย่างมีนัยสำคัญ ($p > 0.05$) เมื่อพิจารณาการเรียงของเส้นใยกล้ามเนื้อ พบว่าไม่มีผลต่ออัตราการแพร่ของน้ำไม่ว่าจะอบแห้งด้วยไอน้ำร้อนยวดยิ่งหรืออากาศร้อน และเมื่อเปรียบเทียบคุณภาพด้านต่าง ๆ พบว่าการเรียงของเส้นใยกล้ามเนื้อให้คุณภาพด้านสีแตกต่างกันเล็กน้อย เนื้อวัวแบบตัดขวางเส้นใยมีความแข็งมากกว่าและหดตัวน้อยกว่าแบบตัดตามเส้นใยอยู่เล็กน้อย เมื่อเทียบกับการอบแห้งแบบขั้นตอนเดียว คุณภาพของเนื้อวัวที่ผ่านการอบแห้งแบบ ๒ ขั้นตอนให้คุณภาพสีของเนื้อวัวหลังการอบแห้งมีสีน้ำตาลอ่อนกว่า การคืนตัวสูงขึ้น และความแข็งลดลง

คำสำคัญ : ความแข็ง, คุณภาพ, การหดตัว, ไอน้ำร้อนยวดยิ่ง, เส้นใยกล้ามเนื้อ, เนื้อวัวแบบตัดขวางเส้นใย

[๑] อาจารย์คณะวิศวกรรมศาสตร์และเทคโนโลยีอุตสาหกรรม มหาวิทยาลัยศิลปากร สนามจันทร์ นครปฐม
[๒] นิสิตปริญญาโท คณะพลังงานและวัสดุ มหาวิทยาลัยเทคโนโลยีพระจอมเกล้าธนบุรี กรุงเทพฯ
[๓] รองศาสตราจารย์ คณะวิศวกรรมศาสตร์ มหาวิทยาลัยเทคโนโลยีพระจอมเกล้าธนบุรี กรุงเทพฯ
[๔] ศาสตราจารย์ คณะพลังงานและวัสดุ มหาวิทยาลัยเทคโนโลยีพระจอมเกล้าธนบุรี กรุงเทพฯ

๑. บทนำ

การถนอมอาหารโดยวิธีการทำให้แห้งเป็นวิธีที่นิยมกันอย่างแพร่หลาย เนื่องจากวิธีดังกล่าวสามารถรักษาคุณภาพอาหารได้เป็นเวลานาน การอบแห้งมีหลายวิธี แต่ละวิธีมีข้อดีและข้อเสียแตกต่างกัน เช่น วิธีการอบแห้งโดยวิธีตากแห้งเป็นวิธีที่ง่ายและประหยัดพลังงาน แต่ใช้เวลาในการอบแห้งนาน การควบคุมคุณภาพของผลิตภัณฑ์ทำได้ยากเนื่องจากขึ้นอยู่กับสภาวะแวดล้อมทางธรรมชาติ สำหรับการอบแห้งโดยการเป่าอากาศผ่านวัสดุชื้น ซึ่งในกรณีนี้พื้นที่ในการอบแห้งอยู่ในขอบเขตจำกัด การควบคุมคุณภาพผลิตภัณฑ์สามารถทำได้ง่ายและให้คุณภาพในด้านความสะอาดมากกว่า

เนื้อวัวเป็นเนื้อสัตว์ชนิดหนึ่งที่นิยมนำมาบริโภคกันอย่างกว้างขวางและเป็นแหล่งอาหารที่มีปริมาณโปรตีนสูง การแปรรูปเนื้อสัตว์เพื่อให้สามารถเก็บรักษาคุณค่าทางอาหารไว้ได้นานและการเพิ่มมูลค่าของผลิตภัณฑ์มีได้หลายวิธี เช่น การตากแห้งโดยใช้แสงแดดซึ่งต้องใช้ระยะเวลาค่อนข้างมาก เนื่องจากการระเหยของน้ำจากเนื้อเยื่อของสัตว์ทำได้ยากกว่าระเหยน้ำจากเซลล์พืช และยังมีปัญหาคุณภาพของผลิตภัณฑ์เนื่องจากฝุ่นและแมลง การแปรรูปอาหารจึงมักจะใช้เครื่องอบแห้งด้วยอากาศร้อน ซึ่งสามารถทำให้ระยะเวลาในการอบแห้งลดลง แต่เมื่อใช้อุณหภูมิของอากาศร้อนสูงเกินไป จะทำให้คุณภาพและคุณค่าทางอาหารของเนื้อสัตว์สูญเสียไป เช่น สีของเนื้อสัตว์อาจเปลี่ยนแปลงจนไม่น่ารับประทาน การอบแห้งด้วยไอน้ำร้อนยวดยิ่งจึงเป็นทางเลือกอีกทางหนึ่ง ซึ่งสามารถจะอบแห้งได้อย่างรวดเร็ว ข้อดีของการใช้ไอน้ำร้อนยวดยิ่งในการอบแห้งคือ ลดปฏิกิริยาการเกิดออกซิเดชัน เป็นผลทำให้ผลิตภัณฑ์ที่ได้มีสีดีขึ้น อัตราการอบแห้งสูง รวมถึงเป็นกระบวนการทำให้ผลิตภัณฑ์อาหารปลอดเชื้อจากจุลินทรีย์ต่าง ๆ ที่ทำให้เกิดโรคอาหารเป็นพิษได้ อย่างไรก็ตาม การอบแห้งโดยไอน้ำร้อนยวดยิ่งก็ยังมีข้อจำกัดบางประการเนื่องจากต้องใช้อุณหภูมิในการอบแห้งที่สูงจึงมีผลทำให้ผลิตภัณฑ์ที่ไม่ทนต่อความร้อนเกิดการเสียหายได้[๑]

ในช่วงระยะทศวรรษที่ผ่านมาได้มีการศึกษาเปรียบเทียบการอบแห้งด้วยอากาศร้อนและไอน้ำร้อนยวดยิ่งกันอย่างมากมาย ซึ่งจากการศึกษาทางด้านจลนพลศาสตร์ของการอบแห้งให้ผลที่ได้คล้ายคลึงกัน[๒, ๓, ๔] ในด้านคุณภาพของผลิตภัณฑ์ต่าง ๆ ที่ได้จากตัวกลางของการอบแห้งทั้งสอง โดยเฉพาะผลิตภัณฑ์อาหารที่มีสตาร์ชเป็นองค์ประกอบ เช่น มันฝรั่ง การอบแห้งด้วยไอน้ำร้อนยวดยิ่งทำให้ผลิตภัณฑ์มีการหดตัว ความหนาแน่นสูงกว่าการอบแห้งด้วยลมร้อน แต่ให้ความเป็นรูพรุนลดต่ำลง หรือกล่าวอีกนัยคือ เนื้อผิวของผลิตภัณฑ์มีความเรียบสม่ำเสมอกว่าการอบด้วยลมร้อน ซึ่งเป็นผลอันเนื่องจากการเกิดเจลาทิไนซ์ของสตาร์ช[๒, ๔, ๖] ในการอบแห้งข้าวเปลือก พบว่า ปริมาณต้นข้าวเพิ่มขึ้นเมื่อใช้ไอน้ำร้อนยวดยิ่ง สาเหตุจากกระบวนการเจลาทิไนเซชันในเมล็ดข้าวทำให้ข้าวเกิดความแข็งเพิ่มขึ้น ทนต่อการขัดสี จึงทำให้ปริมาณต้นข้าวสูงกว่าการอบด้วยลมร้อน[๗] ส่วนในผลิตภัณฑ์เนื้อสัตว์ ทำให้คุณภาพการหดตัวน้อยลงและมีสีของผลิตภัณฑ์ดีขึ้น[๘] เมื่อใช้การอบแห้งด้วยไอน้ำแทนลมร้อน

งานวิจัยนี้เป็นการศึกษาผลของการใช้ตัวกลางในการอบแห้งที่ต่างชนิดกัน ได้แก่ไอน้ำร้อนยวดยิ่งและอากาศร้อน อีกทั้งศึกษาผลของลักษณะการหั่นเนื้อวัวที่มีต่อจลนพลศาสตร์ของการอบแห้ง และคุณภาพของเนื้อวัวหลังการอบแห้ง โดยคุณภาพของเนื้อวัวหลังการอบแห้งที่พิจารณาสำหรับงานวิจัยนี้ ได้แก่ สี การหดตัว การคืนตัว และความแข็ง

๒. อุปกรณ์และวิธีการทดลอง

๒.๑ การเตรียมวัสดุ

นำเนื้อสันนอก (sirloin) ของเนื้อวัวมาหั่นเป็นแผ่นที่มีขนาด ๓ × ๓ ตารางเซนติเมตร และหนา ๐.๓ เซนติเมตร ลักษณะการหั่นเนื้อวัวเป็นแบบตัดขวาง (transverse section) และตัดตามเส้นใยกล้ามเนื้อ (longitudinal section) จากนั้นนำชิ้นตัวอย่างไปคลุกเกลือในอัตราส่วนร้อยละ ๒ โดยมวล ต่อมานำไปแช่เย็นที่อุณหภูมิ ๔ องศาเซลเซียส และนำตัวอย่างออกมาคลุกใหม่ทุก ๆ ๕ นาที เพื่อให้เกลือแทรกซึมเข้าไปในเนื้อวัวอย่างสม่ำเสมอ จนครบ ๒๐ นาที หลังจากคลุกเกลือ เนื้อ

วัวมีค่าความชื้นเริ่มต้นอยู่ในช่วงระหว่าง ๒๔๕-๒๕๕% d.b. ความชื้นของตัวอย่างหาได้โดยการอบในตู้อบลมร้อนที่อุณหภูมิ ๑๐๓ องศาเซลเซียส เป็นระยะเวลา ๗๒ ชั่วโมง

๒.๒ เครื่องอบแห้ง

เครื่องอบแห้งที่ใช้ในการทดลองศึกษาในงานวิจัยนี้เป็นเครื่องอบแห้งแบบถาดโดยใช้ไอน้ำร้อนยวดยิ่งเป็นตัวกลางแสดงดังรูปที่ ๑ ประกอบด้วยห้องอบแห้งขนาด ๓๐×๓๐×๑๐ ลูกบาศก์เซนติเมตร อุปกรณ์ให้ความร้อนขนาด ๑๓.๕ กิโลวัตต์ โดยมีเครื่องควบคุมอุณหภูมิแบบ PID มีความถูกต้อง ± ๑ องศาเซลเซียส พัดลมเป็นแบบเหวี่ยงใบพัดโค้งหลัง มีมอเตอร์ขนาด ๒.๒ กิโลวัตต์ สามารถปรับความเร็วรอบของพัดลมได้ เครื่องกำเนิดไอน้ำออกแบบความดันใช้งานสูงสุด ๓.๕ บาร์ สามารถผลิตไอน้ำได้ ๓๑ กิโลกรัมต่อชั่วโมง

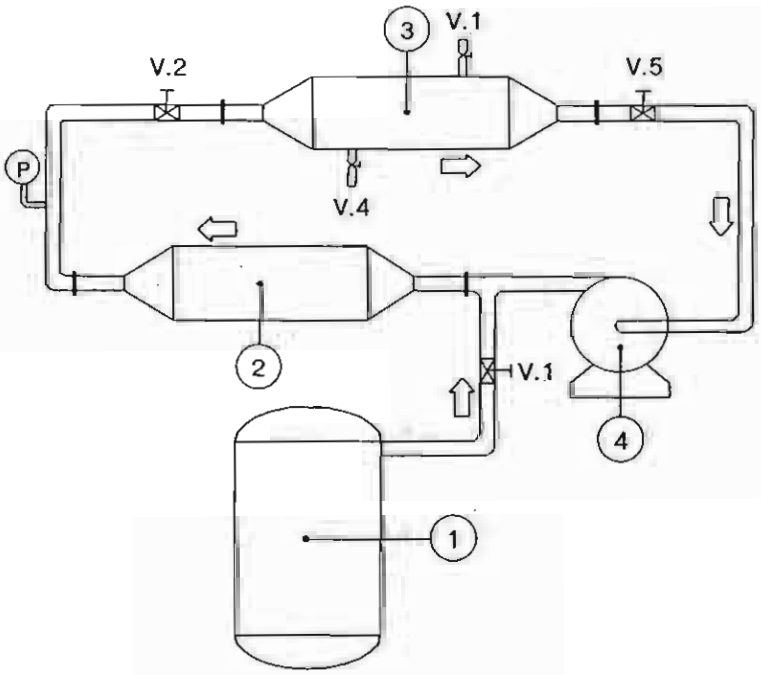
๒.๓ วิธีการอบแห้งเนื้อวัว

นำเนื้อวัวที่เตรียมไว้มาปรับอุณหภูมิให้สูงขึ้นเท่ากับอุณหภูมิห้องก่อนจะนำไปทดลองอบแห้ง ในการอบแห้งได้ใช้อุณหภูมิไอน้ำร้อนยวดยิ่งที่ ๑๓๐, ๑๔๐ และ ๑๕๐ องศาเซลเซียส และความเร็วของไอน้ำร้อนยวดยิ่งเท่ากับ ๒ เมตรต่อวินาที ความดันของระบบเหนือบรรยากาศเล็กน้อย ในการอบแห้งจะนำตัวอย่างออกมาชั่งน้ำหนักด้วยเครื่องชั่ง Sartorius CP-3202 ซึ่งมีค่าความถูกต้องของการอ่าน ± ๐.๐๑ กรัม ทุก ๆ ๕ นาที อบแห้งจนกระทั่งเหลือความชื้นสุดท้ายประมาณ ๑๑% d.b. และเปรียบเทียบกับการอบแห้งด้วยอากาศร้อนที่ภาวะเดียวกัน จากนั้นนำเนื้อวัวที่ผ่านการอบแห้งมาปล่อยให้เย็นตัวลง แล้วจึงนำไปทดสอบคุณภาพต่อไป

สำหรับการอบแห้ง ๒ ขั้นตอน เริ่มจากนำเนื้อวัวที่เตรียมไว้นำมาอบแห้งด้วยไอน้ำร้อนยวดยิ่งจนกระทั่งความชื้นลดลงเหลือประมาณ ๔๓% d.b. จากนั้นนำมาอบแห้งต่อด้วยอากาศร้อนที่อุณหภูมิ ๖๐ ที่ความเร็วลม ๐.๓ เมตรต่อวินาที จนกระทั่งความชื้นสุดท้ายประมาณ ๑๑% d.b แล้วจึงนำเนื้อวัวที่อบแห้งไปทดสอบคุณภาพต่าง ๆ ต่อไป

๒.๔ การทดสอบคุณภาพด้านสีของผลิตภัณฑ์

สีของเนื้อวัวอบแห้งวัดด้วยเครื่องวัดสีอาหาร MINOLTA รุ่น CR-400 โดยมีค่าความคลาดเคลื่อนในการวัดซ้ำ (repeat quality) ของเครื่องวัดสีอยู่ที่ ΔE ๐.๐๗ สีของเนื้อวัววัดจากตัวแปร L, a และ b ซึ่งเป็นระบบ Hunter Lab Color Scale โดยค่า L (lightness parameter) แสดงค่าความสว่าง ส่วนค่า a (redness parameter) แสดงค่าสีแดง (+) และสีเขียว (-) และค่า b (yellowness parameter) แสดงค่าสีเหลือง (+) และสีน้ำเงิน (-) ในการทดสอบจะสุ่มตัวอย่าง ๙ ชิ้น โดย



รูปที่ ๑ ระบบเครื่องอบแห้งแบบไอน้ำร้อนยวดยิ่งและอากาศร้อน (๑) เครื่องกำเนิดไอน้ำ (๒) อุปกรณ์ให้ความร้อน (๓) ห้องอบแห้ง (๔) พัดลม, V = วาล์ว, P = เกจวัดความดัน

ในแต่ละตัวอย่างจะทำการวัดซ้ำ ๓ ครั้ง

๒.๕ การทดสอบคุณภาพด้านการหดตัวของผลิตภัณฑ์

การหดตัวของเนื้อวัวหลังการอบแห้งสามารถทราบได้โดยการแทนที่ปริมาตรของเนื้อวัวในของเหลว n-heptane [$CH_3(CH_2)_5CH_3$] การหดตัวคำนวณจากสมการ(๑)[๑๐]

$$\% \text{ Shrinkage} = \frac{V_o - V}{V_o} \times ๑๐๐ \qquad (๑)$$

โดยที่ V_o, V คือ ปริมาตรของเนื้อวัวก่อนและหลังการอบแห้งตามลำดับ (m^3)

๒.๖ การทดสอบคุณภาพด้านการคืนตัวของผลิตภัณฑ์

ค่าการคืนตัวของเนื้อวัวหลังการอบแห้งเป็นตัวแปรที่สำคัญตัวแปรหนึ่งที่บ่งบอกถึงคุณภาพของผลิตภัณฑ์หลังการอบแห้ง ถ้าค่าการคืนตัวของผลิตภัณฑ์มีค่าสูง แสดงว่าคุณภาพของชิ้นตัวอย่างมีความเสียหายเนื่องจากกระบวนการอบแห้งน้อย ในงานวิจัยนี้การคืนตัวของเนื้อวัวอบแห้งสามารถทราบได้โดยการนำเนื้อวัวหลังการอบแห้งไปแช่ในน้ำร้อนที่อุณหภูมิ ๙๐ ± ๑ องศาเซลเซียส เป็นระยะเวลา ๑๕ นาที จากนั้นนำมาคำนวณหาการคืนตัวของเนื้อวัวได้ดังสมการที่ (๒)[๑๐]

$$\% \text{ rehydration} = \frac{W_t - W_d}{W_d} \times ๑๐๐ \qquad (๒)$$

โดยที่ W_d ,W_t คือ น้ำหนักของเนื้อวัวที่ทำการคืนตัวก่อนและหลังแช่น้ำอุ่น ตามลำดับ, kg

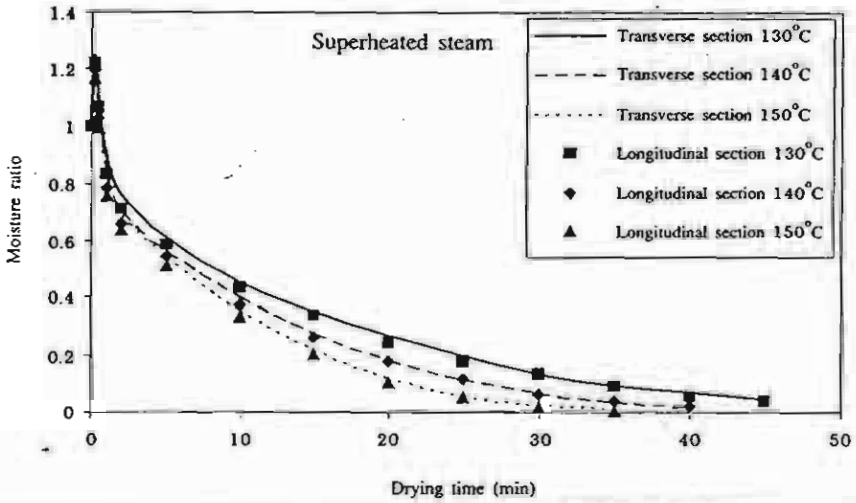
๒.๗ การทดสอบคุณภาพด้านเนื้อสัมผัสของผลิตภัณฑ์

คุณภาพทางเนื้อสัมผัสของเนื้อวัวหลังการอบแห้งสามารถทดสอบด้วยเครื่อง Texture Analyser รุ่น TA-XT ๒ โดยการนำชิ้นตัวอย่างมาทำการทดสอบในลักษณะของแรงกดหัวกดที่ใช้ทดสอบมีขนาดเส้นผ่านศูนย์กลาง ๒ มิลลิเมตร และความเร็วในการกด ๑ มิลลิเมตรต่อวินาที โดยกดจนกระทั่งเนื้อวัวแตกออกจากกันแล้วจึงอ่านค่าสูงสุดซึ่งเป็นค่าความแข็งของเนื้อวัว ในการทดสอบจะสุ่มตัวอย่างในการกดตัวอย่างจำนวน ๙ ชิ้น

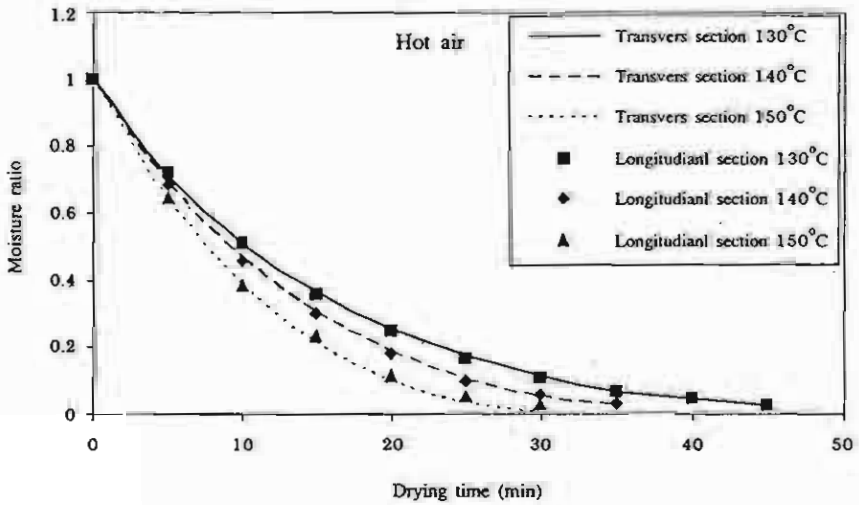
๓. ผลการทดลองและวิจารณ์

๓.๑ ผลของอุณหภูมิตัวกลางต่ออัตราการลดความชื้น

ผลการทดลองการอบแห้งเนื้อวัวด้วยไอน้ำร้อนยวดยิ่งที่อุณหภูมิ ๑๓๐, ๑๔๐ และ ๑๕๐ องศาเซลเซียส มีแสดงในรูปที่ ๒ ซึ่งแสดงความชื้นของเนื้อวัวในรูปของความชื้นไร้หน่วย จากกราฟพบว่าในช่วงแรกของการอบแห้งเนื้อวัวด้วยไอน้ำร้อนยวดยิ่งจะเกิดการควบแน่นของไอน้ำที่บริเวณผิวของเนื้อวัว ซึ่งสามารถสังเกตได้จากช่วงที่ความชื้นของตัวอย่างเพิ่มขึ้น การเพิ่มขึ้นของความชื้นในผลิตภัณฑ์ในทางปฏิบัติไม่เป็นที่ต้องการในกระบวนการอบแห้ง เพราะว่าจะเป็นการเพิ่มระยะเวลาในการอบแห้งให้นานขึ้น สิ้นเปลืองพลังงานเพิ่มขึ้น อย่างไรก็ตาม การควบแน่นของไอน้ำมิใช่จะส่งผลในเชิงลบเพียงอย่างเดียว จากรายงานการวิจัยต่าง ๆ พบว่าปรากฏการณ์ควบแน่นของไอน้ำในช่วงต้นของการอบแห้งกลับมีผลดีต่อผลิตภัณฑ์บางประเภท เช่น ข้าว นั่นคือข้าวที่ผ่านการกระบวนการอบแห้งด้วยวิธีนี้ให้ปริมาณข้าวต้นที่สูงกว่าการอบแห้งด้วยลมร้อนซึ่งเกิดจากเจลาทิไนเซชัน[๑๑,๑๒,๑๓]



รูปที่ ๒ เปรียบเทียบผลของการหั่นเนื้อวัวแบบตัดขวางเส้นใยกับตัดตามเส้นใยที่มีผลต่ออัตราการลดความชื้นของการอบแห้งด้วยไอน้ำร้อนยวดยิ่งที่อุณหภูมิต่าง ๆ



รูปที่ ๓ เปรียบเทียบผลของการหั่นเนื้อวัวแบบตัดขวางเส้นใยกับตัดตามเส้นใยที่มีผลต่ออัตราการลดความชื้นของการอบแห้งด้วยอากาศร้อนที่อุณหภูมิต่าง ๆ

จากรูปจะเห็นว่าในช่วงของการควบแน่น ความชื้นของชิ้นตัวอย่างเพิ่มขึ้นจาก ๑ เป็น ๑.๒ ความชื้นไร้หน่วย ช่วงของการเพิ่มความชื้นนั้นเป็นช่วงระยะเวลาสั้น ๆ จากนั้นจะเป็นช่วงของการลดความชื้นของชิ้นตัวอย่าง จากผลการทดลองที่อุณหภูมิของไอน้ำร้อนยวดยิ่งค่าต่าง ๆ พบว่า การอบแห้งที่อุณหภูมิสูงสามารถลดความชื้นของเนื้อวัวได้เร็วกว่าการอบแห้งที่อุณหภูมิต่ำ เนื่องจากผลต่างของอุณหภูมิระหว่างไอน้ำร้อนยวดยิ่งกับผลิตภัณฑ์มีค่ามากกว่ากรณีที่ใช้อุณหภูมิต่ำในการอบแห้ง ส่งผลให้อัตราการถ่ายเทความร้อนจากไอน้ำไปยังผลิตภัณฑ์มีค่าสูงกว่า ด้วยเหตุผลดังกล่าวทำให้ระยะเวลาในการอบแห้งด้วยไอน้ำร้อนยวดยิ่งที่อุณหภูมิ ๑๕๐ องศาเซลเซียส จะสั้นกว่าการอบแห้งด้วยไอน้ำร้อนยวดยิ่งที่ ๑๓๐ และ ๑๔๐ องศาเซลเซียส สำหรับผลการอบแห้งด้วยอากาศร้อนดังแสดงในรูปที่ ๓ ให้ผลในทำนองเดียวกับกรณีการใช้ไอน้ำร้อนยวดยิ่ง กล่าวคือ การอบแห้งที่อุณหภูมิสูงสามารถลดความชื้นของผลิตภัณฑ์ได้เร็วกว่าการอบแห้งที่อุณหภูมิต่ำ สิ่งหนึ่งที่แตกต่างกันชัดเจนระหว่างการอบแห้งด้วยไอน้ำร้อนยวดยิ่งกับการอบแห้งด้วยอากาศร้อนคือในกรณีที่อบแห้งด้วยอากาศร้อนไม่ปรากฏช่วงการเพิ่มขึ้นของความชื้น

๓.๒ ผลของลักษณะการหั่นเนื้อวัวต่ออัตราการอบแห้ง

นอกจากปัจจัยของอุณหภูมิ รูปที่ ๒ และรูปที่ ๓ ยังแสดงถึงผลของลักษณะของการหั่นเนื้อวัวระหว่างตัดขวาง กับตัดตามเส้นใยกล้ามเนื้อ โดยในกรณีตัดตามเส้นใยแสดงด้วยสัญลักษณ์ต่าง ๆ และตัดขวางแสดงด้วยรูปแบบเส้น จากผลการทดลองที่ได้ พบว่าอัตราการลดความชื้นของเนื้อวัวที่หั่นแบบตัดขวางเส้นใยกับตัดตามเส้นใยนั้น มีค่าใกล้เคียงกันมาก จนเกือบจะทับเป็นเส้นเดียวกัน เนื่องจากเมื่อเนื้อวัวได้รับความร้อนทำให้เนื้อวัวเกิดการสูญเสียความสามารถในการจับน้ำ (water holding capacity, WHC) ทำให้น้ำอิสระ (free water) ซึ่งเป็นน้ำที่ถูกดึงดูดไว้ด้วยแรงตึงผิวถูกปลดปล่อยออกมาจากโปรตีนทั้งหลาย ไม่ว่าจะเป็นไมโอไฟบริลลาโปรตีน (myofibrillar protein) หรือจะเป็นโปรตีนเนื้อเยื่อเกี่ยวพัน (connective tissue protein) ซึ่งในการเคลื่อนที่ของน้ำอิสระที่อยู่ตามโปรตีนต่าง ๆ จะถูกปลดปล่อยออกมาแล้วสามารถเคลื่อนที่ไปได้ทุกทิศทุกทาง ไม่ว่าจะเคลื่อนที่ไปในทิศทางตามยาวของเส้นใยกล้ามเนื้อหรือจะเคลื่อนที่ออกตามแนวรัศมีของเส้นใยกล้ามเนื้อ ตามปรกติแล้วซาร์โคเลมมา (sarcolemma) ซึ่งเป็นผนังของเส้นใยกล้ามเนื้อจะทำหน้าที่ในการปิดกั้นน้ำที่จะออกมาจากเส้นใยกล้ามเนื้อ แต่เมื่อถูกความร้อนซาร์โคเลมมาก็จะสูญเสียสถานภาพไป[๙] ทำให้น้ำออกมาจากเส้นใยกล้ามเนื้อได้ทุกทิศทุกทาง ด้วยเหตุดังกล่าวจึงทำให้อัตราการอบแห้งของลักษณะการหั่นเนื้อวัวแบบตัดขวางเส้นใยกับตัดตามเส้นใยนั้นมีค่าแตกต่างกันอย่างไม่มีนัยสำคัญ

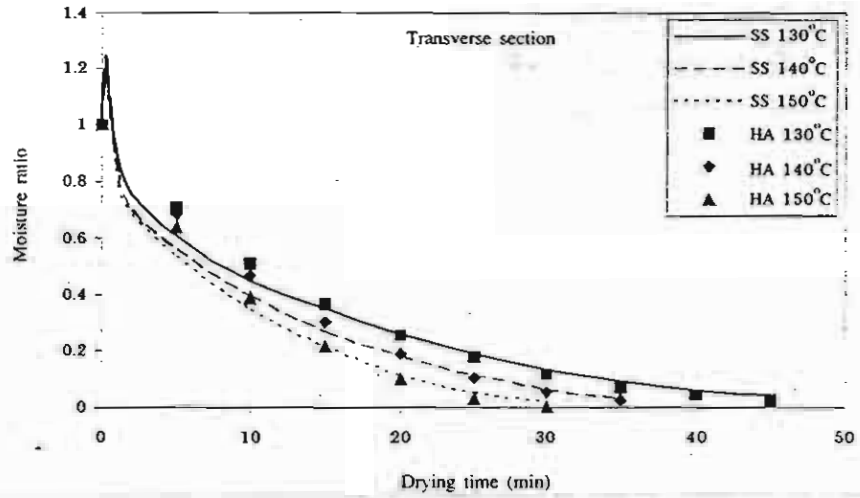
นอกจากนี้ จากข้อมูลการทดลองที่ได้พบว่าระยะเวลาในการอบแห้งเนื้อวัวด้วยไอน้ำร้อนยวดยิ่ง จนกระทั่งเนื้อวัวมีความชื้นประมาณ ๑๑% d.b. มีค่าไม่แตกต่างกันอย่างมีนัยสำคัญ สำหรับการอบแห้งเนื้อวัวที่หั่นแบบตัดขวางกับแบบตัดตามเส้นใย การอบแห้งที่อุณหภูมิ ๑๓๐, ๑๔๐ และ ๑๕๐ องศาเซลเซียส ใช้ระยะเวลาในการอบแห้งประมาณ ๔๓-๔๔, ๓๓-๓๔ และ ๒๕-๒๖ นาที ตามลำดับ

๓.๓ ผลของชนิดตัวกลางที่มีต่ออัตราการลดความชื้น

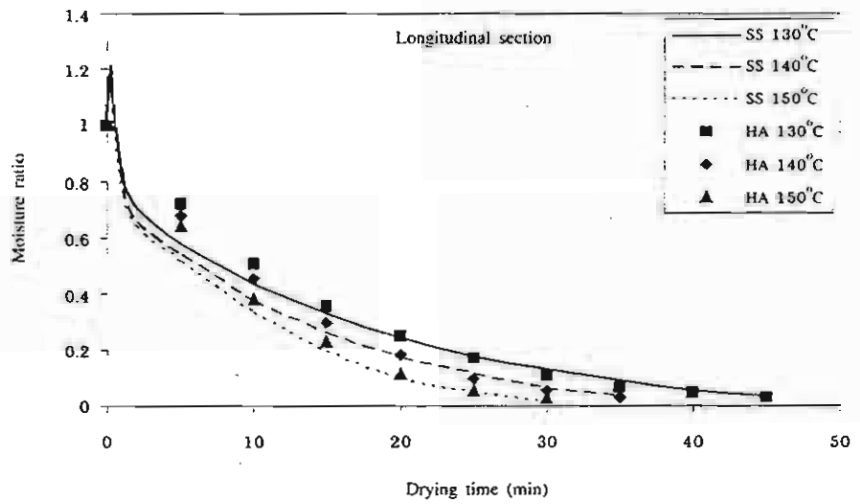
รูปที่ ๔ และรูปที่ ๕ แสดงถึงชนิดของตัวกลางที่ใช้ในการอบแห้งที่มีต่อการลดความชื้น โดยกำหนดให้ผลการทดลองอบแห้งด้วยไอน้ำแสดงด้วยเส้นชนิดต่าง ๆ และการอบแห้งด้วยอากาศแสดงด้วยรูปสัญลักษณ์ จากผลการทดลองพบว่าในช่วง ๒-๓ นาทีแรกของการอบแห้ง ไอน้ำร้อนยวดยิ่งสามารถลดความชื้นของผลิตภัณฑ์ทั้งในกรณีตัดตามและตัดขวางเส้นใยกล้ามเนื้อได้เร็วกว่าในกรณีของการอบแห้งด้วยอากาศร้อนอย่างเห็นได้ชัด แต่หลังจากนั้นการอบแห้งด้วยอากาศร้อนสามารถลดความชื้นผลิตภัณฑ์ได้ค่อนข้างเร็วกว่าเล็กน้อย การที่ไอน้ำร้อนยวดยิ่งสามารถลดความชื้นได้เร็วในช่วงแรกนี้อาจเนื่องมาจากสาเหตุที่อุณหภูมิของเนื้อวัวสูงขึ้นอย่างรวดเร็ว (ดังแสดงในรูปที่ ๖) เป็นผลให้การแพร่ของความชื้นเกิดขึ้นได้เร็วกว่าในกรณีของการอบแห้งด้วยอากาศร้อนที่การเปลี่ยนแปลงของอุณหภูมิชิ้นตัวอย่างอบแห้งเกิดขึ้นช้ากว่า อย่างไรก็ตาม เมื่อพิจารณาตลอดช่วงของการอบแห้งกลับพบว่าการอบแห้งด้วยอากาศร้อนสามารถลดความชื้นของผลิตภัณฑ์ได้ตามที่ต้องการเร็วกว่าการอบแห้งด้วยไอน้ำร้อนยวดยิ่งประมาณ ๒-๓ นาที ภายใต้เงื่อนไขของการอบแห้งที่เหมือนกัน ซึ่งในกรณีนี้อาจกล่าวได้ว่าระยะเวลาในการอบแห้งผลิตภัณฑ์ด้วยไอน้ำร้อนและอากาศร้อนไม่มีความแตกต่างอย่างเห็นได้ชัด

๓.๔ การเปลี่ยนแปลงอุณหภูมิของเนื้อวัวระหว่างการอบแห้ง

รูปที่ ๖ แสดงความสัมพันธ์ระหว่างระยะเวลาในการอบแห้งกับอุณหภูมิของเนื้อวัวด้วยไอน้ำร้อนยวดยิ่งที่อุณหภูมิ ๑๓๐, ๑๔๐ และ ๑๕๐ องศาเซลเซียส พบว่า ในช่วงแรกของการอบแห้ง ซึ่งเป็นช่วงที่เกิดการควบแน่นของไอน้ำนั้น อุณหภูมิของเนื้อวัวจะเพิ่มสูงขึ้นอย่างรวดเร็วจนถึงอุณหภูมิประมาณ ๑๐๐ องศาเซลเซียส ซึ่งเป็นอุณหภูมิจุดเดือดของน้ำ ส่งผลให้อัตราส่วนความชื้นในช่วงแรกของการอบแห้งนี้ลดลงอย่างรวดเร็ว ซึ่งสอดคล้องกับรูปที่ ๔ และรูปที่ ๕ ตามลำดับ ต่อจากนั้นอุณหภูมิของเนื้อวัวจะคงตัวที่อุณหภูมิจุดเดือดของน้ำช่วงระยะเวลาหนึ่ง หลังจากนั้นอุณหภูมิของเนื้อวัวจะค่อย ๆ เพิ่มขึ้นอีกครั้ง จนกระทั่ง



รูปที่ ๔ เปรียบเทียบผลของตัวกลางที่มีผลต่ออัตราการลดความชื้นของเนื้อวัวแบบตัดขวางเส้นใยที่อุณหภูมิต่าง ๆ



รูปที่ ๕ เปรียบเทียบผลของตัวกลางที่มีผลต่ออัตราการลดความชื้นของเนื้อวัวแบบตัดตามเส้นใยที่อุณหภูมิต่าง ๆ

อุณหภูมิในเนื้อวัวมีอุณหภูมิเท่ากับอุณหภูมิของไอน้ำร้อนยวดยิ่งที่ใช้ในการอบแห้ง ส่วนผลการทดลองการอบแห้งเนื้อวัวด้วยอากาศร้อนที่อุณหภูมิ ๑๓๐, ๑๔๐ และ ๑๕๐ องศาเซลเซียส ดังแสดงในรูปที่ ๗ พบว่า ในช่วงแรกของการอบแห้งนั้น อุณหภูมิของเนื้อวัวจะเพิ่มสูงขึ้นแต่ด้วยอัตราที่ช้ากว่าการอบแห้งด้วยไอน้ำร้อนยวดยิ่ง ความแตกต่างดังกล่าวเป็นผลเนื่องจากสัมประสิทธิ์การถ่ายเทความร้อนโดยการควบแน่นของไอน้ำมีค่าสูงกว่าค่าสัมประสิทธิ์การถ่ายเทความร้อนโดยการพาของอากาศมาก จึงทำให้อุณหภูมิผลิตภัณฑ์เพิ่มขึ้นเร็วกว่าในกรณีของไอน้ำร้อน อย่างไรก็ตาม ในตอนท้ายของการอบแห้งอุณหภูมิผลิตภัณฑ์ของการอบแห้งด้วยตัวกลางทั้งสองไม่มีความแตกต่างกันอย่างเห็นได้ชัด

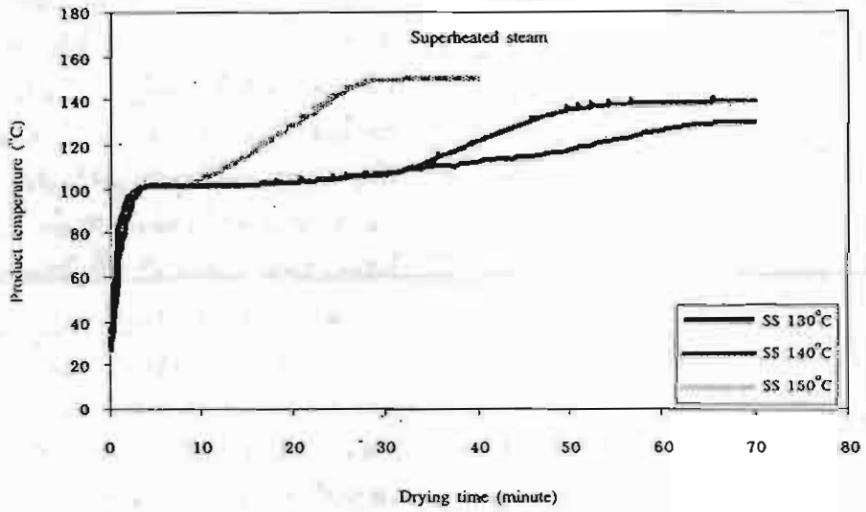
๓.๕ อัตราการอบแห้ง

จากผลการเปลี่ยนแปลงความชื้นของเนื้อวัวด้วยไอน้ำร้อนยวดยิ่งและอากาศร้อน ดังแสดงในรูปที่ ๒ และรูปที่ ๓ ตามลำดับ สามารถนำมาคำนวณหาอัตราการอบแห้งของเนื้อวัวที่อบแห้งด้วยไอน้ำยวดยิ่งและอากาศร้อนที่อุณหภูมิ ๑๓๐, ๑๔๐ และ ๑๕๐ องศาเซลเซียส ได้โดยนำค่าความชื้นที่ระยะเวลาอบแห้งต่าง ๆ มาฟิต (fit) กับสมการถดถอยที่เหมาะสมที่สุด จากนั้นหาอนุพันธ์ของสมการดังกล่าวเทียบกับเวลา ก็จะสามารถทราบอัตราการอบแห้ง ณ ขณะใดขณะหนึ่งได้ ในการคำนวณหาอัตราการอบแห้งเริ่มจากจุดที่มีความชื้นของผลิตภัณฑ์สูงสุดซึ่งเป็นจุดที่การควบแน่นของไอน้ำสิ้นสุดลง[๙๔]

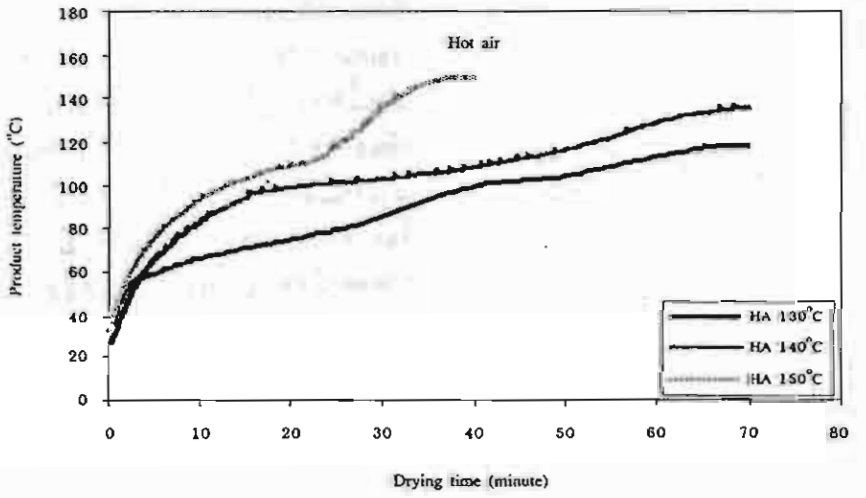
จากอัตราการอบแห้งเนื้อวัวด้วยไอน้ำร้อนยวดยิ่งและอากาศร้อนที่อุณหภูมิ ๑๓๐, ๑๔๐ และ ๑๕๐ องศาเซลเซียส ทั้งแบบตัดขวางเส้นใยและตัดตามเส้นใย ดังแสดงในรูปที่ ๘ และรูปที่ ๙ ตามลำดับ พบว่า การอบแห้ง

เนื้อวัวอยู่ในช่วงของการอบแห้งลดลงเพียงอย่างเดียว และการอบแห้งที่อุณหภูมิ ๑๕๐ องศาเซลเซียส มีอัตราการอบแห้งสูงกว่าการอบแห้งที่อุณหภูมิ ๑๓๐ และ ๑๔๐ องศาเซลเซียส ในทุก ๆ ช่วงของความชื้น

อัตราการอบแห้งลดลงในลักษณะเชิงเส้นตรงตามปริมาณความชื้นของวัสดุที่ลดลงเกือบตลอดช่วงของการอบแห้ง ยกเว้นในช่วงต้นของการอบแห้งด้วยไอน้ำ ซึ่งตรงกับช่วงความชื้นที่สูงกว่า ๑๖๐ (%d.b.) การเปลี่ยนแปลงของอัตราการอบแห้งในช่วงความชื้นสูงดังกล่าวค่อนข้างไวต่อความชื้น ทั้งนี้เป็นผลเนื่องจากช่วงความชื้นดังกล่าวเป็นช่วงของระเหยความชื้นที่เกิดจากชิ้นตัวอย่างดูดซับน้ำจากการควบแน่นของไอน้ำร้อนยวดยิ่ง ปริมาณน้ำที่ดูดซับโดยวัสดุนั้นส่วนใหญ่อยู่บริเวณผิวของวัสดุซึ่งกำจัดได้ง่าย ดังนั้นการเปลี่ยนแปลงของอัตราการอบแห้งกับความชื้นในช่วงดังกล่าวจึงไม่เป็นเชิงเส้นตรง

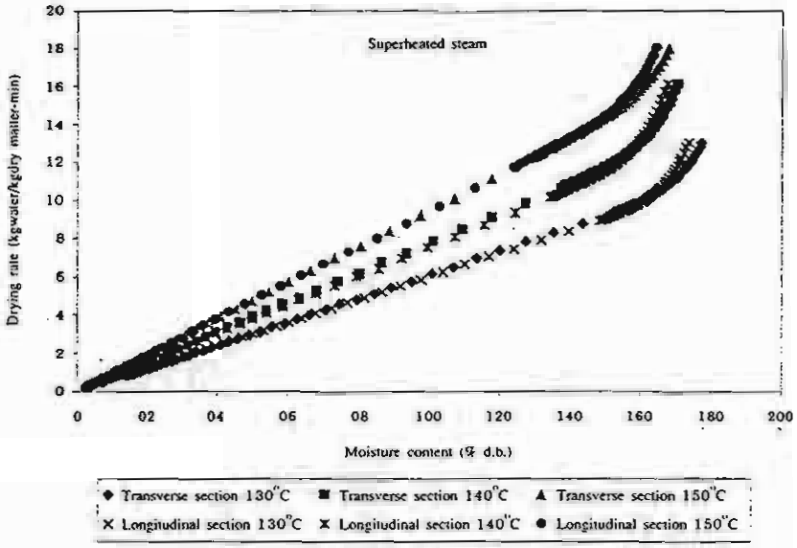


รูปที่ ๖ เปรียบเทียบระยะเวลาในการอบแห้งกับอุณหภูมิของเนื้อวัวที่ทำการอบแห้งด้วยไอน้ำร้อนยวดยิ่งที่อุณหภูมิต่าง ๆ

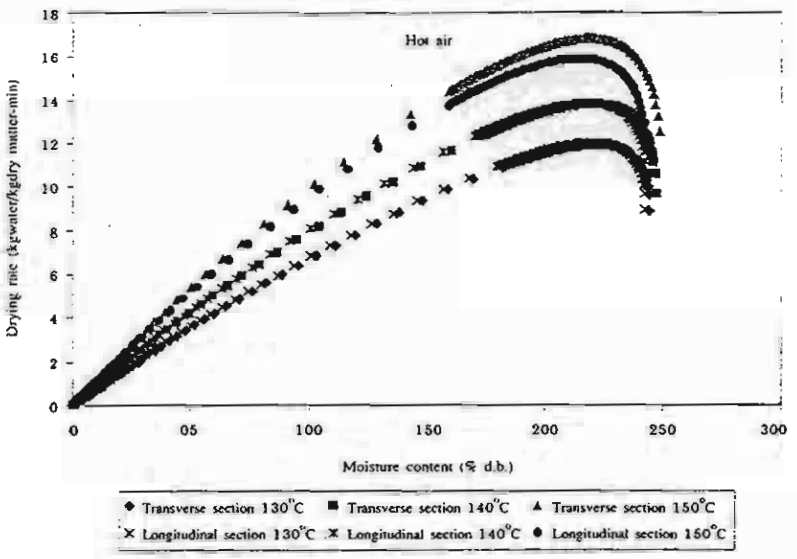


รูปที่ ๗ เปรียบเทียบระยะเวลาในการอบแห้งกับอุณหภูมิของเนื้อวัวที่ทำการอบแห้งด้วยอากาศร้อนที่อุณหภูมิต่าง ๆ

เมื่อเปรียบเทียบลักษณะของเส้นอัตราการอบแห้งกับความชื้นที่ได้จากการอบแห้งด้วยตัวกลางอบแห้งทั้งสอง พบว่าลักษณะของเส้นกราฟของอัตราการอบแห้งสำหรับการอบแห้งด้วยอากาศร้อนและไอน้ำร้อนยวดยิ่งโดยทั่วไปมีลักษณะคล้ายกัน ยกเว้นเฉพาะในช่วงแรกของการอบแห้ง ในกรณีของอากาศร้อนนั้นอัตราการอบแห้งจะเพิ่มขึ้นในขณะที่มีการลดความชื้นของผลิตภัณฑ์ ช่วงที่เกิดขึ้นนี้สามารถเห็นได้ทั่วไปสำหรับการอบแห้งด้วยอากาศร้อน ซึ่งเป็นช่วงเริ่มต้นของการอุ่นวัสดุให้ร้อนขึ้นและใช้เวลาประมาณ ๑ นาทีเศษ ดังนั้น อัตราการอบแห้งที่เพิ่มขึ้นนั้น เป็นผลเนื่องมาจากอุณหภูมิของวัสดุที่สูงขึ้น นอกจากปัจจัยดังกล่าวแล้ว ในช่วงดังกล่าวความชื้นส่วนใหญ่อยู่ใกล้ผิวของวัสดุซึ่งกำจัดได้ง่าย สำหรับในกรณีของไอน้ำร้อนปรากฏว่า



รูปที่ ๘ เปรียบเทียบอัตราการอบแห้งเนื้อวัวด้วยไอน้ำร้อนยวดยิ่งแบบตัดขวางเส้นใยกับตัดตามเส้นใยที่อุณหภูมิต่าง ๆ (ไม่รวมช่วงที่เกิดการควบแน่น)



รูปที่ ๙ เปรียบเทียบอัตราการอบแห้งเนื้อวัวด้วยอากาศร้อนแบบตัดขวางเส้นใยกับตัดตามเส้นใยที่อุณหภูมิต่าง ๆ

ไม่พบช่วงของการเพิ่มขึ้นของอัตราการอบแห้ง ทั้งนี้อาจเนื่องมาจากช่วงของการอุ่นวัสดุนั้นสั้นมาก ทำให้อุณหภูมิของวัสดุสูงขึ้นถึงจุดเดือดอย่างรวดเร็ว

๓.๖ สัมประสิทธิ์การแพร่ประสิทธิผล

ผลการเปลี่ยนแปลงความชื้นตามเวลาทั้งในกรณีของการอบแห้งด้วยไอน้ำร้อนยวดยิ่งและอากาศร้อนดังแสดงในรูปที่ ๒ และรูปที่ ๓ ตามลำดับ และอัตราการอบแห้งของเนื้อวัว

ที่ความชื้นต่าง ๆ ดังแสดงในรูปที่ ๘ และ ๙ แสดงให้เห็นว่าการอบแห้งอยู่ในช่วงของการอบแห้งลดลงเพียงอย่างเดียวและการอบแห้งในช่วงดังกล่าวนี้สามารถอธิบายได้ด้วยกฎข้อที่ ๒ ของฟิค ในกรณีของการอบแห้งเนื้อวัวที่หั่นเป็นชิ้นบาง ๆ นั้น การเคลื่อนที่ของความชื้นส่วนใหญ่เคลื่อนที่ตามความหนาของชิ้นวัสดุ ดังนั้น เราสามารถประมาณได้ว่าการแพร่ของความชื้นเกิดขึ้นในทิศทางเดียว สมการที่ใช้ในการคำนวณหาความชื้นในกรณีนี้แสดงได้ด้วยสมการที่ (๓)[๖]

$$MR = \frac{8}{\pi^2}\sum_{m=0}^{\infty}\left(\frac{1}{(2m+1)^2}\exp\left[-(2m+1)^2\pi^2\frac{Dt}{L^2}\right]\right) \qquad (๓)$$

จากสมการดังกล่าว เราสามารถคำนวณหาค่าสัมประสิทธิ์การแพร่ประสิทธิผลได้เมื่อทราบอัตราส่วนความชื้นไร้หน่วยที่เวลาต่าง ๆ ภายใต้เงื่อนไขของการอบแห้งที่อุณหภูมิคงที่อันหนึ่ง จากผลการทดลองที่ได้เป็นที่ทราบดีว่าเมื่ออุณหภูมิสูงขึ้น อัตราการอบแห้งก็จะเร็วขึ้น ความสัมพันธ์ระหว่างอุณหภูมิที่ใช้ในการอบแห้งกับค่าสัมประสิทธิ์การแพร่ประสิทธิผลสามารถอธิบายด้วยสมการของ Arrhenius คือ

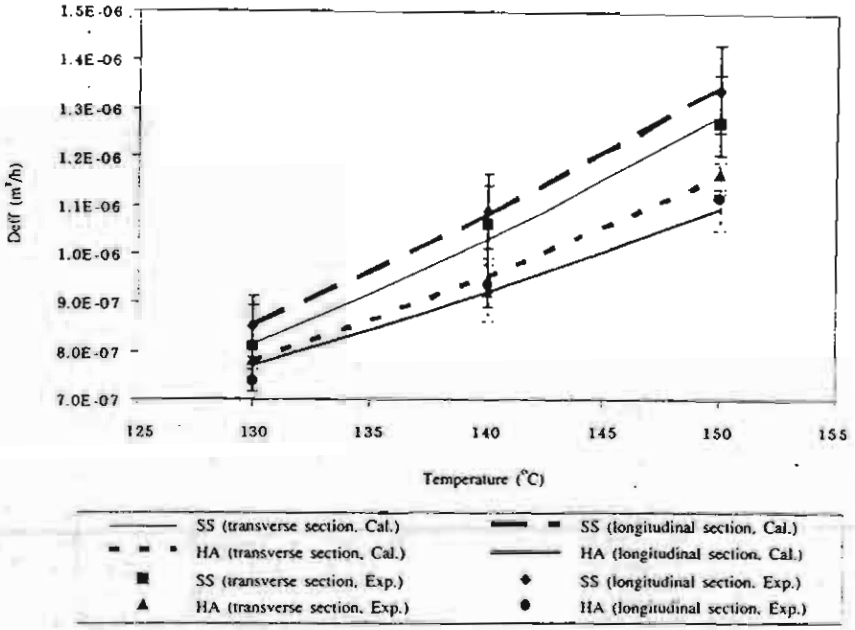
$$D_{eff} = D_0 \exp\left(\frac{-E_a}{RT}\right) \qquad (๔)$$

โดยที่ค่าคงตัว D_0 และ E_a สามารถทราบได้โดยการใช้เทคนิคของสมการถดถอยแบบเชิงเส้นในการประมาณค่าคงตัวดังกล่าว ค่าคงตัวต่าง ๆ ที่ได้จากการทดลองในกรณีต่าง ๆ แสดงในตารางที่ ๑ การที่ค่าของ R^2 เข้าใกล้หนึ่งและ SSE มีค่าน้อยแสดงให้เห็นว่าสมการของ Arrhenius สามารถอธิบายความสัมพันธ์ระหว่างค่าสัมประสิทธิ์การแพร่ประสิทธิผลกับอุณหภูมิได้สอดคล้องกัน อนึ่งการคำนวณหาค่าสัมประสิทธิ์การแพร่ความชื้นภายในเนื้อวัวที่อบแห้งด้วยไอน้ำร้อนยวดยิ่งนี้ จะไม่รวมช่วงที่เกิดการควบแน่นของไอน้ำที่ผิวของเนื้อวัว

รูปที่ ๑๐ แสดงความสัมพันธ์ระหว่างค่าสัมประสิทธิ์การแพร่ประสิทธิผลกับอุณหภูมิในการอบแห้ง พบว่าค่าสัมประสิทธิ์การแพร่ประสิทธิผลของความชื้นของเนื้อวัวที่อบแห้งด้วยไอน้ำร้อนยวดยิ่งมีค่าสูงกว่าที่อบแห้งด้วยอากาศร้อนตลอดช่วงของอุณหภูมิการอบแห้งที่ศึกษา แม้ว่าเวลาในการอบแห้งด้วยอากาศร้อนโดยรวมจะน้อยกว่าเวลาในการอบแห้งด้วยไอน้ำร้อน ที่เป็นเช่นนี้อาจเป็นเพราะช่วงแรกของการระเหยความชื้นของชิ้นตัวอย่างที่

ตารางที่ ๑ ค่าคงที่ของค่าสัมประสิทธิ์การแพร่ประสิทธิผลของการอบแห้งเนื้อวัวด้วยไอน้ำร้อนยวดยิ่งและอากาศร้อน

ตัวกลางอบแห้ง	ลักษณะการหั่น	D_0 ($\times 10^{-3}$ m^2/h)	E_a (kJ/kmol)	R^2 (%)	SSE
ไอน้ำร้อนยวดยิ่ง	ตัดขวางเส้นใย	13.74	32613.15	99.59	0.01
	ตัดตามเส้นใย	12.96	32260.58	99.69	0.0076
อากาศร้อน	ตัดขวางเส้นใย	3.78	28446.75	97.54	0.0634
	ตัดตามเส้นใย	1.38	25104.82	97.72	0.0584



รูปที่ ๑๐ เปรียบเทียบค่าสัมประสิทธิ์การแพร่ประสิทธิผลของการอบแห้งด้วยไอน้ำร้อนยวดยิ่งและอากาศร้อนที่อุณหภูมิต่าง ๆ

อบแห้งด้วยไอน้ำร้อนยวดยิ่งเป็นไปอย่างรวดเร็ว ดังนั้น จึงมีผลกระทบค่อนข้างสูงต่อการคำนวณหาค่าสัมประสิทธิ์การแพร่

๓.๗ คุณภาพด้านสี

จากการทดสอบคุณภาพด้านสี โดยสีเนื้อวัวเริ่มต้นก่อนการอบแห้งมีค่า L, a และ b คือ ๓๔.๔๓, ๙.๕๕ และ ๗.๙๗ ตามลำดับ สีของเนื้อวัวเริ่มต้นมีสีแดงสด เนื่องจากเม็ดสีที่อยู่ในกล้ามเนื้อคือ ไมโอโกลบิน (myoglobin) ซึ่งทำหน้าที่เป็นตัวกักเก็บโมเลกุลออกซิเจนในเซลล์กล้ามเนื้อเพื่อใช้งานต่อไปตามกระบวนการเมแทบอลิซึม ไมโอโกลบินเป็นโปรตีนประเภท conjugated ประกอบไปด้วย ironporphyrin compound และฮีม (heme) อยู่ร่วมกันกับโปรตีนโกลบิน โดยฮีมจะทำหน้าที่ในการยึดเกาะออกซิเจนในขณะที่โปรตีนโกลบินจะทำหน้าที่ห่อหุ้มและปกป้องฮีมไว้ แต่เมื่ออบแห้งเนื้อวัวด้วยไอน้ำร้อนยวดยิ่งหรืออากาศร้อนนั้น เนื้อวัวจะได้รับความร้อนจากตัวกลางดังกล่าว และความร้อนนี้เองจะทำให้โครงสร้างทางเคมีของเนื้อวัวเปลี่ยน Qxymyoglobin ซึ่งมี Fe^{2+} ในสีเนื้อมีสีแดงไปเป็น met-myoglobin ซึ่งมี Fe^{3+} ส่งผลให้สีของเนื้อวัวหลังการอบแห้งมีความสว่างลดต่ำลงและมีสีเนื้อเป็นสีน้ำตาล ดังแสดงในตารางที่ ๒ จากข้อมูลที่แสดงในตารางพบว่าไม่ว่าจะอบแห้งเนื้อวัวด้วยวิธีใด สีของเนื้อวัวหลังการอบแห้งมีสีใกล้เคียงกัน ไม่ว่าจะอบแห้งที่อุณหภูมิสูงหรือต่ำ โดยที่ค่าการเปลี่ยนแปลงคือ ΔL, Δa และ Δb ที่อุณหภูมิต่าง ๆ ไม่มีความแตกต่างกันอย่างมีนัยสำคัญ แต่เมื่อทำการเปรียบเทียบกันระหว่างการอบแห้งเนื้อวัวด้วยไอน้ำร้อนยวดยิ่งกับการอบแห้งด้วยอากาศร้อน พบว่าค่า Δb ซึ่งแสดงการเปลี่ยนแปลงของค่าสีเหลืองต่างกัน โดยการอบแห้งด้วยอากาศร้อนจะมีค่า Δb สูงกว่าการอบแห้งด้วยไอน้ำร้อนยวดยิ่งอยู่เล็กน้อย ขณะที่ค่า ΔL และค่า Δa ไม่มีความแตกต่างกันอย่างมีนัยสำคัญ จากการสังเกตด้วยสายตา พบว่าการอบแห้งเนื้อวัวด้วยไอน้ำร้อนยวดยิ่งจะได้เนื้อวัวหลังการอบแห้งที่มีสีสม่ำเสมอกว่าการอบแห้งด้วยอากาศร้อน ซึ่งสามารถสังเกตได้จากการแสดงค่าของ L ที่ให้ค่าเบี่ยงเบนมาตรฐานของค่า L ในกรณีของไอน้ำร้อนน้อยกว่าในกรณีของอากาศร้อน

ตารางที่ ๒ การทดสอบคุณภาพด้านสีของเนื้อวัวหลังการอบแห้งที่เงื่อนไขต่าง ๆ
ค่าสีเริ่มต้นของเนื้อวัวก่อนการอบแห้ง L = 34.43±0.85, a = 9.55±1.08 และ b = 7.97±0.56

	Color		
	ΔL	Δa	Δb
SS 130°C ตัดขวางเส้นใย	10.51 ± 0.92^{b}	5.33 ± 0.68^{bcd}	1.97 ± 0.59^{ab}
SS 140°C ตัดขวางเส้นใย	11.52 ± 0.76^{cd}	5.03 ± 0.83^{abc}	1.99 ± 0.74^{ab}
SS 150°C ตัดขวางเส้นใย	11.56 ± 0.67^{cd}	5.05 ± 0.65^{abc}	1.67 ± 0.48^{a}
SS 130°C ตัดตามเส้นใย	10.36 ± 0.94^{b}	5.55 ± 0.47^{d}	1.98 ± 0.51^{ab}
SS 140°C ตัดตามเส้นใย	11.12 ± 1.01^{bcd}	5.41 ± 0.41^{cd}	2.08 ± 0.44^{bc}
SS 150°C ตัดตามเส้นใย	11.22 ± 0.66^{bcd}	5.42 ± 0.39^{cd}	1.95 ± 0.49^{ab}
HA 130°C ตัดขวางเส้นใย	10.50 ± 1.43^{b}	4.87 ± 0.66^{a}	2.77 ± 0.60^{de}
HA 140°C ตัดขวางเส้นใย	10.74 ± 1.23^{bc}	5.14 ± 0.48^{abc}	2.82 ± 0.66^{def}
HA 150°C ตัดขวางเส้นใย	10.89 ± 1.02^{bc}	4.95 ± 0.42^{ab}	2.63 ± 0.51^{de}
HA 130°C ตัดตามเส้นใย	10.40 ± 2.11^{b}	5.19 ± 0.59^{abcd}	2.43 ± 0.78^{cd}
HA 140°C ตัดตามเส้นใย	11.14 ± 2.12^{bcd}	5.09 ± 0.73^{abc}	2.75 ± 0.68^{de}
HA 150°C ตัดตามเส้นใย	11.82 ± 0.77^{d}	5.56 ± 0.49^{d}	3.18 ± 0.78^{f}
SS 140°C (43% d.b.) + HA 60°C ตัดขวางเส้นใย	9.41 ± 1.37^{a}	7.21 ± 0.86^{e}	2.97 ± 0.70^{ef}
SS 140°C (43% d.b.) + HA 60°C ตัดตามเส้นใย	9.37 ± 1.23^{a}	7.60 ± 0.38^{f}	3.54 ± 0.37^{g}

อักษรเหมือนกันภายในคอลัมน์เดียวกันหมายถึงไม่มีความแตกต่างอย่างมีนัยสำคัญ ($p > 0.05$)

เมื่อทำการอบแห้งเนื้อวัวแบบ ๒ ขั้นตอน แล้วนำเนื้อวัวหลังการอบแห้งไปเปรียบเทียบกับการอบแห้งเนื้อวัวด้วยไอน้ำร้อนยวดยิ่งหรืออากาศร้อนเพียงอย่างเดียว จากการวิเคราะห์ค่าทางสถิติ พบว่าการอบแห้งแบบ ๒ ขั้นตอนให้คุณภาพทางด้านสีของเนื้อวัวหลังการอบแห้งแตกต่างอย่างมีนัยสำคัญกับการอบแห้งด้วยไอน้ำร้อนยวดยิ่งหรืออากาศร้อนเพียงอย่างเดียว ($p < 0.05$) เนื่องจากในการอบแห้งแบบ ๒ ขั้นตอนนั้นปฏิกิริยา sugar-amine browning ที่อุณหภูมิสูงยังเกิดขึ้นได้ไม่นาน และเมื่อนำเนื้อวัวไปอบแห้งต่อในขั้นตอนที่ ๒ ซึ่งเป็นการอบแห้งที่อุณหภูมิต่ำ จึงทำให้เกิดการเปลี่ยนแปลงสีเพิ่มขึ้นเพียงเล็กน้อยเท่านั้น ดังนั้นวิธีการอบแห้งเนื้อวัวแบบ ๒ ขั้นตอน ให้เนื้อวัวหลังการอบแห้งมีสีน้ำตาลอ่อนกว่าสีของเนื้อวัวหลังการอบแห้งด้วยไอน้ำร้อนยวดยิ่งและอากาศร้อนเพียงอย่างเดียว

๓.๔ การทดสอบคุณภาพด้านการหดตัว

จากผลการทดสอบคุณภาพด้านการหดตัวของเนื้อวัวหลังการอบแห้งด้วยไอน้ำร้อนยวดยิ่งและอากาศร้อน ดังแสดงในตารางที่ ๓ ทำให้พบว่าผลของอุณหภูมิของตัวกลางในการอบแห้งมีผลต่อการหดตัวเล็กน้อย โดยที่อุณหภูมิของตัวกลางในการอบแห้งสูงกว่ามีแนวโน้มว่าเนื้อวัวจะหดตัวมากกว่าการอบแห้งที่อุณหภูมิต่ำ

เนื่องจากการอบแห้งเนื้อวัวที่อุณหภูมิสูงจะทำให้โปรตีนเส้นใยย่อย (myofibrillar protein) คือโปรตีนแอกทินและไมโอซินเกิดการจับตัวกันแน่นกว่าการอบแห้งที่อุณหภูมิต่ำ อย่างไรก็ตามเมื่อวิเคราะห์ค่าทางสถิติแล้วปรากฏว่าอุณหภูมิของตัวกลางในการอบแห้งไม่มีผลต่อการหดตัวอย่างมีนัยสำคัญ เมื่อเปรียบเทียบการหดตัวของเนื้อวัวหลังการอบแห้งระหว่างลักษณะการหั่นแบบตัดขวางเส้นใยกับตัดตามเส้นใยสามารถแบ่งได้เป็น ๒ อย่าง คือในกรณีอบแห้งด้วยอากาศร้อน การหั่นเนื้อวัวแบบตัดตามเส้นใยหดตัวมากกว่าการหั่นแบบตัดขวางเส้นใยอย่างมีนัยสำคัญ แต่เมื่อเปลี่ยนเป็นไอน้ำร้อนยวดยิ่งกลับพบว่าการหดตัวของชิ้นตัวอย่างไม่มีความแตกต่างกันระหว่างกันหั่นตามกับหั่นขวางเส้นใยกล้ามเนื้อ และเมื่อเปรียบเทียบการหดตัวของเนื้อวัวหลังการอบแห้งระหว่างการอบแห้งเนื้อวัวด้วยไอน้ำร้อนยวดยิ่งกับการอบแห้งเนื้อวัวด้วยอากาศร้อนภายใต้อุณหภูมิที่เดียวกัน พบว่าการอบแห้งเนื้อวัวด้วยไอน้ำร้อนยวดยิ่งมีการหดตัวมากกว่าการอบแห้งเนื้อวัวด้วยอากาศร้อน เนื่องจากการอบแห้งเนื้อวัวด้วยไอน้ำร้อนยวดยิ่งจะเกิดการแปรสภาพของคอลลาเจน (collagen) เป็นเจลาติน (gelatin) ในช่วงแรกของการอบแห้งเนื้อวัวด้วยไอน้ำร้อนยวดยิ่งมีลักษณะเป็นความร้อนเปียก (moist heat) อีกทั้งอุณหภูมิของเนื้อวัวยังเพิ่มขึ้นอย่างรวดเร็ว ในขณะนั้นความชื้นที่อยู่ในเนื้อวัวก็ยังเหลืออยู่มาก ภาวะดังกล่าวมีความเหมาะสมอย่างยิ่งต่อการละลายของคอลลาเจนและแปรสภาพเป็นเจลาติน โดยปรกติคอลลาเจนเริ่มเปลี่ยนสภาพที่อุณหภูมิของเนื้อวัวประมาณ ๖๐-๗๐ องศาเซลเซียส [๙๔] ดังนั้น ในการอบแห้งเนื้อวัวด้วยไอน้ำร้อนยวดยิ่งคาดว่าเหลือคอลลาเจนที่อยู่ในเนื้อวัวหลังจากการอบแห้งน้อยมาก ซึ่งต่างกับการอบแห้งเนื้อวัวด้วยอากาศร้อนที่เป็นความร้อนแห้ง (dry heat) จึงทำให้คอลลาเจนแปรสภาพเป็นเจลาตินได้ยาก จึงเป็นเหตุให้เนื้อวัวที่อบแห้งด้วยอากาศร้อนเหลือคอลลาเจนอยู่ในเนื้อวัวเป็นจำนวนมาก

เมื่อทำการอบแห้งเนื้อวัวแบบ ๒ ขั้นตอน แล้วนำเนื้อวัวหลังการอบแห้งไปเปรียบเทียบกับการอบแห้งเนื้อวัวด้วยไอน้ำร้อนยวดยิ่งและอากาศร้อนเพียงอย่างเดียว พบว่า ชิ้นตัวอย่างที่ผ่านการอบแห้งแบบ ๒ ขั้นตอนเกิดการหดตัวน้อยกว่าการอบแห้งด้วยไอน้ำร้อนยวดยิ่งเพียงอย่างเดียว แต่เกิดการหดตัวมากกว่าการอบแห้งด้วยอากาศร้อนเพียงอย่างเดียว

ตารางที่ ๓ การทดสอบคุณภาพด้านการหดตัวของเนื้อวัวหลังการอบแห้งที่เงื่อนไขต่าง ๆ

Drying process	% Shrinkage
SS 130 °C ตัดขวางเส้นใย	0.80 ± 0.42^{de}
SS 140 °C ตัดขวางเส้นใย	70.62 ± 0.19^{d}
SS 150 °C ตัดขวางเส้นใย	72.10 ± 1.06^{ef}
SS 130 °C ตัดตามเส้นใย	71.76 ± 0.99^{de}
SS 140 °C ตัดตามเส้นใย	71.96 ± 0.71^{de}
SS 150 °C ตัดตามเส้นใย	73.38 ± 0.65^{f}
HA 130 °C ตัดขวางเส้นใย	63.58 ± 1.51^{a}
HA 140 °C ตัดขวางเส้นใย	64.07 ± 2.08^{a}
HA 150 °C ตัดขวางเส้นใย	64.32 ± 1.57^{a}

ตารางที่ ๓ การทดสอบคุณภาพด้านการหดตัวของเนื้อวัวหลังการอบแห้งที่เงื่อนไขต่างๆ

Drying process	% Shrinkage
HA 130 °C ตัดตามเส้นใย	66.20 ± 1.43 [b]
HA 140 °C ตัดตามเส้นใย	66.39 ± 0.57 [b]
HA 150 °C ตัดตามเส้นใย	66.78 ± 0.36 [b]
SS 140 °C (43% d.b.) + HA 60 °C ตัดขวางเส้นใย	68.64 ± 1.25 [c]
SS 140 °C (43% d.b.) + HA 60 °C ตัดตามเส้นใย	70.61 ± 1.40 [d]

อักษรเหมือนกันภายในคอลัมน์เดียวกันหมายถึงไม่มีความแตกต่างอย่างมีนัยสำคัญ ($p > 0.05$)

๓.๙ การทดสอบคุณภาพด้านการคืนตัว

ตารางที่ ๔ แสดงผลการทดสอบคุณภาพด้านการคืนตัวของเนื้อวัวหลังการอบแห้งด้วยไอน้ำร้อนยวดยิ่งและอากาศร้อน จากการทดลองพบว่าผลของอุณหภูมิตัวกลางในการอบแห้งมีผลต่อค่าการคืนตัวของเนื้อวัวเพียงเล็กน้อย โดยมีแนวโน้มไปในทิศทางเดียวกันคือ ที่อุณหภูมิของตัวกลางในการอบแห้งต่ำ ชิ้นตัวอย่างสามารถคืนตัวได้มากกว่าการอบแห้งที่อุณหภูมิสูง และเมื่อเปรียบเทียบค่าการคืนตัวของเนื้อวัวหลังการอบแห้งระหว่างลักษณะการหั่นแบบตัดขวางเส้นใยกับตัดตามเส้นใย พบว่าเนื้อวัวที่มีการหั่นแบบตัดขวางเส้นใยและผ่านการอบแห้งด้วยไอน้ำร้อนยวดยิ่งมีค่าการคืนตัวมากกว่าการหั่นแบบตัดตามเส้นใย ในทางตรงกันข้าม ชิ้นเนื้อวัวที่ตัดขวางเส้นใยและอบแห้งด้วยอากาศร้อนสามารถคืนตัวได้มากกว่าแบบตัดตามเส้นใยที่ทุก ๆ อุณหภูมิ อย่างไรก็ตาม เมื่อนำค่าการคืนตัวที่ได้ไปวิเคราะห์ทางสถิติ พบว่าลักษณะการหั่นเนื้อวัวของการอบแห้งด้วยอากาศร้อนไม่มีความแตกต่างของค่าการคืนตัวอย่างมีนัยสำคัญ ($p > 0.05$) แต่มีความแตกต่างอย่างมีนัยสำคัญเมื่อผ่านการอบแห้งด้วยไอน้ำร้อนยวดยิ่ง ($p < 0.05$)

จากการเปรียบเทียบค่าการคืนตัวของเนื้อวัวหลังการอบแห้งระหว่างการอบแห้งเนื้อวัวด้วยไอน้ำร้อนยวดยิ่งกับการอบแห้งเนื้อวัวด้วยอากาศร้อนภายใต้อุณหภูมิเดียวกัน พบว่าการอบแห้งเนื้อวัวด้วยไอน้ำร้อนยวดยิ่งมีค่าการคืนตัวใกล้เคียงกันกับการอบแห้งเนื้อวัวด้วยอากาศร้อน

เมื่อทำการอบแห้งเนื้อวัวแบบ ๒ ขั้นตอน แล้วนำเนื้อวัวหลังการอบแห้งไปทดสอบค่าการคืนตัวโดยเปรียบเทียบกับค่าการคืนตัวของเนื้อวัวที่อบแห้งด้วยไอน้ำร้อนยวดยิ่งและอากาศร้อนเพียงอย่างเดียว พบว่าชิ้นเนื้อวัวที่ผ่านการอบแห้งแบบ ๒ ขั้นตอน มีค่าการคืนตัวสูงกว่าค่าการคืนตัวของเนื้อวัวที่อบแห้งด้วยไอน้ำร้อนยวดยิ่งและอากาศร้อนเพียงอย่างเดียว ซึ่งอาจเนื่องจากในการอบแห้งเนื้อวัวแบบ ๒ ขั้นตอนนั้น โปรตีนต่าง ๆ จะเสียสภาพน้อยกว่า จึงอาจจะทำให้โปรตีนสามารถดึงโมเลกุลของน้ำกลับเข้าในในเนื้อวัวได้มากขึ้น ซึ่งต่างกับเนื้อวัวที่อบแห้งด้วยไอน้ำร้อนยวดยิ่งและอากาศร้อนเพียงอย่างเดียว ที่โปรตีนต่าง ๆ เสียสภาพไปมาก เนื่องจากอบแห้งที่อุณหภูมิสูงเป็นเวลานาน

๓.๑๐ การทดสอบคุณภาพด้านเนื้อสัมผัส

จากผลการทดสอบคุณภาพด้านเนื้อสัมผัสของเนื้อวัวหลังการอบแห้งด้วยไอน้ำร้อนยวดยิ่งและอากาศร้อน ดังแสดงในตารางที่ ๕ พบว่าการอบแห้งที่อุณหภูมิสูงหรืออุณหภูมิต่ำจะให้เนื้อวัวหลังการอบแห้งจะมีค่าความแข็งที่ใกล้เคียงกัน และเมื่อวิเคราะห์ค่าทางสถิติแล้วปรากฏว่า อุณหภูมิของตัวกลางในการอบแห้งนั้น ไม่ทำให้ค่าความแข็งของเนื้อวัวหลังการอบแห้งมี



ตารางที่ ๔ การทดสอบการคืนตัวของเนื้อวัว ที่ผ่านการอบแห้งเงื่อนไขต่าง ๆ

Drying process	% Rehydration
SS 130°C ตัดขวางเส้นใย	59.11 ± 1.96^{fg}
SS 140°C ตัดขวางเส้นใย	58.09 ± 2.82^{efg}
SS 150°C ตัดขวางเส้นใย	55.56 ± 0.71^{cdef}
SS 130°C ตัดตามเส้นใย	51.71 ± 0.23^{abc}
SS 140°C ตัดตามเส้นใย	51.15 ± 0.71^{ab}
SS 150°C ตัดตามเส้นใย	47.78 ± 0.67^{a}
HA 130°C ตัดขวางเส้นใย	60.70 ± 2.85^{g}
HA 140°C ตัดขวางเส้นใย	56.56 ± 3.22^{def}
HA 150°C ตัดขวางเส้นใย	53.76 ± 1.71^{bcd}
HA 130°C ตัดตามเส้นใย	54.10 ± 2.85^{bcde}
HA 140°C ตัดตามเส้นใย	52.75 ± 2.08^{bcd}
HA 150°C ตัดตามเส้นใย	51.52 ± 0.52^{abc}
SS 140°C (43% d.b.) + HA 60°C ตัดขวางเส้นใย	73.17 ± 1.07^{i}
SS 140°C (43% d.b.) + HA 60°C ตัดตามเส้นใย	65.56 ± 0.96^{h}

อักษรเหมือนกันภายในคอลัมน์เดียวกันหมายถึงไม่มีความแตกต่างอย่างมีนัยสำคัญ ($p > 0.05$)

ความแตกต่างกันอย่างมีนัยสำคัญ และเมื่อเปรียบเทียบค่าความแข็งของเนื้อวัวหลังการอบแห้งระหว่างการหั่นแบบตัดขวางเส้นใยกับตัดตามเส้นใย พบว่าการหั่นแบบตัดตามเส้นใยมีค่าความแข็งน้อยกว่าการหั่นแบบตัดขวางเส้นใยอย่างอย่างมาก เนื่องจากเมื่อหัวกดจากเครื่องทดสอบกดลงบนเนื้อวัวหลังการอบแห้งแบบตัดตามเส้นใย ชิ้นเนื้อวัวจะแตกออกจากกันเป็น ๒ ชิ้นส่วนตามแนวยาวของเส้นใยกล้ามเนื้อ ซึ่งเป็นจุดที่แตกง่าย เนื่องจากแรงยึดเหนี่ยวระหว่างโครงสร้างน้อย จึงทำให้ค่าความแข็งที่ได้มีค่าน้อยกว่าเนื้อวัวหลังการอบแห้งแบบตัดขวางเส้นใย เนื้อวัวแบบตัดขวางเส้นใยนี้ จะแตกออกจากกันได้เพราะความเค้นอัด (compressive stress) และแตกออกในลักษณะสุ่ม จึงทำให้ค่าความแข็งที่ได้มีค่ามาก และเมื่อเปรียบเทียบค่าความแข็งของเนื้อวัวหลังการอบแห้งระหว่างเนื้อวัวที่อบแห้งด้วยไอน้ำร้อนยวดยิ่งกับที่อบด้วยอากาศร้อน พบว่าเนื้อวัวที่อบแห้งด้วยไอน้ำร้อนยวดยิ่งมีแนวโน้มว่าจะมีค่าความแข็งมากกว่าเนื้อวัวที่อบแห้งด้วยอากาศร้อน เนื่องจากการอบแห้งด้วยไอน้ำร้อนยวดยิ่งนั้นอุณหภูมิของเนื้อวัวจะเพิ่มขึ้นอย่างรวดเร็ว ซึ่งในขณะนั้นความชื้นที่อยู่ในเนื้อวัวก็ยังเหลืออยู่มาก ภาวะดังกล่าวเหมาะสมอย่างยิ่งต่อการละลายของคอลลาเจนและแปรสภาพเป็นเจลาติน ดังนั้น ในการอบแห้งเนื้อวัวด้วยไอน้ำร้อนยวดยิ่งคาดว่าเหลือคอลลาเจนที่อยู่ในเนื้อวัวหลังจากการอบแห้งน้อยมาก ซึ่งต่างกับการอบแห้งเนื้อวัวด้วยอากาศร้อนที่เป็นความร้อนแห้ง จึงทำให้คอลลาเจนแปรสภาพเป็นเจลาตินได้ยาก และเป็นเหตุให้เนื้อวัวที่อบแห้งด้วยอากาศร้อน

เหลือคอลลาเจนอยู่ในเนื้อวัวเป็นจำนวนมาก ทำให้เนื้อวัวมีค่าความแข็งมากกว่า อย่างไรก็ตาม เมื่อนำค่าความแข็งที่ได้ไปวิเคราะห์ทางสถิติ พบว่าไม่มีความแตกต่างกันอย่างมีนัยสำคัญ ($p > 0.05$) เมื่อทำการอบแห้งเนื้อวัวแบบ ๒ ขั้นตอน แล้วนำเนื้อวัวหลังการอบแห้งไปทดสอบค่าความแข็งเปรียบเทียบกับการอบแห้งเนื้อวัวด้วยไอน้ำร้อนยวดยิ่งเพียงอย่างเดียว พบว่าเนื้อวัวที่อบแห้งแบบ ๒ ขั้นตอนจะมีค่าความแข็งน้อยกว่าเนื้อวัวที่อบแห้งด้วยไอน้ำร้อนยวดยิ่งเพียงอย่างเดียว

๔. สรุปผลการทดลอง

จากผลการทดลองอบแห้งที่อุณหภูมิ ๑๓๐, ๑๔๐ และ ๑๕๐ องศาเซลเซียส พบว่าการอบแห้งที่อุณหภูมิสูงจะมีอัตราการอบแห้งสูงกว่าการอบแห้งที่อุณหภูมิต่ำ ขณะที่คุณภาพด้านสีโดยวัดการเปลี่ยนแปลงสีของตัวแปร L, a และ b การหดตัว และความแข็ง มีค่าไม่แตกต่างกันอย่างมีนัยสำคัญ ($p > 0.05$) เมื่อพิจารณาเปรียบเทียบการอบแห้งด้วยไอน้ำร้อนยวดยิ่งและอากาศร้อนแบบชนิดของตัวกลางในการอบแห้ง พบว่าสัมประสิทธิ์การแพร่ของเนื้อวัวที่อบแห้งด้วยไอน้ำร้อนยวดยิ่งจะมีค่าสูงกว่ากรณีอบแห้งด้วยอากาศร้อน และสีของเนื้อวัวหลังการอบแห้งด้วยไอน้ำร้อนยวดยิ่งมีความสม่ำเสมอกว่า การหดตัวมากกว่า ส่วนการคืนตัวและความแข็งไม่แตกต่างกันอย่างมีนัยสำคัญ ($p > 0.05$) เมื่อพิจารณาการเรียงของเส้นใยกล้ามเนื้อ พบว่าไม่มีผลต่ออัตราการแพร่ของน้ำ ไม่ว่าจะอบแห้งด้วยไอน้ำร้อนยวดยิ่งหรืออากาศร้อน และเมื่อเปรียบเทียบคุณภาพด้านต่าง ๆ พบว่าการเรียงของเส้นใยกล้ามเนื้อให้คุณภาพ

ตารางที่ ๕ การทดสอบคุณภาพด้านเนื้อสัมผัสของเนื้อวัวหลังการอบแห้งที่เงื่อนไขต่างๆ

Drying process	Hardness (N)
SS 130 °C ตัดขวางเส้นใย	59.62 ± 17.24^{cd}
SS 140 °C ตัดขวางเส้นใย	59.57 ± 14.90^{cd}
SS 150 °C ตัดขวางเส้นใย	67.65 ± 12.82^{d}
SS 130 °C ตัดตามเส้นใย	27.09 ± 5.96^{a}
SS 140 °C ตัดตามเส้นใย	31.54 ± 9.96^{a}
SS 150 °C ตัดตามเส้นใย	36.45 ± 10.53^{ab}
HA 130 °C ตัดขวางเส้นใย	47.85 ± 12.15^{bc}
HA 140 °C ตัดขวางเส้นใย	48.67 ± 14.12^{bc}
HA 150 °C ตัดขวางเส้นใย	47.82 ± 9.72^{bc}
HA 130 °C ตัดตามเส้นใย	37.94 ± 14.58^{ab}
HA 140 °C ตัดตามเส้นใย	38.41 ± 18.27^{ab}
HA 150 °C ตัดตามเส้นใย	45.71 ± 14.96^{b}
SS 140 °C (43% d.b.) + HA 60 °C ตัดขวางเส้นใย	31.53 ± 13.17^{a}
SS 140 °C (43% d.b.) + HA 60 °C ตัดตามเส้นใย	25.74 ± 5.44^{a}

อักษรเหมือนกันภายในคอลัมน์เดียวกันหมายถึงไม่มีความแตกต่างอย่างมีนัยสำคัญ ($p > 0.05$)

สีแตกต่างกันเล็กน้อย เนื้อวัวแบบตัดขวางเส้นใยมีความแข็งมากกว่าและหดตัวน้อยกว่าแบบตัดตามเส้นใยอยู่เล็กน้อย เมื่อเทียบกับการอบแห้งแบบขั้นตอนเดียว การอบแห้งแบบ ๒ ขั้นตอน ทำให้สีที่ได้ของเนื้อวัวอบแห้งเป็นสีน้ำตาลอ่อนกว่า การคืนตัวสูงขึ้น ขณะที่ความแข็งของชิ้นเนื้อลดลง

๕. กิตติกรรมประกาศ

ผู้วิจัยขอขอบคุณ สำนักงานกองทุนสนับสนุนการวิจัย (สกว.) ที่ให้ทุนสนับสนุนงานวิจัย จนทำให้งานวิจัยนี้สำเร็จลุล่วงไปด้วยดี

เอกสารอ้างอิง

๑. Mujumdar, AS. Superheated steam drying, Handbook of Industrial Drying; Pub. Marcel Dekker Inc., New York, 1995.

๒. Li, YB, Seyed-Yagoobi, J, Moreira, RG, Yamsaengsung, R. Superheated steam impingement drying of tortilla chips. Drying Technology, 1999; 17(1&2): 191-213.

๓. Tang, Z, Cenkowski, S. Dehydration dynamics of potatoes in superheated steam and hot air. Canadian Agricultural Engineering, 2000; 42(1): 6.1-6.13.

๔. Moreira, RG. Impingement drying of foods using hot air and superheated steam. Journal of Food Engineering, 2001; 49(4): 291-295.

๕. Iyota, N, Nishimura, N, Onuma, T, Nomura, T. Drying of sliced raw potatoes in superheated steam and hot air. Drying Technology, 2001; 19(7): 1411-1424.

๖. Caixeta, AT, Moreira, R, Castell-Perez, ME. Impingement drying of potato chips. Journal of Food Process Engineering, 2002; 25: 63-90.

๗. Rordprapat, W, Nathakaranakule, A, Tia, W, Soponronnarit, S. Comparative study of fluidized bed paddy drying using hot air and superheated steam, Journal of Food Engineering, 2005; 71(1): 28-36.

๘. Prachayawarakorn, S, Soponronnarit, S, Wetchakama, S, Jaisut, D. Desorption isotherms and drying characteristics of shrimp in superheated steam and hot air. Drying Technology, 2002; 20(3): 669-684.

๙. Uengkimbuan, N, Soponronnarit, S, Prachayawarakorn, S, Nathkaranakule, A. Drying kinetic and physical properties of dried pork using two-stage techniques, Proceedings of the 2nd International Conference on Innovations in Food Processing Technology and Engineering , Jan 11-13, 2005; Bangkok, Thailand: 320-328.

๑๐. Maskan, M. Drying, Shrinkage and Rehydration Characteristics of Kiwifruits during Hot Air and Microwave Drying, Journal of Food Engineering, 2001; 48: 177-182.

๑๑. Taechapairoj, C, Dhuchakallaya, I, Soponronnarit, S, Watchcama, S, Prachayawarakorn, S. Superheated Steam Fluidised Bed Paddy Drying, Journal of Food Engineering, 2003; 58: 67-73.

๑๒. Taechapairoj, C, Prachayawarakorn, S, Soponronnarit, S. Characteristic of Rice Dried in Superheated-Steam Fluidized-Bed, Drying Technology, 2004; 22(4): 719-743.

๑๓. สมชาติ โสภณรณฤทธิ์, อธิคม จิรจินดาเถิศ, อดิศักดิ์ นาถกรณกุล, ชัยยงค์ เศชะไพโรจน์, การผลิตข้าวกล้องนึ่งด้วยเทคนิค ฟลูอิไดเซชันโดยใช้ไอน้ำร้อนยวดยิ่ง, วารสารราชบัณฑิตยสถาน, ๒๕๔๘; ๓๐(๑): ๗๖-๘๑.

๑๔. Faustman, C. Postmortem Changes in Muscle Foods, In: Muscle Foods Meat Poultry and Seafood Technology, Kinsman, DM, Kotula, AW, Breidenstein, BC, eds., Chapman & Hall, New York, USA, 1994: 63-78.

๑๕. Tang, Z, Cenkowski, S, Izydorczyk, M. Thin-layer Drying of Spent Grains in Superheated Steam, Journal of Food Engineering, 2004; 67: 457-465.

๑๖. Crank, J. The Mathematics of Diffusion, 2nd ed., J. W. Arrowsmith LTD. Bristol, England, 1975; 44-68.

Abstract Effects of drying medium on drying kinetics and beef quality

Chaiyong Taechapairoj
Siriwat Sinprasert
Somkiat Prachayawarakorn
Somchart Soponronnarit
Fellow of the Academy of Science, The Royal Institute, Thailand

Drying method greatly affects drying kinetics and food quality. To obtain desired quality of meat products for serving as snack food, single-stage drying using superheated steam and hot air as well as two-stage drying were selected to investigate their effects on drying kinetics and quality attributes of beef sliced along the longitudinal and transverse directions of muscle fiber. The experiments were set up at drying temperatures of 130-150°C. The samples with the initial moisture contents of 245-255% d.b. were dried until the moisture content of 11% d.b. was reached. The experimental results showed that an increase in drying temperature significantly reduced drying time. However, qualities in terms of color (L, a, b-values), shrinkage, rehydration and hardness were not significantly different amongst drying temperatures ($p > 0.05$). The effective diffusion coefficient of the meat dried by superheated steam was higher than that dried by hot air. The final product obtained form superheated steam drying had more uniform-color and higher degree of shrinkage than that obtained from hot air drying. The muscle fibre orientation had little effect on drying rate and product color. The meat sliced in the transverse direction had lower degree of shrinkage but higher degree of hardness than longitudinal one. The two-stage drying provided the meat product with a light brown color, a higher rehydration capacity, but a lower value of hardness as compared to single drying stage.

Key words : hardness, quality, shrinkage, superheated steam, texture, transverse

Cataloging in Publication Data
Lectures and workshop exercises on drying of agricultural and marine products: Regional Workshops on Drying Technology. A project activity of the ASEAN SubCommittee on Non-Conventional Energy Research. -- Jakarta: Indonesian Institute of Sciences Press 2003.

251 pp.; 21 cm.

Include index
ISBN 979-98014-0-0

1. Food drying. 2. Food – Preservation

664.028 4

EDITORIAL BOARD

Dr Yeoh Bee Ghin - Malaysia – cum- Chairman, ASEAN SCNCER
Mr Abd Shawal B Yaman - Brunei Darussalam
Dr Bun Narith - Cambodia
Dr Suwarto Martosudirjo, APU - Indonesia
Mr Pho Muangnalad - Lao PDR
Prof Dr Mya Mya Oo - Myanmar
Mr Nonilo A Pena - Philippines
Assoc Prof J C Ho - Singapore
Prof Chullapong Chullabodhi - Thailand
Prof Hoang Ngoc Ha - Viet Nam

First published: October 2003
© ASEAN SCNCER 2003

Index by Kamariah Tambunan, Ade Kohar, Mahmudah
Published by LIPI Press, Jln. Gondangdia Lama 39 Menteng Jakarta, Indonesia

Lectures And Workshop Exercises On Drying Of Agricultural And Marine Products

Regional Workshop On Drying Technology

A Project Activity Of
The ASEAN Subcommittee On Non – Conventional Energy Research

Supported by
The ASEAN Foundation

ASEAN SCNCER 2003

RESEARCH AND DEVELOPMENT WORK ON PADDY DRYING IN SOUTH-EAST ASIA

Somchart Soponronnarit* and Somkiat Prachayawarakorn**

* School of Energy and Materials
** Faculty of Engineering

King Mongkut's University of Technology Thonburi
Suksawat 48 Rd., Bangmod, Thungkru, Bangkok 10140, Thailand
Email: somchart.sop@kmut.ac.th

ABSTRACT

Traced back to the last decade, the research work on paddy drying has been conducted in ASEAN countries especially Thailand, Vietnam and the Philippines, in collaboration with the Australian Center for International Agricultural Research. Recently, the Japan International Research Center on Agricultural Sciences has been co-operating with Thailand to conduct research for reducing post-harvest losses of paddy. Most of the work done and being done concentrates on rapid drying by using fluidization and spouted bed techniques, as well as slow drying in storage which is usually called in-store drying. In addition, a lot of effort has been done for the development of rice husk furnace, which is used cyclone concept.

The fluidized bed paddy dryer has been commercialized since 1995. It has been sold to several countries such as Thailand, Cambodia, French Guyana, Indonesia, Laos, Malaysia, Mexico, Myanmar, the Philippines and Taiwan. More than 200 units have been sold so far. The cyclonic rice husk furnace has also been commercialized in several countries since 1998. More than 100 units have been sold. In-store drying of paddy has been accepted for practicing in rice mill in Thailand though it is not very popular due to the limitation of long-term storage. Some rice mills use the technique of in-store drying for aeration of bulk storage of paddy in order to replace grain turning which has been practiced since very long time.

1. INTRODUCTION

It has been suggested that high moisture paddy should be dried rapidly to approximately 23% moisture content (dry basis[1]) then subjected to ambient air slow drying in storage[1,2]. Following two stage drying, cost and product quality appear to be optimised. The dryers with rapid drying techniques commonly used today are LSU dryer, cross-flow dryer, recirculating batch dryer and fluidised bed dryer. In this paper, the rapid drying using techniques of fluidised bed and spouted bed, slow drying in storage using ambient air or near-ambient air and rice husk furnace which has become increasingly popular are explained.

2. FLUIDISED BED PADDY DRYING

Fluidised bed paddy drying is an alternative to conventional hot air drying. Its advantages are: (1) uniform product moisture content and thus high drying air temperature can be employed but with less over-dried grain; (2) high drying capacity due to better heat and mass transfer; (3) as a result of the advantages 1&2, the fluidised bed dryer is compact and thus a significantly lower initial cost; and (4) significant spin-off in terms of increasing head rice yield and potential for producing aging rice.

2.1. The Development of Fluidised Bed Paddy Dryer

Sutherland and Ghaly[3] were probably the first research group who reported feasibility of using fluidisation technique for paddy drying. Their experimental results showed that head rice yield was 58-61% when paddy was dried from 28.2 to 20.5% but was 15-24% when the final moisture content was 19%. Tumambing and Driscoll[4] found that the drying rate was affected by the drying air temperature and the bed thickness under the experimental conditions as follows: drying air temperature of 40-100°C; bed thickness of 5-20 cm and air velocity of 1.5-2.5 m/s. They also developed a mathematical model for a continuous fluidised bed paddy dryer.

Soponronnarit and Prachayawarakorn[5] reviewed the research and development work on fluidised bed drying of grain, and conducted both experimental and simulation studies on batch fluidised bed paddy drying. Soponronnarit et al.[6] described the development of a cross-flow fluidised bed paddy dryer with a capacity of 200 kg/hour. Experimental results showed that final

[1] Unless otherwise stated, the moisture contents (m.c.) quoted in this paper are dry basis

moisture content of paddy should not be lower than 23% if quality in terms of both whiteness and head yield were to be maintained. Drying air temperature was limited at 115°C. Simulation results indicated that the appropriate operating parameters should be as follows: air speed, 2.3 m/s; bed thickness, 10 cm; and fraction of air recycled of 0.8. With these conditions, energy consumption was close to the minimum, while drying capacity was near maximal. In this study, moisture of paddy was reduced from 30 to 24%. Following the success of the development of the cross-flow fluidised bed paddy dryer, Rice Engineering Supply Co. Ltd., a private company in Thailand, showed their interest in collaborating in the development of a prototype with a capacity of approximately 1 t/hour[7]. The prototype is similar to that later developed for commercial unit as shown in Figure 1. It comprises a drying section, a 7.5 kW backward curved blade centrifugal fan, a diesel fuel-oil burner, and a cyclone. The bed length, width and height of the drying section are 1.7, 0.3 and 1.2 m, respectively. The depth of the paddy bed is controlled by a weir. Paddy is fed in and out by rotary feeders. In operation, hot air (temperature controlled by thermostat) is blown into the drying section through a perforated steel sheet floor. The air and grain flows are perpendicular to each other. A small portion of the air leaving the drying chamber is vented to the atmosphere, while the remainder, after cleaning in a cyclone, is recycled to the dryer, mixed with ambient air and reheated to the desired temperature, respectively. The feed rate of paddy can be varied from less than 1 t/hour to more than 1.5 t/hour. Experimental results showed that the unit operated efficiently and yielded high product quality in terms of head yield and whiteness. In reducing the moisture content from 45 to 24% using air temperature of 100-120°C, fraction of air recycled of 0.66, specific airflow rate of 0.05 kg/s-kg dry matter, superficial air velocity of 3.2 m/s, and bed depth of 0.1 m, total primary energy consumption was 2.32 MJ/kg of water evaporated, of which 0.35 was the primary energy from electricity (electrical energy multiplied by 2.6) and 1.79 was the primary energy in terms of heat energy.

As a result of the success of the prototype, commercial fluidised bed paddy dryers with capacities of 5, 10 and 20 t/hour as shown in Figure 1 are now available. More than 200 units have been sold since the beginning of 1995. The fluidised bed dryer is mainly composed of a drying chamber, a backward curved blade centrifugal

fan, a burner using diesel oil or fuel oil for heating air, and a cyclone. Commercial cyclonic rice husk furnace is now available. More than 100 units have been sold since the beginning of 1998.

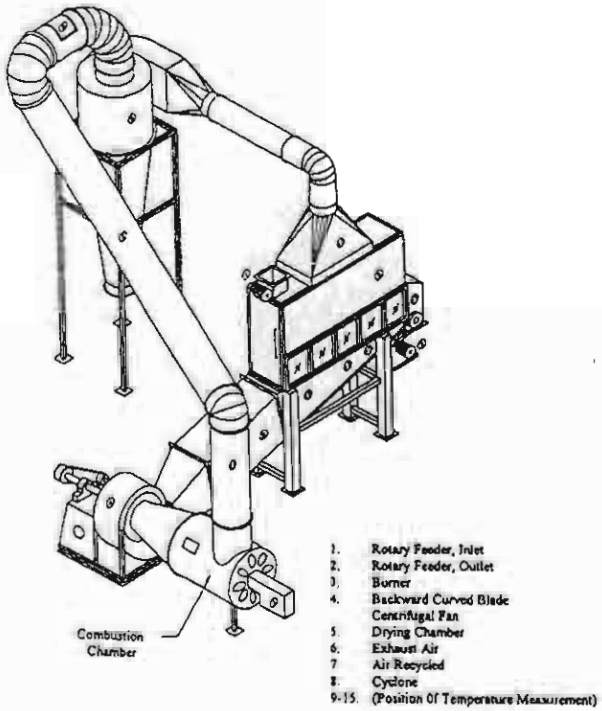


Figure 1 Commercial fluidised bed paddy dryer.

2.2. The Performance of Fluidised Bed Grain Dryer

The minimum fluidised bed velocity for paddy is approximately 1.6 m/s and increases with moisture content[5]. The relationship between pressure drop across the paddy bed and bed velocity is presented in Figure 2.

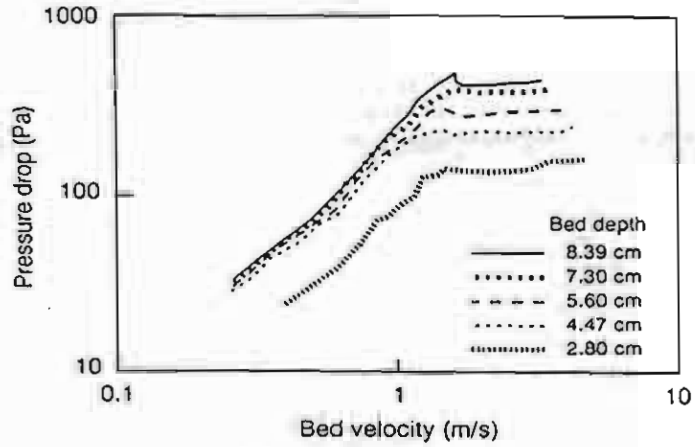


Figure 2 Relationship between bed pressure drop and bed velocity at different bed depths in fluidised bed paddy dryer.

For maize, the minimum fluidised bed velocity increases with moisture content. It varies from 1.5 to1.8 m/s[8]. For soybean, the minimum fluidised bed velocity is 1.9 m/s and varies slightly and inversely with moisture content[9]. The designed fluidised bed velocity is normally 1.5 times of the minimum one.

The performance of commercial fluidised bed paddy dryers with capacities of 2.5-5 t/h and 5-10 t/h are summarized in Table 1[10]. Paddy qualities in terms of head yield and whiteness are all acceptable as compared to paddy dried by ambient air (reference) which is expected to obtain the highest quality. Considering energy consumption, it is relatively low as compared to conventional hot air dryers, except for the case of low inlet paddy moisture content. It is generally recommended to dry paddy from high moisture level to a moisture content of approximately 23% in order to maintain paddy quality. However, it is possible to dry paddy to a lower moisture level if tempering process follows the fluidised bed drying. In addition, as compared to ambient air drying, head yield can be increased if proper drying conditions are provided. The effects of both tempering and drying on paddy quality will be presented in the next section.

Table 1 Performance test results of commercial fluidised bed paddy dryers[10].

Test nos. Testing results	1	2	3	4	5
Drying air temperature (°C)	115	116	120	130	150
Drying air recycled (%)	69	69	69	69	53
Inlet moisture content of paddy (% dry basis)	22.0	26.0	28.7	30.6	27.0
Outlet moisture content of paddy (% dry basis)	20.1	22.5	22.5	23.0	21.0
Outlet paddy temperature (°C)	54.0	52.0	54.0	57.0	63.0
Electrical energy consumed (MJ/kg-water evap.)	0.83	0.43	0.26	0.21	0.15
Thermal energy consumed (MJ/kg-water evap.)	7.80	3.13	2.57	2.21	3.90
Head rice yield (%)					
- dried in fluidised bed dryer	53.2	54.3	53.9	57.0	48.1
- dried by ambient air (reference)	57.4	57.2	53.9	57.0	56.2
Rice whiteness					
- dried in fluidised bed dryer	40.3	40.7	40.0	43.7	36.8
- dried by ambient air (reference)	44.4	44.2	40.1	43.8	42.6
Testing hours	5.0	35.0	46.0	51.0	29.0
Drying capacity (tons/h)	9.5[b]	9.5[b]	9.5[b]	9.5[b]	4.8[a]

Remarks: a = Dryer with capacity of 2.5 – 5.0 tons/h
b = Dryer with capacity of 5.0 – 10.0 tons/h

Soponronnarit et al.[11] investigated in a laboratory how to manage moist paddy by three processes in series, i.e., fluidised bed drying, tempering and ambient air ventilation. Experimental results show that after the three processes, moisture content was reduced from 33% to 16.5% within 53 minutes. During the first process, a fluidised bed dryer with inlet air temperature of 150°C reduced the moisture content of paddy down to 19.5% within 3 minutes. Then the paddy was tempered for 30 minutes. Finally, it was cooled by ambient air with temperature and relative humidity of 30°C and 55-60%, respectively and speed of 0.15 m/s for 20 minutes. Quality of paddy as measured by the head rice yield and whiteness is acceptable.

Soponronnarit et. al.[12] conducted paddy drying using fluidisation technique and paddy tempering following drying in a laboratory and found a significant spin-off. Head yield increases higher than 50% when paddy was dried by fluidisation technique with inlet drying air temperature of 140-150°C and initial moisture content of paddy of 29.9 - 44.9%. As initial moisture content increases, head rice yield increases. Final moisture contents of paddy that can increase head yield to a maximum value are in a range of 23.4 - 28.2%. It is believed that gelatinization especially at the surface of rice kernel is the main factor for increasing head yield. Tempering of paddy after drying can maintain head yield as compared to that without tempering. Rice whiteness of dried paddy is mostly accepted if tempering temperature is not higher than 60°C. For consumer acceptance, tested rice without tempering is not significantly different from that dried by ambient air, while tested rice with tempering, after being cooked, has higher bad smell and lower whiteness. However, this may be solved by reducing tempering time down to 30 minutes.

For other grains, the fluidised bed dryer has a great potential for commercialization. More than ten units have been used in parboiled rice, maize and animal feed (for eliminating trypsin inhibitor) industries. Experimental results obtained from commercial fluidised bed dryers show good performance and good product quality with a significant spin-off that urease activity in soybean kernel could be reduced to an acceptable level as required by animal feed industry.

3. SPOUTED BED DRYER

Spouted bed technique is an alternative way, besides fluidisation, for drying grains that are too coarse and non-uniform in size. The conventional spouted bed shown in Figure 3a has a conical-cylindrical shape[13]. Drying air with a sufficiently high velocity is introduced through a centrally located small opening at the conical base, causing grains to rise rapidly through a hollowed central core, namely spout zone, within the vessel. These grains, after raising a certain height above the bed surface, separate from the air stream and drop into the annulus region. In this region, grains move slowly downward. Some portions of these grains may be re-entrained into the spout region before reaching the bottom, where the mixing of particles is very rigorous. The cyclic and spout

patterns are a very important characteristic of the spouted bed. However, the conventional spouted bed dryers have not been available for industrial applications due to the problems of scale-up and control of cyclic pattern. To overcome such limitations, the modification has been made by inserting the draft plates between the annulus and spout regions. The modified spouted bed dryer is shown in Figure 3b showing that the cyclic movement for grains is improved, comparing to Figure 3a, while the spout characteristic is still maintained[14,15]. The spout and annulus regions that separate definitely by draft plates provide the advantage for drying the heat-sensitive particulate solids in particular paddy, corn and soybean etc.

For the draft plate spouted bed, drying mostly takes place in the spout region since grains are exposed to high air velocity and high temperature whilst drying in the annulus, where the grains and air move in the opposite direction, is really rare because of low air velocity[16]. Such water evaporation rate occurring in this dryer type results in the higher thermal efficiency when compared to the fluidised bed, but the drying capacity becomes relatively lower under the same drying condition[5, 11]. The slow drying rate in the annulus region may reduce the stress inside the grains, thus obtaining the better quality of grains. Madhiyanon et al.[14] conducted the paddy drying experiments in a spouted bed dryer with draft plates. The interesting results are summarised in Table 2. It is seen that thermal energy consumption, in the range of 3.1-3.8 MJ/kg water evaporated at an approximate drying capacity of 3000 kg/h, is relatively comparable to the commercial dryer as previously shown in Table 1. The head rice yield after drying in the spouted bed dryer for each experiment reduces approximately 1% comparing to the sample before drying whilst the reduction in head rice yield from the fluidised bed becomes higher. In addition to higher head rice yield, the rice whiteness is also better. In spite of superior quality of paddy, the spouted bed dryer has not been fully commercialised. This may be because of the relatively low drying rate for this dryer.

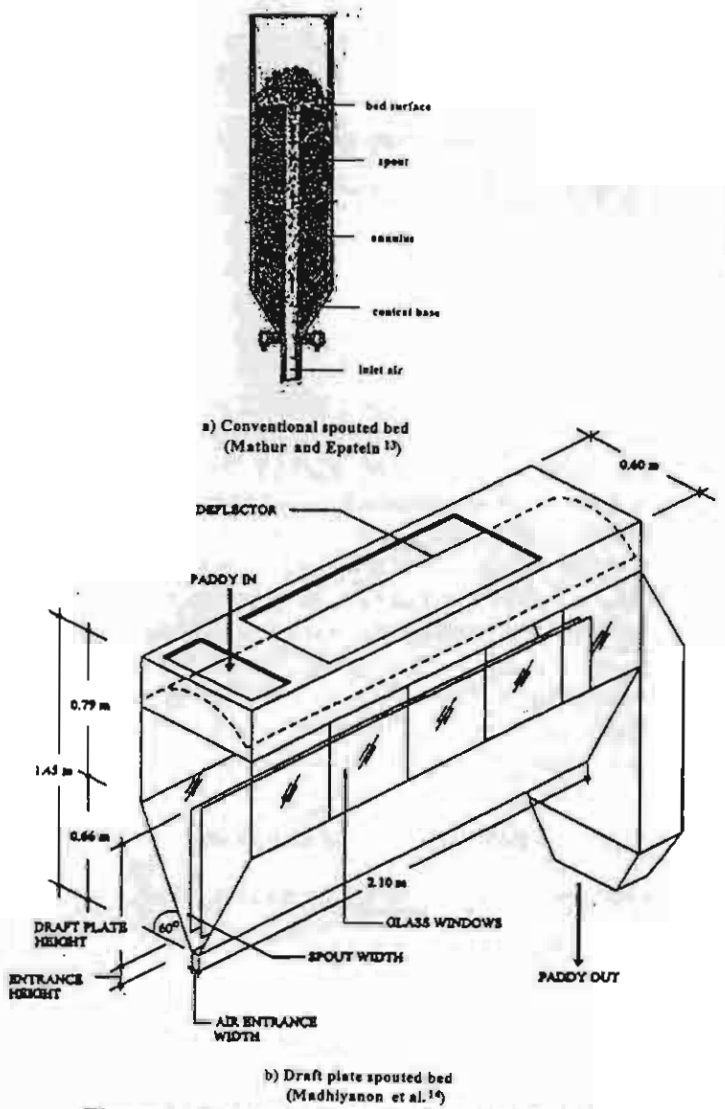


Figure 3 Schematic diagram of spouted bed dryers

Table 2 Summary of paddy drying experiments in the -scale spouted bed (Madhiyanon et al.[14])

Description	Test No.							
	8[a]	9[b]	10[b]	11[c]	12[c]	13[c]	14[c]	15[d]
Feed rate (kg/h)	2470	2440	1990.	2370	2400	3160	3280	3550
Hold-up (kg)	60	360	340	240	210	335	290	310
Residence time (min)	1.5	8.9	10.2	6.0	5.3	6.4	5.3	5.2
Average inlet air temp. (°C)	154	149	141	152	159	154	156	160
Exit grain temp. (°C)	68	71	66	71	68	67	67	68
Average moisture content								
BFD (% dry basis)	26.1	21.7	28.5	22.1	25.0	29.4	28.2	22.8
AFD (% dry basis)	22.7	17.5	23.6	17.1	19.7	25.0	23.3	19.0
Head rice yield								
BFD (%)	56.1	45.9	53.3	49.0	49.6	50.1	54.3	41.2
AFD (%)	58.9	45.7	54.2	47.4	48.4	52.4	55.0	40.8
Whiteness								
BFD	41.9	45.7	44.2	47.6	47.6	47.8	46.4	46.7
AFD	41.6	45.4	45.0	46.8	46.7	47.5	46.3	45.9
Drying rate (kg water/h)	68	87	79	101	106	111	130	101
Energy consumption (MJ/kg water evaporated)								
Heat	6.5	7.0	N/A	4.4	5.2	3.5	3.8	3.1
Electricity	0.60	0.60	0.60	0.50	0.50	0.46	0.40	0.46

AFD, after drying; BFD, before drying; N/A, not available; temp., temperature.

[a]Draft channel blade angle 85°; entrance height, 10 cm.

[b]Draft channel blade angle 89°; entrance height, 10 cm.

[c]Draft channel blade angle 89°; entrance height, 12.5 cm.

[d]Draft channel blade angle 89°; entrance height, 15 cm.

4. IN-STORE DRYING

In-store drying technique, known as the fixed bed grain drying, can be suitably applied for the relatively low initial moisture contents of grains, 22-25% dry basis[17]. This technique offers the superior quality of grains and the effective heat utilisation. Figure 4 shows schematically an in-store drying system of which a bin, a heater unit and a ventilation system are the main component.

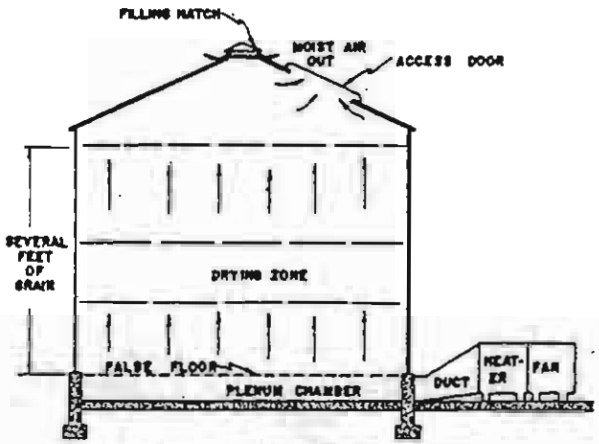


Figure 4 In-store drying system (Brooker et al.[18])

The drying zone starts at the bottom and then moves on the top. A low airflow rate is often used in order to avoid the large pressure drop in the bed. For drying paddy at the initial moisture content between 20% and 22% dry basis under the hot and humid weather, the ambient airflow rate should be in the range between 0.5 and 1.0 m^3/min-m^3 of paddy and the relative humidity should not be higher than 75% [17]. The slightly heated air may be required when the severe air conditions are being encountered. This ensures that the already dried paddy will not be adsorbed the water vapour from the humid air. If the paddy adsorbs the water, it may cause the lower strength of grain[19]. In addition to the cause of such high inlet humidity, the moisture migration within the grain bulk caused by the gradient of temperatures can also occur naturally during the long-term storage, resulting in the grain adsorption, even though air is not blown through the bulk. The proper ventilation can terminate the moisture migration. Soponronnarit et al.[20] studied the field trial of in-store drying and storage using ambient temperature and airflow rate of 0.57 m^3/min-m^3 of paddy. During 19-week storage, the air ventilation was taken twice a week, at least 2 or 3 hours in each time. The moisture migration was not found and the paddy qualities in terms of whiteness and head rice yield obtained did not change, comparing to the samples at the beginning.

Another quality index of commercial interest, besides the head rice yield, is the rice yellowing. The rice yellowing is a serious

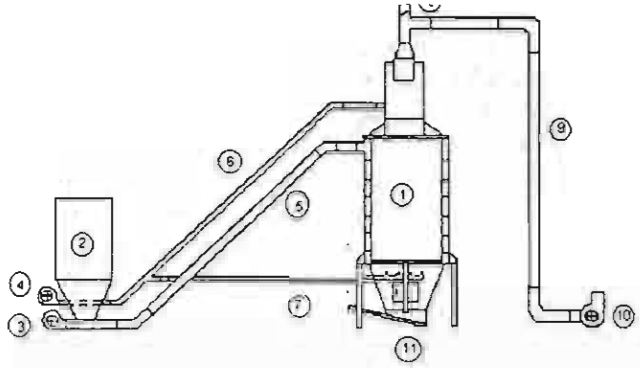
problem in the tropical region. Trashing and drying delays may cause the yellowing[21]. The yellow kernels were found in the moist paddy having the moisture content higher than 25% dry basis, corresponding to the higher water activity of 0.96. The resulting rapid microorganism growth could be occurred and the grains were then heated up to temperatures between 45 and 60°C. Phillips et al.[22] noticed that the kernels at the central area of paddy bulk where high temperature exists had an intense yellow within 2-3 days whereas the kernels at the bulk surface had a fewer yellow. The mechanism of yellowing is not fully understood although a large number of investigations have been attempted to pursue this cause. According to the previous works, we may summarise that the yellowing of paddy is due to the metabolic activities of microbial and the non-enzymatic browning or the Millard reaction[23-25]. Whether the yellowing of paddy takes place by the microorganisms or by the Millard reaction, the moisture content and the temperature are the important factors contributing to the degree of yellowness. The yellowing of rice produced inside the kernels is not uniform, decreasing a degree of yellowness from the surface to the inner layers[25].

Recently, a quantitative study of influences of the water activity temperature and temperature and storage atmosphere on the yellowing of paddy has been studied. Some workers[26,27] reported that the water activity and the temperature strongly affected the degree of yellowness whilst the O_2 was less significant. The yellowing kinetic formulated by Gras et al.[26] was described by the following power law model: $k = \alpha . e^{\beta T}(a_w)^{\gamma}[O_2]^{\delta}$ where k is the rate of yellowing (Hunter b unit/day), T is the absolute temperature (K), a_w is the water activity, O_2 is the oxygen content (mol/m^3) and δ, β, α and γ are the constants. By contrast, Soponronnarit et al.[28] found the yellowing rate followed with the zero order kinetic model, $ln\ k = \alpha - \delta a_w - \varepsilon/T + (\gamma a_w)/T$ where δ, ε, α and γ are the constant values.

5. RICE HUSK FURNACE

Singh et al.[29] designed and tested a cyclonic rice husk furnace for drying one ton of paddy with initial moisture content of 35% down to 14% dry basis. Efficiencies of the furnace were different at various rice husk feed rates and air flow rates. The highest efficiency was 80% with the rice husk feed rate of 20 kg/h and air flow rate of 168 m^3/h. Tumambing[30] investigated the performance of the cyclonic

rice husk furnace of Padicor for paddy drying and found that the combustion efficiency was 98%. Xuan et al.[31] designed and tested two types of rice husk furnace. The first one was a furnace with inclined grate and cylindrical combustion chamber. The upper part of the furnace was a heat exchanger. Inlet air entered at the lower part of inclined grate on which rice husk with a feed rate of 20-25 kg/h was burnt. The efficiency of the furnace was 70%. The second one was a pneumatic-fed cyclonic furnace. It consisted of combustion chamber and rice husk feed system. Rice husk was fed into the combustion chamber with primary air and was burnt. Then it fell down to the lower part of the chamber. The secondary air entered at the upper part of the combustion chamber in tangent direction in order to eliminate dust from flue gas. Rice husk consumption and furnace efficiency were 10-12 kg/h and 75%, respectively. The past research showed that there were several designs of rice husk furnace, i.e. vortex or inclined grate types and direct use of flue gas or indirect use of thermal energy from combustion via heat exchanger. However, acceptance of the furnace was still limited in the experimental sites.



1 combusti chamber
2 ricehusk hopper
3 conveyi fan of rice husk syste
4 conveyi fan of air feeding
5 primary air duct
6 secondary air
7 tertiary air
8 butterfly
9 exit air
10 suctioblowe
11 scre convey

Figure 5 Schematic diagram of the cyclonic rice husk furnace[32]

Soponronnarit et al.[32] reported a success of the development of a commercial-scale prototype of cyclonic rice husk furnace for a commercial fluidized bed paddy dryer with a capacity of 10 tons/h as shown in Figure 5. The furnace consisted of a combustion chamber, feeding systems of air and rice husk, a control system and a suction blower. The combustion chamber was made of steel in cylindrical shape with inner and outer diameters of 1.37 and 1.76 m, respectively and height of 2.75 m. Materials inside the combustion chamber at the lower part from inner layer to outer layer were the following: fire brick, steel, glass fiber and covering steel. There was a grate with diameter of 1.37 m, thickness of 9.5 mm (583 holes/m^2, hole diameter 0.0127 m) and ash paddle with cross-section 50 x 50 mm and length 1.1 m at the lower part of combustion chamber. The primary air duct was connected to the upper part of the combustion chamber in tangential direction. On the upper part of the combustion chamber, a steel cylinder with inner diameter of 0.8 m and height of 1.6 m was installed and connected to the secondary air duct in tangential direction in order to clean up flue gas. The cylinder was insulated with cement 60 mm thick. Rice husk ash was removed from the combustion chamber by the ash paddle followed by a screw conveyor installed under the combustion chamber. The tertiary air duct was connected to the bottom part of the combustion chamber in

order to support complete combustion. The rice husk feeding system consisted of a rice husk hopper with a screw installed at the bottom and driven by a 0.37 kW motor, a 0.152 m diameter primary air duct for pneumatic feed of rice husk and a fan. The secondary air duct was 0.102 m in diameter. The tertiary air duct with diameter of 0.076 m separated from the secondary air duct and then was divided into 4 ducts with distributors at the bottom of the combustion chamber under the grate. Air suction system consisted of a 15 kW blower, a duct with diameter of 0.254 m and a valve for regulating the fraction of fresh air into the combustion chamber.

The experimental results showed that for heights of ash on grate 30, 45, 50 and 60 cm, rice husk feed rates 110-136 kg/h, and excess air 265-350%, the combustion gas temperature was approximately 523-710°C. Thermal efficiency of the furnace system increasing with excess air was approximately 57-73% while carbon conversion efficiency was approximately 89-97%. The height of ash on grate had no effect on the system performance. Financial analysis indicated that the pay-back period of the furnace was 1200 hours, when using in place of the diesel oil burner. Latest information shows that the rice husk furnace has been commercialized for almost 100 units in several countries since 1998.

6. CONCLUSION

The first fluidised bed paddy dryer was first commercialized in Thailand in 1995. It is probably the first commercial large-scale continuous fluidised bed dryer for paddy drying. Since then, more than 200 units with capacities of 5, 10 and 20 t/hour have been sold in Thailand, the Philippines, Indonesia, Malaysia, Myanmar, Laos, Spain, Guyana and Taiwan. Due to high operating cost from using diesel oil, rice husk furnace has become increasingly popular. The cyclonic rice husk furnace as illustrated in this paper has been commercialized for almost 100 units in several countries since the beginning of the year 1998. The fluidised bed paddy dryer is competitive with conventional hot air dryers especially at high moisture level, i.e. low energy consumption, low cost and acceptable paddy quality. Important operating parameters are:drying air temperature of 140 - 150°C, fraction of air recycled of 0.8, air velocity around 2.0 - 2.3 m/s and bed thickness of 10 - 15 cm. Under proper conditions such as high initial moisture content of paddy (higher than 29.9%) and high air temperature (140 - 150°C), head

yield can be increased up to 50% compared to ambient air drying. For consumer acceptance, tested rice with fluidised bed drying is not significantly different from that dried by ambient air.

Spouted bed paddy drying has been researched in the ASEAN region especially in Thailand and Vietnam. It is expected to be an alternative technique besides fluidised bed drying. However, the advantage of using spouted bed technique is not very clear. Therefore, it has still been not commercialised yet.

In-store paddy drying has been accepted for a limited number of rice mill in Thailand due to the requirement of long term storage in spite of its advantage in terms of low energy consumption and high quality product of head rice yield. However, this technique has been successfully in several rice mills for aeration of bulk storage of paddy in order to replace grain turning.

7. ACKNOWLEDGMENT

Thanks are due to the Thailand Research Fund, the Australian Centre for International Agricultural Research and the Japan International Research Center on Agricultural Sciences for financial support to the Research Group on Drying Technology, King Mongkut's University of Technology Thonburi, Thailand.

8. REFERENCES

(1) Soponronnarit, S., Wongvirojtana, P., Nathakaranakule, A, and Prachayawarakorn, S. 1994. Maintaining paddy quality by appropriate ventilation under tropical climate. Proceedings of the 9th International Drying Symposium, Gold Coast, Australia, 1-4 Aug 1994, pp. 825-832

(2) Driscoll, R.H, and Srzednicki, G.S. 1991. Design for a complete grain drying system under Southeast Asian climates. Proceedings of the 12th ASEAN Technical Seminar on Grain Post-harvest Technology, Surabaya, Indonesia, 29-31 Aug 1989.

(3) Sutherland, J.W, and Ghaly, T.F. 1992. Rapid fluid bed drying of paddy rice in the humid tropics. Proceedings of the 13th ASEAN Conference on Grain Post-harvest Technology, Brunei Darussalam, 4-7 Sep 1990.

(4) Tumambing, J.A, and Driscoll, R.H. 1993. Modeling the performance of continuous fluidized bed paddy dryer for rapid pre-drying of paddy. Proceedings of the 14th ASEAN seminar on Grain Post-harvest Technology, Manila, Philippines, 5-8 Nov 1991, pp. 193-213.

(5) Soponronnarit, S. and Prachayawarakorn, S. 1994. Optimum strategy for fluidized bed paddy drying. *Drying Technology*. 12: 1667-1686.

(6) Soponronnarit, S., Prachayawarakorn, S. and Sripawatakul, O. 1996. Development of cross-flow fluidized bed paddy dryer. *Drying Technology*. 14: 2397-2410.

(7) Soponronnarit, S., Yapha, M. and Prachayawarakorn, S. 1995. Cross-flow fluidized bed paddy dryer: prototype and commercialization. *Drying Technology*. 13: 2207-2216.

(8) Soponronnarit, S., Pongtornkulpanich, A. and Prachayawarakorn, S. 1997. Drying characteristics of corn in fluidized bed dryer. *Drying Technology*. 15: 1603-1615.

(9) Soponronnarit, S., Swasdisevi, T., Wetchacama, S. and Wutiwatchai, W. 2000. Fluidised bed drying of soybeans. *J. Stored Products Research*. 37: 133-151.

(10) Soponronnarit, S., Prachayawarakorn, S, and Wangji, M. 1996. Commercial fluidized bed paddy dryer. Proceedings of the 10th International Drying Symposium, Krakow, Poland. 30 July - 2 Aug 1996, Vol. A: 638-644.

(11) Soponronnarit, S., Wetchacama, S., Swasdisevi, T. and Poomsa-ad, N. 1999. Managing moist paddy by drying, tempering and ambient air ventilation. *Drying Technology*. 17: 335-344.

(12) Soponronnarit, S., Taweerattanapanish, A., Wetchacama, S., Kongseri, N, and Wongpiyachon, S. 1998. Spin-off from paddy drying by fluidization technique. Proceedings of the 7th International Working Conference on Stored-Product Protection, Beijing, China, 14-19 Oct 1998.

(13) Mathur,E.B. and Epstein, N. 1974. Spouted Beds. Academic Press, Inc. New York.

(14) Madhiyanon, T., Soponronnarit, S. and Tia, W. 2001. Industrial-scale prototype of continuous spouted bed paddy dryer. *Drying technology*. 19: 207-216.

(15) Hung-Nguyen, L., Driscoll R.H. and Srzednicki, G. S. 2001. Drying of high moisture content paddy in a pilot scale triangular spouted bed dryer. *Drying Technology*. 19: 375-387.

(16) Hung-Nguyen, L., Driscoll, R.H, and Srzednicki, G.S. 1998. Drying characteristics of high moisture paddy in a novel triangular spouted bed dryer. Proceedings of the 11 th Int. Drying Symp. (IDS'98), Thessaloniki, Greece, pp. 1397-1404.

(17) Soponronnarit S, Wongvirojtana, P., Nathakaranakule, A. and Chinsakolthanakorn, S. 1995. Design charts for in-store paddy drying under hot and humid climates. *Agri. Enginnering J.* 4: 147-162.

(18) Brooker, D.B., Bakker-Arkema, F.W. and Hall, C.W. 1992. Drying and storage of grains and oilseeds. Van Nostrand Reinhold Publisher, New York.

(19) Kunze O.R. 1995. Effect of drying on grain quality. Proceedings of the International Conference on Grain Drying in Asia, Bangkok, 17-20 Oct 1995.

(20) Soponronnarit S., Amatachaya, P., Prachayawarakorn, S., Nathakaranakule, A. and Inchan, S. 1997. Field trial of in-store drying and storage. *Kasetsart J.* 18: 86-100.

(21) Mendoza, E.E., Jr. and Rigor, A.C. 1982. Grain quality deterioration in on-farm level of operation. Proceddings of the 5th Annual Workshop on Grain Post-Harvest Technology, pp. 101-107.

(22) Phillips S., Mitfa, R. and Wallbridge, A. 1989. Rice yellowing during drying delays. *J. Stored Product Research*. 25: 155-164.

(23) Quitco, R.T. 1982. Studies of fungal infection and heating of paddy. Proceedings of GASGA Seminar, Paddy Deterioration in the Humid Tropics, Baguio, 1981, Philippines, pp. 52-56, GTZ, Eschborn.

(24) Indudhara Swamy, Y.M., Ali, S.Z. and Bhattacharya, K.R. 1971. Relationship of moisture and temperature to discoloration of rice during storage. *J. Food Sci Technol*. 8:150-152.

(25) Yap, A.B., Juliano, B.O, and Perez, C.M. 1988. Artificial yellowing of rice at 60°C. Proceedings of 11 th ASEAN Technical Seminar on Grain Post-Harvest Technology, Kuala Lumpur, Malaysia, 23-26 Aug 1988.

(26) Gras, P.W., Banks, H.J., Bason, M.L. and Arriola, L.P. 1989. A quantitative study of the influence of temperature, water activity and storage atmosphere on the yellowing of milled rice. *J. Stored Prod Res*. 9: 77-89.

(27) Bason, M.L., Gras, P.W., Banks, H.J. and Esteves, L.A. 1990. A quantitative study of the influence of temperature, water activity and storage atmosphere on the yellowing of paddy endosperm. *J. Cereal Science*. 9: 77-89.

(28) Soponronnarit, S., Srisubati, N. and Yoovidhya, T. 1998. Effect of temperature and relative humidity on yellowing rate of paddy. *J. Stored Product Research*. 34: 323-330

(29) Singh, R., Maherhweri, R.C. and Ojha, T.P. 1980. Development of husk fired furnace. *The British Society for Research in Agricultural Engineering*. India, pp. 109-120.

(30) Tumambing, J.A., 1984. Testing and evaluation of rice hull-fed furnaces for grain drying. National Post Harvest Institute for Research and Extension, the Philippines, pp. 197-214

(31) Xuan, N.V., Vinh, T., Anh, P.T, and Hien, P. 1995. Development of rice husk furnaces for grain drying: Proceedings of the International Conference on Grain Drying in Asia, Bangkok, Thailand, 17-20 Oct 1995, pp. 109-120.

(32) Soponronnarit, S., Swasdisevi, T., Wetchacama, S., Shujinda, A. and Srisawat. A. 2000. Cyclonic rice husk furnace and its application on paddy drying. *International Energy Journal*._1: 67-75.

ANNEX

DEVELOPMENT OF MATHEMATICAL MODEL OF FLUIDISED BED GRAIN DRYING

It was assumed that there is thermal equilibrium between the drying air and the product, and that the air and grain flow were in plug type. Experimental results reported by Sripawatakul[1] indicated that the flow regime of paddy was between near plug flow and high dispersion flow. Though dispersion was a known factor in the fluidised bed, the mathematical model assumed plug flow in order to simplify calculation. The model is similar to that presented by Soponronnarit and Prachayawarakorn[2]. Figure 1 shows control volumes (CVs) for the derivation of energy and mass balance equations.

◂ grain flow; ← air flow; T, temperature; W, humidity ratio; M, grain moisture content; Q, heat; CV, control volume.

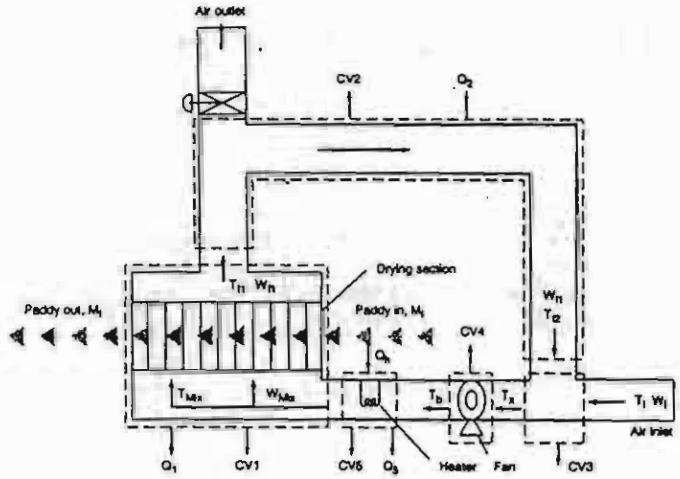


Figure 1 Control volume's of continuous cross-flow fluidised bed drying system

1. Equation of Mean Residence Time

The empirical equation of mean residence time of paddy developed by Sripawatakul[1] was used. It is written as follows:

$$\tau = hu/F \qquad (1)$$

where τ = mean residence time, second (s)
hu = hold up, kg
F = feed rate, kg/s

and $hu = [\{-0.0095000 + 0.59870\ F - (0.00020000 + 0.17360\ F)\ V\} + \{1.1728 - 0.082300\ V + (2.2093 - 0.15050\ V)\ F\}\ h]\ \rho_p A$

where A = paddy bed area, m^2
V = air velocity, m/s
ρ_p = average product density, kg/m^3
h = weir height, m

It is valid for weir heights in the range 0.04 - 0.10 m, air velocities in the range 1.7 - 2.3 m/s, and paddy feed rates in the range 0.025-0.058 kg/s. For a rough calculation, hu is approximately equal to $hA\rho_p$ and can be applied to other grains.

Dividing the paddy bulk into n layers, changes in moisture content of paddy, temperature, and the humidity ratio of air were calculated for each layer. The following basic equations were employed.

2. Equation for the Drying Rate

The empirical equation for fluidised bed paddy drying in the form of the equation of Page[3], developed by Sripawatakul[1], was used. It is written as follows:

$$MR = \exp\{-x(t/60)^y\} \quad (2)$$

where $MR = (M - M_{eq})/(M_{in} - M_{eq})$
t = drying time, s
$x = 0.00163100\ T_{mix} - 1.16202\ (m_{mix}/hu) + 0.00415300\ (m_{mix}/hu)\ T_{mix} + 0.147383\ \ln(m_{mix}/hu) + 0.474743$
$y = -0.00322000\ T_{mix} - 0.835960\ (m_{mix}/hu) + 0.0203190\ (m_{mix}/hu)\ T_{mix} - 0.143150\ \ln(m_{mix}/hu) + 0.548493$

Equation (2) is similar to that developed by Soponronnarit and Prachayawarakorn[2] for higher specific airflow rate (m_{mix}/hu). It is valid for temperatures of 90 - 140°C and specific airflow rates of 0.03 - 0.16 kg/s/kg dry matter of paddy. The symbols are defined as follows:

M = moisture content of paddy at time t, decimal dry basis
M_{in} = moisture content of paddy at the inlet of drying section, decimal dry basis
M_{eq} = equilibrium moisture content, decimal dry basis
T_{mix} = air temperature at the inlet of drying section, °C
m_{mix} = airflow rate at the inlet of drying section, kg/s

During calculation, Equation (2) was differentiated with time, and finite difference was employed to obtain the solution. Equilibrium moisture content was determined using the equation developed by Laithong[4].

For the drying rates of maize and soybean, they are available in Soponronnarit et al.[5] and Soponronnarit et al.[6], respectively.

3. Equation of Mass Conservation

$$W_{fl,i} = R(M_i - M_f) + W_{mix} \quad (3)$$

where
$W_{fl,i}$ = humidity ratio of outlet air at the i^{th} layer, kg water/kg dry air
W_{mix} = humidity ratio of inlet air at the i^{th} layer, kg water/kg dry air
M_i = moisture content of paddy at the inlet of i^{th} layer, decimal dry basis
M_f = moisture content of paddy at the outlet of i^{th} layer, decimal dry basis
R = ratio of dry mass of paddy to mass of dry air.

4. Equation of Energy Conservation

$$T_{fl,i} = [Q_l/m_{mix} + C_a T_{mix} + W_{mix}(h_{fg} + C_v T_{mix}) - W_{fl,i} h_{fg} + RC_{pw} T_{mix}]/(C_a + W_{fl,i} C_v + RC_{pw}) \quad (4)$$

where $T_{fl,i}$ = temperature of outlet air at the i^{th} layer, °C
Q_l = heat loss, kW
C_a = specific heat of dry air, kJ/kg °C
C_v = specific heat of vapour, kJ/kg °C
C_{pw} = specific heat of moist paddy, kJ/kg °C
h_{fg} = latent heat of moisture vaporisation, kJ/kg

Average temperature and humidity ratio of the outlet air from n layers were determined by arithmetic mean.

For other calculations such as mixing of air streams, and consumption of energy at the fan and the heater, solutions can be achieved by the application of first law of thermodynamics [see Soponronnarit and Prachayawarakorn[2] for details].

The equations were solved by iteration. Firstly, the value of exit humidity ratio of air was assumed. The equations presented by Wilhelm[7] were used to determine properties of moist air.

The accuracy of the mathematical model was tested and found to be in good agreement with the experimental results. The model was employed to investigate optimum operating parameters such as air temperature, specific airflow rate, and fraction of air recycled. Details for paddy drying and maize drying are available in Soponronnarit et al.[8] and Soponronnarit et al.[5], respectively.

5. Further Development of the Mathematical Model

In simulation of multi-stage drying including the tempering between each stage, the moisture profile in a grain kernel at the end of each drying stage must be known. Unfortunately, the moisture profile in a grain kernel cannot be predicted by the empirical drying equations such as Equation (2). But, it can be determined only by using a theoretical equation, mostly described by the Fick's unsteady state diffusion equation in which an effective moisture diffusion coefficient is taken into account.

Poomsa-ad et al.[9] developed the mathematical model for the simulation of multi-stage drying including the tempering between each stage. It was assumed that water moves in the combined radial and axial direction and paddy is an isotropic solid. The partial differential equation of moisture diffusion for a single paddy kernel considered geometrically to be a finite cylindrical shape can be written as follows:

$$\frac{\partial M}{\partial t} = D\left[\frac{\partial^2 M}{\partial r^2} + \left(\frac{1}{r}\right)\frac{\partial M}{\partial r} + \frac{\partial^2 M}{\partial z^2}\right] \qquad (5)$$

where

D = effective moisture diffusion coefficient, m/s^2
r = coordinate along the radius of cylinder, m
z = coordinate along the length of cylinder, m

The initial and boundary conditions for paddy drying are given by

$t=0,\ 0 \le r \le r_o$	$M = M_{in}$ or $M = M(r,z)$
$-\ell \le z \le +\ell$	$M = M_{in}$ or $M = M(r,z)$
$t>0,\ r = r_o$	$M = M_{eq}$
$z = \pm\ell$	$M = M_{eq}$
$t>0,\ r = 0$	$\frac{\partial M}{\partial r} = 0$

where ℓ = half length of cylinder, m
r_o = radius of cylinder, m

The effective moisture diffusion coefficient described by the Arrhenius type equation is given as follows:

$$D = 5.41141 \times 10^{-6} \exp\left(\frac{-28436.4}{R(273.15+T)}\right) \qquad (6)$$

where R = universal gas constant, kJ/kmol-K

For tempering process, moisture profile at the end of the first stage drying is used as the initial condition. During this period, the moisture inside a paddy kernel transports to the exterior surface, but it does not evaporate to the environment. The redistribution of moisture inside the kernel can be described again by Eqn. (5) with the new boundary and initial conditions as follows:

$t=0,$	$M = M(r,z)$
$t>0,\ r = r_o$	$\frac{\partial M}{\partial r} = 0$
$z = \pm\ell$	$\frac{\partial M}{\partial z} = 0$
$t>0,\ r = 0$	$\frac{\partial M}{\partial r} = 0$

The finite difference method was employed for solving Equation (5) using proper initial and boundary conditions for each process. The simulation results are in good agreement with the experimental results including a series of drying, tempering and subsequent drying.

REFERENCES

(1) Sripawatakul, O. 1994. Study of drying paddy by cross-flow fluidization technique. Master's thesis, Faculty of Engineering, King Mongkut's Institute of Technology Thonburi, Bangkok, Thailand, in Thai.

(2) Soponronnarit, S. and Prachayawarakorn, S., 1994. Optimum strategy for fluidized bed paddy drying. *Drying Technology.* 12:1667-1686.

(3) Page, G.E. 1949. Factors influencing the maximum rate of drying shelled corn in layers. Unpublished thesis, Master of Science, Purdue University.

(4) Laithong, C. 1987. Study of physico-thermal properties of rough rice. Master's thesis, King Mongkut's Institute of Technology Thonburi, Bangkok, Thailand, in Thai.

(5) Soponronnarit, S., Kittiporn, K. and Prachayawarakorn, S. 1997. Appropriate operating parameters for fluidized bed corn drying. *RERIC International Energy Journal.* 19: 1-13.

(6) Soponronnarit, S., Swasdisevi, T., Wetchacama, S. and Wutiwatchai, W. 2000. Fluidised bed drying of soybeans. *Journal of Stored Product Research.* 37: 133-151

(7) Wilhelm, L.R. 1976. Numerical calculation on psychrometric properties in SI units. *Transactions of the American Society of Agricultural Engineers.* 19: 318-321, 325

(8) Soponronnarit, S., Prachayawarakorn, S. and Sripawatakul, O. 1996. Development of cross-flow fluidized bed paddy dryer. *Drying Technology.* 14: 2397-2410.

(9) Poomsa-ad, N., Soponronnarit, S., Prachayawarakorn, S. and Terdyothin, A. 2002. Effect of tempering on subsequent drying of paddy using fluidisation technique, *Drying Technology.* 20: 195-210.

© ADC'03

FLUIDISED BED GRAIN DRYING

Somchart Soponronnarit

School of Energy and Materials
King Mongkut's University of Technology Thonburi
Suksawat 48 Road, Bangkok 10140, Thailand

The fluidised bed grain dryer is now fully commercialized in several countries. Its potential is great especially for high moisture grains such as paddy, parboiled rice, maize and soybean. Its drying rate is very fast as compared to conventional grain dryers. Consequently, the size of drying unit is very compact relative to its capacity. Its energy consumption is relatively low while grain quality is maintained. In this paper, the research and development effort on fluidised bed grain drying especially in Thailand is described, starting with an experimental batch dryer and culminating with a commercial continuous-flow dryer. A mathematical model of the fluidised bed grain drying system including a series of drying, tempering and ambient air ventilation is also described.

Introduction

It has been suggested that high moisture paddy should be dried quickly to approximately 23% moisture content (dry basis[1]) then subjected to ambient air drying in storage (Soponronnarit et al. 1994; Driscoll and Srzednicki 1991). Following two-stage drying, cost and product quality appear to be optimised. During the first stage, fluidised bed drying is an alternative to conventional hot-air drying. Its advantages are: (1) uniform product moisture content, and thus high drying air temperature can be employed but with less over dried grain; (2) high drying capacity due to better heat and mass transfer; (3) a much smaller drying chamber and thus a

[1] Unless otherwise stated, the moisture contents (m.c.) quoted in this paper are dry basis.

significantly lower initial cost; and (4) significant spin-off in terms of increasing head rice yield and potential for producing aging rice.

Sutherland and Ghaly (1992) were probably the first research group who investigated feasibility of using fluidisation technique for paddy drying. Japanese researcher may have conducted similar research work before. Experimental results reported by Sutherland and Ghaly (1992) showed that head yield was 58-61% when paddy was dried from 28.2 to 20.5% but was 15-24% when the final moisture content was 19%. Tumambing and Driscoll (1993) found that drying rate was affected by drying air temperature and bed thickness under experimental conditions as follows: drying air temperature of 40-100°C; bed thickness of 5-20 cm and air velocity of 1.5-2.5 m/s. They also developed a mathematical model for continuous fluidised bed paddy dryer.

Soponronnarit and Prachayawarakorn (1994) have reviewed the research and development work on fluidised bed drying of grain, and conducted both experimental and simulation studies on batch fluidised bed drying of paddy. Soponronnarit et al. (1996a) described the development of a cross-flow fluidised bed paddy dryer with a capacity of 200 kg/hour (Figure 1).

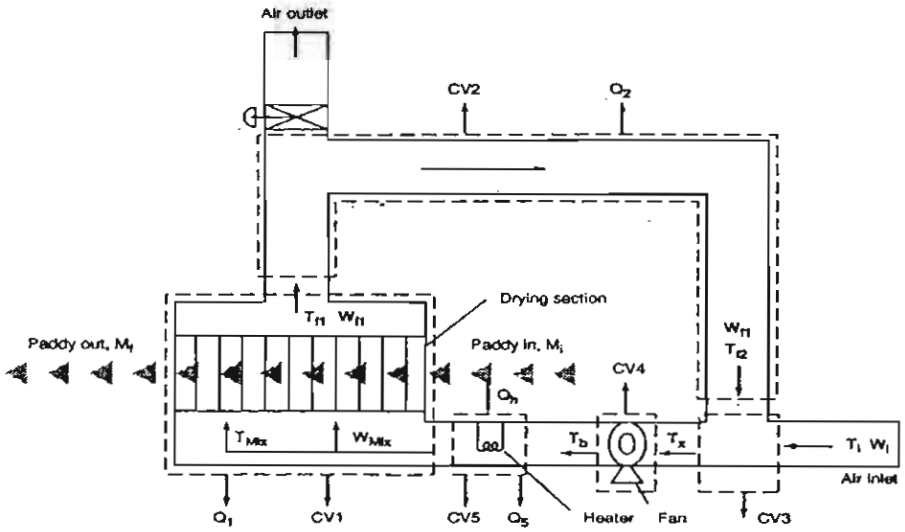


Figure 1. Control volumes of continuous cross-flow fluidised bed drying system: ↓ grain flow; ← air flow; T, temperature; W, humidity ratio; M, grain moisture content; Q, heat; CV, control volume

Experimental results showed that final moisture content of paddy should not be lower than 23% if quality in terms of both whiteness and head yield were to be maintained. Drying air temperature was 115°C. Simulation results indicated that the appropriate operating parameters

should be as follows: air speed, 2.3 m/s; bed thickness, 10 cm; and fraction of air recycled of 0.8. With these conditions, energy consumption was close to the minimum, while drying capacity was near maximal. In this study, moisture of paddy was reduced from 30 to 24%.

Following the success of the development of the cross-flow fluidised bed paddy dryer, Rice Engineering Supply Co. Ltd., a private company in Thailand, showed interest in collaborating in the development of a prototype with a capacity of approximately 1 t/hour (Soponronnarit et al. 1995). The prototype is shown diagrammatically in Figure 2.

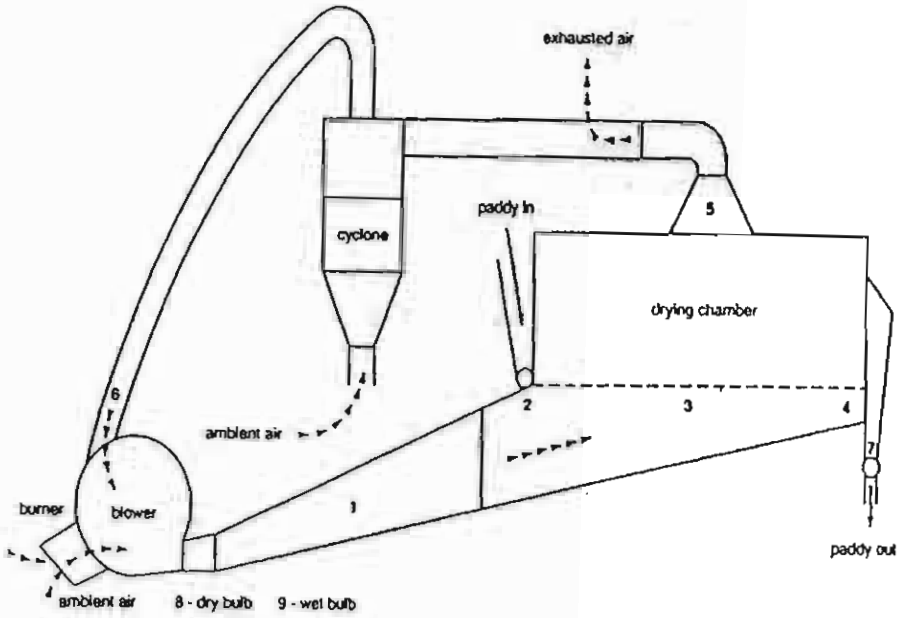


Figure 2. Diagram of fluidised bed paddy dryer

It comprises a drying section, a 7.5 kW backward curved blade centrifugal fan, a diesel fuel-oil burner, and a cyclone. The bed length, width and height of the drying section are 1.7, 0.3 and 1.2 m, respectively. The depth of the paddy bed is controlled by a weir. Paddy is fed in and out by rotary feeders. In operation, hot air (temperature controlled by thermostat) is blown into the drying section through a perforated steel sheet floor. The air and grain flows are perpendicular to each other. A small portion of the air leaving the drying chamber is vented to the atmosphere, while the remainder, after cleaning in a cyclone, is recycled to the dryer, mixed with ambient air and reheating to the desired temperature, respectively. The feed rate of paddy can be varied from less than 1 t/hour to more than 1.5 t/hour. More detail is given in Yapha (1994). Experimental results showed that the unit operated efficiently and yielded high product quality in terms of head yield and whiteness. In reducing the moisture

content from 45 to 24% using air temperature of 100-120°C, fraction of air recycled of 0.66, specific airflow rate of 0.05 kg/s-kg dry matter, superficial air velocity of 3.2 m/s, and bed depth of 0.1 m, total primary energy consumption was 2.32 MJ/kg of water evaporated, of which 0.35 was primary energy from electricity (electrical energy multiplied by 2.6) and 1.79 was primary energy in terms of heat energy.

As a result of the success of the prototype, commercial fluidised bed paddy dryers with capacities of 5, 10 and 20 t/hour as shown in Figure 3 are now available. More than 200 units have been sold since the beginning of 1995. The fluidised bed dryer is mainly composed of a drying chamber, a backward curved blade centrifugal fan, a burner using diesel oil or fuel oil for heating air, and a cyclone or a cyclo-fan. Commercial cyclonic rice husk furnace is now available commercially. More than 100 units have been sold since the beginning of 1999.

Operation of the commercial fluidised bed paddy dryer is similar to the prototype except that a small portion of exhaust air is vented to the atmosphere after being cleaned by the cyclone.

Development of mathematical model

It was assumed that there is thermal equilibrium between the drying air and the product, and that the air and grain flow were in plug type. Experimental results reported by Sripawatakul (1994) indicated that the flow regime of paddy was between near plug flow and high dispersion flow. Though dispersion was a known factor in the fluidised bed, the mathematical model assumed plug flow in order to simplify calculation. The model is similar to that presented by Soponronnarit and Prachayawarakorn (1994). Figure 1 shows control volumes (CVs) for the derivation of energy and mass balance equations.

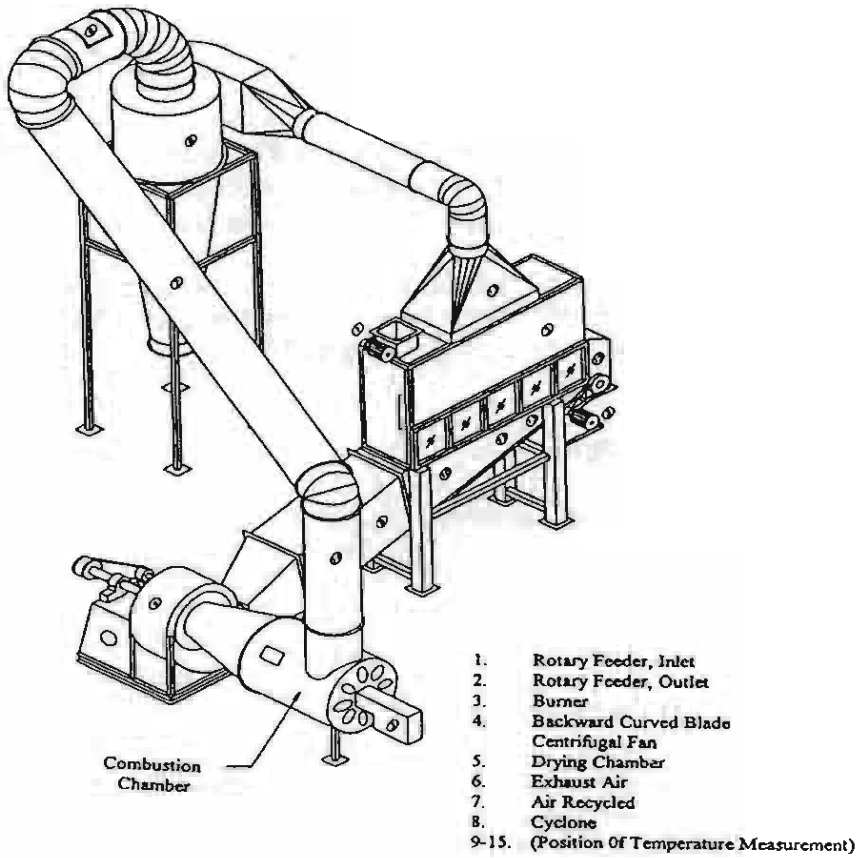


Figure 3. Commercial fluidised bed paddy dryer

Equation of mean residence time

The empirical equation of mean residence time of paddy developed by Sripawatakul (1994) was used. It is written as follows:

$$\tau = hu/F \qquad (1)$$

where τ = mean residence time, second (s)
hu = hold up, kg
F = feed rate, kg/s

and $hu = [\{-0.0095000 + 0.59870\ F - (0.00020000 + 0.17360\ F)\ V\} + \{1.1728 - 0.082300\ V + (2.2093 - 0.15050\ V)\ F\}\ h]\ \rho_p A$

where A = paddy bed area, m^2

V = air velocity, m/s
ρ_p = average product density, kg/m^3
h = weir height, m

It is valid for weir heights in the range 0.04 - 0.10 m, air velocities in the range 1.7 - 2.3 m/s, and paddy feed rates in the range 0.025 - 0.058 kg/s. For a rough calculation, hu is approximately equal to $hA\rho_p$ and can be applied to other grains.

Dividing the paddy bulk into n layers, changes in moisture content of paddy, temperature, and the humidity ratio of air were calculated for each layer. The following basic equations were employed.

Equation for the drying rate

The empirical equation for fluidised bed paddy drying in the form of the equation of Page (1949), developed by Sripawatakul (1994), was used. It is written as follows:

$$MR = \exp\{-x(t/60)^y\} \qquad (2)$$

where $MR = (M - M_{eq})/(M_{in} - M_{eq})$
t= drying time, s
$x = 0.00163100\ T_{mix} - 1.16202\ (m_{mix}/hu) + 0.00415300\ (m_{mix}/hu)\ T_{mix} + 0.147383 \ln (m_{mix}/hu) + 0.474743$
$y = - 0.00322000\ T_{mix} - 0.835960\ (m_{mix}/hu) + 0.0203190\ (m_{mix}/hu)\ T_{mix} -0.143150 \ln (m_{mix}/hu) + 0.548493$

Equation (2) is similar to that developed by Soponronnarit and Prachayawarakorn (1994) for higher specific airflow rate (m_{mix}/hu). It is valid for temperatures of 90 - 140°C and specific airflow rates of 0.03 - 0.16 kg/s/kg dry matter of paddy. The symbols are defined as follows:

M = moisture content of paddy at time t, decimal dry basis
M_{in} = moisture content of paddy at the inlet of drying section, decimal dry basis
M_{eq} = equilibrium moisture content, decimal dry basis
T_{mix} = air temperature at the inlet of drying section, °C
m_{mix} = airflow rate at the inlet of drying section, kg/s

During calculation, Equation (2) was differentiated with time, and finite difference was employed to obtain the solution. Equilibrium moisture content was determined using the equation developed by Laithong (1987).

For the drying rates of maize and soybean, they are available in Soponronnarit et al. (1997a) and Soponronnarit et al. (2000), respectively.

Equation of mass conservation

$$W_{fl,i} = R\,(M_i - M_f) + W_{mix} \qquad (3)$$

where
$W_{fl,i}$ = humidity ratio of outlet air at the i^{th} layer, kg water/kg dry air
W_{mix} = humidity ratio of inlet air at the i^{th} layer, kg water/kg dry air
M_i =moisture content of paddy at the inlet of i^{th} layer, decimal dry basis
M_f=moisture content of paddy at the outlet of i^{th} layer, decimal dry basis
R=ratio of dry mass of paddy to mass of dry air

Equation of energy conservation

$$T_{fl,i} = [Q_l/m_{mix} + C_a T_{mix} + W_{mix}(h_{fg} + C_v T_{mix}) - W_{fl,i} h_{fg} + RC_{pw} T_{mix}]/(C_a + W_{fl,i} C_v + C_{pw}) \qquad (4)$$

where
$T_{fl,i}$ = temperature of outlet air at the i^{th} layer, °C
Q_l = heat loss, kW
C_a = specific heat of dry air, kJ/kg °C
C_v = specific heat of vapour, kJ/kg °C
C_{pw} = specific heat of moist paddy, kJ/kg °C
h_{fg} = latent heat of moisture vaporisation, kJ/kg

Average temperature and humidity ratio of the outlet air from n layers were determined by arithmetic mean. For other calculations such as mixing of air streams, and consumption of energy at the fan and the heater, solutions can be achieved by the application of first law of thermodynamics [see Soponronnarit and Prachayawarakorn (1994) for details].

The equations were solved by iteration. Firstly, the value of exit humidity ratio of air was assumed. The equations presented by Wilhelm (1976) were used to determine properties of moist air.

The accuracy of the mathematical model was tested and found to be in good agreement with the experimental results. The model was employed to investigate optimum operating parameters such as air temperature, specific airflow rate, and fraction of air recycled. Details for paddy drying and maize drying are available in Soponronnarit et al. (1996a) and Soponronnarit et al. (1997a), respectively.

Further development of the mathematical model

In simulation of multi-stage drying including the tempering between each stage, the moisture profile in a grain kernel at the end of each drying stage must be known. Unfortunately, the moisture profile in a grain kernel

cannot be predicted by the empirical drying equations such as Equation (2). But, it can be determined only by using a theoretical equation, mostly described by the Fick's unsteady state diffusion equation in which an effective moisture diffusion coefficient is taken into account.

Poomsa-ad et al. (2002) developed the mathematical model for the simulation of multi-stage drying including the tempering between each stage. It was assumed that water moves in the combined radial and axial direction and paddy is an isotropic solid. The partial differential equation of moisture diffusion for a single paddy kernel considered geometrically to be a finite cylindrical shape can be written as follows:

$$\frac{\partial M}{\partial t} = D\left[\frac{\partial^2 M}{\partial r^2} + \left(\frac{1}{r}\right)\frac{\partial M}{\partial r} + \frac{\partial^2 M}{\partial z^2}\right] \qquad (5)$$

where D = effective moisture diffusion coefficient, m/s^2
r = coordinate along the radius of cylinder, m
z = coordinate along the length of cylinder, m

The initial and boundary conditions for paddy drying are given by

$t = 0,\ 0 \le r \le r_o$	$M = M_{in}$ or	$M = M(r,z)$
$-\ell \le z \le +\ell$	$M = M_{in}$ or	$M = M(r,z)$
$t > 0,\ r = r_o$	$M = M_{eq}$	
$z = \pm\ell$	$M = M_{eq}$	
$t > 0,\ r = 0$	$\frac{\partial M}{\partial r} = 0$	

where ℓ = half length of cylinder, m
r_o = radius of cylinder, m

The effective moisture diffusion coefficient described by the Arrhenius type equation is given as follows:

$$D = 5.41141 \times 10^{-6} \exp\left(\frac{-28436.4}{R(273.15+T)}\right) \qquad (6)$$

where R = universal gas constant, kJ/kmol-K

For tempering process, moisture profile at the end of the first stage drying is used as the initial condition. During this period, the moisture inside a paddy kernel transports to the exterior surface, but it does not evaporate to the environment. The redistribution of moisture inside the kernel can be described again by Eqn. (5) with the new boundary and initial conditions as follows:

$$t = 0, \qquad M = M(r, z)$$

$$t > 0, \; r = r_o \qquad \frac{\partial M}{\partial r} = 0$$

$$z = \pm \ell \qquad \frac{\partial M}{\partial z} = 0$$

$$t > 0, \; r = 0 \qquad \frac{\partial M}{\partial r} = 0$$

The finite difference method was employed for solving Equation (5) using proper initial and boundary conditions for each process. The simulation results are in good agreement with the experimental results including a series of drying, tempering and subsequent drying.

Performance of fluidised bed paddy dryer

Minimum fluidised bed velocity

From the experimental results reported by Soponronnarit and Prachayawarakorn (1994), the minimum fluidised bed velocity for paddy is approximately 1.6 m/s and increases with moisture content. The relationship between pressure drop across the paddy bed and bed velocity is presented in Figure 4.

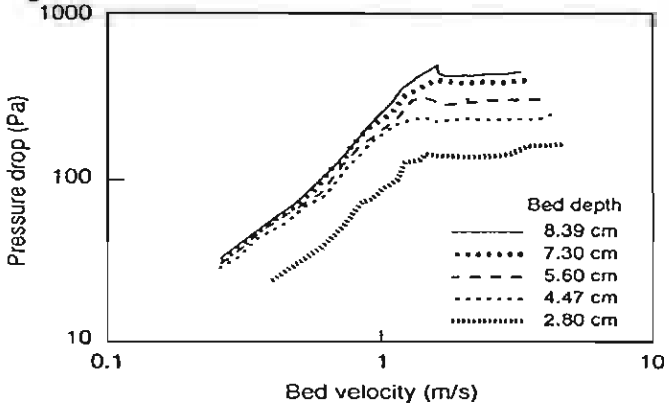


Figure 4. Relationship between bed pressure drop and bed velocity at different bed depths in fluidised bed paddy dryer

For maize, the minimum fluidised bed velocity increases with moisture content. It varies from 1.5 to1.8 m/s as reported by Soponronnarit et al. (1997b). For soybean, Soponronnarit et al. (2000) reported that the minimum fluidised bed velocity is 1.9 m/s and varies slightly and inversely with moisture content.

Experimental results from commercial fluidised bed grain dryers

Experimental results from commercial fluidised bed paddy dryers with capacities of 2.5-5 t/h and 5-10 t/h are summarized in Table 1 (Soponronnarit et al., 1996b). Paddy quality in terms of head yield and whiteness are all acceptable as compared to paddy dried by ambient air (reference) which is expected to obtain highest quality. Considering energy consumption, it is relatively low as compared to conventional hot air dryers, except a case with low inlet paddy moisture content. It is generally recommended to dry paddy from high moisture level to a moisture content of approximately 23% in order to maintain paddy quality. However, it is possible to dry paddy to a lower moisture level if tempering process follows the fluidised bed drying. In addition, as compared to ambient air drying, head yield can be increased if proper drying conditions are provided. The effects of both tempering and drying on paddy quality will be presented in the next section.

Experimental results of maize drying in a commercial fluidised bed dryer are presented in Table 2. At high moisture level of maize, i.e. inlet and exit moisture contents higher than 28% and 19%, respectively, energy consumption is relatively low. The quality in terms of breakage and stress cracks is relatively good and commercially acceptable provided that the exit moisture content of maize is not less than 16.7%.

Table 1. Performance test results of commercial fluidised bed paddy dryers

Test nos. / *Testing results*	*1*	*2*	*3*	*4*	*5*
Drying air temperature (°C)	115	116	120	130	150
Drying air recycled (%)	69	69	69	69	53
Inlet moisture content of Paddy (% dry basis)	22.0	26.0	28.7	30.6	27.0
Outlet moisture content of Paddy (% dry basis)	20.1	22.5	22.5	23.0	21.0
Outlet paddy temperature (°C)	54.0	52.0	54.0	57.0	63.0
Electrical energy consumed (MJ/kg-water evap.)	0.83	0.43	0.26	0.21	0.15
Thermal energy consumed (MJ/kg-water evap.)	7.80	3.13	2.57	2.21	3.90
Head rice yield (%)					
- dried in fluidised bed dryer	53.2	54.3	53.9	57.0	48.1
- dried by ambient air (reference)	57.4	57.2	53.9	57.0	56.2
Rice whiteness					
- dried in fluidised bed dryer	40.3	40.7	40.0	43.7	36.8
- dried by ambient air (reference)	44.4	44.2	40.1	43.8	42.6
Testing hours	5.0	35.0	46.0	51.0	29.0
Drying capacity (tons/h)	9.5[b]	9.5[b]	9.5[b]	9.5[b]	4.8[a]

Remarks: a = Dryer with capacity of 2.5 – 5.0 tons/h
b = Dryer with capacity of 5.0 – 10.0 tons/h

Table 2. Performance test results of commercial fluidised bed maize dryer

Test nos. / *Testing results*	*1*	*2*	*3*	*4*	*5*	*6*	*7*	*8*
• Drying air temperature (°C)	130[a]	130[a]	140[b]	150[a]	150[a]	160[a]	170[c]	175[a]
• Drying air recycled (%)	84	78	78	78	84	78	84	84
• Inlet moisture content of maize (% dry basis)	22.2	38.3	32.7	28.2	18.6	40.3	21.1	22.8
• Outlet moisture content of maize (% dry basis)	19.1	30.8	27.2	19.2	16.7	26.3	14.2	18.2
• Outlet maize temperature (°C)	68	68	74	-	74	-	97	96
• Electrical energy consumed (MJ/kg-water evap.)	1.25	0.60	0.49	0.41	2.05	0.32	-	0.88
• Thermal energy consumed (MJ/kg-water evap.)	15.21	6.67	6.48	5.50	27.83	4.72	-	15.68
• Breakage (% by mass)								
- dried in FBD	1.91	-	-	-	1.81	-	2.82	1.34
- dried by ambient air (reference)	1.04	-	-	-	1.72	-	2.44	1.55
• Stress cracks (% by mass)								
- dried in FBD	0.59	-	-	-	1.03	-	32.69	3.34
- dried by ambient air (reference)	0.19	-	-	-	0.59	-	0.62	0.79
• 'a' Hunter value								
- dried in FBD	11.42	11.26	14.56	11.74	11.13	12.09	8.10	6.93
- dried by ambient air (reference)	10.24	10.85	12.85	10.63	8.84	10.80	7.66	7.69
• 'b' Hunter value								
- dried in FBD	24.52	23.85	27.21	26.55	23.91	25.93	21.61	20.23
- dried by ambient air (reference)	22.84	22.88	28.27	25.46	22.10	28.85	19.86	19.52
• Testing hours	2	6	10	7	2	4	5	7
• Drying capacity (tons/h)	1.8	2.0	3.0	2.0	1.8	1.8	1.6	1.8

Remarks: FBD = Fluidised bed dryer
a = 17 cm bed depth
b = 19 cm bed depth
c = 22 cm bed depth

Experiment of soybean drying in a commercial fluidised bed dryer was conducted (Wangji et al., 1997). The operating parameters are as follows: drying capacity of 2.9 t/h, air flow rate of 3.3 kg/s, bed velocity of 2.9 m/s, bed height of 0.15 m, residence time of 2.35 minutes, fraction of air

recycled of 0.83 and inlet drying air temperatures of 110-140°C. Moisture content of soybean was reduced from 25.3, 29.7, 33.7 and 39.3% to 20.2, 22.0, 22.8 and 23.4%, respectively. Average primary energy consumption of which the majority is from heat energy is 4.62 MJ/kg water evaporated. Average stress cracks after drying is about 12% higher than that before drying. More insight of quality results obtained from lab-scale fluidised bed soybean drying were reported by Soponronnarit et al. (2000). The fluidised bed drying was found to reduce the level of urease activity which is an indirect measure of trypsin inhibitor, with 120°C being the minimum required to reduce the urease activity to an acceptable level (ΔpH less than 0.3). Increased air temperatures caused increased cracking and breakage, with temperature below 140°C giving an acceptable level for animal feed industry in Thailand (Breakage less than 3%). The protein level was not significantly reduced in this temperature range. Details are available in Table 3.

Table 3. Protein solubility in 0.2% KOH and urease activity of high initial moisture soybean dried in fluidised bed dryer

T (°C)	M_i (%d.b.)	M_f (%d.b.)	*Protein* (%)	*Urease activity* (ΔpH)	*Protein solubility* (%)
140	33.5	23.3	40.76	0.67	86.14
130	32.1	22.0	39.75	0.90	86.76
120	33.5	24.0	40.53	0.83	88.96
140	33.5	14.4	40.14	0.10	81.78
130	32.1	12.2	40.67	0.11	81.70
120	33.5	12.8	41.33	0.11	82.43
Initial values			41.45-41.67	1.89 – 2.04	89.94 – 90.07

Remarks: T = Temperature, (°C)
M_i = Initial moisture content, % dry basis
M_f = Final moisture content, % dry basis

Effects of drying, tempering and ambient air ventilation on moisture reduction and quality of paddy

Soponronnarit et al. (1999) investigated in a laboratory how to manage moist paddy by three processes in series, i.e., fluidised bed drying, tempering and ambient air ventilation. Experimental results show that after the three processes, moisture content is reduced from 33% to 16.5% within approximately 53 minutes. During the first process, a fluidised bed dryer with inlet air temperature of 150°C was used to reduce the moisture content of paddy down to 19.5% within 3 minutes. Then the paddy was tempered for 30 minutes. Finally, it was cooled by ambient air (temperature and relative humidity of 30°C and 55-60%, respectively with air velocity of 0.15

m/s) for 20 minutes. Quality of paddy in terms of head rice yield and whiteness is acceptable.

Poomsa-ad et al. (2002) experimentally and mathematically confirmed that the tempering period of 35 minutes is recommended for the two-stage fluidised bed drying. The drying rate during the second stage drying can be improved considerably. This is due to the redistribution of moisture in the grain kernel. The simulation result shows that the moisture is almost uniform after 35 minutes tempering. It should be noted that the recommended tempering period is very much shorter compared to other researches. This is mainly due to significantly higher drying temperature employed in the fluidised bed drying which results in higher grain temperature and thus causes faster moisture diffusion during tempering in case of the fluidised bed drying.

Spin-off from fluidised bed paddy drying

Soponronnarit et. al. (1998) conducted paddy drying using fluidisation technique and paddy tempering following drying in a laboratory and found a significant spin-off. Head yield increases higher than 50% when paddy is dried by fluidisation technique with inlet drying air temperature of 140-150°C and initial moisture content of paddy of 29.9 - 44.9%. As initial moisture content increases, head rice yield increases. Final moisture contents of paddy that can increase head yield to a maximum value are in a range of 23.4 - 28.2%. It is believed that gelatinization especially at the surface of rice kernel is the main factor for increasing head yield. Tempering of paddy after drying can maintain head yield as compared to that without tempering. Rice whiteness of dried paddy is mostly accepted provided that tempering temperature is not higher than 60°C. For consumer acceptance, tested rice without tempering is not significantly different from that dried by ambient air, while tested rice with tempering, after being cooked, has higher bad smell and lower whiteness. However, this may be solved by reducing tempering time down to 30 minutes.

Conclusion

Fluidised bed grain drying has been developed for almost 9 years in Thailand. The first fluidised bed paddy dryer was first commercialized in Thailand in 1995. It is probably the first commercial continuous fluidised bed dryer for paddy drying. Since then, more than 200 commercial units with capacities of 5, 10 and 20 tons/hour have been sold in Thailand, Cambodia, French Guyana, Indonesia, Laos, Malaysia, Mexico, Myanmar, the Philippines and Taiwan.

A basic study including drying kinetics and factors affecting grain quality, moisture reduction rate and energy consumption was conducted for

paddy, maize and soybean. Important results are presented in this paper. The performance of commercial fluidised bed grain dryer was also investigated and presented. Finally, a complete mathematical model for the fluidised bed grain drying system including a series of drying, tempering and subsequent drying was derived.

In conclusion, the fluidised bed paddy dryer is competitive with conventional hot air dryers especially at high moisture level, i.e. low energy consumption, low cost and acceptable paddy quality. Important operating parameters are : drying air temperature of 140 - 150°C, fraction of air recycled of 0.8, air velocity around 2.0 - 2.3 m/s and bed thickness of 10 - 15 cm. Under proper conditions such as high initial moisture content of paddy (higher than 30%) and high air temperature (140 - 150°C), head yield can be increased up to 50% compared to ambient air drying. For consumer acceptance, tested rice with fluidised bed drying is not significantly different from that dried by ambient air.

For other grains, the fluidised bed dryer has a great potential for commercialization. Many units have been used in parboiled rice mills, a few for maize and soybean industries. Experimental results obtained from commercial fluidised bed dryers showed good performance and good product quality with a significant spin-off that urease activity in soybean kernel could be reduced to an acceptable level required by animal feed industry.

Acknowledgment

Thanks are due to the Thailand Research Fund for financial support to the Research Group on Drying Technology, King Mongkut's University of Technology Thonburi, Bangkok, Thailand.

References

Driscoll, R.H. and Srzednicki, G.S., 1991. Design for a complete grain drying system under Southeast Asian climates. In Proceedings of the 12th ASEAN Technical Seminar on Grain Post-harvest Technology. Surabaya, Indonesia.

Laithong, C., 1987. Study of physico-thermal properties of rough rice. Bangkok, Thailand: King Mongkut's Institute of Technology Thonburi, Master Thesis.

Page, G.E., 1949. Factors influencing the maximum rate of drying shelled corn in layers. Purdue University, Unpublished, Master Thesis.

Poomsa-ad, N., Soponronnarit, S., Prachayawarakorn, S. and Terdyothin, A. 2002. Effect of tempering on subsequent drying of paddy using flidisation technique. Drying Technology. 20:195-210.

Soponronnarit, S., Kittiporn, K. and Prachayawarakorn, S., 1997a. Appropriate operating parameters for fluidized bed corn drying. RERIC International Energy Journal. 19:1-13.

Soponronnarit, S., Pongtornkulpanich, A. and Prachayawarakorn, S. 1997b. Drying characteristics of corn in fluidized bed dryer. Drying Technology. 15:1603-1615.

Soponronnarit, S. and Prachayawarakorn, S., 1994. Optimum strategy for fluidized bed paddy drying. Drying Technology. 12:1667-1686.

Soponronnarit, S., Prachayawarakorn, S. and Sripawatakul, O., 1996a. Development of cross-flow fluidized bed paddy dryer. Drying Technology. 14:2397-2410.

Soponronnarit, S., Prachayawarakorn, S. and Wangji, M., 1996b. Commercial fluidized bed paddy dryer. In Proceedings of the 10th International Drying Symposium, 638-644. Krakow, Poland.

Soponronnarit, S., Swasdisevi, T., Wetchacama, S. and Wutiwatchai, W., 2000. Fluidised bed drying of soybeans. Accepted to be published in Journal of Stored Product Research.

Soponronnarit, S., Taweerattanapanish, A., Wetchacama, S., Kongseri, N. and Wongpiyachon, S., 1998. Spin-off from paddy drying by fluidization technique. Keynote paper presented at the 7th International Working Conference on Stored-Product Protection. Beijing, China.

Soponronnarit, S., Wetchacama, S., Swasdisevi, T. and Poomsa-ad, N., 1999. Managing moist paddy by drying, tempering and ambient air ventilation. Drying Technology. 17: 335-344.

Soponronnarit, S., Wongvirojtana, P., Nathakaranakule, A. and Prachayawarakorn, S., 1994. Maintaining paddy quality by appropriate ventilation under tropical climate. In Proceedings of the 9th International Drying Symposium, 825-832. Gold Coast, Australia.

Soponronnarit, S., Yapha, M. and Prachayawarakorn, S., 1995. Cross-flow fluidized bed paddy dryer: prototype and commercialization. Drying Technology. 13:2207-2216.

Sripawatakul, O., 1994. Study of drying paddy by cross-flow fluidization technique. Bangkok, Thailand: King Mongkut's Institute of Technology Thonburi, Master Thesis.

Sutherland, J.W. and Ghaly, T.F., 1992. Rapid fluid bed drying of paddy rice in the humid tropics. In Proceedings of the 13th ASEAN Conference on Grain Post-harvest Technology. Brunei Darussalam.

Tumambing, J.A. and Driscoll, R.H., 1993. Modeling the performance of continuous fluidized bed paddy dryer for rapid pre-drying of paddy. In Proceedings of the 14th ASEAN seminar on Grain Post-harvest Technology, 193-213. Manila, Philippines.

Wangji, M., Soponronnarit, S. and Wetchacama, S., 1997. Soybean drying by fluidization technique. In Proceedings of the Yearly Technical Seminar held by the Thailand Engineering Institute, 534-548. Bangkok, Thailand.

Wilhelm, L.R., 1976. Numerical calculation on psychrometric properties in SI units. Transactions of the American Society of Agricultural Engineers. 19: 318-321, 325

Yapha, M., 1994. Design and testing of pilot continuous fluidized bed paddy dryer. Bangkok, Thailand: King Mongkut's Institute of Technology Thonburi, Master Thesis.

Proceedings of the

3rd Asia-Pacific Drying Conference

1-3 September 2003

Editors

Vinod K. Jindal
Athapol Noomhorm
Imran Ahmad

Asian Institute of Technology

Bangkok, Thailand

MATHEMATICAL MODELLING AND SIMULATION OF FLUIDISED-BED DRYING, TEMPERING AND VENTILATION OF GRAINS

Somchart Soponronnarit[1] and Somkiat Prachayawarakorn[2]

[1]School of Energy and Materials, [2]Faculty of Engineering
King Mongkut's University of Technology Thonburi
Suksawat 48 Road, Bangkok 10140, Thailand

ABSTRACT

The fluidized-bed grain dryer is now fully commercialized in several countries. Its potential is great especially for high moisture grains such as paddy, parboiled rice, maize and soybean. Its drying rate is very fast as compared to conventional grain dryers. Consequently, the size of drying unit is very compact relative to its capacity. Its energy consumption is relatively low while grain quality is maintained. In this paper, the research and development effort on fluidised bed grain drying is described, starting with an experimental batch dryer and culminating with a commercial continuous-flow dryer. A mathematical model of the fluidised bed grain drying system including a series of drying, tempering, ambient air ventilation and head-rice equation is derived. The model provides the useful information about designing and operating condition for the drying system in order to optimize the drying capacity and quality, both of which show the contradict results.

INTRODUCTION

It has been suggested that high moisture paddy should be dried quickly to approximately 23% moisture content (dry basis[1]) then subjected to ambient air drying in storage (Soponronnarit et al. 1994; Driscoll and Srzednicki 1991). Following two-stage drying, cost and product quality appear to be optimised. During the first stage, fluidised bed drying is an alternative to conventional hot-air drying. Its advantages are: (1) uniform product moisture content, and thus high drying air temperature can be employed but with less overdried grain; (2) high drying capacity due to better heat and mass transfer; (3) a much smaller drying chamber and thus a significantly lower initial cost; and (4) significant spin-off in terms of increasing head rice yield and potential for producing aging rice.

Sutherland and Ghaly (1992) were probably the first research group who investigated feasibility of using fluidisation technique for paddy drying. Japanese researcher may have conducted similar research work before. Experimental results reported by Sutherland and Ghaly (1992) showed that head yield was 58-61% when paddy was dried from 28.2 to 20.5% but was 15-24% when the final moisture content was 19%. Tumambing and Driscoll (1993) found that drying rate was affected by drying air temperature and bed thickness under experimental conditions as follows: drying air temperature of 40-100°C; bed thickness of 5-20 cm and air velocity of 1.5-2.5 m/s. They also developed a mathematical model for continuous fluidised bed paddy dryer.

Soponronnarit and Prachayawarakorn (1994) have reviewed the research and development work on fluidised bed drying of grain, and conducted both experimental and simulation studies on batch fluidised bed drying of paddy. Soponronnarit et al. (1996) described the development of a cross-flow fluidised bed paddy dryer with a capacity of 200 kg/hour (Fig.1). Experimental results showed that final moisture content of paddy should not be lower than 23% if quality in terms of both whiteness and head yield were to be maintained. Drying air temperature was 115°C. Simulation results indicated that the appropriate operating parameters should be as follows: air speed, 2.3 m/s; bed thickness, 10 cm; and fraction of air recycled of 0.8. With these conditions, energy consumption was close to the minimum, while drying capacity was near maximal. In this study, moisture of paddy was reduced from 30 to 24%.

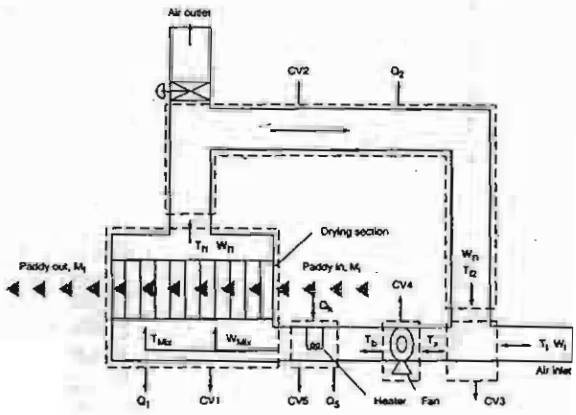
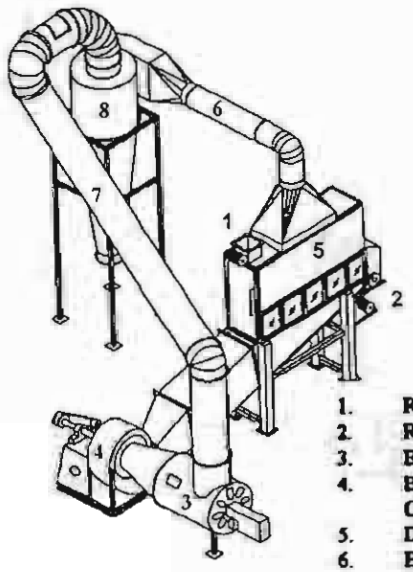


Figure 1 Control volumes of continuous cross-flow fluidised bed drying system: ◂ grain flow; ← air flow; T, temperature; W, humidity ratio; M, grain moisture content; Q, heat; CV, control volume.

Following the success of the development of the cross-flow fluidised bed paddy dryer, Rice Engineering Supply Co. Ltd., a private company in Thailand, showed interest in collaborating in the development of a

[1] Unless otherwise stated, the moisture contents (m.c.) quoted in this paper are dry basis.

prototype with a capacity of approximately 1 t/hour as shown in Figure 2 (Soponronnarit et al. 1995). It comprises a drying section, a 7.5 kW backward curved blade centrifugal fan, a diesel fuel-oil burner, and a cyclone. The bed length, width and height of the drying section are 1.7, 0.3 and 1.2 m, respectively. The depth of the paddy bed is controlled by a weir. Paddy is fed in and out by rotary feeders. In operation, hot air (temperature controlled by thermostat) is blown into the drying section through a perforated steel sheet floor. The air and grain flows are perpendicular to each other. A small portion of the air leaving the drying chamber is vented to the atmosphere, while the remainder, after cleaning in a cyclone, is recycled to the dryer, mixed with ambient air and reheating to the desired temperature, respectively. The feed rate of paddy can be varied from less than 1 t/hour to more than 1.5 t/hour. More detail is given in Yapha (1994). Experimental results showed that the unit operated efficiently and yielded high product quality in terms of head yield and whiteness. In reducing the moisture content from 45 to 24% using air temperature of 100-120°C, fraction of air recycled of 0.66, specific airflow rate of 0.05 kg/s-kg dry matter, superficial air velocity of 3.2 m/s, and bed depth of 0.1 m, total primary energy consumption was 2.32 MJ/kg of water evaporated, of which 0.35 was primary energy from electricity (electrical energy multiplied by 2.6) and 1.79 was primary energy in terms of heat energy.



1. Rotary Feeder, Inlet
2. Rotary Feeder, Outlet
3. Burner
4. Backward Curved Blade Centrifugal Fan
5. Drying Chamber
6. Exhaust Air
7. Air Recycled
8. Cyclone

Figure 2 Commercial fluidised-bed paddy dryer.

As a result of the success of the prototype, commercial fluidised bed paddy dryers with capacities of 5, 10 and 20 t/hour are now available. More than 200 units have been sold since the beginning of 1995. The fluidised bed dryer is mainly composed of a drying chamber, a backward curved blade centrifugal fan, a burner using diesel oil or fuel oil for heating air, and a cyclone or a cyclo-fan. Commercial cyclonic rice husk furnace is now available commercially. More than 200 units have been sold since the beginning of 1999.

Operation of the commercial fluidised bed paddy dryer is similar to the prototype except that a small portion of exhaust air is vented to the atmosphere after being cleaned by the cyclone.

DEVELOPMENT OF MATHEMATICAL MODEL

It was assumed that there is thermal equilibrium between the drying air and the product, and that the air and grain flow were in plug type. Experimental results reported by Sripawatakul (1994) indicated that the flow regime of paddy was between near plug flow and high dispersion flow. Though dispersion was a known factor in the fluidised bed, the mathematical model assumed plug flow in order to simplify calculation. The model is similar to that presented by Soponronnarit and Prachayawarakorn (1994). Figure 1 shows control volumes (CVs) for the derivation of energy and mass balance equations.

Equation of mean residence time

The empirical equation of mean residence time of paddy developed by Sripawatakul (1994) was used. It is written as follows:

$$\tau = hu/F \qquad (1)$$

where τ = mean residence time, second (s)
hu = hold up, kg
F = feed rate, kg/s

and $hu = [\{-0.0095000 + 0.59870\ F - (0.00020000 + 0.17360\ F)\ V\} + \{1.1728 - 0.082300\ V + (2.2093 - 0.15050\ V)\ F\}\ h]\ \rho_p A$

where A = paddy bed area, m^2
V = air velocity, m/s
ρ_p = average product density, kg/m^3
h = weir height, m

It is valid for weir heights in the range 0.04 - 0.10 m, air velocities in the range 1.7 - 2.3 m/s, and paddy feed rates in the range 0.025 - 0.058 kg/s. For a rough calculation, hu is approximately equal to $hA\rho_p$ and can be applied to other grains.

Dividing the paddy bulk into n layers, changes in moisture content of paddy, temperature, and the humidity ratio of air were calculated for each layer. The following basic equations were employed.

Equation for the drying rate

The empirical equation for fluidised bed paddy drying in the form of the equation of Page (1949), developed by Sripawatakul (1994), was used. It is written as follows:

$$MR = \exp\{-x(t/60)^y\} \qquad (2)$$

where $MR = (M - M_{eq})/(M_{in} - M_{eq})$

t = drying time, s

$x = 0.00163100\ T_{mix} - 1.16202\ (m_{mix}/hu) + 0.00415300\ (m_{mix}/hu)\ T_{mix} + 0.147383\ \ln(m_{mix}/hu) + 0.474743$

$y = -0.00322000\ T_{mix} - 0.835960\ (m_{mix}/hu) + 0.0203190\ (m_{mix}/hu)\ T_{mix} - 0.143150\ \ln(m_{mix}/hu) + 0.548493$

Equation (2) is similar to that developed by Soponronnarit and Prachayawarakorn (1994) for higher specific airflow rate (m_{mix}/hu). It is valid for temperatures of 90 - 140°C and specific airflow rates of 0.03 - 0.16 kg/s/kg dry matter of paddy. The symbols are defined as follows:

M = moisture content of paddy at time t, decimal dry basis

M_{in} = moisture content of paddy at the inlet of drying section, decimal dry basis

M_{eq} = equilibrium moisture content, decimal dry basis

T_{mix} = air temperature at the inlet of drying section, °C

m_{mix} = airflow rate at the inlet of drying section, kg/s

During calculation, Equation (2) was differentiated with time, and finite difference was employed to obtain the solution. Equilibrium moisture content was determined using the equation developed by Laithong (1987).

For the drying rates of maize and soybean, they are available in Soponronnarit et al. (1997) and Soponronnarit et al. (2001), respectively.

Equation of mass conservation

$$W_{fl,i} = R_t(M_i - M_f) + W_{mix} \qquad (3)$$

where $W_{fl,i}$ = humidity ratio of outlet air at the i^{th} layer, kg water/kg dry air

W_{mix} = humidity ratio of inlet air at the i^{th} layer, kg water/kg dry air

M_i = moisture content of paddy at the inlet of i^{th} layer, decimal dry basis

M_f = moisture content of paddy at the outlet of i^{th} layer, decimal dry basis

R_t = ratio of dry mass of paddy to mass of dry air.

Equation of energy conservation

$$T_{fl,i} = [Q_l/m_{mix} + C_a T_{mix} + W_{mix}(h_{fg} + C_v T_{mix}) - W_{fl,i} h_{fg} + R_t C_{pw} T_{mix}]/(C_a + W_{fl,i} C_v + R_t C_{pw}) \qquad (4)$$

where $T_{fl,i}$ = temperature of outlet air at the i^{th} layer, °C

Q_l = heat loss, kW

C_a = specific heat of dry air, kJ/kg °C

C_v = specific heat of vapour, kJ/kg °C

C_{pw} = specific heat of moist paddy, kJ/kg °C

h_{fg} = latent heat of moisture vaporisation, kJ/kg

Average temperature and humidity ratio of the outlet air from n layers were determined by arithmetic mean.

For other calculations such as mixing of air streams, and consumption of energy at the fan and the heater, solutions can be achieved by the application of first law of thermodynamics [see Soponronnarit and Prachayawarakorn (1994) for details].

The equations were solved by iteration. Firstly, the value of exit humidity ratio of air was assumed. The equations presented by Wilhelm (1976) were used to determine properties of moist air.

The accuracy of the mathematical model was tested and found to be in good agreement with the experimental results. The model was employed to investigate optimum operating parameters such as air temperature, specific airflow rate, and fraction of air recycled. Details for paddy drying and maize drying are available in Soponronnarit et al. (1996) and Soponronnarit et al. (1997), respectively.

Further development of the mathematical model

In simulation of multi-stage drying including the tempering between each stage, the moisture profile in a grain kernel at the end of each drying stage must be known. Unfortunately, the moisture profile in a grain kernel cannot be predicted by the empirical drying equations such as Equation (2). But, it can be determined only by using a theoretical equation, mostly described by the Fick's unsteady state diffusion equation in which an effective moisture diffusion coefficient is taken into account.

Poomsa-ad et al. (2002) developed the mathematical model for the simulation of multi-stage drying including the tempering between each stage. It was assumed that water moves in the combined radial and axial direction and paddy is an isotropic solid. The partial differential equation of moisture diffusion for a single paddy kernel considered geometrically to be a finite cylindrical shape can be written as follows:

$$\frac{\partial M}{\partial t} = D\left[\frac{\partial^2 M}{\partial r^2} + \left(\frac{1}{r}\right)\frac{\partial M}{\partial r} + \frac{\partial^2 M}{\partial z^2}\right] \qquad (5)$$

where D = effective moisture diffusion coefficient, m/s^2

r = coordinate along the radius of cylinder, m

z = coordinate along the length of cylinder, m

The initial and boundary conditions for paddy drying are given by

$t = 0,\ 0 \le r \le r_o \quad M = M_{in}$ or $M = M(r,z)$

$-\ell \le z \le +\ell \quad M = M_{in}$ or $M = M(r,z)$

$t > 0,\ r = r_o \quad M = M_{eq}$

$$z = \pm \ell \qquad M = M_{eq}$$

$$t > 0, \ r = 0 \qquad \frac{\partial M}{\partial r} = 0$$

where ℓ = half length of cylinder, m
r_o = radius of cylinder, m

The effective moisture diffusion coefficient described by the Arrhenius type equation is given as follows:

$$D = 5.41141 \times 10^{-6} \exp\left(\frac{-28436.4}{R(273.15+T)}\right) \quad (6)$$

where R = universal gas constant, kJ/kmol-K

For tempering process, moisture profile at the end of the first stage drying is used as the initial condition. During this period, the moisture inside a paddy kernel transports to the exterior surface, but it does not evaporate to the environment. The redistribution of moisture inside the kernel can be described again by Equation (5) with the new boundary and initial conditions as follows:

$$t = 0, \qquad M = M(r,z)$$

$$t > 0, \ r = r_o \qquad \frac{\partial M}{\partial r} = 0$$

$$z = \pm \ell \qquad \frac{\partial M}{\partial z} = 0$$

$$t > 0, \ r = 0 \qquad \frac{\partial M}{\partial r} = 0$$

The degree of uniformity of moisture content in this stage is described by the tempering index, I_c,

$$I_c = \frac{(M_{s,t} - M_{s,t=0})}{(M_{s,t=\infty} - M_{s,t=0})} \quad (7)$$

where M_s is the surface moisture content, decimal dry basis. Theoretically, the uniform distribution of moisture, corresponding to the tempering index of unity, required infinite time.

After tempering stage, the grains are cooled to room temperature, using ambient air temperature, to stop formation of yellow pigment. Yellowing can be a severe problem in rice drying because temperature stimulates the development of rice yellowness, a non-enzymatic browning reaction (Taweerattanapanish et al., 1999; Soponronnarit et al., 1998a; Yap et al., 1988). Ventilation was stopped when the grain temperature approached or was slightly above ambient air temperature. While the air ventilated through the heated grains, there was the simultaneous heat and mass transfer from the grain to air, making the air slightly warmer and more humid. The heat-transfer phenomenon in this unit was opposite to that occurring in the dryer section. Assuming that the air flowed through a thin bed in the cross-flow dryer, the outlet-air temperature, T_{ft}, is thus given by

$$T_{ft} = \frac{(C_a T_i + W_i(h_{fg} + C_v T_i) - W_{ft} h_{fg} + R_t C_{pw} \theta_{in})}{(C_a + W_{ft} C_v + R_t C_{pw})} \quad (8)$$

where θ is the grain temperature (°C) and W_{ft} is the outlet humidity ratio at the ventilation unit. Using such a simplified assumption, the properties of air change insignificantly along the bed height, thereby providing economic computation by a single-step approach. For the moisture transport in the ventilation, it is calculated by using Equation (5) again, with the following initial and boundary conditions:

$$t = 0, \qquad M = M(r,z)$$

$$t > 0, \ r = r_o \qquad M = M_{eq}$$

$$z = \pm l \qquad M = M_{eq}$$

In the determination of moisture reduction, the grain temperature is replaced in Equation (6), instead of the inlet-air temperature, because the grain temperature at the beginning of ventilation was approximately 50°C higher than the ambient-air temperature.

Head-rice yield equation

Poomsa-ad et al. (2001) reported that the amount of head rice yield related with tempering time, grain temperature or tempering temperature and the moisture content after fluidised-bed drying. A head rice equation was simply described by

$$RHY = A + Bt + Ct^2 \quad (9)$$

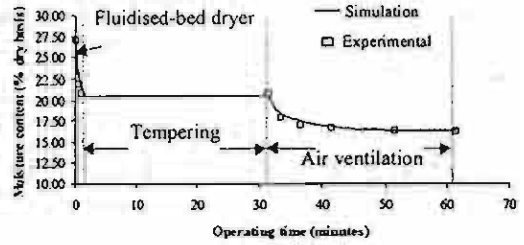
where $A = -39.232 + 8.4227M_f - 0.34060T - 0.029105TM_f$
$B = 25.945 - 1.1878M_f - 0.2443T + 0.012302TM_f$
$C = -0.33610 + 0.015028M_f + 0.003259T - 0.00015762TM_f$

t is the tempering time (minute), M_f is the moisture content (%d.b.) after drying and T is the tempering temperature (°C).

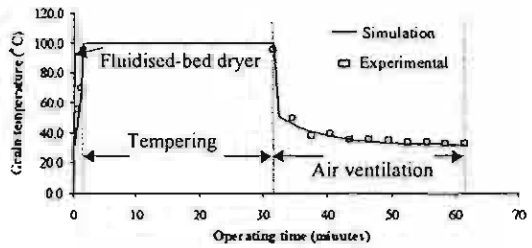
SIMULATION RESULTS

Figure 3 shows the change of moisture content and grain temperature after passing through the units i.e. drying, tempering and ventilation in the process of paddy drying. This experiment was carried out with a batch fluidized-bed drying and the details were given in Poomsa-ad et al. (accepted to be published). As shown in this Figure, the moisture content is reduced from 27.5% d.b. to 22.5% d.b. in the fluidised-bed dryer followed the unchanged value of moisture content in the tempering stage. In the last stage, the moisture content is decreased to 17.5% d.b. The model proposed reasonably predicts

the changes of moisture content and grain temperature at various units of the paddy drying process. As seen in Figure 3b, the temperature steeply drops during a small interval of ventilation, thus causing a high reduction of head rice yield, due to the thermal and moisture gradients, if the grains are not tempered. The poor head-rice yield can be seen in Figure 4 for zero tempering time, with a relative head-rice yield of 20% for the case of B. The relative head-rice yield is defined as the ratio of head-rice yield obtained by drying paddy at high temperature to that at ambient temperature. For the case of A, on the other hand, the head-rice yield quality does not drop although the sample is not subjected to temper.



a) Moisture content



b) Grain temperature

Figure 3 Comparisons of moisture content and grain temperature obtained from the experiment and prediction. (Poomsa-ad et al. (accepted to be published))

The insignificant reduction of head-rice yield for the case of 35% d.b. moisture content is probably attributed to the gelatinization effect, making paddy to withstand the milling forces. When the tempering time increases, the head-rice yield is improved and higher than that at zero tempering time. According to this result, it is questionable whether the paddy should be tempered for how long after drying with fluidised-bed dryer. To answer such a question, the proposed model is used to estimate the suitable tempering time. The criterion indicating the appropriate tempering time is related to the tempering index. Poomsa-ad et al. (2002) recommended the tempering index of 0.95, corresponding to the calculated tempering time of 35 minutes for high-temperature drying. This agrees with the experiment results shown in Figure 4, indicating insignificant change of head-rice yield after tempering for 30 minutes. In addition to the aforementioned quality, the fastest drying rate at the subsequent stage is achieved, giving the benefit of effective energy utilisation. From this figure, it also shows that the head-rice yield equation when included in the heat and mass transfer equations reasonably explains the quality change with the tempering time.

The similar result was also reported by several workers (Steffe et al., 1979; Soponronnarit et al., 1998b; Soponronnarit et al., 1999), showing a higher head-rice yield when the tempering was included between drying stages.

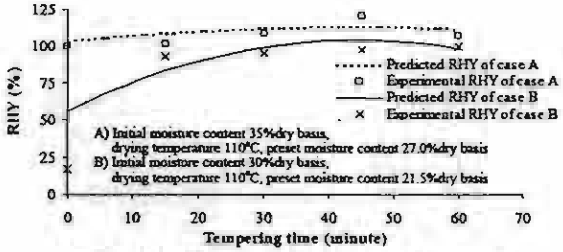


Figure 4 Effect of tempering time on relative head-rice yield (Poomsa-ad et al. (accepted to be published))

SIGNIFICANCE OF SIMULATION RESULTS

Reducing moisture content of paddy by using only fluidised-bed dryer seems an inappropriate method since the transport of water is controlled by internal resistances, resulting in wastage of energy. Besides, the amount of broken rice is enormous, due to excessive stresses produced inside the kernel, and the colour of white rice changes from white to yellow, causing by the non-enzymatic browning reaction (Soponronnarit and Prachayawarakorn, 1994; Sutherland and Ghaly, 1992). To optimise the drying time and energy consumption, along with high head-rice yield, moist paddy should be followed with three stages in series i.e. fluidised bed, tempering and ambient air ventilation to remove its moisture content to a certain level for safe storage. Both experiments and simulations agree well that fluidised-bed dryer, with inlet air temperature of 150°C, is used to decrease the moisture content of paddy to 19.5% d.b. followed with tempering for 30 minutes. In the last stage, the paddy is cooled by ambient air (temperature and relative humidity of 30°C and 55-60%, respectively with air velocity of 0.15 m/s) for 20 minutes. Quality of paddy in terms of head-rice yield and whiteness is acceptable. Under the specified conditions, the thermal and electrical energy consumptions were in the respective ranges of 5-7 MJ/kg-water evaporated and 0.54-0.61 MJ/kg-water evaporated. For drying paddy within high moisture range using fluidized bed technique only, it was reported by Soponronnarit (2000) that energy consumption was lower, i.e. 2.2-3.9 MJ/kg-water evaporated in terms of thermal energy and 0.15-0.43 MJ/kg-water evaporated in terms of electrical energy. Under proper conditions such as high initial moisture content of paddy (higher than 30%) and high air temperature (140 - 150°C), head yield can be increased up to 50% compared to ambient-air drying. For consumer acceptance, tested rice with fluidised bed drying is insignificantly different from that dried by ambient air.

CONCLUSION

Fluidised bed grain drying has been developed for almost 10 years in Thailand. The first fluidised bed paddy dryer was first commercialized in Thailand in 1995. It is probably the first commercial continuous fluidised bed dryer for paddy drying. Since then, more than 200 commercial units with capacities of 5, 10 and 20 tons/hour have been sold in Thailand, Cambodia, Indonesia, Laos, Malaysia, Mexico, Myanmar, the Philippines, Taiwan and Venezuela.

A basic study including drying kinetics and factors affecting grain quality, moisture reduction rate and energy consumption was conducted for paddy, maize and soybean. Important results are presented in this paper. Finally, a complete mathematical model for the fluidised bed grain drying system including a series of drying, tempering and subsequent ventilation was derived.

In conclusion, the fluidised bed paddy dryer is competitive with conventional hot air dryers especially at high moisture level, i.e. low energy consumption, low cost and acceptable paddy quality. Important operating parameters are: drying air temperature of 140 - 150°C, fraction of air recycled of 0.8, air velocity around 2.0 - 2.3 m/s and bed thickness of 10 - 15 cm. Under proper conditions such as high initial moisture content of paddy (higher than 30%) and high air temperature (140 - 150°C), head yield can be increased up to 50% compared to ambient-air drying. For consumer acceptance, tested rice with fluidised bed drying is not significantly different from that dried by ambient air.

ACKNOWLEDGMENT

Thanks are due to the Thailand Research Fund for financial support to the Research Group on Drying Technology, King Mongkut's University of Technology Thonburi, Bangkok, Thailand.

REFERENCES

Driscoll, R.H. and Srzednicki, G.S., 1991, Design for a complete grain drying system under Southeast Asian climates, *Proceedings of the 12th ASEAN Technical Seminar on Grain Post-harvest Technology,* Surabaya, Indonesia, 29-31 August 1989.

Laithong, C., 1987, Study of physico-thermal properties of rough rice, Master's thesis, King Mongkut's Institute of Technology Thonburi, Bangkok, Thailand, in Thai.

Page, G.E., 1949, Factors influencing the maximum rate of drying shelled corn in layers, Unpublished thesis, Master of Science, Purdue University.

Poomsa-ad, N., Soponronnarit, S., Prachayawarakorn, S. and Terdyothin, A. 2002, Effect of tempering on subsequent drying of paddy using flidisation technique, *Drying Technology* **20**, 195-210.

Poomsa-ad, N, Soponronnarit, S., Terdyothin, A. and Prachayawarakorn, S., 2001. Head rice yield after drying by fluidization technique and tempering. Proc. the 2nd Asian-Oceana Drying Conference, 20-23 August 2001, Penang, Malaysia, pp. 717-726.

Poomsa-ad, N., Soponronnarit, S. and Prachayawarakorn, S., Investigation on head-rice yield and operating time in drying process: Experiment and Simulation, *Journal of Stored Product Research.* (Accepted to be published)

Soponronnarit, S., 2000, Fluidised bed grain drying, In: Mujumdar, A. and Suvachittanont, S. (Eds.), *Developments in Drying, Vol. II, Drying of Food and Agro-Products*, pp. 135-148, Kasetsart University press, Bangkok, Thailand.

Soponronnarit, S. and Prachayawarakorn, S., 1994, Optimum strategy for fluidized bed paddy drying, *Drying Technology* **12**, 1667-1686.

Soponronnarit, S., Kittiporn, K. and Prachayawarakorn, S., 1997, Appropriate operating parameters for fluidized bed corn drying, *RERIC International Energy Journal* **19**, 1-13.

Soponronnarit, S., Prachayawarakorn, S. and Sripawatakul, O., 1996, Development of cross-flow fluidized bed paddy dryer, *Drying Technology* **14**, 2397-2410.

Soponronnarit, S., Srisubati, N., Yoovidhya, T., 1998a, Effect of temperature and relative humidity on yellowing rate of paddy. *Journal of Stored Products Research* 34, 323-330.

Soponronnarit, S., Swasdisevi, T., Wetchacama, S. and Wutiwatchai, W., 2001, Fluidised bed drying of soybeans, *Journal of Stored Product Research* **37**, 133-151.

Soponronnarit, S., Taweerattanapanish, A., Wetchacama, S., Kongseri, N. and Wongpiyachon, S., 1998b, Spin-off from paddy drying by fluidization technique, Keynote paper in Proc. at *the 7th International Working Conference on Stored-Product Protection*, Beijing, China, 14-19 October 1998.

Soponronnarit, S., Wetchacama, S., Swasdisevi, T. and Poomsa-ad, N., 1999, Managing moist paddy by drying, tempering and ambient air ventilation, *Drying Technology* **17**, 335-344.

Soponronnarit, S., Wongvirojtana, P., Nathakaranakule, A. and Prachayawarakorn, S., 1994, Maintaining paddy quality by appropriate ventilation under tropical climate, *Proceedings of the 9th International Drying Symposium*, Gold Coast, Australia, 1-4 August 1994, pp. 825-832.

Soponronnarit, S., Yapha, M. and Prachayawarakorn, S., 1995, Cross-flow fluidized bed paddy dryer: prototype and commercialization, *Drying Technology* **13**, 2207-2216.

Sripawatakul, O., 1994, *Study of drying paddy by cross-flow fluidization technique*, Master's thesis, Faculty of Engineering, King Mongkut's Institute of Technology Thonburi, Bangkok, Thailand, in Thai.

Steffe, J.F., Singh, R.P. and Bakshi, A.S., 1979, Influence of tempering time and cooling on rice milling yields and moisture removal, *Trans.of the ASAE*, 17, 1214-1218.

Sutherland, J.W. and Ghaly, T.F., 1992, Rapid fluid bed drying of paddy rice in the humid tropics, *Proceedings of the 13th ASEAN Conference on Grain Post-harvest Technology*, Brunei Darussalam, 4-7 September 1990.

Taweerattanapanish, A., Soponronnarit, S., Wetchacama, S., Kongseri, N., Wongpiyachon, S., 1999. Effects of drying in head rice yield using fluidization technique, *Drying Technology* 17, 345-353.

Tumambing, J.A. and Driscoll, R.H., 1993, Modeling the performance of continuous fluidized bed paddy dryer for rapid pre-drying of paddy, *Proceedings of the 14th ASEAN seminar on Grain Post-harvest Technology*, Manila, Philippines, 5-8 November 1991, pp. 193-213.

Wilhelm, L.R., 1976, Numerical calculation on psychrometric properties in SI units, *Transactions of the American Society of Agricultural Engineers* **19**, 318-321, 325

Yapha, M., 1994, *Design and testing of pilot continuous fluidized bed paddy dryer*, Master's thesis, School of Energy and Materials, King Mongkut's Institute of Technology Thonburi, Bangkok, Thailand, in Thai.

Yap, A.B., Juliano, B.O., Perez, C.M., 1988. Artificial yellowing of rice at 60°C. In: Naewbanij, J.O. (Ed), Proceedings of the Eleventh ASEAN Technical Seminar on Grain Postharvest Technology, 23-26 August, 1988 Kuala Lumpur, Malaysia, ASEAN Grain Postharvest Programme, Bangkok, Thailand, pp. 3-20.

สถานภาพและแนวทางการวิจัยพลังงานหมุนเวียนในประเทศไทย

STATUS AND RESEARCH TRENDS ON RENEWABLE ENERGY IN THAILAND

วารุณี เตีย พิมพร แจ้งพลอย กังสดาล สกุลพงษ์มาลี และสมชาติ โสภณรณฤทธิ์
คณะพลังงานและวัสดุ มหาวิทยาลัยเทคโนโลยีพระจอมเกล้าธนบุรี
91 ถนนประชาอุทิศ แขวงบางมด เขตทุ่งครุ กรุงเทพฯ 10140 โทร.0-2470-8613 โทรสาร.0-2427-9062

Warunee Tia, Pimporn Changploy, Kangsadan Sagulpongmalee, and Somchart Soponronnarit
School of Energy and Materials, King Mongkut's University of Technology Thonburi
Bangmod, Tungkru, Bangkok 10140, Thailand, Tel.0-2470-8613 Fax.0-2427-9062

บทคัดย่อ

พิธีสารเกียวโตเริ่มมีผลบังคับใช้ ประเทศไทยเสี่ยงต่อการถูกจัดให้อยู่ในกลุ่มประเทศที่มีพันธกรณีจะต้องลดปริมาณการปล่อยแก๊สเรือนกระจก เนื่องจากการใช้พลังงานไม่มีประสิทธิภาพ ไม่ประหยัด และใช้พลังงานหมุนเวียนน้อย ทำให้การปล่อยแก๊สเรือนกระจกต่อประชากรของไทยมีค่าเข้าใกล้ค่าเฉลี่ยของโลกในปีฐาน (พ.ศ. ๒๕๓๓) ในบทความนี้จะกล่าวถึงพลังงานหมุนเวียนประเภทต่างๆ เช่น พลังงานมวลชีวภาพ พลังงานแสงอาทิตย์ พลังงานลม พลังน้ำขนาดเล็ก พลังงานความร้อนใต้พิภพ และพลังงานจากมหาสมุทร โดยลำดับจาก ศักยภาพ สถานภาพการใช้ และแนวทางวิจัยในอนาคต

คำสำคัญ: ประเทศไทย, พลังงานหมุนเวียน, ศักยภาพ, สถานภาพ, งานวิจัย

Abstract

Since Kyoto Protocal has come into effect. Thailand risks to be listed in the Kyoto Protocal as one of the countries which has to reduce greenhouse gas emissions. Because of inefficient energy use and less renewable energy utilization in Thailand, the amount of greenhouse gas emissions per capita approached to the average value of the world in 1990 which was used as a basis. Thus this paper presents the potential, status and research trends of renewable energy in Thailand, namely biomass, solar, wind, small-hydro, geothermal, and ocean energy.

Keywords: potential, renewable energy, research, status, Thailand

บทนำ

การใช้พลังงานหมุนเวียนในโลกจะเพิ่มมากขึ้นร้อยละ ๖๐ ในอีก ๒๕ ปีข้างหน้า (พ.ศ. ๒๕๙๓) แต่สัดส่วนของพลังงานหมุนเวียนเมื่อเทียบกับพลังงานทั้งหมดจะไม่เปลี่ยนแปลงมากนัก มวลชีวภาพดั้งเดิมจะมีสัดส่วนร้อยละ ๖ ในขณะที่มวลชีวภาพอื่นร้อยละ ๕ พลังงานจากแหล่งน้ำร้อยละ ๒ ส่วนพลังงานจากลมแสงอาทิตย์ ความร้อนใต้พิภพ น้ำขึ้นน้ำลง และคลื่น รวมกันแล้วร้อยละ ๒ โดยเฉพาะพลังงานจากน้ำขึ้นน้ำลงและคลื่นอาจจะมีบทบาทไม่มากนัก[๑]

ในแง่ของการผลิตกำลัง กำลังงานเขียว (Green power) จะมีสัดส่วนเพิ่มขึ้นร้อยละ ๑๘ ในปี พ.ศ. ๒๕๔๕ เป็นร้อยละ ๑๙ ในปี พ.ศ. ๒๕๙๓ ส่วนใหญ่จะได้จากพลังน้ำ, ลม และมวลชีวภาพ[๑]

มวลชีวภาพหนึ่งในพลังงานหมุนเวียนเพื่อการผลิตกำลังในอนาคตแยกได้เป็น ๓ ประเภท ตามกระบวนการผลิตเรียงลำดับความสำคัญดังนี้ ๑) กระบวนอุณหภาพ ๒) แก๊สจากการกลบฝัง และ ๓) แก๊สชีวภาพ ซึ่งคาดว่าจะมีการติดตั้งในโลกนี้ระหว่างปี พ.ศ. ๒๕๔๗–๒๕๔๖ รวม ๑๒,๑๗๒, ๑,๖๘๐ และ ๕๗๕ MW ตามลำดับ ประเทศในยุโรปตะวันตก อเมริกาเหนือและเอเชีย จะมีกำลังการติดตั้งจากสูงไปต่ำตามลำดับสำหรับภูมิภาคอื่นจะมีการติดตั้งไม่มากนัก[๑]

พิธีสารเกียวโตเริ่มมีผลบังคับใช้ตั้งแต่เดือนกุมภาพันธ์ พ.ศ. ๒๕๔๘ ชี้ให้เห็นว่าพลังงานหมุนเวียนจะเริ่มมีบทบาทสำคัญมากขึ้นในอนาคต แม้ว่าประเทศไทยจะยังไม่มีพันธกรณีที่จะต้องลดปริมาณการปล่อยแก๊สเรือนกระจก แต่จากการใช้พลังงานหมุนเวียนน้อย และการใช้พลังงานฟอสซิลซึ่งส่วนใหญ่นำเข้า เพิ่มขึ้นมากอย่างไม่มีประสิทธิภาพ จะทำให้การปล่อยแก๊สเรือนกระจกต่อประชากรของไทยสูงกว่าค่าเฉลี่ยของโลกในปีฐาน (พ.ศ. ๒๕๓๓) คือ ๓.๙ ตันคาร์บอนไดออกไซด์เทียบเท่าต่อคนก่อนปี ๒๕๔๓ ซึ่งจะทำให้เสี่ยงต่อการถูกจัดให้อยู่ในกลุ่มประเทศที่มีพันธกรณี[๒]

ในบทความนี้จะกล่าวถึง ศักยภาพ การใช้และแนวทางวิจัยพลังงานมวลชีวภาพ พลังงานแสงอาทิตย์ พลังงานลม พลังน้ำขนาดเล็ก พลังงานความร้อนใต้พิภพ และพลังงานจากมหาสมุทร

วิธีดำเนินงานวิจัย

แหล่งพลังงานหมุนเวียนที่กล่าวถึงในบทความนี้ ได้แก่ พลังงานมวลชีวภาพ พลังงานแสงอาทิตย์ พลังงานลม พลังน้ำขนาดเล็ก พลังงานความร้อนใต้พิภพ และพลังงานจากมหาสมุทร

งานวิจัยนี้ได้เก็บรวบรวมข้อมูลจากแหล่งต่างๆ ได้แก่ รายงาน และบทความวิจัย เพื่อนำมาศึกษาและเสนอแนวทางวิจัย ซึ่งมีรายละเอียดดังนี้

ก. ศึกษาศักยภาพของแหล่งพลังงานหมุนเวียนในประเทศไทย ศักยภาพของแหล่งพลังงานหมุนเวียน ขึ้นอยู่กับลักษณะภูมิประเทศและภูมิอากาศของแต่ละพื้นที่

ข. ศึกษาสถานภาพการใช้พลังงานหมุนเวียนของประเทศไทย

ค. ศึกษาสถานภาพงานวิจัยที่ผ่านมา

ง. วิเคราะห์ข้อมูล ศักยภาพของแหล่งพลังงาน สถานภาพการใช้และงานวิจัยพลังงานที่ผ่านมา นำมาสรุปเสนอเป็นแนวทางงานวิจัยที่ควรดำเนินการต่อไป

ผลการศึกษาและวิจารณ์

๑. พลังงานมวลชีวภาพ

๑.๑ ศักยภาพมวลชีวภาพของประเทศไทย

ปริมาณมวลชีวภาพจากวัสดุเหลือใช้ทางการเกษตรขึ้นอยู่กับผลผลิตทางการเกษตรและการใช้ในแต่ละปี ในปี ๒๕๔๓ ได้มีการประเมินศักยภาพมวลชีวภาพจากวัสดุเหลือใช้ทางการเกษตร[๓] ๑๐ ชนิด ดังแสดงในตารางที่ ๑ จะเห็นได้ว่ามีปริมาณมวลชีวภาพเหลือใช้ทางเกษตรที่ยังไม่ได้นำมาใช้เป็นเชื้อเพลิงยังมีอยู่อีกมากคิดเป็นพลังงานรวมทั้งสิ้น ๖๐๔,๘๒๒×๑๐[๖] จูล

มูลสัตว์ น้ำเสียจากโรงงานอุตสาหกรรม และขยะ สามารถนำมาผลิตเป็นแก๊สชีวภาพได้ ในปี ๒๕๔๓ ได้มีการประเมินศักยภาพศักยภาพการผลิตแก๊สชีวภาพจากมูลสัตว์ ๖ ชนิดดังแสดงในตารางที่ ๒ มีศักยภาพรวมทั้งสิ้น ๑๑,๗๕๐×๑๐[๖]จูล (คิดที่ค่าความร้อนแก๊สชีวภาพผลิตจากมูลสัตว์เท่ากับ ๒๑ เมกะจูลต่อลบ.ม.) สำหรับน้ำเสียในโรงงานอุตสาหกรรม ๑๑ ประเภท ดังแสดงในตารางที่ ๓ มีศักยภาพรวมทั้งสิ้น ๑๐,๔๔๖×๑๐[๖]จูล (คิดที่ค่าความร้อนแก๊สชีวภาพผลิตจากน้ำเสียเท่ากับ ๒๔ เมกะจูลต่อลบ.ม.) จะเห็นได้ว่าโรงงานแป้งมันและโรงงานน้ำตาลมีศักยภาพสูงมาก ในส่วนของการผลิตแก๊สชีวภาพจากการฝังกลบขยะมีศักยภาพรวมทั้งสิ้น ๒๓,๐๙๒×๑๐[๖] จูล (คิดที่ค่าความร้อนแก๊สชีวภาพผลิตจากขยะเท่ากับ ๑๙.๕ เมกะจูลต่อลบ.ม.) ดังแสดงในตารางที่ ๔ ศักยภาพรวมของการผลิตแก๊สชีวภาพจากมูลสัตว์ น้ำเสียจากโรงงานอุตสาหกรรม และขยะที่ได้จากการฝังกลบรวมทั้งหมดเท่ากับ ๔๔,๒๘๘×๑๐[๖] เมกะจูลต่อปี ถึงแม้ว่าศักยภาพที่ได้จากการฝังกลบจะมีค่ามาก แต่ในปัจจุบันการรวบรวมทำได้ยาก ดังนั้นจึงจะพิจารณาการผลิตแก๊สชีวภาพจากมูลสัตว์ น้ำเสียจากโรงงานอุตสาหกรรม เป็นสำคัญ

มวลชีวภาพสำหรับการผลิตไบโอดีเซล ประเทศไทยมีพืชน้ำมันที่ทำการเกษตรอย่างเป็นระบบและเชิงพาณิชย์ ได้แก่ ถั่วเหลือง ถั่วลิสง ปาล์มน้ำมัน งา มะพร้าว ละหุ่ง ซึ่งมีผลผลิตดังแสดงในตารางที่ ๕ จะเห็นได้ว่าปาล์มน้ำมันมีศักยภาพสูงที่สุด การนำน้ำมันพืชมาใช้มีปัญหาหลักคือ ความหนืด การนำน้ำมันพืชมาสังเคราะห์เป็นเอสเตอร์หรือไบโอดีเซล จะทำให้ความหนืดลดลง มีความคงตัวมากขึ้นเมื่ออุณหภูมิเปลี่ยน จุดวาบไฟของไบโอดีเซลสูงกว่าน้ำมันดีเซล จึงมีความปลอดภัยในการใช้และการขนส่ง[๔] นอกจากนี้ไบโอดีเซลยังมีค่าซีเทนสูงกว่าน้ำมันดีเซล กล้าณรงค์ ศรีรอด และคณะ[๖] ได้ศึกษาพื้นที่ที่เหมาะสมและพื้นที่ปลูกจริงของปาล์มน้ำมัน พบว่า สามารถขยายพื้นที่เพาะปลูกได้อีก ๑๑,๙๙๓,๒๑๔ ไร่ ต้นทุนการผลิตไบโอดีเซลอยู่ในช่วง ๔.๐๐-๑๙.๕๐ บาทต่อลิตร ขึ้นกับราคาวัตถุดิบ ต้นทุนสำหรับกระบวนการ Transesterification อยู่ในช่วง ๒.๕๐- ๓.๐๐ บาทต่อลิตร[๖]

สำหรับเอทธานอลสามารถผลิตได้จากผลผลิตทางเกษตรและวัสดุเหลือใช้ทางการเกษตร[๗] ได้แก่ วัตถุดิบประเภทแป้ง เช่น มันสำปะหลัง วัตถุดิบประเภทน้ำตาล เช่น อ้อย กากน้ำตาล และเศษวัสดุที่เป็นเซลลูโลส เช่น ฟางข้าว ขี้เลื่อย เป็นต้น สำหรับประเทศไทยวัตถุดิบที่เหมาะสมและสามารถนำมาผลิตเอทธานอล ได้แก่ มันสำปะหลัง กากน้ำตาล และอ้อย พื้นที่เพาะปลูกมันสำปะหลังของประเทศไทยประมาณ ๖.๕ ล้านไร่ จะผลิตมันสำปะหลังได้ ๒๐ ล้านตันต่อปี (เมื่อคิดที่ปริมาณผลผลิต ๓ ตันต่อไร่) หัวมันสำปะหลังได้นำมาใช้ในภาคอุตสาหกรรมผลิตแป้งมันสำปะหลังประมาณ ๘ ล้านตันต่อปี ผลิตมันเส้น/มันอัดเม็ดอีกประมาณ ๘ ล้านตันต่อปี จะทำให้มีหัวมันสำปะหลังเหลืออยู่ประมาณ ๔ ล้านตันต่อปี สามารถนำไปผลิตเป็นเอทธานอลได้ ๑.๘๓ ล้านลิตรต่อวัน[๙] การใช้มันสำปะหลังควรใช้ในรูปของมันเส้นเพราะสามารถแปรรูปได้ง่าย และสามารถเก็บไว้ใช้ได้ตลอดปี ต้นทุนการผลิตเอทธานอลจากมันสดอยู่ในช่วง ๑๑.๙ ถึง ๑๙.๓ บาทต่อลิตร (ที่ราคามันสำปะหลังในช่วง ๑,๐๐๐-๑,๔๐๐ บาท/ตัน) และจากมันเส้น ๑๑.๔๔-๑๒.๔๔ บาทต่อลิตร[๙] (ที่ราคามันสำปะหลังเส้นอยู่ในช่วง ๒,๔๐๐-๒,๙๐๐ บาท/ตัน) ปัจจุบันสามารถใช้เทคโนโลยีการผลิตเอทธานอลโดยวิธี Simultaneous Saccharification and Fermentation (SSF) สามารถลดต้นทุนการผลิตเอทธานอลลงได้ร้อยละ ๒๕ ในส่วนของต้นทุนการหมักปกติ

การใช้อ้อยเป็นวัตถุดิบในการผลิตเอทธานอลนั้นไม่เหมาะสม เนื่องจากปริมาณอ้อยไม่เพียงพอต่อความต้องการของอุตสาหกรรมน้ำตาล กากน้ำตาลเป็นผลพลอยได้จากการผลิตน้ำตาล ในการผลิตน้ำตาลจากอ้อยประมาณ ๕๐ ล้านตันต่อปี จะได้กากน้ำตาลประมาณร้อยละ ๕ หรือประมาณ ๒.๕ ล้านตันต่อปี กากน้ำตาลนำไปใช้ในอุตสาหกรรมอาหารภายในประเทศประมาณ ๑.๕ ล้านตัน และส่งออกประมาณ ๑ ล้านตัน กากน้ำตาลมีราคาต่ำกว่าราคาของเอทธานอลมาก กากน้ำตาล ๑ ล้านตันสามารถผลิตเอทธานอลได้ประมาณ ๘๐๐,๐๐๐ ลิตรต่อวัน ต้นทุนการผลิตเอทธานอลจากกากน้ำตาลอยู่ในช่วง ๑๑.๓ - ๑๕.๓ บาทต่อลิตร[๙] (ที่ราคากากน้ำตาลอยู่ในช่วง ๑,๕๐๐-๒,๕๐๐ บาทต่อตัน)

๑.๒ สถานภาพการใช้พลังงานมวลชีวภาพของประเทศไทย

ในปี ๒๕๔๖ ประเทศไทยได้จัดหามวลชีวภาพของแข็งมาใช้ในพลังงานขั้นต้น รวมทั้งสิ้น ๑๔,๘๑๘ พันตันเทียบเท่าน้ำมันดิบ[๑๐] คิดเป็นร้อยละ ๑๖.๐ ของการจัดหาพลังงานขั้นต้นทั้งหมดของประเทศ ซึ่งส่วนใหญ่ผลิตได้ภายในประเทศ รวมทั้งสิ้น ๑๔,๘๐๔ พันตันเทียบเท่าน้ำมันดิบ[๑๐] ได้แก่ไม้ฟืนร้อยละ ๖๘.๓ ที่เหลือเป็น ชานอ้อย และแกลบ คิดเป็นสัดส่วนร้อยละ ๒๒.๒ และ ๙.๕ ตามลำดับ ประมาณร้อยละ ๖๔.๑ ของไม้ฟืนนำไปใช้ในการแปรรูปเป็นถ่านไม้[๑๑] มีการนำเข้าถ่านไม้และฟืน เล็กน้อยรวมทั้งสิ้น ๑๗ พันตันเทียบเท่าน้ำมันดิบ[๑๐] และมีการส่งออกถ่านไม้รวมทั้งสิ้น 3 พันตันเทียบเท่าน้ำมันดิบ[๑๐] รัฐได้สนับสนุนให้มีการใช้มวลชีวภาพเป็นเชื้อเพลิงในการผลิตไฟฟ้า โดยรับซื้อไฟฟ้าจากผู้ผลิตรายเล็กและเล็กมากที่ใช้พลังงานนอกรูปแบบเป็นเชื้อเพลิง ในปี ๒๕๔๖ มีการใช้แกลบ ชานอ้อย ฟืน ขยะ และวัสดุเหลือทิ้งทางการเกษตรอื่นๆ เป็นเชื้อเพลิงในการผลิตไฟฟ้ารวมทั้งสิ้น ๓,๐๖๗ พันตัน[๑๐] ซึ่งส่วนใหญ่ผลิตจากโรงงานน้ำตาล นอกจากนี้ยังมีการใช้แบล็คลิเคอ ๙,๔๐๔×๑๐[๖]จูล[๑๐] ในโรงงาน

กระดาษ และแก๊สเหลือใช้จากกระบวนการผลิตปิโตรเคมี อีกประมาณ ๖๙๙×๑๐[๑๖] จูล[๑๐] มาใช้เป็นเชื้อเพลิงในการผลิตไฟฟ้า สำหรับการใช้มวลชีวภาพของแข็งในพลังงานขั้นสุดท้ายในสาขาเศรษฐกิจต่างๆ รวมทั้งสิ้น ๙,๗๕๑ พันตันเทียบเท่าน้ำมันดิบ[๙] ได้แก่ ไม้ (ร้อยละ ๓๕.๙) ถ่านไม้ (ร้อยละ ๒๔.๒) ชานอ้อย (ร้อยละ ๒๑.๙) และแกลบ (ร้อยละ ๑๐.๒) ซึ่งใช้ในครัวเรือนประมาณร้อยละ ๕๒.๖ ส่วนใหญ่ใช้ไม้และถ่านไม้ ส่วนที่เหลืออีกร้อยละ ๔๗.๔ ใช้ในภาคอุตสาหกรรมซึ่งส่วนใหญ่ใช้ชานอ้อย แกลบ และไม้

สำหรับไบโอดีเซล ในปี ๒๕๔๖ ประเทศไทยมีกำลังผลิตติดตั้งโรงงานสกัดน้ำมันปาล์มดิบภายในประเทศรวมทั้งสิ้น ๘๗๘,๙๘๑.๘ ตัน เกือบทั้งหมดถูกใช้ไปเพื่อการบริโภค มีศักยภาพเพื่อมาใช้เป็นเชื้อเพลิงได้ ๑๗,๔๓๕.๖ ตัน หรือ เท่ากับ ๑๖.๓ พันตันเทียบเท่าน้ำมันดิบ[๑๑]

สำหรับเอทานอล ปัจจุบันมีโรงงานผลิตเอทานอลที่ได้รับอนุญาตจากสำนักงานคณะกรรมการเอทานอลแห่งชาติรวม ๒๔ โรง มีกำลังการผลิตรวม ๔,๑๑๐,๐๐๐ ลิตรต่อวัน[๑๒] ซึ่งเริ่มเดินระบบแล้ว ๒ โรง มีกำลังผลิตรวม ๑๒๔,๐๐๐ ลิตรต่อวัน[๑๒]

สำหรับแก๊สชีวภาพ ในปี ๒๕๔๖ ประเทศไทยมีระบบผลิตก๊าซชีวภาพจากการเลี้ยงสัตว์มีทั้งประเภทครัวเรือนและเพื่อการค้า รวม ๑๒๒,๘๕๔ ลบ.ม. ส่วนน้ำเสียในโรงงานอุตสาหกรรมจากข้อมูลของกรมพัฒนาพลังงานทดแทนและอนุรักษ์พลังงาน สามารถผลิตก๊าซชีวภาพได้ประมาณ ๖๑,๓๒๐ ลบ.มต่อวัน[๑๓] ที่ค่าความร้อนของก๊าซชีวภาพจากน้ำเสียมีค่าเท่ากับ ๒๔ เมกะจูลต่อลบ.ม. จะได้เป็นพลังงานรวมประมาณ ๑,๔๗๑,๖๘๐ เมกกะจูลต่อวัน

๑.๓ สถานภาพงานวิจัยด้านพลังงานมวลชีวภาพของประเทศไทย

งานวิจัยด้านเชื้อเพลิงมวลชีวภาพของแข็ง ได้มีการปรับปรุงเตาเผาไหม้มวลชีวภาพเพื่อให้มีประสิทธิภาพสูงขึ้น เช่น เตาถ่านไม้[๑๔] เตาเผาแกลบแบบไซโคลน[๑๔] เตาฟลูอิดไดซ์เบด[๑๖] เนื่องจากมวลชีวภาพเป็นเชื้อเพลิงแข็งจึงได้มีการวิจัยเพื่อเปลี่ยนให้เป็นเชื้อเพลิงก๊าซก่อนที่จะมีการเผาไหม้เพื่อให้ใช้ประโยชน์ได้กว้างมากขึ้น[๑๗] สำหรับการนำมวลชีวภาพมาเป็นเชื้อเพลิงในการผลิตไฟฟ้าได้มีงานวิจัยที่ประเมินหาศักยภาพด้านเทคนิคและเศรษฐศาสตร์ของการใช้ระบบผลิตไฟฟ้าและความร้อนร่วมของโรงงานสกัดน้ำมันปาล์ม[๑๙] โรงสีข้าว[๑๙] โรงงานน้ำตาล[๒๐] โรงงานไม้ยางพารา[๒๑] ถ้าพบว่าเดิมโรงงานบางแห่งได้มีการผลิตกำลังงานจากมวลชีวภาพอยู่แล้ว แต่ใช้ไอน้ำที่ความดันไม่สูงมากนัก ก็จะพิจารณาปรับปรุงระบบให้ใช้ไอน้ำที่ความดันสูงขึ้นเพื่อจะผลิตกำลังงานไฟฟ้าได้มากขึ้น นอกจากนี้ยังมีงานวิจัยเพื่อนำความร้อนจากการเผาไหม้ไปใช้ประโยชน์ เช่น การอบแห้งข้าวเปลือก[๒๒]

งานวิจัยด้านไบโอดีเซล มีการวิจัยด้านกระบวนการผลิตไบโอดีเซลจากน้ำมันพืชชนิดต่างๆเช่นน้ำมันปาล์ม[๒๓] น้ำมันพืชใช้แล้ว[๒๔] พบว่าไบโอดีเซลมีสมบัติสามารถใช้กับเครื่องยนต์ดีเซลได้ และมีงานวิจัยที่ทดสอบการใช้งานน้ำมันไบโอดีเซลกับเครื่องยนต์เพื่อดูสมรรถนะและปัญหาต่างๆที่อาจจะเกิดได้ นอกจากนี้มีการทดลองนำน้ำมันดีเซลไปผสมกับน้ำมันพืชชนิดต่างๆโดยตรงในสัดส่วนต่างๆ[๒๔,๒๖] แล้วไปทดสอบเดินเครื่องยนต์ พบว่า ปริมาณควันดำขึ้นอยู่กับสัดส่วนน้ำมันพืชที่ผสม อย่างไรก็ดีการทดสอบกับเครื่องยนต์ส่วนใหญ่เป็นการทดสอบระยะสั้น

งานวิจัยด้านเอทานอล มีการวิจัยหาแนวทางลดต้นทุนในกระบวนการผลิตในการกลั่นโดยใช้พลังงานแสงอาทิตย์มาเสริม[๒๗] และการหมัก[๒๘] การประเมินความเป็นไปได้ในการผลิตเอทานอลจากผลผลิตทางเกษตร[๒๙,๓๐] และนำเอทานอลไปใช้เป็นเชื้อเพลิงในเครื่องยนต์ก๊าซโซลีนเพื่อทดสอบสมรรถนะและการสึกหรอของเครื่องยนต์ นอกจากนี้ยังมีงานวิจัยด้านบูรณาการกระบวนการผลิตเอทานอลกับโรงน้ำตาล และโรงงานแป้งมันสำปะหลัง[๓๑] สามารถลดต้นทุนค่าขนส่งวัตถุดิบ ส่วนการบูรณาการด้านพลังงานสามารถลดต้นทุนด้านพลังงานได้

งานวิจัยด้านแก๊สชีวภาพ ได้มีการวิจัยระบบผลิตแก๊สชีวภาพจากมูลสัตว์ และน้ำเสียจากอุตสาหกรรมทั้งระบบเดี่ยวๆของแต่ละแห่ง และระบบบำบัดรวมขนาดใหญ่[๓๒,๓๓] รวมถึงการใช้ประโยชน์จากแก๊สชีวภาพ และการวิเคราะห์ความคุ้มค่าทางการเงินของการลงทุน

๑.๔ แนวทางวิจัยพลังงานมวลชีวภาพของประเทศไทย

ปัญหาโดยทั่วไปของการใช้มวลชีวภาพ คือ แหล่งมวลชีวภาพที่นำมาใช้ได้มีไม่สม่ำเสมอ เปลี่ยนแปลงตามฤดูกาลโดยเฉพาะจากอุตสาหกรรมเกษตร โดยส่วนใหญ่มวลชีวภาพแต่ละชนิดจะปลูกและมีผลผลิตตามฤดูกาล และยังขึ้นอยู่กับสภาพอากาศ นอกจากนี้ยังขึ้นอยู่กับราคา และความต้องการของตลาดซึ่งส่งผลให้เกษตรกรเปลี่ยนชนิดของพืชที่เพาะปลูก และการเปลี่ยนแปลงพื้นที่การเกษตรไปใช้ประโยชน์ด้านอื่นอีกด้วย เนื่องจากมวลชีวภาพมีอยู่อย่างกระจัดกระจาย ทำให้รวบรวมได้ยาก และมีปริมาตรมาก ทำให้ค่าขนส่งสูง ดังนั้นการพัฒนาเพื่อนำมวลชีวภาพที่ยังไม่ได้ใช้มาผลิตพลังงานได้เพิ่มขึ้นจึงควรมีการวิจัยด้านการจัดการมวลชีวภาพที่ใช้เป็นวัตถุดิบ เช่น การจัดหา รวบรวม และจัดเก็บ เพื่อสามารถนำมาผลิตพลังงานได้ต่อเนื่องไม่ขาดช่วง และมีต้นทุนวัตถุดิบต่ำ นอกจากนี้ควรมีการวิจัยเชิงนโยบายเพื่อหามาตรการส่งเสริม เพื่อจูงใจให้มีการใช้มวลชีวภาพเป็นพลังงานทดแทนมากขึ้น

ในการใช้มวลชีวภาพเป็นเชื้อเพลิงควรทำการวิจัยเพื่อเพิ่มประสิทธิภาพเตาหรือห้องเผาไหม้มวลชีวภาพและควรใช้กับเชื้อเพลิงมวลชีวภาพได้หลายๆ ประเภท เนื่องจากเตาเผามวลชีวภาพแต่ละเตาจะออกแบบมาเพื่อใช้กับมวลชีวภาพแต่ละชนิด ดังนั้นถ้ามวลชีวภาพชนิดดังกล่าวมีปริมาณไม่เพียงพอจำเป็นต้องพึ่งพามวลชีวภาพประเภทอื่น ก็จะทำให้ได้ประสิทธิภาพในการเผาไหม้ต่ำ นอกจากนี้ควรมีการศึกษาการเผาไหม้มวลชีวภาพร่วมกับเชื้อเพลิงเชิงพาณิชย์บางชนิด เช่น ถ่านหิน เพื่อหาแนวทางเสริมการให้ใช้เชื้อเพลิงมวลชีวภาพทดแทน ถึงแม้จะมีเชื้อเพลิงมวลชีวภาพไม่เพียงพออย่างต่อเนื่องตลอดช่วงความต้องการใช้งาน และควรมีการศึกษาความเป็นไปได้ของการผลิตไฟฟ้าจากเชื้อเพลิงมวลชีวภาพที่ยังไม่ได้นำมาใช้ให้มากขึ้น

สำหรับไบโอดีเซลจากการศึกษาพบว่า ปาล์มน้ำมันมีศักยภาพมากที่สุด ประเทศไทยถึงแม้จะมีพื้นที่ที่เหมาะสมในการปลูกปาล์มน้ำมันหลายพื้นที่ แต่มีข้อจำกัดบางประการทำให้ไม่ได้ใช้พื้นที่เหล่านั้นในการเพาะปลูก และเมื่อเปรียบเทียบกับต่างประเทศ ประเทศไทยยังมี

ผลผลิตต่อไร่ต่ำทำให้ต้นทุนการผลิตมีค่าสูง เนื่องจากการจัดการหลังการเก็บเกี่ยวยังไม่ดีพอจึงทำให้คุณภาพปาล์มน้ำมันที่สกัดได้ยังไม่ดีเท่าที่ควร ดังนั้นควรมีงานวิจัยด้านการเกษตรเพื่อใช้พื้นที่ในการเพาะปลูกที่เหมาะสม การคัดเลือกและปรับปรุงพันธุ์ปาล์ม เพื่อหาวิธีขยายพันธุ์ที่ดี การถ่ายทอดเทคโนโลยีสู่ชาวไร่ เทคโนโลยีการเก็บเกี่ยวและหลังการเก็บเกี่ยว เพื่อควบคุมคุณภาพของปาล์มน้ำมัน ทั้งหมดนี้เพื่อเพิ่มผลผลิตต่อไร่ให้มีค่าสูงขึ้น ลดต้นทุนของวัตถุดิบ และให้ได้ผลผลิตที่มีคุณภาพ นอกจากนี้ควรมีการศึกษาวิจัยเพื่อลดค่าใช้จ่ายในกระบวนการผลิตไบโอดีเซล เนื่องจากไบโอดีเซลที่ผลิตมาจากวัตถุดิบหลายชนิดที่มีคุณภาพและต้นทุนการผลิตแตกต่างกัน จึงควรมีการศึกษาเพื่อกำหนดมาตรฐานคุณภาพของไบโอดีเซล และควรมีการศึกษาผลระยะยาวของเครื่องยนต์ที่ใช้ไบโอดีเซลเป็นเชื้อเพลิง

การวิจัยด้านเอทานอล จากการศึกษาข้อมูล พบว่าวัตถุดิบที่เหมาะสมจะนำมาผลิตเอทานอล ได้แก่ มันสำปะหลัง และกากน้ำตาล เพราะไม่มีผลกระทบกับการบริโภค สำหรับมันสำปะหลังควรศึกษาวิธีการวางแผนการกำหนดพื้นที่เพาะปลูกเพื่อให้เก็บเกี่ยวผลผลิตได้อย่างต่อเนื่อง และควรมีการวิจัยเพื่อกำหนดมาตรฐานอัตราส่วนผสมระหว่างเอทานอลกับน้ำมันเบนซิน และควรมีการศึกษาผลระยะยาวเครื่องยนต์ที่ใช้น้ำมันเบนซินผสมนี้ด้วย

สำหรับแก๊สชีวภาพ ยังมีโรงงานและฟาร์มเป็นจำนวนมากที่มีศักยภาพ แต่ยังไม่มีระบบการผลิตแก๊สชีวภาพ จึงควรมีงานวิจัยด้านการศึกษาความเป็นไปได้ของการผลิตและประยุกต์ใช้แก๊สชีวภาพในรูปแบบต่างๆ เพื่อให้ได้รูปแบบ ขนาดระบบ และการนำไปใช้ประโยชน์ได้อย่างเหมาะสม ในฟาร์มเลี้ยงสัตว์บางแห่งยังพบว่ามีปัญหาในด้านความเสียหายของอุปกรณ์ที่ใช้เนื่องจากเกิดการกัดกร่อนที่เกิดจากไฮโดรเจนซัลไฟด์ (H_2S) เมื่อรวมกับน้ำจะเป็นกรดซัลฟิวริกมีฤทธิ์สามารถกัดกร่อนโลหะได้ ซึ่งขึ้นอยู่กับองค์ประกอบทางเคมีของแก๊สชีวภาพที่ได้จากมูลสัตว์หรือน้ำเสียจากโรงงานอุตสาหกรรม จึงควรมีแนวทางวิจัยของระบบกำจัดก๊าซไฮโดรเจนซัลไฟด์ในแก๊สชีวภาพด้วย

นอกจากนี้ควรมีงานวิจัยเชิงนโยบายและมาตรการต่างๆของประเทศที่ประสพความสำเร็จในการใช้พลังงานมวลชีวภาพ เช่น มาตรการภาษีด้านต่างๆ โดยเฉพาะภาษีแก๊สคาร์บอนไดอ๊อกไซด์

๒. พลังงานแสงอาทิตย์

๒.๑ ศักยภาพพลังงานแสงอาทิตย์ในประเทศไทย

พื้นที่ส่วนใหญ่ของประเทศไทยมีความเข้มแสงอาทิตย์สูงสุด อยู่ในช่วงเดือนเมษายน และพฤษภาคม โดยมีค่าอยู่ช่วง ๒๐ - ๒๔ เมกะจูล/ตารางเมตร-วัน[๔] พื้นที่ที่ได้รับความเข้มแสงอาทิตย์สูงสุดเฉลี่ยทั้งปี ได้แก่ ภาคตะวันออกเฉียงเหนือ และภาคกลางบางส่วน ความเข้มแสงอาทิตย์เฉลี่ยต่อปีของพื้นที่ทั่วประเทศมีค่าเท่ากับ ๑๗.๕ เมกะจูล/ตารางเมตร-วัน[๕] ศักยภาพพลังงานแสงอาทิตย์เมื่อคิดจากร้อยละ ๑ ของพื้นที่ทั้งหมด คิดเป็น ๕๕๔,๐๗๑ พันตันเทียบเท่าน้ำมันดิบ[๕]

๒.๒ การใช้พลังงานแสงอาทิตย์ในประเทศไทย

ในปี ๒๕๔๖ ประเทศไทยมีการใช้พลังงานแสงอาทิตย์ในรูปความร้อนรวมทั้งสิ้น ๕,๗๙๙,๑๒๕ เมกะจูล และไฟฟ้า ๕,๙๑๔.๒ เมกะวัตต์ชั่วโมง[๖] ส่วนใหญ่ใช้ในภาคเหนือ ในสาขาเศรษฐกิจ บ้านอยู่อาศัยและธุรกิจการค้า

เครื่องทำน้ำร้อนพลังงานแสงอาทิตย์เป็นที่ยอมรับในเชิงพาณิชย์แล้ว มีใช้ในบ้านเรือน โรงแรม โรงพยาบาล มียอดจำหน่ายประมาณ ๔,๐๐๐-๑๐,๐๐๐ ตารางเมตรต่อปี รวมพื้นที่ติดตั้งตัวรับรังสีอาทิตย์ชนิดแผ่นราบประมาณ ๕๐,๐๐๐ ตารางเมตร[๗] ซึ่งมีทั้งนำเข้าจากต่างประเทศและผลิตเองในท้องถิ่น แต่จำนวนยอดจำหน่ายในแต่ละปียังเพิ่มขึ้นไม่มากนัก แสดงว่าการยอมรับมีจำกัดและยังไม่แพร่หลายเท่าที่ควร เนื่องจากสาเหตุหลายประการ เช่น มีราคาสูงกว่าเครื่องทำน้ำร้อนจากไฟฟ้าและแก๊สหุงต้ม ความไม่สม่ำเสมอของการใช้งานหรือต้องใช้งานควบคู่กับพลังงานชนิดอื่น เครื่องที่ผลิตในประเทศของบางบริษัทมีคุณภาพต่ำ ทำให้ขาดความเชื่อถือในระยะยาว บริการหลังการขายยังไม่ดี รวมทั้งมาตรการสนับสนุนจากภาครัฐยังมีความจูงใจไม่เพียงพอ

เครื่องอบแห้งพลังงานแสงอาทิตย์ยังไม่เป็นที่ยอมรับในเชิงพาณิชย์ มีการใช้งานสำหรับอบแห้งพืชผลทางการเกษตรเป็นส่วนใหญ่ มีขนาดเล็กและการยอมรับยังอยู่ในวงจำกัด และยังไม่สามารถใช้ในเชิงอุตสาหกรรมได้ การอบแห้งผลิตภัณฑ์แต่ละครั้งได้ในปริมาณที่ไม่มากนัก และระยะเวลาที่ใช้ใกล้เคียงกับวิธีตากกลางแจ้งแต่มีการลงทุนสูงกว่า

สำหรับเครื่องกลั่นน้ำพลังงานแสงอาทิตย์ ยังไม่มีข้อมูลการนำไปใช้งาน ประสิทธิภาพยังไม่สูงเพียงพอที่จะนำไปใช้งานได้จริงและไม่คุ้มค่าในเชิงพาณิชย์ รวมถึงยังไม่มีความต้องการและความจำเป็นในการนำมาใช้งานสำหรับประเทศไทย และยังมีปัญหาด้านคุณภาพของน้ำกลั่นที่ผลิตได้ว่าจะเหมาะสมสำหรับการนำไปใช้ประโยชน์ด้านใด

เครื่องทำความเย็นด้วยพลังงานแสงอาทิตย์ในประเทศไทยยังอยู่ในขั้นตอนของการวิจัยเพื่อศึกษาสมรรถนะเท่านั้น ยังไม่มีข้อมูลสำหรับการนำมาใช้งานจริง เนื่องจากหลักการทำงานของระบบจะค่อนข้างซับซ้อนต้องใช้อุปกรณ์ที่ได้มาตรฐานและทันสมัย รวมถึงความก้าวหน้าของเทคโนโลยีที่ยังไม่ได้รับการพัฒนาเท่าที่ควร จึงทำให้เครื่องทำความเย็นพลังงานแสงอาทิตย์ยังมีประสิทธิภาพต่ำ มีราคาค่อนข้างสูงกว่าเครื่องทำความเย็นในระบบเดิมอยู่มาก

การนำเซลล์แสงอาทิตย์มาใช้ในประเทศไทยส่วนใหญ่นำไปใช้ในพื้นที่ห่างไกลที่ระบบสายส่งไปไม่ถึง เนื่องจากต้นทุนในการผลิตไฟฟ้ายังคงสูงกว่าที่ซื้อจากสายส่งอยู่มาก มีการผลิตไฟฟ้าจากเซลล์แสงอาทิตย์สำหรับงานในระบบโทรคมนาคม ระบบประจุแบตเตอรี่หมู่บ้านห่างไกล ระบบสูบน้ำในหมู่บ้านห่างไกล ระบบสอนหนังสือทางไกล ระบบผลิตไฟฟ้าผสมผสานในพื้นที่ห่างไกล เช่น ที่ภูเก็ตมีระบบผลิตไฟฟ้าร่วม เซลล์แสงอาทิตย์กำลังผลิต ๑๑.๓๔ กิโลวัตต์และกังหันลมกำลังการผลิต ๑๗๐ กิโลวัตต์[๖] ปัจจุบันโรงไฟฟ้าเซลล์แสงอาทิตย์ขนาดใหญ่ที่สุดในประเทศ คือ โรงไฟฟ้าเซลล์แสงอาทิตย์ผาปองที่มีขนาด ๒,๔๐๐ กิโลวัตต์ ผลิตเพื่อจำหน่ายไฟฟ้าให้จังหวัดแม่ฮ่องสอน[๗] นอกจากนี้ยังมีการใช้เซลล์แสงอาทิตย์ในงานอื่นๆ เช่น ไฟสัญญาณ สถานีอนามัย

สำหรับเทคโนโลยีการติดตั้งเซลล์แสงอาทิตย์ในประเทศไทยมีอยู่ด้วยกัน ๓ แบบ คือ Solar home system (SHM), Roof-top PV และ

Centralised PV โดย Solar home system จะเป็นการติดตั้งที่ไม่ต่อเข้าระบบสายส่งของการไฟฟ้า (Stand alone) ซึ่งมักจะติดตั้งในชนบทห่างไกลที่สายส่งเข้าไปไม่ถึงหรือหน่วยงานสาธิตต่างๆ ส่วน Roof-top PV และ Centralised PV จะเป็นการติดตั้งที่ต่อเข้าระบบสายส่ง โดย Centralised PV จะเป็นการติดตั้งเพื่อผลิตกระแสไฟฟ้าเข้าระบบของการไฟฟ้าฝ่ายผลิตแห่งประเทศไทยและการไฟฟ้าส่วนภูมิภาค ซึ่งจะมีขนาดใหญ่กว่า Roof-top PV ซึ่งจะติดตั้งตามหน่วยงานต่างๆ ที่ได้รับการคัดเลือก

รัฐได้มีนโยบายสนับสนุนให้มีการติดตั้งระบบผลิตไฟฟ้าด้วยเซลล์แสงอาทิตย์ โดยได้ออกระเบียบให้การไฟฟ้าฝ่ายผลิตแห่งประเทศไทยรับซื้อไฟฟ้าจากผู้ผลิตไฟฟ้าพลังงานหมุนเวียนขนาดเล็กมาก ดังนั้น บ้านพักอาศัย หน่วยงาน หรือ สถานประกอบการที่มีการติดตั้งระบบผลิตไฟฟ้าด้วยเซลล์แสงอาทิตย์ สามารถขายไฟฟ้ากลับเข้าสายส่งไฟฟ้าได้ ในปี ๒๕๔๖ มีการผลิตไฟฟ้าด้วยพลังงานแสงอาทิตย์ รวมทั้งสิ้น ๕,๙๑๙.๒ เมกกะวัตต์ชั่วโมง ประมาณร้อยละ ๕๗ ผลิตในภาคเหนือ รองลงมาคือ ภาคกลาง ภาคใต้และภาคตะวันออกเฉียงเหนือ ร้อยละ ๒๑.๓, ๑๖.๒ และ ๕.๕ ตามลำดับ[๗]

๒.๓ สถานภาพงานวิจัยด้านพลังงานแสงอาทิตย์ของประเทศไทย

มีการวิจัยและพัฒนาการผลิตน้ำร้อนด้วยแสงอาทิตย์มาเป็นเวลานาน ปัจจุบันมีใช้งานในเชิงพาณิชย์ งานวิจัยส่วนใหญ่เป็นการพัฒนาและทดสอบสมรรถนะของตัวรับรังสี[๘,๙,๑๐,๑๑,๑๒] นอกจากนี้ยังมีงานวิจัยระบบทำน้ำร้อนด้วยแสงอาทิตย์และการศึกษาปัญหาและอุปสรรคของการใช้งาน งานวิจัยด้านการอบแห้งด้วยแสงอาทิตย์ส่วนใหญ่เป็นการศึกษาสมรรถนะของเครื่องอบแห้งชนิดต่างๆ ให้เหมาะสมกับผลิตภัณฑ์ที่นำมาทำการอบแห้ง[๑๓,๑๔,๑๕,๑๖] เช่น กล้วยน้ำว้า เนื้อสัตว์ ปลา กระเทียม นอกจากนี้ยังมีงานวิจัยด้านการใช้พลังงานแสงอาทิตย์ร่วมกับแหล่งพลังงานอื่นในการให้ความร้อน เช่น ไอน้ำ, แก๊สปิโตรเลียมเหลว, แก๊สชีวภาพ และมีงานวิจัยเกี่ยวกับตัวรับรังสีอาทิตย์ที่ใช้ร่วมกับห้องอบแห้ง และการใช้หินเป็นตัวกักเก็บความร้อน ถึงแม้จะมีงานวิจัยเกี่ยวกับเครื่องอบแห้งแสงอาทิตย์มากมาย แต่ยังไม่มีการนำมาใช้ประโยชน์อย่างแพร่หลาย โดยเฉพาะในระดับอุตสาหกรรม เนื่องจากความไม่สม่ำเสมอของพลังงานแสงอาทิตย์ ดังนั้นถ้าต้องการควบคุมอุณหภูมิจะต้องใช้ร่วมกับแหล่งพลังงานอื่น ทำให้มีการลงทุนสูงขึ้น

มีงานวิจัยด้านสมรรถนะของเครื่องกลั่นพลังงานแสงอาทิตย์ในรูปแบบต่างๆ[๑๗,๑๘,๑๙,๒๐] เช่น แบบผิวดั้งฝาครอบอคริลิค แบบกระจกเอียง และใช้ผิวดูดความร้อนชนิดต่างๆ นอกจากนี้ยังมีงานวิจัยที่ศึกษาตัวรับรังสีอาทิตย์แบบต่างๆ ที่นำมาใช้ร่วมกับเครื่องกลั่นน้ำเพื่อเพิ่มสมรรถนะของเครื่องกลั่นน้ำ[๒๑] และมีงานวิจัยที่พัฒนาเครื่องกลั่นด้วยแสงอาทิตย์สำหรับผลิตภัณฑ์อื่น เช่น เอธานอล[๒๒,๒๓,๒๔]

งานวิจัยด้านเครื่องทำความเย็นด้วยแสงอาทิตย์ส่วนใหญ่จะเป็นการศึกษาสมรรถนะและความเป็นไปได้ของระบบ เช่น การศึกษาเครื่องทำความเย็นแบบดูดซึม การศึกษาสมรรถนะของระบบทำความเย็นแบบดูดซับด้วยแสงอาทิตย์ที่ใช้ถ่านกัมมันต์-เมธานอลเป็นสารคู่ทำงาน[๒๕,๒๖,๒๗] พบว่าสามารถทำความเย็นได้อุณหภูมิต่ำถึง – ๗.๖ องศาเซลเซียส แต่สัมประสิทธิสมรรถนะการทำความเย็นของระบบยังมีค่าต่ำอยู่มากคือ ๐.๐๘๓๐

เนื่องจากประเทศไทยไม่ใช่ผู้นำในการผลิตเซลล์แสงอาทิตย์ ประกอบกับการวิจัยในการพัฒนาเซลล์แสงอาทิตย์มีระบบที่ยุ่งยากและซับซ้อน และต้องใช้อุปกรณ์ที่ได้มาตรฐานและทันสมัยมาก จึงทำให้งานวิจัยส่วนใหญ่จะเน้นการศึกษาพารามิเตอร์ คุณภาพ สมรรถนะของการนำไปใช้ในงานต่างๆ เช่น การศึกษาพารามิเตอร์ของระบบผลิตไฟฟ้าแบบผสมผสานที่ประกอบด้วย เซลล์แสงอาทิตย์ พลังงานลม และเครื่องยนต์ดีเซลเพื่อใช้งานในพื้นที่ห่างไกล[๔] การศึกษาคุณภาพของกำลังไฟฟ้าที่ผลิตได้จากระบบผลิตไฟฟ้าแบบผสมผสาน[๔] การจัดการระบบผลิตสูบน้ำด้วยเซลแสงอาทิตย์[๕] ศึกษาระบบที่เชื่อมโยงกับสายส่ง[๖] การประจุแบตเตอรี่[๖] อย่างไรก็ดี สำนักงานพัฒนาวิทยาศาสตร์และเทคโนโลยีแห่งชาติ (สวทช) ได้รับเงินสนับสนุนให้ทำวิจัยและผลิตเซลล์แสงอาทิตย์ขึ้นในประเทศไทย โดยคาดว่าจะสามารถผลิตเซลล์แบบอะมอร์ฟัสซิลิกอนให้มีประสิทธิภาพได้ถึง 10%[๓] โดยจะพัฒนาเซลล์แบบผลึกควบคู่กันไป

จากการศึกษาสถานภาพการใช้ สถานภาพด้านงานวิจัยพลังงานแสงอาทิตย์ และการวิเคราะห์ความเป็นไปได้ทางเศรษฐศาสตร์ของเครื่องทำน้ำร้อนพลังงานแสงอาทิตย์ เครื่องอบแห้งพลังงานแสงอาทิตย์ เครื่องกลั่นน้ำพลังงานแสงอาทิตย์ เครื่องทำความเย็นพลังงานแสงอาทิตย์และเซลล์แสงอาทิตย์ จึงสามารถสรุปตามสถานภาพต่างๆ ได้ดังตารางที่ ๖

๒.๔ ข้อจำกัดและปัญหาการใช้พลังงานแสงอาทิตย์ของประเทศไทย

ถึงแม้ว่าประเทศไทยจะมีศักยภาพของพลังงานแสงอาทิตย์เพียงพอสำหรับการนำไปใช้ประโยชน์ในด้านต่างๆ แต่ยังมีการใช้งานไม่มากเท่าที่ควร ปัญหาของงานวิจัยด้านพลังงานแสงอาทิตย์มีทั้งที่เป็นภาพรวมของประเทศและตามสถานภาพการใช้งานของอุปกรณ์แต่ละอย่าง

การใช้พลังงานแสงอาทิตย์ด้านความร้อน เนื่องจากความไม่สม่ำเสมอและความไม่แน่นอนของแหล่งพลังงานแสงอาทิตย์ ทำให้เกิดปัญหาในการใช้งานและข้อจำกัดต่างๆดังนี้ ไม่สามารถใช้งานได้อย่างต่อเนื่อง ไม่สามารถควบคุมอุณหภูมิได้ตามต้องการ ซึ่งจะส่งผลกระทบโดยตรงต่อคุณภาพผลิตภัณฑ์สำหรับกรณีเครื่องอบแห้งและเครื่องทำความเย็น ดังนั้นถ้าจะแก้ไขปัญหาเหล่านี้จะต้องคิดอุปกรณ์เพิ่มเพื่อใช้แหล่งพลังงานอื่นเสริมซึ่งจะทำให้ระบบมีต้นทุนสูงขึ้น นอกจากนี้สมรรถนะของบางอุปกรณ์ยังต่ำอยู่มากเช่น เครื่องกลั่นน้ำ และเครื่องทำความเย็น ทำให้ไม่น่าสนใจที่จะนำมาใช้งาน

สำหรับการนำแสงอาทิตย์มาผลิตไฟฟ้าด้วยเซลล์แสงอาทิตย์ มีปัญหาด้านราคาแผงเซลล์และระบบที่มีค่าสูง และประสิทธิภาพเซลล์แสงอาทิตย์ต่ำ ประกอบความไม่สม่ำเสมอและความไม่แน่นอนของแหล่งพลังงานแสงอาทิตย์ ทำให้ต้นทุนไฟฟ้าที่ผลิตได้ยังสูงกว่าราคาไฟฟ้าที่ซื้อจากการไฟฟ้ามาก ดังนั้นจึงทำให้เกิดข้อจำกัดของการนำไปใช้งาน ซึ่งส่วนใหญ่จะนำไปใช้ในพื้นที่ที่ห่างไกลระบบสายส่งไปไม่ถึง จึงทำการใช้งานได้ไม่อย่างแพร่หลาย

๒.๕ แนวทางงานวิจัยพลังงานแสงอาทิตย์ในประเทศไทย

จากการศึกษาสถานภาพงานวิจัยด้านพลังงานแสงอาทิตย์ พบว่า ประเทศไทยมีการทำงานวิจัยด้านนี้มาเป็นเวลานาน แต่ถ้าพิจารณาถึงปัญหาและข้อจำกัดของการใช้งาน ความเป็นไปได้ทางเทคนิคและเศรษฐศาสตร์แล้ว พบว่า ควรมีวิจัยด้านเพิ่มประสิทธิภาพ สมรรถนะ และหาแนวทางลดต้นทุนของระบบ/อุปกรณ์ที่ใช้พลังงานแสงอาทิตย์ และควรพัฒนาหาวัสดุที่ผลิตได้ในประเทศมาใช้เพื่อลดต้นทุน ควรมีงานวิจัยหาแนวทางพัฒนาระบบที่จะสามารถเก็บความร้อนและไฟฟ้าที่ผลิตได้จากพลังงานแสงอาทิตย์เพื่อให้มาการใช้งานได้อย่างต่อเนื่องอย่างสม่ำเสมอ และการวิจัยที่จะหาแหล่งพลังงานอื่นที่ราคาถูกมาใช้ผสมผสานเพื่อให้การใช้งานของระบบเป็นไปได้อย่างเสถียร และควรมีงานวิจัยทั้งทางด้านเทคนิคและเศรษฐศาสตร์เพื่อขยายโอกาสที่จะพัฒนาอุปกรณ์และการประยุกต์ใช้ในงานใหม่ๆต่างๆได้อย่างเหมาะสม ให้ได้กว้างขวางมากยิ่งขึ้น โดยเฉพาะเงื่อนไขที่เหมาะสมและความคุ้มค่าของการใช้เซลล์แสงอาทิตย์ นอกจากนี้ควรมีงานวิจัยเชิงนโยบายและมาตรการต่างๆของประเทศที่ประสพความสำเร็จในการใช้พลังงานแสงอาทิตย์ เช่น มาตรการภาษีด้านต่างๆ โดยเฉพาะภาษีนก๊สคาร์บอนไดอ๊อกไซด์

๓. พลังน้ำ

๓.๑ สถานการณ์ และการใช้พลังน้ำในประเทศไทย

ศักยภาพพลังน้ำประเมินจากเขื่อนที่ผลิตไฟฟ้าที่ดำเนินการแล้วในปัจจุบันมีกำลังผลิตติดตั้งรวมทั้งสิ้น ๒,๙๗๓ เมกกะวัตต์[๖๐] คิดเป็นสัดส่วนร้อยละ ๑๒ ของกำลังผลิตติดตั้งโรงไฟฟ้าของภาครัฐ[๙] ส่วนใหญ่กว่าร้อยละ ๘๐ อยู่ทางภาคเหนือและภาคกลางของประเทศ ในปี พ.ศ. ๒๕๔๖ สามารถผลิตไฟฟ้าได้รวมทั้งสิ้น ๗,๒๙๙ ล้านกิโลวัตต์วัตต์ชั่วโมง คิดเทียบเท่าพลังงานปฐมภูมิ ๑,๖๑๖ พันตันเทียบเท่าน้ำมันดิบ[๙] ในจำนวนนี้เป็นโรงไฟฟ้าพลังน้ำที่มีขนาดเล็กกว่า ๑๒ เมกกะวัตต์อยู่ ๖๙ เมกกะวัตต์ สามารถผลิตไฟฟ้าได้ ๑๙๐ ล้านกิโลวัตต์วัตต์ชั่วโมง

ปัจจุบันการหาแหล่งเพื่อพัฒนาเขื่อนขนาดใหญ่ในประเทศคงเป็นไปได้ยาก ที่มีศักยภาพมากเป็นลุ่มน้ำระหว่างประเทศ ซึ่งในการพัฒนาเพื่อผลิตไฟฟ้าจะต้องเป็นไปในลักษณะความร่วมและถือกรรมสิทธิ์ร่วมระหว่างประเทศ ดังนั้นการพัฒนาแหล่งพลังน้ำขนาดเล็กในประเทศไทยเพื่อผลิตไฟฟ้าจึงเป็นแหล่งพลังงานหมุนเวียนที่สำคัญอย่างหนึ่ง การใช้แหล่งพลังน้ำขนาดเล็กในการผลิตไฟฟ้าเป็นการใช้น้ำในลำน้ำธรรมชาติเป็นพลังงานโดยสร้างเขื่อนปิดกั้นแม่น้ำไว้ให้มีระดับสูงจนมีปริมาณน้ำและแรงดันเพียงพอที่จะหมุนกังหันน้ำ และเครื่องกำเนิดไฟฟ้าที่อยู่ท้ายน้ำที่มีระดับต่ำกว่า วิธีนี้เหมาะสมกับพื้นที่แถบชนบทที่สายไฟฟ้าส่งเข้าไปไม่ถึง โรงไฟฟ้าพลังน้ำขนาดเล็กแปลตามปริมาณน้ำได้เป็น ๓ ประเภท[๖๔] ได้แก่ โรงไฟฟ้าแบบมีน้ำไหลผ่านตลอดปี (Run-of-river hydro plant) โรงไฟฟ้าแบบนี้ไม่มีอ่างเก็บน้ำ ส่วนใหญ่จะติดตั้งอยู่กับเขื่อนผันน้ำชลประทานซึ่งมีน้ำไหลผ่านตลอดปี โรงไฟฟ้าแบบมีอ่างเก็บน้ำขนาดเล็ก (Regulating pond hydro plant) และโรงไฟฟ้าแบบสูบกลับ (Pumped storage plant) ส่วนใหญ่โครงการไฟฟ้าพลังน้ำขนาดเล็กจะเป็นโรงไฟฟ้าแบบมีน้ำไหลผ่านตลอดปี โรงไฟฟ้าแบบนี้ไม่มีอ่างเก็บน้ำ และมีผลกระทบต่อสิ่งแวดล้อมน้อย

จากการศึกษาเบื้องต้น ด้วยแผนที่และการสำรวจภาคสนามในบางพื้นที่ รวมทั้งพิจารณาจากการศึกษาโครงการไฟฟ้าพลังน้ำของหน่วยงานอื่นๆ ซึ่งในการศึกษาได้พิจารณาโรงไฟฟ้า ๓ รูปแบบ พบว่าทั่วประเทศไทยมีที่ตั้งโครงการไฟฟ้าพลังน้ำที่น่าจะเป็นไปได้ ๑,๑๓๖ แห่ง[๖๔] ปัจจุบันกรมพัฒนาพลังงานทดแทนและอนุรักษ์พลังงานได้คัดเลือกเพื่อพัฒนาโครงการโรงไฟฟ้าพลังน้ำขนาดเล็กเพื่อที่จะสร้างในอนาคต ๒๔ โครงการ รวมกำลังการผลิตติดตั้งทั้งหมด ๖๖.๑๓ เมกกะวัตต์คาดว่าจะผลิตไฟฟ้าได้ ๒๙๑ ล้านกิโลวัตต์ชั่วโมง ประมาณการเงินลงทุนรวมทั้งสิ้น ๔,๒๙๓ ล้านบาท[๙๐]

๓.๒ สถานภาพงานวิจัยด้านพลังน้ำขนาดเล็กของประเทศไทย

การวิจัยด้านพลังน้ำขนาดเล็กของประเทศไทย มีงานวิจัยเกี่ยวกับการประเมินเชิงเทคนิคของโครงการพัฒนาพลังน้ำขนาดเล็กในประเทศที่กำลังพัฒนาและในประเทศที่พัฒนาแล้ว พบว่า มีแนวโน้มที่จะเพิ่มศักยภาพมากขึ้น[๖๔] ส่วนการศึกษาทางด้านโยธามีการศึกษาในเรื่องของวัสดุที่นำมาใช้และมาตรฐาน ปัจจัยสำคัญในการเลือกใช้วัสดุอุปกรณ์นั้นๆขึ้นอยู่กับงบประมาณการลงทุน สภาพภูมิอากาศ ความยากง่ายในการสรรหาวัสดุอุปกรณ์มาใช้ในโครงการ การขนย้ายและการติดตั้ง มีการวิจัยด้านการจัดสรรน้ำเพื่อประโยชน์สูงสุดในการจัดการอ่างเก็บน้ำ ทั้งนี้เพื่อวางแผนและจัดการน้ำที่เหมาะสมเพื่อให้มีการใช้น้ำที่มีอยู่ตามธรรมชาติให้มีประสิทธิภาพและเกิดประโยชน์สูงสุด[๖๖]

๓.๓ แนวทางงานวิจัยพลังน้ำขนาดเล็กในประเทศไทย

การสร้างเขื่อนขนาดใหญ่เป็นไปได้ยาก ควรเน้นพลังน้ำขนาดเล็ก เนื่องจากโรงไฟฟ้าพลังน้ำขนาดเล็กส่วนใหญ่เป็นแบบมีน้ำไหลผ่านตลอดปี (Run-of-river hydro power plant) ควรมีการวิจัยเพื่อเพิ่มประสิทธิภาพของกังหันที่มีความสูงของหัวน้ำที่ต่ำ ส่วนด้านวัสดุอุปกรณ์ ควรตั้งมาตรฐานของวัสดุอุปกรณ์ต่างๆของโรงไฟฟ้าพลังน้ำขนาดเล็ก เพื่อให้เหมาะสมกับความสูงของหัวน้ำที่มีความแตกต่างกันในแต่ละโครงการ ซึ่งจะทำให้ผลิตพลังงานได้ประสิทธิภาพสูงสุด การก่อสร้างโรงไฟฟ้าพลังน้ำใช้เงินลงทุนสูงมาก ดังนั้นควรมีการศึกษาวิจัยเพื่อหาแนวทางลดต้นทุน นอกจากนี้ควรมีการวิจัยเกี่ยวกับการจัดสรรน้ำมาใช้ประโยชน์ให้ได้มากที่สุด และควรศึกษาความเป็นไปได้ของการผลิตไฟฟ้าจากเขื่อนหรือฝายน้ำขนาดเล็กที่ก่อสร้างใช้งานอยู่แล้ว ที่สร้างขึ้นเพื่อการชลประทานและการเกษตร ทั้งนี้เพื่อเพิ่มประโยชน์การใช้ทรัพยากรให้ได้หลายวัตถุประสงค์ เช่น เขื่อนป่าสักชลสิทธิ์ ในโครงการพระราชดำริ ที่เริ่มสร้างขึ้นเพื่อการอุปโภค การเกษตร อุตสาหกรรม คมนาคม บรรเทาอุทกภัย ปัจจุบันกำลังดำเนินการติดตั้งกังหันน้ำ และเครื่องกำเนิดไฟฟ้า ขนาดกำลังผลิตสูงสุด ๖.๗ เมกกะวัตต์ และคาดว่าจะเริ่มผลิตไฟฟ้าจำหน่ายได้ในปี พ.ศ. ๒๕๔๘ นอกจากนี้ควรมีงานวิจัยเชิงนโยบายในความร่วมมือกับประเทศเพื่อนบ้าน

๔. พลังงานลม

๔.๑ ศักยภาพพลังงานลมของประเทศไทย

กรมพัฒนาพลังงานทดแทนและอนุรักษ์พลังงานได้จัดทำแผนที่ศักยภาพพลังงานลมมาตั้งแต่ปี ๒๕๑๙ และได้มีการจัดทำใหม่ในปี ๒๕๔๔[๖๗] ซึ่งสรุปได้ว่า ประเทศไทยได้รับอิทธิพลลมมรสุมตะวันออกเฉียงเหนือที่พัดผ่านประเทศไทยจากทะเลจีนใต้ ในเดือนพฤศจิกายนถึงมีนาคม และอิทธิพลลมมรสุมตะวันตกเฉียงใต้พัดผ่านประเทศไทยในเดือนพฤษภาคมถึงตุลาคม พื้นที่ที่ได้รับอิทธิพลทั้งลมมรสุมตะวันออกเฉียงเหนือและลมมรสุมตะวันตกเฉียงใต้เป็นบริเวณเทือกเขาทอดยาวขวางทิศทางลม ทำให้เป็นพื้นที่ที่มีลมพัดแรงเกือบตลอดทั้งปี ที่ยอดเขามีความเร็วลมประมาณ ๗.๐ เมตร/วินาที ขึ้นไป ได้แก่ จังหวัด สุราษฎร์ พังงา กระบี่ นครศรีธรรมราช

สำหรับพื้นที่ที่ได้รับอิทธิพลลมมรสุมตะวันออกเฉียงเหนือ โดยมีทิศทางลมพัดจากทะเลเข้าสู่ฝั่งความเร็วลมเฉลี่ยทั้งปี ๖.๔ เมตร/วินาที (ที่ความสูง ๕๐ เมตร จากพื้นดิน) ขึ้นไป ในพื้นที่ภาคใต้บริเวณชายฝั่งทะเลตะวันออก ได้แก่ จังหวัดนครศรีธรรมราช สงขลา และปัตตานี ส่วนพื้นที่ที่ได้รับอิทธิพลลมมรสุมตะวันตกเฉียงใต้ กำลังลมแรงบนยอดเขามีความเร็วลมประมาณ ๖.๕ เมตร/วินาที ขึ้นไป ได้แก่ พื้นที่บนเทือกเขาด้านทิศตะวันตก ตั้งแต่จังหวัดเพชรบุรี กาญจนบุรี และจังหวัดตาก ส่วนอุทยานแห่งชาติดอยอินทนนท์ จังหวัดเชียงใหม่ ก็ได้รับอิทธิพลจากความกดอากาศสูงจากประเทศสาธารณรัฐประชาชนจีนและลมมรสุมตะวันตกเฉียงใต้ทำให้มีความเร็วลมประมาณ ๖.๔ เมตร/วินาที ขึ้นไป

ส่วนแหล่งที่มีศักยภาพพลังงานลมรองลงมา ได้แก่ ความเร็วลมเฉลี่ย ๔.๔ เมตร/วินาที ขึ้นไป (ที่ความสูง ๕๐ เมตร จากพื้นดิน) ซึ่งเกิดจากอิทธิพลลมมรสุมตะวันออกเฉียงเหนือ พบว่า อยู่ที่ อ่าวไทยฝั่งตะวันตก ตั้งแต่ จังหวัดสุราษฎร์ธานี ชุมพร ประจวบคีรีขันธ์ เพชรบุรี และบริเวณที่สูงบนยอดเขาในภาคเหนือ จังหวัดเชียงใหม่ และภาคตะวันออกเฉียงเหนือ จังหวัดเพชรบูรณ์ และ เลย และแหล่งที่มีศักยภาพรองลงมาซึ่งได้รับอิทธิพลจากลมมรสุมตะวันตกเฉียงใต้ ได้แก่ ภาคใต้ฝั่งตะวันตก ตั้งแต่ จังหวัดสตูล ตรัง กระบี่ ภูเก็ต พังงา และอ่าวไทยฝั่งตะวันออก จังหวัดชลบุรี และระยอง

๔.๒ การใช้พลังงานลมในประเทศไทย

เนื่องจากพลังงานลมขึ้นอยู่กับความเร็วและมวลของอากาศ ดังนั้นการนำพลังงานลมมาใช้ประโยชน์จะต้องเลือกพื้นที่ที่มีศักยภาพความเร็วลมสูงจึงจะได้พลังงานมาก พลังงานลมสามารถเปลี่ยนเป็นพลังงานกล หรือพลังงานไฟฟ้าได้โดยใช้กังหันลมเป็นอุปกรณ์เปลี่ยนพลังงาน ทั้งนี้สามารถจำแนกตามลักษณะการใช้ประโยชน์ได้เป็น ๒ ประเภทหลักๆได้แก่ กังหันลมเพื่อการสูบน้ำและกังหันลมเพื่อการผลิตไฟฟ้า

ประเทศไทยมีการใช้กังหันลมเพื่อการสูบน้ำ ๓ แบบ[๖๕] ได้แก่ กังหันลมใบเรือ กังหันลมใบพัด และกังหันลมหลายใบ กังหันลมสองชนิดแรกเป็นแบบดั้งเดิมที่ใบพัดของกังหันทำด้วยเสื่อลำแพน ผ้า ใบ ไม้ และสังกะสี ซึ่งกังหันลมชนิดใบเรือส่วนใหญ่ใช้ในนาเกลือ กังหันลมชนิดใบพัดส่วนใหญ่ใช้ในนาข้าว กังหันลมทั้งสองชนิดนี้มีความสามารถในการยกระดับน้ำไม่เกิน 2 เมตร สามารถผลิตสร้างเองได้และราคาไม่แพง สำหรับกังหันลมชนิดหลายใบส่วนใหญ่ใช้ในการสูบน้ำเพื่อการอุปโภคและบริโภค มีความสามารถในการยกระดับน้ำได้สูงกว่าสองชนิดแรก ราคากังหันลมชนิดนี้ขึ้นอยู่กับขนาดและจำนวนใบกังหันลม และจะมีราคาแพงกว่ากังหันลมสองแบบแรก สำหรับเครื่องสูบน้ำที่ใช้คู่กับกังหันลมมีการใช้อยู่ ๒ แบบ คือ แบบระหัดและแบบสูบชัก โดยเครื่องสูบน้ำแบบระหัดจะทำจากไม้ใช้ร่วมกับกังหันลมชนิดใบเรือและใบพัด เพื่อวิดน้ำเข้านาเกลือและนาข้าว ส่วนเครื่องสูบน้ำแบบสูบชักทำจากโลหะใช้ร่วมกับกังหันลมชนิดหลายใบ กรรมวิธีการผลิตใช้เทคนิคค่อนข้างซับซ้อนและยุ่งยากกว่าแบบระหัด ส่วนใหญ่บริษัทจำหน่ายกังหันลมคู่กับเครื่องสูบน้ำ

ในปีพ.ศ. ๒๕๔๖ ประเทศไทยมีกำลังผลิตติดตั้งกังหันลมเพื่อผลิตไฟฟ้ารวมทั้งสิ้น ๑๙๕.๙ กิโลวัตต์[๖๖] ซึ่งส่วนใหญ่อยู่ในภาคใต้ (๑๙๒.๓ กิโลวัตต์) มีส่วนน้อยอยู่ในภาคตะวันออกเฉียงเหนือ (๒.๕ กิโลวัตต์) และภาคใต้ (๐.๙ กิโลวัตต์) การไฟฟ้าฝ่ายผลิตได้สร้างสถานีสาธิตพลังงานทดแทนที่แหลมพรหมเทพ จ.ภูเก็ต ซึ่งเป็นการผลิตไฟฟ้าร่วมระหว่างพลังงานลม ๑๙๒ กิโลวัตต์ และเซลล์แสงอาทิตย์ขนาด ๑๑.๓๙ กิโลวัตต์

๔.๓ สถานภาพงานวิจัยด้านพลังงานลมของประเทศไทย

จากการศึกษาข้อมูลงานวิจัยด้านพลังงานลมของประเทศไทย สามารถแบ่งงานวิจัยออกเป็น ๒ ประเภท ได้แก่ งานวิจัยด้านสมรรถนะของกังหันลมเพื่อการสูบน้ำ และงานวิจัยด้านสมรรถนะของการผลิตพลังงานไฟฟ้าจากพลังงานลม

ด้านการสูบน้ำ มีการทดสอบสมรรถนะกังหันลม ๔ ใบ กังหันลมหลายใบ การศึกษาความเค้นในใบของกังหันลมแกนหมุนแนวดิ่งการศึกษาแบบจำลองไฟไนท์เอเลเมนท์ของใบพัดกังหันลมแบบคาร์เรียส และการศึกษา Laminar separation bubble บนใบพัดของกังหันลม[๖๙-๗๒] การทดสอบสมรรถนะของโรเตอร์กังหันลมที่มีใช้อยู่ในประเทศไทย ๖ แบบ ได้แก่ กังหันลมหลายใบ กังหันลมล้อจักรยาน กังหันลมนาข้าว ๒ ใบ กังหันลมนาข้าว ๔ ใบ กังหันลมนาเกลือ ๖ ใบ และกังหันลมปัตตานี ๒ ใบ โดยแบบสร้างจำลองทางคณิตศาสตร์ เพื่อหาอัตราส่วนความเร็วปลายใบที่ให้ค่าสัมประสิทธิ์กำลังงานสูงสุดของกังหันแต่ละแบบ จากผลการทดสอบที่ได้ทำให้สามารถเลือกใช้กังหันลมแต่ละแบบให้เหมาะสมกับศักยภาพลมของแต่ละพื้นที่

ด้านการผลิตไฟฟ้า มีการทดสอบแบบจำลองสมรรถนะกังหันลมแบบใจโร-โรเตอร์ชนิดใบตรง[๗๓] ศึกษาสมรรถนะของกังหันลมแบบคาร์เรียส[๗๔] ซึ่งเป็นกังหันลมแบบแนวดิ่ง มีการทดสอบโดยใช้เครื่องกำเนิดไฟฟ้าในรถยนต์กับกังหันลม[๗๕] เนื่องจากหาง่ายและมีราคาถูก นอกจากนี้มีการศึกษาพารามิเตอร์ของระบบผลิตไฟฟ้าแบบผสมผสานที่ประกอบด้วย พลังงานลม เซลล์แสงอาทิตย์ และเครื่องยนต์ดีเซลเพื่อใช้งานในพื้นที่ห่างไกล[๗๖] นอกจากนี้ยังมีงานวิจัยระบบผลิตและสำรองไฟฟ้าด้วยพลังงานลม[๗๗] โดยดัดแปลงกังหันนาเกลือแบบหมุนรับลมตามทิศทางมาใช้สำหรับผลิตไฟฟ้า ศึกษาความสัมพันธ์ระหว่างความเร็วลมรอบของกังหันลม

ประเทศไทยมีการใช้กังหันลมเพื่อผลิตพลังงานไฟฟ้าโดยการนำเข้าจากต่างประเทศ เนื่องประเทศไทยยังไม่มีโรงงานผลิตกังหันลม

เพื่อผลิตกระแสไฟฟ้าภายในประเทศ ดังนั้นราคาพลังงานไฟฟ้าที่ผลิตจากพลังงานลมจึงสามารถอ้างอิงราคาพลังงานของต่างประเทศได้ จะมีราคาสูงกว่าเพราะต้องรวมค่าขนส่ง ค่าติดตั้ง อัตราแลกเปลี่ยนเงินตรา ภาษีนำเข้าอุปกรณ์ของประเทศไทย รวมถึงค่าอะไหล่ที่ต้องนำเข้าและการซ่อมแซมบำรุงรักษา จากข้อมูลของการไฟฟ้าฝ่ายผลิตแห่งประเทศไทย[๗] เกี่ยวกับการวิเคราะห์ทางเศรษฐศาสตร์ของการผลิตไฟฟ้าจากกังหันลม พบว่าบริเวณที่มีความเร็วลมเฉลี่ย ๔.๕ เมตร/วินาที ขึ้นไปมีแนวโน้มว่าต้นทุนไฟฟ้าที่ผลิตได้สามารถแข่งขันกับการผลิตไฟฟ้าโดยใช้เครื่องยนต์ดีเซล หรือการขยายสายส่งเป็นระยะทางไกล

จากการศึกษาศักยภาพ สถานภาพการใช้ สถานภาพงานวิจัย และการวิเคราะห์ทางเศรษฐศาสตร์ ของพลังงานลมที่นำมาใช้สำหรับเพื่อการสูบน้ำและผลิตไฟฟ้า สามารถสรุปสถานภาพได้ตารางที่ ๗

๔.๔ แนวทางงานวิจัยด้านพลังงานลมในประเทศไทย

ข้อจำกัดสำคัญของการใช้ประโยชน์จากพลังงานลม คือ ค่าความเร็วลม สำหรับการใช้พลังลมเพื่อการสูบน้ำ ถึงแม้จะต้องการความเร็วลมไม่สูงมากนักแต่ในพื้นที่ที่ความเร็วลมต่ำมากก็ไม่สามารถทำได้เช่นกัน และที่สำคัญจะต้องเป็นพื้นที่ที่ไม่มีสิ่งกีดขวางเส้นทางลมและห่างจากชุมชนพอสมควร ส่วนกังหันลมเพื่อการผลิตพลังงานไฟฟ้าจำเป็นต้องใช้พื้นที่ที่มีศักยภาพความเร็วลมสูง เช่น ชายฝั่งทะเล จึงทำให้สามารถติดตั้งได้เฉพาะบางพื้นที่เท่านั้น

จากการศึกษาข้างต้นพบว่า สิ่งสำคัญของการนำพลังงานลมมาใช้ประโยชน์ด้านพลังงาน ได้แก่ ค่าความเร็วลมของพื้นที่นั้นๆ ต้องเหมาะสมสำหรับการใช้งาน เนื่องจากกังหันลมแต่ละชนิดแต่ละแบบจะมีค่าความเร็วเริ่มต้นของการทำงานต่างกัน ดังนั้นการติดตั้งกังหันลมในแต่ละพื้นที่จะต้องทำการศึกษาศักยภาพความเร็วลมก่อนเป็นอันดับแรก เนื่องจากข้อมูลด้านความเร็วลมที่ระดับความสูงมากกว่า ๕๐ เมตรจากพื้นดินยังไม่มี ดังนั้นจึงควรสนับสนุนให้มีการศึกษา รวมถึงการศึกษาความเป็นไปได้ทางเทคนิคและเศรษฐศาสตร์ สำหรับการติดตั้งกังหันลมในพื้นที่ที่มีความเร็วลมสูง โดยใช้แบบจำลองทางคณิตศาสตร์เพื่อศึกษาตัวแปรต่างๆ ที่มีผลต่อทางเทคนิคและเศรษฐศาสตร์ของกังหันลม เนื่องจากประเทศไทยไม่ใช้ผู้ผลิตกังหันลมเพื่อผลิตไฟฟ้าจึงต้องนำเข้าจากต่างประเทศ จึงทำให้ยังคงมีปัญหาทางด้านเศรษฐศาสตร์ในการนำมาใช้งาน ดังนั้นควรมีการศึกษาความเป็นไปได้ที่จะพัฒนาอุตสาหกรรมการผลิตกังหันลมเพื่อผลิตไฟฟ้าภายในประเทศในอนาคต

จากสถานภาพของงานวิจัยด้านพลังงานลมเพื่อการสูบน้ำของประเทศไทย ส่วนใหญ่จะเน้นไปในด้านงานวิจัยเพื่อทดสอบสมรรถนะของกังหันลม เนื่องจากกังหันลมมีหลายแบบซึ่งเหมาะสมกับการทำงานแต่ละแบบไม่เหมือนกัน ดังนั้นควรมีงานวิจัยด้านการประยุกต์ใช้กังหันลมกับอุปกรณ์ที่ใช้พลังงานกล การเก็บรวบรวมข้อมูลสถานภาพการใช้กังหันลมเพื่อการสูบน้ำ ณ สภาวะปัจจุบันจะมีประโยชน์อย่างมากต่อการกำหนดแผนพัฒนาและส่งเสริมการใช้กังหันลมเพื่อการสูบน้ำต่อไป

นอกจากนี้ควรมีงานวิจัยเชิงนโยบายด้านมาตรการจูงใจและส่งเสริมการผลิตและติดตั้งกังหันเพื่อการสูบน้ำและเพื่อการผลิตไฟฟ้า เช่น การให้คำปรึกษาด้านเทคนิคและอุปกรณ์ที่เกี่ยวข้องกับกังหันลม การลดภาษีนำเข้าวัสดุ อุปกรณ์ การกำหนดพื้นที่ที่มีศักยภาพเพื่อให้มีการลงทุนของภาคเอกชนในการผลิตไฟฟ้าจำหน่ายเข้าระบบ

๕. พลังงานความร้อนใต้พิภพ

พลังงานความร้อนใต้พิภพ หมายถึง พลังงานธรรมชาติที่เกิดจากความร้อนที่ถูกกักเก็บอยู่ภายใต้ผิวโลก สามารถนำไปใช้ประโยชน์ได้ โดยอุณหภูมิใต้ผิวโลกจะเพิ่มขึ้นตามความลึก ตามปกติแหล่งพลังงานนี้จะอยู่ในรูปของ น้ำพุร้อน หรือน้ำร้อนจากใต้ดิน โดยแหล่งพลังงานความร้อนใต้พิภพที่พบในโลกแบ่งตามลักษณะการเกิดได้ ๓ ลักษณะ[๙] คือ

- แหล่งที่เป็นไอน้ำส่วนใหญ่ (Steam dominated) เป็นแหล่งกักเก็บความร้อนที่ประกอบด้วยไอน้ำมากกว่าร้อยละ ๙๕ โดยทั่วไปมักจะเป็นแหล่งที่มีความสัมพันธ์ใกล้ชิดกับหินหลอมเหลวร้อนที่แทรกดันขึ้นมาอยู่ในระดับตื้นๆ โดยอุณหภูมิของไอน้ำร้อนสูงกว่า ๒๔๐ องศาเซลเซียส แหล่งที่เป็นไอน้ำส่วนใหญ่พบน้อยมาก แต่สามารถนำมาใช้ผลิตกระแสไฟฟ้าได้มากที่สุด เช่น The Geyser Field ในรัฐแคลิฟอร์เนีย ประเทศสหรัฐอเมริกา และ Larderello ประเทศ อิตาลี เป็นต้น

- แหล่งที่เป็นน้ำร้อนส่วนใหญ่ (Hot water dominated) เป็นแหล่งกักเก็บสะสมความร้อนที่ประกอบไปด้วยน้ำร้อนเป็นส่วนใหญ่ อุณหภูมิน้ำร้อนจะมีตั้งแต่ ๑๐๐ องศาเซลเซียส ขึ้นไป ระบบนี้จะพบมากที่สุด เช่น Cerro prieto ประเทศเม็กซิโก Hatchobaru ประเทศญี่ปุ่น และ Wairakei ในประเทศนิวซีแลนด์

- แหล่งหินร้อนแห้ง (Hot dry rock) เป็นแหล่งสะสมความร้อนที่เป็นหินเนื้อแน่น แต่ไม่มีน้ำร้อนหรือไอน้ำไหลหมุนเวียนอยู่ ดังนั้นถ้าจะนำมาใช้จำเป็นต้องทำชั้นหินร้อนให้มีรอยแตกแล้วจึงอัดน้ำเย็นลงไปทางหลุมเจาะ ให้น้ำได้รับความร้อนจากหินร้อน โดยไหลหมุนเวียนภายในรอยแตกที่กระทำขึ้น จากนั้นก็ทำการสูบน้ำนี้ขึ้นมาทางหลุมเจาะอีกหลุมหนึ่ง

๕.๑ ศักยภาพของพลังงานความร้อนใต้พิภพที่พบในประเทศไทย

แหล่งพลังงานความร้อนใต้พิภพของประเทศไทย จัดอยู่ในแหล่งกักเก็บอุณหภูมิต่ำ คือ มีอุณหภูมิน้อยกว่า ๑๒๕ องศาเซลเซียส โดยแหล่งเก็บสะสมความร้อนจะประกอบไปด้วยน้ำร้อนเป็นส่วนใหญ่ อุณหภูมิน้ำร้อนจะมีค่ามากกว่า ๘๐ องศาเซลเซียส สรุปผลจากการสำรวจแหล่งพลังงานความร้อนใต้พิภพของประเทศไทย[๙] พบว่า มีแหล่งส่วนใหญ่อยู่ทางภาคเหนือและอุณหภูมิต่ำกว่า ๑๐๐ องศาเซลเซียส และประเทศไทยมีศักยภาพเชิงความร้อนรวมทั้งสิ้น ๔๒๗ พันตันเทียบเท่าน้ำมันดิบ จากเกณฑ์การพิจารณาศักยภาพพลังงานความร้อนใต้พิภพในประเทศไทยที่สามารถนำมาผลิตไฟฟ้า ได้แก่ อุณหภูมิ อยู่ในช่วง ๑๐๐-๑๕๐ องศาเซลเซียส ขนาดของแหล่งกักเก็บจะต้องมีความลึกไม่เกิน ๐-๒๐๐ เมตรจากพื้นดิน ความดันของไอน้ำ และลักษณะของแหล่งประกอบไปด้วยน้ำร้อนหรือไอน้ำเป็นส่วนใหญ่

๕.๒ การนำความร้อนใต้พิภพมาใช้ประโยชน์ในประเทศไทย

ความร้อนใต้พิภพที่นำมาใช้ประโยชน์ในประเทศไทย มีอยู่เพียงที่เดียว ซึ่งเป็นโครงการสาธิตของการไฟฟ้าฝ่ายผลิต คือ ที่อำเภอฝาง จ. เชียงใหม่ เพื่อใช้ในการผลิตไฟฟ้ามีกำลังการผลิตติดตั้ง ๓๐๐ kW ซึ่งเป็นโรงไฟฟ้าระบบ ๒ วงจร[๙] ที่ใช้แหล่งพลังงานความร้อนที่มีอุณหภูมิต่ำ ใช้น้ำร้อนจากหลุมเจาะระดับตื้นที่มีอุณหภูมิ ๑๓๐ องศาเซลเซียส ผลิตได้ประมาณปีละ ๑.๒ ล้านกิโลวัตต์ชั่วโมง จะถูกส่งเข้าสู่ระบบของการไฟฟ้าส่วนภูมิภาคเพื่อจ่ายให้ผู้ใช้ไฟฟ้าต่อไป และได้นำน้ำร้อนที่ผ่านการใช้งานในระบบผลิตไฟฟ้าแล้วไปใช้ให้ความร้อนในการอบแห้ง ห้องเย็น กิจการเพื่อกายบำบัด และเป็นสถานที่ท่องเที่ยว ส่วนแหล่งพลังงานความร้อนใต้พิภพอื่นๆ ที่มีศักยภาพ เช่น ที่สันกำแพงนั้น ได้มีการเจาะสำรวจแต่ยังไม่มีการติดตั้งกำลังการผลิต ส่วนแหล่งพลังงานความร้อนใต้พิภพที่อำเภอป่าแป๋และเทพพนม ยังพบปัญหาหลายอย่าง คือ อยู่ในเขตอุทยานแห่งชาติ ดังนั้นการพัฒนาแหล่งพัฒนาแหล่งความร้อนใต้พิภพจะเป็นไปได้ยาก ส่วนที่อำเภอแม่จันนั้น อยู่ในพื้นที่ที่มีการจ่ายไฟฟ้าถึงอยู่แล้ว ต้นทุนของการผลิตไฟฟ้าด้วยพลังงานความร้อนใต้พิภพจะมีค่าสูงกว่า ดังนั้นจึงยังไม่มีการพัฒนา

แหล่งความร้อนใต้พิภพในประเทศไทย ส่วนใหญ่เป็นแหล่งกักเก็บที่มีอุณหภูมิต่ำ ดังนั้นควรพิจารณาในการนำมาใช้ประโยชน์โดยตรงเป็นแหล่งให้ความร้อน ซึ่งเป็นการใช้ประโยชน์ของความร้อนจากน้ำร้อนโดยตรง ความร้อนที่ใช้อยู่ในช่วงประมาณ ๒๐-๑๕๐ องศาเซลเซียส[๙] สามารถนำมาใช้ประโยชน์ต่างๆ ได้ เช่น สามารถนำไปใช้ในการอบแห้ง และเป็นแหล่งให้พลังงานแก่ห้องเย็นสำหรับเก็บรักษาพืชผลทางการเกษตรได้ นำไปใช้ในกิจการเพื่อกายบำบัด

ปัญหาที่สำคัญอีกอย่างหนึ่งของการใช้งานคือ น้ำพุร้อนที่โผล่ขึ้นมาให้เห็นตามผิวดิน อาจไม่ได้อยู่เหนือแหล่งที่กำเนิดและกักเก็บพลังงาน ดังนั้นจึงไม่สามารถประเมินถึงศักยภาพของแหล่งพลังงานความร้อนใต้พิภพได้อย่างแน่นชัดว่ามีปริมาณเท่าไรและจะหมดเมื่อไร จึงยากที่จะประเมินว่าเหมาะสม คุ้มค่าที่จะนำมาใช้หรือไม่

๕.๓ แนวทางวิจัยพลังงานความร้อนใต้พิภพในประเทศไทย

ข้อจำกัดของการใช้พลังงานความร้อนใต้พิภพ คือ จะมีการปล่อยแก๊สคาร์บอนไดออกไซด์ ซัลเฟอร์ไดออกไซด์ และมีเทน ในน้ำแร่ร้อน ยังประกอบด้วยสารละลายซิลิกา โลหะหนัก โซเดียมและโพแทซเซียมคลอไรด์ บางครั้งอาจมีคาร์บอร์เนตด้วย ซึ่งอาจมีผลกระทบต่อสิ่งแวดล้อม อาจมีการทรุดตัวของพื้นดินในแหล่งพลังงานความร้อนใต้พิภพที่มีน้ำเป็นส่วนใหญ่ จากศักยภาพแหล่งพลังงานความร้อนใต้พิภพในประเทศไทย จะเห็นได้ว่าเป็นแหล่งกักเก็บที่มีอุณหภูมิต่ำ ดังนั้น ควรมีแนวทางวิจัยในการศึกษาความเป็นไปได้ในการนำความร้อนจากน้ำร้อนไปใช้ประโยชน์โดยตรงแทน โดยพัฒนาแหล่งพลังงานและศึกษาผลกระทบทางด้านสิ่งแวดล้อมด้วย

๖. พลังงานจากมหาสมุทร

มหาสมุทรสามารถผลิตพลังงานได้ ๒ รูปแบบ คือ พลังงานความร้อนที่ได้จากแสงอาทิตย์ และพลังงานกลที่ได้จากน้ำขึ้นน้ำลง และคลื่น

๖.๑ ศักยภาพการผลิตไฟฟ้าด้วยความร้อนจากมหาสมุทรในประเทศไทย (OTEC)[๑๐]

พื้นผิวโลกกว่าร้อย ๗๐ เป็นมหาสมุทร ดังนั้นมหาสมุทรจึงเป็นเสมือนตัวเก็บรังสีอาทิตย์ ขนาดใหญ่ การผลิตไฟฟ้าด้วยความร้อนจากมหาสมุทร จะอาศัยความแตกต่างระหว่างอุณหภูมิน้ำทะเลส่วนบนที่มีความลึกไม่เกิน ๕๐ เมตร ซึ่งเป็นส่วนที่สะสมพลังงานจากแสงอาทิตย์ มีอุณหภูมิประมาณ ๒๕-๓๐ องศาเซลเซียส และอุณหภูมิของน้ำทะเลส่วนล่างที่มีความลึกประมาณ ๑,๐๐๐ เมตร มีอุณหภูมิประมาณ ๕ องศาเซลเซียส

บริเวณที่เหมาะสมในการพัฒนาระบบ OTEC[๙๑] คือ ชายฝั่งที่มีความลาดชันสูง ลึกมากกว่า ๑,๐๐๐ เมตร และไม่ควรอยู่อยู่ห่างจากชายฝั่งเกิน ๕๐ กิโลเมตร นอกจากนี้กระแสลมและกระแสน้ำก็มีอิทธิพลต่อการพัฒนาด้วย กล่าวคือ กระแสน้ำที่มีความเร็วมากกว่า ๑.๙๒ กิโลเมตรต่อชั่วโมง หรือบริเวณที่มีกระแสลมที่มีความเร็วสูงกว่า ๔๖.๔ กิโลเมตรต่อชั่วโมง จะไม่เหมาะสมต่อการติดตั้งโรงไฟฟ้า OTEC

การผลิตไฟฟ้าจากพลังงานความร้อนจากมหาสมุทร (OTEC) มีระบบวัฏจักรการทำงาน แบ่งออกได้เป็น ๓ ระบบ คือ[๙๒] ระบบวัฏจักรเปิด ระบบวัฏจักรปิด และแบบลูกผสม ซึ่งทั้ง ๓ ระบบจะมีส่วนประกอบที่สำคัญอยู่ ๓ ส่วน คือ เครื่องระเหย เครื่องควบแน่น กังหันไอน้ำและเครื่องกำเนิดไฟฟ้า การทำงานของระบบผลิตไฟฟ้าด้วยความร้อนจากมหาสมุทร OTEC จะคล้ายคลึงกับโรงไฟฟ้าทั่วไป แต่ต่างกันที่ไม่มีการเผาไหม้เชื้อเพลิงเนื่องจากใช้ความร้อนจากน้ำมหาสมุทรส่วนบนเป็นต้นกำเนิดพลังงาน จึงไม่มีต้นทุนของค่าเชื้อเพลิง โรงไฟฟ้าแบบนี้จะใช้ผลิตไฟฟ้าในช่วงภาระฐาน แต่ประสิทธิภาพของระบบการผลิตจะต่ำประมาณร้อยละ ๖.๘-๙.๐ ซึ่งขึ้นกับค่าความแตกต่างของอุณหภูมิของน้ำที่ใช้ในระบบ ปัจจุบันการออกแบบโรงไฟฟ้ามี ๒ ลักษณะ คือ แบบที่ตั้งบนชายฝั่ง และแบบลอยน้ำ

จากข้อมูลของกรมอุทกศาสตร์ กองทัพเรือ ในด้านของอุณหภูมิของน้ำทะเลที่ระดับผิวน้ำ และที่ความลึกในระดับต่างๆ สามารถสรุปได้ดังตารางที่ ๔

พื้นท้องทะเลอ่าวไทยมีลักษณะคล้ายแอ่งน้ำ ส่วนที่ลึกสุดอยู่ตรงกลางและมีความลึกประมาณ ๘๓ เมตร เมื่อน้ำลงต่ำสุด ความลึกเฉลี่ยของอ่าวตอนกลางและตอนล่าง ประมาณ ๕๐ เมตร บริเวณปากอ่าวไทยที่ต่อกับทะเลจีนใต้ลึกประมาณ ๔๐ เมตร[๙๓] และด้านฝั่งทะเลอันดามัน พบว่าในระดับความลึก ๑,๐๐๐ เมตร อยู่ห่างชายฝั่ง ๒๒๐-๓๒๐ กิโลเมตร ซึ่งอยู่ในเขตน่านน้ำสากล และอยู่ห่างจากชายฝั่งมาก

เมื่อพิจารณาข้อมูลด้านพลังงานความร้อนจากมหาสมุทรดังแสดงในตารางที่ ๔ พบว่าประเทศไทยไม่มีศักยภาพเพียงพอในการพัฒนาระบบพลังงานความร้อนจากมหาสมุทร ทั้งในด้านความเหมาะสมของของอุณหภูมิระหว่างผิวน้ำ และอุณหภูมิใต้ผิวน้ำที่ความลึกของท้องมหาสมุทร รวมถึงลักษณะชายฝั่งของประเทศไทยที่ไม่มี

ความลาดชันที่เพียงพอที่จะทำให้ท้องมหาสมุทรมีความลึกในระดับที่สามารถนำมาใช้ประโยชน์ได้

๖.๒ พลังงานน้ำขึ้น-น้ำลง (Tidal Energy)

น้ำขึ้น-น้ำลง เป็นปรากฏการณ์ธรรมชาติอย่างหนึ่งของโลก ซึ่งการเกิดจากการเพิ่มขึ้นและลดลงของระดับน้ำ[๖] เป็นผลมาจากการเปลี่ยนแปลงแรงโน้มถ่วงและแรงจลน์ของดวงอาทิตย์ ดวงจันทร์และโลก เมื่อโคจรมาอยู่ในตำแหน่งต่างๆกัน โดยเมื่อดวงอาทิตย์และดวงจันทร์เข้าใกล้โลกและโคจรอยู่ในแนวเดียวกันจะทำให้เกิดน้ำขึ้น และเมื่อแรงดึงดูดของดวงอาทิตย์และดวงจันทร์ทำมุม ๙๐ องศา เมื่อเปรียบเทียบกับโลก จะทำให้เกิดน้ำลง

บริเวณที่เหมาะสมในการผลิตไฟฟ้าจากพัฒนาระบบพลังงานน้ำขึ้น-น้ำลง[๗] อยู่ที่แนวเส้นรุ้งที่ ๔๐-๖๐ องศา โดยลักษณะของชายฝั่งทะเลบริเวณปากอ่าวควรมีลาดชันสูงเพื่อสามารถสร้างเป็นอ่างเก็บน้ำได้ ความแตกต่างของระดับน้ำขึ้น-น้ำลง มีค่า ๔-๑๑ เมตร

จากข้อมูลของกรมอุทกศาสตร์ในปี พ.ศ. ๒๕๒๔-๒๕๓๖ สามารถสรุปเป็นข้อมูลของระดับน้ำขึ้น-น้ำลงสูงสุด และข้อมูลของระดับน้ำขึ้น-ลง ต่ำสุด ได้ดังตารางที่ ๙

เมื่อพิจารณาข้อมูลระดับน้ำขึ้น-น้ำลง จะเห็นได้ว่าค่าความแตกต่างของระดับน้ำขึ้น-น้ำลง ยังไม่อยู่ในเกณฑ์ที่เหมาะสม โดยค่าของความแตกต่างของระดับน้ำขึ้น-น้ำลง ทั้งในบริเวณอ่าวไทย และฝั่งทะเลอันดามันนั้นอยู่ในเกณฑ์ต่ำ และสภาพภูมิประเทศของไทย ในบริเวณปากแม่น้ำจะมีลักษณะราบเรียบ ไม่เอื้ออำนวยในการสร้างอ่างเก็บน้ำได้ ดังนั้นจึงสรุปได้ว่าประเทศไทยไม่มีศักยภาพเพียงพอในการพัฒนาระบบพลังงานน้ำขึ้น-น้ำลง

๖.๓ พลังงานจากคลื่น

คลื่น เป็นปรากฏการณ์ธรรมชาติในทะเลที่เกิดขึ้นตลอดเวลา โดยคลื่นเกิดจากลมที่พัดผ่านผิวมหาสมุทรและทะเล ขนาดของคลื่นจะใหญ่หรือเล็ก จะขึ้นอยู่กับความเร็วลม และระยะทางของลมที่พัดผ่านเหนือผิวน้ำ

เทคโนโลยีการแปลงพลังงานจากคลื่นทะเลเพื่อผลิตพลังงานนั้น ใช้หลักการแปลงพลังงานจลน์ของคลื่นทะเลเพื่อผลิตพลังงาน[๘] โดยพลังงานที่อยู่ในคลื่นทะเลจะประกอบไปด้วย พลังงาน ๒ ส่วน ได้แก่ พลังงานศักย์และพลังงานจลน์ พลังงานศักย์เป็นพลังงานเกี่ยวข้องกับรูปแบบของคลื่นหรือความสูงของคลื่น ส่วนพลังงานจลน์เป็นพลังงานที่เกี่ยวข้องกับการเคลื่อนที่ของคลื่น หรือความเร็วของน้ำทะเลที่ประกอบกันเป็นคลื่น

จากข้อมูลของกรมอุทกศาสตร์ในปี พ.ศ. ๒๕๒๔-๒๕๓๖ สามารถสรุปเป็นข้อมูลของระดับความสูงของคลื่น และคาบคลื่น ของฝั่งอ่าวไทยและฝั่งทะเลอันดามัน ได้ดังตารางที่ ๑๐

จากการพิจารณาความสูงของคลื่นและคาบคลื่น รวมถึงเทคโนโลยีที่จะนำมาผลิตพลังงานจากคลื่น โดยฝั่งอ่าวไทยมีความสูงของคลื่นไม่เกิน ๒ เมตร และฝั่งทะเลอันดามันมีความสูงของคลื่นไม่เกิน ๔ เมตร ซึ่งไม่เพียงพอในการนำมาใช้ประโยชน์และจากสถานภาพของเทคโนโลยีในการนำพลังงานคลื่นมาผลิตเป็นไฟฟ้า ยังไม่มีเทคโนโลยีที่รองรับการผลิตพลังงานจากความสูงคลื่นเพียง ๒-๔ เมตร

สรุป

ด้านพลังงานมวลชีวภาพ พบว่า ยังมีแหล่งมวลชีวภาพอีกมากที่ยังไม่ได้นำมาใช้เป็นเชื้อเพลิง ข้อจำกัดโดยทั่วไปของการใช้มวลชีวภาพ คือ แหล่งวัตถุดิบที่นำมาใช้มีปริมาณเปลี่ยนแปลงตามฤดูกาล เก็บรวมยาก และมีต้นทุนสูง ดังนั้นเพื่อลดข้อจำกัดของแหล่งพลังงานมวลชีวภาพ ควรมีแนวทางวิจัยด้านการจัดการแหล่งวัตถุดิบและการลดต้นทุนวัตถุดิบที่นำมาใช้ผลิตพลังงาน การเพิ่มประสิทธิภาพการเปลี่ยนรูปพลังงานมวลชีวภาพ รวมทั้งหาแนวทางเพิ่มการใช้มวลชีวภาพที่ยังไม่มีการพัฒนานำมาใช้มาผลิตพลังงาน นอกจากนี้ควรมีงานวิจัยเชิงนโยบายและมาตรการต่างๆ โดยเฉพาะมาตรการภาษีด้านต่างๆ โดยเฉพาะภาษีแก๊สคาร์บอนไดอ๊อกไซด์

ด้านพลังงานแสงอาทิตย์ พบว่า มีการทำงานวิจัยด้านนี้มาเป็นเวลานาน แต่ข้อจำกัดของการใช้งาน ควรมีวิจัยด้านเพิ่มประสิทธิภาพ สมรรถนะ และหาแนวทางลดต้นทุนของระบบ/อุปกรณ์ที่ใช้พลังงานแสงอาทิตย์ ควรมีงานวิจัยทั้งทางด้านเทคนิคและเศรษฐศาสตร์เพื่อขยายโอกาสที่จะพัฒนาอุปกรณ์และการประยุกต์ใช้ในงานใหม่ๆต่างๆ ได้อย่างเหมาะสมให้ได้กว้างขวางมากยิ่งขึ้น โดยเฉพาะเงื่อนไขที่เหมาะสมและความคุ้มค่าของการใช้เซลล์แสงอาทิตย์ นอกจากนี้ควรมีงานวิจัยเชิงนโยบายและมาตรการต่างๆของประเทศที่ประสพความสำเร็จในการใช้พลังงานแสงอาทิตย์ เช่น มาตรการภาษีด้านต่างๆ โดยเฉพาะภาษีแก๊สคาร์บอนไดอ๊อกไซด์

ด้านไฟฟ้าพลังน้ำ พบว่า การสร้างเขื่อนขนาดใหญ่เป็นไปได้ยาก ควรเน้นพลังน้ำขนาดเล็ก นอกจากนี้ควรมีงานวิจัยเชิงนโยบายในความร่วมมือกับประเทศเพื่อนบ้าน

ด้านพลังงานลม พบว่า ข้อมูลด้านความเร็วลมที่ระดับความสูงมากกว่า ๕๐ เมตรจากพื้นดินยังไม่มี ดังนั้นจึงควรสนับสนุนให้มีการศึกษา รวมถึงการศึกษาความเป็นไปได้ทางเทคนิคและเศรษฐศาสตร์ สำหรับการติดตั้งกังหันลมในพื้นที่ที่มีความเร็วลมสูง นอกจากนี้ควรมีงานวิจัยเชิงนโยบายด้านมาตรการจูงใจและส่งเสริมการผลิตและติดตั้งกังหันเพื่อการสูบน้ำและเพื่อการผลิตไฟฟ้า

พลังงานความร้อนใต้พิภพในประเทศไทยมีศักยภาพต่ำ ส่วนพลังงานจากมหาสมุทรไม่น่าจะมีศักยภาพ

กิตติกรรมประกาศ

ผู้เขียนใคร่ขอบคุณสำนักงานกองทุนสนับสนุนการวิจัยที่ให้การสนับสนุนทุนวิจัย

เอกสารอ้างอิง

๑. Anon, 2004. Refocus, Nov./Dec., pp. 4, 42-44.

๒. นิรนาม ๒๕๔๗ สถานภาพปัจจุบันและข้อเสนอสู่อนาคต ด้านเชื้อเพลิงและเทคโนโลยีเชื้อเพลิง หน้า ๔.

๓. กรมพัฒนาพลังงานทดแทนและอนุรักษ์พลังงาน, ศักยภาพพลังงานชีวมวล, http://203.150.24.8/dede/renew/bio_p.htm ,เมษายน ๒๕๔๗.

๔. สำนักงานเศรษฐกิจการเกษตร, สถิติการเกษตรของประเทศไทยปีเพาะปลูก พ.ศ. ๒๕๔๔-๒๕๔๕, http://oae.go.th/statistic/yearbook/2001-02/ , เมษายน ๒๕๔๗.

๕. สุรกิตติ ศรีกุล, สุนีย์ นิเทศพัตรพงศ์ และ ชาย โฆรวิส., เอกสารประกอบการประชุมระดมความคิด เรื่อง แนวทางการวิจัยและพัฒนาไบโอดีเซลสู่เชิงพาณิชย์, สำนักงานคณะกรรมการวิจัยแห่งชาติ, ๒๕๔๔, หน้า B-๑-B-๑๔.

๖. กล้าณรงค์ ศรีรอต , พูนศุข ประเสริฐสรรพ์ , สมพร อิศวิลานนท์ และเกื้อกูล ปิยะจอมขวัญ, *รายงานการวิจัยการศึกษาสถานภาพวัตถุดิบที่จะนำมาใช้ในอุตสาหกรรมการผลิตไบโอดีเซล*, สำนักงานคณะกรรมการวิจัยแห่งชาติ, กรุงเทพฯ, ๒๕๔๔, ๑๑๒ หน้า.

๗. คณะกรรมาธิการพลังงาน สภาผู้แทนราษฎร, *วัตถุดิบสำหรับผลิตเอทานอล*, พลังงานทดแทน เอทานอล และไบโอดีเซล, กรุงเทพฯ, ๒๕๔๔, หน้า ๑๓๗-๑๓๙.

๘. กล้าณรงค์ ศรีรอต , เจริญศักดิ์ โรจนฤทธิ์พิเชษฐ์ , เอ็จ สโรบล , พิพัฒน์ วีระถาวร และ เกื้อกูล ปิยะจอมขวัญ, *รายงานการวิจัยการศึกษาสถานภาพวัตถุดิบที่จะนำมาใช้ในอุตสาหกรรมการผลิตแก๊สโซฮอล์*, สำนักงานคณะกรรมการวิจัยแห่งชาติ, กรุงเทพฯ, ๒๕๔๔, ๑๑๔ หน้า.

๙. รายงานพลังงานของประเทศไทย ๒๕๔๖, กรมพัฒนาพลังงานทดแทน และ อนุรักษ์พลังงาน กระทรวงพลังงาน, กรุงเทพฯ.

๑๐. รายงานไฟฟ้าของประเทศปี ๒๕๔๔, กรมพัฒนาพลังงานทดแทนและอนุรักษ์พลังงาน, กรุงเทพ, ๒๕๔๖.

๑๑. รายงานพลังงานทดแทนของประเทศไทย ๒๕๔๖, กรมพัฒนาพลังงานทดแทน และอนุรักษ์ พลังงาน กระทรวงพลังงาน, กรุงเทพฯ.

๑๒. http://www.dede.go.th/dede/index.php?id=172, 2005.

๑๓. กรมพัฒนาพลังงานทดแทนและอนุรักษ์พลังงาน, สถานภาพการใช้พลังงานชีวมวล:น้ำเสียในโรงงานอุตสาหกรรม, มกราคม ๒๕๔๖, http://๒๐๓.๑๔๐.๒๔.๘/renew/status.asp.

๑๔. ภาณุวัณท์ คล้ายวงศ์วาลย์, วิทยานิพนธ์ปริญญาวิทยาศาสตรมหาบัณฑิต, *มหาวิทยาลัยเทคโนโลยีพระจอมเกล้าธนบุรี*, กรุงเทพฯ., ๒๕๔๖.

๑๕. บุญเรือง ศรีสวัสดิ์, การปรับปรุงสมรรถนะเตาเผาแกลบ, วิทยานิพนธ์ปริญญาวิทยาศาสตรมหาบัณฑิต, *มหาวิทยาลัยเทคโนโลยีพระจอมเกล้าธนบุรี*, กรุงเทพฯ,๒๕๔๑.

๑๖. สุวิทย์ เตีย , ภัทวุฒิ พุกอมรพันธ์ , พรเทพ จิตวุฒิไกร , แสง แซ่เล้า และ ทนงค์ ฉายาวัฒนะ, "การเผาไหม้เชื้อเพลิงในเตาฟลูอิดไดซ์เบด", *วารสารวิจัยและพัฒนา มจธ.*, ๒๕๔๒, ปีที่ ๒๒,ฉบับที่ ๒, หน้า ๔๗-๖๓.

๑๗. นิรมล ชุลีเลิศวิทยาภรณ์ และคณะ, ๒๕๓๗, การหาสภาวะที่ผลิตก๊าซคาร์บอนมอนนอกไซด์ที่ดีที่สุดของเครื่องผลิตก๊าซชีวมวลแบบไหลขึ้นโดยวิธีการค้นหาแบบ Simplex, รายงานการประชุมทางวิชาการ คณะวิศวกรรมศาสตร์, มหาวิทยาลัยเทคโนโลยีพระจอมเกล้าธนบุรี, ๙-๑๑ พฤษภาคม ๒๕๓๗, หน้า๙๗.

๑๘. สุรศักดิ์ สุรนันทชัย., การวิเคราะห์ระบบผลิตพลังงานร่วมในโรงงานปาล์มน้ำมัน, วิทยานิพนธ์ปริญญาวิศวกรรมศาสตรมหาบัณฑิต, *สถาบันเทคโนโลยีพระจอมเกล้าธนบุรี*, กรุงเทพฯ, ๒๕๓๕.

๑๙. วารุณี เตีย , สมชาติ โสภณรณฤทธิ์ และ ยุวดี เรืองเดช, "ศักยภาพการผลิตไฟฟ้าและความร้อนร่วมในโรงสีข้าวขาวของประเทศไทย", *วิศวกรรมสาร ฉบับวิจัยและพัฒนา*, ๒๕๔๕, ปีที่ ๑๓, ฉบับที่ ๒, หน้า ๔๐-๔๗.

๒๐. จิระพันธุ์ เนื่องจากนิล, บูรณาการระบบพลังงานความร้อนและไฟฟ้าในโรงงานน้ำตาล, วิทยานิพนธ์ปริญญาวิศวกรรมศาสตรมหาบัณฑิต, *มหาวิทยาลัยเทคโนโลยีพระจอมเกล้าธนบุรี*, กรุงเทพฯ, ๒๕๔๒.

๒๑. สุธีระ ประเสริฐสรรพ์, การจำลองโรงจักรผลิตพลังงานร่วมความร้อนและไฟฟ้าโดยชีวมวล, สำนักงานคณะกรรมการนโยบายแห่งชาติ, ๒๕๔๒, ๑๔๓ หน้า.

๒๒. เอกรินทร์ โบษกรนัฏ, สมชาติโสภณรณฤทธิ์, และ วารุณี เตีย, การอบแห้งข้าวนึ่งด้วยเครื่องอบแห้งฟลูอิดไดซ์เบด, รายงานการประชุมวิชาการสมาคมวิศวกรรมเกษตรแห่งประเทศไทย ครั้งที่ ๔, ๒๕๔๖, หน้า ๒๙๗-๓๐๔.

๒๓. กนกอร รจนากิจ , พงษ์ศักดิ์ คำมูล และ จินดา เจริญพรพาณิชย์, การทำไบโอดีเซลจากไขมันปาล์มบริสุทธิ์เป็นเชื้อเพลิงในเครื่องยนต์จุดระเบิดด้วยการอัด, รายงานการประชุมวิชาการเครือข่ายวิศวกรรมเครื่องกลแห่งประเทศไทย ครั้งที่ ๑๖, ๒๕๔๕, หน้า ๖๖-๗๑.

๒๔. วัชระ ลอยสมุทร , อุพารวิศว์ ครองยุทธ , สุรชัย ฝั้นแก้ว และ ศิริกุล จันทร์สว่าง, การปรับปรุงน้ำมันพืชใช้แล้วเป็นเชื้อเพลิงในเครื่องยนต์ดีเซล, *RSU JET*, ๒๕๔๒, ฉบับที่ ๓, เล่มที่ ๓, หน้า ๓๔-๓๗.

๒๕. สุพัฒน์ หวังวงศ์วัฒนา, "ผลกระทบของการใช้น้ำมันดีเซลผสมน้ำมันพืช ต่อเครื่องยนต์และมลพิษทางอากาศ", เอกสารประกอบการสัมมนาเรื่องแนวทางการวิจัยและพัฒนาไบโอดีเซลไปสู่เชิงพาณิชย์, สำนักงานคณะกรรมการวิจัยแห่งชาติ, ๒๕๔๔, หน้าF-๑-F-๗.

๒๖. อภิชิต เสมศรี , มณฑล ใจกุศล และ จินดา เจริญพร พาณิชย์, การใช้น้ำมันพืชผสมสำหรับเครื่องยนต์ดีเซลขนาดเล็กแบบฉีดตรงเข้าห้องเผาไหม้, รายงานการประชุมวิชาการเครือข่ายวิศวกรรมเครื่องกลแห่งประเทศไทย ครั้งที่ ๑๖, ๒๕๔๕, หน้า ๑๓๙-๑๔๓.

๒๗. ธีระพงษ์ ว่องรัตนไพศาล , ทนงเกียรติ เกียรติศิริโรจน์ และ ณัฐ วรยศ, เอกสารประกอบการสัมมนาเผยแพร่ผลงานวิจัยด้านพลังงานทดแทน เรื่อง การผลิตเอทานอลโดยใช้พลังงานแสงอาทิตย์ในรูปความร้อน, สำนักงานคณะกรรมการวิจัยแห่งชาติ, ๒๕๔๖, หน้า B-๑-B-๑๓.

๒๘. เจริญศักดิ์ โรจนฤทธิ์พิเชษฐ์ , กล้าณรงค์ ศรีรอด , สุวิทย์ เดีย , มณเฑียร นิติวรรัตน์ , เกื้อกูล ปิยะจอมขวัญ , สุทธิพันธ์ แก้วสมพงษ์ และ สิทธิโชค วัลลภาทิตย์., เอกสารประกอบการสัมมนาเผยแพร่ผลงานวิจัยด้านพลังงานทดแทน เรื่อง โครงการศึกษาต้นแบบโรงงานเอทานอลโดยการพัฒนาเทคโนโลยีการผลิตจากมันเส้น, สำนักงานคณะกรรมการวิจัยแห่งชาติ, ๒๕๔๖, หน้า A-๑-A-๕

๒๙. สุวิทย์ เดีย , บุณยพัต สุภานิช และ สุทธิดา สาย, แบบสรุปผลการวิจัย เรื่อง โครงการประเมินความเป็นไปได้ของการผลิตเชื้อเพลิงเอทานอลจากผลผลิตทางการเกษตรของประเทศไทย, สำนักงานคณะกรรมการวิจัยแห่งชาติ, ๒๕๔๔, ๖ หน้า.

๓๐. สุวิทย์ เดีย, การสัมมนาเรื่องศักยภาพของประเทศไทยในการผลิตเอทานอลเพื่อทดแทนการนำเข้า, กลุ่มงานเกษตรและอุตสาหกรรมเกษตร, กองโครงการและประสานงานวิจัย สำนักงานคณะกรรมการวิจัยแห่งชาติ, ๒๕๔๔, หน้า D-๑ – D-๑๙.

๓๑. บุณยพัตร สุภานิช , สุวิทย์ เดีย และปนัดดา ภูอากาศ, เอกสารประกอบการสัมมนาเผยแพร่ผลงานวิจัยด้านพลังงานทดแทน เรื่อง การบูรณาการกระบวนการผลิตเอทานอลกับโรงงานน้ำตาลและโรงงานแป้งมันสำปะหลัง และการประเมินเทคโนโลยีในการทำเอทานอลให้บริสุทธิ์, สำนักงานคณะกรรมการวิจัยแห่งชาติ, ๒๕๔๖, หน้า C-๑-C-๑๓

๓๒. อาณัติ มีป้อม, การศึกษาความเป็นไปได้ในการจัดตั้งระบบบำบัดน้ำเสียรวมเพื่อการผลิตก๊าซชีวภาพในจังหวัดนครปฐม ๑) ของเสียที่เกิดจากฟาร์มเลี้ยงสุกรและโรงงานอุตสาหกรรมอาหารขนาดกลางและเล็ก, วิทยานิพนธ์ปริญญาโทวิทยาศาสตรมหาบัณฑิต, *มหาวิทยาลัยเทคโนโลยีพระจอมเกล้าธนบุรี*, กรุงเทพฯ, ๒๕๔๔.

๓๓. นันทนิตย์ ทัศน์เอี่ยม, การเปรียบเทียบการผลิตก๊าซชีวภาพจากน้ำบึบเปลือกสับปะรดในถังปฏิกรณ์แบบชั้นกรองระหว่างกระบวนการหมักแบบขั้นตอนเดียวและสองขั้นตอน, วิทยานิพนธ์ปริญญาวิทยาศาสตรมหาบัณฑิต, *มหาวิทยาลัยเทคโนโลยีพระจอมเกล้าธนบุรี*, กรุงเทพฯ, ๒๕๓๑.

๓๔. เสริม จันทร์ฉาย และจรุงแสง ลักษณบุญส่ง, แผนที่ศักยภาพพลังงานแสงอาทิตย์จากข้อมูลดาวเทียมสำหรับประเทศไทย, กรมพัฒนาและส่งเสริมพลังงานร่วมกับภาควิชาฟิสิกส์ คณะวิทยาศาสตร์ มหาวิทยาลัยศิลปากร, หน้า ๘๒-๘๙.

๓๕. http://www.nepo.go.th/vrs/VRS44-07-Solar.html, 2001.

๓๖. http://www.egat.or.th/rdo/energy/phuket.html, 2005.

๓๗. http://www.egat.co.th/information/powerplant/solarcell.htm, 2005.

๓๘. คณะทำงานพลังงานแสงอาทิตย์ในรูปความร้อน, ๒๕๔๐, รายงานการประชุมคณะทำงานพลังงานแสงอาทิตย์ในรูปความร้อน, คณะอนุกรรมการประสานงานการวิจัยและพัฒนาพลังงานทดแทน, สำนักงานคณะกรรมการวิจัยแห่งชาติ, หน้า ๒-๔.

๓๙. สุรสิทธิ์ ประสารปราน, ๒๕๓๐, ระบบทำน้ำร้อนด้วยแสงอาทิตย์ที่มีตัวรับรังสีแบบอีทไปป์-เซอร์มัลไดอด, วิทยานิพนธ์ปริญญาวิทยาศาสตรมหาบัณฑิต สาขาวิชาเทคโนโลยีพลังงาน คณะพลังงานและวัสดุ สถาบันเทคโนโลยีพระจอมเกล้าธนบุรี.

๔๐. สุคนธ์ อาจฤทธิ์, ๒๕๒๔, ตัวรับแสงอาทิตย์แผ่นราบแบบเพิ่มผิวโค้งสะท้อนแสง, วิทยานิพนธ์ปริญญาวิทยาศาสตรมหาบัณฑิต สาขาเทคโนโลยีพลังงาน คณะพลังงานและวัสดุ , สถาบันเทคโนโลยีพระจอมเกล้าธนบุรี, ๙๓ หน้า.

๔๑. ประวิทย์ ถีถะแก้ว, ๒๕๒๔, สมรรถภาพของระบบทำน้ำร้อนด้วยแสงอาทิตย์ที่ใช้ชุดรับรังสีแผ่นราบกระจก ๒ ชั้น, วิทยานิพนธ์ปริญญาวิทยาศาสตรมหาบัณฑิต สาขาเทคโนโลยีพลังงาน คณะพลังงานและวัสดุ, สถาบันเทคโนโลยีพระจอมเกล้าธนบุรี, ๑๐๔ หน้า.

๔๒. สมนึก บุญญศาสตร์พันธุ์, ๒๕๒๗, ระบบทำน้ำร้อนด้วยแสงอาทิตย์ที่อุณหภูมิสูงด้วยตัวรับรังสีแบบแผ่นเรียบ, วิทยานิพนธ์ปริญญาวิศวกรรมศาสตรมหาบัณฑิต สาขาเทคโนโลยีพลังงาน คณะพลังงานและวัสดุ, สถาบันเทคโนโลยีพระจอมเกล้าธนบุรี, ๙๔ หน้า.

๔๓. สุขฤดี สุขใจ, ๒๕๓๔, สมรรถนะของเครื่องอบแห้งกล้วยน้ำว้าด้วยแสงอาทิตย์แบบหมุนเวียนและแบบต่อเนื่อง, วิทยานิพนธ์ปริญญาวิศวกรรมศาสตรมหาบัณฑิต สาขาเทคโนโลยีพลังงาน คณะพลังงานและวัสดุ, สถาบันเทคโนโลยีพระจอมเกล้าธนบุรี, ๑๔๔ หน้า.

๔๔. วรวิทย์ รุ่งจิวารักษ์, ๒๕๓๘, การศึกษาระบบอบแห้งกล้วยน้ำว้าด้วยแสงอาทิตย์ขนาดอุตสาหกรรม, วิทยานิพนธ์ปริญญาวิศวกรรมศาสตรมหาบัณฑิต สาขาวิชาเทคโนโลยีพลังงาน คณะพลังงานและวัสดุ สถาบันเทคโนโลยีพระจอมเกล้าธนบุรี, ๑๘๔ หน้า.

๔๕. ณัฐวุฒิ คุษฎี, ๒๕๓๔, การพัฒนาระบบอบแห้งผลไม้โดยใช้พลังงานแสงอาทิตย์เป็นพลังงานเสริม, วิทยานิพนธ์ปริญญาวิศวกรรมศาสตรมหาบัณฑิต สาขาวิชาเทคโนโลยีพลังงาน

คณะพลังงานและวัสดุ สถาบันเทคโนโลยีพระจอมเกล้าธนบุรี, ๑๐๗ หน้า.

๔๖. พจนา วงษ์ศิริ, ๒๕๒๔, การอบแห้งผลิตภัณฑ์อาหารโดยใช้เครื่องอบแห้งแสงอาทิตย์แบบมีตัวรับรังสี, วิทยานิพนธ์ปริญญาวิศวกรรมศาสตรมหาบัณฑิต สาขาวิชาเทคโนโลยีพลังงาน คณะพลังงานและวัสดุ สถาบันเทคโนโลยีพระจอมเกล้าธนบุรี, ๗๙ หน้า.

๔๗. อานนท์ โพธิ์หอม, ๒๕๒๐, เครื่องกลั่นน้ำด้วยแสงอาทิตย์, โครงการปริญญาวิศวกรรมศาสตรมหาบัณฑิต ภาควิชาวิศวกรรมเครื่องกล คณะวิศวกรรมศาสตร์ สถาบันเทคโนโลยีพระจอมเกล้าธนบุรี, ๙๘ หน้า.

๔๘. ทนงเกียรติ เกียรติศิริโรจน์, ๒๕๒๓, การศึกษาเครื่องกลั่นน้ำแสงอาทิตย์แบบรีเจนเนเรทิฟ,วารสารวิจัยและพัฒนา สจธ., ฉบับที่ ๔, เล่มที่ ๒, หน้า ๑-๘.

๔๙. ศิริชัย เทพา, ๒๕๓๒, เครื่องกลั่นน้ำผิวตั้งฝาครอบอคริลิค, วารสารวิจัยและพัฒนา สจธ., ฉบับที่ ๑๒, เล่มที่ ๑, หน้า ๑๖-๓๙.

๕๐. อานนท์ โพธิ์หอม, ๒๕๒๑, เครื่องกลั่นน้ำด้วยแสงอาทิตย์แบบอยู่กับที่, Seminar on Solar Energy and Applications, Technological Promotion Association (Thai-Japan) and King Mongkut's Institute of Technology, Thailand, หน้า ๗.

๕๑. สมชาย โสภณศิริกุล, ๒๕๔๓, การปรับปรุงสมรรถนะของเครื่องกลั่นน้ำ, วิทยานิพนธ์ปริญญาวิทยาศาสตรมหาบัณฑิต สาขาวิชาเทคโนโลยีพลังงาน คณะพลังงานและวัสดุ สถาบันเทคโนโลยีพระจอมเกล้าธนบุรี, ๑๐๙ หน้า.

๕๒. มานะ คงดีจันทร์, ๒๕๓๔, การกลั่นเอธานอลจากวัตถุดิบการเกษตรโดยพลังงานแสงอาทิตย์, วิทยานิพนธ์ปริญญาวิศวกรรมศาสตรมหาบัณฑิต สาขาวิชาเทคโนโลยีพลังงาน คณะพลังงานและวัสดุ สถาบันเทคโนโลยีพระจอมเกล้าธนบุรี, ๑๑๐ หน้า.

๕๓. จีรศักดิ์ จิระวารี และวีระชัย แก่นทรัพย์, ๒๕๒๓, การกลั่นแอลกอฮอล์ด้วยตัวรับรังสีแผ่นราบ, โครงงานปริญญาวิศวกรรมศาสตรบัณฑิต ภาควิชาวิศวกรรมเครื่องกล คณะวิศวกรรมศาสตร์ สถาบันเทคโนโลยีพระจอมเกล้าธนบุรี, ๘๔ หน้า.

๕๔. ณัฐ วรยศ, ๒๕๔๔, การศึกษาความเป็นไปได้ในการกลั่นเอทธานอลด้วยพลังงานแสง อาทิตย์, เอกสารประกอบการสัมมนาเรื่องศักยภาพของประเทศไทยในการผลิตเอทธานอลเพื่อทดแทนการนำเข้า, กลุ่มงานเกษตรและอุตสาหกรรมเกษตร กองโครงการและประสานงานวิจัย สำนักงานคณะกรรมการวิจัยแห่งชาติ, หน้า E-๑-E-๖.

๕๕. ทวีศักดิ์ ศรีภูสิตโต และคณะ, ๒๕๓๑, Solar Adsorption Refrigeration, โครงงานปริญญาวิศวกรรมศาสตรบัณฑิต ภาควิชาวิศวกรรมเครื่องกล คณะวิศวกรรมศาสตร์ สถาบันเทคโนโลยีพระจอมเกล้าธนบุรี, ๗๕ หน้า.

๕๖. พิทยา กิ่งชม และคณะ, ๒๕๓๒, การศึกษาเครื่องทำความเย็นแบบดูดเกาะ, โครงงานปริญญาวิศวกรรมศาสตรมหาบัณฑิต สายวิชาวิศวกรรมเครื่องกล คณะวิศวกรรมศาสตร์ สถาบันเทคโนโลยีพระจอมเกล้าธนบุรี, ๖๖ หน้า.

๕๗. ทนงเกียรติ เกียรติศิริโรจน์, ๒๕๓๕, การศึกษาสมรรถนะของระบบทำความเย็นแสง อาทิตย์ที่ใช้ถ่านกัมมันต์-เมธานอลเป็นสารคู่ทำงาน, วิศวกรรมสารฉบับวิจัยและพัฒนา, ฉบับที่ ๓, เล่มที่ ๑, หน้า ๖๑-๖๙.

๕๘. Boonbumroong, U., et al., Suwannakum, T., Pongchawee, D., Pengma, S., Kitikara, K., and Sripadungtum, P., 2004, Parametric Study of a PV/Wind/Diesel Hybrid System for Kohjik Island, 14th International Photovoltaic Science and Engineering Conference, 26-30 January, Chulalongkorn University, Bangkok, pp.841-842.

๕๙. Somsak, T., Boonbumroong, U., Tanchareon, S., Jeenkaokam, N., and Jivacate, C., 2004, PV-Diesel Stand Alone Hybrid System at Royal Project Research Station: Observations on Power Quality, 14th International Photovoltaic Science and Engineering Conference, 26-30 January, Chulalongkorn University, Bangkok, pp.843-846.

๖๐. Thianphu, A., 2004, Management of PV Water Pumping system, 14th International Photovoltaic Science and Engineering Conference, 26-30 January, Chulalongkorn University, Bangkok, pp.889-890.

๖๑. Sangpanich, U., Thongpron, J., Kitikara, K., and Jivacate, C., 2004, Power Quality of Four Rooftop Grid-Connected Photovoltaic System In Thailand, 14th International Photovoltaic Science and Engineering Conference, 26-30 January, Chulalongkorn University, Bangkok, pp.139-140.

๖๒. Buranasajja, S. and Seingsanor, S., 2004, Photovoltaic Battery Charging System in Thailand: a Case Study of Ban Bon Khao Kangriang, 14th International Photovoltaic Science and Engineering Conference, 26-30 January, Chulalongkorn University, Bangkok, pp.945-946.

๖๓. คณะอนุกรรมการส่งเสริมการใช้พลังงานหมุนเวียน, ๒๕๔๔, เอกสารประกอบการประชุม เรื่องแผนพัฒนาพลังงานหมุนเวียนในช่วงปี ๒๕๔๕-๒๕๔๙, สำนักงานคณะกรรมการนโยบายแห่งชาติ.

๖๔. แผนปฏิบัติการเทคโนโลยีไฟฟ้าพลังน้ำขนาดเล็ก ๕ ปี (๒๕๔๕-๒๕๔๙) กรมพัฒนาพลังงานทดแทนและอนุรักษ์พลังงาน.

๖๕. ทวีป ชัยสมภพ และจักรี คุปต์อัครภิญโญ, ๒๕๔๖, "การประเมินเชิงเทคโนโลยีของโครงการพัฒนาพลังน้ำขนาดเล็กในประเทศที่กำลังพัฒนาและในประเทศที่พัฒนาแล้ว", การสัมมนาเผยแพร่ผลงานวิจัยด้านพลังงานทดแทน, วันที่ ๒๕ กันยายน ๒๕๔๖, โรงแรมรามาการ์เดนส์, หน้า ๑๓๘-๑๔๗.

๖๖. ธนะ บุญญสิริกูล, ๒๕๔๔, "การออกแบบนโยบายจัดสรรน้ำเพื่อประโยชน์สูงสุดในการจัดการอ่างเก็บน้ำ", การประชุมสัมมนาวิชาการและนิทรรศการด้านพลังน้ำ, ครั้งที่ ๑, วันที่ ๖-๗ กุมภาพันธ์ ๒๕๔๔, การไฟฟ้าฝ่ายผลิตแห่งประเทศไทย, หน้า ๓-๑๓ – ๓-๑๙.

๖๗. กรมพัฒนาส่งเสริมพลังงาน, 2544, เอกสารโครงการจัดทำแผนที่ศักยภาพพลังงานลมในประเทศ.

๖๘. คณะทำงานพลังงานลม, ๒๕๔๑, นโยบายแผนและแนวทางการวิจัยและพัฒนาพลังงานทดแทน : พลังงานลม, คณะอนุกรรมการประสานงานการวิจัยและพัฒนาพลังงานทดแทน,สำนักงานคณะกรรมการวิจัยแห่งชาติ, ๑๔ หน้า.

๖๙. องอาจ คงฤทธิ์ และคณะ, ๒๕๒๔, การนำอุโมงค์มาทดสอบกังหันลม ๘ ใบ, โครงงาน ปริญญาวิศวกรรมศาสตรบัณฑิต ภาควิชาวิศวกรรมเครื่องกล คณะวิศวกรรมศาสตร์ สถาบันเทคโนโลยีพระจอมเกล้าธนบุรี, ๔๒ หน้า.

๗๐. ประจัญ เพชรไวฑูรย์, ๒๕๓๐, การศึกษาความเค้นในใบของกังหันลมแกนหมุนแนวดิ่ง, วิทยานิพนธ์ปริญญาวิศวกรรมศาสตรมหาบัณฑิต สาขาวิชาเทคโนโลยีพลังงาน คณะพลังงานและวัสดุ สถาบันเทคโนโลยีพระจอมเกล้าธนบุรี, ๑๓๙ หน้า.

๗๑. สมชาย ชูชีพกุล, ๒๕๓๓, แบบจำลองไฟไนท์เอเลเมนท์ของใบพัดกังหันลมแบบดาร์เรียส, "วารสารวิจัยและพัฒนา สจช.," ฉบับที่ ๑๓, เล่มที่ ๒, หน้า ๑-๑๖.

๗๒. สุกฤษณ์ โรจนวิไลกุล สุทธิชัย ศิริพรอดุลศิลป์ และเอกภพ จันทร์ศุภมงคล, ๒๕๔๒, การศึกษา Laminar Separation Brbble บนใบพัดของกังหันลม, โครงงานปริญญาวิศวกรรมศาสตรมหาบัณฑิต ภาควิชาวิศวกรรมเครื่องกล คณะวิศวกรรมศาสตร์ มหาวิทยาลัยเทคโนโลยีพระจอมเกล้าธนบุรี, ๑๔๑ หน้า.

๗๓. เกรียงศักดิ์ ขุนไชย, ๒๕๒๗, ระบบผลิตไฟฟ้าจากกังหันลมแบบไจโร-โรเตอร์(ระยะ๒), วิทยานิพนธ์ปริญญาวิทยาศาสตรมหาบัณฑิต สาขาวิชาเทคโนโลยีพลังงาน คณะพลังงานและวัสดุ สถาบันเทคโนโลยีพระจอมเกล้าธนบุรี, ๑๕๒ หน้า.

๗๔. มนชัย เหลืองวัฒนวิไล และคณะ, ๒๕๓๔, กังหันลมผลิตกระแสไฟฟ้าแบบดาร์เรียส,โครงงานปริญญาวิศวกรรมศาสตรบัณฑิต ภาควิชาวิศวกรรมเครื่องกล คณะวิศวกรรมศาสตร์ สถาบันเทคโนโลยีพระจอมเกล้าธนบุรี, ๔๔ หน้า.

๗๕. อนุวัตต์ จางวนิชเลิศ และประภาษ ไพรสุวรรณ, ๒๕๓๔, การพัฒนาเครื่องกำเนิด กระแสไฟฟ้าด้วยพลังงานลม, พลังงานลม เครื่องกำเนิดกระแสไฟฟ้า ไฟฟ้ารถยนต์ Electric generators, การประชุมวิชาการทางวิศวกรรมไฟฟ้า ครั้งที่ ๒๐ เล่ม ๓, หน้า ๓๙๖-๓๙๑.

๗๖. อนุวัตน์ จางวนิชเลิศ และประภาษ ไพรสุวรรณ, ๒๕๔๑, "ระบบผลิตและสำรองกระแสไฟฟ้าด้วยพลังงานลม, "วิศวสารลาดกระบัง, ปีที่ 14, ฉบับที่ ๑, หน้า ๑-๙.

๗๗. กองพัฒนาพลังงานทดแทน, สำนักงานวิจัยและพัฒนา การไฟฟ้าฝ่ายผลิต, ๒๕๔๒, การผลิตไฟฟ้าจากกังหันลม, "วารสารประสิทธิภาพพลังงาน," ฉบับที่ ๔๖, หน้า ๓๓-๓๙.

๗๘. กองพัฒนาพลังงานทดแทน, ๒๕๔๒, "พลังงานความร้อนใต้พิภพ", พลังงานความร้อนใต้พิภพ, การไฟฟ้าฝ่ายผลิตแห่งประเทศไทย.

๗๙. http://www.dmr.go.th/HOTSPING/THAIHOTSP.htm, 2002.

๘๐. http://www.egat.or.th/rdo/energy/gerohermal_plant.htm, 2002.

๘๑. มานพ รักษาสกุลวงศ์ และศิริพร สูงปานเขา, ๒๕๔๔, "พลังงานความร้อนใต้พิภพ", ข่าวสารการธรณี, ปีที่ ๔๗, ฉบับที่ ๒, หน้า ๔๑-๔๙.

๘๒. http://www.nrel.gov/clean_energy/ocean.html, 2005.

๘๓. สุรชัย ประเสริฐวิกัย, ๒๕๔๐, "พลังงานความร้อนจากมหาสมุทร...สำคัญที่ผลพลอยได้", วารสารการไฟฟ้าฝ่ายผลิต, ปีที่ ๖, เล่มที่ ๓, หน้า ๓๘-๔๔.

๘๔. คณะวิศวกรรมศาสตร์ มหาวิทยาลัยเชียงใหม่, ๒๕๔๑, รายงานฉบับสมบูรณ์ โครงการศึกษาเบื้องต้น ศักยภาพและความเหมาะสมในการพัฒนาพลังงานจากทะเล, กรมพัฒนาพลังงานทดแทนและอนุรักษ์พลังงาน, ๖๒ หน้า.

๘๕. มนูวดี หังสพฤกษ์, ๒๕๔๓, "สมุทรศาสตร์กายภาพของอ่าวไทย", วารสารราชบัณฑิตยสถาน, ปีที่ ๒๕, หน้า ๑๖๘-๑๗๙.

๘๖. ประวิทย์ ถีตะแก้ว, ๒๕๒๖, "พลังงานน้ำขึ้นน้ำลง", พลังงาน, หน้า ๒๕๓-๒๖๑.

ตารางที่ ๑ ศักยภาพพลังงานจากวัสดุเหลือใช้ทางการเกษตร พ.ศ. ๒๕๔๓

ชนิด	ผลผลิต/ปี (พันตัน)	วัสดุเหลือใช้	ปริมาณวัสดุเหลือใช้ (พันตัน)	แฟคเตอร์วัสดุเหลือใช้ที่ยังไม่มีการใช้	ปริมาณวัสดุเหลือใช้ที่ยังไม่มีการใช้ (พันตัน)	ค่าพลังงานความร้อน (MJ/kg)	ศักยภาพพลังงาน (*10^6 MJ)
อ้อย	๕๓,๔๖๔	ชานอ้อย ส่วนยอดและใบ	๑๕,๕๖๗ ๑๖,๑๕๕	๐.๒๐๗ ๐.๙๕๖	๓,๒๒๒ ๑๕,๙๒๙	๑๔.๔๐ ๑๗.๓๙	๔๖,๔๐๑ ๒๗๗,๐๐๖
ข้าว	๒๔,๑๗๒	แกลบ ฟาง (ส่วนบน)	๕,๕๖๐ ๑๐,๘๐๕	๐.๔๙๓ ๐.๖๘๔	๒,๗๔๑ ๗,๓๙๑	๑๔.๒๗ ๑๐.๒๔	๓๙,๑๑๒ ๗๕,๖๗๙
ปาล์มน้ำมัน	๓,๒๕๖	ทะลายเปล่า เส้นใยปาล์ม กะลาปาล์ม ก้าน ทะลายตัวผู้	๑,๓๙๕ ๔๗๙ ๑๖๐ ๘,๔๗๙ ๗๕๙	๐.๕๘๔ ๐.๑๓๔ ๐.๐๓๗ ๑.๐๐๐ ๑.๐๐๐	๘๑๔ ๖๔ ๖ ๘,๔๗๙ ๗๕๙	๑๗.๘๖ ๑๗.๖๒ ๑๘.๔๖ ๙.๘๓ ๑๖.๓๓	๑๔,๕๓๕ ๑,๑๓๐ ๑๐๙ ๘๓,๓๔๕ ๑๒,๓๘๙
มันสำปะหลัง	๑๙,๐๖๔	ลำต้น	๑,๖๗๘	๐.๔๐๗	๖๘๓	๑๘.๔๒	๑๒,๕๗๗
ข้าวโพด	๔,๒๘๖	ซังข้าวโพด	๑,๑๗๐	๐.๖๗๐	๗๘๔	๑๘.๐๔	๑๔,๑๔๒
มะพร้าว	๑,๔๐๐	เปลือก กะลา ทะลาย ทางมะพร้าว	๕๐๗ ๒๒๗ ๖๙ ๓๑๕	๐.๕๙๕ ๐.๓๗๘ ๐.๘๔๓ ๐.๘๐๙	๓๐๒ ๘๕ ๕๘ ๒๕๕	๑๖.๒๓ ๑๗.๙๓ ๑๕.๔๐ ๑๖.๐๐	๕,๘๙๔ ๑,๕๑๘ ๘๙๑ ๓,๐๗๗
ถั่วเหลือง	๓๑๙	ลำต้น,ใบ,เปลือก	๘๔๙	๐.๗๖๐	๖๔๖	๑๙.๔๔	๑๒,๕๕๑
ข้าวฟ่าง	๑๔๒	ใบ,ต้น	๑๗๘	๐.๖๔๘	๑๑๕	๑๙.๒๓	๒,๒๑๕
ฝ้าย	๓๖	ลำต้น	๑๑๖	๑.๐๐๐	๑๑๖	๑๔.๔๙	๑,๖๙๖
ถั่วลิสง	๑๓๘	เปลือก	๔๕	๑.๐๐๐	๔๕	๑๒.๖๖	๕๖๔
รวม							๖๐๔,๘๒๒

ที่มา : กรมพัฒนาและส่งเสริมพลังงาน[๓]

ตารางที่ ๒ ศักยภาพการผลิตแก๊สชีวภาพจากมูลสัตว์ ปี พ.ศ.๒๕๔๓

ชนิดสัตว์	จำนวน (ตัว)	ปริมาณมูลสัตว์ (กก./ตัว/วัน)	อัตราส่วนมูลที่เก็บได้	อัตราส่วนของแข็งระเหย (%)	อัตราส่วนแก๊สชีวภาพที่ผลิตได้ (ลบ.ม./กก. ของแข็งระเหย)	ปริมาณแก๊สชีวภาพ (10^6 ลบ.ม./ปี)	ศักยภาพพลังงาน (*10^{6}MJ)
สุกร	๗,๗๖๑,๐๕๖	๒.๐	๐.๘	๒๔.๘๔	๐.๒๑๗	๑๓๔.๖๗	๒,๘๒๘
โคเนื้อ	๔,๔๐๐,๖๑๔	๕.๐	๐.๕	๑๓.๓๗	๐.๓๐๗	๑๘๓.๕๕	๓,๘๕๕
โคนม	๓๐๗,๙๒๗	๑๕	๐.๘	๑๓.๓๗	๐.๓๐๗	๕๕.๓๖	๑,๑๖๓
กระบือ	๑,๗๐๒,๒๒๓	๘.๐	๐.๕	๑๓.๖๔	๐.๒๘๖	๙๖.๙๕	๒,๐๓๖
ไก่	๑๗๒,๒๔๗,๕๖๑	๐.๐๓	๐.๘	๒๒.๓๔	๐.๒๔๒	๘๑.๕๗	๑,๗๑๓
เป็ด	๒๗,๘๘๔,๐๔๑	๐.๐๓	๐.๔	๑๗.๔๔	๐.๓๑๐	๖.๖๐	๑๓๙
ช้าง	๒,๑๗๘	๔๐	๐.๕	๒๑.๖๑	๐.๒๔๑	๐.๘๓	๑๗
รวม						๕๕๙.๕๔	๑๑,๗๕๐

ที่มา : กรมพัฒนาและส่งเสริมพลังงาน[๓]

ตารางที่ ๓ ศักยภาพการผลิตแก๊สชีวภาพจากน้ำเสียอุตสาหกรรมปี ๒๕๔๓

ประเภทอุตสาหกรรม	หน่วย	ผลผลิต (หน่วย/ปี)	น้ำเสีย/ผลผลิต (ลบ.ม./ตัน)	ปริมาณน้ำเสีย (ลบ.ม./ปี)	แก๊สชีวภาพ (ลบ.ม./ปี)	ศักยภาพพลังงาน ($*10^6$MJ)
โรงฆ่าสัตว์	ตัน	๒๒๔,๘๔๖	๗๔.๕๔	๑๖,๘๓๔,๕๖๑	๑๔,๓๙๐,๐๕๕	๓๖๙
โรงงานน้ำตาล	ตัน	๖,๔๔๗,๐๐๐	๑๑.๘๒	๗๖,๒๐๓,๕๔๐	๘๙,๓๗๑,๕๑๒	๒,๑๔๕
โรงงานสุรา	ลิตร	๗๕,๓๘๐,๐๐๐	๓.๔๐	๒๕๖,๒๗๒	๒,๕๙๓,๖๗๕	๖๒
โรงงานเบียร์	ลิตร	๑,๑๖๕,๐๐๐,๐๐๐	๔.๑๒	๔,๗๙๙,๘๐๐	๕,๕๔๖,๓๗๑	๑๐๙
โรงงานน้ำนมดิบ	ตัน	๔๙๑,๓๗๐	๔.๐๕	๑,๙๙๐,๐๔๙	๑,๐๑๔,๗๒๕	๒๔
โรงงานสับปะรดกระป๋อง	ตัน	๓๙๑,๒๘๒	๔.๙๘	๑,๙๕๘,๕๘๔	๑๒,๘๔๙,๗๔๕	๓๐๘
โรงงานอาหารทะเลแช่แข็ง	ตัน	๔๙๕,๑๗๔	๓๑.๑๔	๑๕,๔๑๙,๗๑๘	๑๖,๐๓๖,๕๐๗	๓๘๕
โรงงานอาหารทะเลกระป๋อง	ตัน	๕๕๘,๒๙๗	๓๑.๑๔	๑๗,๓๘๕,๓๖๙	๔๗,๒๙๕,๑๕๗	๑.๑๓๔
โรงงานน้ำอัดลม	ตัน	๑,๓๘๑,๐๐๐	๙.๓๐	๑๒,๘๕๓,๓๐๐	๑๒,๒๔๗,๓๗๑	๒๙๔
โรงงานแป้งมัน	ตัน	๒,๒๒๔,๑๒๔	๒๔.๗๒	๕๕,๐๐๕,๐๙๐	๑๖๖,๒๖๙,๓๗๖	๓,๙๙๐
โรงงานน้ำมันปาล์ม	ตัน	๓,๒๕๖,๐๐๐	๑.๐๐	๓,๒๕๖,๐๐๐	๖๗,๗๒๔,๘๐๐	๑,๖๒๔
รวม					๔๓๕,๓๒๙,๕๐๒	๑๐,๔๔๖

ที่มา : กรมพัฒนาและส่งเสริมพลังงาน[๓]

ตารางที่ ๔ ศักยภาพการผลิตแก๊สชีวภาพจากขยะที่ได้จากการฝังกลบ ปี ๒๕๔๓

ภูมิภาค	ปริมาณขยะ (ตัน/ปี)	สัดส่วนขยะที่ฝังกลบ(%)	ปริมาณขยะที่ฝังกลบ (ตัน/ปี)	ปริมาณแก๊สชีวภาพจากการฝังกลบ ($*10^6$ลบ.ม.)	พลังงานจากแก๊สชีวภาพจากการฝังกลบ ($*10^6$ MJ)
กรุงเทพและปริมณฑล	๓,๓๓๒,๔๕๐	๘๕	๒,๘๓๒,๕๘๓	๒๘๓.๒๖	๕,๕๒๓.๓๙
เขตเทศบาลและเมืองพัทยา					
-ภาคกลางและตะวันออก	๑,๘๖๘,๘๐๐	๘๕	๑,๕๘๘,๔๘๐	๑๕๘.๘๕	๓,๐๙๗.๕๔
-ภาคเหนือ	๗๓๗,๖๖๔	๘๕	๖๒๗,๐๑๕	๖๒.๗๐	๑,๒๒๒.๖๘
-ภาคตะวันออกเฉียงเหนือ	๙๘๙,๑๔๐	๘๕	๘๔๐,๗๗๘	๘๔.๐๘	๑,๖๓๙.๕๒
-ภาคใต้	๗๐๕,๙๑๐	๘๕	๖๐๐,๐๒๔	๖๐.๐๐	๑,๑๗๐.๐๕
นอกเขตเทศบาล	๖,๒๙๘,๐๗๕	๘๕	๕,๓๕๓,๓๖๔	๕๓๕.๓๔	๑๐,๔๓๙.๐๖
รวม	๑๓,๙๓๒,๐๕๐		๑๑,๘๕๒,๓๖๔	๑,๑๘๔	๒๓,๐๗๒.๓๗

ที่มา : กรมพัฒนาและส่งเสริมพลังงาน[๓]

ตารางที่ ๕ พื้นที่และผลผลิตของพืชน้ำมันที่สำคัญของไทย ปีเพาะปลูก ๒๕๔๔/๒๕๔๕

พืชน้ำมัน	พื้นที่เพาะปลูก (*พันไร่)	ผลผลิต (พันตัน)	ผลผลิต/ไร่ (กก./ไร่)
ปาล์มน้ำมัน	๑,๔๕๗	๔,๐๘๙	๒,๘๐๗
มะพร้าว	๒,๐๓๗	๑,๓๙๖	๖๘๕
ถั่วเหลือง	๑,๓๒๔	๒๙๒	๒๒๗
ถั่วลิสง	๕๒๑	๑๒๙	๒๔๒
งา	๓๙๔	๓๙	๙๙
ละหุ่ง	๘๔	๙	๑๐๗

ที่มา : สำนักงานเศรษฐกิจการเกษตร[๔]

ตารางที่ ๖ สรุปสถานภาพของพลังงานแสงอาทิตย์ของประเทศไทย

ลักษณะการใช้	สถานภาพ						
	งานวิจัยพื้นฐาน	งานวิจัยและพัฒนา	การออกแบบทางวิศวกรรมและงานสาธิต	คุ้มค่าทางเศรษฐศาสตร์	มีจำหน่ายแบบตามใบสั่ง	ไม่เป็นเชิงพาณิชย์	มีการใช้ในเชิงพาณิชย์
เครื่องทำน้ำร้อน		X	X	X			X
เครื่องอบแห้ง		X	X	X	X		
เครื่องกลั่นน้ำ		X		X	X		
เครื่องทำความเย็น		X				X	
เซลล์แสงอาทิตย์		X	X	X (เฉพาะพื้นที่)			X

หมายเหตุ : X หมายถึง มีสถานภาพตามหัวข้อในแนวตั้ง

ตารางที่ ๗ สรุปสถานภาพของพลังงานลมของประเทศไทย

ลักษณะการใช้งาน	สถานภาพ			
	ศักยภาพทางเทคนิค	มีการใช้งานอย่างแพร่หลาย	โครงการสาธิต	มีจำหน่ายเชิงพาณิชย์
กังหันลมเพื่อการสูบน้ำ	X	X		X
กังหันลมเพื่อผลิตไฟฟ้า	X		X	

หมายเหตุ X หมายถึง มีสถานภาพตามหัวข้อในแนวตั้ง

ตารางที่ ๘ อุณหภูมิของน้ำทะเลในบริเวณอ่าวไทย

ช่วงเวลา	อุณหภูมิ (องศาเซลเซียส)		
	ผิว	ลึก ๓๐ ม.	ลึก ๕๐ ม.
มี.ค. – เม.ย.	๒๙.๐๐	๒๘.๑๗	๒๗.๙๕
พ.ค. – ก.ย.	๓๐.๐๔	๒๙.๔๘	๒๘.๕๔
พ.ย. – ก.พ.	๒๘.๓๕	๒๘.๒๔	๒๗.๙๖

ที่มา : โครงการศึกษาเบื้องต้นศักยภาพและความเหมาะสมในการพัฒนาพลังงานจากทะเล[๔๔]

ตารางที่ ๙ ความแตกต่างของระดับน้ำขึ้น-น้ำลงของทะเล

ช่วงเวลา	ความแตกต่างของระดับน้ำขึ้น-น้ำลง สูงสุด		ความแตกต่างของระดับน้ำขึ้น-น้ำลง ต่ำสุด	
	สถานี	ความแตกต่าง (เมตร)	สถานี	ความแตกต่าง (เมตร)
อ่าวไทย				
มี.ค. – เม.ย.	มหาชัย	๒.๕๘	สงขลา	๐.๘๔
พ.ค. – ก.ย.	มหาชัย	๒.๗๖	สงขลา	๐.๘๕
พ.ย. – ก.พ.	หัวหิน	๒.๗๔	สงขลา	๑.๐๒
ทะเลอันดามัน				
มี.ค. – เม.ย.	เกาะตะเภาน้อย	๒.๙๗	ทับละมุ	๒.๗๗
พ.ค. – ก.ย.	เกาะตะรุเตา	๒.๙๑	ทับละมุ	๒.๖๕
พ.ย. – ก.พ.	เกาะตะรุเตา	๒.๙๓	เกาะตะเภาน้อย	๒.๕๑

ที่มา : โครงการศึกษาเบื้องต้นศักยภาพและความเหมาะสมในการพัฒนาพลังงานจากทะเล[๔๔]

ตารางที่ ๑๐ ระดับความสูงของคลื่นและคาบคลื่น

ช่วงเวลา	ความสูงคลื่น (เมตร)	คาบคลื่น (วินาที)
อ่าวไทย		
มี.ค. – เม.ย.	๐.๑ – ๐.๗	๒-๔
พ.ค. – ก.ย.	๐.๑ – ๑.๒	๒-๖
พ.ย. – ก.พ.	๐.๑ – ๑.๗	๒-๖
ทะเลอันดามัน		
พ.ค. – ก.ย.	๐.๑ – ๐.๓	๒-๕
พ.ย. – ก.พ.	๐.๕ – ๔.๕	๔-๗

ที่มา : โครงการศึกษาเบื้องต้นศักยภาพและความเหมาะสมในการพัฒนาพลังงานจากทะเล[๔๔]

Proceedings of the 4th Asia Pacific Drying Conference, Kolkata, India, 13-15 December 2005

New Method for Producing Parboiled Rice Under High-Temperature Superheated-steam Fluidization

S. Soponronnarit, S. Prachayawarakorn[1] and C.Taechapairoj[2]

School of Energy and Materials, [1]Faculty of Engineering,
King Mongkut's University of Tech., Thonburi, Bangkok 10140, Thailand
[2]Faculty of Engineering and Ind. Tech., Silpakorn University, Nakhon Phathom 73000, Thailand
E-mail: somchart.sop@kmutt.ac.th

ABSTRACT

In order to extremely shorten a long process time of parboiled-rice production, a new method for parboiling paddy and brown rice using superheated-steam fluidization was investigated. The experimental conditions were carried out at the initial moisture contents of 39-42.5% dry basis (d.b.), bed heights of 8-15 cm, superheated-steam temperatures of 120-170°C with a constant pressure of 106.1 kPa and a fixed superficial velocity of 3.1 and 3.9 m/s for paddy and brown rice, respectively. The experimental results showed that the inlet temperature had much more effect on moisture removal than the bed height. For the rice quality, reducing moisture content to 28 and 18% d.b., in case of brown rice and paddy, respectively, resulted in higher percentage of head rice yield and lower percentage of white belly (<1.5%). The whiteness of polished rice, obtained from the parboiled paddy and brown rice, became significantly darker when affected by increased inlet temperature. SEM figures of the parboiled rice indicated a complete gelatinization of starch granules. Additionally, peak viscosity, breakdown viscosity, and setback viscosity of rice flour were found lower than those of raw rice.

Keywords: Drying; Quality; Scanning Electron Microscopy (SEM); Viscosity

INTRODUCTION

Parboiling of rough rice is a hydro-thermal process aimed at improving milling, nutritional, resistance to spoilage by insects and mold, and organoleptic attributes of rice. It is an alternative method for prolonging shelf life rice storage. Additionally, it reduces broken grain, increases head rice yield and reduces nutritional loss during polishing process.[1] In the traditional parboiling process, paddy is steeped in water until attaining the moisture content approximate 30% wet basis (w.b.). This stage is taken overnight or longer in water at ambient temperature. It is then followed by boiling or steaming the steeped rice at 100°cC to gelatinize the starch, resulting in the grain swelling and the hull's lemma and palea separating. The parboiled rice is then cooled and dried before storing and milling. In the modern process, the stages are similar to the first one, except for the soaking stage in which paddy is immersed in hot water in order to reduce the sour odour and accelerate transport of water into kernel.[2] After soaking in hot water, paddy is left to cool down to environmental temperature for 2 hours to allow water to enter the core part of rice grain.

The drying method is the key factor influencing the milling quality of rice.[3] Several drying methods have been used for drying parboiled rice such as shade or sun drying, hot air drying, vacuum drying and superheated-steam drying.[1, 4, 5]

Fluidisation technique is an effective drying method, in which air and solid particles are rigorously mixed. It has been suggested that high moisture paddy should be dried quickly to approximate 23% d.b. to prevent the yellowing of rice kernels which is easily occurred at high moisture level and then subjected to ambient air drying in a storage bin until its moisture content is down to 16% d.b.[6] Sutherland & Ghaly[7] undertook an intensive investigation into the feasibility of using a hot-air fluidized-bed drying technique for paddy. Their experiments showed that the head rice yield related to the final moisture content: the head rice yield was 58-61% when paddy was

dried from 28.2 to 20.5% d.b. but was 15-24% for final moisture content lower than 20% d.b.

The drying medium which is used for carrying the evaporated water and fluidizing solid particles could be hot air or superheated steam. Superheated-steam drying offers many important advantages over hot air drying. Firstly, the energy supplied to the dryer can be reduced economically by recycling the exhaust steam in a closed loop. Secondly, the energy from the exhaust steam resulting from the evaporation of moisture inside the solids can be recovered and used in the other sections. Lastly, environmental pollution or odour emission to the atmosphere can be eliminated since drying occurs in a closed chamber without air.

The purpose of this work is to produce the parboiled rice from paddy and brown rice using superheated-steam fluidized bed. The characteristics of rice such as pasting properties and microstructure are investigated. In addition, the head rice yield, whiteness and white belly of rice are also determined.

MATERIALS AND METHODS

A batch superheated steam fluidized dryer is shown in Fig. 1. The system of the fluidised-bed dryer consists of five main components: a cylindrical chamber with an 15 cm inner diameter and a 100 cm height, a 13.5 kW electrical heater for converting saturated steam to the superheated steam, a backward-curved blade centrifugal fan driven by a 2.2 kW motor, a reverse flow cyclone and a small boiler with a 31 kg/h capacity of generated steam. A PID controller with an accuracy of ± 1°C was used to control the steam temperature. Before using steam for drying, hot air was used for warming up the system until the temperature in every part reached the desired temperature. Then, the steam was replaced accordingly. The steam generator was generated the saturated steam at 106 kPa (absolute pressure) with the corresponding temperature of 101°C. When the saturated steam was flown through the electrical heaters, the additional heat was supplied to rise the steam temperature to the required level. It was subsequently flown through the fluidized bed dryer. The dust particles and the immature grains being suspended in the exhaust steam were

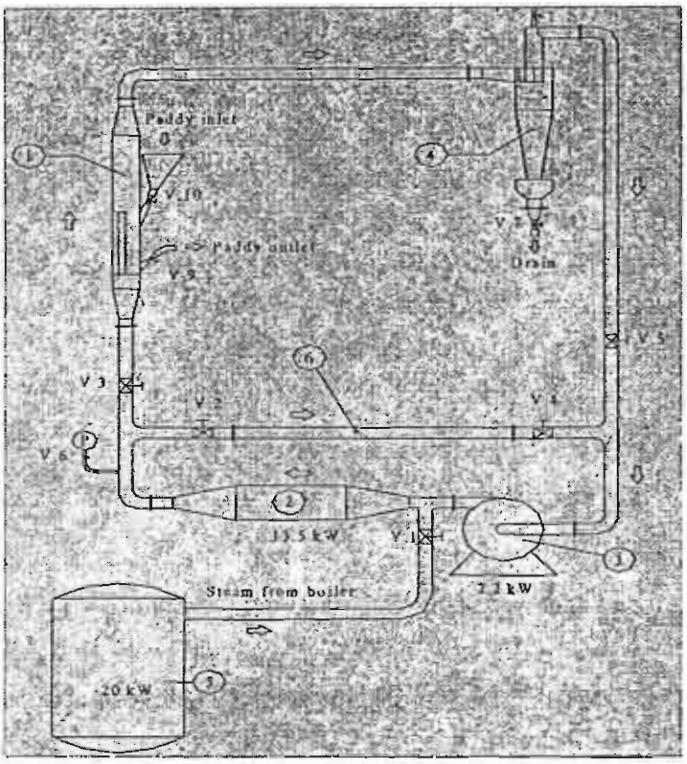


Fig. 1: A Schematic Diagram of Superheated Steam Fluidised Bed dryer System.

collected at the cyclone. Finally, the cleanning exhaust steam was reused again.

Long grain paddy of Chainat1 (CNT1) variety from Pathum Thani Rice Research Center, Pathum Thani Province, Thailand. Paddy was soaked at temperature of 80°C for 3.5 h. Then, the water was drained out and tempered at same tank for 1 h. The drying conditions were set up as follows: initial moisture contents of 41-42.5% d.b., superheated steam temperatures of 150-170°C, bed heights of 10-15 cm, at superficial velocity of 3.1 m/s.

Brown rice was prepared from long grain paddy of Chainat1 (CNT1) variety. It was soaked in hot water temperature of 70°C for 1 h before draining and tempering to ambient temperature for 30 minutes. The drying conditions were set at initial moisture contents of 37.5 – 40% d.b., superheated steam temperatures of 120 – 160°C, bed depths of 8-12 cm at superficial velocity of 3.9 m/s.

Temperatures at different positions of drying chamber were measured by Chromel-Alumel thermocouples (Type K) connected to

a data logger with an accuracy of ± 1°C (COMARK Model 8510, England). The grain, with a mass of 1 kg, was dried until reaching the predetermined time and then withdrawn from dryer at the valve V.9 to determine the moisture content and grain temperature. To measure grain temperature, the kernels were fully packed in a well-insulated container. After that, the sample was kept in polypropylene bag and left in the environmental condition until the grain temperature approached the ambient temperature. Then, it was spread on a sieve and ventilated by an ambient airflow until its moisture content reached 16 % dry basis. Finally, a 300 g sample was kept in a seal plastic bag for 2 weeks before testing head rice yield, whiteness and white belly.

The moisture content of paddy and brown rice were determined by an electrical air oven at a temperature of 103°C for 72 h. (AOAC, 1995)[8] Paddy qualities in terms of head rice yield and whiteness were quantitatively determined and compared to the reference sample (paddy dried by the ambient air). The methods were followed with the guideline of the Ministry of Agriculture and Cooperatives, Thailand. Head rice is defined as milled rice having kernel length of at least 75% of its original length. The individual head rice kernels after milling were graded manually to check for the white belly. Kernel that has an opaque white area exceeding 50% of its total area was categorized as white belly (Ministry of Commerce Thailand, 1997).[9]

The color of rice samples was measured by a Kett digital whiteness meter (Model C – 300). Before measuring the color of sample, the whiteness meter was calibrated with a white colored reference, presenting a standard value of 86.3.

SCANNING ELECTRON MICROSCOPY

Structural changes of kernels were investigated by scanning electron microscopy (SEM) (JSM – 5600LV, Japan). The rice kernel was broken along the cross-sectional axis. Samples were placed on adhesive tape attached to a circular aluminum specimen stub, coated with gold layer using a sputter-coater and photographed at an accelerator potential of 10 kV.

RVA MEASUREMENT

All rice flour samples were prepared by grinding rice with a laboratory model hammer mill (Retsch Mühle, type SK1, Germany) with a mesh opening of 800 mm. Pasting properties of rice flour were determined by a Rapid Visco Analyser model-4 (Newport Scientific Pty Ltd., Warriewood, Australia) utilizing Thermocline. Following AACC Method 61 – 02 (AACC, 1995)[10], the sample (3 g, 14% moisture basis) was mixed with distilled water in a RVA aluminum canister to make the total weight of slurry 28 g. The mixture was stirred at 900 rpm for 10 s and then changed to 160 rpm. The mixture was held at 50°C for 1 min and then heated to 95°C at 12°C/min. After that, holding at 95°C for 2.5 min, followed by cooling down to 50°C at 12°C/min and kept for 2.1 min. These tests were done in duplication. A plot of paste viscosity in arbitrary RVA unit (RVU) versus time was used to determine the peak viscosity (PV), temperature at peak viscosity (P_{temp}), trough final viscosity (FV), breakdown viscosity (BKV = PV- trough) and setback viscosity (SBV = FV – trough). The first point at which the viscosity increases to 1 RVU/s or faster is defined as the onset gelatinization temperature of rice flour (P_{Temp}). Peak viscosity (PV) indicates the water-biding capacity of the mixture. It is often correlated with the final product quality, and also provides an indication of the viscous load likely to be encountered by a cook. Breakdown viscosity measures the degree of disintegration of the granules or paste stability. Setback viscosity is a measure of gelling or retrogradation tendency.

RESULTS AND DISCUSSION

Drying Curve

Fig. 2 shows the relationship between grain moisture content, temperature and drying time. At the initial stage of drying, a region where the uptake of moisture into grains can be observed, typically of the order of 1 – 2% moisture content dry basis, since the flowing steam contacting with a low initial temperature of paddy is condensed. The amount of water uptake is slightly dependent on the steam temperature, as observed from the experiments.

Because of rapid release of heat vaporisation by condensation, the grain temperature rapidly increases. As shown in Figs. 2a and 2c,

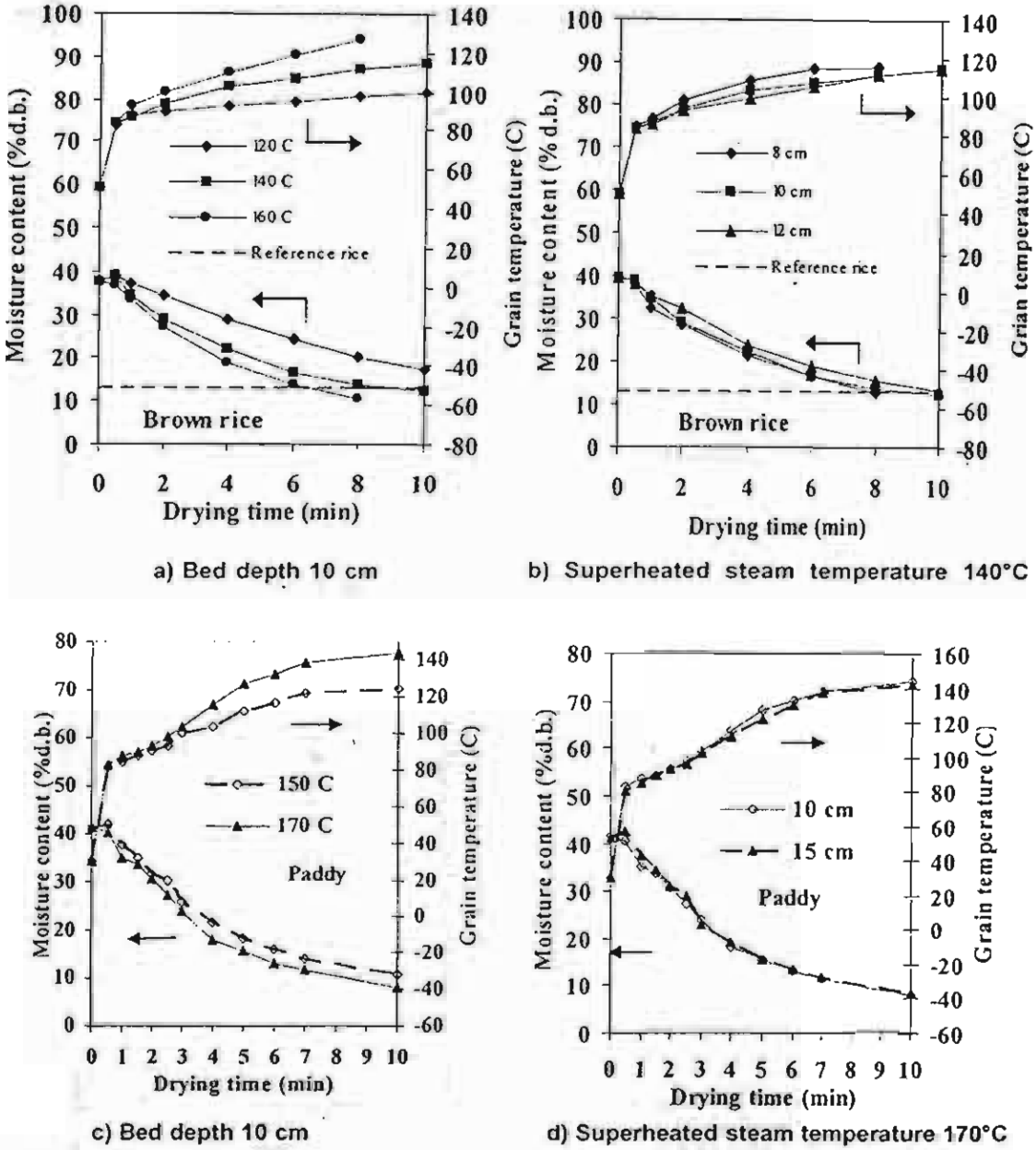


Fig. 2: Effect of Superheated Steam Temperatures and Bed Depths on Moisture Content and Grain Temperature

the grain temperature is slightly above 80°C in the first minute of drying time and then relatively rises to 100°C in 3 or 4 minutes. Afterwards, the grain temperature rapidly increases and higher grain temperatures follow with higher steam temperatures, resulting in the relative difference of moisture content.

The effect of bed depth on drying rate and grain temperature were of less significant than that of superheated steam temperature (Figs. 2b and 2d).

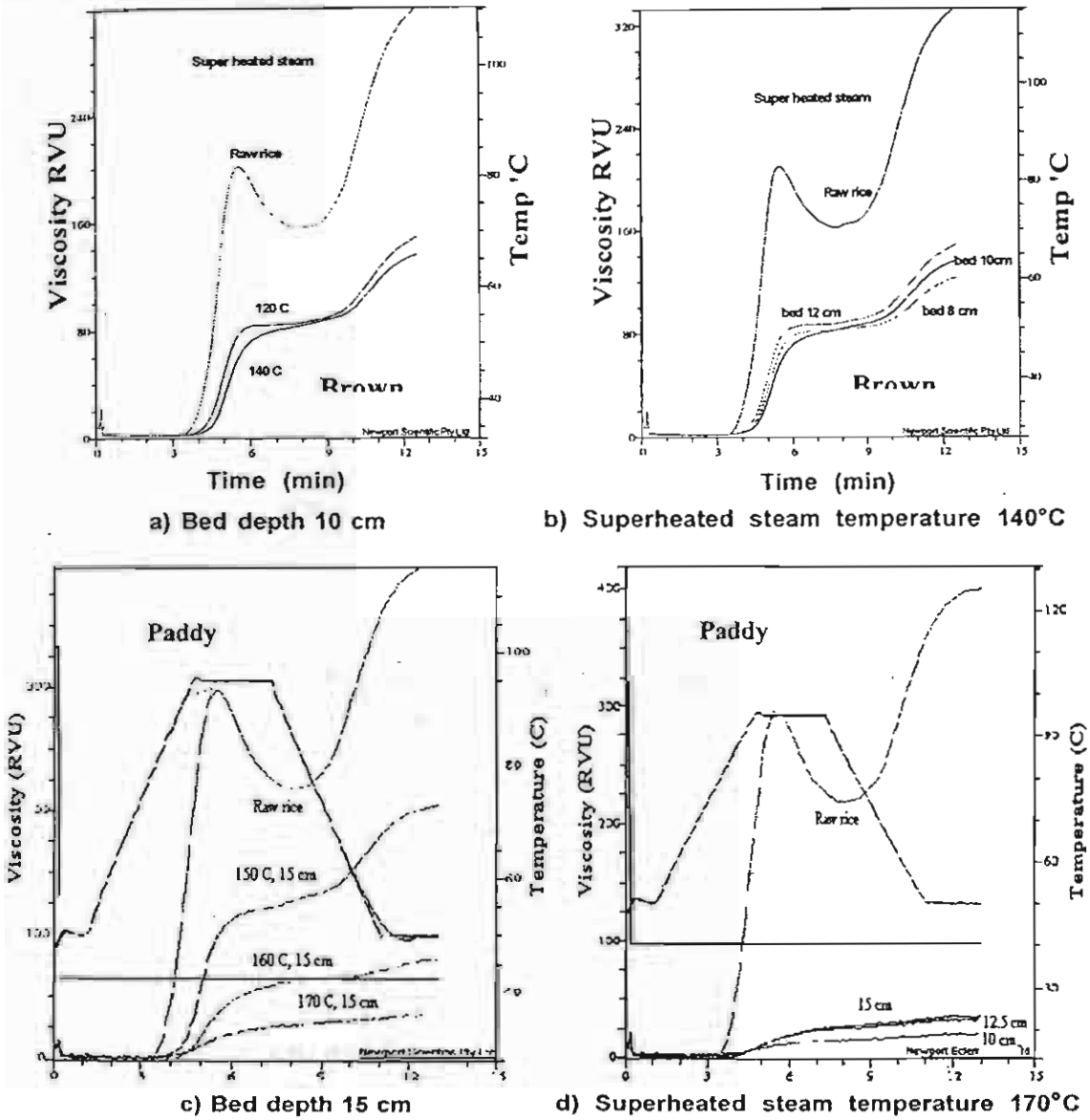


Fig. 3: Viscograph of Raw Rice Flour and Rice Flour Dried by Superheated Steam.

PASTING PROPERTIES

Pasting curve of viscosity determined by RVA represents the viscosity of starch during heating cycle, which shows the integrity of starch granules and hydration properties resulting from the native properties of starch or from the molecular interactions during drying.

Pasting properties of raw rice, brown rice and paddy dried by superheated steam are shown in Fig. 4. It was clearly seen that the characteristic properties of dried brown rice and paddy totally differed from those of raw rice. The PV, BKV, FV and SBV of treated rice flour are remarkably smaller than those of the raw rice flour. Decrease in PV of dried rice was due to its loss of water binding capacity as a result of partial gelatinization. The treated samples possess low firmness texture, as indicated by the low FV and SBV. It was also found that the effect of temperature on pasting properties of dried material was more pronounced than that of the bed depth, especially for the paddy. The differences between the pasting properties of the raw rice flour and dried rice flour increased with increasing drying temperature. This is because the degrees of reassociation of starch molecules depend on the degree of heat treatment.

HEAD RICE YIELD

The relationship between head rice yield and final moisture content of brown rice grain at various superheated steam temperatures and bed depths are presented in Figs. 4a and 4b. Drying brown rice with superheated steam at an initial stage provided higher head rice yield compared to that of reference sample. An increase in head rice yield, closed to that of reference rice, was apparent at the final rice moisture content of 28 – 29% d.b. This improvement was caused by stronger structure of rice starch as a result of gelatinization process (Fig. 5c). Furthermore, the denaturation of protein and diffused into inter-granular space of starch increase the binding effect. With higher moisture content, rice starch dried by superheated steam was more rapidly gelatinized, thus, stronger structure was obtained. When rice grain with moisture content of lower than 28% d.b. was exposed to longer heating period, rice grain temperature will be increased resulting in more porosities within rice starch, high moisture and temperature gradient causing stress development inside the kernels. As a result, rice kernel are more susceptible to physical damage during milling process leading to lower head rice yield. At a given final moisture content, head rice yield increased with increasing superheated steam temperature and bed depth.

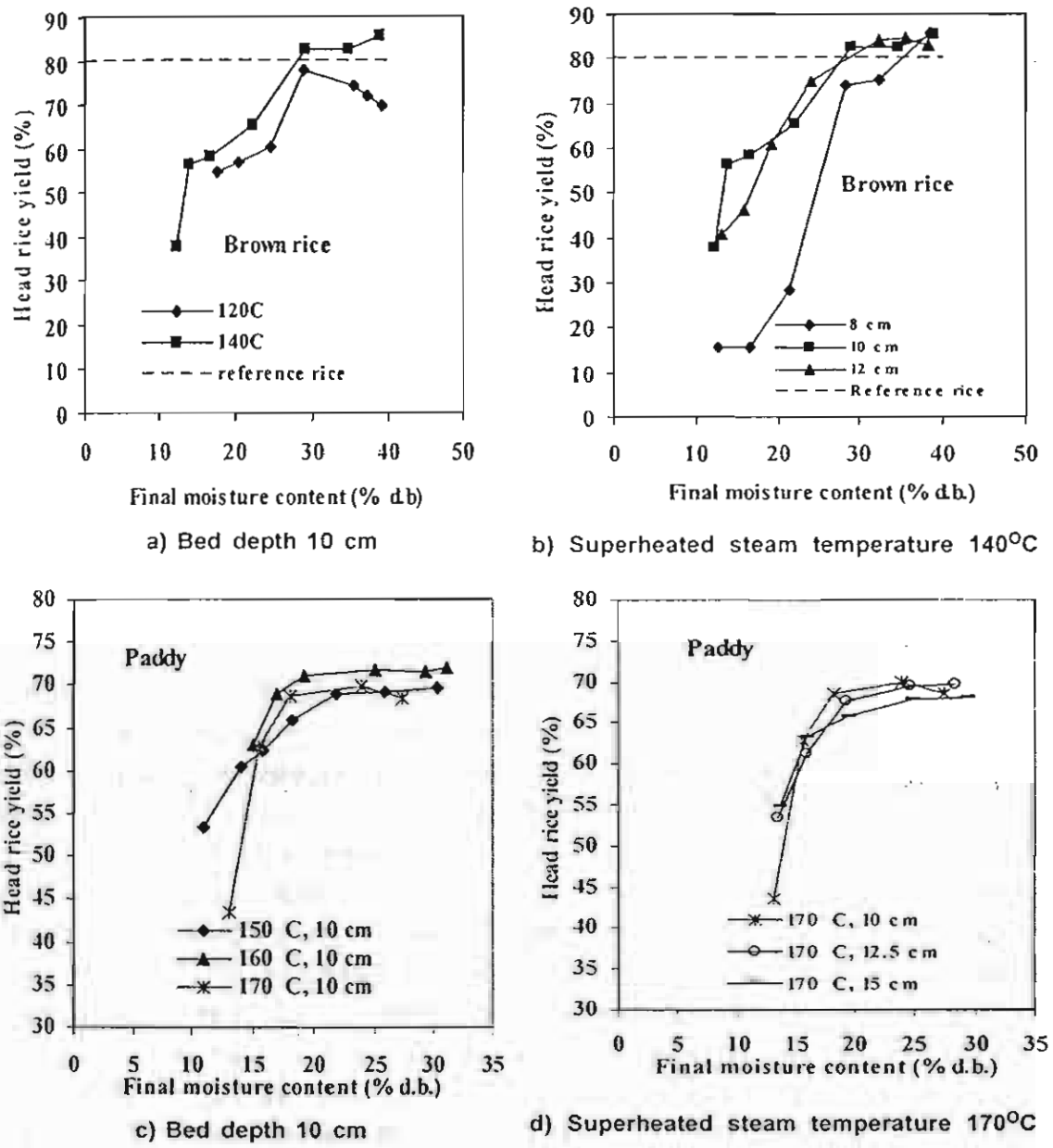
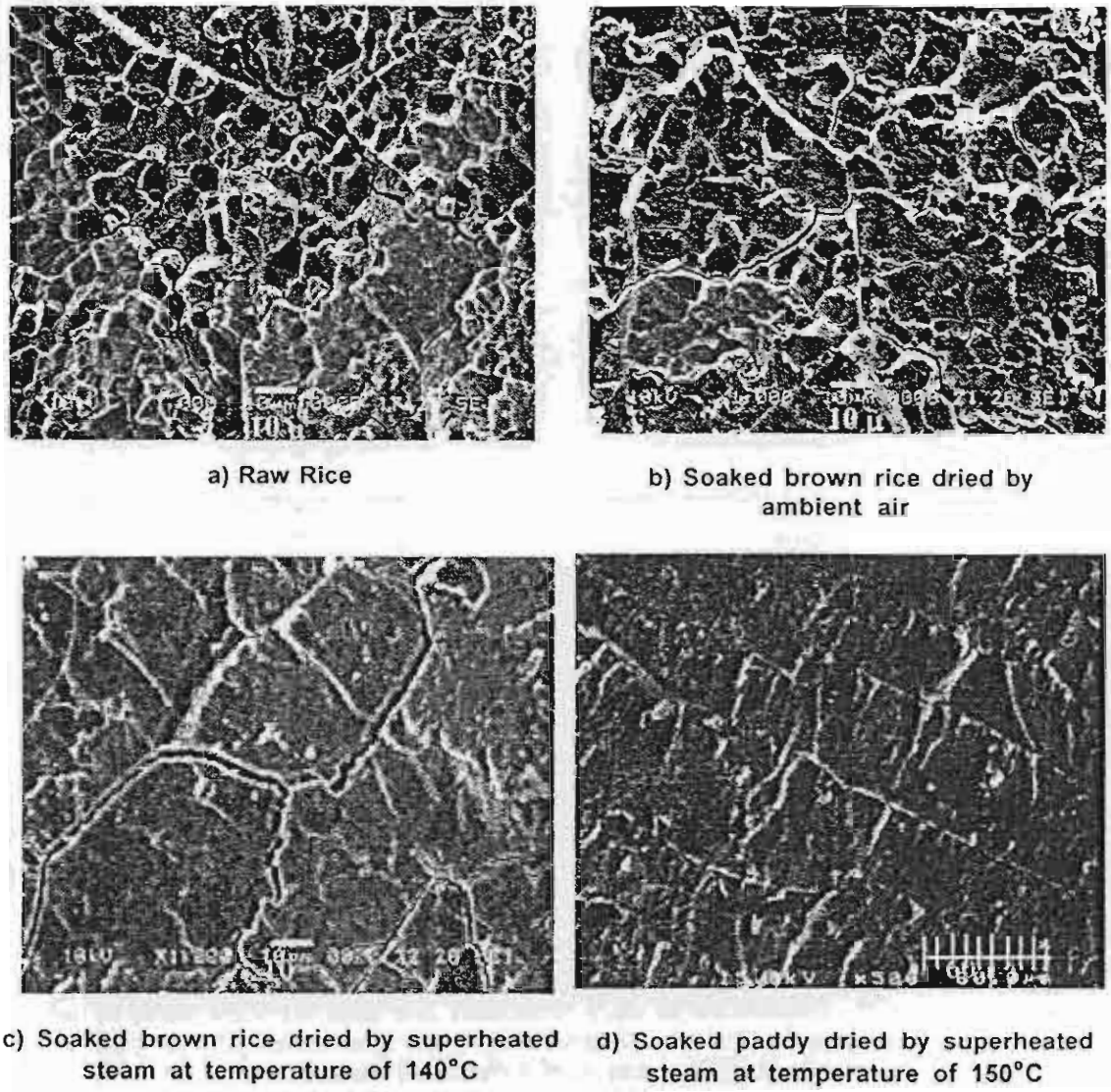


Fig. 4: Relationship between Head Rice Yield and Final Moisture Content During Drying in Superheated Steam at Different Bed Depths and Steam Temperature.

The relationship between head rice yield and final moisture content of paddy in the superheated-steam fluidized-bed dryer at different drying conditions is shown in Figs. 4c-4d. The head rice yield slightly changes when the paddy is dried from 41 – 42.5% to 18% d.b. The head rice obtained is in the narrow range of 65 to 70, which is 70% higher than that of the control samples. The higher head rice yield is



a) Raw Rice

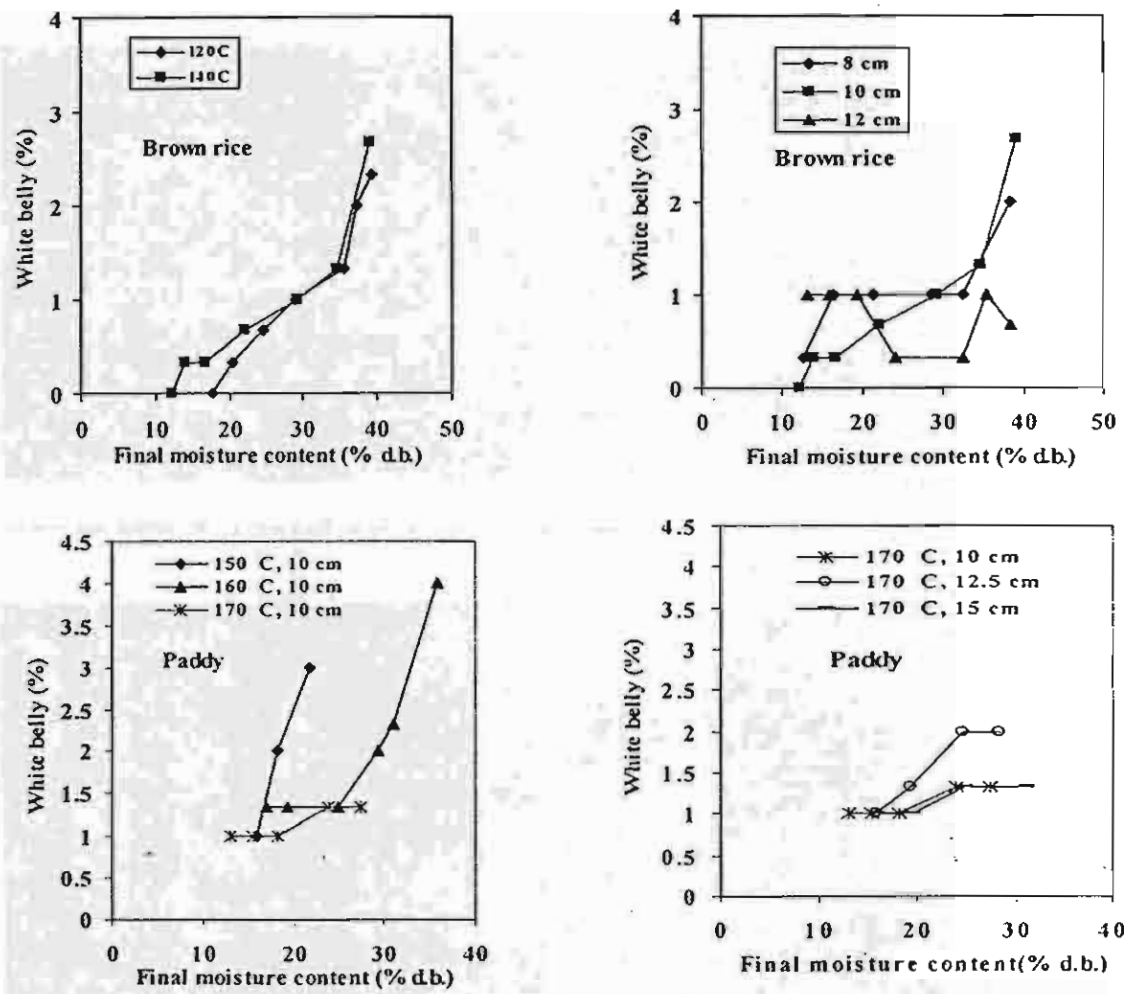
b) Soaked brown rice dried by ambient air

c) Soaked brown rice dried by superheated steam at temperature of 140°C

d) Soaked paddy dried by superheated steam at temperature of 150°C

Fig. 5: Scanning Electron Micrographs of Rice at Different Processes

because the swelling effect causes the starch granules approaching together and thus resistant to deformation by strengthening the intra-molecular binding forces (Fig. 5d). This explanation can be indicated by the low SBV, FV and trough of dried rice flour in RVA measurement. However, when the moisture content reduces below 18% d.b., the head rice yield rapidly decreases. This may be caused by the prevalent contribution of stress forces taken place by moisture gradient, leading to fissure development inside the grain kernels.



c) Bed depth 10 cm

d) Superheated steam temperature 170°C

Fig. 6: Relationship between White Belly Percentage and Final Moisture Content During Drying in Superheated Steam at Different Drying Temperatures and Bed Depths (white Belly Percentage of Reference Rice = 20%).

WHITE BELLY

White belly is considered a poor characteristic of parboiled rice caused by incomplete gelatinization of rice starch. It is described as dully white spot with porosities between the starch granules. White belly is usually found at the core of rice kernel. Fig. 6 shows the relationship between white belly and final moisture content of brown rice and paddy at various superheated steam temperatures and bed depths. The percentage of white belly was calculated by the number of white belly kernels divided by the total number of head rice kernels. The percentage of white belly kernels reduces with decrease in final

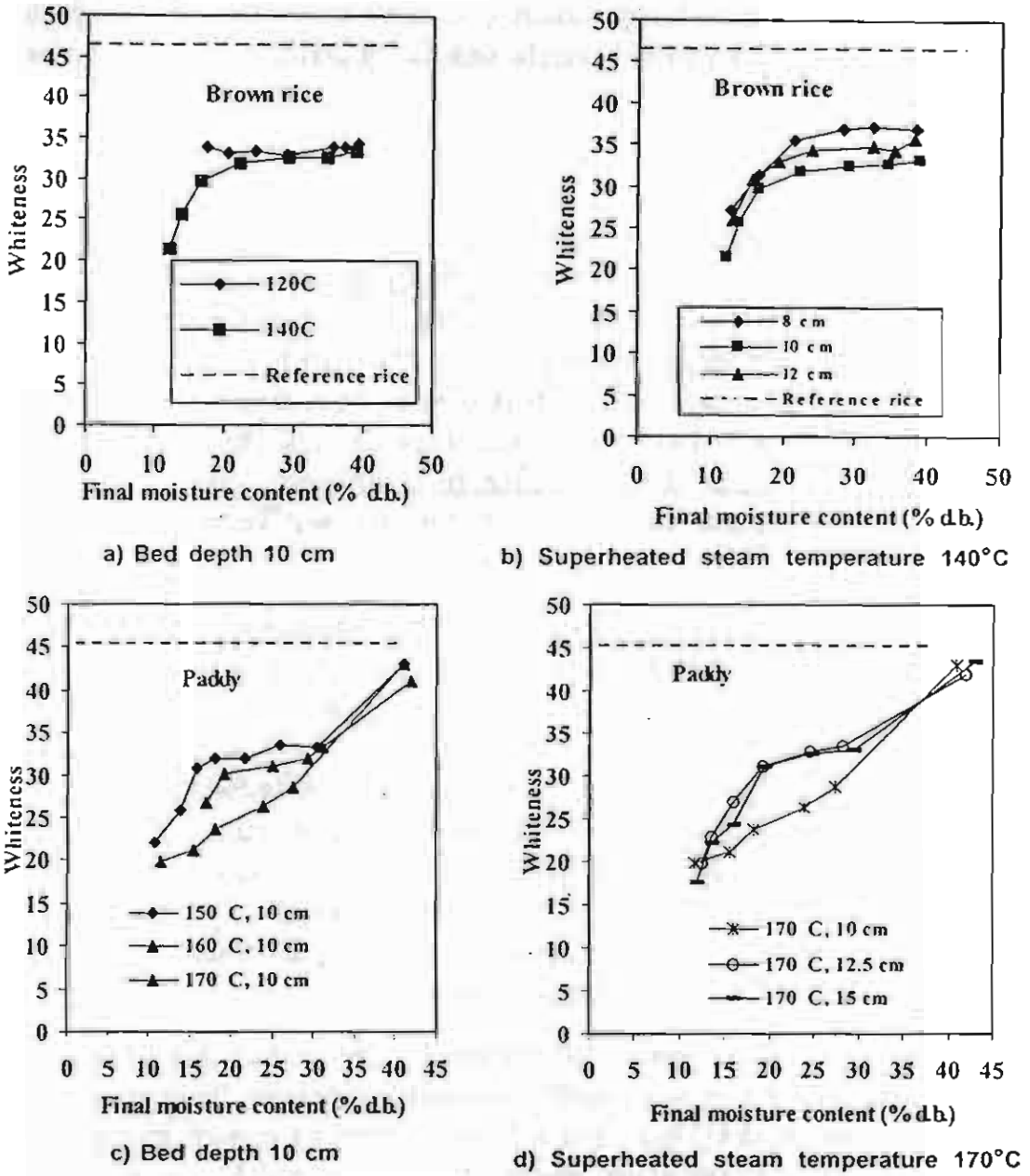


Fig. 7: Relationship between Whiteness and Final Moisture Content During Drying in Superheated Steam at Different Drying Temperatures and Bed Depths.

moisture content or, in other words, with increase in drying time. When drying temperature is changed, the percentage of white belly is changed in a way that higher temperature provides the smaller number of white belly kernels as shown in Figs 6a and 6c. The bed depth has a rather small effect, with the value lying between 1 and 2% for the bed depths of 8 to 15 cm as illustrated in Figs. 6b and 6d.

According to the white belly results, it may be indirectly used to indicate how well the grain kernels can be gelatinized, besides the accurate method.

RICE WHITENESS

Compared with reference rice, dried brown rice gave lower whiteness value (Fig. 7). The dark colour of dried grain was caused by maillard browning reaction between reducing sugar and amino acid activated by heat. Figs. 7a and 7b show the relationship between the whiteness and final moisture content of brown rice at various temperatures and bed depths. Superheated steam temperature did not show significant effect on the whiteness. The decrease in whiteness was found only when the final moisture content of brown rice was lower than 20% d.b.

The change of the colour of paddy samples at steam temperatures of 150, 160 and 170°C and initial moisture content of 42% d.b. are shown in Figs. 7c and 7d. The rice whiteness at the first 2 minutes of drying steeply drops from the original values, 41 – 43, to approximately 30. Such a rapid change in the colour is due to the steam condensation onto the paddy surface. The resulting bran and colour pigments covered around kernel are dissolved and then adsorbed by the endosperm: the amounts of bran after milling for the dried samples are in order of 5.3 to 7.1%, which is approximately 2 times lower than the original value of the reference samples.

In addition to the dissolved pigments, the colour development might be caused by non-enzymatic browning reaction. This reaction seems to be enhanced by high grain temperature as shown in Fig. 6c, where the higher temperature causes the lower whiteness. For the bed depth effect, the slightly low value of whiteness is obtained with the use of thin bed depth.

CONCLUSION

From the study of superheated steam fluidized bed drying of parboiled paddy and brown rice, it was found that superheated steam temperature was the most significant effect on drying rate while bed depth was of

minor importance. The head rice yield considerately decreased when final moisture content of rice grain were lower than 28 and 18% d.b. in case of brown rice and paddy, respectively, resulted in higher percentage of head rice yield and lower percentage white belly. The whiteness of polished rice, obtained from the parboiled paddy and brown rice, were apparently darkened at high temperature. According to the viscosity properties of rice starch, superheated steam drying provided lower PV, BKV and SBV compared with raw rice.

ACKNOWLEDGEMENT

The authors would like to express sincerely thanks to Thailand Research Fund for financial support and Institute of Food Research and Product Development, Kasetsart University for physical properties testing machine.

REFERENCES

1. Bhattacharya, K.R., 1985, Parboiling of rice. In B.O. Juliano (Ed.), *Rice : Chemistry and Technology* (pp. 289-348), St. Paul, Mn, USA: American Association of Cereal Chemists
2. Gariboldi, F., 1974, Rice Parboiling, FAO Agricultural Development Paper No. 97, Food and Agriculture Organization of the United Nations, Rome, Italy.
3. Bhattacharya, K.R. and Indudhara Swamy, Y.M., 1967, Conditions of drying parboiled paddy for optimum milling quality. *Cereal Chemistry* 44: 592-600.
4. Taechapairoj, C., Prachayawarakorn, S. and Soponronarit, S., 2004, Characteristics of rice dried in superheated steam fluidised bed, *Drying Technology* 22(4): 719-743.
5. Soponronarit, S., Taechapairoj, C. and Prachayawarakorn, S., 2004, New technique producing parboiled rice, *The Journal of the Royal Institute of Thailand* 29(1): 78-86.
6. Soponronnarit, S. and Prachayawarakorn, S., 1994, Optimum strategy for fluidised bed paddy drying, *Drying Technology* 12 (7): 1667-1686.
7. Sutherland, J.W. and Ghaly, T.F., 1990, Rapid fluid-bed drying of paddy rice in the humid tropics, *Presented the 13th ASEAN Seminar on Grain Postharvest*